Université de Montréal

Étude du rôle de la conformation des glycoprotéines de l'enveloppe du VIH-1 dans la réponse cytotoxique cellulaire dépendante des anticorps

par
Jérémie Prévost

Département de microbiologie, infectiologie et immunologie
Faculté de médecine

Thèse présentée en vue de l'obtention du grade de
Philosophiae Doctor (Ph.D.)
en Microbiologie et Immunologie

Juin, 2022

Université de Montréal
Faculté des études supérieures et postdoctorales
Département de microbiologie, infectiologie et immunologie, Faculté de médecine

Cette thèse intitulée :

Étude du rôle de la conformation des glycoprotéines de l'enveloppe du VIH-1 dans la réponse cytotoxique cellulaire dépendante des anticorps

Présentée par
Jérémie Prévost

a été évaluée par un jury composé des personnes suivantes :

Dr Jacques Thibodeau
Président-rapporteur

Dr Andrés Finzi
Directeur de recherche

Dr Roger Lippé
Membre du jury

Dr Olivier Schwartz
Examinateur externe

Dre Marylise Duperthuy
Représentante du doyen

RÉSUMÉ

En l'absence d'un vaccin efficace et avec des thérapies antirétrovirales incapables d'éradiquer le virus, le VIH-1 reste un problème de santé publique mondial. Des immunothérapies à base d'anticorps sont à l'étude pour éliminer les réservoirs cellulaires, qui représentent un obstacle incontournable à la guérison du VIH-1. Les glycoprotéines d'enveloppe du VIH-1 (Env) représentent le seul antigène du virus exposé à la surface des cellules infectées et constituent donc la principale cible des anticorps. L'Env non-liée adopte sa conformation « fermée », reconnue préférentiellement par les anticorps neutralisants. L'interaction avec CD4 fait passer Env dans sa conformation « ouverte », exposant des épitopes conservés reconnus par les anticorps non-neutralisants (nnAbs) présents dans le sérum d'individus infectés par le VIH-1 (sérums VIH+). Les nnAbs peuvent éliminer les cellules infectées par la cytotoxicité cellulaire dépendante des anticorps (ADCC). Cependant, les protéines accessoires Nef et Vpu diminuent l'expression de surface de CD4 et BST-2 afin d'évader à la reconnaissance et l'élimination des cellules infectées par les nnAbs. Dans cette thèse, nous caractérisons en détail la contribution d'Env, Nef et Vpu pour échapper aux réponses humorales et explorons de nouvelles stratégies pour sensibiliser les cellules infectées à l'ADCC.

Pour quantifier plus adéquatement la réponse ADCC, nous avons identifié des biais dans les tests largement utilisés, notamment pour évaluer les corrélats de protection vaccinale. Il s'agit de l'incapacité à faire la distinction entre l'élimination des cellules infectées et des cellules non-infectées, et l'utilisation de constructions virales comportant un gène rapporteur empêchant l'expression de Nef. En utilisant un nouveau marquage intracellulaire, nous avons confirmé l'effet protecteur de Nef et Vpu contre l'ADCC.

Ensuite, nous avons étudié les déterminants d'Env et Vpu modulant la susceptibilité des cellules infectées à l'ADCC médiée par les nnAbs. Certaines caractéristiques structurelles d'Env modulent ses transitions conformationnelles, incluant le domaine d'association du trimère, le site de clivage de la furine et la cavité Phe43. L'altération de ces composantes augmente la sensibilité des cellules infectées à l'ADCC par les sérums VIH+. Outre l'inhibition de CD4 et BST-2, Vpu cible également NTB-A et PVR, des ligands de récepteurs activateurs des cellules NK. Cependant, la polyfonctionnalité de Vpu est compromise par l'augmentation de BST-2 par les interférons de type I (IFN-I), sensibilisant ainsi les cellules infectées aux réponses NK. En utilisant un modèle de

souris humanisée, nous validons l'importance de Vpu pour échapper à la pression immunitaire des nnAbs *in vivo*.

Enfin, nous avons exploré de nouvelles stratégies pour sensibiliser les cellules infectées à l'ADCC en modulant la conformation d'Env avec des mimétiques moléculaires de CD4 (CD4mc). Nous avons identifié des résidus bordant la cavité Phe43 modulant la sensibilité au CD4mc. L'accumulation d'Env induite par les IFN-I augmente la capacité du CD4mc à sensibiliser les cellules infectées à l'ADCC par les sérums VIH+.

Globalement, cette thèse dévoile une caractérisation approfondie des déterminants viraux et cellulaires modulant la susceptibilité des cellules infectées par le VIH-1 aux réponses humorales. Une meilleure compréhension de ces mécanismes est nécessaire pour développer des nouvelles stratégies capables d'éradiquer les réservoirs viraux.

Mots-clés: VIH-1, ADCC, Env, glycoprotéine, Vpu, Nef, CD4, BST-2, anticorps, cellules NK

ABSTRACT

In the absence of an effective vaccine and with antiretroviral therapies unable to eradicate the virus, HIV-1 remains a global public health problem. Antibody-based immunotherapies are currently being investigated to eliminate cellular reservoirs, which represent a major obstacle towards an HIV-1 cure. HIV-1 envelope glycoproteins (Env) represent the only virus-specific antigen exposed at the surface of infected cells and therefore is the main target for antibodies. In its unliganded form, Env samples a 'closed' conformation, preferentially recognized by neutralizing antibodies. Interaction with CD4 drives Env into its 'open' conformation, exposing conserved epitopes recognized by non-neutralizing antibodies (nnAbs) present in sera from HIV-1 infected individuals (HIV+ sera). NnAbs can eliminate infected cells by antibody-dependent cellular cytotoxicity (ADCC). However, HIV-1 encodes for the accessory proteins Nef and Vpu which decrease cell surface levels of CD4 and BST-2, thus avoiding recognition and elimination of infected cells by nnAbs. In this thesis, we characterize in detail the contribution of Env, Nef, and Vpu to evade humoral responses and explore new strategies for sensitizing infected cells to ADCC.

In an effort to develop a more adequate quantification of ADCC responses, we identified major biases in widely used assays, including the ones used to assess correlates of vaccine protection. These include the inability to distinguish between the elimination of infected and uninfected cells and the use of viral constructs coding for a reporter gene that prevents Nef expression. Using a novel intracellular staining, we confirmed the protective effect of Nef and Vpu against ADCC responses.

Next, we studied the different Env and Vpu determinants modulating the susceptibility of infected cells to nnAbs-mediated ADCC responses. Certain Env structural features modulate its conformational transitions, including the trimer association domain, the furin cleavage site and the Phe43 cavity. Alterations of these components increase the susceptibility of HIV-1-infected cells to ADCC mediated by HIV+ sera. In addition to inhibiting CD4 and BST-2, Vpu also targets NTB-A and PVR, which act as ligands for NK cell activating receptors. However, we found that the polyfunctionality of Vpu can be compromised by the upregulation of BST-2 by type I interferons (IFN-I), thereby sensitizing infected cells to NK cell responses. Using a humanized mouse model, we validate the importance of Vpu to escape the immune pressure of nnAbs *in vivo*.

Finally, we explored new strategies to bypass the protective effect of Vpu and Nef and sensitize HIV-1-infected cells to ADCC by modulating Env conformation using small CD4-mimetic compounds (CD4mc). We identified a network of residue lining the Phe43 cavity that modulates Env sensitivity to CD4mc. The enhanced surface expression of Env by type I IFNs boosts the ability of CD4mc to sensitize HIV-1-infected cells to ADCC by HIV+ sera.

Overall, this thesis sheds light on a thorough characterization of viral and cellular determinants modulating the susceptibility of HIV-1-infected cells to humoral responses. A better understanding of these mechanisms is needed to develop new strategies able to eradicate viral reservoirs.

Keywords: HIV-1, ADCC, Env, glycoprotein, Vpu, Nef, CD4, BST-2, antibody, NK cells

TABLE DES MATIÈRES

LISTE DES FIGURES ET TABLEAUX

CHAPITRE I – INTRODUCTION

(ARTICLE 1) ***Impact of HIV-1 Envelope Conformation on ADCC Responses***

CHAPITRE III – MÉTHODES DE QUANTIFICATION DE LA RÉPONSE ADCC

(ARTICLE 2) ***Uninfected Bystander Cells Impact the Measurement of HIV-Specific Antibody-Dependent Cellular Cytotoxicity Responses***

LISTE DES ABRÉVIATIONS

6HB	*6-Helix Bundle*
Ad26	Adénovirus de sérotype 26
ADCC	Cytotoxicité cellulaire dépendante des anticorps (*antibody-dependent cellular cytotoxicity*)
ADCML	Lyse par le complément dépendante des anticorps (*antibody-dependent complement-mediated lysis*)
ADCP	Phagocytose dépendante des anticorps (*antibody-dependant cellular phagocytosis*)
ADN	Acide désoxyribonucléique
ADNdb	ADN double brin
ALIX	*ALG-2-interacting protein X*
ALLINI	Inhibiteur allostérique de l'intégrase (*Allosteric integrase inhibitor*)
ALVAC	Virus canarypox vivant atténué (*Attenuated live vaccinia*)
aNAb	Anticorps neutralisant autologue
AP1	Protéine activatrice 1 (*Activator protein 1*)
AP-1	Complexe de protéines adaptatrices de la clathrine 1 (*Adaptor Protein 1*)
AP-2	Complexe de protéines adaptatrices de la clathrine 2 (*Adaptor Protein 2*)
APOBEC3	*Apolipoprotein B mRNA-editing enzyme catalytic polypeptide-like 3*
ARN	Acide ribonucléique
ARNm	ARN messager
ARNPII	ARN polymérase II
ARNsb	ARN simple brin
ARNv	ARN viral
ARNt(Lys3)	ARN de transfert 3 pour la lysine
ART	Thérapie antirétrovirale (*Antiretroviral therapy*)
ARV	Antirétroviraux
ATR	*Ataxia telangiectasia-mutated and Rad3-related protein*
AZT	Azidothymidine
BCL-2	*B cell lymphoma-2*
BICD2	*Bicaudal D2*

bNAb	Anticorps neutralisant à large spectre (*Broadly neutralizing antibody*)
β-TrCP	*Beta-transducin repeat containing protein*
CA	Capside virale
CARD8	*Caspase recruitment domain family member 8*
Cas9	*CRISPR associated protein 9*
CBFβ	*Core-binding factor subunit beta*
CCDC137	*Coiled-coil domain containing 137*
CCL	Chimiokine C-C (*C-C chemokine ligand*)
CCR	Récepteur de chimiokine C-C (*C-C chemokine receptor*)
CD	Cluster de différentiation
CD3ζ	Chaîne zeta du TCR
CD4BS	Site de liaison à CD4 (*CD4 binding site*)
CD4i	Induits par CD4 (*CD4-induced*)
CD4mc	Mimétique moléculaire de CD4 (*CD4 mimetic compound*)
CD62L	L-sélectine
CDC	*Center for Disease Control and Prevention*
CDK	Protéine kinase dépendante de la cycline (*Cyclin-dependent kinase*)
CDR	*Complementarity Determining Regions*
CDS	Senseur d'ADN cytosolique (*Cytosolic DNA sensor*)
cGAS	*cyclic GMP–AMP synthase*
CHAMP	*Control of HIV after Antiretroviral Medication Pause*
CKII	*Casein kinase II*
CLR	Lectine de type C (*C-type lectin receptor*)
CMH-I	Complexe majeur d'histocompatibilité de classe I
CMH-II	Complexe majeur d'histocompatibilité de classe II
CMV	Cytomégalovirus
COPI	*Coatomer protein complex I*
CoRBS	Site de liaison au corécepteur (*Coreceptor binding site*)
COVID-19	*Coronavirus Disease 2019*
CpG	Cytosine–phosphate–guanine
CPSF6	*Cleavage and polyadenylation specific factor 6*

CRF	Forme recombinante en circulation (*circulating recombinant form*)
CRISPR	*Clustered Regularly Interspaced Short Palindromic Repeats*
CRM1	*Chromosome maintenance gene 1*
CST7	*Cystatin-7*
CT	Queue cytoplasmique (*Cytoplasmic tail*)
CTL	Lymphocyte T cytotoxique (*Cytotoxic T lymphocyte*)
CTLA-4	*Cytotoxic T-lymphocyte-associated protein 4*
CUL	*Cullin*
CXCR	Récepteur de chimiokine C-X-C (*C-X-C chemokine receptor*)
CypA	Cyclophiline A
CycT1	Cycline T1
DAP	*DNAX-activating protein*
DART	*Dual-affinity re-targeting molecule*
DCAF1	*DDB1 and CUL4 associated factor 1*
DDB1	*DNA damage-binding protein 1*
DC-SIGN	*Dendritic cell–specific intercellular adhesion molecular-3-grabbing non-integrin*
DNAM-1	*DNAX accessory molecule 1*
dNTP	Désoxyribonucléotide triphosphate
ELISA	*Enzyme-linked immunosorbent assay*
ELOB	*Elongin B*
ELOC	*Elongin C*
Env	Glycoprotéines d'enveloppe virale
ERAD	Système de dégradation de protéines associé au réticulum endoplasmique (*ER-associated protein degradation*)
ESCRT	*Endosomal Sorting Complex Required for Transport*
EXO1	Exonucléase 1
Fab	Fragment liant l'antigène (*Fragment antigen-binding*)
Fc	Fragment cristallisable
FcεRIγ	Chaîne γ du récepteur Fc des immunoglobulines E
FcR	Récepteur Fc
FcγR	Récepteur Fc des immunoglobulines G

FDR	Facteur de restriction
FEZ1	*Fasciculation and elongation protein zeta 1*
FSS	Signal de changement de cadre de lecture (*Frameshifting signal*)
Fv	Fragment variable
Gag	*Group-Specific Antigen*
GALT	*Gut-associated lymphoid tissue*
GBP5	*Guanylate binding protein 5*
GM-CSF	*Granulocyte-macrophage colony-stimulating factor*
GPI	Glycosylphosphatidilinositol
gp41	Glycoprotéine d'enveloppe de 41 KDa
gp120	Glycoprotéine d'enveloppe de 120 KDa
gp140	Glycoprotéine d'enveloppe de 140 KDa dont le site clivage de la furine, le domaine transmembranaire et la queue cytoplasmique ont été enlevés
gp160	Glycoprotéine d'enveloppe de 160 KDa
GTP	Guanosine triphosphate
GvHD	Réaction du greffon contre l'hôte
H3K36me3	Histone 3 Lysine 36 triméthylée
HARSAH	Hommes ayant des relations sexuelles avec des hommes
HDAC	Histone désacétylase
HLA	*Human Leukocyte Antigen*
HLTF	*Helicase like transcription factor*
HR1	*Helical heptad repeat 1*
HR2	*Helical heptad repeat 2*
HSPG	*Heparan sulfate proteoglycan*
HTLV-III	Virus T-lymphotropique humain de type III (*Human T-lymphotropic virus III*)
HVTN	*HIV Vaccine Trials Network*
IAVI	*International AIDS Vaccine Initiative*
ICAM	*Intercellular adhesion molecule*
IFI16	*Interferon gamma inducible protein 16*
IFITM	*Interferon-induced transmembrane protein*
IFNAR	Récepteur de l'interféron-α/β

IFN-I	Interféron de type I
Ig	Immunoglobuline
IκB	*Inhibitor of nuclear factor kappa B*
IL	Interleukine
IMC	Clone moléculaire infectieux (*Infectious molecular clone*)
IN	Intégrase
INSTI	Inhibiteur du transfert de brin par l'intégrase (*Integrase strand transfer inhibitor*)
IP_6	Inositol hexaphosphate
ISG	Gène induit par l'interféron (*Interferon-stimulated gene*)
ITAM	*Immunoreceptor tyrosine-based activation motif*
ITIM	*Immunoreceptor tyrosine-based inhibitory motif*
ITSS	Infection transmissible sexuellement ou par le sang
JAK	*Janus kinase*
LAG3	*Lymphocyte-activation gene 3*
LAV	Virus associé aux lymphadénopathies (*Lymphadenopathy associated virus*)
LEDGF	*Lens epithelium-derived growth factor*
LFA-1	*Lymphocyte function-associated antigen 1*
LLP	Peptide lytique lentiviral (*Lentiviral lytic peptide*)
LP-98	Lipopeptide 98
LPS	Lipopolysacharride
LPA	Agent promouvant la latence (*Latency-Promoting Agents*)
LRA	Agent réactivateur de la latence (*Latency-Reversing Agent*)
L-SIGN	*liver/lymph node-specific ICAM-3 grabbing non-integrin*
LTNP	*Long term non-progressors*
LTR	*Long Terminal Repeat*
MA	Matrice
MAC	Complexe d'attaque membranaire (*Membrane attack complex*)
mAb	Anticorps monoclonal (*monoclonal antibody*)
M-CSF	*Macrophage colony-stimulating factor*
MDA5	*Melanoma differentiation-associated protein 5*
MICA	*MHC class I chain-related molecule A*

MIP	Protéine inflammatoire des macrophages (*Macrophage Inflammatory Protein*)
mL	millilitre
µL	microlitre
MPER	*Membrane-proximal external region*
MT	Microtubule
MVA	*Modified Vaccinia Virus Ankara*
MX2	*Myxovirus resistance protein 2*
NAb	Anticorps neutralisant
NC	Nucléocapside
Nef	*Negative factor*
NES	Signal d'export nucléaire (*Nuclear export signal*)
NFAT	*Nuclear factor of activated T cells*
NF-κB	*Nuclear factor-kappa B*
NHP	primate non-humain (*Non-human primate*)
NK	*Natural Killer*
NKT	*Natural Killer T*
NKG2D	*Natural Killer Group 2D*
NLR	Récepteur de type NOD (*NOD-like receptor*)
NLRP3	*NLR family pyrin domain containing protein 3*
NLS	Signal de localisation nucléaire (*Nuclear localisation signal*)
NRTI	Inhibiteur nucléosidique de la transcriptase inverse (*Nucleoside reverse transcriptase inhibitor*)
NNRTI	Inhibiteur non nucléosidique de la transcriptase inverse (*Non-nucleoside reverse transcriptase inhibitor*)
NPC	Complexe de pore nucléaire (*Nuclear pore complex*)
NPL4	*Nuclear protein localization protein 4*
NTB-A	*NK-T-B antigen*
NUP	Nucléoporine
ONUSIDA	Programme commun de l'Organisation des Nations Unis sur le VIH/SIDA
ORF	Cadre de lecture ouvert (*Open Reading Frame*)
p6	Protéine de 6 kDa dérivé de Gag

PAMP	Motif moléculaire associé aux pathogènes (*Pathogen-associated molecular pattern*)
PBS	Site de liaison de l'amorce (*Primer Binding Site*)
PD-1	*Programmed cell death 1*
pDC	Cellule dendritique plasmacytoïde
PKC	Protéine kinase C
PI	Inhibiteur de protéase
PIC	Complexe de pré-intégration (*Pre-Integration Complex*)
PI(4,5)P_2	Phosphatidylinositol-4,5-bisphosphate
Pol	Polymérase
PP2A	Protéine phosphatase 2A
PPARγ	*Peroxisome proliferator-activated receptor gamma*
PPP2R5	Complexe régulateur de PP2A
PPT	Tract de polypurine (*PolyPurine Tract*)
PPTc	Tract central de polypurine (*central PolyPurine Tract*)
PR	Protéase
PRR	Récepteur de reconnaissance de motifs moléculaires (*Pattern recognition receptor*)
$Pr55^{Gag}$	Précurseur Gag de 55 kDa
$Pr160^{Gag-Pol}$	Précurseur Gag-Pol de 160 kDa
PrEP	prophylaxie pré-exposition (*Pre-exposure prophylaxis*)
PS	Peptide signal
PSGL-1	*P-selectin glycoprotein ligand-1*
P-TEFb	*Positive transcription elongation factor b*
PVR	Récepteur du virus de la poliomyélite (*Polio virus receptor*)
PVVIH	Personne vivant avec le VIH
Rab11-FIP1C	*Ras-associated binding protein 11 family interacting protein 1C*
Rab14	*Ras-associated binding protein 14*
rAd5	Vecteur adénoviral recombinant de sérotype 5
Ran	*Ras-related nuclear protein*
RANTES	*Regulated upon activation, normal T cell expressed and presumably secreted*
RBX	*Ring-box protein*

RE	Réticulum endoplasmique
RER	Réticulum endoplasmique rugueux
Rev	*Regulator of expression of virion proteins*
rhCD4	CD4 de macaque rhésus
RIDS	*Residual immune dysregulation syndrome*
RIG-I	*Retinoic acid-inducible gene I*
RING	*Really interesting new gene*
RLR	Récepteur de tpye RIG-I (*RIG-I-like receptor*)
RRE	Élément de réponse à Rev (*Rev-responsive element*)
RT	Transcriptase inverse (*Reverse transcriptase*)
RTC	Complexe de rétrotranscription (*Reverse transcription complex*)
SAMHD1	*Sterile Alpha Motif and Histidine Aspartate domain-containing protein 1*
sCD4	CD4 soluble
SCF	Complexe E3 ubiquitine ligase Skp1/Cullin 1/F-box
SERINC3	*Serine incorporator 3*
SERINC5	*Serine incorporator 5*
SERPINB9	*Serine proteinase inhibitor B9*
SIGLEC	*Sialic acid-binding immunoglobulin-like lectin*
SHIV	Virus chimérique d'immunodéficience humaine/simienne (*Simian-human immunodeficiency virus*)
SIDA	Syndrome d'immunodéficience acquise
SIRPα	*Signal-regulatory protein alpha*
SIV	Virus d'immunodéficience simienne (*simian immunodeficiency virus*)
SKP1	*S-phase kinase-associated protein 1*
SLAM	*Signaling lymphocytic activation molecule*
SLFN11	Schlafen 11
SLX4	*Structure-specific endonuclease subunit 4*
SMAC	*Second mitochondria-derived activator of caspases*
smFRET	*Single molecule Förster resonance energy transfer*
SNAT1	*Sodium-coupled neutral amino acid transporter 1*
SNP	Polymorphisme mononucléotidique (*Single nucleotide polymorphism*)

SOSIP.664	Trimère d'Env soluble (gp140) stabilisé par un pont disulfure (SOS) et la mutation I559P (IP) dans la gp41
Sp1	Protéine de spécificité 1 (*Specificity protein 1*)
SP1	Peptide intercalaire 1 (*Spacer Peptide 1*)
SP2	Peptide intercalaire 2 (*Spacer Peptide 2*)
SPRY	Spla and ryanodine receptor
SRAS-CoV-2	Coronavirus du syndrome respiratoire aigu sévère 2
SRG-15	Modèle de souris humanisée (SIRPα$^{h/m}$ Rag2$^{-/-}$ Il2rg$^{-/-}$ IL-15$^{h/m}$)
STAT	*Signal transducer and activator of transcription*
STING	*Stimulator of interferon genes*
T20	Enfuvirtide
TAR	Élément de réponse de trans-activation (*Trans-Activating Response element*)
Tat	Transactivateur transcriptionnel
T_{CM}	Lymphocyte T mémoire central
TCR	Récepteur des lymphocytes T (*T cell receptor*)
T_{EM}	Lymphocyte T mémoire effecteur
T/F	Transmis/fondateur
T_{FH}	Lymphocyte T folliculaire auxiliaire
TGN	Réseau *trans*-Golgi (*Trans-Golgi network*)
Th	Lymphocyte T auxiliaire (*T helper cell*)
TIGIT	*T cell immunoreceptor with Ig and ITIM domains*
TIM-3	*T cell immunoglobulin and mucin domain-containing protein 3*
TLR	Récepteur de type Toll (*Toll-like receptor*)
TNPO3	Transportine-3
TRIM5α	*Tripartite motif-containing protein 5 isoform α*
T_{RM}	Lymphocyte T mémoire résident
T_{SCM}	Lymphocyte T mémoire progéniteur
Tsg101	*Tumour Susceptibility Gene 101*
T_{TM}	Lymphocyte T mémoire transitionnel
Ub	Ubiquitine
UFD1L	*Ubiquitin fusion degradation 1 like*

ULBP	*UL16 binding protein*
UNG2	*Uracil-DNA glycosylase 2*
URF	Forme recombinante unique (*Unique recombinant form*)
U.S. FDA	*United States Food and Drug Administration*
VCP	*Valosin-containing protein*
Vif	*Virus infectivity factor*
VIH-1	Virus de l'immunodéficience humaine de type 1
VIH-2	Virus de l'immunodéficience humaine de type 2
VISCONTI	*Viro-immunological sustained control after treatment interruption*
Vpr	*Viral protein R*
Vpu	*Viral protein U*
Vpx	*Viral protein X*
ZAP	*Zinc finger antiviral protein*
ZFN	Nucléase à doigt de zinc (*Zinc finger nuclease*)

REMERCIEMENTS

Tout d’abord, je tiens à remercier mon directeur de recherche, le Dr Andrés Finzi, pour son support exceptionnel et son immense générosité. Andrés, merci de m’avoir accueilli dans ton laboratoire, de m’avoir attribué ta confiance et de m’avoir permis de m’épanouir et de repousser mes limites. Merci pour ta passion contagieuse de la recherche fondamentale, pour la liberté que tu m'as donnée pour poursuivre mes propres idées et pour ta façon de toujours me donner l’heure juste. Tu m’as offert des opportunités en or de participer à des projets stimulants, de présenter mes travaux dans des conférences nationales et internationales, et de collaborer avec des chercheurs de renom. J’ai tout simplement adoré ces sept années sous ta supervision et je quitte ton laboratoire grandi et prêt à affronter de nouveaux défis. Que dire de plus, merci pour tout!

Je suis sincèrement reconnaissant envers les Instituts de recherche en santé du Canada (IRSC), le Département de microbiologie, infectiologie et immunologie de l'Université de Montréal et le programme de bourse de stage d’été COPSÉ pour leur soutien financier durent mes études universitaires. Je veux également remercier tous les volontaires qui nous ont généreusement fourni des échantillons biologiques pour ces projets. Je profite de l'occasion pour remercier tous les collaborateurs qui ont contribué à mes recherches, spécialement Dr Daniel Kaufmann, Dr Jimmy Dikeakos, Dr Matthew Parsons, Dre Marzena Pazgier, Dr Walther Mothes, Dr Joseph Sodroski et Dr Stuart Neil, ainsi que les professeurs qui m'ont soutenu pendant ma formation académique, en particulier les membres de mon comité d'examen pré-doctoral, Dr Daniel Lamarre, Dr Nicolas Chomont et Dr David Evans, ainsi que les membres du jury ayant accepté de réviser cette thèse, Dr Jacques Thibodeau, Dr Roger Lippé, Dr Olivier Schwartz et Dre Marylise Duperthuy. À cet égard, je remercie sincèrement tous les scientifiques qui, au fil des ans, m'ont enseigné et ont contribué à façonner le scientifique que je suis aujourd'hui, notamment Dre Catherine Paradis-Bleau, ma première mentore, pour avoir contribué à éveiller mon intérêt pour le domaine de la recherche scientifique.

J'aimerais également exprimer ma gratitude à tous les membres actuels et passés du laboratoire Finzi, pour leur aide et leur soutien technique ainsi que pour avoir fait du laboratoire un environnement de travail aussi agréable. Un merci tout particulier au Dr Jonathan Richard pour avoir été mon mentor au quotidien, je lui dois une bonne partie de ma réussite. Je me souviens

encore des innombrables et interminables discussions sur la science, le sport et la vie, de nos nombreuses plaisanteries et de ta passion pour la musique suédoise! Je remercie également Mathieu Coutu, Dr Shilei Ding et Dre Halima Medjahed pour avoir été des collègues agréables à côtoyer et des aides inestimables depuis mon arrivée au laboratoire. Un grand merci à mes chers amis, Dre Elsa Brunet-Ratnasingham, Dre Julia Nießl, Dre Myriam Verly et Gérémy Sannier, je suis très reconnaissant d'avoir pu partager l'expérience des études doctorales avec vous et d'avoir pu créer de merveilleux souvenirs tous ensemble!

Enfin, j'aimerais adresser mes plus sincères remerciements à ma famille, à ma belle-famille et à mes amis proches qui m'ont fourni support et encouragements tout au long de cette aventure, sans toujours savoir ou comprendre sur quoi je travaillais sans compter les heures. Un merci spécial à ma femme, la Dre Sai Priya Anand, sans qui cette expérience n'aurait jamais été la même. Merci d'être une présence aussi rayonnante dans ma vie, merci pour ton support indéfectible, ta compréhension, ton écoute et ton amour. Je suis si heureux de partager ma vie et ma passion pour la science avec toi. Qui sait ce que le futur nous réserve?

CHAPITRE I - INTRODUCTION

Depuis le début du XX^{e} siècle, trois grandes pandémies d'origine virale ont été particulièrement meurtrières. Toutes ont été causées par des transmissions zoonotiques de virus à ARN enveloppés. Tout d'abord, à la fin de la Première Guerre mondiale, la pandémie d'influenza A H1N1 de 1918-1919, appelée la « grippe espagnole », éclate et on estime qu'un tiers de la population mondiale (soit environ 500 millions de personnes) ait été infecté et qu'environ 50 millions d'individus en soient décédés, touchant particulièrement les adolescents et jeunes adultes (1). Par la suite, au début des années 1980, un nombre croissant de manifestations cliniques du syndrome de l'immunodéficience acquise (SIDA) dans la communauté homosexuelle marque le début d'une pandémie causée par le virus de l'immunodéficience humaine de type 1 (VIH-1) qui n'est toujours pas résolue à ce jour. Autour de 79 millions de personnes ont contracté ce virus dans les quarante dernières années et près de la moitié en sont décédées en date de l'année 2020 (2). Finalement, un nouveau coronavirus infectant l'humain fait son apparition à la fin de l'année 2019; il s'agit du SRAS-CoV-2, l'agent étiologique de la COVID-19, une maladie se caractérisant par un syndrome de détresse respiratoire aigu dans les cas plus sévères, spécialement chez les personnes âgées. En date de juin 2022, on dénombre environ 547 millions d'infections par le SRAS-CoV-2 et au moins 6 millions de morts mondialement (3). Le bilan provisoire de cette troisième pandémie montre un taux de mortalité largement inférieur aux deux précédentes pandémies, notamment en raison du développement de vaccins et de thérapies efficaces en l'espace d'une année, du jamais vu. Ces avancés historiques ont largement bénéficié de la recherche effectuée lors des précédentes pandémies et épidémies causées par des virus, dont celles causées par l'influenza A, le VIH-1, le virus de l'hépatite C, le virus de la rage, le virus Ebola, le virus Zika et les coronavirus pathogènes (SRAS, MERS).

Parmi ces trois virus, le VIH-1 se démarque puisqu'il cause une infection chronique due à l'intégration de son génome dans l'ADN de son hôte, ce qui rend son élimination particulièrement difficile. Contrairement à l'influenza ou au SRAS-CoV-2, il n'existe toujours pas de vaccin efficace capable de prévenir ou de guérir l'infection par le VIH-1. Les personnes infectées sont traitées à l'aide de la thérapie antirétrovirale (ART) qui est capable de réprimer la réplication du virus, mais incapable d'éliminer le virus de l'organisme. Il est donc essentiel de développer de nouvelles approches thérapeutiques afin d'éradiquer le VIH-1 dans le but d'obtenir une cure fonctionnelle.

1.1 Le VIH-1 et le SIDA

1.1.1 Épidémiologie

Depuis son identification il y a près de quatre décennies, le VIH représente toujours un enjeu important de santé publique puisque les plus récents rapports publiés en 2020 par l'organisme ONUSIDA font état d'environ 37,7 millions de personnes vivant avec le VIH (PVVIH) à travers le monde, dont 36 millions d'adultes et 1,7 million d'enfants (2). Ces nombres ne cessent d'augmenter, en raison des effets du traitement par ART sur l'espérance de vie, et un taux soutenu de nouvelles infections, avec 1,5 million de personnes nouvellement infectées en 2020 (2). Bien que le traitement par ART ait considérablement augmenté l'espérance de vie et amélioré la santé des PVVIH, seule la moitié des personnes infectées dans le monde reçoit un traitement efficace (2). On dénombre 680 000 décès reliés au VIH/SIDA en 2020 uniquement (2). En 2014, ONUSIDA et ses partenaires ont fixé l'objectif 90-90-90 pour l'année 2020 : diagnostiquer 90 % de toutes les PVVIH, traiter 90 % des personnes qui connaissent leur statut, et supprimer le virus à des niveaux indétectables chez 90 % des personnes sous traitement (2, 4-6). Bien que les objectifs aient été presque atteints en 2020 (2), plusieurs obstacles se posent maintenant devant le nouvel objectif ambitieux adopté pour 2030 (95-95-95), notamment le nombre élevé de cas non-diagnostiqués (environ 16% des infections), le manque d'accès au traitement (chez 13% des cas diagnostiqués), l'adhésion au traitement de manière durable ainsi que la présence de toxicité ou de multirésistance à des classes d'antirétroviraux (ARV) chez certains PVVIH (7-9). Il est donc peu probable que le traitement par ART soit suffisant pour mettre fin à l'épidémie actuelle.

Dû à son mode de transmission, le VIH-1 fait partie des infections transmissibles sexuellement ou par le sang (ITSS), ce qui veut dire qu'il peut se propager par voie sexuelle, percutanée ou périnatale (10, 11). La très grande majorité des adultes (80%) contractent le VIH-1 à la suite d'une exposition aux muqueuses anale, vaginale ou pénienne (10, 11). Les populations les plus à risque de contracter le virus sont donc les hommes ayant des relations sexuelles avec des hommes (HARSAH), les transgenres, les travailleurs du sexe et les utilisateurs de drogues injectables (UDI) ainsi que leurs partenaires sexuelles. Ces populations clés sont responsables de la majorité des nouveaux cas enregistrés dans les dernières années dans les pays développés (2).

Or, ce sont les pays en développement qui connaissent les plus hauts taux de transmission, morbidité et mortalité liées au VIH-1; les taux de prévalence les plus élevés sont enregistrés chez les jeunes adultes hétérosexuels en Afrique subsaharienne (2). Afin de ralentir le rythme des nouvelles infections par le VIH-1, on mise sur plusieurs mesures au niveau de la prévention, notamment sur le port du condom, la circoncision et la prise d'ARV sous forme de prophylaxie préexposition (PrEP), mais leur application et leur accessibilité sont encore sous optimales, particulièrement dans les pays en développement (12-16). Tout comme le diagnostic et le traitement, ces mesures préventives ont été ralenties dans le contexte de la pandémie de COVID-19, ce qui pourrait aggraver la situation dans les régions endémiques (17-22). Le besoin d'un vaccin abordable et accessible est criant dans ces populations où le fardeau socio-économique, la criminalisation et la stigmatisation liés aux PVVIH sont toujours omniprésents (23-27).

1.1.2 Découverte et avancées scientifiques

C'est dès 1981 que les premiers cas cliniques du syndrome d'immunodéficience acquise (SIDA) sont répertoriés, principalement chez de jeunes hommes homosexuels qui succombent à des infections opportunistes inhabituelles et à des tumeurs malignes rares (28-30). L'épidémie se propage ensuite chez les toxicomanes et les hémophiles, puis à la population générale, menant à la pire pandémie virale depuis la « grippe espagnole » (31-33). Au début de l'année 1983, un nouveau rétrovirus humain, appelé à l'époque « virus associé aux lymphadénopathies » (LAV), est isolé à l'Institut Pasteur, en France, par l'équipe du Dr Luc Montagnier et Dre Françoise Barré-Sinoussi (prix Nobel de médecine de 2008), à partir d'une culture dérivée d'un échantillon de biopsie de ganglion lymphatique d'un patient présentant une lymphadénopathie généralisée (34). La découverte du VIH-1 comme agent étiologique du SIDA est confirmée en 1984 par le groupe américain du Dr Robert C. Gallo qui le nomme « virus T-lymphotrope humain de type 3 » (HTLV-III) à cause de son apparente similarité avec les rétrovirus humains HTLV-I et HTLV-II (35-37). Or, LAV et HTLV-III s'avère éventuellement être des souches d'un seul et même virus qui est renommé VIH par le Comité international de taxonomie des virus en 1986 (38). Dans la même année, un autre rétrovirus humain morphologiquement similaire, mais génétiquement distinct, est isolé chez des patients atteints du SIDA en Afrique de l'Ouest et qui sera désigné VIH de type 2 (VIH-2) (39, 40).

Les premiers tests diagnostiques par ELISA sont mis au point dès 1984 (41-43) et approuvés par la *Food and Drug administration* (FDA) américaine en 1985 pour réaliser de vastes études séro-épidémiologiques et des criblages des banques de sang (44, 45). Le clonage moléculaire du VIH-1 (46-48) et le séquençage du génome viral en 1985 (49, 50) ont ensuite permis de développer des tests de charge virale et de résistance pour suivre les patients infectés par le VIH-1. Le premier médicament antirétroviral, un analogue nucléosidique appelé azidothymidine (AZT ou zidovudine/ZDV), originellement développé comme potentiel traitement anti-cancer, est approuvé par la FDA en 1987 comme traitement contre le VIH-1 (51, 52). Dans les années qui suivent, le développement de nouveaux inhibiteurs de la transcription virale (53-55) et nouvelles classes d'ARV (56, 57) permet l'élaboration de thérapies combinant deux (bithérapie) ou trois ARV (trithérapie), ce qui s'avère grandement efficace comparativement aux monothérapies déjà en place (58-64). Peu à peu, les études cliniques montrent que la prise systématique d'une thérapie combinatoire permet de supprimer la charge virale à des niveaux indétectables, ce qui empêche la transmission du virus à un partenaire sexuel non-infecté (65, 66). En 2012, les cliniciens commencent à utiliser ART comme traitement préventif (PrEP) contre le VIH-1, ce qui réduit les risques de transmission sexuelle avec une efficacité de 99% (67-71). Pour ce qui est du développement d'un vaccin prophylactique, les premiers essais vaccinaux de phase III débutent à la fin des années 1990 et sont menés par la compagnie de biotechnologie VaxGen (72, 73). Ils testent l'efficacité d'un vaccin sous-unitaire appelé AIDSVAX en Amérique du Nord/Europe (Vax004) et en Thaïlande (Vax003), mais les résultats publiés en 2005-2006 ne montrent aucune protection vaccinale contre l'infection par le VIH-1 (74, 75). Après l'échec consécutif de deux autres vaccins (76, 77), ceux-ci à base de vecteur adénoviral, la publication en 2009 des résultats de l'essai clinique RV144 mené en Thaïlande sont encourageants, quoique modestes. Le vaccin combinant un vecteur à base de poxvirus (ALVAC-HIV) et le vaccin AIDSVAX montre une efficacité vaccinale de 31,2 % à 42 mois post-vaccination par rapport au groupe contrôle (78). La même année, on rapporte pour la première fois la guérison complète d'un patient infecté par le VIH-1, dit « le patient de Berlin » (79, 80). Après son diagnostic de séropositivité, ce patient développe une leucémie et reçoit une greffe de cellules souches ayant la particularité d'être réfractaires au VIH-1 à cause d'une mutation dans le gène *ccr5*. Ce succès inattendu mène à la guérison de trois autres patients à ce jour : le patient de Londres (81), le patient de Düsseldorf (82) et la patiente de New York (83). En revanche, l'application de ce type

d'intervention est extrêmement limitée, ce qui souligne encore le besoin d'un traitement thérapeutique efficace, accessible et applicable à grande échelle.

1.1.3 Origine et classification

Le VIH est un virus enveloppé appartenant au genre lentivirus au sein de la famille des rétrovirus (*Retroviridae*). Cette famille de virus se distingue par sa capacité à transcrire son génome composé d'acide ribonucléique simple brin (ARNsb) en acide désoxyribonucléique double brin (ADNdb) à l'aide de sa transcriptase inverse (84, 85) ainsi que par sa capacité à intégrer son génome dans l'ADN cellulaire de l'hôte (86, 87). Il existe deux espèces de lentivirus retrouvées chez l'humain, le VIH-1 et le VIH-2, provoquant tous les deux le SIDA. Le VIH-1 est le virus responsable de la pandémie, tandis que les infections par le VIH-2 sont restreintes à des zones endémiques en Afrique de l'Ouest (88, 89). Cette différence s'explique par un faible taux de transmission et une progression de la maladie plus lente chez les individus infectés par le VIH-2 en raison de leur charge virale réduite (90-94). Depuis leurs découvertes, la possibilité que l'origine de ces virus soit due à des transmissions zoonotiques est étudiée. Le premier virus apparenté au VIH a été identifié pour la première fois chez des macaques en captivité, souffrant de symptômes semblables à ceux du SIDA (95). Depuis, des virus d'immunodéficience simienne (SIV) ont été retrouvés chez plus de 40 espèces de primates de l'Ancien Monde, notamment chez des hôtes naturels du virus tels que les singes verts africains (genre *Chlorocebus*), les singes mangabeys (genre *Cercocebus*) et les guenons arboricoles (genre *Cercopithecus*), dont les populations peuvent atteindre plus de 50% de prévalence (96-99). Curieusement, on constate que ces virus semblent largement non-pathogènes chez leurs hôtes naturels et qu'ils ne causent pas le SIDA, malgré des charges virales élevées (100-104).

À notre connaissance actuelle, seules trois espèces de primates (chimpanzés, gorilles et mangabeys) ont transmis leur virus à l'homme (**Figure 1.1.1**). Le VIH-1 se divise en quatre lignées phylogénétiquement distinctes, dont chacune est issue de transmissions distinctes d'un SIV à l'homme. Les virus du groupe M (majeur), à l'origine de la pandémie mondiale (>98% des infections), résultent d'un seul évènement de transmission provenant d'une souche de SIV présente chez le chimpanzé d'Afrique centrale (SIVcpzPtt ; *Pan troglodytes troglodytes*), survenu il y a environ un siècle dans le sud-est du Cameroun, suivi d'une phase de propagation initiale à

Kinshasa, en République Démocratique du Congo (99, 105-107). Les souches de VIH-1 du groupe N (non-M, non-O, nouveau), détectées chez une vingtaine d'individus, proviennent également d'une souche de SIVcpzPtt (99), tandis que celles du groupe O (*outlier*) et P sont originaires de virus infectant les gorilles des plaines occidentales (SIVgor), eux-mêmes issus de souches provenant des chimpanzés (108-111). Comme le chimpanzé n'est pas un hôte naturel du virus, il est proposé que le SIVcpz soit dérivé d'une recombinaison entre un ancêtre des SIV retrouvés aujourd'hui chez les guenons (SIVgsn/mon/mus), et d'un précurseur du SIV présent chez les mangabeys (SIVrcm), compte tenu de la discordance existant entre les parties 5' et 3' de son génome (98, 112).

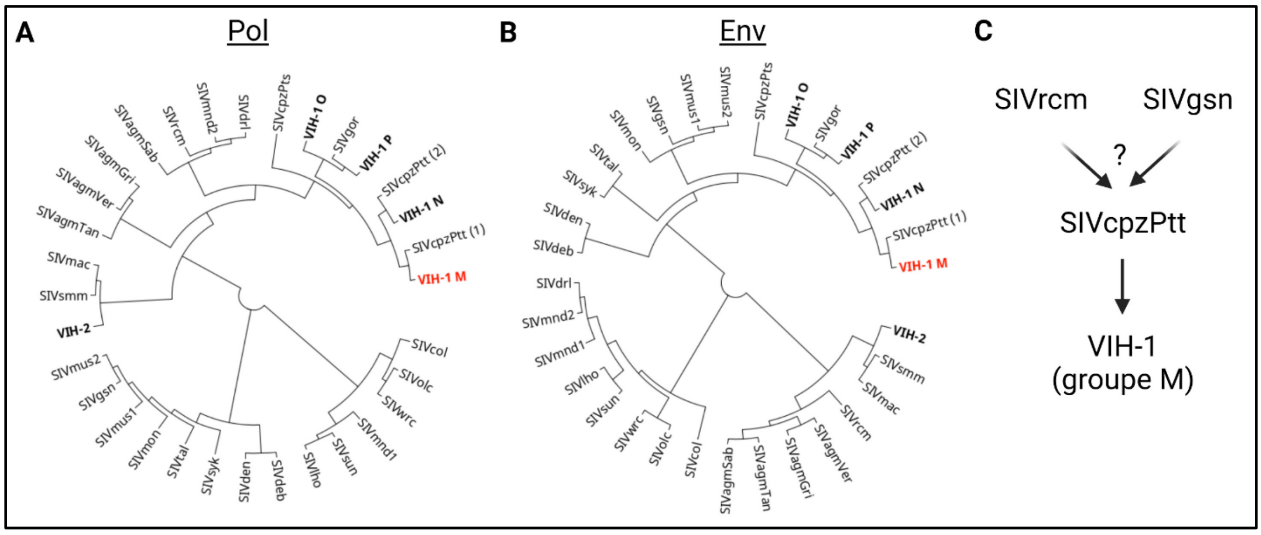

Figure 1.1.1 – Phylogénie du VIH-1
Arbre phylogénétique des virus de l'immunodéficience humaine et simienne. Cladogramme circulaire montrant la proximité génétique des séquences de (**A**) la polyprotéine Pol (1003 acides aminés) et (**B**) de la glycoprotéine Env (856 acides aminés) obtenus à partir de séquences des différents lentivirus de primates provenant de la base de données VIH du Laboratoire National de Los Alamos (www.hiv.lanl.gov/content/sequence/HIV/mainpage.html). Une séquence complète du génome d'une souche représentative a été utilisée pour chaque virus. L'alignement des séquences et la génération des cladogrammes ont été réalisés à l'aide du logiciel Geneious Prime version 2022.0.2 (https://www.geneious.com). Les différentes souches de VIH sont écrites en gras et la souche pandémique (VIH-1 groupe M) est mise en évidence en rouge. (**C**) Possible évènement de recombinaison entre SIVrcm et SIVgsn menant à la génération de SIVcpzPtt et transmission à l'homme menant à la pandémie de VIH-1 du groupe M. Diagramme créé avec BioRender.com.

Pour ce qui est du VIH-2, il se divise en neuf groupes (A à I) qui sont issus de neuf transmissions zoonotiques de SIV infectant les mangabeys (SIVsmm) (113). Ces virus ont

également une proximité génétique avec les isolats de SIV retrouvés chez les macaques (SIVmac) en 1985. Comme le macaque n'est pas un hôte naturel du SIV, des études ultérieures ont confirmé que le SIVmac a été généré par la transmission accidentelle du SIVsmm provenant de mangabeys dans des centres de primates américains (114). Puisque l'infection des macaques par le SIV est associée au développement rapide d'une maladie s'apparentant au SIDA, ce modèle est toujours utilisé aujourd'hui pour comprendre la pathogenèse du VIH-1 ainsi que pour l'élaboration de vaccins et de traitements contre ce virus (115).

Au fur et à mesure que le VIH-1 de groupe M s'est répandu dans le monde, sa diffusion a impliqué des événements fondateurs qui ont conduit à la prédominance de différentes lignées (sous-types) du groupe M dans différentes zones géographiques. En raison de la grande diversité génétique du VIH-1, le groupe M peut aujourd'hui être classé en neuf sous-types/clades (A-D, F-H, J, K), et plus d'une centaine de formes recombinantes circulantes (CRFs) et de formes recombinantes uniques (URFs) générées par des événements de recombinaison chez des individus infectés par plusieurs clades en même temps (88, 116). De nos jours, les sous-types les plus répandus dans le monde sont les clades C (46,6%), B (12,1%), A (10,2%), G (4,6%) et D (2,6%) (117). Les sous-types A et D sont originaires d'Afrique centrale, mais ont finalement établi des épidémies en Afrique de l'Est (118), tandis que le sous-type C a été introduit en Afrique australe, où il prédomine, d'où il s'est propagé en Inde par la suite (119, 120). Le sous-type B, qui représente la grande majorité des infections par le VIH-1 sur le continent américain, en Europe et en Australie, est issu d'une souche africaine unique qui semble s'être d'abord répandue en Haïti dans les années 1960, puis aux États-Unis et dans d'autres pays occidentaux (121). Le sous-type G est principalement retrouvé en Afrique de l'Ouest (122). D'autre part, l'effet fondateur se dissipe graduellement dans les dernières données causant une augmentation de la diversité génétique du VIH-1 (123). On note également la montée des cas par des CRFs au cours des dernières années, représentant environ 17% des infections (117). On documente des épidémies grandissantes des souches CRF01_AE en Asie du Sud-Est et en Chine (124, 125), CRF02_AG en Afrique de l'Ouest (126) et CRF07_BC en Chine (127). Cette large diversité génétique du VIH-1 à l'échelle mondiale constitue un obstacle majeur au développement de nouveaux vaccins et traitements efficaces contre ce virus.

1.1.4 Génome et structure

Le génome du VIH-1 est constitué de deux copies d'ARNsb non-épissée à polarité positive et d'une longueur de 9,2 kilobases (kb) chacune qui sont encapsidées dans le noyau de la particule virale (128, 129). La taille de l'ARN génomique du VIH-1 est limitée en raison de la fidélité de sa transcriptase inverse et de sa capacité d'encapsidation (130-132), forçant le virus à adopter plusieurs stratégies afin d'optimiser l'utilisation de ses séquences codantes, notamment par l'utilisation des trois cadres de lecture, le chevauchement des différents gènes, la synthèse de polyprotéines et l'épissage alternatif des ARN messagers (ARNm) (133-135). L'ARN viral (ARNv) génomique est coiffé à l'extrémité 5' et polyadénylé à l'extrémité 3' (136, 137), comme les autres ARNm eucaryotes, et les deux extrémités de l'ARNv sont flanquées de longues séquences répétées terminales (LTR) composées de séquences non-traduites en 5' et 3' (élément U) et de séquences répétées inversées (élément R) (138). Lors de l'infection, l'ARNv est rétrotranscrit en ADNdb, ce qui mène à la duplication des éléments U de part et autre du génome (U3-R-U5), formant ainsi le promoteur de la transcription des gènes viraux à l'extrémité 5' (138). Chaque ARNv comporte neuf cadres de lecture ouverts (ORFs) qui se chevauchent et codent pour quinze protéines virales différentes (**Figure 1.1.2**) (128).

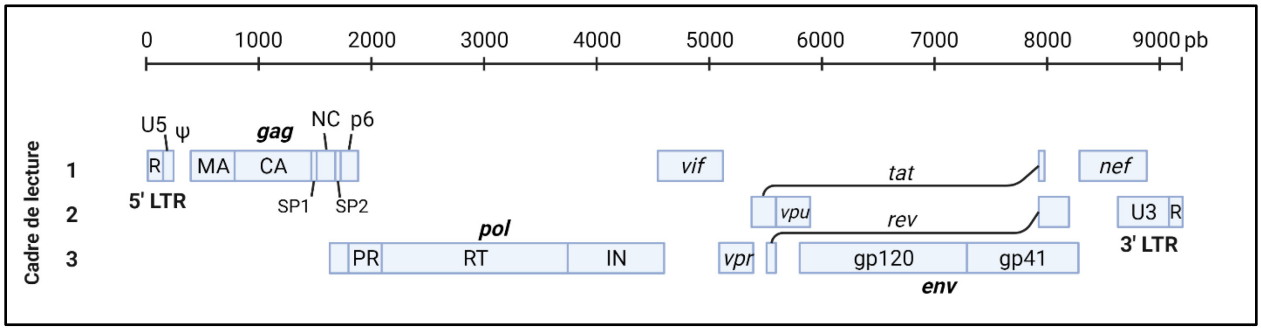

Figure 1.1.2 - Organisation génomique du VIH-1
L'organisation du génome du VIH-1 de 9,2 kb avec les extrémités 5' et 3' composées de longues répétitions terminales (LTR) et les différents ORFs répartis sur les trois différents cadres de lecture, ceux-ci codant pour les protéines et polyprotéines virales. U5 : région non-traduite en 5'; U3 : région non-traduite en 3'; R : séquence répétée inversée; ψ : séquence d'encapsidation; *gag* : gène codant pour les protéines structurelles; *pol* : gène codant pour les enzymes; *env* : gène codant pour les glycoprotéines de surface; MA : matrice; CA : capside; NC : nucléocapside; SP1 : peptide intercalaire 1; SP2 : peptide intercalaire 2; PR : protéase; RT : transcriptase inverse; IN : intégrase; pb : paires de bases. Le génome de la souche HXB2 a servi de référence pour cette figure (128) Diagramme créé avec BioRender.com.

Les trois principaux produits structurels et enzymatiques du génome du VIH-1 sont Gag (*group-specific antigen*), Pol (polymérase) et Env (enveloppe), qui sont d'abord transcrits sous forme de longues polyprotéines, et ensuite clivés en différentes protéines fonctionnelles par la protéase virale (PR) dans le cas de Gag et Pol, ou par une protéase cellulaire de type furine pour Env (139-141). À la suite de son clivage, le précurseur Gag ($Pr55^{Gag}$) génère les protéines de la matrice (MA, p17), la capside (CA, p24), la nucléocapside (NC, p7) et la protéine p6 (142). Il existe également des peptides intercalaires (SP1 et SP2), qui jouent un rôle dans la régulation de l'assemblage du virion et de la maturation de la capside (143, 144). Alternativement, la production du précurseur Gag-Pol ($Pr160^{gag\text{-}pol}$) survient lors du décalage (*frameshift*) des ribosomes à la jonction entre les gènes *gag* et *pol*, permettant l'expression des enzymes virales telles que la protéase (PR, p12), la transcriptase inverse (RT) comprenant un domaine RNase H (p65) ou non (p51) ainsi que l'intégrase (IN, p32) (145, 146). Le gène *env* code pour le précurseur des glycoprotéines d'enveloppe (gp160), qui est clivé pour former les sous-unités externes (SU; gp120) et transmembranaire (TM; gp41) (147). En plus des protéines structurelles, le génome du VIH-1 code pour les protéines régulatrices Tat (transactivateur transcriptionnel) et Rev (régulateur de l'expression des protéines virales) qui sont nécessaires à la transcription et l'export des ARNv du noyau (148, 149), ainsi que les protéines accessoires Vif (*viral infectivity factor*), Vpr (*viral protein r*), Vpu (*viral protein u*) et Nef (*negative factor*), qui ont un impact sur l'infectivité et la pathogenèse du virus (150-153). De son côté, le VIH-2 ne code pas pour Vpu, mais plutôt pour Vpx (*viral protein x*), expliquant partiellement sa pathogénicité réduite (154).

Les particules virales du VIH-1 sont de forme sphérique et leur diamètre moyen qui varie de 100 à 145 nm (**Figure 1.1.3**) (155-157). Chaque virion est entouré d'une bicouche lipidique qui provient de la membrane cytoplasmique de la cellule hôte (158, 159). Au cours de son assemblage, le VIH-1 incorpore 7 à 10 trimères d'Env, formés de trois hétérodimères de gp120 et de gp41 liés de manière non-covalente (160-162) et environ 2000 à 3000 copies des polyprotéines Gag et Gag-Pol, à un ratio de 20:1, qui s'assemble à la membrane cytoplasmique en particules virales immatures (157-159, 161, 163). La génération des particules virales pleinement infectieuses et morphologiquement matures nécessite une libération des protéines structurelles individuelles de Gag dans une série d'étapes de clivage étroitement régulées et catalysées par PR (164). Chez le virion mature, la surface interne de la membrane virale est tapissée de protéines MA assemblées

sous forme d'hexamères de trimères et qui reste ancrées dans la membrane via un groupement myristoyl dans leur portion N-terminale (165). MA permet l'incorporation d'Env dans les particules virales en interagissant avec sa queue cytoplasmique (162, 166). À l'intérieur du virion, les protéines CA s'arrangent sous forme d'hexamères ou de pentamères, qui seront assemblés ensemble pour former une capside de forme conique composée d'environ 1500 monomères de CA (167-170). À l'intérieur de la capside, les protéines NC se lient à l'ARNv dimérisé via son interaction avec la séquence d'encapsidation Psi (ψ) et possèdent également une activité de chaperonne des acides nucléiques qui favorisent la stabilité du génome avant l'initiation de la rétrotranscription (171-173). Le complexe ribonucléoprotéique (RNP) formé par l'ARNv et NC contient également les enzymes RT et IN qui seront nécessaire pour répliquer son génome sous forme d'ADNdb et de l'intégrer dans l'ADN de la cellule hôte lors de l'infection (174, 175). Certaines protéines accessoires sont également incorporées dans les virions : Vif, via son interaction avec l'ARNv (176), Vpr, via son interaction avec la protéine p6 (177, 178), et Nef, grâce à la myristoylation de sa partie N-terminale (179).

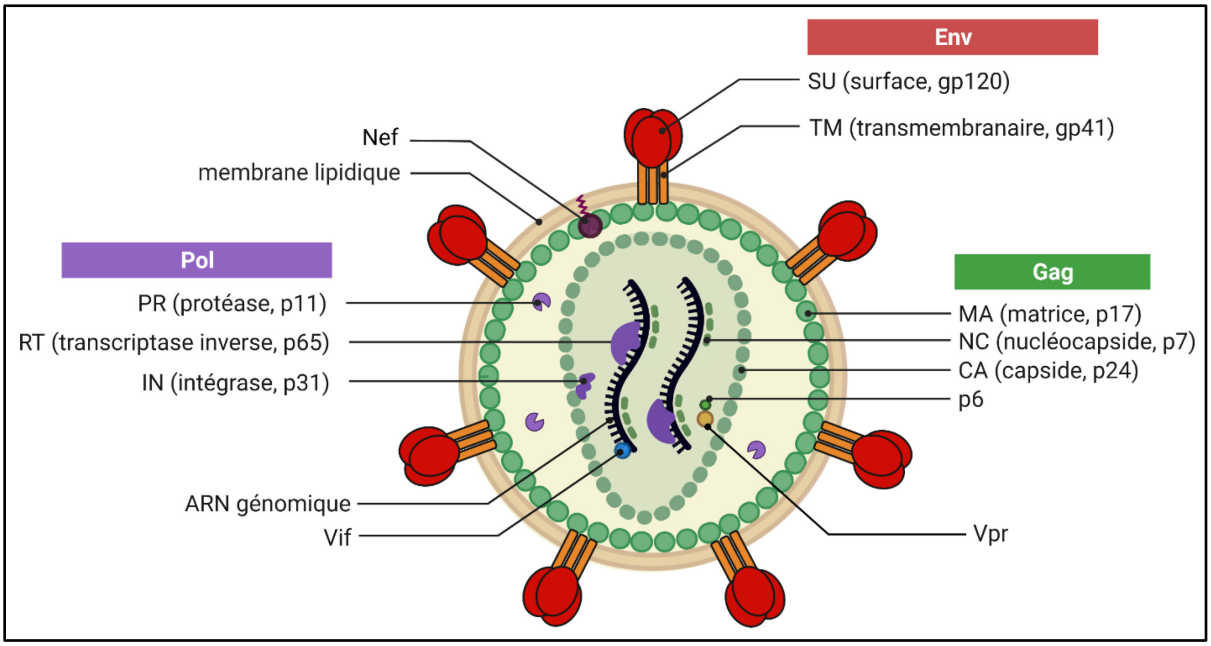

Figure 1.1.3 - Structure du virion mature du VIH-1
Vue schématique de la particule mature du VIH-1 détaillant les protéines virales et la structure du virion. L'Env du VIH-1, composé de complexes trimériques de gp120 et gp41, est le seul antigène viral présent sur le feuillet externe de la membrane lipidique. La queue cytoplasmique de la gp41 interagit avec MA. Les protéines CA forment une capside conique qui contient un dimère d'ARNv lié par la protéine NC. La protéine p6, les enzymes PR, RT et IN ainsi que les protéines accessoires Vif, Vpr et Nef sont également présents dans le virus. Diagramme créé avec BioRender.com.

1.1.5 Cycle de réplication

Lors de l'infection, le VIH-1 prend le contrôle de la cellule et détourne de nombreuses protéines de l'hôte afin d'assurer un cycle de réplication efficace. Le cycle de réplication du VIH-1 peut être divisé en deux phases distinctes : la phase précoce et la phase tardive. Le stade précoce comprend toutes les étapes allant de l'entrée du virus à l'intégration de l'ADN viral. La phase tardive comprend la transcription de l'ADN proviral, la traduction des ARNm viraux, l'assemblage du virus et la relâche de virions matures (**Figure 1.1.4**).

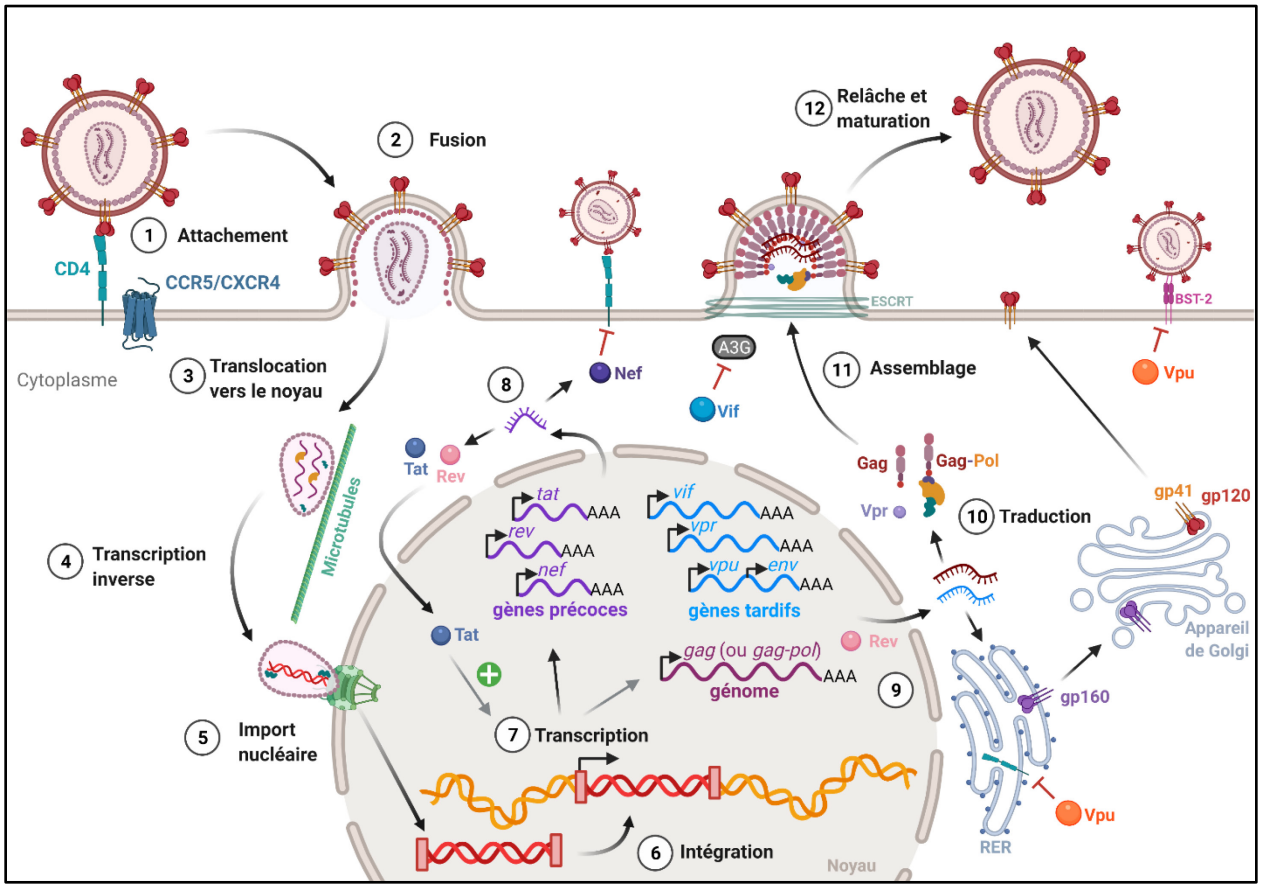

Figure 1.1.4 - Cycle de réplication du VIH-1
Représentation schématique des principales étapes de la réplication virale : (**1**) attachement du virus via l'interaction avec le récepteur CD4, (**2**) fusion et entrée, (**3**) translocation de la capside virale vers le noyau le long des microtubules, (**4**) rétrotranscription de l'ARNsb génomique en ADNdb, (**5**) désassemblage de la capside et import nucléaire du complexe de pré-intégration (PIC), (**6**) intégration dans l'ADN cellulaire, (**7**) transcription, (**8**) export nucléaire des transcrits multi-épissés et (**9**) non-épissés ou mono-épissés, (**10**) traduction des protéines virales dans le cytoplasme ou le réticulum endoplasmique rugueux (RER), (**11**) assemblage et bourgeonnement, et (**12**) relâche et maturation des virions. A3G: APOBEC3G. Diagramme créé avec BioRender.com.

1.1.5.1 Glycoprotéines d'enveloppe et entrée virale

Le cycle de réplication du VIH-1 débute par l'entrée du virus dans une cellule cible de l'hôte, un processus nécessitant la fusion entre les membranes du virus et de la cellule, ce qui est médié par les glycoprotéines d'enveloppe virale (Env) (**Figure 1.1.5**). Bien que chaque virion possède en moyenne 7 à 10 trimères d'Env à sa surface, la plupart des souches de VIH-1 ne nécessitent en moyenne que 2 ou 3 trimères fonctionnels afin d'initier l'infection (180, 181). Dans son processus de biosynthèse, Env est traduit sous forme d'un précurseur inactif (gp160) dans le réticulum endoplasmique, qui est par la suite clivé par la signal peptidase pour enlever le peptide signal en N-terminale et par la furine cellulaire afin de générer deux sous-unités fonctionnelles associées de manière non-covalente : la gp120 et la gp41 (141, 182, 183). L'Env fonctionnelle est assemblée sous forme d'un trimère comprenant trois sous-unités gp120 qui contiennent les sites de liaison aux récepteurs de l'hôte et trois sous-unités gp41 qui comprennent la machinerie de fusion (184-186). La sous-unité gp120 de Env est constituée de cinq régions constantes (C1 à C5) et de cinq régions variables (V1 à V5) (187, 188). La structure globale de la gp120 est composée d'un domaine interne hautement conservé interagissant avec la gp41 et d'un domaine externe variable et lourdement glycosylé (185, 189-191). La sous-unité gp41 est composée d'un domaine extracellulaire, d'un domaine transmembranaire et d'une longue queue cytoplasmique en C-terminale (192-195). Le domaine extracellulaire de la gp41 contient les régions importantes pour le processus de fusion, notamment le peptide de fusion et les régions de répétitions d'heptades (HR1 et HR2) (196). L'énergie nécessaire au processus de fusion provient du repliement d'Env qui est déclenché par ses récepteurs de manière séquentielle, ce qui fait passer Env d'une conformation pré-fusion métastable à haute énergie vers un état post-fusion stable de basse énergie (197, 198).

Le processus d'entrée débute par l'attachement de la particule virale à la cellule cible. L'attachement peut être relativement non spécifique, l'Env interagissant avec les protéoglycanes faits de sulfate d'héparane (HSPG) chargés négativement de la surface cellulaire (199-201), des lectines de type C telles que DC-SIGN et L-SIGN (202-204) et des lectines de type SIGLEC (205). L'incorporation de molécules d'adhésion cellulaires telles que ICAM-1, CD44 et CD62L dans la particule virale permet également de favoriser la rétention des virions à la surface des cellules via l'interaction avec leur récepteur respectif (206-208). Les protéines TIM peuvent également

favoriser l'attachement en interagissant avec les phosphatidylsérines exposées sur le feuillet externe de la membrane virale (209). L'attachement du VIH-1 à la cellule hôte par l'un de ces mécanismes amène Env à proximité de son récepteur et de ses corécepteurs, ce qui augmente l'efficacité de l'infection (210, 211).

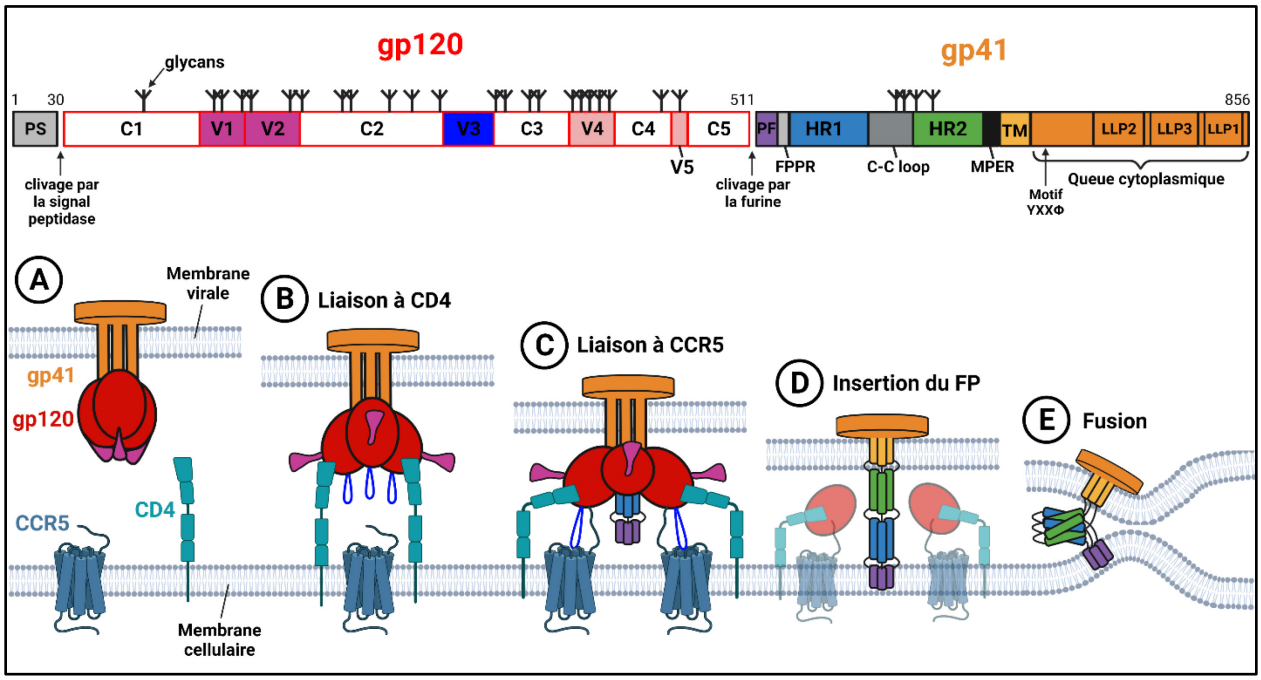

Figure 1.1.5 – Les glycoprotéines d'enveloppe et l'entrée du VIH-1
Les glycoprotéines d'Env sont clivées par la signal peptidase et la furine cellulaire en deux sous-unités fonctionnelles (gp120 et gp41). Env possède environ 27 sites de glycosylation recouvrant sa surface protéique. La sous-unité gp120 est composée de cinq régions constantes (C1-C5) et de cinq domaines variables (V1-V5). La sous-unité gp41 est composée d'un ectodomaine, d'un domaine transmembranaire (TM), et d'une queue cytoplasmique en C-terminale. Dans l'ectodomaine se trouvent le peptide de fusion, les régions de répétition d'heptades (HR1 et HR2), et la région externe proximale à la membrane (MPER). Dans la queue C-terminale se trouvent les séquences peptidiques lytiques du lentivirus (LLP1, LLP2 et LLP3), et le motif d'endocytose YXXΦ (près de l'extrémité N-terminale). PS : peptide signal; FPPR : *fusion peptide proximal region*; C-C loop : boucle disulfure. (**A**) L'entrée commence par (**B**) la liaison de la gp120 à son récepteur CD4, ce qui déclenche l'ouverture d'Env, ce qui permet (**C**) la liaison de la gp120 à son corécepteur CCR5 (ou CXCR4). (**D**) La liaison du corécepteur libère le peptide de fusion qui s'insère dans la membrane cellulaire. (**E**) Suite au détachement de la gp120, la gp41 se replie sur elle-même grâce aux régions complémentaires HR1 et HR2, formant le faisceau à 6 hélices (6HB) nécessaire à la fusion des membranes virale et cellulaire. Diagramme créé avec BioRender.com.

Le récepteur primaire du VIH-1 est CD4 (212, 213), une glycoprotéine de surface cellulaire contenant quatre domaines de type immunoglobuline (D1 à D4), avec D1 à l'extrémité distale de la membrane (214). Son interaction avec la sous-unité gp120 est essentielle pour initier le processus de fusion du virus en induisant des changements de conformation d'Env pour exposer le site de liaison du corécepteur (215-218). Le site de liaison au CD4 (CD4BS) d'Env représente un arrangement quaternaire très complexe de cinq boucles différentes qui se rencontrent pour former cette structure hautement conservée. Trois de ces boucles convergent pour former la cavité Phe43 : la boucle de liaison au CD4 (région C3), la boucle β20-β21 (région C4) et la boucle de sortie du domaine externe (région C5) (219). Deux autres boucles en périphérie de la cavité Phe43 sont également impliquées dans la liaison au CD4 : la boucle D (région C2) et la boucle V5 (219). La cavité Phe43 est une structure hautement conservée du domaine externe où le résidu Phe43 du CD4 s'insère et établit de nombreux contacts avec des résidus conservés de la gp120 (219). Cette interaction provoque des changements conformationnels majeurs menant à « l'ouverture » du trimère d'Env, notamment grâce au réarrangement de la boucle V1/V2 située à l'apex du trimère, s'éloignant de l'axe central du trimère (220, 221). Ce réarrangement permet ainsi l'exposition de la boucle V3 et la formation d'une passerelle en feuillet β (*bridging sheet*) entre le domaine externe et interne à la base de la boucle V1/V2 (220, 221). Ces deux éléments structuraux forment ensemble le site de liaison au corécepteur (222-224), soit CCR5 (225-231) ou CXCR4 (232, 233). Ces changements conformationnels induits par le CD4 sont guidés par les couches topologiques 1, 2 et 3 du domaine interne de la gp120 (234-237). La liaison du corécepteur déclenche d'autres changements de conformation au sein de la gp41 qui favorisent la libération du peptide de fusion hydrophobe de la gp41 qui s'insère dans la membrane de la cellule hôte (238). Le détachement de la gp120 permet l'adoption d'une structure intermédiaire allongée par la gp41 (239), et les régions HR1 et HR2 de chaque sous-unité se replient pour former un trimère de structures en épingle à cheveux (6HB) grâce à leur surface complémentaire (194, 240, 241). Ainsi, le 6HB est composé d'un trimère de HR1 entouré de trois hélices HR2 disposées de manière antiparallèle (196). Cela permet de rapprocher la membrane virale et la membrane cible, puis de former le pore de fusion, ce qui entraîne la libération de la capside virale dans le cytoplasme de la cellule cible (242-244). Comme ce processus est indépendant du pH (245, 246), l'entrée du VIH-1 se fait souvent au niveau de la membrane cytoplasmique, mais peut également se faire dans les compartiments endosomaux dans certains types cellulaires, notamment les macrophages (247-253).

La présence du récepteur et des corécepteurs dicte la permissivité et le tropisme cellulaire du VIH-1. En effet, le VIH-1 cible de manière préférentielle les lymphocytes T $CD4^+$, dû à la forte densité d'expression de CD4 à leur surface, mais peut également cibler d'autres cellules du système immunitaire telles que les macrophages et les cellules dendritiques (254). Les souches virales sont classées en fonction de l'utilisation des corécepteurs : celles utilisant le récepteur CCR5 sont appelées isolats R5 et celles qui utilisent le récepteur CXCR4 sont appelées isolats X4 (255). Une classe distincte de souches à tropisme mixte utilise les deux récepteurs et est appelée isolats R5X4 (255). Les souches R5 possèdent une capacité de réplication supérieure à celle des souches X4 dans des conditions homéostatiques et sont les principales souches transmises entre individus (256, 257). L'expression de chacun de ces corécepteurs dicte également la susceptibilité d'un type cellulaire à l'infection. Par exemple, CCR5 est surtout exprimé sur les lymphocytes T CD4+ mémoires ou activés, les macrophages et les cellules dendritiques, tandis que CXCR4 est exprimé principalement sur les lymphocytes T CD4+ naïves (254). Parmi les lymphocytes T CD4+, les sous-types cellulaires à différentiation Th1 et Th17 sont les plus susceptibles à l'infection grâce à leur forte expression de CCR5 et CXCR4 (256, 258, 259).

1.1.5.2 Étapes précoces du cycle de réplication

Après avoir pénétré dans la cellule hôte, la capside doit être acheminée vers le noyau afin de pouvoir intégrer le génome viral dans l'ADN cellulaire. La capside étant trop grande pour diffuser librement dans le cytoplasme encombré, le VIH-1 utilise le réseau de microtubules (MT) en induisant sa stabilisation et en détournant les protéines motrices pour assurer le transport actif de la capside virale vers le noyau (260-262). Le trafic le long du réseau des MT est réalisé par les moteurs de dynéine et de kinésine et constitue un moyen primaire de transport cytoplasmique dans les cellules (263). La dynéine facilite les mouvements vers l'intérieur en direction du noyau, tandis que les kinésines médient les mouvements vers la périphérie cellulaire (263). La capside du VIH-1 se sert des deux types de moteur pour obtenir un mouvement rétrograde net en se liant à leur protéine adaptatrice respective, BICD2 et FEZ1 (264-267). Ce transport bidirectionnel permet d'éviter les obstacles stériques et est modulé par le VIH-1 via la phosphorylation de FEZ1, permettant d'activer ou de désactiver le moteur de kinésine (268). Durant son transport vers le noyau, la capside s'associe également avec d'autres facteurs cellulaires tels que l'inositol

hexaphosphate (IP_6) et la cyclophiline A (CypA), deux facteurs lui permettant de garder son intégrité structurelle jusqu'à son arrimage au complexe du pore nucléaire (NPC) (269-274).

Pendant le processus de translocation vers le noyau, l'ARNv du VIH-1 est converti en ADN par le complexe de rétrotranscription (RTC), dirigé par la RT avec la contribution de la protéine NC qui agit à titre de chaperonne aidant au repliement adéquat des acides nucléiques (275, 276). La RT possède deux activités enzymatiques comprenant une activité d'ADN polymérase, qui peut utiliser l'ARN ou l'ADN comme matrice, et une activité RNase H, qui dégrade exclusivement l'ARN dans le contexte d'un duplex d'ARN/ADN (138). Pour commencer ce processus, l'ARN de transfert Lys3 ($ARNt^{Lys3}$) d'origine cellulaire est utilisé comme amorce pour se lier au site de liaison de l'amorce (PBS) présent dans l'élément U5 de l'extrémité 5' de l'ARNv (175, 277). Des pores présents dans la capside, situés au centre des hexamères de CA, permettent l'import sélectif de désoxynucléotides triphosphates (dNTPs), nécessaires à la polymérisation de l'ADNv (278, 279). La RT catalyse alors la synthèse de l'ADN pendant que son activité RNase H dégrade progressivement l'extrémité 5' restante de l'ARN matrice du complexe ARN/ADN pour libérer l'ADNsb à polarité négative (280-282). Lorsque la transcription inverse de l'extrémité 5′ est terminée, l'élément R du brin d'ADN nouvellement synthétisé s'hybride alors à l'élément R présent à l'extrémité 3' de l'ARNv dans un processus appelé transfert du premier brin (283). Comme le VIH porte deux copies de l'ARN génomique, le transfert du premier brin peut se produire en *cis* ou en *trans*, ce qui explique les possibilités de recombinaison virale (284, 285). Ce transfert d'ADN permet la synthèse complète du premier brin d'ADNv, tout en dégradant l'ARN matrice, à l'exception du tract de polypurine (PPT), qui est résistant à l'activité de la RNase H et qui servira d'amorce pour produire le second brin d'ADN à polarité positive (286, 287). Le VIH-1 possède deux séquences PPT, l'une étant situé près de l'extrémité 3' de l'ARNv et l'autre étant présent dans la région centrale du génome (PPTc) (288). La synthèse du second brin d'ADNv est initiée lorsque la RT utilise les séquences PPT comme amorce (289), ce qui permet l'élongation jusqu'à la séquence PBS présente à l'extrémité 3', où l'$ARNt^{Lys3}$ est dégradé par la RNase H (290, 291). Ceci permet l'hybridation des séquences PBS complémentaires présentes aux extrémités 3' et 5' dans un processus appelé transfert du second brin, permettant de compléter la synthèse des deux brins d'ADNv (283). Le produit final est un ADNdb avec les régions U3, R et U5 formant les LTR aux extrémités et flanquant les régions codantes du génome (138). Les possibilités de

recombinaison et la fidélité déficiente de RT pendant le processus de rétrotranscription contribuent à la grande diversité génétique du VIH-1 (292). Suite à la rétrotranscription, le complexe pré-intégration (PIC) s'assemble à partir de l'ADNv nouvellement synthétisé; celui-ci comporte également les protéines virales IN, RT, MA, et Vpr (293-295).

La complétion du processus de rétrotranscription est coordonnée avec l'initiation du processus de désassemblage de la capside virale (296-298). Les études récentes favorisent un modèle dans lequel le désassemblage de la capside se produit après la translocation nucléaire en fournissant des preuves convaincantes que la transcription inverse se finalise dans le noyau et que la capside entière pénètre dans le noyau et reste intacte jusqu'à ce qu'elle se désassemble et libère le PIC près des sites d'intégration (299-303). Pour ce faire, la capside s'arrime au NPC via sa capture par la protéine NUP358 présente dans les filaments cytoplasmiques du NPC (304, 305). La capside interagit ensuite de manière séquentielle avec la protéine NUP153 du panier nucléaire du NPC (306-309), puis avec le complexe CPSF6/TNPO3 permettant son passage à travers l'enveloppe nucléaire et sa relâche dans le noyau (310-316). Bien que la taille du pore nucléaire limite habituellement la pénétration de macromolécules ayant une taille excédant 40 nm, il existe une certaine hétérogénéité au niveau de la taille du NPC, qui peut se dilater jusqu'à environ 64 nm de diamètre, permettant ainsi le passage de capside virale complète (~60 nm) (303, 317, 318). Un remodelage de la capside par la protéine CPSF6 facilite également le passage à travers du NPC (319-321).

La dernière étape précoce du cycle de réplication du VIH-1 est l'intégration de l'ADNv dans le génome de la cellule hôte (322). L'enzyme virale IN joue un rôle crucial dans ce processus, ainsi que la protéine cellulaire LEDGF/p75, en plus d'autres protéines virales (MA, NC et Vpr) qui contribuent à accroître l'efficacité de l'intégration (323-327). LEDGF facilite l'attachement et empêche la circularisation de l'ADN et la formation de cercles 2-LTR puisque cette forme du génome ne peut pas être intégrée (328). Lors de la première étape de l'intégration, l'intégrase retire deux nucléotides de chaque extrémité 3′ de l'ADNdb (329, 330). Dans la deuxième étape, appelée transfert de brin d'ADN, les extrémités 3′ de l'ADNv induisent une cassure double brin de l'ADN cellulaire et sont jointes de manière covalente à chaque brin (331). Finalement, les interstices dus aux deux nucléotides supplémentaires présents aux extrémités 5′ de l'ADNv sont réparées par des

enzymes cellulaires pour achever l'intégration (332). Il a été suggéré que l'intégration se produit de préférence au niveau des régions de la chromatine actives sur le plan transcriptionnel et près du NPC (333-335). Ce processus est facilité par l'interaction de LEDGF avec les nucléosomes H3K36me3, enrichis dans les régions d'euchromatine riches en gènes et où la machinerie de réparation de l'ADN est recrutée en grande proportion (336-339).

1.1.5.3 Étapes tardives du cycle de réplication

Après l'intégration, l'ADN viral intégré est appelé " provirus " et sert de matrice pour la transcription de toutes les protéines virales structurelles, régulatrices et accessoires. La transcription virale initiale est médiée par l'ARN polymérase II cellulaire (ARNPII) et est rendue possible par l'interaction directe entre des facteurs de transcription cellulaires et les éléments régulateurs en *cis* situés dans le promoteur du LTR (340). Ces éléments comprennent une boîte TATA non-canonique, trois sites de liaison de la protéine de spécificité 1 (Sp1) en tandem et deux sites de liaison du facteur nucléaire kappa B (NF-κB) hautement conservés et essentiels à la transcription virale (341-344). D'autres facteurs de transcription tels que NFAT, AP1 et plusieurs autres modulent l'activité du promoteur sans toutefois être essentiels à la transcription virale (345, 346). Les ARNm produits sont de pleine longueur (9,2 kb) et doivent éviter la machinerie d'épissage afin de rester ainsi. Ces ARN non-épissés sont les ARNm codant pour les gènes *gag* et *pol* et servent également d'ARN génomique qui sera incorporé dans les nouveaux virions (347, 348). Tous les autres transcrits viraux sont donc le résultat de l'épissage. Trois de ces ARNm sont complètement épissés et codent pour les gènes précoces (*tat*, *rev*, *nef*), tandis que trois autres transcrits sont partiellement épissés (*vif*, *vpr*, *vpu/env*) et codent pour les gènes tardifs (347, 348). Certains mécanismes cellulaires préviennent toutefois l'export nucléaire des ARNm non-épissés et partiellement épissés à cause de la présence d'introns, permettant uniquement l'export des ARNm complètement épissés au début du processus de transcription (133). Les protéines virales Tat, Rev et Nef sont produites en premier lieu par des ribosomes cytoplasmiques et les protéines régulatrices Tat et Rev sont importées dans le noyau via des signaux de localisation nucléaire (NLS) leur permettant de lier une variété d'importines (349-353). L'accumulation de Tat dans le noyau stimule davantage la transcription à partir du LTR par une boucle de rétroaction positive (354-356). Tat se lie à l'élément de réponse à la transactivation (TAR), une structure d'ARN en épingle liée au LTR proviral en aval du site d'initiation de la transcription (357, 358).

Subséquemment, Tat recrute le facteur positif d'élongation de la transcription (P-TEFb), composé de la cycline T1 (CycT1) et de la kinase 9 dépendante de la cycline (CDK9) qui médie l'hyperphosphorylation de la queue C-terminale de l'ARNPII, améliorant ainsi sa processivité et sa capacité d'élongation (358-360). L'export nucléaire des transcrits non-épissés ou partiellement épissés est rendu possible par la protéine Rev qui se multimérise et se lie à la séquence RRE chevauchant le gène *env* et présente dans tous ces ARNm (361, 362). Rev contient un signal d'export nucléaire (NES) qui sert d'adaptateur au complexe CRM1/RanGTP et qui permet le transport actif vers le cytoplasme des ARNm viraux tardifs (363-365). Ceux-ci permettront la production des protéines virales Gag, Gag-Pol, Vif et Vpr par les ribosomes cytoplasmiques ainsi que Vpu et Env par les ribosomes associés au réticulum endoplasmique (366).

Le VIH-1 optimise la capacité codante de son génome en traduisant différentes protéines à partir d'un même ARNm. C'est le cas de l'ARNm bicistronique *vpu*/*env* qui code à la fois pour les deux protéines transmembranaires du VIH-1 (367, 368). Bien que le gène *env* soit situé en aval de *vpu* dans la séquence de l'ARNm, la traduction d'Env est favorisée puisque le codon d'initiation de Vpu est précédé d'une séquence Kozak faible et qu'il est chevauché par un ORF de six nucléotides dans un cadre de lecture différent, permettant aux ribosomes de court-circuiter le gène *vpu* pour traduire *env* (369, 370). Un autre exemple est le cas de l'ARN génomique qui sert à produire les polyprotéines Gag et Gag-Pol (145). La polyprotéine Gag-Pol, qui est synthétisée dans un ratio de 1:20 par rapport à Gag, est traduite grâce au signal de changement de cadre de lecture (FSS) qui coïncide avec un décalage ribosomal d'un seul nucléotide à la jonction entre *gag* et *pol* (145, 163, 371, 372).

Après sa synthèse par les ribosomes cytoplasmiques, la polyprotéine $Pr55^{Gag}$ coordonne l'assemblage des particules virales (373, 374). L'extrémité N-terminale de MA est myristoylée et Gag est ancrée à la membrane cytoplasmique dans des sites riches en phosphatidylinositol-4,5-bisphosphate [$PI(4,5)P_2$] et en cholestérol (375-378). Ces régions sont connues sous le nom de microdomaines lipidiques ou « radeaux lipidiques », à partir desquels le bourgeonnement viral se fait, et sont enrichies en cholestérol, en sphingolipides et en protéines ancrées par un groupement glycosylphosphatidylinositol (GPI) (379-381). Le domaine CA favorise la multimérisation de Gag avec l'aide d'IP_6 (272, 382-385) pendant que le domaine p6 permet l'incorporation de Vpr (178,

386-390) et que le domaine NC conduit l'empaquetage de l'ARNv génomique dimérique, en interagissant avec la séquence d'encapsidation ψ (129, 172, 391).

Pendant ce temps, le précurseur d'Env de 160 kDa (gp160), une glycoprotéine transmembranaire de type I, est synthétisé à partir de l'ARNm bicistronique *vpu*/*env*, dans le réticulum endoplasmique rugueux (RER) (392). La gp160 comprend un peptide signal (PS) à son extrémité N-terminale qui la cible à la membrane du RER, et ce peptide est clivé par les signal peptidases cellulaires après la traduction (393-396). Le clivage du PS sert de point de contrôle du repliement adéquat de la protéine, qui se fait à l'aide de chaperonnes cellulaires et nécessite la formation de plusieurs ponts disulfures intramoléculaires afin de maintenir sa structure tertiaire (397-400). La gp160 s'oligomérise alors sous forme de trimère et subit des modifications post-traductionnelles, majoritairement via la glycosylation de résidus asparagines avec des chaînes latérales d'oligomannoses (N-glycans) (184, 397, 401). Ensuite, au cours de son trafic à travers le réseau *trans*-Golgi (TGN), les chaînes latérales d'oligosaccharides sont coupées, des glycans complexes sont ajoutés (402-404) et les proprotéines convertases cellulaires, telles que la furine et les protéases de type furine, catalysent le clivage protéolytique de la gp160 pour produire les sous-unités fonctionnelles (gp120 et gp41), qui restent associées de manière non covalente (189, 405-410). La furine reconnaît et clive en aval du motif polybasique hautement conservé à la jonction gp120-gp41 (^{508}REKR^{511}), ce qui libère le peptide de fusion hydrophobe à l'extrémité N-terminale de la gp41 essentiel au processus de fusion virale (141, 182, 183, 411, 412). Suite à sa biosynthèse, Env est transloqué vers la surface cellulaire où elle sera soit incorporée aux virions bourgeonnants, soit rapidement internalisée (413). La queue cytoplasmique (CT) d'Env contient un motif d'endocytose à base de tyrosine (^{712}YXXΦ^{715} ; où X représente n'importe quel acide aminé et Φ un acide aminé hydrophobe) qui interagit avec le complexe de protéines adaptatrices de la clathrine 2 (AP-2) (414, 415). L'Env internalisée passe par les compartiments de recyclage endosomaux et est dirigée vers les sites d'assemblage des virions par le complexe Rab11-FIP1C/Rab14 (416-418). La rétention d'Env dans les plateformes d'assemblage virales est facilitée par un motif d'interaction avec le cholestérol (^{679}LWYIK^{683}) dans sa région externe proximale à la membrane (MPER), par au moins un site de palmitoylation dans sa CT et par son interaction avec la protéine virale MA (413, 419-424).

La fin du cycle de réplication du virus implique le bourgeonnement et la relâche des virions nouvellement formés. Le domaine p6 à l'extrémité C-terminale de Gag sert d'adapteur pour recruter la machinerie ESCRT, qui est composée de protéines cellulaires qui aident au processus de scission membranaire (425-427). Le motif PTAP de p6 interagit avec la protéine TSG101, une composante du complexe ESCRT-I tandis que son motif YPXL se lie à la protéine ALIX, une protéine qui interagit directement avec les complexes ESCRT-I et ESCRT-III (428-433). Les virions libérés subissent un processus de maturation, qui débute par le clivage autocatalytique du domaine PR de Gag-Pol (434-436). L'enzyme PR est une protéase aspartique qui s'assemble sous forme d'homodimère, dans lequel le site actif est situé dans une cavité à l'interface du dimère (437-440). Dans une séquence ordonnée, PR clive des sites prédéfinis dans les polyprotéines Gag et Gag-Pol pour libérer les protéines structurelles MA, CA, SP1, NC, SP2 et p6 ainsi que les enzymes PR, RT et IN (139, 441, 442). Le clivage de la PR déclenche des changements morphologiques dans le virion, notamment via la formation d'une capside en forme de fullerène conique et par le compactage de l'ARNv, ce qui donne des particules virales infectieuses matures (142, 165, 443, 444).

1.1.5.4 Facteurs de restriction

Les facteurs de restriction sont des protéines de l'immunité innée de la cellule hôte qui interfèrent avec des étapes spécifiques du cycle de réplication des virus, bloquant ainsi l'infection. Les facteurs de restriction partagent un certain nombre de caractéristiques et la définition la plus stricte stipule que ce sont des gènes exprimés de manière constitutive, inductible par la réponse interféron de type I (IFN-I) et hautement conservé grâce à une pression sélective positive. Les facteurs de restriction représentent des barrières de transmission inter-espèces, mais ils sont inactifs contre les virus de type sauvage dans leur hôte naturel grâce à l'antagonisme par une protéine accessoire virale ou le recrutement d'un partenaire cellulaire (445). Il existe quatre facteurs de restriction canoniques connus pour inhiber la réplication du VIH-1: APOBEC3G, TRIM5α, SAMHD1 et BST-2 (446-451).

APOBEC3G appartient à une famille d'enzymes de type cytidine désaminases d'ADNsb capable d'inhiber l'étape de la transcription inverse (446). Son mécanisme de restriction débute par son incorporation dans les particules virales via sa multimérisation sur l'ARNv génomique

(452, 453). Dans les cellules nouvellement infectées, APOBEC3G provoque un phénomène d'hypermutation du génome pendant la rétrotranscription en catalysant la désamination des cytidines en uridines (C→U) dans l'ADNsb naissant (454-456). Par conséquent, ce mécanisme d'édition de l'ADN proviral mène à des transitions G→A sur le brin codant qui conduise à l'introduction de substitutions non-synonymes et de codons de terminaison prématurés, pouvant causer des défauts lors de la transcription et de la traduction du provirus (454, 455, 457, 458). Le locus humain du gène APOBEC3 comporte sept cytidine désaminases (APOBEC3A, -3B, -3C, -3D, -3F, -3G, -3H), certaines ayant également une activité antivirale contre le VIH-1 (459, 460). Les protéines APOBEC3 sont exprimées dans de nombreux types de cellules, notamment dans les cellules hématopoïétiques (461-463). La protéine accessoire Vif du VIH-1 a évolué pour contrer l'activité antivirale d'APOBEC3G et d'autres membres de la famille APOBEC en induisant leur dégradation par le protéasome, réduisant ainsi leurs niveaux d'incorporation dans les virions nouvellement produits (459, 464-468).

TRIM5α appartient à une grande famille d'enzyme de type E3 ubiquitine (Ub) ligase et inhibe la réplication du VIH-1 en accélérant le processus de désassemblage de la capside virale, entravant la transcription inverse et la translocation du génome vers le noyau (447). Sa topologie comprend entre autres un domaine RING E3 Ub ligase en N-terminal, un domaine de dimérisation central, et un domaine SPRY en C-terminal qui est capable d'interagir avec la capside du VIH-1 (469-472). Donc, TRIM5α cause le désassemblage prématuré de la capside dans le cytoplasme en s'y liant directement via son domaine SPRY et en se multimérisant pour former une vaste structure hexagonale (473-475). TRIM5α recrute ensuite la machinerie d'ubiquitination permettant la dégradation de la capside par le protéasome (476-478). À cause d'une certaine redondance génique, TRIM5α peut également former des hétéro-oligomères avec d'autres protéines de la famille TRIM et conserver son activité antivirale (479-481). Or, en plus de stabiliser la capside virale lors de l'infection, le recrutement de CypA protège également de la restriction par TRIM5α en compétitionnant pour la liaison à CA (482, 483). Fait intéressant, chez plusieurs espèces de singes, le domaine SPRY de TRIM5α a été remplacé par un domaine de cyclophiline A (TRIM-CypA), ce qui lui confère une résistance accrue à l'infection par le VIH-1 (484-490).

SAMHD1 est une dNTP hydrolase présente dans le noyau qui entrave également la transcription inverse du VIH-1 en réduisant le pool de dNTPs intracellulaire disponible (448, 491, 492). L'activité de SAMHD1 est inhibée par la phosphorylation de son résidu T592 par les kinases CDK1/2 pendant l'initiation de la phase S du cycle cellulaire (493, 494) et déphosphorylée par la phosphatase PP2A à la fin de la phase M (495). La phosphorylation de SAMHD1 peut notamment être augmentée par les cytokines de type γc comme l'interleukine-2 (IL-2), l'IL-7 et l'IL-15 qui régulent la prolifération homéostatique des lymphocytes T $CD4^+$ (496, 497). La protéine accessoire Vpx du VIH-2 est connue pour sa capacité à induire la dégradation de SAMHD1 par le protéasome (449). Du côté du VIH-1, il ne possède pas de gène encodant pour Vpx, mais pourrait compenser ce manque en induisant un arrêt du cycle cellulaire en phase G2/M par Vpr et en dégradant PP2A par l'entremise de Vif, afin de piéger SAMHD1 dans son état phosphorylé (498-504). SAMHD1 est exprimé de façon ubiquitaire dans les cellules myéloïdes et lymphocytaires, mais confère une résistance au VIH-1 uniquement dans les cellules différentiées terminales (e.g. cellule dendritique) ou quiescentes (e.g. lymphocyte T naïf) qui sont dans la phase G0/G1 (505-507).

BST-2, aussi connue comme tétherine, est une protéine transmembranaire qui ancre les particules virales bourgeonnantes à la surface des cellules infectées, empêchant la relâche du virus (450, 451). Cette fonction est assurée par sa topologie unique, avec la présence d'un domaine transmembranaire en N-terminal, de cystéines dans son domaine extracellulaire permettant sa dimérisation, et d'une ancre lipidique GPI en C-terminal, qui permet de fixer une extrémité de la protéine à la membrane plasmique et l'autre à la membrane virale (508, 509). BST-2 exerce une activité antivirale contre un large spectre de virus enveloppés (510-521). Notamment, les lentivirus de primates ont évolué vers trois protéines virales différentes pour échapper à la restriction de BST-2. La protéine Vpu du VIH-1 surmonte la restriction du BST-2 humain par sa séquestration dans le TGN et les compartiments endosomaux et la promotion de sa dégradation par le protéasome et les lysosomes (522-530). Les glycoprotéines d'Env du VIH-2 et de souches de SIV reliées sont également capables d'antagoniser BST-2 via une interaction entre leurs domaines transmembranaires respectifs (531-534). Pour la plupart des SIV, la protéine Nef cible une séquence dans la queue cytoplasmique de BST-2 simien favorisant son endocytose et sa dégradation lysosomale (535). Comme le BST-2 humain est dépourvu de cette séquence, cela lui

confère une résistance à l'antagonisme du Nef encodé par les différentes souches de SIV (536-538). Le gène *bst2* possède un codon d'initiation alternatif permettant la génération d'une isoforme courte résistante à Vpu, ayant une troncature de 12 acides aminés dans sa queue cytoplasmique par rapport à son isoforme longue (539, 540). De son côté, l'isoforme longue de BST-2 possède la capacité d'induire l'activation de la cascade de signalisation pro-inflammatoire NF-κB via la détection de virions attachés à la surface cellulaire, dévoilant une fonction supplémentaire de BST-2 en tant que senseur viral dans l'immunité innée au-delà de son activité de restriction (541, 542). L'activation de la voie NF-kB par BST-2 est également abrogée par Vpu (543, 544). En plus d'être augmenté par les IFN-I, BST-2 peut également être induit par l'IL-27 via des voies de signalisation JAK-STAT redondantes dans les cellules myéloïdes et les lymphocytes T (545).

Dans le domaine de la recherche sur le VIH-1, les modèles de primates non-humains (NHP), comme le macaque, sont largement utilisés pour mimer l'infection par le VIH-1 (115). Comme le VIH-1 est incapable d'antagoniser les quatre facteurs de restriction principaux chez le macaque, l'utilisation de ce modèle d'infection nécessite l'utilisation de constructions virales hybrides, appelées virus de l'immunodéficience humaine et simienne (SHIV) (447, 526, 536, 546-548). Ces virus sont typiquement composés d'une souche de SIVmac où l'on substitue uniquement le segment génique *env* du VIH-1 afin d'obtenir une infection productive (549).

1.1.5.5 Facteurs de résistance

De surcroît, il existe également plusieurs facteurs de résistance cellulaires capables d'inhiber un large éventail de processus du cycle de réplication du VIH-1, sans toutefois remplir tous les critères pour être considérés comme des facteurs de restriction. Le fait que les IFN-I inhibent fortement la réplication du VIH-1 suggère la présence de facteurs antiviraux additionnels provenant des gènes induits par l'IFN (ISG) (550-555). Les protéines de la famille IFITM (IFITM1, IFITM2, IFITM3) et de la famille GBP (GBP2, GBP5) sont connues pour interférer avec l'entrée virale du VIH-1 (556, 557). Les IFITMs affectent à la fois la biosynthèse d'Env dans la cellule infectée productrice et le processus de fusion dans la cellule cible (558-561). GBP2/5 sont des inhibiteurs de la furine cellulaire, affectant également la synthèse de trimère d'Env fonctionnels (562, 563). L'activité antivirale de ces deux familles de protéines peut être surmontée par le VIH-1 par des mutations d'Env ou en augmentant l'expression d'Env, respectivement (564-566).

Ensuite, il y a la protéine MX2 qui est capable de bloquer l'import nucléaire du PIC par sa liaison à la capside virale et par une potentielle compétition pour la liaison à la protéine Nup153 du panier du NPC (321, 567-572). Les protéines ZAP et SLFN11 sont des facteurs antiviraux posant des contraintes au niveau de la séquence du génome viral et affectant les étapes tardives de transcription et de traduction (573-575). ZAP est une polymérase d'ADP-ribose capable de reconnaître et cliver les ARNm contenant des îlots de dinucléotides CpG (576-580), tandis que SLFN11 digère certains ARNt de type II (573, 581). Le VIH-1 est capable d'échapper à ces deux facteurs par la limitation du contenu en nucléotides CG et par une utilisation biaisée de certains codons dans son génome (582, 583). Outre les ISGs, il existe également des facteurs de résistance intrinsèques exprimés de manière constitutive qui inhibent la réplication du VIH-1. Les protéines SERINC3 et SERINC5 sont incorporées au niveau de la particule virale et réduisent l'efficacité de l'entrée virale (584-587). Cette famille de protéines à dix passages transmembranaires, une caractéristique typique des enzymes de type flippase, jouerait potentiellement un rôle visant à réduire l'exposition des phosphatidylsérines sur le feuillet externe de la membrane virale, ce qui est essentiel au processus de fusion (253, 588, 589). Les lentivirus de primates (HIV-1, HIV-2 et SIVs) utilisent la protéine accessoire Nef afin d'exclure SERINC3 et SERINC5 des virions bourgeonnants (590, 591). Les protéines TIMs possèdent un domaine pouvant se lier aux phosphatidylsérines de la membrane virale et ainsi limiter la relâche virale dans un mécanisme indépendant de BST-2 (209). Cependant, le VIH-1 régule négativement les niveaux de surface de cette famille de protéines en utilisant les protéines accessoire Vpu pour cibler TIM-3 et Nef pour cibler TIM-1 (592, 593). Malgré la présence d'une variété de facteurs antiviraux cellulaires, le VIH-1 a évolué de sorte qu'il puisse contrecarrer ces mécanismes de défense et répliquer efficacement dans les cellules hôtes.

1.1.6 Protéines accessoires

Les protéines accessoires du VIH-1 (Vif, Vpr, Vpu, Nef) ne sont pas nécessaires à la réplication du VIH-1 *in vitro*, mais sont essentielles pour la réplication virale efficace *in vivo*. Les protéines accessoires manipulent de nombreuses voies et processus cellulaires pour créer un environnement propice à la réplication virale, en surmontant les mécanismes de défense antiviraux de l'immunité innée et adaptative. Ces petites protéines polyvalentes se servent des complexes de protéines adaptatrices de clathrine (Nef, Vpu) et de la machinerie d'ubiquitination (Vif, Vpr, Vpu),

afin d'induire la relocalisation ou la dégradation par le protéasome ou les lysosomes d'une grande variété de facteurs cellulaires.

1.1.6.1 Vif

Vif est une protéine cytoplasmique de 23 kDa qui est exprimée tard dans le cycle de réplication virale. Vif joue un rôle prépondérant dans la pathogenèse lentivirale *in vivo* puisque son absence empêche complètement la réplication virale dans les modèles d'infection de NHP ou de souris humanisées (594-597). La principale fonction de Vif est d'antagoniser les facteurs de restriction de la famille APOBEC3 pour assurer la production de virons infectieux (446). Vif interagit directement avec APOBEC3G et recrute le complexe E3 Ub ligase ELOC/ELOB/CUL5/RBX2 pour polyubiquitiner APOBEC3G, ce qui conduit à sa dégradation par le protéasome (467, 598-601). Ce processus nécessite également le cofacteur cellulaire non-canonique CBFβ pour stabiliser Vif et son assemblage avec la E3 Ub ligase (602-607). Certaines fonctions secondaires de Vif incluent l'induction d'un arrêt du cycle cellulaire en phase G2/M par la dégradation de plusieurs complexes régulateurs hétérotrimériques de la phosphatase PP2A (PPP2R5) (501-504, 608), l'inhibition de l'autophagie (609) et l'inhibition de la réponse interféron (610-612).

1.1.6.2 Vpr

Vpr est une protéine nucléaire de 14 kDa dont la fonction est la plus énigmatique. Sa présence semble jouer un rôle plus prépondérant dans l'infection de cellules myéloïdes et sa délétion *in vivo* atténue modestement la pathogénèse du virus (613-617). Vpr interagit avec DCAF1, un adaptateur permettant de recruter le complexe E3 Ub ligase DCAF1/DDB1/CUL4A/RBX1 (618-622). Le recrutement de la E3 Ub ligase par Vpr a différents effets biologiques, notamment l'induction d'un arrêt du cycle cellulaire en phase G2/M des cellules infectées et l'activation de la voie des dommages à l'ADN médiée par ATR (498-500, 623, 624), ce qui mène à la reprogrammation du transcriptome de la cellule infectée et l'augmentation de l'activité transcriptionnelle du promoteur du LTR (625-629). Ce processus active les mécanismes d'apoptose cellulaire qui sont également contrecarrés par Vpr (630-633). Une conséquence connue de l'activation de la voie des dommages à l'ADN est d'accroître la sensibilité des cellules infectées à la destruction par les cellules NK en induisant l'expression de ligands de stress à la surface des

cellules infectées (634-636). De nombreuses protéines cellulaires jouant un rôle dans les différentes voies de réparation de l'ADN, y compris la glycosylase d'uracile UNG2 (637, 638), le complexe SLX4 (639, 640), l'hélicase HLTF (327, 641, 642), l'exonucléase EXO1 (643), ont été signalées comme étant dégradées par Vpr, mais n'ayant que peu d'effet sur le cycle cellulaire et l'expression génique (644, 645). La récente identification du facteur CCDC137 comme cible cellulaire dégradée par Vpr pourrait être la pièce manquante puisque sa déplétion récapitule entièrement le phénotype induit par Vpr (644, 646).

1.1.6.3 Vpu

Vpu est une protéine transmembranaire de 16 kDa produite à partir d'un ARNm bicistronique codant également pour Env, ce qui suggère que l'expression de Vpu et d'Env est coordonnée pendant l'infection par le VIH-1 (151, 153, 367, 368). L'expression de Vpu est spécifique au VIH-1 et aux SIV apparentés, incluant ses précurseurs SIVcpz et SIVgor, ainsi que les ancêtres du SIVcpz (SIVgsn/mon/mus/den) (109, 647-651). Sa topologie consiste en un court peptide luminal en N-terminal, un domaine transmembranaire sous forme d'hélice α inclinée à 25° et d'un domaine cytoplasmique hydrophile composé de deux hélices α amphiphiles partiellement enfouies dans la membrane lipidique (652). Les hélices 2 et 3 sont connectées par une boucle flexible comportant une séquence hautement conservée (^{51}DSGNES^{56}), qui comprend une paire de sérines (S52 et S56) qui sont phosphorylées par la caséine kinase II (CKII) (653-656). Ce motif de phosphosérine interagit avec l'adaptateur β-TrCP, qui permet le recrutement de la E3 Ub ligase β-TrCP/SKP1/CUL1/RBX1 ($SCF^{\beta\text{-}TrCP}$) (657, 658). L'hélice 3 comporte également un motif d'endocytose dileucine non-classique (^{59}EXXXLV^{64}) lui permettant de lier le complexe de protéines adaptatrices de clathrine AP-1 (659-661). Vpu se localise principalement dans des compartiments intracellulaires, notamment, le réticulum endoplasmique (RE), le TGN et les endosomes (522, 654, 662, 663).

La protéine Vpu du VIH-1 possède deux fonctions principales : l'augmentation de l'infectivité des virions par la dégradation du récepteur CD4 (664) et l'augmentation de la relâche des virions par l'antagonisme du facteur de restriction BST-2 (450, 451). Des modèles d'infection *in vivo* ont confirmé le rôle de Vpu dans la promotion de la réplication virale dans la phase initiale de l'infection et de la persistance de la virémie à long terme grâce à sa capacité à réguler

négativement CD4 et BST-2 (665-669). En ciblant le CD4 nouvellement synthétisé, Vpu prévient la formation de complexes Env-CD4 dans le RE, ce qui pourrait affecter la stabilité, la maturation, le trafic et l'incorporation de Env vers les sites d'assemblage viraux (670). La dégradation de CD4 médiée par Vpu est initiée par l'interaction entre l'hélice 2 de Vpu et une hélice α située dans la région proximale à la membrane dans la queue cytoplasmique du CD4 (671-678), suivi de la polyubiquitination de CD4 par la E3 Ub ligase $SCF^{\beta\text{-}TrCP}$ (657, 679, 680). La polyubiquitination de CD4 favorise le recrutement du complexe de dislocase VCP-UFD1L-NPL4 de la voie de dégradation associée au RE (ERAD), qui permet l'extraction du CD4 de la membrane et son acheminement au protéasome pour sa dégradation (679, 681, 682). De son côté, le mécanisme par lequel Vpu antagonise BST-2 est associé à une réduction des niveaux de BST-2 à la surface cellulaire en ciblant le BST-2 nouvellement synthétisé ou recyclé vers la membrane cytoplasmique (530, 683). Vpu et BST-2 interagissent directement par l'intermédiaire de leurs domaines transmembranaires respectifs, ce qui dépend d'un sillon hydrophobe formé par les résidus A10, A14, A18 et W22 dans l'hélice transmembranaire de Vpu (684, 685). Le BST-2 est ensuite séquestré dans le TGN et les compartiments endosomaux riches en clathrine grâce au recrutement du complexe AP-1 (522, 527, 659). En induisant la polyubiquitination de la queue cytoplasmique de BST-2, Vpu redirige BST-2 vers une voie de dégradation endosomale dépendante des ESCRTs qui se termine par sa dégradation dans les lysosomes (523, 525, 686-688).

En plus de CD4 et BST-2, Vpu module à la baisse une variété de protéines cellulaires transmembranaires à l'aide de son domaine transmembranaire ou de ses partenaires cellulaires afin d'améliorer l'efficacité du cycle de réplication viral et la survie des cellules infectées (**Figure 1.1.6**). D'abord, la régulation négative du récepteur de phosphatidylsérine TIM-3 est un autre mécanisme par lequel Vpu augmente la relâche virale (209, 593). La capacité de Vpu à augmenter l'infectivité des virions passe également par l'exclusion de PSGL-1 et CD43, des protéines hautement glycosylées empêchant l'attachement à la surface des cellules cibles (689-691), ainsi que les tétraspanines, une famille de molécules affectant le processus de fusion (692-695). Ensuite, Vpu est capable d'altérer l'activation des lymphocytes T $CD4^+$ infectées en ciblant des cofacteurs du récepteur des lymphocytes T (TCR) comme CD4, CD28 et TIM-3 (593, 696-698), en dégradant le transporteur d'alanine SNAT1, important pour l'immunométabolisme des cellules en prolifération (699), et en interrompant la voie de signalisation NF-κB, par son antagonisme de

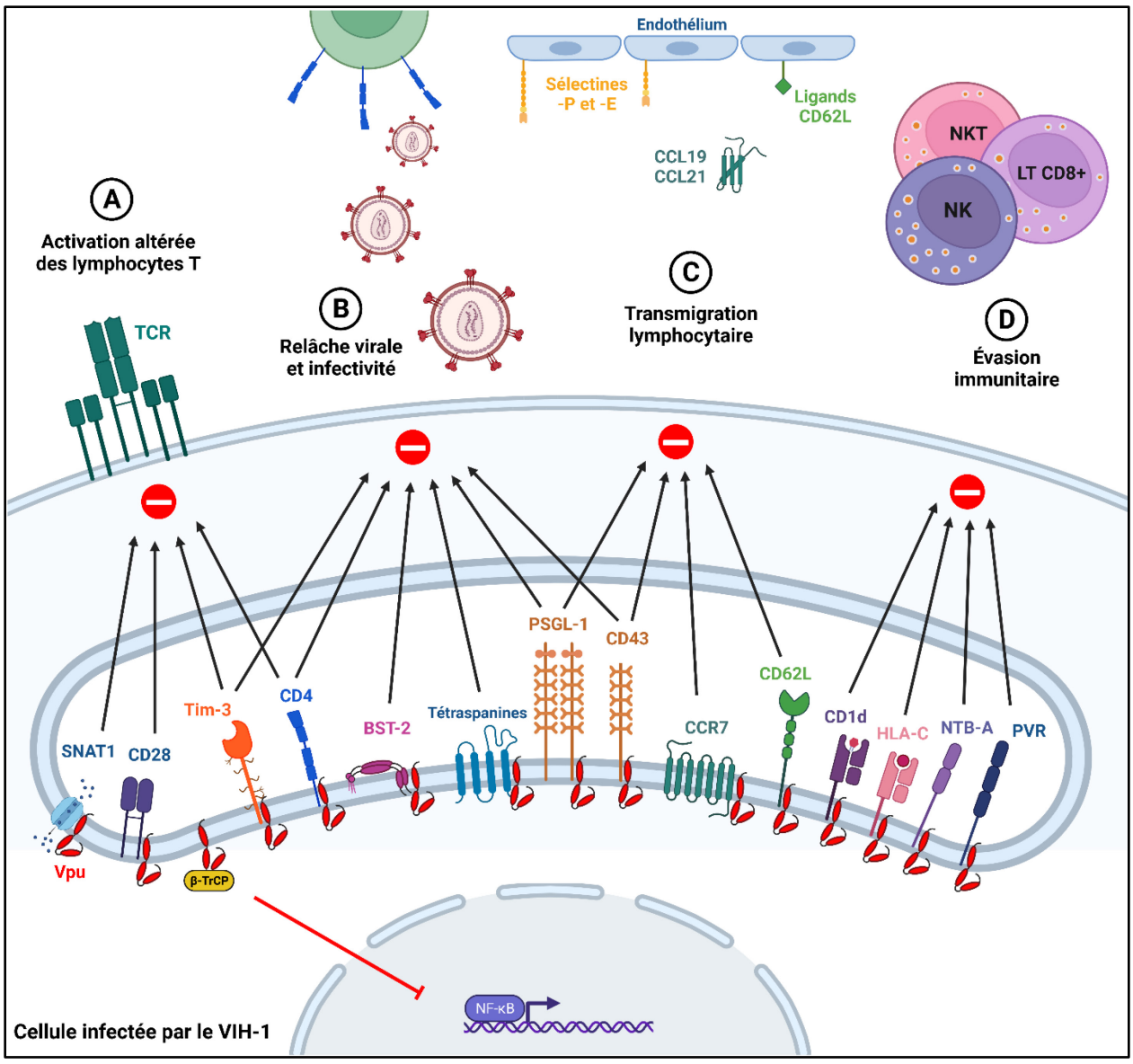

Figure 1.1.6 - Fonctions de Vpu dans les cellules infectées par le VIH-1

Par sa capacité à recruter les protéines adaptatrices de clathrine et une E3 ubiquitine ligase, Vpu est capable de cibler une vaste gamme de protéines cellulaires transmembranaires dans les différents compartiments de la voie de sécrétion. (**A**) Vpu peut interférer avec l'activation des lymphocytes T infectés en interférant avec la voie de signalisation du TCR (NF-κB), des cofacteurs du TCR (CD4, CD28, TIM-3) ou l'immunométabolisme (SNAT1). (**B**) Vpu augmente aussi la relâche virale (BST-2, TIM-3) et l'infectivité des particules virales relâchées (CD4, PSGL-1, CD43 et les tétraspanines). (**C**) Une autre de ses fonctions est de bloquer la migration trans-endothéliale lymphocytaire vers les tissus (PSGL-1, CD43, CCR7, CD62L). (**D**) Finalement, Vpu joue un rôle dans l'évasion immunitaire des cellules infectées en régulant négativement les ligands de récepteurs activateurs des cellules NKT (CD1d), lymphocytes T [LT] $CD8^+$ (HLA-C) et cellules NK (NTB-A, PVR). Diagramme créé avec BioRender.com.

BST-2 et par la séquestration de la protéine adaptatrice β-TrCP, ce qui empêche la dégradation de IκB (540, 543, 544, 700, 701). D'autre part, Vpu prévient la migration trans-endothéliale vers les tissus en ciblant le récepteur de chimiokine CCR7, nécessaire au « homing » des cellules vers les ganglions lymphatiques via un gradient chimiotactique de CCL19 et CCL21 (702, 703), et en inhibant l'exposition de surface de la sélectine-L (CD62L) et des ligands pour la sélectine-P et la sélectine-E (PSGL-1, CD43), des molécules d'adhésion importantes pour le processus de roulement sur l'endothélium (704-706). Finalement, Vpu contribue à l'évasion de différentes réponses immunitaires innées et adaptatives notamment en modulant à la baisse les ligands des récepteurs activateurs des cellules NK (NTB-A, PVR), des cellules NKT (CD1d) et des cellules T CD8+ cytotoxiques (HLA-C) (707-713).

1.1.6.4 Nef

Nef est une protéine de 27 kDa produite à partir de transcriptions virales précoces (133, 714). Nef joue un rôle important dans la pathogenèse du VIH-1 en favorisant la réplication et la propagation virales *in vivo* et en permettant l'évasion immunitaire des cellules infectées. Les patients infectés par le VIH-1 portant des gènes *nef* mutants ou défectueux présentent une progression de la maladie beaucoup plus lente (715-721). De même, les modèles de NHP et de souris humanisées infectés par un lentivirus n'exprimant pas Nef développent de faibles charges virales et ne développe pas le SIDA (722-725). De manière remarquable, l'expression de Nef induit à elle seule un syndrome semblable au SIDA chez des souris transgéniques, ce qui suggère un rôle direct de Nef dans la pathogenèse du VIH-1 (726-729). Nef est une protéine cytoplasmique dont l'extrémité N-terminale est myristoylée ce qui permet son association avec la membrane plasmique et son incorporation dans les virions (730-732). La topologie de Nef consiste en une région flexible en N-terminale servant de commutateur moléculaire, un noyau globulaire et une longue boucle flexible permettant la liaison aux complexes adaptateurs de clathrine AP-1 et AP-2, via un motif dileucine (^{160}EXXXLL^{165}) hautement conservé en C-terminale (733-736).

Tout comme Vpu, Nef interfère avec le trafic intracellulaire d'une multitude de protéines de l'hôte, ses principales fonctions étant la régulation négative de l'expression de surface du récepteur CD4 (737) et du complexe majeur d'histocompatibilité de classe I (CMH-I) (738). Contrairement à Vpu, Nef cible les molécules de CD4 déjà présentes à la surface des cellules

infectées et induit leur endocytose par les puits de clathrine en liant la queue cytoplasmique de CD4 et en recrutant le complexe AP-2 (736, 739-745). Le CD4 internalisé est ensuite redirigé vers les lysosomes pour être dégradé grâce à son transport rétrograde par les vésicules COPI (746, 747). La régulation négative de CD4 par Nef permet de prévenir la surinfection de la cellule, d'améliorer la relâche et l'infectivité des particules virales bourgeonnantes et d'évader la réponse anticorps non-neutralisante (748-759). D'une manière similaire à CD4, Nef entraîne également la régulation négative des facteurs de résistance SERINC3 et SERINC5 via le recrutement du complexe AP-2 afin d'améliorer l'infectivité virale (584, 585, 760, 761). Afin d'évader la réponse immunitaire à médiation cellulaire, Nef limite la présentation antigénique en modulant à la baisse les molécules classiques du CMH-I, soit HLA-A et HLA-B, afin de protéger les cellules infectées de la reconnaissance par les lymphocytes T $CD8^+$ cytotoxiques (CTL) (738, 762). Cette spécificité de Nef est dictée par la présence d'un résidu tyrosine dans la queue cytoplasmique des molécules du CMH-I, absent chez HLA-C, mais présent chez HLA-A, HLA-B, HLA-E et CD1d (763-767). Contrairement à CD4, Nef interfère avec le trafic intracellulaire des molécules du CMH-I nouvellement synthétisées via le recrutement du complexe AP-1 à l'aide son motif dileucine et le remodelage de son noyau globulaire afin d'accommoder la queue cytoplasmique du CMH-I (768-772). À l'instar de CD4, les molécules du CMH-I transitent par les vésicules COPI pour être finalement dégradées dans les lysosomes (738, 747). De plus, Nef module à la baisse l'expression de plusieurs molécules du CMH-I non-classiques telles que ULBP1, ULBP2 et MICA, qui agissent comme ligands du récepteur activateur NKG2D, afin de protéger les cellules infectées de l'élimination par les cellules NK (773, 774). En plus du récepteur CD4 et des molécules du CMH-I, les fonctions complémentaires de Nef et Vpu permettent de cibler plusieurs autres substrats de manière redondante, notamment CD28, CD62L, CD1d, PVR et les tétraspanines (693, 696, 704, 708, 764, 765). Nef semble également impliquer dans d'autres processus cellulaires incluant l'altération des voies de signalisation NFAT et NF-κB (543, 775-778), la répression de l'autophagie (779, 780) et la sécrétion de vésicules extracellulaires (781, 782).

1.1.7 Pathogénèse du VIH-1

La transmission du VIH-1 résulte d'un contact direct avec les fluides corporels d'une personne infectée, notamment le sang, les fluides vaginaux, les fluides pré-séminaux, le sperme, les fluides rectaux et le lait maternel. Les principales sources de transmission sont les rapports

sexuels non protégés et le virus est transmis par les voies génitales ou la muqueuse rectale. Les autres formes de transmission comprennent la transmission de la mère à l'enfant pendant la grossesse et l'allaitement, les transfusions sanguines et le partage d'aiguilles ou de seringues (783). Bien que l'inoculum lors de la transmission contienne un mélange de quasi-espèces de VIH-1 génétiquement diverses, l'initiation de l'infection commence généralement à partir d'un seul virus appelé « virus transmis fondateur » (T/F) (257). Ces virus T/F présentent généralement un tropisme CCR5, une infection préférentielle des lymphocytes T $CD4^+$, une infectivité et une capacité de réplication accrues, une résistance aux IFN-I et des glycoprotéines Env possédant des boucles variables plus courtes et moins de sites de N-glycosylation (257, 564, 784-794). Une fois l'infection établie, la manifestation clinique de l'infection par le VIH-1 non-traitée peut être décrite en trois grandes étapes : la phase aiguë, la phase chronique et la phase SIDA (**Figure 1.1.7**).

1.1.7.1 Phases de l'infection

La phase aiguë (également appelée primo-infection) dure quelques semaines après l'exposition au virus. La période initiale entre le moment où la première cellule est infectée et celui où le virus est détectable pour la première fois dans le sang est appelée la phase d'éclipse et dure environ 1 à 3 semaines (795-800). Pendant cette phase silencieuse, le virus se propage dans les lymphocytes T $CD4^+$ des muqueuses et des ganglions lymphatiques drainants (801). Une fois que la charge virale devient détectable dans le plasma sanguin, elle augmente de manière exponentielle pour atteindre plusieurs millions de copies par millilitre (mL) en raison de la réplication du virus dans les tissus lymphoïdes associés à l'intestin (GALT) et dans le sang périphérique, ce qui cause une déplétion significative des lymphocytes T $CD4^+$ dans ces tissus (802-809). L'infection primaire déclenche également la réponse immunitaire adaptative par la libération de cytokines pro-inflammatoires, ce qui permet un certain contrôle de la charge virale et la récupération partielle des niveaux de lymphocytes T $CD4^+$ en périphérie (810-812). L'apparition séquentielle de marqueurs viraux et immunitaires quantifiables dans le sang a permis l'établissement d'un système de classification des différents stades de l'infection aiguë appelés « stades Fiebig » (813). Suite à la détection de l'ARN viral (Fiebig I), on détecte séquentiellement l'apparition l'antigène de capside (Fiebig II) et d'anticorps spécifiques au VIH-1, appelée la séroconversion, détectable par ELISA (Fiebig III) ou par immunobuvardage de type Western (Fiebig IV, V et VI) (813). C'est pendant cette phase précoce que les réservoirs viraux sont rapidement établis (814-816).

L'infection progresse ensuite vers une phase chronique asymptomatique de durée variable (2 à 12 ans) qui se caractérise par une virémie plasmatique relativement stable et qui voit la population virale homogène entrer dans une phase de diversification (817, 818). Cela s'accompagne d'une perte d'intégrité de la muqueuse gastro-intestinale et de la translocation microbienne, ce qui contribue à l'induction d'une réponse inflammatoire persistante et d'une activation immunitaire chronique, qui sont associées à leur tour à la progression de la maladie et à la déplétion des lymphocytes T CD4+ infectés et non-infectés (819-822).

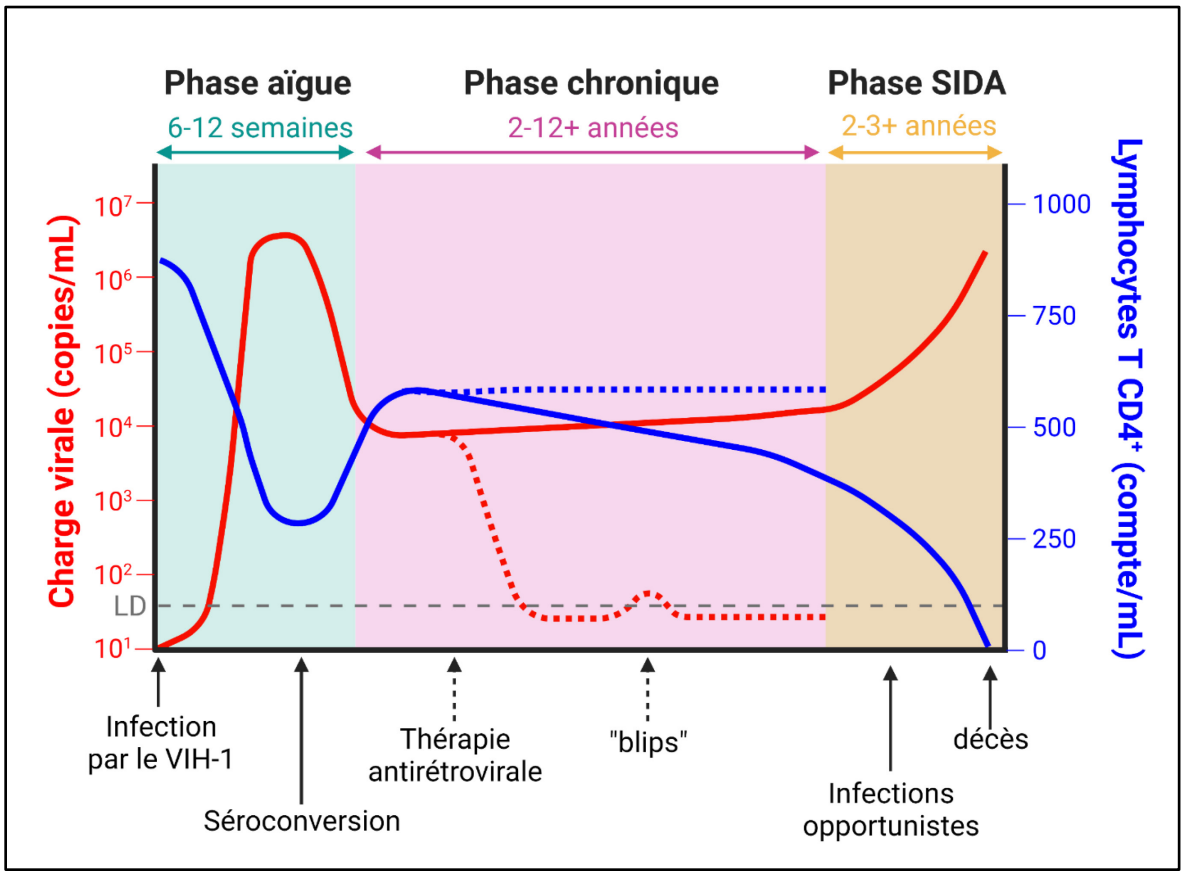

Figure 1.1.7 - Stades de l'infection par le VIH-1.
La manifestation clinique de l'infection typique par le VIH-1 peut être séparée en plusieurs phases : la phase aiguë où la virémie atteint son paroxysme et le nombre de lymphocytes T $CD4^+$ diminue de manière drastique, la phase chronique où la charge virale et les niveaux de lymphocytes T $CD4^+$ se stabilisent et la phase SIDA où l'individu subit une perte accélérée des lymphocytes T $CD4^+$ et une augmentation importante de la virémie, ce qui mène au décès à la suite d'infections opportunistes. La réponse immunitaire adaptative et la séroconversion arrivent vers de la fin de la phase aiguë et permet une certaine réduction de la virémie et la récupération de comptes de lymphocyte T $CD4^+$ plus élevés. L'utilisation de la thérapie antirétrovirale permet de garder des taux stables de lymphocytes $CD4^+$ et une virémie indétectable, malgré la présence de « blips » occasionnels (823). LD : limite de détection. Figure inspirée de (824). Diagramme créé avec BioRender.com.

Différents mécanismes ont été décrits pour expliquer la déplétion des lymphocytes T $CD4^+$, notamment les effets cytopathiques directs du virus via la formation de syncytia ou l'induction de l'apoptose, ou encore leur élimination par les cellules NK et les lymphocytes T $CD8^+$ cytotoxiques (825-827). Cependant, la déplétion des lymphocytes T $CD4^+$ ne se limite pas seulement aux cellules infectées et serait majoritairement due à l'élimination de cellules non-infectées (828). Plusieurs protéines virales dont la gp120 soluble peuvent être libérées dans la circulation et induire l'apoptose ou la pyroptose des cellules non-infectées en se liant aux récepteurs de surface ou par absorption intracellulaire (829-833). La liaison de la gp120 soluble au CD4 présent à la surface des lymphocytes T $CD4^+$ non-infectées permet également leur reconnaissance par les anticorps présents dans le sérum des personnes infectées, ce qui peut mener à leur élimination par les cellules effectrices du système immunitaire (834).

Au cours du dernier stade clinique de l'infection, le SIDA, le décès des personnes infectées est associé au développement de cancers et d'infections opportunistes en raison de l'effondrement du système immunitaire. Cliniquement, un individu infecté par le VIH-1 progresse vers la phase SIDA lorsque le nombre de lymphocytes T $CD4^+$ est inférieur à 200 cellules par microlitre (µL) et que la charge virale remonte, ce qui est habituellement dû à l'apparition de virus à tropisme CXCR4 (835-837). L'utilisation de la thérapie antirétrovirale permet de contrôler la charge virale à des niveaux indétectables et de stabiliser les comptes de lymphocytes T $CD4^+$ chez la majorité des individus infectés, freinant ainsi la progression vers la phase SIDA (838, 839). Un sous-ensemble représentant environ 5% des personnes infectées par le VIH-1, appelées « non-progresseur à long terme » (LTNP), est capable de maintenir des niveaux de lymphocytes T $CD4^+$ stables et une faible virémie plasmatique en absence d'ART (840). Il existe également une minorité d'individus infectés (moins de 1%), appelés contrôleurs élites, qui peuvent supprimer la virémie à des niveaux indétectables, préserver un taux élevé de lymphocytes T $CD4^+$, et passer des décennies sans traitement sans jamais évoluer vers la phase SIDA (841). Ce groupe de patients exceptionnels, somme toute très hétérogène, est actuellement à l'étude comme modèle de guérison fonctionnelle de l'infection par le VIH-1 (842-847).

1.1.7.2 Réservoirs

Bien que la déplétion sélective des lymphocytes T $CD4^+$ soit l'une des caractéristiques principales de l'infection par le VIH-1, certaines cellules infectées avec de l'ADN proviral intégré réussissent à survivre, et ce, même en présence d'ART (848). Plusieurs facteurs biologiques permettent la persistance de ces cellules qui forme le réservoir viral, soit leur localisation anatomique, leur susceptibilité à l'infection, leur durée de vie, leur état d'activation ainsi que la latence virale. Une cartographie détaillée de la distribution du VIH-1 dans l'organisme a permis de constater un enrichissement du virus dans les ganglions lymphatiques et de manière prédominante dans le GALT, bien que le virus puisse être détecté dans à peu près tous les organes du corps (849-854). Dans l'état d'inflammation chronique de l'infection par le VIH-1, des centres germinatifs se forment dans les follicules de lymphocytes B au sein des structures lymphoïdes afin de générer une réponse humorale (855). Ces structures contiennent des lymphocytes T $CD4^+$ folliculaires auxiliaires (T_{FH}) activés, hautement susceptibles à l'infection, mais excluent activement la présence de cellules effectrices, offrant ainsi au virus un sanctuaire immunitaire favorisant la réplication (851, 856-860). Les testicules et le cerveau comptent également parmi les sanctuaires immunitaires potentiels du VIH-1 (861, 862). En plus de l'absence de cellules effectrices, la pénétration sous-optimale des médicaments antiviraux dans ces mêmes tissus est un autre facteur pouvant contribuer à la persistance des réservoirs (863-865). Au niveau cellulaire, les réservoirs sont particulièrement enrichis chez les lymphocytes T $CD4^+$ mémoires à longue durée de vie qui sont retrouvés en circulation (T_{CM}, T_{TM}, T_{EM} et T_{SCM}) ou qui résident dans les tissus (T_{RM}), ces derniers dérivant majoritairement des lymphocytes Th17 présents dans la lamina propria de l'intestin (866-875). La susceptibilité accrue des lymphocytes Th17 est caractérisée par un certain niveau constant d'activation et d'un niveau élevé d'expression du corécepteur CCR5 et de l'intégrine $\alpha4\beta7$ (259, 876-886). En plus de la longue durée de vie des lymphocytes T mémoires, la persistance du réservoir est assurée par une expansion clonale massive et soutenue des cellules infectées via trois mécanismes principaux: l'intégration du provirus dans les gènes associés à la croissance cellulaire, la prolifération homéostatique et la prolifération induite par la spécificité antigénique du TCR (866, 887-895). En plus des cellules actives sur le plan réplicatif, il existe également un pool de cellules infectées de manière latente, comportant un provirus intégré intact, peu actif sur le plan transcriptionnel et ne produisant pas de virions infectieux, mais ayant la capacité de le faire après stimulation (848, 896-901). Le phénomène de latence est multifactoriel

et peut être affecté notamment par l'expression de molécules de point de contrôle immunitaire (PD-1, CTLA-4, LAG3, TIGIT, TIM-3) (851, 902-905), et par des modifications épigénétiques provoquant l'extinction transcriptionnelle de l'ADN proviral par le compactage de la chromatine (906-915).

Bien que le VIH-1 puisse infecter d'autres types cellulaires comme les macrophages, monocytes et cellules dendritiques, la présence d'un réservoir viral dans les cellules myéloïdes reste un sujet controversé et peu étudié comparativement aux lymphocytes T $CD4^+$. Malgré la présence de macrophages tissulaires à longue durée de vie, les présentes études suggèrent un apport minimal de ces cellules à la persistance virale (916-918). Au final, l'incapacité du système immunitaire et du traitement ART à éliminer le réservoir viral hétérogène reste un des problèmes majeurs à l'éradication du VIH-1 de l'organisme et nécessite l'élaboration de stratégies de guérison novatrices afin de résoudre ce casse-tête.

1.2 Réponses immunitaires contre l'infection par le VIH-1

La réponse immunitaire contre le VIH-1 consiste en une réponse innée qui est peu spécifique, mais qui sert de première ligne de défense protégeant l'hôte contre le virus, sans aucune exposition préalable. Ces premiers mécanismes antiviraux sont orchestrés en grande partie par les IFN-I, qui induisent un état antiviral chez les cellules cibles par l'induction de gènes codant pour des facteurs de restriction et de résistance au virus. Celle-ci est suivi de la réponse adaptative qui est hautement spécifique et implique le recrutement de cellules effectrices capable d'éliminer les cellules infectées directement grâce à la reconnaissance d'anomalies à la surface cellulaire (réponse à médiation cellulaire) ou par le biais d'anticorps capables de neutraliser le virus et de recruter les cellules effectrices exprimant les récepteurs Fc (réponse humorale). Le VIH-1 a développé plusieurs mécanismes moléculaires permettant d'échapper à ces différentes réponses immunitaires afin de se répliquer efficacement et persister dans l'organisme.

1.2.1 Réponses innées

Les infections virales sont détectées par des composantes du système immunitaire inné par l'intermédiaire de récepteurs de reconnaissance de motifs moléculaires (PRR) capables de reconnaître les motifs moléculaires associés aux agents pathogènes (PAMP). Parmi les PRR, on

compte notamment les récepteurs de type Toll (TLR), les récepteurs de type RIG-I (RLR), les senseurs d'ADN cytosolique (CDS), les lectines de type C (CLR) et les récepteurs de type NOD (NLR). L'activation de ces récepteurs déclenche des cascades de signalisation convergentes qui aboutissent à la relocalisation nucléaire de facteurs de transcription, stimulant un nouveau programme transcriptionnel qui mène à la libération de cytokines pro-inflammatoires, de chimiokines et d'interférons afin d'amorcer la réponse antivirale (919, 920). Dans l'infection par le VIH-1, les cellules dendritiques plasmacytoïdes (pDC) jouent un rôle prépondérant dans l'activation d'une réponse inflammatoire efficace grâce à l'expression constitutive d'une vaste gamme de PRR (921-928). Dépendamment du mode d'entrée virale, l'ARNv simple brin peut être détecté dans les endosomes par les TLR7 et TLR8, ce qui mène au recrutement de l'adaptateur MyD88 et à la translocation nucléaire de NF-κB et d'un homodimère d'IRF7 (929-937). La translocation microbienne induite par le VIH-1 contribue également à l'inflammation en activant des TLR de surface reconnaissant des produits bactériens comme les lipopolysaccharides (LPS) ou le peptidoglycane (938). La détection du génome viral peut également se faire via les senseurs présents dans le cytoplasme par la détection de l'ARNv simple brin par les RLR (RIG-I, MDA5) ou par la détection de l'ADNv double brin par les CDS (IFI16, cGAS) (939-944). La signalisation des RLR passe par l'adaptateur MAVS, présent sur les mitochondries, et mène à l'import nucléaire de NF-κB et d'un hétérodimère d'IRF3 et IRF7, tandis que la signalisation des CDS passe par STING et mène à l'import nucléaire de NF-κB et d'un homodimère d'IRF3 (945, 946).

Le VIH-1 est toutefois connu pour sa capacité à échapper à la détection du système immunitaire inné (947). En plus de la séquestration de RIG-I grâce à la protéase virale, la présence d'une coiffe, d'une queue polyadénylée et de sites de méthylation sur l'ARNv rend l'activation des RLR peu efficace (948-950). La stabilité remarquable de la capside virale joue également un rôle majeur pour protéger le génome viral des différents senseurs d'acides nucléiques durant la rétrotranscription et plus particulièrement les CDS (951-954). Le VIH-1 agit également en aval des cascades de signalisation des PRR en bloquant la translocation nucléaire des facteurs de transcription IRF3, IRF7 et NF-κB grâce à plusieurs mécanismes impliquant les protéines accessoires Vif, Vpr et Vpu (544, 610, 612, 955-958). En plus du génome viral, plusieurs protéines du VIH-1 peuvent agir en tant que PAMP, incluant Env et PR. La reconnaissance des N-glycans présents sur la gp120 par les récepteurs CLR a un rôle ambigu dans l'activation de l'immunité

innée puisque sa liaison à DC-SIGN stimule la voie NF-κB, tandis que la liaison à BDCA-2 inhibe la signalisation des TLR endosomaux (959-963). Une régulation adéquate de l'activité enzymatique de PR est également très importante puisque son activation prématurée peut être détectée par CARD8, une composante de l'inflammasome, menant ainsi à l'activation de la caspase-1 qui déclenche la relâche des cytokines pro-inflammatoires IL-1β et IL-18 et induit la mort cellulaire par pyroptose (964). Dans l'ensemble, le VIH-1 contrôle efficacement l'activation des différents PRR lors de l'infection productive, suggérant la présence d'infection abortive comme source plus plausible de la stimulation de l'immunité innée antivirale (965-967).

1.2.1.1 Réponse interféron

Les IFN-I forment une famille de cytokines pléiotropes, pro-inflammatoires et immunomodulatrices, qui induisent un état antiviral par la régulation positive de centaines d'ISGs. Le génome humain code pour 17 IFN-I différents, dont 13 types d'IFN-α, ainsi que l'IFN-β, l'IFN-ε, l'IFN-κ et l'IFN-ω (968, 969). En réponse aux infections virales, Les IFN-I sont rapidement sécrétés puis signalent de manière autocrine et paracrine en se liant au récepteur hétérodimérique de l'interféron-α/β (IFNAR) exprimé de manière ubiquitaire (970). L'engagement d'IFNAR active une voie de transduction intracellulaire de type JAK-STAT, qui débute par la phosphorylation des tyrosine kinases JAK1 et TYK2, ce qui permettra l'import nucléaire d'un complexe phosphorylé formé par STAT1, STAT2 et IRF9 (971, 972) et l'induction d'un profil transcriptionnel antiviral caractérisé par l'expression des différents facteurs de restriction (APOBEC3s, TRIM5α, SAMHD1, BST-2) et de plusieurs facteurs de résistance (IFITMs, MX2, GBP2/5, ZAP, SLFN11) (973). Par contre, les protéines accessoires du VIH-1 sont capables d'interférer avec la signalisation d'IFNAR en induisant la dégradation de STAT1 par le protéasome ou en inhibant sa phosphorylation (611, 974). Bien que tous les sous-types d'IFN-I se lient au même récepteur, ils diffèrent dans leur affinité pour l'IFNAR et déclenchent différents schémas d'expression des ISGs, ce qui suggère qu'ils varient dans leur activité et leur puissance *in vivo* (975-978). En effet, l'IFN-β et l'IFN-α14 semblent être les sous-types ayant le plus grand potentiel antiviral tant *in vitro* qu'*in vivo* (979-984).

Des études dans des modèles *in vivo* ont démontré l'importance des IFN-I pour limiter la transmission du VIH-1 et pour contrôler la phase aiguë de l'infection par le VIH-1 en limitant la

charge virale, l'établissement du réservoir et l'évolution de la maladie (985-990). Cependant, une réponse soutenue à l'IFN-I est préjudiciable, car elle contribue à augmenter l'inflammation systémique chronique et la diminution des comptes de lymphocytes T $CD4^+$ (990-992). La déplétion des pDCs productrices d'IFN-I chez les patients infectés a été corrélée avec une augmentation de la charge virale, tandis que les niveaux élevés de pDCs retrouvés chez les contrôleurs élites contribuent au contrôle de la réplication du VIH-1 (993-995). Certaines études cliniques ont évalué les avantages thérapeutiques de l'administration d'IFN-I à des individus infectés par le VIH-1 sous traitement ART. Lors d'interruptions planifiées du traitement antirétroviral, l'administration d'IFN-α2 a permis de prolonger le contrôle viral, d'atténuer le rebond de la virémie et de diminuer la taille du réservoir (996-1002). Afin de mieux comprendre la pression exercée par l'IFN-I *in vivo*, des études récentes ont évalué la sensibilité du virus circulant à l'IFN-α2 et l'IFN-β lors de différentes phases de l'infection. Ces études ont montré que les virus T/F sont hautement résistants à l'IFN-I et que cette résistance constitue un déterminant majeur de l'aptitude à la transmission du VIH-1 et de la réplication lors de la phase aiguë de l'infection (564, 789, 790, 792, 1003). En revanche, les virus isolés au cours de la phase chronique deviennent généralement sensibles à l'IFN-I, mais cette sensibilité est perdue lors de la progression vers la phase SIDA (792, 1003-1005). Parallèlement, le virus présent lors du traitement suppressif par ART est relativement sensible à l'IFN-I, tandis que l'interruption du traitement donne lieu à une recrudescence de virus à très haut degré de résistance à l'IFN-I (1003). Somme toute, la résistance à la réponse interféron semble donner un avantage sélectif aux quasi-espèces pendant les phases exponentielles de réplication, soit lors de la transmission ou du rebond viral post-traitement.

1.2.2 Réponses à médiation cellulaire

Lors de la phase aiguë de l'infection par le VIH-1, deux types cellulaires sont principalement responsables du contrôle initial de la virémie grâce à leur capacité à éliminer les cellules infectées par une réponse cytotoxique directe : les lymphocytes T $CD8^+$ appartenant à l'immunité adaptative et les cellules NK appartenant à l'immunité innée.

1.2.2.1 Lymphocytes T CD8$^+$

Une réponse antivirale robuste par les lymphocytes T CD8+ cytotoxiques (CTL) est mise en place au cours de la phase précoce de l'infection par le VIH-1 et est responsable en grande partie de la diminution de la charge virale initiale (825, 1006-1008). La réponse CTL est initialement dirigée contre un nombre restreint d'épitopes linéaires présents dans les protéines Env et Nef de la souche T/F qui sont présentés au TCR par le CMH-I à la surface des cellules infectées (1009-1011). Cette pression immunitaire force une sélection rapide de mutations non-synonymes dans les épitopes ciblés permettant d'échapper à la reconnaissance par les CTL (1009, 1012, 1013). La magnitude de la réponse précoce des CTL spécifiques au VIH-1 influence les niveaux auxquels la charge virale se stabilise pendant la phase chronique, un déterminant important de la progression de la maladie (1014, 1015). Pendant la phase chronique de l'infection, la réponse CTL se diversifient et ciblent d'autres antigènes viraux, dont Gag (1016-1020). Le contrôle de la virémie par les CTL est hautement dépendant des variations alléliques du CMH-I présentes chez l'individu infecté et le développement d'un statut de contrôleur élite est plus souvent lié à l'expression des allèles HLA-B*57 et HLA-B*27 (1021-1025). Ces deux allèles sont capables de présenter des épitopes conservés de la capside virale importants pour la liaison à CypA et l'introduction de mutations échappatoires dans ces épitopes diminue grandement la capacité du virus à se répliquer et augmente la restriction par TRIM5α (1026-1031). En outre, les lymphocytes T CD8+ spécifiques au VIH-1 possédant des capacités cytotoxiques, prolifératives et polyfonctionnelles ont été corrélées avec un meilleur contrôle de la virémie et des réservoirs pendant la phase chronique ou sous traitement ART (1032-1040). En plus des fonctions cytolytiques, les lymphocytes T CD8$^+$ peuvent utiliser des mécanismes antiviraux non-lytiques faisant intervenir des molécules solubles, telles que les chimiokines MIP-1α, MIP-1β et RANTES, pouvant se lier au récepteur CCR5 et limiter l'infection par le VIH-1 en diminuant les niveaux de surface du récepteur ou compétitionner pour la liaison d'Env à son corécepteur principal (1041, 1042). Cependant, le VIH-1 réussit à échapper à la réponse des lymphocytes T CD8$^+$ malgré l'étendue de leurs activités antivirales. Les facteurs contribuant à cette évasion immunitaire comprennent la modulation à la baisse des molécules classiques du CMH-I par Nef et Vpu (711, 712, 738, 762, 763), l'inaccessibilité des CTL à certains sites anatomiques de réplication virale comme les centres germinatifs (856, 859, 1043-1045) et l'épuisement immunitaire causée par la persistance antigénique et l'inflammation chronique (905, 1046-1049).

1.2.2.2 Cellules NK

Les cellules NK sont un sous-ensemble de lymphocytes de l'immunité innée, capables, lorsqu'elles sont matures et éduquées, de répondre rapidement à la présence d'une infection sans qu'une exposition préalable à un antigène soit nécessaire. Elles exercent des fonctions effectrices et immunorégulatrices s'apparentant à celles des lymphocytes T $CD8^+$ dans la réponse précoce aux infections virales (1050). Elles peuvent être divisées en deux sous-populations principales basées sur le niveau d'expression du marqueur CD56: les cellules NK $CD56^{haut}$, située dans les organes lymphoïdes secondaires, produisant des cytokines (IFN-γ, TNF-α) et les chimiokines pro-inflammatoires (MIP-1α, MIP-1β, RANTES) (1051, 1052), et les cellules NK $CD56^{bas}$, plus nombreuses en circulation, ayant un plus grand potentiel cytolytique (1053, 1054). Les cellules $CD56^{bas}$ cytotoxiques sont caractérisées par expression de la molécule CD16, un récepteur activateur de faible affinité pour la région constante Fc des anticorps de type IgG, ce qui leur permet d'avoir une activité de cytotoxicité cellulaire dépendante des anticorps (ADCC) (1055). Ces cellules NK effectrices comportent des granules cytolytiques, composées notamment de perforines et de granzymes, dont le contenu sera relargué dans la synapse immunologique lors de la reconnaissance de ligands de récepteurs activateurs ou d'anticorps opsonisés à la surface d'une cellule infectée (1056). La perforine s'insère dans la membrane cible et s'assemble sous forme de pores permettant le passage vers le cytoplasme des granzymes, des sérine protéases capables d'induire l'apoptose de la cellule via l'activation de la voie des caspases (1057). L'activité des cellules NK est modulée par une série de cytokines incluant les IFN-I, les cytokines γc comme l'IL-2, l'IL-15 et l'IL-21 ainsi que l'IL-12 et l'IL-18 (1058-1060). L'IL-15 joue un rôle particulièrement important puisqu'elle régule la génération, la différentiation et la survie des cellules NK, en plus d'augmenter ses capacités d'activation, de cytotoxicité et d'immunorégulation (1061-1064).

Le déclenchement de la dégranulation des cellules NK au contact des cellules cibles est contrôlé par l'équilibre des signaux reçus par les récepteurs activateurs et inhibiteurs présents à leur surface (**Figure 1.1.8**). De façon générale, les récepteurs activateurs s'associent avec des protéines adaptatrices intracellulaires possédant un motif d'activation de type ITAM comme DAP12, CD3ζ et FcεRIγ (1065-1067), tandis que les récepteurs inhibiteurs possèdent un ou plusieurs motifs d'inhibition de type ITIM dans leur queue cytoplasmique (1068). Lors de

l'engagement de ces récepteurs, les motifs ITAM permettent le recrutement de tyrosine kinases déclenchant des voies de signalisation menant à la dégranulation (1069), tandis que les motifs ITIM recrutent des phosphatases qui répriment les cascades de phosphorylation nécessaires à l'activation des fonctions effectrices (1070). Les principaux signaux inhibiteurs des cellules NK proviennent des récepteurs KIR à longue queue cytoplasmique qui reconnaissent les molécules classiques du CMH-I (HLA-A, HLA-B, HLA-C), et du récepteur hétérodimérique CD94-NKG2A reconnaissant HLA-E, une molécule non-classique du CMH-I présentant le peptide signal clivé à partir des molécules HLA-A/B/C (1071, 1072). Certains récepteurs activateurs comme les récepteurs KIR à courte queue cytoplasmique et le complexe CD94-NKG2C partagent une spécificité commune avec les récepteurs inhibiteurs pour la liaison des molécules du CMH-I, mais leurs interactions sont de moindre affinité (1073, 1074). De façon similaire, le récepteur activateur DNAM-1 partage la liaison du ligand de stress PVR avec la molécule de point de contrôle immunitaire TIGIT dans un système favorisant l'interaction PVR-TIGIT (1075-1077). Parmi les récepteurs activateurs principaux, on retrouve le récepteur homodimérique NKG2D qui s'associe à la protéine adaptatrice DAP10 et qui reconnaît une variété de molécules du CMH-I non-classiques, incluant les ULBP1-6, MICA et MICB, exprimées en réponse à certains stress cellulaires (1078). Les récepteurs naturels de cytotoxicité (NCR) tels que NKp30, NKp44 et NKp46 sont des récepteurs activateurs dont les ligands sont méconnus (1079). Il a été suggéré que NKp30 se lie à la molécule de stress B7-H6 (1080), tandis que NKp44 se lie à certaines molécules du CMH-II, plus particulièrement des allèles de HLA-DP capables de présenter des peptides endogènes (1081, 1082). Le facteur P de la voie alterne du complément (aussi appelé properdine) a récemment été montré comme étant un ligand du récepteur NKp46 (1083). Il a été suggéré que le facteur P puisse agir en tant que PRR étant donné sa capacité à interagir avec de nombreuses protéines virales, bactériennes et parasitaires (1084). Les cellules NK expriment également les récepteurs de la famille SLAM incluant NTB-A et 2B4, dont les ligands respectifs sont NTB-A et CD48 (1085, 1086). Ces récepteurs coactivateurs ne peuvent induire la dégranulation seuls, toutefois leur stimulation conjointe avec les différents récepteurs activateurs montre un effet synergique permettant une activation plus efficace des cellules NK (1087).

Comme le VIH-1 affecte l'expression de surface du CMH-I afin d'évader la réponse CTL, cela cause un débalancement de la réponse NK puisque la perte des signaux inhibiteurs favorise

leur activation (1088). De surcroît, l'expression de surface de la majorité des ligands des récepteurs activateurs est induite par l'infection par le VIH-1, notamment par l'activation de la voie des dommages à l'ADN par Vpr et par l'activation de la voie de stress du RE, potentiellement causée

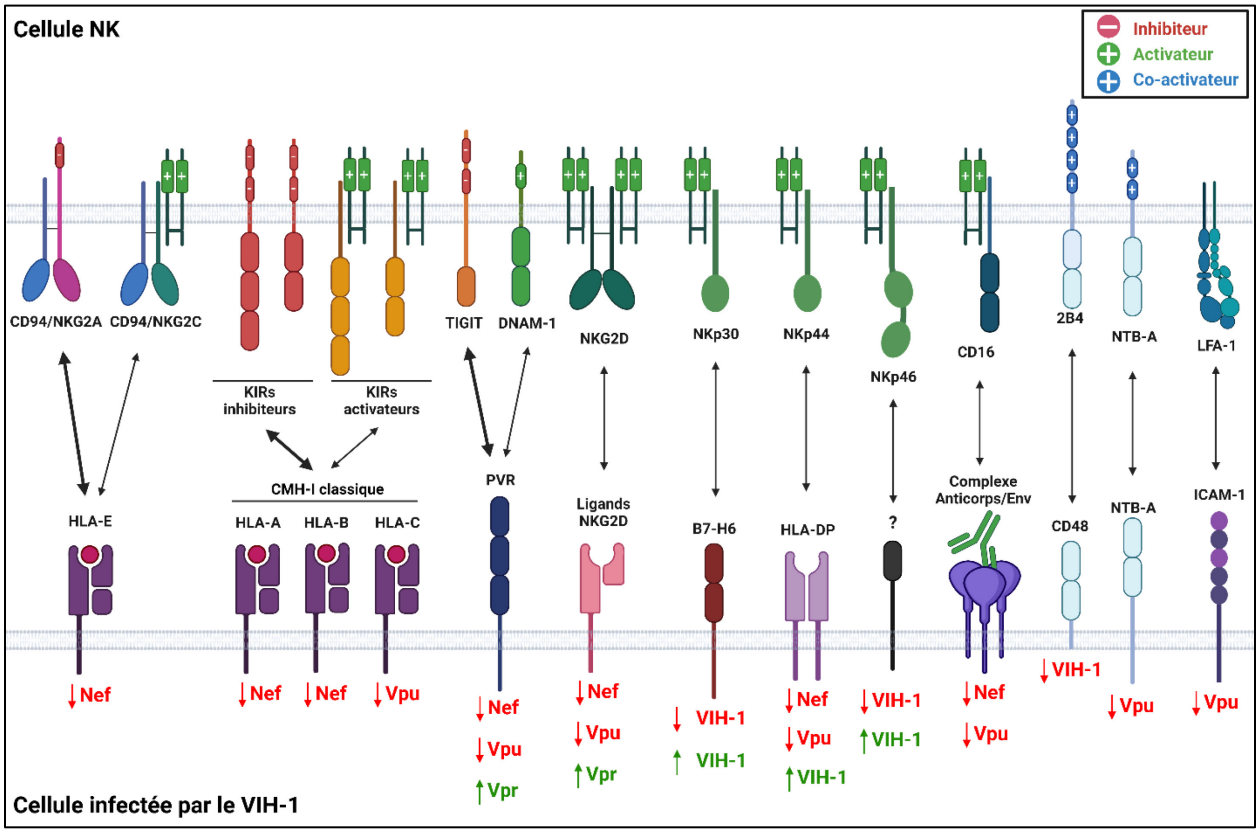

Figure 1.1.8 - Les récepteurs des cellules NK et la modulation de leurs ligands par le VIH-1 et ses protéines accessoires.

Les fonctions effectrices des cellules NK sont régulées par une balance de signaux provenant de récepteurs activateurs et inhibiteurs. Les récepteurs inhibiteurs de type KIR et CD94-NKG2A reconnaissent des molécules du CMH-I (HLA-A, HLA-B, HLA-C, HLA-E) qui peuvent également être reconnues par des récepteurs activateurs de moindre affinité, les KIRs activateurs et CD94-NKG2C, respectivement. Les récepteurs activateurs (NKG2D, DNAM-1, NKp30, NK44, NKp46) reconnaissent principalement des molécules de surface induites par l'infection virale (ULBPs, MICA/B, PVR, B7-H6, HLA-DP) via un stress cellulaire qui peut dépendre de la protéine accessoire Vpr ou des anticorps liés à un antigène viral (Env) dans le cas du récepteur Fc CD16. Le récepteur inhibiteur TIGIT lie également PVR et compétitionne avec DNAM-1 par son affinité supérieure. Les récepteurs de type SLAM (NTB-A, 2B4) servent de récepteurs coactivateurs grâce à leur synergie avec les différents récepteurs activateurs. L'intégrine LFA-1 favorise la formation de la synapse immunologique et la polarisation de la cellule NK en interagissant avec ICAM-1. Le VIH-1 est capable de réguler négativement la quasi-totalité des ligands de cellules NK, autant activateurs qu'inhibiteurs, via les protéines accessoires Nef et Vpu. Figure inspirée de (1089). Diagramme créé avec BioRender.com.

par des protéines d'Env mal repliées (634-636, 1090-1093). Étant donné que la somme de ces effets sur la balance des signaux est défavorable pour la survie de la cellule infectée, le VIH-1 a développé de nombreuses stratégies pour évader la réponse NK. Les protéines accessoires Nef et Vpu agissent de manière redondante afin d'altérer le trafic vers la surface cellulaire de PVR, des ligands de NKG2D et des molécules matures du CMH-II incluant HLA-DP (708, 773, 1094-1097). L'expression de surface des ligands des récepteurs activateurs NKp30 et NKp46 ainsi que des récepteurs coactivateurs 2B4 et NTB-A est également connue pour être supprimée lors de l'infection par le VIH-1 (699, 707, 1098). La réponse anticorps chez les individus infectés, principalement dirigée contre Env, est peu efficace pour reconnaître les cellules infectées, notamment à cause de l'endocytose constitutive d'Env et du ciblage de CD4 et BST-2 par Nef et Vpu, ce qui ne permet pas la formation d'une quantité suffisante de complexes immuns pour activer CD16 (756, 1099-1102). En plus de limiter l'activation de la cellule NK, le VIH-1 altère la formation de la synapse immunologique et la polarisation des granules lytiques par LFA-1 en modulant à la baisse les niveaux de surface de la molécule d'adhésion ICAM-1 (1103, 1104). Dans l'ensemble, le VIH-1 réussit à atténuer la réponse NK en rétablissant une balance des signaux lui étant favorable.

Lors de la phase aiguë de l'infection par le VIH-1, les cellules NK jouent un rôle critique dans l'établissement de la réponse immunitaire. La production massive d'IFN-I et d'IL-15 en réponse à l'infection permet l'activation et l'expansion rapide des cellules NK cytotoxiques avant l'établissement de la réponse adaptative médiée par les lymphocytes T $CD8^+$ et les anticorps (986, 1105, 1106). Les cellules NK contribuent au contrôle initial de la virémie grâce à leur activité cytolytique, mais également en stimulant la réponse CTL par la sécrétion d'IFN-γ, et en relâchant les différentes chimiokines liant CCR5 (1105, 1107, 1108). Le contrôle de la charge virale est associé à l'expression du récepteur de chimiokine CXCR5 par les cellules NK, leur permettant de migrer vers les follicules B dans les ganglions lymphatiques, où se trouvent des cellules T_{FH} infectées (1109-1111). La combinaison des récepteurs KIR et des allèles du CMH-I exprimés chez les individus infectés semble également jouer un rôle important dans le contrôle de l'infection. En effet, la co-expression du récepteur activateur KIR3DS1 et de certains allèles HLA-B chez les individus infectés corrèle avec de meilleures fonctions effectrices et une progression plus lente vers la phase SIDA (1112, 1113). L'expression homozygote du KIR3DS1 est également enrichie

chez les personnes séronégatives hautement exposées au VIH-1, qui possède une résistance naturelle à l'infection (1114, 1115). La progression vers la phase chronique de l'infection chez les individus virémiques est généralement associée avec la dysfonction des cellules NK caractérisée par une perte de leurs activités cytolytiques et immunorégulatrices (1116-1118). Ceci est notamment lié à la diminution de l'expression de nombreux récepteurs activateurs tels que NKG2D, NKp30, NKp44 et NKp46 (1119-1124). Cependant, le traitement ART semble permettre un rétablissement de l'expression de ces récepteurs et de restaurer les fonctions effectrices des cellules NK (1120, 1123).

1.2.3 Réponses humorales

Comme le trimère d'Env du VIH-1 est le seul antigène viral exposé à la surface des particules virales et des cellules infectées, il représente la cible principale de la réponse humorale via la génération d'anticorps neutralisants et non-neutralisants par les lymphocytes B. Au courant de l'infection par le VIH-1, les anticorps spécifiques pour Env sont détectables dès la phase aiguë, environ deux ou trois semaines suivant l'infection (1125). La réponse anticorps initiale est constituée d'immunoglobulines (Ig)M dirigées contre la gp41 des souches T/F (1125). Au cours des semaines suivantes, on peut détecter des réponses de type IgG et IgA dans le sang et les muqueuses grâce à la commutation de classe (1125), et un élargissement dans la spécificité des épitopes reconnus notamment contre l'extrémité de la boucle V3 et la passerelle en feuillet β (*bridging sheet*) de la gp120, deux composantes importantes pour l'interaction avec le corécepteur (1126-1128). Cependant, ces épitopes immunodominants ne sont pas exposés dans la conformation pré-fusion d'Env, appelée conformation « fermée », et donc génèrent des anticorps non-neutralisants (nnAbs) n'ayant aucun impact détectable sur la charge virale (1125). Des anticorps neutralisants ciblant uniquement la souche T/F autologue sont détectables dans les premiers mois après l'infection et reconnaissent principalement les régions variables V1/V2 et V3 d'Env, mais ceux-ci conduisent à la sélection de mutations échappatoires (1129-1138). Comme les souches T/F ont généralement moins de sites de N-glycosylation, cela génère des brèches dans le bouclier de glycans d'Env qui sont très immunogéniques et propices à la génération d'anticorps neutralisants autologues (aNAbs) (786, 793, 1139, 1140). Un processus de coévolution entre le virus et l'hôte est enclenché après la réponse anticorps initiale. Pendant la phase chronique, la sélection répétée de mutations échappatoires chez le virus augmente de plus en plus la maturation des anticorps afin

de s'adapter aux changements dans les épitopes reconnus par les NAbs (1141-1146). Chez moins de 10% des d'individus infectés de façon chronique, des anticorps neutralisants à large spectre (bNAbs) qui ciblent des épitopes conservés dans plusieurs souches peuvent être produits lors d'une exposition virale prolongée (1147, 1148).

1.2.3.1 Structure des IgG

Les anticorps de type IgG spécifiques au VIH-1 représentent la population isotypique majoritaire des anticorps présents en circulation suite à l'infection et peuvent exercer une multitude de fonctions antivirales incluant la neutralisation des virions et l'élimination des cellules infectées en recrutant des cellules effectrices du système immunitaire (1149). Les IgG sont composées de deux chaînes légères (κ ou λ) et deux chaînes lourdes (γ) qui sont liées entre elles de manière symétrique par des ponts disulfures pour former deux domaines fonctionnels : le fragment de liaison à l'antigène (Fab) et le fragment cristallisable (Fc) (**Figure 1.1.9**). Le fragment Fab contient notamment de régions hautement variables à son extrémité qui peuvent être mutées génétiquement par un processus d'hypermutation somatique (1150). Chacun des domaines variables des chaînes lourdes et légères est composé de trois régions déterminant la complémentarité (CDR), qui forment ensemble le paratope, et qui interagissent avec un antigène via un épitope spécifique (1151). Ce fragment est le déterminant majeur de la capacité neutralisante d'un anticorps. Le fragment Fc des IgG, formé par les domaines C_H2 et C_H3 de la chaîne lourde, est constitué d'une séquence et d'une structure conservées déterminant les fonctionnalités effectrices de l'anticorps et peut être catégorisé en quatre sous-classes isotypiques (IgG1, IgG2, IgG3, IgG4) (1152). Ce fragment possède des domaines structuraux lui permettant d'interagir avec la molécule C1q pour déclencher la cascade du complément (1153) et avec les récepteurs Fc des IgG (FcγRs) pour recruter des cellules effectrices de l'immunité innée (1154). Le site de liaison aux FcγRs comporte notamment la présence d'un glycan (N297) à l'interface des domaines C_H2 (1155). Un troisième site chevauchant les domaines C_H2 et C_H3 permet de prolonger la demi-vie des anticorps par sa liaison au récepteur Fc néonatal (FcRn), présent principalement dans le système endosomal de plusieurs types cellulaires, en empêchant leur dégradation par les lysosomes, ce qui permet le recyclage des IgG vers la circulation (1156, 1157). Les fragments Fab et Fc sont reliés par une région charnière qui assure une flexibilité moléculaire permettant la liaison bivalente des portions Fab et l'accessibilité de la portion Fc pour ses récepteurs (1158, 1159).

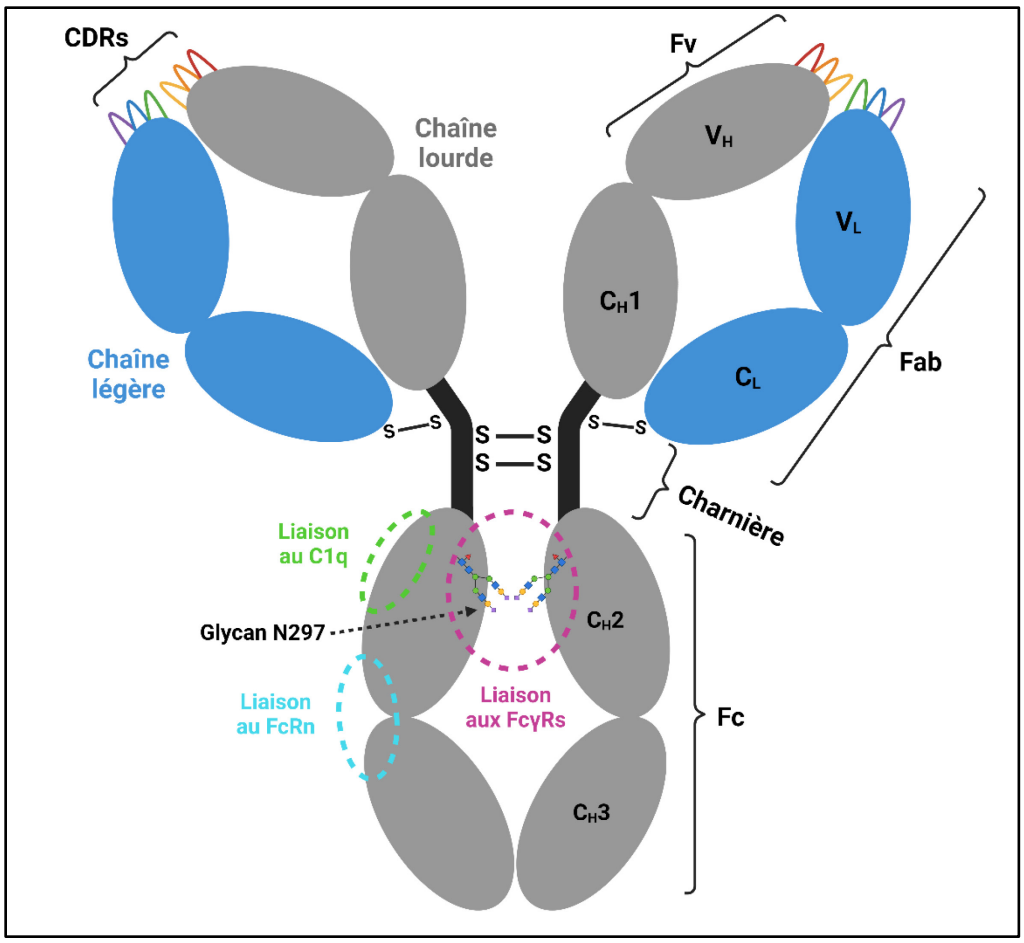

Figure 1.1.9 - Structure des anticorps de type IgG1.
Une molécule d'IgG1 possède un poids moléculaire de 150 kDa et est composée de deux chaînes lourdes (H) identiques de 50 kDa, et de deux chaînes légères (L) identiques de 25 kDa, qui sont reliées par des ponts disulfures (S—S). La portion Fab permet la liaison à un antigène via les régions déterminant la complémentarité (CDRs) situées dans le fragment variable (Fv) des chaînes lourdes et légères (V_H et V_L). La portion Fc est formée de régions constantes (C_H2 et C_H3) et sert d'adaptateur capable de recruter les cellules effectrices par la liaison aux récepteurs Fc des IgG (FcγRs) et le système du complément par la liaison au C1q. Le glycan N297 se situe à l'interface avec les FcγRs et contribuent à leur interaction. Un troisième site permet le recyclage et la transcytose des IgG par la liaison au FcRn. La portion charnière assure une certaine flexibilité permettant la liaison bivalente des portions Fab et l'accessibilité de la portion Fc pour ses récepteurs. Diagramme créé avec BioRender.com.

1.2.3.2 Anticorps neutralisants et non-neutralisants

La caractérisation d'un vaste panel de souches d'Env du VIH-1 provenant de différents clades, localisations géographiques et stades de l'infection a permis de démontrer que les isolats du VIH-1 présentent un spectre de sensibilité à la neutralisation par le plasma d'individus infectés

par le VIH-1 (plasma VIH$^+$) qui peut être classé en trois niveaux (tiers) distincts (1160, 1161). Le tiers 1, le plus sensible à la neutralisation, représente une fraction très mineure des souches en circulation et est particulièrement enrichi en isolats adaptés en laboratoire et en souches à tropisme X4. Le tiers 2, modérément sensible à la neutralisation, et le tiers 3, le plus résistant à la neutralisation, englobent la majorité des souches en circulation incluant les souches T/F. La conformation adoptée par Env semble être le facteur déterminant pour dicter la résistance à la neutralisation puisque les souches d'Env du tiers 1 présentent une propension à adopter la conformation « ouverte » d'Env, tandis que les souches d'Env des tiers 2 et 3 sont stabilisées dans la conformation « fermée » (217, 1162).

Les bNAbs générés contre le VIH-1 ciblent des épitopes relativement conservés sur le trimère d'Env pré-fusion et possèdent des capacités neutralisantes contre des souches virales hétérologues de tiers 2 et 3 (**Figure 1.1.10**). Ils bloquent donc l'entrée du virus en empêchant soit la liaison au récepteur CD4, soit les changements de conformation d'Env nécessaire à la fusion (217, 1163-1165). Les bNAbs peuvent être classés en fonction des épitopes distincts qu'ils ciblent sur le trimère d'Env : le site de liaison à CD4 (CD4BS) (1166-1171), la boucle V2 situé à l'apex du trimère (V2 apex) (1143, 1172-1174), les glycans à la base de la boucle V3 (V3 glycan) (1173, 1175, 1176), la façade silencieuse (1177, 1178), l'interface entre la gp120 et la gp41 (1179-1182), et la région externe proximale à la membrane (MPER) de la gp41 (1183-1186). Deux nouvelles classes de bNAbs récemment identifiées reconnaissent le corridor V2/V5 et la couronne de la boucle V3 (1187, 1188). Comme les bNAbs reconnaissent principalement la forme « fermée » d'Env, leurs épitopes se trouvent généralement dans les régions variables, ou à proximité, et comportent la présence d'un ou de plusieurs glycans (1189, 1190). Afin d'accommoder ces contraintes, la majorité des bNAbs possèdent une ou plusieurs particularités inhabituelles expliquant leur rareté. Ceux-ci incluent des niveaux très élevés d'hypermutation somatique dus à de multiples cycles de maturation de l'affinité, des CDR3 de la chaîne lourde exceptionnellement longues et la présence de polyréactivité ou d'autoréactivité (1191). Les bNAbs isolés jusqu'à présent se présentent généralement sous forme d'IgG chez des individus virémiques, mais plusieurs études récentes ont permis l'identification de bNAbs chez des individus contrôlant leur charge virale, notamment sous forme d'IgA (1176, 1188, 1192-1194). L'anticorps 2G12 est un cas particulier puisque son épitope est composé exclusivement de glycans et qu'il définit une catégorie

d'anticorps naturels dont les deux portions Fab s'assemblent sous forme d'un dimère formant un paratope unique pouvant reconnaître des glycans du non-soi (1195-1197).

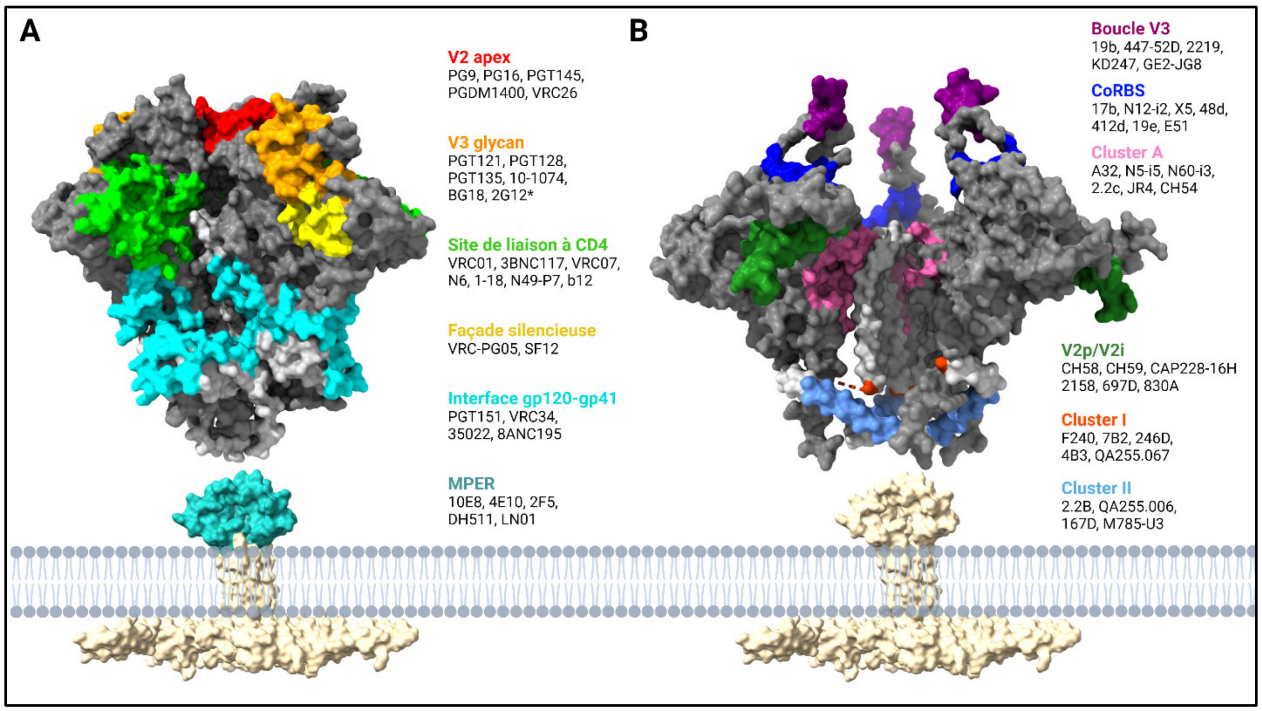

Figure 1.1.10 - Les épitopes d'Env reconnus par les bNAbs et les nnAbs
(**A**) Le trimère d'Env pré-fusion assume une conformation dite « fermée » qui est reconnue préférentiellement par les bNAbs et (**B**) la liaison à CD4 permet l'adoption de la conformation dite « ouverte » est reconnue préférentiellement par les nnAbs. Les épitopes reconnus par les différentes classes de bNAbs et nnAbs sont indiqués par un code de couleur et chaque classe est accompagnée d'une liste des anticorps prototypiques lui appartenant. L'épitope du cluster A définit par l'anticorps C11 n'est pas indiqué puisqu'il n'est pas formé dans la structure d'Env « ouverte » représentée ici. (**A-B**) Les représentations structurelles ont été générées à l'aide du logiciel ChimeraX v1.3 à partir de structures disponibles dans la base de données RCSB PDB. La structure d'Env liée à PG16 (PDB 6ULC) et un modèle de la structure d'Env liée à CD4 et 17b (PDB 3J70) servent de canevas de référence pour les conformations fermée et ouverte, respectivement. Les densités associées aux anticorps et au CD4 ont été enlevées pour une question de clarté. La sous-unité gp120 est illustrée en gris foncé et l'ectodomaine de la gp41 est illustré en gris pâle. La structure du domaine transmembranaire de la gp41 flanqué du MPER et de la queue cytoplasmique (PDB 7LOI) est illustrée en beige. *L'épitope de 2G12 inclut seulement des glycans. Diagramme créé avec BioRender.com.

Les études sur des modèles animaux ont permis de démontrer que l'administration prophylactique de bNAbs protégeait contre l'acquisition de l'infection et que leur utilisation thérapeutique permettait de supprimer la charge virale à des niveaux indétectables (1171, 1176, 1178, 1198-1206). Des anticorps ciblant le CD4BS (VRC01, 3BNC117, VRC07-523, N6), la

région V3 glycan (10-1074, PGT121) ainsi que la région V2 apex (PGDM1400) sont actuellement à l'étude dans de multiples essais cliniques chez l'humain en tant qu'agents thérapeutiques pour contrôler la virémie et éliminer les réservoirs viraux (ClinicalTrials.gov : NCT03837756, NCT02664415, NCT04871113, NCT04983030). Des études portant sur l'administration de bNAbs à des participants infectés ont montré une diminution rapide et un contrôle transitoire de la charge virale plasmatique, mais l'apparition de mutations échappatoires a rendu les bNAbs inefficaces (1207-1211). Pour remédier à ce problème, l'utilisation de combinaisons de bNAbs de plusieurs spécificités différentes est dorénavant privilégiée et permet un contrôle du rebond viral sur une période prolongée après l'interruption du traitement (1212-1214). Comme le déclin des niveaux de bNAbs dans l'organisme est un facteur limitant, les plus récentes études ont mis à l'essai des bNAbs dont la portion Fc est modifiée pour augmenter la demi-vie de l'anticorps via des mutations augmentant l'affinité pour le FcRn (ClinicalTrials.gov : NCT03554408, NCT05079451, NCT04811040, NCT04319367, NCT04212091, NCT03565315).

Au cours de l'infection naturelle, la majorité des anticorps ciblent la conformation « ouverte » d'Env, et présentent donc une activité neutralisante faible ou nulle contre les souches primaires du VIH-1 (1215, 1216). Les épitopes de ces anticorps non-neutralisants sont dissimulés dans la conformation « fermée » du trimère d'Env et nécessitent l'interaction d'Env avec son récepteur CD4 afin de déclencher les changements de conformation nécessaire à l'exposition de ces épitopes dits induits par CD4 (CD4i) (216, 220, 221, 1217, 1218). Or, lors de l'infection productive, les protéines accessoires Nef et Vpu se chargent de réguler négativement l'expression de CD4 à la surface des cellules et dans les compartiments intracellulaires afin de prévenir son interaction avec Env et ainsi exposer les épitopes CD4i facilement reconnus par le plasma VIH^+ (756, 757). Parmi les nnAbs les plus communs dirigés contre la gp120 (**Figure 1.1.10**), on note les nnAbs reconnaissant l'extrémité de la boucle V3 (1219-1221), un épitope polymorphique de la boucle V2 (V2p/V2i) (1222-1224), la passerelle en feuillet β du site de liaison au corécepteur (CoRBS) (219, 223, 1225-1227), le domaine interne de la gp120 (Cluster A) (1228-1232). Contrairement aux deux autres classes, les anticorps contre le CoRBS et le cluster A reconnaissent des épitopes situés dans les régions constantes qui sont particulièrement conservés à travers les différents isolats du VIH-1 (1233). Du côté de la gp41, les nnAbs reconnaissent principalement l'épitope du cluster I, situé dans la boucle disulfure entre HR1 et HR2 (1234-1236), ainsi que

l'épitope du cluster II correspondant à l'hélice α formée par HR2 (1237). Comme il existe des interactions non-covalentes entre les sous-unités gp120 et gp41, il peut en résulter une dissociation spontanée de la gp120 de la gp41, ce qui mène à la relâche de gp120 soluble de la surface des cellules infectées (234, 409, 410). Par conséquent, des niveaux significatifs de gp120 soluble peuvent être trouvés en circulation dans le sang et les tissus des individus infectés par le VIH-1 (1238-1240). La gp120 soluble peut interagir avec le CD4 présent à la surface des cellules non-infectées et exposer des épitopes CD4i facilement accessible aux nnAbs, permettant une redirection de la réponse immunitaire vers les cellules non-infectées (834, 1241, 1242). Le relargage de la gp120 laisse également un trimère de gp41 exposé à la surface des cellules infectées qui est hautement reconnu par les nnAbs (1243). Comme l'effet antiviral des nnAbs s'est avéré très limité dans les modèles animaux, aucun essai clinique n'utilise présentement ce type d'anticorps (1234, 1242, 1244-1248).

1.2.3.3 Fonctions effectrices des anticorps et récepteurs Fc

Il existe divers mécanismes immunitaires médiés par la portion Fc des IgG lesquels pouvant mener à l'élimination des cellules infectées lorsqu'elles sont opsonisées par une quantité suffisante d'anticorps. Ceux-ci incluent la cytotoxicité cellulaire dépendante des anticorps (ADCC), la phagocytose cellulaire dépendante des anticorps (ADCP) et la lyse par le complément dépendante des anticorps (ADCML) (**Figure 1.1.11**). Ces fonctions effectrices Fc-dépendantes peuvent être médiées autant par les bNAbs que les nnAbs, à la condition que leurs épitopes respectifs soient exposés à la surface des cellules infectées.

Les récepteurs Fc (FcR), forment une famille de récepteurs de surface cellulaire qui se lient spécifiquement à la partie Fc des anticorps de type IgG (FcγR), de type IgA (FcαR) et de type IgE (FcεR). Il existe six membres de la famille des FcγRs dont les récepteurs activateurs FcγRI (CD64), FcγRIIa (CD32a), FcγRIIc (CD32c), FcγRIIIa (CD16a) et FcγRIIIb (CD16b), ainsi que le récepteur inhibiteur FcγRIIb (CD32b); chacun possédant un profil d'expression cellulaire et des fonctions différentes dans la réponse immunitaire (1249). À l'exception du FcγRI, les FcγRs ont une faible affinité pour les IgG et n'engagent pas les IgG monomères dans des conditions physiologiques (1249). Ces récepteurs détectent plutôt la présence de complexes immuns multimériques, ce qui fournit une avidité suffisante aux monomères de FcγR pour s'agglomérer et

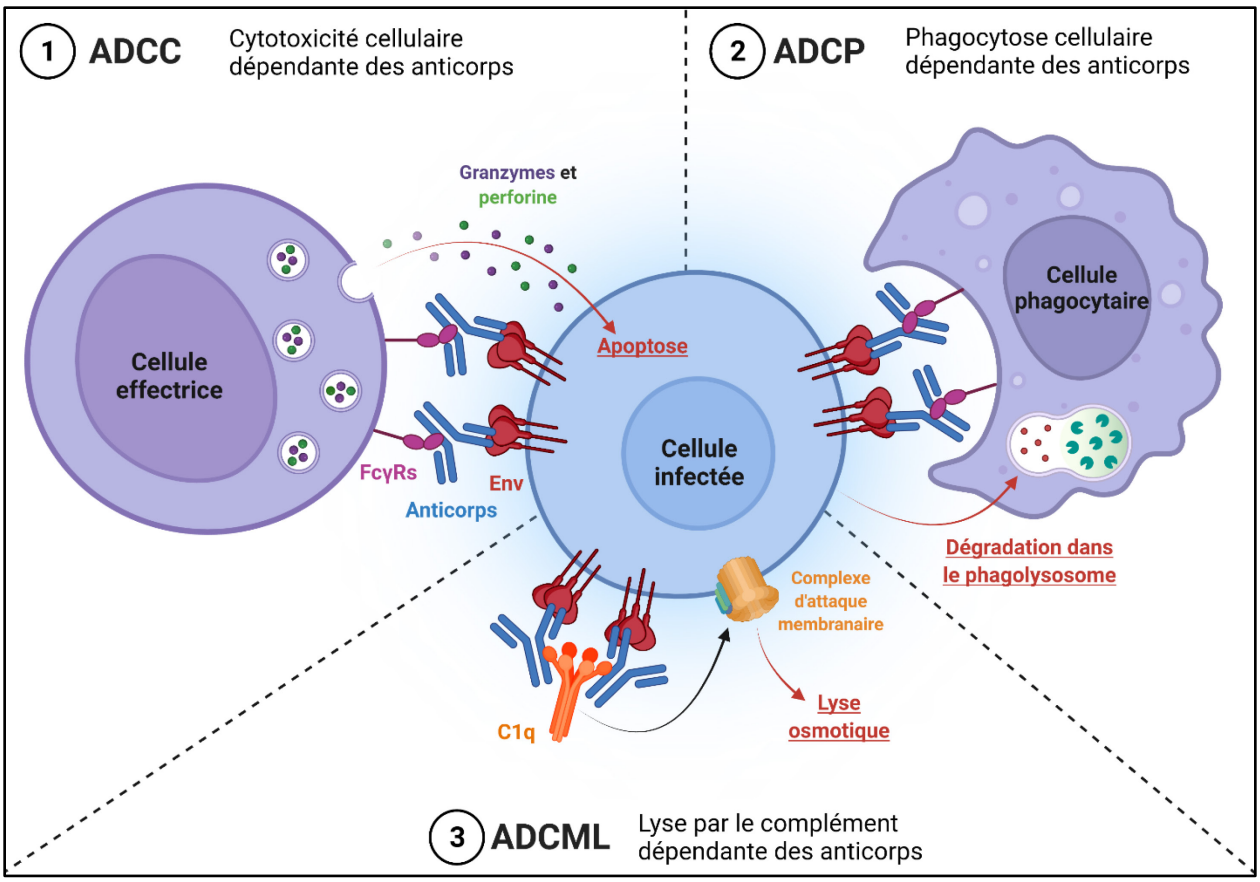

Figure 1.1.11 - Fonctions effectrices médiées par le fragment Fc des IgG.
Représentation schématique des processus d'élimination des cellules infectées médiés par la portion Fc des anticorps. (**1**) La cytotoxicité cellulaire dépendante des anticorps (ADCC) dépend du recrutement de cellules effectrices comme les cellules NK capables d'induire l'apoptose des cellules infectées par la dégranulation de granzymes et perforines. (**2**) La phagocytose cellulaire dépendante des anticorps (ADCP) dépend du recrutement de cellules phagocytaires capables de dégrader la cellule infectée via une voie d'endocytose menant au phagolysosome. (**3**) La lyse par le complément dépendante des anticorps (ADCML) dépend du recrutement du complexe d'attaque membranaire menant à la lyse osmotique des cellules infectées. Diagramme créé avec BioRender.com.

déclencher l'activation de la cellule effectrice via des motifs ITAM (1250, 1251). De plus, les FcγRs possèdent une affinité supérieure pour les portions Fc des isotypes IgG1 et IgG3 comparativement aux IgG2 et IgG4 (1252). Plusieurs facteurs peuvent influencer l'activation des fonctions effectrices Fc-dépendantes dans le contexte de l'infection par le VIH-1. En ce sens, la stœchiométrie et l'orientation des anticorps liés à l'antigène représentent des paramètres importants pouvant dicter l'accessibilité des domaines Fc pour engager les FcγRs (1227, 1228). L'interaction IgG-FcγR est également influencée par la composition du glycan N297 de la portion Fc,

notamment par l'absence de fucose qui permet une meilleure affinité pour le FcγRIIIa, et donc une fonctionnalité supérieure (1253-1256). La magnitude des fonctions effectrices est également influencée par la présence de polymorphismes mononucléotidiques (SNP) dans les allèles du FcγRIIIa (V/F158) et du FcγRIIa (H/R131) qui module l'affinité globale pour la portion Fc et la spécificité isotypique pour les IgG (1257-1259).

La réponse ADCC est médiée par des cellules effectrices, typiquement par les cellules NK, mais également par les monocytes, les macrophages et les neutrophiles, qui s'activent via l'engagement du récepteur activateur FcγRIIIa et libèrent des molécules cytotoxiques pour éliminer les cellules infectées par un virus (1260). Dans le cas des cellules NK, il s'agit de granules cytolytiques comportant des granzymes et perforines qui sont capables d'induire l'apoptose de la cellule infectée. Certains récepteurs activateurs des cellules NK, tel que NKG2D, peuvent agir à titre de corécepteur à CD16 pour faciliter le déclenchement de la réponse ADCC (1087, 1261). La réponse ADCP est médiée par des cellules phagocytaires incluant les monocytes, les macrophages, les cellules dendritiques, les neutrophiles et les éosinophiles, principalement via l'activation du FcγRIIa ou du FcγRI (1262). L'engagement du FcγR permet l'internalisation de la cellule infectée et sa dégradation dans les phagolysosomes. En plus de mener à l'élimination de la cellule infectée, cela stimule la présentation antigénique aux lymphocytes T $CD4^+$ et $CD8^+$ par les cellules présentatrices d'antigènes (1263). Les réponses ADCC et ADCP peuvent également être médiées par l'interaction des IgA-avec le FcαR présents à la surface de certaines cellules myéloïdes (1264-1267). Enfin, la réponse ADCML ne nécessite pas de cellules effectrices, mais dépend plutôt de l'activation de la cascade du complément (1268). La voie classique du complément est initiée par la reconnaissance des IgG agglomérés à la surface des cellules infectées par la molécule C1q, ce qui mène à la formation de la C3 convertase (1269). Le clivage du facteur C3 en C3a et C3b permet la déposition du C3b à la surface de la cellule infectée, se liant à la C3 convertase pour former la C5 convertase (1270). Le clivage du facteur C5 déclenche l'assemble du complexe d'attaque membranaire (MAC) par les facteurs C5b, C6, C7 et C8, qui servent de plateforme pour l'oligomérisation du facteur C9 sous forme de pore transmembranaire permettant la lyse osmotique de la cellule infectée (1271). Toutefois, la présence de CD59 à la surface cellulaire empêche la lyse en inhibant la polymérisation du MAC (1272-1276). Dans l'article de revue présent à la fin du chapitre I (**article 1**), la contribution des fonctions effectrices Fc-dépendantes des anticorps au

niveau de la protection contre la transmission du VIH-1, le contrôle de la virémie et la progression de la maladie est discutée en détail. On y retrouve également un sommaire des différents mécanismes utilisés par le VIH-1 pour évader les réponses humorales neutralisantes et non-neutralisantes. Le développement de nouvelles stratégies expérimentales afin d'optimiser l'élimination des cellules infectées par les nnAbs et les bNAbs y est également présenté.

1.3 Traitements contre le VIH-1

En 2022, aucun vaccin efficace ou traitement menant à la guérison de l'infection par le VIH-1 n'ont été établis. Bien que les symptômes de la maladie et la charge virale puissent être supprimés par le traitement ART, la nécessité d'un traitement curatif demeure, car les personnes infectées abritent toujours des cellules réservoirs infectées (1277). Ainsi, le succès du traitement ART a transformé l'infection par le VIH-1 d'une maladie mortelle en une maladie chronique, ce qui rend nécessaire la prise d'ARV à vie pour empêcher le rebond viral à partir des réservoirs. Cependant, la thérapie à vie nécessite une adhésion stricte au traitement et peut occasionner des effets secondaires indésirables dus à sa toxicité et l'apparition de multirésistance aux ARV (1278, 1279). Avec la suppression de la réplication du VIH-1 induite par le traitement ART, le nombre de lymphocytes T $CD4^+$ en circulation se stabilise à des niveaux relativement normaux chez la majorité des individus infectés. Cependant, de nombreux patients traités ne réussissant pas à récupérer des comptes normaux de lymphocytes T $CD4^+$ présentent un syndrome de dysrégulation immunitaire résiduelle (RIDS), qui se caractérise par une inflammation et une coagulopathie accrues, associées à une morbidité et une mortalité élevées (1280). Plusieurs stratégies vaccinales et thérapeutiques sont actuellement à l'essai dans le début d'éradiquer le VIH-1 pour de bon.

1.3.1 Thérapie antirétrovirale

La compréhension de la biologie du VIH-1 a conduit à la découverte de médicaments antirétroviraux ciblant diverses étapes du cycle de réplication, notamment l'entrée, la transcription inverse, la décapsidation, l'intégration et la maturation, et au moins trente d'entre eux sont actuellement approuvés par la U.S. FDA (1281). Les premiers ARVs ont été développés pour inhiber l'activité des différentes enzymes du VIH-1 (RT, IN, PR) et sont encore aujourd'hui les plus utilisés dans les traitements ART combinatoires (1282). Les inhibiteurs nucléosidiques de la transcriptase inverse (NRTI) sont des analogues de nucléosides qui peuvent être incorporés dans

le génome viral lors de la rétrotranscription et provoquer la terminaison de la synthèse d'ADN en raison de l'absence ou le remplacement du groupement hydroxyle en 3' (1283, 1284). Les inhibiteurs non-nucléosidiques de la transcriptase inverse (NNRTI) perturbent l'activité catalytique de la RT par leur interaction avec un site allostérique qui déforme la cavité du site actif (1285, 1286). Les inhibiteurs du transfert de brin par l'intégrase (INSTI) se lient au complexe formé par l'IN et l'ADNv, et interagissent avec les ions de magnésium qui servent de cofacteurs du site actif permettant la capture de l'ADN cellulaire (1287, 1288). Une nouvelle classe d'inhibiteurs allostériques de l'intégrase (ALLINI) bloquant l'interaction avec LEDGF et induisant la mutimérisation aberrante d'IN est présentement à l'étude (1289-1292). Les inhibiteurs de protéase (PI) s'insèrent dans la cavité à l'interface du dimère de PR et interagissent avec les résidus d'aspartates conservés du site catalytique (1293, 1294). Le processus de maturation est également ciblé par une nouvelle classe d'inhibiteurs perturbant spécifiquement le clivage entre CA et SP1 et ceux-ci sont présentement en phase clinique (1295-1297). Suivant les recommandations du *Center for Disease Control and Prevention* (CDC), la trithérapie conventionnelle est composée de deux NRTIs en combinaison avec un NNRTI, un INSTI ou un PI (1298). Or, l'émergence de multirésistance chez certains patients a forcé le développement de nouvelles classes d'inhibiteurs ciblant les protéines structurelles du VIH-1. Les inhibiteurs d'entrée peuvent agir au niveau de l'attachement ou de la fusion virale en ciblant Env ou un de ses récepteurs (1299). La plus récente classe d'inhibiteurs ayant démontré son efficacité est dirigée contre la capside virale, et ceux-ci empêchent la décapsidation et la relâche de l'ADNv dans le noyau en augmentant la stabilité de la capside (1300-1304). Il n'existe toujours pas d'inhibiteurs autorisés ciblant les protéines régulatrices (Tat, Rev) ou les protéines accessoires (Vif, Vpr, Vpu, Nef) du VIH-1. Une seule molécule ciblant Vpu (BIT225) est actuellement testée en essai clinique, mais avec une activité antivirale mitigée (1305-1309).

1.3.1.1 Inhibiteurs d'entrée virale

La caractérisation du mécanisme multifactoriel d'entrée du VIH-1 dans la cellule hôte a révélé une série de processus critiques qui pourraient être perturbés par des moyens pharmacologiques. En plus des anticorps neutralisants, plusieurs molécules ont été développées pour bloquer l'entrée du VIH-1 dans les cellules cibles, connues collectivement sous le nom d'inhibiteurs d'entrée, mais constituant un groupe complexe de médicaments dont les mécanismes

d'action sont multiples et dépendent de l'étape du processus d'entrée à laquelle ils agissent et de la protéine ciblée. Il existe présentement quatre inhibiteurs de l'entrée du VIH-1 approuvés par la U.S. FDA qui se répartissent en quatre classes distinctes : les inhibiteurs d'attachement, les inhibiteurs post-attachement, les antagonistes de CCR5 et les inhibiteurs de fusion.

L'inhibiteur d'attachement fostemsavir (BMS-663068) a été approuvé en 2020 pour le traitement de l'infection par le VIH-1 chez les personnes ayant développé une résistance à plusieurs ARV et disposant d'options de traitement limitées (1310). Temsavir (BMS-626529), le composé actif du promédicament fostemsavir, empêche l'interaction entre Env et CD4 en s'insérant sous la boucle β20-β21 du CD4BS de la gp120, de manière orthogonale à la cavité Phe43 hydrophobe (1311). Cet inhibiteur maintient le trimère d'Env dans sa conformation « fermée » en empêchant la liaison à CD4 de manière allostérique et en prévenant la formation du site de liaison au corécepteur (217, 1311-1314). De même, la cavité Phe43 est ciblée par plusieurs autres composés présentement en développement pré-clinique, mais ceux-ci agissent plutôt en tant qu'agoniste de CD4 (**Figure 1.1.12**). À l'instar de CD4, les miniprotéines de CD4 et les mimétiques moléculaires de CD4 (CD4mc) s'insèrent directement dans la cavité Phe43 et déclenchent des changements de conformation exposant les épitopes CD4i (1315-1317). En plus de compétitionner avec CD4 pour son site de liaison, l'activation prématurée de la conformation « ouverte » d'Env par les CD4mc provoque le détachement de la gp120, ce qui inactive Env de manière irréversible (1318-1320). Les études utilisant les CD4mc dans des modèles animaux ont démontré que ces composés étaient capables de prévenir l'infection par le VIH-1, contrôler la charge virale et réduire la taille des réservoirs viraux lorsqu'utilisés en combinaison avec des anticorps non-neutralisants (1321-1325). Ces inhibiteurs ont été optimisés afin de présenter un large groupement hydrophobe se projetant profondément dans la cavité Phe43 et leur permettant d'atteindre le fond de la cavité où se trouve le résidu 375 (1326-1328). Ces projections pénètrent plus profondément dans la cavité Phe43 que le résidu Phe43 lui-même, ce qui rend ces molécules plus sensibles aux changements survenant dans la cavité, comme la présence de résidus volumineux à la position 375 capables de remplir la cavité (1226, 1320, 1329-1332). La majorité des souches du VIH-1 en circulation présentent un petit résidu sérine à cette position (Ser375), avec l'exception du clade CRF01_AE qui possèdent un résidu histidine largement conservé (His375), ce qui leur confère une résistance aux CD4mc, mais également à temsavir (1328, 1333, 1334).

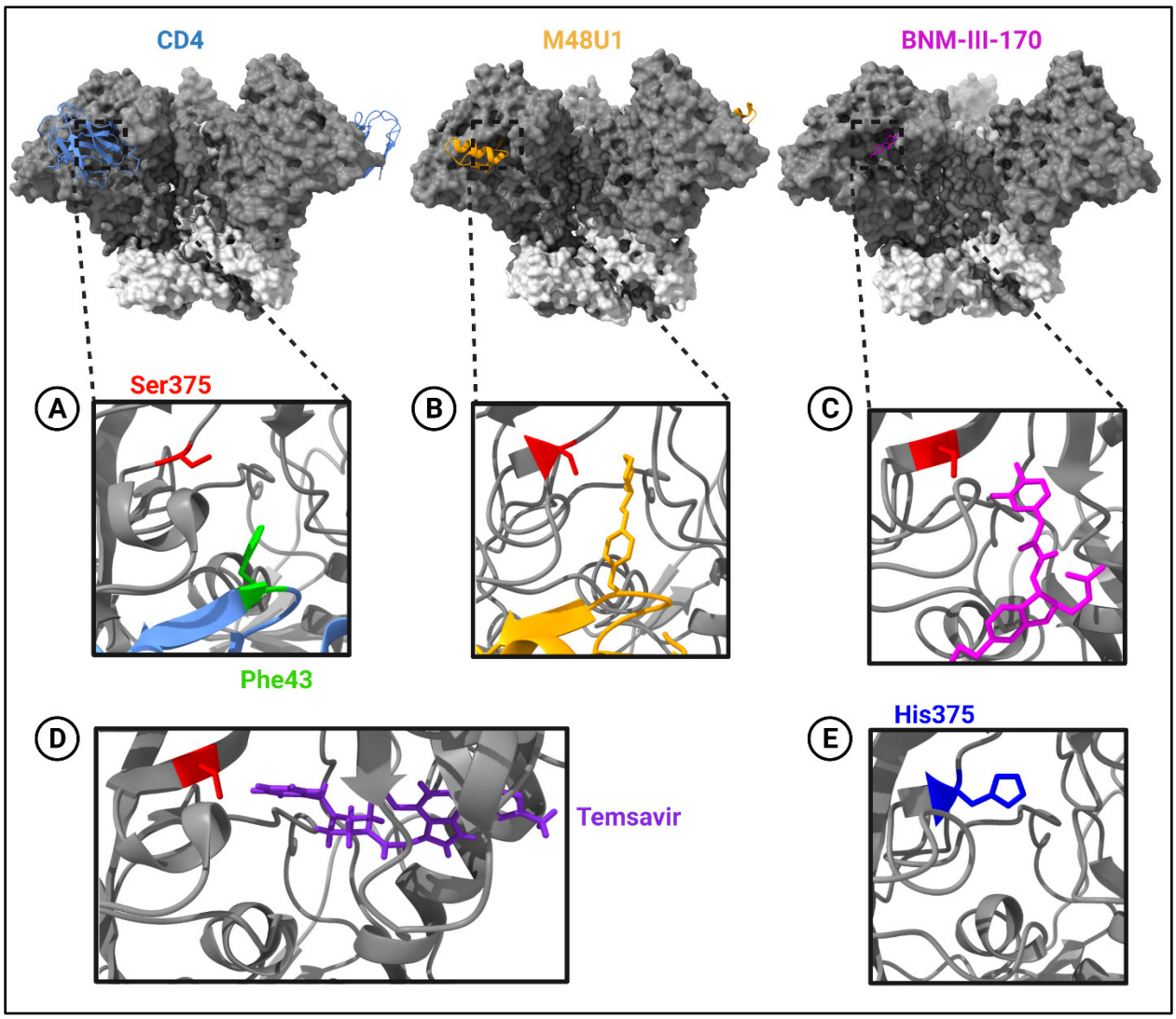

Figure 1.1.12 – Inhibiteurs d'entrée ciblant la cavité Phe43 de l'Env du VIH-1.
(**A**) Le récepteur CD4 interagit avec l'Env du VIH-1 via l'insertion de son résidu Phe43 dans la cavité Phe43 de la gp120. Plusieurs inhibiteurs d'entrée ciblent également cette cavité. (**B**) Les miniprotéines de CD4 (comme M48U1) et (**C**) les mimétiques moléculaires de CD4 (comme BNM-III-170) s'insèrent dans cette cavité et permettent l'adoption de la conformation « ouverte ». (**D**) La molécule temsavir s'insère de manière orthogonale à l'ouverture de la cavité Phe43 et stabilise la conformation « fermée ». (**E**) Contrairement, aux autres clades du VIH-1 qui possèdent une sérine en position 375, l'Env des souches CRF01_AE possède une histidine à cette position. Les représentations structurelles ont été générées à l'aide du logiciel ChimeraX v1.3 à partir de structures disponibles dans la base de données RCSB PDB. Les structures utilisées sont celles d'une Env du clade A liée à CD4 et E51 (PDB : 6U0L), M48U1 et 17b (PDB : 7LOK), BNM-III-170 et 17b (PDB : 7LO6) ou temsavir, PGT122 et 35022 (PDB : 5U7O) ainsi que la structure d'une Env du clade CRF01_AE liée à 8ANC195 (PDB : 6NQD). Pour CD4, la densité visible provient uniquement de son domaine D1. Les densités associées aux anticorps ont été enlevées pour une question de clarté. La sous-unité gp120 est illustrée en gris foncé et la gp41 est illustrée en gris pâle. Diagramme créé avec BioRender.com.

L'ibalizumab, premier anticorps monoclonal de type IgG4 approuvé en 2018 pour le traitement de l'infection par le VIH-1, est un inhibiteur d'entrée post-attachement dirigé contre CD4 qui bloque l'entrée du VIH-1 dans les cellules cibles tout en préservant sa fonction immunitaire normale (1335). L'ibalizumab se lie au domaine D2 de CD4, permettant la liaison du domaine D1 à l'Env du VIH-1, mais empêchant les étapes ultérieures nécessaires à l'entrée du virus (1336). Son utilisation dans la trithérapie est également réservée pour le traitement d'infections multirésistantes en échec de leur traitement ART initial (1337, 1338). Le maraviroc, approuvé en 2007, appartient à la classe des antagonistes de CCR5 et son utilisation est strictement limitée aux individus infectés par des souches à tropisme R5 (1339, 1340). Cette molécule s'insère dans la pochette hydrophobe centrale du CCR5, délimitée par ses sept hélices transmembranaires, et compétitionne directement pour l'interaction entre CCR5 et la boucle V3 de la gp120 (224, 1341). Des antagonistes de CXCR4 ont été développés de manière similaire, mais ont échoué dans les essais cliniques (1342, 1343). Également capable de bloquer l'interaction entre Env et CCR5, le leronlimab, un anticorps monoclonal de type IgG4, est présentement en essai clinique pour être utilisé chez les patients dont la charge virale est indétectable (1344, 1345). Du côté des inhibiteurs de fusion, on retrouve l'enfuvirtide (T20), premier ARV ciblant l'entrée approuvé en 2003, qui est un peptide de 36 acides aminés analogue au domaine HR2 de la gp41 capable d'empêcher les réarrangements structurels nécessaires à la formation du 6HB en se liant de manière complémentaire au domaine HR1 (1346, 1347). Son utilisation dans le traitement ART est devenue très limitée à cause de l'émergence rapide de mutations échappatoires et une demi-vie très courte dans l'organisme (1348-1350). Les inhibiteurs de fusion de deuxième génération comme l'albuvirtide, un peptide de HR2 couplé à l'albumine, et le LP-98, un peptide complémentaire à HR1 couplé au cholestérol, ont démontré une activité antivirale et une demi-vie supérieures comparativement au T20 et sont présentement en développement clinique et pré-clinique, respectivement (1351-1353).

1.3.2 Stratégies de vaccination contre le VIH-1

Un vaccin préventif efficace n'a toujours pas été trouvé et, à ce jour, plusieurs candidats ont fait l'objet d'essais cliniques de phases 2 et 3, parmi lesquels seul l'essai vaccinal RV144 a démontré une efficacité modeste de 31,2 % sur un suivi de trois ans (78). Les deux premiers essais d'efficacité (Vax003 et Vax004) visaient à induire une réponse humorale contre un vaccin bivalent

composé de gp120 monomériques recombinantes (AIDSVAX) (72). Malheureusement, l'analyse des données en a révélé que les deux vaccins n'arrivaient pas à produire des bNAbs chez les vaccinés et donc ne prévenaient pas l'acquisition du VIH-1 ou la progression de la maladie (74, 75). Par la suite, les essais vaccinaux STEP et Phambili visaient à induire une réponse à médiation cellulaire par les lymphocytes $CD8^+$ en utilisant des vecteurs adénoviraux recombinants (rAd5) codant pour les protéines virales Gag, Pol et Nef (1354, 1355). Ces essais n'ont démontré aucune protection globale, augmentant même le risque d'infection chez les individus présentant une immunité préexistante contre le vecteur (76, 77, 1356). De manière similaire, l'essai vaccinal HVTN 505 (*HIV Vaccine Trials Network 505*) proposait un vaccin à base d'ADN recombinant codant pour les protéines Gag, Pol, Env et Nef, suivi d'une dose de rappel avec un rAd5 exprimant Gag, Pol et Env; toutefois, cet essai n'a démontré aucune efficacité (1357).

En utilisant une approche pour induire une réponse immunitaire humorale et cellulaire, l'essai vaccinal RV144 réalisé en Thaïlande était basé sur un vaccin combinant un vecteur poxvirus recombinant (ALVAC-HIV) encodant les gènes structuraux *gag*, *pol* et *env*, suivi de doses de rappel avec de la gp120 recombinante (AIDSVAX). Cette étude a fourni les premières preuves cliniques de l'efficacité d'un vaccin contre le VIH-1 en démontrant une efficacité de 60,5 % au cours de la première année, qui est ensuite descendue à 31,2 % trois ans après la vaccination (78, 1358). Les corrélats immunitaires de la protection observée étaient principalement les réponses IgG spécifiques à la boucle V1/V2 de la gp120 et une forte réponse ADCC chez les participants ayant une réponse IgA réduite (1359, 1360). Le déclin rapide de l'efficacité du vaccin RV144 a mené à de nouvelles études (RV305 et RV306) dans le but d'administrer des doses de rappel du vaccin afin de fournir une protection plus durable, mais les réponses immunitaires induites se sont avérées transitoires (1361, 1362). Les résultats prometteurs de l'essai RV144 ont suscité l'intérêt d'évaluer son efficacité contre d'autres clades. En fait, le vaccin du RV144 était conçu à l'origine pour protéger contre l'infection par les souches du clade CRF01_AE circulants en Thaïlande et a été adapté plus tard pour cibler les souches du clade C dans l'essai vaccinal HVTN 702 (Uhombo) réalisé en Afrique du Sud (1363). Cet essai vaccinal a récemment été interrompu en 2020 pour cause de futilité après qu'une analyse intermédiaire n'ait révélé aucune prévention de l'infection (1364). Les essais vaccinaux en cours misent maintenant sur l'induction d'une réponse immunitaire à large spectre. Les essais HVTN 705 (Imbokodo) et HVTN 706 (Mosaico) sont

conçus à partir d'un vaccin à base de vecteurs adénoviraux (Ad26) codant pour les protéines Gag, Pol et Env et un rappel à base de protéines d'Env recombinantes (gp140), dont les séquences ont été optimisées *in silico* afin de refléter la diversité des différents clades (1365-1367). Bien que l'essai HVTN 706 ne soit toujours pas terminé (ClinicalTrials.gov : NCT03964415), l'essai HVTN 705 a été interrompu en août 2021 à cause d'une efficacité vaccinale insuffisante (25,2 %) deux ans après le début de la vaccination (1368). Le dernier essai vaccinal en lice (PrEPVacc) mise sur l'utilisation de plusieurs stratégies déjà éprouvées (vaccin à ADN, vecteur poxvirus (MVA) et protéines recombinantes d'Env) en combinaison avec un traitement ART préventif (PrEP) (ClinicalTrials.gov : NCT04066881). Les résultats de cette étude sont attendus pour 2023.

Les défis à relever pour développer un vaccin efficace sont principalement dus à la variabilité du virus, en particulier d'Env, ainsi qu'à l'identification concluante des corrélats immunitaires de protection. Si un vaccin pouvait stimuler la production de bNAbs, il pourrait possiblement conférer une protection contre l'infection par le VIH-1 (1369). Le développement d'un immunogène à partir du trimère d'Env représente un des enjeux principaux dans l'élaboration des approches vaccinales de nouvelles générations. Plusieurs défis se sont imposés dans la caractérisation de l'arrangement structurel d'un trimère d'Env pré-fusion soluble, en raison de sa conformation métastable, sa lourde glycosylation et l'interaction non-covalente entre les différentes sous-unités du trimère. Depuis 2013, une forme soluble du trimère d'Env (connue sous le nom de SOSIP.664), dérivée de la séquence de l'isolat de clade A BG505 et stabilisée par l'introduction de ponts disulfure artificiels entre les sous-unités gp120 et gp41 (SOS), grâce aux mutations A501C et T605C, en combinaison avec la mutation I559P (IP) dans le domaine HR1, est utilisée pour des études structurelles (185, 186). Bien que le trimère reste intact en solution, l'introduction des mutations SOSIP entraîne une déstabilisation de la conformation native d'Env et un profil de glycosylation aberrant (403, 1370-1373). Les études utilisant le trimère SOSIP.664 en tant qu'immunogène vaccinal dans des modèles animaux ont montré qu'il induisait presque uniquement des anticorps neutralisants autologues ou dirigés contre la base du trimère (1140, 1374-1376). Un autre défi dans la génération de bNAbs par vaccination est la stimulation des lignées germinales de lymphocytes B naïfs codant pour les précurseurs de bNAbs. En ce moment, l'approche privilégiée pour la génération de bNAbs passe par l'activation des lignées germinales suivie d'une maturation séquentielle guidée par des immunogènes trimériques d'Env (1377-1383).

Bien que ces stratégies aient donné des résultats mitigés dans les modèles animaux, les premiers essais cliniques de phase 1 sont présentement en cours afin d'évaluer leur efficacité pour induire des bNAbs chez l'humain, notamment via l'utilisation de vaccins à base d'ARNm (ClinicalTrials.gov : NCT03547245, NCT04224701, NCT05001373, NCT05217641) qui ont montré des résultats prometteurs dans des études pré-cliniques (1384-1386).

1.3.3 Stratégies de guérison du VIH-1

En termes généraux, pour obtenir une guérison du VIH-1, il faut soit une éradication complète du réservoir latent (guérison stérilisante), soit un contrôle à long terme de la réplication virale en l'absence d'ART (guérison fonctionnelle). En 2022, quatre personnes sont considérées guéries du VIH-1 : le « patient de Berlin », le « patient de Londres », le patient de « Düsseldorf » et la « patiente de New York » (79-83). Tous ont développé une leucémie myéloïde aiguë ou un lymphome de Hodgkin et ont été traités par des immunosuppresseurs, suivis d'une transplantation allogénique de cellules souches hématopoïétiques en utilisant des donneurs présentant une mutation homozygote du gène CCR5 ($CCR5^{\Delta32/\Delta32}$), ce qui confère une résistance à l'infection du VIH-1 par les souches à tropisme R5 (1387-1389). Le traitement antirétroviral a été interrompu plusieurs mois après la transplantation et les quatre individus étaient en rémission avec une charge virale plasmatique indétectable. Cependant, ce traitement n'est pas une option viable pour toutes les personnes infectées, étant donné le risque élevé de complications pendant la transplantation de cellules souches et la difficulté de trouver des donneurs histocompatibles et homozygotes pour la mutation $CCR5^{\Delta32/\Delta32}$ (1390). Entre autres, un autre patient traité avec des cellules souches $CCR5^{\Delta32/\Delta32}$ a souffert d'un éventuel rebond viral de souches à tropisme X4 (1391). Basé sur ces succès, des stratégies de guérison utilisant la thérapie génique visent à d'introduire la mutation $CCR5^{\Delta32/\Delta32}$. À cet effet, plusieurs méthodes moléculaires permettant la modification du génome de l'hôte sont à l'essai, telles que les nucléases à doigt de zinc (ZFN) ou la technologie CRISPR-Cas9, mais leurs taux de modification *in vivo* restent insuffisants pour le moment pour conférer une résistance complète à l'infection (1392, 1393).

De manière encourageante, deux cas de guérison spontanée ont été caractérisés chez des contrôleurs élites exceptionnels dans la dernière année : la patiente de San Francisco et la patiente d'Esperanza (846, 847). En absence de traitement ART, ces dernières ne présentent aucune virémie

détectable depuis 12 ans et 8 ans, respectivement, et aucun provirus intact compétent pour la réplication n'a été détecté dans plus d'un milliard de cellules de sang périphériques analysées (846, 847). Étant donné la complexité associée à l'élimination complète des réservoirs viraux, la guérison fonctionnelle semble une approche plus réaliste. La diminution de la taille des réservoirs du VIH-1 de manière préventive ou active pourrait être suffisante afin de permettre au système immunitaire de contrôler la réplication virale et d'empêcher la progression de la maladie en l'absence du traitement ART. Notamment, l'initiation de la thérapie antirétrovirale dans la phase précoce de l'infection a été liée à la réduction de l'établissement des réservoirs du VIH-1 (1394-1396) et à un contrôle prolongé du rebond viral suite à l'interruption du traitement ART chez les contrôleurs post-traitement, tels qu'observés chez trois cas pédiatriques infectés de manière périnatale et traités intensivement dès leurs premiers mois de vie(1397-1399) et chez des patients adultes de la cohorte « *Viro-Immunologic Sustained Control after Treatment Interruption* » (VISCONTI) et de la cohorte « *Control of HIV After Antiretroviral Medication Pause* » (CHAMP) (1025, 1400). Cependant, un rebond viral a fini par se produire éventuellement dans ces cas (1401).

Les plus récentes stratégies thérapeutiques expérimentales pour permettre une guérison fonctionnelle se classent dans deux idéologies différentes : les stratégies « *shock and kill* » qui visent l'élimination active des réservoirs et les stratégies « *block and lock* » qui visent plutôt à bloquer l'expression virale de manière permanente. Les stratégies « *shock and kill* » nécessitent la réactivation de l'expression du provirus à partir de son état latent à l'aide d'agents d'inversion de la latence (LRA) en présence de traitement ART pour empêcher l'infection de nouvelles cellules (1402). Certaines molécules agissant sur le plan épigénétique sont utilisées pour prévenir la formation d'hétérochromatine, incluant des inhibiteurs d'histone désacétylase (HDAC) comme le vorinostat, le panabinostat et la romidepsine (1403-1405), tandis que d'autres agissent au niveau de l'activation transcriptionnelle du provirus via la libération du complexe P-TEFb actif (1406) et l'activation de la voie NF-κB; ceux-ci incluent les agonistes de la protéine kinase C (PKC) comme la bryostatine, la prostratine et l'ingénol (1407, 1408), les mimétiques de SMAC (1409) et les agonistes de TLR (1410-1413). Suite à la réactivation de l'expression virale, les réservoirs cellulaires doivent être éliminés par le système immunitaire. L'élimination des cellules infectées peut être augmentée par l'administration de bNAbs, de lymphocytes exprimant un récepteur antigénique chimérique ou d'immunomodulateurs augmentant les fonctions effectrices, incluant

les agonistes de TLR, les IFN-I et l'IL-15 (1199, 1410, 1414-1418). Les stratégies « *block and lock* » visent à réduire au silence la transcription du VIH-1 en bloquant le promoteur dans une latence profonde à l'aide d'agents favorisant la latence (LPA) (1419). Les inhibiteurs de Tat, les inhibiteurs de kinase et les ARN d'interférence sont des exemples de LPA (1420-1424). En stimulant la latence virale et en la rendant irréversible, il pourrait être possible d'arrêter le traitement ART sans rebond viral et d'établir une rémission prolongée sans médicament.

ARTICLE 1

Impact de la conformation de l'enveloppe du VIH-1 dans la réponse ADCC

Impact of HIV-1 Envelope Conformation on ADCC Responses

Auteurs:

Jonathan Richard[1,2,*], Jérémie Prévost[1,2,*], Nirmin Alsahafi[1,3], Shilei Ding[1,2], Andrés Finzi[1,2,3]

Affiliations:

[1]Centre de Recherche du CHUM, Montreal, QC, Canada; [2]Department of Microbiology, Infectiology and Immunology, Université de Montréal, Montreal, QC, Canada; [3]Department of Microbiology and Immunology, McGill University, Montreal, QC, Canada; *contribution égale

Contribution des auteurs:

Rédaction - version originale: **Tous les auteurs**; Rédaction - révision et édition: **Tous les auteurs**; Visualisation: J.R. et **J.P.**; Supervision: A.F.; Obtention du financement: A.F.

Statut: Cet article a été publié dans *Trends in Microbiology* en avril 2018.
https://doi.org/10.1016/j.tim.2017.10.007

Commentaire :

Cette revue de littérature présente un sommaire des principaux concepts abordés dans les prochains chapitres de cette thèse concernant la réponse anticorps dirigée contre les glycoprotéines d'enveloppe du VIH-1. On y aborde les rôles clés joués par la conformation d'Env et de l'expression des protéines accessoires Nef et Vpu. Ceux-ci dictent la reconnaissance antigénique par les différentes classes d'anticorps neutralisants (bNAbs) et non-neutralisants (nnAbs) et la susceptibilité des cellules infectées à la réponse ADCC. Nous explorons les différentes stratégies expérimentales utilisées afin d'optimiser l'élimination des cellules infectées par les bNAbs et les nnAbs. Cet article présente également une comparaison détaillée des différentes techniques de laboratoire utilisées pour mesurer la réponse ADCC et de leur pertinence biologique.

1.4.1 RÉSUMÉ

Les glycoprotéines d'enveloppe du VIH-1 (Env) représentent le seul antigène spécifique du virus exposé à la surface des cellules infectées. Dans sa forme non-liée, l'Env de virus primaires adopte la conformation « fermée » (conformation 1), qui est reconnue préférentiellement par les anticorps neutralisants à large spectre (bNAbs). L'interaction avec CD4 fait passer Env dans une conformation intermédiaire « partiellement ouverte » (conformation 2), puis dans la conformation « ouverte » liée à CD4 (conformation 3). De nouvelles données suggèrent l'existence d'un lien entre la conformation d'Env et la réponse cytotoxique cellulaire dépendante des anticorps (ADCC). Les cellules infectées par le VIH-1 exposant Env dans la conformation liée à CD4 sont sensibles à l'ADCC médiée par les anticorps non-neutralisants (nnAbs) et le sérum d'individus infectés par le VIH. Les cellules exposant Env dans la conformation « fermée » sont sensibles à l'ADCC médiée par les bNAbs. Nous examinons ici comment la conformation d'Env affecte la réponse ADCC et sa quantification *in vitro*.

1.4.2 ABSTRACT

HIV-1 envelope glycoproteins (Env) represent the only virus-specific antigen exposed at the surface of infected cells. In its unliganded form, Env from primary viruses samples a 'closed' conformation (State 1), which is preferentially recognized by broadly neutralizing antibodies (bNAbs). CD4 engagement drives Env into an intermediate 'partially open' (State 2) and then into the 'open' CD4-bound conformation (State 3). Emerging evidence suggests a link between Env conformation and Ab-dependent cellular cytotoxicity (ADCC). HIV-1-infected cells exposing Env in the CD4-bound conformation are susceptible to ADCC mediated by CD4-induced Abs and HIV^+ sera. Cells exposing State 1 Env are susceptible to ADCC mediated by bNAbs. Here, we discuss how Env conformation affects ADCC responses and *in vitro* measurements.

1.4.3 MAIN TEXT

Impact of Antibody-Dependent Cellular Cytotoxicity on HIV-1 Replication and Transmission

HIV-1 continues to infect more than 1.8 million individuals annually, with an estimated total of 36.7 million people living with this virus in 2016[i]. Enormous effort has been made to improve the clinical management of HIV/AIDS through highly active antiretroviral therapy (HAART). Accordingly, HIV-1 infection can be controlled with HAART and, in most cases, allows for a significant increase in the life expectancy of infected individuals [1]. However, viral rebounds can occur upon HAART interruption due to the presence of latent viral reservoirs [2,3], persisting mainly in long-lived memory $CD4^+$ T cells [4]. Efforts to design efficient preventive or curative strategies have yet to produce results in the clinic. Identifying and characterizing the immune functions needed to establish a protective immunity and understanding how the virus responds and protects itself from these immune functions represent a highly complex, multifaceted problem.

At the time of writing, only one anti-HIV-1 vaccine trial, the RV144 Thai trial (see Glossary), has presented a modest (31.2%) efficacy in preventing infection by HIV-1 [5]. Interestingly, correlates of protection in this trial suggested that increased ADCC could be linked with decreased HIV-1 acquisition [6] and Abs with potent ADCC activity were isolated from some RV144 vaccinees [7]. ADCC is thought to represent an important immune effector function in the protection and control of different viral infections and could be mediated by natural killer (NK) cells, monocytes/macrophages, or neutrophils [8–11]. Decreased viral load, rate of disease progression, and decreased mother–child transmission correlated with Fc-mediated effector functions in HIV-1 and simian immunodeficiency virus (SIV) infections in some [12–22], but not in all studies [23–25]. Of note, Fc-mediated effector functions appear to be important against not only infected cells, but also free virus [26]. While some studies failed to show that passive administration of non-neutralizing Abs (nnAbs) presenting ADCC activity could confer protection against SIV or simian-HIV (SHIV) challenges in macaque models [27–30], a recent study clearly indicated that nnAbs could alter the course of HIV-1 infection in humanized mice [31]. Supporting an important role of ADCC in preventing viral transmission, a recent pentavalent HIV-1 vaccine

was shown to protect 55% of pentavalent vaccine-immunized rhesus macaques from SHIV challenge. Systems serology of the Ab responses in this study identified ADCC activity as one of the four main immunological parameters able to predict decreased infection risk [32].

Env Conformation

The HIV-1 Env trimer mediates viral entry. HIV-1 Env is formed by three exterior gp120 and three transmembrane gp41 subunits, which are noncovalently associated [33–35]. Interaction of gp120 with the CD4 receptor triggers major conformational changes in Env, including movement of the V1/V2 and V3 loops, and formation of the co-receptor binding site (CoRBS) and the bridging sheet [36–43]. CD4 interaction also leads to the exposure of the gp41 helical heptad repeat (HR1) [44]. CCR5 or CXCR4 co-receptor interaction with gp120 promotes additional conformational changes in gp41, resulting in the formation of a six-helix bundle formed by HR1 and HR2 heptad repeats and in the fusion of viral and cellular membranes.

Env is a metastable molecule that transits from its unliganded 'closed' high-energy conformation (State 1) to its 'open' CD4-bound low-energy conformation (State 3). CD4 engagement drives Env into an intermediate 'partially open' conformation (State 2) and then into State 3 [45,46]. Env represents the only virus-specific antigen exposed at the surface of infected cells and, thus, represents a major target for ADCC. The unliganded Env of most primary clinical HIV1 isolates assumes a 'closed' State 1 conformation, which renders them relatively resistant to Ab attack (**Figure 1.2.1**) [46]. Despite different modes of recognition, multiple bNAbs preferentially recognize and stabilize this 'closed' conformation. By contrast, CD4 binding 'opens' Env by reorganizing the V1/V2 and V3 loops, resulting in the adoption of the CD4-bound conformation, referred to as State 3 (**Figure 1.2.1**) [45,46]. This conformation is efficiently recognized by ADCC-mediating Abs present in sera from HIV-1-infected individuals [47]. To avoid the exposure of these vulnerable epitopes, Env tightly controls its transition from State 1 to States 2/3. For instance, the V1/V2 and V3 loops have a critical role in keeping the trimer 'closed' [48–50], with well-conserved V2 residues restraining Env from sampling downstream States 2/3 conformations [45]. Additional elements participate in keeping Env in State 1, including the Phe43 cavity, a highly conserved approximately 150-$Å^3$ pocket located at the interface between the inner and outer domain of the gp120, which allows engagement to CD4 via its Phe43 residue [51].

Within this cavity, residue 375 impacts the conformation spontaneously sampled by Env. Most HIV-1 group M Envs have an 'empty' Phe43 cavity due to the presence of a small residue, such as serine, at position 375 (S375), which favors the adoption of State 1, therefore preventing transitions to downstream conformations [52,53] (**Figure 1.2.1**). Interestingly, substitution of S375 by large hydrophobic residues, such as histidine or tryptophan, 'fills' the Phe43 cavity and predisposes Env to spontaneously assume a state closer to the CD4-bound conformation [52] (**Figure 1.2.1**). Accordingly, CRF01_AE Envs, which have a naturally occurring Phe43 cavity-filling residue at this position (H375), are better recognized by CD4-induced (CD4i) Abs than CRF01_AE Envs having this residue replaced by a serine (H375S), resulting in enhanced ADCC responses mediated by HIV^+ sera and anti-cluster A Abs [54].

Besides binding CD4, the Phe43 cavity is also the target of small CD4-mimetic compounds (CD4mc), which block the gp120–CD4 interaction, inducing thermodynamic changes in gp120 similar to those observed upon CD4 binding [55,56] and forcing Env to sample State 2/3 conformations [46] (**Figure 1.2.1**). In agreement with the susceptibility of the CD4-bound conformation of Env to ADCC responses [47], CD4mc sensitize HIV-1-infected cells to ADCC mediated by Abs present in sera, cervicovaginal fluids, and breast milk from HIV-1-infected individuals [57,58].

The conformation sampled by Env results from the balance between elements preventing the spontaneous adoption of the CD4-bound conformation, such as the V1/V2 V3 loops and S375 within the Phe43 cavity, and other elements facilitating this transition. Three topological layers (Layers 1, 2, and 3) in the gp120 inner domain facilitate Env transition to the CD4-bound conformation [53,59]. Accordingly, mutation of highly conserved residues at the interface between these layers, such as tryptophan 69 (W69, conservation of 99.8% based on the Los Alamos HIV database), decreases the adoption of this conformation and the recognition by CD4i ADCC-mediating Abs [60,61].

Role of HIV-1 Accessory Proteins in ADCC Responses

HIV-1 limits the Env–CD4 interaction by downregulating CD4 and preventing Env accumulation at the surface of infected cells [47,61–64] (**Figure 1.2.2**). HIV-1 uses the accessory

proteins Nef and Vpu to reduce the surface expression of CD4, thus preventing the exposure of CD4i Env epitopes [47,61]. In addition to its role in preventing CD4 accumulation at the cell surface [65], Vpu promotes viral release by counteracting the restriction factor BST-2, thus preventing the accumulation of nascent virions on the surface of infected cells [66,67]. Supporting the role of Vpu in limiting antigen accumulation at the surface of infected cells, several studies showed that Vpu reduces Env recognition by ADCC-mediating Abs [47,61–64]. HIV-1 also controls Env accumulation at the cell surface through efficient Env internalization, which in turns limits ADCC responses [68]. Beside its capacity to limit ADCC responses by downregulating CD4 [61,69], Nef also interferes with NK cell activation by decreasing the expression of ligands for the NK cell receptor NKG2D [70]. Since NKG2D acts as a co-receptor for the CD16/Fc receptor (FcR) to mediate ADCC against HIV-1-infected cells [71], Nef-mediated downregulation of NKG2D ligands also contributes to protection from ADCC responses [72] (**Figure 1.2.2**). Together, these observations demonstrate the central role of Nef and Vpu in protecting HIV-1-infected cells from ADCC. Targeting these accessory proteins might help develop new strategies to eliminate HIV-1-infected cells.

CD4-Induced Antibodies

One consequence of Env binding to CD4 is the exposure of numerous Env CD4i epitopes. Several families of Abs recognize different CD4i epitopes, including anti-CoRBS, anti-V1V2, anti-V3, anti-gp41, and anti-cluster A Abs. Here, we discuss the impact of two CD4i families of Abs (anti-cluster A and anti-CoRBS) on ADCC responses.

Anti-cluster A Antibodies

Binding to CD4 causes conformational changes in Env and results in the exposure of concealed epitopes, including those located in the gp120 inner domain cluster A region. This region comprises the N- and C-terminal of gp120, the seven-stranded β-sandwich, and gp120 layers 1 and 2 [73]. This region was defined initially by the recognition of the A32 Ab [74,75], which binds the interface of gp120 inner domain layer 1 and layer 2, and C11, which is reported to bind the N termini [53,73,75–77]. Crystal structures of anti-cluster A N5i5 and 2.2c Abs in complex with gp120 cores and CD4 identified α0 and α1 helices in the C1 region as being critical for binding [78]. Importantly, the generation of a disulfide-linked stabilized gp120 inner domain

(ID) recently allowed the co-crystallization of A32 [79]. This new structure provided detailed information about the A32 epitope and confirmed previous mutagenesis data [53,60] that identified residue W69 as a key contact residue involved in ADCC responses mediated by anti-cluster A Abs [60]. While anti-cluster A Abs are unable to neutralize viral particles and, therefore, are known as nnAbs, several studies indicate that they can mediate potent ADCC if target cells expose Env in its CD4-bound conformation [47,54,57,60,61,69,79,80]. However, since their epitopes are occluded in the unliganded trimer, target cells exposing Env in State 1, such as cells infected with primary viruses, are resistant to ADCC mediated by these Abs [47,57,58,60,61,64,69,81–84] (**Figure 1.2.2**).

Co-receptor Binding Site Antibodies

The CoRBS comprises the V3 loop and the 'bridging sheet', a structure formed by b-sheets from the V1/V2 loop stem and the β20-β21 loop, which come together upon CD4 binding [51]. Since CoRBS Abs recognize this bridging sheet, which is exposed after CD4 binding, they are also known as CD4i Abs. Similar to anti-cluster A Abs, CoRBS Abs were shown to poorly recognize HIV-1-infected cells exposing Env in State 1 [60,81,84–86]. In addition, cells infected with viruses defective for Nef and Vpu are readily recognized by CoRBS Abs (**Figure 1.2.3**, Key Figure). However, despite good recognition of infected cells, CoRBS Abs are unable to mediate potent ADCC [60,80,84,85] (see **Outstanding Questions**). This paradox (i.e., good recognition of target cells but no ADCC activity) could be explained by the different angles of approach used by anti-cluster A Abs and CoRBS Abs to engage with Env and, therefore, expose their Fc portion to effector cells and crosslink the FcR [78].

Broadly Neutralizing Antibodies

Despite targeting different Env elements, such as the CD4-binding site (CD4BS) (e.g., VRC01, 3BNC117), the gp120–gp41 interface (e.g., PGT151, 8ANC195), the gp41 membrane-proximal external region (MPER) (e.g., 10E8, 4E10), the variable loops V1/V2 (e.g., PG9, PG16) or V3 (e.g., PGT121, PGT126), most bNAbs preferentially recognize Env State 1 [46] (**Figure 1.2.3**). While several of these bNAbs were shown to mediate ADCC against cells infected with wildtype viruses (i.e., encoding functional Nef and Vpu proteins), including those recognizing the CD4-binding site (e.g., 3BNC117, NIH45-46), quaternary epitopes formed by the V1/V2 and V3

variable loops (e.g., PG9, PGT121-126) or the gp120–gp41 interface (e.g., PGT151), other bNAbs recognizing the gp41 MPER region (e.g., 10E8, 4E10, 2F5) failed to do so [84–89]. As described above, good recognition of Env at the surface of infected cells does not necessarily translate into potent ADCC responses: for example, 2G12 recognizes infected cells efficiently but fails to mediate potent ADCC [23,60,80,84,85], highlighting the importance of Fc engagement by effector cells. Accordingly, the ability of the CD4BS b12 Ab to protect rhesus macaques from SHIV challenge correlated with its capacity to engage FcR [26,90]. Similarly, a recent study described how the Fc portion of another CD4BS bNAb (3BNC117) was required to control HIV-1 replication in a humanized mouse model [91].

Measuring ADCC

Several approaches have been developed to measure ADCC responses against HIV-1. These methods were recently described in detail elsewhere [11,92] and are summarized in **Table 1.2.1**. They commonly use T cells either pulsed with soluble HIV-1 Env recombinant proteins (gp120 or gp140), with AT-2-inactivated viruses or infected with different viral strains, as target cells. The selection of targets cells must be done carefully because they define the type of Env epitopes that drive the ADCC response being measured. For instance, in target cells pulsed with soluble Env or inactivated viral particles, Env interacts with CD4 at the cell surface and, thus, samples the CD4-bound conformation [73,93,94]. This is not representative of productively HIV-1-infected cells, where the Env–CD4 interaction is prevented by the actions of Nef and Vpu [47,60,61,69]. As stated above, several bNAbs preferentially recognize quaternary epitopes in the unbound closed trimeric Env but not in monomeric gp120 [95–98] (**Figure 1.2.3**). Moreover, in pulsed T cells, CD4BS Abs compete with CD4 for the gp120 CD4BS [99–101] (**Figure 1.2.3**). By contrast, CD4i ADCC-mediating Abs, naturally present in HIV^+ sera, efficiently recognize both trimeric and monomeric CD4-bound Envs [60,61,80,93,102] (**Figure 1.2.3**). Therefore, ADCC assays using T cells coated with soluble Envs, pulsed with inactivated viruses or infected with strains defective for Nef and/or Vpu, preferentially measure ADCC responses mediated by CD4i Abs or HIV^+ sera, but underestimate the responses mediated by bNAbs, particularly those targeting the CD4BS.

While HIV-1-infected cells are protected from ADCC mediated by CD4i Abs and most HIV$^+$ sera [47,57,58,60,61,64,69,81–84], gp120 shed from productively infected cells binds CD4 on uninfected bystander CD4$^+$ T cells, sensitizing them to ADCC mediated by these Abs [83] (**Figure 1.2.4**), thus influencing *in vitro* ADCC measurements. Of note, shed gp120 binding to uninfected bystander CD4$^+$ was shown to be abrogated by CD4mc, which bind to the CD4-binding site required for the CD4 interaction [83]. Assays measuring ADCC in the total population cannot distinguish responses directed against infected cells versus uninfected bystander cells. For instance, GranToxiLux [7,23,80,103], RFADCC [73,94,104], and Chromium release [15,88,105] assays do not differentiate ADCC responses against infected versus uninfected bystander cells. Similarly, NK cell activation assays [13,106,107] cannot determine which cell population activates NK cells. Therefore, these methods overestimate ADCC responses mediated by Abs recognizing the CD4-bound conformation of Env. Enrichment of HIV-1-infected cells before ADCC measurements could improve the specificity of these assays [88].

Measurement of productively infected cell elimination by ADCC was reported using a T cell line expressing a Tat-driven luciferase gene. In this assay, Luciferase is only expressed upon productive HIV-1 infection and elimination of infected cells is calculated by the loss of luciferase activity [108]. Similarly, calculating the loss of the percentage of infected cells using GFP-expressing virus [47,58,60,61,64,83,86] or through intracellular detection of p24 [23,57,58,69,81–83,85] can also evaluate the elimination of productively infected cells. In agreement with the ability of HIV-1 to prevent exposure of CD4i Env epitopes [47,61], studies using these assays reported that productively infected cells are mainly resistant to ADCC mediated by anti-cluster A Abs or HIV$^+$ sera [47,57,58,60,61,64,69,81–84]. Another advantage of these assays is that they can measure the ADCC activity of bNAbs [60,81,84–87]. Since there is not a clear consensus on the best ADCC assay to use to measure anti-HIV ADCC responses [109], assay specificities should be carefully considered when interpreting results from different studies (see **Outstanding Questions**). These differences could explain, at least in part, the discrepancies concerning the ability or inability of anti-cluster A and HIV+ sera to mediate ADCC responses against HIV-1-infected cells.

New Strategies to Eliminate Infected Cells

In recent years, several approaches have been developed to eliminate HIV-1-infected cells through Ab attack. These approaches either allow Ab recognition of the closed Env or exposition of vulnerable ADCC-mediating CD4i Env epitopes. The Env trimer in its 'closed' state is known to be susceptible to bNabs. The need to achieve better neutralization breath and potency led to the generation of bispecific Abs (bsAbs). Traditionally, bsAbs were engineered to target a combination of two Env epitopes, including the CD4BS, V3 glycans, V2 apex, gp120– gp41 interface or gp41 MPER (**Figure 1.2.5**) [110–113]. Alternatively, bsAbs were also developed to target an Env epitope on one arm and viral receptors on the other arm (**Figure 1.2.5**) [114,115]. Generally, bsAbs displayed superior neutralization profiles compared with their single parental bNabs. Furthermore, several groups generated bispecific proteins (bsp) with the capacity to target CD4BS and CoRBS [116–121]. Notably, the bsp eCD4-Ig, a fusion of CD4-Ig with a small CCR5-mimetic sulfopeptide (**Figure 1.2.5**), was shown to be broader and more potent than any bNAbs, while providing protection against multiple SHIV challenges in macaque [118]. Importantly, bsAbs and bsp often contain an IgG Fc portion that not only improves their stability, solubility, and half-life, but also allows the recruitment and activation of FcR-bearing effector cells [122]. In that context, bsAbs and bsp showed potent ADCC activity against HIV-1-infected cells both *in vitro* and *in vivo* [113,116,118].

Another generation of bispecific Abs has been developed to target HIV-1 Env and simultaneously recruit cytotoxic T cells (**Figure 1.2.5**). These bsAbs, termed 'bispecific T cell engagers' (BiTEs) or 'dual-affinity retargeting molecules' (DARTs) comprise one arm targeting HIV-1 Env, while the other arm is directed to the CD3 receptor. These recombinant proteins were demonstrated to be capable of redirecting normal resting cytotoxic T cells to eliminate HIV-infected cells without prior *in vitro* sensitization [123–125]. Alternatively, Berger and colleagues recently reported the development of a new bispecific chimeric antigen receptor (CAR) targeting Env. Its expression on $CD8^+$ T cells allowed efficient elimination of HIV-1-infected $CD4^+$ T cells [126].

Increasing evidence suggests that Abs naturally elicited during HIV-1-infection preferentially recognize Env in its CD4-bound conformation [47,127]. Stemming from these observations, CD4mc were used to modulate the Env conformation at the surface of HIV-1-

infected cells, leading to the unmasking of CD4i epitopes [58]. This approach efficiently sensitized primary $CD4^+$ T cells infected with HIV-1 primary isolates to ADCC. Strikingly, it also sensitized endogenously infected ex vivo-amplified primary CD4+ T cells to ADCC mediated by autologous sera and effector cells. This suggests that all the elements required to eliminate HIV-1- infected cells by ADCC are already present in infected individuals. CD4mc bring the last piece to the puzzle, by opening Env and allowing Ab recognition and recruitment of effector cells. However, exposure of the epitopes recognized by these commonly elicited Abs requires the sequential opening of the Env trimer. This could be achieved with CD4mc, which initially open the Env trimer to allow binding of CoRBS Abs, but not of anti-cluster A Abs. CoRBS Abs binding then opens the trimer to expose anti-cluster A epitopes and sensitize HIV-1-infected cells to ADCC (**Figure 1.2.5B**) [57]. The fact that these two classes of CD4i nnAb recognize highly conserved Env epitopes [60,61,128] suggests that this strategy represents a broad and potent approach to unlock the Env trimer and eliminate infected cells by ADCC. We note that these nnAbs are easily elicited by immunization [129,130].

While these approaches represent promising tools for HIV-1 eradication, their ability to reduce the size of the HIV-1 reservoir in vivo remains to be proven. Notably, it is still unclear whether the level of Env present at the surface of reactivated latently infected cells is sufficient for the strategies described above (see **Outstanding Questions**). In this context, enhancing Env accumulation at the cell surface through BST-2 upregulation (via IFN type 1 or IL-27), shown to bolster ADCC responses [63,82], might complement these promising approaches.

Concluding Remarks

To activate effector cells and mediate ADCC, Abs must first recognize their target, in this case Env. Since Env conformation greatly affects the recognition of HIV-1-infected cells by all the Abs directed against it, the dynamic conformational landscape of Env should be taken into account not only when measuring ADCC responses in vitro, but also when developing strategies aimed at bolstering this immune response.

1.4.4 TRENDS

- bNAbs preferentially recognize Env in its 'closed' conformation, while non-neutralizing CD4-induced Abs target the 'open' CD4-bound conformation.

- Env tightly controls its transition from the unbound to the CD4-bound conformation to avoid recognition by host CD4-induced Abs.

- Nef and Vpu accessory proteins protect HIV-1-infected cells from ADCC by preventing Env–CD4 interactions and by reducing the expression levels of cell surface NKG2D ligands.

- Gp120 shed from infected cells binds CD4 on uninfected bystander $CD4^+$ T cells, sensitizing them to ADCC and influencing in vitro ADCC measurements.

- Targeting the Env 'closed' conformation with bispecific Abs and/or proteins or exposing vulnerable ADCC-mediating epitopes using CD4 mimetics are emerging approaches to eliminate HIV-1-infected cells.

1.4.5 OUTSTANDING QUESTIONS

- Is there a threshold of Env recognition required for ADCC responses?

- What dictates differential ADCC activity of anti-Env Abs recognizing Env to similar extents?

- What is the best way to measure anti-Env ADCC responses *in vitro*?

- Is the level of Env present at the surface of reactivated latently infected cells sufficient for Ab attack?

1.4.6 GLOSSARY

Antibody-dependent cellular cytotoxicity (ADCC)

An adaptive host immune response that results in the lysis of target cells exposing cell surface antigens bound by specific Abs. Cross-linking of FcR expressed on effector cells, such as natural killer (NK) cells and monocytes, triggers the release of cytotoxic molecules, leading to cytolysis of the target cells.

Antibody Fc portion

The tail region of an Ab that binds to FcR on effector cells and some components of the complement system. Ab isotypes (IgG, IgM, IgA, IgE, and IgD) dictate the immune response to be triggered. For example, ADCC is mainly driven by IgG1 and IgG3.

Broadly neutralizing antibodies (bNAbs)

Abs with exceptional breath and potency able to neutralize viral particles from a broad range of viral isolates.

CD4-induced antibodies (CD4i Abs)

Abs recognizing an epitope that is occluded in the unliganded Env trimer. CD4 interaction is required for the exposure of their epitopes.

Small CD4 mimetic compounds (CD4mc)

Small compounds of low molecular weight that interact within the gp120 Phe 43 cavity and induce conformational changes similar to those induced by CD4.

Fc receptor (FcR)

Protein present at the surface of certain immune effector cells (e.g., NK cell, macrophages, monocytes, and neutrophils) that can interact with the Fc portion of Abs.

Non-neutralizing antibodies (nnAbs)

Abs unable to neutralize viral particles from HIV-1 isolates, mainly because their epitopes are not exposed in the unliganded Env trimer present at the surface of virions.

RV144 vaccine trial

HIV-1 vaccine trial performed in Thailand using the ALVAC canarypox vector encoding some HIV-1 genes (*gag*, *pol*, and *env*) and followed by a bivalent AIDSVAX B/E gp120 boost. It is the only human vaccine trial to date that has provided some degree of protection against HIV-1 transmission (31.2%).

1.4.7 ACKNOWLEDGMENTS

This work was supported by a CIHR foundation grant #352417 and by an amfAR Innovation Grant#109343-59-RGRL with support from FAIR to A.F. A.F. is the recipient of a Canada Research Chair on Retroviral Entry. J.R. is the recipient of a Mathilde Krim Fellowship in Basic Biomedical Research from amfAR. J.P. is the recipient of a CIHR Fellowship Award. N.A. is the recipient of a King Abdullah scholarship for higher education from the Saudi Government. S.D. is the recipient of a FRSQ postdoctoral fellowship award. Our funding sources had no role in data collection, analysis, or interpretation, and were not involved in the writing of this manuscript.

1.4.8 RESOURCES

[i]www.unaids.org/sites/default/files/media_asset/20170720_Data_book_2017_en.pdf

1.4.9 REFERENCES

1. Antiretroviral Therapy Cohort Collaboration (2008) Life expectancy of individuals on combination antiretroviral therapy in high-income countries: a collaborative analysis of 14 cohort studies. Lancet 372, 293–299
2. Chun, T.W. et al. (1997) Quantification of latent tissue reservoirs and total body viral load in HIV-1 infection. Nature 387, 183–188
3. Finzi, D. et al. (1997) Identification of a reservoir for HIV-1 in patients on highly active antiretroviral therapy. Science 278, 1295–1300
4. Chomont, N. et al. (2009) HIV reservoir size and persistence are driven by T cell survival and homeostatic proliferation. Nat. Med. 15, 893–900
5. Rerks-Ngarm, S. et al. (2009) Vaccination with ALVAC and AIDSVAX to prevent HIV-1 infection in Thailand. N. Engl. J. Med. 361, 2209–2220

6. Haynes, B.F. et al. (2012) Immune-correlates analysis of an HIV1 vaccine efficacy trial. N. Engl. J. Med. 366, 1275–1286
7. Bonsignori, M. et al. (2012) Antibody-dependent cellular cytotoxicity-mediating antibodies from an HIV-1 vaccine efficacy trial target multiple epitopes and preferentially use the VH1 gene family. J. Virol. 86, 11521–11532
8. Kohl, S. (1991) Role of antibody-dependent cellular cytotoxicity in defense against herpes simplex virus infections. Rev. Infect. Dis. 13, 108–114
9. Beltran, D. and Lopez-Verges, S. (2014) NK cells during Dengue disease and their recognition of Dengue virus-infected cells. Front. Immunol. 5, 192
10. Jegaskanda, S. et al. (2013) Antibody-dependent cellular cytotoxicity is associated with control of pandemic H1N1 influenza virus infection of macaques. J. Virol. 87, 5512–5522
11. Kramski, M. et al. (2013) HIV-specific antibody immunity mediated through NK cells and monocytes. Curr. HIV Res. 11, 388– 406
12. Banks, N.D. et al. (2002) Sustained antibody-dependent cell-mediated cytotoxicity (ADCC) in SIV-infected macaques correlates with delayed progression to AIDS. AIDS Res. Hum. Retroviruses 18, 1197–1205
13. Sun, Y. et al. (2011) Antibody-dependent cell-mediated cytotoxicity in simian immunodeficiency virus-infected rhesus monkeys. J. Virol. 85, 6906–6912
14. Alpert, M.D. et al. (2012) ADCC develops over time during persistent infection with live-attenuated SIV and is associated with complete protection against SIV(mac)251 challenge. PLoS Pathog. 8, e1002890
15. Baum, L.L. et al. (1996) HIV-1 gp120-specific antibody-dependent cell-mediated cytotoxicity correlates with rate of disease progression. J. Immunol. 157, 2168–2173
16. Forthal, D.N. et al. (1999) Antibody-dependent cellular cytotoxicity independently predicts survival in severely immunocompromised human immunodeficiency virus-infected patients. J. Infect. Dis. 180, 1338–1341
17. Ljunggren, K. et al. (1990) Antibodies mediating cellular cytotoxicity and neutralization correlate with a better clinical stage in children born to human immunodeficiency virus-infected mothers. J. Infect. Dis. 161, 198–202
18. Chung, A.W. et al. (2011) Activation of NK cells by ADCC antibodies and HIV disease progression. J. Acquir. Immune Defic. Syndr. 58, 127–131

19. Mabuka, J. et al. (2012) HIV-specific antibodies capable of ADCC are common in breastmilk and are associated with reduced risk of transmission in women with high viral loads. PLoS Pathog. 8, e1002739
20. Milligan, C. et al. (2015) Passively acquired antibody-dependent cellular cytotoxicity (ADCC) activity in HIV-infected infants is associated with reduced mortality. Cell Host Microbe 17, 500–506
21. Milligan, C. and Overbaugh, J. (2014) The role of cell-associated virus in mother-to-child HIV transmission. J. Infect. Dis. 210 (Suppl 3), S631–S640
22. Reh, L. et al. (2015) Capacity of broadly neutralizing antibodies to inhibit HIV-1 Cell-Cell transmission is strain- and epitope-dependent. PLoS Pathog. 11, e1004966
23. Smalls-Mantey, A. et al. (2012) Antibody-dependent cellular cytotoxicity against primary HIV-infected CD4+ T cells is directly associated with the magnitude of surface IgG binding. J. Virol. 86, 8672-8680
24. Dalgleish, A. et al. (1990) Failure of ADCC to predict HIV-associated disease progression or outcome in a haemophiliac cohort. Clin. Exp. Immunol. 81, 5–10
25. Koup, R.A. et al. (1989) Antigenic specificity of antibody-dependent cell-mediated cytotoxicity directed against human immunodeficiency virus in antibody-positive sera. J. Virol. 63, 584– 590
26. Hessell, A.J. et al. (2007) Fc receptor but not complement binding is important in antibody protection against HIV. Nature 449, 101–104
27. Dugast, A.S. et al. (2014) Lack of protection following passive transfer of polyclonal highly functional low-dose non-neutralizing antibodies. PLoS One 9, e97229
28. Nakane, T. et al. (2013) Limited impact of passive non-neutralizing antibody immunization in acute SIV infection on viremia control in rhesus macaques. PLoS One 8, e73453
29. Moog, C. et al. (2014) Protective effect of vaginal application of neutralizing and nonneutralizing inhibitory antibodies against vaginal SHIV challenge in macaques. Mucosal. Immunol. 7, 46–56
30. Astronomo, R.D. et al. (2016) Neutralization takes precedence over IgG or IgA isotype-related functions in mucosal HIV-1 antibody-mediated protection. EBioMedicine 14, 97–111

31. Horwitz, J.A. et al. (2017) Non-neutralizing antibodies alter the course of HIV-1 infection in vivo. Cell 170, 637–648 e10
32. Bradley, T. et al. (2017) Pentavalent HIV-1 vaccine protects against simian-human immunodeficiency virus challenge. Nat. Commun. 8, 15711
33. Allan, J.S. et al. (1985) Major glycoprotein antigens that induce antibodies in AIDS patients are encoded by HTLV-III. Science 228, 1091–1094
34. Robey, W.G. et al. (1985) Characterization of envelope and core structural gene products of HTLV-III with sera from AIDS patients. Science 228, 593–595
35. Wyatt, R. and Sodroski, J. (1998) The HIV-1 envelope glycoproteins: fusogens, antigens, and immunogens. Science 280, 1884–1888
36. Alkhatib, G. et al. (1996) CC CKR5: a RANTES, MIP-1alpha, MIP-1beta receptor as a fusion cofactor for macrophage-tropic HIV-1. Science 272, 1955–1958
37. Choe, H. et al. (1996) The beta-chemokine receptors CCR3 and CCR5 facilitate infection by primary HIV-1 isolates. Cell 85, 1135–1148
38. Deng, H. et al. (1996) Identification of a major co-receptor for primary isolates of HIV-1. Nature 381, 661–666
39. Doranz, B.J. et al. (1996) A dual-tropic primary HIV-1 isolate that uses fusin and the beta-chemokine receptors CKR-5, CKR-3, and CKR-2b as fusion cofactors. Cell 85, 1149–1158
40. Dragic, T. et al. (1996) HIV-1 entry into CD4+ cells is mediated by the chemokine receptor CC-CKR-5. Nature 381, 667–673
41. Feng, Y. et al. (1996) HIV-1 entry cofactor: functional cDNA cloning of a seven-transmembrane, G protein-coupled receptor. Science 272, 872–877
42. Wu, L. et al. (1996) CD4-induced interaction of primary HIV-1 gp120 glycoproteins with the chemokine receptor CCR-5. Nature 384, 179–183
43. Trkola, A. et al. (1996) CD4-dependent, antibody-sensitive interactions between HIV-1 and its co-receptor CCR-5. Nature 384, 184–187
44. Furuta, R.A. et al. (1998) Capture of an early fusion-active conformation of HIV-1 gp41. Nat. Struct. Biol. 5, 276–279
45. Herschhorn, A. et al. (2016) Release of gp120 restraints leads to an entry-competent intermediate state of the HIV-1 envelope glycoproteins. MBio 7, e01598–16

46. Munro, J.B. et al. (2014) Conformational dynamics of single HIV1 envelope trimers on the surface of native virions. Science 346, 759–763
47. Veillette, M. et al. (2015) The HIV-1 gp120 CD4-bound conformation is preferentially targeted by antibody-dependent cellular cytotoxicity-mediating antibodies in sera from HIV-1-infected individuals. J. Virol. 89, 545–551
48. Kwon, Y.D. et al. (2012) Unliganded HIV-1 gp120 core structures assume the CD4-bound conformation with regulation by quaternary interactions and variable loops. Proc. Natl. Acad. Sci. U.S.A. 109, 5663–5668
49. Liu, J. et al. (2008) Molecular architecture of native HIV-1 gp120 trimers. Nature 455, 109–113
50. Mao, Y. et al. (2012) Subunit organization of the membrane-bound HIV-1 envelope glycoprotein trimer. Nat. Struct. Mol. Biol. 19, 893–899
51. Kwong, P.D. et al. (1998) Structure of an HIV gp120 envelope glycoprotein in complex with the CD4 receptor and a neutralizing human antibody. Nature 393, 648–659
52. Xiang, S.H. et al. (2002) Mutagenic stabilization and/or disruption of a CD4-bound state reveals distinct conformations of the human immunodeficiency virus type 1 gp120 envelope glycoprotein. J. Virol. 76, 9888–9899
53. Finzi, A. et al. (2010) Topological layers in the HIV-1 gp120 inner domain regulate gp41 interaction and CD4-triggered conformational transitions. Mol. Cell 37, 656–667
54. Prevost, J. et al. (2017) Influence of the envelope gp120 Phe 43 cavity on HIV-1 sensitivity to antibody-dependent cell-mediated cytotoxicity responses. J. Virol. 91, e02452–16
55. Schon, A. et al. (2006) Thermodynamics of binding of a low-molecular-weight CD4 mimetic to HIV-1 gp120. Biochemistry 45, 10973–10980
56. Melillo, B. et al. (2016) Small-Molecule CD4-Mimics: Structure-Based Optimization of HIV-1 Entry Inhibition. ACS Med. Chem. Lett. 7, 330–334
57. Richard, J. et al. (2016) Co-receptor binding site antibodies enable CD4-mimetics to expose conserved anti-cluster A ADCC epitopes on HIV-1 envelope glycoproteins. EBioMedicine 12, 208–218
58. Richard, J. et al. (2015) CD4 mimetics sensitize HIV-1-infected cells to ADCC. Proc. Natl. Acad. Sci. U. S. A. 112, E2687– E2694

59. Desormeaux, A. et al. (2013) The highly conserved layer-3 component of the HIV-1 gp120 inner domain is critical for CD4-required conformational transitions. J. Virol. 87, 2549–2562
60. Ding, S. et al. (2015) A highly conserved residue of the HIV-1 gp120 inner domain is important for antibody-dependent cellular cytotoxicity responses mediated by anti-cluster A antibodies. J. Virol. 90, 2127–2134
61. Veillette, M. et al. (2014) Interaction with cellular CD4 exposes HIV-1 envelope epitopes targeted by antibody-dependent cell-mediated cytotoxicity. J. Virol. 88, 2633–2644
62. Alvarez, R.A. et al. (2014) HIV-1 Vpu antagonism of tetherin inhibits antibody-dependent cellular cytotoxic responses by natural killer cells. J. Virol. 88, 6031–6046
63. Arias, J.F. et al. (2014) Tetherin antagonism by Vpu protects HIV-infected cells from antibody-dependent cell-mediated cytotoxicity. Proc. Natl. Acad. Sci. U. S. A. 111, 6425–6430
64. Pham, T.N. et al. (2014) HIV Nef and Vpu protect HIV-infected CD4+ T cells from antibody-mediated cell lysis through downmodulation of CD4 and BST2. Retrovirology 11, 15
65. Lama, J. et al. (1999) Cell-surface expression of CD4 reduces HIV-1 infectivity by blocking Env incorporation in a Nef- and Vpu-inhibitable manner. Curr. Biol. 9, 622–631
66. Neil, S.J. et al. (2008) Tetherin inhibits retrovirus release and is antagonized by HIV-1 Vpu. Nature 451, 425–430
67. Van Damme, N. et al. (2008) The interferon-induced protein BST-2 restricts HIV-1 release and is downregulated from the cell surface by the viral Vpu protein. Cell Host Microbe 3, 245– 252
68. von Bredow, B. et al. (2015) Envelope glycoprotein internalization protects human and simian immunodeficiency virus infected cells from antibody-dependent cell-mediated cytotoxicity. J. Virol. 89, 10648–10655
69. Alsahafi, N. et al. (2015) Nef proteins from HIV-1 elite controllers are inefficient at preventing antibody-dependent cellular cytotoxicity. J. Virol. 90, 2993–3002
70. Cerboni, C. et al. (2007) Human immunodeficiency virus 1 Nef protein downmodulates the ligands of the activating receptor NKG2D and inhibits natural killer cell-mediated cytotoxicity. J. Gen. Virol. 88 (Pt 1), 242–250

71. Parsons, M.S. et al. (2016) NKG2D acts as a co-receptor for natural killer cell-mediated anti-HIV-1 antibody-dependent cellular cytotoxicity. AIDS Res. Hum. Retroviruses 32, 1089–1096
72. Alsahafi, N. et al. (2017) Impaired downregulation of NKG2D ligands by Nef protein from elite controllers sensitizes HIV-1- infected cells to ADCC. J. Virol. 91, e00109–17
73. Guan, Y. et al. (2013) Diverse specificity and effector function among human antibodies to HIV-1 envelope glycoprotein epitopes exposed by CD4 binding. Proc. Natl. Acad. Sci. U. S. A. 110, E69–E78
74. Robinson, J.E. et al. (1992) Distinct antigenic sites on HIV gp120 identified by a panel of human monoclonal antibodies. J. Cell. Biochem. 449 (Suppl. 16E), Q449
75. Wyatt, R. et al. (1995) Involvement of the V1/V2 variable loop structure in the exposure of human immunodeficiency virus type 1 gp120 epitopes induced by receptor binding. J. Virol. 69, 5723–5733
76. Moore, J.P. et al. (1994) Probing the structure of the human immunodeficiency virus surface glycoprotein gp120 with a panel of monoclonal antibodies. J. Virol. 68, 469–484
77. Moore, J.P. et al. (1994) Immunological evidence for interactions between the first, second, and fifth conserved domains of the gp120 surface glycoprotein of human immunodeficiency virus type 1. J. Virol. 68, 6836–6847
78. Acharya, P. et al. (2014) Structural definition of an antibody-dependent cellular cytotoxicity response implicated in reduced risk for HIV-1 infection. J. Virol. 88, 12895–12906
79. Tolbert, W.D. et al. (2016) Paring down HIV Env: design and crystal structure of a stabilized inner domain of HIV-1 gp120 displaying a major ADCC target of the A32 region. Structure 24, 697–709
80. Ferrari, G. et al. (2011) An HIV-1 gp120 envelope human monoclonal antibody that recognizes a C1 conformational epitope mediates potent antibody-dependent cellular cytotoxicity (ADCC) activity and defines a common ADCC epitope in human HIV-1 serum. J. Virol. 85, 7029–7036
81. Bruel, T. et al. (2017) Lack of ADCC breadth of human non-neutralizing anti-HIV-1 antibodies. J. Virol. 91, e02440–16

82. Richard, J. et al. (2017) BST-2 expression modulates small CD4-mimetic sensitization of HIV-1-infected cells to antibody-dependent cellular cytotoxicity. J. Virol. 91, e00219–17
83. Richard, J. et al. (2016) Small CD4 mimetics prevent HIV-1 uninfected bystander CD4 + T cell killing mediated by antibody-dependent cell-mediated cytotoxicity. EBioMedicine 3, 122–134
84. von Bredow, B. et al. (2016) Comparison of antibody-dependent cell-mediated cytotoxicity and virus neutralization by HIV-1 Env-specific monoclonal antibodies. J. Virol. 90, 6127–6139
85. Mujib, S. et al. (2017) Comprehensive cross-clade characterization of antibody-mediated recognition, complement-mediated lysis, and cell-mediated cytotoxicity of HIV-1 envelope-specific antibodies toward eradication of the HIV-1 reservoir. J. Virol. 91, e00634–17
86. Pham, T.N. et al. (2016) Enhancing virion tethering by BST2 sensitizes productively and latently HIV-infected T cells to ADCC mediated by broadly neutralizing antibodies. Sci. Rep. 6, 37225
87. Bruel, T. et al. (2016) Elimination of HIV-1-infected cells by broadly neutralizing antibodies. Nat. Commun. 7, 10844
88. Tomescu, C. et al. (2017) IFN-alpha augments natural killer-mediated antibody-dependent cellular cytotoxicity of HIV-1- infected autologous CD4+ T cells regardless of major histocompatibility complex class 1 downregulation. AIDS 31, 613–622
89. Falkowska, E. et al. (2014) Broadly neutralizing HIV antibodies define a glycan-dependent epitope on the prefusion conformation of gp41 on cleaved envelope trimers. Immunity 40, 657–668
90. Hessell, A.J. et al. (2009) Effective, low-titer antibody protection against low-dose repeated mucosal SHIV challenge in macaques. Nat. Med. 15, 951–954
91. Bournazos, S. et al. (2014) Broadly neutralizing anti-HIV-1 antibodies require Fc effector functions for in vivo activity. Cell 158, 1243–1253
92. Veillette, M. et al. (2016) Role of HIV-1 envelope glycoproteins conformation and accessory proteins on ADCC responses. Curr. HIV Res. 14, 9–23
93. Richard, J. et al. (2014) Flow cytometry-based assay to study HIV-1 gp120 specific antibody-dependent cellular cytotoxicity responses. J. Virol. Methods 208, 107–114

94. Orlandi, C. et al. (2016) A new cell line for high throughput HIV-specific antibody-dependent cellular cytotoxicity (ADCC) and cell-to-cell virus transmission studies. J. Immunol. Methods 433, 51–58
95. Blattner, C. et al. (2014) Structural delineation of a quaternary, cleavage-dependent epitope at the gp41-gp120 interface on intact HIV-1 Env trimers. Immunity 40, 669–680
96. Doria-Rose, N.A. et al. (2014) Developmental pathway for potent V1V2-directed HIV-neutralizing antibodies. Nature 509, 55–62
97. Huang, J. et al. (2014) Broad and potent HIV-1 neutralization by a human antibody that binds the gp41-gp120 interface. Nature 515, 138–142
98. Walker, L.M. et al. (2009) Broad and potent neutralizing antibodies from an African donor reveal a new HIV-1 vaccine target. Science 326, 285–289
99. Julien, J.P. et al. (2013) Broadly neutralizing antibody PGT121 allosterically modulates CD4 binding via recognition of the HIV-1 gp120 V3 base and multiple surrounding glycans. PLoS Pathog 9, e1003342
100. Thali, M. et al. (1992) Discontinuous, conserved neutralization epitopes overlapping the CD4-binding region of human immunodeficiency virus type 1 gp120 envelope glycoprotein. J. Virol. 66, 5635–5641
101. Wu, X. et al. (2010) Rational design of envelope identifies broadly neutralizing human monoclonal antibodies to HIV-1. Science 329, 856–861
102. Williams, K.L. et al. (2015) HIV-specific CD4-induced antibodies mediate broad and potent antibody-dependent cellular cytotoxicity activity and are commonly detected in plasma from HIV-infected humans. EBioMedicine 2, 1464–1477
103. Pollara, J. et al. (2011) High-throughput quantitative analysis of HIV-1 and SIV-specific ADCC-mediating antibody responses. Cytometry A 79, 603–612
104. Gomez-Roman, V.R. et al. (2006) A simplified method for the rapid fluorometric assessment of antibody-dependent cell-mediated cytotoxicity. J. Immunol. Methods 308, 53–67
105. Tyler, D.S. et al. (1990) Alterations in antibody-dependent cellular cytotoxicity during the course of HIV-1 infection. Humoral and cellular defects. J. Immunol. 144, 3375–3384
106. Johansson, S.E. et al. (2011) NK cell function and antibodies mediating ADCC in HIV-1-infected viremic and controller patients. Viral Immunol. 24, 359–368

107. Stratov, I. et al. (2008) Robust NK cell-mediated human immunodeficiency virus (HIV)-specific antibody-dependent responses in HIV-infected subjects. J. Virol. 82, 5450–5459
108. Alpert, M.D. et al. (2012) A novel assay for antibody-dependent cell-mediated cytotoxicity against HIV-1- or SIV-infected cells reveals incomplete overlap with antibodies measured by neutralization and binding assays. J. Virol. 86, 12039–12052
109. Lewis, G.K. et al. (2017) Beyond viral neutralization. AIDS Res. Hum. Retroviruses 33, 760–764
110. Asokan, M. et al. (2015) Bispecific antibodies targeting different epitopes on the HIV-1 envelope exhibit broad and potent neutralization. J. Virol. 89, 12501–12512
111. Bournazos, S. et al. (2016) Bispecific anti-HIV-1 antibodies with enhanced breadth and potency. Cell 165, 1609–1620
112. Galimidi, R.P. et al. (2015) Intra-spike crosslinking overcomes antibody evasion by HIV-1. Cell 160, 433–446
113. Mabondzo, A. et al. (1994) Antibody-dependent cellular cytotoxicity and neutralization of human immunodeficiency virus type 1 by high affinity cross-linking of gp41 to human macrophage Fc IgG receptor using bispecific antibody. J. Gen. Virol. 75 (Pt 6), 1451–1456
114. Huang, Y. et al. (2016) Engineered bispecific antibodies with exquisite HIV-1-neutralizing activity. Cell 165, 1621–1631
115. Pace, C.S. et al. (2013) Bispecific antibodies directed to CD4 domain 2 and HIV envelope exhibit exceptional breadth and picomolar potency against HIV-1. Proc. Natl. Acad. Sci. U. S. A. 110, 13540–13545
116. Bardhi, A. et al. (2017) Potent in vivo NK cell-mediated elimination of HIV-1-infected cells mobilized by a gp120-bispecific and hexavalent broadly neutralizing fusion protein. J. Virol. 91, e00937–17
117. Chen, W. et al. (2014) Exceptionally potent and broadly cross-reactive, bispecific multivalent HIV-1 inhibitors based on single human CD4 and antibody domains. J. Virol. 88, 1125–1139
118. Gardner, M.R. et al. (2015) AAV-expressed eCD4-Ig provides durable protection from multiple SHIV challenges. Nature 519, 87–91

119. Lagenaur, L.A. et al. (2010) sCD4-17b bifunctional protein: extremely broad and potent neutralization of HIV-1 Env pseudotyped viruses from genetically diverse primary isolates. Retrovirology 7, 11
120. Sun, M. et al. (2014) Rational design and characterization of the novel, broad and potent bispecific HIV-1 neutralizing antibody iMabm36. J. Acquir. Immune Defic. Syndr. 66, 473–483
121. West, A.P., Jr et al. (2010) Evaluation of CD4-CD4i antibody architectures yields potent, broadly cross-reactive anti-human immunodeficiency virus reagents. J. Virol. 84, 261–269
122. Liu, H. et al. (2017) Fc Engineering for developing therapeutic bispecific antibodies and novel scaffolds. Front. Immunol. 8, 38
123. Pegu, A. et al. (2015) Activation and lysis of human CD4 cells latently infected with HIV-1. Nat. Commun. 6, 8447
124. Sloan, D.D. et al. (2015) Targeting HIV reservoir in infected CD4 T cells by Dual-Affinity Re-targeting Molecules (DARTs) that bind HIV envelope and recruit cytotoxic T cells. PLoS Pathog. 11, e1005233
125. Sung, J.A. et al. (2015) Dual-Affinity Re-Targeting proteins direct T cell-mediated cytolysis of latently HIV-infected cells. J. Clin. Invest. 125, 4077–4090
126. Liu, L. et al. (2015) Novel CD4-based bispecific chimeric antigen receptor designed for enhanced anti-HIV potency and absence of HIV entry receptor activity. J. Virol. 89, 6685–6694
127. Decker, J.M. et al. (2005) Antigenic conservation and immunogenicity of the HIV coreceptor binding site. J. Exp. Med. 201, 1407–1419
128. Thali, M. et al. (1993) Characterization of conserved human immunodeficiency virus type 1 gp120 neutralization epitopes exposed upon gp120-CD4 binding. J. Virol. 67, 3978–3988
129. Ding, S. et al. (2017) Short communication: small-molecule CD4 mimetics sensitize HIV-1-infected cells to antibody-dependent cellular cytotoxicity by antibodies elicited by multiple envelope glycoprotein immunogens in nonhuman primates. AIDS Res. Hum. Retroviruses 33, 428–431
130. Madani, N. et al. (2016) Antibodies elicited by multiple envelope glycoprotein immunogens in primates neutralize primary human immunodeficiency viruses (HIV-1) sensitized by CD4-mimetic compounds. J. Virol. 90, 5031–5046

1.4.10 FIGURES

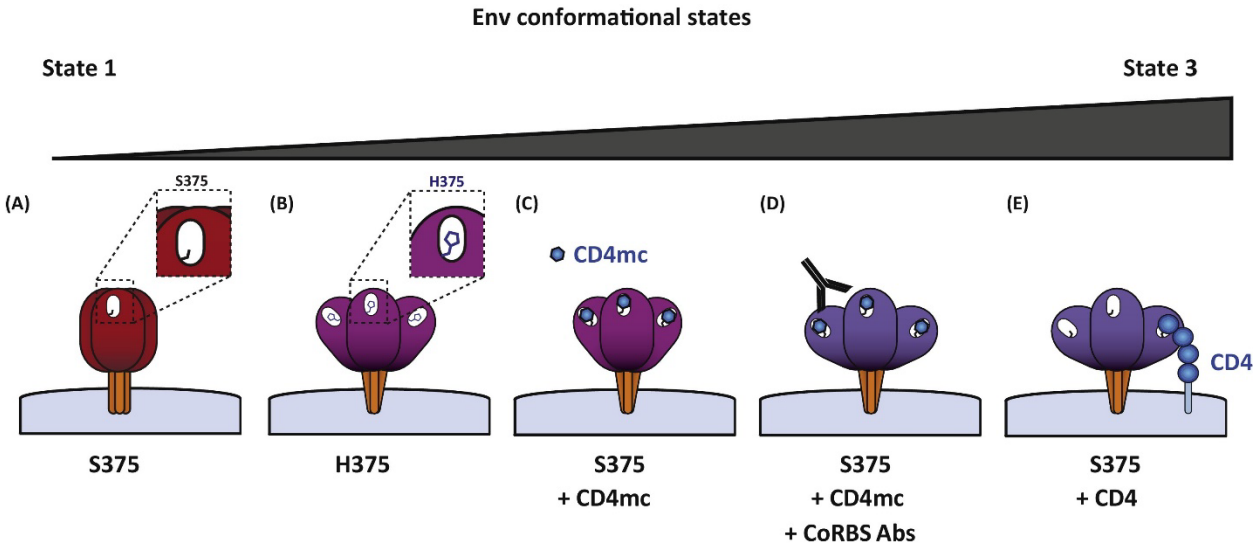

Figure 1.2.1 - HIV-1 Envelope Glycoproteins (Env) Conformational Landscape.
The Phe43 cavity (in white) modulates Env conformation. A small residue at position 375, such as serine (S375), favors a 'closed' (State 1) conformation (**A**). Larger hydrophobic residues at this position, such as histidine (H375), can trigger Env to sample more 'open' conformations (**B**), closer to the CD4-bound state (State 3) induced by interaction with membrane-anchored CD4 (**E**). CD4 mimetics (CD4mc) trigger conformational changes that initially 'open' the Env trimer and stabilize Env in State 2/3 conformations (**C**). Antibodies against the co-receptor binding site (CoRBS) prompt the Env trimer to reach conformations closer to State 3 in the presence of CD4mc (**D**).

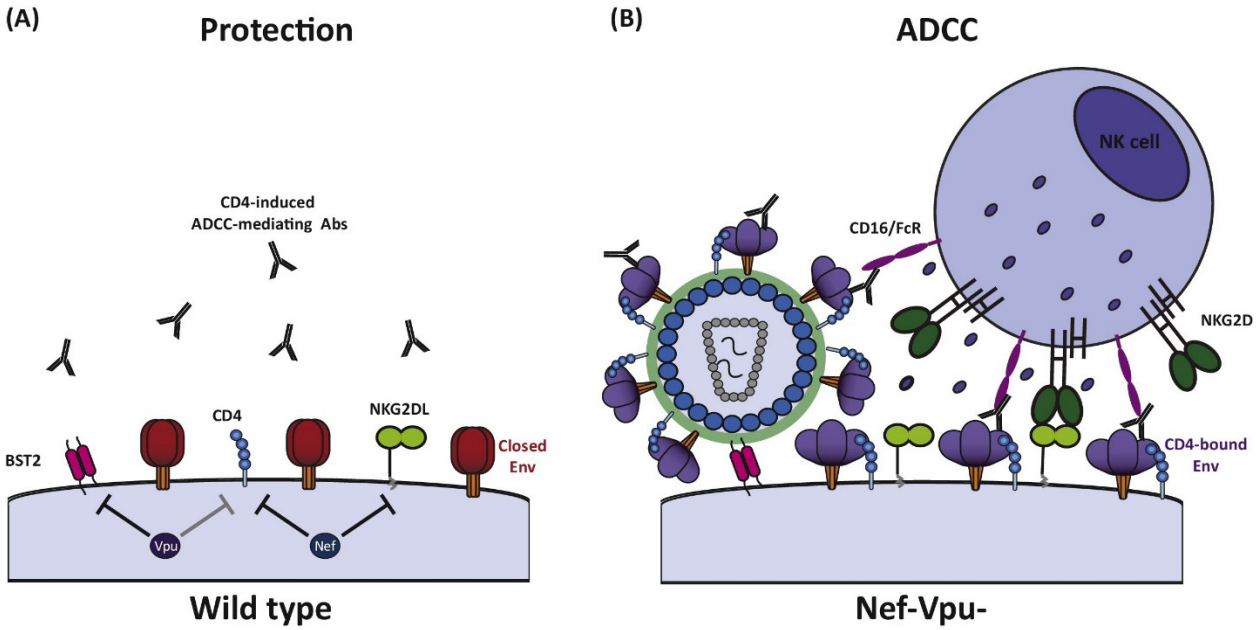

Figure 1.2.2 - Nef and Vpu Accessory Proteins Protect Infected Cells from Antibody-Dependent Cellular Cytotoxicity (ADCC) Responses.
To prevent the exposure of vulnerable CD4-induced ADCC-mediating epitopes, the virus controls the level of cell surface CD4 through the action of Nef and Vpu and limits HIV-1 envelope glycoprotein (Env) accumulation through Vpu-mediated BST-2 downmodulation (**A**). Without the action of these accessory proteins, Env and CD4 can interact at the cell surface, thus sensitizing infected cells to ADCC mediated by CD4-induced (CD4i) antibodies (**B**). Nef also limits NKG2D ligands (NKG2DL) expression at the surface of infected cells (**A**), preventing the interaction with the NKG2D receptor present on effector cells, which acts as a co-receptor for ADCC mediated by CD16/ FcR (**B**).

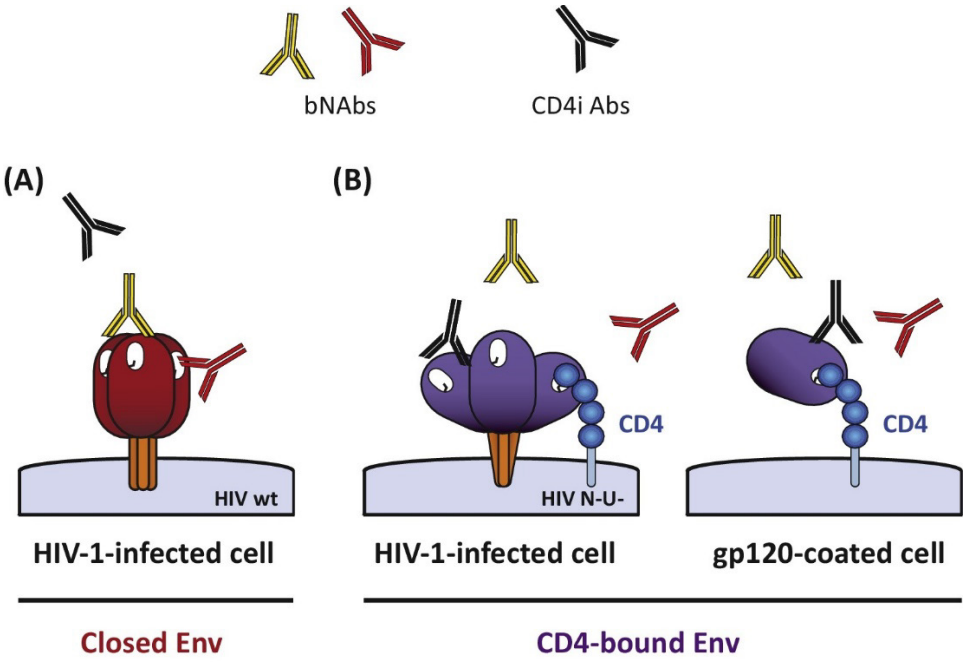

Figure 1.2.3 - Different Modes of HIV-1 Envelope Glycoprotein (Env) Recognition at the Surface of HIV-1-Infected or gp120-Coated Cells.
(**A**) Broadly neutralizing antibodies (bNAbs) preferentially bind to the 'closed' State 1 trimer. (**B**) By contrast, CD4i Abs bind to Env sampling the 'open' CD4-bound conformation. This conformation is achieved upon Env–CD4 interaction at the surface of cells infected with viruses defective for Nef and Vpu ($N^{-}U^{-}$) or in gp120-coated cells.

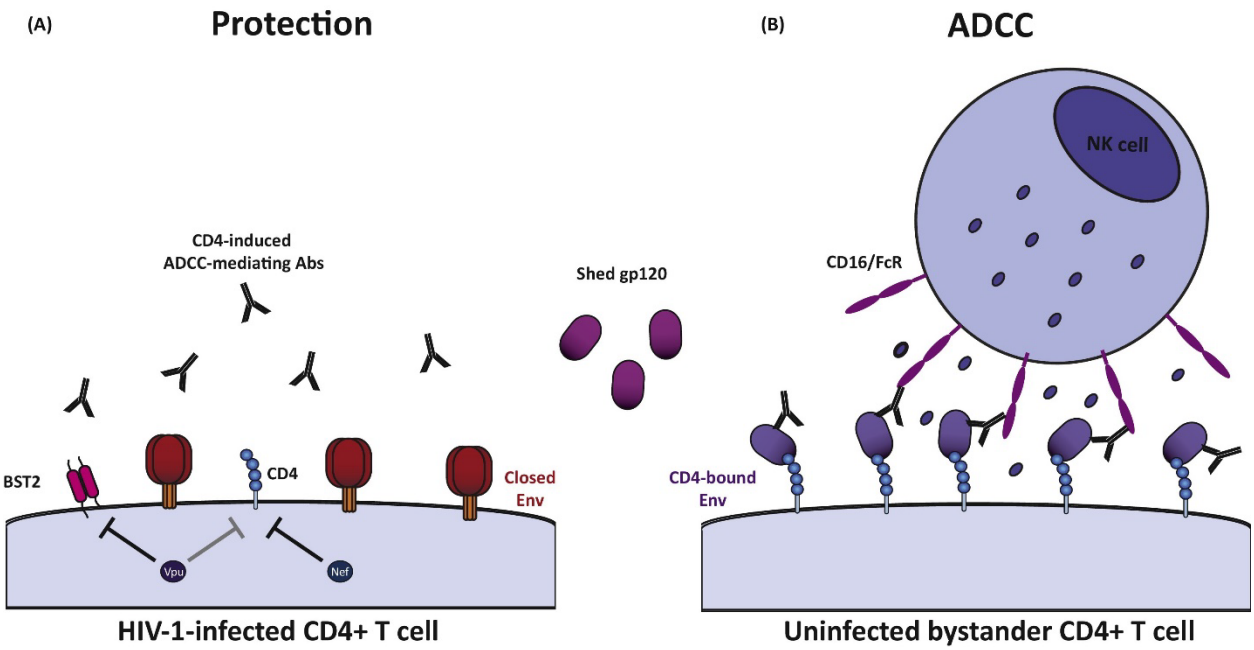

Figure 1.2.4 - Interaction of Shed gp120 with CD4 Sensitizes Uninfected Bystander Cells to Antibody-Dependent Cellular Cytotoxicity (ADCC) Responses.
While infected cells are mainly protected from ADCC mediated by CD4-induced (CD4i) antibodies (Abs) due to the actions of Nef and Vpu (**A**), uninfected bystander cells become susceptible to ADCC upon soluble gp120 interaction with CD4 (**B**). Due to its noncovalent association with gp41, gp120 sheds from the surface of productively infected cells. Upon interaction with the CD4 receptor present at the surface of uninfected bystander cells, gp120 samples the CD4-bound conformation, resulting in the exposure of vulnerable CD4i epitopes and leading to the sensitization of these cells to ADCC responses.

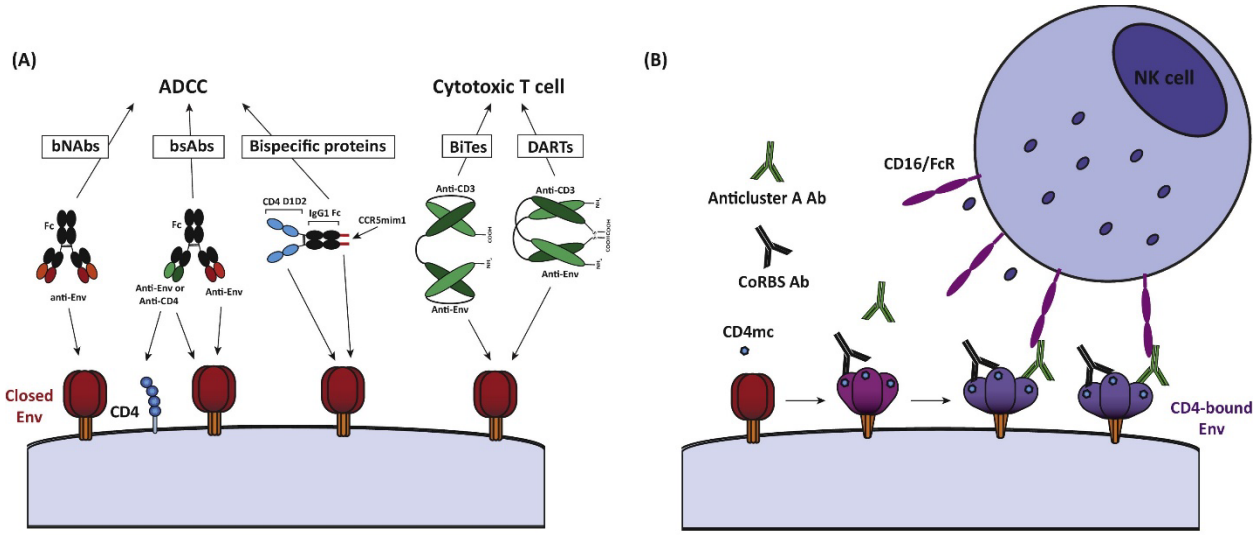

Figure 1.2.5 - Emerging Approaches to Eliminate HIV-1-Infected Cells through Antibody (Ab) Attack.

(**A**) Broadly neutralizing Abs (bNAbs), bispecific Abs (bsAbs), or bispecific proteins preferentially recognize the HIV-1 envelope glycoprotein (Env) 'closed' conformation by targeting one or two different Env epitopes. Alternatively, bsAbs can also include one arm directed against viral receptors (CD4 or CCR5). These constructs contain an IgG Fc domain that allows the recruitment and activation of FcR-bearing effector cells. Similarly, bispecific T cell engagers (BiTEs) or dual-affinity retargeting molecules (DARTs) comprise one arm targeting Env, while the other arm allows the recruitment and activation of cytotoxic T cells by targeting CD3. (**B**) CD4 mimetics (CD4mc) sensitize HIV-1-infected cells to antibody-dependent cellular cytotoxicity (ADCC) mediated by sera from patients with HIV-1. CD4mc initially open the trimeric Env to allow the binding of co-receptor binding site (CoRBS) Abs, which expose cluster A epitopes. Anti-cluster A Abs recruit effector cells and mediate ADCC.

Table 1.2.1 - Description of ADCC assays.

Assay	Target cells	Description	Readout	Measured Population	ADCC responses with anti-Cluster A Abs or HIV+ sera	References
Chromium release assay	Pulsed with soluble Env or HIV-1-infected cells	Targets cells are labeled with the radioactive ^{51}Chromium. ADCC-mediated target cell killing measured by the release of the radioactive isotope into the cell culture supernatant	Target cell elimination	Total population	+	[15, 88, 105]
NK cell activation assay	Pulsed with soluble Env or HIV-1-infected cells	Ab-dependent activation of NK cell functions assessed by detection of intracellular IFN-γ, cell-surface expression of CD107a or by measuring the loss of intracellular granzyme B	Activation of NK cell functions	Total population	+	[13, 106, 107]
ADCC GranToxiLux assay	Pulsed with soluble Env or HIV-1-infected cells	Target cells incubated with a cell-permeable fluorogenic peptide substrate that generates fluorescent signal when hydrolyzed by granzyme B. Level of target cells that receive granzyme B from effector cells is determined by flow cytometry	Delivery of granzyme B into target cell	Total population	+	[7, 23, 80, 103]
Rapid and Fluorometric ADCC (RFADCC) assay	Pulsed with soluble Env or inactivated virus or HIV-1-infected cells	Target cells stained with membrane dye (PKH-26) and a viability dye (CFSE). ADCC-mediated target cell killing is calculated by the emergence of a cell population positively labeled by membrane dye that loses the viability dye (PKH-26+ CFSE-)	Target cell permeabilization	Total population	+	[73, 94, 104]
Luciferase assay	HIV-1-infected cells	Target cell expressing luciferase from Tat-inducible promoter upon HIV-1 infection. ADCC-mediated target cell killing is measured by the dose-dependent loss of luciferase activity	HIV-1-infected cell elimination	Infected cell population	-	[63, 84, 108]
Infected-cell elimination assay	HIV-1-infected cells	Measurement of HIV-1-infected cell elimination by ADCC assessed by calculating the loss of the percentage of infected cells using GFP-expressing viruses or detection of intracellular p24	HIV-1-infected cell elimination	Infected cell population	-	[47, 57, 58, 60, 61, 64, 69, 81, 82, 85]

CHAPITRE II - HYPOTHÈSES ET OBJECTIFS

Les études structurelles et biophysiques ont clairement démontré que le trimère d'Env des isolats primaires du VIH-1 adoptent préférentiellement la conformation « fermée » et que les épitopes des nnAbs y sont inaccessibles à moins qu'Env interagisse avec son récepteur CD4 (185, 186, 190, 216-218, 220, 221, 1217, 1218, 1425). Or, le rôle des nnAbs dans l'élimination des cellules infectées par le VIH-1 reste un sujet controversé. En effet, de nombreuses études *in vitro* tendent à démontrer que les nnAbs, et plus particulièrement ceux reconnaissant le domaine interne de la gp120, sont de puissants effecteurs de la réponse ADCC (1228, 1229, 1235, 1360, 1426-1433), tandis que d'autres ont prouvé que les cellules infectées par le VIH-1 évadent substantiellement la pression immunitaire par les nnAbs, notamment grâce à la régulation négative de CD4 et BST-2 par les protéines accessoires Nef et Vpu (756-758, 1099-1101, 1241, 1434-1436). De plus, cette discordance s'applique également aux études *in vivo*. Bien que la majorité des études dans des modèles animaux ont noté que les nnAbs jouent un rôle négligeable dans la prévention de l'infection et le contrôle de la charge virale (1234, 1244-1248, 1323, 1437), deux études phares ont mis en lumière leur potentiel antiviral dans un contexte prophylactique ou thérapeutique (1242, 1359). Afin de réconcilier ces résultats divergents, l'objectif principal de cette thèse de doctorat est d'apporter une compréhension approfondie des facteurs gouvernant la conformation d'Env et la capacité des nnAbs à médier la réponse ADCC afin de pouvoir exploiter leurs activités effectrices contre le VIH-1. Cet objectif s'articule autour de quatre thèmes généraux qui seront abordés dans les chapitres qui suivent :

1. *Comment quantifier la réponse ADCC in vitro?*

Une variété de méthodes *in vitro* est utilisée pour quantifier la réponse ADCC contre les cellules infectées par le VIH-1. L'utilisation de certaines de ces techniques favorisent la détection d'une forte réponse ADCC par les nnAbs, tandis que d'autres montrent que les cellules infectées sont résistantes à ces anticorps. En fait, ces techniques diffèrent notamment par la nature des cellules cibles et des constructions virales utilisées, mais surtout dans la manière de mesurer l'ADCC puisque certaines méthodes ne prennent pas en compte la conformation d'Env présentée par les cellules cibles. Dans le **chapitre III**, nous nous concentrons sur une analyse comparative détaillée des méthodes de quantification de la réponse ADCC les plus utilisées dans la littérature et nous suggérons des modifications expérimentales afin d'éviter les biais inhérents à certaines techniques.

2. *Quelles propriétés structurelles d'Env affectent sa conformation et la réponse ADCC médiée par les nnAbs?*

En absence de Nef et Vpu, l'interaction entre Env et CD4 à la surface des cellules infectées induit des changements conformationnels permettant l'exposition des épitopes reconnus par les nnAbs, ce qui les rend hautement susceptibles à la réponse ADCC. Chez un virus de type sauvage, l'Env non-liée adopte préférentiellement sa conformation « fermée », mais l'introduction de mutations dans certains de ses domaines structuraux conservés peut forcer l'adoption spontanée de sa conformation « ouverte ». Dans le **chapitre IV**, l'objectif est de caractériser les déterminants structuraux d'Env affectant sa reconnaissance par les nnAbs et d'identifier des polymorphismes naturels pouvant rendre certaines souches plus susceptibles à la réponse ADCC.

3. *Quelles fonctions de Vpu contribuent à protéger les cellules infectées de la réponse ADCC?*

La protéine accessoire Vpu cible de manière simultanée un large éventail de protéines transmembranaires afin d'évader les réponses immunitaires innées et adaptatives. La régulation négative de la plupart d'entre elles dépend uniquement d'une interaction avec le domaine transmembranaire de Vpu. Le **chapitre V** a pour but d'étudier la dynamique de la polyfonctionnalité de Vpu et de l'importance de la somme de ces fonctions pour protéger les cellules infectées de la réponse ADCC et promouvoir la réplication du VIH-1 *in vivo* en présence de nnAbs.

4. *Comment cibler les cellules infectées avec des nnAbs en utilisant de nouvelles approches expérimentales?*

À l'instar de CD4, les CD4mc s'insèrent dans la cavité Phe43 de la gp120 et déclenchent l'ouverture du trimère d'Env, rendant les cellules infectées susceptibles à la réponse ADCC médiée par les nnAbs. Les récentes études pré-cliniques ont montré des résultats prometteurs, mais une compréhension plus approfondie des potentiels mécanismes de résistance du VIH-1 à ces molécules est nécessaire. Dans le **chapitre VI**, nous caractérisons des résidus polymorphiques d'Env modulant son interaction avec les CD4mc et nous élaborons de nouvelles stratégies pour augmenter leur capacité antivirale en combinaison avec les nnAbs.

Articles présentés dans les chapitres suivants

CHAPITRE III - MÉTHODES DE QUANTIFICATION DE LA RÉPONSE ADCC

Article 2: *Uninfected Bystander Cells Impact the Measurement of HIV-Specific Antibody-Dependent Cellular Cytotoxicity Responses*

Article 3: *Incomplete Downregulation of CD4 Expression Affects HIV-1 Env Conformation and Antibody-Dependent Cellular Cytotoxicity Responses*

Article 4: *Detection of the HIV-1 accessory proteins Nef and Vpu by flow cytometry represents a new tool to study their functional interplay within a single infected CD4+ T cell*

CHAPITRE IV - RÔLE DE LA CONFORMATION D'ENV DANS LA RÉPONSE ADCC

Article 5: *Envelope glycoproteins sampling states 2/3 are susceptible to ADCC by sera from HIV-1-infected individuals*

Article 6: *HIV-1 envelope glycoproteins proteolytic cleavage protects infected cells from ADCC mediated by plasma from infected individuals*

Article 7: *Influence of the Envelope gp120 Phe43 Cavity on HIV-1 Sensitivity to Antibody-Dependent Cell-Mediated Cytotoxicity Responses*

CHAPITRE V - RÔLE DE LA PROTÉINE ACCESSOIRE VPU DANS LA RÉPONSE ADCC

Article 8: *Upregulation of BST-2 by Type I Interferons Reduces the Capacity of Vpu to Protect HIV-1-Infected Cells from NK Cell Responses*

Article 9: *HIV-1 Vpu restricts Fc-mediated effector functions in vivo*

CHAPITRE VI - UTILISATION DES MIMÉTIQUES MOLÉCULAIRES DE CD4 POUR OUVRIR ENV

Article 10: *The HIV-1 Env gp120 Inner Domain Shapes the Phe43 Cavity and the CD4 Binding Site*

Article 11: *BST-2 Expression Modulates Small CD4-Mimetic Sensitization of HIV-1-Infected Cells to Antibody-Dependent Cellular Cytotoxicity*

CHAPITRE III - MÉTHODES DE QUANTIFICATION DE LA RÉPONSE ADCC

3.1 Préambule

Dans ce chapitre, nous décortiquons les différentes méthodes de quantification de la réponse ADCC dirigée contre les cellules infectées par le VIH-1 utilisées en laboratoire et afin d'identifier les plus rigoureuses ayant une pertinence biologique. Afin de remplir ces critères, ces techniques doivent être capables de mesurer spécifiquement l'élimination des cellules productivement infectées par des virus pleinement infectieux. Lors de notre analyse comparative, nous avons identifié plusieurs biais importants dans certaines techniques largement utilisées, y compris celles utilisées pour évaluer les corrélats de la protection vaccinale, menant à une surestimation de la capacité antivirale des nnAbs présents dans le sérum d'individus infectés par le VIH-1 (sérum VIH+). Nous avons développé des protocoles améliorés pour quantifier la réponse ADCC dans des conditions biologiquement pertinentes. Dans l'**article 2**, nous avons noté que certaines méthodes d'ADCC ne discernent pas l'élimination des cellules infectées par rapport aux cellules non-infectées. Ainsi, ces tests détectent une forte réponse ADCC médiée par les nnAbs, qui est principalement dirigée contre les cellules non-infectées recouvertes de gp120 soluble liée au CD4 présent à leur surface. Nous avons caractérisé en détail les populations cellulaires reconnues par les nnAbs et 99% d'entre elles se sont avérées non-infectées. Afin de résoudre ce problème, nous avons adapté ces techniques afin d'y inclure une étape préalable d'enrichissement rapide des cellules productivement infectées. Dans l'**article 3**, nous avons découvert que certains clones moléculaires infectieux (IMC) du VIH-1 comportant un gène rapporteur pour faciliter l'analyse à haut débit présentent une suppression incomplète des niveaux de CD4 à la surface des cellules infectées en raison d'une perte d'expression de Nef. Ceci entraîne une augmentation de la sensibilité des cellules infectées à l'ADCC médiée par les nnAbs. L'insertion du gène rapporteur dans le provirus doit se faire en combinaison avec des stratégies moléculaires permettant de maintenir l'expression de Nef. Nous montrons que l'insertion d'un site interne de liaison des ribosomes (IRES) en aval du gène rapporteur est capable de restaurer l'expression de Nef, ce qui se traduit par une résistance des cellules infectées à l'ADCC médiée par les nnAbs. Dans l'**article 4**, nous avons élaboré un nouveau marquage intracellulaire capable de détecter Nef et Vpu dans leur forme native par cytométrie en flux, ce qui nous a permis de confirmer que la régulation négative de CD4 par ces deux protéines représente le facteur principal dictant la susceptibilité des cellules infectées à l'ADCC médiée par les sérums VIH+. Ce nouvel outil peut également servir à surveiller l'expression adéquate de Nef et Vpu dans les constructions virales.

ARTICLE 2

Les cellules non-infectées affectent la quantification de la réponse ADCC contre les cellules infectées par le VIH-1

Uninfected Bystander Cells Impact the Measurement of HIV-Specific Antibody-Dependent Cellular Cytotoxicity Responses

Auteurs:

Jonathan Richard[1,2], Jérémie Prévost[1,2], Amy E. Baxter[1,2], Benjamin von Bredow[3], Shilei Ding[1,2], Halima Medjahed[1], Gloria G. Delgado[1], Nathalie Brassard[1], Christina M. Stürzel[4], Frank Kirchhoff[4], Beatrice H. Hahn[5], Matthew S. Parsons[6], Daniel E. Kaufmann[1,7,8], David T. Evans[3,9], Andrés Finzi[1,2,10]

Affiliations:

[1]Centre de Recherche du CHUM, Montreal, QC, Canada; [2]Department of Microbiology, Infectiology and Immunology, Université de Montréal, Montreal, QC, Canada; [3]Department of Pathology and Laboratory Medicine, University of Wisconsin, Madison, WI, USA; [4]Institute of Molecular Virology, Ulm University Medical Center, Ulm, Germany; [5]Departments of Medicine and Microbiology, Perelman School of Medicine, University of Pennsylvania, Philadelphia, PA, USA; [6]Department of Microbiology and Immunology, The University of Melbourne, at The Peter Doherty Institute for Infection and Immunity, Melbourne, VIC, Australia; [7]Department of Medicine, Université de Montréal, Montreal, QC, Canada; [8]Center for HIV/AIDS Vaccine Immunology and Immunogen Discovery, The Scripps Research Institute, La Jolla, CA, USA; [9]Wisconsin National Primate Research Center, University of Wisconsin, Madison, WI, USA; [10]Department of Microbiology and Immunology, McGill University, Montreal, QC, Canada.

Contribution des auteurs:

Conceptualisation: J.R., **J.P.**, M.S.P. et A.F.; Méthodologie: J.R., **J.P.**, A.E.B., B.V.B., M.S.P., D.E.K., D.T.E. et A.F.; Recherche: J.R., **J.P.**, A.E.B., B.V.B., S.D. et M.S.P.; Ressources: H.M., G.G.D., N.B., C.M.S., F.K., B.H.H., D.E.K. et A.F.; Analyse formelle: J.R.; Visualisation: J.R. et A.E.B.; Supervision: D.E.K., D.T.E. et A.F.; Obtention du financement: M.S.P., D.E.K., D.T.E. et A.F.; Rédaction - version originale: J.R. et A.F.; Rédaction - révision et édition: **Tous les auteurs**.

Statut: Cet article a été publié dans *mBio*, le 20 mars 2018.

https://doi.org/10.1128/mBio.00358-18

3.2.1 RÉSUMÉ

La conformation des glycoprotéines d'enveloppe (Env) du VIH-1 a un impact considérable sur la reconnaissance des anticorps et la réponse cytotoxique cellulaire dépendante des anticorps (ADCC). En l'absence du récepteur CD4 à la surface cellulaire, l'Env des virus primaires adopte une conformation « fermée » qui dissimule les épitopes induits par CD4 (CD4i). Le virus contrôle l'expression de CD4 par l'action des protéines accessoires Nef et Vpu, protégeant ainsi les cellules infectées de la réponse ADCC. Cependant, la gp120 excrétée par les cellules infectées peut se lier au CD4 présent sur les cellules non-infectées, les sensibilisant ainsi à l'ADCC médiée par les anticorps CD4i. Nous avons donc émis l'hypothèse que ces cellules non-infectées avoisinantes pourraient avoir un impact sur l'interprétation des mesures d'ADCC. Pour étudier cette hypothèse, nous avons évalué la capacité des anticorps contre les épitopes CD4i (nnAbs) et des anticorps neutralisants à large spectre (bNAbs) à médier l'ADCC mesuré par cinq techniques d'ADCC couramment utilisées dans le domaine. Nos résultats indiquent que les cellules non-infectées recouvertes de gp120 sont reconnues efficacement par les nnAbs, mais pas par les bNAbs. Par conséquent, les cellules non-infectées affectent considérablement les mesures d'ADCC *in vitro* effectuées avec des techniques qui ne permettent pas de différencier la réponse ADCC dirigée contre les cellules infectées par rapport aux cellules non-infectées. De plus, en utilisant une technique de cytométrie en flux pouvant détecter l'ARNm du virus, permettant ainsi de détecter les cellules infectées de manière productive, nous avons constaté que la grande majorité des cellules infectées par le VIH-1 provenant de cultures *in vitro* ou d'échantillons *ex vivo* provenant de personnes infectées par le VIH-1 sont CD4 négatives et n'exposent donc pas des niveaux significatifs d'épitopes CD4i. Dans l'ensemble, nos résultats indiquent que les techniques d'ADCC incapables de différencier les réponses contre les cellules infectées et non-infectées surestiment les réponses médiées par les anticorps CD4i.

3.2.2 ABSTRACT

The conformation of the HIV-1 envelope glycoprotein (Env) substantially impacts antibody recognition and antibody-dependent cellular cytotoxicity (ADCC) responses. In the absence of the CD4 receptor at the cell surface, primary Envs sample a "closed" conformation that occludes CD4-induced (CD4i) epitopes. The virus controls CD4 expression through the actions of Nef and Vpu accessory proteins, thus protecting infected cells from ADCC responses. However,

gp120 shed from infected cells can bind to CD4 present on uninfected bystander cells, sensitizing them to ADCC mediated by CD4i antibodies (Abs). Therefore, we hypothesized that these bystander cells could impact the interpretation of ADCC measurements. To investigate this, we evaluated the ability of antibodies to CD4i epitopes and broadly neutralizing Abs (bNAbs) to mediate ADCC measured by five ADCC assays commonly used in the field. Our results indicate that the uninfected bystander cells coated with gp120 are efficiently recognized by the CD4i ligands but not the bNAbs. Consequently, the uninfected bystander cells substantially affect in vitro measurements made with ADCC assays that fail to identify responses against infected versus uninfected cells. Moreover, using an mRNA flow technique that detects productively infected cells, we found that the vast majority of HIV-1-infected cells in in vitro cultures or ex vivo samples from HIV-1-infected individuals are CD4 negative and therefore do not expose significant levels of CD4i epitopes. Altogether, our results indicate that ADCC assays unable to differentiate responses against infected versus uninfected cells overestimate responses mediated by CD4i ligands.

3.2.3 IMPORTANCE

Emerging evidence supports a role for antibody-dependent cellular cytotoxicity (ADCC) in protection against HIV-1 transmission and disease progression. However, there are conflicting reports regarding the ability of non-neutralizing antibodies targeting CD4-inducible (CD4i) Env epitopes to mediate ADCC. Here, we performed a side-by-side comparison of different methods currently being used in the field to measure ADCC responses to HIV-1. We found that assays which are unable to differentiate virus-infected from uninfected cells greatly overestimate ADCC responses mediated by antibodies to CD4i epitopes and underestimate responses mediated by broadly neutralizing antibodies (bNAbs). Our results strongly argue for the use of assays that measure ADCC against HIV-1-infected cells expressing physiologically relevant conformations of Env to evaluate correlates of protection in vaccine trials.

3.2.4 INTRODUCTION

Antibody-dependent cellular cytotoxicity (ADCC) represents a major effector mechanism used by the immune system to target and eliminate virally infected cells. Besides being incorporated into viral particles, the HIV-1 envelope glycoprotein (Env) trimer represents the only virus-specific target exposed on the surface of infected cells and thus represents a major target for ADCC (1). Emerging evidence suggests that Env conformation plays a critical role in the susceptibility of HIV-1-infected cells to ADCC (2, 3). HIV-1 Env is a metastable molecule, which is driven by CD4 receptor engagement to transition from its unliganded "closed" high-energy conformation (state 1) into an intermediate "partially open" conformation (state 2) and then into a more open CD4-bound conformation (state 3) (4). Interaction of Env with the CD4 receptor was reported to be critical for the exposure of epitopes for ADCC-mediating antibodies (Abs) (5–7). Accordingly, ADCC-mediating Abs naturally present in sera from HIV-1- infected individuals (HIV^+ sera) preferentially target HIV-1-infected cells that present Env in states 2 and 3 (5, 8). In line with this observation, ADCC activity present in sera from HIV-1-infected individuals (HIV^+ sera) is predominantly mediated by the anti-cluster A Abs (5, 9–11, 14). These non-neutralizing antibodies (nnAbs) target a highly conserved region in the gp120 inner domain that is buried inside the closed unliganded Env and becomes exposed only upon CD4 engagement (6, 7, 10–14). Thus, cells infected with primary viruses that expose Env in its closed unliganded conformation are largely resistant to ADCC induced by these nnAbs (7, 10, 15–19).

To protect HIV-1-infected cells from ADCC by naturally occurring CD4-induced (CD4i) Abs, the virus has evolved several strategies to limit the adoption of the CD4-bound conformation and thus prevent exposure of vulnerable CD4i epitopes. HIV-1 limits Env-CD4 interaction by both downregulating CD4 and preventing Env accumulation at the surface of infected cells (5, 7, 20–22). Two accessory proteins, Nef and Vpu, reduce cell surface expression of CD4 (5, 7), while Env accumulation is tightly controlled through efficient internalization (22) and Vpu-mediated BST-2 downregulation (20, 21, 23). Therefore, Nef and Vpu play a central role in protecting HIV-infected cells from ADCC by averting the premature exposure of vulnerable epitopes.

While HIV-1-infected cells are generally protected from ADCC, we recently found that uninfected bystander $CD4^+$ T cells are susceptible to ADCC mediated by CD4i ligands (16). It has

been well established that due to its noncovalent association with gp41, gp120 sheds from the surface of productively infected cells (13, 24, 25). Binding of shed gp120 to the CD4 receptor on the surface of uninfected bystander cells exposes vulnerable CD4i ADCC epitopes and results in the sensitization of these cells to ADCC (16). However, the extent to which exposure of these CD4i epitopes on uninfected bystander cells impacts *in vitro* measurements of ADCC has not yet been determined. Many ADCC assays measure killing of total cell population and thus are unable to differentiate ADCC responses against HIV-infected cells from those against uninfected bystander cells. Here, we compared different ADCC assays currently used in the field for their ability to measure HIV-1-infected cell-specific responses. We found that uninfected bystander cells greatly impact *in vitro* measurements of ADCC by introducing a significant bias toward CD4i Abs.

3.2.5 RESULTS

Differential recognition of uninfected bystander cells and infected cells by ADCC-mediating Abs.

We first explored the capacity of different ADCC-mediating Abs to recognize uninfected bystander cells versus productively infected cells. To this end, we infected primary $CD4^+$ T cells from HIV-1-uninfected individuals with a previously reported wild-type (WT) HIV-1 strain that encodes all accessory proteins as well as a *gfp* reporter gene and the R5-tropic (ADA) envelope (NL4.3 ADA green fluorescent protein [GFP]) (7, 16). In this system, productively infected cells are GFP^+, whereas GFP^- cells represent the uninfected bystander cells. Forty-eight hours post-infection, the average percentage of infected cells was 12.6%. At this step, cells were incubated with HIV^+ sera, the nnAb A32, or a broadly neutralizing Ab (bNAb) (either PGT126 or 3BNC117). The cluster A-specific monoclonal antibody (mAb) A32 recognizes a highly conserved CD4i epitope located at the interface of the gp120 inner domain layers 1 and 2 (7, 11–13). As previously reported, productively infected (GFP^+) cells were poorly recognized by A32 as well as HIV^+ sera (16), while mock-infected cells were not recognized (**Fig. 3.1.1A to C**). This weak recognition of infected cells is likely due to the efficient downregulation of CD4 by Nef and Vpu (see **Fig. 3.1.S1** in the supplemental material), which permits Env to retain its "closed" conformation. In contrast, uninfected bystander (GFP^-) cells from the same culture were readily recognized by A32 and HIV^+

sera (**Fig. 3.1.1A and B**). As most cells present in the culture are gp120-coated uninfected bystander cells (16), strong binding was detected for A32 and HIV$^+$ sera when Ab binding was measured for the total cell population (i.e., both uninfected and infected cells) (**Fig. 3.1.1B**). Of note, sera from HIV-1-uninfected individuals (HIV$^-$ sera) did not react with any cell population (**Fig. 3.1.1C**).

In contrast to nnAbs, bNAbs preferentially recognize Env in its closed conformation (4). PGT126 binds a conserved region at the V3 loop stem near the N332 glycosylation site (26–28), while 3BNC117 recognizes the CD4-binding site (29). Both bNAbs were previously found to mediate ADCC against HIV-1-infected cells (18, 21, 30–32). Consistent with these findings, PGT126 and 3BNC117 efficiently recognized productively infected cells (GFP$^+$) but not the uninfected GFP$^-$ cells (**Fig. 3.1.1A and B**). As expected, since the majority of the cells in the culture are not recognized by these Abs, the overall (total) signal obtained with these Abs was lower than the signal obtained with A32 or HIV$^+$ sera (**Fig. 3.1.1B**). In agreement with the role of Nef and Vpu in preventing the formation of CD4i epitopes through CD4 downregulation (**Fig. 3.1.S1**), deletion of these accessory genes dramatically increased recognition of infected (GFP$^+$) cells by A32 and HIV$^+$ sera (**Fig. 3.1.1C**). To rule out the possibility that these phenotypes were related to the viral strain used, we also used primary CD4$^+$ T cells infected with the transmitted founder (TF) virus CH77 and obtained similar recognition patterns (**Fig. 3.1.S2**). Altogether, these results indicate that CD4i ligands recognize uninfected bystander cells coated with shed gp120 more efficiently than Abs preferentially recognizing the closed trimer.

Assays measuring ADCC against productively infected cells reveal greater killing of infected cells by bNAbs than by CD4i Abs.

To evaluate the potential impact of the uninfected bystander cell population on ADCC, we compared different assays currently used in the field to detect ADCC responses against WT-infected cells using the A32, PGT126, or 3BNC117 MAb or human sera. We initially tested assays designed to distinguish ADCC responses against infected cells from those against uninfected bystander cells. These included the fluorescence-activated cell sorting (FACS)-based infected-cell elimination (ICE) assay, in which ADCC-mediated elimination of productively infected cells is determined by calculating the loss of infected cells using a GFP-expressing virus (5, 7, 10, 16) or

by measuring intracellular HIV-1 p24 antigen (10, 15, 17, 32). Using primary $CD4^+$ T cells infected with the NL4.3 ADA GFP WT virus as target cells and autologous peripheral blood mononuclear cells (PBMCs) as effector cells, we found that WT-infected cells were significantly more susceptible to ADCC mediated by PGT126 and 3BNC117 than to that mediated by A32 (**Fig. 3.1.2A**). Furthermore, WT-infected cells were largely resistant to ADCC responses mediated by A32 (**Fig. 3.1.2B**, gray bars) and responses mediated by HIV^+ sera were comparable to those seen with HIV^- sera (**Fig. 3.1.2C**, gray circles). Again, deletion of *nef* and *vpu* genes drastically increased ADCC responses mediated by A32 and HIV^+ sera (**Fig. 3.1.2B and C**, black bars and circles, respectively), confirming the dependence of this killing on Env-CD4 interaction.

Measurement of ADCC-mediated elimination of infected cells was also conducted using a luciferase assay (33). In this assay, infected CEM.NKr-CCR5-sLTR-Luc cells expressing a Tat-driven luciferase reporter gene serve as target cells, while human PBMCs or a $CD16^+$ NK cell line is used as effector cells (18, 21, 22, 33). As luciferase is expressed only upon productive HIV-1 infection, elimination of infected cells can be calculated by the loss of luciferase activity. Since this assay measures the elimination of productively infected (Tat-expressing) cells, we observed ADCC responses very similar to those obtained with the FACS-based ICE assay (compare **Fig. 3.1.2A to C** with **D to F**; **Fig. 3.1.S3**). ADCC responses mediated by PGT126 and 3BNC117 were significantly higher than those obtained with A32. HIV^+ sera and A32 mediated robust ADCC responses only against cells infected with the *nef- vpu-* virus (**Fig. 3.1.2E and F**). Similar results were obtained using target cells infected with the transmitted founder CH77 virus (**Fig. 3.1.S4**). These results confirm the increased ability of bNAbs to mediate ADCC responses against infected cells compared to CD4i Abs.

Assays measuring ADCC activities on the total cell population overestimate the responses mediated by CD4i Abs.

The two assays described above are able to distinguish between HIV-1-infected and uninfected bystander cells. Other ADCC methods, however, assess killing on the total cell population (i.e., uninfected and infected cells). Given that the binding of shed gp120 on uninfected bystander cells enables recognition of these cells by CD4i Abs but not bNAbs, we hypothesized that these assays would primarily detect killing of bystander cells.

To investigate this, we performed a similar series of experiments as in **Fig. 3.1.2** but measured ADCC using assays that detect killing within the total cell population: the granzyme B assay and the NK cell activation assay. The granzyme B assay (GranToxiLux or Pantoxilux assay) detects granzyme B activity in target cells upon incubation with NK cells and Abs or sera (34–36). Since this assay is not compatible with the permeabilization step required to perform intracellular p24 staining, the user cannot differentiate productively infected cells from uninfected bystander cells. Similarly, the NK cell activation assay, which measures NK activation markers (CD107a and interferon gamma [IFN-γ]), is unable to determine which cell population (infected or uninfected) leads to NK cell activation (20, 37–40). The ADCC responses detected with the granzyme B and NK cell activation assays were strikingly different from those measured with the FACS-based ICE and luciferase assays (compare **Fig. 3.1.2 to 3.1.3A to F**). Strong responses were detected against WT-infected targets using A32, while weak responses were observed with PGT126 and 3BNC117 (**Fig. 3.1.3A and D**). Similarly, robust granzyme B activity and NK cell activation were detected with HIV^+ sera in the context of WT-infected target cells but not with HIV^- sera (**Fig. 3.1.3C and F**), while both assays were unable to detect the protective effect of Nef and Vpu accessory proteins on ADCC responses (**Fig. 3.1.3B, C, E, and F and 3.1.S5**). Results obtained with granzyme B and NK activation were similar to those obtained with the FACS-based ICE assay when responses were calculated for the total population (GFP^- and GFP^+) rather than by gating on productively infected (GFP^+) cells (**Fig. 3.1.3G to I**). Moreover, while assays measuring the elimination of productively infected cells (FACS-based and luciferase assays) showed a positive correlation between antibody binding and ADCC (**Fig. 3.1.4A and B**), no such correlation was observed with assays that measured killing of total targets (granzyme B, NK activation, or FACS-based ICE on total cell population) (**Fig. 3.1.4C to E**). Thus, assays relying on the assessment of ADCC responses on the total cell population overestimate ADCC responses mediated by CD4i Abs and at the same time underestimate responses mediated by bNAbs.

Most ADCC activity detected using total cell target population is directed against uninfected bystander cells.

Since A32 and HIV$^+$ sera preferentially recognize uninfected bystander cells (**Fig. 3.1.1**), we hypothesized that most of the ADCC responses detected with the granzyme B and NK activation assays were directed against such cells. To test this possibility, uninfected bystander cells (GFP$^-$ CD4$^+$) were removed from the infected coculture using beads coated with an anti-CD4 antibody that does not compete for gp120 binding (see Materials and Methods) (**Fig. 3.1.5A**). These uninfected bystander cells were replaced by the same number of autologous mock-infected cells (i.e., never exposed to HIV) prior to ADCC measurements. Importantly, this procedure did not affect the percentage of productively infected cells (percent GFP$^+$ CD4$^-$) in the cell culture (**Fig. 3.1.5A and B**). As expected, the replacement of uninfected bystander cells by mock-infected cells did not alter recognition of infected GFP$^+$ cells but decreased the proportion of uninfected bystander cells recognized by A32 (**Fig. 3.1.5C and D**). This replacement also dramatically reduced ADCC responses mediated by both A32 and HIV$^+$ sera using both the granzyme B and NK cell activation assays (**Fig. 3.1.6**). Finally, removal of bystander cells resulted in a positive correlation between the abilities of A32 and HIV$^+$ sera to recognize infected cells and trigger ADCC responses (**Fig. 3.1.6E**). Thus, uninfected bystander cells greatly influence the measurement of ADCC responses by assays that cannot distinguish infected from uninfected cells.

Measurement of ADCC responses using gp120-coated cells preferentially detects CD4i-mediated ADCC responses.

Cells coated with recombinant gp120 are frequently used as target cells to assess the ADCC activity of monoclonal antibodies (mAbs) or sera from HIV-1-infected or vaccinated individuals (9, 14, 34, 40–50). In these assays, CD4$^+$ target cells are incubated with recombinant gp120 monomers, which adopt a CD4-bound conformation on the target cells and expose surfaces of the protein that are normally occluded in native Env trimers (51). We thus evaluated Ab binding and ADCC responses using gp120-coated target cells. The NK cell-resistant cell line CEM.NKr was coated with recombinant gp120 and subsequently used as target cells to measure ADCC (41). As predicted from results in **Fig. 3.1.1**, gp120-coated CEM.NKr cells were efficiently recognized by A32 and HIV$^+$ sera but not by HIV$^-$ sera (**Fig. 3.1.7A and B**) or PGT126 and 3BNC117 (**Fig. 3.1.7A and B**). This was also the case when the rapid fluorometric ADCC assay (RFADCC assay) (41), which uses gp120-coated target cells to detect ADCC responses, was used for analysis (12, 14, 40, 43, 44, 52). As presented in **Fig. 3.1.7C and D and 3.1.S6**, robust responses were detected

with A32 and HIV$^+$ sera but not with PGT126, 3BNC117, or HIV$^-$ sera (**Fig. 3.1.7C and D**). Thus, gp120-coated target cells detected ADCC responses largely mediated by CD4i antibodies and not by bNAbs capable of recognizing functional Env trimers, such as antibodies to the CD4-binding site or to a proteoglycan epitope in the V3 region.

A32 preferentially recognizes CD4$^+$ p24$^-$ cells not expressing HIV-1 *gag-pol* mRNA.

Our results suggest that A32 preferentially targets uninfected bystander cells rather than productively infected cells (**Fig. 3.1.2 and 3.1.5**), although anti-cluster A Abs, such as A32, were initially identified as potent ADCC-mediating Abs (9, 14). Therefore, we could not exclude the possibility that the cells detected as bystander cells in our assays were infected but below the limit of detection. To investigate this possibility, we used a previously described RNA-flow fluorescence *in situ* hybridization (FISH) method (53, 54). This method identifies productively infected cells by visualizing cellular HIV-1 *gag-pol* mRNA by *in situ* RNA hybridization and intracellular Ab staining for the HIV-1 p24 protein. This approach is 1,000-fold more sensitive than p24 staining alone, with a detection limit of 0.5 to 1 *gag-pol* mRNA$^+$/p24 protein$^+$ infected cell per million CD4$^+$ T cells (53, 54). The sensitivity of the assay is high, since a cell is reliably identified as *gag-pol* mRNA$^+$ if it contains more than 20 copies of HIV-1 mRNA. Thus, this technique can distinguish infected cells from uninfected bystander cells with high specificity and sensitivity.

For these experiments, primary CD4$^+$ T cells were infected with the NL4.3 ADA GFP WT virus, and 48 h post-infection, the average percentage of infection was 8.0%. Infected cells were stained first with A32 before staining for phenotypic markers, such as CD4. Cells were then fixed and permeabilized to allow detection of the HIV-1 p24 antigen and *gag-pol* mRNA. We first tested whether CD4 T cells recognized by A32 were positive for *gag-pol* mRNA (**Fig. 3.1.8A and 3.1.B**) but found that less than 2% of these cells contained p24 protein or *gag-pol* mRNA. In contrast, the vast majority of A32- negative cells were positive for p24 protein (73.03%) or gag-pol mRNA (78.04%). This confirmed that the vast majority of CD4$^+$ T cells recognized by A32 are uninfected bystander cells.

It remained possible, however, that the cells detected as p24^{-} *gag-pol* mRNA^{-} were in a very early stage of infection, before viral protein and mRNA could be detected. Indeed, previous studies have suggested that A32-like epitopes become transiently exposed during viral entry (55, 56). To investigate this possibility, uninfected bystander (GFP^{-}) cells were sorted by flow cytometry to determine how many could become productively infected. After 5 additional days in cell culture, less than 3% of sorted GFP^{-} cells became infected (**Fig. 3.1.S7**). Thus, most cells recognized by A32 are neither productively infected nor in a very early stage of infection.

Since Env-CD4 interaction is critical for exposure of the A32 epitope (5–7), we next analyzed the RNA-flow FISH results based on p24 and CD4 expression. As shown in **Fig. 3.1.8C and D**, CD4^{+} p24^{-} cells were efficiently recognized by A32 (blue bars) but remained almost exclusively negative for *gag-pol* mRNA (red bars). Inversely, the CD4^{-} p24^{+} population was largely positive for *gag-pol* mRNA but was not recognized by A32. More recent studies suggested that the A32 epitope could be exposed on a fraction of p24^{+} cells because of residual CD4 expression (42, 57, 58). Therefore, we next quantified the recognition by A32 and infection of these p24^{+} CD4^{+} cells by RNA-flow FISH (dark gray box, **Fig. 3.1.8C**). Although this rare population was indeed recognized, only a fraction of A32-positive cells was productively infected (~20%). Similar results were obtained with primary CD4^{+} T cells infected with an X4-tropic virus (**Fig. 3.1.S8**). Finally, we determined the proportion of *gag-pol* mRNA^{+} cells that were both p24^{+} and CD4^{+} and found less than 5% of such cells that could be recognized by A32 (**Fig. 3.1.8E**). We also performed the reverse analysis by first identifying A32^{+} CD4^{+} T cells and then determining how many of those cells were both p24 and CD4 positive. Since only ~1% of such cells were CD4^{+} p24^{+} (**Fig. 3.1.8F**), it seems clear that A32^{+} cells represent only a minuscule fraction of productively HIV-1-infected CD4^{+} T cells.

To determine whether *gag-pol* mRNA-containing CD4^{+} p24^{+} cells were present in the peripheral blood of HIV-1-infected individuals, we isolated CD4^{+} T cells from the blood of untreated chronically HIV-1-infected individuals, rested them overnight without stimulation, and then performed the RNA-flow FISH assay (**Fig. 3.1.9A and B**). Again, the CD4^{+} p24^{+} cell population represented only a minimal fraction of the *gag-pol* mRNA^{+} cells. Therefore, *in vivo* A32 is unlikely to recognize most HIV-1-infected cells.

3.2.6 DISCUSSION

The conformation adopted by Env at the cell surface has considerable influence on Ab recognition and ADCC responses (2). In its unliganded form, Env from most primary virus samples adopts a "closed" trimeric conformation, preferentially recognized by bNAbs but not by CD4i Abs, which are abundant in plasma from most HIV-1-infected individuals (2, 4, 10, 15–18, 23, 59, 60, 86). One of the mechanisms that HIV-1 has developed to avoid exposing Env CD4i epitopes is the downregulation of CD4 cell surface expression. This is achieved in a two-step process. First, during the early phases of the HIV-1 replication cycle, Nef downregulates CD4 from the plasma membrane. Second, Vpu, expressed from a bicistronic mRNA also coding for Env, induces CD4 degradation through an endoplasmic reticulum (ER)-associated protein degradation (ERAD) mechanism in the ER (61). The action of Vpu liberates Env from CD4-dependent retention in the ER (62), allowing its trafficking to the plasma membrane in a "closed" conformation in which CD4i epitopes are occluded by oligomerization. These epitopes, however, are exposed in shed gp120 monomers that are released by the dissociation of the non-covalent gp120-gp41 interactions. Interestingly, *in vitro* experiments have shown that the binding of shed gp120 to uninfected bystander $CD4^+$ T cells enables recognition of these cells by CD4i antibodies (16). Of note, this was seen using a variety of HIV-1 variants, including primary or transmitted founder viruses (**Fig. 3.1.1 and 3.1.S2**) (16, 17, 58, 63), as well as simian-human immunodeficiency virus (SHIV) infectious molecular clones (16).

Here, we demonstrate that the uninfected bystander $CD4^+$ T cell population, which is coated with shed gp120, represents a confounding factor when measuring ADCC responses *in vitro*. Using assays that are unable to differentiate infected from uninfected cell populations, we observed strong killing mediated by A32 and HIV^+ sera (**Fig. 3.1.3**). This ADCC activity was not correlated with the inability of these antibodies to recognize infected cells (**Fig. 3.1.1 and 3.1.4**). Replacement of gp120-coated uninfected bystander $CD4^+$ T cells with autologous mock-infected cells confirmed that most of the detected activities were directed against uninfected $CD4^+$ T cells (**Fig. 3.1.5 and 3.1.6**). Using a sensitive RNA-flow FISH method, we next showed that A32 preferentially recognizes $CD4^+$ cells that are negative for HIV-1 p24 and *gag-pol* mRNA (**Fig. 3.1.8**), while fewer than 2% of productively infected cells ($p24^+$ *gag-pol* $mRNA^+$) were recognized

by this antibody. Although this population remains to be defined further, these cells likely represent virus-coated cells on which the A32 epitope has been transiently exposed as a result of the high density of Env-CD4 interactions, a possibility supported by the fact that they do not form a distinct population in FACS analyses but form a shoulder of the p24-negative population. The extent to which this cell population exists *in vivo*, and the ability of Fcγ receptor-bearing cells to gain access to CD4i epitopes, remains unknown. In contrast, the vast majority of productively infected cells were $CD4^-$, both *in vitro* and in *ex vivo* samples from HIV-1-infected individuals. Consistent with poor recognition of infected cells by A32 and HIV^+ sera, *in vitro* assays able to determine ADCC responses against infected cells failed to detect robust ADCC responses mediated by these ligands (**Fig. 3.1.2**). This was not due to a lack of sensitivity, since these assays readily detected ADCC responses mediated by the bNAbs PGT126 and 3BNC117 (**Fig. 3.1.2**). Thus, assays measuring responses on the total population missed the ADCC activity mediated by these bNAbs.

The results of our study highlight the difficulties in selecting an appropriate assay to measure ADCC. If ADCC is measured on the total population (granzyme B and NK cell activation), A32 and HIV^+ sera appear to mediate a stronger ADCC response than PGT126 and 3BNC117. On the other hand, assays that can evaluate responses against infected cells show the opposite: PGT126 and 3BNC117 mediate significantly higher ADCC responses than A32 and HIV^+ sera. It seems clear that ligand recognition of gp120-coated uninfected bystander $CD4^+$ T cells is, at least in part, responsible for these differences. Indeed, removal of these cells significantly reduced the ADCC activity detected for A32 and HIV^+ sera. Therefore, the differential recognition of the uninfected bystander cell population by any given ligand has a significant impact on *in vitro* ADCC measurements. It is well established that HIV-1 accessory proteins Nef and Vpu protect HIV-1-infected cells from ADCC responses (5, 7, 10, 15, 19–21, 64, 65). Assays measuring the elimination of infected cells were able to confirm these observations (**Fig. 3.1.2, 3.1.S3, and 3.1.S4**), while those that measure the total population (granzyme B and NK cell activation) failed to do so (**Fig. 3.1.3**). Thus, the presence of gp120-coated uninfected bystander $CD4^+$ T cells confounds *in vitro* ADCC measurements.

Previous reports demonstrated that the majority of ADCC activity present in HIV$^+$ sera is mediated by anti-cluster A antibodies (9–11, 14). These antibodies preferentially target Env in its CD4-bound conformation (5, 8). Intriguingly, we observed variable ADCC activity among the different HIV$^+$ sera tested (**Fig. 3.1.2, 3.1.3, and 3.1.6**). It is possible that differences in their concentration in sera account for some of this variability. However, we cannot rule out that the presence of additional ADCC-mediating Abs that do not require the CD4-bound conformation of Env to recognize infected cells, or that target the gp41, might also contribute to this variable ADCC activity.

While passive administration of ADCC-mediating nnAbs, including A32, has failed to protect macaques against simian immunodeficiency virus (SIV) or SHIV challenges (66–70), several studies have identified ADCC responses measured against total cell population or gp120-coated target cells as correlates of protection in these same animal models (45, 71–74). Moreover, CD4i vaccines have been reported to protect macaques from viral challenge (45, 72). Since Env conformation greatly influences ADCC responses (8), it is possible that the conformation of Env in the challenge viruses impacted the reported protection efficacy. It is conceivable that the Env of these challenge stocks sampled a slightly more "open" conformation, readily recognized by CD4i Abs but not present in primary viruses (8). For example, non-neutralizing CD4i Abs with ADCC activity, in the presence of low levels in plasma of IgA Env-specific Abs, inversely correlated with HIV-1 acquisition in the RV144 trial (75). A recent study suggested that the presence of a naturally occurring histidine at position 375 (H375) in the Phe43 cavity of the predominant strain (CRF01_AE) replicating in Thailand might have contributed to the efficacy of the trial by spontaneously exposing epitopes recognized by ADCC-mediating antibodies elicited by the RV144 vaccine regimen (76). Our results warrant further studies to assess the conformation of Envs of current SHIVs used in vaccine efficacy studies.

Since Env conformation and the nature of target cells greatly influence ADCC results, our study highlights the need for careful assay selection. Assays measuring ADCC responses on the total cell population (**Fig. 3.1.3 to 3.1.6**) or using target cells coated with recombinant gp120 (**Fig. 3.1.7**) or infected with viruses defective for Nef and Vpu expression (**Fig. 3.1.2**) favor the detection of ADCC responses mediated by CD4i Abs over those induced by bNAbs. Assays measuring

ADCC responses on the infected-cell population are better suited to evaluate responses mediated by Abs recognizing the CD4-binding site or trimeric Env. Thus, these parameters must be carefully considered before selecting assays for characterizing HIV-1-specific ADCC responses when evaluating responses mediated by monoclonal Abs, mechanisms of immune evasion, or correlates of vaccine protection.

3.2.7 MATERIALS AND METHODS

Ethics statement

Written informed consent was obtained from all study participants (the Montreal Primary HIV Infection Cohort [77, 78] and the Canadian Cohort of HIV Infected Slow Progressors [79–81]), and research adhered to the ethical guidelines of the Centre de Recherche du CHUM (CRCHUM) and was reviewed and approved by the CRCHUM institutional review board (ethics committee approval number CE 16.164-CA). Research adhered to the standards indicated by the Declaration of Helsinki. All participants were adult and provided informed written consent prior to enrollment in accordance with institutional review board approval.

Cell lines and isolation of primary cells

HEK293T human embryonic kidney cells (obtained from ATCC) and CEM.NKr-CCR5-sLTR-Luc cells were grown as previously described (7, 15). Primary human PBMCs, NK cells, and $CD4^+$ T cells were isolated, activated, and cultured as previously described (7, 15) and detailed in the supplemental material.

Viral production and infections

To achieve the same level of infection among the different IMCs (infectious molecular clones) tested, vesicular stomatitis virus G (VSVG)-pseudotyped HIV-1 viruses were produced and titrated as previously described (5). Viruses were then used to infect activated primary CD4 T cells from healthy HIV-1-negative donors or CEM.NKr-CCR5-sLTR-Luc cells by spin infection at 800 × g for 1 h in 96-well plates at 25°C.

Antibodies and sera

A detailed list of the Abs used for cell surface staining, ADCC measurement, and RNA flow analysis is presented in the supplemental material. Sera from HIV-infected and uninfected donors were collected, heat inactivated, and conserved as previously described (7, 15). A random number generator (QuickCalcs; GraphPad, San Diego, CA) was used to randomly select a number of sera for each experiment.

Plasmids and site-directed mutagenesis

pNL43-ADA(Env)-GFP.IRES.Nef proviral vectors containing intact or defective *nef* and *vpu* genes, as well as the VSVG-encoding plasmid (pSVCMV-IN-VSV-G), were previously described (5). The plasmid encoding the HIV-1 transmitted founder (TF) IMC CH77 containing intact or defective *nef* and *vpu* genes was previously described (10, 15, 82–85).

Flow cytometry analysis of cell surface staining

Cell surface staining was performed as previously described (5, 15). Binding of HIV-1-infected cells by sera (1:1,000 dilution), anti-Env MAbs (A32, PGT126, or 3BNC117) (5 µg/ml), or anti-CD4 mAbs (1 µg/ml) was performed at 48 h post-infection. Cells infected with HIV-1 primary isolates were stained intracellularly for HIV-1 p24, using the Cytofix/Cytoperm fixation/permeabilization kit (BD Biosciences, Mississauga, ON, Canada) and the fluorescent anti-p24 mAb (phycoerythrin [PE]-conjugated anti-p24, clone KC57; Beckman Coulter/Immunotech). The percentage of infected cells ($p24^+$ or GFP^+ cells) was determined by gating the living cell population on the basis of the AquaVivid viability dye staining. Samples were analyzed on an LSR II cytometer (BD Biosciences), and data analysis was performed using FlowJo vX.0.7 (Tree Star, Ashland, OR, USA).

Replacement of uninfected bystander cells by autologous mock cells

Uninfected bystander cells (GFP^- $CD4^{high}$ T cells) were removed from the target cell population using the Dynabeads CD4-positive selection kit (Invitrogen) at a ratio of 25 µl of beads per million cells. Enrichment of infected primary GFP^+ $CD4^{low}$ T cells was assessed by cell surface staining with the anti-CD4 OKT4 Ab (**Fig. 3.1.5A**). Uninfected bystander cells were then replaced by the same number of autologous mock cells prior to staining with A32 or performing ADCC measurements.

ADCC measurements

ADCC responses were measured at 48 h post-infection, as described in detail in the supplemental material. For the FACS-based, granzyme B, and NK cell activation assays, mAbs were used at 5 µg/ml and human sera were used at a 1:1,000 dilution. For the luciferase assay, mAbs were used at 0.0024, 0.0098, 0.0390, 0.1563, 0.6250, 2.5, 10, or 40 µg/ml and human sera were used at a dilution of 1:100, 1:400, 1:1,600, 1:6,400, 1:25,600, 1:102,400, 1:409,600, or 1:1,638,400. For the RFADCC assay, mAbs were used at 0.008, 0.04, 0.2, 1, and 5 µg/ml and human sera were used at a dilution of 1:100, 1:400, 1:1,600, 1:6,400, or 1:25,600.

RNA-flow analysis

Samples were processed using the HIV RNA/Gag RNA flow assay as previously described (53, 54). Briefly, for *in vitro* studies, primary $CD4^+$ T cells infected for 48 h were collected and indirectly surface stained for HIV Env using A32 (as described above) before further staining for phenotypic markers. For *ex vivo* studies, $CD4^+$ T cells were isolated from chronically HIV-infected, untreated individuals and rested overnight in the presence of antiretrovirals (zidovudine [AZT] plus T20) in order to block new cycles of infection. In all experiments, cells were labeled with a viability dye (eFluor 506 fixable viability dye; ThermoFisher Scientific) and surface stained for phenotypic markers (CD3, CD4, and exclusion [CD8, CD14, and CD19]), before fixation, permeabilization, and intracellular staining for HIV p24. HIV *gag-pol* mRNA was labeled using the ThermoFisher PrimeFlow kit using probes designed against JR-CSF (53, 54). Samples were acquired on a BD LSR II cytometer (BD Biosciences), and data analysis was performed using FlowJo vX.0.7 (Tree Star).

Statistical analyses

Statistics were analyzed using GraphPad Prism version 6.0.1 (GraphPad, San Diego, CA). Every data set was tested for statistical normality, and this information was used to apply the appropriate (parametric or nonparametric) statistical test. P values of < 0.05 were considered significant.

3.2.8 ACKNOWLEDGMENTS

We thank Dominique Gauchat from the CRCHUM Flow Cytometry Platform for technical assistance, Mario Legault for cohort coordination and clinical samples, IAVI for PGT126, and Michel Nussenzweig for 3BNC117. This work was supported by CIHR foundation grant 352417 to A.F. Support for this work was also provided by amfAR Innovation grant 109343-59-RGRL with support from FAIR to A.F. and by NIH R01 to A.F. and Marzena Pazgier (AI129769). This study was also supported by NIH AI100645 and AI100663 Centers for HIV/AIDS Vaccine Immunology and Immunogen Design (CHAVI-ID) and by R01 AI 114266 to B.H.H. and the BEAT-HIV Delaney Consortium (UM1 AI 126620). Work by D.T.E. and B.V.B. was supported by National Institutes of Health grants AI121135, AI095098, AI098485, AI055332, and OD011106. F.K. is supported by the DFG CRC 1279 and ERC advanced grant 323035. M.S.P. is funded by grant 1124680 from the National Health and Medical Research Council. A.F. is the recipient of Canada Research Chair on Retroviral Entry RCHS0235. J.R. is the recipient of a Mathilde Krim Fellowship in Basic Biomedical Research from amfAR. J.P. and A.E.B. are recipients of CIHR Fellowship Awards. S.D. is the recipient of an FRSQ postdoctoral fellowship award. D.E.K. is supported by an FRSQ Senior Research Scholar Award. C.M.S. is supported by the German Research Foundation (DFG) and an ERC advanced grant (antivirome). D.T.E. is an Elizabeth Glaser Scientist of the Elizabeth Glaser Pediatric AIDS Foundation. The funders had no role in study design, data collection and analysis, decision to publish, or preparation of the manuscript.

3.2.9 REFERENCES

1. Checkley MA, Luttge BG, Freed EO. 2011. HIV-1 envelope glycoprotein biosynthesis, trafficking, and incorporation. J Mol Biol 410:582– 608.
2. Richard J, Prévost J, Alsahafi N, Ding S, Finzi A. 2017. Impact of HIV-1 envelope conformation on ADCC responses. Trends Microbiol 26:253-265
3. Veillette M, Richard J, Pazgier M, Lewis GK, Parsons MS, Finzi A. 2016. Role of HIV-1 envelope glycoproteins conformation and accessory proteins on ADCC responses. Curr HIV Res 14:9 –23.

4. Munro JB, Gorman J, Ma X, Zhou Z, Arthos J, Burton DR, Koff WC, Courter JR, Smith AB, III, Kwong PD, Blanchard SC, Mothes W. 2014. Conformational dynamics of single HIV-1 envelope trimers on the surface of native virions. Science 346:759 –763.
5. Veillette M, Coutu M, Richard J, Batraville LA, Dagher O, Bernard N, Tremblay C, Kaufmann DE, Roger M, Finzi A. 2015. The HIV-1 gp120 CD4-bound conformation is preferentially targeted by antibody-dependent cellular cytotoxicity-mediating antibodies in sera from HIV-1-infected individuals. J Virol 89:545–551.
6. Veillette M, Coutu M, Richard J, Batraville LA, Désormeaux A, Roger M, Finzi A. 2014. Conformational evaluation of HIV-1 trimeric envelope glycoproteins using a cell-based ELISA assay. J Vis Exp (91):e51995.
7. Veillette M, Désormeaux A, Medjahed H, Gharsallah NE, Coutu M, Baalwa J, Guan Y, Lewis G, Ferrari G, Hahn BH, Haynes BF, Robinson JE, Kaufmann DE, Bonsignori M, Sodroski J, Finzi A. 2014. Interaction with cellular CD4 exposes HIV-1 envelope epitopes targeted by antibody-dependent cell-mediated cytotoxicity. J Virol 88:2633–2644.
8. Prévost J, Richard J, Ding S, Pacheco B, Charlebois R, Hahn BH, Kaufmann DE, Finzi A. 2018. Envelope glycoproteins sampling states 2/3 are susceptible to ADCC by sera from HIV-1-infected individuals. Virology 515: 38 – 45.
9. Ferrari G, Pollara J, Kozink D, Harms T, Drinker M, Freel S, Moody MA, Alam SM, Tomaras GD, Ochsenbauer C, Kappes JC, Shaw GM, Hoxie JA, Robinson JE, Haynes BF. 2011. An HIV-1 gp120 envelope human monoclonal antibody that recognizes a C1 conformational epitope mediates potent antibody-dependent cellular cytotoxicity (ADCC) activity and defines a common ADCC epitope in human HIV-1 serum. J Virol 85: 7029 – 7036.
10. Ding S, Veillette M, Coutu M, Prévost J, Scharf L, Bjorkman PJ, Ferrari G, Robinson JE, Stürzel C, Hahn BH, Sauter D, Kirchhoff F, Lewis GK, Pazgier M, Finzi A. 2015. A highly conserved residue of the HIV-1 gp120 Inner domain is important for antibody-dependent cellular cytotoxicity responses mediated by anti-cluster A antibodies. J Virol 90:2127–2134.
11. Tolbert WD, Gohain N, Veillette M, Chapleau JP, Orlandi C, Visciano ML, Ebadi M, DeVico AL, Fouts TR, Finzi A, Lewis GK, Pazgier M. 2016. Paring down HIV Env: design

and crystal structure of a stabilized inner domain of HIV-1 gp120 displaying a major ADCC target of the A32 region. Structure 24:697–709.

12. Acharya P, Tolbert WD, Gohain N, Wu X, Yu L, Liu T, Huang W, Huang CC, Kwon YD, Louder RK, Luongo TS, McLellan JS, Pancera M, Yang Y, Zhang B, Flinko R, Foulke JS, Jr., Sajadi MM, Kamin-Lewis R, Robinson JE, Martin L, Kwong PD, Guan Y, DeVico AL, Lewis GK, Pazgier M. 2014. Structural definition of an antibody-dependent cellular cytotoxicity response implicated in reduced risk for HIV-1 infection. J Virol 88:12895–12906.
13. Finzi A, Xiang SH, Pacheco B, Wang L, Haight J, Kassa A, Danek B, Pancera M, Kwong PD, Sodroski J. 2010. Topological layers in the HIV-1 gp120 inner domain regulate gp41 interaction and CD4-triggered conformational transitions. Mol Cell 37:656 – 667.
14. Guan Y, Pazgier M, Sajadi MM, Kamin-Lewis R, Al-Darmarki S, Flinko R, Lovo E, Wu X, Robinson JE, Seaman MS, Fouts TR, Gallo RC, DeVico AL, Lewis GK. 2013. Diverse specificity and effector function among human antibodies to HIV-1 envelope glycoprotein epitopes exposed by CD4 binding. Proc Natl Acad Sci USA 110:E69 –E78.
15. Richard J, Veillette M, Brassard N, Iyer SS, Roger M, Martin L, Pazgier M, Schön A, Freire E, Routy JP, Smith AB, III, Park J, Jones DM, Courter JR, Melillo BN, Kaufmann DE, Hahn BH, Permar SR, Haynes BF, Madani N, Sodroski JG, Finzi A. 2015. CD4 mimetics sensitize HIV-1-infected cells to ADCC. Proc Natl Acad Sci USA 112:E2687–E2694.
16. Richard J, Veillette M, Ding S, Zoubchenok D, Alsahafi N, Coutu M, Brassard N, Park J, Courter JR, Melillo B, Smith AB, III, Shaw GM, Hahn BH, Sodroski J, Kaufmann DE, Finzi A. 2016. Small CD4 mimetics prevent HIV-1 uninfected bystander CD4 T cell killing mediated by antibody-dependent cell-mediated cytotoxicity. EBioMedicine 3:122–134.
17. Bruel T, Guivel-Benhassine F, Lorin V, Lortat-Jacob H, Baleux F, Bourdic K, Noël N, Lambotte O, Mouquet H, Schwartz O. 2017. Lack of ADCC breadth of human non-neutralizing anti-HIV-1 antibodies. J Virol 91: e02440-16.
18. von Bredow B, Arias JF, Heyer LN, Moldt B, Le K, Robinson JE, Zolla-Pazner S, Burton DR, Evans DT. 2016. Comparison of antibody-dependent cell-mediated cytotoxicity and virus neutralization by HIV-1 Env-specific monoclonal antibodies. J Virol 90:6127– 6139.

19. Alsahafi N, Ding S, Richard J, Markle T, Brassard N, Walker B, Lewis GK, Kaufmann DE, Brockman MA, Finzi A. 2015. Nef proteins from HIV-1 elite controllers are inefficient at preventing antibody-dependent cellular cytotoxicity. J Virol 90:2993–3002.
20. Alvarez RA, Hamlin RE, Monroe A, Moldt B, Hotta MT, Rodriguez Caprio G, Fierer DS, Simon V, Chen BK. 2014. HIV-1 Vpu antagonism of tetherin inhibits antibody-dependent cellular cytotoxic responses by natural killer cells. J Virol 88:6031– 6046.
21. Arias JF, Heyer LN, von Bredow B, Weisgrau KL, Moldt B, Burton DR, Rakasz EG, Evans DT. 2014. Tetherin antagonism by Vpu protects HIV-infected cells from antibody-dependent cell-mediated cytotoxicity. Proc Natl Acad Sci USA 111:6425– 6430.
22. von Bredow B, Arias JF, Heyer LN, Gardner MR, Farzan M, Rakasz EG, Evans DT. 2015. Envelope glycoprotein internalization protects human and simian immunodeficiency virus-infected cells from antibody-dependent cell-mediated cytotoxicity. J Virol 89:10648 – 10655.
23. Richard J, Prévost J, von Bredow B, Ding S, Brassard N, Medjahed H, Coutu M, Melillo B, Bibollet-Ruche F, Hahn BH, Kaufmann DE, Smith AB, III, Sodroski J, Sauter D, Kirchhoff F, Gee K, Neil SJ, Evans DT, Finzi A. 2017. BST-2 expression modulates small CD4-mimetic sensitization of HIV-1-infected cells to antibody-dependent cellular cytotoxicity. J Virol 91:e00219-17.
24. Helseth E, Olshevsky U, Furman C, Sodroski J. 1991. Human immunodeficiency virus type 1 gp120 envelope glycoprotein regions important for association with the gp41 transmembrane glycoprotein. J Virol 65: 2119 –2123.
25. Yang X, Mahony E, Holm GH, Kassa A, Sodroski J. 2003. Role of the gp120 inner domain beta-sandwich in the interaction between the human immunodeficiency virus envelope glycoprotein subunits. Virology 313: 117–125.
26. Pejchal R, Doores KJ, Walker LM, Khayat R, Huang PS, Wang SK, Stanfield RL, Julien JP, Ramos A, Crispin M, Depetris R, Katpally U, Marozsan A, Cupo A, Maloveste S, Liu Y, McBride R, Ito Y, Sanders RW, Ogohara C, Paulson JC, Feizi T, Scanlan CN, Wong CH, Moore JP, Olson WC, Ward AB, Poignard P, Schief WR, Burton DR, Wilson IA. 2011. A potent and broad neutralizing antibody recognizes and penetrates the HIV glycan shield. Science 334:1097–1103.

27. Walker LM, Huber M, Doores KJ, Falkowska E, Pejchal R, Julien JP, Wang SK, Ramos A, Chan-Hui PY, Moyle M, Mitcham JL, Hammond PW, Olsen OA, Phung P, Fling S, Wong CH, Phogat S, Wrin T, Simek MD, Protocol G Principal Investigators, Koff WC, Wilson IA, Burton DR, Poignard P. 2011. Broad neutralization coverage of HIV by multiple highly potent antibodies. Nature 477:466 – 470.
28. Sok D, Doores KJ, Briney B, Le KM, Saye-Francisco KL, Ramos A, Kulp DW, Julien JP, Menis S, Wickramasinghe L, Seaman MS, Schief WR, Wilson IA, Poignard P, Burton DR. 2014. Promiscuous glycan site recognition by antibodies to the high-mannose patch of gp120 broadens neutralization of HIV. Sci Transl Med 6:236ra63.
29. Scheid JF, Mouquet H, Ueberheide B, Diskin R, Klein F, Oliveira TY, Pietzsch J, Fenyo D, Abadir A, Velinzon K, Hurley A, Myung S, Boulad F, Poignard P, Burton DR, Pereyra F, Ho DD, Walker BD, Seaman MS, Bjorkman PJ, Chait BT, Nussenzweig MC. 2011. Sequence and structural convergence of broad and potent HIV antibodies that mimic CD4 binding. Science 333:1633–1637.
30. Bournazos S, Klein F, Pietzsch J, Seaman MS, Nussenzweig MC, Ravetch JV. 2014. Broadly neutralizing anti-HIV-1 antibodies require Fc effector functions for in vivo activity. Cell 158:1243–1253.
31. Lu CL, Murakowski DK, Bournazos S, Schoofs T, Sarkar D, HalperStromberg A, Horwitz JA, Nogueira L, Golijanin J, Gazumyan A, Ravetch JV, Caskey M, Chakraborty AK, Nussenzweig MC. 2016. Enhanced clearance of HIV-1-infected cells by broadly neutralizing antibodies against HIV-1 in vivo. Science 352:1001–1004.
32. Bruel T, Guivel-Benhassine F, Amraoui S, Malbec M, Richard L, Bourdic K, Donahue DA, Lorin V, Casartelli N, Noël N, Lambotte O, Mouquet H, Schwartz O. 2016. Elimination of HIV-1-infected cells by broadly neutralizing antibodies. Nat Commun 7:10844.
33. Alpert MD, Heyer LN, Williams DE, Harvey JD, Greenough T, Allhorn M, Evans DT. 2012. A novel assay for antibody-dependent cell-mediated cytotoxicity against HIV-1- or SIV-infected cells reveals incomplete overlap with antibodies measured by neutralization and binding assays. J Virol 86:12039 –12052.
34. Pollara J, Hart L, Brewer F, Pickeral J, Packard BZ, Hoxie JA, Komoriya A, Ochsenbauer C, Kappes JC, Roederer M, Huang Y, Weinhold KJ, Tomaras GD, Haynes BF, Montefiori

DC, Ferrari G. 2011. High-throughput quantitative analysis of HIV-1 and SIV-specific ADCC-mediating antibody responses. Cytometry A 79:603–612.

35. Konstantinus IN, Gamieldien H, Mkhize NN, Kriek JM, Passmore JA. 2016. Comparing high-throughput methods to measure NK cell-mediated antibody dependent cellular cytotoxicity during HIV-infection. J Immunol Methods 434:46 –52.
36. Smalls-Mantey A, Doria-Rose N, Klein R, Patamawenu A, Migueles SA, Ko SY, Hallahan CW, Wong H, Liu B, You L, Scheid J, Kappes JC, Ochsenbauer C, Nabel GJ, Mascola JR, Connors M. 2012. Antibody-dependent cellular cytotoxicity against primary HIV-infected CD4 T cells is directly associated with the magnitude of surface IgG binding. J Virol 86:8672– 8680.
37. Sun Y, Asmal M, Lane S, Permar SR, Schmidt SD, Mascola JR, Letvin NL. 2011. Antibody-dependent cell-mediated cytotoxicity in simian immunodeficiency virus-infected rhesus monkeys. J Virol 85:6906 – 6912.
38. Johansson SE, Rollman E, Chung AW, Center RJ, Hejdeman B, Stratov I, Hinkula J, Wahren B, Kärre K, Kent SJ, Berg L. 2011. NK cell function and antibodies mediating ADCC in HIV-1-infected viremic and controller patients. Viral Immunol 24:359 –368.
39. Stratov I, Chung A, Kent SJ. 2008. Robust NK cell-mediated human immunodeficiency virus (HIV)-specific antibody-dependent responses in HIV-infected subjects. J Virol 82:5450 –5459.
40. Ackerman ME, Mikhailova A, Brown EP, Dowell KG, Walker BD, BaileyKellogg C, Suscovich TJ, Alter G. 2016. Polyfunctional HIV-specific antibody responses are associated with spontaneous HIV control. PLoS Pathog 12:e1005315.
41. Gómez-Román VR, Florese RH, Patterson LJ, Peng B, Venzon D, Aldrich K, Robert-Guroff M. 2006. A simplified method for the rapid fluorometric assessment of antibody-dependent cell-mediated cytotoxicity. J Immunol Methods 308:53– 67.
42. Orlandi C, Flinko R, Lewis GK. 2016. A new cell line for high throughput HIV-specific antibody-dependent cellular cytotoxicity (ADCC) and cellto-cell virus transmission studies. J Immunol Methods 433:51–58.
43. Ruiz MJ, Ghiglione Y, Falivene J, Laufer N, Holgado MP, Socías ME, Cahn P, Sued O, Giavedoni L, Salomón H, Gherardi MM, Rodríguez AM, Turk G. 2016. Env-specific IgA

from viremic HIV-Infected subjects compromises antibody-dependent cellular cytotoxicity. J Virol 90:670 – 681.

44. Williams KL, Cortez V, Dingens AS, Gach JS, Rainwater S, Weis JF, Chen X, Spearman P, Forthal DN, Overbaugh J. 2015. HIV-specific CD4-induced antibodies mediate broad and potent antibody-dependent cellular cytotoxicity activity and are commonly detected in plasma from HIV-infected humans. EBioMedicine 2:1464 –1477.
45. Bradley T, Pollara J, Santra S, Vandergrift N, Pittala S, Bailey-Kellogg C, Shen X, Parks R, Goodman D, Eaton A, Balachandran H, Mach LV, Saunders KO, Weiner JA, Scearce R, Sutherland LL, Phogat S, Tartaglia J, Reed SG, Hu SL, Theis JF, Pinter A, Montefiori DC, Kepler TB, Peachman KK, Rao M, Michael NL, Suscovich TJ, Alter G, Ackerman ME, Moody MA, Liao HX, Tomaras G, Ferrari G, Korber BT, Haynes BF. 2017. Pentavalent HIV-1 vaccine protects against simian-human immunodeficiency virus challenge. Nat Commun 8:15711.
46. Jensen SS, Fomsgaard A, Borggren M, Tingstedt JL, Gerstoft J, Kronborg G, Rasmussen LD, Pedersen C, Karlsson I. 2015. HIV-specific antibody-dependent cellular cytotoxicity (ADCC)-mediating antibodies decline while NK cell function increases during antiretroviral therapy (ART). PLoS One 10:e0145249.
47. Jensen SS, Hartling HJ, Tingstedt JL, Larsen TK, Nielsen SD, Pedersen C, Fomsgaard A, Karlsson I. 2015. HIV-specific ADCC improves after antiretroviral therapy and correlates with normalization of the NK cell phenotype. J Acquir Immune Defic Syndr 68:103–111.
48. Shen X, Basu R, Sawant S, Beaumont D, Kwa SF, LaBranche C, Seaton KE, Yates NL, Montefiori DC, Ferrari G, Wyatt LS, Moss B, Alam SM, Haynes BF, Tomaras GD, Robinson HL. 2017. HIV-1 gp120 protein and MVAgp140 boost immunogens increase immunogenicity of a DNA/MVA HIV-1 vaccine. J Virol 91:e1077-17.
49. Ake JA, Schuetz A, Pegu P, Wieczorek L, Eller MA, Kibuuka H, Sawe F, Maboko L, Polonis V, Karasavva N, Weiner D, Sekiziyivu A, Kosgei J, Missanga M, Kroidl A, Mann P, Ratto-Kim S, Eller LA, Earl P, Moss B, Dorsey-Spitz J, Milazzo M, Ouedraogo GL, Rizvi F, Yan J, Khan AS, Peel S, Sardesai NY, Michael NL, Ngauy V, Marovich M, Robb ML. 2017. Safety and immunogenicity of PENNVAX-G DNA prime administered by Biojector 2000 or CELLECTRA electroporation device with modified vaccinia Ankara-CMDR boost. J Infect Dis 216:1080 –1090.

50. Karlsson I, Borggren M, Jensen SS, Heyndrickx L, Stewart-Jones G, Scarlatti G, Fomsgaard A. 2018. Immunization with clinical HIV-1 Env proteins induces broad antibody dependent cellular cytotoxicity-mediating antibodies in a rabbit vaccination model. AIDS Res Hum Retroviruses 34: 206 –217.
51. Richard J, Veillette M, Batraville LA, Coutu M, Chapleau JP, Bonsignori M, Bernard N, Tremblay C, Roger M, Kaufmann DE, Finzi A. 2014. Flow cytometry-based assay to study HIV-1 gp120 specific antibody-dependent cellular cytotoxicity responses. J Virol Methods 208:107–114.
52. Mabuka J, Nduati R, Odem-Davis K, Peterson D, Overbaugh J. 2012. HIV-specific antibodies capable of ADCC are common in breastmilk and are associated with reduced risk of transmission in women with high viral loads. PLoS Pathog 8:e1002739.
53. Baxter AE, Niessl J, Fromentin R, Richard J, Porichis F, Charlebois R, Massanella M, Brassard N, Alsahafi N, Delgado GG, Routy JP, Walker BD, Finzi A, Chomont N, Kaufmann DE. 2016. Single-cell characterization of viral translation-competent reservoirs in HIV-infected individuals. Cell Host Microbe 20:368 –380.
54. Baxter AE, Niessl J, Fromentin R, Richard J, Porichis F, Massanella M, Brassard N, Alsahafi N, Routy JP, Finzi A, Chomont N, Kaufmann DE. 2017. Multiparametric characterization of rare HIV-infected cells using an RNAflow FISH technique. Nat Protoc 12:2029 –2049.
55. Mengistu M, Ray K, Lewis GK, DeVico AL. 2015. Antigenic properties of the human immunodeficiency virus envelope glycoprotein gp120 on virions bound to target cells. PLoS Pathog 11:e1004772.
56. Mengistu M, Tang AH, Foulke JS, Jr, Blanpied TA, Gonzalez MW, Spouge JL, Gallo RC, Lewis GK, DeVico AL. 2017. Patterns of conserved gp120 epitope presentation on attached HIV-1 virions. Proc Natl Acad Sci USA 114:E9893–E9902.
57. Gohain N, Tolbert WD, Orlandi C, Richard J, Ding S, Chen X, Bonsor DA, Sundberg EJ, Lu W, Ray K, Finzi A, Lewis GK, Pazgier M. 2016. Molecular basis for epitope recognition by non-neutralizing anti-gp41 antibody F240. Sci Rep 6:36685.
58. Tolbert WD, Gohain N, Alsahafi N, Van V, Orlandi C, Ding S, Martin L, Finzi A, Lewis GK, Ray K, Pazgier M. 2017. Targeting the late stage of HIV-1 entry for antibody-

dependent cellular cytotoxicity: structural basis for Env epitopes in the C11 region. Structure 25:1719 –1731.e4.

59. Richard J, Pacheco B, Gohain N, Veillette M, Ding S, Alsahafi N, Tolbert WD, Prévost J, Chapleau JP, Coutu M, Jia M, Brassard N, Park J, Courter JR, Melillo B, Martin L, Tremblay C, Hahn BH, Kaufmann DE, Wu X, Smith AB, III, Sodroski J, Pazgier M, Finzi A. 2016. Co-receptor binding site antibodies enable CD4-mimetics to expose conserved anti-cluster A ADCC epitopes on HIV-1 envelope glycoproteins. EBioMedicine 12: 208 – 218.
60. Mujib S, Liu J, Rahman AKMN, Schwartz JA, Bonner P, Yue FY, Ostrowski MA. 2017. Comprehensive cross-clade characterization of antibody-mediated recognition, complement-mediated lysis, and cell-mediated cytotoxicity of HIV-1 envelope-specific antibodies toward eradication of the HIV-1 reservoir. J Virol 91:e00634-17.
61. Magadán JG, Pérez-Victoria FJ, Sougrat R, Ye Y, Strebel K, Bonifacino JS. 2010. Multilayered mechanism of CD4 downregulation by HIV-1 Vpu involving distinct ER retention and ERAD targeting steps. PLoS Pathog 6:e1000869.
62. Kimura T, Nishikawa M, Ohyama A. 1994. Intracellular membrane traffic of human immunodeficiency virus type 1 envelope glycoproteins: vpu liberates Golgi-targeted gp160 from CD4-dependent retention in the endoplasmic reticulum. J Biochem 115:1010 –1020.
63. Horwitz JA, Bar-On Y, Lu CL, Fera D, Lockhart AAK, Lorenzi JCC, Nogueira L, Golijanin J, Scheid JF, Seaman MS, Gazumyan A, Zolla-Pazner S, Nussenzweig MC. 2017. Non-neutralizing antibodies alter the course of HIV-1 infection in vivo. Cell 170:637– 648.e10.
64. Janvier K, Craig H, Le Gall S, Benarous R, Guatelli J, Schwartz O, Benichou S. 2001. Nef-induced CD4 downregulation: a diacidic sequence in human immunodeficiency virus type 1 Nef does not function as a protein sorting motif through direct binding to beta-COP. J Virol 75:3971–3976.
65. Pham TN, Lukhele S, Hajjar F, Routy JP, Cohen ÉA. 2014. HIV Nef and Vpu protect HIV-infected CD4 T cells from antibody-mediated cell lysis through down-modulation of CD4 and BST2. Retrovirology 11:15.
66. Dugast AS, Chan Y, Hoffner M, Licht A, Nkolola J, Li H, Streeck H, Suscovich TJ, Ghebremichael M, Ackerman ME, Barouch DH, Alter G. 2014. Lack of protection

following passive transfer of polyclonal highly functional low-dose non-neutralizing antibodies. PLoS One 9:e97229.

67. Nakane T, Nomura T, Shi S, Nakamura M, Naruse TK, Kimura A, Matano T, Yamamoto H. 2013. Limited impact of passive non-neutralizing antibody immunization in acute SIV infection on viremia control in rhesus macaques. PLoS One 8:e73453.

68. Moog C, Dereuddre-Bosquet N, Teillaud JL, Biedma ME, Holl V, Van Ham G, Heyndrickx L, Van Dorsselaer A, Katinger D, Vcelar B, Zolla-Pazner S, Mangeot I, Kelly C, Shattock RJ, Le Grand R. 2014. Protective effect of vaginal application of neutralizing and non-neutralizing inhibitory antibodies against vaginal SHIV challenge in macaques. Mucosal Immunol 7:46 –56.

69. Santra S, Tomaras GD, Warrier R, Nicely NI, Liao HX, Pollara J, Liu P, Alam SM, Zhang R, Cocklin SL, Shen X, Duffy R, Xia SM, Schutte RJ, Pemble CW, IV, Dennison SM, Li H, Chao A, Vidnovic K, Evans A, Klein K, Kumar A, Robinson J, Landucci G, Forthal DN, Montefiori DC, Kaewkungwal J, Nitayaphan S, Pitisuttithum P, Rerks-Ngarm S, Robb ML, Michael NL, Kim JH, Soderberg KA, Giorgi EE, Blair L, Korber BT, Moog C, Shattock RJ, Letvin NL, Schmitz JE, Moody MA, Gao F, Ferrari G, Shaw GM, Haynes BF. 2015. Human non-neutralizing HIV-1 envelope monoclonal antibodies limit the number of founder viruses during SHIV mucosal infection in rhesus macaques. PLoS Pathog 11:e1005042.

70. Astronomo RD, Santra S, Ballweber-Fleming L, Westerberg KG, Mach L, Hensley-McBain T, Sutherland L, Mildenberg B, Morton G, Yates NL, Mize GJ, Pollara J, Hladik F, Ochsenbauer C, Denny TN, Warrier R, Rerks-Ngarm S, Pitisuttithum P, Nitayapan S, Kaewkungwal J, Ferrari G, Shaw GM, Xia SM, Liao HX, Montefiori DC, Tomaras GD, Haynes BF, McElrath JM. 2016. Neutralization takes precedence over IgG or IgA isotype-related functions in mucosal HIV-1 antibody-mediated protection. EBioMedicine 14:97–111.

71. Gómez-Román VR, Patterson LJ, Venzon D, Liewehr D, Aldrich K, Florese R, Robert-Guroff M. 2005. Vaccine-elicited antibodies mediate antibody-dependent cellular cytotoxicity correlated with significantly reduced acute viremia in rhesus macaques challenged with SIVmac251. J Immunol 174:2185–2189.

72. Fouts TR, Bagley K, Prado IJ, Bobb KL, Schwartz JA, Xu R, Zagursky RJ, Egan MA, Eldridge JH, LaBranche CC, Montefiori DC, Le Buanec H, Zagury D, Pal R, Pavlakis GN, Felber BK, Franchini G, Gordon S, Vaccari M, Lewis GK, DeVico AL, Gallo RC. 2015. Balance of cellular and humoral immunity determines the level of protection by HIV vaccines in rhesus macaque models of HIV infection. Proc Natl Acad Sci USA 112:E992–E999.

73. Huang Y, Ferrari G, Alter G, Forthal DN, Kappes JC, Lewis GK, Love JC, Borate B, Harris L, Greene K, Gao H, Phan TB, Landucci G, Goods BA, Dowell KG, Cheng HD, Bailey-Kellogg C, Montefiori DC, Ackerman ME. 2016. Diversity of antiviral IgG effector activities observed in HIV-infected and vaccinated subjects. J Immunol 197:4603– 4612.

74. Florese RH, Demberg T, Xiao P, Kuller L, Larsen K, Summers LE, Venzon D, Cafaro A, Ensoli B, Robert-Guroff M. 2009. Contribution of non-neutralizing vaccine-elicited antibody activities to improved protective efficacy in rhesus macaques immunized with Tat/Env compared with multigenic vaccines. J Immunol 182:3718 –3727.

75. Haynes BF, Gilbert PB, McElrath MJ, Zolla-Pazner S, Tomaras GD, Alam SM, Evans DT, Montefiori DC, Karnasuta C, Sutthent R, Liao HX, DeVico AL, Lewis GK, Williams C, Pinter A, Fong Y, Janes H, DeCamp A, Huang Y, Rao M, Billings E, Karasavvas N, Robb ML, Ngauy V, de Souza MS, Paris R, Ferrari G, Bailer RT, Soderberg KA, Andrews C, Berman PW, Frahm N, De Rosa SC, Alpert MD, Yates NL, Shen X, Koup RA, Pitisuttithum P, Kaewkungwal J, Nitayaphan S, Rerks-Ngarm S, Michael NL, Kim JH. 2012. Immune-correlates analysis of an HIV-1 vaccine efficacy trial. N Engl J Med 366:1275–1286.

76. Prévost J, Zoubchenok D, Richard J, Veillette M, Pacheco B, Coutu M, Brassard N, Parsons MS, Ruxrungtham K, Bunupuradah T, Tovanabutra S, Hwang KK, Moody MA, Haynes BF, Bonsignori M, Sodroski J, Kaufmann DE, Shaw GM, Chenine AL, Finzi A. 2017. Influence of the envelope gp120 Phe43 cavity on HIV-1 sensitivity to antibody-dependent cell-mediated cytotoxicity responses. J Virol 91:e02452-16.

77. Fontaine J, Chagnon-Choquet J, Valcke HS, Poudrier J, Roger M, Montreal Primary HIV Infection and Long-Term Non-Progressor Study Groups. 2011. High expression levels of B lymphocyte stimulator (BLyS) by dendritic cells correlate with HIV-related B-cell disease progression in humans. Blood 117:145–155.

78. Fontaine J, Coutlée F, Tremblay C, Routy JP, Poudrier J, Roger M, Montreal Primary HIV Infection and Long-Term Non-progressor Study Groups. 2009. HIV infection affects blood myeloid dendritic cells after successful therapy and despite non-progressing clinical disease. J Infect Dis 199:1007–1018.

79. International HIV Controllers Study, Pereyra F, Jia X, McLaren PJ, Telenti A, de Bakker PI, Walker BD, Ripke S, Brumme CJ, Pulit SL, Carrington M, Kadie CM, Carlson JM, Heckerman D, Graham RR, Plenge RM, Deeks SG, Gianniny L, Crawford G, Sullivan J, Gonzalez E, Davies L, Camargo A, Moore JM, Beattie N, Gupta S, Crenshaw A, Burtt NP, Guiducci C, Gupta N, Gao X, Qi Y, Yuki Y, Piechocka-Trocha A, Cutrell E, Rosenberg R, Moss KL, Lemay P, O'Leary J, Schaefer T. 2010. The major genetic determinants of HIV-1 control affect HLA class I peptide presentation. Science 330: 1551–1557.

80. Kamya P, Boulet S, Tsoukas CM, Routy JP, Thomas R, Côté P, Boulassel MR, Baril JG, Kovacs C, Migueles SA, Connors M, Suscovich TJ, Brander C, Tremblay CL, Bernard N, Canadian Cohort of HIV Infected Slow Progressors. 2011. Receptor-ligand requirements for increased NK cell polyfunctional potential in slow progressors infected with HIV-1 co-expressing KIR3DL1*h/*y and HLA-B*57. J Virol 85:5949 –5960.

81. 81. Peretz Y, Ndongala ML, Boulet S, Boulassel MR, Rouleau D, Côté P, Longpré D, Routy JP, Falutz J, Tremblay C, Tsoukas CM, Sékaly RP, Bernard NF. 2007. Functional T cell subsets contribute differentially to HIV peptide-specific responses within infected individuals: correlation of these functional T cell subsets with markers of disease progression. Clin Immunol 124:57– 68.

82. Ochsenbauer C, Edmonds TG, Ding H, Keele BF, Decker J, Salazar MG, Salazar-Gonzalez JF, Shattock R, Haynes BF, Shaw GM, Hahn BH, Kappes JC. 2012. Generation of transmitted/founder HIV-1 infectious molecular clones and characterization of their replication capacity in CD4 T lymphocytes and monocyte-derived macrophages. J Virol 86:2715–2728.

83. Bar KJ, Tsao CY, Iyer SS, Decker JM, Yang Y, Bonsignori M, Chen X, Hwang KK, Montefiori DC, Liao HX, Hraber P, Fischer W, Li H, Wang S, Sterrett S, Keele BF, Ganusov VV, Perelson AS, Korber BT, Georgiev I, McLellan JS, Pavlicek JW, Gao F, Haynes BF, Hahn BH, Kwong PD, Shaw GM. 2012. Early low-titer neutralizing antibodies impede HIV-1 replication and select for virus escape. PLoS Pathog 8:e1002721.

84. Parrish NF, Gao F, Li H, Giorgi EE, Barbian HJ, Parrish EH, Zajic L, Iyer SS, Decker JM, Kumar A, Hora B, Berg A, Cai F, Hopper J, Denny TN, Ding H, Ochsenbauer C, Kappes JC, Galimidi RP, West AP, Jr., Bjorkman PJ, Wilen CB, Doms RW, O'Brien M, Bhardwaj N, Borrow P, Haynes BF, Muldoon M, Theiler JP, Korber B, Shaw GM, Hahn BH. 2013. Phenotypic properties of transmitted founder HIV-1. Proc Natl Acad Sci USA 110:6626 – 6633.

85. Fenton-May AE, Dibben O, Emmerich T, Ding H, Pfafferott K, AasaChapman MM, Pellegrino P, Williams I, Cohen MS, Gao F, Shaw GM, Hahn BH, Ochsenbauer C, Kappes JC, Borrow P. 2013. Relative resistance of HIV-1 founder viruses to control by interferon-alpha. Retrovirology 10: 146.

86. Decker JM, Bibollet-Ruche F, Wei X, Wang S, Levy DN, Wang W, Delaporte E, Peeters M, Derdeyn CA, Allen S, Hunter E, Saag MS, Hoxie JA, Hahn BH, Kwong PD, Robinson JE, Shaw GM. 2005. Antigenic conservation and immunogenicity of the HIV coreceptor binding site. J Exp Med 201:1407–1419.

3.2.10 FIGURES

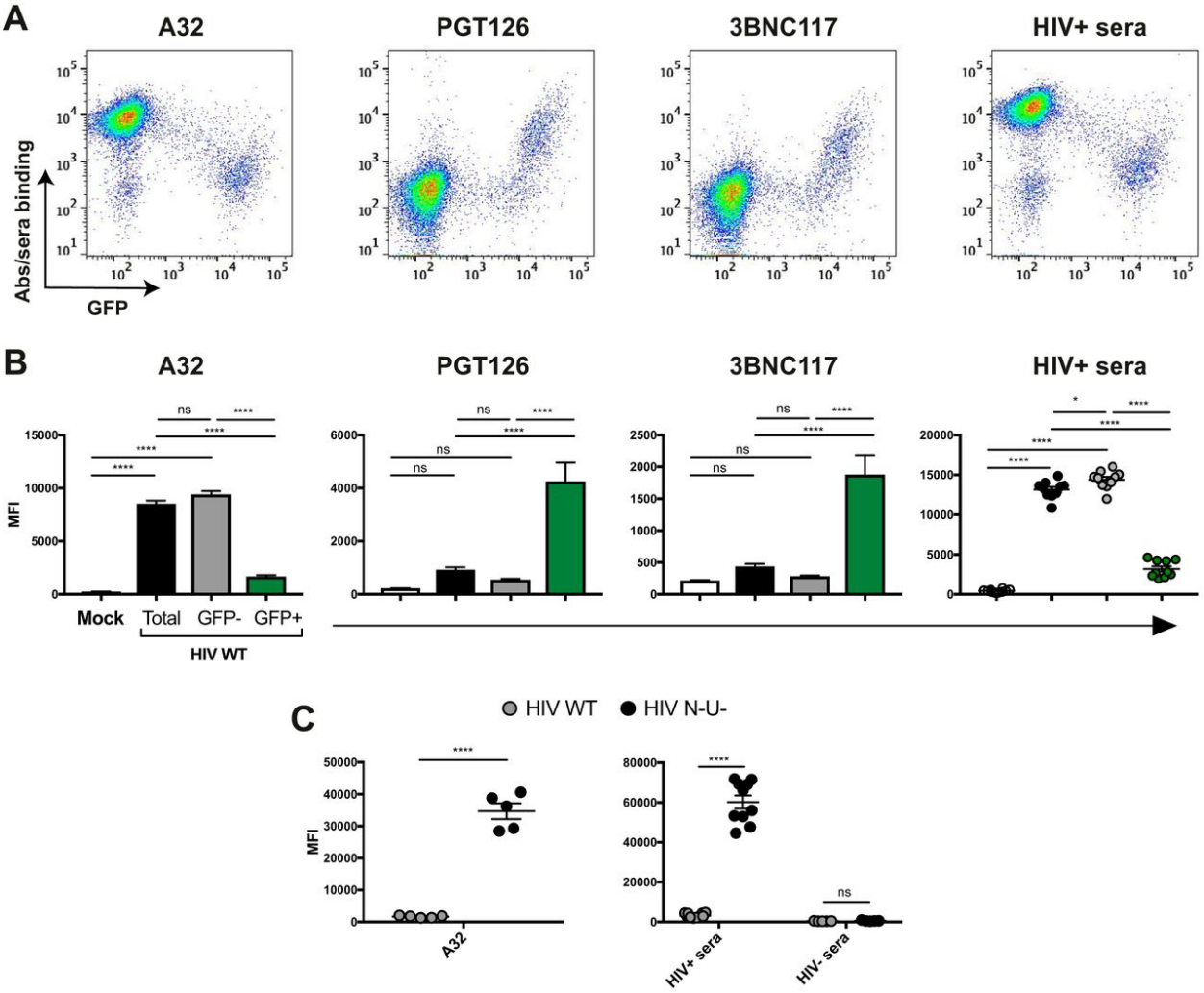

Figure 3.1.1 - Differential recognition of infected and uninfected bystander cells by ADCC-mediating Abs.

Primary $CD4^+$ T cells were mock infected or infected with the NL4.3 ADA GFP virus, either wild type (HIV WT) or defective for Nef and Vpu expression (HIV N^- U^-). Forty-eight hours post-infection, cells were stained with the anti-Env Ab (5 µg/ml) A32, PGT126, or 3BNC117 or sera (1:1,000 dilution) from 10 HIV-1-infected (HIV^+ sera) or 5 uninfected (HIV^- sera) individuals, followed by appropriate secondary Abs. (**A**) Dot plots depicting representative staining of WT-infected cells. (**B**) Mean fluorescence intensities (MFI) obtained for at least 5 independent stainings with the different Abs and 10 HIV^+ or 5 HIV^- sera. (**C**) Graphs represent the MFI obtained for 5 independent staining experiments with A32 and 10 HIV^+ or 5 HIV^- sera on cells infected with WT and N^- U^- virus. Error bars indicate means +/- standard errors of the means. Statistical significance was tested using ordinary one-way analysis of variance (**B**) or unpaired t test or Mann-Whitney test (**C**) (*, $P < 0.05$; ****, $P < 0.0001$; ns, nonsignificant).

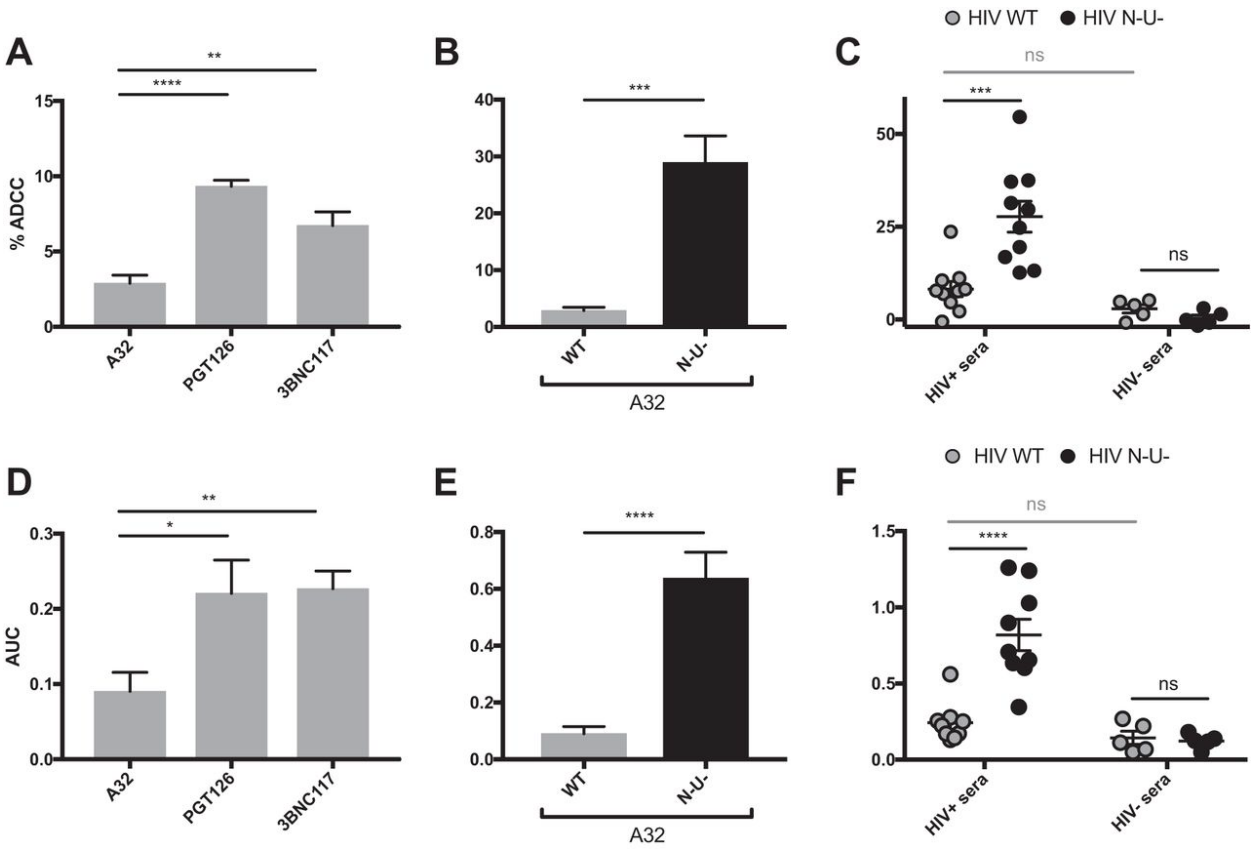

Figure 3.1.2 - ADCC responses detected with assays measuring the elimination of infected cells.

Primary $CD4^+$ T cells (**A to C**) or CEM.NKr-CCR5-sLTR-Luc cells (**D to F**) infected with the NL4.3 ADA GFP virus, either wild-type (HIV WT) (depicted in gray) or defective for Nef and Vpu expression (HIV N^- U^-) (depicted in black) were used as target cells with the FACS-based infected-cell elimination assay (**A to C**) or the luciferase assays (**D to F**). (**A and D**) ADCC responses detected with the anti-Env Abs A32, PGT126, and 3BNC117 against cells infected with the WT virus. (**B, C, E, and F**) ADCC responses detected with A32 (**B and E**) or HIV and HIV sera (**C and F**) against cells infected with WT or N^- U^- viruses. All graphs shown represent ADCC responses obtained from at least 5 independent experiments. For the FACS-based assay, mAbs were used at 5 µg/ml and human sera were used at a 1:1,000 dilution. For the luciferase assay, area under the curve (AUC) values were calculated using increased concentrations of mAbs (0.0024, 0.0098, 0.0390, 0.1563, 0.6250, 2.5, and 10 µg/ml) and increased dilutions of human sera (1:100, 1:400, 1:1,600, 1:6,400, 1:25,600, and 1:102,400). Error bars indicate means +/- standard errors of the means. Statistical significance was tested using unpaired t test or Mann-Whitney test (*, $P < 0.05$; **, $P < 0.01$; ***, $P < 0.001$; ****, $P < 0.0001$; ns, nonsignificant).

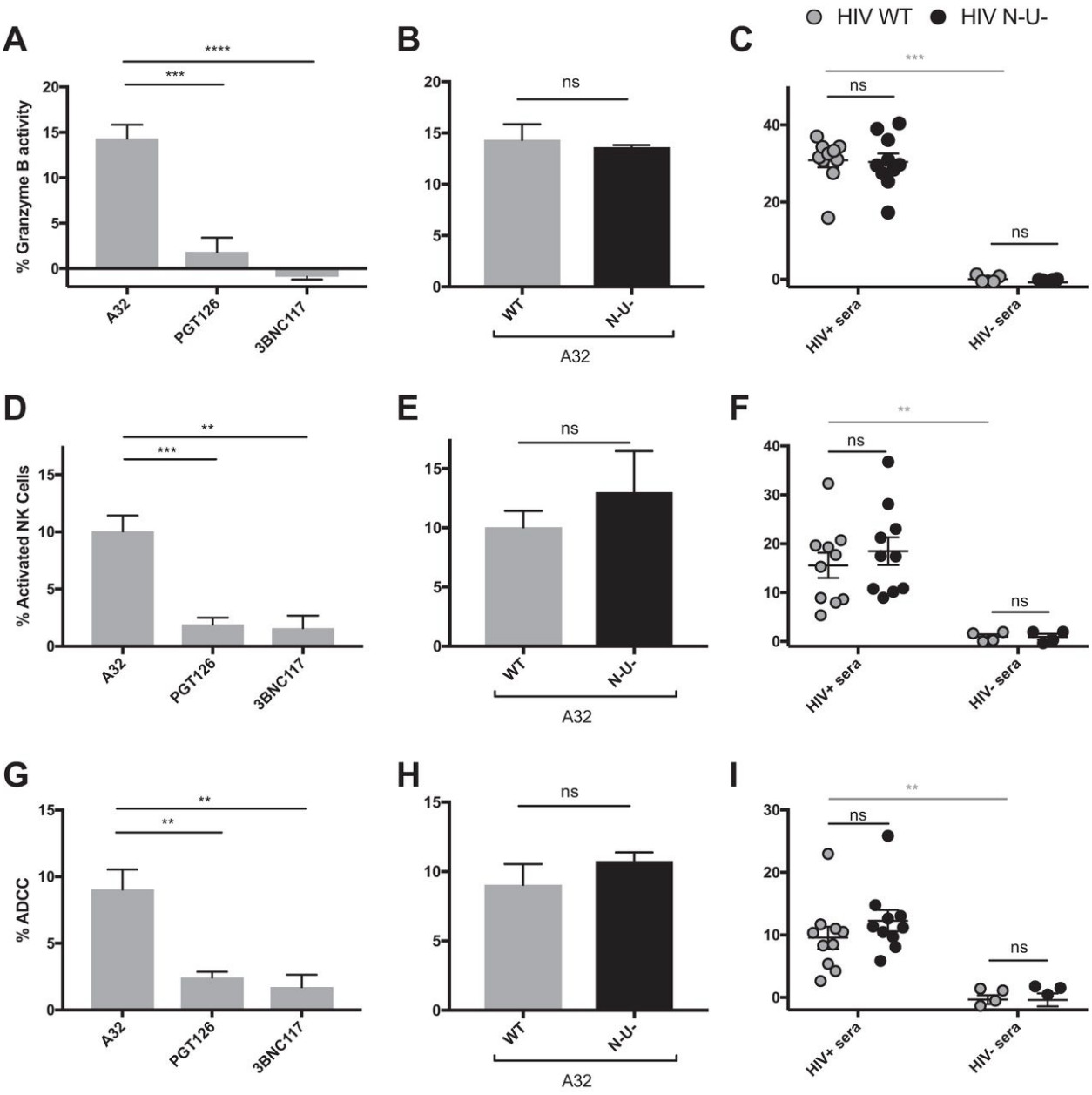

Figure 3.1.3 - ADCC responses detected with assays relying on the total cell population. Primary $CD4^+$ T cells infected with the NL4.3 ADA GFP virus, either wild-type (HIV WT) (depicted in gray) or defective for Nef and Vpu expression (HIV N^- U^-) (depicted in black), were used as target cells in the granzyme B assay (**A to C**), the NK cell activation assay (**D to F**), or FACS-based assays (gating on the total cell population) (**G to I**). (**A, D, and G**) ADCC responses detected with the anti-Env mAbs (5 µg/ml) A32, PGT126, and 3BNC117 against cells infected with WT virus. (**B, C, E, F, H, and I**) ADCC responses mediated by A32 (**B, E, and H**) or HIV^+ and HIV^- sera (1:1,000 dilution) (**C, F, and I**) against cells infected with WT or N^- U^- virus. All graphs shown represent ADCC responses obtained for at least 5 independent experiments. Error bars indicate means +/- standard errors of the means. Statistical significance was tested using unpaired t test or Mann-Whitney test (*, $P < 0.05$; **, $P < 0.01$; ***, $P < 0.001$; ****, $P < 0.0001$; ns, nonsignificant).

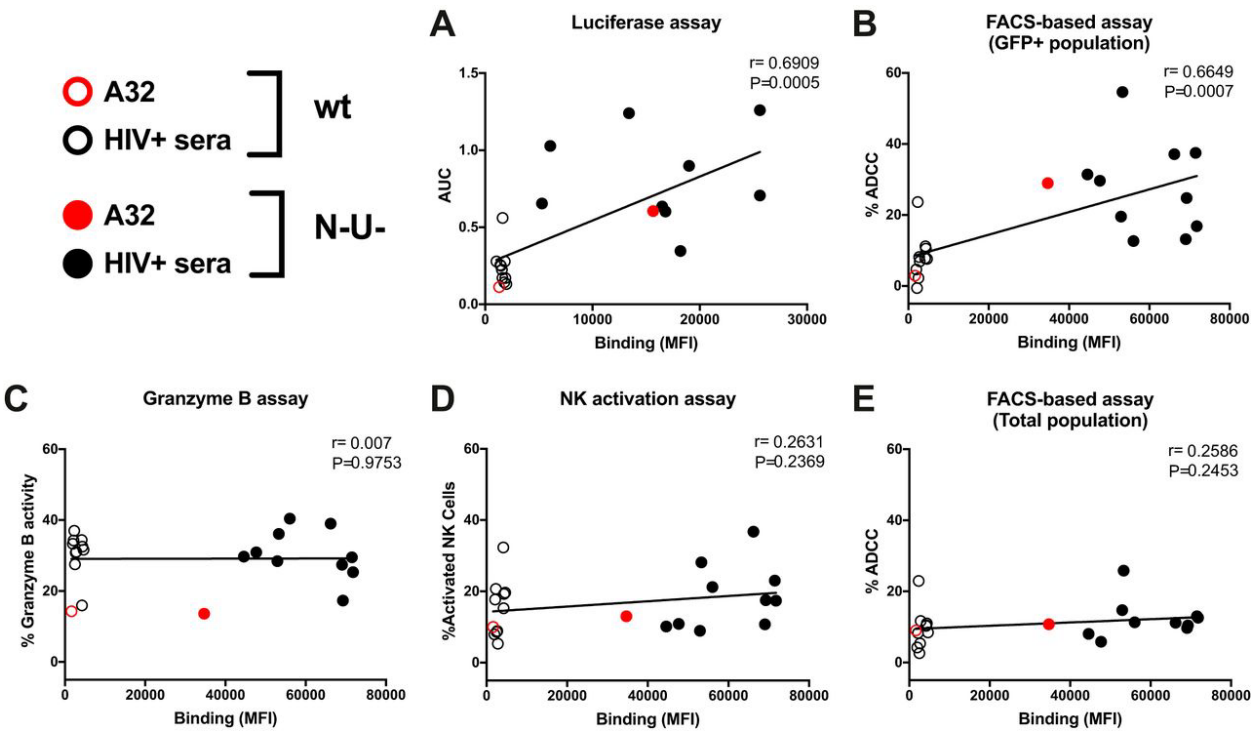

Figure 3.1.4 - Recognition of infected cells correlates with ADCC responses when using assays measuring the elimination of the infected-cell population.
Correlation between the ability of A32 and HIV^+ sera to recognize cells infected with NL4.3 ADA GFP, either wild-type (WT) or defective for Nef and Vpu expression (N^- U^-), and the ADCC responses detected against these cells using the luciferase assays (**A**), the FACS-based assay (on the GFP cell population) (**B**), the granzyme B assay (**C**), the NK cell activation assay (**D**), or the FACS-based assay (**E**) (on the total cell population) was calculated using a Pearson correlation test.

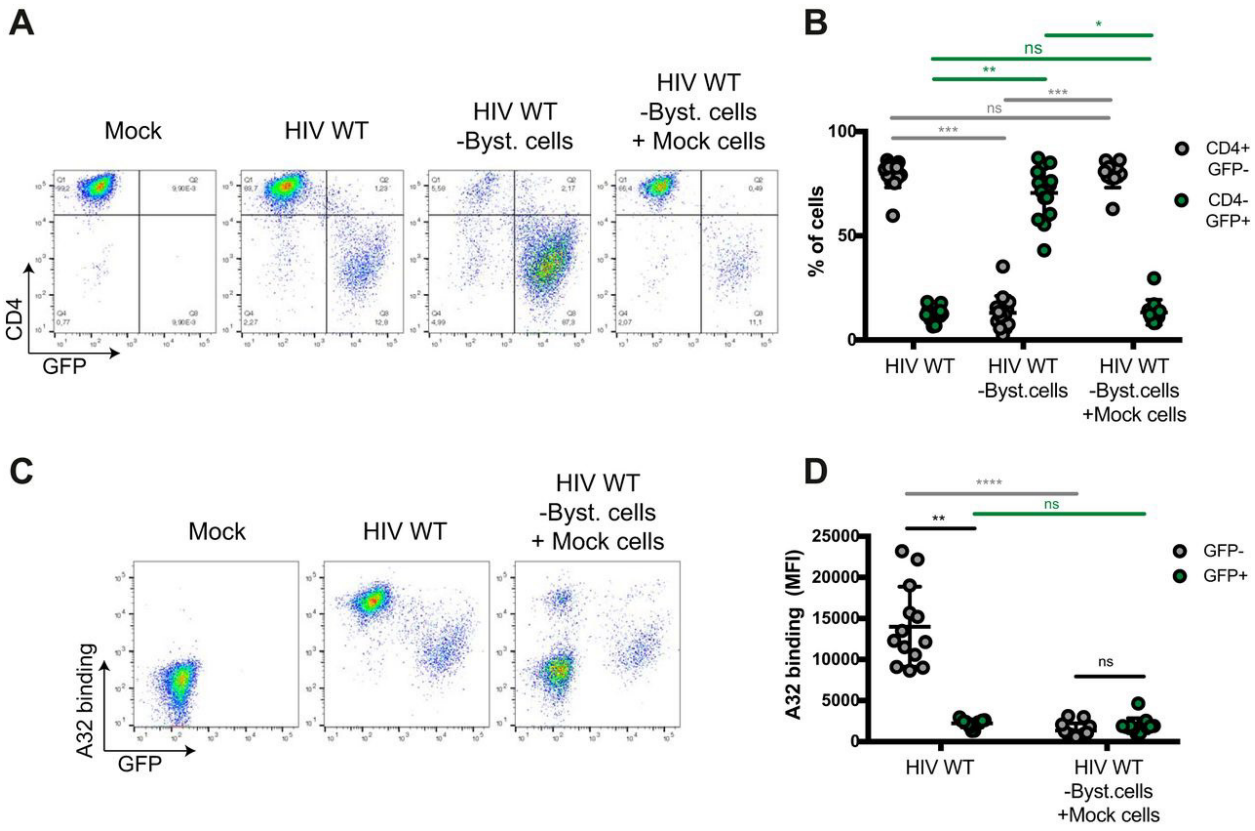

Figure 3.1.5 - Replacement of uninfected bystander cells by autologous mock-infected cells reduces the proportion of cells recognized by A32.

Primary $CD4^+$ T cells were mock infected (Mock) or infected with the NL4.3 ADA GFP WT virus (HIV WT). Forty-eight hours post-infection, uninfected bystander CD4 cells were removed (HIV WT -Byst. cells) and replaced by the same number of autologous mock-infected cells (HIV WT -Byst. cells + Mock cells). Cells were stained with anti-CD4 (1 µg/ml) and A32 (5 µg/ml) Abs. (**A and C**) Representative staining for CD4 (**A**) and A32 (**C**). (**B**) Percentage of CD4 GFP and CD4 GFP cells. (**D**) MFI obtained for the A32 staining for at least 13 independent experiments. Error bars indicate means +/- standard errors of the means. Statistical significance was tested using a Kruskal-Wallis test (*, $P < 0.05$; **, $P < 0.01$; ***, $P < 0.001$; ****, $P < 0.0001$; ns, nonsignificant).

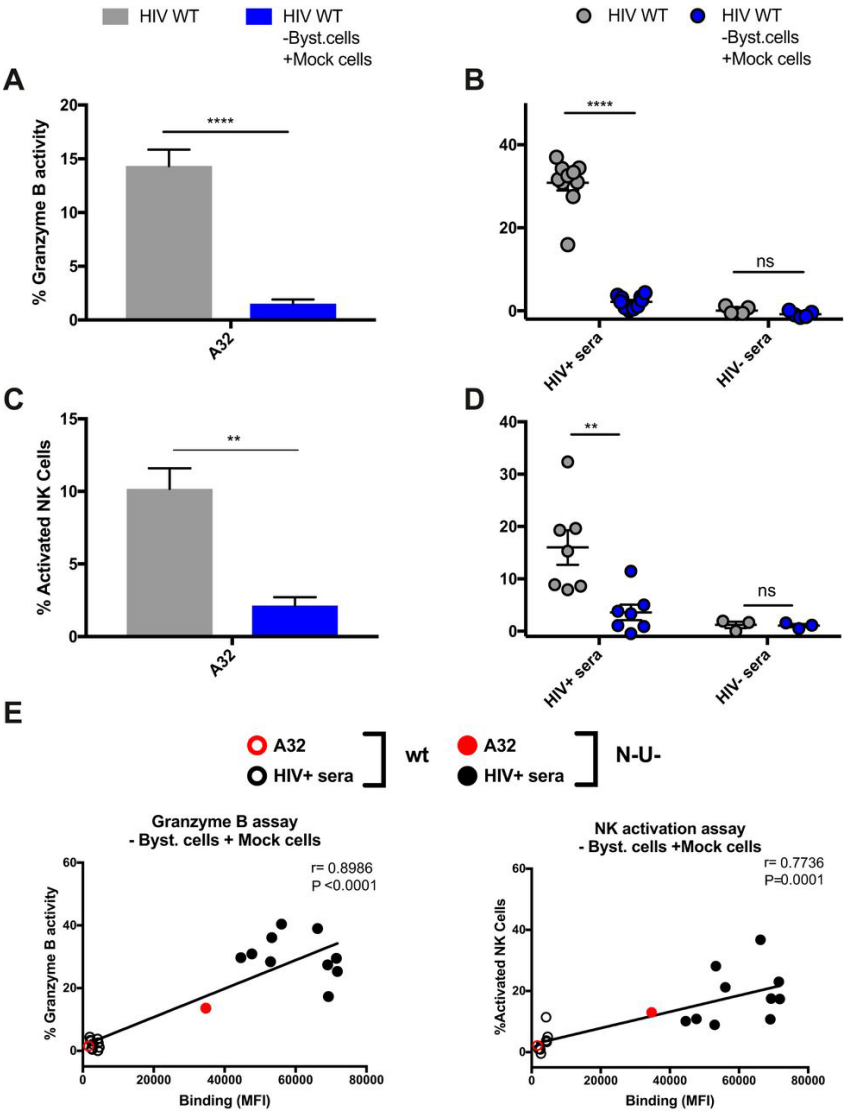

Figure 3.1.6 - Replacement of uninfected bystander cells by autologous mock-infected cells strongly reduces the ADCC responses detected with granzyme B and NK cell activation assays.

Primary $CD4^+$ T cells were mock infected (Mock) or infected with the NL4.3 ADA GFP WT virus (HIV WT). Forty-eight hours post-infection, uninfected bystander $CD4^+$ T cells were removed and replaced by the same number of autologous mock-infected cells (HIV WT -Byst. cells Mock cells) prior to ADCC measurements with the granzyme B assay (**A and B**) and the NK cell activation assay (**C and D**). (**A and C**) ADCC responses detected with A32 (5 µg/ml). (**B and D**) Responses mediated by HIV^+ and HIV^- sera (1:1,000 dilution). (**E**) A correlation between the ability of A32 and HIV sera to recognize infected cells and the ADCC responses detected with the granzyme B and NK cell activation assay was observed when the uninfected bystander $CD4^+$ T cells were replaced by autologous mock-infected cells in the context of a WT infection. All graphs shown represent ADCC responses obtained in at least 5 independent experiments. Error bars indicate means +/- standard errors of the means. Statistical significance was tested using unpaired t test or Mann-Whitney test (**A to D**) and a Pearson correlation test (**E**) (**, $P < 0.01$; ****, $P < 0.0001$; ns, nonsignificant).

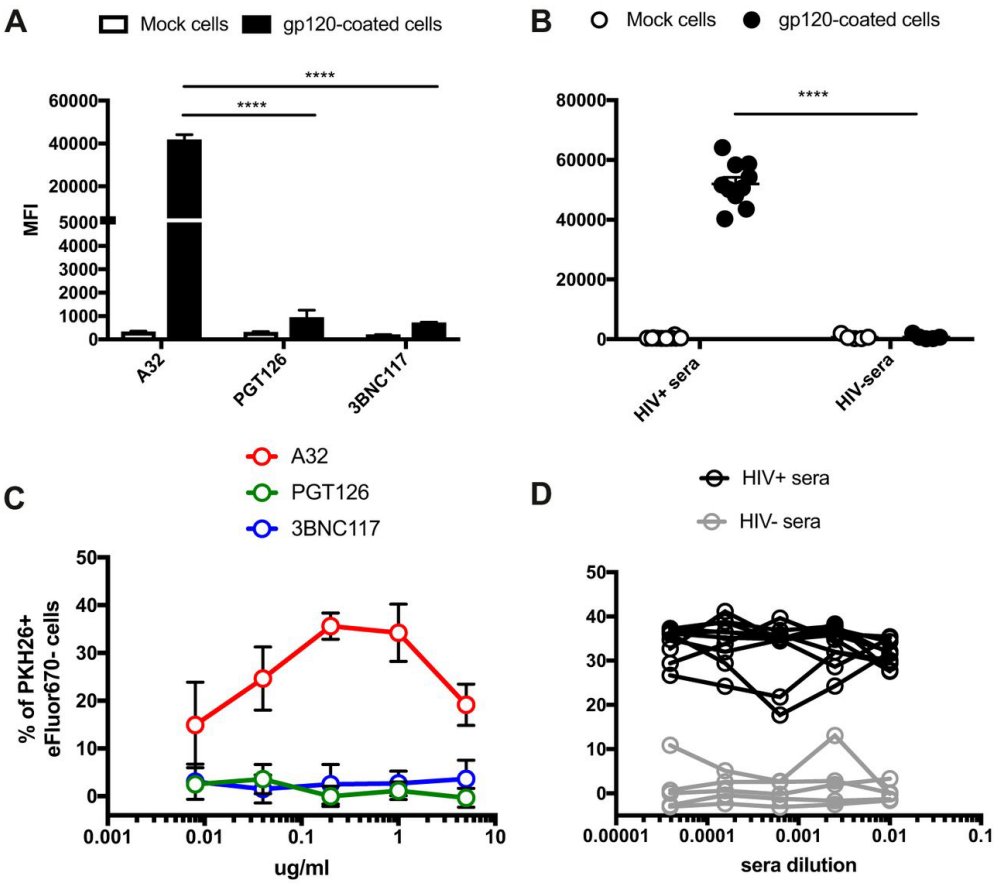

Figure 3.1.7 - Measurement of ADCC responses against gp120-coated target cells.
(**A and B**) Recognition of gp120-coated CEM.NKr cells by A32, PGT126, or 3BNC117 (**A**) and HIV or HIV sera (**B**). (**C and D**) ADCC responses detected using the RFADCC assay against gp120-coated cells with the anti-Env Ab A32, PGT126, or 3BNC117 (0.008, 0.04, 0.2, 1, and 5 µg/ml) (**C**) and HIV^+ or HIV^- sera (1:100, 1:400, 1:1,600, 1:6,400, and 1:25,600 dilutions) (**D**). All graphs shown represent staining and ADCC responses obtained in at least 3 independent experiments. Error bars indicate means +/- standard errors of the means. Statistical significance was tested using unpaired t test (****, $P < 0.0001$).

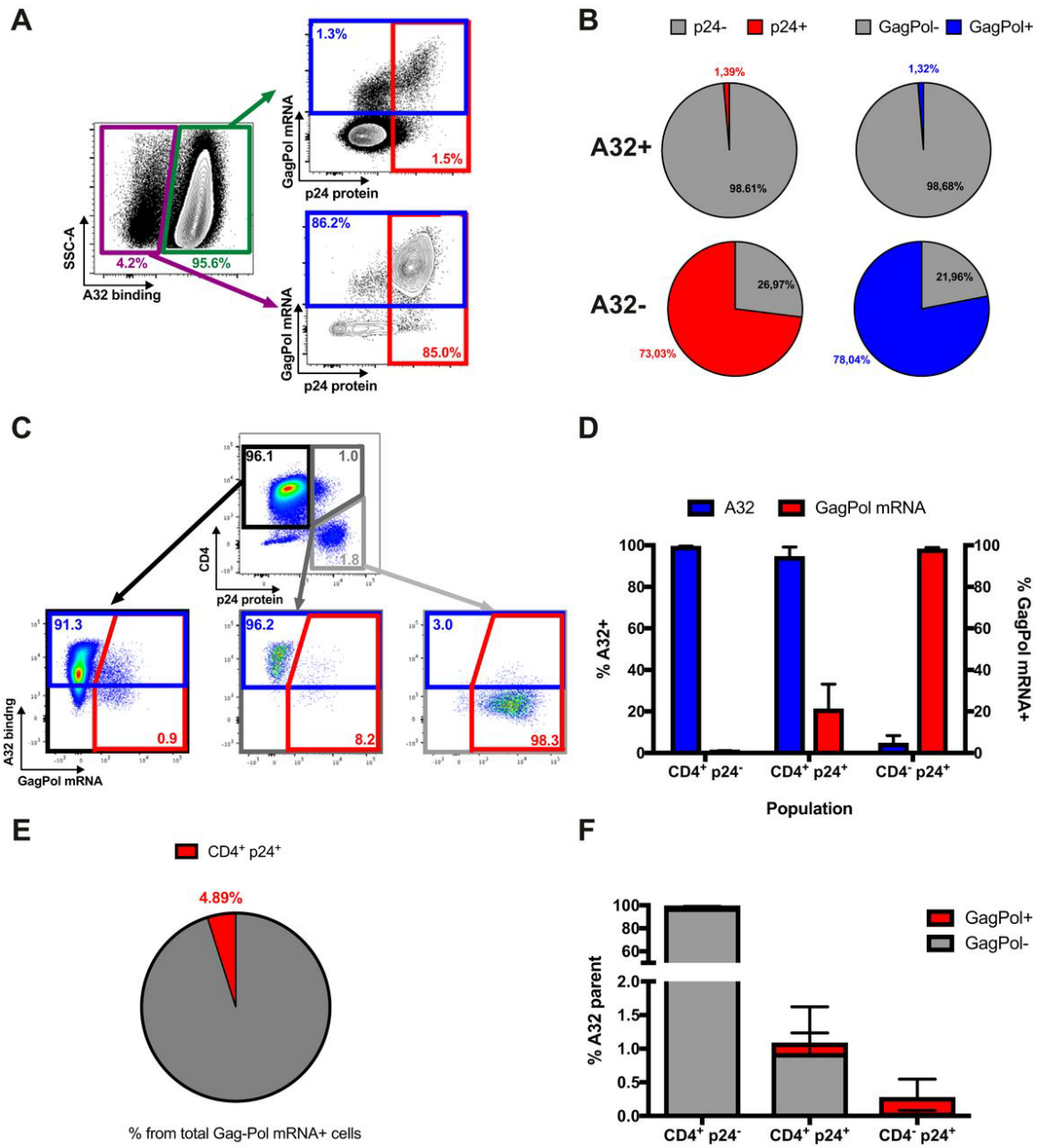

Figure 3.1.8 - A32 preferentially binds to cells that are CD4$^+$ p24$^-$ *gag-pol* mRNA$^-$.
(**A and B**) Primary CD4$^+$ T cells infected with NL3.4 ADA GFP WT virus were stained with A32, followed by appropriate secondary Abs. Cells were then stained for phenotypic markers (see Materials and Methods) prior to detection of HIV-1 p24 and *gag-pol* mRNA by RNA-flow FISH. (**A**) Example of flow cytometry gating strategy based on A32 binding. (**B**) Quantification of the percentage of cells positive for HIV-1 p24 or *gag-pol* mRNA based on A32 binding. (**C**) Example of flow cytometry gating based on p24 and CD4 expression. (**D**) Quantification of the percentage of cells positive for A32 binding and *gag-pol* mRNA based on CD4 and p24 levels. (**E**) Quantification of the percentage of p24$^+$ CD4$^+$ cells among the cells positive for *gag-pol* mRNA. (**F**) Quantification of the percentage of cells that are CD4$^+$ p24$^-$, CD4$^+$ p24$^+$, or CD4$^-$ p24$^+$ among the cells recognized by A32. Error bars indicate means +/- standard errors of the means of at least 4 independent experiments.

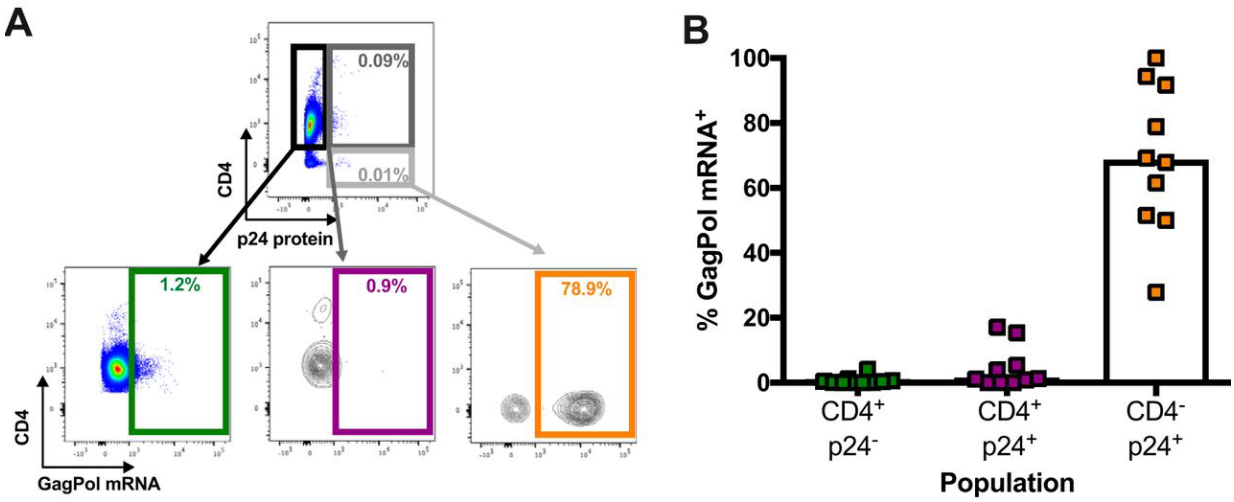

Figure 3.1.9 - The CD4$^+$ p24$^+$ cell population represents a minimal fraction of the *gag-pol* mRNA$^+$ cells in HIV-1-infected individuals.
CD4$^+$ T cells isolated from chronically HIV-infected, untreated individuals were rested overnight. Cells were then stained for phenotypic markers (see Materials and Methods) prior to detection of HIV-1 p24 and *gag-pol* mRNA by RNA-flow FISH. (**A**) Example of flow cytometry gating based on p24 and CD4 expression. (**B**) Quantification of the percentage of cells positive for *gag-pol* mRNA based on CD4 and p24 levels. Error bars indicate means +/- standard errors of the means of data obtained with 10 HIV-1-infected individuals.

3.2.11 SUPPLEMENTAL MATERIAL

Primary cells

PBMC were obtained by leukapheresis. NK cells and $CD4^+$ T lymphocytes were purified from resting PBMCs by negative selection using immunomagnetic beads per the manufacturer's instructions (StemCell Technologies, Vancouver, BC). NK cells were cultured overnight in RPMI 1640 complete medium supplemented with 20% fetal bovine serum and 100 µg/mL penicillin-streptomycin before use. $CD4^+$ T lymphocytes were activated with phytohemagglutinin-L (10 µg/mL) for 48 hours and then maintained in RPMI 1640 complete medium supplemented with rIL-2 (100 U/mL).

Antibodies

The following Abs were used as first Ab for cell surface staining: 1 µg/mL mouse anti-CD4 mAb OKT4 (14-0048-82; eBiosciences), 5 µg/mL human anti-HIV-1 Env mAbs A32, PGT126 (kindly provided by the International AIDS Vaccine Initiative), 3BNC117 (kindly provided by M.C. Nussenzweig, The Rockefeller University, New York, NY), 1 µg/mL of either Alexa Fluor 647-conjugated goat anti-mouse or goat anti-human Abs (Thermo Fisher Scientific) were used as secondary Abs. The following Abs were used for the NK cell activation assay: APC-conjugated anti-CD107a (BD Biosciences, H4A3), BV421-conjugated anti-CD3 (Biolegend, UCHT1), PE-conjugated anti-CD56 (BD Biosciences, NCAM16.2) and PE-Cy7-conjugated anti-IFNγ (BD Biosciences, B27). The following Abs were used for RNA-flow analysis: BUV395-conjugated anti-CD3 (BD Biosciences, UCHT1), PE-Cy7-conjugated anti-CD4 (BD Biosciences, RPA-T4) BV510-conjugated anti-CD8 (Biolegend, SK1), BV510-conjugated anti-CD14 (Biolegend, M5E2) BV510-conjugated anti-CD19 (Biolegend, H1B19) and PE-conjugated anti-p24 (Beckman Coulter/Immunotech, KC57), while AquaVivid (Thermo Fisher Scientific) was used as viability dye.

ADCC measurements

FACS-based assay

Measurement of ADCC using the FACS-based assay was performed at 48h post-infection as previously described (1-3). Briefly, infected primary $CD4^+$ T cells were stained with viability

(AquaVivid; Thermo Fisher Scientific) and cellular (cell proliferation dye eFluor670; eBioscience) markers and used as target cells. Autologous PBMC effectors cells, stained with another cellular marker (cell proliferation dye eFluor450; eBioscience), were added at an effector: target ratio of 10:1 in 96-well V-bottom plates (Corning, Corning, NY). A 1:1,000 final dilution of sera or 5 µg/ml of ADCC-mediating mAbs were added to appropriate wells and cells were incubated for 15 min at room temperature. The plates were subsequently centrifuged for 1 min at 300 × g, and incubated at 37°C, 5% CO2 for 5 to 6 h before being fixed in a 2% PBS-formaldehyde solution containing 5x104 flow cytometry particles/ml (AccuCount blank particles; 5.3 µm; Spherotech). Samples were analyzed on an LSRII cytometer (BD Biosciences) and acquisition was set to acquire 1,000 flow cytometry particles, which allows the calculation of relative cell counts (2). Data analysis was performed using FlowJo vX.0.7 (Tree Star). The percentage of ADCC was calculated with the following formula: (relative count of GFP^+ cells in targets plus effectors) - (relative count of GFP^+ cells in targets plus effectors plus Abs or sera) / (relative count of GFP^+ cells in targets) by gating infected live target cells. For cells infected with HIV-1 primary isolates, infected cells were identified by intracellular staining for HIV-1 p24. In that context, the percentage of ADCC was calculated with the following formula: (% of $p24^+$ cells in Targets plus Effectors) − (% of $p24^+$ cells in Targets plus Effectors plus sera) / (% of $p24^+$ cells in Targets) by gating on infected lived target cells.

Granzyme B assay

Measurement of ADCC response using the Granzyme B assay was performed 48h post-infection according to the manufacturer's instructions (OncoImmunin, Gaithersburg, MD) and as previously described (4, 5). Briefly, infected primary $CD4^+$ T cells were stained with a fluorescent target cell marker (TFL4; OncoImmunin, Gaithersburg, MD) and a viability marker (NFL1; OncoImmunin or AquaVivid; Thermo Fisher Scientific). Rested autologous purified NK cells were used as effector cells. Target and effector cells were counted and adjusted to reach a final effector: target ratio of 10:1. Twenty-five µl of each effector and target cell suspension and 75 µl of Granzyme B substrate (OncoImmunin) was dispensed into each well of a 96-well V-bottom plate (Corning). A 1:1,000 final dilution of sera or 5 µg/ml or ADCC-mediating Abs were added to appropriate wells and cells were incubated for 15 min at room temperature. The plates were subsequently centrifuged for 1 min at 300 × g and incubated for 1 h at 37°C and 5% CO_2. After

two washes, cells were acquired on an LSRII cytometer (BD Biosciences) and data analysis was performed using FlowJo vX.0.7 (Tree Star). The percentage of Ab or sera-induced Granzyme B activity was calculated with the following formula: (Percentage of Granzyme B^+ target cells in targets plus effectors plus Abs or sera) - (Percentage of Granzyme B^+ target cells in targets plus effectors) per the gating strategy presented in **Fig 3.1.S5**.

NK cell activation assay

Measurement of ADCC response using the NK cell activation assay was performed using a modified version of a previously described protocol (6). Briefly, primary $CD4^+$ T cells infected for 48h were co-cultured with autologous PBMC at an effector: target ratio of 5:1 in the presence of a 1:1,000 final dilution of sera or 5 µg/ml or ADCC-mediating Abs, anti-CD107a, Brefeldin A (Sigma) (5µg/ml) and Monensin (BD Biosciences) (6µg/ml) for 5h at 37ºC. Control conditions included incubation of PBMC alone or incubation of PBMC with mock cells in the presence of sera or ADCC-mediating Abs. After incubation cells were surface stained with anti-CD3 and anti-CD56 Abs. Next, cells were fixed and permeabilized using the Cytofix/Cytoperm Fixation/Permeabilization Kit (BD Biosciences) and stained with anti-IFNγ Ab. Samples were analyzed on an LSRII cytometer (BD Biosciences) and data analysis was performed using FlowJo vX.0.7 (Tree Star). The percentage of Ab or sera-induced NK cell activation was calculated with the following formula: (Percentage of NK cells ($CD3^-$ $CD56^+$) positive for CD107a and/or IFNγ in targets plus effectors plus Abs or sera) - (Percentage of NK cells ($CD3^-$ $CD56^+$) positive for CD107a and/or IFNγ in targets plus effectors) according to the gating strategy presented in **Fig 3.1.S5**.

Luciferase assay

Measurement of ADCC responses using the Luciferase assay was performed as previously described (7). Briefly, CEM.NKR-CCR5-sLTR-Luc target cells, which express luciferase (Luc) under the control of a Tat-inducible promoter, were infected and used as target cells at 48h post-infection. Primary human PBMCs or NK cell line expressing human CD16 were used as effector cells. Target and effector cells were co-cultured for 6-8h, in triplicate, at an effector: target ratio of 10:1 in the presence of different concentrations of Abs (0.0024, 0.0098, 0.0390, 0.1563, 0.6250, 2.5, 10 or 40 µg/ml) or different dilution of human sera (1:100, 1:400, 1:1,600, 1:6,400, 1:25,600,

1:102,400, 1:409,600 or 1:1,638,400). The dose-dependent loss of Luc activity was measured as an indication of sera or Ab-mediated killing of productively-infected cells. Infected target cells incubated with effector cells in the absence of sera or Ab were used to measure maximal Luc activity, and uninfected target cells cultured with effector cells were used to determine background Luc activity. Area under the curve (AUC) values for ADCC were calculated as previously described (7). For experiments involving CH77 wt and $N^{-}U^{-}$ viruses, the *vif* gene was deleted by site-directed mutagenesis. The nucleotides 62 and 63 in *vif* were deleted, causing a frameshift that resulted in an early stop codon (W21*) while preserving the *pol* open reading frame.

RFADCC assay

CEM.NKR-CCR5-sLTR-Luc target cells were coated or not with 1 µg/ml of recombinant gp120 protein derived from the HIV-1 YU2 strain for 30 minutes at 37°C, 5% CO_2. Cells were then double stained with PKH26 red fluorescent cell linker (Sigma-Aldrich, USA) and the cellular proliferation marker eFluor670 (eBioscience) as previously described (2, 8, 9) Cells were then dispensed together with different concentration of Abs (0.008, 0.04, 0.2, 1 and 5 µg/ml) or different dilutions of sera (1:100, 1:400, 1:1,600, 1:6,400 and 1:25,600). After 15 min at room temperature, effector cells (Rested primary PBMCs) were added at an effector: target ratio of 50:1. Plates were centrifuged for 1 min at 300 × g and incubated for 4 h at 37°C. Cells were washed, fixed and acquired on an LSRII cytometer (BD Biosciences). Data analysis was performed using FlowJo vX.0.7 (Tree Star). The percentage of cytotoxicity was calculated with the following formula: (Percentage of cells that remained $PKH26^{+}$ but that had lost the proliferation dye ($eFluor670^{-}$) in target cells coated with recombinant gp120 plus effectors plus Abs or sera) - (Percentage of cells that remained $PKH26^{+}$ but that had lost the proliferation dye ($eFluor670^{-}$) in target cells plus effectors plus Abs or sera) according to the gating strategy presented in **Fig 3.1.S6**.

3.2.12 SUPPLEMENTAL REFERENCES

1. Veillette M, Desormeaux A, Medjahed H, Gharsallah NE, Coutu M, Baalwa J, Guan Y, Lewis G, Ferrari G, Hahn BH, Haynes BF, Robinson JE, Kaufmann DE, Bonsignori M, Sodroski J, Finzi A. 2014. Interaction with cellular CD4 exposes HIV-1 envelope epitopes targeted by antibody-dependent cell-mediated cytotoxicity. J Virol 88:2633-44.

2. Richard J, Veillette M, Batraville LA, Coutu M, Chapleau JP, Bonsignori M, Bernard N, Tremblay C, Roger M, Kaufmann DE, Finzi A. 2014. Flow cytometry-based assay to study HIV-1 gp120 specific antibody-dependent cellular cytotoxicity responses. J Virol Methods 208:107-14.
3. Richard J, Veillette M, Brassard N, Iyer SS, Roger M, Martin L, Pazgier M, Schon A, Freire E, Routy JP, Smith AB, III, Park J, Jones DM, Courter JR, Melillo BN, Kaufmann DE, Hahn BH, Permar SR, Haynes BF, Madani N, Sodroski JG, Finzi A. 2015. CD4 mimetics sensitize HIV-1-infected cells to ADCC. Proc Natl Acad Sci USA 112:E2687-94.
4. Pollara J, Hart L, Brewer F, Pickeral J, Packard BZ, Hoxie JA, Komoriya A, Ochsenbauer C, Kappes JC, Roederer M, Huang Y, Weinhold KJ, Tomaras GD, Haynes BF, Montefiori DC, Ferrari G. 2011. High-throughput quantitative analysis of HIV-1 and SIV-specific ADCC-mediating antibody responses. Cytometry A 79:603-12.
5. Konstantinus IN, Gamieldien H, Mkhize NN, Kriek JM, Passmore JA. 2016. Comparing high-throughput methods to measure NK cell-mediated antibody-dependent cellular cytotoxicity during HIV- infection. J Immunol Methods 434:46-52.
6. Gooneratne SL, Richard J, Lee WS, Finzi A, Kent SJ, Parsons MS. 2015. Slaying the Trojan horse: natural killer cells exhibit robust anti-HIV-1 antibody-dependent activation and cytolysis against allogeneic T cells. J Virol 89:97-109.
7. Alpert MD, Heyer LN, Williams DE, Harvey JD, Greenough T, Allhorn M, Evans DT. 2012. A novel assay for antibody-dependent cell-mediated cytotoxicity against HIV-1- or SIV-infected cells reveals incomplete overlap with antibodies measured by neutralization and binding assays. J Virol 86:12039-52.
8. Gomez-Roman VR, Florese RH, Patterson LJ, Peng B, Venzon D, Aldrich K, Robert-Guroff M. 2006. A simplified method for the rapid fluorometric assessment of antibody-dependent cell-mediated cytotoxicity. J Immunol Methods 308:53-67.
9. Ruiz MJ, Ghiglione Y, Falivene J, Laufer N, Holgado MP, Socias ME, Cahn P, Sued O, Giavedoni L, Salomon H, Gherardi MM, Rodriguez AM, Turk G. 2016. Env-Specific IgA from Viremic HIV-Infected Subjects Compromises Antibody-Dependent Cellular Cytotoxicity. J Virol 90:670-81.

3.2.13 SUPPLEMENTAL FIGURES

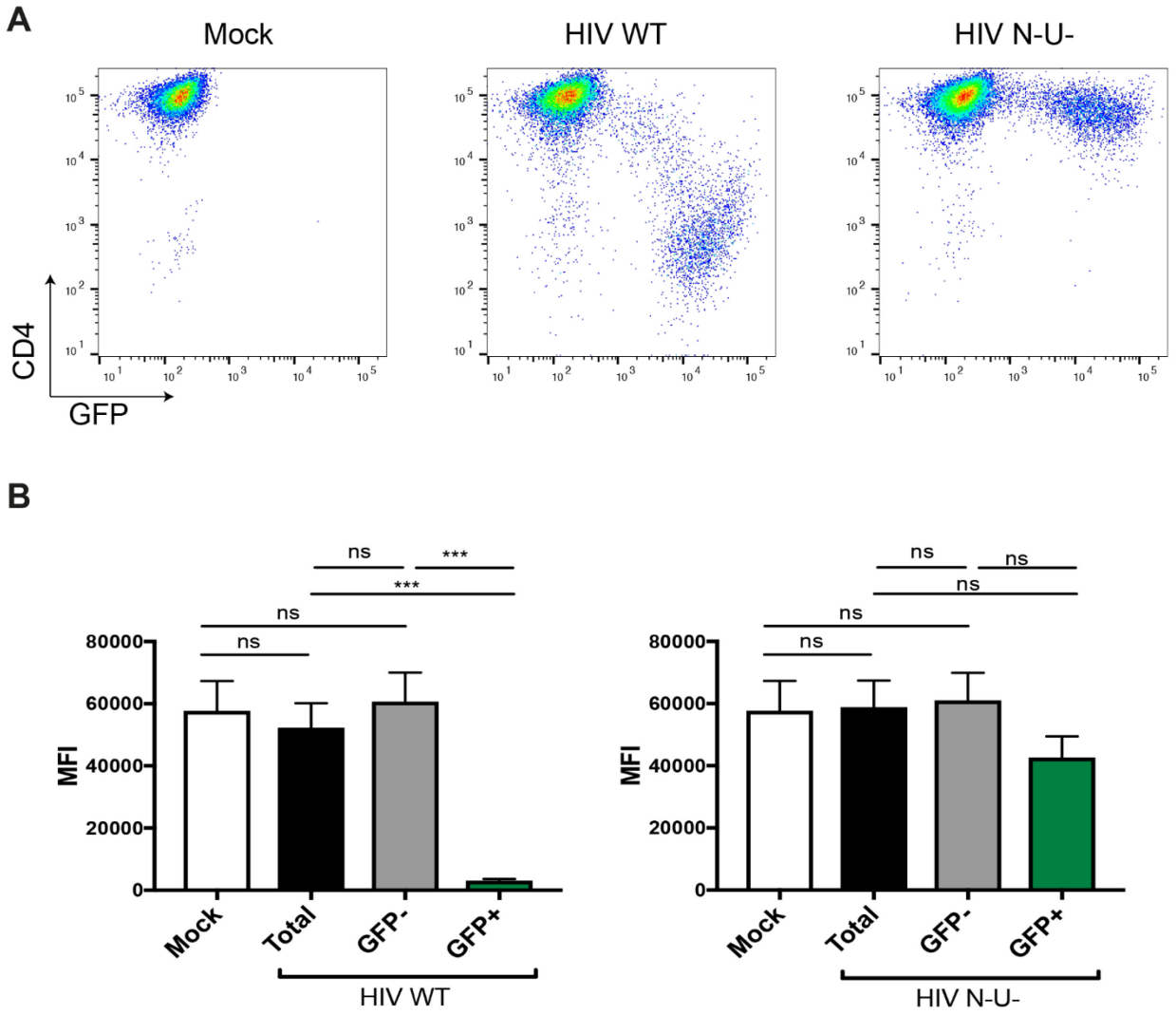

Figure 3.1.S1 - Level of cell-surface CD4 on infected and uninfected cells.
Cell-surface staining of primary $CD4^+$ T cells mock-infected (Mock) or infected with the NL4.3 ADA GFP virus, either wild-type (HIV WT) or defective for Nef and Vpu expression (HIV N^-U^-) with the anti-CD4 OKT4 Ab (1µg/ml) (**A**) Dot plots depicting representative staining. (**B**) Mean Fluorescence Intensity (MFI) obtained for at least 5 different experiments. Error bars indicate means ± standard errors of the means. Statistical significance was tested using ordinary one-way ANOVA. (***, $P < 0.001$, ns: nonsignificant).

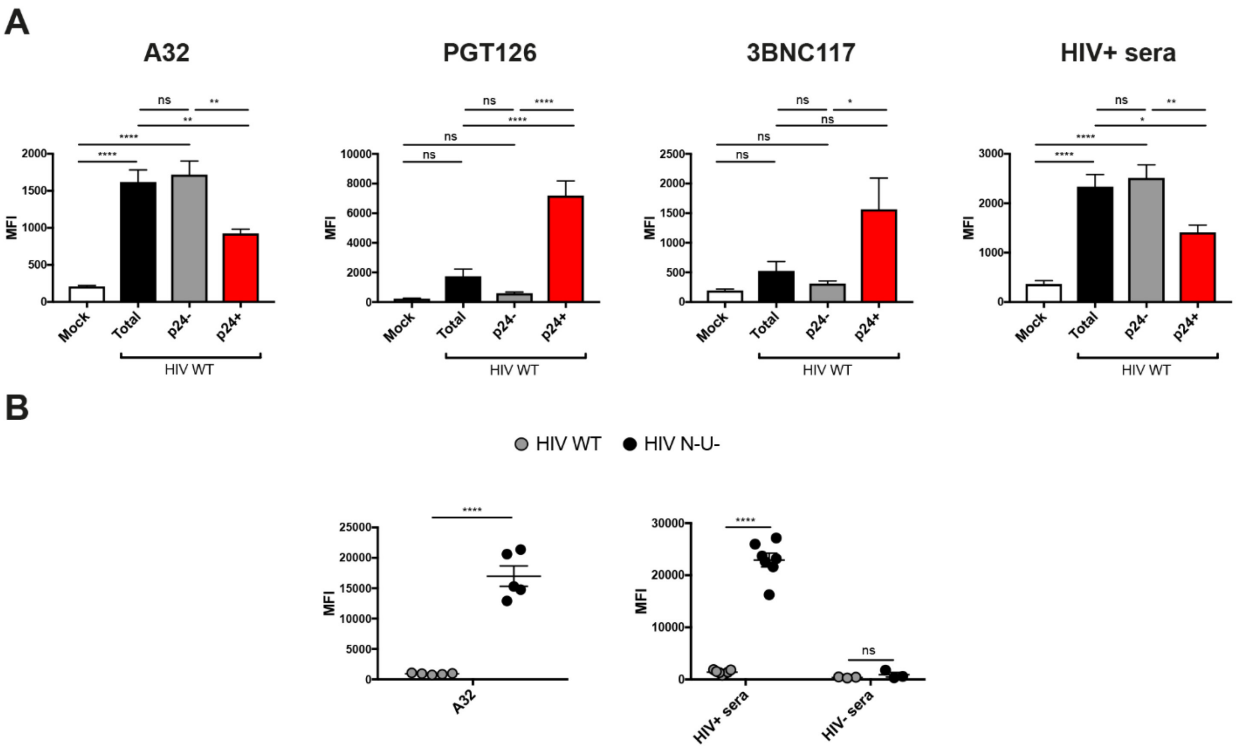

Figure 3.1.S2 - Recognition of primary CD4$^+$ T cells infected with the transmitted/founder virus CH77.

Primary CD4$^+$ T cells were mock-infected or infected with the transmitted/founder virus CH77, either wild-type (HIV WT) or defective for Nef and Vpu expression (HIV N$^-$U$^-$). Forty-eight hours post-infection, cells were stained with A32, PGT126, 3BNC117 (5 µg/ml) or sera from 10 HIV-1-infected individuals (HIV$^+$ sera) or 5 uninfected individuals (HIV$^-$ sera) (1:1000 dilution), followed with appropriate secondary Abs. Shown in (**A**) are the mean fluorescence intensities (MFI) obtained for at least 5 independent stains with the different Abs, with 10 HIV$^+$ or 5 HIV$^-$ sera on cells infected with WT virus. Graphs shown in (**B**) represent the MFI obtained for 5 independent stains with A32, with 10 HIV$^+$ sera or 5 HIV$^-$ sera on cells infected with WT and N$^-$U$^-$ virus. Error bars indicate means ± standard errors of the means. Statistical significance was tested using (**A**) ordinary one-way ANOVA, (**B**) unpaired t test or Mann-Whitney test (*, $P < 0.05$, (**, $P < 0.01$, ****, $P < 0.0001$, ns: non-significant).

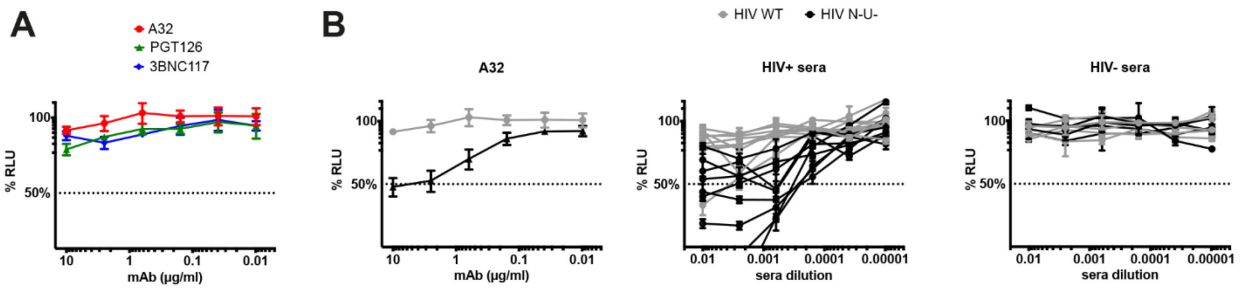

Figure 3.1.S3 - ADCC responses detected by the Luciferase assays.
Representation of the ADCC responses detected by the Luc assay (presented in Fig 3.1.2) as the loss of luciferase signal (RLU). (**A**) ADCC responses mediated by A32, PGT126 and 3BNC117 (0.0024, 0.0098, 0.0390, 0.1563, 0.6250, 2.5 and 10 µg/ml) against cells infected with NL4.3 ADA GFP WT. (**B**) ADCC responses mediated by A32 (0.0024, 0.0098, 0.0390, 0.1563, 0.6250, 2.5 and 10 µg/ml), HIV^+ or HIV^- sera (1:100, 1:400, 1:1,600, 1:6,400, 1:25,600 and 1:102,400) against cells infected with NL4.3 ADA GFP WT (HIV WT) or defective for Nef and Vpu expression (HIV N^-U^-). Error bars indicate means +/- standard errors of the means.

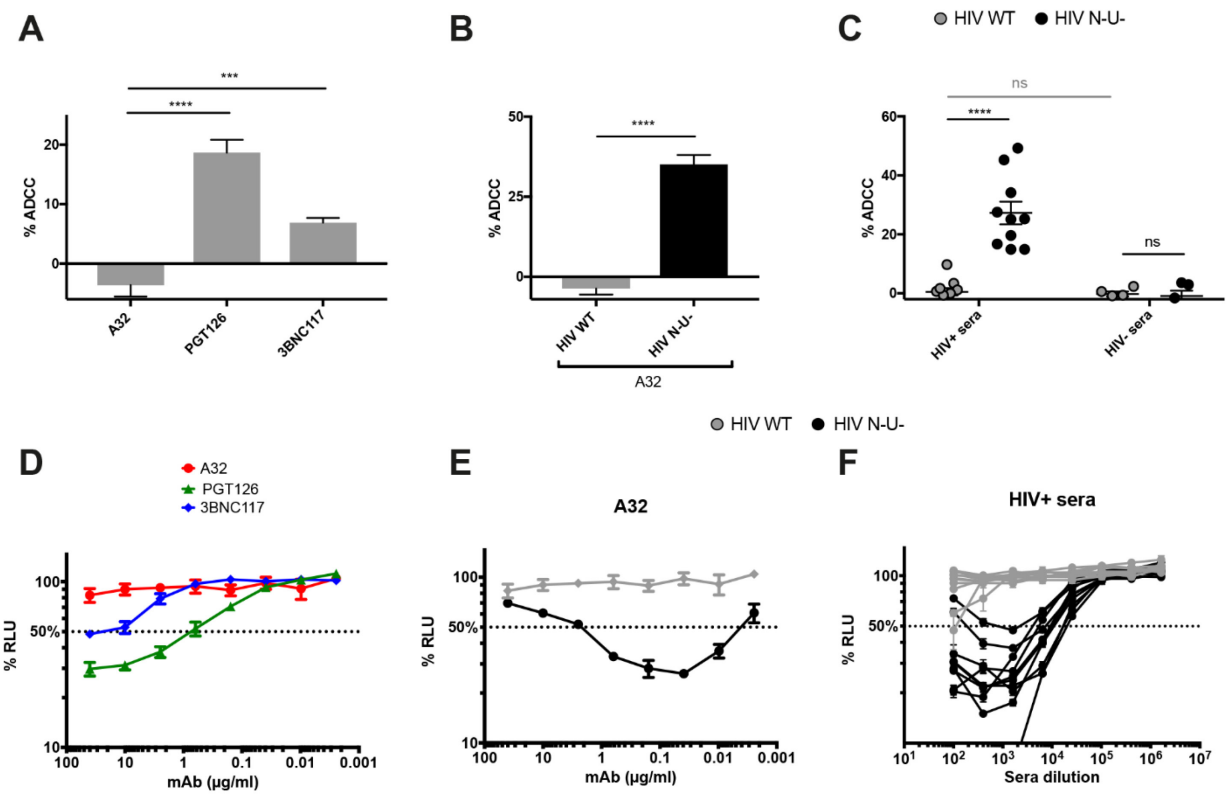

Figure 3.1.S4 - ADCC responses detected with the FACS-based and Luciferase assays against cells infected with the transmitted/founder virus CH77.

(**A-C**) Primary $CD4^+$ T cells or (**D-F**) CEM.NKR-CCR5-sLTR-Luc cells infected with the transmitted/founder virus CH77, either wild-type (HIV WT) (depicted in gray) or defective for Nef and Vpu expression (HIV N^-U^-) (depicted in black) were used as target cells with the (**A-C**) FACS-based infected cell elimination assay or (**D-F**) the Luciferase assays. Shown in (**A,D**) are ADCC responses mediated by A32, PGT126 and 3BNC117 against cells infected with WT virus, and in (**B,C,E,F**) ADCC responses mediated by (**B,E**) A32 or (**C,F**) HIV^+ and HIV^- sera against cells infected with WT or N^-U^- virus. (**A-C**) All graphs shown represent ADCC responses obtained from at least 5 independent experiments. (**D-F**) ADCC responses presented as loss of luciferase signal (RLU) in triplicate. For the FACS-based assay, mAbs were used at 5 µg/ml and human sera at a 1:1,000 dilution. For the Luciferase assay, mAbs were used at 0.0024, 0.0098, 0.0390, 0.1563, 0.6250, 2.5, 10 and 40 µg/ml and human sera at a dilution of 1:100, 1:400, 1:1,600, 1:6,400, 1:25,600, 1:102,400, 1:409,600 and 1:1,638,400. Error bars indicate means +/- standard errors of the means. Statistical significance was tested using unpaired t test (***, P <0.001, ****, P <0.0001, ns: non-significant).

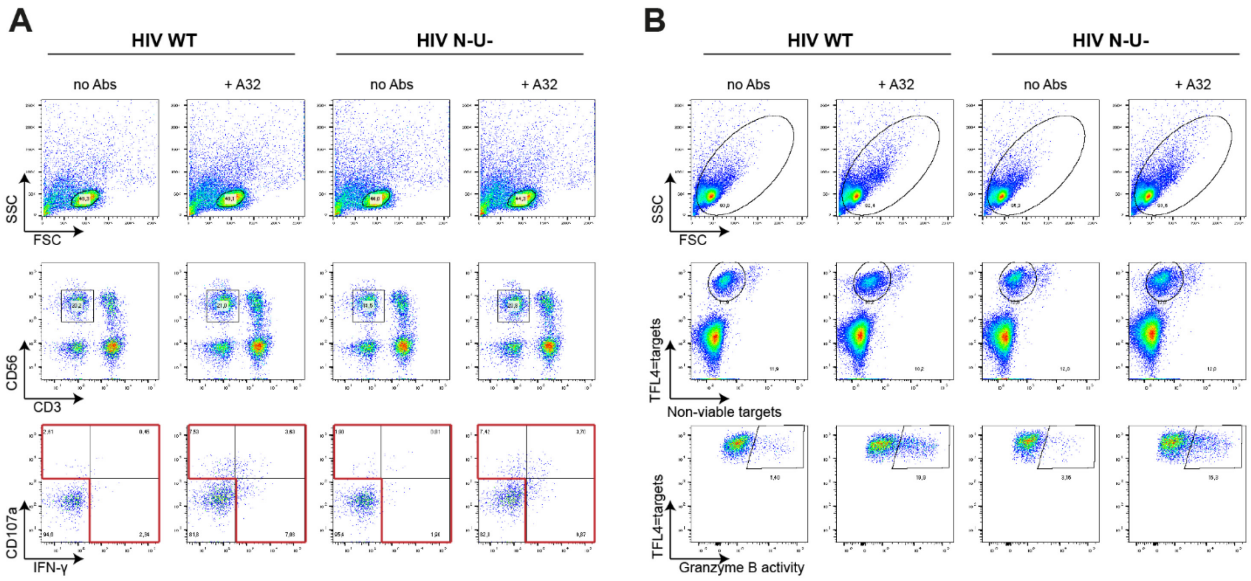

Figure 3.1.S5 - Gating strategy used for the NK cell activation and Granzyme B assays. Gating strategy and dot plots depicting a representative detection of (**A**) NK cell activation and (**B**) granzyme B activity in the context of cells infected with NL4.3 ADA GFP virus, either WT (HIV WT) or defective for Nef and Vpu expression (HIV $N^{-}U^{-}$) in the presence or absence of A32.

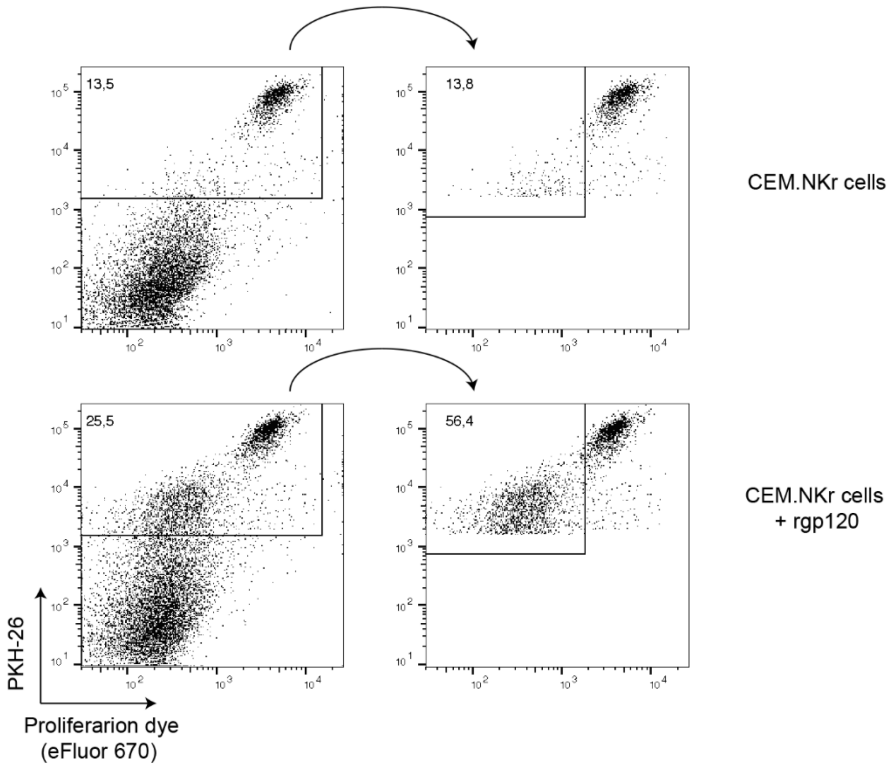

Figure 3.1.S6 - Gating strategy used for the RFADCC assays.
Gating strategy and dot plots depicting representative detection of responses mediated by A32 against target cells coated or not with recombinant gp120 using the RFADCC assay.

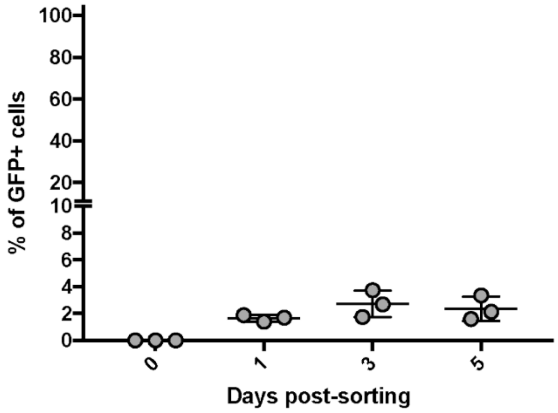

Figure 3.1.S7 - The vast majority of uninfected bystander CD4$^+$ T cells remain uninfected after 5 days in culture.

Primary CD4$^+$ T cells were infected with the NL4.3 ADA GFP WT. Forty-eight hours post-infection, the GFP$^-$ cell population was sorted by flow cytometry and kept in culture for 5 days. The vast majority of cells (>96%) remained negative for GFP after 5 days of culture. Error bars indicate means +/- standard errors of the means for 3 independent experiments.

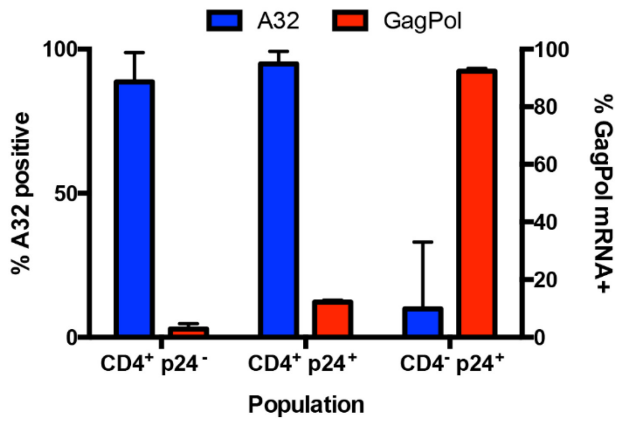

Figure 3.1.S8 - Characterization of cells infected with the X4-tropic NL4.3 virus by RNA Flow FISH method.
Quantification of the percentage of cells positive for A32 binding and *gag-pol* mRNA based on CD4 and p24 levels among primary $CD4^+$ T cells infected with the X4-tropic NL4.3 WT virus. Error bars indicate means ± standard errors of the means of at least 4 independent experiments.

ARTICLE 3

La suppression incomplète des niveaux de CD4 sur les cellules infectées affecte la conformation de l'enveloppe du VIH-1 et la réponse ADCC

Incomplete Downregulation of CD4 Expression Affects HIV-1 Env Conformation and Antibody-Dependent Cellular Cytotoxicity Responses

Auteurs:

Jérémie Prévost[1,2], Jonathan Richard[1,2], Halima Medjahed[1], Audrey Alexander[3], Jennifer Jones[3], John C. Kappes[3], Christina Ochsenbauer[3], Andrés Finzi[1,2,4]

Affiliations:

[1]Centre de Recherche du CHUM, Montreal, QC, Canada; [2]Department of Microbiology, Infectious Diseases and Immunology, Université de Montréal, Montreal, QC, Canada; [3]Department of Medicine, University of Alabama at Birmingham, Birmingham, AL, USA; [4]Department of Microbiology and Immunology, McGill University, Montreal, QC, Canada.

Contribution des auteurs:

Conceptualisation: **J.P.** et A.F.; Méthodologie: **J.P.** et A.F.; Recherche: **J.P.**, J.R., A.A. et J.J.; Ressources: H.M., J.C.K., C.O., et A.F.; Analyse formelle: **J.P.**; Visualisation: **J.P.**; Supervision: J.C.K., C.O., et A.F.; Obtention du financement: J.C.K., C.O., et A.F.; Rédaction - version originale: **J.P.** et A.F.; Rédaction - révision et édition: **Tous les auteurs**.

Statut: Cet article a été publié dans *Journal of Virology*, le 13 juin 2018.
https://doi.org/10.1128/JVI.00484-18

3.3.1 RÉSUMÉ

Les cellules infectées par le VIH-1 exprimant à leur surface les glycoprotéines d'enveloppe (Env) dans la conformation liée à CD4 sont ciblées par la réponse cytotoxique cellulaire dépendante des anticorps (ADCC) médiée par les anticorps induits par CD4 (CD4i) et les sérums d'individus infectés par le VIH-1 (sérums VIH$^+$). En régulant négativement l'expression de surface de CD4, Nef empêche l'interaction Env-CD4, protégeant ainsi les cellules infectées par le VIH-1 de l'ADCC. Les clones moléculaires infectieux (IMCs) du VIH-1 sont largement utilisés pour mesurer l'ADCC. Afin de faciliter l'identification des cellules infectées et l'analyse ADCC à haut débit, des gènes rapporteurs (par exemple, le gène de la luciférase de Renilla [LucR]) sont souvent introduits dans les constructions IMC. Nous avons évalué la susceptibilité des lymphocytes T CD4$^+$ infectés par le VIH-1 à la réponse ADCC en utilisant un panel d'IMCs parentaux et de dérivés qui expriment le gène rapporteur LucR, en utilisant différentes stratégies moléculaires, dont une spécifiquement conçue pour conserver l'expression de Nef. Nous avons constaté que dans certaines de ces constructions, l'expression de Nef dans les lymphocytes T CD4$^+$ était sous-optimale et que, par conséquent, la régulation négative de CD4 était incomplète. Les molécules CD4 restant à la surface des cellules entraînent l'exposition des épitopes CD4i sur Env et une augmentation importante de la sensibilité des cellules infectées à l'ADCC. On constate également que les cellules infectées avec l'IMC parental sont protégées contre la réponse ADCC puisqu'elles présentent une forte diminution des niveaux de CD4. Cette différence entre le virus parental et le virus déficient pour l'expression de Nef est indépendante de la souche d'Env exprimée, mais elle est plutôt corrélée aux niveaux d'expression de surface de CD4. Dans l'ensemble, nos résultats indiquent qu'il faut faire preuve de prudence lors de la sélection des IMCs pour mesurer la réponse ADCC et que la régulation négative du CD4 doit être prise en considération avant de tirer des conclusions sur la nature et l'ampleur de la réponse ADCC.

3.3.2 ABSTRACT

HIV-1-infected cells expressing envelope glycoproteins (Env) in the CD4-bound conformation on their surfaces are targeted by antibody-dependent cellular cytotoxicity (ADCC) mediated by CD4-induced (CD4i) antibodies and sera from HIV-1-infected individuals (HIV$^+$ sera). By downregulating the surface expression of CD4, Nef prevents Env-CD4 interaction, thus protecting HIV-1-infected cells from ADCC. HIV-1 infectious molecular clones (IMCs) are

widely used to measure ADCC. In order to facilitate the identification of infected cells and high-throughput ADCC analysis, reporter genes (e.g., the Renilla luciferase [LucR] gene) are often introduced into IMC constructs. We evaluated the susceptibility of HIV-1-infected CD4 T lymphocytes to ADCC using a panel of parental IMCs and derivatives that expressed the LucR reporter gene, utilizing different molecular strategies, including one specifically designed to retain Nef expression. We found that in some of these constructs, Nef expression in CD4 T cells was suboptimal, and consequently, CD4 downregulation was incomplete. CD4 molecules remaining on the cell surface resulted in the exposure of ADCC-mediating CD4i epitopes on Env and a dramatic increase in the susceptibility of the infected cells to ADCC. Strikingly, protection from ADCC was observed when cells were infected with the parental IMC, which exhibited strong CD4 downregulation. This discrepancy between the parental and Nef-impaired viruses was independent of the strains of Env expressed, but rather, it was correlated with the levels of CD4 surface expression. Overall, our results indicate that caution should be taken when selecting IMCs for ADCC measurements and that CD4 downregulation needs to be carefully monitored when drawing conclusions about the nature and magnitude of ADCC

3.3.3 IMPORTANCE

In-depth understanding of the susceptibility of HIV-1-infected cells to ADCC might help establish correlates of vaccine protection and guide the development of HIV-1 vaccine strategies. Different ADCC assays have been developed, including those using infectious molecular clones (IMCs) carrying a LucR reporter gene that greatly facilitates large-scale quantitative analysis. We previously reported different molecular strategies for introducing LucR while maintaining Nef expression and function and, consequently, CD4 surface downregulation. Here, we demonstrate that utilizing IMCs that exhibit impaired Nef expression can have undesirable consequences due to incomplete CD4 downregulation. CD4 molecules remaining on the cell surface resulted in the exposure of ADCC-mediating CD4i epitopes on Env and a dramatic increase in the susceptibility of the infected cells to ADCC. Overall, our results indicate that CD4 downregulation needs to be carefully monitored when drawing conclusions about the nature and magnitude of ADCC.

3.3.4 INTRODUCTION

Recent efforts aimed at understanding antibody-dependent cellular cytotoxicity (ADCC) against HIV-1-infected cells uncovered several strategies put in place by the virus to limit exposure of vulnerable CD4-induced (CD4i) epitopes. Interaction of Env with the CD4 receptor was reported to be critical for exposing epitopes recognized by ADCC-mediating antibodies (Abs) (1–3). HIV-1 achieves protection from ADCC by limiting Env-CD4 interaction by downregulating CD4 and preventing Env accumulation at the surface of infected cells (1, 3–7). Two accessory proteins, Nef and Vpu, impact ADCC sensitivity via reduction of cell surface expression of CD4 (1, 3), while Env accumulation is tightly controlled through efficient internalization (6) and Vpu-mediated BST-2 downregulation (4, 5, 7). Therefore, these accessory proteins protect HIV-1-infected cells from ADCC mediated by CD4i non-neutralizing Abs (nnAbs). Thus, cells infected with primary viruses coding for functional Nef and Vpu proteins are largely resistant to ADCC induced by these nnAbs (3, 7–13). These findings are in agreement with structural information indicating that ADCC-mediating nnAbs target a highly conserved region in the gp120 inner domain that is buried inside the untriggered Env trimer and becomes exposed only upon CD4 engagement (2, 3, 8, 14–17). Thus, it is to be expected that in the presence of functional Vpu and Nef, HIV-1-infected cells will be largely refractory to CD4i nnAb-mediated ADCC. Several studies, however, have reported ADCC activity by such antibodies against HIV-1-infected cells (18–33), suggesting the CD4i epitopes were accessible. Since all of these studies used HIV-1 infectious molecular clones (IMCs) carrying the Renilla luciferase (LucR) reporter gene for sensitive quantification of infection and infection inhibition, we wondered whether the molecular design of the LucR reporter IMC might have impaired Nef functions that impacted the conformation sampled by Env at the surface of infected cells. Of note, the original reporter IMC strategy encompassed an isogenic proviral backbone from which heterologous env strains could be expressed in cis and encoding LucR in frame with a T2A “ribosome-skipping” peptide intended to drive Nef expression (referred to as Env-IMC-LucR.T2A) (34). Supporting the possibility of Env conformation being impacted, we previously reported that the strategy used to create LucR reporter IMCs can affect Nef expression on CD4 T cells (35), which in turn may affect the Env conformation due to incomplete CD4 downregulation (1, 3, 13, 36). Of note, we found that a revised molecular strategy utilizing a modified encephalomyocarditis virus (EMCV) internal ribosome entry site (IRES) element in lieu of T2A (Env-IMC-LucR.6ATRi) can normalize Nef

expression and function compared to the Env-IMC-LucR.T2A molecular strategy (35, 37). In order to test this possibility, we evaluated the CD4i nnAb binding and ADCC susceptibility of primary CD4 T cells infected with panels of parental IMCs and LucR-reporter IMC derivatives in which different strategies to drive Nef expression were applied. Cells infected with certain LucR viruses that exhibited physiological levels of Nef expression downregulated surface CD4 efficiently, though not always completely. Consequently, their levels of CD4i nnAb binding were similar to that of cells infected with the parental viruses, as were their levels of protection against ADCC by CD4i antibodies. However, importantly, we found that in some IMC-LucR constructs, Nef expression in CD4 T cells was suboptimal, and consequently, CD4 downregulation from the cell surface was less efficient. This allowed Env-CD4 engagement and the exposure of CD4i epitopes otherwise occluded on cells infected with parental IMCs. Consequently, while cells infected with parental IMCs presented robust CD4 downregulation and were protected from ADCC mediated by the antibody A32 and HIV+ sera, cells infected with the LucR reporter IMCs that displayed impaired Nef expression (i.e., encoding LucR.T2A) were highly susceptible to ADCC mediated by these ligands.

3.3.5 RESULTS

Molecular strategies for Nef expression in reporter HIV-1 affect CD4 downregulation.

HIV-1 IMCs carrying panels of heterologous HIV-1 env sequences (Env-IMCs) in an isogenic backbone and expressing the Renilla luciferase (LucR) reporter, which allows highly sensitive, quantitative readout of productive infection (34), have been widely used to evaluate the susceptibility of HIV-1-infected cells to ADCC mediated by vaccine-elicited antibodies and several CD4i nnAbs (18–33). However, we previously reported that some of these LucR reporter IMCs, particularly those utilizing a ribosome-skipping T2A peptide strategy to link Renilla luciferase with Nef (Env-IMC-LucR.T2A), were unable to fully downregulate CD4 due to impaired Nef expression in CD4 T cells (35). In a modified molecular approach, we introduced a bicistronic LucR.IRES-nef cassette in lieu of LucR.T2A-nef by utilizing the EMCV-modified 6ATR IRES element (6ATRi) to drive nef expression (Env-IMC-LucR.6ATRi) and showed that it can normalize Nef expression and function compared to the T2A molecular strategy (35, 37). **Figure 3.2.1** schematically illustrates these molecular approaches. In this study, we aimed to

elucidate whether different strategies to drive Nef expression affect the sensitivity of reporter HIV-1 IMCs to ADCC compared to their parental non-reporter IMCs. To this end, we first compared the abilities of a panel of IMCs (described in Materials and Methods) to downregulate CD4. In addition to previously reported replication-competent Env-IMC and Env-IMC-LucR.T2A viruses, we included an expanded panel of Env-IMC-LucR.6ATRi viruses carrying further transmitted/founder (T/F) and reference env strains, as well as novel full-length T/F IMCs into which the LucR.6ATRi cassette was inserted. In order to evaluate the abilities of the different parental and LucR IMCs to downregulate CD4 from the cell surface, primary CD4 T cells from HIV-1-uninfected individuals were infected as described in Materials and Methods and 48 h later incubated with the anti-CD4 antibody OKT4. The infected cells were identified by intracellular p24 staining and analyzed by flow cytometry as indicated in Materials and Methods. To help visualize the impact that the LucR.T2A cloning strategy had on CD4 downregulation, representative flow cytometry dot plots are provided in **Fig. 3.2.2A**. Cells infected ($p24^+$) with the parental CH058.c T/F virus exhibited robust CD4 downregulation (**Fig. 3.2.2A**, left). This was recapitulated with a pNL4.3-based Env-IMC expressing the CH058 Env (**Fig. 3.2.2A**, center). However, in the strain-matched Env-IMC-LucR.T2A virus (NL-LucR.T2A-B.CH058.ecto), CD4 downregulation was dramatically reduced (**Fig. 3.2.2A and B**). This finding was consistent with what we previously described for the BaL env-bearing counterpart, NL-LucR.T2A-BaL.ecto, and matched the Nef-minus control (**Fig. 3.2.2C**) (35). The same impairment of CD4 downregulation compared to parental Env-IMC was observed with additional Env-IMC-LucR.T2A viruses expressing different T/F and reference strain Envs (CH040, YU2, SF162, and BaL), indicating that the observed effect was independent of the Env being expressed (**Fig. 3.2.2C**). Notably, the T2A strategy to drive Nef expression also adversely affected CD4 downregulation when LucR.T2A was introduced into the parental CH077.t T/F IMC (**Fig. 3.2.2C**), indicating that the lack of functional Nef expression and CD4 downregulation is not exclusive to the laboratory-adapted pNL4.3 backbone. Interestingly, introduction of the LucR.6ATRi element into two T/F IMCs (CH077.t and CH0505s) or several Env-IMC proviruses allowed downregulation of CD4 to physiological levels, similar to their parental counterparts, but not always as efficiently (**Fig. 3.2.2C**, compare CH040, CH077, and CH505). As expected, and in agreement with our previous publication (35), impaired CD4 downregulation was strongly correlated with deficient Nef expression in T cells

(**Fig. 3.2.2D and E**) and with deficient Nef-mediated major histocompatibility complex class I (MHC-I) downregulation (not shown).

CD4 downregulation affects Env conformation and ADCC responses.

We previously established that inefficient CD4 downregulation results in Env-CD4 interaction that causes exposure of Env CD4i epitopes on the surfaces of infected cells (1, 3, 13). Nevertheless, Nef-impaired Env-IMC-LucR.T2A viruses have been used to assess CD4i nnAb-mediated ADCC *in vitro*, while Env strain-matched reporter viruses utilizing the 6ATRi element to drive Nef expression had not yet been investigated for ADCC assays. We therefore investigated whether the impaired CD4 downregulation observed for some LucR reporter IMCs (**Fig. 3.2.2A to C**) was sufficient to alter Env conformation. Primary $CD4^+$ T cells were infected with the same panels of viruses described above. Exposure of CD4i epitopes was monitored with the nnAb antibody, A32, which recognizes an anti-cluster A epitope normally occluded in the untriggered trimer (2, 3, 8, 14–17), as well as with sera from HIV-1-infected individuals (HIV^+ sera). Dramatic differences in Env recognition by A32 (**Fig. 3.2.3A to C**) and HIV^+ sera (**Fig. 3.2.3E to G**) were observed among the different panels of IMCs expressing the same Env. For example, cells infected with the wild-type CH058.c T/F IMC or its cognate non-reporter Env-IMC were poorly recognized by these ligands (**Fig. 3.2.3A and E**), but when the same Env was expressed in the context of the Env-IMC-LucR.T2A backbone, Env was much more readily recognized by the ligands (mean fluorescence intensities [MFI] were 3- to 5-fold higher) (**Fig. 3.2.3B and F**). Varying degrees of significant increases in Ab binding were also seen for the other T2A-encoding IMCs compared to their Env strain-matched parental viruses and were consistent with the extent of Nef-deficient virus (**Fig. 3.2.3C and G**, panel of BaL Env-expressing IMCs). With regard to Ab binding, LucR.6ATRi-containing reporter IMCs closely resembled parental viruses (**Fig. 3.2.3C and G**). Accordingly, highly significant correlations ($P < 0.0001$) were established between the amounts of CD4 detected on the cell surface and Env recognition by A32 (**Fig. 3.2.3D**) and HIV^+ sera (**Fig. 3.2.3H**). Importantly, increased Env recognition translated into higher susceptibility to ADCC (**Fig. 3.2.4**). Cells infected with the parental IMC were completely (encoding T/F Env strains) or largely (encoding chronic and laboratory-adapted strains, YU-2, SF162, and BaL) resistant to ADCC mediated by these ligands, and LucR.6ATRi-encoding reporter counterparts displayed similar or slightly higher ADCC than the respective parental strain. In contrast, cells infected with

viruses unable to efficiently downregulate CD4 were highly susceptible. Again, strong ($r = 0.76$) and highly significant ($P < 0.0001$) correlations were established between cell surface CD4 levels and ADCC mediated by A32 (**Fig. 3.2.4B**) and HIV$^+$ sera (**Fig. 3.2.4D**). These results strongly advocate for careful characterization of the CD4 downregulation properties of any HIV-1 IMC, including reporter viruses, chosen and intended to measure ADCC, as any IMC with impaired Nef (or Vpu) function may have dramatic effects on Env conformation and thus introduce significant bias toward non-neutralizing CD4i Abs.

Impaired downregulation of NKG2D ligands modulates ADCC responses.

While antibody recognition of target cells is absolutely required for ADCC responses, additional interactions between target and effector cells have been shown to be necessary to activate effector cells, including NK cells. For example, NK cell effector functions are modulated by a balance between signals delivered through inhibitory (e.g., KIR and CD94/NKG2A), activating (e.g., CD16, NKG2D, DNAM-1, and NKp46), or coactivating (e.g., NTB-A and 2B4) receptors that either suppress or enhance NK cell activity (38). It has been shown that Nef decreases the expression of NKG2D ligands (MICA, ULBP1, and ULBP2) (39, 40), thus preventing their interaction with the NK cell-activating NKG2D receptor. Since the NKG2D receptor is known to modulate ADCC responses against HIV-1-infected cells (36, 41), we evaluated the capacities of IMCs expressing T/F Envs CH058, CH040, and CH077 to downregulate NKG2D ligands. To evaluate this, primary CD4 T cells were isolated from non-HIV-infected individuals and infected with these IMCs as described above. The cultures were then stained with a recombinant human NKG2D-Fc chimera that recognizes several NKG2D ligands (41–44) or with a matched isotype control. Infected cells within these cultures were identified by intracellular p24 staining. As previously reported (45), HIV-1 infection enhanced NKG2D-Fc detection compared to mock-infected cells (**Fig. 3.2.5A**). This enhancement, however, was significantly greater when cells were infected with IMCs comprising the LucR.T2A element and was correlated with CD4 levels present at the cell surface (**Fig. 3.2.5B**). We next addressed whether the increased expression of NKG2D ligands enhanced susceptibility to ADCC mediated by A32 and HIV$^+$ sera. As previously reported (1, 3, 8, 13, 36) and shown in **Fig. 3.2.4**, cells infected with the parental viruses were not sensitive to ADCC mediated by A32 (**Fig. 3.2.5C**) or antibodies within HIV$^+$ sera (**Fig. 3.2.5D**), using autologous peripheral blood mononuclear cells

(PBMCs) as effector cells. Supporting Nef's role in evading ADCC (1, 3, 8, 13, 36, 41), cells infected by IMCs with impaired Nef expression (i.e., LucR.T2A viruses) were more susceptible to ADCC mediated by either A32 (**Fig. 3.2.5C**) or HIV$^+$ sera (**Fig. 3.2.5D**). In agreement with a role for NKG2D ligands in ADCC responses against HIV-1-infected cells (36, 41), addition of a blocking anti-NKG2D antibody, but not an isotype control, significantly decreased the susceptibility of Env-IMC LucR.T2A-infected cells to ADCC mediated by A32 and antibodies contained within HIV$^+$ sera (**Fig. 3.2.5C and D**). Altogether, these results indicate that, in addition to the exposure of ADCC-mediating epitopes induced by the presence of CD4 at the cell surface, the accumulation of NKG2D-activating ligands promotes NK cell cytotoxicity for cells infected with IMCs unable to express physiological levels of Nef.

3.3.6 DISCUSSION

While ADCC responses against HIV-1 have been associated with protection against HIV-1 transmission and disease progression (23, 46–51), there are conflicting reports regarding the ability of non-neutralizing CD4i Abs to mediate ADCC. Consistent with the occluded nature of the epitopes recognized by these Abs, several groups have shown that cells infected with full-length HIV-1 are resistant to ADCC mediated by the Abs (3, 8–13). However, CD4i Abs have also been reported to mediate potent ADCC (18–23, 52–59). Part of this conundrum was recently explained by performing a side-by-side comparison of the different assays used to measure ADCC responses (60). It was shown that assays that do not differentiate virus-infected from uninfected cells (granzyme B and NK cell activation) or that rely on gp120-coated cells (rapid fluorometric antibody-dependent cellular cytotoxicity [RFADCC] assay) overestimate ADCC responses mediated by antibodies to CD4i epitopes. These assays are severely biased in favor of CD4i antibodies as a consequence of the coating of uninfected bystander cells by shed gp120 (10, 60). However, this did not explain why additional studies found strong ADCC of these Abs when measuring their activities against cells infected with full-length IMC LucR.T2A viruses (18–33), in which the readout was sensitive detection of a provirally encoded LucR reporter gene (i.e., avoiding measurement of bystander killing) and a molecular strategy utilizing a T2A ribosome-skipping peptide intended to provide Nef expression. Since increasing evidence supports a role of Env conformation in the susceptibility of HIV-1-infected cells to ADCC (61–64), we explored the possibility that Env conformation at the surface of cells infected with these reporter viruses might

differ from those of the parental viruses due to altered interactions with CD4. We first evaluated the abilities of these viruses to downregulate the CD4 receptor in comparison with their parental IMCs. In agreement with our previous report (35), we found that the presence of the T2A peptide did not, as intended, support Nef expression in primary T cells, and consequently, CD4 downregulation was impaired. The remaining levels of CD4 at the surface of cells infected with these LucR.T2A reporter IMCs were sufficient to expose CD4i epitopes on Env, permitting recognition by A32 and HIV$^+$ sera. An alternative molecular strategy to achieve LucR, as well as Nef, expression (6ATRi) largely, but not fully, resolved these deficiencies. In marked contrast to Nef-deficient viruses, cells infected with the parental IMCs (e.g., T/F IMC, CH058.c, CH040.c, CH077.t, and CH0505s) exhibited robust CD4 downregulation and thus did not expose the epitopes. Accordingly, cells infected with the parental viruses were resistant to ADCC mediated by these ligands (**Fig. 3.2.4 and 3.2.5**). In addition, we observed that IMCs with impaired Nef expression were unable to fully downregulate NKG2D ligands, thus contributing to the enhanced susceptibility of these cells to CD4i antibody-mediated ADCC responses (**Fig. 3.2.5**). For example, cells infected with CH058 Env-IMC were more susceptible to ADCC mediated by A32 and HIV$^+$ sera than those infected with the parental virus (**Fig. 3.2.4 and 3.2.5**). This could be at least partially explained by the presence of higher levels of NKG2D ligands at the surfaces of CH058 Env-IMC-infected cells (**Fig. 3.2.5A**). Interestingly, we also found that some Env-IMCs, including CH058, failed to downregulate the restriction factor BST-2 to the same extent as the parental virus, resulting in increased Env levels at the cell surface (**Fig. 3.2.6**) and explaining the better recognition of these infected cells by A32 and HIV$^+$ sera (**Fig. 3.2.3B and F**). Therefore, our results strongly advocate for carefully controlling for Nef expression and function, as well as BST-2 downregulation and Env expression, when selecting IMCs to measure ADCC.

The establishment of a large panel of viruses has proven extremely useful to standardize neutralization assessments of anti-Env antibodies and to evaluate their breadth and potency (65–67). Similar efforts are being considered for evaluating the breadth of ADCC responses against HIV-1-infected cells (68). One attractive strategy might be to generate large panels of reporter IMCs expressing Envs from circulating strains, which offers the advantage of highly sensitive, quantitative, and rapid assay readout, which avoids inadvertent measurement of bystander killing. The fact that this strategy worked well for neutralization assays (69–71) does not, however,

guarantee that it will be the same for ADCC without undertaking further extensive optimization for ADCC assay-specific criteria. We believe that assays to measure Ab and effector cell interactions with infected cells are significantly more complex than those assessing Ab neutralization of viral particles because, in addition to Env expression and conformation, additional players, such as NKG2D ligands, can affect the readout of the assay. Therefore, our results strongly suggest that additional efforts should be devoted to identify and optimize reporter IMC strategies that ensure wildtype-like Nef expression and function before developing them into Env strain panels. We found LucR reporter IMCs encoding the modified EMCV IRES 6ATRi element expressed levels of Nef, and mediated CD4 downregulation, similarly to the cognate parental viruses. Consequently, Env conformation was less affected than with LucR IMCs utilizing the T2A peptide approach. Nevertheless, small but significant differences remained and varied depending on the 6ATRi-containing IMC that was used. For example, when 6ATRi was introduced in the pNL4.3 backbone coding for BaL Env, ADCC responses were similar to those obtained for the non-reporter pNL4.3. However, in the context of IMCs coding for CH040, CH077, and CH505 Envs, ADCC susceptibility was significantly higher than for their parental counterparts (**Fig. 3.2.4**). While small differences in CD4 and NKG2D ligand downregulation might partially explain these differences, additional parameters, including Env expression and Vpr-mediated upregulation of NKG2D ligands (45), could also affect ADCC responses and should be carefully evaluated. Our results highlight just some of the important elements of the intrinsic complexity in the interplay between Env and accessory proteins in modulating the susceptibility of infected cells to ADCC. A better comprehension of the susceptibility of HIV-1-infected cells to ADCC might help us better understand the correlates of vaccine protection and guide the development of HIV eradication strategies. Our results strongly advocate for carefully measuring parameters that may affect Env conformation and accessory protein function when measuring anti-HIV ADCC responses.

3.3.7 MATERIALS AND METHODS

Ethics statement

Written informed consent was obtained from all study participants (the Montreal Primary HIV Infection Cohort [72, 73] and the Canadian Cohort of HIV Infected Slow Progressors [74–76]), and the research adhered to the ethical guidelines of Centre de Recherche du CHUM (CRCHUM) and was reviewed and approved by the CRCHUM Institutional Review Board (ethics committee approval number CE 16.164 -CA). The research adhered to the standards indicated by the Declaration of Helsinki. All the participants were adults and provided written informed consent prior to enrollment, in accordance with Institutional Review Board approval.

Cell lines and isolation of primary cells

HEK293T human embryonic kidney cells (obtained from the ATCC) were grown as previously described (3, 9). TZM-bl cells were cultured as we described previously (77). Primary human PBMCs and $CD4^+$ T cells were isolated, activated, and cultured as previously described (3, 9). Briefly, PBMCs were obtained by leukapheresis, and $CD4^+$ T lymphocytes were purified from resting PBMCs by negative selection using immunomagnetic beads (StemCell Technologies, Vancouver, BC, Canada) according to the manufacturer's instructions and were activated with phytohemagglutinin-L (10 µg/ml) for 48 h and then maintained in RPMI 1640 complete medium supplemented with recombinant interleukin 2 (rIL-2) (100 U/ml).

Proviral constructs

We previously reported the generation of proviral plasmids of IMCs of T/F clade B HIV-1 strains pCH040.c, pCH058.c, and pCH077.t (accession numbers JN944939, JN944940, and JN944941) (78), and that of the brain-derived HIV-1 strain YU-2 (79), in which vpu was corrected to yield pYU-2c, and the clade C T/F IMC pCH0505.s (80) was also previously described. Proviral constructs, referred to collectively as Env-IMCs, comprising an HIV-1 NL4.3 (M19921.2)-based isogenic backbone engineered for the insertion of heterologous env strain sequences and expression in cis of full-length Env, were previously described (34). The proviral plasmids of replication-competent Env-IMCs utilized in this study are those encoding the Env ectodomain of T/F strains (pNL-B.CH040.ecto, pNL-B.CH058.ecto, pNL-CH077.ecto, and pNL-

C.CH0505s.ecto) and reference strains (pNL-B.YU-2.ecto, pNL-B.SF162.ecto, and pNL-B.BaL.ecto). In the same study, we reported the construction of env strain-matched, replication-competent reporter virus derivatives of Env-IMCs that encode Renilla luciferase (LucR) followed in frame by a ribosome-skipping T2A peptide intended to drive Nef expression, collectively referred to as Env-IMCLucR.T2A viruses (34). The proviral plasmids utilized here were pNL-LucR.T2A-B.CH040.ecto, pNL-LucR.T2AB.CH058.ecto, pNL-LucR.T2A-CH077.ecto, pNL-LucR.T2A-B.YU-2.ecto, pNL-LucR.T2A-B.SF162.ecto, pNL-LucR.T2AB.BaL.ecto, and pNL-LucR.T2A-B.Bal.ecto-Nefstop (34). In a modified molecular approach, we replaced the bicistronic LucR.T2A-nef fragment with a bicistronic LucR.IRES-nef cassettes utilizing the EMCV-modified 6ATR IRES element (6ATRi) to drive nef expression, resulting in Env-IMC-LucR.6ATRi viruses (35). The LucR reporter virus derivatives of CH077.t and CH0505.s T/F IMCs included in this study were constructed similarly to IMC-LucR.T2A (CH077.t-LucRT2A [81]) or IMC-LucR.6ATRi (CH077.t-LucR.6ATRi and CH0505.s-LucR.6ATRi [data not shown]). Of note, while the parental IMCs code for parental Nef proteins, Env-IMC, Env-IMC-LucR.T2A, and Env-IMC-LucR.6ATRi code for the pNL4.3 Nef protein.

Virus production and infections

To achieve similar levels of infection among the different IMCs tested, vesicular stomatitis virus G (VSVG)-pseudotyped HIV-1 isolates were produced and titrated as previously described (1). The viruses were then used to infect activated primary CD4 T cells from healthy HIV-1-negative donors by spin infection at 800 × g for 1 h in 96-well plates at 25°C. The percentages of infected cells, as evaluated by intracellular p24 staining, were below 15% for all the viruses tested and typically reached 10%.

Antibodies and sera

The following Abs were used as primary Abs for cell surface staining: mouse anti-CD4 mAb OKT4 (recognizing the D3 domain of CD4; BioLegend); rabbit anti-BST-2 Ab (sc-99191; Santa Cruz); allophycocyanin (APC)-conjugated mouse anti- MHC-I (clone G46-2.6, recognizing a monomorphic epitope on HLA-A, HLA-B, and HLA-C; BD Biosciences); anti-HIV-1 Env 2G12, 10e8, and A32 mAbs (NIH AIDS Reagent Program); and NKG2D-IgG Fc fusion protein (recognizing NKG2D ligands MICA, MICB, and ULBPs; R&D Systems) or its matched IgG Fc

fusion protein (R&D Systems) as a control. Goat anti-mouse and anti-human antibodies precoupled to Alexa Fluor 647 (Invitrogen) were used as secondary antibodies in flow cytometry experiments. Sera from chronically HIV-infected donors were collected, heat inactivated, and conserved as previously described (3, 9). A random number generator (QuickCalcs; GraphPad, San Diego, CA, USA) was used to randomly select a number of sera for each experiment. Antibodies for Western blotting are described below.

Flow cytometry analysis

Cell surface staining was performed as previously described (1, 9). Binding of cell surface CD4 (OKT4; 1 g/ml), MHC-I (clone G46-2.6), and NKG2DL by NKG2D-Fc chimera protein (5 µg/ml) and HIV-1 Env by sera (1:1,000 dilution) or anti-Env mAb A32 (5 µg/ml) was performed at 48 h post-infection. Infected cells were identified by intracellular staining of HIV-1 p24 using a Cytofix/ Cytoperm fixation/permeabilization kit (BD Biosciences, Mississauga, ON, Canada) and a fluorescent anti-p24 mAb (phycoerythrin [PE]-conjugated anti-p24, clone KC57; Beckman Coulter/Immunotech). The percentage of infected cells ($p24^+$) was determined by gating the live-cell population on the basis of viability dye staining (Aqua Vivid; Thermo Fisher Scientific). Samples were acquired on an LSRII cytometer (BD Biosciences), and data analysis was performed using FlowJo vX.0.7 (Tree Star, Ashland, OR, USA).

FACS-based ADCC assay

Measurement of ADCC using a fluorescence-activated cell sorting (FACS)- based assay was performed at 48 h post-infection (hpi) as previously described (3, 9, 82). Briefly, infected primary CD4 T cells were stained with AquaVivid viability dye and cell proliferation dye (eFluor670; eBioscience) and used as target cells. Autologous effector PBMCs, stained with another cellular marker (cell proliferation dye eFluor450; eBioscience), were added at an effector/target ratio of 10:1 in 96-well V-bottom plates (Corning, Corning, NY). A 1:1,000 final dilution of sera or 5 µg/ml of ADCC-mediating mAb was added to appropriate wells, and the cells were incubated for 15 min at room temperature. The plates were subsequently centrifuged for 1 min at 300 × g and incubated at 37°C and 5% CO_2 for 5 to 6 h before being fixed in a 2% phosphate-buffered saline (PBS)-formaldehyde solution. Alternatively, effector cells were preincubated in the presence of purified anti-human CD314 (NKG2D; R&D Systems) or its matched IgG isotype

control (10 µg/ml) prior being incubated with target cells for NKG2D blockade experiments. Samples were acquired on an LSRII cytometer (BD Biosciences), and data analysis was performed using FlowJo vX.0.7 (Tree Star). The percentage of ADCC was calculated with the following formula: (percent $p24^+$ cells in targets plus effectors) × (percent $p24^+$ cells in targets plus effectors plus Abs) / (percent $p24^+$ cells in targets) by gating on infected live target cells.

Western blotting

CD8-depleted, CD3/CD28 Dynabeads (Gibco, Life Technologies)-activated CD4 T cells from 4 healthy non-HIV-infected donors were pooled and infected as described above (with VSV-G-pseudotyped virions). The percentage and total number of infected $CD4^+$ T cells were determined at 72 hpi via intracellular p24 staining and flow cytometric analysis (essentially as described above). Aliquots of the cells were lysed with Laemmli sample buffer at a final concentration of 0.5×10^4 infected cells/µl of lysate. Equal amounts (either 10 µl or 20 µl) of lysate from each sample were loaded in parallel for p24 and Nef detection. The procedures for sample sonication, denaturing SDS-PAGE, and Western blotting were essentially as we described previously (35). Here, we used the following primary antibodies: polyclonal rabbit HIV-1 Nef antiserum (obtained from the NIH AIDS Reagent Program, Division of AIDS, NIAID, NIH; contributed by Ronald Swanstrom; catalog no. 2949; lot 10-070932) at 1:1,000 dilution to visualize Nef protein and mouse mAb to HIV-1 p24 (Gag), prepared from the HIV-1 p24 hybridoma (clone 183-H12-5C; obtained from the NIH AIDS Reagent Program, Division of AIDS, NIAID, NIH; contributed by Bruce Chesebro and Hardy Chen; catalog no. 1513) (83) and used at 1:1,000 dilution to probe for p24/Gag.

Statistical analyses

Statistics were analyzed using GraphPad Prism version 6.0.1 (GraphPad, San Diego, CA, USA). Every data set was tested for statistical normality, and the information was used to apply the appropriate (parametric or nonparametric) statistical test. P values of < 0.05 were considered significant; significance values are indicated as *, $P < 0.05$; **, $P < 0.01$, ***, $P < 0.001$; ****, $P < 0.0001$.

3.3.8 ACKNOWLEDGEMENTS

We thank Dominique Gauchat from the CRCHUM Flow Cytometry Platform for technical assistance and Mario Legault for cohort coordination and clinical samples. This work was supported by CIHR foundation grant 352417 to A.F. Support for the work was also provided by NIH R01 to A.F. and Marzena Pazgier (AI129769). The study was also supported by NIH AI100645 Center for HIV/AIDS Vaccine Immunology and Immunogen Design (CHAVI-ID) subawards to A.F. and J.C.K.; an original CHAVI (U01- AI067854) subaward to J.C.K.; and a subcontract to C.O. from the Comprehensive Antibody Vaccine Immune Monitoring Consortium (CA-VIMC) (grant 1032144), which is part of the Collaboration for AIDS Vaccine Discovery (CAVD)/CAVIMC, funded by the Bill and Melinda Gates Foundation. A.F. is the recipient of a Canada Research Chair on Retroviral Entry (RCHS0235). J.P. is the recipient of a CIHR Fellowship Award. J.R. is the recipient of a Mathilde Krim Fellowship in Basic Biomedical Research from amfAR. The funders had no role in study design, data collection and analysis, decision to publish, or preparation of the manuscript.

3.3.9 REFERENCES

1. Veillette M, Coutu M, Richard J, Batraville LA, Dagher O, Bernard N, Tremblay C, Kaufmann DE, Roger M, Finzi A. 2015. The HIV-1 gp120 CD4-bound conformation is preferentially targeted by antibody-dependent cellular cytotoxicity-mediating antibodies in sera from HIV-1-infected individuals. J Virol 89:545–551.
2. Veillette M, Coutu M, Richard J, Batraville LA, Desormeaux A, Roger M, Finzi A. 2014. Conformational evaluation of HIV-1 trimeric envelope glycoproteins using a cell-based ELISA assay. J Vis Exp 14:51995.
3. Veillette M, Desormeaux A, Medjahed H, Gharsallah NE, Coutu M, Baalwa J, Guan Y, Lewis G, Ferrari G, Hahn BH, Haynes BF, Robinson JE, Kaufmann DE, Bonsignori M, Sodroski J, Finzi A. 2014. Interaction with cellular CD4 exposes HIV-1 envelope epitopes targeted by antibody-dependent cell-mediated cytotoxicity. J Virol 88:2633–2644.
4. Alvarez RA, Hamlin RE, Monroe A, Moldt B, Hotta MT, Rodriguez Caprio G, Fierer DS, Simon V, Chen BK. 2014. HIV-1 Vpu antagonism of tetherin inhibits antibody-dependent cellular cytotoxic responses by natural killer cells. J Virol 88:6031– 6046.

5. Arias JF, Heyer LN, von Bredow B, Weisgrau KL, Moldt B, Burton DR, Rakasz EG, Evans DT. 2014. Tetherin antagonism by Vpu protects HIV-infected cells from antibody-dependent cell-mediated cytotoxicity. Proc Natl Acad Sci USA 111:6425– 6430.
6. von Bredow B, Arias JF, Heyer LN, Gardner MR, Farzan M, Rakasz EG, Evans DT. 2015. Envelope glycoprotein internalization protects human and simian immunodeficiency virus infected cells from antibody-dependent cell-mediated cytotoxicity. J Virol 89:10648 – 10655.
7. Richard J, Prevost J, von Bredow B, Ding S, Brassard N, Medjahed H, Coutu M, Melillo B, Bibollet-Ruche F, Hahn BH, Kaufmann DE, Smith AB, III, Sodroski J, Sauter D, Kirchhoff F, Gee K, Neil SJ, Evans DT, Finzi A. 2017. BST-2 expression modulates small CD4-mimetic sensitization of HIV-1-infected cells to antibody-dependent cellular cytotoxicity. J Virol 91:e00219-17.
8. Ding S, Veillette M, Coutu M, Prevost J, Scharf L, Bjorkman PJ, Ferrari G, Robinson JE, Sturzel C, Hahn BH, Sauter D, Kirchhoff F, Lewis GK, Pazgier M, Finzi A. 2016. A highly conserved residue of the HIV-1 gp120 inner domain is important for antibody-dependent cellular cytotoxicity responses mediated by anti-cluster A antibodies. J Virol 90:2127–2134.
9. Richard J, Veillette M, Brassard N, Iyer SS, Roger M, Martin L, Pazgier M, Schon A, Freire E, Routy JP, Smith AB, III, Park J, Jones DM, Courter JR, Melillo BN, Kaufmann DE, Hahn BH, Permar SR, Haynes BF, Madani N, Sodroski JG, Finzi A. 2015. CD4 mimetics sensitize HIV-1-infected cells to ADCC. Proc Natl Acad Sci USA 112:E2687–E2694.
10. Richard J, Veillette M, Ding S, Zoubchenok D, Alsahafi N, Coutu M, Brassard N, Park J, Courter JR, Melillo B, Smith AB, III, Shaw GM, Hahn BH, Sodroski J, Kaufmann DE, Finzi A. 2016. Small CD4 mimetics prevent HIV-1 uninfected bystander CD4 T cell killing mediated by antibody-dependent cell-mediated cytotoxicity. EBioMedicine 3:122–134.
11. Bruel T, Guivel-Benhassine F, Lorin V, Lortat-Jacob H, Baleux F, Bourdic K, Noel N, Lambotte O, Mouquet H, Schwartz O. 2017. Lack of ADCC breadth of human non-neutralizing anti-HIV-1 antibodies. J Virol 91: e02440-16.

12. von Bredow B, Arias JF, Heyer LN, Moldt B, Le K, Robinson JE, Zolla-Pazner S, Burton DR, Evans DT. 2016. Comparison of antibody-dependent cell-mediated cytotoxicity and virus neutralization by HIV-1 Env-specific monoclonal antibodies. J Virol 90:6127– 6139.
13. Alsahafi N, Ding S, Richard J, Markle T, Brassard N, Walker B, Lewis GK, Kaufmann DE, Brockman MA, Finzi A. 2015. Nef proteins from HIV-1 elite controllers are inefficient at preventing antibody-dependent cellular cytotoxicity. J Virol 90:2993–3002.
14. Acharya P, Tolbert WD, Gohain N, Wu X, Yu L, Liu T, Huang W, Huang CC, Kwon YD, Louder RK, Luongo TS, McLellan JS, Pancera M, Yang Y, Zhang B, Flinko R, Foulke JS, Jr, Sajadi MM, Kamin-Lewis R, Robinson JE, Martin L, Kwong PD, Guan Y, DeVico AL, Lewis GK, Pazgier M. 2014. Structural definition of an antibody-dependent cellular cytotoxicity response implicated in reduced risk for HIV-1 infection. J Virol 88:12895–12906.
15. Finzi A, Xiang SH, Pacheco B, Wang L, Haight J, Kassa A, Danek B, Pancera M, Kwong PD, Sodroski J. 2010. Topological layers in the HIV-1 gp120 inner domain regulate gp41 interaction and CD4-triggered conformational transitions. Mol Cell 37:656 – 667.
16. Tolbert WD, Gohain N, Veillette M, Chapleau JP, Orlandi C, Visciano ML, Ebadi M, DeVico AL, Fouts TR, Finzi A, Lewis GK, Pazgier M. 2016. Paring down HIV Env: design and crystal structure of a stabilized inner domain of HIV-1 gp120 displaying a major ADCC target of the A32 region. Structure 24:697–709.
17. Guan Y, Pazgier M, Sajadi MM, Kamin-Lewis R, Al-Darmarki S, Flinko R, Lovo E, Wu X, Robinson JE, Seaman MS, Fouts TR, Gallo RC, DeVico AL, Lewis GK. 2013. Diverse specificity and effector function among human antibodies to HIV-1 envelope glycoprotein epitopes exposed by CD4 binding. Proc Natl Acad Sci USA 110:E69 –E78.
18. Tomaras GD, Ferrari G, Shen X, Alam SM, Liao HX, Pollara J, Bonsignori M, Moody MA, Fong Y, Chen X, Poling B, Nicholson CO, Zhang R, Lu X, Parks R, Kaewkungwal J, Nitayaphan S, Pitisuttithum P, Rerks-Ngarm S, Gilbert PB, Kim JH, Michael NL, Montefiori DC, Haynes BF. 2013. Vaccine-induced plasma IgA specific for the C1 region of the HIV-1 envelope blocks binding and effector function of IgG. Proc Natl Acad Sci USA 110: 9019 –9024.
19. Pollara J, Bonsignori M, Moody MA, Liu P, Alam SM, Hwang KK, Gurley TC, Kozink DM, Armand LC, Marshall DJ, Whitesides JF, Kaewkungwal J, Nitayaphan S,

Pitisuttithum P, Rerks-Ngarm S, Robb ML, O'Connell RJ, Kim JH, Michael NL, Montefiori DC, Tomaras GD, Liao HX, Haynes BF, Ferrari G. 2014. HIV-1 vaccine-induced C1 and V2 Env-specific antibodies synergize for increased antiviral activities. J Virol 88:7715–7726.

20. Permar SR, Fong Y, Vandergrift N, Fouda GG, Gilbert P, Parks R, Jaeger FH, Pollara J, Martelli A, Liebl BE, Lloyd K, Yates NL, Overman RG, Shen X, Whitaker K, Chen H, Pritchett J, Solomon E, Friberg E, Marshall DJ, Whitesides JF, Gurley TC, Von Holle T, Martinez DR, Cai F, Kumar A, Xia SM, Lu X, Louzao R, Wilkes S, Datta S, Sarzotti-Kelsoe M, Liao HX, Ferrari G, Alam SM, Montefiori DC, Denny TN, Moody MA, Tomaras GD, Gao F, Haynes BF. 2015. Maternal HIV-1 envelope-specific antibody responses and reduced risk of perinatal transmission. J Clin Invest 125:2702–2706.
21. Santra S, Tomaras GD, Warrier R, Nicely NI, Liao HX, Pollara J, Liu P, Alam SM, Zhang R, Cocklin SL, Shen X, Duffy R, Xia SM, Schutte RJ, Pemble CW IV, Dennison SM, Li H, Chao A, Vidnovic K, Evans A, Klein K, Kumar A, Robinson J, Landucci G, Forthal DN, Montefiori DC, Kaewkungwal J, Nitayaphan S, Pitisuttithum P, Rerks-Ngarm S, Robb ML, Michael NL, Kim JH, Soderberg KA, Giorgi EE, Blair L, Korber BT, Moog C, Shattock RJ, Letvin NL, Schmitz JE, Moody MA, Gao F, Ferrari G, Shaw GM, Haynes BF. 2015. Human non-neutralizing HIV-1 envelope monoclonal antibodies limit the number of founder viruses during SHIV mucosal infection in rhesus macaques. PLoS Pathog 11:e1005042.
22. Sung JA, Pickeral J, Liu L, Stanfield-Oakley SA, Lam CK, Garrido C, Pollara J, LaBranche C, Bonsignori M, Moody MA, Yang Y, Parks R, Archin N, Allard B, Kirchherr J, Kuruc JD, Gay CL, Cohen MS, Ochsenbauer C, Soderberg K, Liao HX, Montefiori D, Moore P, Johnson S, Koenig S, Haynes BF, Nordstrom JL, Margolis DM, Ferrari G. 2015. Dual-affinity re-targeting proteins direct T cell-mediated cytolysis of latently HIV-infected cells. J Clin Invest 125:4077– 4090.
23. Bradley T, Pollara J, Santra S, Vandergrift N, Pittala S, Bailey-Kellogg C, Shen X, Parks R, Goodman D, Eaton A, Balachandran H, Mach LV, Saunders KO, Weiner JA, Scearce R, Sutherland LL, Phogat S, Tartaglia J, Reed SG, Hu SL, Theis JF, Pinter A, Montefiori DC, Kepler TB, Peachman KK, Rao M, Michael NL, Suscovich TJ, Alter G, Ackerman ME, Moody MA, Liao HX, Tomaras G, Ferrari G, Korber BT, Haynes BF. 2017.

Pentavalent HIV-1 vaccine protects against simian-human immunodeficiency virus challenge. Nat Commun 8:15711.

24. Huang Y, Ferrari G, Alter G, Forthal DN, Kappes JC, Lewis GK, Love JC, Borate B, Harris L, Greene K, Gao H, Phan TB, Landucci G, Goods BA, Dowell KG, Cheng HD, Bailey-Kellogg C, Montefiori DC, Ackerman ME. 2016. Diversity of antiviral IgG effector activities observed in HIV-infected and vaccinated subjects. J Immunol 197:4603– 4612.
25. Viegas EO, Tembe N, Nilsson C, Meggi B, Maueia C, Augusto O, Stout R, Scarlatti G, Ferrari G, Earl PL, Wahren B, Andersson S, Robb ML, Osman N, Biberfeld G, Jani I, Sandstrom E. 27 November 2017. Intradermal HIV-1 DNA immunization using needle-free zetajet injection followed by HIV-modified vaccinia virus Ankara vaccination is safe and immunogenic in Mozambican young adults: A phase I randomized controlled trial . AIDS Res Hum Retroviruses 34:193-205.
26. Meyerhoff RR, Scearce RM, Ogburn DF, Lockwood B, Pickeral J, Kuraoka M, Anasti K, Eudailey J, Eaton A, Cooper M, Wiehe K, Montefiori DC, Tomaras G, Ferrari G, Alam SM, Liao HX, Korber B, Gao F, Haynes BF. 2017. HIV-1 consensus envelope-induced broadly binding antibodies. AIDS Res Hum Retroviruses 33:859 – 868.
27. Joachim A, Munseri PJ, Nilsson C, Bakari M, Aboud S, Lyamuya EF, Tecleab T, Liakina V, Scarlatti G, Robb ML, Earl PL, Moss B, Wahren B, Mhalu F, Ferrari G, Sandstrom E, Biberfeld G. 2017. Three-year durability of immune responses induced by HIV-DNA and HIV-modified vaccinia virus Ankara and effect of a late HIV-modified vaccinia virus Ankara boost in Tanzanian volunteers. AIDS Res Hum Retroviruses 33:880 – 888.
28. Costa MR, Pollara J, Edwards RW, Seaman MS, Gorny MK, Montefiori DC, Liao HX, Ferrari G, Lu S, Wang S. 2016. Fc receptor-mediated activities of Env-specific human monoclonal antibodies generated from volunteers receiving the DNA prime-protein boost HIV vaccine DP6-001. J Virol 90:10362–10378.
29. Joachim A, Bauer A, Joseph S, Geldmacher C, Munseri PJ, Aboud S, Missanga M, Mann P, Wahren B, Ferrari G, Polonis VR, Robb ML, Weber J, Tatoud R, Maboko L, Hoelscher M, Lyamuya EF, Biberfeld G, Sandstrom E, Kroidl A, Bakari M, Nilsson C, McCormack S. 2016. Boosting with subtype C CN54rgp140 protein adjuvanted with glucopyranosyl lipid adjuvant after priming with HIV-DNA and HIV-MVA is safe and enhances immune responses: a phase I trial. PLoS One 11:e0155702.

30. Pollara J, McGuire E, Fouda GG, Rountree W, Eudailey J, Overman RG, Seaton KE, Deal A, Edwards RW, Tegha G, Kamwendo D, Kumwenda J, Nelson JA, Liao HX, Brinkley C, Denny TN, Ochsenbauer C, Ellington S, King CC, Jamieson DJ, van der Horst C, Kourtis AP, Tomaras GD, Ferrari G, Permar SR. 2015. Association of HIV-1 envelope-specific breast milk IgA responses with reduced risk of postnatal mother-to-child transmission of HIV-1. J Virol 89:9952–9961.
31. Wise MC, Hutnick NA, Pollara J, Myles DJ, Williams C, Yan J, LaBranche CC, Khan AS, Sardesai NY, Montefiori D, Barnett SW, Zolla-Pazner S, Ferrari G, Weiner DB. 2015. An enhanced synthetic multiclade DNA prime induces improved cross-clade-reactive functional antibodies when combined with an adjuvanted protein boost in nonhuman primates. J Virol 89:9154 –9166.
32. Dennison SM, Anasti KM, Jaeger FH, Stewart SM, Pollara J, Liu P, Kunz EL, Zhang R, Vandergrift N, Permar S, Ferrari G, Tomaras GD, Bonsignori M, Michael NL, Kim JH, Kaewkungwal J, Nitayaphan S, Pitisuttithum P, Rerks-Ngarm S, Liao HX, Haynes BF, Alam SM. 2014. Vaccine-induced HIV-1 envelope gp120 constant region 1-specific antibodies expose a CD4-inducible epitope and block the interaction of HIV-1 gp140 with galactosylceramide. J Virol 88:9406 –9417.
33. Ferrari G, Pollara J, Kozink D, Harms T, Drinker M, Freel S, Moody MA, Alam SM, Tomaras GD, Ochsenbauer C, Kappes JC, Shaw GM, Hoxie JA, Robinson JE, Haynes BF. 2011. An HIV-1 gp120 envelope human monoclonal antibody that recognizes a C1 conformational epitope mediates potent antibody-dependent cellular cytotoxicity (ADCC) activity and defines a common ADCC epitope in human HIV-1 serum. J Virol 85: 7029 – 7036.
34. Edmonds TG, Ding H, Yuan X, Wei Q, Smith KS, Conway JA, Wieczorek L, Brown B, Polonis V, West JT, Montefiori DC, Kappes JC, Ochsenbauer C. 2010. Replication competent molecular clones of HIV-1 expressing Renilla luciferase facilitate the analysis of antibody inhibition in PBMC. Virology 408:1–13.
35. Alberti MO, Jones JJ, Miglietta R, Ding H, Bakshi RK, Edmonds TG, Kappes JC, Ochsenbauer C. 2015. Optimized replicating renilla luciferase reporter HIV-1 utilizing novel internal ribosome entry site elements for native Nef expression and function. AIDS Res Hum Retroviruses 31: 1278 –1296.

36. Alsahafi N, Richard J, Prevost J, Coutu M, Brassard N, Parsons MS, Kaufmann DE, Brockman M, Finzi A. 2017. Impaired downregulation of NKG2D ligands by Nef protein from elite controllers sensitizes HIV-1- infected cells to ADCC. J Virol 91:e00109-17.
37. Cavrois M, Banerjee T, Mukherjee G, Raman N, Hussien R, Rodriguez BA, Vasquez J, Spitzer MH, Lazarus NH, Jones JJ, Ochsenbauer C, McCune JM, Butcher EC, Arvin AM, Sen N, Greene WC, Roan NR. 2017. Mass cytometric analysis of HIV entry, replication, and remodeling in tissue CD4 T cells. Cell Rep 20:984 –998.
38. Lanier LL. 2008. Up on the tightrope: natural killer cell activation and inhibition. Nat Immunol 9:495–502.
39. Cerboni C, Neri F, Casartelli N, Zingoni A, Cosman D, Rossi P, Santoni A, Doria M. 2007. Human immunodeficiency virus 1 Nef protein downmodulates the ligands of the activating receptor NKG2D and inhibits natural killer cell-mediated cytotoxicity. J Gen Virol 88:242–250.
40. Norman JM, Mashiba M, McNamara LA, Onafuwa-Nuga A, Chiari-Fort E, Shen W, Collins KL. 2011. The antiviral factor APOBEC3G enhances the recognition of HIV-infected primary T cells by natural killer cells. Nat Immunol 12:975–983.
41. Parsons MS, Richard J, Lee WS, Vanderven H, Grant MD, Finzi A, Kent SJ. 2016. NKG2D acts as a co-receptor for natural killer cell-mediated antiHIV-1 antibody-dependent cellular cytotoxicity. AIDS Res Hum Retroviruses 32:1089 –1096.
42. Ward J, Davis Z, DeHart J, Zimmerman E, Bosque A, Brunetta E, Mavilio D, Planelles V, Barker E. 2009. HIV-1 Vpr triggers natural killer cellmediated lysis of infected cells through activation of the ATR-mediated DNA damage response. PLoS Pathog. 5:e1000613.
43. Ward J, Bonaparte M, Sacks J, Guterman J, Fogli M, Mavilio D, Barker E. 2007. HIV modulates the expression of ligands important in triggering natural killer cell cytotoxic responses on infected primary T-cell blasts. Blood 110:1207–1214.
44. Fogli M, Mavilio D, Brunetta E, Varchetta S, Ata K, Roby G, Kovacs C, Follmann D, Pende D, Ward J, Barker E, Marcenaro E, Moretta A, Fauci AS. 2008. Lysis of endogenously infected CD4 T cell blasts by rIL-2 activated autologous natural killer cells from HIV-infected viremic individuals. PLoS Pathog 4:e1000101.

45. Richard J, Sindhu S, Pham TN, Belzile JP, Cohen EA. 2010. HIV-1 Vpr up-regulates expression of ligands for the activating NKG2D receptor and promotes NK cell-mediated killing. Blood 115:1354 –1363.
46. Baum LL, Cassutt KJ, Knigge K, Khattri R, Margolick J, Rinaldo C, Kleeberger CA, Nishanian P, Henrard DR, Phair J. 1996. HIV-1 gp120- specific antibody-dependent cell-mediated cytotoxicity correlates with rate of disease progression. J Immunol 157:2168 – 2173.
47. Ljunggren K, Moschese V, Broliden PA, Giaquinto C, Quinti I, Fenyo EM, Wahren B, Rossi P, Jondal M. 1990. Antibodies mediating cellular cytotoxicity and neutralization correlate with a better clinical stage in children born to human immunodeficiency virus-infected mothers. J Infect Dis 161:198 –202.
48. Chung AW, Navis M, Isitman G, Wren L, Silvers J, Amin J, Kent SJ, Stratov I. 2011. Activation of NK cells by ADCC antibodies and HIV disease progression. J Acquir Immune Defic Syndr 58:127–131.
49. Mabuka J, Nduati R, Odem-Davis K, Peterson D, Overbaugh J. 2012. HIV-specific antibodies capable of ADCC are common in breastmilk and are associated with reduced risk of transmission in women with high viral loads. PLoS Pathog 8:e1002739.
50. Haynes BF, Gilbert PB, McElrath MJ, Zolla-Pazner S, Tomaras GD, Alam SM, Evans DT, Montefiori DC, Karnasuta C, Sutthent R, Liao HX, DeVico AL, Lewis GK, Williams C, Pinter A, Fong Y, Janes H, DeCamp A, Huang Y Rao M, Billings E, Karasavvas N, Robb ML, Ngauy V, de Souza MS, Paris R, Ferrari G, Bailer RT, Soderberg KA, Andrews C, Berman PW, Frahm N, De Rosa SC, Alpert MD, Yates NL, Shen X, Koup RA, Pitisuttithum P, Kaewkungwal J, Nitayaphan S, Rerks-Ngarm S, Michael NL, Kim JH. 2012. Immune-correlates analysis of an HIV-1 vaccine efficacy trial. N Engl J Med 366:1275–1286.
51. Bonsignori M, Pollara J, Moody MA, Alpert MD, Chen X, Hwang KK, Gilbert PB, Huang Y, Gurley TC, Kozink DM, Marshall DJ, Whitesides JF, Tsao CY, Kaewkungwal J, Nitayaphan S, Pitisuttithum P, Rerks-Ngarm S, Kim JH, Michael NL, Tomaras GD, Montefiori DC, Lewis GK, Devico A, Evans DT, Ferrari G, Liao HX, Haynes BF. 2012. Antibody-dependent cellular cytotoxicity-mediating antibodies from an HIV-1 vaccine

efficacy trial target multiple epitopes and preferentially use the VH1 gene family. J Virol 86:11521–11532.

52. Pollara J, Bonsignori M, Moody MA, Pazgier M, Haynes BF, Ferrari G. 2013. Epitope specificity of human immunodeficiency virus-1 antibody dependent cellular cytotoxicity [ADCC] responses. Curr HIV Res 11: 378 –387.
53. Phillips B, Fouda GG, Eudailey J, Pollara J, Curtis AD, II, Kunz E, Dennis M, Shen X, Bay C, Hudgens M, Pickup D, Alam SM, Ardeshir A, Kozlowski PA, Van Rompay KKA, Ferrari G, Moody MA, Permar S, De Paris K. 2017. Impact of poxvirus vector priming, protein coadministration, and vaccine intervals on HIV gp120 vaccine-elicited antibody magnitude and function in infant macaques. Clin Vaccine Immunol 24:e00231-17.
54. Shubin Z, Li W, Poonia B, Ferrari G, LaBranche C, Montefiori D, Zhu X, Pauza CD. 2017. An HIV Envelope gp120-Fc fusion protein elicits effector antibody responses in rhesus macaques. Clin Vaccine Immunol 24: e00028-17.
55. Zurawski G, Shen X, Zurawski S, Tomaras GD, Montefiori DC, Roederer M, Ferrari G, Lacabaratz C, Klucar P, Wang Z, Foulds KE, Kao SF, Yu X, Sato A, Yates NL, LaBranche C, Stanfield-Oakley S, Kibler K, Jacobs B, Salazar A, Self S, Fulp W, Gottardo R, Galmin L, Weiss D, Cristillo A, Pantaleo G, Levy Y. 2017. Superiority in rhesus macaques of targeting HIV-1 Env gp140 to CD40 versus LOX-1 in combination with replication-competent NYVAC-KC for induction of Env-specific antibody and T cell responses. J Virol 91:e01596-16.
56. Fong Y, Shen X, Ashley VC, Deal A, Seaton KE, Yu C, Grant SP, Ferrari G, de Camp AC, Bailer RT, Koup RA, Montefiori D, Haynes BF, Sarzotti-Kelsoe M, Graham BS, Carpp LN, Hammer SM, Sobieszczyk M, Karuna S, Swann E, DeJesus E, Mulligan M, Frank I, Buchbinder S, Novak RM, McElrath MJ, Kalams S, Keefer M, Frahm NA, Janes HE, Gilbert PB, Tomaras GD. 2018. Vaccine-induced antibody responses modify the association between T-cell immune responses and HIV-1 infection risk in HVTN 505. J Infect Dis 217:1280 –1288.
57. Ackerman ME, Mikhailova A, Brown EP, Dowell KG, Walker BD, Bailey-Kellogg C, Suscovich TJ, Alter G. 2016. Polyfunctional HIV-specific antibody responses are associated with spontaneous HIV control. PLoS Pathog 12:e1005315.

58. Chung AW, Kumar MP, Arnold KB, Yu WH, Schoen MK, Dunphy LJ, Suscovich TJ, Frahm N, Linde C, Mahan AE, Hoffner M, Streeck H, Ackerman ME, McElrath MJ, Schuitemaker H, Pau MG, Baden LR, Kim JH, Michael NL, Barouch DH, Lauffenburger DA, Alter G. 2015. Dissecting polyclonal vaccine-induced humoral immunity against HIV using systems serology. Cell 163:988 –998.
59. Williams KL, Cortez V, Dingens AS, Gach JS, Rainwater S, Weis JF, Chen X, Spearman P, Forthal DN, Overbaugh J. 2015. HIV-specific CD4-induced antibodies mediate broad and potent antibody-dependent cellular cytotoxicity activity and are commonly detected in plasma from HIV-infected humans. EBioMedicine 2:1464 –1477.
60. Richard J, Prévost J, Baxter AE, von Bredow B, Ding S, Medjahed H, Delgado GG, Brassard N, Stürzel CM, Kirchhoff F, Hahn BH, Parsons MS, Kaufmann DE, Evans DT, Finzi A. 2018. Uninfected bystander cells impact the measurement of HIV-specific ADCC responses. mBio 9:e00358-18.
61. Richard J, Prevost J, Alsahafi N, Ding S, Finzi A. 2018. Impact of HIV-1 envelope conformation on ADCC responses. Trends Microbiol 26: 253–265.
62. Veillette M, Richard J, Pazgier M, Lewis GK, Parsons MS, Finzi A. 2016. Role of HIV-1 envelope glycoproteins conformation and accessory proteins on ADCC responses. Curr HIV Res 14:9 –23.
63. Prevost J, Richard J, Ding S, Pacheco B, Charlebois R, Hahn BH, Kaufmann DE, Finzi A. 2018. Envelope glycoproteins sampling states 2/3 are susceptible to ADCC by sera from HIV-1-infected individuals. Virology 515: 38 – 45.
64. Prevost J, Zoubchenok D, Richard J, Veillette M, Pacheco B, Coutu M, Brassard N, Parsons MS, Ruxrungtham K, Bunupuradah T, Tovanabutra S, Hwang KK, Moody MA, Haynes BF, Bonsignori M, Sodroski J, Kaufmann DE, Shaw GM, Chenine AL, Finzi A. 2017. Influence of the envelope gp120 Phe43 cavity on HIV-1 sensitivity to antibody-dependent cell-mediated cytotoxicity responses. J Virol 91:e02452-16.
65. Hraber P, Rademeyer C, Williamson C, Seaman MS, Gottardo R, Tang H, Greene K, Gao H, LaBranche C, Mascola JR, Morris L, Montefiori DC, Korber B. 2017. Panels of HIV-1 subtype C Env reference strains for standardized neutralization assessments. J Virol 91:e00991-17.

66. Seaman MS, Janes H, Hawkins N, Grandpre LE, Devoy C, Giri A, Coffey RT, Harris L, Wood B, Daniels MG, Bhattacharya T, Lapedes A, Polonis VR, McCutchan FE, Gilbert PB, Self SG, Korber BT, Montefiori DC, Mascola JR. 2010. Tiered categorization of a diverse panel of HIV-1 Env pseudoviruses for assessment of neutralizing antibodies. J Virol 84:1439 –1452.
67. Mascola JR, D'Souza P, Gilbert P, Hahn BH, Haigwood NL, Morris L, Petropoulos CJ, Polonis VR, Sarzotti M, Montefiori DC. 2005. Recommendations for the design and use of standard virus panels to assess neutralizing antibody responses elicited by candidate human immunodeficiency virus type 1 vaccines. J Virol 79:10103–10107.
68. Lewis GK, Pazgier M, Evans D, Ferrari G, Bournazos S, Parsons MS, Bernard NF, Finzi A. 2017. Beyond viral neutralization. AIDS Res Hum Retroviruses 33:760 –764.
69. Montefiori DC, Karnasuta C, Huang Y, Ahmed H, Gilbert P, de Souza MS, McLinden R, Tovanabutra S, Laurence-Chenine A, Sanders-Buell E, Moody MA, Bonsignori M, Ochsenbauer C, Kappes J, Tang H, Greene K, Gao H, LaBranche CC, Andrews C, Polonis VR, Rerks-Ngarm S, Pitisuttithum P, Nitayaphan S, Kaewkungwal J, Self SG, Berman PW, Francis D, Sinangil F, Lee C, Tartaglia J, Robb ML, Haynes BF, Michael NL, Kim JH. 2012. Magnitude and breadth of the neutralizing antibody response in the RV144 and Vax003 HIV-1 vaccine efficacy trials. J Infect Dis 206: 431– 441.
70. Sarzotti-Kelsoe M, Daniell X, Todd CA, Bilska M, Martelli A, LaBranche C, Perez LG, Ochsenbauer C, Kappes JC, Rountree W, Denny TN, Montefiori DC. 2014. Optimization and validation of a neutralizing antibody assay for HIV-1 in A3R5 cells. J Immunol Methods 409:147–160.
71. Ochsenbauer C, Kappes JC. 2009. New virologic reagents for neutralizing antibody assays. Curr Opin HIV AIDS 4:418 – 425.
72. Fontaine J, Chagnon-Choquet J, Valcke HS, Poudrier J, Roger M. 2011. High expression levels of B lymphocyte stimulator (BLyS) by dendritic cells correlate with HIV-related B-cell disease progression in humans. Blood 117:145–155.
73. Fontaine J, Coutlee F, Tremblay C, Routy JP, Poudrier J, Roger M. 2009. HIV infection affects blood myeloid dendritic cells after successful therapy and despite nonprogressing clinical disease. J Infect Dis 199: 1007–1018.

74. International HIV Controllers Study, Pereyra F, Jia X, McLaren PJ, Telenti A, de Bakker PI, Walker BD, Ripke S, Brumme CJ, Pulit SL, Carrington M, Kadie CM, Carlson JM, Heckerman D, Graham RR, Plenge RM, Deeks SG, Gianniny L, Crawford G, Sullivan J, Gonzalez E, Davies L, Camargo A, Moore JM, Beattie N, Gupta S, Crenshaw A, Burtt NP, Guiducci C, Gupta N, Gao X, Qi Y, Yuki Y, Piechocka-Trocha A, Cutrell E, Rosenberg R, Moss KL, Lemay P, O'Leary J, Schaefer T, Verma P, Toth I, Block B, Baker B, Rothchild A, Lian J, Proudfoot J, Alvino DM, Vine S, Addo MM, et al. 2010. The major genetic determinants of HIV-1 control affect HLA class I peptide presentation. Science 330:1551–1557.
75. Kamya P, Boulet S, Tsoukas CM, Routy JP, Thomas R, Cote P, Boulassel MR, Baril JG, Kovacs C, Migueles SA, Connors M, Suscovich TJ, Brander C, Tremblay CL, Bernard N. 2011. Receptor-ligand requirements for increased NK cell polyfunctional potential in slow progressors infected with HIV-1 co-expressing KIR3DL1*h/*y and HLA-B*57. J Virol 85: 5949 –5960.
76. Peretz Y, Ndongala ML, Boulet S, Boulassel MR, Rouleau D, Cote P, Longpre D, Routy JP, Falutz J, Tremblay C, Tsoukas CM, Sekaly RP, Bernard NF. 2007. Functional T cell subsets contribute differentially to HIV peptide-specific responses within infected individuals: correlation of these functional T cell subsets with markers of disease progression. Clin Immunol 124:57– 68.
77. Wei X, Decker JM, Liu H, Zhang Z, Arani RB, Kilby JM, Saag MS, Wu X, Shaw GM, Kappes JC. 2002. Emergence of resistant human immunodeficiency virus type 1 in patients receiving fusion inhibitor (T-20) monotherapy. Antimicrob Agents Chemother 46:1896 – 1905.
78. Ochsenbauer C, Edmonds TG, Ding H, Keele BF, Decker J, Salazar MG, Salazar-Gonzalez JF, Shattock R, Haynes BF, Shaw GM, Hahn BH, Kappes JC. 2012. Generation of transmitted/founder HIV-1 infectious molecular clones and characterization of their replication capacity in CD4 T lymphocytes and monocyte-derived macrophages. J Virol 86:2715–2728.
79. Li Y, Kappes JC, Conway JA, Price RW, Shaw GM, Hahn BH. 1991. Molecular characterization of human immunodeficiency virus type 1 cloned directly from uncultured

human brain tissue: identification of replication-competent and -defective viral genomes. J Virol 65:3973–3985.

80. Gao F, Bonsignori M, Liao HX, Kumar A, Xia SM, Lu X, Cai F, Hwang KK, Song H, Zhou T, Lynch RM, Alam SM, Moody MA, Ferrari G, Berrong M, Kelsoe G, Shaw GM, Hahn BH, Montefiori DC, Kamanga G, Cohen MS, Hraber P, Kwong PD, Korber BT, Mascola JR, Kepler TB, Haynes BF. 2014. Cooperation of B cell lineages in induction of HIV-1-broadly neutralizing antibodies. Cell 158:481– 491.
81. Naarding MA, Fernandez N, Kappes JC, Hayes P, Ahmed T, Icyuz M, Edmonds TG, Bergin P, Anzala O, Hanke T, Clark L, Cox JH, Cormier E, Ochsenbauer C, Gilmour J. 2014. Development of a luciferase based viral inhibition assay to evaluate vaccine induced CD8 T-cell responses. J Immunol Methods 409:161–173.
82. Richard J, Veillette M, Batraville LA, Coutu M, Chapleau JP, Bonsignori M, Bernard N, Tremblay C, Roger M, Kaufmann DE, Finzi A. 2014. Flow cytometry-based assay to study HIV-1 gp120 specific antibody-dependent cellular cytotoxicity responses. J Virol Methods 208:107–114.
83. Chesebro B, Wehrly K, Nishio J, Perryman S. 1992. Macrophage-tropic human immunodeficiency virus isolates from different patients exhibit unusual V3 envelope sequence homogeneity in comparison with T-cell-tropic isolates: definition of critical amino acids involved in cell tropism. J Virol 66:6547– 6554.
84. Richard J, Pacheco B, Gohain N, Veillette M, Ding S, Alsahafi N, Tolbert WD, Prevost J, Chapleau JP, Coutu M, Jia M, Brassard N, Park J, Courter JR, Melillo B, Martin L, Tremblay C, Hahn BH, Kaufmann DE, Wu X, Smith AB, III, Sodroski J, Pazgier M, Finzi A. 2016. Co-receptor binding site antibodies enable CD4-mimetics to expose conserved anti-cluster A ADCC epitopes on HIV-1 envelope glycoproteins. EBioMedicine 12: 208 – 218.

3.3.10 FIGURES

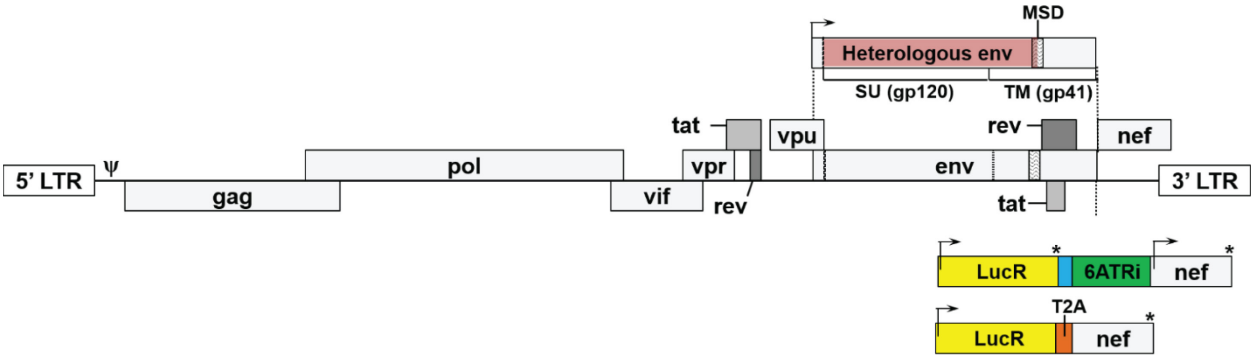

Figure 3.2.1 - Schematic representation of HIV-1 IMC, Env-IMC, and their LucR reporter virus derivatives.
Shown is the HIV-1 proviral genome representing either a full-length IMC (e.g., T/F strain) or a pNL4.3-based isogenic backbone engineered to encode the Env ectodomain (i.e., SU/gp120 and the extracellular and part of the membrane-spanning domain [MSD] portion of TM/gp41; shaded in pink) of heterologous HIV-1 strains. The cytoplasmic tail of Env is derived from backbone strain NL4-3, as is the signal peptide sequence. Also shown is how IMCs were modified for reporter gene expression by the insertion into the IMC backbone of the *Renilla* luciferase (LucR) open reading frame (yellow), followed by either the previously described 26-nucleotide (nt) IRES spacer region (blue) and the modified EMCV IRES element, 6ATRi (green), which drives expression of wild-type Nef; a 3-amino-acid-long functional deletion mutant (not shown); or the T2A ribosome-skipping peptide sequence (orange) in frame with *nef*. The arrows indicate translation start sites. *, stop codon. The molecular strategies are based on those we previously described (34, 35). LTR, long terminal repeat; ψ, Psi packaging element.

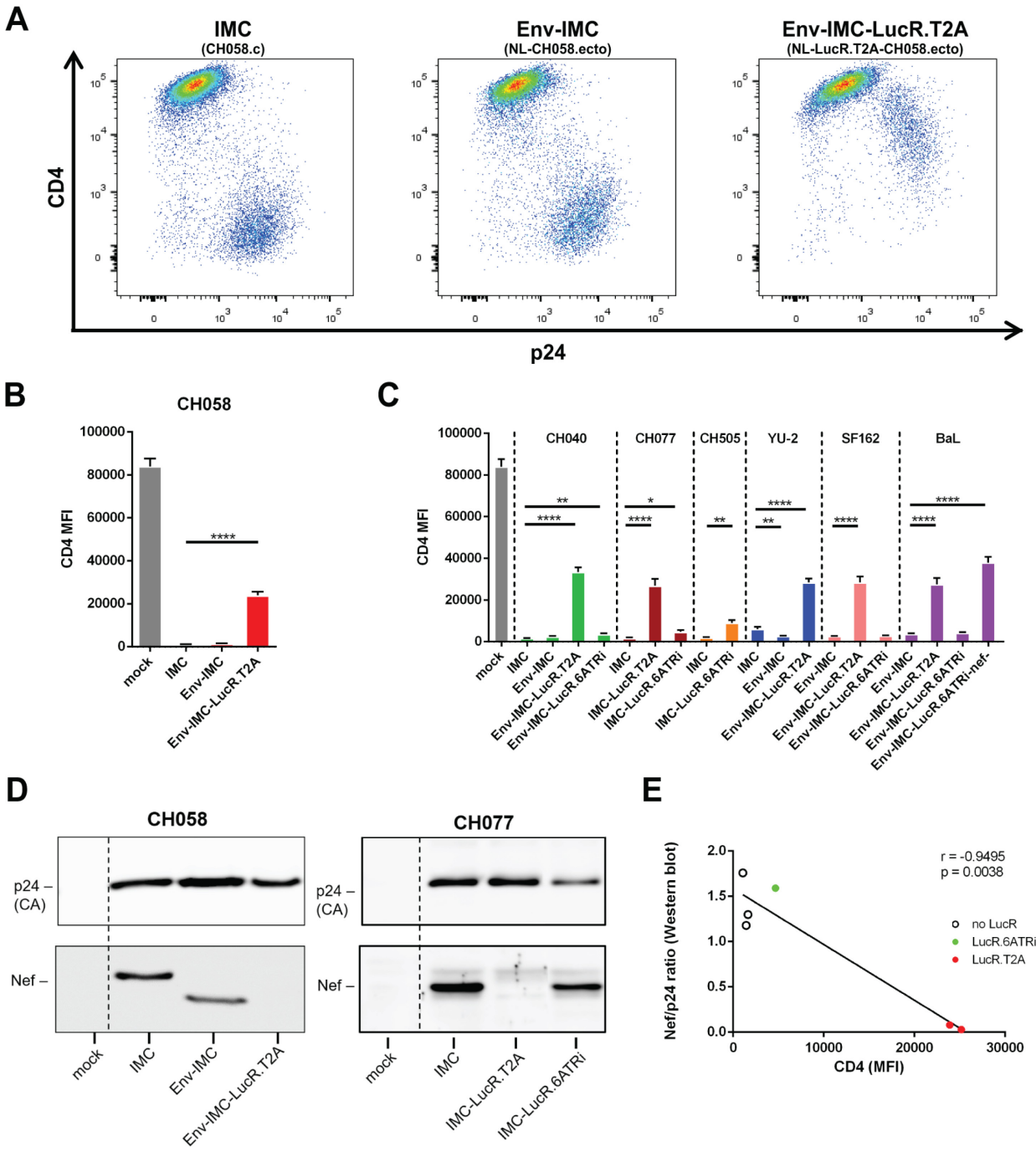
A
IMC
(CH058.c)
Env-IMC
(NL-CH058.ecto)
Env-IMC-LucR.T2A
(NL-LucR.T2A-CH058.ecto)
CD4
p24
B
CH058
CD4 MFI
mock
IMC
Env-IMC
Env-IMC-LucR.T2A
C
CH040
CH077
CH505
YU-2
SF162
BaL
CD4 MFI
mock
IMC
Env-IMC
Env-IMC-LucR.T2A
Env-IMC-LucR.6ATRi
IMC-LucR.T2A
IMC-LucR.6ATRi
Env-IMC-LucR.6ATRi-nef-
D
CH058
CH077
p24 –
(CA)
Nef –
mock
IMC
Env-IMC
Env-IMC-LucR.T2A
IMC-LucR.6ATRi
E
Nef/p24 ratio (Western blot)
CD4 (MFI)
r = -0.9495
p = 0.0038
no LucR
LucR.6ATRi
LucR.T2A

Figure 3.2.2 - Impact of the molecular strategy for LucR element insertion on Nef expression from reporter HIV-1 and CD4 downregulation.

Cell surface staining with anti-CD4 antibody OKT4 of primary $CD4^+$ T cells either mock infected or infected with IMCs expressing different Env strains (CH058, CH040, CH077, CH505, YU-2, SF162, and BaL) and expressing or not the LucR reporter. (**A to C**) Histograms depicting representative CD4 stainings (**A**) and the MFI of the infected ($p24^+$) population obtained in at least 5 independent experiments (**B and C**). (**D**) Nef expression from cells infected with the indicated parental and LucR IMCs encoding CH058 or CH077 Env was monitored by Western blotting with antibodies directed against CA/p24 (for normalization) and Nef. (**E**) Nef expression levels correlated with detection of CD4 at the surfaces of infected ($p24^+$) cells using a Pearson correlation test. The data are shown as means and standard errors of the mean (SEM). Statistical significance was tested using an unpaired t test (*, $P < 0.05$; **, $P < 0.01$; ****, $P < 0.0001$).

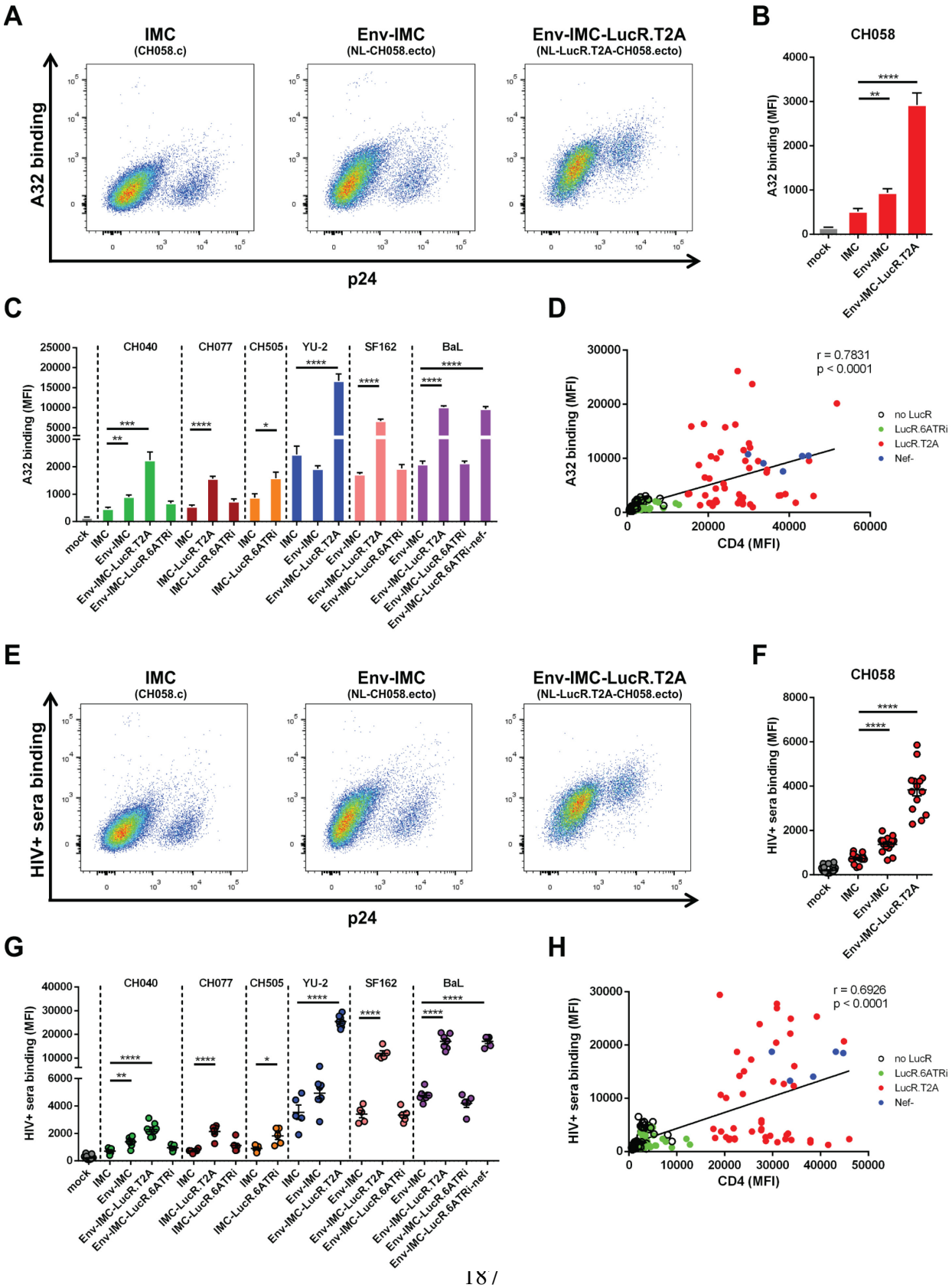
A
IMC
(CH058.c)
Env-IMC
(NL-CH058.ecto)
Env-IMC-LucR.T2A
(NL-LucR.T2A-CH058.ecto)
A32 binding
p24
B
CH058
A32 binding (MFI)
mock
IMC
Env-IMC
Env-IMC-LucR.T2A
C
CH040
CH077
CH505
YU-2
SF162
BaL
A32 binding (MFI)
mock
IMC
Env-IMC
Env-IMC-LucR.T2A
Env-IMC-LucR.6ATRi
IMC-LucR.T2A
IMC-LucR.6ATRi
Env-IMC-LucR.6ATRi-nef-
D
r = 0.7831
p < 0.0001
A32 binding (MFI)
CD4 (MFI)
no LucR
LucR.6ATRi
LucR.T2A
Nef-
E
IMC
(CH058.c)
Env-IMC
(NL-CH058.ecto)
Env-IMC-LucR.T2A
(NL-LucR.T2A-CH058.ecto)
HIV+ sera binding
p24
F
CH058
HIV+ sera binding (MFI)
mock
IMC
Env-IMC
Env-IMC-LucR.T2A
G
CH040
CH077
CH505
YU-2
SF162
BaL
HIV+ sera binding (MFI)
mock
IMC
Env-IMC
Env-IMC-LucR.T2A
Env-IMC-LucR.6ATRi
IMC-LucR.T2A
IMC-LucR.6ATRi
Env-IMC-LucR.6ATRi-nef-
H
r = 0.6926
p < 0.0001
HIV+ sera binding (MFI)
CD4 (MFI)
no LucR
LucR.6ATRi
LucR.T2A
Nef-

Figure 3.2.3 - Impact of the molecular strategy for LucR reporter element insertion on Env conformation.

Cell surface staining of primary CD4 T cells either mock infected or infected with IMCs expressing different Env strains (CH058, CH040, CH077, CH505, YU-2, SF162, and BaL) and expressing or not the LucR reporter gene with A32 (**A to D**) or HIV^+ sera (**E to H**). (**A to C and E to G**) Histograms depicting representative A32 or HIV^+ serum staining (**A and E**) and the MFI in the infected ($p24^+$) population (**B, C, F, and G**) obtained in at least 5 independent experiments. (**D and H**) Spearman rank correlations between the levels of cell surface CD4 (detected with the anti-CD4 Ab OKT4) and Env staining performed with A32 or HIV^+ sera using different IMC constructs. The data are shown as means and SEM. Statistical significance was tested using an unpaired t test (**B, C, F, and G**) or a Spearman correlation test (**D and H**) (*, $P < 0.05$; **, $P < 0.01$; ***, $P < 0.001$; ****, $P < 0.0001$).

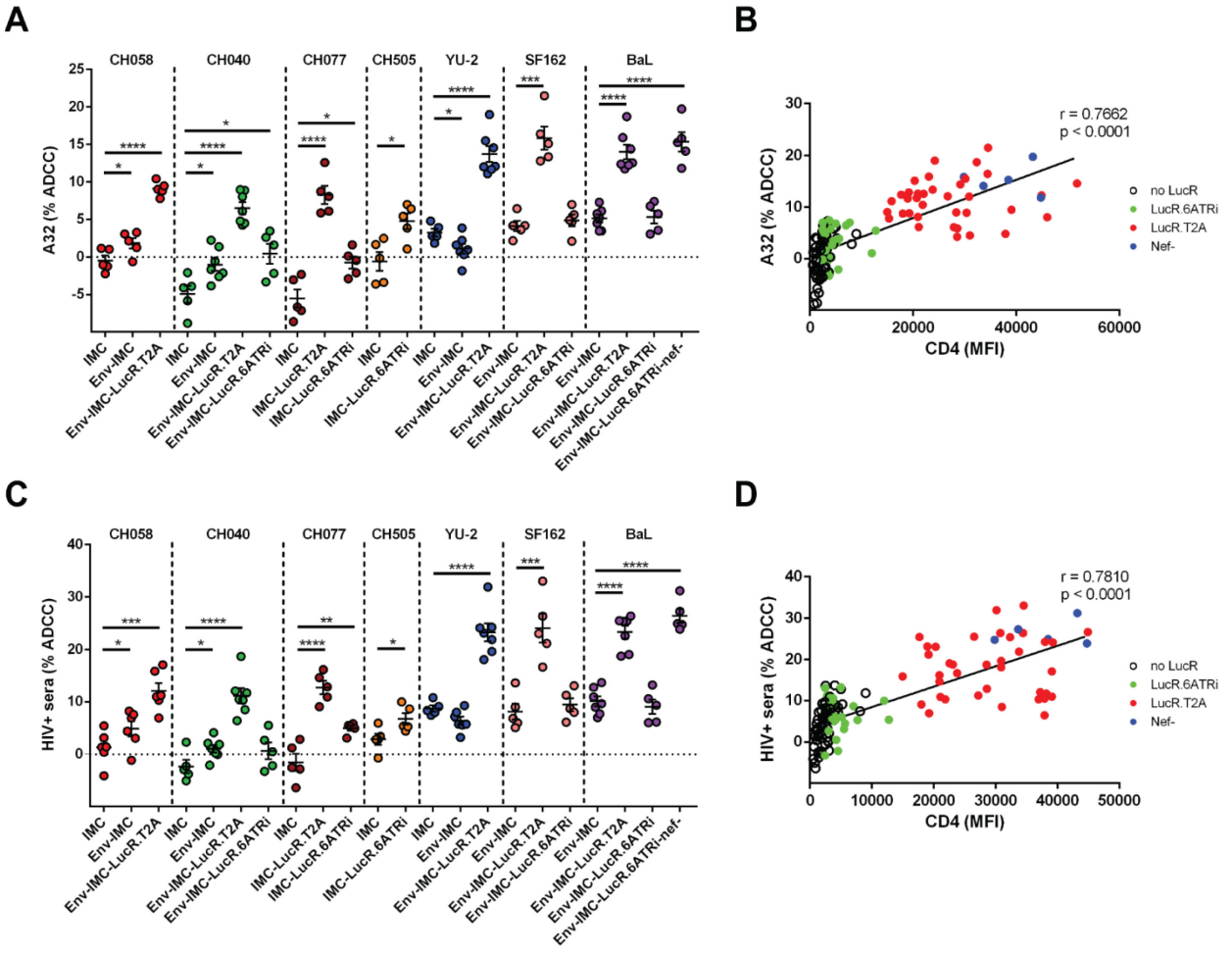

Figure 3.2.4 - Susceptibility of cells infected with different parental and reporter IMCs to ADCC mediated by A32 and HIV$^+$ sera.

Primary CD4$^+$ T cells infected with IMCs expressing different Env strains (CH058, CH040, CH077, CH505, YU-2, SF162, and BaL) and expressing or not the LucR reporter gene were used as target cells, and autologous PBMCs were used as effector cells in a well-established FACS-based ADCC assay (1, 9, 10, 60, 84). (**A and C**) Percentages of ADCC-mediated killing obtained with A32 or HIV$^+$ sera from 5 HIV-1-infected individuals obtained in at least 5 independent experiments. (**B and D**) Correlations between levels of cell surface CD4 and ADCC responses mediated by A32 or HIV$^+$ sera, using the same panel of IMC constructs, detected with the FACS-based ADCC assay. Statistical significance was tested using an unpaired t test (**A and C**), a Pearson correlation test (**B**), or a Spearman rank correlation test (**D**) (*, $P < 0.05$; **, $P < 0.01$; ***, $P < 0.001$; ****, $P < 0.0001$).

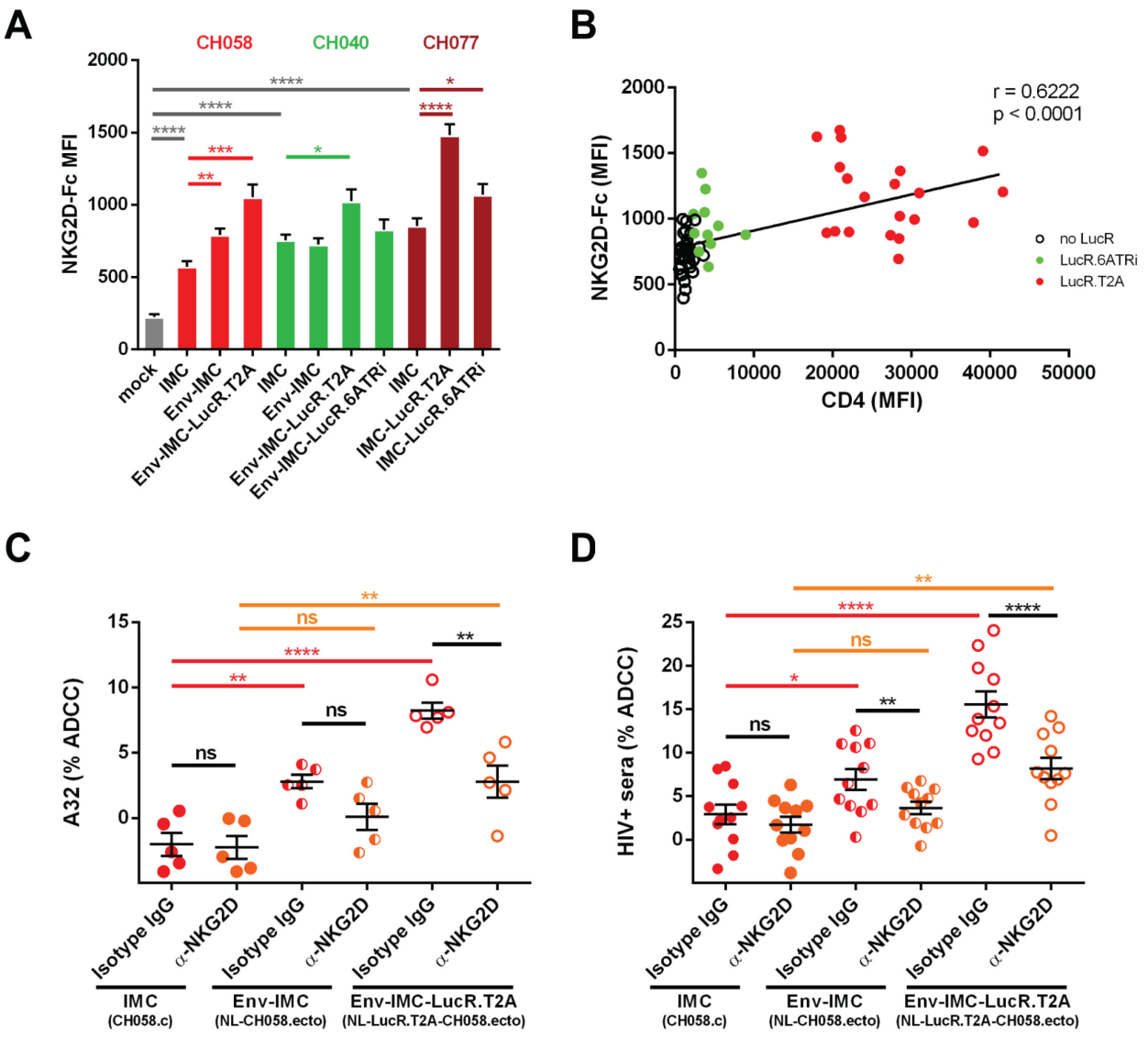

Figure 3.2.5 - Effect of the molecular strategy for LucR reporter element insertion on the expression of NKG2D ligands.

Shown are the results of cell surface staining of primary $CD4^+$ T cells either mock infected or infected with IMC constructs expressing different Env strains (CH058, CH040, and CH077) and expressing or not the LucR reporter gene with an NKG2D-Fc chimera protein that binds to NKG2D ligands. (**A**) MFI in the infected ($p24^+$) population obtained in at least 5 independent experiments. (**B**) Spearman rank correlation between CD4 levels and NKG2D ligand expression. (**C and D**) ADCC responses obtained in the presence of an anti-NKG2D Ab or its isotype control, as described in Materials and Methods. The data are shown as means and SEM. Statistical significance was tested using an unpaired t test (**A**), a Spearman correlation test (**B**), or an unpaired (**C**) or a paired (**D**) one-way analysis of variance (ANOVA) with a Holm-Sidak post-test (*, $P < 0.05$; **, $P < 0.01$; ***, $P < 0.001$; ****, $P < 0.0001$; ns, nonsignificant).

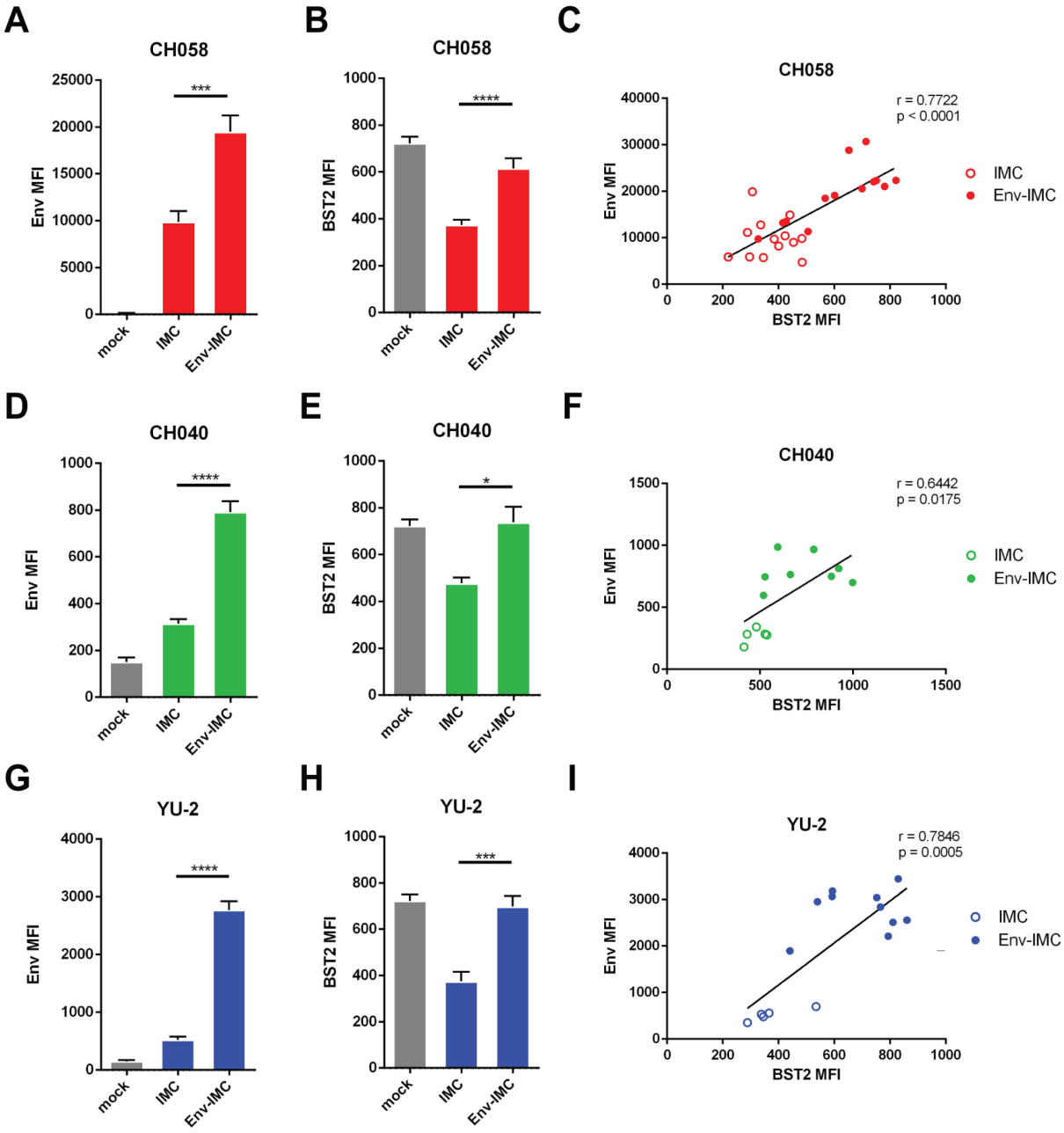

Figure 3.2.6 - Impact of the proviral backbone on BST-2 downregulation and Env detection at the cell surface.

Shown are the results of cell surface staining of primary $CD4^+$ T cells either mock infected or infected with IMC constructs expressing different Envs (CH058, CH40, and YU2) with the conformation-independent anti-Env 2G12 (**A**), 10E8 (**B and C**), or anti-BST-2 (**D to F**). (**A to F**) MFI in the infected ($p24^+$) population obtained in at least 5 independent experiments. (**G to I**) Correlations between the levels of cell surface BST-2 and Env staining performed with 2G12 or 10E8 using different IMC constructs. The data are shown as means and SEM. Statistical significance was tested using an unpaired t test (**A to F**) or a Pearson correlation test (**G to I**) (*, $P < 0.05$; ***, $P < 0.001$; ****, $P < 0.0001$).

ARTICLE 4

La détection des protéines accessoires Nef et Vpu du VIH-1 par cytométrie en flux représente un nouvel outil pour étudier simultanément leur interaction fonctionnelle au sein d'une seule cellule infectée

Detection of the HIV-1 Accessory Proteins Nef and Vpu by Flow Cytometry Represents a New Tool to Study their Functional Interplay within a Single Infected CD4$^+$ T cell

Auteurs:

Jérémie Prévost[1,2,*], Jonathan Richard[1,2,*], Romain Gasser[1,2], Halima Medjahed[1], Frank Kirchhoff[3], Beatrice H. Hahn[4], John C. Kappes[5], Christina Ochsenbauer[5], Ralf Duerr[6], Andrés Finzi[1,2,7]

Affiliations:

[1]Centre de Recherche du CHUM, Montreal, QC, Canada; [2]Département de Microbiologie, Infectiologie et Immunologie, Université de Montréal, Montreal, QC, Canada; [3]Institute of Molecular Virology, Ulm University Medical Center, Ulm, Germany; [4]Departments of Medicine and Microbiology, Perelman School of Medicine, University of Pennsylvania, Philadelphia, PA, USA; [5]Department of Medicine, University of Alabama at Birmingham, Birmingham, AL, USA; [6]Department of Microbiology, New York University School of Medicine, New York, NY, USA; [7]Department of Microbiology and Immunology, McGill University, Montreal, QC, Canada; *contribution égale

Contribution des auteurs:

Conceptualisation: **J.P.**, J.R. et A.F.; Méthodologie: **J.P.**, J.R. et A.F.; Recherche: **J.P.**, J.R. et R.G.; Ressources: H.M., F.K., B.H.H., J.C.K., C.O. et A.F.; Analyse formelle: **J.P.**, J.R. et R.D.; Visualisation: **J.P.**; Supervision: A.F.; Obtention du financement: J.C.K., C.O. et A.F.; Rédaction - version originale: **J.P.**, J.R., B.H.H. et A.F.; Rédaction - révision et édition: **Tous les auteurs**.

Statut: Cet article a été publié dans *Journal of Virology*, le 26 janvier 2022.
https://doi.org/10.1128/jvi.01929-21

3.4.1 RÉSUMÉ

Les protéines accessoires Nef et Vpu du VIH-1 sont connues pour protéger les cellules infectées des réponses de cytotoxicité cellulaire dépendant des anticorps (ADCC) en limitant l'exposition des épitopes de l'enveloppe (Env) induits par CD4 (CD4i) à la surface des cellules. Bien que les deux protéines ciblent le récepteur CD4 de l'hôte pour le dégrader, l'étendue de leur redondance fonctionnelle est inconnue. Nous avons développé une technique de coloration intracellulaire qui permet la détection intracellulaire de Nef et Vpu dans les lymphocytes T $CD4^+$ primaires par cytométrie de flux. Grâce à cette méthode, nous montrons que l'expression combinée de Nef et de Vpu prédit la susceptibilité des lymphocytes T $CD4^+$ primaires infectés par le VIH-1 à l'ADCC par le plasma VIH+. Nous montrons également que Vpu ne peut pas compenser l'absence de Nef, ce qui explique pourquoi certains clones moléculaires infectieux qui portent un gène rapporteur LucR en amont de Nef rendent les cellules infectées plus sensibles à la réponse ADCC. Notre méthode représente donc un nouvel outil pour disséquer l'activité biologique de Nef et Vpu dans le contexte d'autres protéines cellulaires et virales au sein d'un même lymphocyte T $CD4^+$ infecté.

3.4.2 ABSTRACT

The HIV-1 Nef and Vpu accessory proteins are known to protect infected cells from antibody-dependent cellular cytotoxicity (ADCC) responses by limiting exposure of CD4-induced (CD4i) envelope (Env) epitopes at the cell surface. Although both proteins target the host receptor CD4 for degradation, the extent of their functional redundancy is unknown. Here, we developed an intracellular staining technique that permits the intracellular detection of both Nef and Vpu in primary $CD4^+$ T cells by flow cytometry. Using this method, we show that the combined expression of Nef and Vpu predicts the susceptibility of HIV-1-infected primary $CD4^+$ T cells to ADCC by HIV^+ plasma. We also show that Vpu cannot compensate for the absence of Nef, thus providing an explanation for why some infectious molecular clones that carry a LucR reporter gene upstream of Nef render infected cells more susceptible to ADCC responses. Our method thus represents a new tool to dissect the biological activity of Nef and Vpu in the context of other host and viral proteins within single infected $CD4^+$ T cells.

3.4.3 IMPORTANCE

HIV-1 Nef and Vpu exert several biological functions that are important for viral immune evasion, release, and replication. Here, we developed a new method allowing simultaneous detection of these accessory proteins in their native form together with some of their cellular substrates. This allowed us to show that Vpu cannot compensate for the lack of a functional Nef, which has implications for studies that use Nef-defective viruses to study ADCC responses.

3.4.4 INTRODUCTION

The human immunodeficiency virus type 1 (HIV-1) genome encodes four accessory proteins (Vif, Vpr, Vpu, and Nef), which are dispensable for viral replication *in vitro* but required for efficient replication, restriction factor counteraction, and immune evasion *in vivo* (1–7). Among them, Nef and Vpu are well known for their role in subverting the host cell protein trafficking machinery (8, 9).

HIV-1 Nef is a small cytoplasmic protein of 27 kDa produced from early viral transcripts (10) which requires a myristoyl group on its N-terminus to traffic to intracellular and plasma membranes (11). Nef harbors a highly conserved dileucine motif in its C-terminal flexible loop that is responsible for the interaction with clathrin adaptor protein complexes (AP-1, AP-2, and AP-3) (12). Among these, interaction with AP-2 is required to downregulate the CD4 receptor from the surface of infected cells (13, 14) and target it for degradation in lysosomal compartments (15, 16).

HIV-1 Vpu is a small type I transmembrane protein of 16 kDa produced late in the viral replication cycle (17, 18) and contains a short luminal N-terminal peptide followed by a single helical transmembrane domain and a C-terminal cytoplasmic domain (19–21). The cytoplasmic domain comprises two a-helices linked by a flexible loop known for its interaction with the $SCF^{\beta TRCP}$ E3 ubiquitin ligase complex via a conserved phosphoserine motif ($DS^{P}GNES^{P}$) (22, 23). Vpu mainly localizes within intracellular compartments, notably, the endoplasmic reticulum (ER) and the *trans*-Golgi network (TGN) (24–26). Like Nef, Vpu also induces degradation of newly synthesized CD4 by directing it through an ER-associated pathway (ERAD) for further proteasomal degradation (22, 27–29). In addition, Vpu sequesters the restriction factor BST-2 in

the TGN using its transmembrane domain and thereby increasing the release of progeny virions (30–33).

CD4 downregulation by Nef and Vpu was previously reported to be critical for efficient viral replication in T cells by enhancing virion release and infectivity and by preventing superinfection (34–39). CD4 downregulation is critical for immune evasion since the anti-Env antibody (Ab) response is dominated by non-neutralizing antibodies (nnAbs) that target Env in its "open" CD4-bound conformation (40–42). The interaction between CD4 and Env at the surface of HIV-1-infected cells has been shown to promote nnAbs binding to Env, leading to the elimination of infected cells through Fc-mediated effector functions, including antibody-dependent cellular cytotoxicity (ADCC) and complement-dependent cytotoxicity (41, 43, 44). Nef and Vpu limit the presence of Env-CD4 complexes at the cell surface and thus protect infected cells against ADCC (41, 43, 45).

In previous studies, Nef and Vpu expression was mostly examined in transfected cell lines, frequently using tagged proteins (30, 31, 46, 47) or by performing Western blot analysis and immunofluorescence microscopy in infected primary cells (48–53). However, both proteins are small, intracellularly located, and present in small amounts, rendering their detection difficult. To facilitate their analysis in primary $CD4^+$ T cells, we developed an intracellular staining technique to detect Nef and Vpu expression by flow cytometry, which allows the simultaneous detection of these proteins together with host and viral proteins within a single infected cell. Using this method, we show that Nef and Vpu expression predicts the susceptibility of HIV-1-infected primary $CD4^+$ T cells to ADCC by HIV^+ plasma. We also explain why decreased Nef expression in widely used reporter viruses increases the susceptibility of infected cells to ADCC responses.

3.4.5 RESULTS

Intracellular detection of Nef and Vpu in HIV-1-infected primary $CD4^+$ T cells.

To facilitate detection of intracellular Nef, we obtained a polyclonal Nef antiserum through the NIH AIDS Reagent Program, which was generated by immunization of rabbits with a recombinant clade B Nef consensus protein produced in *Escherichia coli* (54). In previous studies,

this antibody detected native Nef proteins by Western blotting and immunofluorescence microscopy in both transfected and infected cells (48, 55–57). Given the scarcity of anti-Vpu antibodies, we immunized rabbits with a peptide corresponding to the clade B Vpu C-terminal region (residues 69 to 81). A similar approach was previously used to generate a polyclonal antibody capable of detecting Vpu by Western blotting and immunofluorescence microscopy (24, 58).

We first evaluated the ability of both Nef and Vpu antisera to recognize their cognate antigen using HEK 293T cells transfected with plasmids expressing the Nef or Vpu proteins from the transmitted/founder (T/F) virus CH058 (59, 60). Cells were permeabilized and stained with the antisera 48 h post-transfection, followed by detection with a fluorescently labeled anti-rabbit secondary antibody. As expected, the Nef antiserum recognized only Nef-transfected cells, while the Vpu antiserum recognized only Vpu-transfected cells (**Fig. 3.3.1A to C**). To evaluate whether our method detected Nef and Vpu when expressed in a biologically relevant culture system, we infected primary $CD4^+$ T cells with CH058 infectious molecular clones (IMC) encoding Nef and/or Vpu proteins. While wild-type (WT)-infected cells were efficiently recognized by both Nef and Vpu antisera, abrogation of Nef (**Fig. 3.3.1D and E**) or Vpu (**Fig. 3.3.1F and G**) expression prevented the recognition of productively infected cells as identified by Gag protein intracellular staining ($p24^+$). Of note, mock-infected or uninfected bystander cells ($p24^-$) were not detected by either antiserum, further confirming their specificity (**Fig. 3.3.1D to G**).

We next examined the antiserum binding to Nef and Vpu proteins from different HIV-1 clades and groups as well as from closely related simian immunodeficiency viruses (SIV). Primary $CD4^+$ T cells were infected with a panel of HIV-1 IMCs representing clades B, C, A1, and CRF01_AE. As expected, both Nef and Vpu antisera recognized their respective antigen in cells infected with clade B viruses since both were raised against clade B immunogens (**Fig. 3.3.1H and I**). The anti-Nef polyclonal antibody was also able to recognize Nef proteins from group M clades C, A1, and CRF01_AE as well as the Nef from a group O isolate. This recognition extended even to the Nef protein of a related SIVcpzPts strain (isolate TAN2) but not to chimeric simian-human immunodeficiency viruses (SHIV) which express an SIVmac Nef (**Fig. 3.3.1H**). The Vpu antiserum was less cross-reactive and failed to detect Vpu from clade C viruses (**Fig. 3.3.1I**). These

findings confirmed the specificity and cross-reactivity of the intracellular detection of Nef and Vpu using infected primary $CD4^+$ T cells.

Measuring CD4 and BST-2 downregulation in infected primary $CD4^+$ T cells with or without Nef and Vpu expression.

The efficient detection of Nef and Vpu at the single cell level by flow cytometry allowed us to combine this approach with the quantification of CD4 and BST-2 expression levels on the cell surface. Productively-infected cells ($p24^+$) expressing both Nef and Vpu had little detectable CD4 and BST-2 compared to uninfected cells (**Fig. 3.3.2A**). In contrast, cells infected with Vpu- or Nef-defective viruses differed in the extent of CD4 and BST-2 downregulation (**Fig. 3.3.2A**).

Vpu targets CD4 and BST-2 by different mechanisms. First, Vpu interacts with multiple transmembrane proteins, including BST-2, through its transmembrane domain (TMD), which sequesters these proteins in perinuclear compartments (32, 33, 61–64). Second, Vpu downregulates CD4 by interaction of its cytoplasmic domain with the cytoplasmic tail of CD4 (65–70). Consistent with these different interaction modes, Vpu-mediated CD4 and BST-2 degradation involves independent pathways (proteasomal and lysosomal degradation, respectively), both of which depend on polyubiquitination by the $SCF^{\beta TRCP}$ E3 ubiquitin ligase complex, recruited by Vpu using its highly conserved phosphoserine motif (22, 26, 71, 72). To examine whether we could measure the expression and activity of Vpu mutants by flow cytometry, we introduced mutations at critical residues of the Vpu TMD (A14L/A18L) or its phosphoserine motif (S52A/S56A). CH058 IMCs coding for wild-type or mutated Vpu proteins were used to infect primary $CD4^+$ T cells. While the TMD mutations did not affect Vpu expression, the phosphoserine mutations led to a significant accumulation of intracellular Vpu proteins (**Fig. 3.3.2B**), most likely because Vpu is degraded together with its target protein as a ubiquitinated complex (24, 73, 74). Despite a higher expression level, the Vpu phosphoserine mutant was unable to downregulate CD4 and was marginally diminished in its capacity to antagonize BST-2 (**Fig. 3.3.2C to F**). This is consistent with studies demonstrating that the recruitment of the $SCF^{\beta TRCP}$ E3 ubiquitin ligase complex and the degradation of BST-2 by Vpu is dissociable from its capacity to antagonize the restriction factor (32, 72, 75–77). In contrast, the Vpu TMD mutations did not affect Vpu's ability to target CD4 but completely abrogated its capacity to downregulate BST-2

(**Fig. 3.3.2C to F**). Together, these results emphasize the need for measuring Nef and Vpu expression when studying their biological functions.

Nef and Vpu expression inversely correlates with ADCC responses.

CD4 downregulation by Nef and Vpu together with Vpu-mediated BST-2 antagonism were found to be critical factors preventing the exposure of vulnerable CD4-induced Env epitopes, thus protecting HIV-1-infected cells from ADCC (41, 43, 45, 78–81). To investigate the link between Nef and Vpu expression and HIV-1-infected cell immune evasion, we infected activated primary $CD4^+$ T cells from five HIV-negative individuals with two clade B IMCs, CH058 T/F and JR-FL, encoding functional or defective *nef* and *vpu* genes. Focusing on the productively infected cells ($p24^+$), we performed a comprehensive characterization of the patterns of viral protein expression, including cell-surface Env (detected with the conformation-independent Ab 2G12), intracellular Nef, and Vpu in combination with cell-surface levels of CD4 and BST-2. We also measured the specific recognition and elimination of infected cells by ADCC using the CD4-induced (CD4i) A32 monoclonal Ab (mAb). This antibody binds the cluster A region of the gp120, which is occluded in the "closed" trimer and therefore, can only bind Env in the "open" CD4-bound conformation. We also tested 25 different plasma samples from chronically HIV-1-infected individuals. As expected, Nef was only expressed by WT and Vpu^- constructs, while Vpu was only expressed by WT and Nef^- constructs (**Fig. 3.3.3A**). Consistent with previous reports (43, 78, 79), deletion of Nef strongly impaired CD4 downregulation by both viruses but did not affect Env or BST-2 cell-surface levels. Vpu deletion mitigated CD4 downregulation to a lesser extent than Nef and abrogated BST-2 downmodulation, resulting in an overall increase in the amount of cell-surface Env (**Fig. 3.3.3B**). The cumulative effect of Nef and Vpu on cell-surface levels of Env, CD4, and BST-2 prevented the recognition of infected cells and protected them from ADCC responses mediated by A32 and HIV^+ plasma (**Fig. 3.3.3C and D**). In contrast, abrogation of Nef or Vpu expression resulted in increased recognition and susceptibility of infected cells to ADCC mediated by nnAbs (**Fig. 3.3.3C and D**). We performed correlation analyses to measure the level of association between the different cellular, virological, and immunological variables (**Fig. 3.3.3E and F**). We found that both Nef and Vpu established a large network of inverse correlations with cellular and immunological factors. Interestingly, Env levels hardly contributed to the network and were poorly associated with the immunological outcome, thus indicating that the overall amount

of Env present at the surface does not dictate ADCC responses mediated by CD4i Abs or HIV$^+$ plasma but, rather, the conformation Env occupies. Apart from antibody binding, ADCC responses mediated by nnAbs correlated strongly with CD4 and Nef levels (**Fig. 3.3.3E and F**). Overall, Nef and Vpu expression inversely correlates with the susceptibility of HIV-1-infected cells to ADCC mediated by CD4i Abs and HIV$^+$ plasma.

Impaired Nef expression from IMC LucR.T2A constructs enhance the susceptibility of infected cells to ADCC.

Infectious molecular clones encoding the Renilla luciferase (LucR) reporter gene upstream of the *nef* sequence and a T2A ribosome-skipping peptide to drive Nef expression are widely employed to quantify anti-HIV-1 ADCC responses (82–95). Despite evidence that Nef-mediated CD4 downregulation is impaired when using these IMCs (55, 80), a series of recent studies have hypothesized that Vpu can compensate for the absence of Nef expression and completely downregulate CD4 on its own (96–100). To evaluate this hypothesis, we used our intracellular staining to measure Nef and Vpu expression levels and study their impact on ADCC responses mediated by nnAbs against cells infected with IMC-LucR.T2A constructs. Primary CD4$^+$ T cells were infected with NL4.3-based IMCs that do (Env-IMC-LucR.T2A) or do not encode (Env-IMC) a LucR.T2A cassette. These IMCs express the Env ectodomain from two clade B viruses, CH058 T/F and YU-2. Consistent with the lack of Nef detection by Western blotting (55, 80), insertion of the LucR.T2A cassette also impaired the detection of Nef by flow cytometry, while Vpu expression remained unchanged (**Fig. 3.3.4A and B**). However, we noted an accumulation of cell-surface CD4 for Env-IMC-LucR.T2A compared to *nef*-intact constructs (~20-fold higher) (**Fig. 3.3.4C**), which resulted in a significantly increased recognition and susceptibility of infected cells to ADCC responses mediated by A32 mAb and HIV$^+$ plasma (**Fig. 3.3.4D and E**). Of note, both the binding and the ADCC responses mediated by nnAbs were strongly associated with CD4 levels and inversely correlated with Nef expression (**Fig. 3.3.4F and G**). In contrast, these variables were poorly correlated with Vpu expression. Based on these data, it seems clear that Vpu expression alone is not sufficient to prevent ADCC-mediated killing of infected cells and that HIV-1 requires both Nef and Vpu for efficient humoral response evasion.

Nef, Vpu, and CD4 levels predict ADCC responses mediated by HIV$^+$ plasma.

We next used univariate multiple linear regression (MLR) analysis to evaluate the capacity of different variables to predict ADCC responses mediated by HIV^+ plasma. This model is based on the hypothesis that a linear relationship exists between the dependent variable quantified empirically and the independent variables that serve as predictive variables. In our model, the dependent variable is the ADCC responses mediated by plasma from HIV-1 donors (ADCC HIV^+ plasma), and the independent variables are the cellular, virological, and immunological factors measured on infected cells. To run the MLR model, we combined data obtained with the different viral constructs (**Fig. 3.3.3 and 3.3.4**) and plotted the mean ADCC obtained with 25 HIV^+ plasma samples against a single virus on the *x* axis and the associated predicted ADCC value based on one or more independent variables on the *y* axis. When looking at cellular factors, we noticed that only CD4 accurately predicts ADCC responses mediated by HIV^+ plasma, independent of the viral strain (**Fig. 3.3.5A**). Even though BST-2 displayed a strong correlation with ADCC responses (**Fig. 3.3.3E**), it was not predictive. When focusing on virological variables, we observed that Nef is the only significant ADCC predictive variable, albeit not as good as CD4 (**Fig. 3.3.5A and B**). However, combinations of Nef with Vpu or Env increased its predictive scores, reaching similar levels as CD4 when combined with Vpu (**Fig. 3.3.5B**). Of note, the strength of the prediction was not further improved when combining all three virological variables altogether. As for immunological variables, their capacity to predict ADCC by HIV^+ plasma was found to be equivalent or even higher than for cellular and virological factors (**Fig. 3.3.5C**). Indeed, the binding of HIV^+ plasma predicted ADCC values with a similar score as CD4 or Nef and Vpu combined, while the binding of A32 predicted ADCC by HIV^+ plasma even better (**Fig. 3.3.5A to C**). This could be explained by the fact that A32-like Abs present in plasma from infected individuals are from the main class of Abs (anti-cluster A Abs) mediating ADCC responses against infected cells (41, 81, 82, 92, 101). In line with this interpretation, ADCC mediated by A32 was found to have a near-perfect predictive ability, suggesting that factors other than antibody binding are presumably needed to fully explain the ADCC phenotypes observed (**Fig. 3.3.5C**).

3.4.6 DISCUSSION

Unlike simple retroviruses, HIV-1 and related SIVs encode multiple accessory proteins that promote viral replication and immune evasion (102). Among them, Nef and Vpu modulate the expression, trafficking, localization, and function of several host cell surface proteins, including

the viral receptor CD4, restriction factors, and homing receptors (28, 30, 31, 63, 70, 103–107). They also modulate a wide range of immunoreceptors to evade immune responses mediated by $CD8^+$ T, NK, and NKT cells (108–116). Most of these host cell proteins are naturally expressed on primary $CD4^+$ T cells, the preferential target of HIV-1. The detection of Nef and Vpu has previously been done in transfected cells (30, 31, 47, 49, 50, 117), which results in the overexpression of the viral proteins compared to infected primary $CD4^+$ T cells. Moreover, tagged viral proteins are frequently used to facilitate their detection (30, 31, 47, 49, 50, 117). Protein overexpression and/or tag insertion have the potential to impact the trafficking and functions of these accessory proteins. To study Nef and Vpu's biological activities in a physiologically relevant system, we developed an intracellular staining method to detect native Nef and Vpu proteins in HIV-1-infected primary $CD4^+$ T cells by flow cytometry. Using Nef and Vpu antisera, we detected both viral proteins with high specificity in cells productively infected ($p24^+$) with multiple IMCs. The Nef antiserum was cross-reactive, detecting Nef from group M (clades B, C, A1, and CRF01_AE) from a group O isolate and from a closely related SIVcpz strain. In contrast, the Vpu antiserum recognized only clade B Vpu proteins, consistent with the fact that we used a peptide from the C-terminal region of clade B Vpu. This region is highly variable among group M viruses (118). More conserved regions of Vpu map to the transmembrane domain of the protein and the βTRCP binding site (119, 120). However, these regions are either buried in the plasma membrane or occluded by cellular partners and thus are not readily accessible for antibody recognition. While the generation of a broad Vpu antiserum is challenging, it may be possible to generate clade-specific Vpu antisera by immunization using peptides corresponding to the C-terminal region specific for a given clade.

Nef and Vpu intracellular detection by flow cytometry represents an excellent tool to study their biological activities in HIV-1-infected primary $CD4^+$ T cells. This method allows for the detection of cell-surface substrates or antibody recognition of surface Env and the concomitant detection of Nef and Vpu expression within a single infected cell (**Fig. 3.3.2A**). Infected $CD4^+$ T cells represent the most relevant system to study the complex interplay between these two accessory proteins and the wide range of host cell factors naturally expressed by T cells. Recent findings revealed that modulation of BST-2 levels by type I IFNs impacts the capacity of Vpu to downregulate NTB-A, PVR, CD62L, and TIM-3, thus reducing its polyfunctionality (64, 70). Nef

and Vpu also display overlapping functions, as they share the capacity to downregulate several cell-surface proteins, including CD4, PVR, CD62L, and CD28 (8, 57, 63, 113, 121). The expression levels of one viral protein could therefore modulate the biological activities of the other, making it essential to study their functions in a context where both viral proteins are expressed simultaneously at physiological levels. Thus, our intracellular staining measuring Nef/Vpu expression and functionality in HIV-1-infected cells represents a new approach to better characterize their functional interplay.

Increasing evidence points toward Env conformation on the surface of infected cells as a critical parameter of ADCC susceptibility to HIV^+ plasma (41, 122–124). Non-neutralizing antibodies in the plasma from HIV-1-infected individuals target epitopes that are only exposed when Env interacts with cell-surface CD4, thus adopting the open CD4-bound conformation (41, 43). Nef and Vpu contribute to protect HIV-1-infected cells from ADCC by limiting Env-CD4 interaction via CD4 downregulation and BST-2 antagonism (41, 43, 45, 78, 79). Here, we confirm and extend previous observations by showing that Nef and Vpu expression predicts the susceptibility of HIV-1-infected primary $CD4^+$ T cells to ADCC responses. In agreement with recent studies (45, 80), we found that CD4 accurately predicted the susceptibility of infected cells to ADCC (**Fig. 3.3.5**). Given its enhanced capacity to downregulate CD4 compared to Env or Vpu (34, 41, 43, 121), Nef represents the main viral factor influencing ADCC responses mediated by CD4-induced ligands (**Fig. 3.3.5B**). On the contrary, BST-2 and Env expression, alone or in combination, were unable to accurately predict the susceptibility of infected cells to ADCC. These results are consistent with previous reports suggesting that Env conformation and CD4 reactivity, rather than overall cell-surface Env levels, drive ADCC responses mediated by HIV^+ plasma (41, 43, 123–125). This is also in agreement with recent work showing that BST-2 upregulation by type I IFNs enhances cell-surface Env levels without increasing the susceptibility of infected cells to ADCC mediated by HIV^+ plasma, unless CD4-mimetics are used to "open-up" Env and stabilize the CD4-bound conformation (126).

A series of recent studies using LucR.T2A IMCs have hypothesized that Vpu can compensate for the absence of Nef expression by fully downregulating cell-surface CD4 (96–100). Our results show that this is not the case. Consistent with its role in targeting CD4 already present

at the plasma membrane, the impact of Nef on CD4 downmodulation is more prominent (**Fig. 3.3.2 and 3.3.3**) (34, 41, 43, 121). In its absence, Vpu was unable to fully downregulate CD4, thus sensitizing infected cells to ADCC responses. These results highlight the importance of selecting full-length unmutated IMCs with proper Nef and Vpu expression to generate biologically relevant ADCC measurements. For example, a recent manuscript recently reported no differences in ADCC susceptibility between cells infected with clade B, clade C, or CRF01_AE IMCs (127), while previous studies have shown otherwise (123, 128). In this article (127), the authors use functionally Nef-defective LucR.T2A IMCs, which results in incomplete CD4 downregulation and therefore exposure of Env in its CD4-bound conformation at the cell surface (**Fig. 3.3.4**) (80). Thus, it is not surprising that the usage of Nef-defective viruses skews ADCC responses in favor of nnAbs and mitigates the intrinsic differences that exist between Env from different clades. Fortunately, several alternatives to the use of LucR.T2A IMCs are available to measure ADCC against productively infected cells (129), including the infected cell elimination (ICE) assay, which measures the loss of productively infected cells ($p24^+$) by flow cytometry and allows the utilization of unmodified IMCs. Utilization of an NK cell-resistant T cell line expressing a Tat-driven luciferase reporter gene (CEM.NKr-CCR5-sLTR-Luc) as target cells also represents an option (130). Finally, luciferase reporter IMCs (referred to as LucR.6ATRi IMCs) expressing similar levels of Nef as those obtained with unmodified IMCs are also available. These IMCs utilize a modified encephalomyocarditis virus (EMCV) internal ribosome entry site (IRES) element in lieu of T2A (55, 80). Thus, LucR.6ATRi reporter viruses represent a biologically relevant alternative to LucR.T2A IMCs when measuring ADCC mediated by nnAbs and plasma collected from infected or vaccinated individuals.

3.4.7 MATERIALS AND METHODS

Ethics statement

Written informed consent was obtained from all study participants (the Montreal Primary HIV Infection Cohort [131, 132] and the Canadian Cohort of HIV Infected Slow Progressors [133–135]), and research adhered to the ethical guidelines of CRCHUM and was reviewed and approved by the CRCHUM institutional review board (ethics committee, approval number CE 16.164-CA). Research adhered to the standards indicated by the Declaration of Helsinki. All participants were adults and provided informed written consent prior to enrollment, in accordance with institutional review board approval.

Cell lines and isolation of primary cells

HEK293T human embryonic kidney cells (obtained from ATCC) were grown as previously described (136). Primary human peripheral blood mononuclear cells (PBMCs) and $CD4^+$ T cells were isolated, activated, and cultured as previously described (43). Briefly, PBMCs were obtained by leukapheresis from HIV-negative individuals (4 males and 1 female), and $CD4^+$ T lymphocytes were purified from resting PBMCs by negative selection using immunomagnetic beads per the manufacturer's instructions (StemCell Technologies, Vancouver, BC) and were activated with phytohemagglutinin-L (10 µg/mL) for 48 h and then maintained in RPMI 1640 complete medium supplemented with rIL-2 (100 U/mL).

Plasmids and proviral constructs

The vesicular stomatitis virus G (VSV-G)-encoding plasmid was previously described (137). Transmitted/founder (T/F) and chronic infectious molecular clones (IMCs) of patients CH040, CH058, CH077, CH131, CH141, CH167, CH185, CH198, CH236, CH269, CH293, CH440, CH470, CH505, CH534, CH850, CM235, MCST, REJO, RHGA, RHPA, STCO, SUMA, TRJO, WARO, WITO, WR27, 40061, 703357, and 851891 were inferred, constructed, and biologically characterized as previously described (123, 138–147). The IMCs encoding HIV-1 reference strains AD8, JR-FL, JR-CSF, NL4-3, and YU-2 were described elsewhere (148–153). HIV-1 group O (RBF206), SIVcpz (TAN2), and chimeric SIVmac/HIV-1 IMC constructs ($SHIV_{AD8\text{-}EO}$ and SHIV.AE.40100) were generated as previously published (154–157). CH058

IMCs defective for Vpu and/or Nef expression were previously described (59). To generate a *nef*-defective JR-FL IMC, a frameshift mutation was introduced at the unique XhoI restriction site within the *nef* gene, resulting in a premature stop codon at position 47. To generate *vpu*-defective JR-FL IMCs, two stop-codons were introduced directly after the start-codon of *vpu* using the QuikChange II XL site-directed mutagenesis protocol (Agilent Technologies, Santa Clara, CA). The presence of the desired mutations was determined by automated DNA sequencing. Proviral constructs, collectively referred to as Env-IMCs, comprising an HIV-1 NL4.3-based isogenic backbone engineered for the insertion of heterologous *env* strain sequences and expression in *cis* of full-length Env (pNL.CH058.ecto and pNL.YU-2.ecto), were previously described (48). In the same study, isogenic proviral constructs encoding *Renilla* luciferase (LucR) followed in-frame by a ribosome-skipping T2A peptide intended to drive Nef expression were also reported (collectively referred to as Env-IMC-LucR.T2A) (48). Construction of plasmids encoding CH058 Vpu and CH058 Nef in the pCGCG-IRES-eGFP expression vector was previously described (59, 60).

Viral production and infections

To achieve a similar level of infection in primary $CD4^+$ T cells among the different IMCs tested, VSV-G-pseudotyped HIV-1 viruses were produced and titrated as previously described (123). Viruses were then used to infect activated primary $CD4^+$ T cells from healthy HIV-1-negative donors by spin infection at 800 × g for 1 h in 96-well plates at 25°C.

Antibodies and plasma

The following Abs were used to assess cell-surface Env staining: A32, 2G12 (NIH AIDS Reagent Program), and PGT135 (IAVI). Mouse anti-human CD4 (clone OKT4; Thermo Fisher Scientific, Waltham, MA, USA) and mouse anti-human BST-2 (clone RS38E, PE-Cy7-conjugated; BioLegend, San Diego, CA, USA) were also used as primary antibodies for cell-surface staining. Goat anti-mouse and anti-human antibodies precoupled to Alexa Fluor 647 (Invitrogen, Rockford, IL, USA) were used as secondary antibodies in flow cytometry experiments. Plasma from HIV-infected individuals was collected, heat-inactivated, and conserved at -80°C until use. Rabbit antisera raised against a Nef consensus protein (NIH AIDS Reagent Program) or against a Vpu C-terminal peptide (70) were used as primary antibodies in intracellular staining. Brilliant Violet 421 (BV421)-conjugated donkey anti-rabbit antibodies (BioLegend) were

used as secondary antibodies to detect Nef and Vpu antisera binding by flow cytometry. To avoid any potential cross-reactivity with the anti-rabbit secondary antibodies used for intracellular staining, mouse monoclonal antibodies were used to detect CD4 and BST-2 proteins.

Flow cytometry analysis of cell-surface and intracellular staining

Cell-surface staining of infected cells was performed as previously described (41). Binding of cell-surface HIV-1 Env by anti-Env mAbs (5µg/mL) or HIV^+ plasma (1:1,000 dilution) was performed at 48 h post-infection. Infected cells were then permeabilized using the Cytofix/Cytoperm fixation/permeabilization kit (BD Biosciences, Mississauga, ON, Canada) and stained intracellularly using phycoerythrin (PE)-conjugated mouse anti-p24 mAb (clone KC57; Beckman Coulter, Brea, CA, USA; 1:100 dilution) in combination with Nef or Vpu rabbit antisera (1:1,000 dilution). The percentage of infected cells ($p24^+$) was determined by gating on the living cell population according to viability dye staining (Aqua Vivid; Thermo Fisher Scientific). Alternatively, intracellular staining was assessed on 293T expressing Nef or Vpu proteins. Briefly, 2 × 106 293T cells were transfected with 7 µg of Nef or Vpu expressor with the calcium-phosphate method. At 48 h post-transfection, 293T cells were stained intracellularly with rabbit antisera raised against Nef or Vpu (1:1,000). Samples were acquired on an LSR II cytometer (BD Biosciences), and data analysis was performed using FlowJo v10.5.3 (Tree Star, Ashland, OR, USA).

FACS-based ADCC assay

Measurement of ADCC using the fluorescence-activated cell sorter (FACS)-based assay was performed at 48 h post-infection as previously described (43, 122). Briefly, HIV-1-infected primary $CD4^+$ T cells were stained with Aqua Vivid viability dye and cell proliferation dye eFluor 670 (Thermo Fisher Scientific) and used as target cells. Autologous PBMC effector cells, stained with cell proliferation dye eFluor 450 (Thermo Fisher Scientific), were added at an effector:target ratio of 10:1 in 96-well V-bottom plates (Corning, Corning, NY). A 1:1,000 final dilution of plasma or 5 µg/mL of A32 mAb was added to the appropriate wells, and cells were incubated for 5 min at room temperature. The plates were subsequently centrifuged for 1 min at 300 × g and incubated at 37°C, 5% CO_2, for 5 h before being fixed in a 2% phosphate-buffered saline (PBS)-formaldehyde solution. Samples were acquired on an LSR II cytometer (BD Biosciences), and

data analysis was performed using FlowJo v10.5.3 (Tree Star). The percentage of ADCC was calculated with the following formula: (% of $p24^+$ cells in targets plus effectors) - (% of $p24^+$ cells in targets plus effectors plus plasma)/(% of $p24^+$ cells in targets) by gating on infected live target cells. Negative ADCC values can be observed when uninfected $p24^+$ cells are eliminated in a larger proportion than infected $p24^+$ cells as previously reported (158, 159).

Software scripts and visualization

Correlograms were generated using the corrplot package in R v4.1.012 and RStudio v1.4.1106 (160, 161). Correlation networks were created using the ggraph and igraph packages in R in undirected mode, clustered based on the igraph layout "star." Edges are weighted according to *P* values (inversely). Edges are only shown if *P* is < 0.05, and nodes without edges were removed. Nodes are sized according to the *r* values of connecting edges. Multiple linear regression analyses were performed using GraphPad Prism software (v9.1.0). The coefficient of determination (R^2) was used as a metric to measure the proportion of the variation observed with the dependent variable that can be explained by the variation in the independent variables. Since R^2 values usually increase when more predictive variables are added to the model, we also measured the adjusted R^2 (adj. R^2) to account for this caveat. Individual values for each virus and every parameter were used to generate the correlograms and correlation networks, while multiple linear regression analyses were performed using mean values.

Statistical analysis

Statistics were analyzed using Prism v9.1.0 (GraphPad, San Diego, CA, USA). Every data set was tested for statistical normality, and this information was used to apply the appropriate (parametric or nonparametric) statistical test. *P* values of < 0.05 were considered significant; significance values are indicated as *, $P < 0.05$; **, $P < 0.01$; ***, $P < 0.001$; ****, $P < 0.0001$.

3.4.8 ACKNOWLEDGMENTS

We thank the CRCHUM BSL3 and Flow Cytometry Platforms for technical assistance and Mario Legault from the FRQS AIDS and Infectious Diseases network for cohort coordination and clinical samples. We thank the following collaborators for kindly providing some infectious molecular clones: Dennis Burton (The Scripps Research Institute) for JR-FL, Malcom A. Martin

(NIAID) for $SHIV_{AD8-EO}$, George M. Shaw (UPenn) for SHIV.AE.40100, and Sodsai Tovanabutra (US MHRP) for the $HIV\text{-}1_{WR27}$, $HIV\text{-}1_{703357}$, $HIV\text{-}1_{40061}$, $HIV\text{-}1_{CM235}$, and $HIV\text{-}1_{851891}$ IMCs. We thank MédiMabs for their scientific and technical support during the development of the Vpu antiserum. This study was supported by grants from the National Institutes of Health to A.F., C.O. and J.C.K. (R01 AI148379), to A.F. (R01 AI129769 and R01 AI150322), and to B.H.H. (R01 AI162646 and UM1 AI164570). This work was also partially supported by 1UM1AI164562-01, co-funded by the National Heart, Lung, and Blood Institute, National Institute of Diabetes and Digestive and Kidney Diseases, National Institute of Neurological Disorders and Stroke, National Institute on Drug Abuse, and the National Institute of Allergy and Infectious Diseases, a CIHR foundation grant (no. 352417), a CIHR Team grant (no.422148), and a Canada Foundation for Innovation grant (no. 41027) to A.F. A.F. is the recipient of a Canada Research Chair on Retroviral Entry (no. RCHS0235 950-232424). F.K. is supported by the Deutsche Forschungsgemeinschaft (CRC 1279 and SPP 1923). J.P. is the recipient of a CIHR doctoral fellowship. The funders had no role in study design, data collection and analysis, the decision to publish, or preparation of the manuscript.

3.4.9 REFERENCES

1. Desrosiers RC, Lifson JD, Gibbs JS, Czajak SC, Howe AY, Arthur LO, Johnson RP. 1998. Identification of highly attenuated mutants of simian immunodeficiency virus. J Virol 72:1431–1437.
2. Dave VP, Hajjar F, Dieng MM, Haddad E, Cohen EA. 2013. Efficient BST2 antagonism by Vpu is critical for early HIV-1 dissemination in humanized mice. Retrovirology 10:128.
3. Sato K, Misawa N, Fukuhara M, Iwami S, An DS, Ito M, Koyanagi Y. 2012. Vpu augments the initial burst phase of HIV-1 propagation and downregulates BST2 and CD4 in humanized mice. J Virol 86:5000–5013.
4. Sato K, Misawa N, Iwami S, Satou Y, Matsuoka M, Ishizaka Y, Ito M, Aihara K, An DS, Koyanagi Y. 2013. HIV-1 Vpr accelerates viral replication during acute infection by exploitation of proliferating $CD4^+$ T cells in vivo. PLoS Pathog 9:e1003812.
5. Crotti A, Neri F, Corti D, Ghezzi S, Heltai S, Baur A, Poli G, Santagostino E, Vicenzi E. 2006. Nef alleles from human immunodeficiency virus type 1-infected long-term-non-

progressor hemophiliacs with or without late disease progression are defective in enhancing virus replication and CD4 down-regulation. J Virol 80:10663–10674.

6. Rucker E, Grivel JC, Munch J, Kirchhoff F, Margolis L. 2004. Vpr and Vpu are important for efficient human immunodeficiency virus type 1 replication and $CD4^+$ T-cell depletion in human lymphoid tissue ex vivo. J Virol 78:12689–12693.
7. Kirchhoff F, Greenough TC, Brettler DB, Sullivan JL, Desrosiers RC. 1995. Absence of intact nef sequences in a long-term survivor with non-progressive HIV-1 infection. N Engl J Med 332:228–232.
8. Haller C, Muller B, Fritz JV, Lamas-Murua M, Stolp B, Pujol FM, Keppler OT, Fackler OT. 2014. HIV-1 Nef and Vpu are functionally redundant broad-spectrum modulators of cell surface receptors, including tetraspanins. J Virol 88:14241–14257.
9. Tokarev A, Guatelli J. 2011. Misdirection of membrane trafficking by HIV-1 Vpu and Nef: keys to viral virulence and persistence. Cell Logist 1: 90–102.
10. Purcell DF, Martin MA. 1993. Alternative splicing of human immunodeficiency virus type 1 mRNA modulates viral protein expression, replication, and infectivity. J Virol 67:6365–6378.
11. Bentham M, Mazaleyrat S, Harris M. 2006. Role of myristoylation and N-terminal basic residues in membrane association of the human immunodeficiency virus type 1 Nef protein. J Gen Virol 87:563–571.
12. Craig HM, Reddy TR, Riggs NL, Dao PP, Guatelli JC. 2000. Interactions of HIV-1 nef with the mu subunits of adaptor protein complexes 1, 2, and 3: role of the dileucine-based sorting motif. Virology 271:9–17.
13. Chaudhuri R, Lindwasser OW, Smith WJ, Hurley JH, Bonifacino JS. 2007. Downregulation of CD4 by human immunodeficiency virus type 1 Nef is dependent on clathrin and involves direct interaction of Nef with the AP2 clathrin adaptor. J Virol 81:3877–3890.
14. Ren X, Park SY, Bonifacino JS, Hurley JH. 2014. How HIV-1 Nef hijacks the AP-2 clathrin adaptor to downregulate CD4. Elife 3:e01754.
15. Aiken C, Konner J, Landau NR, Lenburg ME, Trono D. 1994. Nef induces CD4 endocytosis: requirement for a critical dileucine motif in the membrane-proximal CD4 cytoplasmic domain. Cell 76:853–864.

16. Rhee SS, Marsh JW. 1994. Human immunodeficiency virus type 1 Nef-induced down-modulation of CD4 is due to rapid internalization and degradation of surface CD4. J Virol 68:5156–5163.
17. Schwartz S, Felber BK, Pavlakis GN. 1992. Mechanism of translation of monocistronic and multicistronic human immunodeficiency virus type 1 mRNAs. Mol Cell Biol 12:207–219.
18. Krummheuer J, Johnson AT, Hauber I, Kammler S, Anderson JL, Hauber J, Purcell DF, Schaal H. 2007. A minimal uORF within the HIV-1 vpu leader allows efficient translation initiation at the downstream env AUG. Virology 363:261–271.
19. Wray V, Federau T, Henklein P, Klabunde S, Kunert O, Schomburg D, Schubert U. 1995. Solution structure of the hydrophilic region of HIV-1 encoded virus protein U (Vpu) by CD and 1H NMR spectroscopy. Int J Pept Protein Res 45:35–43.
20. Maldarelli F, Chen MY, Willey RL, Strebel K. 1993. Human immunodeficiency virus type 1 Vpu protein is an oligomeric type I integral membrane protein. J Virol 67:5056–5061.
21. Marassi FM, Ma C, Gratkowski H, Straus SK, Strebel K, Oblatt-Montal M, Montal M, Opella SJ. 1999. Correlation of the structural and functional domains in the membrane protein Vpu from HIV-1. Proc Natl Acad Sci USA 96:14336–14341.
22. Margottin F, Bour SP, Durand H, Selig L, Benichou S, Richard V, Thomas D, Strebel K, Benarous R. 1998. A novel human WD protein, h-beta TrCp, that interacts with HIV-1 Vpu connects CD4 to the ER degradation pathway through an F-box motif. Mol Cell 1:565–574.
23. Coadou G, Evrard-Todeschi N, Gharbi-Benarous J, Benarous R, Girault JP. 2002. HIV-1 encoded virus protein U (Vpu) solution structure of the 41-62 hydrophilic region containing the phosphorylated sites Ser52 and Ser56. Int J BiolMacromol 30:23–40.
24. Dube M, Roy BB, Guiot-Guillain P, Mercier J, Binette J, Leung G, Cohen EA. 2009. Suppression of tetherin-restricting activity upon human immunodeficiency virus type 1 particle release correlates with localization of Vpu in the trans-Golgi network. J Virol 83:4574–4590.
25. Klimkait T, Strebel K, Hoggan MD, Martin MA, Orenstein JM. 1990. The human immunodeficiency virus type 1-specific protein vpu is required for efficient virus maturation and release. J Virol 64:621–629.

26. Schubert U, Strebel K. 1994. Differential activities of the human immunodeficiency virus type 1-encoded Vpu protein are regulated by phosphorylation and occur in different cellular compartments. J Virol 68:2260–2271.
27. Schubert U, Anton LC, Bacik I, Cox JH, Bour S, Bennink JR, Orlowski M, Strebel K, Yewdell JW. 1998. CD4 glycoprotein degradation induced by human immunodeficiency virus type 1 Vpu protein requires the function of proteasomes and the ubiquitin-conjugating pathway. J Virol 72: 2280–2288.
28. Willey RL, Maldarelli F, Martin MA, Strebel K. 1992. Human immunodeficiency virus type 1 Vpu protein induces rapid degradation of CD4. J Virol 66:7193–7200.
29. Magadan JG, Perez-Victoria FJ, Sougrat R, Ye Y, Strebel K, Bonifacino JS. 2010. Multilayered mechanism of CD4 downregulation by HIV-1 Vpu involving distinct ER retention and ERAD targeting steps. PLoS Pathog 6:e1000869.
30. Neil SJ, Zang T, Bieniasz PD. 2008. Tetherin inhibits retrovirus release and is antagonized by HIV-1 Vpu. Nature 451:425–430.
31. Van Damme N, Goff D, Katsura C, Jorgenson RL, Mitchell R, Johnson MC, Stephens EB, Guatelli J. 2008. The interferon-induced protein BST-2 restricts HIV-1 release and is downregulated from the cell surface by the viral Vpu protein. Cell Host Microbe 3:245–252.
32. Dube M, Roy BB, Guiot-Guillain P, Binette J, Mercier J, Chiasson A, Cohen EA. 2010. Antagonism of tetherin restriction of HIV-1 release by Vpu involves binding and sequestration of the restriction factor in a perinuclear compartment. PLoS Pathog 6:e1000856.
33. Hauser H, Lopez LA, Yang SJ, Oldenburg JE, Exline CM, Guatelli JC, Cannon PM. 2010. HIV-1 Vpu and HIV-2 Env counteract BST-2/tetherin by sequestration in a perinuclear compartment. Retrovirology 7:51.
34. Wildum S, Schindler M, Munch J, Kirchhoff F. 2006. Contribution of Vpu, Env, and Nef to CD4 down-modulation and resistance of human immunodeficiency virus type 1-infected T cells to superinfection. J Virol 80:8047–8059.
35. Ding S, Gasser R, Gendron-Lepage G, Medjahed H, Tolbert WD, Sodroski J, Pazgier M, Finzi A. 2019. CD4 incorporation into HIV-1 viral particles exposes envelope epitopes recognized by CD4-induced antibodies. J Virol 93:e01403-19.

36. Bour S, Perrin C, Strebel K. 1999. Cell surface CD4 inhibits HIV-1 particle release by interfering with Vpu activity. J Biol Chem 274:33800–33806.
37. Cortes MJ, Wong-Staal F, Lama J. 2002. Cell surface CD4 interferes with the infectivity of HIV-1 particles released from T cells. J Biol Chem 277: 1770–1779.
38. Lama J, Mangasarian A, Trono D. 1999. Cell-surface expression of CD4 reduces HIV-1 infectivity by blocking Env incorporation in a Nef- and Vpu-inhibitable manner. Curr Biol 9:622–631.
39. Levesque K, Zhao YS, Cohen EA. 2003. Vpu exerts a positive effect on HIV-1 infectivity by down-modulating CD4 receptor molecules at the surface of HIV-1-producing cells. J Biol Chem 278:28346–28353.
40. Decker JM, Bibollet-Ruche F, Wei X, Wang S, Levy DN, Wang W, Delaporte E, Peeters M, Derdeyn CA, Allen S, Hunter E, Saag MS, Hoxie JA, Hahn BH, Kwong PD, Robinson JE, Shaw GM. 2005. Antigenic conservation and immunogenicity of the HIV coreceptor binding site. J Exp Med 201:1407–1419.
41. Veillette M, Coutu M, Richard J, Batraville LA, Dagher O, Bernard N, Tremblay C, Kaufmann DE, Roger M, Finzi A. 2015. The HIV-1 gp120 CD4-bound conformation is preferentially targeted by antibody-dependent cellular cytotoxicity-mediating antibodies in sera from HIV-1-infected individuals. J Virol 89:545–551.
42. Guan Y, Pazgier M, Sajadi MM, Kamin-Lewis R, Al-Darmarki S, Flinko R, Lovo E, Wu X, Robinson JE, Seaman MS, Fouts TR, Gallo RC, DeVico AL, Lewis GK. 2013. Diverse specificity and effector function among human antibodies to HIV-1 envelope glycoprotein epitopes exposed by CD4 binding. Proc Natl Acad Sci USA 110:E69–E78.
43. Veillette M, Desormeaux A, Medjahed H, Gharsallah NE, Coutu M, Baalwa J, Guan Y, Lewis G, Ferrari G, Hahn BH, Haynes BF, Robinson JE, Kaufmann DE, Bonsignori M, Sodroski J, Finzi A. 2014. Interaction with cellular CD4 exposes HIV-1 envelope epitopes targeted by antibody-dependent cell-mediated cytotoxicity. J Virol 88:2633–2644.
44. Dufloo J, Guivel-Benhassine F, Buchrieser J, Lorin V, Grzelak L, Dupouy E, Mestrallet G, Bourdic K, Lambotte O, Mouquet H, Bruel T, Schwartz O. 2020. Anti-HIV-1 antibodies trigger non-lytic complement deposition on infected cells. EMBO Rep 21:e49351.

45. Alsahafi N, Ding S, Richard J, Markle T, Brassard N, Walker B, Lewis GK, Kaufmann DE, Brockman MA, Finzi A. 2015. Nef proteins from HIV-1 elite controllers are inefficient at preventing antibody-dependent cellular cytotoxicity. J Virol 90:2993–3002.
46. Schaefer MR, Wonderlich ER, Roeth JF, Leonard JA, Collins KL. 2008. HIV-1 Nef targets MHC-I and CD4 for degradation via a final common beta-COP-dependent pathway in T cells. PLoS Pathog 4:e1000131.
47. Dikeakos JD, Atkins KM, Thomas L, Emert-Sedlak L, Byeon IJ, Jung J, Ahn J, Wortman MD, Kukull B, Saito M, Koizumi H, Williamson DM, Hiyoshi M, Barklis E, Takiguchi M, Suzu S, Gronenborn AM, Smithgall TE, Thomas G. 2010. Small molecule inhibition of HIV-1-induced MHC-I down-regulation identifies a temporally regulated switch in Nef action. Mol Biol Cell 21:3279–3292.
48. Edmonds TG, Ding H, Yuan X, Wei Q, Smith KS, Conway JA, Wieczorek L, Brown B, Polonis V, West JT, Montefiori DC, Kappes JC, Ochsenbauer C. 2010. Replication competent molecular clones of HIV-1 expressing Renilla luciferase facilitate the analysis of antibody inhibition in PBMC. Virology 408:1–13.
49. Atkins KM, Thomas L, Youker RT, Harriff MJ, Pissani F, You H, Thomas G. 2008. HIV-1 Nef binds PACS-2 to assemble a multikinase cascade that triggers major histocompatibility complex class I (MHC-I) down-regulation: analysis using short interfering RNA and knock-out mice. J Biol Chem 283:11772–11784.
50. Lenassi M, Cagney G, Liao M, Vaupotic T, Bartholomeeusen K, Cheng Y, Krogan NJ, Plemenitas A, Peterlin BM. 2010. HIV Nef is secreted in exosomes and triggers apoptosis in bystander $CD4^+$ T cells. Traffic 11: 110–122.
51. Komoto S, Tsuji S, Ibrahim MS, Li YG, Warachit J, Taniguchi K, Ikuta K. 2003. The vpu protein of human immunodeficiency virus type 1 plays a protective role against virus-induced apoptosis in primary CD4(1) T lymphocytes. J Virol 77:10304–10313.
52. Miyagi E, Andrew AJ, Kao S, Strebel K. 2009. Vpu enhances HIV-1 virus release in the absence of Bst-2 cell surface down-modulation and intracellular depletion. Proc Natl Acad Sci USA 106:2868–2873.
53. Chu H, Wang JJ, Qi M, Yoon JJ, Chen X, Wen X, Hammonds J, Ding L, Spearman P. 2012. Tetherin/BST-2 is essential for the formation of the intracellular virus-containing compartment in HIV-infected macrophages. Cell Host Microbe 12:360–372.

54. Shugars DC, Smith MS, Glueck DH, Nantermet PV, Seillier-Moiseiwitsch F, Swanstrom R. 1993. Analysis of human immunodeficiency virus type 1 nef gene sequences present in vivo. J Virol 67:4639–4650.
55. Alberti MO, Jones JJ, Miglietta R, Ding H, Bakshi RK, Edmonds TG, Kappes JC, Ochsenbauer C. 2015. Optimized replicating Renilla luciferase reporter HIV-1 utilizing novel internal ribosome entry site elements for native Nef expression and function. AIDS Res Hum Retroviruses 31:1278–1296.
56. Jacob RA, Edgar CR, Prevost J, Trothen SM, Lurie A, Mumby MJ, Galbraith A, Kirchhoff F, Haeryfar SMM, Finzi A, Dikeakos JD. 2021. The HIV-1 accessory protein Nef increases surface expression of the checkpoint receptor Tim-3 in infected CD4(1) T cells. J Biol Chem 297:101042.
57. Pawlak EN, Dirk BS, Jacob RA, Johnson AL, Dikeakos JD. 2018. The HIV-1 accessory proteins Nef and Vpu downregulate total and cell surface CD28 in CD4(1) T cells. Retrovirology 15:6.
58. Cohen EA, Terwilliger EF, Sodroski JG, Haseltine WA. 1988. Identification of a protein encoded by the vpu gene of HIV-1. Nature 334:532–534.
59. Heigele A, Kmiec D, Regensburger K, Langer S, Peiffer L, Sturzel CM, Sauter D, Peeters M, Pizzato M, Learn GH, Hahn BH, Kirchhoff F. 2016. The potency of Nef-mediated SERINC5 antagonism correlates with the prevalence of primate lentiviruses in the wild. Cell Host Microbe 20:381–391.
60. Kmiec D, Iyer SS, Sturzel CM, Sauter D, Hahn BH, Kirchhoff F. 2016. Vpu-mediated counteraction of tetherin is a major determinant of HIV-1 interferon resistance. mBio 7:e00934-16.
61. Bolduan S, Hubel P, Reif T, Lodermeyer V, Hohne K, Fritz JV, Sauter D, Kirchhoff F, Fackler OT, Schindler M, Schubert U. 2013. HIV-1 Vpu affects the anterograde transport and the glycosylation pattern of NTB-A. Virology 440:190–203.
62. Bolduan S, Reif T, Schindler M, Schubert U. 2014. HIV-1 Vpu mediated downregulation of CD155 requires alanine residues 10, 14 and 18 of the transmembrane domain. Virology 464–465:375–384.

63. Vassena L, Giuliani E, Koppensteiner H, Bolduan S, Schindler M, Doria M. 2015. HIV-1 Nef and Vpu interfere with L-selectin (CD62L) cell surface expression to inhibit adhesion and signaling in infected $CD4^+$ T lymphocytes. J Virol 89:5687–5700.
64. Prevost J, Pickering S, Mumby MJ, Medjahed H, Gendron-Lepage G, Delgado GG, Dirk BS, Dikeakos JD, Sturzel CM, Sauter D, Kirchhoff F, Bibollet-Ruche F, Hahn BH, Dube M, Kaufmann DE, Neil SJD, Finzi A, Richard J. 2019. Upregulation of BST-2 by type I interferons reduces the capacity of Vpu to protect HIV-1-infected cells from NK cell responses. mBio 10:e01113-19.
65. Bour S, Schubert U, Strebel K. 1995. The human immunodeficiency virus type 1 Vpu protein specifically binds to the cytoplasmic domain of CD4: implications for the mechanism of degradation. J Virol 69:1510–1520.
66. Chen MY, Maldarelli F, Karczewski MK, Willey RL, Strebel K. 1993. Human immunodeficiency virus type 1 Vpu protein induces degradation of CD4 in vitro: the cytoplasmic domain of CD4 contributes to Vpu sensitivity. J Virol 67:3877–3884.
67. Lenburg ME, Landau NR. 1993. Vpu-induced degradation of CD4: requirement for specific amino acid residues in the cytoplasmic domain of CD4. J Virol 67:7238–7245.
68. Vincent MJ, Raja NU, Jabbar MA. 1993. Human immunodeficiency virus type 1 Vpu protein induces degradation of chimeric envelope glycoproteins bearing the cytoplasmic and anchor domains of CD4: role of the cytoplasmic domain in Vpu-induced degradation in the endoplasmic reticulum. J Virol 67:5538–5549.
69. Margottin F, Benichou S, Durand H, Richard V, Liu LX, Gomas E, Benarous R. 1996. Interaction between the cytoplasmic domains of HIV-1 Vpu and CD4: role of Vpu residues involved in CD4 interaction and in vitro CD4 degradation. Virology 223:381–386.
70. Prevost J, Edgar CR, Richard J, Trothen SM, Jacob RA, Mumby MJ, Pickering S, Dube M, Kaufmann DE, Kirchhoff F, Neil SJD, Finzi A, Dikeakos JD. 2020. HIV-1 Vpu downregulates Tim-3 from the surface of infected CD4(1) T cells. J Virol 94:e01999-19.
71. Binette J, Dube M, Mercier J, Halawani D, Latterich M, Cohen EA. 2007. Requirements for the selective degradation of CD4 receptor molecules by the human immunodeficiency virus type 1 Vpu protein in the endoplasmic reticulum. Retrovirology 4:75.
72. Mitchell RS, Katsura C, Skasko MA, Fitzpatrick K, Lau D, Ruiz A, Stephens EB, Margottin-Goguet F, Benarous R, Guatelli JC. 2009. Vpu antagonizes BST-2-mediated

restriction of HIV-1 release via beta-TrCP and endo-lysosomal trafficking. PLoS Pathog 5:e1000450.

73. Gustin JK, Douglas JL, Bai Y, Moses AV. 2012. Ubiquitination of BST-2 protein by HIV-1 Vpu protein does not require lysine, serine, or threonine residues within the BST-2 cytoplasmic domain. J Biol Chem287:14837–14850.
74. Belaidouni N, Marchal C, Benarous R, Besnard-Guerin C. 2007. Involvement of the betaTrCP in the ubiquitination and stability of the HIV-1 Vpu protein. Biochem Biophys Res Commun 357:688–693.
75. Kueck T, Neil SJ. 2012. A cytoplasmic tail determinant in HIV-1 Vpu mediates targeting of tetherin for endosomal degradation and counteracts interferon-induced restriction. PLoS Pathog 8:e1002609.
76. Kueck T, Foster TL, Weinelt J, Sumner JC, Pickering S, Neil SJ. 2015. Serine phosphorylation of HIV-1 Vpu and its binding to tetherin regulates interaction with clathrin adaptors. PLoS Pathog 11:e1005141.
77. Mangeat B, Gers-Huber G, Lehmann M, Zufferey M, Luban J, Piguet V. 2009. HIV-1 Vpu neutralizes the antiviral factor Tetherin/BST-2 by binding it and directing its beta-TrCP2-dependent degradation. PLoS Pathog 5:e1000574.
78. Arias JF, Heyer LN, von Bredow B, Weisgrau KL, Moldt B, Burton DR, Rakasz EG, Evans DT. 2014. Tetherin antagonism by Vpu protects HIV-infected cells from antibody-dependent cell-mediated cytotoxicity. Proc Natl Acad Sci USA 111:6425–6430.
79. Alvarez RA, Hamlin RE, Monroe A, Moldt B, Hotta MT, Rodriguez Caprio G, Fierer DS, Simon V, Chen BK. 2014. HIV-1 Vpu antagonism of tetherin inhibits antibody-dependent cellular cytotoxic responses by natural killer cells. J Virol 88:6031–6046.
80. Prevost J, Richard J, Medjahed H, Alexander A, Jones J, Kappes JC, Ochsenbauer C, Finzi A. 2018. Incomplete downregulation of CD4 expression affects HIV-1 Env conformation and antibody-dependent cellular cytotoxicity responses. J Virol 92:e00484-18.
81. Ding S, Veillette M, Coutu M, Prevost J, Scharf L, Bjorkman PJ, Ferrari G, Robinson JE, Sturzel C, Hahn BH, Sauter D, Kirchhoff F, Lewis GK, Pazgier M, Finzi A. 2016. A highly conserved residue of the HIV-1 gp120 inner domain is important for antibody-dependent cellular cytotoxicity responses mediated by anti-cluster A antibodies. J Virol 90:2127–2134.

82. Ferrari G, Pollara J, Kozink D, Harms T, Drinker M, Freel S, Moody MA, Alam SM, Tomaras GD, Ochsenbauer C, Kappes JC, Shaw GM, Hoxie JA, Robinson JE, Haynes BF. 2011. An HIV-1 gp120 envelope human monoclonal antibody that recognizes a C1 conformational epitope mediates potent antibody-dependent cellular cytotoxicity (ADCC) activity and defines a common ADCC epitope in human HIV-1 serum. J Virol 85:7029–7036.

83. Tomaras GD, Ferrari G, Shen X, Alam SM, Liao HX, Pollara J, Bonsignori M, Moody MA, Fong Y, Chen X, Poling B, Nicholson CO, Zhang R, Lu X, Parks R, Kaewkungwal J, Nitayaphan S, Pitisuttithum P, Rerks-Ngarm S, Gilbert PB, Kim JH, Michael NL, Montefiori DC, Haynes BF. 2013. Vaccine-induced plasma IgA specific for the C1 region of the HIV-1 envelope blocks binding and effector function of IgG. Proc Natl Acad Sci U S A 110:9019–9024.

84. Pollara J, Bonsignori M, Moody MA, Liu P, Alam SM, Hwang KK, Gurley TC, Kozink DM, Armand LC, Marshall DJ, Whitesides JF, Kaewkungwal J, Nitayaphan S, Pitisuttithum P, Rerks-Ngarm S, Robb ML, O'Connell RJ, Kim JH, Michael NL, Montefiori DC, Tomaras GD, Liao HX, Haynes BF, Ferrari G. 2014. HIV-1 vaccine-induced C1 and V2 Env-specific antibodies synergize for increased antiviral activities. J Virol 88:7715–7726.

85. Santra S, Tomaras GD, Warrier R, Nicely NI, Liao HX, Pollara J, Liu P, Alam SM, Zhang R, Cocklin SL, Shen X, Duffy R, Xia SM, Schutte RJ, Pemble Iv CW, Dennison SM, Li H, Chao A, Vidnovic K, Evans A, Klein K, Kumar A, Robinson J, Landucci G, Forthal DN, Montefiori DC, Kaewkungwal J, Nitayaphan S, Pitisuttithum P, Rerks-Ngarm S, Robb ML, Michael NL, Kim JH, Soderberg KA, Giorgi EE, Blair L, Korber BT, Moog C, Shattock RJ, Letvin NL, Schmitz JE, Moody MA, Gao F, Ferrari G, Shaw GM, Haynes BF. 2015. Human non-neutralizing HIV-1 envelope monoclonal antibodies limit the number of founder viruses during SHIV mucosal infection in rhesus macaques. PLoS Pathog 11:e1005042.

86. Huang Y, Ferrari G, Alter G, Forthal DN, Kappes JC, Lewis GK, Love JC, Borate B, Harris L, Greene K, Gao H, Phan TB, Landucci G, Goods BA, Dowell KG, Cheng HD, Bailey-Kellogg C, Montefiori DC, Ackerman ME. 2016. Diversity of antiviral IgG effector activities observed in HIV-infected and vaccinated subjects. J Immunol 197:4603–4612.

87. Costa MR, Pollara J, Edwards RW, Seaman MS, Gorny MK, Montefiori DC, Liao HX, Ferrari G, Lu S, Wang S. 2016. Fc receptor-mediated activities of Env-specific human monoclonal antibodies generated from volunteers receiving the DNA prime-protein boost HIV vaccine DP6-001. J Virol 90:10362–10378.
88. Bradley T, Pollara J, Santra S, Vandergrift N, Pittala S, Bailey-Kellogg C, Shen X, Parks R, Goodman D, Eaton A, Balachandran H, Mach LV, Saunders KO, Weiner JA, Scearce R, Sutherland LL, Phogat S, Tartaglia J, Reed SG, Hu SL, Theis JF, Pinter A, Montefiori DC, Kepler TB, Peachman KK, Rao M, Michael NL, Suscovich TJ, Alter G, Ackerman ME, Moody MA, Liao HX, Tomaras G, Ferrari G, Korber BT, Haynes BF. 2017. Pentavalent HIV-1 vaccine protects against simian-human immunodeficiency virus challenge. Nat Commun 8:15711.
89. Meyerhoff RR, Scearce RM, Ogburn DF, Lockwood B, Pickeral J, Kuraoka M, Anasti K, Eudailey J, Eaton A, Cooper M, Wiehe K, Montefiori DC, Tomaras G, Ferrari G, Alam SM, Liao HX, Korber B, Gao F, Haynes BF. 2017. HIV-1 consensus envelope-induced broadly binding antibodies. AIDS Res Hum Retroviruses 33:859–868.
90. Sung JA, Pickeral J, Liu L, Stanfield-Oakley SA, Lam CK, Garrido C, Pollara J, LaBranche C, Bonsignori M, Moody MA, Yang Y, Parks R, Archin N, Allard B, Kirchherr J, Kuruc JD, Gay CL, Cohen MS, Ochsenbauer C, Soderberg K, Liao HX, Montefiori D, Moore P, Johnson S, Koenig S, Haynes BF, Nordstrom JL, Margolis DM, Ferrari G. 2015. Dual-affinity retargeting proteins direct T cell-mediated cytolysis of latently HIV-infected cells. J Clin Invest 125:4077–4090.
91. Tuyishime M, Garrido C, Jha S, Moeser M, Mielke D, LaBranche C, Montefiori D, Haynes BF, Joseph S, Margolis DM, Ferrari G. 2020. Improved killing of HIV-infected cells using three neutralizing and non-neutralizing antibodies. J Clin Invest 130:5157–5170.
92. Bonsignori M, Pollara J, Moody MA, Alpert MD, Chen X, Hwang KK, Gilbert PB, Huang Y, Gurley TC, Kozink DM, Marshall DJ, Whitesides JF, Tsao CY, Kaewkungwal J, Nitayaphan S, Pitisuttithum P, Rerks-Ngarm S, Kim JH, Michael NL, Tomaras GD, Montefiori DC, Lewis GK, Devico A, Evans DT, Ferrari G, Liao HX, Haynes BF. 2012. Antibody-dependent cellular cytotoxicity-mediating antibodies from an HIV-1 vaccine efficacy trial target multiple epitopes and preferentially use the VH1 gene family. J Virol 86:11521–11532.

93. Cheng HD, Dowell KG, Bailey-Kellogg C, Goods BA, Love JC, Ferrari G, Alter G, Gach J, Forthal DN, Lewis GK, Greene K, Gao H, Montefiori DC, Ackerman ME. 2021. Diverse antiviral IgG effector activities are predicted by unique biophysical antibody features. Retrovirology 18:35.
94. Mitchell JL, Pollara J, Dietze K, Edwards RW, Nohara J, N'Guessan KF, Zemil M, Buranapraditkun S, Takata H, Li Y, Muir R, Kroon E, Pinyakorn S, Jha S, Manasnayakorn S, Chottanapund S, Thantiworasit P, Prueksakaew P, Ratnaratorn N, Nuntapinit B, Fox L, Tovanabutra S, Paquin-Proulx D, Wieczorek L, Polonis VR, Maldarelli F, Haddad EK, Phanuphak P, Sacdalan CP, Rolland M, Phanuphak N, Ananworanich J, Vasan S, Ferrari G, Trautmann L. 2021. Anti-HIV antibody development up to one year after antiretroviral therapy initiation in acute HIV infection. J Clin Invest 132:e150937.
95. Mielke D, Bandawe G, Zheng J, Jones J, Abrahams MR, Bekker V, Ochsenbauer C, Garrett N, Abdool Karim S, Moore PL, Morris L, Montefiori D, Anthony C, Ferrari G, Williamson C. 2021. ADCC-mediating non-neutralizing antibodies can exert immune pressure in early HIV-1 infection. PLoS Pathog 17:e1010046.
96. Pollara J, Jones DI, Huffman T, Edwards RW, Dennis M, Li SH, Jha S, Goodman D, Kumar A, LaBranche CC, Montefiori DC, Fouda GG, Hope TJ, Tomaras GD, Staats HF, Ferrari G, Permar SR. 2019. Bridging vaccine-induced HIV-1 neutralizing and effector antibody responses in rabbit and rhesus macaque animal models. J Virol 93:e02119-18.
97. Fisher L, Zinter M, Stanfield-Oakley S, Carpp LN, Edwards RW, Denny T, Moodie Z, Laher F, Bekker LG, McElrath MJ, Gilbert PB, Corey L, Tomaras G, Pollara J, Ferrari G. 2019. Vaccine-induced antibodies mediate higher antibody-dependent cellular cytotoxicity after interleukin-15 pretreatment of natural killer effector cells. Front Immunol 10:2741.
98. Lewis GK, Ackerman ME, Scarlatti G, Moog C, Robert-Guroff M, Kent SJ, Overbaugh J, Reeves RK, Ferrari G, Thyagarajan B. 2019. Knowns and unknowns of assaying antibody-dependent cell-mediated cytotoxicity against HIV-1. Front Immunol 10:1025.
99. Easterhoff D, Pollara J, Luo K, Tolbert WD, Young B, Mielke D, Jha S, O'Connell RJ, Vasan S, Kim J, Michael NL, Excler J-L, Robb ML, Rerks-Ngarm S, Kaewkungwal J, Pitisuttithum P, Nitayaphan S, Sinangil F, Tartaglia J, Phogat S, Kepler TB, Alam SM, Wiehe K, Saunders KO, Montefiori DC, Tomaras GD, Moody MA, Pazgier M, Haynes

BF, Ferrari G. 2020. Boosting with AIDSVAX B/E enhances Env constant region 1 and 2 antibody-dependent cellular cytotoxicity breadth and potency. J Virol 94:e01120-19.

100. Tolbert WD, Van V, Sherburn R, Tuyishime M, Yan F, Nguyen DN, Stanfield-Oakley S, Easterhoff D, Bonsignori M, Haynes BF, Moody MA, Ray K, Ferrari G, Lewis GK, Pazgier M. 2020. Recognition patterns of the C1/C2 epitopes involved in Fc-mediated response in HIV-1 natural infection and the RV114 vaccine trial. mBio 11:e00208-20.
101. Madani N, Princiotto AM, Mach L, Ding S, Prevost J, Richard J, Hora B, Sutherland L, Zhao CA, Conn BP, Bradley T, Moody MA, Melillo B, Finzi A, Haynes BF, Smith AB, III, Santra S, Sodroski J. 2018. A CD4-mimetic compound enhances vaccine efficacy against stringent immunodeficiency virus challenge. Nat Commun 9:2363.
102. Strebel K. 2013. HIV accessory proteins versus host restriction factors. Curr Opin Virol 3:692–699.
103. Ramirez PW, Famiglietti M, Sowrirajan B, DePaula-Silva AB, Rodesch C, Barker E, Bosque A, Planelles V. 2014. Downmodulation of CCR7 by HIV-1 Vpu results in impaired migration and chemotactic signaling within $CD4^+$ T cells. Cell Rep 7:2019–2030.
104. Usami Y, Wu Y, Gottlinger HG. 2015. SERINC3 and SERINC5 restrict HIV-1 infectivity and are counteracted by Nef. Nature 526:218–223.
105. Rosa A, Chande A, Ziglio S, De Sanctis V, Bertorelli R, Goh SL, McCauley SM, Nowosielska A, Antonarakis SE, Luban J, Santoni FA, Pizzato M. 2015. HIV-1 Nef promotes infection by excluding SERINC5 from virion incorporation. Nature 526:212–217.
106. Liu Y, Fu Y, Wang Q, Li M, Zhou Z, Dabbagh D, Fu C, Zhang H, Li S, Zhang T, Gong J, Kong X, Zhai W, Su J, Sun J, Zhang Y, Yu XF, Shao Z, Zhou F, Wu Y, Tan X. 2019. Proteomic profiling of HIV-1 infection of human $CD4^+$ T cells identifies PSGL-1 as an HIV restriction factor. Nat Microbiol 4:813–825.
107. Fu Y, He S, Waheed AA, Dabbagh D, Zhou Z, Trinite B, Wang Z, Yu J, Wang D, Li F, Levy DN, Shang H, Freed EO, Wu Y. 2020. PSGL-1 restricts HIV-1 infectivity by blocking virus particle attachment to target cells. Proc Natl Acad Sci USA 117:9537–9545.
108. Schwartz O, Marechal V, Le Gall S, Lemonnier F, Heard JM. 1996. Endocytosis of major histocompatibility complex class I molecules is induced by the HIV-1 Nef protein. Nat Med 2:338–342.

109. Collins KL, Chen BK, Kalams SA, Walker BD, Baltimore D. 1998. HIV-1 Nef protein protects infected primary cells against killing by cytotoxic T lymphocytes. Nature 391:397–401.
110. Cerboni C, Neri F, Casartelli N, Zingoni A, Cosman D, Rossi P, Santoni A, Doria M. 2007. Human immunodeficiency virus 1 Nef protein downmodulates the ligands of the activating receptor NKG2D and inhibits natural killer cell-mediated cytotoxicity. J Gen Virol 88:242–250.
111. Fausther-Bovendo H, Sol-Foulon N, Candotti D, Agut H, Schwartz O, Debre P, Vieillard V. 2009. HIV escape from natural killer cytotoxicity: nef inhibits NKp44L expression on $CD4^+$ T cells. AIDS 23:1077–1087.
112. Shah AH, Sowrirajan B, Davis ZB, Ward JP, Campbell EM, Planelles V, Barker E. 2010. Degranulation of natural killer cells following interaction with HIV-1-infected cells is hindered by downmodulation of NTB-A by Vpu. Cell Host Microbe 8:397–409.
113. Matusali G, Potesta M, Santoni A, Cerboni C, Doria M. 2012. The human immunodeficiency virus type 1 Nef and Vpu proteins downregulate the natural killer cell-activating ligand PVR. J Virol 86:4496–4504.
114. Apps R, Del Prete GQ, Chatterjee P, Lara A, Brumme ZL, Brockman MA, Neil S, Pickering S, Schneider DK, Piechocka-Trocha A, Walker BD, Thomas R, Shaw GM, Hahn BH, Keele BF, Lifson JD, Carrington M. 2016. HIV-1 Vpu mediates HLA-C downregulation. Cell Host Microbe 19: 686–695.
115. Moll M, Andersson SK, Smed-Sorensen A, Sandberg JK. 2010. Inhibition of lipid antigen presentation in dendritic cells by HIV-1 Vpu interference with CD1d recycling from endosomal compartments. Blood 116:1876–1884.
116. Chen N, McCarthy C, Drakesmith H, Li D, Cerundolo V, McMichael AJ, Screaton GR, Xu XN. 2006. HIV-1 down-regulates the expression of CD1d via Nef. Eur J Immunol 36:278–286.
117. Pacyniak E, Gomez ML, Gomez LM, Mulcahy ER, Jackson M, Hout DR, Wisdom BJ, Stephens EB. 2005. Identification of a region within the cytoplasmic domain of the subtype B Vpu protein of human immunodeficiency virus type 1 (HIV-1) that is responsible for retention in the Golgi complex and its absence in the Vpu protein from a subtype C HIV-1. AIDS Res Hum Retroviruses 21:379–394.

118. Sharma S, Jafari M, Bangar A, William K, Guatelli J, Lewinski MK. 2019. The C-terminal end of HIV-1 Vpu has a clade-specific determinant that antagonizes BST-2 and facilitates virion release. J Virol 93:e02315-18.
119. Pickering S, Hue S, Kim EY, Reddy S, Wolinsky SM, Neil SJ. 2014. Preservation of tetherin and CD4 counteractivities in circulating Vpu alleles despite extensive sequence variation within HIV-1 infected individuals. PLoS Pathog 10:e1003895.
120. Iwami S, Sato K, Morita S, Inaba H, Kobayashi T, Takeuchi JS, Kimura Y, Misawa N, Ren F, Iwasa Y, Aihara K, Koyanagi Y. 2015. Pandemic HIV-1 Vpu overcomes intrinsic herd immunity mediated by tetherin. Sci Rep 5:12256.
121. Chen BK, Gandhi RT, Baltimore D. 1996. CD4 down-modulation during infection of human T cells with human immunodeficiency virus type 1 involves independent activities of vpu, env, and nef. J Virol 70:6044–6053.
122. Richard J, Veillette M, Brassard N, Iyer SS, Roger M, Martin L, Pazgier M, Schon A, Freire E, Routy JP, Smith AB, III, Park J, Jones DM, Courter JR, Melillo BN, Kaufmann DE, Hahn BH, Permar SR, Haynes BF, Madani N, Sodroski JG, Finzi A. 2015. CD4 mimetics sensitize HIV-1-infected cells to ADCC. Proc Natl Acad Sci USA 112:E2687–E2694.
123. Prevost J, Zoubchenok D, Richard J, Veillette M, Pacheco B, Coutu M, Brassard N, Parsons MS, Ruxrungtham K, Bunupuradah T, Tovanabutra S, Hwang KK, Moody MA, Haynes BF, Bonsignori M, Sodroski J, Kaufmann DE, Shaw GM, Chenine AL, Finzi A. 2017. Influence of the envelope gp120 Phe43 cavity on HIV-1 sensitivity to antibody-dependent cell-mediated cytotoxicity responses. J Virol 91:e02452-16.
124. Prevost J, Richard J, Ding S, Pacheco B, Charlebois R, Hahn BH, Kaufmann DE, Finzi A. 2018. Envelope glycoproteins sampling states 2/3 are susceptible to ADCC by sera from HIV-1-infected individuals. Virology 515:38–45.
125. Alsahafi N, Bakouche N, Kazemi M, Richard J, Ding S, Bhattacharyya S, Das D, Anand SP, Prevost J, Tolbert WD, Lu H, Medjahed H, Gendron-Lepage G, Ortega Delgado GG, Kirk S, Melillo B, Mothes W, Sodroski J, Smith AB, III, Kaufmann DE, Wu X, Pazgier M, Rouiller I, Finzi A, Munro JB. 2019. An asymmetric opening of HIV-1 Envelope mediates antibody-dependent cellular cytotoxicity. Cell Host Microbe 25:578–587.e5.

126. Richard J, Prevost J, von Bredow B, Ding S, Brassard N, Medjahed H, Coutu M, Melillo B, Bibollet-Ruche F, Hahn BH, Kaufmann DE, Smith AB, III, Sodroski J, Sauter D, Kirchhoff F, Gee K, Neil SJ, Evans DT, Finzi A. 2017. BST-2 expression modulates small CD4-mimetic sensitization of HIV-1-infected cells to antibody-dependent cellular cytotoxicity. J Virol 91:e00219-17.
127. Mielke D, Stanfield-Oakley S, Borate B, Fisher LH, Faircloth K, Tuyishime M, Greene K, Gao H, Williamson C, Morris L, Ochsenbauer C, Tomaras G, Haynes BF, Montefiori D, Pollara J, deCamp AC, Ferrari G. 2021. Selection of HIV Envelope strains for standardized assessments of vaccine-elicited antibody-dependent cellular cytotoxicity (ADCC)-mediating antibodies. J Virol 96:e0164321.
128. Prevost J, Tolbert WD, Medjahed H, Sherburn RT, Madani N, Zoubchenok D, Gendron-Lepage G, Gaffney AE, Grenier MC, Kirk S, Vergara N, Han C, Mann BT, Chenine AL, Ahmed A, Chaiken I, Kirchhoff F, Hahn BH, Haim H, Abrams CF, Smith AB, III, Sodroski J, Pazgier M, Finzi A. 2020. The HIV-1 Env gp120 inner domain shapes the Phe43 cavity and the CD4 binding site. mBio 11:e00280-20.
129. Richard J, Prevost J, Alsahafi N, Ding S, Finzi A. 2018. Impact of HIV-1 Envelope conformation on ADCC responses. Trends Microbiol 26:253–265.
130. Alpert MD, Heyer LN, Williams DE, Harvey JD, Greenough T, Allhorn M, Evans DT. 2012. A novel assay for antibody-dependent cell-mediated cytotoxicity against HIV-1- or SIV-infected cells reveals incomplete overlap with antibodies measured by neutralization and binding assays. J Virol 86:12039–12052.
131. Fontaine J, Chagnon-Choquet J, Valcke HS, Poudrier J, Roger M, Montreal Primary HIV Infection and Long-Term Non-Progressor Study Groups. 2011. High expression levels of B lymphocyte stimulator (BLyS) by dendritic cells correlate with HIV-related B-cell disease progression in humans. Blood 117:145–155.
132. Fontaine J, Coutlee F, Tremblay C, Routy JP, Poudrier J, Roger M, Montreal Primary HIV Infection and Long-Term Non-progressor Study Groups. 2009. HIV infection affects blood myeloid dendritic cells after successful therapy and despite non-progressing clinical disease. J Infect Dis 199: 1007–1018.
133. Pereyra F, Jia X, McLaren PJ, Telenti A, de Bakker PIW, Walker BD, Ripke S, Brumme CJ, Pulit SL, Carrington M, Kadie CM, Carlson JM, Heckerman D, Graham RR, Plenge

RM, Deeks SG, Gianniny L, Crawford G, Sullivan J, Gonzalez E, Davies L, Camargo A, Moore JM, Beattie N, Gupta S, Crenshaw A, Burtt NP, Guiducci C, Gupta N, Gao X, Qi Y, Yuki Y, Piechocka-Trocha A, Cutrell E, Rosenberg R, Moss KL, Lemay P, O'Leary J, Schaefer T, Verma P, Toth I, Block B, Baker B, Rothchild A, Lian J, Proudfoot J, Alvino DML, Vine S, Addo MM, Allen TM, International HIV Controllers Study, et al. 2010. The major genetic determinants of HIV-1 control affect HLA class I peptide presentation. Science 330:1551–1557.

134. Kamya P, Boulet S, Tsoukas CM, Routy JP, Thomas R, Cote P, Boulassel MR, Baril JG, Kovacs C, Migueles SA, Connors M, Suscovich TJ, Brander C, Tremblay CL, Bernard N, Canadian Cohort of HIV Infected Slow Progressors. 2011. Receptor-ligand requirements for increased NK cell polyfunctional potential in slow progressors infected with HIV-1 co-expressing KIR3DL1*h/*y and HLA-B*57. J Virol 85:5949–5960.
135. Peretz Y, Ndongala ML, Boulet S, Boulassel MR, Rouleau D, Cote P, Longpre D, Routy JP, Falutz J, Tremblay C, Tsoukas CM, Sekaly RP, Bernard NF. 2007. Functional T cell subsets contribute differentially to HIV peptide-specific responses within infected individuals: correlation of these functional T cell subsets with markers of disease progression. Clin Immunol 124:57–68.
136. Finzi A, Xiang SH, Pacheco B, Wang L, Haight J, Kassa A, Danek B, Pancera M, Kwong PD, Sodroski J. 2010. Topological layers in the HIV-1 gp120 inner domain regulate gp41 interaction and CD4-triggered conformational transitions. Mol Cell 37:656–667.
137. Emi N, Friedmann T, Yee JK. 1991. Pseudotype formation of murine leukemia virus with the G protein of vesicular stomatitis virus. J Virol 65:1202–1207.
138. Salazar-Gonzalez JF, Salazar MG, Keele BF, Learn GH, Giorgi EE, Li H, Decker JM, Wang S, Baalwa J, Kraus MH, Parrish NF, Shaw KS, Guffey MB, Bar KJ, Davis KL, Ochsenbauer-Jambor C, Kappes JC, Saag MS, Cohen MS, Mulenga J, Derdeyn CA, Allen S, Hunter E, Markowitz M, Hraber P, Perelson AS, Bhattacharya T, Haynes BF, Korber BT, Hahn BH, Shaw GM. 2009. Genetic identity, biological phenotype, and evolutionary pathways of transmitted/founder viruses in acute and early HIV-1 infection. J Exp Med 206:1273–1289.
139. Ochsenbauer C, Edmonds TG, Ding H, Keele BF, Decker J, Salazar MG, Salazar-Gonzalez JF, Shattock R, Haynes BF, Shaw GM, Hahn BH, Kappes JC. 2012. Generation of

transmitted/founder HIV-1 infectious molecular clones and characterization of their replication capacity in CD4 T lymphocytes and monocyte-derived macrophages. J Virol 86:2715–2728.

140. Parrish NF, Wilen CB, Banks LB, Iyer SS, Pfaff JM, Salazar-Gonzalez JF, Salazar MG, Decker JM, Parrish EH, Berg A, Hopper J, Hora B, Kumar A, Mahlokozera T, Yuan S, Coleman C, Vermeulen M, Ding H, Ochsenbauer C, Tilton JC, Permar SR, Kappes JC, Betts MR, Busch MP, Gao F, Montefiori D, Haynes BF, Shaw GM, Hahn BH, Doms RW. 2012. Transmitted/founder and chronic subtype C HIV-1 use CD4 and CCR5 receptors with equal efficiency and are not inhibited by blocking the integrin alpha4beta7. PLoS Pathog 8:e1002686.
141. Parrish NF, Gao F, Li H, Giorgi EE, Barbian HJ, Parrish EH, Zajic L, Iyer SS, Decker JM, Kumar A, Hora B, Berg A, Cai F, Hopper J, Denny TN, Ding H, Ochsenbauer C, Kappes JC, Galimidi RP, West AP Jr, Bjorkman PJ, Wilen CB, Doms RW, O'Brien M, Bhardwaj N, Borrow P, Haynes BF, Muldoon M, Theiler JP, Korber B, Shaw GM, Hahn BH. 2013. Phenotypic properties of transmitted founder HIV-1. Proc Natl Acad Sci U S A 110:6626–6633.
142. Fenton-May AE, Dibben O, Emmerich T, Ding H, Pfafferott K, Aasa-Chapman MM, Pellegrino P, Williams I, Cohen MS, Gao F, Shaw GM, Hahn BH, Ochsenbauer C, Kappes JC, Borrow P. 2013. Relative resistance of HIV-1 founder viruses to control by interferon-alpha. Retrovirology 10:146.
143. Liao HX, Lynch R, Zhou T, Gao F, Alam SM, Boyd SD, Fire AZ, Roskin KM, Schramm CA, Zhang Z, Zhu J, Shapiro L, Mullikin JC, Gnanakaran S, Hraber P, Wiehe K, Kelsoe G, Yang G, Xia SM, Montefiori DC, Parks R, Lloyd KE, Scearce RM, Soderberg KA, Cohen M, Kamanga G, Louder MK, Tran LM, Chen Y, Cai F, Chen S, Moquin S, Du X, Joyce MG, Srivatsan S, Zhang B, Zheng A, Shaw GM, Hahn BH, Kepler TB, Korber BT, Kwong PD, Mascola JR, Haynes BF, NISC Comparative Sequencing Program. 2013. Co-evolution of a broadly neutralizing HIV-1 antibody and founder virus. Nature 496:469–476.
144. Gao F, Bonsignori M, Liao HX, Kumar A, Xia SM, Lu X, Cai F, Hwang KK, Song H, Zhou T, Lynch RM, Alam SM, Moody MA, Ferrari G, Berrong M, Kelsoe G, Shaw GM, Hahn BH, Montefiori DC, Kamanga G, Cohen MS, Hraber P, Kwong PD, Korber BT,

Mascola JR, Kepler TB, Haynes BF. 2014. Cooperation of B cell lineages in induction of HIV-1-broadly neutralizing antibodies. Cell 158:481–491.

145. Salminen MO, Ehrenberg PK, Mascola JR, Dayhoff DE, Merling R, Blake B, Louder M, Hegerich S, Polonis VR, Birx DL, Robb ML, McCutchan FE, Michael NL. 2000. Construction and biological characterization of infectious molecular clones of HIV-1 subtypes B and E (CRF01_AE) generated by the polymerase chain reaction. Virology 278:103–110.
146. Chenine AL, Merbah M, Wieczorek L, Molnar S, Mann B, Lee J, O'Sullivan AM, Bose M, Sanders-Buell E, Kijak GH, Herrera C, McLinden R, O'Connell RJ, Michael NL, Robb ML, Kim JH, Polonis VR, Tovanabutra S. 2018. Neutralization sensitivity of a novel HIV-1 CRF01_AE panel of infectious molecular clones. J Acquir Immune Defic Syndr 78:348–355.
147. Peachman KK, Karasavvas N, Chenine AL, McLinden R, Rerks-Ngarm S, Jaranit K, Nitayaphan S, Pitisuttithum P, Tovanabutra S, Zolla-Pazner S, Michael NL, Kim JH, Alving CR, Rao M. 2015. Identification of new regions in HIV-1 gp120 variable 2 and 3 loops that bind to alpha4beta7 integrin receptor. PLoS One 10:e0143895.
148. O'Brien WA, Koyanagi Y, Namazie A, Zhao JQ, Diagne A, Idler K, Zack JA, Chen IS. 1990. HIV-1 tropism for mononuclear phagocytes can be determined by regions of gp120 outside the CD4-binding domain. Nature 348:69–73.
149. Li Y, Kappes JC, Conway JA, Price RW, Shaw GM, Hahn BH. 1991. Molecular characterization of human immunodeficiency virus type 1 cloned directly from uncultured human brain tissue: identification of replication-competent and -defective viral genomes. J Virol 65:3973–3985.
150. Theodore TS, Englund G, Buckler-White A, Buckler CE, Martin MA, Peden KW. 1996. Construction and characterization of a stable full-length macrophage-tropic HIV type 1 molecular clone that directs the production of high titers of progeny virions. AIDS Res Hum Retroviruses 12:191–194.
151. Krapp C, Hotter D, Gawanbacht A, McLaren PJ, Kluge SF, Sturzel CM, Mack K, Reith E, Engelhart S, Ciuffi A, Hornung V, Sauter D, Telenti A, Kirchhoff F. 2016. Guanylate binding protein (GBP) 5 is an interferon-inducible inhibitor of HIV-1 infectivity. Cell Host Microbe 19:504–514.

152. Koyanagi Y, Miles S, Mitsuyasu RT, Merrill JE, Vinters HV, Chen IS. 1987. Dual infection of the central nervous system by AIDS viruses with distinct cellular tropisms. Science 236:819–822.
153. Adachi A, Gendelman HE, Koenig S, Folks T, Willey R, Rabson A, Martin MA. 1986. Production of acquired immunodeficiency syndrome-associated retrovirus in human and nonhuman cells transfected with an infectious molecular clone. J Virol 59:284–291.
154. Mack K, Starz K, Sauter D, Langer S, Bibollet-Ruche F, Learn GH, Sturzel CM, Leoz M, Plantier JC, Geyer M, Hahn BH, Kirchhoff F. 2017. Efficient Vpu-mediated tetherin antagonism by an HIV-1 group O strain. J Virol 91:e02177-16.
155. Takehisa J, Kraus MH, Decker JM, Li Y, Keele BF, Bibollet-Ruche F, Zammit KP, Weng Z, Santiago ML, Kamenya S, Wilson ML, Pusey AE, Bailes E, Sharp PM, Shaw GM, Hahn BH. 2007. Generation of infectious molecular clones of simian immunodeficiency virus from fecal consensus sequences of wild chimpanzees. J Virol 81:7463–7475.
156. Shingai M, Donau OK, Schmidt SD, Gautam R, Plishka RJ, Buckler-White A, Sadjadpour R, Lee WR, LaBranche CC, Montefiori DC, Mascola JR, Nishimura Y, Martin MA. 2012. Most rhesus macaques infected with the CCR5-tropic SHIV(AD8) generate cross-reactive antibodies that neutralize multiple HIV-1 strains. Proc Natl Acad Sci USA 109:19769–19774.
157. Li H, Wang S, Lee FH, Roark RS, Murphy AI, Smith J, Zhao C, Rando J, Chohan N, Ding Y, Kim E, Lindemuth E, Bar KJ, Pandrea I, Apetrei C, Keele BF, Lifson JD, Lewis MG, Denny TN, Haynes BF, Hahn BH, Shaw GM. 2021. New SHIVs and improved design strategy for modeling HIV-1 transmission, immunopathogenesis, prevention, and cure. J Virol 109:e00071-21.
158. Richard J, Veillette M, Ding S, Zoubchenok D, Alsahafi N, Coutu M, Brassard N, Park J, Courter JR, Melillo B, Smith AB, 3rd, Shaw GM, Hahn BH, Sodroski J, Kaufmann DE, Finzi A. 2016. Small CD4 mimetics prevent HIV-1 uninfected bystander CD4 1 T cell killing mediated by antibody-dependent cell-mediated cytotoxicity. EBioMedicine 3:122–134.
159. Richard J, Prevost J, Baxter AE, von Bredow B, Ding S, Medjahed H, Delgado GG, Brassard N, Sturzel CM, Kirchhoff F, Hahn BH, Parsons MS, Kaufmann DE, Evans DT,

Finzi A. 2018. Uninfected bystander cells impact the measurement of HIV-specific antibody-dependent cellular cytotoxicity responses. mBio 9:e00358-18.

160. R Core Team. 2013. R: a language and environment for statistical computing. R Foundation for Statistical Computing, Vienna, Austria.
161. RStudio team. 2015. RStudio: integrated development for R. RStudio, Inc., Boston, MA.

3.4.10 FIGURES

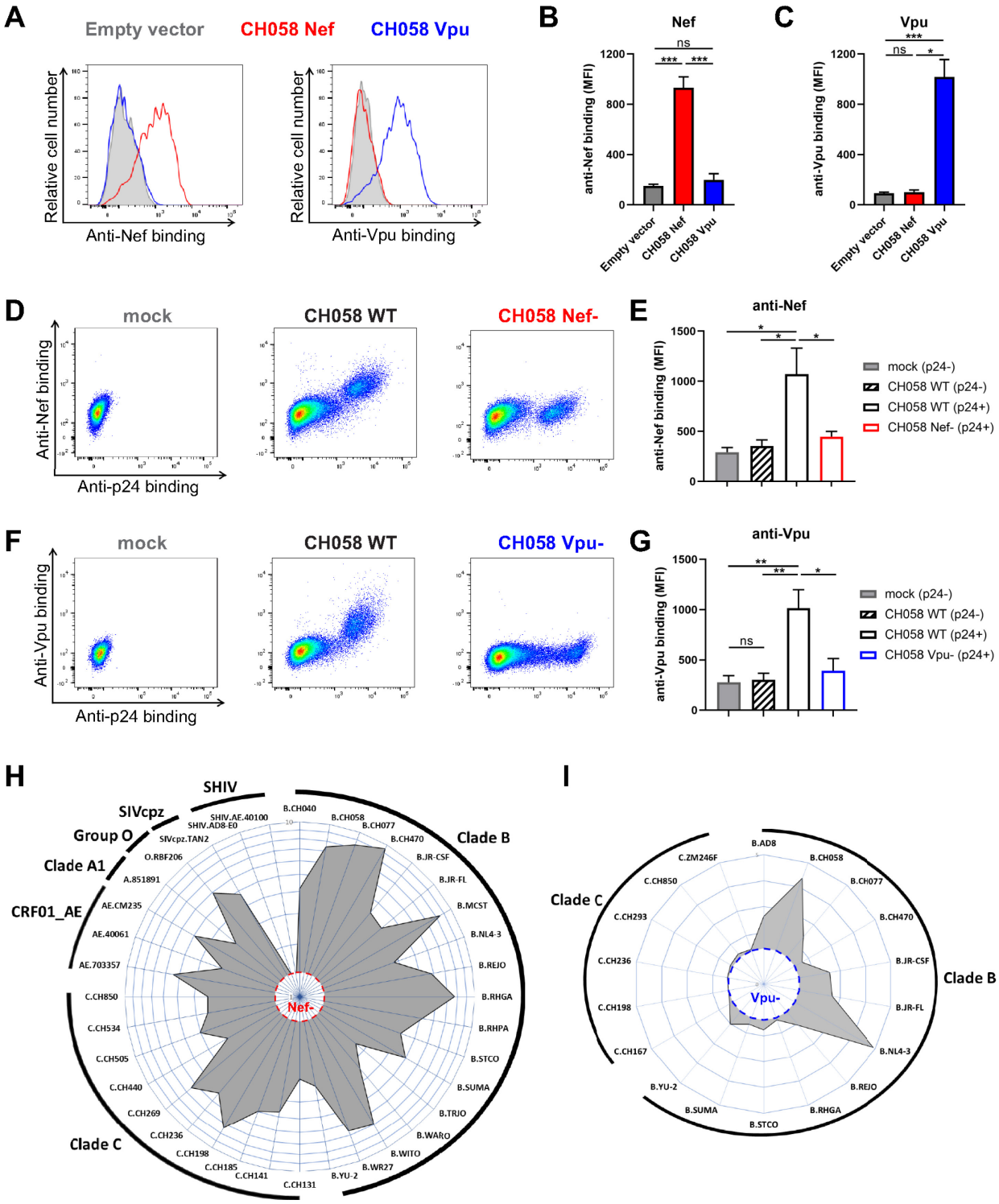

Figure 3.3.1 - Intracellular detection of Nef and Vpu in infected primary CD4$^+$ T cells.
(**A-C**) 293T cells transfected with an empty vector or a plasmid-expressing either CH058 Nef or CH058 Vpu. 48 hours post-transfection, cells were permeabilized and stained with rabbit polyclonal antisera raised against Nef and Vpu to detect their respective intracellular expression. Antiserum binding was detected using donkey anti-rabbit BV421 secondary Abs. (**A**) Histograms depicting representative staining and (**B-C**) Median fluorescence intensities (MFI) obtained for multiple independent stainings using (**B**) anti-Nef or (**C**) anti-Vpu. (**D-G**) Primary CD4$^+$ T cells mock-infected or infected with CH058 T/F WT, Nef-or Vpu-, were stained to detect the intracellular expression of Nef or Vpu. (**D,F**) Dot plots (left) and histograms (right) depicting representative (**D**) Nef and (**F**) Vpu staining. (**E,G**) The graphs show the MFI obtained from different cell populations using cells from five different donors using (**E**) anti-Nef or (**G**) anti-Vpu. Error bars indicate means ± standard errors of the means (SEM). Statistical significance was tested using an unpaired t test or a Mann-Whitney U test based on statistical normality (*, $P < 0.05$; **, $P < 0.01$; ***, $P < 0.001$; ns, nonsignificant). (**H-I**) Primary CD4$^+$ T cells were infected with a panel of viruses from different clades (A1, B, C, CRF01_AE), group (M, O) and host (HIV-1, SIVcpz, SHIV). The radar plots indicate the level of specific recognition of infected cells (MFI normalized to uninfected cells) using the (**H**) anti-Nef or (**I**) anti-Vpu antisera. The limit of detection was determined using (**H**) cells infected with CH058 Nef-for Nef staining and using (**I**) cells infected with CH058 Vpu-for Vpu staining.

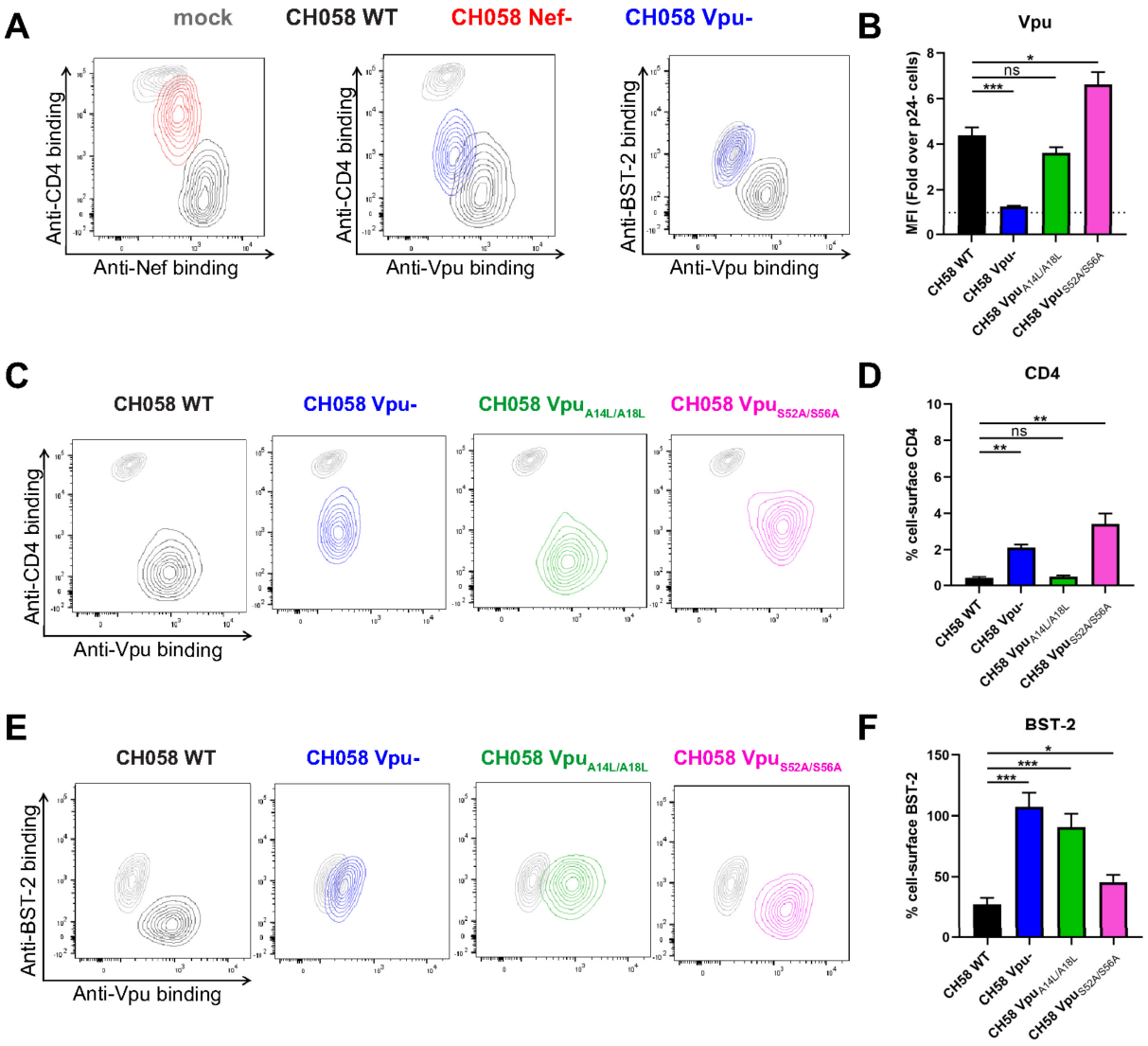

Figure 3.3.2 - Concomitant detection of intracellular Nef and Vpu and cell-surface CD4 and BST-2.

Primary $CD4^+$ T cells infected with CH058T/F WT, Nef-, Vpu-, Vpu A14L/A18L or Vpu S52A/S56A viruses were stained for cell-surface CD4 and BST-2 prior to detection of intracellular Nef or Vpu expression. (**A,C,E**) Contour plots depicting representative cell-surface CD4 or BST-2 detection in combination with Nef or Vpu intracellular detection. Mock-infected cells were used as a control and are shown in grey. (**B,D,F**) The graphs show the results obtained from five independent experiments. CD4 and BST-2 levels were reported as a percentage of detection at the surface of infected $p24^+$ cells compared to uninfected $p24^-$ cells. Error bars indicate means +/- standard errors of the means (SEM). Statistical significance was tested using an unpaired t test or a Mann-Whitney U test based on statistical normality (*, $P < 0.05$; **, $P < 0.01$; ***, $P < 0.001$; ns, nonsignificant).

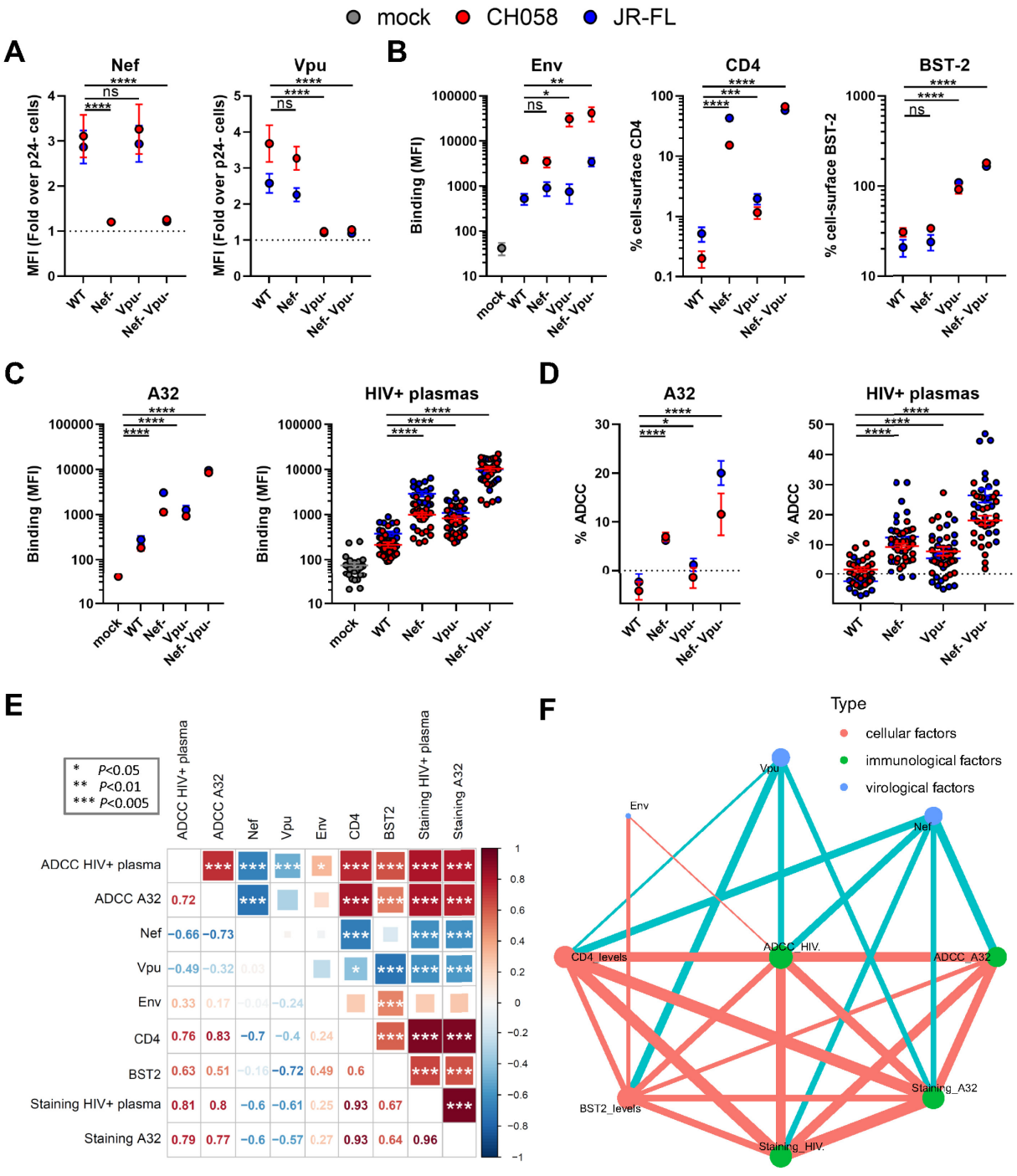
mock
CH058
JR-FL
A
Nef
Vpu
MFI (Fold over p24- cells)
WT
Nef-
Vpu-
Nef- Vpu-
B
Env
CD4
BST-2
Binding (MFI)
% cell-surface CD4
% cell-surface BST-2
mock
C
A32
HIV+ plasmas
D
% ADCC
E
* P<0.05
** P<0.01
*** P<0.005
ADCC HIV+ plasma
ADCC A32
Nef
Vpu
Env
CD4
BST2
Staining HIV+ plasma
Staining A32
F
Type
cellular factors
immunological factors
virological factors
CD4_levels
ADCC_HIV.
ADCC_A32
BST2_levels
Staining_HIV.
Staining_A32

Figure 3.3.3 - Nef and Vpu intracellular detection inversely correlates with the recognition of infected cells and their susceptibility to ADCC responses mediated by HIV$^+$ plasma.
(**A and B**) Primary CD4$^+$ T cells were mock-infected (gray) or infected with CH058 T/F (red) or JR-FL (blue) viruses (WT, Nef$^-$, Vpu$^-$, Nef$^-$ Vpu$^-$), and stained for (A) intracellular Nef or Vpu expression in combination with (**B**) cell-surface staining of Env (using the anti-Env 2G12 mAb), CD4, and BST-2. (**C and D**) The ability of the anti-Env A32 mAb and 25 different HIV$^+$ plasma samples to (**C**) recognize infected cells and (**D**) eliminate infected cells by ADCC was also measured. (**A to D**) The graphs show the MFI obtained on the infected (p24$^+$) cell population using cells from five different donors. Error bars indicate means +/- standard errors of the means (SEM). Statistical significance was tested using an unpaired t test or a Mann-Whitney U test based on statistical normality (*, $P < 0.05$; **, $P < 0.01$; ***, $P < 0.001$; ns, nonsignificant). (**E**) Correlograms summarize pairwise correlations among all immunological, virological, and cellular variables obtained from infected primary CD4$^+$ T cells (shown in panels **A to D**). Squares are color-coded according to the magnitude of the correlation coefficient (r), and the square dimensions are inversely proportional with the P values. Red squares represent a positive correlation between two variables, and blue squares represent negative correlations. Asterisks indicate all statistically significant correlations (*, $P < 0.05$; **, $P < 0.01$; ***, $P < 0.005$). Correlation analysis was done using nonparametric Spearman rank tests. (**F**) Correlation networks were generated using data shown in panel E. Each node (circle) represents a cellular (red), an immunological (green), or a virological (blue) feature measured on infected cells. Nodes are connected with edges (lines) if they are significantly correlated ($P < 0.05$); nodes without edges were removed. Edges are weighted according to P values (inversely). Red edges represent a positive correlation between two variables, and blue edges represent negative correlations. Nodes are sized according to the r values of connecting edges.

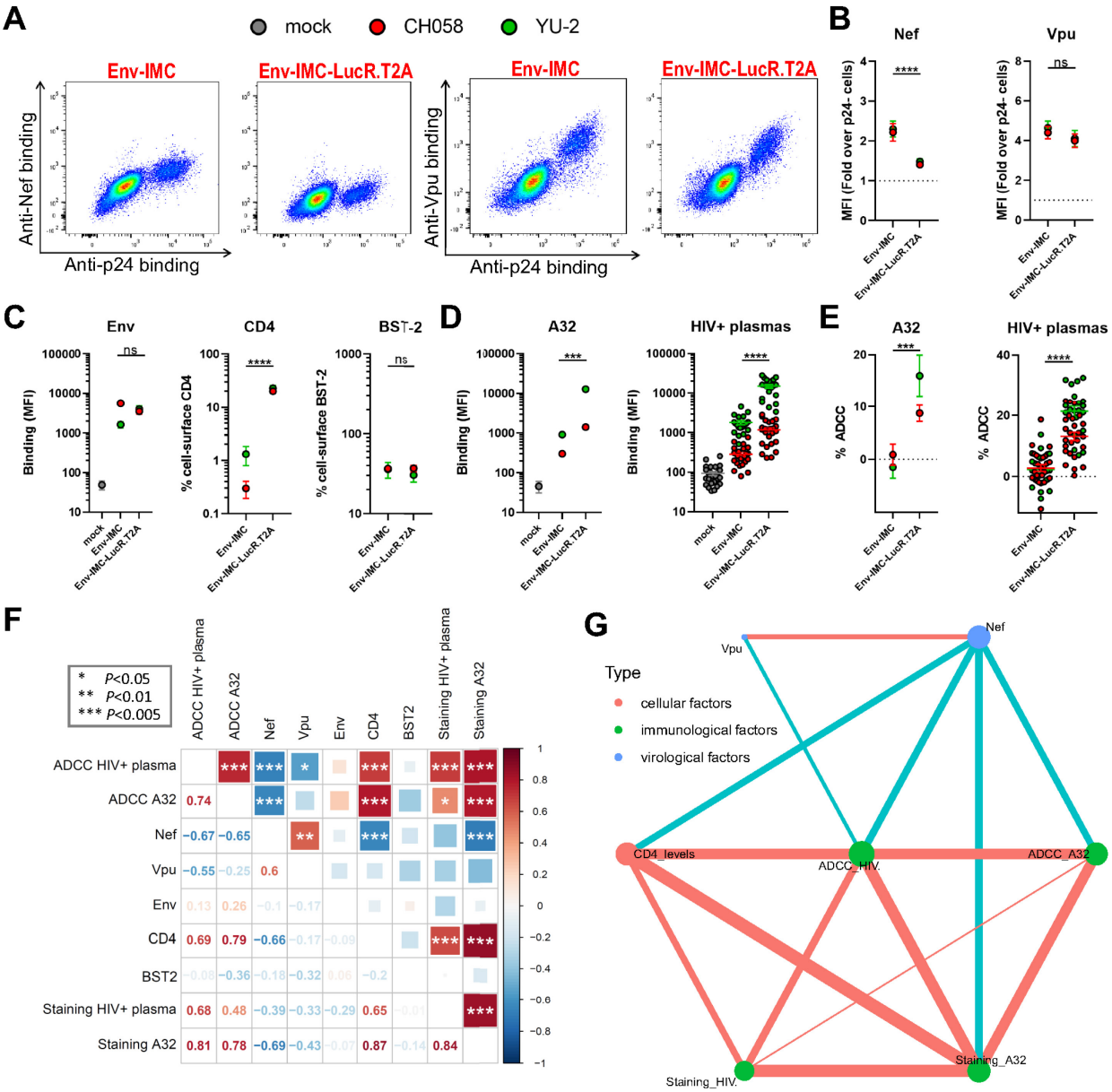
A
mock
CH058
YU-2
Env-IMC
Env-IMC-LucR.T2A
Anti-Nef binding
Anti-p24 binding
Anti-Vpu binding
B
Nef
Vpu
MFI (Fold over p24- cells)
****
ns
C
Env
CD4
BST-2
Binding (MFI)
% cell-surface CD4
% cell-surface BST-2
D
A32
HIV+ plasmas
***
E
% ADCC
F
* P<0.05
** P<0.01
*** P<0.005
ADCC HIV+ plasma
ADCC A32
Nef
Vpu
Env
CD4
BST2
Staining HIV+ plasma
Staining A32
G
Type
cellular factors
immunological factors
virological factors
CD4_levels
ADCC_HIV.
ADCC_A32
Staining_HIV.
Staining_A32

Figure 3.3.4 - Lack of Nef expression in primary CD4$^+$ T cells infected with LucR.T2A IMC results in enhanced ADCC.

Primary CD4$^+$ T cells mock-infected (gray) or infected with chimeric IMCs expressing CH058 Env (red) or YU-2 Env (green) and expressing or not the LucR reporter gene. (**A**) Dot plots depicting representative stainings of intracellular Nef or Vpu expression. (B and C) Detection by flow cytometry of (**B**) intracellular Nef or Vpu expression in combination with (**C**) cell-surface staining of Env (using anti-Env mAbs 2G12 (CH058) or PGT135 (YU-2)), CD4, and BST-2. (**D and E**) The ability of the A32 mAb and 25 HIV$^+$ plasma to (**D**) recognize infected cells and (**E**) eliminate infected cells by ADCC was also measured. (**B to E**) The graphs show the MFI obtained on the infected (p24$^+$) cell population using cells from five different donors. Error bars indicate the means +/- standard errors of the means (SEM). Statistical significance was tested using an unpaired t test or a Mann-Whitney U test based on statistical normality (*, $P < 0.05$; **, $P < 0.01$; ***, $P < 0.001$; ns, nonsignificant). (**F**) Correlograms summarize pairwise correlations among all immunological, virological, and cellular variables obtained from infected primary CD4$^+$ T cells (shown in panels **B to E**). Squares are color-coded according to the magnitude of the correlation coefficient (r), and the square dimensions are inversely proportional with the P values. Red squares represent a positive correlation between two variables, and blue squares represent negative correlations. Asterisks indicate all statistically significant correlations (*, $P < 0.05$; **, $P < 0.01$; ***, $P < 0.005$). Correlation analysis was done using non-parametric Spearman rank tests. (**G**) Correlation networks were generated using data shown in panel **F**. Each node (circle) represents a cellular (red), an immunological (green), or a virological (blue) feature measured on infected cells. Nodes are connected with edges (lines) if they are significantly correlated ($P < 0.05$); nodes without edges were removed. Edges are weighted according to P values (inversely). Red edges represent a positive correlation between two variables, and blue edges represent negative correlations. Nodes are sized according to the r values of connecting edges.

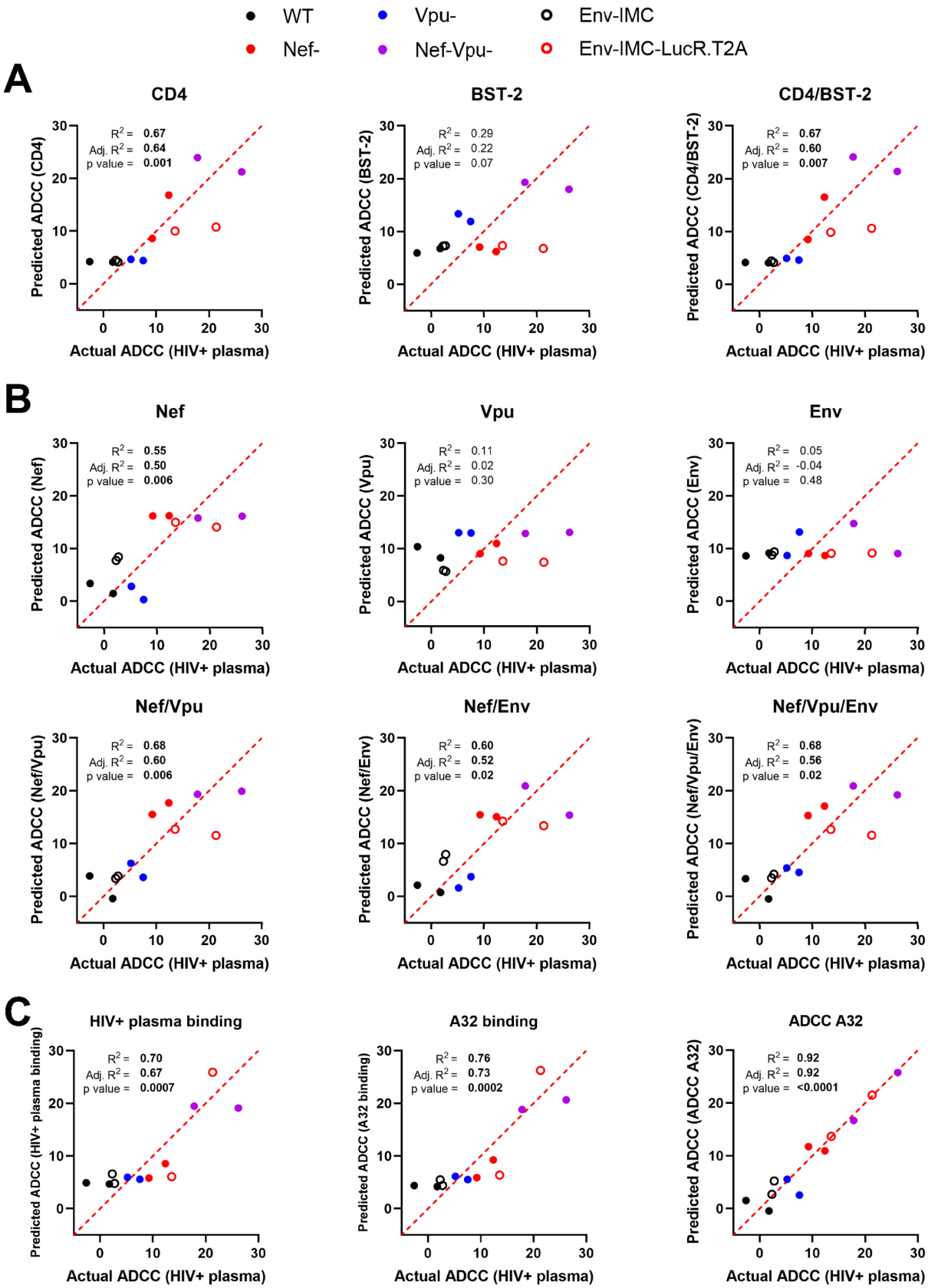
WT
Vpu-
Env-IMC
Nef-
Nef-Vpu-
Env-IMC-LucR.T2A
A
CD4
R² = 0.67
Adj. R² = 0.64
p value = 0.001
Predicted ADCC (CD4)
Actual ADCC (HIV+ plasma)
BST-2
R² = 0.29
Adj. R² = 0.22
p value = 0.07
Predicted ADCC (BST-2)
Actual ADCC (HIV+ plasma)
CD4/BST-2
R² = 0.67
Adj. R² = 0.60
p value = 0.007
Predicted ADCC (CD4/BST-2)
Actual ADCC (HIV+ plasma)
B
Nef
R² = 0.55
Adj. R² = 0.50
p value = 0.006
Predicted ADCC (Nef)
Actual ADCC (HIV+ plasma)
Vpu
R² = 0.11
Adj. R² = 0.02
p value = 0.30
Predicted ADCC (Vpu)
Actual ADCC (HIV+ plasma)
Env
R² = 0.05
Adj. R² = -0.04
p value = 0.48
Predicted ADCC (Env)
Actual ADCC (HIV+ plasma)
Nef/Vpu
R² = 0.68
Adj. R² = 0.60
p value = 0.006
Predicted ADCC (Nef/Vpu)
Actual ADCC (HIV+ plasma)
Nef/Env
R² = 0.60
Adj. R² = 0.52
p value = 0.02
Predicted ADCC (Nef/Env)
Actual ADCC (HIV+ plasma)
Nef/Vpu/Env
R² = 0.68
Adj. R² = 0.56
p value = 0.02
Predicted ADCC (Nef/Vpu/Env)
Actual ADCC (HIV+ plasma)
C
HIV+ plasma binding
R² = 0.70
Adj. R² = 0.67
p value = 0.0007
Predicted ADCC (HIV+ plasma binding)
Actual ADCC (HIV+ plasma)
A32 binding
R² = 0.76
Adj. R² = 0.73
p value = 0.0002
Predicted ADCC (A32 binding)
Actual ADCC (HIV+ plasma)
ADCC A32
R² = 0.92
Adj. R² = 0.92
p value = <0.0001
Predicted ADCC (ADCC A32)
Actual ADCC (HIV+ plasma)

Figure 3.3.5 - Prediction of ADCC responses mediated by HIV$^+$ plasma using multiple linear regression models.

Multiple linear regression analysis to identify variables that can predict the ADCC responses mediated by HIV1 plasma against primary CD4$^+$ T cells infected by different viral constructs (WT, Nef–, Vpu–, Nef-Vpu–, Env-IMC, Env-IMC-LucR.T2A) from different HIV-1 strains (CH058, JR-FL, YU-2). Each dot represents a single virus where the average of ADCC obtained with 25 different HIV1 plasma samples (dependent variable) is plotted on the x axis and the predicted ADCC value based on one or more independent parameters is plotted on the y axis. (**A to C**) Predictors include (**A**) cellular variables, (**B**) virological variables, and (**C**) immunological variables. Multiple linear regression analyses were performed using the GraphPad Prism software (v 9.1.0). P values below 0.05 are considered significant and are highlighted in bold. The coefficient of multiple correlation (R^2) indicates the goodness of fit of the multiple regression linear model. The adjusted R^2 (Adj. R^2) is used to compare the fits of models across experiments with different numbers of data points and independent variables.

CHAPITRE IV - RÔLE DE LA CONFORMATION D'ENV DANS LA RÉPONSE ADCC

4.1 Préambule

Dans ce chapitre, nous décrivons que la régulation négative de CD4 par les protéines Nef et Vpu n'est pas suffisante pour protéger les cellules infectées de la réponse ADCC médiée par les nnAbs. En fait, le facteur déterminant dictant la liaison des nnAbs est la conformation adoptée par Env à la surface de la cellule, et bien que celle-ci puisse être modulée par son interaction avec CD4, elle peut également varier de manière spontanée. Chez les isolats primaires du VIH-1, le trimère d'Env non-liée est maintenu dans un état « fermée » métastable de haute énergie qui peut transitionner vers des conformations « ouvertes » de plus basse énergie de manière dynamique. Nous avons caractérisé plusieurs domaines structuraux qui agissent de concert afin de limiter l'adoption de la conformation « ouverte » de manière spontanée, protégeant ainsi les cellules infectées de l'ADCC médiée par les nnAbs. Dans l'**article 5**, nous avons étudié un résidu conservé du domaine d'association du trimère (L193), qui contribue à stabiliser la conformation « fermée » en gardant les boucles V1/V2 ancrées à l'apex du trimère d'Env. La mutation de ce résidu permet d'augmenter la propension d'Env à adopter sa conformation « ouverte », ce qui se traduit par une augmentation de la susceptibilité des cellules infectées à être éliminées par la réponse ADCC médiée par le sérum VIH^{+}. Dans l'**article 6**, nous avons étudié l'impact du clivage protéolytique du précurseur d'Env sur l'évasion des nnAbs. L'absence de clivage rend l'Env plus flexible et plus disposée à adopter la conformation « ouverte », rendant les cellules infectées plus susceptibles aux activités effectrices Fc-dépendantes des nnAbs présents dans le sérum VIH^{+}. Cette flexibilité peut être exploitée grâce des petites molécules ciblant la cavité Phe43 afin de favoriser soit la conformation « ouverte » ou « fermée », ceci ayant pour effet d'augmenter ou de bloquer l'ADCC médiée par les nnAbs, respectivement. Dans l'**article 7**, nous avons étudié un résidu de la cavité Phe43 (S375), une structure critique pour l'interaction avec CD4 et qui sert de point de contrôle important dans le déclenchement des changements de conformation d'Env. La substitution de ce petit résidu par de larges résidus hydrophobes permet de « remplir » la cavité Phe43, prédisposant Env à adopter spontanément la conformation « ouverte » et augmentant la susceptibilité des cellules infectées à la réponse ADCC médiée par les nnAbs. Le résidu S375 est conservé dans la majorité des souches du VIH-1 du groupe M en circulation, à l'exception du clade CRF01_AE qui possède naturellement une histidine à cette position. Cette souche est prédominante en Thaïlande, là où l'essai vaccinal RV144 a eu lieu, ce qui pourrait expliquer pourquoi les corrélats de protection de cette étude incluaient la réponse ADCC médiée par les nnAbs.

ARTICLE 5

Les glycoprotéines d'enveloppe adoptant les conformations 2 et 3 sont plus susceptibles à la réponse ADCC médiée par le sérum d'individus infectés

Envelope Glycoproteins Sampling States 2/3 are Susceptible to ADCC by Sera from HIV-1-Infected Individuals

Auteurs:

Jérémie Prévost[1,2], Jonathan Richard[1,2], Shilei Ding[1,2], Beatriz Pacheco[1], Roxanne Charlebois[1], Beatrice H. Hahn[3], Daniel E. Kaufmann[1,4,5], and Andrés Finzi[1,2,6]

Affiliations:

[1]Centre de Recherche du CHUM, QC, Canada; [2]Department of Microbiology, Infectiology and Immunology, Université de Montréal, Montreal, QC, Canada; [3]Departments of Medicine and Microbiology, Perelman School of Medicine, University of Pennsylvania, Philadelphia, PA, USA; [4]Department of Medicine, Université de Montréal, Montreal, QC, Canada; [5]Center for HIV/AIDS Vaccine Immunology and Immunogen Discovery, The Scripps Research Institute, La Jolla, CA, USA; [6]Department of Microbiology and Immunology, McGill University, Montreal, QC, Canada.

Contribution des auteurs:

Conceptualisation: **J.P.** et A.F.; Méthodologie: **J.P.** J.R. et A.F.; Recherche: **J.P.**, J.R. et S.D; Ressources: B.P., R.C., B.H.H., D.E.K. et A.F.; Analyse formelle: **J.P.**; Visualisation: **J.P.**; Supervision: A.F.; Obtention du financement: D.E.K. et A.F.; Rédaction - version originale: **J.P.** et A.F.; Rédaction - révision et édition: **Tous les auteurs**.

Statut: Cet article a été publié dans *Virology* en février 2018

https://doi.org/10.1016/j.virol.2017.12.002

4.2.1 RÉSUMÉ

Une analyse récente de la dynamique des glycoprotéines d'enveloppe (Env) du VIH-1 a montré que le trimère d'Env non-lié peut potentiellement adopter trois conformations : la conformation "fermée" métastable (conformation 1), la conformation "ouverte" liée aux CD4 (conformation 3) et une conformation intermédiaire "partiellement ouverte" (conformation 2). Le VIH-1 a développé plusieurs mécanismes pour éviter l'ouverture d'Env afin d'échapper aux réponses immunitaires telles que la réponse cytotoxique cellulaire dépendante des anticorps (ADCC), qui cible de préférence Env dans la conformation liée à CD4 à la surface des cellules infectées. Nous avons profité d'une mutation bien caractérisée dans le domaine d'association du trimère de la gp120 pour modifier la conformation d'Env et évaluer son impact sur la réponse ADCC. Nous avons constaté que les cellules infectées par des virus exprimant Env stabilisée dans les conformations 2/3 deviennent très sensibles à la réponse ADCC médiée par les sérums d'individus infectés par le VIH-1. Nos résultats indiquent que la conformation adoptée spontanément par le trimère d'Env à la surface des cellules infectées a un impact significatif sur la réponse ADCC.

4.2.2 ABSTRACT

Recent analysis of HIV-1 envelope glycoproteins (Env) dynamics showed that the unliganded Env trimer can potentially sample three conformations: a metastable "closed" conformation (State 1), an "open" CD4-bound conformation (State 3), and an intermediate "partially open" conformation (State 2). HIV-1 evolved several mechanisms to avoid "opening" its Env in order to evade immune responses such as antibody-dependent cellular cytotoxicity (ADCC), which preferentially targets Envs in the CD4-bound conformation on the surface of infected cells. Here we took advantage of a well-characterized single-residue change in the gp120 trimer association domain to modify Env conformation and evaluate its impact on ADCC responses. We found that cells infected with viruses expressing Env stabilized in States 2/3 become highly susceptible to ADCC responses by sera from HIV-1-infected individuals. Our results indicate that the conformations spontaneously sampled by the Env trimer at the surface of infected cells has a significant impact on ADCC responses.

4.2.3 INTRODUCTION

The entry of human immunodeficiency virus (HIV-1) into the host cell is mediated by the viral envelope glycoproteins (Envs), which are derived by proteolytic cleavage of a trimeric gp160 Env precursor (Allan et al., 1985; Robey et al., 1985; Wyatt and Sodroski, 1998). The mature Env complex is composed of three gp120 surface subunits and three gp41 transmembrane subunits. Env is a metastable molecule which transits from its unliganded "closed" high energy conformation (State 1) to an "open" CD4-bound low energy conformation (State 3). CD4 engagement drives Env into an intermediate "partially open" conformation and then into State 3, a pre-hairpin intermediate conformation (Herschhorn et al., 2016; Munro et al., 2014). CCR5 or CXCR4 coreceptor interaction with the gp120 promotes additional conformational changes in gp41 resulting in the formation of a six-helix bundle formed by HR1 and HR2 heptad repeats resulting in the fusion of viral and cellular membranes (Chan et al., 1997; Lu et al., 1995; Weissenhorn et al., 1997). Env represents the only virus-specific antigen exposed at the surface of infected cells and thus is a major target for antibody-mediated immune responses, including antibody-dependent cellular cytotoxicity (ADCC). The unliganded Env of most primary HIV-1 isolates assumes a "closed" State 1 conformation (Julien et al., 2013; Liu et al., 2008; Lyumkis et al., 2013; Mao et al., 2012; Munro et al., 2014; Pancera et al., 2014; White et al., 2010), which renders the trimer relatively resistant to antibody attack. Env interaction with CD4 (Veillette et al., 2015, 2014b), large alterations in the Phe43 cavity (Prevost et al., 2017) and small CD4-mimetics (CD4mc) (Richard et al., 2016a, 2015) have been shown to trigger Env to sample downstream conformations and render HIV-1-infected cells susceptible to ADCC responses. Thus, downstream conformations from State 1 appear to be preferentially recognized by ADCC-mediating antibodies that are present in the sera of HIV-1-infected individuals (Veillette et al., 2015). In order to limit the recognition of Env at the surface of infected cells, HIV-1 has evolved sophisticated mechanisms to efficiently internalize Env (von Bredow et al., 2015), to counteract the host restriction factor BST-2 with the viral Vpu protein (Alvarez et al., 2014; Arias et al., 2014; Veillette et al., 2014b), and to downregulate CD4 using Nef and Vpu (Veillette et al., 2015, 2014b). Moreover, multiple intermolecular interactions within the Env trimer contribute to the maintenance of this relatively "antibody-resistant" State 1 conformation, including the gp120 β20–β21 element and the V1V2 and V3 variable loops (Herschhorn et al., 2017, 2016; Kwon et al., 2012). For example, mutation of "restraining" residues within V1V2 were shown to enable Env to

spontaneously sample lower energy State 2 and 3 conformations. These Env variants were reported to be more susceptible to neutralization by State 2/3-preferring ligands such as soluble CD4 (sCD4), small CD4 mimetics (CD4mc) and CD4-induced (CD4i) antibodies (Herschhorn et al., 2016). However, their impact on ADCC responses remains unknown. Here we tested the influence of a V2 State 2/3-stabilizing Env mutation, L193A, on ADCC responses mediated by sera from HIV-1-infected individuals.

4.2.4 MATERIALS AND METHODS

Cell lines and isolation of primary cells

293T human embryonic kidney (obtained from ATCC, Cat# CRL-3216, RRID: CVCL 0063), and primary $CD4^+$ T cells were grown as previously described (Richard et al., 2010; Veillette et al., 2014b). $CD4^+$ T lymphocytes were purified from resting PBMCs by negative selection and activated as previously described (Richard et al., 2015). Research adhered to the ethical guidelines of CRCHUM and was reviewed and approved by the CRCHUM institutional review board (ethics committee). Research adhered to the standards indicated by the Declaration of Helsinki.

Viral production and infections

In order to achieve the same level of infection among the different mutants tested, vesicular stomatitis virus G (VSVG)-pseudotyped HIV-1 viruses were produced and titrated as described (Veillette et al., 2015). Viruses were used to infect primary $CD4^+$ T cells from healthy HIV-negative donors by spin infection at 800 × g for 1 h in 96-well plates at 25 °C. Under these conditions we obtained equivalent levels of infection for all viruses tested.

Antibodies and sera

The following antibodies were used to assess Env cell-surface staining: conformation-independent anti-gp120 outer-domain 2G12 (NIH AIDS Reagent Program), State 1- preferring anti-gp120 antibodies VRC03 (NIH AIDS Reagent Program), PGT151 (IAVI) and PG9 (Polymun), State 2/3-preferring anti-gp120 antibodies 17b, 19b, A32, F105 and anti-gp41 antibodies 7B2 and F240 (NIH AIDS Reagent Program). The monoclonal antibody anti-CD4

OKT4 (BioLegend) binds to the D3 domain of CD4 and was used to measure cell-surface levels of CD4, as described (Veillette et al., 2014b). Secondary antibodies goat anti-mouse and anti-human coupled to Alexa Fluor 647 (Invitrogen) were used in flow cytometry experiments. Sera from HIV-infected and healthy donors were collected, heat-inactivated and conserved at − 80 °C until use. Written Informed consent was obtained from all study participants (the Montreal Primary HIV Infection Cohort (Fontaine et al., 2011, 2009) and the Canadian Cohort of HIV Infected Slow Progressors (International et al., 2010; Kamya et al., 2011; Peretz et al., 2007)). A random number generator (GraphPad, QuickCalcs) was used to randomly select a number of sera for each experiment.

Plasmids

The plasmid encoding the HIV-1 transmitted founder (TF) infectious molecular clone (IMC) CH58 and CH77 were previously described (Bar et al., 2012; Fenton-May et al., 2013; Ochsenbauer et al., 2012; Parrish et al., 2013; Richard et al., 2015). Individual Env mutations were introduced using the QuikChange II XL site-directed mutagenesis protocol (Stratagene) and verified by sequencing.

Flow cytometry analysis of cell-surface staining

Using the standard calcium phosphate method, 7 µg of each IMC was transfected into 2 × 10^6 293T cells. At 48 h post transfection, 293T cells were stained with anti-Env antibodies (5 µg/mL) followed by intracellular p24 staining (PE-anti-p24, clone KC57; Beckman Coulter/Immunotech, Hialeah, FL; 1:100 final dilution), to identify transfected cells. Alternatively, to evaluate soluble CD4 (sCD4) binding to the different Envs expressed at the cell surface, transfected 293T cells were incubated with sCD4 (5 µg/mL), followed with a staining by the monoclonal anti-CD4 OKT4 antibody.

Cell-surface staining of primary $CD4^+$ T cells was performed as previously described (Richard et al., 2015; Veillette et al., 2015). MFI histograms show signal on live infected populations. Binding of HIV-1-infected cells by HIV^+ sera (1:1000 dilution) or anti-Env mAbs (5 µg/mL) were performed 48 h after infection. The percentage of infected cells ($p24^+$ cells) was determined by gating the living cell population based on viability dye staining (Aqua Vivid,

Thermo Fisher Scientific, Cat# L43957). Samples were analyzed on an LSRII cytometer (BD Biosciences, Mississauga, ON, Canada) and data analysis was performed using FlowJo v10.0.7 (Tree Star, Ashland, OR, USA).

ADCC responses

Measurement of ADCC-mediated killing was performed with a previously described assay (Richard et al., 2015). Primary $CD4^+$ T cells isolated from five healthy HIV-negative donors were infected for 48 h with the different IMCs. In order to avoid the potential bias induced by the presence of gp120-coated uninfected bystander $CD4^+$ T cells in ADCC measurements (Richard et al., 2016b), $CD4^{high}$ T cells were removed from the target cell population using Dynabeads® $CD4^+$ positive selection kit (Invitrogen) at a ratio of 25 µl of beads per million cells. Of note, these beads do not distinguish between $p24^+$ and $p24^-$ cells. Their capacity to enrich CD4low cells is based in their ability to select for $CD4^{high}$ cells. Negative selection of $CD4^{low}$ T cells was assessed by double staining with anti-CD4 OKT4 mAb and anti-p24 mAb (KC57, Beckman Coulter). Productively-infected primary CD4 T cells ($CD4^{low}$, $p24^+$) were incubated with autologous PBMC in presence of HIV^+ or HIV^- sera (1:1000) for 5 h at 37 °C. Cytometry beads were used to normalize the number of productively-infected cells left after the ADCC reaction, as described (Richard et al., 2014, 2016b). The percentage of cytotoxicity (% ADCC) was calculated with the following formula: (Normalized number of Targets plus Effectors) − (Normalized number of Targets plus Effectors plus serum)/(Normalized number of Targets) by gating infected lived target cells.

Immunoprecipitation of envelope glycoproteins

3×10^5 293T cells were transfected by the calcium phosphate method with the different IMCs. One day after transfection, cells were metabolically labeled for 16 h with 100 µCi/mL [^{35}S] methionine-cysteine ([^{35}S] Protein Labeling Mix; PerkinElmer) in Dulbecco's modified Eagle's medium lacking methionine and cysteine and supplemented with 5% dialyzed fetal bovine serum. Cells were subsequently lysed in RIPA buffer (140 mM NaCl, 8 mM Na_2HPO_4, 2 mM NaH_2PO_4, 1% NP40, 0.05% sodium dodecyl sulfate (SDS)). Precipitation of radiolabeled envelope glycoproteins from cell lysates or medium was performed with a mixture of sera from HIV-1-infected individuals in the presence of 50 µl of 10% Protein A-Sepharose (American BioSciences) at 4 °C. The association index is a measure of the ability of the mutant gp120 molecule to remain

associated with the Env trimer complex on the expressing cell, relative to that of the wild-type Env trimers. The association index is calculated as follows: association index = ([mutant gp120] cell × [wildtype gp120] supernatant) / ([mutant gp120] supernatant × [wild-type gp120] cell).

Statistical analyses

Statistics were analyzed using GraphPad Prism version 6.01 (GraphPad, San Diego, CA, USA). P values < 0.05 were considered significant; significance values are indicated as * $p < 0.05$, ** $p < 0.01$, *** $p < 0.001$, **** $p < 0.0001$.

4.2.5 RESULTS

Effect of L193A on HIV-1 Env conformation.

A recent report identified a series of State 1 restraining residues located in the V1V2 variable regions that when mutated enabled Env to spontaneously sample downstream conformations (Herschhorn et al., 2016). Based on its marked States 2/3 phenotype, mutation L193A was selected and introduced into primary transmitted/founder (TF) infectious molecular clones (IMCs) CH58 and CH77. These IMCs were chosen because they have been extensively characterized and shown to be resistant to ADCC mediated by HIV^+ sera and anti-cluster A antibodies (Ding et al., 2016b, 2016c; Richard et al., 2016a, 2017a, 2015a, 2016b). In order to confirm that mutation L193A triggered Env to sample State 2/3 conformations, primary $CD4^+$ T cells infected with wild type CH58, CH77 and L193A variants were incubated with a panel of conformational specific ligands and assessed by flow cytometry. Since it has been reported that small amounts of CD4 at the surface of cells are sufficient to affect Env conformation (Veillette et al., 2014a, 2014b), we first assessed Env conformation using CD4 negative cells (293T). As shown in **Fig. 4.1.1A–B**, State 1-preferring ligands (PG9, VRC03 and PGT151) recognized L193A variants of CH58 and CH77 IMCs less efficiently than the corresponding wild type viruses. This was associated with a significant increase in their recognition by State 2/3-preferring ligands (19b, 17b, 7B2, F240, F105, sCD4, A32). Of note, PG9 did not recognize CH58 Env; VRC03 did not recognize CH77 Env, and therefore were not included for these viruses.

We then evaluated whether the State 2/3-like conformation of L193A variants was maintained at the surface of primary CD4+ T cells, a biologically-relevant model for ADCC responses (Lewis et al., 2015; Veillette et al., 2016). Primary $CD4^+$ T cells from 3 healthy HIV-1 negative donors were infected with WT CH58 and CH77, and their L193A variants. Env conformation was evaluated with the same panel of ligands described above. Consistent with efficient CD4 down-regulation by Nef and Vpu accessory proteins, productively-infected cells ($p24^+$) expressed almost no CD4 at their surface (data not shown). In agreement with Env sampling a "closed" State 1 conformation, Env at the surface of wildtype-infected $CD4^+$ T cells were efficiently recognized by State 1 but not States 2/3- preferring ligands (**Fig. 4.1.1C–D**). In contrast, primary $CD4^+$ T cells infected with L193A variants were efficiently recognized by State 2/3-preferring ligands (**Fig. 4.1.1C–D**). Altogether, these results support previous observations indicating that L193A stabilizes Env in a State 2/3-like conformation (Herschhorn et al., 2016).

Subunit association of L193A variants.

When performing Env staining at the surface of productively-infected ($p24^+$) primary CD4+ T cells, we observed a decreased signal for L193A variants when using the conformationally independent anti-gp120 outer domain 2G12 antibody (**Fig. 4.1.2A–B**) (Veillette et al., 2015, 2014a, 2014b). Since decreased Env detection at the surface of HIV-1-infected cells could be explained by enhanced gp120 shedding, we decided to directly examine whether introduction of the L193A mutation results in such a phenotype. Briefly, 293T cells were transfected with wild-type CH58 and CH77, and their L193A variants. Transfected cells were metabolically-labeled 24 h later and released and cell-associated gp120 molecules were quantified after immunoprecipitation from medium and cell lysates, as described (Ding et al., 2016a; Finzi et al., 2010). Introduction of the L193A mutation resulted in a significant increase in gp120 shedding in both IMCs (**Fig. 4.1.2C–F**), suggesting decreased trimer stability. These results are consistent with a role of the V1V2 variable regions in maintaining trimer stability (Herschhorn et al., 2016; Medjahed et al., 2013).

Impact of the L193A mutation on ADCC responses mediated by HIV^+ sera.

We then evaluated whether introduction of L193A into CH58 and CH77 IMCs affected Env recognition and ADCC responses mediated by sera from HIV-1 infected individuals. Primary

$CD4^+$ T cells isolated from 5 HIV-1 negative donors were infected with wild-type and L193A mutant CH58 and CH77 viruses. Two days post-infection cells were stained with sera from 10 HIV-1-infected individuals or 5 healthy HIV-1-negative individuals. In agreement with Env being stabilized in a State 2/3 conformation, infected cells expressing the L193A variants were more efficiently detected by HIV^+ sera tested than their WT counterparts (**Fig. 4.1.3**). As expected, sera from HIV-1 negative donors did not bind to HIV-1- infected cells (not shown). We next evaluated whether enhanced recognition of HIV-1- infected cells by HIV^+ sera translated into increased susceptibility to ADCC responses. However, since L193A induces gp120 shedding (**Fig. 4.1.2**) and this shed gp120 affects ADCC measurements by binding to uninfected bystander $CD4^+$ T cells (Richard et al., 2016b), we decided to modify a previously-described FACS-based ADCC assay (Richard et al., 2014, 2015). Briefly, primary $CD4^+$ T cells were infected with the different IMCs for 48 h. Uninfected bystander $CD4^+$ T cells were removed using beads coated with an anti-CD4 antibody which does not compete for gp120 binding (**Fig. 4.1.4A–D**). As shown in **Fig. 4.1.4**, $CD4^{high}$ T cell depletion removed more than 90% of uninfected $CD4^+$ T cells ($p24^-$ $CD4^+$) (**Fig. 4.1.4** and not shown), leaving the vast majority of productively-infected cells ($p24^+$ $CD4^-$). Enriched productively-infected cells were then used to assess ADCC responses mediated by HIV^+ sera. In agreement with poor recognition of wild-type Envs by State 2/3-preferring ligands (**Fig. 4.1.1**) and HIV^+ sera (**Fig. 4.1.3**), we observed low ADCC activity against cells infected with wild-type viruses (**Fig. 4.1.4E–F**). In contrast, infected cells expressing the L193A variant were significantly more susceptible to ADCC responses, indicating that Env State 2/3 conformations are more susceptible to ADCC mediated by antibodies present in HIV^+ sera.

4.2.6 DISCUSSION

The unliganded HIV-1 Env trimer can potentially sample three conformations: a metastable "closed" conformation (State 1), an "open" CD4-bound conformation (State 3), and an intermediate "partially open" conformation (State 2) (Herschhorn et al., 2016; Munro et al., 2014). Along with extensive glycosylation and a variable protein surface, Env conformational flexibility contributes to the ability of HIV-1 to evade the host's antibody response. Recent evidence suggests that HIV-1 developed additional mechanisms to avoid "opening" the Env which otherwise results in the exposure of vulnerable epitopes. Recognition of these conserved epitopes by host-elicited antibodies not only results in viral neutralization but also in the elimination of HIV-1 infected cells

by Fc-mediated effector functions (Lewis et al., 2017; Madani et al., 2016; Richard et al., 2016a, 2017a, 2015; Tolbert et al., 2017; Veillette et al., 2015, 2014b). HIV-1 restrains its envelope glycoproteins from sampling downstream conformation and exposing these epitopes by downregulating the CD4 receptor from the surface of the cell (Veillette et al., 2015, 2014b), by keeping small residues in its Env Phe43 cavity (Prevost et al., 2017) and by maintaining multiple intramolecular and intermolecular interactions within the Env trimer (Bradley et al., 2016; Cimbro et al., 2016; Duenas-Decamp et al., 2016; Herschhorn et al., 2016; Kwon et al., 2012; O'Rourke et al., 2012). A recent mutagenesis study showed that subtle losses of key molecular contacts resulting from single-residue changes in the gp120 trimer association domain release Env to assume one or more intermediate states (Herschhorn et al., 2016). We took advantage of the detailed conformational dynamic characterization by single-molecule Fluorescence Resonance Energy Transfer (smFRET) of the L193A mutation (Herschhorn et al., 2016) to explore the sensitivity of these intermediate states to ADCC responses. This mutant was shown to spontaneously sample a State 2/3-like conformation and was reported to be more susceptible to neutralization by State 2/3-preferring ligands, including sCD4, CD4mc and CD4i antibodies. In agreement with these results, we found that introduction of the L193A mutation in two primary IMCs resulted in Env sampling intermediate State 2/3 conformations at the surface of infected cells based on their efficient recognition by a panel of State 2/3-recognizing ligands. This was accompanied with a significant increase in gp120 shedding, suggesting that Env States 2/3 are overall less stable, which is consistent with a role of the V1V2 variable regions in maintaining trimer stability (Medjahed et al., 2013). Since binding of shed gp120 to uninfected bystander $CD4^+$ T cells can affect in vitro measurements of ADCC activity (Richard et al., 2016b), we decided to modify a previously-described FACS-based ADCC assay (Richard et al., 2014, 2015) by removing $p24^-$ $CD4^{high}$ cells. This was necessary because the presence of uninfected bystander $CD4^+$ T cells ($p24^-$ $CD4^{high}$), which are coated with gp120 shed from productively infected cells (Richard et al., 2016b), induces a strong bias by exposing CD4i epitopes that are normally occluded in productively-infected cells and therefore overestimate the ADCC activity of CD4i antibodies present in sera from HIV-1-infected individuals. By removing these cells, we obtained an homogenous population of productively-infected, $p24^+$ $CD4^{low}$, cells. Primary $CD4^+$ T cells infected with wild-type CH58 and CH77 were resistant to ADCC mediated by HIV^+ sera. This is consistent with the recognition of these infected cells by State 1-preferring ligands and the

concomitant occlusion of CD4i epitopes in primary Envs (Ding et al., 2016b; Richard et al., 2015; Veillette et al., 2015, 2014b; von Bredow et al., 2016). In marked contrast, infected cells expressing the L193A variant were significantly more susceptible to ADCC responses mediated by sera from several HIV-1-infected individuals. Altogether, our results indicate that the conformation spontaneously sampled by Env at the surface of infected cells has a significant impact on ADCC responses. This information might be useful in understanding the role of ADCC responses in HIV-1 transmission in animal studies.

4.2.7 ACKNOWLEDGMENTS

The authors thank Dominique Gauchat from the CRCHUM Flow Cytometry Platform for technical assistance, Mario Legault for cohort coordination and clinical samples and Marzena Pazgier for discussions on Env conformational states. This work was supported by a CIHR Foundation Grant #352417 to A.F. Support for this work was also provided by an amfAR Innovation Grant #109343-59-RGRL with support from FAIR to A.F. and by NIH R01 to M.P. and A.F. (AI129769). This study was also supported by NIH AI100645 and AI100663 Center for HIV/AIDS Vaccine Immunology and Immunogen Design (CHAVI-ID). A.F. is the recipient of a Canada Research Chair on Retroviral Entry. J.R. is the recipient of a Mathilde Krim Fellowships in Basic Biomedical Research from amfAR. J.P. is the recipient of a CIHR Fellowship Award. S.D. is the recipient of a FRSQ postdoctoral fellowship award. D.E.K is supported by a FRQS Senior Research Scholar Award. Our funding sources had no role in data collection, analysis or interpretation, and were not involved in the writing of this manuscript.

4.2.8 REFERENCES

Allan JS, Coligan JE, Barin F, McLane MF, Sodroski JG, Rosen CA, Haseltine WA, Lee TH, Essex M. Major glycoprotein antigens that induce antibodies in AIDS patients are encoded by HTLV-III. Science. 1985; 228:1091–1094.

Alvarez RA, Hamlin RE, Monroe A, Moldt B, Hotta MT, Rodriguez Caprio G, Fierer DS, Simon V, Chen BK. HIV-1 Vpu antagonism of tetherin inhibits antibody-dependent cellular cytotoxic responses by natural killer cells. J Virol. 2014; 88:6031–6046.

Arias JF, Heyer LN, von Bredow B, Weisgrau KL, Moldt B, Burton DR, Rakasz EG, Evans DT. Tetherin antagonism by Vpu protects HIV-infected cells from antibody-dependent cell-mediated cytotoxicity. Proc Natl Acad Sci USA. 2014; 111:6425–6430.

Bar KJ, Tsao CY, Iyer SS, Decker JM, Yang Y, Bonsignori M, Chen X, Hwang KK, Montefiori DC, Liao HX, Hraber P, Fischer W, Li H, Wang S, Sterrett S, Keele BF, Ganusov VV, Perelson AS, Korber BT, Georgiev I, McLellan JS, Pavlicek JW, Gao F, Haynes BF, Hahn BH, Kwong PD, Shaw GM. Early low-titer neutralizing antibodies impede HIV-1 replication and select for virus escape. PLoS Pathog. 2012; 8:e1002721.

Bradley T, Trama A, Tumba N, Gray E, Lu X, Madani N, Jahanbakhsh F, Eaton A, Xia SM, Parks R, Lloyd KE, Sutherland LL, Scearce RM, Bowman CM, Barnett S, Abdool-Karim SS, Boyd SD, Melillo B, Smith AB, III, Sodroski J, Kepler TB, Alam SM, Gao F, Bonsignori M, Liao HX, Moody MA, Montefiori D, Santra S, Morris L, Haynes BF. Amino acid changes in the HIV-1 gp41 membrane proximal region control virus neutralization sensitivity. EBioMedicine. 2016; 12:196– 207.

Chan DC, Fass D, Berger JM, Kim PS. Core structure of gp41 from the HIV envelope glycoprotein. Cell. 1997; 89:263–273. [PubMed: 9108481] Cimbro R, Peterson FC, Liu Q, Guzzo C, Zhang P, Miao H, Van Ryk D, Ambroggio X, Hurt DE, De Gioia L, Volkman BF, Dolan MA, Lusso P. Tyrosine-sulfated V2 peptides inhibit HIV-1 infection via coreceptor mimicry. EBioMedicine. 2016; 10:45–54.

Ding S, Tolbert WD, Prevost J, Pacheco B, Coutu M, Debbeche O, Xiang SH, Pazgier M, Finzi A. A highly conserved gp120 inner domain residue modulates Env conformation and trimer stability. J Virol. 2016a; 90:8395-409.

Ding S, Veillette M, Coutu M, Prevost J, Scharf L, Bjorkman PJ, Ferrari G, Robinson JE, Sturzel C, Hahn BH, Sauter D, Kirchhoff F, Lewis GK, Pazgier M, Finzi A. A highly conserved residue of the HIV-1 gp120 inner domain is important for antibody-dependent cellular cytotoxicity responses mediated by anti-cluster A antibodies. J Virol. 2016b; 90:2127–2134.

Ding S, Verly MM, Princiotto A, Melillo B, Moody T, Bradley T, Easterhoff D, Roger M, Hahn BH, Madani N, Smith AB, III, Haynes BF, Sodroski JMD, Finzi A. Small molecule CD4-mimetics sensitize HIV-1-infected cells to ADCC by antibodies elicited by multiple

envelope glycoprotein immunogens in non-human primates. AIDS Res Hum Retroviruses. 2016c; 33:428-431.

Duenas-Decamp M, Jiang L, Bolon D, Clapham PR. Saturation mutagenesis of the HIV-1 envelope CD4 binding loop reveals residues controlling distinct trimer conformations. PLoS Pathog. 2016; 12:e1005988.

Fenton-May AE, Dibben O, Emmerich T, Ding H, Pfafferott K, Aasa-Chapman MM, Pellegrino P, Williams I, Cohen MS, Gao F, Shaw GM, Hahn BH, Ochsenbauer C, Kappes JC, Borrow P. Relative resistance of HIV-1 founder viruses to control by interferon-alpha. Retrovirology. 2013; 10:146.

Finzi A, Xiang SH, Pacheco B, Wang L, Haight J, Kassa A, Danek B, Pancera M, Kwong PD, Sodroski J. Topological layers in the HIV-1 gp120 inner domain regulate gp41 interaction and CD4-triggered conformational transitions. Mol Cell. 2010; 37:656–667.

Fontaine J, Chagnon-Choquet J, Valcke HS, Poudrier J, Roger M, Montreal Primary HIVI, Long-Term Non-Progressor Study, G. High expression levels of B lymphocyte stimulator (BLyS) by dendritic cells correlate with HIV-related B-cell disease progression in humans. Blood. 2011; 117:145–155.

Fontaine J, Coutlee F, Tremblay C, Routy JP, Poudrier J, Roger M, Montreal Primary HIVI, Long Term Non-progressor Study, G. HIV infection affects blood myeloid dendritic cells after successful therapy and despite non-progressing clinical disease. J Infect Dis. 2009; 199:1007–1018.

Herschhorn A, Gu C, Moraca F, Ma X, Farrell M, Smith AB, III, Pancera M, Kwong PD, Schon A, Freire E, Abrams C, Blanchard SC, Mothes W, Sodroski JG. The beta20-beta21 of gp120 is a regulatory switch for HIV-1 Env conformational transitions. Nat Commun. 2017; 8:1049.

Herschhorn A, Ma X, Gu C, Ventura JD, Castillo-Menendez L, Melillo B, Terry DS, Smith AB, III, Blanchard SC, Munro JB, Mothes W, Finzi A, Sodroski J. Release of gp120 restraints leads to an entry-competent intermediate state of the HIV-1 envelope glycoproteins. mBio. 2016; 7:e01598-16.

International HIV Controllers Study, Pereyra F, Jia X, McLaren PJ, Telenti A, de Bakker PI, Walker BD, Ripke S, Brumme CJ, Pulit SL, Carrington M, Kadie CM, Carlson JM, Heckerman D, Graham RR, Plenge RM, Deeks SG, Gianniny L, Crawford G, Sullivan J,

Gonzalez E, Davies L, Camargo A, Moore JM, Beattie N, Gupta S, Crenshaw A, Burtt NP, Guiducci C, Gupta N, Gao X, Qi Y, Yuki Y, Piechocka-Trocha A, Cutrell E, Rosenberg R, Moss KL, Lemay P, O'Leary J, Schaefer T, Verma P, Toth I, Block B, Baker B, Rothchild A, Lian J, Proudfoot J, Alvino DM, Vine S, Addo MM, et al. 2010. The major genetic determinants of HIV-1 control affect HLA class I peptide presentation. Science 330:1551–1557.

Julien JP, Cupo A, Sok D, Stanfield RL, Lyumkis D, Deller MC, Klasse PJ, Burton DR, Sanders RW, Moore JP, Ward AB, Wilson IA. Crystal structure of a soluble cleaved HIV-1 envelope trimer. Science. 2013; 342:1477-83.

Kamya P, Boulet S, Tsoukas CM, Routy JP, Thomas R, Cote P, Boulassel MR, Baril JG, Kovacs C, Migueles SA, Connors M, Suscovich TJ, Brander C, Tremblay CL, Bernard N, Canadian Cohort of, H.I.V.I.S.P. Receptor-ligand requirements for increased NK cell polyfunctional potential in slow progressors infected with HIV-1 co-expressing KIR3DL1*h/*y and HLA-B*57. J Virol. 2011; 85:5949–5960.

Kwon YD, Finzi A, Wu X, Dogo-Isonagie C, Lee LK, Moore LR, Schmidt SD, Stuckey J, Yang Y, Zhou T, Zhu J, Vicic DA, Debnath AK, Shapiro L, Bewley CA, Mascola JR, Sodroski JG, Kwong PD. Unliganded HIV-1 gp120 core structures assume the CD4-bound conformation with regulation by quaternary interactions and variable loops. Proc Natl Acad Sci USA. 2012; 109:5663–5668.

Lewis GK, Finzi A, DeVico AL, Pazgier M. Conformational masking and receptor-dependent unmasking of highly conserved Env epitopes recognized by non-neutralizing antibodies that mediate potent ADCC against HIV-1. Viruses. 2015; 7:5115–5132.

Lewis GK, Pazgier M, Evans D, Ferrari G, Bournazos S, Parsons MS, Bernard NF, Finzi A. Beyond viral neutralization. AIDS Res Hum Retroviruses. 2017 Liu J, Bartesaghi A, Borgnia MJ, Sapiro G, Subramaniam S. Molecular architecture of native HIV-1 gp120 trimers. Nature. 2008; 455:109–113.

Lu M, Blacklow SC, Kim PS. A trimeric structural domain of the HIV-1 transmembrane glycoprotein. Nat Struct Biol. 1995; 2:1075–1082.

Lyumkis D, Julien JP, de Val N, Cupo A, Potter CS, Klasse PJ, Burton DR, Sanders RW, Moore JP, Carragher B, Wilson IA, Ward AB. Cryo-EM structure of a fully glycosylated soluble cleaved HIV-1 envelope trimer. Science. 2013; 342:1484-90.

Madani N, Princiotto AM, Easterhoff D, Bradley T, Luo K, Williams WB, Liao HX, Moody MA, Phad GE, Vazquez Bernat N, Melillo B, Santra S, Smith AB, III, Karlsson Hedestam GB, Haynes B, Sodroski J. Antibodies elicited by multiple envelope glycoprotein immunogens in primates neutralize primary human immunodeficiency viruses (HIV-1) sensitized by CD4-mimetic compounds. J Virol. 2016; 90:5031–5046.

Mao Y, Wang L, Gu C, Herschhorn A, Xiang SH, Haim H, Yang X, Sodroski J. Subunit organization of the membrane-bound HIV-1 envelope glycoprotein trimer. Nat Struct Mol Biol. 2012; 19:893– 899.

Medjahed H, Pacheco B, Desormeaux A, Sodroski J, Finzi A. The HIV-1 gp120 major variable regions modulate cold inactivation. J Virol. 2013; 87:4103–4111.

Munro JB, Gorman J, Ma X, Zhou Z, Arthos J, Burton DR, Koff WC, Courter JR, Smith AB, III, Kwong PD, Blanchard SC, Mothes W. Conformational dynamics of single HIV-1 envelope trimers on the surface of native virions. Science. 2014; 346:759–763.

O'Rourke SM, Schweighardt B, Phung P, Mesa KA, Vollrath AL, Tatsuno GP, To B, Sinangil F, Limoli K, Wrin T, Berman PW. Sequences in glycoproteingp41, the CD4 binding site, and the V2 domain regulate sensitivity and resistance of HIV-1 to broadly neutralizing antibodies. J Virol. 2012; 86:12105–12114.

Ochsenbauer C, Edmonds TG, Ding H, Keele BF, Decker J, Salazar MG, Salazar-Gonzalez JF, Shattock R, Haynes BF, Shaw GM, Hahn BH, Kappes JC. Generation of transmitted/founder HIV-1 infectious molecular clones and characterization of their replication capacity in CD4 T lymphocytes and monocyte-derived macrophages. J Virol. 2012; 86:2715–2728.

Pancera M, Zhou T, Druz A, Georgiev IS, Soto C, Gorman J, Huang J, Acharya P, Chuang GY, Ofek G, Stewart-Jones GB, Stuckey J, Bailer RT, Joyce MG, Louder MK, Tumba N, Yang Y, Zhang B, Cohen MS, Haynes BF, Mascola JR, Morris L, Munro JB, Blanchard SC, Mothes W, Connors M, Kwong PD. Structure and immune recognition of trimeric pre-fusion HIV-1 Env. Nature. 2014; 514:455–461.

Parrish NF, Gao F, Li H, Giorgi EE, Barbian HJ, Parrish EH, Zajic L, Iyer SS, Decker JM, Kumar A, Hora B, Berg A, Cai F, Hopper J, Denny TN, Ding H, Ochsenbauer C, Kappes JC, Galimidi RP, West AP Jr, Bjorkman PJ, Wilen CB, Doms RW, O'Brien M, Bhardwaj N,

Borrow P, Haynes BF, Muldoon M, Theiler JP, Korber B, Shaw GM, Hahn BH. Phenotypic properties of transmitted founder HIV-1. Proc Natl Acad Sci USA. 2013; 110:6626–6633.

Peretz Y, Ndongala ML, Boulet S, Boulassel MR, Rouleau D, Cote P, Longpre D, Routy JP, Falutz J, Tremblay C, Tsoukas CM, Sekaly RP, Bernard NF. Functional T cell subsets contribute differentially to HIV peptide-specific responses within infected individuals: correlation of these functional T cell subsets with markers of disease progression. Clin Immunol. 2007; 124:57–68.

Prevost J, Zoubchenok D, Richard J, Veillette M, Pacheco B, Coutu M, Brassard N, Parsons MS, Ruxrungtham K, Bunupuradah T, Tovanabutra S, Hwang KK, Moody MA, Haynes BF, Bonsignori M, Sodroski J, Kaufmann DE, Shaw GM, Chenine AL, Finzi A. Influence of the envelope gp120 Phe43 cavity on HIV-1 sensitivity to antibody-dependent cell-mediated cytotoxicity responses. J Virol. 2017; 91:e02452-16.

Richard J, Pacheco B, Gohain N, Veillette M, Ding S, Alsahafi N, Tolbert WD, Prevost J, Chapleau JP, Coutu M, Jia M, Brassard N, Park J, Courter JR, Melillo B, Martin L, Tremblay C, Hahn BH, Kaufmann DE, Wu X, Smith AB, III, Sodroski J, Pazgier M, Finzi A. Co-receptor Binding Site Antibodies Enable CD4-Mimetics to Expose Conserved Anti-cluster A ADCC Epitopes on HIV-1 Envelope Glycoproteins. EBioMedicine. 2016a; 12:208-218.

Richard J, Prevost J, von Bredow B, Ding S, Brassard N, Medjahed H, Coutu M, Melillo B, Bibollet-Ruche F, Hahn BH, Kaufmann DE, Smith AB, III, Sodroski J, Sauter D, Kirchhoff F, Gee K, Neil SJ, Evans DT, Finzi A. BST-2 expression Modulates small CD4-mimetic sensitization of HIV-1- infected cells to antibody-dependent cellular cytotoxicity. J Virol. 2017; 91:e00219-17.

Richard J, Sindhu S, Pham TN, Belzile JP, Cohen EA. HIV-1 Vpr up-regulates expression of ligands for the activating NKG2D receptor and promotes NK cell-mediated killing. Blood. 2010; 115:1354–1363.

Richard J, Veillette M, Batraville LA, Coutu M, Chapleau JP, Bonsignori M, Bernard N, Tremblay C, Roger M, Kaufmann DE, Finzi A. Flow cytometry-based assay to study HIV-1gp120 specific antibody-dependent cellular cytotoxicity responses. J Virol Methods. 2014; 208:107–114.

Richard J, Veillette M, Brassard N, Iyer SS, Roger M, Martin L, Pazgier M, Schon A, Freire E, Routy JP, Smith AB, III, Park J, Jones DM, Courter JR, Melillo BN, Kaufmann DE, Hahn

BH, Permar SR, Haynes BF, Madani N, Sodroski JG, Finzi A. CD4 mimetics sensitize HIV-1-infected cells to ADCC. Proc Natl Acad Sci USA. 2015; 112:E2687–E2694.

Richard J, Veillette M, Ding S, Zoubchenok D, Alsahafi N, Coutu M, Brassard N, Park J, Courter JR, Melillo B, Smith AB, III, Shaw GM, Hahn BH, Sodroski J, Kaufmann DE, Finzi A. Small CD4 mimetics prevent HIV-1 uninfected bystander CD4 + T cell killing mediated by antibody-dependent cell-mediated cytotoxicity. EBioMedicine. 2016b; 3:122–134.

Robey WG, Safai B, Oroszlan S, Arthur LO, Gonda MA, Gallo RC, Fischinger PJ. Characterization of envelope and core structural gene products of HTLV-III with sera from AIDS patients. Science. 1985; 228:593–595.

Tolbert WD, Gohain N, Alsahafi N, Van V, Orlandi C, Ding S, Martin L, Finzi A, Lewis GK, Ray K, Pazgier M. Targeting the late stage of HIV-1 entry for antibody-dependent cellular cytotoxicity: structural basis for Env epitopes in the C11 region. Structure. 2017; 25:1719-1731.e4.

Veillette M, Coutu M, Richard J, Batraville LA, Dagher O, Bernard N, Tremblay C, Kaufmann DE, Roger M, Finzi A. The HIV-1 gp120 CD4-bound conformation is preferentially targeted by antibody-dependent cellular cytotoxicity-mediating antibodies in sera from HIV-1-infected individuals. J Virol. 2015; 89:545–551.

Veillette M, Coutu M, Richard J, Batraville LA, Desormeaux A, Roger M, Finzi A. Conformational evaluation of HIV-1 trimeric envelope glycoproteins using a cell-based ELISA assay. J Vis Exp: JoVE. 2014a; 14:51995.

Veillette M, Desormeaux A, Medjahed H, Gharsallah NE, Coutu M, Baalwa J, Guan Y, Lewis G, Ferrari G, Hahn BH, Haynes BF, Robinson JE, Kaufmann DE, Bonsignori M, Sodroski J, Finzi A. Interaction with cellular CD4 exposes HIV-1 envelope epitopes targeted by antibody-dependent cell-mediated cytotoxicity. J Virol. 2014b; 88:2633–2644.

Veillette M, Richard J, Pazgier M, Lewis GK, Parsons MS, Finzi A. Role of HIV-1 Envelope Glycoproteins Conformation and Accessory Proteins on ADCC Responses. Curr HIV Res. 2016; 14:9–23.

von Bredow B, Arias JF, Heyer LN, Gardner MR, Farzan M, Rakasz EG, Evans DT. Envelope glycoprotein internalization protects human and simian immunodeficiency virus infected cells from antibody-dependent cell-mediated cytotoxicity. J Virol. 2015; 89:10648-55.

von Bredow B, Arias JF, Heyer LN, Moldt B, Le K, Robinson JE, Zolla-Pazner S, Burton DR, Evans DT. Comparison of antibody-dependent cell-mediated cytotoxicity and virus neutralization by HIV-1 Env-specific monoclonal antibodies. J Virol. 2016; 90:6127–6139.

Weissenhorn W, Dessen A, Harrison SC, Skehel JJ, Wiley DC. Atomic structure of the ectodomain from HIV-1 gp41. Nature. 1997; 387:426–430.

White TA, Bartesaghi A, Borgnia MJ, Meyerson JR, de la Cruz MJ, Bess JW, Nandwani R, Hoxie JA, Lifson JD, Milne JL, Subramaniam S. Molecular architectures of trimeric SIV and HIV-1 envelope glycoproteins on intact viruses: strain-dependent variation in quaternary structure. PLoS Pathog. 2010; 6:e1001249.

Wyatt R, Sodroski J. The HIV-1 envelope glycoproteins: fusogens, antigens, and immunogens. Science. 1998; 280:1884–1888.

4.2.9 FIGURES

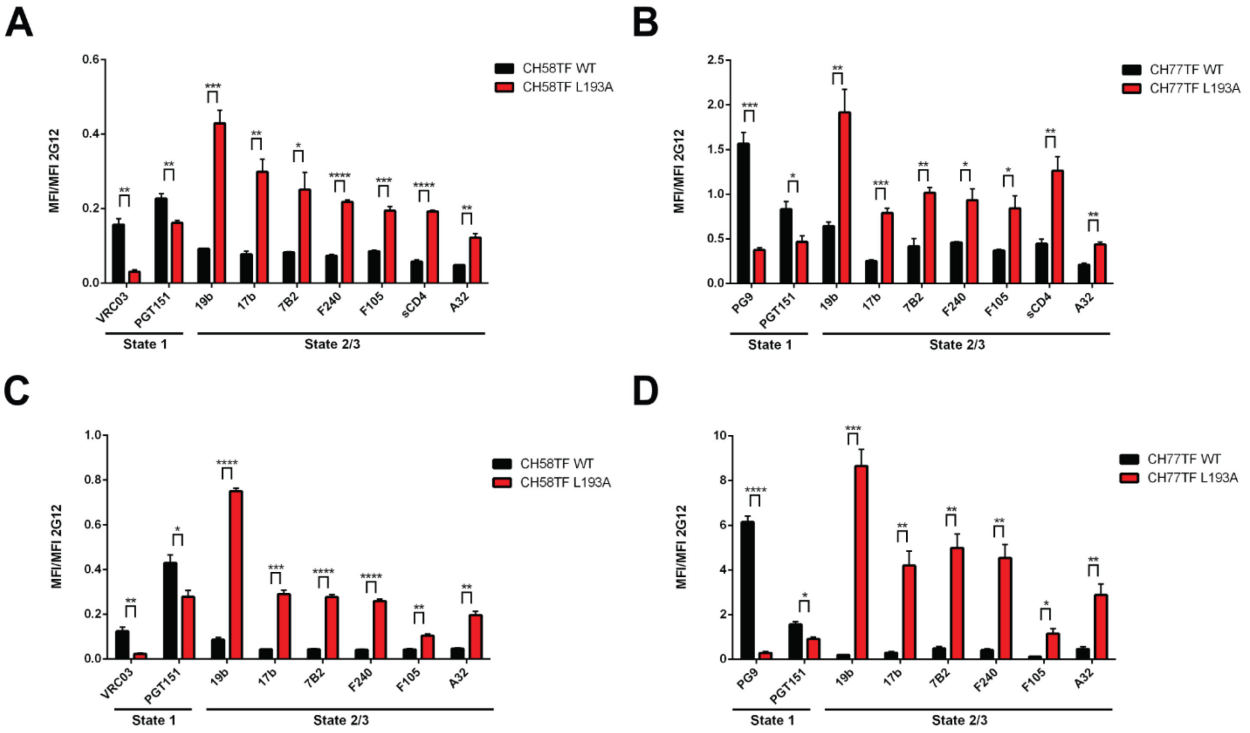

Figure 4.1.1 - HIV-1 Env L193A variant is stabilized in a State 2/3-like conformation. Cell-surface staining of 293T transfected cells (A, B) or primary $CD4^+$ T cells infected (C, D) with transmitted-founder IMCs CH58 and CH77 WT or L193A variants using State 1-preferring antibodies (VRC03, PGT151, PG9) or State 2/3-preferring antibodies (19b, 17b, 7B2, F240, F105, A32). Assessment of sCD4 binding (followed by anti-CD4 OKT4 mAb staining) was performed in 293T cells only. Shown are the mean fluorescence intensities (MFI) obtained in the infected (p24+) population for staining obtained in at least 3 independent experiments. Error bars indicate mean +/- SEM. Statistical significance was tested using an unpaired two-tailed t-test (*, $P < 0.05$, **, $P < 0.01$, ***, $P < 0.001$, ****, $P < 0.0001$).

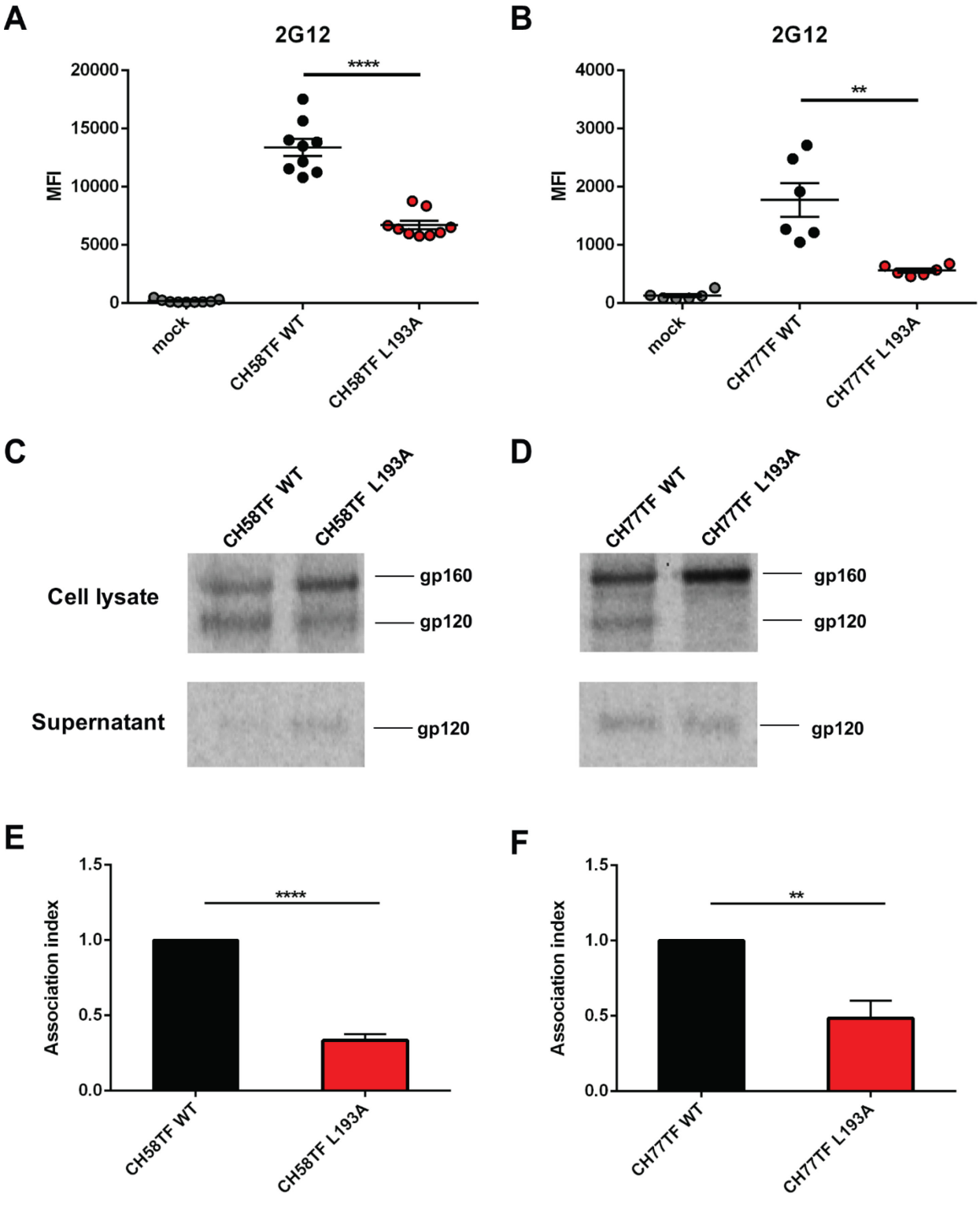
A
2G12
MFI
20000
15000
10000
5000
0
****
mock
CH58TF WT
CH58TF L193A
B
2G12
MFI
4000
3000
2000
1000
0
**
mock
CH77TF WT
CH77TF L193A
C
CH58TF WT
CH58TF L193A
Cell lysate
gp160
gp120
Supernatant
gp120
D
CH77TF WT
CH77TF L193A
gp160
gp120
gp120
E
Association index
1.5
1.0
0.5
0.0
****
CH58TF WT
CH58TF L193A
F
Association index
1.5
1.0
0.5
0.0
**
CH77TF WT
CH77TF L193A

Figure 4.1.2 - Introduction of the L193A change induces gp120 shedding.
Cell-surface staining of primary $CD4^+$ T cells, either mock-infected or infected with transmitted-founder IMCs CH58, CH77 WT or L193A variants, with the conformation-independent anti-gp120 2G12 mAb (**A, B**). The mean fluorescence intensities (MFI) on infected ($p24^+$) cells obtained in at least 6 independent experiments are shown. In order to evaluate the impact of the L193A change on gp120 shedding, 293T cells were transfected with WT or L193A variants and metabolically-labeled with ^{35}S. Cell lysates and supernatants (**C, D**) were immunoprecipitated with sera from HIV-1-infected patients. The precipitated proteins were loaded onto SDS-PAGE gels and analyzed by autoradiography and densitometry to calculate their association indexes (**E, F**). The association index is a measure of the ability of the mutant gp120 molecule to remain associated with the envelope glycoprotein complex on the expressing cell relative to that of the wild-type envelope glycoproteins. Shown are association indexes calculated in 3 independent experiments. Error bars indicate mean ± SEM. Statistical significance was tested using an unpaired two-tailed ttest (**, $P < 0.01$, ****, $P < 0.0001$).

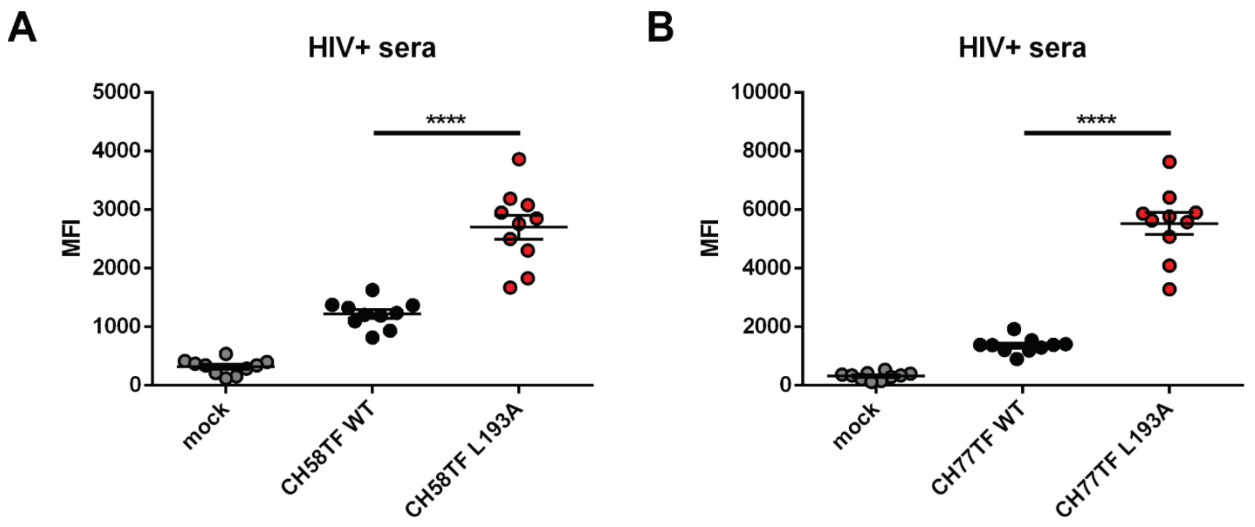

Figure 4.1.3 - Recognition of HIV-1-infected cells by sera from HIV-1-infected and uninfected individuals.

Cell surface staining of primary $CD4^+$ T cells either mock-infected or infected with transmitted-founder CH58, CH77 WT or L193A variants with sera from 10 HIV-1-infected individuals (**A, B**). The mean fluorescence intensities (MFI) when gating in the infected ($p24^+$) cell population obtained in at least 5 independent experiments are shown. Error bars indicate mean +/- SEM. Statistical significance was tested using a paired two-tailed t-test (****, $P < 0.0001$).

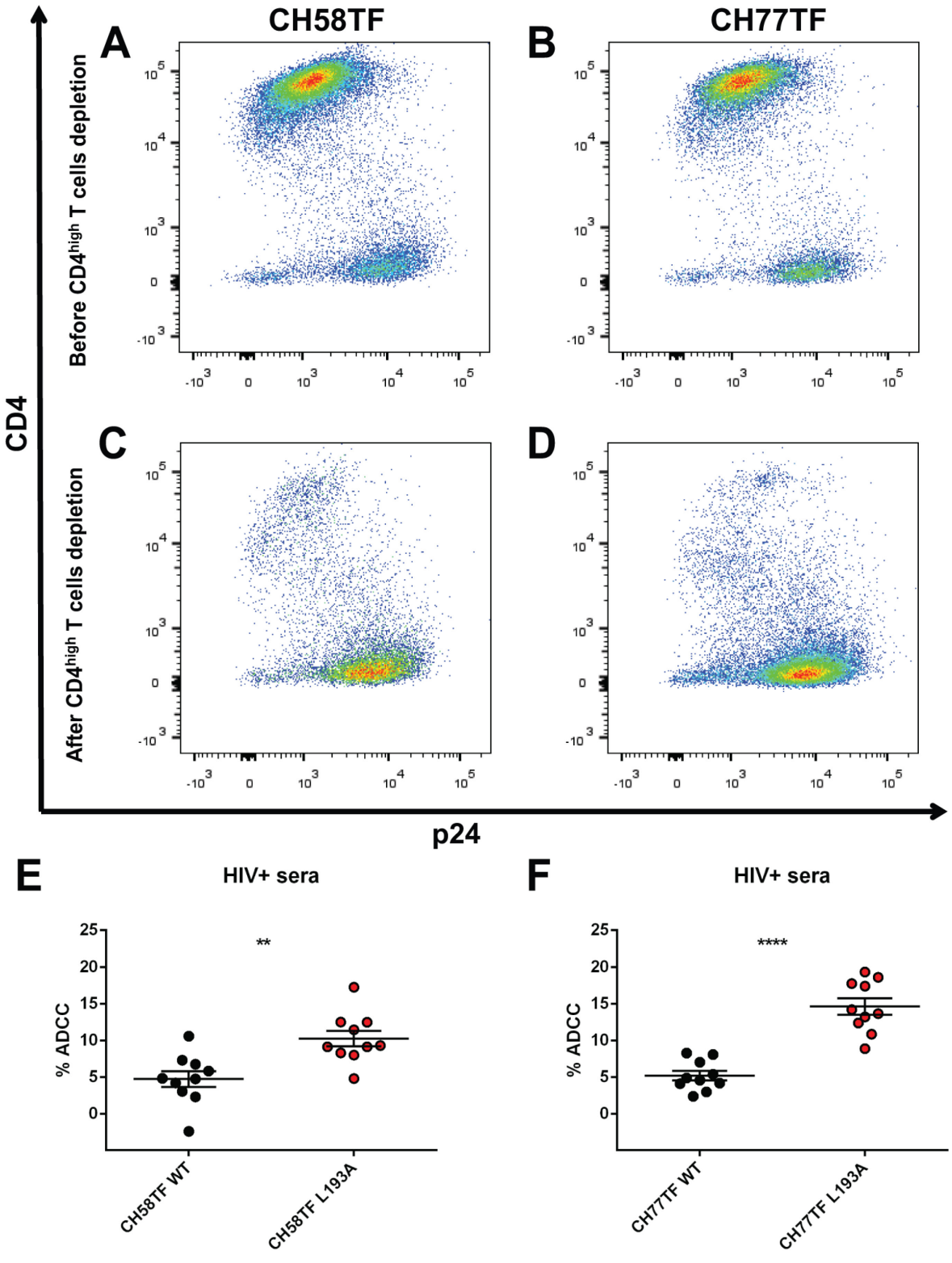
CH58TF
CH77TF
A
B
C
D
Before CD4high T cells depletion
After CD4high T cells depletion
CD4
p24
E
F
HIV+ sera
HIV+ sera
% ADCC
% ADCC
**
****
CH58TF WT
CH58TF L193A
CH77TF WT
CH77TF L193A

Figure 4.1.4 - Cells expressing Env stabilized in States 2/3 are more susceptible to ADCC responses mediated by HIV$^+$ sera.
Primary CD4$^+$ T cells infected with transmitted-founder CH58, CH77 WT or L193A variants were stained with anti-CD4 OKT4 mAb before (**A, B**) or after (**C, D**) removal of uninfected bystander CD4high cell, as described in material and methods. (**E, F**) Enriched productively-infected cells (p24$^+$ CD4^{low}) were used as target cells and incubated with autologous PBMC (used as effector cells) in the presence of sera from 10 HIV-1-infected individuals. The percentage of ADCC was calculated as described in material and methods. Results are representative of those obtained in at least 5 independent experiments. Error bars indicate mean ± SEM. (**E,F**) statistical significance was tested using a paired two-tailed t-test (**, $P < 0.01$, ****, $P < 0.0001$).

ARTICLE 6

Le clivage protéolytique des glycoprotéines d'enveloppe du VIH-1 protège les cellules infectées de la réponse ADCC médiée par le plasma d'individus infectés

HIV-1 Envelope Glycoproteins Proteolytic Cleavage Protects Infected Cells from ADCC Mediated by Plasma from Infected Individuals

Auteurs:

Jérémie Prévost[1,2], Halima Medjahed[1], Dani Vézina[1], Hung-Ching Chen[3], Beatrice H. Hahn[4], Amos B. Smith III[3], Andrés Finzi[1,2]

Affiliations:

[1]Centre de Recherche du CHUM, Montreal, QC, Canada; [2]Département de Microbiologie, Infectiologie et Immunologie, Université de Montréal, Montreal, QC, Canada; [3]Department of Chemistry, School of Arts and Sciences, University of Pennsylvania, Philadelphia, PA, USA; [4]Departments of Medicine and Microbiology, Perelman School of Medicine, University of Pennsylvania, Philadelphia, PA, USA.

Contribution des auteurs:

Conceptualisation: **J.P.** et A.F.; Méthodologie: **J.P.** et A.F.; Recherche: **J.P.**, H.M. et D.V.; Ressources: H.-C.C., B.H.H., A.B.S. et A.F.; Analyse formelle: **J.P.**; Visualisation: **J.P.**; Supervision: A.F.; Obtention du financement: B.H.H., A.B.S. et A.F.; Rédaction - version originale: **J.P.** et A.F.; Rédaction - révision et édition: **Tous les auteurs**.

Statut : Cet article a été publié dans *Viruses*, le 6 novembre 2021
https://doi.org/10.3390/v13112236

4.3.1 RÉSUMÉ

Les glycoprotéines d'enveloppe du VIH-1 (Env) sont synthétisées dans le réticulum endoplasmique sous la forme d'un précurseur trimérique de gp160, qui nécessite le clivage protéolytique par une protéase cellulaire de type furine pour assurer la fusion virus-cellule. L'Env est flexible sur le plan de la conformation, mais contrôle sa transition de la conformation "fermée" non-liée (conformation 1) aux conformations liées à CD4 (conformations 2/3), qui sont nécessaires à la fusion. Entre autres, le VIH-1 a développé plusieurs mécanismes qui réduisent l'ouverture prématurée d'Env, afin d'empêcher l'exposition d'épitopes hautement conservés reconnus par des anticorps non-neutralisants (nnAbs) capables de médier la réponse cytotoxique cellulaire dépendante des anticorps (ADCC). Le clivage d'Env diminue ses transitions conformationnelles favorisant l'adoption de la conformation "fermée". Ici, nous avons modifié le site de clivage de la gp160 par la furine afin d'empêcher le clivage de l'Env et d'examiner son impact sur la réponse ADCC médiée par le plasma d'individus infectés par le VIH-1. Nous avons constaté que les lymphocytes T $CD4^+$ primaires infectés exprimant l'Env non-clivée, mais pas de type sauvage, sont reconnus efficacement par les nnAbs et deviennent très sensibles à la réponse ADCC médiée par le plasma d'individus infectés par le VIH-1. Ainsi, le VIH-1 limite l'exposition de l'Env non-clivée à la surface des cellules infectées, du moins en partie pour échapper à la réponse ADCC.

4.3.2 ABSTRACT

The HIV-1 envelope glycoprotein (Env) is synthesized in the endoplasmic reticulum as a trimeric gp160 precursor, which requires proteolytic cleavage by a cellular furin protease to mediate virus-cell fusion. Env is conformationally flexible but controls its transition from the unbound "closed" conformation (State 1) to downstream CD4-bound conformations (States 2/3), which are required for fusion. In particular, HIV-1 has evolved several mechanisms that reduce the premature "opening" of Env which exposes highly conserved epitopes recognized by non-neutralizing antibodies (nnAbs) capable of mediating antibody-dependent cellular cytotoxicity (ADCC). Env cleavage decreases its conformational transitions favoring the adoption of the "closed" conformation. Here we altered the gp160 furin cleavage site to impair Env cleavage and to examine its impact on ADCC responses mediated by plasma from HIV-1-infected individuals. We found that infected primary $CD4^+$ T cells expressing uncleaved, but not wildtype, Env are efficiently recognized by nnAbs and become highly susceptible to ADCC responses mediated by

plasma from HIV-1-infected individuals. Thus, HIV-1 limits the exposure of uncleaved Env at the surface of HIV-1-infected cells at least in part to escape ADCC responses.

4.3.3 INTRODUCTION

The human immunodeficiency virus type 1 (HIV-1) envelope glycoprotein (Env) is a class I viral membrane fusion protein which mediates viral entry using the CD4 cellular receptor. The envelope gp160 precursor is synthesized in the endoplasmic reticulum (ER) and oligomerizes as a trimer [1,2]. Subsequently, the trimeric Env traffics through the trans-Golgi network (TGN) to reach the plasma membrane and to be incorporated into nascent HIV-1 virions [3–5]. During its transit through the secretory pathway, Env undergoes important post-translational modifications, including N-linked and O-linked glycosylation as well as proteolytic cleavage [6–10]. The addition of high-mannose oligosaccharides takes place in the ER and these glycans are further processed to acquire complex modifications in the TGN [11]. Concomitantly, proprotein convertases present in the TGN, including furin and furin-like proteases, catalyze the cleavage of the immature gp160 polyprotein [12–15] into two functional non-covalently linked subunits: the exterior gp120 subunit, which is responsible for viral attachment and the transmembrane gp41 subunit, which mediates membrane fusion. The human furin protein is part of the subtilisin-like serine endoprotease family and recognizes polybasic motifs, having Arg-X-Lys/Arg-Arg (RXK/RR) as a consensus cleavage site [16]. HIV-1 Env possesses a highly conserved furin cleavage site at the gp120-gp41 junction (^{508}REKR^{511}) which is adjacent to the hydrophobic fusion peptide at the gp41 N-terminus, with furin cleavage being essential for viral infectivity [6,8,17,18]. A putative secondary furin cleavage site (^{500}KAKR^{503}), located a few residues upstream of the primary cleavage site, has been described but its function remains unclear [17,19].

The functional mature Env trimer is known to sample different conformations ranging from the pre-fusion “closed” metastable conformation (State 1) to the CD4-bound “open” conformation (State 3), transitioning through an intermediate asymmetric conformation (State 2) [20,21]. Env glycoproteins from primary isolates preferentially adopt the State 1 conformation, which is preferentially recognized by broadly neutralizing antibodies (bNAbs) [20,22–24] and can be triggered into downstream conformations by CD4 binding, which exposes highly conserved epitopes targeted by non-neutralizing antibodies (nnAbs) [20,25,26]. These nnAbs are rapidly

elicited upon infection and vaccination [27–32] and mediate potent Fc-effector functions, including antibody-dependent cellular cytotoxicity (ADCC) [26,33–38]. The binding of Env to CD4 on the surface of HIV-1-infected cells stabilizes Env in State 2A, which is highly susceptible to nnAbs-mediated ADCC [26,39,40]. However, HIV-1 has evolved to prevent the premature adoption of the CD4-bound conformation by downregulating and degrading pre-existing and newly-synthesized CD4 through its accessory proteins Nef and Vpu [26,35,41,42]. Small CD4 mimetic compounds (CD4mc) are being developed to "open up" Env, with the goal of harnessing the potential of nnAbs responses for prevention [31,32,38,43–46] and eradication [36,40,47–53] strategies. Another class of Env antagonists known as conformational blockers, which includes the FDA-approved drug Temsavir, prevents Env transitions to downstream conformations by stabilizing Env State 1 [20,22,54,55].

Besides Env-CD4 interaction, there are also structural features of HIV-1 Env that can modulate the sensitivity of HIV-1 to ADCC responses mediated by nnAbs present in plasma from infected individuals. Natural polymorphisms in the Phe43 cavity (notably in CRF01_AE strains) and mutations of conserved residues in the trimer association domain have been shown to modulate Env conformation [25,56–59] and as a result, the susceptibility of cells infected with these viruses to ADCC responses [51,60,61]. Similarly, proteolytic cleavage has been reported to stabilize a "closed" Env conformation [62–65], since mutations in the furin cleavage site resulted in the spontaneous sampling of downstream conformations, including Env State 2A [40,55,63]. Here we evaluate the impact of altering the Env furin cleavage site on the susceptibility of infected primary $CD4^+$ T cells to ADCC responses mediated by HIV^+ plasma.

4.3.4 MATERIALS AND METHODS

Ethics Statement

Written informed consent was obtained from all study participants (the Montreal Primary HIV Infection Cohort [66,67] and the Canadian Cohort of HIV Infected Slow Progressors [68–70]), and research adhered to the ethical guidelines of CRCHUM and was reviewed and approved by the CRCHUM institutional review board (ethics committee, approval number CE 16.164-CA). The research adhered to the standards indicated by the Declaration of Helsinki. All participants

were adults and provided informed written consent prior to enrolment in accordance with Institutional Review Board approval.

Cell Lines and Primary Cells

293T human embryonic kidney cells (obtained from ATCC) and TZM-bl cells (NIH AIDS Reagent Program) were maintained at 37 °C under 5% CO_2 in Dulbecco's Modified Eagle Medium (DMEM) (Wisent, St. Bruno, QC, Canada), supplemented with 5% fetal bovine serum (FBS) (VWR, Radnor, PA, USA) and 100 U/mL penicillin/streptomycin (Wisent). 293T cells were derived from 293 cells, into which the simian virus 40 T-antigen was inserted. TZM-bl were derived from HeLa cells and were engineered to stably express high levels of human CD4 and CCR5 and to contain the firefly luciferase reporter gene under the control of the HIV-1 promoter [71]. Primary human PBMCs and $CD4^+$ T cells were isolated, activated, and cultured as previously described [26]. Briefly, PBMCs were obtained by leukapheresis from six HIV-negative individuals (all males), and primary $CD4^+$ T lymphocytes were purified from resting PBMCs by negative selection using immunomagnetic beads per the manufacturer's instructions (StemCell Technologies, Vancouver, BC, Canada) and were activated with phytohemagglutinin-L (10 µg/mL) for 48 h and then maintained in RPMI-1640 (Thermo Fisher Scientific, Waltham, MA, USA) complete medium supplemented with rIL-2 (100 U/mL).

Antibodies and Sera

The following Abs were used to assess Env conformation at the cell surface: conformation-independent anti-gp120 outer-domain 2G12 (NIH AIDS Reagent Program), broadly- neutralizing antibodies anti-CD4 binding site VRC03 (NIH AIDS Reagent Program), anti-V2 apex PG9 (Polymun Scientific, Klosterneuburg, Austria), anti-V3 glycan PGT126, antigp41-gp120 interface PGT151 (IAVI), anti-V3 glycan 10-1074 (kindly provided by Michel Nussenzweig) and anti-fusion peptide VRC34 (kindly provided by John Mascola) as well as non-neutralizing antibodies anti-gp41 C-C loop F240, anti-V3 crown 19b, anti-coreceptor binding site 17b, anti-cluster A A32 and C11 (NIH AIDS Reagent Program). The HIV-IG polyclonal antibody consists of anti-HIV immunoglobulins purified from a pool of plasma from HIV^+ asymptomatic donors (NIH AIDS Reagent Program). Goat anti-human and anti-mouse antibodies pre-coupled to Alexa Fluor 647 (Invitrogen, Rockford, IL, USA) were used as secondary antibodies in flow cytometry

experiments. Plasma from HIV-infected individuals was collected, heat-inactivated and conserved at −80 ◦C until use. In most experiments, the 2G12 monoclonal Ab (mAb) was used to normalize Env expression because of its conformation independence. Both viruses used in the study (CH058 and CH077) are well recognized by 2G12 despite polymorphism found at position 295 in CH077 Env.

Small Molecules

The small-molecule CD4-mimetic compound BNM-III-170 was synthesized as described previously [72]. The HIV-1 attachment inhibitor Temsavir (BMS-626529) was purchased from APExBIO (Houston, TX, USA). The compounds were dissolved in dimethyl sulfoxide (DMSO) at a stock concentration of 10 mM and diluted to 50 µM in phosphate-buffered saline (PBS) for cell-surface staining and virus capture assay or in RPMI-1640 complete medium for ADCC assays.

Plasmids and Proviral Constructs

The vesicular stomatitis virus G (VSV-G)-encoding plasmid was previously described [73]. Transmitted/Founder (T/F) infectious molecular clones (IMCs) of patients CH058 and CH077 were previously reported [74–77]. To generate IMCs encoding for cleavage-deficient Env, two mutations (R508S/R511S) were introduced in the furin cleavage site (^{508}REKR^{511}) using the QuikChange II XL site-directed mutagenesis protocol (Agilent Technologies, Santa Clara, CA). The presence of the desired mutations was determined by automated DNA sequencing.

Radioactive Labeling and Immunoprecipitation of Envelope Glycoproteins

293T cells (3×10^5) were transfected by the calcium phosphate method with the different IMCs. One day after transfection, cells were metabolically labeled for 16 h with 100 µCi/mL of [^{35}S] methionine-cysteine ([^{35}S] Protein Labeling Mix; PerkinElmer, Waltham, MA, USA) in DMEM lacking methionine and cysteine and supplemented with 5% dialyzed fetal bovine serum. Cells were subsequently lysed in RIPA buffer (140 mM NaCl, 8 mM Na_2HPO_4, 2 mM NaH_2PO_4, 1% NP40, 0.05% sodium dodecyl sulfate (SDS), 1.2 mM sodium deoxycholate). Precipitation of radiolabeled envelope glycoproteins from the whole-cell lysates or found in the supernatant was performed with a pool of sera from HIV-1-infected individuals in the presence of 50 µL of 10% Protein A-Sepharose (Cytiva, Marlborough, MA) at 4 ◦C. The precipitated proteins were loaded

onto SDS-PAGE gels and analyzed by autoradiography and densitometry to calculate their processing indexes. The processing index is a measure of the conversion of the mutant gp160 Env precursor to mature gp120, relative to wild-type Env trimers. The processing index is calculated with the following formula: processing index = ([total gp120] mutant × [gp160] WT) / ([gp160] mutant × [total gp120] WT).

Viral Production and Infections

VSV-G-pseudotyped HIV-1 viruses were produced and concentrated as previously described [60]. Viruses were then used to infect activated primary $CD4^+$ T cells from healthy HIV-1 negative donors by spin infection at 800 × g for 1 h in 96-well plates at 25 °C. Viral preparations were titrated directly on primary $CD4^+$ T cells to achieve similar levels of infection among the different IMCs tested (around 10% of $p24^+$ cells). To assess viral infectivity, TZM-bl reporter cells were seeded at a density of 2×10^4 cells/well in 96-well luminometer-compatible tissue culture plates (PerkinElmer) 24 h before infection. Normalized amounts of viruses (according to reverse transcriptase activity [78]) in a final volume of 100 µL were then added to the target cells and incubated for 48 h at 37 °C. The medium was then removed from each well, and the cells were lysed by the addition of 30 µL of passive lysis buffer (Promega, Madison, WI, USA) and one freeze-thaw cycle. An LB 941 TriStar luminometer (Berthold Technologies, Bad Wildbad, Germany) was used to measure the luciferase activity of each well after the addition of 100 µL of luciferin buffer (15 mM $MgSO_4$, 15 mM KH_2PO_4 [pH 7.8], 1 mM ATP, and 1 mM 170 dithiothreitol) and 50 µL of 1 mM D-luciferin potassium salt (Prolume, Pinetop, AZ, USA).

Virus Capture Assay

The HIV-1 virus capture assay was previously reported [79]. Pseudoviral particles were produced by transfecting 2×10^6 293T cells with pNL4.3 R-E- Luc (NIH AIDS Reagent Program) (3.5 µg), HIV-1_{CH058} (3.5 µg), and VSV-G (1 µg) using the standard calcium phosphate method. Forty-eight hours later, virus-containing supernatant was collected, and cell debris were removed by centrifugation (1500 rpm for 10 min). Anti-Env antibodies was immobilized on white MaxiSorp ELISA plates (Thermo Fisher Scientific) at a concentration of 5 µg/mL in 100 µL of PBS overnight at 4 °C. Unbound antibodies were removed by washing twice the plates twice with PBS. Plates were subsequently blocked with 3% bovine serum albumin (BSA) in PBS for 1 h at room

temperature. After washing plates twice with PBS, 200 µL of virus-containing supernatants were added to the wells. After 4 to 6 h incubation, virions were removed, and the wells were washed three times with PBS. Virus capture by any given antibody was visualized by adding 1×10^4 293T cells per well in complete DMEM. To measure recombinant virus infectivity, 1×10^4 293T cells were directly mixed with 100 µL of virus-containing supernatants per well. Forty-eight hours post-infection, cells were lysed by the addition of 30 µL of passive lysis buffer (Promega) and one freeze-thaw cycle. An LB 941 TriStar luminometer (Berthold Technologies) was used to measure the luciferase activity of each well after the addition of 100 µL of luciferin buffer (15 mM $MgSO_4$, 15 mM KH_2PO_4 [pH 7.8], 1 mM ATP, and 1 mM dithiothreitol) and 50 µL of 1 mM D-luciferin potassium salt (Prolume).

Flow Cytometry Analysis of Cell-Surface and Intracellular Staining

Cell-surface staining of HIV-1-transfected and HIV-1-infected cells was executed as previously described [35,61]. For transfected cells, we used the standard calcium phosphate method to transfect 7 µg of each IMC into 2×10^6 293T cells. Binding of cell-surface HIV-1 Env by anti-Env mAbs (5 µg/mL) or HIV^+ plasma (1:1000 dilution) was performed at 48 h post-transfection. Similarly, cell-surface staining of infected cells was performed at 48 h post-infection. After cell-surface staining, transfected cells and infected cells were permeabilized using the Cytofix/Cytoperm Fixation/Permeabilization Kit (BD Biosciences, Mississauga, ON, Canada) and stained intracellularly using PE-conjugated mouse anti-p24 mAb (clone KC57; Beckman Coulter, Brea, CA, USA; 1:100 dilution). The percentage of transfected or infected cells ($p24^+$) was determined by gating on the living cell population according to a viability dye staining (Aqua Vivid, Thermo Fisher Scientific). Samples were acquired on an LSRII cytometer (BD Biosciences), and data analysis was performed using FlowJo v10.5.3 (Tree Star, Ashland, OR, USA).

FACS-Based ADCC Assay

Measurement of ADCC using the FACS-based assay was performed at 48 h post-infection as previously described [26,36]. Briefly, HIV-1-infected primary $CD4^+$ T cells were stained with AquaVivid viability dye and cell proliferation dye eFluor670 (Thermo Fisher Scientific) and used as target cells. Autologous PBMC effectors cells, stained with the cell proliferation dye eFluor450

(Thermo Fisher Scientific), were added at an effector: target ratio of 10:1 in 96-well V-bottom plates (Corning, Glendale, AZ, USA). A 1:1000 final dilution of HIV^+ plasma was added to appropriate wells and cells were incubated for 5 min at room temperature. The plates were subsequently centrifuged for 1 min at 300 × g and incubated at 37 °C, 5% CO_2 for 5 h before being fixed in a 2% PBS-formaldehyde solution. Samples were acquired on an LSRII cytometer (BD Biosciences) and data analysis was performed using FlowJo v10.5.3 (Tree Star). The percentage of ADCC was calculated with the following formula: (% of $p24^+$ cells in Targets plus Effectors) − (% of $p24^+$ cells in Targets plus Effectors plus sera) / (% of $p24^+$ cells in Targets) by gating on infected lived target cells.

Statistical Analysis

Statistics were analyzed using GraphPad Prism version 9.1.0 (GraphPad, San Diego, CA, USA). Every data set was tested for statistical normality and this information was used to apply the appropriate (parametric or nonparametric) statistical test. p values < 0.05 were considered significant; significance values are indicated as * $p < 0.05$, ** $p < 0.01$, *** $p < 0.001$, **** $p < 0.0001$.

4.3.5 RESULTS

Conformation of HIV-1 Uncleaved Env at the Surface of Infected Cells and Viral Particles.

To study the role of the furin cleavage site on Env conformation, we performed mutagenesis on the infectious molecular clones (IMCs) of clade B transmitted/founder (T/F) viruses CH058 and CH077. Envs from both viruses were previously shown to preferentially sample the "closed" State 1 conformation [61]. We introduced substitutions in the primary cleavage site at position 508 and 511 (**Figure 4.2.1A**), to replace the highly conserved arginine residues with serine residues (R508S/R511S; referred as Cl− mutant), a double mutant known to efficiently abrogate furin-dependant Env processing [64,80–82]. We used protein radioactive labelling of 293T cells transfected with the different IMC constructs followed by Env immunoprecipitation to confirm the effect of the mutations on Env cleavage (**Figure 4.2.1B–E**). As expected, Env glycoproteins expressed from the wild-type (WT) construct were efficiently cleaved while their cleavage-deficient (Cl−) counterpart yielded little to no detectable gp120 in

the 293T whole-cell lysates (**Figure 4.2.1B,D**). Although we observed some soluble gp120 in the supernatant of CH058-transfected cells, this was likely due to the presence of a second upstream cleavage site, which matched the furin consensus sequence (RAKR). The supernatant of CH077-transfected cells did not contain gp120 consistent with an altered upstream cleavage site (KAKR) (**Figure 4.2.1A**). Of note, two bands of gp160 with distinct molecular weights were observed in cells transfected with Cl− variants, a phenotype previously observed that was linked to a difference in Env trafficking and localization [83–85].

Subsequently, we evaluated the ability of a panel of bNAbs and nnAbs to recognize the cleaved (WT) and uncleaved (Cl−) Env at the surface of 293T cells. We selected these cells since they do not express CD4 and it has been well documented that the presence of CD4 affects Env conformation [26,35,86]. Cells were transfected with the different IMC constructs and virus-expressing cells were identified using Gag p24 staining (**Figure 4.2.1F,G**). Cell-surface Env expression was normalized using the conformation-independent 2G12 antibody. Cells expressing WT Env were preferentially recognized by the bNAbs preferring the State 1 conformation (PGT126, VRC03, PG9) and recognizing the fusion peptide (PGT151, VRC34) compared to those expressing the respective cleavage site mutants (**Figure 4.2.1F,G**). Conversely, the binding of nnAbs targeting the downstream conformations States 2/3 (19b, F240, 17b) and State 2A (A32, C11) was significantly enhanced on cells expressing uncleaved Env (**Figure 4.2.1F,G**). To confirm this phenotype in a physiologically more relevant culture system, we infected activated primary $CD4^+$ T cells with the different primary IMCs. Of note, all viruses were pseudotyped with the VSV G glycoprotein to normalize the level of infection and to compensate for the inability of uncleaved Env to mediate viral fusion. Consistent with the 293T results, productively-infected cells ($p24^+$ $CD4^{low}$) were more efficiently recognized by bNAbs when expressing cleaved Env, and by nnAbs when expressing uncleaved Env (**Figure 4.2.1H,I**). Overall, these results support and extend previous observations indicating that furin cleavage favors the adoption of the native "closed" conformation at the cell surface [40,65,84].

We next investigated the effect of furin cleavage on Env conformation at the surface of viral particles, since the viral membrane is known to be enriched in cholesterol, a lipid known to stabilize Env State 1 conformation by interacting with the gp41 membrane-proximal external

region (MPER) [87–89]. Since virions expressing the Env Cl−variants were unable to infect even highly permissive cells, we used a recently developed virus capture assay [79] (**Figure 4.2.2A**). Specifically, we generated luciferase reporter pseudovirions that contained both HIV-1 Env and VSV G glycoproteins, thus allowing captured virions to infect 293T cells in an Env-independent manner (i.e., 293T infection is driven by the incorporated VSV G glycoprotein, **Figure 4.2.2B**). Virions harboring WT Env were captured more efficiently by bNAbs, while virions harboring uncleaved Env were primarily bound by nnAbs (**Figure 4.2.2C**). The recognition of pseudovirions was also assessed using purified anti-HIV-1 immunoglobulins from HIV^+ asymptomatic donors (HIV-IG) [90]. Since the vast majority of naturally-elicited antibodies targets Env in its "open" conformation [26,27,34], HIV-IG polyclonal antibodies captured viral particles displaying immature Env in a larger proportion (**Figure 4.2.2D**). HIV-IG specific capture of uncleaved or cleaved Env could be further increased using the small molecule CD4mc BNM-III-170, which stabilizes the CD4-bound conformation (**Figure 4.2.2D**). Alternatively, treatment with the conformational blocker Temsavir decreased the capacity of HIV-IG to capture viral particles bearing Cl− Envs (**Figure 4.2.2D**), in agreement with its capacity to stabilize the "closed" conformation [20,22,55]. These results indicate that uncleaved Env can be forced into "open" or "closed" conformations using small molecule Env antagonists.

Impact of HIV-1 Env Proteolytic Cleavage on ADCC Responses Mediated by HIV^+ Plasma.

Knowing that alterations in the furin cleavage site increase the exposure of downstream conformations at the surface of infected cells and lentiviral particles, we sought to determine whether the presence of uncleaved Env at the surface of infected cells could also affect ADCC responses mediated by plasma from HIV-1-infected donors. Activated primary $CD4^+$ T cells were infected with WT or cleavage defective CH058 and CH077 and then examined for their susceptibility to ADCC killing following incubation with plasma from 15 different chronically HIV-1-infected individuals. As expected, HIV^+ plasma binding was significantly higher on infected cells expressing cleavage-deficient Env compared to WT Env (**Figure 4.2.3A,B**). Moreover, inhibition of Env cleavage led to strong ADCC responses, while WT-infected cells were protected from these responses mediated by HIV^+ plasma (**Figure 4.2.3C,D**). Treatment with BNM-III-170 was found to enhance the binding of HIV^+ plasma on both WT and Cl− mutant infected cells, consistent with its ability to expose CD4i epitopes. Accordingly, CD4mc addition

induced a potent ADCC response against WT-infected cells, but marginally enhanced the ADCC response against cells expressing cleavage-deficient Env, suggesting that CD4i epitope exposure by uncleaved Env is sufficient to trigger the elimination of infected cells by ADCC. Conversely, the addition of State 1-stabilizing molecule Temsavir protected Cl− expressing cells from ADCC by decreasing the binding of HIV^+ plasma to uncleaved Env (**Figure 4.2.3A–D**). Of note, Temsavir did not impact HIV^+ plasma mediated ADCC against WT infected cells since they are known to already express the Env in the "closed" conformation [26,35–37,40,60,61,86,91,92]. Altogether, our results demonstrate the importance for HIV-1 to limit the presence of Env gp160 precursor at the surface of infected cells to evade nnAbs-mediated ADCC responses.

4.3.6 DISCUSSION

In this study, we show that uncleaved HIV-1 Env trimers display conformational flexibility which favors the sampling of downstream "more open" conformations at the surface of infected cells and pseudoviral particles. Cell-surface expression of uncleaved gp160 leads to an efficient recognition of infected cells by non-neutralizing CD4i antibodies naturally present in plasma from HIV-1-infected individuals and as a consequence, leads to a significantly higher susceptibility to ADCC responses. Conversely, efficient cleavage by endogenous furin allows Env trimers to sample a metastable "closed" conformation (State 1), thus protecting HIV-1-infected cells from ADCC responses mediated by HIV^+ plasma. Beyond the well-established role of furin cleavage on viral infectivity, efficient proteolytic cleavage of Env trimers thus appears to allow HIV-1 to evade humoral immune responses. These results are important in the context of recent findings showing that several interferon-inducible cellular antiviral factors affect Env gp160 precursor processing [93–97]. Among them, IFITM proteins impair Env cleavage through direct interaction with Env, while GBP2 and GBP5 restrict furin protease activity [93,96]. The antiviral activity of both families of proteins can be overcome by HIV-1 through Env substitutions or by increasing Env expression through the deletion of the accessory Vpu protein, respectively [97–100]. According to the Los Alamos National Laboratory HIV sequence database, very few mutations are naturally found in the furin cleavage site, especially for the basic residues found at positions 508, 510, and 511 which are more than 99.7% conserved. Given the importance of an effective Env cleavage to generate infectious viral particles, therapeutic interventions designed to specifically inhibit this proteolytic cleavage could result in a loss in infectivity with a concomitant

increase in ADCC responses against infected cells. A recent study has shown that conformational blockers, such as Temsavir, can interfere with proper Env cleavage by reducing its conformational flexibility [63]. Additional drugs inhibiting directly the furin protease activity, including the synthetic peptide Dec-RVKR-CMK and the serine protease inhibitor α_1-PDX, are also being investigated, but their in vivo efficacy and toxicity remain to be determined [12,13,101–105]. If these broad-spectrum inhibitors end up being well-tolerated and exhibit good pharmacokinetic properties, they may also be useful as therapeutics against other viral infections, including Influenza A, Ebola, Respiratory syncytial virus (RSV), and SARS-CoV-2, where the acquisition of a furin cleavage site in the respective fusion glycoproteins appears to confer a higher level of infectivity [106–110].

4.3.7 ACKNOWLEDGMENTS

The authors thank the CRCHUM BSL3 and Flow Cytometry Platforms for technical assistance, Mario Legault from the FRQS AIDS and Infectious Diseases network for cohort coordination and clinical samples. We thank Michel Nussenzweig (The Rockefeller University) for 10-1074 and John Mascola (VRC, NIAID) for VRC34. The graphical abstract was prepared using illustrations from BioRender.com. This study was supported by grants from the National Institutes of Health to A.F. (R01 AI148379, R01 AI129769, and R01 AI150322) and BHH (R01 AI162646 and UM1 AI164570). Support for this work was also provided by P01 GM56550/AI150471 to A.B.S. and A.F. This work was partially supported by 1UM1AI164562-01, co-funded by National Heart, Lung and Blood Institute, National Institute of Diabetes and Digestive and Kidney Diseases, National Institute of Neurological Disorders and Stroke, National Institute on Drug Abuse and the National Institute of Allergy and Infectious Diseases, by a CIHR Foundation grant #352417, a CIHR Team Grant #422148 and a Canada Foundation for Innovation grant #41027 to A.F. A.F. is the recipient of a Canada Research Chair on Retroviral Entry #RCHS0235 950-232424. J.P. is the recipient of a CIHR doctoral fellowship. The funders had no role in study design, data collection and analysis, decision to publish, or preparation of the manuscript.

4.3.8 REFERENCES

1. Earl, P.L.; Doms, R.W.; Moss, B. Oligomeric structure of the human immunodeficiency virus type 1 envelope glycoprotein. Proc. Natl. Acad. Sci. USA 1990, 87, 648–652.
2. Earl, P.L.; Moss, B.; Doms, R.W. Folding, interaction with GRP78-BiP, assembly, and transport of the human immunodeficiency virus type 1 envelope protein. J. Virol. 1991, 65, 2047–2055.
3. Kantanen, M.L.; Leinikki, P.; Kuismanen, E. Endoproteolytic cleavage of HIV-1 gp160 envelope precursor occurs after exit from the trans-Golgi network (TGN). Arch. Virol. 1995, 140, 1441–1449.
4. Qi, M.; Williams, J.A.; Chu, H.; Chen, X.; Wang, J.J.; Ding, L.; Akhirome, E.; Wen, X.; Lapierre, L.A.; Goldenring, J.R.; et al. Rab11-FIP1C and Rab14 direct plasma membrane sorting and particle incorporation of the HIV-1 envelope glycoprotein complex. PLoS Pathog. 2013, 9, e1003278.
5. Kirschman, J.; Qi, M.; Ding, L.; Hammonds, J.; Dienger-Stambaugh, K.; Wang, J.J.; Lapierre, L.A.; Goldenring, J.R.; Spearman, P. HIV-1 Envelope Glycoprotein Trafficking through the Endosomal Recycling Compartment Is Required for Particle Incorporation. J. Virol. 2018, 92, e01893-17.
6. Freed, E.O.; Myers, D.J.; Risser, R. Mutational analysis of the cleavage sequence of the human immunodeficiency virus type 1 envelope glycoprotein precursor gp160. J. Virol. 1989, 63, 4670–4675.
7. Bosch, V.; Pawlita, M. Mutational analysis of the human immunodeficiency virus type 1 env gene product proteolytic cleavage site. J. Virol. 1990, 64, 2337–2344.
8. McCune, J.M.; Rabin, L.B.; Feinberg, M.B.; Lieberman, M.; Kosek, J.C.; Reyes, G.R.; Weissman, I.L. Endoproteolytic cleavage of gp160 is required for the activation of human immunodeficiency virus. Cell 1988, 53, 55–67.
9. Leonard, C.K.; Spellman, M.W.; Riddle, L.; Harris, R.J.; Thomas, J.N.; Gregory, T.J. Assignment of intrachain disulfide bonds and characterization of potential glycosylation sites of the type 1 recombinant human immunodeficiency virus envelope glycoprotein (gp120) expressed in Chinese hamster ovary cells. J. Biol. Chem. 1990, 265, 10373–10382.

10. Bernstein, H.B.; Tucker, S.P.; Hunter, E.; Schutzbach, J.S.; Compans, R.W. Human immunodeficiency virus type 1 envelope glycoprotein is modified by O-linked oligosaccharides. J. Virol. 1994, 68, 463–468.
11. Dewar, R.L.; Vasudevachari, M.B.; Natarajan, V.; Salzman, N.P. Biosynthesis and processing of human immunodeficiency virus type 1 envelope glycoproteins: Effects of monensin on glycosylation and transport. J. Virol. 1989, 63, 2452–2456.
12. Hallenberger, S.; Bosch, V.; Angliker, H.; Shaw, E.; Klenk, H.D.; Garten, W. Inhibition of furin-mediated cleavage activation of HIV-1 glycoprotein gp160. Nature 1992, 360, 358–361.
13. Decroly, E.; Vandenbranden, M.; Ruysschaert, J.M.; Cogniaux, J.; Jacob, G.S.; Howard, S.C.; Marshall, G.; Kompelli, A.; Basak, A.; Jean, F.; et al. The convertases furin and PC1 can both cleave the human immunodeficiency virus (HIV)-1 envelope glycoprotein gp160 into gp120 (HIV-1 SU) and gp41 (HIV-I TM). J. Biol. Chem. 1994, 269, 12240–12247.
14. Decroly, E.; Wouters, S.; Di Bello, C.; Lazure, C.; Ruysschaert, J.M.; Seidah, N.G. Identification of the paired basic convertases implicated in HIV gp160 processing based on in vitro assays and expression in CD4(+) cell lines. J. Biol. Chem. 1996, 271, 30442–30450.
15. Decroly, E.; Benjannet, S.; Savaria, D.; Seidah, N.G. Comparative functional role of PC7 and furin in the processing of the HIV envelope glycoprotein gp160. FEBS Lett. 1997, 405, 68–72.
16. Molloy, S.S.; Thomas, L.; VanSlyke, J.K.; Stenberg, P.E.; Thomas, G. Intracellular trafficking and activation of the furin proprotein convertase: Localization to the TGN and recycling from the cell surface. EMBO J. 1994, 13, 18–33.
17. Dubay, J.W.; Dubay, S.R.; Shin, H.J.; Hunter, E. Analysis of the cleavage site of the human immunodeficiency virus type 1 glycoprotein: Requirement of precursor cleavage for glycoprotein incorporation. J. Virol. 1995, 69, 4675–4682.
18. Herrera, C.; Klasse, P.J.; Michael, E.; Kake, S.; Barnes, K.; Kibler, C.W.; Campbell-Gardener, L.; Si, Z.; Sodroski, J.; Moore, J.P.; et al. The impact of envelope glycoprotein cleavage on the antigenicity, infectivity, and neutralization sensitivity of Env-pseudotyped human immunodeficiency virus type 1 particles. Virology 2005, 338, 154–172.

19. Pasquato, A.; Dettin, M.; Basak, A.; Gambaretto, R.; Tonin, L.; Seidah, N.G.; Di Bello, C. Heparin enhances the furin cleavage of HIV-1 gp160 peptides. FEBS Lett. 2007, 581, 5807–5813.
20. Munro, J.B.; Gorman, J.; Ma, X.; Zhou, Z.; Arthos, J.; Burton, D.R.; Koff, W.C.; Courter, J.R.; Smith, A.B., III; Kwong, P.D.; et al. Conformational dynamics of single HIV-1 envelope trimers on the surface of native virions. Science 2014, 346, 759–763.
21. Ma, X.; Lu, M.; Gorman, J.; Terry, D.S.; Hong, X.; Zhou, Z.; Zhao, H.; Altman, R.B.; Arthos, J.; Blanchard, S.C.; et al. HIV-1 Env trimer opens through an asymmetric intermediate in which individual protomers adopt distinct conformations. eLife 2018, 7, e34271.
22. Lu, M.; Ma, X.; Castillo-Menendez, L.R.; Gorman, J.; Alsahafi, N.; Ermel, U.; Terry, D.S.; Chambers, M.; Peng, D.; Zhang, B.; et al. Associating HIV-1 envelope glycoprotein structures with states on the virus observed by smFRET. Nature 2019. 568, 415-419.
23. Li, Z.; Li, W.; Lu, M.; Bess, J., Jr.; Chao, C.W.; Gorman, J.; Terry, D.S.; Zhang, B.; Zhou, T.; Blanchard, S.C.; et al. Subnanometer structures of HIV-1 envelope trimers on aldrithiol-2-inactivated virus particles. Nat. Struct. Mol. Biol. 2020, 27, 726–734.
24. Stadtmueller, B.M.; Bridges, M.D.; Dam, K.M.; Lerch, M.T.; Huey-Tubman, K.E.; Hubbell, W.L.; Bjorkman, P.J. DEER Spectroscopy Measurements Reveal Multiple Conformations of HIV-1 SOSIP Envelopes that Show Similarities with Envelopes on Native Virions. Immunity 2018, 49, 235–246.e234.
25. Finzi, A.; Xiang, S.H.; Pacheco, B.; Wang, L.; Haight, J.; Kassa, A.; Danek, B.; Pancera, M.; Kwong, P.D.; Sodroski, J. Topological layers in the HIV-1 gp120 inner domain regulate gp41 interaction and CD4-triggered conformational transitions. Mol. Cell 2010, 37, 656–667.
26. Veillette, M.; Desormeaux, A.; Medjahed, H.; Gharsallah, N.E.; Coutu, M.; Baalwa, J.; Guan, Y.; Lewis, G.; Ferrari, G.; Hahn, B.H.; et al. Interaction with cellular CD4 exposes HIV-1 envelope epitopes targeted by antibody-dependent cell-mediated cytotoxicity. J. Virol. 2014, 88, 2633–2644.
27. Decker, J.M.; Bibollet-Ruche, F.; Wei, X.; Wang, S.; Levy, D.N.; Wang, W.; Delaporte, E.; Peeters, M.; Derdeyn, C.A.; Allen, S.; et al. Antigenic conservation and immunogenicity of the HIV coreceptor binding site. J. Exp. Med. 2005, 201, 1407–1419.

28. Tomaras, G.D.; Yates, N.L.; Liu, P.; Qin, L.; Fouda, G.G.; Chavez, L.L.; Decamp, A.C.; Parks, R.J.; Ashley, V.C.; Lucas, J.T.; et al. Initial B-cell responses to transmitted human immunodeficiency virus type 1: Virion-binding immunoglobulin M (IgM) and IgG antibodies followed by plasma anti-gp41 antibodies with ineffective control of initial viremia. J. Virol. 2008, 82, 12449–12463.
29. Tomaras, G.D.; Haynes, B.F. HIV-1-specific antibody responses during acute and chronic HIV-1 infection. Curr. Opin. HIV AIDS 2009, 4, 373–379.
30. Davis, K.L.; Gray, E.S.; Moore, P.L.; Decker, J.M.; Salomon, A.; Montefiori, D.C.; Graham, B.S.; Keefer, M.C.; Pinter, A.; Morris, L.; et al. High titer HIV-1 V3-specific antibodies with broad reactivity but low neutralizing potency in acute infection and following vaccination. Virology 2009, 387, 414–426.
31. Madani, N.; Princiotto, A.M.; Easterhoff, D.; Bradley, T.; Luo, K.; Williams, W.B.; Liao, H.X.; Moody, M.A.; Phad, G.E.; Vazquez Bernat, N.; et al. Antibodies Elicited by Multiple Envelope Glycoprotein Immunogens in Primates Neutralize Primary Human Immunodeficiency Viruses (HIV-1) Sensitized by CD4-Mimetic Compounds. J. Virol. 2016, 90, 5031–5046.
32. Madani, N.; Princiotto, A.M.; Mach, L.; Ding, S.; Prevost, J.; Richard, J.; Hora, B.; Sutherland, L.; Zhao, C.A.; Conn, B.P.; et al. A CD4-mimetic compound enhances vaccine efficacy against stringent immunodeficiency virus challenge. Nat. Commun. 2018, 9, 2363.
33. Ferrari, G.; Pollara, J.; Kozink, D.; Harms, T.; Drinker, M.; Freel, S.; Moody, M.A.; Alam, S.M.; Tomaras, G.D.; Ochsenbauer, C.; et al. An HIV-1 gp120 envelope human monoclonal antibody that recognizes a C1 conformational epitope mediates potent antibody-dependent cellular cytotoxicity (ADCC) activity and defines a common ADCC epitope in human HIV-1 serum. J. Virol. 2011, 85, 7029–7036.
34. Guan, Y.; Pazgier, M.; Sajadi, M.M.; Kamin-Lewis, R.; Al-Darmarki, S.; Flinko, R.; Lovo, E.; Wu, X.; Robinson, J.E.; Seaman, M.S.; et al. Diverse specificity and effector function among human antibodies to HIV-1 envelope glycoprotein epitopes exposed by CD4 binding. Proc. Natl. Acad. Sci. USA 2013, 110, E69–E78.
35. Veillette, M.; Coutu, M.; Richard, J.; Batraville, L.A.; Dagher, O.; Bernard, N.; Tremblay, C.; Kaufmann, D.E.; Roger, M.; Finzi, A. The HIV-1 gp120 CD4-Bound Conformation Is

Preferentially Targeted by Antibody-Dependent Cellular Cytotoxicity-Mediating Antibodies in Sera from HIV-1-Infected Individuals. J. Virol. 2015, 89, 545–551.

36. Richard, J.; Veillette, M.; Brassard, N.; Iyer, S.S.; Roger, M.; Martin, L.; Pazgier, M.; Schon, A.; Freire, E.; Routy, J.P.; et al. CD4 mimetics sensitize HIV-1-infected cells to ADCC. Proc. Natl. Acad. Sci. USA 2015, 112, E2687–E2694.
37. Ding, S.; Veillette, M.; Coutu, M.; Prevost, J.; Scharf, L.; Bjorkman, P.J.; Ferrari, G.; Robinson, J.E.; Sturzel, C.; Hahn, B.H.; et al. A Highly Conserved Residue of the HIV-1 gp120 Inner Domain Is Important for Antibody-Dependent Cellular Cytotoxicity Responses Mediated by Anti-Cluster A Antibodies. J. Virol. 2016, 90, 2127–2134.
38. Ding, S.; Verly, M.M.; Princiotto, A.; Melillo, B.; Moody, T.; Bradley, T.; Easterhoff, D.; Roger, M.; Hahn, B.H.; Madani, N.; et al. Small Molecule CD4-Mimetics Sensitize HIV-1-infected Cells to ADCC by Antibodies Elicited by Multiple Envelope Glycoprotein Immunogens in Non-Human Primates. AIDS Res. Hum. Retrovir 2016, 33, 428-431
39. Veillette, M.; Coutu, M.; Richard, J.; Batraville, L.A.; Desormeaux, A.; Roger, M.; Finzi, A. Conformational evaluation of HIV-1 trimeric envelope glycoproteins using a cell-based ELISA assay. J. Vis. Exp. 2014, 14, 51995
40. Alsahafi, N.; Bakouche, N.; Kazemi, M.; Richard, J.; Ding, S.; Bhattacharyya, S.; Das, D.; Anand, S.P.; Prevost, J.; Tolbert, W.D.; et al. An Asymmetric Opening of HIV-1 Envelope Mediates Antibody-Dependent Cellular Cytotoxicity. Cell Host. Microbe. 2019, 25, 578–587.e575.
41. Willey, R.L.; Maldarelli, F.; Martin, M.A.; Strebel, K. Human immunodeficiency virus type 1 Vpu protein induces rapid degradation of CD4. J. Virol. 1992, 66, 7193–7200.
42. Rhee, S.S.; Marsh, J.W. Human immunodeficiency virus type 1 Nef-induced down-modulation of CD4 is due to rapid internalization and degradation of surface CD4. J. Virol. 1994, 68, 5156–5163.
43. Madani, N.; Schon, A.; Princiotto, A.M.; Lalonde, J.M.; Courter, J.R.; Soeta, T.; Ng, D.; Wang, L.; Brower, E.T.; Xiang, S.H.; et al. Small-molecule CD4 mimics interact with a highly conserved pocket on HIV-1 gp120. Structure 2008, 16, 1689–1701.
44. Madani, N.; Princiotto, A.M.; Schon, A.; LaLonde, J.; Feng, Y.; Freire, E.; Park, J.; Courter, J.R.; Jones, D.M.; Robinson, J.; et al. CD4-mimetic small molecules sensitize

human immunodeficiency virus to vaccine-elicited antibodies. J. Virol. 2014, 88, 6542–6555.

45. Madani, N.; Princiotto, A.M.; Zhao, C.; Jahanbakhshsefidi, F.; Mertens, M.; Herschhorn, A.; Melillo, B.; Smith, A.B., III; Sodroski, J. Activation and Inactivation of Primary Human Immunodeficiency Virus Envelope Glycoprotein Trimers by CD4-Mimetic Compounds. J. Virol. 2017, 91, e01880-16.
46. Princiotto, A.M.; Vrbanac, V.D.; Melillo, B.; Park, J.; Tager, A.M.; Smith, A.B., III; Sodroski, J.; Madani, N. A Small-Molecule CD4-Mimetic Compound Protects Bone Marrow-Liver-Thymus Humanized Mice From HIV-1 Infection. J. Infect. Dis. 2018, 218, 471–475.
47. Lee, W.S.; Richard, J.; Lichtfuss, M.; Smith, A.B., III; Park, J.; Courter, J.R.; Melillo, B.N.; Sodroski, J.G.; Kaufmann, D.E.; Finzi, A.; et al. Antibody-Dependent Cellular Cytotoxicity against Reactivated HIV-1-Infected Cells. J. Virol. 2015, 90, 2021–2030.
48. Richard, J.; Pacheco, B.; Gohain, N.; Veillette, M.; Ding, S.; Alsahafi, N.; Tolbert, W.D.; Prevost, J.; Chapleau, J.P.; Coutu, M.; et al. Co-receptor Binding Site Antibodies Enable CD4-Mimetics to Expose Conserved Anti-Cluster A ADCC Epitopes on HIV-1 Envelope Glycoproteins. EBioMedicine 2016, 12, 208–218.
49. Anand, S.P.; Prevost, J.; Baril, S.; Richard, J.; Medjahed, H.; Chapleau, J.P.; Tolbert, W.D.; Kirk, S.; Smith, A.B., III; Wines, B.D.; et al. Two Families of Env Antibodies Efficiently Engage Fc-Gamma Receptors and Eliminate HIV-1-Infected Cells. J. Virol. 2019, 93, e01823-18.
50. Ding, S.; Grenier, M.C.; Tolbert, W.D.; Vezina, D.; Sherburn, R.; Richard, J.; Prevost, J.; Chapleau, J.P.; Gendron-Lepage, G.; Medjahed, H.; et al. A New Family of Small-Molecule CD4-Mimetic Compounds Contacts Highly Conserved Aspartic Acid 368 of HIV-1 gp120 and Mediates Antibody-Dependent Cellular Cytotoxicity. J. Virol. 2019, 93, e01325-19.
51. Prevost, J.; Tolbert, W.D.; Medjahed, H.; Sherburn, R.T.; Madani, N.; Zoubchenok, D.; Gendron-Lepage, G.; Gaffney, A.E.; Grenier, M.C.; Kirk, S.; et al. The HIV-1 Env gp120 Inner Domain Shapes the Phe43 Cavity and the CD4 Binding Site. mBio 2020, 11, e00280-20.

52. Vezina, D.; Gong, S.Y.; Tolbert, W.D.; Ding, S.; Nguyen, D.; Richard, J.; Gendron-Lepage, G.; Melillo, B.; Smith, A.B., III; Pazgier, M.; et al. Stabilizing the HIV-1 envelope glycoprotein State 2A conformation. J. Virol. 2020, 95, e01620-20.
53. Rajashekar, J.K.; Richard, J.; Beloor, J.; Prevost, J.; Anand, S.P.; Beaudoin-Bussieres, G.; Shan, L.; Herndler-Brandstetter, D.; Gendron-Lepage, G.; Medjahed, H.; et al. Modulating HIV-1 envelope glycoprotein conformation to decrease the HIV-1 reservoir. Cell Host Microbe 2021, 29, 904–916.e906.
54. Zou, S.; Zhang, S.; Gaffney, A.; Ding, H.; Lu, M.; Grover, J.R.; Farrell, M.; Nguyen, H.T.; Zhao, C.; Anang, S.; et al. Long-Acting BMS-378806 Analogues Stabilize the State-1 Conformation of the Human Immunodeficiency Virus (HIV-1) Envelope Glycoproteins. J. Virol. 2020. 94, e00148-20.
55. Lu, M.; Ma, X.; Reichard, N.; Terry, D.S.; Arthos, J.; Smith, A.B., III; Sodroski, J.G.; Blanchard, S.C.; Mothes, W. Shedding-Resistant HIV-1 Envelope Glycoproteins Adopt Downstream Conformations That Remain Responsive to Conformation-Preferring Ligands. J. Virol. 2020, 94, e00597-20.
56. Xiang, S.H.; Kwong, P.D.; Gupta, R.; Rizzuto, C.D.; Casper, D.J.; Wyatt, R.; Wang, L.; Hendrickson, W.A.; Doyle, M.L.; Sodroski, J. Mutagenic stabilization and/or disruption of a CD4-bound state reveals distinct conformations of the human immunodeficiency virus type 1 gp120 envelope glycoprotein. J. Virol. 2002, 76, 9888–9899.
57. Herschhorn, A.; Ma, X.; Gu, C.; Ventura, J.D.; Castillo-Menendez, L.; Melillo, B.; Terry, D.S.; Smith, A.B., III; Blanchard, S.C.; Munro, J.B.; et al. Release of gp120 Restraints Leads to an Entry-Competent Intermediate State of the HIV-1 Envelope Glycoproteins. mBio 2016, 7, e01598-16.
58. Desormeaux, A.; Coutu, M.; Medjahed, H.; Pacheco, B.; Herschhorn, A.; Gu, C.; Xiang, S.H.; Mao, Y.; Sodroski, J.; Finzi, A. The highly conserved layer-3 component of the HIV-1 gp120 inner domain is critical for CD4-required conformational transitions. J. Virol. 2013, 87, 2549–2562.
59. Vilmen, G.; Smith, A.C.; Benet, H.C.; Shukla, R.K.; Larue, R.C.; Herschhorn, A.; Sharma, A. Conformation of HIV-1 Envelope governs rhesus CD4 usage and simian-human immunodeficiency virus replication. mBio 2022, 13, e0275221.

60. Prevost, J.; Zoubchenok, D.; Richard, J.; Veillette, M.; Pacheco, B.; Coutu, M.; Brassard, N.; Parsons, M.S.; Ruxrungtham, K.; Bunupuradah, T.; et al. Influence of the Envelope gp120 Phe43 Cavity on HIV-1 Sensitivity to Antibody-Dependent Cell-Mediated Cytotoxicity Responses. J. Virol. 2017, 91, e02452-16.
61. Prevost, J.; Richard, J.; Ding, S.; Pacheco, B.; Charlebois, R.; Hahn, B.H.; Kaufmann, D.E.; Finzi, A. Envelope glycoproteins sampling states 2/3 are susceptible to ADCC by sera from HIV-1-infected individuals. Virology 2018, 515, 38–45.
62. Castillo-Menendez, L.R.; Witt, K.; Espy, N.; Princiotto, A.; Madani, N.; Pacheco, B.; Finzi, A.; Sodroski, J. Comparison of Uncleaved and Mature Human Immunodeficiency Virus Membrane Envelope Glycoprotein Trimers. J. Virol. 2018, 92, e00277-18.
63. Zhang, S.; Wang, K.; Wang, W.L.; Nguyen, H.T.; Chen, S.; Lu, M.; Go, E.P.; Ding, H.; Steinbock, R.T.; Desaire, H.; et al. Asymmetric structures and conformational plasticity of the uncleaved full-length human immunodeficiency virus (HIV-1) envelope glycoprotein trimer. J. Virol. 2021, 95, e0052921.
64. Ringe, R.P.; Sanders, R.W.; Yasmeen, A.; Kim, H.J.; Lee, J.H.; Cupo, A.; Korzun, J.; Derking, R.; van Montfort, T.; Julien, J.P.; et al. Cleavage strongly influences whether soluble HIV-1 envelope glycoprotein trimers adopt a native-like conformation. Proc. Natl. Acad. Sci. USA 2013, 110, 18256–18261.
65. Chakrabarti, B.K.; Pancera, M.; Phogat, S.; O'Dell, S.; McKee, K.; Guenaga, J.; Robinson, J.; Mascola, J.; Wyatt, R.T. HIV type 1 Env precursor cleavage state affects recognition by both neutralizing and nonneutralizing gp41 antibodies. AIDS Res. Hum. Retrovir. 2011, 27, 877–887.
66. Fontaine, J.; Chagnon-Choquet, J.; Valcke, H.S.; Poudrier, J.; Roger, M. High expression levels of B lymphocyte stimulator (BLyS) by dendritic cells correlate with HIV-related B-cell disease progression in humans. Blood 2011, 117, 145–155.
67. Fontaine, J.; Coutlee, F.; Tremblay, C.; Routy, J.P.; Poudrier, J.; Roger, M. HIV infection affects blood myeloid dendritic cells after successful therapy and despite non-progressing cl.inical disease. J. Infect. Dis. 2009, 199, 1007–1018.
68. International, H.I.V.C.S.; Pereyra, F.; Jia, X.; McLaren, P.J.; Telenti, A.; de Bakker, P.I.; Walker, B.D.; Ripke, S.; Brumme, C.J.; Pulit, S.L.; et al. The major genetic determinants of HIV-1 control affect HLA class I peptide presentation. Science 2010, 330, 1551–1557.

69. Kamya, P.; Boulet, S.; Tsoukas, C.M.; Routy, J.P.; Thomas, R.; Cote, P.; Boulassel, M.R.; Baril, J.G.; Kovacs, C.; Migueles, S.A.; et al. Receptor-ligand requirements for increased NK cell polyfunctional potential in slow progressors infected with HIV-1 co-expressing KIR3DL1*h/*y and HLA-B*57. J. Virol. 2011, 85, 5949–5960.
70. Peretz, Y.; Ndongala, M.L.; Boulet, S.; Boulassel, M.R.; Rouleau, D.; Cote, P.; Longpre, D.; Routy, J.P.; Falutz, J.; Tremblay, C.; et al. Functional T cell subsets contribute differentially to HIV peptide-specific responses within infected individuals: Correlation of these functional T cell subsets with markers of disease progression. Clin. Immunol. 2007, 124, 57–68.
71. Platt, E.J.; Wehrly, K.; Kuhmann, S.E.; Chesebro, B.; Kabat, D. Effects of CCR5 and CD4 cell surface concentrations on infections by macrophagetropic isolates of human immunodeficiency virus type 1. J. Virol. 1998, 72, 2855–2864.
72. Chen, J.; Park, J.; Kirk, S.M.; Chen, H.C.; Li, X.; Lippincott, D.J.; Melillo, B.; Smith, A.B., III. Development of an Effective Scalable Enantioselective Synthesis of the HIV-1 Entry Inhibitor BNM-III-170 as the Bis-Trifluoroacetate Salt. Org. Process. Res. Dev. 2019, 23, 2464–2469.
73. Emi, N.; Friedmann, T.; Yee, J.K. Pseudotype formation of murine leukemia virus with the G protein of vesicular stomatitis virus. J. Virol. 1991, 65, 1202–1207.
74. Salazar-Gonzalez, J.F.; Salazar, M.G.; Keele, B.F.; Learn, G.H.; Giorgi, E.E.; Li, H.; Decker, J.M.; Wang, S.; Baalwa, J.; Kraus, M.H.; et al. Genetic identity, biological phenotype, and evolutionary pathways of transmitted/founder viruses in acute and early HIV-1 infection. J. Exp. Med. 2009, 206, 1273–1289.
75. Ochsenbauer, C.; Edmonds, T.G.; Ding, H.; Keele, B.F.; Decker, J.; Salazar, M.G.; Salazar-Gonzalez, J.F.; Shattock, R.; Haynes, B.F.; Shaw, G.M.; et al. Generation of Transmitted/Founder HIV-1 Infectious Molecular Clones and Characterization of Their Replication Capacity in CD4 T Lymphocytes an.nd Monocyte-Derived Macrophages. J. Virol. 2012, 86, 2715–2728.
76. Parrish, N.F.; Gao, F.; Li, H.; Giorgi, E.E.; Barbian, H.J.; Parrish, E.H.; Zajic, L.; Iyer, S.S.; Decker, J.M.; Kumar, A.; et al. Phenotypic properties of transmitted founder HIV-1. Proc. Natl. Acad. Sci. USA 2013, 110, 6626–6633.

77. Fenton-May, A.E.; Dibben, O.; Emmerich, T.; Ding, H.; Pfafferott, K.; Aasa-Chapman, M.M.; Pellegrino, P.; Williams, I.; Cohen, M.S.; Gao, F.; et al. Relative resistance of HIV-1 founder viruses to control by interferon-alpha. Retrovirology 2013, 10, 146.
78. Rho, H.M.; Poiesz, B.; Ruscetti, F.W.; Gallo, R.C. Characterization of the reverse transcriptase from a new retrovirus (HTLV) produced by a human cutaneous T-cell lymphoma cell line. Virology 1981, 112, 355–360.
79. Ding, S.; Gasser, R.; Gendron-Lepage, G.; Medjahed, H.; Tolbert, W.D.; Sodroski, J.; Pazgier, M.; Finzi, A. CD4 Incorporation into HIV-1 Viral Particles Exposes Envelope Epitopes Recognized by CD4-Induced Antibodies. J. Virol. 2019, 93, e01403-19.
80. Si, Z.; Phan, N.; Kiprilov, E.; Sodroski, J. Effects of HIV type 1 envelope glycoprotein proteolytic processing on antigenicity. AIDS Res. Hum. Retrovir. 2003, 19, 217–226.
81. Yang, X.; Kurteva, S.; Lee, S.; Sodroski, J. Stoichiometry of antibody neutralization of human immunodeficiency virus type 1. J. Virol. 2005, 79, 3500–3508.
82. Brandenberg, O.F.; Magnus, C.; Rusert, P.; Regoes, R.R.; Trkola, A. Different infectivity of HIV-1 strains is linked to number of envelope trimers required for entry. PLoS Pathog. 2015, 11, e1004595.
83. Stieh, D.J.; King, D.F.; Klein, K.; Aldon, Y.; McKay, P.F.; Shattock, R.J. Discrete partitioning of HIV-1 Env forms revealed by viral capture. Retrovirology 2015, 12, 81.
84. Zhang, S.; Nguyen, H.T.; Ding, H.; Wang, J.; Zou, S.; Liu, L.; Guha, D.; Gabuzda, D.; Ho, D.D.; Kappes, J.C.; et al. Dual Pathways of Human Immunodeficiency Virus Type 1 Envelope Glycoprotein Trafficking Modulate the Selective Exclusion of Uncleaved Oligomers from Virions. J. Virol. 2021, 95, e01369-20.
85. Anand, S.P.; Prévost, J.; Descôteaux-Dinelle, J.; Richard, J.; Nguyen, D.N.; Medjahed, H.; Chen, H.-C.; Smith, A.B.; Pazgier, M.; Finzi, A. HIV-1 Envelope Glycoprotein Cell Surface Localization Is Associated with Antibody-Induced Internalization. Viruses 2021, 13, 1953.
86. Alsahafi, N.; Ding, S.; Richard, J.; Markle, T.; Brassard, N.; Walker, B.; Lewis, G.K.; Kaufmann, D.E.; Brockman, M.A.; Finzi, A. Nef Proteins from HIV-1 Elite Controllers Are Inefficient at Preventing Antibody-Dependent Cellular Cytotoxicity. J. Virol. 2016, 90, 2993–3002.

87. Aloia, R.C.; Tian, H.; Jensen, F.C. Lipid composition and fluidity of the human immunodeficiency virus envelope and host cell plasma membranes. Proc. Natl. Acad. Sci. USA 1993, 90, 5181–5185.
88. Vishwanathan, S.A.; Thomas, A.; Brasseur, R.; Epand, R.F.; Hunter, E.; Epand, R.M. Large changes in the CRAC segment of gp41 of HIV do not destroy fusion activity if the segment interacts with cholesterol. Biochemistry 2008, 47, 11869–11876.
89. Salimi, H.; Johnson, J.; Flores, M.G.; Zhang, M.S.; O'Malley, Y.; Houtman, J.C.; Schlievert, P.M.; Haim, H. The lipid membrane of HIV-1 stabilizes the viral envelope glycoproteins and modulates their sensitivity to antibody neutralization. J. Biol. Chem. 2020, 295, 348–362.
90. Cummins, L.M.; Weinhold, K.J.; Matthews, T.J.; Langlois, A.J.; Perno, C.F.; Condie, R.M.; Allain, J.P. Preparation and characterization of an intravenous solution of IgG from human immunodeficiency virus-seropositive donors. Blood 1991, 77, 1111–1117.
91. Prevost, J.; Richard, J.; Medjahed, H.; Alexander, A.; Jones, J.; Kappes, J.C.; Ochsenbauer, C.; Finzi, A. Incomplete Downregulation of CD4 Expression Affects HIV-1 Env Conformation and Antibody-Dependent Cellular Cytotoxicity Responses. J. Virol. 2018, 92, e00484-18.
92. Alsahafi, N.; Richard, J.; Prevost, J.; Coutu, M.; Brassard, N.; Parsons, M.S.; Kaufmann, D.E.; Brockman, M.; Finzi, A. Impaired downregulation of NKG2D ligands by Nef protein from elite controllers sensitizes HIV-1-infected cells to ADCC. J. Virol. 2017, 91, e00109-17.
93. Braun, E.; Hotter, D.; Koepke, L.; Zech, F.; Gross, R.; Sparrer, K.M.J.; Muller, J.A.; Pfaller, C.K.; Heusinger, E.; Wombacher, R.; et al. Guanylate-Binding Proteins 2 and 5 Exert Broad Antiviral Activity by Inhibiting Furin-Mediated Processing of Viral Envelope Proteins. Cell Rep. 2019, 27, 2092-2104.e10.
94. Lodermeyer, V.; Suhr, K.; Schrott, N.; Kolbe, C.; Sturzel, C.M.; Krnavek, D.; Munch, J.; Dietz, C.; Waldmann, T.; Kirchhoff, F.; et al. 90K, an interferon-stimulated gene product, reduces the infectivity of HIV-1. Retrovirology 2013, 10, 111.
95. Tada, T.; Zhang, Y.; Koyama, T.; Tobiume, M.; Tsunetsugu-Yokota, Y.; Yamaoka, S.; Fujita, H.; Tokunaga, K. MARCH8 inhibits HIV-1 infection by reducing virion incorporation of envelope glycoproteins. Nat. Med. 2015, 21, 1502–1507.

96. Yu, J.; Li, M.; Wilkins, J.; Ding, S.; Swartz, T.H.; Esposito, A.M.; Zheng, Y.M.; Freed, E.O.; Liang, C.; Chen, B.K.; et al. IFITM Proteins Restrict HIV-1 Infection by Antagonizing the Envelope Glycoprotein. Cell Rep. 2015, 13, 145–156.
97. Wang, Y.; Pan, Q.; Ding, S.; Wang, Z.; Yu, J.; Finzi, A.; Liu, S.L.; Liang, C. The V3 Loop of HIV-1 Env Determines Viral Susceptibility to IFITM3 Impairment of Viral Infectivity. J. Virol. 2017, 91, e02441-16.
98. Foster, T.L.; Wilson, H.; Iyer, S.S.; Coss, K.; Doores, K.; Smith, S.; Kellam, P.; Finzi, A.; Borrow, P.; Hahn, B.H.; et al. Resistance of Transmitted Founder HIV-1 to IFITM-Mediated Restriction. Cell Host Microbe 2016, 20, 429–442.
99. Drouin, A.; Migraine, J.; Durand, M.A.; Moreau, A.; Burlaud-Gaillard, J.; Beretta, M.; Roingeard, P.; Bouvin-Pley, M.; Braibant, M. Escape of HIV-1 envelope glycoprotein from the restriction of infection by IFITM3. J. Virol. 2020, 95, e01994-20.
100. Krapp, C.; Hotter, D.; Gawanbacht, A.; McLaren, P.J.; Kluge, S.F.; Sturzel, C.M.; Mack, K.; Reith, E.; Engelhart, S.; Ciuffi, A.; et al. Guanylate Binding Protein (GBP) 5 Is an Interferon-Inducible Inhibitor of HIV-1 Infectivity. Cell Host Microbe 2016, 19, 504–514.
101. Jean, F.; Stella, K.; Thomas, L.; Liu, G.; Xiang, Y.; Reason, A.J.; Thomas, G. alpha1-Antitrypsin Portland, a bioengineered serpin highly selective for furin: Application as an antipathogenic agent. Proc. Natl. Acad. Sci. USA 1998, 95, 7293–7298.
102. Khatib, A.M.; Siegfried, G.; Prat, A.; Luis, J.; Chretien, M.; Metrakos, P.; Seidah, N.G. Inhibition of proprotein convertases is associated with loss of growth and tumorigenicity of HT-29 human colon carcinoma cells: Importance of insulin-like growth factor-1 (IGF-1) receptor processing in IGF-1-mediated functions. J. Biol. Chem. 2001, 276, 30686–30693.
103. Bassi, D.E.; Lopez De Cicco, R.; Mahloogi, H.; Zucker, S.; Thomas, G.; Klein-Szanto, A.J. Furin inhibition results in absent or decreased invasiveness and tumorigenicity of human cancer cells. Proc. Natl. Acad. Sci. USA 2001, 98, 10326–10331.
104. Kibler, K.V.; Miyazato, A.; Yedavalli, V.S.; Dayton, A.I.; Jacobs, B.L.; Dapolito, G.; Kim, S.J.; Jeang, K.T. Polyarginine inhibits gp160 processing by furin and suppresses productive human immunodeficiency virus type 1 infection. J. Biol. Chem. 2004, 279, 49055–49063.
105. Remacle, A.G.; Gawlik, K.; Golubkov, V.S.; Cadwell, G.W.; Liddington, R.C.; Cieplak, P.; Millis, S.Z.; Desjardins, R.; Routhier, S.; Yuan, X.W.; et al. Selective and potent furin

inhibitors protect cells from anthrax without significant toxicity. Int. J. Biochem. Cell Biol. 2010, 42, 987–995.

106. Klenk, H.D.; Rott, R. The molecular biology of influenza virus pathogenicity. Adv. Virus Res. 1988, 34, 247–281.

107. Volchkov, V.E.; Feldmann, H.; Volchkova, V.A.; Klenk, H.D. Processing of the Ebola virus glycoprotein by the proprotein convertase furin. Proc. Natl. Acad. Sci. USA 1998, 95, 5762–5767.

108. Rawling, J.; Cano, O.; Garcin, D.; Kolakofsky, D.; Melero, J.A. Recombinant Sendai viruses expressing fusion proteins with two furin cleavage sites mimic the syncytial and receptor-independent infection properties of respiratory syncytial virus. J. Virol. 2011, 85, 2771–2780.

109. Johnson, B.A.; Xie, X.; Bailey, A.L.; Kalveram, B.; Lokugamage, K.G.; Muruato, A.; Zou, J.; Zhang, X.; Juelich, T.; Smith, J.K.; et al. Loss of furin cleavage site attenuates SARS-CoV-2 pathogenesis. Nature 2021, 591, 293–299.

110. Sasaki, M.; Toba, S.; Itakura, Y.; Chambaro, H.M.; Kishimoto, M.; Tabata, K.; Intaruck, K.; Uemura, K.; Sanaki, T.; Sato, A.; et al. SARS-CoV-2 Bearing a Mutation at the S1/S2 Cleavage Site Exhibits Attenuated Virulence and Confers Protective Immunity. mBio 2021, 12, e0141521.

4.3.9 FIGURES

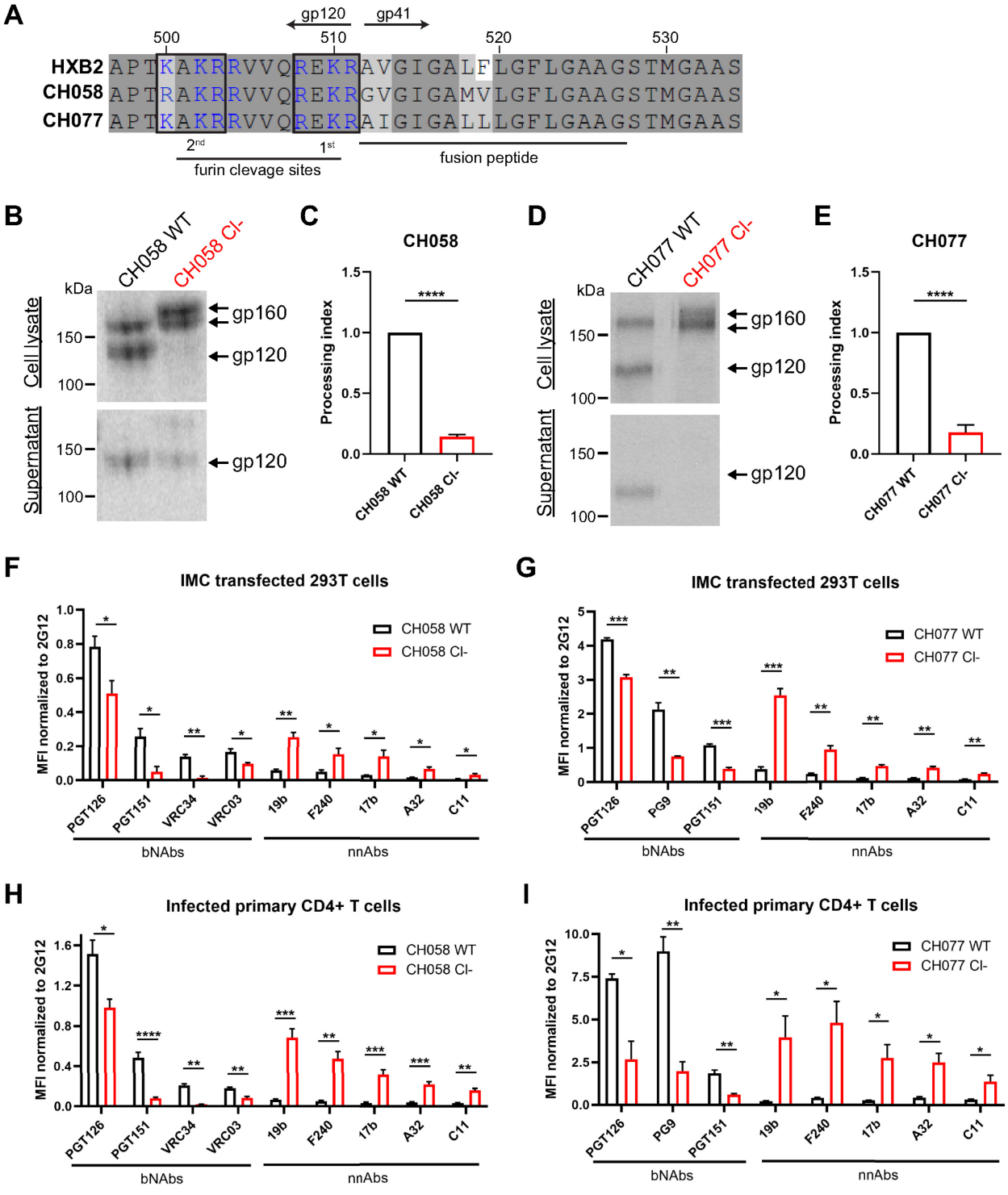
A
gp120
gp41
500
510
520
530
HXB2 APTKAKRRVVQREKRAVGIGALFLGFLGAAGSTMGAAS
CH058 APTRAKRRVVQREKRGVGIGAMVLGFLGAAGSTMGAAS
CH077 APTKAKRRVVQREKRAIGIGALLLGFLGAAGSTMGAAS
2nd
1st
furin clevage sites
fusion peptide
B
CH058 WT
CH058 Cl-
kDa
Cell lysate
Supernatant
150
100
gp160
gp120
gp120
C
CH058
Processing index
****
CH058 WT
CH058 Cl-
D
CH077 WT
CH077 Cl-
kDa
Cell lysate
Supernatant
150
100
gp160
gp120
gp120
E
CH077
Processing index
****
CH077 WT
CH077 Cl-
F
IMC transfected 293T cells
MFI normalized to 2G12
CH058 WT
CH058 Cl-
PGT126
PGT151
VRC34
VRC03
19b
F240
17b
A32
C11
bNAbs
nnAbs
G
IMC transfected 293T cells
MFI normalized to 2G12
CH077 WT
CH077 Cl-
PGT126
PG9
PGT151
19b
F240
17b
A32
C11
bNAbs
nnAbs
H
Infected primary CD4+ T cells
MFI normalized to 2G12
CH058 WT
CH058 Cl-
PGT126
PGT151
VRC34
VRC03
19b
F240
17b
A32
C11
bNAbs
nnAbs
I
Infected primary CD4+ T cells
MFI normalized to 2G12
CH077 WT
CH077 Cl-
PGT126
PG9
PGT151
19b
F240
17b
A32
C11
bNAbs
nnAbs

Figure 4.2.1 - Proteolytic cleavage stabilizes Env in its "closed" conformation.
(**A**) Sequence alignment of the HIV-1 Env furin cleavage site region from primary viruses CH058 (GenBank accession number JN944940) and CH077 (GenBank accession number JN944941) with the HXB2 reference strain (GenBank accession number K03455). Putative furin cleavage sequences are highlighted by black boxes. Positively charged residues (arginine and lysine) are shown in blue. Residue numbering is based on the HXB2 strain. Identical residues are shaded in dark gray, and conserved residues are shaded in light gray. (**B–E**) 293T cells were transfected with primary IMCs (**B,C**) CH058, (**D,E**) CH077 WT or their cleavage-deficient (Cl−) variants and metabolically labeled with [^{35}S]-methionine and [^{35}S]-cysteine. (**B,D**) Cell lysates and supernatants were immunoprecipitated with plasma from HIV-1-infected individuals. The precipitated proteins were loaded onto SDS-PAGE gels and analyzed by autoradiography and densitometry to calculate their processing indexes. The processing index is a measure of the conversion of the mutant gp160 Env precursor to mature gp120, relative to the wild-type Env trimer. (**C,E**) Shown is the average of processing indexes calculated in 3 independent experiments. (**F–I**) Cell-surface staining of (**F,G**) IMC transfected 293T cells (**H,I**) or primary CD4$^+$ T cells infected with IMCs (**F,H**) CH058 and (**G,I**) CH077 WT or their cleavage-deficient (Cl−) variants using a panel of anti-Env bNAbs (PGT126, PG9, PGT151, VRC34, VRC03) and nnAbs (19b, F240, 17b, A32, C11). Shown are the mean fluorescence intensities (MFI) using the different antibodies normalized to the signal obtained with the conformation-independent 2G12 mAb. MFI values were measured on the transfected or infected (p24$^+$) population for staining obtained in at least 3 independent experiments. Error bars indicate the mean ± SEM. Statistical significance was tested using an unpaired t-test (*. $P < 0.05$, **, $P < 0.01$, ***, $P < 0.001$, ****, $P < 0.0001$).

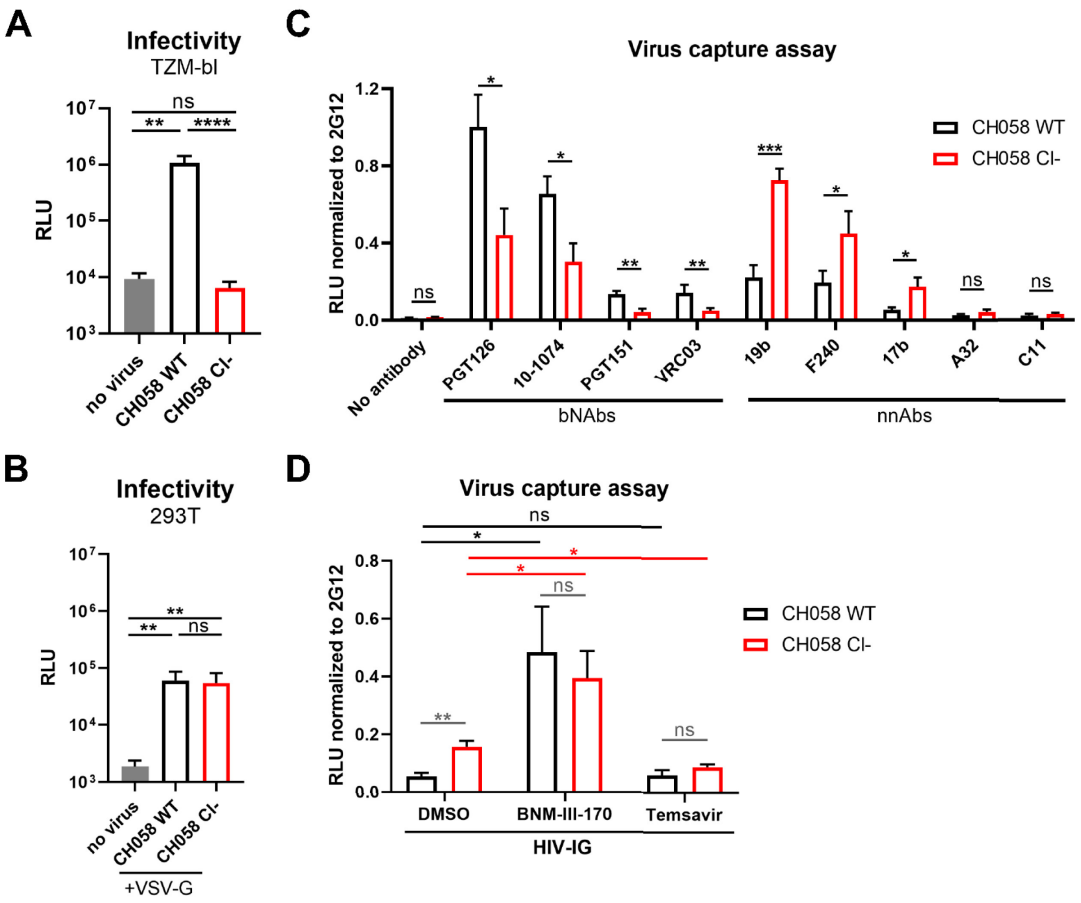

Figure 4.2.2 - Virions displaying uncleaved Env are better recognized by nnAbs.
(**A**) Viral infectivity was assessed by incubating TZM-bl target cells with HIV-1 CH058 virions expressing the wild-type (WT) or cleavage-deficient (Cl−) Env glycoprotein for 48 h. Viral preparations were normalized according to reverse transcriptase activity. (**B**) VSV-G-pseudotyped viral particles encoding the luciferase gene (Luc+) and bearing HIV-1 CH058 Env wildtype (WT) or its cleavage-deficient mutant (Cl−) were used to infect 293T cells to determine their infectivity in a single-round infection. (**C,D**) These recombinant pseudovirions were further tested for virus capture by (**C**) a panel of anti-Env bNAbs (PGT126, PG9, PGT151, VRC34, VRC03) and nnAbs (19b, F240, 17b, A32, C11) or (**D**) HIV-IG. RLU values obtained using the different antibodies were normalized to the signal obtained with the conformation-independent 2G12 mAb. Data shown are the mean +/- SEM from at least three independent experiments. Statistical significance was tested using an unpaired t-test or a Mann–Whitney U-test based on statistical normality (*, P < 0.05; **, P < 0.01; ***, P < 0.001; ****. P < 0.0001; ns, nonsignificant).

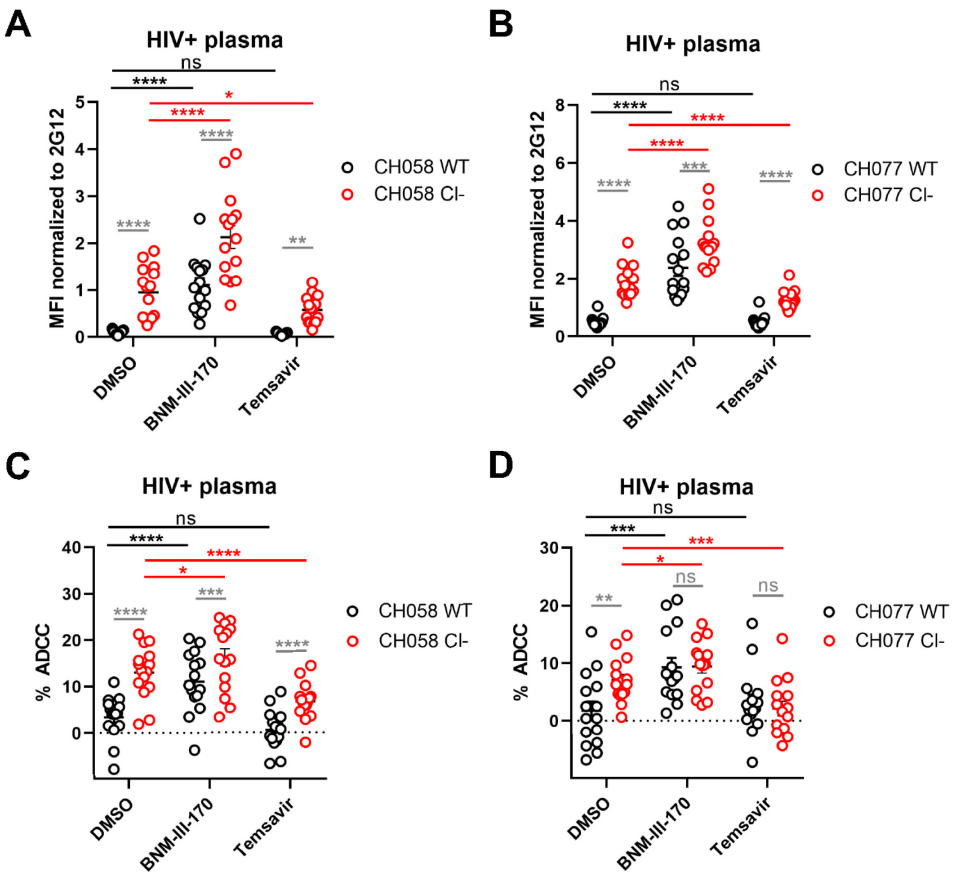

Figure 4.2.3 - Env cleavage protects HIV-1-infected cells from ADCC mediated by HIV$^+$ plasma.

(**A,B**) Cell surface staining of primary CD4+T cells infected with primary HIV-1 viruses (**A**) CH058 and (**B**) CH077 WT or their cleavage-deficient (Cl−) variants using plasma from 15 different HIV-1-infected individuals in the presence of 50 µM of CD4mc BNM-III-170, conformational blocker Temsavir or an equivalent volume of the vehicle (DMSO). The graphs show the MFI obtained on the infected (p24$^+$) cell population. (**C,D**) Primary CD4+ T cells infected with (**C**) CH058 and (**D**) CH077 viruses were also used as target cells, and autologous PBMCs were used as effector cells in a FACS-based ADCC assay. The graphs shown represent the percentages of ADCC mediated by 15 different HIV$^+$ plasma in the presence of 50 µM of CD4mc BNM-III-170, attachment inhibitor Temsavir or an equivalent volume of the vehicle (DMSO). All results were obtained using cells from at least three different donors. Error bars indicate the means +/- SEM. Statistical significance was tested using a repeated measures one-way ANOVA with a Holm–Sidak post-test (*, $P < 0.05$; **, $P < 0.01$; ***, $P < 0.001$; ****, $P < 0.0001$; ns, nonsignificant).

4.3.10 GRAPHICAL ABSTRACT

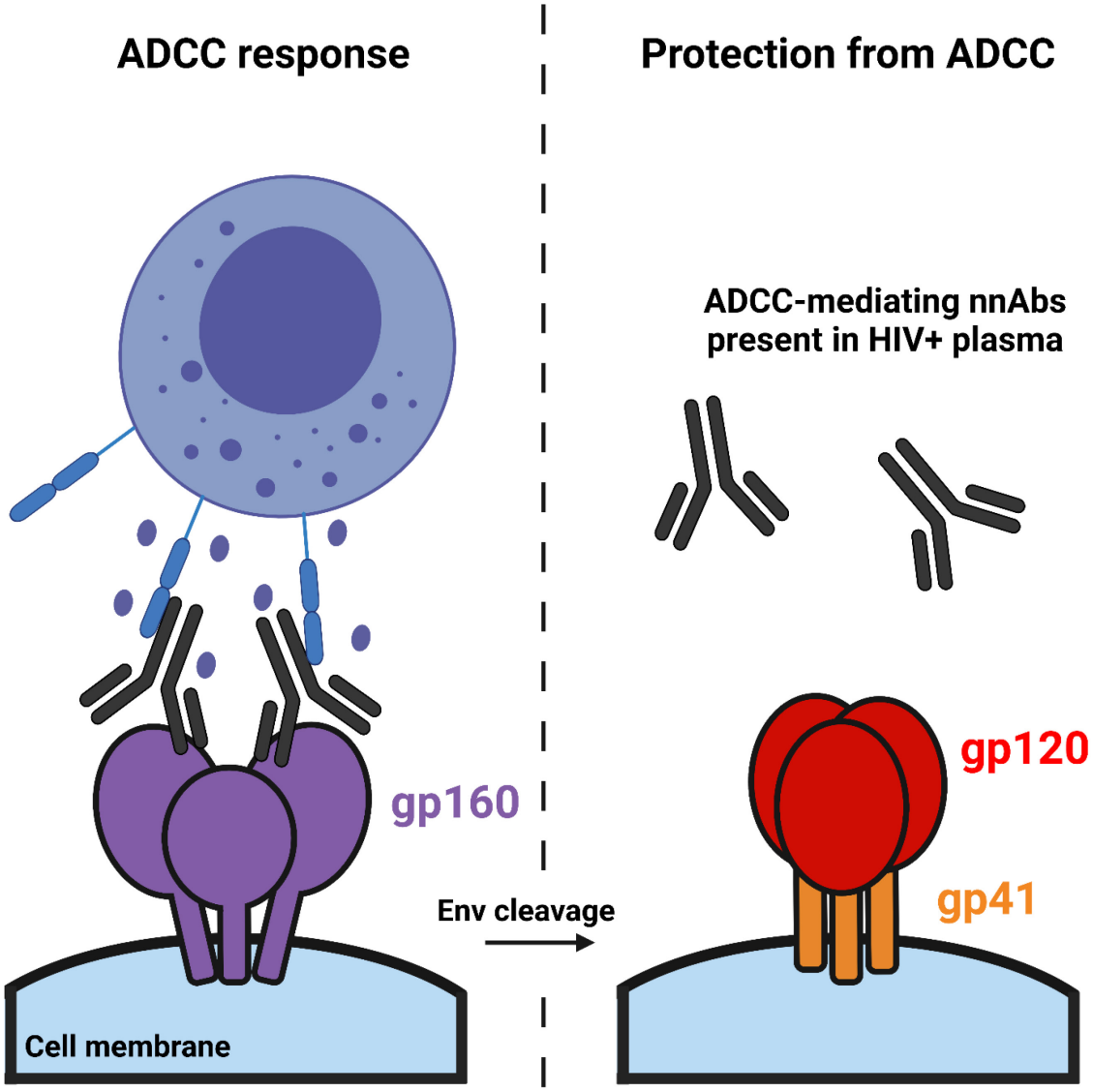

Figure 4.2.4 - Graphical abstract
Proteolytic cleavage of HIV-1 Env protects infected cells from ADCC mediated by non-neutralizing antibodies present in plasma from infected individuals.

ARTICLE 7

L'influence de la cavité Phe43 de l'enveloppe du VIH-1 dans la sensibilité des cellules infectées à la réponse ADCC

Influence of the Envelope gp120 Phe43 Cavity on HIV-1 Sensitivity to Antibody Dependent Cell-Mediated Cytotoxicity Responses

Auteurs:

Jérémie Prévost[1,2], Daria Zoubchenok[1,2], Jonathan Richard[1,2], Maxime Veillette[1,2], Beatriz Pacheco[1], Mathieu Coutu[1], Nathalie Brassard[1], Matthew S. Parsons[3], Kiat Ruxrungtham[4,5], Torsak Bunupuradah[4], Sodsai Tovanabutra[14,15], Kwan-Ki Hwang[6,7], M. Anthony Moody[6,8], Barton F. Haynes[6], Mattia Bonsignori[6], Joseph Sodroski[9,10], Daniel E. Kaufmann[1,11,12], George M. Shaw[13], Agnès L. Chenine[14,15], Andrés Finzi[1,2,16]

Affiliations:

[1]Centre de Recherche du CHUM, Montreal, QC, Canada; [2]Department of Microbiology, Infectiology and Immunology, Université de Montréal, Montreal, QC, Canada; [3]Department of Microbiology and Immunology, University of Melbourne, Peter Doherty Institute for Infection and Immunity, Melbourne, VIC, Australia; [4]HIVNAT, Thai Red Cross AIDS Research Center, Bangkok, Thailand; [5]Allergy and Clinical Immunology Division, Department of Medicine, Chula Vaccine Research Center, Faculty of Medicine, Chulalongkorn University, Bangkok, Thailand; [6]Duke Human Vaccine Institute, Duke University Medical Center, Durham, North Carolina, USA; [7]Department of Medicine, Duke University Medical Center, Durham, North Carolina, USA; [8]Department of Pediatrics, Duke University Medical Center, Durham, North Carolina, USA; [9]Department of Cancer Immunology and Virology, Dana-Farber Cancer Institute, and Department of Microbiology and Immunobiology, Division of AIDS, Harvard Medical School, Boston, Massachusetts, USA; [10]Department of Immunology and Infectious Diseases, Harvard T. H. Chan School of Public Health, Boston, Massachusetts, USA; [11]Department of Medicine, Université de Montréal, Montreal, QC, Canada; [12]Center for HIV/AIDS Vaccine Immunology and Immunogen Discovery, The Scripps Research Institute, La Jolla, California, USA; [13]Departments of Medicine and Microbiology, Perelman School of Medicine, University of Pennsylvania, Philadelphia, Pennsylvania, USA; [14]U.S. Military HIV Research Program, Walter Reed Army Institute of Research, Silver Spring, Maryland, USA; [15]Henry M. Jackson Foundation for the Advancement of the Military Medicine, Bethesda, Maryland, USA; [16]Department of Microbiology and Immunology, McGill University, Montreal, QC, Canada.

Contribution des auteurs:

Conceptualisation: **J.P.**, M.V. et A.F.; Méthodologie: **J.P.** et A.F.; Recherche: **J.P.**, D.Z. et J.R.; Ressources: M.V., B.P., M.C., N.B., M.S.P., K.R., T.B., S.T., K.K.H., M.A.M., B.F.H., M.B., D.E.K., G.M.S., A.L.C. et A.F.; Analyse formelle: **J.P.**; Visualisation: **J.P.**; Supervision: A.F.; Obtention du financement: B.F.H., J.G.S., D.E.K. et A.F.; Rédaction - version originale: **J.P.**, J.S. et A.F.; Rédaction - révision et édition: **Tous les auteurs**.

Statut: Cet article a été publié dans *Journal of Virology*, le 13 mars 2017.
https://doi.org/10.1128/JVI.02452-16

4.4.1 RÉSUMÉ

Les cellules infectées par le VIH-1 qui présentent à leur surface des glycoprotéines d'enveloppe (Env) dans la conformation liée à CD4 sont préférentiellement ciblées par la réponse cytotoxique cellulaire dépendante des anticorps (ADCC). Le VIH-1 a développé des mécanismes sophistiqués pour éviter l'exposition des épitopes d'Env médiant l'ADCC en régulant négativement CD4 et en limitant la quantité totale d'Env à la surface des cellules. Chez le VIH-1, la substitution de la sérine 375 pour un large résidu tels que l'histidine ou le tryptophane (S375H/W) dans la cavité Phe43 de la gp120, où le résidu Phe43 de CD4 entre en contact avec la gp120, entraîne l'adoption spontané de la conformation liée à CD4 d'Env. Alors que le résidu S375 est bien conservé dans la majorité des isolats de VIH-1 du groupe M, les souches recombinantes CRF01_ AE ont une histidine naturellement présente à cette position (H375). Il est intéressant de noter que le clade CRF01_AE est la souche prédominante en circulation en Thaïlande, où l'essai vaccinale RV144 a eu lieu. Dans cet essai clinique, qui a donné lieu à un degré de protection modeste, la réponse ADCC a été identifiée comme un corrélat de protection. Nous étudions ici l'influence de la cavité Phe43 sur la réponse ADCC. Le remplissage de cette cavité par un résidu histidine ou tryptophane chez une souche d'Env ayant naturellement un résidu sérine à cette position (S375H/W) augmente la susceptibilité des cellules infectées par le VIH-1 à l'ADCC. À l'inverse, le remplacement de H375 par un résidu sérine (H375S) chez la souche CRF01_AE diminue l'efficacité de la réponse ADCC. Nos résultats soulèvent la possibilité que la présence de H375 dans la souche en circulation où s'est déroulé l'essai clinique RV144 ait contribué à l'efficacité observée du vaccin.

4.4.2 ABSTRACT

HIV-1-infected cells presenting envelope glycoproteins (Env) in the CD4-bound conformation on their surface are preferentially targeted by antibody-dependent cellular-mediated cytotoxicity (ADCC). HIV-1 has evolved sophisticated mechanisms to avoid the exposure of Env ADCC epitopes by downregulating CD4 and by limiting the overall amount of Env on the cell surface. In HIV-1, substitution of large residues such as histidine or tryptophan for serine 375 (S375H/W) in the gp120 Phe43 cavity, where Phe43 of CD4 contacts gp120, results in the spontaneous sampling of an Env conformation closer to the CD4-bound state. While residue S375 is well conserved in the majority of group M HIV-1 isolates, CRF01_ AE strains have a naturally

occurring histidine at this position (H375). Interestingly, CRF01_AE is the predominant circulating strain in Thailand, where the RV144 trial took place. In this trial, which resulted in a modest degree of protection, ADCC responses were identified as being part of the correlate of protection. Here we investigate the influence of the Phe43 cavity on ADCC responses. Filling this cavity with a histidine or tryptophan residue in Env with a natural serine residue at this position (S375H/W) increased the susceptibility of HIV-1-infected cells to ADCC. Conversely, the replacement of His375 by a serine residue (H375S) within HIV-1 CRF01_AE decreased the efficiency of the ADCC response. Our results raise the intriguing possibility that the presence of His375 in the circulating strain where the RV144 trial was held contributed to the observed vaccine efficacy.

4.4.3 IMPORTANCE

HIV-1-infected cells presenting Env in the CD4-bound conformation on their surface are preferentially targeted by ADCC mediated by HIV-positive (HIV^+) sera. Here we show that the gp120 Phe43 cavity modulates the propensity of Env to sample this conformation and therefore affects the susceptibility of infected cells to ADCC. CRF01_AE HIV-1 strains have an unusual Phe43 cavity-filling His375 residue, which increases the propensity of Env to sample the CD4-bound conformation, thereby increasing susceptibility to ADCC.

4.4.4 INTRODUCTION

Entry is the first step of the human immunodeficiency virus type 1 (HIV-1) replication cycle and requires the mature viral envelope glycoproteins (Env), which results from the proteolytic cleavage of the gp160 precursor Env into the exterior gp120 and transmembrane gp41 subunits. These subunits are linked by noncovalent bonds, allowing conformational changes of the Env trimer during the entry process (1–3). The gp120 exterior subunit mediates the initial interaction with the CD4 receptor. gp120 residue 375 is located in what is known as the Phe43 cavity, where Phe43 of CD4 makes numerous contacts with conserved gp120 residues critical for CD4 binding (4). Some gp120 residues that line this cavity contribute to an aromatic array that helps stabilize the CD4-bound conformation (1, 4, 5). Upon CD4 binding, major conformational changes expose the binding site for coreceptor (i.e., CCR5 and CXCR4) interaction (6). Upon coreceptor engagement, additional conformational changes in gp41 bring together the viral

envelope and the target cell membranes (7, 8). It has been shown that some of these conformational rearrangements could be impacted by large alterations in the Phe43 cavity. The replacement of the well-conserved group M serine at position 375 by a large hydrophobic residue such as tryptophan fills the Phe43 cavity; this substitution alters the Env conformation by predisposing gp120 to spontaneously assume a state closer to the CD4-bound conformation (9). In agreement with the important role played by Env conformation in the CD4 interaction (1, 9–11), a recent study using the simian-human immunodeficiency virus (SHIV) model in rhesus macaques showed that the replacement of residue 375 by larger hydrophobic or basic amino acids enhanced the affinity of Env for macaque CD4 and allowed better infection of macaque T lymphocytes in culture and in vivo (12), highlighting the importance of this residue for viral replication.

Besides its potential involvement in viral replication, the CD4-bound conformation of HIV-1 Env represents a major target of antibodies (Abs) present in sera of HIV-1- infected individuals that mediate antibody-dependent cellular cytotoxicity (ADCC) (13). It has been shown that HIV-1 minimizes the exposure of this ADCC-susceptible Env conformation using a highly sophisticated strategy to keep Env on the surface of infected cells in the unbound "closed" conformation. HIV-1 accomplishes this through its accessory proteins Nef and Vpu, which decrease the overall amounts of Env (via Vpu-mediated BST-2 downregulation) and CD4 at the cell surface (13–16). In addition, decreased amounts of Env at the cell surface due to efficient internalization also help the virus to avoid ADCC responses (17). In agreement with the need for HIV-1 to avoid exposing Env in the CD4-bound conformation, it was recently shown that forcing Env to adopt this conformation with small CD4-mimetic compounds (CD4mcs) sensitizes HIV-1-infected cells to ADCC responses (18–20). Accordingly, we recently reported that the transition of Env to the CD4-bound conformation is required for efficient interactions with ADCC-mediating antibodies (14). We reported that the replacement of serine 375 by a tryptophan residue (S375W) enhanced the exposure of epitopes recognized by anti-cluster A antibodies, known to mediate potent ADCC responses (13, 14, 18, 20–26). Thus, the transition of Env from the unbound to the CD4-bound conformation appears to be a prerequisite for the exposure of inner-domain ADCC epitopes. However, how the presence of naturally occurring Phe43 cavity-filling residues affects ADCC responses remains unknown.

While Ser375 is well conserved in the majority of group M HIV-1 isolates, we noticed that CRF01_AE Env possess a Phe43 cavity-filling residue at position 375 (His375) (27). CRF01_AE is the predominant circulating strain in Thailand, where the RV144 clinical vaccine trial took place. In this trial, which resulted in a modest degree of clinical protection, ADCC responses were identified as a correlate of protection (28), raising the intriguing possibility that naturally occurring His375 in CRF01_AE Env might have contributed to this outcome. Here we explored the influence of the integrity of the Phe43 cavity on ADCC responses.

4.4.5 RESULTS

Comparison of residue 375 flanking the Phe43 cavity among HIV-1 strains.

The vast genetic variability of HIV-1 resulted in its classification into 4 major groups, groups M, N, O, and P. Group M, or "main" group, viruses are responsible for the majority of the global HIV-1 pandemic. Group M is comprised of nine major subtypes and circulating recombinant forms (CRFs) (29–33). To determine the variance in residue 375 among HIV-1 Env, we analyzed all available group M sequences in the NIH Los Alamos HIV database. Interestingly, while the vast majority (84%) of group M strains have a serine at position 375 (S375) and another 9% have a closely related T375 substitution (**Fig. 4.3.1A to D and F to H**), nearly all CRF01_AE Env have a large basic aromatic histidine residue at this position. Indeed, alignments revealed 99% conservation for H375 in CRF01_AE strains (**Fig. 4.3.1E**), clearly differentiating them from the other circulating strains of group M.

Effect of Phe43 cavity-filling changes on recognition and ADCC-mediated killing of HIV-1-infected cells.

It has been shown that the replacement of serine 375 by a histidine or tryptophan residue fills the Phe43 cavity and predisposes Env to assuming a slightly more CD4-bound-like conformation (9). Moreover, it has been shown that sampling of the CD4-bound conformation results in an enhanced exposure of epitopes recognized by anti-cluster A antibodies (14, 34). To evaluate whether this enhanced recognition translates into enhanced susceptibility to ADCC, primary CD4 T cells from healthy HIV-1-negative donors were infected with HIV-1 NL4-3-GFP infectious molecular clones (IMCs) expressing wild-type (WT) strain ADA Env or mutant Env

with a histidine (S375H) or a tryptophan (S375W) substitution at position 375. In parallel, primary CD4 T cells were infected with SHIVs expressing clade C and D HIV-1 Env with the same substitutions in residue 375 (WT and S375H and S375W mutants). Since it is now well established that CD4 present on the cell surface affects Env conformation by forcing it to assume the CD4-bound conformation (13, 14, 21, 22, 35), we first evaluated the ability of all the IMCs to downregulate CD4. **Figure 4.3.2** shows that all IMCs tested, independently of the residue present at position 375, efficiently downregulated CD4 from the cell surface (**Fig. 4.3.2A to C**). Therefore, any detected effects on Env conformation cannot be attributed to differential CD4 downregulation but rather to the nature of the residue present within the Phe43 cavity. Since Env levels present on the cell surface have been shown to affect ADCC responses (17), we verified the overall amount of Env present on the surface of infected cells. Env levels present on the cell surface were unaffected by the nature of the residue present at position 375. Indeed, we detected similar levels of Env expression using the gp120 outer-domain-specific 2G12 antibody for clade B and D Env (**Fig. 4.3.2D and F**). Due to the poor recognition of clade C Env by the 2G12 antibody, we utilized the broadly neutralizing anti-gp41 10e8 antibody to measure clade C Env expression (**Fig. 4.3.2E**). No effect of the changes at residue 375 on Env expression on the surface of cells infected with a SHIV expressing a clade C Env was observed (**Fig. 4.3.2E**). In agreement with an effect on Env conformation, we observed that in all the cases, filling of the Phe43 cavity by the replacement of residue 375 with a histidine or a tryptophan residue significantly increased the binding of Env by CD4-induced (CD4i) antibodies that recognize the coreceptor binding site (CoRBS) (17b) or the cluster A epitope (A32) (**Fig. 4.3.2G to L**). Interestingly, we observed that Env with a "filled" Phe43 cavity (S375H and S375W mutants) were also recognized significantly better by HIV-positive (HIV^+) sera than those with an "empty" Phe43 cavity (S375) (**Fig. 4.3.2M to O**), thus supporting the notion that the CD4-bound conformation affects the recognition of Env by ADCC-mediating CD4i antibodies and antibodies within HIV^+ sera (13).

To evaluate whether the enhanced recognition of HIV-1-infected cells by A32 and antibodies within HIV^+ sera translated into increased susceptibility to ADCC responses, we used a previously described fluorescence-activated cell sorter (FACS)-based ADCC assay (18, 21). Briefly, primary $CD4^+$ T cells infected for 48 h were incubated with autologous peripheral blood mononuclear cells (PBMCs) (effector-to-target cell ratio of 10:1) in the presence of A32 or HIV^+

sera (1:1,000). The percentage of cytotoxicity was calculated as described previously (18). In agreement with the poor recognition of infected cells expressing wild-type Env (S375), we observed low ADCC activity mediated by A32 (**Fig. 4.3.3A to C**) or sera from 15 HIV-1-infected individuals (**Fig. 4.3.3D to F**). However, replacing S375 with a histidine or tryptophan residue resulted in a significant increase in susceptibility to ADCC for the three IMCs tested. Of note, no staining of infected cells or ADCC responses were observed when sera from healthy HIV-1-negative donors were used (not shown).

The Phe43 cavity modulates recognition of CRF01_AE HIV-1-infected cells by CD4i antibodies and HIV$^+$ sera.

CRF01_AE HIV-1 isolates have a highly conserved histidine residue at Env position 375 (**Fig. 4.3.1E**), which was recently shown to be important for CD4 interaction (27) but also to confer strong resistance to the BMS-599793 entry inhibitor (36). To evaluate whether His375 influences the recognition of infected cells by ADCC-mediating antibodies and HIV$^+$ sera, His375 in the CRF01_AE 703357 strain was replaced by a serine (H375S). This strain was identified in the RV144 cohort and submitted to GenBank.

CRF01_AE IMCs were used to infect primary CD4 T cells from healthy uninfected donors. The impact of residue 375 on Env conformation was evaluated with CD4i 17b and A32 antibodies as well as sera from clade B- and CRF01_AE-infected individuals. The nature of the residue at position 375 did not affect CD4 downregulation (**Fig. 4.3.4A**) or Env expression, as evaluated by the binding of the 10e8 antibody (**Fig. 4.3.4B**). In contrast to the limited recognition of clade B, C, and D HIV-1-infected cells by A32, 17b, and antibodies within HIV$^+$ sera (**Fig. 4.3.2**) (13, 18, 20, 22, 37), cells infected with wild-type CRF01_AE Env (H375) were better recognized by both CD4i monoclonal antibodies (mAbs) as well as polyclonal sera (**Fig. 4.3.4C to F**). Strikingly, the replacement of His 375 by a serine residue (H375S) significantly decreased the recognition of infected cells by these ligands (**Fig. 4.3.4**). Overall, these results suggest that the recognition of wild-type CRF01_AE HIV-1 by CD4i antibodies and antibodies within HIV$^+$ sera is enhanced by the Phe43 cavity-filling histidine residue at 375. H375 functions as a proxy of small CD4mcs, which were recently shown to push Env into the CD4-bound conformation and sensitize HIV-1-infected cells to ADCC (18).

The Phe43 cavity modulates recognition of CRF01_AE HIV-1-infected cells by serum antibodies isolated from RV144 vaccinees.

A correlation between high levels of ADCC-mediating antibodies and HIV-1 acquisition in the RV144 vaccine trial was suggested for a subset of individuals with low plasma IgA anti-Env antibody levels (26, 28). ADCC-mediating mAbs targeting multiple epitopes were isolated from memory B cells of RV144 vaccine recipients (26, 38). Importantly, we demonstrated that the vaccine-induced ADCC-mediating antibodies directed against A32-blockable conformational epitopes poorly recognize Env on the surface of HIV-1-infected cells (clade B) unless the CD4 receptor was present on the surface of infected cells. This was achieved by deleting the *nef* and *vpu* genes (14). Since the predominantly circulating strain in Thailand is a CRF01_AE HIV-1 strain, which has a histidine at residue 375, we asked whether these antibodies, thought to have protected against HIV-1 transmission in RV144 recipients, recognized CRF01_AE HIV-1-infected cells in a manner dependent on Env residue 375. Wild-type (H375) or H375S mutant CRF01_AE IMCs were used to infect primary CD4 T cells from healthy uninfected donors. **Figure 4.3.5** shows that 11/12 (91.7%) A32-blockable antibodies induced by the RV144 vaccine recognized CRF01_AE HIV-1-infected cells expressing wild-type Env H375 significantly better than they recognized cells infected with the H375S counterpart.

Residue 375 modulates ADCC responses against CRF01_AE HIV-1-infected cells by CD4i antibodies, antibodies within HIV$^+$ sera, and antibodies from RV144 vaccinees.

To assess whether the recognition of CRF01_AE HIV-1-infected cells by A32, antibodies within HIV$^+$ sera, and antibodies from RV144 vaccinees correlated with ADCC responses, primary CD4 T cells were infected as described above, and ADCC was measured as described in Materials and Methods. **Figure 4.3.6** shows that wild-type (H375) CRF01_AE HIV-1-infected cells were readily susceptible to ADCC mediated by A32 and antibodies within HIV$^+$ sera from individuals infected with clade B and CRF01_AE HIV-1 strains. This result contrasts with the relatively poor ADCC activity observed for these antibodies against primary CD4 T cells infected with wild-type (S375) HIV-1 strains from clades B, C, and D (**Fig. 4.3.3**). ADCC responses directed against CRF01_AE HIV-1- infected cells depended on the presence of His375, as cells infected with the H375S virus variant were significantly less sensitive to ADCC. Similar results were observed

when ADCC experiments were done using the majority of RV144 anti-cluster A antibodies (CH29, CH38, CH40, CH51, CH52, CH54, CH77, CH80, and CH94) (**Fig. 4.3.7**).

4.4.6 DISCUSSION

Renewed interest in the Fc-mediated functions of antibodies such as ADCC stems in part from observed correlations with the control or prevention of HIV-1 infection. Fc-mediated effector functions were found to inversely correlate with viral loads or disease progression in simian immunodeficiency virus (SIV)-infected macaques (39–41) as well as in HIV-1-infected individuals (42–46). Furthermore, analysis of correlates of immune protection in the recent RV144 vaccine trial suggested that high levels of ADCC-mediating Abs correlated with decreased HIV-1 acquisition when combined with low plasma IgA anti-Env antibody levels (28, 47). Moreover, the CD4-bound conformation of Env was recently shown to be a major target of ADCC-mediating antibodies present in the sera of HIV-1-infected individuals (13). Accordingly, here we report that the size of the residue located within the Phe43 cavity of Env modulates the recognition and killing of HIV-1-infected cells by antibodies within HIV^+ sera and ADCC-mediating monoclonal antibodies, including those isolated from RV144 vaccinees. Altogether, our results suggest a model (**Fig. 4.3.8**) where the conformation spontaneously sampled by Env at the surface of infected cells has a significant impact on ADCC susceptibility. Env with an empty Phe43 cavity are protected from such responses due to the adoption of a conformation similar to that of the unliganded closed state (state 1) and the ability of Nef and Vpu to downregulate CD4 from the cell surface (14). This state 1 conformation of Env could be modulated by CD4mcs (18) or by naturally occurring Phe43 cavity-filling residues, which shift Env conformation toward the CD4-bound state. The CD4-bound Env conformation efficiently exposes anti-cluster A epitopes, known to be recognized by antibodies present in the majority of HIV-1-infected individuals and to mediate potent ADCC responses (13, 14, 18, 20–26). Therefore, our results raise the intriguing possibility that histidine 375 present in the predominant strain replicating in Thailand might have contributed to the efficacy of the trial by spontaneously exposing epitopes recognized by ADCC-mediating antibodies elicited by the RV144 vaccine regimen.

Since the first emergence of CRF01_AE HIV-1 strains in Africa and subsequent spread to Asia, where it established a major epidemic, this virus has become the dominant strain in many

Asian countries, including southern China and Thailand (48–50). Why CRF01_AE HIV-1 was able to spread so rapidly is unclear at the moment, but high viral loads and short survival times have been associated with CRF01_AE infection compared with the values seen for HIV-1 infections in the Western world (51–53). Additional work is needed to assess the evolutionary selective pressures that resulted in the fixation of a histidine residue at position 375 in this rapidly spreading viral strain. Substitutions of large residues like histidine at this position have been shown to result in SHIVs that bind rhesus macaque CD4 and replicate in monkeys more efficiently (12). Apparently, the advantages of the S375W change in specific hosts (rhesus monkeys and some southern Chinese and Thai individuals) outweigh negative consequences such as enhanced susceptibility of HIV-1-infected cells to ADCC responses. Our results warrant further studies that assess potential host factors that drive HIV-1 variation in the Phe43 cavity. The importance of the variation in residue 375 to susceptibility to the protective efficacy of HIV-1 vaccine-induced antibody responses also merits additional investigation.

4.4.7 MATERIALS AND METHODS

Plasmids and site-directed mutagenesis

Individual Env mutations were introduced in the previously described pNL43-ADA(Env)-GFP.IRES.Nef proviral vector (14) by using the QuikChange II XL site-directed mutagenesis protocol (Stratagene). The plasmids encoding SHIV clade C strain CH505, SHIV clade D strain 191859, and their variants were previously described (12). The sequence of HIV-1 CRF01_AE transmitted-founder (T/F) clone 703357 was derived by using a single-genome amplification (SGA) strategy. The entire DNA sequence including both long terminal repeats (LTRs) was cloned into pUC57 to generate a full-length infectious molecular clone (FLIMC) (GenBank accession numbers JX448154 and JX448164). Single mutations were then introduced into FLIMC 703357.

Cell lines and isolation of primary cells

293T human embryonic kidney cells were obtained from the ATCC and were grown as previously described (14). PBMCs from healthy donors were obtained under research regulations approved by the Centre de Recherche du CHUM (CRCHUM); written informed consent was

obtained from each individual. $CD4^+$ T cells were purified from rested PBMCs by negative selection and activated as previously described (18).

Virus production and infections

In order to achieve the same level of infection among the different mutants tested, vesicular stomatitis virus G (VSVG)-pseudotyped HIV-1 clones were produced, as previously described (14). This was necessary since mutations at residue 375 were shown to affect CD4 binding and infectivity in CRF01_AE strains (27). Briefly, proviral vectors and a VSVG-encoding plasmid were co-transfected into 293T cells by standard calcium phosphate transfection. Two days after transfection, cell supernatants were harvested, clarified by low-speed centrifugation (5 min at 1,500 rpm), and concentrated by ultracentrifugation for 1 h at 4°C at 100,605 × g over a 20% sucrose cushion. Pellets were resuspended in fresh RPMI, and aliquots were stored at -80°C until use. Viruses were then used to infect ~10 to 15% of primary CD4 T cells by spinoculation at 800 × g for 1 h in 96-well plates at 25°C.

Antibodies and sera

The gp120 outer-domain-specific 2G12 and the anti-gp41 10E8 antibodies were obtained from the NIH AIDS and Research and Reference Reagent Program. Anti-gp120 cluster A antibody A32 and coreceptor binding site antibody 17b were previously reported (14, 24, 54, 55). A32-blockable conformational epitope ADCC-mediating antibodies isolated from recipients of the RV144 ALVAC-HIV AIDSVAX B/E vaccine (CH29, CH38, CH40, CH51, CH52, CH54, CH77, CH80, CH81, CH89, CH91, and CH94) were previously described (14, 26). Sera from HIV-infected individuals (**Table 4.3.1**) were collected, heat inactivated, and stored as previously described (18). Written informed consent was obtained from all study participants (the Montreal Primary HIV Infection Cohort [56, 57] and the Canadian Cohort of HIV Infected Slow Progressors [58–60]), and research adhered to the ethical guidelines of the CRCHUM and was reviewed and approved by the CRCHUM institutional review board (ethics committee). Additional serum samples were acquired from HIV-1-infected individuals from Thailand who were enrolled in the HIV STAR study, as previously described (61) (**Table 4.3.2**). The Thai Ministry of Public Health and local ethics committees approved the collection of these samples. All donors provided informed consent. Research adhered to the standards indicated by the Declaration of Helsinki. All

sera were heat inactivated for 30 min at 56°C and stored at 4°C until they were ready for use in subsequent experiments. A randomnumber generator (QuickCalcs; GraphPad) was used to randomly select a number of serum samples for each experiment. Anti-CD4 monoclonal antibody OKT4 (BioLegend) binds to the D3 domain of CD4 and was used to measure cell surface levels of CD4, as described previously (14). Goat anti-mouse and anti-human antibodies coupled to Alexa Fluor 647 (Invitrogen) were used as secondary antibodies in flow cytometry experiments.

Flow cytometry analysis of cell surface staining and ADCC responses

Cell surface staining was performed as previously described, and mean fluorescence intensity (MFI) histograms show signals on live infected populations (13, 18). Binding of HIV-1-infected cells by HIV^+ sera (1:1,000 dilution) or anti-CD4 (OKT4) or anti-Env mAbs (5 µg/ml) was performed 48 h after in vitro infection. Detection of green fluorescent protein-positive (GFP^+), $p24^+$, or $p27^+$ infected cells was performed as described previously (37). The percentage of infected cells (i.e., GFP^+, $p24^+$, or $p27^+$ cells) was determined by gating the living cell population based on viability dye staining (Aqua Vivid, catalog number L43957; Thermo Fisher Scientific). Samples were analyzed on an LSRII cytometer (BD Biosciences, Mississauga, ON, Canada), and data analysis was performed by using FlowJo v10.0.7 (Tree Star, Ashland, OR, USA).

Measurement of ADCC-mediated killing was performed by using a previously described assay (18). Briefly, primary $CD4^+$ T cells infected for 48 h with the different molecularly cloned viruses described above were incubated with autologous PBMCs (effector-to-target cell ratio of 10:1) in the presence of A32, RV144 antibodies (5 µg/ml), or HIV^+ sera (1:1,000). The percentage of cytotoxicity was calculated as described previously (18).

Statistical analyses

Statistics were analyzed by using GraphPad Prism version 6.0.1 (GraphPad, San Diego, CA, USA). P values of < 0.05 were considered significant; significance values are indicated in the figure legends.

4.4.8 ACKNOWLEDGMENTS

We thank Elizabeth Carpelan for help with manuscript preparation. We thank Dominique Gauchat from the CRCHUM Flow Cytometry Platform for technical assistance and Mario Legault for cohort coordination and clinical samples. This work was supported by CIHR Foundation grant 352417, by amfAR innovation grant 109343-59-RGRL with support from FAIR to A.F., and by the FRQS AIDS and Infectious Diseases Network. A.F. is the recipient of a Canada research chair on retroviral entry. D.Z. is the recipient of FRQS master award 30888. M.V. was supported by CIHR doctoral research award 291485. J.R. is the recipient of CIHR fellowship award 135349. M.S.P. is the recipient of CIHR fellowship award 135451. D.E.K. is supported by a research scholar career award of the Quebec Health Research Fund (FRQS). This study was also supported by CIHR grant MOP93770, NIH grants AI100645 and AI100663, the Center for HIV/AIDS Vaccine Immunology and Immunogen Design (CHAVI-ID), National Institutes of Health grant GM56550, the late William F. McCarty-Cooper, and NIH grant R01AI116274. Our funding sources had no role in data collection, analysis, or interpretation and were not involved in the writing of the manuscript. The opinions expressed here are those of the authors and should not be construed as official or representing the views of the U.S. Department of Defense or Department of the Army. Mention of trade names, commercial products, or organizations does not imply endorsement by the U.S. government.

4.4.9 REFERENCES

1. Finzi A, Xiang SH, Pacheco B, Wang L, Haight J, Kassa A, Danek B, Pancera M, Kwong PD, Sodroski J. 2010. Topological layers in the HIV-1 gp120 inner domain regulate gp41 interaction and CD4-triggered conformational transitions. Mol Cell 37:656 – 667.
2. Helseth E, Olshevsky U, Furman C, Sodroski J. 1991. Human immunodeficiency virus type 1 gp120 envelope glycoprotein regions important for association with the gp41 transmembrane glycoprotein. J Virol 65: 2119 –2123.
3. Yang X, Mahony E, Holm GH, Kassa A, Sodroski J. 2003. Role of the gp120 inner domain beta-sandwich in the interaction between the human immunodeficiency virus envelope glycoprotein subunits. Virology 313: 117–125.

4. Kwong PD, Wyatt R, Robinson J, Sweet RW, Sodroski J, Hendrickson WA. 1998. Structure of an HIV gp120 envelope glycoprotein in complex with the CD4 receptor and a neutralizing human antibody. Nature 393: 648 – 659.
5. Pancera M, Majeed S, Ban YE, Chen L, Huang CC, Kong L, Kwon YD, Stuckey J, Zhou T, Robinson JE, Schief WR, Sodroski J, Wyatt R, Kwong PD. 2010. Structure of HIV-1 gp120 with gp41-interactive region reveals layered envelope architecture and basis of conformational mobility. Proc Natl Acad Sci USA 107:1166 –1171.
6. Wyatt R, Moore J, Accola M, Desjardin E, Robinson J, Sodroski J. 1995. Involvement of the V1/V2 variable loop structure in the exposure of human immunodeficiency virus type 1 gp120 epitopes induced by receptor binding. J Virol 69:5723–5733.
7. Lu M, Blacklow SC, Kim PS. 1995. A trimeric structural domain of the HIV-1 transmembrane glycoprotein. Nat Struct Biol 2:1075–1082.
8. Weissenhorn W, Dessen A, Harrison SC, Skehel JJ, Wiley DC. 1997. Atomic structure of the ectodomain from HIV-1 gp41. Nature 387:426 – 430.
9. Xiang SH, Kwong PD, Gupta R, Rizzuto CD, Casper DJ, Wyatt R, Wang L, Hendrickson WA, Doyle ML, Sodroski J. 2002. Mutagenic stabilization and/or disruption of a CD4-bound state reveals distinct conformations of the human immunodeficiency virus type 1 gp120 envelope glycoprotein. J Virol 76:9888 –9899.
10. Desormeaux A, Coutu M, Medjahed H, Pacheco B, Herschhorn A, Gu C, Xiang SH, Mao Y, Sodroski J, Finzi A. 2013. The highly conserved layer-3 component of the HIV-1 gp120 inner domain is critical for CD4-required conformational transitions. J Virol 87:2549 – 2562.
11. Finzi A, Pacheco B, Xiang SH, Pancera M, Herschhorn A, Wang L, Zeng X, Desormeaux A, Kwong PD, Sodroski J. 2012. Lineage-specific differences between human and simian immunodeficiency virus regulation of gp120 trimer association and CD4 binding. J Virol 86:8974 – 8986.
12. Li H, Wang S, Kong R, Ding W, Lee FH, Parker Z, Kim E, Learn GH, Hahn P, Policicchio B, Brocca-Cofano E, Deleage C, Hao X, Chuang GY, Gorman J, Gardner M, Lewis MG, Hatziioannou T, Santra S, Apetrei C, Pandrea I, Alam SM, Liao HX, Shen X, Tomaras GD, Farzan M, Chertova E, Keele BF, Estes JD, Lifson JD, Doms RW, Montefiori DC, Haynes BF, Sodroski JG, Kwong PD, Hahn BH, Shaw GM. 2016. Envelope residue 375

substitutions in simian-human immunodeficiency viruses enhance CD4 binding and replication in rhesus macaques. Proc Natl Acad Sci USA 113: E3413–E3422.

13. Veillette M, Coutu M, Richard J, Batraville LA, Dagher O, Bernard N, Tremblay C, Kaufmann DE, Roger M, Finzi A. 2015. The HIV-1 gp120 CD4-bound conformation is preferentially targeted by antibody-dependent cellular cytotoxicity-mediating antibodies in sera from HIV-1-infected individuals. J Virol 89:545–551.
14. Veillette M, Desormeaux A, Medjahed H, Gharsallah NE, Coutu M, Baalwa J, Guan Y, Lewis G, Ferrari G, Hahn BH, Haynes BF, Robinson JE, Kaufmann DE, Bonsignori M, Sodroski J, Finzi A. 2014. Interaction with cellular CD4 exposes HIV-1 envelope epitopes targeted by antibody-dependent cell-mediated cytotoxicity. J Virol 88:2633–2644.
15. Arias JF, Heyer LN, von Bredow B, Weisgrau KL, Moldt B, Burton DR, Rakasz EG, Evans DT. 2014. Tetherin antagonism by Vpu protects HIV-infected cells from antibody-dependent cell-mediated cytotoxicity. Proc Natl Acad Sci USA 111:6425– 6430.
16. Alvarez RA, Hamlin RE, Monroe A, Moldt B, Hotta MT, Rodriguez Caprio G, Fierer DS, Simon V, Chen BK. 2014. HIV-1 Vpu antagonism of tetherin inhibits antibody-dependent cellular cytotoxic responses by natural killer cells. J Virol 88:6031– 6046.
17. von Bredow B, Arias JF, Heyer LN, Gardner MR, Farzan M, Rakasz EG, Evans DT. 2015. Envelope glycoprotein internalization protects human and simian immunodeficiency virus infected cells from antibody-dependent cell-mediated cytotoxicity. J Virol 89:10648-55.
18. Richard J, Veillette M, Brassard N, Iyer SS, Roger M, Martin L, Pazgier M, Schon A, Freire E, Routy JP, Smith AB, III, Park J, Jones DM, Courter JR, Melillo BN, Kaufmann DE, Hahn BH, Permar SR, Haynes BF, Madani N, Sodroski JG, Finzi A. 2015. CD4 mimetics sensitize HIV-1-infected cells to ADCC. Proc Natl Acad Sci USA 112:E2687–E2694.
19. Lee WS, Richard J, Lichtfuss M, Smith AB, III, Park J, Courter JR, Melillo BN, Sodroski JG, Kaufmann DE, Finzi A, Parsons MS, Kent SJ. 2015. Antibody-dependent cellular cytotoxicity against reactivated HIV-1-infected cells. J Virol 90:2021–2030.
20. Richard J, Pacheco B, Gohain N, Veillette M, Ding S, Alsahafi N, Tolbert WD, Prevost J, Chapleau JP, Coutu M, Jia M, Brassard N, Park J, Courter JR, Melillo B, Martin L, Tremblay C, Hahn BH, Kaufmann DE, Wu X, Smith AB, III, Sodroski J, Pazgier M, Finzi A. 2016. Co-receptor binding site antibodies enable CD4-mimetics to expose conserved

anti-cluster A ADCC epitopes on HIV-1 envelope glycoproteins. EBioMedicine 12:208-218.

21. Richard J, Veillette M, Batraville LA, Coutu M, Chapleau JP, Bonsignori M, Bernard N, Tremblay C, Roger M, Kaufmann DE, Finzi A. 2014. Flow cytometry-based assay to study HIV-1 gp120 specific antibody-dependent cellular cytotoxicity responses. J Virol Methods 208:107–114.
22. Ding S, Veillette M, Coutu M, Prevost J, Scharf L, Bjorkman PJ, Ferrari G, Robinson JE, Sturzel C, Hahn BH, Sauter D, Kirchhoff F, Lewis GK, Pazgier M, Finzi A. 2016. A highly conserved residue of the HIV-1 gp120 inner domain is important for antibody-dependent cellular cytotoxicity responses mediated by anti-cluster A antibodies. J Virol 90:2127–2134.
23. Tolbert WD, Gohain N, Veillette M, Chapleau JP, Orlandi C, Visciano ML, Ebadi M, DeVico AL, Fouts TR, Finzi A, Lewis GK, Pazgier M. 2016. Paring down HIV Env: design and crystal structure of a stabilized inner domain of HIV-1 gp120 displaying a major ADCC target of the A32 region. Structure 24:697–709.
24. Guan Y, Pazgier M, Sajadi MM, Kamin-Lewis R, Al-Darmarki S, Flinko R, Lovo E, Wu X, Robinson JE, Seaman MS, Fouts TR, Gallo RC, DeVico AL, Lewis GK. 2013. Diverse specificity and effector function among human antibodies to HIV-1 envelope glycoprotein epitopes exposed by CD4 binding. Proc Natl Acad Sci USA 110:E69 –E78.
25. Ferrari G, Pollara J, Kozink D, Harms T, Drinker M, Freel S, Moody MA, Alam SM, Tomaras GD, Ochsenbauer C, Kappes JC, Shaw GM, Hoxie JA, Robinson JE, Haynes BF. 2011. An HIV-1 gp120 envelope human monoclonal antibody that recognizes a C1 conformational epitope mediates potent antibody-dependent cellular cytotoxicity (ADCC) activity and defines a common ADCC epitope in human HIV-1 serum. J Virol 85: 7029 – 7036.
26. Bonsignori M, Pollara J, Moody MA, Alpert MD, Chen X, Hwang KK, Gilbert PB, Huang Y, Gurley TC, Kozink DM, Marshall DJ, Whitesides JF, Tsao CY, Kaewkungwal J, Nitayaphan S, Pitisuttithum P, Rerks-Ngarm S, Kim JH, Michael NL, Tomaras GD, Montefiori DC, Lewis GK, Devico A, Evans DT, Ferrari G, Liao HX, Haynes BF. 2012. Antibody-dependent cellular cytotoxicity-mediating antibodies from an HIV-1 vaccine

efficacy trial target multiple epitopes and preferentially use the VH1 gene family. J Virol 86:11521–11532.

27. Zoubchenok D, Veillette M, Prevost J, Sanders-Buell E, Wagh K, Korber B, Chenine AL, Finzi A. 2016. Histidine 375 modulates CD4 binding in HIV-1 CRF01_AE envelope glycoproteins. J Virol 91:e02151-16.
28. Haynes BF, Gilbert PB, McElrath MJ, Zolla-Pazner S, Tomaras GD, Alam SM, Evans DT, Montefiori DC, Karnasuta C, Sutthent R, Liao HX, DeVico AL, Lewis GK, Williams C, Pinter A, Fong Y, Janes H, DeCamp A, Huang Y, Rao M, Billings E, Karasavvas N, Robb ML, Ngauy V, de Souza MS, Paris R, Ferrari G, Bailer RT, Soderberg KA, Andrews C, Berman PW, Frahm N, De Rosa SC, Alpert MD, Yates NL, Shen X, Koup RA, Pitisuttithum P, Kaewkungwal J, Nitayaphan S, Rerks-Ngarm S, Michael NL, Kim JH. 2012. Immune-correlates analysis of an HIV-1 vaccine efficacy trial. N Engl J Med 366:1275–1286.
29. McCutchan FE. 2006. Global epidemiology of HIV. J Med Virol 78(Suppl 1):S7–S12.
30. Burke DS. 1997. Recombination in HIV: an important viral evolutionary strategy. Emerg Infect Dis 3:253–259.
31. Taylor BS, Hammer SM. 2008. The challenge of HIV-1 subtype diversity. N Engl J Med 359:1965–1966.
32. Hemelaar J. 2012. The origin and diversity of the HIV-1 pandemic. Trends Mol Med 18:182–192.
33. Hemelaar J. 2013. Implications of HIV diversity for the HIV-1 pandemic. J Infect 66:391–400.
34. Veillette M, Coutu M, Richard J, Batraville LA, Desormeaux A, Roger M, Finzi A. 14 September 2014. Conformational evaluation of HIV-1 trimeric envelope glycoproteins using a cell-based ELISA assay. J Vis Exp 14:51995.
35. Veillette M, Richard J, Pazgier M, Lewis GK, Parsons MS, Finzi A. 2016. Role of HIV-1 envelope glycoproteins conformation and accessory proteins on ADCC responses. Curr HIV Res 14:9 –23.
36. Schader SM, Colby-Germinario SP, Quashie PK, Oliveira M, Ibanescu RI, Moisi D, Mesplede T, Wainberg MA. 2012. HIV gp120 H375 is unique to HIV-1 subtype

CRF01_AE and confers strong resistance to the entry inhibitor BMS-599793, a candidate microbicide drug. Antimicrob Agents Chemother 56:4257– 4267.

37. Richard J, Veillette M, Ding S, Zoubchenok D, Alsahafi N, Coutu M, Brassard N, Park J, Courter JR, Melillo B, Smith AB, III, Shaw GM, Hahn BH, Sodroski J, Kaufmann DE, Finzi A. 2016. Small CD4 mimetics prevent HIV-1 uninfected bystander CD4 T cell killing mediated by antibody-dependent cell-mediated cytotoxicity. EBioMedicine 3:122–134.
38. Liao HX, Bonsignori M, Alam SM, McLellan JS, Tomaras GD, Moody MA, Kozink DM, Hwang KK, Chen X, Tsao CY, Liu P, Lu X, Parks RJ, Montefiori DC, Ferrari G, Pollara J, Rao M, Peachman KK, Santra S, Letvin NL, Karasavvas N, Yang ZY, Dai K, Pancera M, Gorman J, Wiehe K, Nicely NI, Rerks-Ngarm S, Nitayaphan S, Kaewkungwal J, Pitisuttithum P, Tartaglia J, Sinangil F, Kim JH, Michael NL, Kepler TB, Kwong PD, Mascola JR, Nabel GJ, Pinter A, Zolla-Pazner S, Haynes BF. 2013. Vaccine induction of antibodies against a structurally heterogeneous site of immune pressure within HIV-1 envelope protein variable regions 1 and 2. Immunity 38:176 –186.
39. Sun Y, Asmal M, Lane S, Permar SR, Schmidt SD, Mascola JR, Letvin NL. 2011. Antibody-dependent cell-mediated cytotoxicity in simian immunodeficiency virus-infected rhesus monkeys. J Virol 85:6906 – 6912.
40. Banks ND, Kinsey N, Clements J, Hildreth JE. 2002. Sustained antibody-dependent cell-mediated cytotoxicity (ADCC) in SIV-infected macaques correlates with delayed progression to AIDS. AIDS Res Hum Retroviruses 18:1197–1205.
41. Alpert MD, Harvey JD, Lauer WA, Reeves RK, Piatak M, Jr, Carville A, Mansfield KG, Lifson JD, Li W, Desrosiers RC, Johnson RP, Evans DT. 2012. ADCC develops over time during persistent infection with live-attenuated SIV and is associated with complete protection against SIV(mac)251 challenge. PLoS Pathog 8:e1002890.
42. Baum LL, Cassutt KJ, Knigge K, Khattri R, Margolick J, Rinaldo C, Kleeberger CA, Nishanian P, Henrard DR, Phair J. 1996. HIV-1 gp120- specific antibody-dependent cell-mediated cytotoxicity correlates with rate of disease progression. J Immunol 157:2168 – 2173.
43. Forthal DN, Landucci G, Haubrich R, Keenan B, Kuppermann BD, Tilles JG, Kaplan J. 1999. Antibody-dependent cellular cytotoxicity independently predicts survival in severely

immunocompromised human immunodeficiency virus-infected patients. J Infect Dis 180:1338 –1341.

44. Ljunggren K, Moschese V, Broliden PA, Giaquinto C, Quinti I, Fenyo EM, Wahren B, Rossi P, Jondal M. 1990. Antibodies mediating cellular cytotoxicity and neutralization correlate with a better clinical stage in children born to human immunodeficiency virus-infected mothers. J Infect Dis 161:198 –202.
45. Chung AW, Navis M, Isitman G, Wren L, Silvers J, Amin J, Kent SJ, Stratov I. 2011. Activation of NK cells by ADCC antibodies and HIV disease progression. J Acquir Immune Defic Syndr 58:127–131.
46. Mabuka J, Nduati R, Odem-Davis K, Peterson D, Overbaugh J. 2012. HIV-specific antibodies capable of ADCC are common in breastmilk and are associated with reduced risk of transmission in women with high viral loads. PLoS Pathog 8:e1002739.
47. Tomaras GD, Ferrari G, Shen X, Alam SM, Liao HX, Pollara J, Bonsignori M, Moody MA, Fong Y, Chen X, Poling B, Nicholson CO, Zhang R, Lu X, Parks R, Kaewkungwal J, Nitayaphan S, Pitisuttithum P, Rerks-Ngarm S, Gilbert PB, Kim JH, Michael NL, Montefiori DC, Haynes BF. 2013. Vaccine-induced plasma IgA specific for the C1 region of the HIV-1 envelope blocks binding and effector function of IgG. Proc Natl Acad Sci USA 110:9019-24
48. Li X, Li W, Zhong P, Fang K, Zhu K, Musa TH, Song Y, Du G, Gao R, Guo Y, Yan W, Xuan Y, Wei P. 2016. Nationwide trends in molecular epidemiology of HIV-1 in China. AIDS Res Hum Retroviruses 32:851-9.
49. Zhong P, Pan Q, Ning Z, Xue Y, Gong J, Zhen X, Zhou L, Sheng F, Zhang W, Gai J, Cheng H, Yue Q, Xing H, Zhuang M, Lu W, Shao Y, Kang L. 2007. Genetic diversity and drug resistance of human immunodeficiency virus type 1 (HIV-1) strains circulating in Shanghai. AIDS Res Hum Retroviruses 23:847– 856.
50. He X, Xing H, Ruan Y, Hong K, Cheng C, Hu Y, Xin R, Wei J, Feng Y, Hsi JH, Takebe Y, Shao Y, Group for HIV Molecular Epidemiology Survey. 2012. A comprehensive mapping of HIV-1 genotypes in various risk groups and regions across China based on a nationwide molecular epidemiologic survey. PLoS One 7:e47289.

51. Hu DJ, Vanichseni S, Mastro TD, Raktham S, Young NL, Mock PA, Subbarao S, Parekh BS, Srisuwanvilai L, Sutthent R, Wasi C, Heneine W, Choopanya K. 2001. Viral load differences in early infection with two HIV-1 subtypes. AIDS 15:683– 691.
52. Rangsin R, Piyaraj P, Sirisanthana T, Sirisopana N, Short O, Nelson KE. 2007. The natural history of HIV-1 subtype E infection in young men in Thailand with up to 14 years of follow-up. AIDS 21(Suppl 6):S39 –S46.
53. Rangsin R, Chiu J, Khamboonruang C, Sirisopana N, Eiumtrakul S, Brown AE, Robb M, Beyrer C, Ruangyuttikarn C, Markowitz LE, Nelson KE. 2004. The natural history of HIV-1 infection in young Thai men after seroconversion. J Acquir Immune Defic Syndr 36:622–629.
54. Robinson JE, Holton D, Elliott S, Ho DD. 1992. Distinct antigenic sites on HIV gp120 identified by a panel of human monoclonal antibodies. J Cell Biochem Suppl 16E:Q449.
55. Zhang W, Godillot AP, Wyatt R, Sodroski J, Chaiken I. 2001. Antibody 17b binding at the coreceptor site weakens the kinetics of the interaction of envelope glycoprotein gp120 with CD4. Biochemistry 40:1662–1670.
56. Fontaine J, Chagnon-Choquet J, Valcke HS, Poudrier J, Roger M, Montreal Primary HIV Infection and Long-Term Non-Progressor Study Groups. 2011. High expression levels of B lymphocyte stimulator (BLyS) by dendritic cells correlate with HIV-related B-cell disease progression in humans. Blood 117:145–155.
57. Fontaine J, Coutlee F, Tremblay C, Routy JP, Poudrier J, Roger M, Montreal Primary HIV Infection and Long-Term Non-progressor Study Groups. 2009. HIV infection affects blood myeloid dendritic cells after successful therapy and despite non-progressing clinical disease. J Infect Dis 199:1007–1018.
58. Peretz Y, Ndongala ML, Boulet S, Boulassel MR, Rouleau D, Cote P, Longpre D, Routy JP, Falutz J, Tremblay C, Tsoukas CM, Sekaly RP, Bernard NF. 2007. Functional T cell subsets contribute differentially to HIV peptide-specific responses within infected individuals: correlation of these functional T cell subsets with markers of disease progression. Clin Immunol 124:57– 68.
59. Kamya P, Boulet S, Tsoukas CM, Routy JP, Thomas R, Cote P, Boulassel MR, Baril JG, Kovacs C, Migueles SA, Connors M, Suscovich TJ, Brander C, Tremblay CL, Bernard N, Canadian Cohort of HIV Infected Slow Progressors. 2011. Receptor-ligand requirements

for increased NK cell polyfunctional potential in slow progressors infected with HIV-1 co-expressing KIR3DL1*h/*y and HLA-B*57. J Virol 85:5949 –5960.

60. International HIV Controllers Study, Pereyra F, Jia X, McLaren PJ, Telenti A, de Bakker PI, Walker BD, Ripke S, Brumme CJ, Pulit SL, Carrington M, Kadie CM, Carlson JM, Heckerman D, Graham RR, Plenge RM, Deeks SG, Gianniny L, Crawford G, Sullivan J, Gonzalez E, Davies L, Camargo A, Moore JM, Beattie N, Gupta S, Crenshaw A, Burtt NP, Guiducci C, Gupta N, Gao X, Qi Y, Yuki Y, Piechocka-Trocha A, Cutrell E, Rosenberg R, Moss KL, Lemay P, O'Leary J, Schaefer T, Verma P, Toth I, Block B, Baker B, Rothchild A, Lian J, Proudfoot J, Alvino DM, Vine S, Addo MM, et al. 2010. The major genetic determinants of HIV-1 control affect HLA class I peptide presentation. Science 330:1551–1557.
61. Bunupuradah T, Chetchotisakd P, Ananworanich J, Munsakul W, Jirajariyavej S, Kantipong P, Prasithsirikul W, Sungkanuparph S, Bowonwatanuwong C, Klinbuayaem V, Kerr SJ, Sophonphan J, Bhakeecheep S, Hirschel B, Ruxrungtham K, HIV STAR Study Group. 2012. A randomized comparison of second-line lopinavir/ritonavir monotherapy versus tenofovir/lamivudine/lopinavir/ritonavir in patients failing NNRTI regimens: the HIV STAR study. Antivir Ther 17:1351–1361.

4.4.10 FIGURES

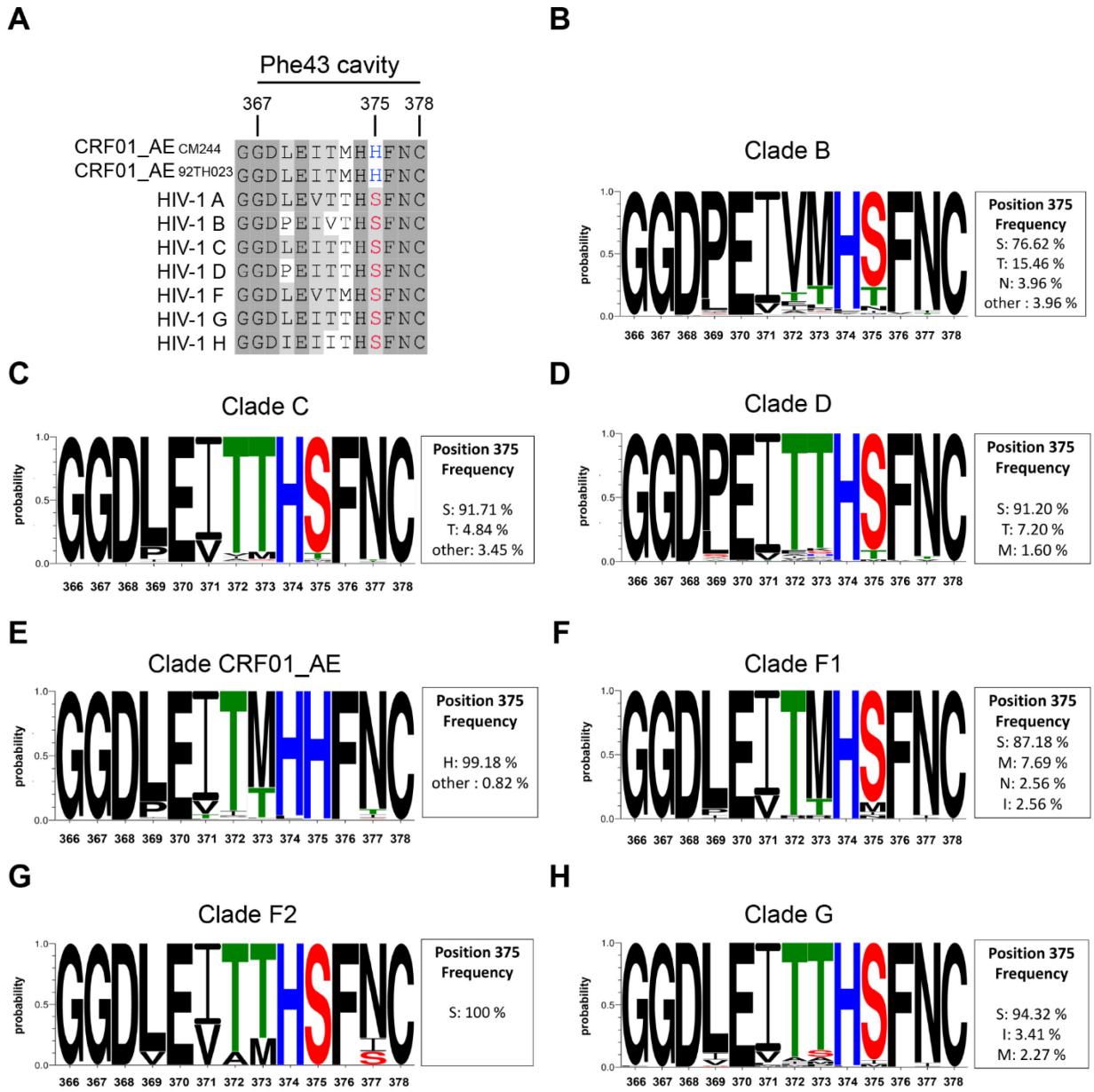

Figure 4.3.1 - Sequence alignment of gp120 residues flanking the Phe43 cavity of different HIV-1 isolates.

(**A**) Primary sequence alignment of gp120 residues flanking the Phe43 cavity based on a single representative sequence from each clade, including HIV-1 clade A (GenBank accession number ABB29387.1), HIV-1 clade B (accession number K03455), HIV-1 clade C (accession number AAB36507.1), HIV-1 clade D (accession number P04581.1), HIV-1 clade F (accession number ACR27173.1), HIV-1 clade G (accession number ACO91925.1), and HIV-1 clade H (accession number AAF18394.1), and two CRF01_AE strains, CM244 (accession number AY713425) and 92TH023. Residue numbering is based on that of the HXBc2 strain of HIV-1. Identical residues are shaded in dark gray, and conserved residues are shaded in light gray. S375 is shown in red, and H375 is shown in blue. (**B to H**) Logo depictions of the frequency of each amino acid from the Phe43 cavity at positions 366 to 378 in isolates from clade B, clade C, clade D, CRF01_AE, clade F1, clade F2, and clade G. The height of the letter indicates its frequency within the clade. The box beside each logo indicates the frequency of all the amino acids at position 375. The 2016 Los Alamos database-curated Env alignment was used as the basis for this figure, which contains 4,397 amino acid HIV-1 group M sequences (1,897 of subtype B, 1,363 of subtype C, 125 of subtype D, 39 of subtype F1, 9 of subtype F2, 88 of subtype G, and 486 of CRF01_AE).

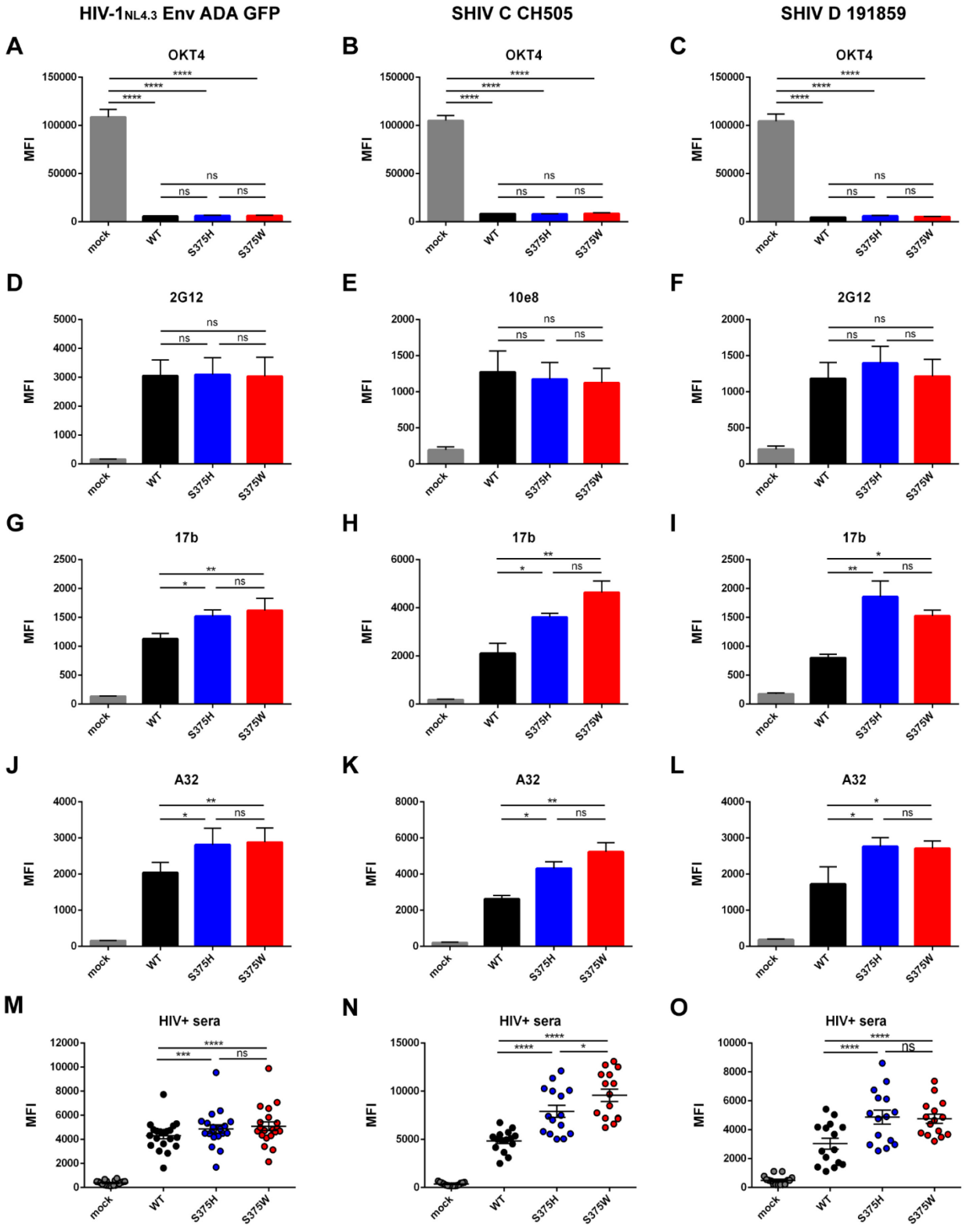
HIV-1NL4.3 Env ADA GFP
SHIV C CH505
SHIV D 191859
A
OKT4
B
OKT4
C
OKT4
D
2G12
E
10e8
F
2G12
G
17b
H
17b
I
17b
J
A32
K
A32
L
A32
M
HIV+ sera
N
HIV+ sera
O
HIV+ sera
MFI
mock
WT
S375H
S375W
ns

Figure 4.3.2 - The Phe43 cavity modulates recognition of clade B, C, and D HIV-1-infected cells by CD4i antibodies and antibodies within HIV$^+$ sera.
Shown are data for cell surface staining of primary CD4$^+$ T cells that were either mock infected or infected with HIV-1 NL4.3-GFP expressing the primary R5 ADA Env (clade B) or SHIV expressing either CH505 (clade C) or 191859 (clade D) Env with anti-CD4 antibody OKT4 (**A to C**); the Env-specific antibody 2G12 (**D and F**) or 10E8 (**E**), which are not influenced by changes in residue 375; CD4i antibodies 17b (**G to I**) and A32 (**J to L**); and antibodies within HIV$^+$ sera (**M to O**). Shown are the MFIs obtained from at least 3 independent experiments. Error bars indicate means +/- standard errors of the means. Statistical significance was tested by using paired one-way analysis of variance with a Holm-Sidak post-test (*, $P < 0.05$; **, $P < 0.01$; ***, $P < 0.001$; ****, $P < 0.0001$; ns, nonsignificant).

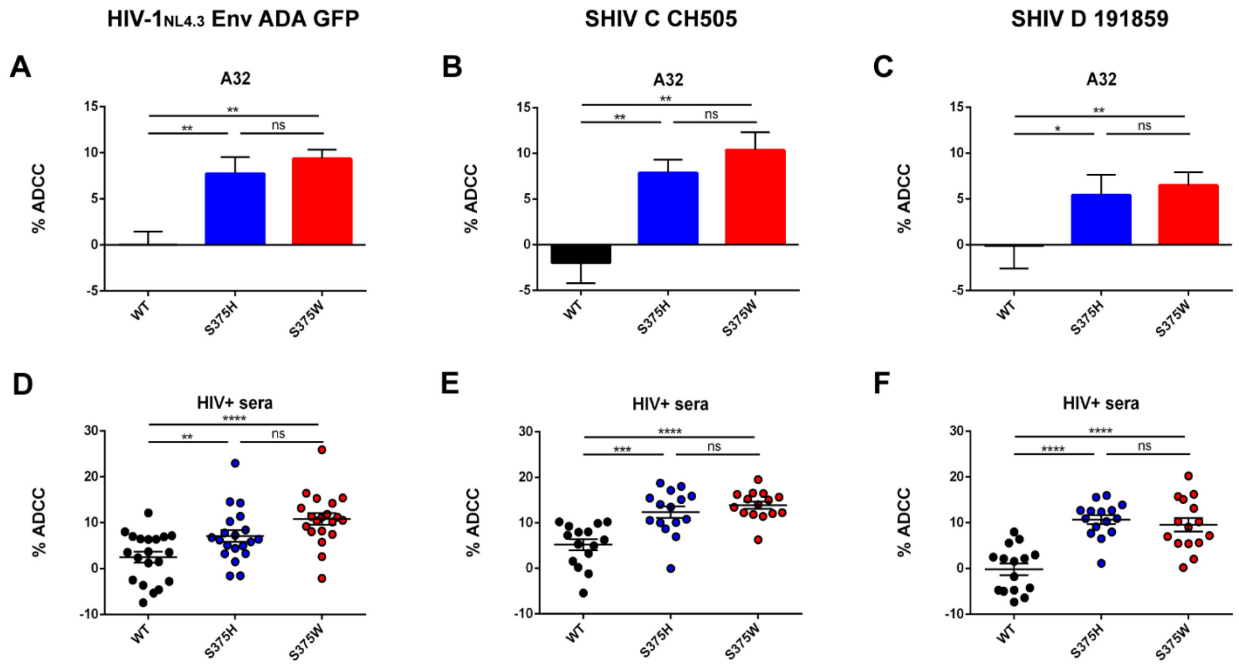

Figure 4.3.3 - The Phe43 cavity modulates ADCC responses mediated by the A32 antibody and antibodies within HIV$^+$ sera.

Primary CD4$^+$ T cells infected with NL4.3-GFP expressing the primary R5 ADA Env (clade B) or SHIV expressing either CH505 (clade C) or 191859 (clade D) Env were used as target cells and autologous PBMCs were used as effector cells in our FACS-based ADCC assay, as described in Materials and Methods. Shown are the percentages of ADCC activity in the presence of anti-cluster A monoclonal antibody A32 (**A to C**) or in the presence of HIV sera from HIV-1 clade B-infected individuals (**D to F**). These results are representative of those obtained in at least 3 independent experiments. Error bars indicate means +/- standard errors of the means. Statistical significance was tested by using paired one-way analysis of variance with a Holm-Sidak post-test (*, $P < 0.05$; **, $P < 0.01$; ***, $P < 0.001$; ****, $P < 0.0001$; ns, nonsignificant).

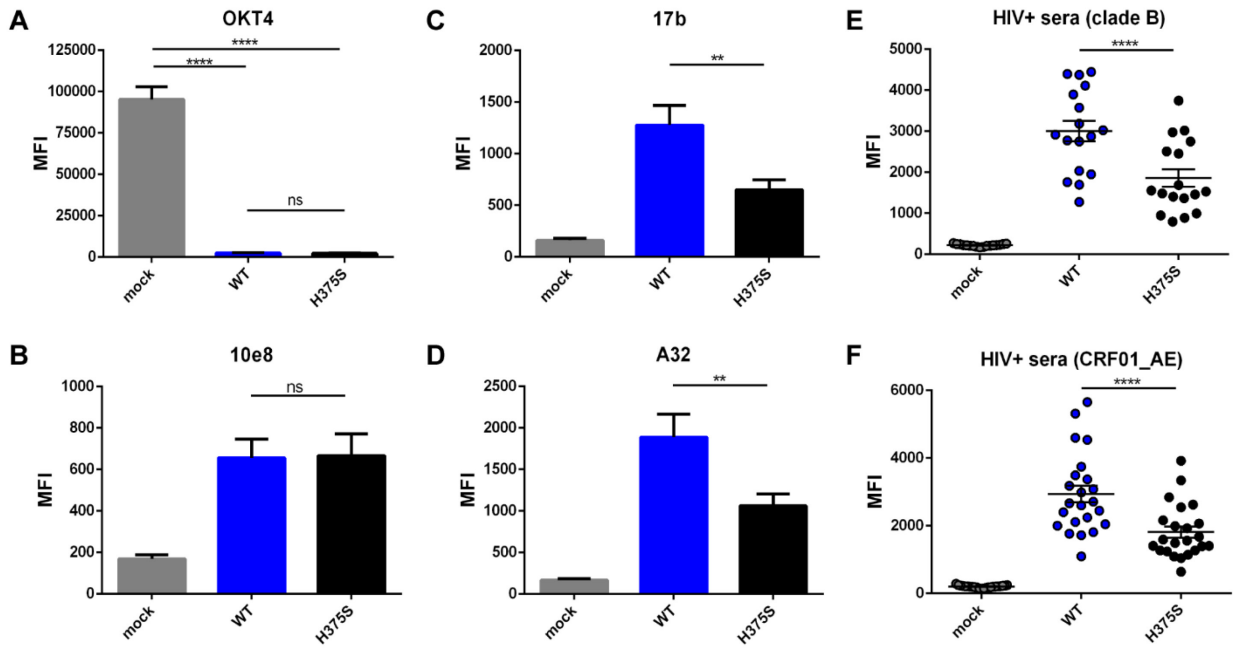

Figure 4.3.4 - The Phe43 cavity modulates the recognition of CRF01_AE HIV-1-infected primary CD4$^+$ T cells by CD4i antibodies and HIV$^+$ sera.
Shown are data for cell surface staining of primary CD4$^+$ T cells that were either mock infected or infected with the WT or the H375S variant of CRF01_AE transmitted-founder HIV-1 (IMC 703357) with anti-CD4 antibody OKT4 (**A**), conformation-insensitive Env-specific antibody 10E8 (**B**), CD4i antibodies 17b (**C**) and A32 (**D**), and sera from individuals infected with HIV-1 clade B (**E**) or HIV-1 CRF01_AE (**F**). Shown are the MFIs obtained in at least 4 independent experiments. Error bars indicate means +/- standard errors of the means. Statistical significance was tested by using an unpaired two-tailed t test for mAbs or a paired two-tailed t test for HIV$^+$ sera (*, $P < 0.05$; ****, $P < 0.0001$; ns, nonsignificant).

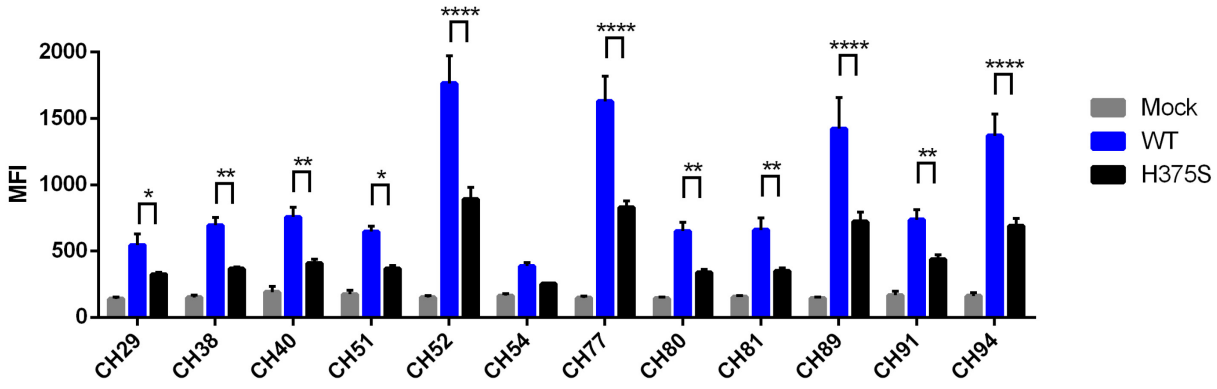

Figure 4.3.5 - The Phe43 cavity modulates the recognition of CRF01_AE HIV-1-infected primary CD4$^+$ T cells by antibodies isolated from RV144 vaccinees.
Shown are data for cell surface staining of primary CD4$^+$ T cells that were either mock infected or infected with the WT or an H375S mutant of CRF01_AE transmitted-founder HIV-1 (IMC 703357) with A32-blockable mAbs isolated from RV144 vaccinees (CH29, CH38, CH40, CH51, CH52, CH54, CH77, CH80, CH81, CH89, CH91, and CH94). Shown are the MFIs obtained in at least 5 independent experiments. Error bars indicate means +/- standard errors of the means. Statistical significance was tested by using an unpaired two-tailed t test (*, $P < 0.05$; **, $P < 0.01$; ****, $P < 0.0001$).

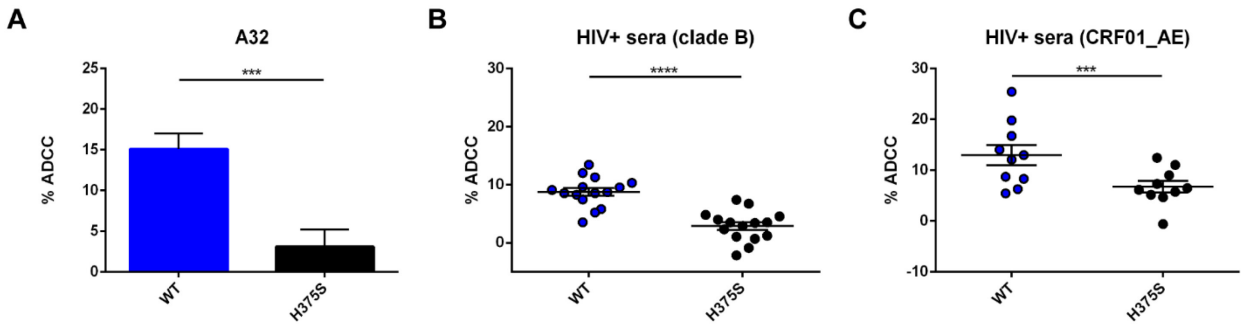

Figure 4.3.6 - Histidine 375 modulates ADCC responses against CRF01_AE HIV-1-infected cells mediated by the A32 antibody and HIV$^+$ sera.

Primary CD4$^+$ T cells infected with WT and H375S mutant CRF01_AE transmitted-founder HIV-1 (IMC 703357) were used as target cells and autologous PBMCs were used as effector cells in our FACS-based ADCC assay, as described in Materials and Methods. Shown are the percentages of ADCC activity by A32 (**A**) or by antibodies in sera from HIV-1 clade B-infected (**B**) or CRF01_AE HIV-1-infected (**C**) individuals. These results are representative of data from at least 4 independent experiments. Error bars indicate means +/- standard errors of the means. Statistical significance was tested by using an unpaired two-tailed t test for A32 or a paired two-tailed t test for HIV$^+$ sera (***, $P < 0.001$; ****, $P < 0.0001$).

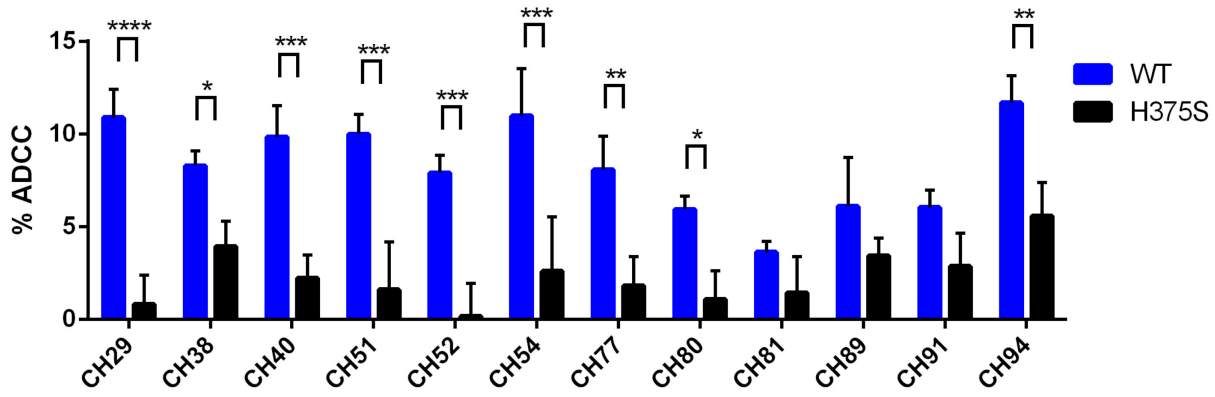

Figure 4.3.7 - Histidine 375 modulates ADCC responses against CRF01_AE HIV-1-infected cells mediated by antibodies isolated from RV144 vaccinees.
Primary $CD4^+$ T cells infected with the WT or the H375S variant of CRF01_AE transmitted-founder HIV-1 (IMC 703357) were used as target cells, with autologous PBMCs as effector cells, in our FACS-based ADCC assay. Shown are the percentages of ADCC activity in the presence of the A32-blockable monoclonal antibodies (CH29, CH38, CH40, CH51, CH52, CH54, CH77, CH80, CH81, CH89, CH91, and CH94) isolated from RV144 vaccinees. These results are representative of those obtained in at least 5 independent experiments. Error bars indicate means +/- standard errors of the means. Statistical significance was tested by using an unpaired two-tailed t test (*, $P < 0.05$; **, $P < 0.01$; ***, $P < 0.001$; ****, $P < 0.0001$).

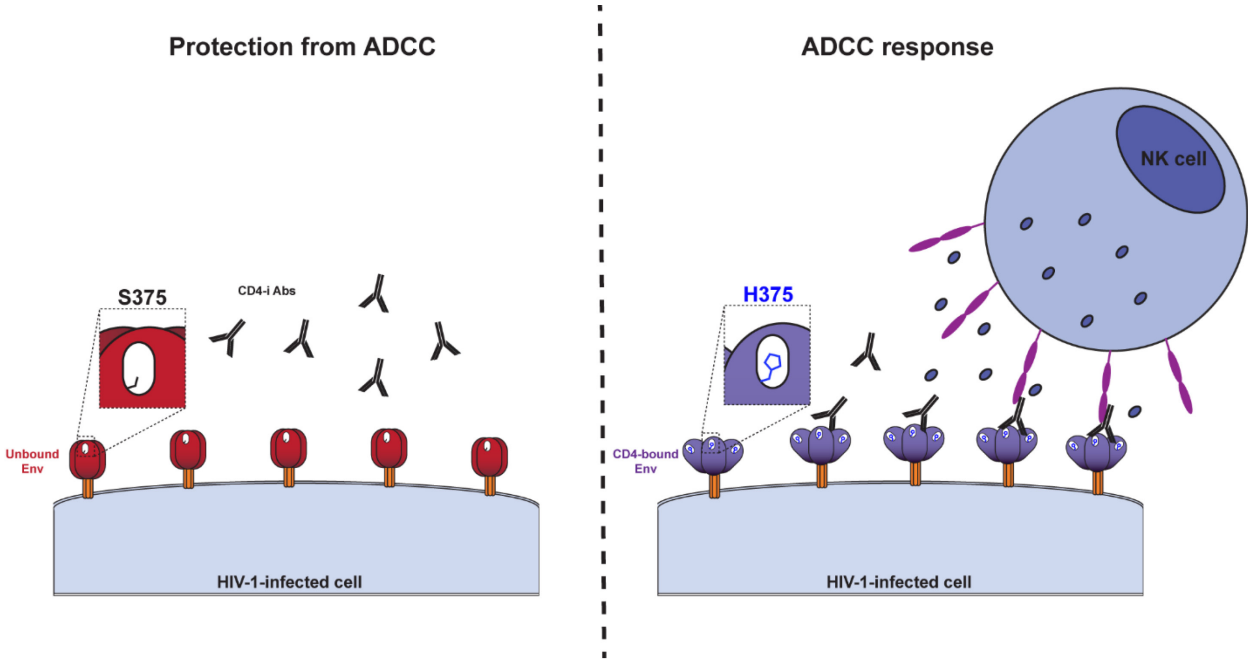

Figure 4.3.8 - The Phe43 cavity modulates HIV-1 Env conformation and ADCC responses. Flanking the Phe43 cavity, the identity of residue 375 modulates the transition of Env to the CD4-bound conformation. The presence of a serine residue at this position keeps Env in its unliganded, closed state (state 1), thus preventing the exposure of highly conserved epitopes recognized by anti-cluster A antibodies. The presence of a larger residue within the cavity, such as the naturally occurring histidine at position 375, shifts Env conformation to a state closer to the CD4-bound state, thus more readily exposing cluster A epitopes and enhancing the susceptibility of infected cells to ADCC mediated by antibodies in HIV^+ sera.

Table 4.3.1 - Characteristics of HIV-1 clade B-infected sera donors

Donor ID	CD4 count (cells / mm^3)	Viral load (copies / ml)
1	410	260
2	692	<50
3	680	633
4	620	<40
5	580	1477
6	670	58475
7	592	13520
8	810	42
9	780	949
10	1307	3387
11	780	905
12	800	7206
13	747	3098
14	920	277
15	790	22045
16	1009	67
17	830	674
18	1029	3779
19	647	961
20	420	1112
21	460	180763

Table 4.3.2 - Characteristics of HIV-1 CRF01_AE-infected sera donors

Donor ID	CD4 count (cells / mm^3)	Viral load (copies / ml)
1	436	29600
2	200	87300
3	775	<40
4	266	43700
5	119	9260
6	369	<50
7	505	2470
8	208	<50
9	690	<50
10	358	<50
11	76	14000
12	610	<40
13	529	<50
14	362	1450
15	282	<50
16	488	67
17	180	<50
18	448	<40
19	424	61
20	273	<50
21	519	<50
22	388	<50
23	413	<40

CHAPITRE V - RÔLE DE LA PROTÉINE ACCESSOIRE VPU DANS LA RÉPONSE ADCC

5.1 Préambule

Dans ce chapitre, nous caractérisons la polyfonctionnalité de Vpu lui permettant de promouvoir l'évasion de la réponse humorale non-neutralisante en antagonisant CD4 et BST-2, ainsi que la réponse cytotoxique directe médiée par les cellules NK en ciblant NTB-A et PVR. En comprenant les déterminants dictant la capacité de Vpu à cibler toutes ces protéines transmembranaires simultanément, nous avons pu établir que certains de ces substrats sont ciblés de manière préférentielle. À partir de ces informations, nous avons développé des stratégies pour augmenter l'élimination des cellules infectées par ADCC en affectant directement la polyfonctionnalité de Vpu ou en contournant son effet protecteur en augmentant le potentiel antiviral des nnAbs. Dans l'**article 8**, nous avons observé que les IFN-I empêchaient Vpu de moduler à la baisse les niveaux de surface de NTB-A et PVR, mais pas de BST-2 ou CD4. Comme BST-2 et CD4 sont préférentiellement ciblés par Vpu, l'augmentation de BST-2 par les IFN-I a pour effet de compétitionner pour la liaison au domaine transmembranaire de Vpu, nécessaire pour l'interaction et la régulation négative de NTB-A et PVR. Puisque ceux-ci sont des ligands pour les récepteurs activateurs NTB-A et DNAM-1, qui agissent également comme corécepteurs de CD16, le traitement par les IFN-I sensibilise les cellules infectées par le VIH-1 aux réponses cytotoxiques directes et dépendantes des anticorps médiées par les cellules NK. Dans l'**article 9**, nous avons étudié l'importance de Vpu pour évader la réponse nnAbs dans le contexte d'une infection *in vivo*. Une étude publiée en 2017 par *Horwitz et al.* a démontré que les nnAbs peuvent altérer le cours de l'infection via leurs fonctions effectrices Fc-dépendantes dans un modèle de souris humanisée. Afin de comprendre ce phénotype, nous nous sommes intéressés plus particulièrement au virus utilisé dans cette étude. Celui-ci s'est avérée être dépourvu de l'expression du gène *vpu*, ce qui pourrait être responsable de la capacité des nnAbs à éliminer efficacement les cellules infectées dans ce modèle *in vivo*. En effet, lorsque nous avons rétabli l'expression de Vpu, les cellules infectées deviennent résistantes aux réponses effectrices médiée par les nnAbs *in vitro* et la charge virale n'est plus affectée par les nnAbs chez des souris humanisées. Afin de rendre les nnAbs plus efficaces à médier l'ADCC contre un virus de type sauvage, nous avons optimisé une stratégie permettant d'exposer Env dans sa conformation « ouverte » et d'augmenter l'interaction avec le récepteur CD16 des cellules effectrices.

ARTICLE 8

L'augmentation de l'expression de BST-2 par les interférons de type I réduit la capacité de Vpu à protéger les cellules infectées par le VIH-1 des réponses cytotoxiques médiées les cellules NK

Upregulation of BST-2 by Type I Interferons Reduces the Capacity of Vpu To Protect HIV-1-Infected Cells from NK Cell Responses

Auteurs:

Jérémie Prévost[1,2], Suzanne Pickering[3], Mitchell J. Mumby[4], Halima Medjahed[1], Gabrielle Gendron-Lepage[1], Gloria G. Delgado[1], Brennan S. Dirk[4], Jimmy D. Dikeakos[4], Christina M. Stürzel[5], Daniel Sauter[5], Frank Kirchhoff[5], Frederic Bibollet-Ruche[6,7], Beatrice H. Hahn[6,7], Mathieu Dubé[1], Daniel E. Kaufmann[1,8,9], Stuart J. D. Neil[3], Andrés Finzi[1,2,10], Jonathan Richard[1,2]

Affiliations:

[1]Centre de Recherche du CHUM, Montreal, QC, Canada; [2]Département de Microbiologie, Infectiologie et Immunologie, Université de Montréal, Montreal, QC, Canada; [3]Department of Infectious Disease, King's College London School of Life Sciences and Medicine, Guy's Hospital, London, United Kingdom; [4]Department of Microbiology and Immunology, Schulich School of Medicine and Dentistry, The University of Western Ontario, London, ON, Canada; [5]Institute of Molecular Virology, Ulm University Medical Center, Ulm, Germany; [6]Department of Medicine, Perelman School of Medicine, University of Pennsylvania, Philadelphia, PA, USA; [7]Department of Microbiology, Perelman School of Medicine, University of Pennsylvania, Philadelphia, PA, USA; [8]Department of Medicine, Université de Montréal, Montreal, QC, Canada; [9]Center for HIV/AIDS Vaccine Immunology and Immunogen Discovery, The Scripps Research Institute, La Jolla, CA, USA; [10]Department of Microbiology and Immunology, McGill University, Montreal, QC, Canada.

Contribution des auteurs:

Conceptualisation: **J.P.**, A.F. et J.R.; Méthodologie: **J.P.**, S.P., M.D., D.E.K., S.J.D.N., A.F. et J.R.; Recherche: **J.P.**, S.P., M.J.M., B.S.D. et J.R.; Ressources: H.M., G.G.-L., G.G.D., C.M.S., D.S., F.K., F.B.-R., B.H.H., D.E.K. et A.F.; Analyse formelle: **J.P.** et J.R.; Visualisation: **J.P.** et J.R.; Supervision: J.D.D., D.E.K., S.J.D.N. et A.F.; Obtention du financement: B.H.H., D.E.K, S.J.D.N., A.F. et J.R.; Rédaction - version originale: **J.P.**, A.F. et J.R.; Rédaction - révision et édition: **Tous les auteurs**.

Statut: Cet article a été publié dans *mBio*, le 18 juin 2019

https://doi.org/10.1128/mBio.01113-19

5.2.1 RÉSUMÉ

La protéine accessoire Vpu du VIH-1 favorise le relargage viral en régulant négativement le facteur de restriction BST-2. En plus, Vpu favorise l'évasion des cellules NK en modulant à la baisse les niveaux de surface des protéines NTB-A et PVR, ligands connus des récepteurs des cellules NK NTB-A et DNAM-1, respectivement. Bien qu'il ait été établi que le domaine transmembranaire (TMD) de Vpu est nécessaire pour l'interaction et la séquestration intracellulaire de BST-2, NTB-A et PVR, la manière dont Vpu parvient à cibler ces protéines simultanément n'est pas claire. Dans cette étude, nous montrons que lorsqu'augmenté, BST-2 est préférentiellement ciblé par Vpu par rapport à ses autres substrats. Nous avons constaté que la régulation à la hausse de la BST-2 par l'interféron de type I (IFN) réduit considérablement la capacité de Vpu à réguler à la baisse NTB-A et PVR. Nos résultats suggèrent que l'occupation du TMD de Vpu par BST-2 affecte sa capacité à réguler négativement d'autres substrats dépendant du TMD. En conséquence, la suppression de BST-2 augmente la capacité de Vpu à réguler négativement NTB-A et PVR en présence d'IFN de type I. De plus, nous montrons que l'expression du BST-2 humain, mais pas celle de son orthologue chez le macaque, diminue la capacité de Vpu à réguler négativement NTB-A. Nous montrons également que les IFN de type I sensibilisent efficacement les cellules infectées par le VIH-1 aux réponses directes et dépendantes des anticorps des cellules NK médiées par NTB-A et DNAM-1. Dans l'ensemble, nos résultats révèlent que les IFN de type I diminuent la polyfonctionnalité de Vpu, réduisant ainsi sa capacité à protéger les cellules infectées par le VIH-1 des réponses cytotoxiques médiées par les cellules NK.

5.2.2 ABSTRACT

The HIV-1 accessory protein Vpu enhances viral release by counteracting the restriction factor BST-2. Furthermore, Vpu promotes NK cell evasion by downmodulating cell surface NTB-A and PVR, known ligands of the NK cell receptors NTB-A and DNAM-1, respectively. While it has been established that Vpu's transmembrane domain (TMD) is required for the interaction and intracellular sequestration of BST-2, NTB-A, and PVR, it remains unclear how Vpu manages to target these proteins simultaneously. In this study, we show that upon upregulation, BST-2 is preferentially downregulated by Vpu over its other TMD substrates. We found that type I interferon (IFN)-mediated BST-2 upregulation greatly impairs the ability of Vpu to downregulate NTB-A and PVR. Our results suggest that occupation of Vpu by BST-2 affects its ability to

downregulate other TMD substrates. Accordingly, knockdown of BST-2 increases Vpu's potency to downmodulate NTB-A and PVR in the presence of type I IFN treatment. Moreover, we show that expression of human BST-2, but not that of the macaque orthologue, decreases Vpu's capacity to downregulate NTB-A. Importantly, we show that type I IFNs efficiently sensitize HIV-1-infected cells to NTB-A- and DNAM-1-mediated direct and antibody-dependent NK cell responses. Altogether, our results reveal that type I IFNs decrease Vpu's polyfunctionality, thus reducing its capacity to protect HIV-1-infected cells from NK cell responses.

5.2.3 IMPORTANCE

The restriction factor BST-2 and the NK cell ligands NTB-A and PVR are among a growing list of membrane proteins found to be downregulated by HIV-1 Vpu. BST-2 antagonism enhances viral release, while NTB-A and PVR downmodulation contributes to NK cell evasion. However, it remains unclear how Vpu can target multiple cellular factors simultaneously. Here we provide evidence that under physiological conditions, BST-2 is preferentially targeted by Vpu over NTB-A and PVR. Specifically, we show that type I IFNs decrease Vpu's polyfunctionality by upregulating BST-2, thus reducing its capacity to protect HIV-1-infected cells from NK cell responses. This indicates that there is a hierarchy of Vpu substrates upon IFN treatment, revealing that for the virus, targeting BST-2 as part of its resistance to IFN takes precedence over evading NK cell responses. This reveals a potential weakness in HIV-1's immunoevasion mechanisms that may be exploited therapeutically to harness NK cell responses against HIV-1.

5.2.4 INTRODUCTION

Robust type I interferon (IFN) responses are among the earliest host immune defenses observed during acute HIV-1 infection (1). Interferons play a central role in early antiviral immune responses and efficiently suppress HIV-1 replication in vitro. A part of their antiviral activity depends on the induction of interferon-stimulated genes (ISGs), including restriction factors, such as APOBEC3, TRIM5, SAMHD1, or BST-2 (bone marrow stromal cell antigen 2), that inhibit various steps of the viral replication cycle (2). For instance, BST-2, also known as Tetherin, CD317, or HM1.24, inhibits the release of HIV-1 by trapping newly formed virions at the surface of infected cells (3, 4). BST-2 is a dimeric glycoprotein that consists of an N-terminal cytoplasmic tail, a conventional transmembrane (TM) alpha-helix, a coiled-coil extracellular domain, and a C-

terminal glycosylphosphatidylinositol (GPI) anchor (5, 6). This unique topology allows BST-2 dimers to cross-link budding virions at the surface of infected cells by incorporating one of their membrane-associated domains into the viral membrane, preferentially the GPI anchor, while the other membrane-associated domain remains associated with the cell membrane (7).

BST-2 antagonism is a highly conserved function among primate lentiviruses (8). In the case of HIV-1, the small accessory protein Vpu acts as a viral antagonist of BST-2 (3, 4). Vpu-mediated BST-2 downregulation requires a physical interaction between the transmembrane domains (TMDs) of the two proteins (9–11). This interaction is mediated by residues A10, A14, A18, and W22 from the highly conserved alanine face of the TMD of Vpu (9, 10). Although the precise mechanism(s) used by Vpu to antagonize BST-2 is not completely understood, the current consensus points toward a subversion of BST-2 trafficking. Vpu has been shown to block newly synthesized as well as recycled BST-2 from trafficking to the plasma membrane (12, 13). To achieve this, Vpu hijacks the AP-1-dependent membrane trafficking pathway and forces BST-2 into clathrin-rich domains of endosomes and the *trans*-Golgi network (TGN) (14–16). Subsequently, Vpu targets BST-2 to an ESCRT-dependent endosomal degradation pathway through a mechanism that depends on a highly conserved DSGNES motif located in the cytoplasmic tail of Vpu (17–19). Phosphorylation of the serine residues of this motif allows the recruitment of the β-TrCP subunit of the $SCF^{\beta\text{-}TrCP1/2}$ E3 ubiquitin ligase complex, leading to the ubiquitination and degradation of BST-2 in lysosomes (20, 21). Increasing evidence suggests that the recruitment of β-TrCP and the degradation of BST-2 by Vpu are dissociable from its ability to antagonize BST-2 (11, 14, 15, 18, 19, 22), although this is subject to debate (23).

In addition to BST-2, Vpu downmodulates a variety of cellular transmembrane proteins, including the viral receptor CD4 (24, 25) and proteins involved in NK cell-mediated immune responses (26, 27). Vpu contributes to NK cell evasion by downmodulating the NK cell ligands NTB-A and PVR from the surface of HIV-1-infected cells (26, 27). NTB-A (NK, T, and B cell antigen, also known as CD352 and SLAMF6) is a type 1 TM protein that belongs to the signaling lymphocytic activation molecules (SLAM) family of receptors found on the surface of all human NK, T, and B cells (28). One interesting feature of this family of receptors is their preference for homophilic interactions. In NK cells, NTB-A functions as a coactivating receptor, and a

homophilic NTB-A–NTB-A interaction triggers NK cell cytotoxicity (29, 30). The downregulation of NTB-A from the surface of HIV-1-infected cells by Vpu was found to prevent NK cell degranulation, thus protecting infected cells from NK cell-mediated lysis (27). Unlike BST-2, Vpu does not enhance NTB-A degradation (27, 31). Instead, Vpu seems to alter the anterograde trafficking of NTB-A, resulting in its sequestration in perinuclear compartments (31). Vpu's anti-NTB-A activity also appears to require a physical interaction between the TMDs of the two proteins (27).

PVR (polio virus receptor, also known as CD155) is a nectin-like protein that serves as a specific ligand for DNAM-1 (DNAX accessory molecule 1, also known as CD226), an adhesion molecule expressed by multiple cell types, including NK and $CD8^+$ T cells. DNAM-1 functions as an activating NK cell receptor, and consequently, its stimulation enhances NK cell-mediated cytotoxicity and cytokine production (32, 33). To reduce the susceptibility of HIV-1-infected cells to NK cell-mediated lysis, Vpu and Nef were shown to downregulate cell surface PVR in an additive manner (26). Similar to the fate of NTB-A in the presence of Vpu, PVR accumulates within perinuclear compartments upon Vpu expression (34). Interestingly, Vpu-mediated downregulation of PVR depends on the same key TM residues, A10, A14, and A18, known to be crucial for BST-2 interaction (34).

While it has been established that Vpu's TMD is required for the interaction and intracellular sequestration of BST-2, NTB-A, and PVR, it remains unclear how Vpu manages to target these different proteins using the same TMD. In this study, we show that the upregulation of BST-2 by type I IFNs greatly impairs the ability of Vpu to downregulate NTB-A and PVR from the surface of infected primary $CD4^+$ T cells. Accumulation of NTB-A and PVR at the surface of HIV-1-infected cells leads to an enhancement in direct and antibody (Ab)-dependent NK cell-mediated killing.

5.2.5 RESULTS

Type I IFNs enhance NTB-A and PVR levels at the surface of HIV-1-infected cells.

Since Vpu utilizes the same domain to target BST-2, NTB-A, and PVR, we speculated that the upregulation of one of these substrates could affect/compete with the downregulation of the other substrates. As BST-2 is an ISG, we decided to upregulate its expression using type I IFNs. Activated primary $CD4^+$ T cells isolated from healthy HIV-1-negative individuals were mock infected or infected with the transmitted/ founder (TF) virus CH58 (CH58 TF). At 24 h post-infection, cells were treated or not with type I IFNs (alpha2a interferon [IFN-α2a] or IFN-β), and the cell surface levels of the three TM proteins were monitored 24 h after IFN treatment by flow cytometry (see **Fig. 5.1.S1** in the supplemental material). In the absence of IFN treatment, the virus was able to downregulate the three TM proteins from the surface of infected (p24-positive [$p24^+$]) cells, in contrast to uninfected p24-negative ($p24^-$) cells (**Fig. 5.1.1A and B**), in a Vpu-dependent manner (**Fig. 5.1.S2**). Strikingly, IFN-α2a or IFN-β treatment significantly abrogated the ability of the virus to downregulate NTB-A and PVR, but not BST-2, from the cell surface (Fig. 1A and B). As previously reported (35), BST-2 levels on all cell populations were significantly enhanced upon IFN-α2a or IFN-β treatment, but this increase was less pronounced on the infected p24 cells (**Fig. 5.1.1C and D**), suggesting that the virus still manages to downregulate this restriction factor upon type I IFN treatment (**Fig. 5.1.1B**). On the other hand, even though NTB-A and PVR levels stayed relatively stable on mock-infected and uninfected bystander cells, the levels for these two ligands at the surface of infected cells were significantly enhanced upon IFN-α2a or IFN-β treatment (**Fig. 5.1.1C and D**). Similar results were obtained with different IFN-α subtypes (IFN-α1, IFN-α6, IFN-α8, IFN-α14, IFN-α16, and IFN-α17), and their ability to upregulate NTB-A and PVR positively correlated with their capacity to enhance BST-2 levels in p24+ cells (**Fig. 5.1.1E**). Among all type I IFNs tested, IFN-β was identified to be the most potent cytokine mediating the upregulation of these three substrates. Therefore, this cytokine was subsequently used to test additional viruses. Similar results were obtained using a panel of transmitted/founder (TF) and 6-month (6mo) consensus and chronic (Chr) viruses from clades B and C (**Fig. 5.1.2**). Enhancement of cell surface BST-2, NTB-A, and PVR was observed with all viruses tested upon treatment with IFN-β (**Fig. 5.1.2A**). Again, from the three TM proteins tested, BST-2 remained the only one to be efficiently downregulated by all the viruses (**Fig. 5.1.2B**). In agreement with the results shown

in **Fig. 5.1.1E**, a strong positive correlation between BST-2 levels and cell surface NTB-A and PVR was observed (**Fig. 5.1.2C**). Altogether, these results demonstrate that type I IFNs affect the capacity of HIV-1 to downregulate NTB-A and PVR.

Type I IFNs reduce the capacity of Vpu to downregulate NTB-A and PVR.

Since Vpu is involved in BST-2, NTB-A, and PVR downregulation (**Fig. 5.1.S2**), we further investigated the role of this accessory protein in the observed phenotype. Primary $CD4^+$ T cells were infected with either wildtype (WT) or *vpu*-defective CH58 TF viruses, and the effect of IFN-β on cell surface expression of NTB-A and PVR was evaluated by flow cytometry. Consistent with the data shown in **Fig. 5.1.1 and 5.1.2**, IFN- significantly enhanced NTB-A and PVR levels on WT-infected cells (**Fig. 5.1.3A to C**). In contrast, no significant increase was observed when cells were infected with the vpu-defective virus, suggesting that the effect of IFN- treatment depends on Vpu expression. The HIV-1 accessory protein Nef contributes to HIV-1-mediated PVR downregulation but not NTB-A or BST-2 downregulation (**Fig. 5.1.S2**). To evaluate the effect of IFN- on Nef-mediated PVR downregulation, we also tested the effect of IFN- treatment on cells infected with a nef-defective variant of CH58 TF. In contrast to Vpu, Nef expression did not alter the capacity of IFN- to enhance cell surface NTB-A and PVR (**Fig. 5.1.3A to C**). Taken together, these data suggest that IFN- impairs specifically the ability of Vpu to downregulate the NK cell ligands NTB-A and PVR, but not BST-2.

BST-2 impairs Vpu's ability to downregulate cell surface NTB-A and PVR.

Since only BST-2 remains efficiently downregulated by Vpu upon IFN treatment, we explored the role of a Vpu–BST-2 functional interaction in the IFN-induced upregulation of NTB-A and PVR. Primary $CD4^+$ T cells, mock infected or infected with HIV-1 CH58 TF, were electroporated with small interfering RNAs (siRNAs) targeting BST-2 mRNA or nontargeting (NT) siRNAs prior to IFN-β treatment. Electroporation with siRNA targeting BST-2 prevented IFN-induced BST-2 upregulation in the context of both mock-infected and CH58 TF-infected cells (**Fig. 5.1.4A and B**). While BST-2 knockdown had no effect on NTB-A and PVR expression in mock-infected cells, it significantly reduced the enhancement of cell surface NTB-A and PVR detected upon type I IFN treatment in infected ($p24^+$) cells. This suggests that Vpu partially recovers its ability to downregulate these NK cell ligands upon IFN treatment, provided that BST-

2 is depleted. Of note, BST-2 levels and cell surface NTB-A or PVR expression correlated significantly (**Fig. 5.1.4C**). These results demonstrate that Vpu's ability to downregulate cell surface NTB-A and PVR can be impaired in a BST-2-dependent manner.

To evaluate if BST-2 expression is sufficient to impair Vpu's ability to downregulate NTB-A, we co-transfected HEK293T cells with plasmids coding for Vpu, NTB-A, and human or rhesus macaque BST-2. Rhesus macaque BST-2 cannot be counteracted by HIV-1 Vpu due to key mutations in its TMD (36, 37). In this system, we observed a robust Vpu-mediated NTB-A downregulation (**Fig. 5.1.5A**). In agreement with results obtained with infected primary cells, increasing amounts of human BST-2 but not of rhesus macaque BST-2 progressively abrogated the ability of Vpu to downregulate NTB-A (**Fig. 5.1.5A**). This confirms that BST-2 expression is sufficient to abrogate the capacity of Vpu to target NTB-A, provided that the BST-2 being expressed is susceptible to Vpu.

To evaluate if this phenotype was specific to BST-2 expression, we determined whether enhanced expression of NTB-A affected the ability of Vpu to counteract BST-2 and enhance viral release. As expected, BST-2 expression potently reduced HIV-1 particle release, and this was partially overcome by Vpu (**Fig. 5.1.5B**). In contrast to the impact of BST-2 expression on Vpu-mediated NTB-A downregulation, increasing amounts of NTB-A did not affect the capacity of Vpu to enhance viral release upon BST-2 expression (**Fig. 5.1.5B**). Consistent with these findings, electroporation of siRNA against NTB-A did not enhance the capacity of Vpu to control BST-2 or PVR cell surface levels in the absence or presence of type I IFNs (**Fig. 5.1.5C**). These observations support a model where Vpu preferentially targets BST-2 over NTB-A.

BST-2 upregulation by type I IFNs affects the ability of Vpu to downmodulate CD62L but not CD4.

To confirm that BST-2 expression affects the ability of Vpu to downregulate substrates that depend on its TMD, we evaluated the effect of IFN- treatment on two other Vpu substrates: CD4 and CD62L. Consistent with the involvement of the cytoplasmic domain of Vpu for CD4 downregulation and not its TMD (38), CD4 levels on HIV-1-infected primary $CD4^+$ T cells were not affected by IFN- treatment (**Fig. 5.1.6A**) even in the absence of Nef (**Fig. 5.1.S3**). In contrast,

IFN-β treatment significantly enhanced the cell surface levels of CD62L (**Fig. 5.1.6A**). As expected, mutation of Vpu's TMD (A14L/A18L) abrogated Vpu's capacity to downregulate CD62L but not CD4, confirming the requirement of Vpu's TMD for Vpu-mediated CD62L downregulation (**Fig. 5.1.6B**). We then characterized CD62L expression in mock-infected, bystander, and infected primary $CD4^+$ T cells. We found that IFN-β enhanced CD62L expression on all these populations but did so more significantly on the infected cell population (**Fig. 5.1.7A and B**). Similar to what we observed for NTB-A and PVR, IFN-β specifically impaired the ability of Vpu to downregulate CD62L, and this activity was significantly enhanced by BST-2 depletion (**Fig. 5.1.7C to E**). In summary, these results suggest that occupation of Vpu's TMD by BST-2 affects Vpu's capacity to target multiple substrates.

IFN-β sensitizes HIV-1-infected cells to NK cell responses in an NTB-A- and DNAM-1-dependent manner.

To evaluate the functional consequences of type I IFN-mediated impairment of NTB-A and PVR downregulation, we characterized their contribution in stimulating NK cell cytotoxic activity using a redirection degranulation assay. Fc gamma receptor-positive ($Fc\gamma R^+$) P815 cells were incubated with antibodies known to engage NTB-A or DNAM-1 or with their matched IgG isotypes. The cells were then incubated with human primary NK cells. In this assay, the Fc portion of the Ab interacts with the FcγR present on P815 target cells, thus allowing NK cell activation through a single receptor or a combination of receptors (here, NTB-A and/or DNAM-1). NK cell degranulation was monitored by detection of cell surface CD107a. Consistent with previous reports (39), the stimulation of either NTB-A or DNAM-1 receptors alone was not sufficient to trigger NK cell degranulation (**Fig. 5.1.8A**). However, the combination of NTB-A and DNAM-1 Abs resulted in a significant increase in NK cell degranulation (**Fig. 5.1.8A and B**), indicating that there is a functional interplay between these receptors to stimulate NK cells. Accordingly, we found that these receptors also positively modulated NK-mediated antibody-dependent cellular cytotoxicity (ADCC) (**Fig. 5.1.8C and D**). Even though stimulation through CD16 was sufficient to induce NK cell degranulation, addition of an anti-NTB-A Ab, an anti-DNAM-1 Ab, or both increased significantly the magnitude of NK cell degranulation (**Fig. 5.1.8C and D**). Altogether, these results indicate that the stimulation of NK cells via DNAM-1 and NTB-A is sufficient to trigger both direct and Ab-dependent NK cell responses.

The potential contribution of NTB-A and PVR in HIV-1-infected cell susceptibility to NK cells was evaluated using a direct killing assay. Primary $CD4^+$ T cells infected with CH58 TF WT virus or its *vpu*-defective counterpart were used as targets in the presence of increasing amounts of autologous primary NK cells. Confirming the protective effect of Vpu expression on NK cell-mediated killing (26, 27), WT-infected cells were less susceptible to autologous NK cell responses than cells infected with a *vpu*-defective virus (**Fig. 5.1.9A**). Interestingly, treatment of WT-infected cells with IFN-β significantly increased their susceptibility to autologous NK cell lysis (**Fig. 5.1.9A**) to levels similar to those reached with *vpu*-defective virus-infected cells. Strikingly, this increase in direct NK cell lysis could be abrogated when NK cells were preincubated with a combination of blocking antibodies against the NK cell receptors NTB-A and DNAM-1 (**Fig. 5.1.9A**). Similarly, the capacity of 3BNC117, a broadly neutralizing antibody (bNAb; targeting the CD4-binding site), to mediate ADCC against HIV-1-infected cells was significantly enhanced upon IFN-β treatment (**Fig. 5.1.9B**). IFN-treated infected cells remained less susceptible to ADCC than cells infected with a *vpu*-defective virus. This is consistent with the capacity of the WT virus to downregulate BST-2 despite IFN treatment (**Fig. 5.1.1A and B**). BST-2 downregulation facilitates viral release, thus decreasing the accumulation of Env at the cell surface (**Fig. 5.1.S4**). However, the ADCC responses directed against WT-infected cells treated with IFN or cells infected with a *vpu*-defective virus were significantly decreased by the addition of blocking antibodies against NTB-A and DNAM-1 (**Fig. 5.1.9B**). Taken together, these results reveal that IFN- enhances the susceptibility of HIV-1-infected cells to autologous NK cell responses in an NTB-A- and DNAM-1-dependent manner.

5.2.6 DISCUSSION

Vpu is known to downregulate several membrane proteins from the cell surface of HIV-1-infected $CD4^+$ T cells. The TMD of Vpu has been shown to be required to downregulate several of them, including BST-2 (9–11), NTB-A (27), PVR (34), and CD62L (**Fig. 5.1.6**). How Vpu manages to target these different substrates using the same domain has not been established. Here we provide the first evidence that under physiologically relevant conditions, BST-2 is preferentially downregulated by Vpu over its other TMD substrates. Specifically, we show that type I IFNs decrease Vpu's polyfunctionality by upregulating BST-2, thus reducing its capacity to

downmodulate the NK cell ligands NTB-A and PVR. Importantly, we show that type I IFNs efficiently sensitize HIV-1-infected cells to both direct and antibody-dependent NK cell responses.

Our results support a model in which the specific occupancy of Vpu's TMD by BST-2 prevents its ability to target other TM proteins. Consistent with this model, Vpu's ability to downregulate CD4 was not affected by IFN-β treatment. This activity of Vpu involves the cytoplasmic domain of the viral protein rather than its TMD (38) (**Fig. 5.1.6B**). Consequently, the capacity of Vpu to target CD4 is unlikely to be impacted by the occupation of its TMD by BST-2. While studies have suggested that the Vpu–BST-2 interaction could occur within post-endoplasmic reticulum membranes (40), we cannot rule out the possibility that Vpu could also interact with CD4 and BST-2 in a successive manner. However, supporting our model, we found that the IFN-induced upregulation of BST-2 affected the ability of Vpu to downmodulate another substrate that depends on the integrity of Vpu's TMD: the CD62L homing receptor (**Fig. 5.1.6 and 5.1.7**). Our findings therefore raise the intriguing possibility that numerous Vpu functions relying on its TMD could be affected by the upregulation of BST-2. One distinctive feature of group M Vpu proteins is their capacity to target BST-2 to an ESCRT-dependent endosomal degradation pathway. However, increasing evidence suggests that BST-2 counteraction by Vpu results from the subversion of BST-2 trafficking prior to its degradation. While BST-2 degradation by Vpu does not appear to be required to counteract BST-2 (11, 14, 15, 18, 19, 22), it could represent an effective mechanism to unleash Vpu's TMD to interact with other cellular substrates. One could speculate that Vpu's polyfunctionality could therefore rely on its ability to degrade BST-2.

Our results provide the first indication that that there is a hierarchy of Vpu targets under type I IFN responses. In contrast to NTB-A, PVR, and CD62L, both CD4 and BST-2 remain efficiently targeted by Vpu despite IFN treatment, which further supports the notion that these two proteins represent the major targets of Vpu (**Fig. 5.1.1, 5.1.2, and 5.1.6**). BST-2 counteraction and CD4 downregulation were found to be critical for viral egress and immune evasion. Vpu antagonism of BST-2 plays a crucial role in enhancing virus replication and release in human $CD4^+$ T cells, particularly in the presence of IFN (41). This activity of Vpu was recently identified to be a major determinant of HIV-1 IFN resistance (41). CD4 degradation by Vpu also participates in the release of fully infectious viral particles by preventing the intracellular interaction between

CD4 and Env (24, 25). Finally, both of Vpu's activities contribute to protect HIV-1-infected cells from ADCC responses by preventing the exposure of ADCC-mediating Env epitopes (42).

The reason for this preference of Vpu for BST-2 over NTB-A and PVR remains to be determined. One can speculate that Vpu's TMD could have a higher affinity for BST-2's TMD than for NTB-A's or PVR's TMD. A recent study by Cole et al. characterized the heterooligomer formation between the TMD of Vpu and its substrates in a lipid environment using Förster resonance energy transfer (FRET) (43). Data from this study show that peptides of Vpu's TMD have a lower affinity for TMD peptides of NTB-A, PVR, and BST-2 than for known TM helix dimers (43). The interaction between Vpu and dimeric BST-2, however, remained more energetically favorable than Vpu–NTB-A and Vpu-PVR interactions, potentially due to the additive effects of multiple TMD-TMD interactions (43). BST-2 forms disulfide-linked dimers, and BST-2 dimerization is required for its antiviral function (7, 44–46). The preference of Vpu for BST-2 could therefore result from its higher affinity for BST-2 dimers than for other monomeric substrates. In the study of Cole et al., PVR and NTB-A TMDs were found to compete with BST-2 TMD for the binding of the Vpu TMD peptide in a lipid environment (43). It is possible that this reduced Vpu–BST-2 interaction detected in the presence of NTB-A's or PVR's TMD is not sufficient to have a significant impact on Vpu function. This apparent contradiction could be explained if the affinity of TMD peptides artificially embedded in a lipid environment did not recapitulate the affinity and/or function of this domain expressed within the full protein. In that regard, our results using infected primary $CD4^+$ T cells or Vpu-expressing cells revealed that NTB-A expression has no effect on the capacity of Vpu to antagonize BST-2 (**Fig. 5.1.5B and C**). Inversely, BST-2 expression greatly reduced the capacity of Vpu to downregulate NTB-A and PVR (**Fig. 5.1.4 and 5.1.5**).

HIV/simian immunodeficiency virus infection is followed by an intense cytokine storm involving type I IFNs. An intact IFN response during the acute phase of infection appears to be crucial for viral control (47). While BST-2 expression is upregulated upon HIV-1 infection by endogenous type I IFNs, a recent study revealed that basal BST-2 levels are sufficient to suppress HIV-1 replication (48). The counteraction of BST-2 by Vpu consequently confers a selective advantage for viral spread *in vivo*, at least in humanized mice (48–50). Our observation that Vpu

preferentially targets BST-2 over other TM proteins (NTB-A, PVR, and CD62L) upon IFN treatment raises the possibility that the polyfunctionality of Vpu could be reduced during acute HIV-1 infection. The upregulation of BST-2 observed during this stage of infection (47, 48) could impact the capacity of Vpu to target multiple TM proteins. This could explain why studies using humanized mouse models of acute HIV-1 infection failed to detect the Vpu-mediated downregulation of NTB-A *in vivo*, despite detecting it *in vitro* (49, 50). In these mouse models, strong type I IFN responses and subsequent BST-2 upregulation were detected upon HIV-1 infection (48). It is then conceivable that the capacity of Vpu to target NTB-A *in vivo* could have been impacted by type I IFN-mediated BST-2 upregulation. Resistance to type 1 IFNs represents a key determinant of HIV-1 transmission fitness. Transmitted/founder (TF) viruses are phenotypically distinct, and increased IFN resistance represents their most distinguishing property (41, 51–54). However, resistance to IFNs is not static during the course of HIV-1 infection. Previous studies revealed that IFN resistance declines rapidly within the first 6 months of infection (53, 54) but then tends to increase again at later stages of disease progression (53). In this study, we found that type I IFNs affect the downregulation of NTB-A and PVR by HIV-1, including by viruses that differ in their sensitivity to IFNs (**Fig. 5.1.2**). All tested viruses, including TF, 6-month, and chronic viruses, were found to be sensitive, at different levels, to this IFN activity. This suggests that type I IFNs could differentially affect Vpu polyfunctionality at different stages of infection. Future studies using longitudinally linked viruses are needed to determine whether the capacity of Vpu to downmodulate NTB-A and PVR upon IFN treatment varies during the course of infection.

We also found that type I IFNs enhance the susceptibility of HIV-1-infected cells to NK cell responses. We demonstrated that stimulation of human NK cells via the NTB-A and DNAM-1 receptors is sufficient to induce NK cell degranulation. We also provide evidence that NTB-A and DNAM-1 are critical players for NK cell-mediated ADCC. We found that there is a functional interplay between these receptors together with CD16 to enhance NK cell degranulation, suggesting that they act as coreceptors of CD16. By preventing Vpu's ability to downregulate NTB-A and PVR, type I IFNs impair Vpu's capacity to protect infected cells from NK responses. Importantly, we found that type I IFNs efficiently sensitize cells infected with an IFN-resistant TF virus (CH58 TF) (41, 53, 54) to autologous NK cell lysis. This suggests that, for the virus, targeting

BST-2 as part of its resistance to type I IFNs takes precedence over protecting HIV-1-infected cells from NK cell responses, at least early in infection, when type I IFN responses play an important role in systemic viral control.

Our findings further support the idea that type I IFNs could be utilized to harness NK cell responses against HIV-1-infected cells. Stimulation with IFN-α was found to augment NK cell cytokine secretion, polyfunctionality, and degranulation, as well as the capacity of NK cells to lyse autologous HIV-1-infected cells (55–57). Additionally, type I IFNs enhance the susceptibility of HIV-1-infected cells to ADCC responses by increasing the level of ADCC-mediating Env epitopes on infected cells (35, 58). Now we demonstrate that this increase in ADCC responses also depends on the capacity of type I IFNs to prevent Vpu-mediated NTB-A and PVR downmodulation (**Fig. 5.1.9B**). Altogether, this suggests that type I IFNs could both directly enhance NK cell effector function and also augment the susceptibility of infected cells to NK cells. Interestingly, administration of IFN-α during chronic HIV-1 infection was found to enhance BST-2 expression and tended to decrease HIV-1 replication (59–61). Studies also revealed that treatment with IFN-α leads to a moderate but sustained decline of integrated HIV-1 DNA in $CD4^+$ T cells (60, 62). While all studies to date in chronic infection have used IFN-α2a, other IFN-α subtypes, as well as IFN-β, have been shown to be more potent at upregulating BST-2 and restricting HIV-1 infection (**Fig. 5.1.1**) (52, 63, 64). Consequently, whether these cytokines would have a more pronounced effect on viral replication and the clearance of the viral reservoir *in vivo* remains to be determined.

In summary, we demonstrate that type I IFN-mediated upregulation of BST-2 greatly impairs Vpu's polyfunctionality. Upon type I IFN treatment, Vpu preferentially targets BST-2 over the NK cell ligands NTB-A and PVR, thus reducing its ability to protect HIV-1-infected cells from NK cell responses.

5.2.7 MATERIALS AND METHODS

Ethics statement

Written informed consent was obtained from all study participants, and the research adhered to the ethical guidelines of CRCHUM and was reviewed and approved by the CRCHUM Institutional

Review Board (Ethics Committee approval number CE 16.164-CA). The research adhered to the standards indicated by the Declaration of Helsinki. All participants were adults and provided informed written consent prior to enrollment, in accordance with Institutional Review Board approval.

Cell culture and isolation of primary cells.

HEK293T human embryonic kidney cells and P815 mouse lymphoblast-like mastocytoma cells (obtained from ATCC) were grown as previously described (39, 65). Primary human peripheral blood mononuclear cells (PBMCs), $CD4^+$ T cells, and NK cells were isolated, activated, and cultured as previously described (66, 67). Briefly, PBMCs were obtained by Ficoll density gradient from whole-blood samples obtained from 9 different HIV-1-negative donors. $CD4^+$ T lymphocytes and NK cells were purified from resting PBMCs by negative selection using immunomagnetic beads per the manufacturer's instructions (StemCell Technologies, Vancouver, BC, Canada). CD4 T cells were activated with phytohemagglutinin-L (10 µg/ml) for 48 h and then maintained in RPMI 1640 complete medium supplemented with recombinant interleukin-2 (100 U/ml; R&D Systems) (see **Fig. 5.1.S1** in the supplemental material). NK cells were isolated and rested overnight in RPMI 1640 complete medium on the day prior to the redirection and killing assays.

Proviral constructs and plasmids

Transmitted/founder (TF) viruses and the corresponding 6-month (6mo) consensus and chronic (Chr) infectious molecular clones (IMCs) of patients CH40, CH58, CH77, CH167, CH198, CH236, CH470, CH505, CH850, and STCO were inferred, constructed, and biologically characterized (51, 53, 68–71). CH58 IMCs defective for Vpu and/or Nef expression or harboring the TMD mutations A14L/A18L, as well as the NL4.3 proviral construct defective for Vpu expression, were previously described (41, 72, 73). The plasmids expressing hemagglutinin (HA)-tagged Vpu 2_87 (pCR3.1- Vpu2_87-HA), human BST-2 (pCR3.1-human Tetherin), rhesus macaque BST-2 (pCR3.1-rhesus Tetherin), NTB-A (pQCXIP_human SLAM6/NTB-A), or green fluorescent protein (GFP) (pCR3.1-GFP) were previously described (14, 36, 74).

Viral production and infections

To achieve similar levels of infection among all viruses tested, vesicular stomatitis virus G (VSV-G)-pseudotyped HIV-1 isolates were produced in HEK293T cells and titrated in activated primary $CD4^+$ T cells to achieve a 10 to 20% infection. Viruses were then used to infect activated primary $CD4^+$ T cells from healthy HIV-1-negative donors by spin infection at 800 × g for 1 h in 96-well plates at 25°C. All experiments using VSV-G-pseudotyped HIV-1 isolates were done in a biosafety level 3 laboratory following manipulation protocols accepted by the CRCHUM Biosafety Committee, which respects the requirements of the Public Health Agency of Canada.

Antibodies

A detailed list of the Abs used for cell surface staining and measurement of NK cell responses is presented in Text S1 in the supplemental material.

Flow cytometry analysis of cell surface staining

Cell surface stainings were performed as previously described (66) and detailed in **Text S1** in the supplemental material. The percentage of BST-2, NTB-A, and PVR levels detected on infected $p24^+$ cells relative to uninfected $p24^-$ cells was calculated with the following formula: (MFI detected on $p24^+$ cells/MFI detected on $p24^-$ cells) × 100, where MFI represents the mean fluorescence intensity.

Type I IFN treatments

Type I IFNs were titrated to identify the optimal concentrations that efficiently enhanced cell surface BST-2 levels on HIV-1-infected primary $CD4^+$ T cells. IFN-β (Rebif; EMD Serono Inc.) (52) was added to the cells at 1 ng/ml. All different IFN-α subtypes tested (PBL Assay Science) were reconstituted in RPMI 1640 complete medium at 1×10^7 U/ml, aliquoted, and stored at -80°C. IFN-α was then added to the cells at 1,000 U/ml. Type I IFNs were added to the cells at 24 h post-infection, 24 h before cell surface staining or killing assays.

siRNA electroporation

Primary $CD4^+$ T cells mock infected or infected with CH58 TF were electroporated with pools of 4 siRNAs to silence BST-2 (ON-TARGETplus Human BST-2 siRNA-SMART pool; Dharmacon) or NTB-A (ON-TARGETplus Human SLAMF6 siRNA-SMART pool; Dharmacon)

expression. Briefly, at 24 h post-infection, infected or mock-infected primary $CD4^+$ T cells were resuspended at a concentration of 5×10^7 cells/ml in Opti-MEM medium (Invitrogen), and 55 µl of the cell suspension was transferred into a 1-mm electroporation cuvette (Harvard Apparatus). Pools of nontargeting (NT) siRNA or siRNA targeting BST-2 or NTB-A sequences were then added to the cells (150 pmol/3×10^6 cells). Further, cells were electroporated at 250 V for 2 ms using a BTX Gemini X2 electroporation system (Harvard Apparatus). Subsequently, electroporated cells were resuspended in RPMI 1640 complete medium and were treated or not with IFN-β (1 ng/ml).

BST-2/NTB-A competition assay

HEK293T cells were seeded at 1.5×10^5 cells per well of a 24-well plate the day before transfection. Cells were co-transfected with 50 ng of an NTB-A-expressing plasmid (pQCXIP_human SLAM6/NTB-A), 40 ng of an Vpu-expressing plasmid (pCR3.1-Vpu2_87-HA), and 150 ng of a GFP-expressing plasmid (pCR3.1-GFP) in the presence of increasing concentrations of human or rhesus macaque BST-2-expressing plasmids (pCR3.1-human Tetherin or pCR3.1-rhesus Tetherin) (0, 10, 20, 50, 100 or 200 ng) using the Lipofectamine 2000 reagent (Invitrogen). At 2 days post-transfection, cell surface NTB-A levels were monitored by flow cytometry as described above. The fluorescence of stained cells was detected by two-color flow cytometry, and Vpu-mediated NTB-A downmodulation was calculated as described previously (74). Briefly, the mean fluorescence intensities were determined for cells showing specific ranges of GFP expression. The fluorescence values obtained for cells co-transfected with the NTB-A, Vpu, and GFP expressors with or without the human or rhesus macaque BST-2 expressors were compared with the corresponding values for number obtained for cells co-transfected with the NTB-A and GFP expressors to determine the efficiency of NTB-A downmodulation by Vpu. The same GFP gating was used in all calculations.

Viral release assay

Subconfluent HEK293T cells were plated in 24-well plates and transfected with NL4.3 ΔVpu proviral construct (500 ng) with or without human the BST-2-expressing plasmid (50 ng; pCR3.1-human Tetherin) in the presence of the Vpu-expressing plasmid (50 ng; pCR3.1-Vpu2_87-HA) and increasing concentrations of the NTB-A-expressing plasmid (0, 50, 100, and

200 ng; pQCXIP_human SLAM6/NTB-A) using 2 µl the Lipofectamine 2000 reagent (Thermo Fisher Scientific). The medium was replaced at 16 h post-transfection, and the supernatants were harvested at 24 h after the medium change and filtered. The infectivity of viral supernatants was determined by infecting TZM-bl cells, and β-galactosidase activity was assayed as previously described (14).

Measurement of NK cell responses

Direct and antibody-dependent NK cell responses were measured using the NK cell redirection degranulation assay, the NK cell direct killing assay, and the fluorescence-activated cell sorting (FACS)-based ADCC assay as described in detail in Text S1 in the supplemental material.

Statistical analysis

Statistics were analyzed using GraphPad Prism (version 6.0.1) software (GraphPad, San Diego, CA, USA). Every data set was tested for statistical normality, and this information was used to apply the appropriate (parametric or nonparametric) statistical test. *P* values of < 0.05 were considered significant; significance values are indicated in the figure legends.

5.2.8 ACKNOWLEDGMENTS

We thank Dominique Gauchat from the CRCHUM Flow Cytometry Platform for technical assistance and Michel Nussenzweig for 3BNC117. Figure 5.1.S1 in the supplemental material was prepared using images from Servier Medical Art by Servier, which is licensed under a Creative Commons Attribution 3.0 Unported License. This work was supported by CIHR foundation grant number 352417 to A.F., by an American Foundation for AIDS Research (amfAR) Mathilde Krim Fellowship in Basic Biomedical Research to J.R., and by grants from the NIH to B.H.H. (R01 AI 114266, UM1 AI 26620, R01 AI 111789) and to D.E.K. (AI100663, CHAVI-ID). J.P. is the recipient of a CIHR doctoral fellowship. S.P. and S.J.D.N. are supported by Wellcome Trust Senior Research Fellowship WT098049AIA. D.E.K. is supported by a senior research scholar award of the Quebec Health Research Fund (FRQS). A.F. is the recipient of a Canada Research Chair on Retroviral Entry (number RCHS0235 950-232424). The funders had no role in study design, data collection and analysis, the decision to publish, or preparation of the manuscript.

5.2.9 REFERENCES

1. Stacey AR, Norris PJ, Qin L, Haygreen EA, Taylor E, Heitman J, Lebedeva M, DeCamp A, Li D, Grove D, Self SG, Borrow P. 2009. Induction of a striking systemic cytokine cascade prior to peak viremia in acute human immunodeficiency virus type 1 infection, in contrast to more modest and delayed responses in acute hepatitis B and C virus infections. J Virol 83:3719 –3733.
2. Doyle T, Goujon C, Malim MH. 2015. HIV-1 and interferons: who's interfering with whom? Nat Rev Microbiol 13:403– 413.
3. Neil SJ, Zang T, Bieniasz PD. 2008. Tetherin inhibits retrovirus release and is antagonized by HIV-1 Vpu. Nature 451:425– 430.
4. Van Damme N, Goff D, Katsura C, Jorgenson RL, Mitchell R, Johnson MC, Stephens EB, Guatelli J. 2008. The interferon-induced protein BST-2 restricts HIV-1 release and is downregulated from the cell surface by the viral Vpu protein. Cell Host Microbe 3:245–252.
5. Kupzig S, Korolchuk V, Rollason R, Sugden A, Wilde A, Banting G. 2003. Bst-2/HM1.24 is a raft-associated apical membrane protein with an unusual topology. Traffic 4:694 –709.
6. Hinz A, Miguet N, Natrajan G, Usami Y, Yamanaka H, Renesto P, Hartlieb B, McCarthy AA, Simorre JP, Gottlinger H, Weissenhorn W. 2010. Structural basis of HIV-1 tethering to membranes by the BST-2/tetherin ectodomain. Cell Host Microbe 7:314 –323.
7. Venkatesh S, Bieniasz PD. 2013. Mechanism of HIV-1 virion entrapment by tetherin. PLoS Pathog 9:e1003483.
8. Sauter D. 2014. Counteraction of the multifunctional restriction factor tetherin. Front Microbiol 5:163.
9. Vigan R, Neil SJ. 2010. Determinants of tetherin antagonism in the transmembrane domain of the human immunodeficiency virus type 1 Vpu protein. J Virol 84:12958 –12970.
10. Skasko M, Wang Y, Tian Y, Tokarev A, Munguia J, Ruiz A, Stephens EB, Opella SJ, Guatelli J. 2012. HIV-1 Vpu protein antagonizes innate restriction factor BST-2 via lipid-embedded helix-helix interactions. J Biol Chem 287:58 – 67.
11. Dube M, Roy BB, Guiot-Guillain P, Binette J, Mercier J, Chiasson A, Cohen EA. 2010. Antagonism of tetherin restriction of HIV-1 release by Vpu involves binding and

sequestration of the restriction factor in a perinuclear compartment. PLoS Pathog 6:e1000856.

12. Schmidt S, Fritz JV, Bitzegeio J, Fackler OT, Keppler OT. 2011. HIV-1 Vpu blocks recycling and biosynthetic transport of the intrinsic immunity factor CD317/tetherin to overcome the virion release restriction. mBio 2:e00036-11.
13. Dube M, Paquay C, Roy BB, Bego MG, Mercier J, Cohen EA. 2011. HIV-1 Vpu antagonizes BST-2 by interfering mainly with the trafficking of newly synthesized BST-2 to the cell surface. Traffic 12:1714 –1729.
14. Kueck T, Foster TL, Weinelt J, Sumner JC, Pickering S, Neil SJ. 2015. Serine phosphorylation of HIV-1 Vpu and its binding to Tetherin regulates interaction with clathrin adaptors. PLoS Pathog 11:e1005141.
15. Kueck T, Neil SJ. 2012. A cytoplasmic tail determinant in HIV-1 Vpu mediates targeting of tetherin for endosomal degradation and counteracts interferon-induced restriction. PLoS Pathog 8:e1002609.
16. Jia X, Weber E, Tokarev A, Lewinski M, Rizk M, Suarez M, Guatelli J, Xiong Y. 2014. Structural basis of HIV-1 Vpu-mediated BST2 antagonism via hijacking of the clathrin adaptor protein complex 1. Elife 3:e02362.
17. Douglas JL, Viswanathan K, McCarroll MN, Gustin JK, Fruh K, Moses AV. 2009. Vpu directs the degradation of the human immunodeficiency virus restriction factor BST-2/Tetherin via a beta-TrCP-dependent mechanism. J Virol 83:7931–7947.
18. Mangeat B, Gers-Huber G, Lehmann M, Zufferey M, Luban J, Piguet V. 2009. HIV-1 Vpu neutralizes the antiviral factor Tetherin/BST-2 by binding it and directing its beta-TrCP2-dependent degradation. PLoS Pathog 5:e1000574.
19. Mitchell RS, Katsura C, Skasko MA, Fitzpatrick K, Lau D, Ruiz A, Stephens EB, Margottin-Goguet F, Benarous R, Guatelli JC. 2009. Vpu antagonizes BST-2-mediated restriction of HIV-1 release via beta-TrCP and endolysosomal trafficking. PLoS Pathog 5:e1000450.
20. Gustin JK, Douglas JL, Bai Y, Moses AV. 2012. Ubiquitination of BST-2 protein by HIV-1 Vpu protein does not require lysine, serine, or threonine residues within the BST-2 cytoplasmic domain. J Biol Chem 287: 14837–14850.

21. Tokarev AA, Munguia J, Guatelli JC. 2011. Serine-threonine ubiquitination mediates downregulation of BST-2/tetherin and relief of restricted virion release by HIV-1 Vpu. J Virol 85:51– 63.
22. Agromayor M, Soler N, Caballe A, Kueck T, Freund SM, Allen MD, Bycroft M, Perisic O, Ye Y, McDonald B, Scheel H, Hofmann K, Neil SJ, Martin-Serrano J, Williams RL. 2012. The UBAP1 subunit of ESCRT-I interacts with ubiquitin via a SOUBA domain. Structure 20:414 – 428.
23. Song YE, Cyburt D, Lucas TM, Gregory DA, Lyddon TD, Johnson MC. 2018. betaTrCP is Required for HIV-1 Vpu Modulation of CD4, GaLV Env, and BST-2/Tetherin. Viruses 10:E573.
24. Willey RL, Maldarelli F, Martin MA, Strebel K. 1992. Human immunodeficiency virus type 1 Vpu protein induces rapid degradation of CD4. J Virol 66:7193–7200.
25. Willey RL, Maldarelli F, Martin MA, Strebel K. 1992. Human immunodeficiency virus type 1 Vpu protein regulates the formation of intracellular gp160-CD4 complexes. J Virol 66:226 –234.
26. Matusali G, Potesta M, Santoni A, Cerboni C, Doria M. 2012. The human immunodeficiency virus type 1 Nef and Vpu proteins downregulate the natural killer cell-activating ligand PVR. J Virol 86:4496 – 4504.
27. Shah AH, Sowrirajan B, Davis ZB, Ward JP, Campbell EM, Planelles V, Barker E. 2010. Degranulation of natural killer cells following interaction with HIV-1-infected cells is hindered by downmodulation of NTB-A by Vpu. Cell Host Microbe 8:397– 409.
28. Bottino C, Falco M, Parolini S, Marcenaro E, Augugliaro R, Sivori S, Landi E, Biassoni R, Notarangelo LD, Moretta L, Moretta A. 2001. NTB-A [correction of GNTB-A], a novel SH2D1A-associated surface molecule contributing to the inability of natural killer cells to kill Epstein-Barr virus-infected B cells in X-linked lymphoproliferative disease. J Exp Med 194:235–246.
29. Falco M, Marcenaro E, Romeo E, Bellora F, Marras D, Vely F, Ferracci G, Moretta L, Moretta A, Bottino C. 2004. Homophilic interaction of NTBA, a member of the CD2 molecular family: induction of cytotoxicity and cytokine release in human NK cells. Eur J Immunol 34:1663–1672.

30. Flaig RM, Stark S, Watzl C. 2004. Cutting edge: NTB-A activates NK cells via homophilic interaction. J Immunol 172:6524 – 6527.
31. Bolduan S, Hubel P, Reif T, Lodermeyer V, Hohne K, Fritz JV, Sauter D, Kirchhoff F, Fackler OT, Schindler M, Schubert U. 2013. HIV-1 Vpu affects the anterograde transport and the glycosylation pattern of NTB-A. Virology 440:190 –203.
32. Bottino C, Castriconi R, Pende D, Rivera P, Nanni M, Carnemolla B, Cantoni C, Grassi J, Marcenaro S, Reymond N, Vitale M, Moretta L, Lopez M, Moretta A. 2003. Identification of PVR (CD155) and Nectin-2 (CD112) as cell surface ligands for the human DNAM-1 (CD226) activating molecule. J Exp Med 198:557–567.
33. Shibuya A, Campbell D, Hannum C, Yssel H, Franz-Bacon K, McClanahan T, Kitamura T, Nicholl J, Sutherland GR, Lanier LL, Phillips JH. 1996. DNAM-1, a novel adhesion molecule involved in the cytolytic function of T lymphocytes. Immunity 4:573–581.
34. Bolduan S, Reif T, Schindler M, Schubert U. 2014. HIV-1 Vpu mediated downregulation of CD155 requires alanine residues 10, 14 and 18 of the transmembrane domain. Virology 464-465:375–384.
35. Richard J, Prevost J, von Bredow B, Ding S, Brassard N, Medjahed H, Coutu M, Melillo B, Bibollet-Ruche F, Hahn BH, Kaufmann DE, Smith AB, III, Sodroski J, Sauter D, Kirchhoff F, Gee K, Neil SJ, Evans DT, Finzi A. 2017. BST-2 expression modulates small CD4-mimetic sensitization of HIV-1-infected cells to antibody-dependent cellular cytotoxicity. J Virol 91:e00219-17.
36. McNatt MW, Zang T, Hatziioannou T, Bartlett M, Fofana IB, Johnson WE, Neil SJ, Bieniasz PD. 2009. Species-specific activity of HIV-1 Vpu and positive selection of tetherin transmembrane domain variants. PLoS Pathog 5:e1000300.
37. Yoshida T, Kao S, Strebel K. 2011. Identification of residues in the BST-2 TM domain important for antagonism by HIV-1 Vpu using a gain-of-function approach. Front Microbiol 2:35.
38. Schubert U, Bour S, Ferrer-Montiel AV, Montal M, Maldarell F, Strebel K. 1996. The two biological activities of human immunodeficiency virus type 1 Vpu protein involve two separable structural domains. J Virol 70:809 – 819.
39. Davis ZB, Sowrirajan B, Cogswell A, Ward JP, Planelles V, Barker E. 2016. CD155 on HIV-infected cells is not modulated by HIV-1 Vpu and Nef but synergizes with NKG2D

ligands to trigger NK cell lysis of autologous primary HIV-infected cells. AIDS Res Hum Retroviruses 33:0375.

40. Skasko M, Tokarev A, Chen CC, Fischer WB, Pillai SK, Guatelli J. 2011. BST-2 is rapidly down-regulated from the cell surface by the HIV-1 protein Vpu: evidence for a post-ER mechanism of Vpu-action. Virology 411:65–77.
41. Kmiec D, Iyer SS, Sturzel CM, Sauter D, Hahn BH, Kirchhoff F. 2016. Vpu-mediated counteraction of Tetherin is a major determinant of HIV-1 interferon resistance. mBio 7:e00934-16.
42. Richard J, Prevost J, Alsahafi N, Ding S, Finzi A. 2017. Impact of HIV-1 envelope conformation on ADCC responses. Trends Microbiol 26: 253–265.
43. Cole GB, Reichheld SE, Sharpe S. 2017. FRET analysis of the promiscuous yet specific interactions of the HIV-1 Vpu transmembrane domain. Biophys J 113:1992–2003.
44. Andrew AJ, Miyagi E, Kao S, Strebel K. 2009. The formation of cysteine-linked dimers of BST-2/tetherin is important for inhibition of HIV-1 virus release but not for sensitivity to Vpu. Retrovirology 6:80.
45. Fitzpatrick K, Skasko M, Deerinck TJ, Crum J, Ellisman MH, Guatelli J. 2010. Direct restriction of virus release and incorporation of the interferon-induced protein BST-2 into HIV-1 particles. PLoS Pathog 6:e1000701.
46. Perez-Caballero D, Zang T, Ebrahimi A, McNatt MW, Gregory DA, Johnson MC, Bieniasz PD. 2009. Tetherin inhibits HIV-1 release by directly tethering virions to cells. Cell 139:499 –511.
47. Sandler NG, Bosinger SE, Estes JD, Zhu RT, Tharp GK, Boritz E, Levin D, Wijeyesinghe S, Makamdop KN, del Prete GQ, Hill BJ, Timmer JK, Reiss E, Yarden G, Darko S, Contijoch E, Todd JP, Silvestri G, Nason M, Norgren RB, Jr, Keele BF, Rao S, Langer JA, Lifson JD, Schreiber G, Douek DC. 2014. Type I interferon responses in rhesus macaques prevent SIV infection and slow disease progression. Nature 511:601– 605.
48. Yamada E, Nakaoka S, Klein L, Reith E, Langer S, Hopfensperger K, Iwami S, Schreiber G, Kirchhoff F, Koyanagi Y, Sauter D, Sato K. 2018. Human-specific adaptations in Vpu conferring anti-tetherin activity are critical for efficient early HIV-1 replication in vivo. Cell Host Microbe 23: 110 –120.e7.

49. Sato K, Misawa N, Fukuhara M, Iwami S, An DS, Ito M, Koyanagi Y. 2012. Vpu augments the initial burst phase of HIV-1 propagation and downregulates BST2 and CD4 in humanized mice. J Virol 86:5000 –5013.
50. Dave VP, Hajjar F, Dieng MM, Haddad E, Cohen EA. 2013. Efficient BST2 antagonism by Vpu is critical for early HIV-1 dissemination in humanized mice. Retrovirology 10:128.
51. Parrish NF, Gao F, Li H, Giorgi EE, Barbian HJ, Parrish EH, Zajic L, Iyer SS, Decker JM, Kumar A, Hora B, Berg A, Cai F, Hopper J, Denny TN, Ding H, Ochsenbauer C, Kappes JC, Galimidi RP, West AP, Jr, Bjorkman PJ, Wilen CB, Doms RW, O'Brien M, Bhardwaj N, Borrow P, Haynes BF, Muldoon M, Theiler JP, Korber B, Shaw GM, Hahn BH. 2013. Phenotypic properties of transmitted founder HIV-1. Proc Natl Acad Sci USA 110:6626 – 6633.
52. Iyer SS, Bibollet-Ruche F, Sherrill-Mix S, Learn GH, Plenderleith L, Smith AG, Barbian HJ, Russell RM, Gondim MV, Bahari CY, Shaw CM, Li Y, Decker T, Haynes BF, Shaw GM, Sharp PM, Borrow P, Hahn BH. 2017. Resistance to type 1 interferons is a major determinant of HIV-1 transmission fitness. Proc Natl Acad Sci USA 114:E590 –E599.
53. Fenton-May AE, Dibben O, Emmerich T, Ding H, Pfafferott K, Aasa-Chapman MM, Pellegrino P, Williams I, Cohen MS, Gao F, Shaw GM, Hahn BH, Ochsenbauer C, Kappes JC, Borrow P. 2013. Relative resistance of HIV-1 founder viruses to control by interferon-alpha. Retrovirology 10: 146.
54. Foster TL, Wilson H, Iyer SS, Coss K, Doores K, Smith S, Kellam P, Finzi A, Borrow P, Hahn BH, Neil S. 2016. Resistance of transmitted founder HIV-1 to IFITM-mediated restriction. Cell Host Microbe 20:429 – 442.
55. Tomescu C, Mavilio D, Montaner LJ. 2015. Lysis of HIV-1-infected autologous CD4 primary T cells by interferon-alpha-activated NK cells requires NKp46 and NKG2D. AIDS 29:1767–1773.
56. Kwaa AKR, Talana CAG, Blankson JN. 2019. Interferon-alpha enhances NK cell function and the suppressive capacity of HIV-specific CD8 T cells. J Virol 93:e01541-18.
57. Tomescu C, Tebas P, Montaner LJ. 2017. IFN-alpha augments natural killer-mediated antibody-dependent cellular cytotoxicity of HIV-1- infected autologous CD4 T cells regardless of major histocompatibility complex class 1 downregulation. AIDS 31:613–622.

58. Arias JF, Heyer LN, von Bredow B, Weisgrau KL, Moldt B, Burton DR, Rakasz EG, Evans DT. 2014. Tetherin antagonism by Vpu protects HIV-infected cells from antibody-dependent cell-mediated cytotoxicity. Proc Natl Acad Sci USA 111:6425– 6430.
59. Asmuth DM, Murphy RL, Rosenkranz SL, Lertora JJ, Kottilil S, Cramer Y, Chan ES, Schooley RT, Rinaldo CR, Thielman N, Li XD, Wahl SM, Shore J, Janik J, Lempicki RA, Simpson Y, Pollard RB, AIDS Clinical Trials Group A5192 Team. 2010. Safety, tolerability, and mechanisms of antiretroviral activity of pegylated interferon alfa-2a in HIV-1-monoinfected participants: a phase II clinical trial. J Infect Dis 201:1686 –1696.
60. Azzoni L, Foulkes AS, Papasavvas E, Mexas AM, Lynn KM, Mounzer K, Tebas P, Jacobson JM, Frank I, Busch MP, Deeks SG, Carrington M, O'Doherty U, Kostman J, Montaner LJ. 2013. Pegylated interferon alfa-2a monotherapy results in suppression of HIV type 1 replication and decreased cell-associated HIV DNA integration. J Infect Dis 207:213–222.
61. Pillai SK, Abdel-Mohsen M, Guatelli J, Skasko M, Monto A, Fujimoto K, Yukl S, Greene WC, Kovari H, Rauch A, Fellay J, Battegay M, Hirschel B, Witteck A, Bernasconi E, Ledergerber B, Gunthard HF, Wong JK, Swiss H. 2012. Role of retroviral restriction factors in the interferon-alpha-mediated suppression of HIV-1 in vivo. Proc Natl Acad Sci USA 109:3035–3040.
62. Sun H, Buzon MJ, Shaw A, Berg RK, Yu XG, Ferrando-Martinez S, Leal M, Ruiz-Mateos E, Lichterfeld M. 2014. Hepatitis C therapy with interferon-alpha and ribavirin reduces CD4 T-cell-associated HIV-1 DNA in HIV-1/ hepatitis C virus-coinfected patients. J Infect Dis 209:1315–1320.
63. Harper MS, Guo K, Gibbert K, Lee EJ, Dillon SM, Barrett BS, McCarter MD, Hasenkrug KJ, Dittmer U, Wilson CC, Santiago ML. 2015. Interferon-alpha subtypes in an ex vivo model of acute HIV-1 infection: expression, potency and effector mechanisms. PLoS Pathog 11:e1005254.
64. Lavender KJ, Gibbert K, Peterson KE, Van Dis E, Francois S, Woods T, Messer RJ, Gawanbacht A, Muller JA, Munch J, Phillips K, Race B, Harper MS, Guo K, Lee EJ, Trilling M, Hengel H, Piehler J, Verheyen J, Wilson CC, Santiago ML, Hasenkrug KJ, Dittmer U. 2016. Interferon alpha subtype-specific suppression of HIV-1 infection in vivo. J Virol 90:6001– 6013.

65. Veillette M, Desormeaux A, Medjahed H, Gharsallah NE, Coutu M, Baalwa J, Guan Y, Lewis G, Ferrari G, Hahn BH, Haynes BF, Robinson JE, Kaufmann DE, Bonsignori M, Sodroski J, Finzi A. 2014. Interaction with cellular CD4 exposes HIV-1 envelope epitopes targeted by antibody-dependent cell-mediated cytotoxicity. J Virol 88:2633–2644.
66. Richard J, Veillette M, Brassard N, Iyer SS, Roger M, Martin L, Pazgier M, Schon A, Freire E, Routy JP, Smith AB, III, Park J, Jones DM, Courter JR, Melillo BN, Kaufmann DE, Hahn BH, Permar SR, Haynes BF, Madani N, Sodroski JG, Finzi A. 2015. CD4 mimetics sensitize HIV-1-infected cells to ADCC. Proc Natl Acad Sci USA 112:E2687–E2694.
67. Richard J, Prevost J, Baxter AE, von Bredow B, Ding S, Medjahed H, Delgado GG, Brassard N, Sturzel CM, Kirchhoff F, Hahn BH, Parsons MS, Kaufmann DE, Evans DT, Finzi A. 2018. Uninfected bystander cells impact the measurement of HIV-specific antibody-dependent cellular cytotoxicity responses. mBio 9:e00358-18.
68. Salazar-Gonzalez JF, Salazar MG, Keele BF, Learn GH, Giorgi EE, Li H, Decker JM, Wang S, Baalwa J, Kraus MH, Parrish NF, Shaw KS, Guffey MB, Bar KJ, Davis KL, Ochsenbauer-Jambor C, Kappes JC, Saag MS, Cohen MS, Mulenga J, Derdeyn CA, Allen S, Hunter E, Markowitz M, Hraber P, Perelson AS, Bhattacharya T, Haynes BF, Korber BT, Hahn BH, Shaw GM. 2009. Genetic identity, biological phenotype, and evolutionary pathways of transmitted/founder viruses in acute and early HIV-1 infection. J Exp Med 206:1273–1289.
69. Ochsenbauer C, Edmonds TG, Ding H, Keele BF, Decker J, Salazar MG, Salazar-Gonzalez JF, Shattock R, Haynes BF, Shaw GM, Hahn BH, Kappes JC. 2012. Generation of transmitted/founder HIV-1 infectious molecular clones and characterization of their replication capacity in CD4 T lymphocytes and monocyte-derived macrophages. J Virol 86:2715–2728.
70. Bar KJ, Tsao CY, Iyer SS, Decker JM, Yang Y, Bonsignori M, Chen X, Hwang KK, Montefiori DC, Liao HX, Hraber P, Fischer W, Li H, Wang S, Sterrett S, Keele BF, Ganusov VV, Perelson AS, Korber BT, Georgiev I, McLellan JS, Pavlicek JW, Gao F, Haynes BF, Hahn BH, Kwong PD, Shaw GM. 2012. Early low-titer neutralizing antibodies impede HIV-1 replication and select for virus escape. PLoS Pathog 8:e1002721.

71. Liao HX, Lynch R, Zhou T, Gao F, Alam SM, Boyd SD, Fire AZ, Roskin KM, Schramm CA, Zhang Z, Zhu J, Shapiro L, Mullikin JC, Gnanakaran S, Hraber P, Wiehe K, Kelsoe G, Yang G, Xia SM, Montefiori DC, Parks R, Lloyd KE, Scearce RM, Soderberg KA, Cohen M, Kamanga G, Louder MK, Tran LM, Chen Y, Cai F, Chen S, Moquin S, Du X, Joyce MG, Srivatsan S, Zhang B, Zheng A, Shaw GM, Hahn BH, Kepler TB, Korber BT, Kwong PD, Mascola JR, Haynes BF. 2013. Co-evolution of a broadly neutralizing HIV-1 antibody and founder virus. Nature 496:469 – 476.

72. Heigele A, Kmiec D, Regensburger K, Langer S, Peiffer L, Sturzel CM, Sauter D, Peeters M, Pizzato M, Learn GH, Hahn BH, Kirchhoff F. 2016. The potency of Nef-mediated SERINC5 antagonism correlates with the prevalence of primate lentiviruses in the wild. Cell Host Microbe 20: 381–391.

73. Neil SJ, Eastman SW, Jouvenet N, Bieniasz PD. 2006. HIV-1 Vpu promotes release and prevents endocytosis of nascent retrovirus particles from the plasma membrane. PLoS Pathog 2:e39.

74. Sauter D, Unterweger D, Vogl M, Usmani SM, Heigele A, Kluge SF, Hermkes E, Moll M, Barker E, Peeters M, Learn GH, Bibollet-Ruche F, Fritz JV, Fackler OT, Hahn BH, Kirchhoff F. 2012. Human tetherin exerts strong selection pressure on the HIV-1 group N Vpu protein. PLoS Pathog 8:e1003093.

5.2.10 FIGURES

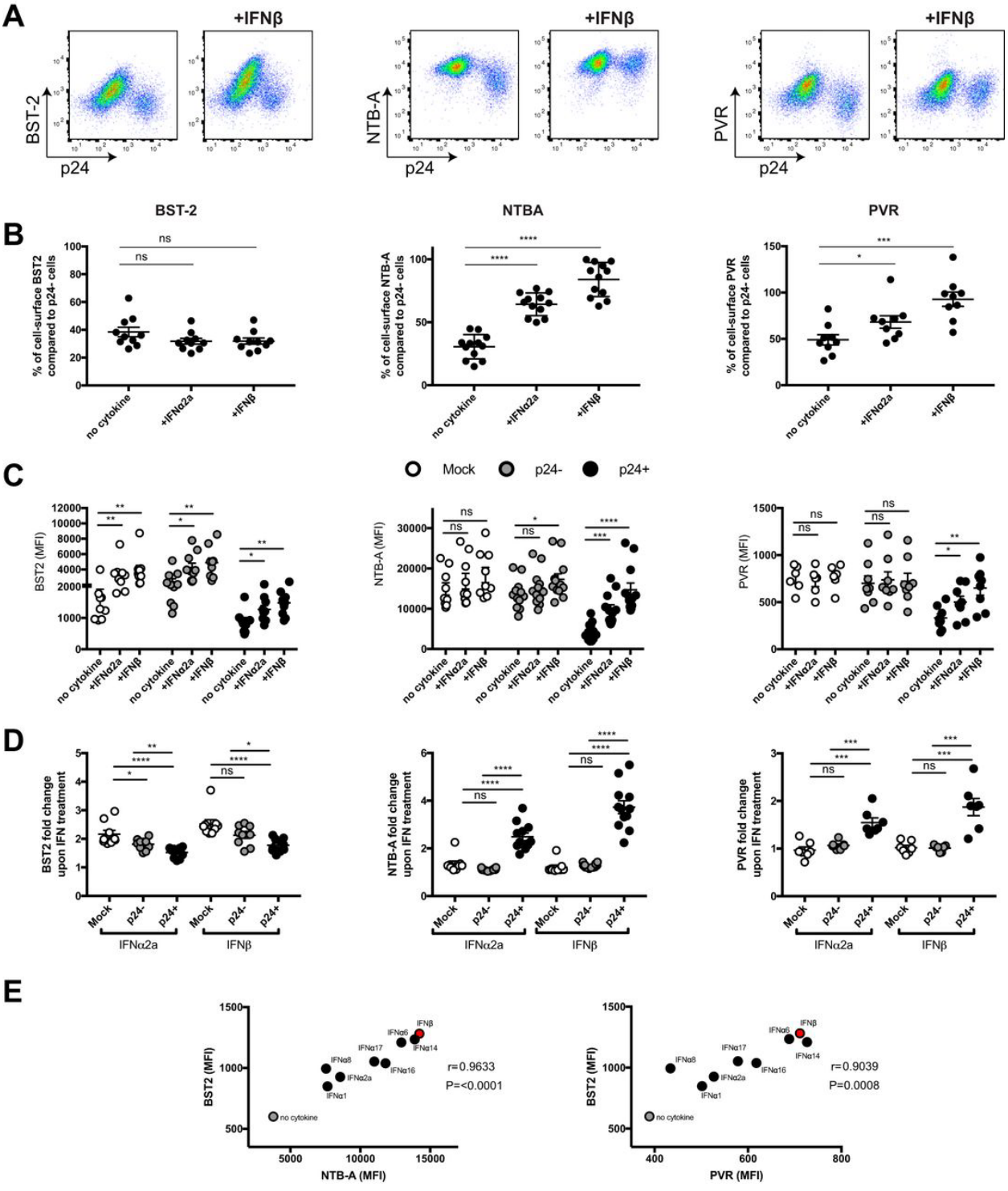

Figure 5.1.1 - Type I IFNs enhance cell surface NTB-A and PVR on HIV-1-infected cells. Primary $CD4^+$ T cells were mock infected or infected with the CH58 transmitted/founder virus (CH58 TF) and either mock treated or treated for 24 h with type I IFNs (IFN-α, IFN-β). At 48 h post-infection, cells were stained with anti-BST-2, anti-NTB-A, or anti-PVR Abs, followed by the appropriate secondary Abs. (**A**) Dot plot depicting representative stainings with or without IFN-β treatment. (**B to D**) The graphs shown represent the percentage of median fluorescence intensities (MFI) detected on the $p24^+$ population over the MFI detected on the $p24^-$ population (**B**), the MFI obtained on mock-infected cells, uninfected $p24^-$ cells, or infected $p24^+$ cells (**C**), or the fold change in MFI upon IFN treatment for at least 6 independent experiments (**D**). Error bars indicate means +/- standard errors of the means (SEM). Statistical significance was tested using an unpaired t test or the Mann-Whitney test based on statistical normality (*, $P < 0.05$; **, $P < 0.01$; ***, $P < 0.001$; ****, $P < 0.0001$; ns, nonsignificant). (**E**) Correlations between the levels of cell surface BST-2 and the levels of NTB-A or PVR on the infected ($p24^+$) population upon treatment with different type I IFNs was calculated using a Pearson correlation test.

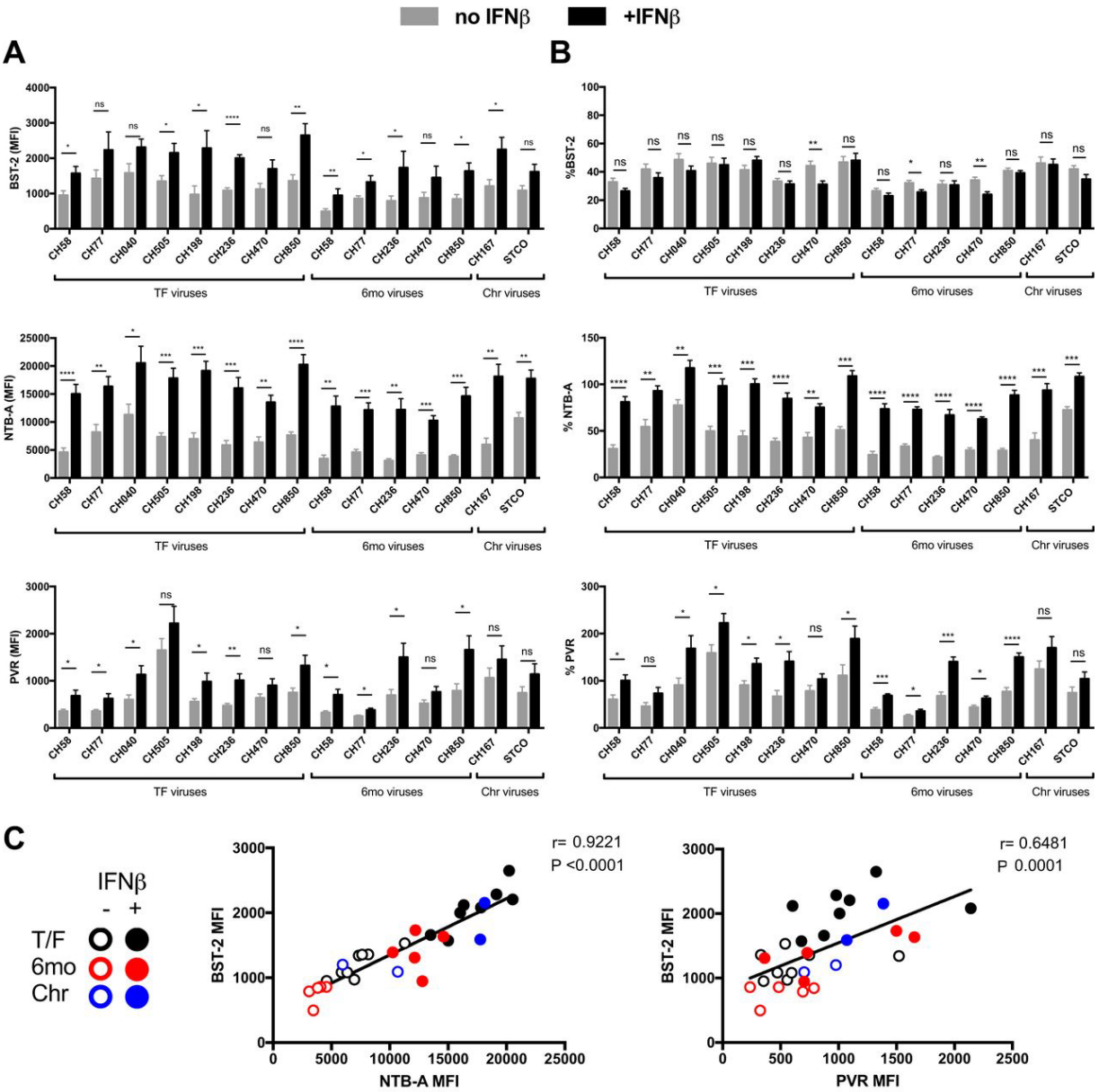

Figure 5.1.2 - IFN-β enhances cell surface NTB-A and PVR on cells infected with TF, 6-month (6mo), and chronic (Chr) viruses.

Primary CD4$^+$ T cells were infected with different transmitted/founder (TF) (CH58, CH77, CH40, CH505, CH198, CH236, CH470, CH850), 6-month (CH58, CH77, CH236, CH470, CH850), and chronic viruses (CH167, STCO) and either mock treated or treated for 24 h with IFN-β. At 48 h post-infection, cells were stained with anti-BST-2, anti-NTB-A, or anti-PVR Abs, followed by the appropriate secondary Abs. The graphs shown represent the MFI obtained on infected (p24$^+$) cells (**A**) or the percentage of the MFI on the p24$^+$ population over the MFI on the p24$^-$ population (**B**). These graphs represent data obtained from at least 5 independent experiments. Error bars indicate means +/- SEM. Statistical significance was tested using an unpaired t test or the Mann-Whitney test based on statistical normality (*, $P < 0.05$; **, $P < 0.01$; ***, $P < 0.001$; ****, $P < 0.0001$; ns, nonsignificant). (**C**) Correlations between the levels of cell surface BST-2 and the levels of NTB-A or PVR on the infected (p24$^+$) population of the different viruses tested upon treatment with different type I IFNs were tested using the Spearman rank correlation test.

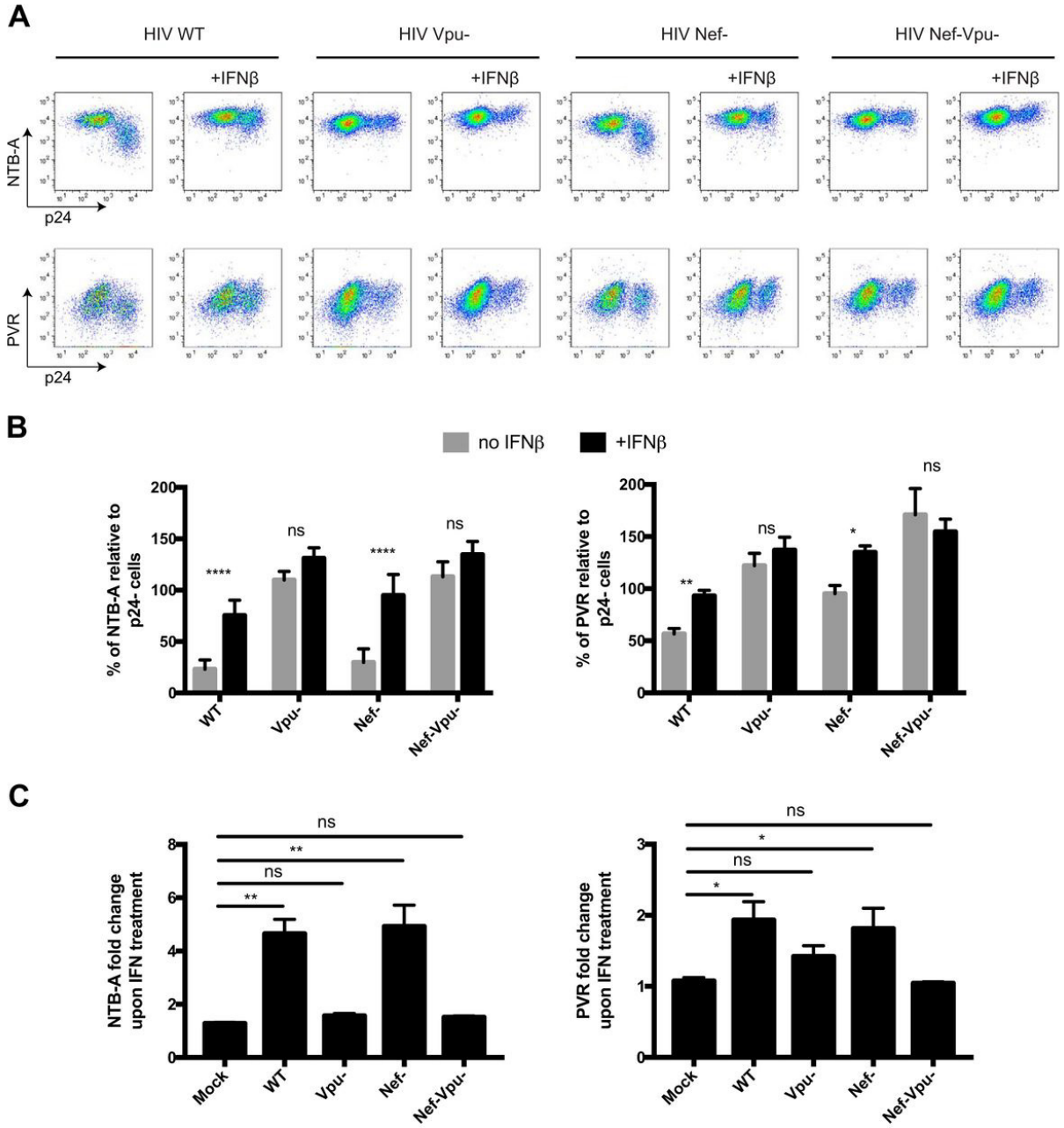

Figure 5.1.3 - IFN-β impairs Vpu's ability to downregulate cell surface NTB-A and PVR.
Primary $CD4^+$ T cells were infected with CH58 TF virus either WT or defective for Nef and/or Vpu expression. At 24 h post-infection, infected cells were either mock treated or treated for 24 h with IFN-. At 48 h post-infection, cells were stained with anti-NTB-A or anti-PVR Abs, followed by the appropriate secondary Abs. (**A**) Dot plot depicting representative stainings with or without IFN-β treatment. (**B and C**) The graphs shown represent the percentage of MFI on the $p24^+$ population over the MFI on the $p24^-$ population (**B**) or the fold change in MFI upon IFN treatment on the different populations (**C**). All graphs shown represent data obtained from at least 5 independent experiments. Error bars indicate means +/- SEM. Statistical significance was tested using a multiple t test, correcting for multiple comparisons using the Bonferroni-Dunn method (**B**), and a Kruskal-Wallis test (**C**) (*, $P < 0.05$; **, $P < 0.01$; ****, $P < 0.0001$; ns, nonsignificant).

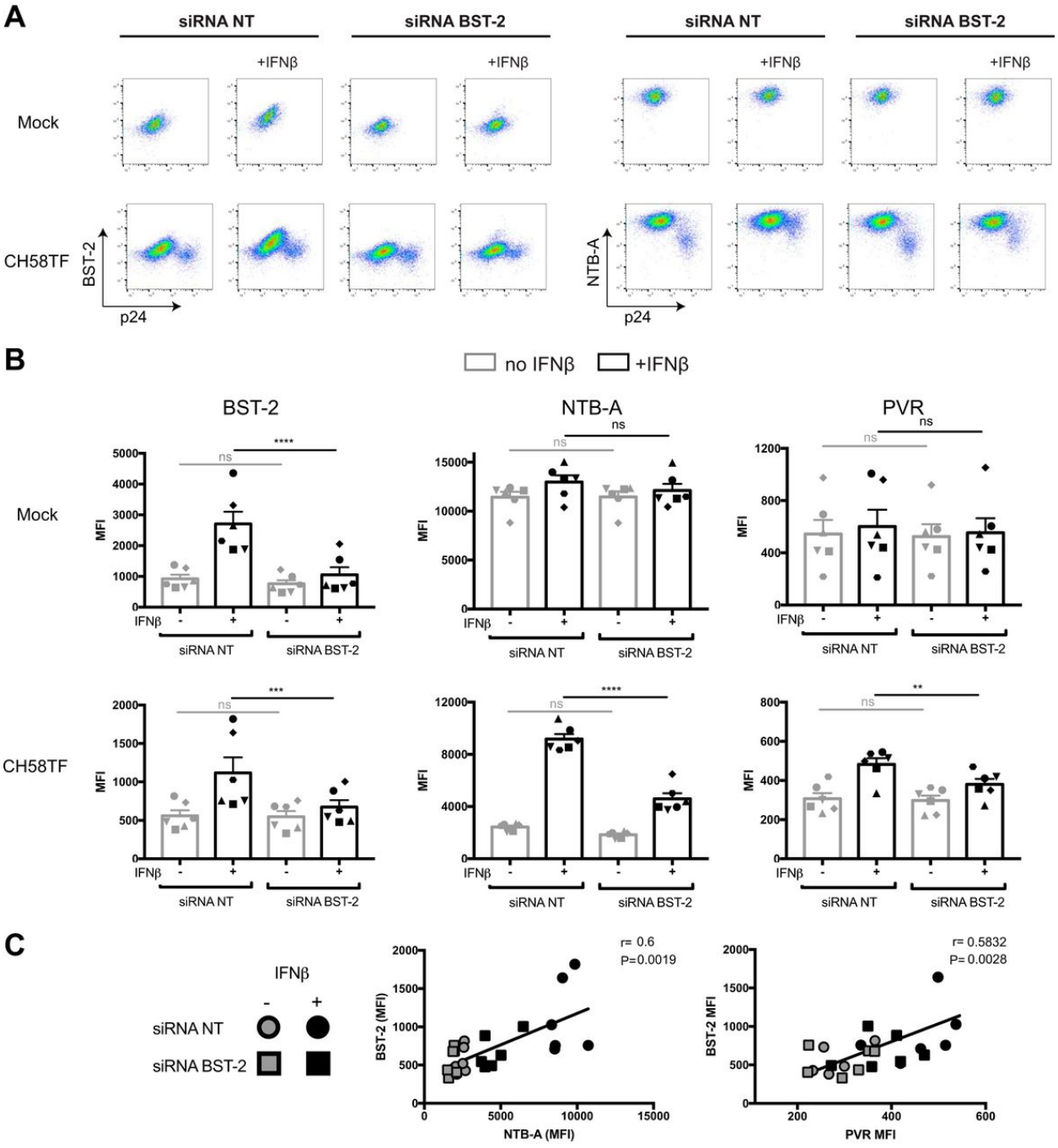
A
siRNA NT
siRNA BST-2
siRNA NT
siRNA BST-2
+IFNβ
+IFNβ
+IFNβ
+IFNβ
Mock
CH58TF
BST-2
p24
NTB-A
p24
B
no IFNβ
+IFNβ
BST-2
NTB-A
PVR
Mock
CH58TF
MFI
IFNβ
siRNA NT
siRNA BST-2
ns
****
***
**
C
IFNβ
siRNA NT
siRNA BST-2
r= 0.6
P=0.0019
BST-2 (MFI)
NTB-A (MFI)
r= 0.5832
P= 0.0028
BST-2 MFI
PVR MFI

Figure 5.1.4 - IFN-β enhances cell surface NTB-A and PVR in a BST-2-dependent manner. Primary $CD4^+$ T cells were mock infected or infected with CH58 TF WT virus. At 24 h post-infection, infected cells were electroporated with siRNAs targeting BST-2 mRNA or nontargeting siRNAs, followed by treatment (or not) with IFN-. At 48 h post-infection, cells were stained with anti-BST-2, anti-NTB-A, or anti-PVR Abs, followed by the appropriate secondary Abs. (**A**) Dot plot depicting representative stainings. (**B**) The graphs shown represent the MFI obtained on mock-infected or infected ($p24^+$) cells in 6 independent experiments. Statistical significance was tested using a paired one-way analysis of variance (**, $P < 0.01$; ***, $P < 0.001$; ****, $P < 0.0001$; ns, nonsignificant). (**C**) Correlations between the levels of cell surface BST-2 and the levels of NTB-A or PVR on the infected ($p24^+$) population upon siRNA electroporation and treatment with IFNβ were tested using Spearman rank correlation test.

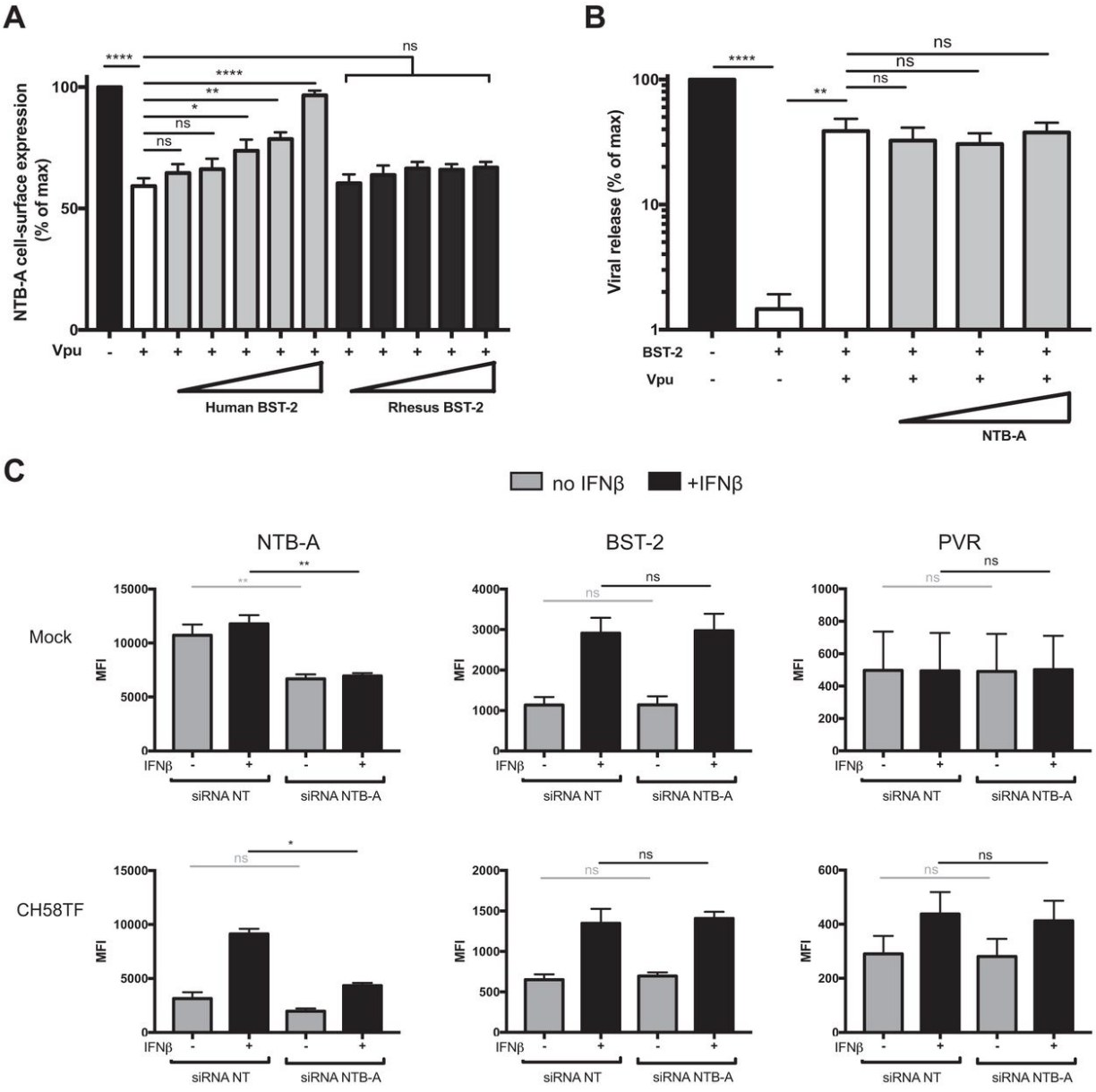
A
NTB-A cell-surface expression (% of max)
Vpu
Human BST-2
Rhesus BST-2
B
Viral release (% of max)
BST-2
Vpu
NTB-A
C
no IFNβ
+IFNβ
NTB-A
BST-2
PVR
Mock
CH58TF
MFI
IFNβ
siRNA NT
siRNA NTB-A

Figure 5.1.5 - Expression of human BST-2 alone is sufficient to impair the ability of Vpu to downregulate NTB-A.
(**A**) HEK293T cells were co-transfected with plasmids expressing Vpu (40 ng), NTB-A (50 ng), and GFP (150 ng) in the presence of increasing concentration of a human or rhesus macaque BST-2 expression vector (0, 10, 20, 50, 100, 200 ng). At 2 days post-transfection, cells were stained with anti-NTB-A Abs, followed by the appropriate secondary Abs. These data sets are representative of those from 5 independent experiments. (**B**) HEK293T cells were co-transfected with plasmids harboring a NL4.3 ΔVpu proviral construct (500 ng), human BST-2 (50 ng), and Vpu (40 ng) in the presence of increasing concentrations of the NTB-A expression vector (0, 50, 100, and 200 ng). Cell culture supernatants containing released infectious virions were harvested at 48 h after transfection and assayed for infectivity on TZM-bl cells. These data sets are representative of those from 4 independent experiments. (**C**) Primary $CD4^+$ T cells were mock infected or infected with CH58 TF WT virus. At 24 h post-infection, infected cells were electroporated with siRNAs targeting NTB-A mRNA or nontargeting siRNAs, followed by treatment (or not) with IFN-β. At 48 h post-infection, cells were stained with anti-BST-2, anti-NTB-A, or anti-PVR Abs, followed by the appropriate secondary Abs. The graphs shown represent the MFIs obtained in 3 independent experiments. Statistical significance was tested using an unpaired t test or a Mann-Whitney test based on statistical normality (**A and B**) or a paired one-way analysis of variance (**C**) (*, $P < 0.05$; **, $P < 0.01$; ****, $P < 0.0001$; ns, nonsignificant).

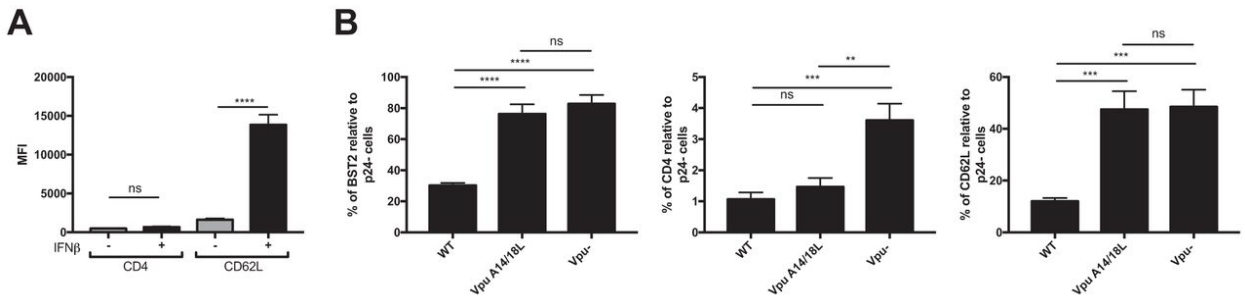

Figure 5.1.6 - Type I IFNs enhance cell surface CD62L but not CD4 on HIV-1-infected cells. (**A**) Primary $CD4^+$ T cells were infected with CH58 TF virus and either mock treated or treated for 24 h with IFN-β. At 48 h post-infection, cells were stained with anti-CD4 or anti-CD62L Abs, followed by the appropriate secondary Abs. The graph shown represents the median fluorescence intensities (MFI) detected on $p24^+$ cells. (**B**) Primary $CD4^+$ T cells were infected with CH58 TF virus expressing the Vpu WT or Vpu A14/18L or CH58 TF virus defective for Vpu expression (Vpu). At 48 h post-infection, cells were stained with anti-BST-2, anti-CD4, or anti-CD62L Abs, followed by the appropriate secondary Abs. The graphs shown represent the percentage of BST-2, CD4, and CD62L detected on the $p24^+$ cells relative to the $p24^-$ cells. All these graphs represent data obtained in at least 6 independent experiments. Error bars indicate means +/- SEM. Statistical significance was tested using an unpaired t test or the Mann-Whitney test based on statistical normality (**, $P < 0.01$; ***, $P < 0.001$; ****, $P < 0.0001$; ns, nonsignificant).

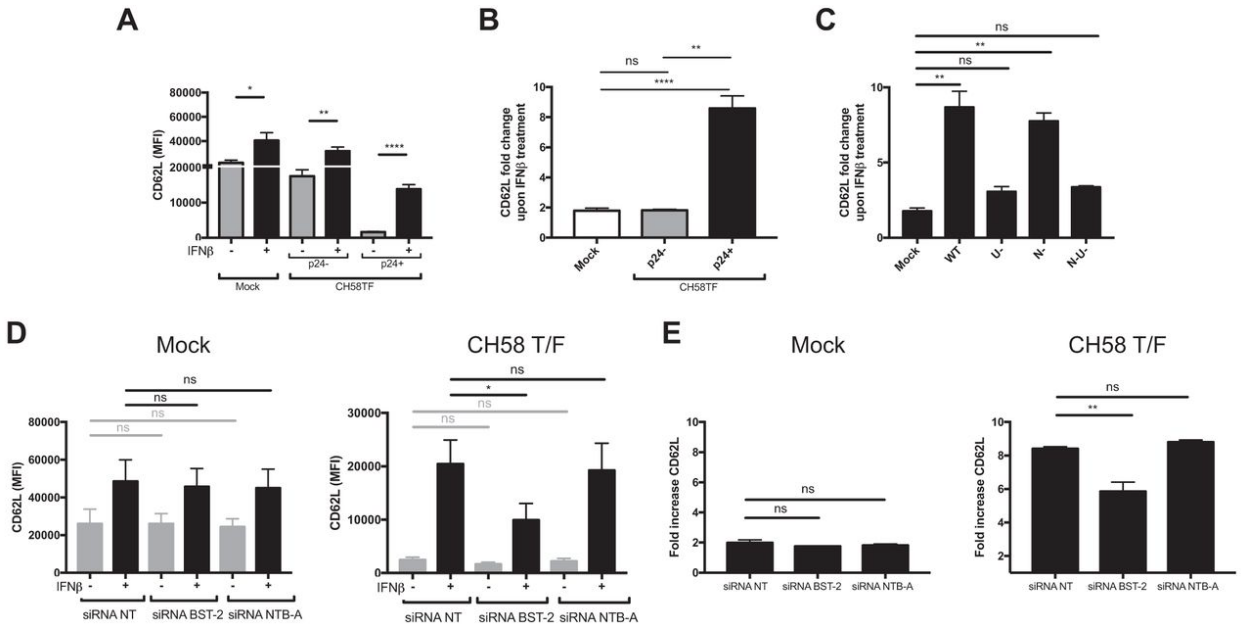

Figure 5.1.7 - Type I IFN-induced BST-2 upregulation prevents the capacity of Vpu to downregulate CD62L.

(**A to C**) Primary $CD4^+$ T cells were infected with CH58 TF virus, either WT or defective for Nef and/or Vpu expression. At 24 h post-infection, infected cells were either mock treated or treated for 24 h with IFN-β. At 48 h post-infection, cells were stained with anti-CD62L Abs, followed by the appropriate secondary Abs. (**A to C**) The graphs shown represent the median fluorescence intensities (MFI) (**A**), the fold change in MFI upon IFN treatment detected on mock-infected, $p24^-$, and $p24^+$ cells in the context of WT infection (**B**), and the fold change in MFI upon IFN treatment detected on $p24^+$ cells in the context of infection with WT virus and virus lacking Vpu (U^-), Nef (N^-), and both Nef and Vpu (N^-U^-) (**C**). (**D and E**) Primary $CD4^+$ T cells were mock infected or infected with CH58 TF WT virus. At 24 h post-infection, cells were electroporated with siRNAs targeting BST-2 or NTB-A mRNA or nontargeting siRNAs, followed by treatment (or not) with IFN-β. At 48 h post-infection, cells were stained with anti-CD62L Abs, followed by the appropriate secondary Abs. The graphs shown represent the median fluorescence intensities (MFI) (**D**) or the fold change in MFI upon IFN treatment detected on mock-infected or $p24^+$ virus-infected cells (**E**). All these graphs represent data obtained in at least 3 independent experiments. Error bars indicate means +/- SEM. Statistical significance was tested using an unpaired t test or the Mann-Whitney test based on statistical normality (**A and B**), a Kruskal-Wallis test (**C**), or a paired one-way analysis of variance (**D and E**) (*, $P < 0.05$; **, $P < 0.01$; ****, $P < 0.0001$; ns, nonsignificant).

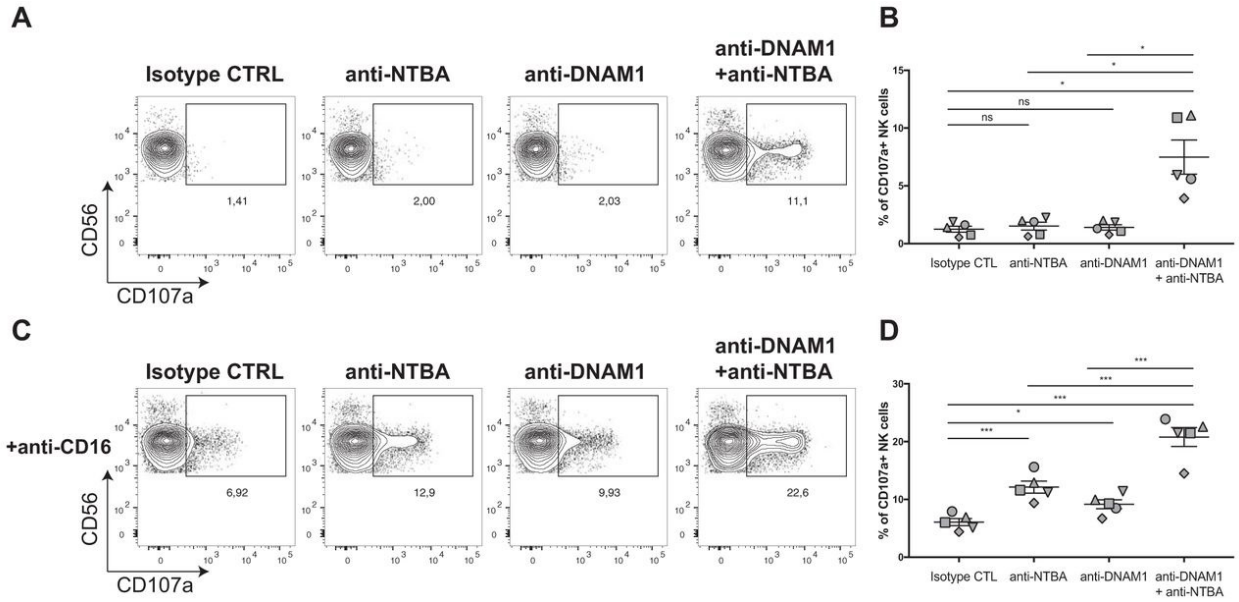

Figure 5.1.8 - Stimulation of NK cells via NTB-A and DNAM-1 induces direct and Ab-dependent NK cell responses.

(**A and B**) P815 cells were incubated with anti-NTB-A Abs and/or anti-DNAM-1 Abs or a matched IgG isotype control prior to being mixed with purified NK cells and incubated for 4 h. (**C and D**) Alternatively, P815 cells were also incubated with anti-CD16 Abs. $CD3^-$ $CD56^+$ cells were evaluated for the percentage of cell surface CD107a expression. (**A and C**) Dot plots depict representative NK cell stimulation. (**B and D**) The graphs shown represent the percentage of CD107a expression among $CD3^-$ $CD56^+$ NK cells obtained in 5 independent experiments. Statistical significance was tested using a paired t test (*, $P < 0.05$; ***, $P < 0.001$; ns, nonsignificant). CTRL and CTL, control.

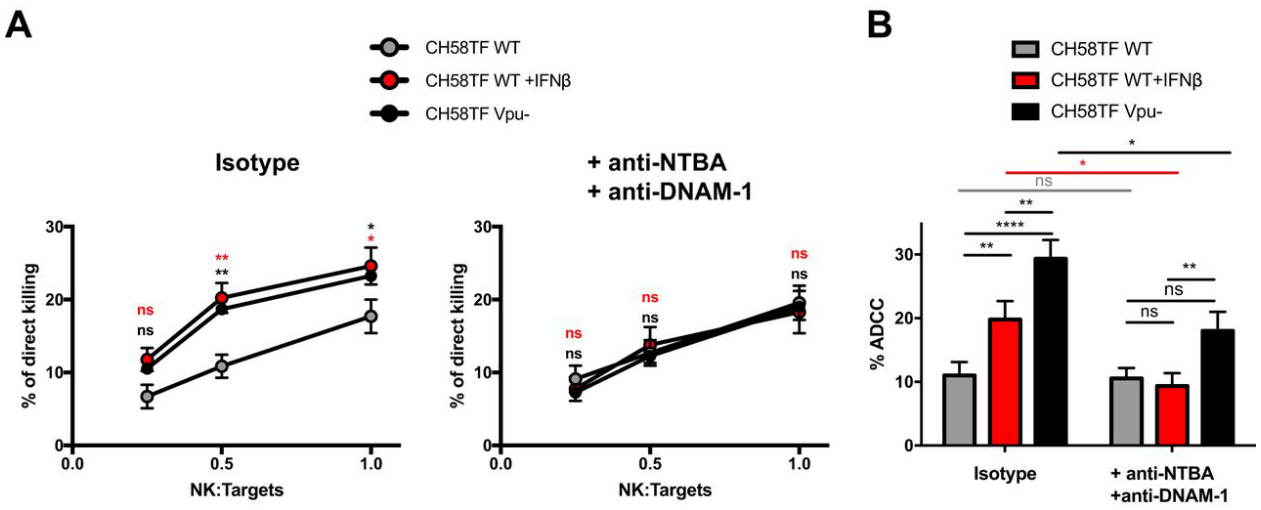

Figure 5.1.9 - Type I IFNs sensitize HIV-1-infected cells to NK cell responses in an NTB-A- and DNAM-1-dependent manner.

(**A**) Primary $CD4^+$ T cells infected with CH58 TF WT virus (treated or not with IFN-β) or its *vpu*-defective counterpart (Vpu) were used as target cells, while autologous NK cells were used as effector cells to perform a direct killing assay. NK cells were preincubated in the presence of anti-NTB-A and anti-DNAM-1 or their matched IgG isotype controls prior to incubation with target cells for 5 h at different NK cell/target cell ratios (1:4, 1:2, 1:1). The graphs shown represent the percentages of direct killing obtained from 3 independent experiments done in triplicate. (**B**) Alternatively, autologous PBMCs were used as effector cells in a well-established FACS-based ADCC assay. Autologous PBMCs were preincubated in the presence of anti-NTB-A and anti-DNAM-1 or their matched IgG isotype controls prior to incubation with target cells for 5 h. The graph shown represents the percentages of ADCC obtained with bNAb 3BNC117 in the presence or absence of blocking Abs. Statistical significance was tested using an unpaired t test (*, $P < 0.05$; **, $P < 0.01$; ****, $P < 0.0001$; ns, nonsignificant).

5.2.11 SUPPLEMENTAL MATERIAL

Flow cytometry analysis of cell-surface staining

Binding of antibodies to cell-surface NTB-A (10 µg/mL), PVR (10 µg/mL), rabbit polyclonal anti-BST-2 (1:2,000 dilution), CD62L (1 µg/mL), CD4 (1 µg/mL) and anti-HIV-1 Env mAb 3BNC117 (0.5 µg/mL) was performed at 48h post-infection. Infected cells were stained intracellularly for HIV-1 p24, using the Cytofix/Cytoperm Fixation/ Permeabilization Kit (BD Biosciences, Mississauga, ON, Canada) and the fluorescent anti-p24 mAb (PE-conjugated anti-p24, clone KC57; Beckman Coulter/Immunotech). The percentage of infected cells ($p24^+$) was determined by gating the living cell population using a viability dye staining (Aqua Vivid, Thermo Fisher Scientific). Samples were acquired on an LSRII cytometer (BD Biosciences), and data analysis was performed using FlowJo vX.0.7 (Tree Star, Ashland, OR, USA).

Antibodies

The following Abs were used as primary Abs for cell-surface staining: mouse anti-human CD352 (NTB-A) (clone NT-7, Biolegend), mouse anti-human CD155 (PVR) (clone SKII.4, Biolegend), rabbit polyclonal anti-human BST2 antiserum (NIH AIDS Reagent Program), mouse anti-CD4 (clone OKT4, eBioscience), mouse anti-CD62L (clone LT-TD180, Invitrogen), anti-HIV-1 Env mAb 3BNC117 (NIH AIDS Reagent Program). Goat anti-mouse and anti-human antibodies pre-coupled to Alexa Fluor 647 (Invitrogen) and BrillantViolet 421-conjugated donkey anti-rabbit antibodies (Biolegend) were used as secondary antibodies in flow cytometry experiments. The following Abs were used for redirection assays and/or killing blockade experiments: PE-anti-human CD56 (clone NCAM16.2, BD Biosciences), APC-anti-human CD107a (clone H4A3, BD Biosciences), BUV395-anti-human CD3 (clone UCHT1, BD Biosciences), mouse anti-human CD352 (NTB-A) (clone NT-7, Biolegend), mouse anti-human CD226 (clone DX11, BD Pharmingen), mouse anti-human CD16 (clone 3G8, Biolegend) and their matched IgG isotype control (clone MOPC-21, Biolegend).

Redirection assays

P815 cells were incubated with 5 µg/ml of purified anti-NTB-A Abs and/or anti-DNAM-1 Abs or their matched IgG isotype control Abs, in the presence or not of 0.5 µg/ml of anti-CD16

Abs, for 30 min at 4°C. The P815 cells (2×10^5) were then mixed with purified NK cells (1×10^5) and incubated for 4hr at 37°C, 5% CO_2. After 4h of coincubation, the cells were stained with fluorochrome-conjugated anti-CD3, CD56 and CD107a. $CD3^-$ $CD56^+$ cells were evaluated for the percentage of cell-surface CD107a expression.

NK cell direct killing assay

Infected primary $CD4^+$ T cells were stained with a viability dye (AquaVivid; ThermoFisher Scientific) and cell proliferation dye (eFluor670; eBioscience) and used as target cells. Autologous purified NK cells, stained with another cellular marker (cell proliferation dye eFluor450; eBioscience), were added at different NK: target ratios (1:4, 1:2, 1:1) in 96-well V-bottom plates (Corning, Corning, NY). NK cells were preincubated in the presence of anti-NTB-A and anti-DNAM-1 or their matched IgG isotype control (10 µg/mL) prior being incubated with target cells. The plates were subsequently centrifuged for 1 min at 300 × g, and incubated at 37°C, 5% CO_2 for 5 to 6 h before being fixed in a 2% PBS-formaldehyde solution. Infected cells were identified by intracellular staining for HIV-1 p24 as described above. Samples were acquired on an LSRII cytometer (BD Biosciences) and data analysis was performed using FlowJo vX.0.7 (Tree Star). The percentage of direct killing was calculated with the following formula: (% of $p24^+$ cells in Targets) − (% of $p24^+$ cells in Targets plus Effectors) / (% of $p24^+$ cells in Targets) by gating on infected lived target cells.

FACS-based ADCC assay

Measurement of ADCC using a FACS-based assay was performed at 48h post-infection as previously described (1). Briefly, infected primary $CD4^+$ T cells were stained with viability dye (AquaVivid; ThermoFisher Scientific) and cell proliferation dye (eFluor670; eBioscience) and used as target cells. Autologous PBMC effectors cells, stained with another cellular marker (cell proliferation dye eFluor450; eBioscience), were added at an effector: target ratio of 10:1 in 96-well V-bottom plates (Corning, Corning, NY). ADCC-mediating mAb 3BNC117 (0.5 µg/ml) was added to appropriate wells and cells were incubated for 15 min at room temperature. The plates were subsequently centrifuged for 1 min at 300 × g, and incubated at 37°C, 5% CO_2 for 5 to 6 h before being fixed in a 2% PBS-formaldehyde solution. Infected cells were identified by intracellular staining for HIV-1 p24 as described above. Alternatively, effector cells were

preincubated in the presence of anti-NTB-A and anti-DNAM-1 antibodies or their matched IgG isotype control (10 μg/mL) prior being incubated with target cells for blockade experiments. Samples were acquired on an LSRII cytometer (BD Biosciences) and data analysis was performed using FlowJo vX.0.7 (Tree Star). The percentage of ADCC was calculated with the following formula: (% of $p24^+$ cells in Targets plus Effectors) − (% of $p24^+$ cells in Targets plus Effectors plus Abs) / (% of $p24^+$ cells in Targets) by gating on infected lived target cells.

5.2.12 SUPPLEMENTAL REFERENCES

1. Richard J, Veillette M, Brassard N, Iyer SS, Roger M, Martin L, et al. CD4 mimetics sensitize HIV-1-infected cells to ADCC. Proc Natl Acad Sci U S A. 2015;112(20):E2687-94.

5.2.13 SUPPLEMENTAL FIGURES

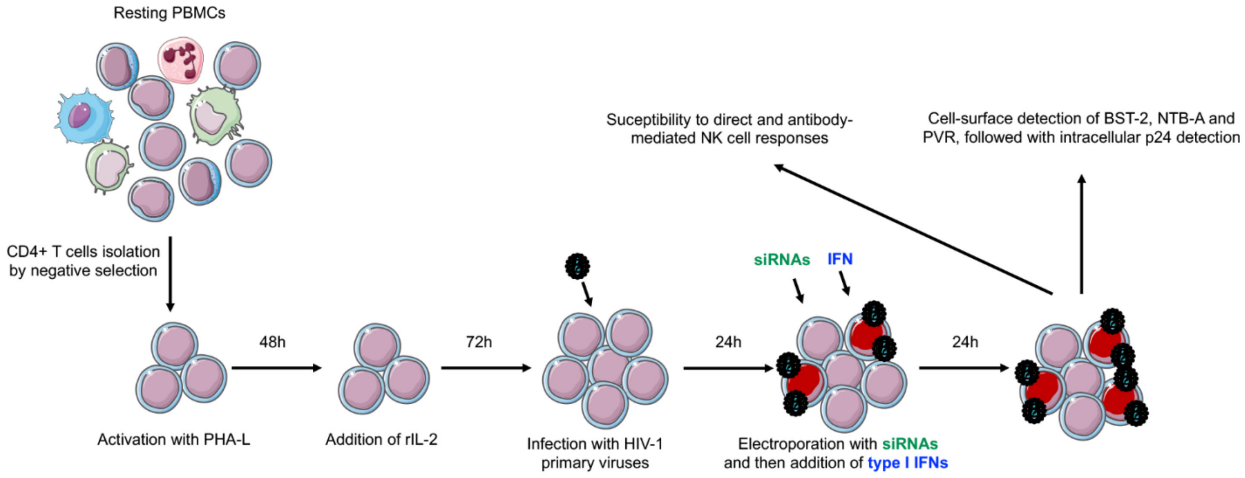

Figure 5.1.S1 - Experimental procedures.
$CD4^+$ T lymphocytes were purified from resting PBMCs by negative selection using immunomagnetic beads. Purified $CD4^+$ T cells were activated with phytohemagglutinin-L (PHA-L) (10 µg/ mL) for 48 hours and then maintained in RPMI 1640 complete medium supplemented with rIL-2 (100 U/mL) for 72 hours. Activated $CD4^+$ T cells were then infected with VSV-G pseudotyped HIV-1 primary viruses by spin-infection. Twenty hours post-infection, infected cells were electroporated with selected siRNAs prior treatment with type I IFNs. Forty-eight hours post-infection, the susceptibility of infected cells to NK cells responses, as well as cell-surface levels of BST-2, NTB-A and PVR were assessed by flow cytometry.

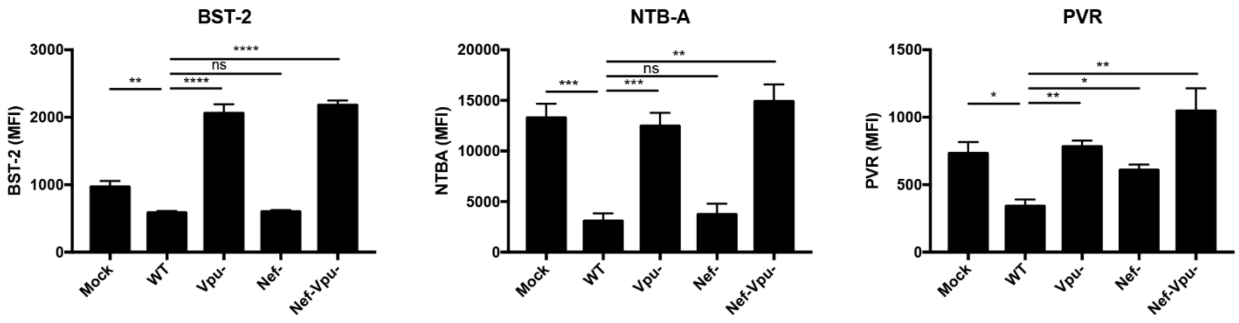

Figure 5.1.S2 - Role of Vpu and Nef in HIV-1-mediated downregulation of cell-surface BST-2, NTB-A and PVR.

Primary $CD4^+$ T cells were infected with CH58 T/F WT or variants defective for Nef and/or Vpu expression. Forty-eight hours post-infection, cells were stained with anti-BST-2, anti-NTBA or anti-PVR Abs, followed with appropriate secondary Abs. The graphs shown represent the median fluorescence intensities (MFI) detected on $p24^-$ cells for mock-infected cells and the infected population ($p24^+$) for HIV-1-infected cells. Statistical significance was tested using unpaired t test (*, $P < 0.05$, **, $P < 0.01$, ***, $P < 0.001$, ****, $P < 0.0001$, ns: non-significant).

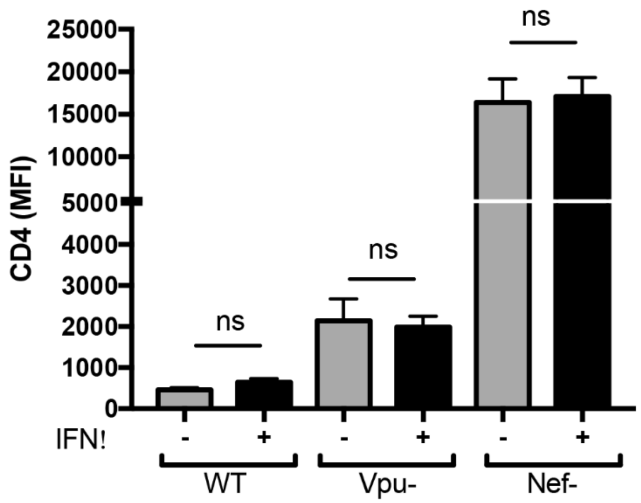

Figure 5.1.S3 - Effect of IFN-β on cell-surface CD4 levels.
Primary $CD4^+$ T cells were infected with CH58 T/F, either WT or defective for Vpu or Nef expression. Twenty-four hours post-infection, infected cells were either mock-treated or treated for 24h with IFN-β. Forty-eight hours post-infection, cells were stained with anti-CD4 Abs, followed with appropriate secondary Abs. The graphs shown represent median fluorescence intensities detected on the p24+ population. Error bars indicate means +/- SEM. Statistical significance was tested using unpaired t test or Mann-Whitney test based on parametric test (ns: non-significant).

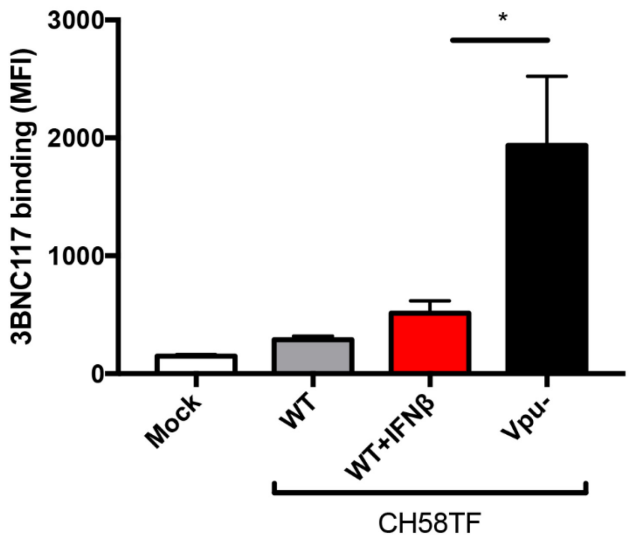

Figure 5.1.S4 - Recognition of HIV-1-infected cells by bNAb 3BNC117 upon treatment with IFNβ.

Primary $CD4^+$ T cells were infected with CH58 T/F WT (treated or not with IFN-β for 24h) or a variant defective for Vpu expression. Forty-eight hours post-infection, cells were stained with anti-Env bNAb 3BNC117 (0.5 μg/mL), followed with appropriate secondary Abs. Statistical significance was tested using unpaired t test (*, $P < 0.05$)

ARTICLE 9

La protéine accessoire Vpu du VIH-1 limite les fonctions effectrices des anticorps *in vivo*

HIV-1 Vpu restricts Fc-mediated effector functions in vivo

Auteurs:

Jérémie Prévost[1,2], Sai Priya Anand[1,3], Jyothi Krishnaswamy Rajashekar[4], Li Zhu[4], Jonathan Richard[1,2], Guillaume Goyette[1], Halima Medjahed[1], Gabrielle Gendron-Lepage[1], Hung-Ching Chen[5], Yaozong Chen[6], Joshua A. Horwitz[7,17], Michael W. Grunst[4], Susan Zolla-Pazner[8], Barton F. Haynes[9,10], Dennis R. Burton[11,12,13], Richard A. Flavell[14], Frank Kirchhoff[15], Beatrice H. Hahn[16], Amos B. Smith III[5], Marzena Pazgier[6], Michel C. Nussenzweig[7], Priti Kumar[4], Andrés Finzi[1,2,3]

Affiliations:

[1]Centre de Recherche du CHUM, Montreal, QC, Canada; [2]Département de Microbiologie, Infectiologie et Immunologie, Université de Montréal, Montreal, QC, Canada; [3]Department of Microbiology and Immunology, McGill University, Montreal, QC, Canada; [4]Department of Internal Medicine, Yale University School of Medicine, New Haven, CT, USA; [5]Department of Chemistry, University of Pennsylvania, Philadelphia, PA, USA; [6]Infectious Diseases Division, Department of Medicine, Uniformed Services University of the Health Sciences, Bethesda, MD, USA; [7]Laboratory of Molecular Immunology, The Rockefeller University, New York, NY, USA; [8]Department of Medicine, Division of Infectious Diseases, Icahn School of Medicine at Mount Sinai, New York, NY, USA; [9]Duke Human Vaccine Institute, Departments of Medicine and Immunology, Duke University School of Medicine, Durham, NC, USA; [10]Consortium for HIV/AIDS Vaccine Development (CHAVD), Duke University, Durham, NC, USA; [11]Department of Immunology and Microbiology, The Scripps Research Institute, La Jolla, CA, USA; [12]Consortium for HIV/AIDS Vaccine Development (CHAVD), The Scripps Research Institute, La Jolla, CA, USA; [13]Ragon Institute of Massachusetts General Hospital, Massachusetts Institute of Technology, Harvard University, Cambridge, MA, USA; [14]Department of Immunobiology, Yale University School of Medicine, New Haven, CT, USA; [15]Institute of Molecular Virology, Ulm University Medical Center, Ulm, Germany; [16]Departments of Medicine and Microbiology, Perelman School of Medicine, University of Pennsylvania, Philadelphia, PA, USA; [17]Current affiliation: Molecular Biology & Virology Group, PureTech Health LLC, Boston, MA, USA.

Contribution des auteurs:

Conceptualisation: **J.P.** et A.F.; Méthodologie: **J.P.**, J.K.R., P.K. et A.F.; Recherche: **J.P.**, S.P.A., J.K.R., L.Z., J.R., Y.C. et M.W.G.; Ressources: **J.P.**, G.G., H.M., G.G.-L., H.-C.C., J.A.H., S.Z.-P., B.F.H., D.R.B., R.A.F., F.K., B.H.H., A.B.S., M.P., M.C.N., P.K. et A.F.; Analyse formelle: **J.P.**; Visualisation: **J.P.**; Supervision: A.B.S., M.P., M.C.N., P.K. et A.F.; Obtention du financement: A.B.S., M.P., P.K. et A.F.; Rédaction - version originale: **J.P.**, B.H.H. et A.F.; Rédaction - révision et edition: **Tous les auteurs**.

Statut: Cet article a été publié dans *Cell Reports*, le 8 novembre 2022.
https://doi.org/10.1016/j.celrep.2022.111624

5.3.1 RÉSUMÉ

Les anticorps non-neutralisants (nnAbs) peuvent éliminer les cellules infectées par le VIH-1 par le biais de la réponse cytotoxique cellulaire dépendante des anticorps (ADCC) et ont été identifiés comme un corrélat de protection dans l'essai vaccinal RV144. Il a récemment été démontré que les fonctions effectrices médiées par les nnAbs peuvent altérer le cours de l'infection par le VIH-1 *in vivo* lorsqu'utilisés contre un virus défectif pour l'expression de la protéine accessoire Vpu. Vpu étant connu pour réguler à la baisse le CD4 à la surface des cellules infectées et que CD4 peut déclencher des changements de conformation de la glycoprotéine de l'enveloppe virale (Env), nous nous sommes demandé si l'absence d'expression de Vpu était liée à l'activité antivirale observée médiée par les nnAbs. Nous avons constaté que la restauration de l'expression de Vpu réduit considérablement la reconnaissance des nnAbs par les cellules infectées, les rendant ainsi résistantes à la réponse ADCC. De plus, l'administration de nnAbs à des souris humanisées réduit la charge virale uniquement chez les animaux infectés par un virus déficient pour Vpu, mais pas par un virus de type sauvage. L'administration de mimétiques moléculaires de CD4, connus pour "ouvrir" Env et exposer les épitopes des nnAbs, rend les virus de type sauvage sensibles aux fonctions effectrices des nnAbs. Enfin, les fonctions effectrices Fc-dépendantes des nnAbs sont observées uniquement sur les cellules exprimant Env dans la conformation "ouverte". Ce travail souligne l'importance de l'évasion de la réponse humorale par Vpu.

5.3.2 ABSTRACT

Non-neutralizing antibodies (nnAbs) can eliminate HIV-1-infected cells via antibody-dependent cellular cytotoxicity (ADCC) and were identified as a correlate of protection in the RV144 vaccine trial. Fc-mediated effector functions of nnAbs were recently shown to alter the course of HIV-1 infection *in vivo* using a *vpu*-defective virus. Since Vpu is known to downregulate cell surface CD4, which triggers conformational changes in the viral envelope glycoprotein (Env), we ask whether the lack of Vpu expression was linked to the observed nnAbs activity. We found that restoring Vpu expression greatly reduces nnAb recognition of infected cells, rendering them resistant to ADCC responses. Moreover, administration of nnAbs in humanized mice reduces viral loads only in animals infected with a *vpu*-defective but not with a wildtype virus.CD4-mimetics administration, known to “open” Env and expose nnAb epitopes, renders wildtype viruses

sensitive to nnAbs Fc-effector functions. This work highlights the importance of Vpu-mediated evasion of humoral responses.

5.3.3 INTRODUCTION

Human immunodeficiency virus type 1 (HIV-1) envelope glycoproteins (Env) mediate viral entry into target cells. Env is synthesized as a trimeric gp160 precursor, which is further cleaved into two subunits linked by non-covalent bonds: the exterior gp120 and the transmembrane gp41 subunits (Earl et al., 1990; Freed et al., 1989; McCune et al., 1988). During the entry process, the gp120 subunit sequentially interacts with the CD4 surface molecule as well as one of its co-receptors (CCR5 or CXCR4) (Kwong et al., 1998; Shaik et al., 2019; Wu et al., 2010a), allowing the gp41 subunit to mediate fusion between the viral and target cell lipid membranes (Chan et al., 1997; Weissenhorn et al., 1997). Since Env is the sole viral antigen exposed at the surface of virions and infected cells, it represents the main target for humoral responses. Fusion-competent Env trimers can sample different conformations. Broadly neutralizing antibodies (bNAbs) mainly recognize the pre-fusion "closed" conformation (Li et al., 2020; Lu et al., 2019; Munro et al., 2014; Stadtmueller et al., 2018), while non-neutralizing antibodies (nnAbs) mainly bind to "open" CD4-bound conformations (Alsahafi et al., 2019; Jette et al., 2021; Munro et al., 2014; Yang et al., 2019). Primary difficult-to-neutralize HIV-1 isolates favor the pre-fusion “closed” conformation, thus exposing Env regions that are heavily glycan shielded (Doores, 2015; Lee et al., 2016; Li et al., 2020).

Since antiretroviral therapy (ART) is unable to eradicate HIV-1 reservoirs, monotherapy or combination of bNAbs targeting the CD4-binding site (3BNC117, VRC01, VRC07-523), the V3 glycan supersite (10-1074, PGT121) and the V2 apex (PGDM1400) are currently under investigation in multiple clinical trials as therapeutic agents to reduce or eliminate cellular reservoirs through Fc-mediated effector functions (NCT02140255, NCT03837756, NCT04319367, NCT03721510). Thus far, results have shown that bNAbs can control HIV-1 viremia and delay viral rebound upon treatment interruption in HIV-1 infected individuals (Bar et al., 2016; Caskey et al., 2015; Caskey et al., 2017; Lynch et al., 2015; Scheid et al., 2016). Similar outcomes were also observed in non-human primates (NHP) and humanized mice (Barouch et al., 2013; Bolton et al., 2016; Freund et al., 2017; Halper-Stromberg et al., 2014; Hessell et al., 2016;

Horwitz et al., 2013; Klein et al., 2012; Nishimura et al., 2017; Parsons et al., 2019; Schommers et al., 2020; Schoofs et al., 2019; Shingai et al., 2013). *In vivo* studies in animal models have demonstrated that Fc-mediated effector functions are required for the optimal therapeutic activity of bNAbs (Asokan et al., 2020; Bournazos et al., 2014; Halper-Stromberg et al., 2014; Lu et al., 2016; Wang et al., 2020). However, bNAbs rarely arise during natural infection and have yet to be consistently elicited by vaccination (Landais and Moore, 2018; Pauthner et al., 2019).

Given the difficulty of eliciting bNAbs *in vivo*, nnAbs have been evaluated as a potential alternative. nnAbs represent the majority of antibodies in the plasma of HIV-1-infected individuals and are easily elicited by vaccination (Beaudoin-Bussieres et al., 2020; Davis et al., 2009; Decker et al., 2005; Madani et al., 2016; Madani et al., 2018; Tomaras and Haynes, 2009; Tomaras et al., 2008; Visciano et al., 2019). Despite poor neutralization capacity, nnAbs can mediate other functions, such as the elimination of HIV-1-infected cells by antibody-dependent cellular cytotoxicity (ADCC) or antibody-dependent cellular phagocytosis (ADCP). Among these functions, ADCC was associated with the protection observed in the RV144 vaccine trial (Haynes et al., 2012a; Rerks-Ngarm et al., 2009). Thus, several studies have examined the antiviral effects of nnAbs in non-human primates and humanized mice. These included prophylactic administration of nnAbs targeting the CD4-binding site (b6), the V3 loop (KD-247, 2219), the V1V2 region (830A, 2158), the gp120 cluster A (A32) and the gp41 immunodominant region (246D, 4B3, F240, 7B2). The results from these studies showed a reduction in the number of transmitted/founder (T/F) viruses and/or plasma viral loads after challenge with lab-adapted tier 1 viruses (Burton et al., 2011; Eda et al., 2006; Hessell et al., 2018; Hioe et al., 2022; Moog et al., 2014; Santra et al., 2015). Finally, therapeutic administration of large quantities of the monoclonal anti-gp41 246D nnAb to humanized mice infected with a *vpu*-deleted tier 2 HIV-1 molecular clone (HIV-$1_{NL4/3}$YU2) led to the elimination of infected cells and selected for escape mutations that stabilized Env "closed" conformation in an Fc-dependent manner, suggesting a protective effect (Horwitz et al., 2017). However, other studies administrating a cocktail of nnAbs (A32 and 17b) to humanized mice infected with a wild-type tier 2 HIV-1 strain (JR-CSF) had no impact on viral replication, except when combined with a small CD4 mimetic compound (CD4mc) that "open-up" the trimer and expose these otherwise occluded epitopes (Rajashekar et al., 2021).

Differences between the various nnAb studies could be attributed to the specificity of the antibodies (anti-gp41 vs anti-gp120), the humanized mouse model used or specific viral determinants. In particular, certain studies were conducted using an infectious molecular clone (IMC) of HIV-1 that expressed a tier 2 Env (YU2) lacked a functional Vpu (HIV-$1_{NL4/3}$YU2). However, Vpu plays an important role in downregulating cell surface CD4, which can bind and trigger conformational changes in the viral Env, therefore exposing vulnerable epitopes (Prevost et al., 2022; Veillette et al., 2015; Veillette et al., 2014). We thus asked whether the lack of a functional Vpu was responsible for the observed nnAbs activity by comparing isogenic viruses that differed solely in Vpu expression. Importantly, we tested the influence of Vpu expression on nnAb function not only *in vitro* but also in humanized mice. We found that anti-gp41 246D nnAb mediates potent ADCC responses against HIV-$1_{NL4/3}$YU2, but not its Vpu+ counterpart. Accordingly, 246D was found to alter viral replication *in vivo* only in absence of Vpu. These data thus provide conclusive evidence that Vpu allows HIV-1 to evade humoral responses *in vivo* and emphasizes the need to use fully functional IMCs to assess nnAb Fc-mediated effector functions.

5.3.4 RESULTS

Elicitation of anti-gp41 non-neutralizing antibodies following HIV-1-infection.

First, we characterized the susceptibility of the HIV-$1_{NL4/3}$YU2 IMC to nnAbs-mediated Fc-effector responses to confirm previous observations (Horwitz et al., 2017). To do so, we used plasma samples from a cross-sectional cohort of 50 HIV-1-infected individuals (HIV^+ plasma) which were grouped according to the inferred time post-infection and ART treatment (**Table 5.2.S1**). The nnAbs present in the HIV^+ plasma from this cohort were previously shown to mediate potent ADCC responses against infected cells presenting Env in the "open" CD4-bound conformation (Ding et al., 2016a; Richard et al., 2015; Veillette et al., 2015). We infected primary $CD4^+$ T cells with the HIV-$1_{NL4/3}$YU2 IMC and evaluated the ability of HIV^+ plasma to recognize and eliminate infected cells. Consistent with its susceptibility to nnAbs, HIV-$1_{NL4/3}$YU2-infected primary $CD4^+$ T cells were efficiently recognized (**Figure 5.2.1A**) and susceptible to ADCC (**Figure 5.2.1B**) mediated by all the tested plasma samples, with a significant increase of activity starting six months post-infection. Similar levels of activity were also present in plasma from ART-treated individuals (**Figure 5.2.1A-B**).

Since the HIV-$1_{NL4/3}$YU2 IMC has been reported to be sensitive to anti-gp41 Fc-mediated antiviral activity *in vivo* (Horwitz et al., 2017), we evaluated the contribution of anti-gp41 nnAbs present in HIV^+ plasma to infected-cell recognition and ADCC activity by performing binding competition experiments (**Figure 5.2.1C-D**). We focused on two main classes of anti-gp41 nnAbs based on observations from previous studies showing potent ADCC responses (Ding et al., 2016a; Gohain et al., 2016; Moog et al., 2014; Santra et al., 2015; Sojar et al., 2019; von Bredow et al., 2016; Williams et al., 2019; Yang et al., 2018): the anti-cluster II Abs targeting the heptad repeat region 2 (HR2) (Frey et al., 2010) and anti-cluster I Abs targeting the disulfide loop region (C-C loop) (Gohain et al., 2016; Santra et al., 2015) (**Figure 5.2.S1A**). Anti-gp41 cluster II nnAbs, inferred from binding competition experiments using the prototypic anti-cluster II 2.2B nnAb, were elicited in the acute phase of the infection (within 90 days) (**Figure 5.2.1C**). Elicitation of anti-gp41 cluster I nnAbs appears to take more time as revealed in binding competition experiments using the prototypic F240 anti-cluster I nnAb. While some competition with F240 binding was observed within the first three months post-infection, it culminates in the chronic phase of the infection (more than 2 years) (**Figure 5.2.1D**). In agreement with previous studies showing potent ADCC activity by anti-cluster I gp41 monoclonal Abs (Ding et al., 2016a; Gohain et al., 2016; Moog et al., 2014; Santra et al., 2015; von Bredow et al., 2016; Williams et al., 2019), we observed that blockade with anti-cluster I gp41 F240 Fab fragment significantly decreased plasma binding, FcγRIIIa engagement and ADCC responses against HIV-$1_{NL4/3}$YU2 infected cells (**Figure 5.2.1E-G**).

Vpu protects HIV-1-infected cells from recognition and Fc-effector functions mediated by anti-Env antibodies *in vitro* and *ex vivo*.

Since the HIV-$1_{NL4/3}$YU2 does not express the accessory protein Vpu due to a mutation in the start codon of the *vpu* gene (Horwitz et al., 2017), we asked whether the efficient recognition and ADCC-mediated elimination of HIV-$1_{NL4/3}$YU2 infected primary $CD4^+$ T cells by nnAbs was linked to the lack of Vpu expression by this IMC. We restored the *vpu* open reading frame (ORF, **Figure 5.2.2A**) and infected primary $CD4^+$ T cells using both Vpu-negative (Vpu-) and Vpu-positive (Vpu+) constructs. Using a recently developed FACS-based intracellular staining method (Prevost et al., 2022), we confirmed Vpu expression upon restoration of the *vpu* ORF (**Figure 5.2.2B**). We also confirmed by intracellular staining the equivalent expression of Nef in both IMCs

(**Figure 5.2.2B**). Vpu efficiently downregulated cell-surface CD4 and BST-2 (**Figure 5.2.2C**). We also measured cell surface expression of NTB-A and PVR, which were shown to modulate ADCC responses against HIV-1-infected cells (Prevost et al., 2019) and are downregulated by Vpu (Matusali et al., 2012; Shah et al., 2010). As expected, Vpu expression significantly downregulated their expression from the surface of primary $CD4^+$ T cells from five different healthy individuals (**Figure 5.2.2D-E**).

We next evaluated the effect of Vpu on the recognition and elimination of infected cells by nnAbs. Consistent with the observed downmodulation of CD4 and BST-2, Vpu expression strongly reduced the recognition of infected cells by monoclonal antibodies (mAb) targeting the anti-gp41 cluster I (246D), the gp120 cluster A (A32) or by polyclonal HIV+ plasma (**Figure 5.2.3A**). We extended these results to a panel of 27 nnAbs and 10 HIV+ plasma which yielded the same results (**Figure 5.2.3B-C**). As a measure of this panel of nnAbs to mediate Fc-effector functions, we examined their ability to interact with a soluble dimeric FcγRIIIa protein. This recombinant protein is used as a surrogate of FcγR clustering which is required to trigger Fc-effector functions (Anand et al., 2019; Wines et al., 2017; Wines et al., 2016). Consistent with a significant reduction in the recognition of infected cells by nnAbs, we observed that Vpu expression diminished the ability of all mAbs and HIV+ plasma to engage with FcγRIIIa (**Figure 5.2.3D-E**) and to mediate ADCC (**Figure 5.2.3F-G**). We noted that nnAbs targeting the gp41 were more potent at engaging soluble dimeric FcγRIIIa and mediating ADCC against cells infected with the vpu-defective IMC than the panel of anti-gp120 nnAbs tested (**Figure 5.2.S2A-C**).

Vpu facilitates viral release by downregulating the restriction factor BST-2 (Neil et al., 2008; Van Damme et al., 2008). Multiple studies have shown that this activity decreases the overall amount of Env at the cell surface, consequently decreasing the susceptibility of infected cells to ADCC (Alvarez et al., 2014; Arias et al., 2014; Pham et al., 2016; Richard et al., 2017; Veillette et al., 2014). Since the *vpu*-defective HIV-$1_{NL4/3}$YU2 was used to evaluate the *in vivo* activity of several bNAbs (Bournazos et al., 2016; Bournazos et al., 2014; Diskin et al., 2013; Freund et al., 2015; Freund et al., 2017; Halper-Stromberg et al., 2014; Horwitz et al., 2013; Klein et al., 2012; Klein et al., 2014; Lu et al., 2016; Schommers et al., 2020; Schoofs et al., 2019; Vanshylla et al., 2021), we tested whether their binding to infected cells was also influenced by Vpu expression.

Consistent with decreased Env expression on cells infected with a Vpu+ virus, we observed a significant reduction in CD4-binding site (3BNC117), V3 glycan (10-1074) and V2-apex (PG16) bNAb binding (**Figure 5.2.4A**). The phenotype was validated using a panel of 35 bNAbs targeting different epitopes, indicative of an overall reduction of cell-surface Env expression in the presence of a functional Vpu (**Figure 5.2.4B-C**). Accordingly, infected cells were significantly less susceptible to bNAbs-mediated Fc-effector functions (**Figure 5.2.4D-G**). Among the different classes of bNAbs, antibodies targeting the V3 glycan supersite, the CD4-binding site and the V2 apex demonstrated stronger ADCC-mediated killing of cells infected with the *vpu*-defective HIV-$1_{NL4/3}$YU2, compared with antibodies known to interact with the gp120 silent face, the gp120-gp41 interface or the gp41 membrane-proximal external region (MPER), despite similar levels of Env recognition (**Figure 5.2.S2D-F**). These findings support previous observations indicating that in addition to Env recognition, the angle of approach of the antibody is important to mediate ADCC as it modulates the exposure of the Fc region required to activate effector cells (Acharya et al., 2014; Tolbert et al., 2020).

Since all coding regions of the HIV-$1_{NL4/3}$YU2 IMC other than the env gene are derived from a lab-adapted proviral backbone, we wished to test unmodified HIV-1 primary isolates. Primary $CD4^+$ T cells were infected with a panel of 13 infectious molecular clones coding for Vpu or not. This panel includes transmitted/founder (T/F) viruses, molecular clones derived during chronic infection, and IMCs from lab-adapted strains as controls (**Figure 5.2.5A-B**). Vpu expression consistently reduced nnAbs (246D and M785U3) and bNAbs (3BNC117 and 10-1074) recognition of infected cells, which in turn protected infected cells from ADCC responses mediated by all antibodies tested (**Figure 5.2.5A-B**). Env polymorphisms present in CH167 (E460), REJO (N334) and CH293 (T332, N334) viruses abrogated the capacity of bNAbs 3BNC117 or 10-1074 to recognize infected cells. Of note, while Vpu expression has a profound effect in the recognition of infected cells by all tested anti-Env antibodies, it did not affect their neutralization profile (**Figure 5.2.S1B-C**).

To extend our observations to a more physiological model, we expanded patient-derived infected CD4+ T cells. Briefly, we isolated and activated primary $CD4^+$ T cells from five ART-treated HIV-1-infected individuals. Viral replication upon reactivation was monitored by

intracellular p24 staining and flow cytometry (**Figure 5.2.5C**). These endogenously-infected cells were protected from Fc-mediated effector functions mediated by nnAb 246D but remained susceptible to bNAb PGT121 (**Figure 5.2.5C**), in agreement with our in vitro results generated using a Vpu+ IMC (**Figure 5.2.5A-B**).

Vpu expression limits the antiviral activity of the 246D antibody in HIV-1-infected humanized mice.

To determine the impact of Vpu expression on 246D antiviral activities *in vivo*, we infected SRG-15 (SIRPA$^{h/m}$ Rag2$^{-/-}$ Il2rg$^{-/-}$ IL15$^{h/m}$) humanized mice (hu-mice) with HIV-1$_{NL4/3}$YU2 or its *vpu*-competent counterpart. Similar to a previously used humanized mouse model (Horwitz et al., 2017), this hu-mice model supports HIV-1 replication and Fc-effector functions *in vivo* (Herndler-Brandstetter et al., 2017; Rajashekar et al., 2021). Immunodeficient mice engrafted with human peripheral blood lymphocytes (hu-PBL) were infected intraperitoneally (I.P.) with 30,000 plaque-forming units (PFU) of either virus (**Figure 5.2.6A**). Half of each cohort received subcutaneous (S.C.) injections of the 246D nnAb at days 2, 4 and 6 post-infection. Infected humanized mice were then monitored for plasma viral loads (PVLs). Both viruses replicated efficiently in SRG-15 hu-PBL mice, reaching on average 1×10^7 viral RNA copies/mL of plasma at 3 days post-infection (P.I.) (**Figure 5.2.6B**). While PVLs in mice infected with HIV-1$_{NL4/3}$YU2 stabilized after day 3, infection with the Vpu+ variant further increased PVLs to 3.5×10^7 copies/mL by day 10. A single administration of the 246D nnAb at day 2 resulted in a significant reduction in PVLs (~36-fold decrease) in hu-mice infected with the vpu-defective virus but not significantly in those infected with the *vpu*-competent virus (**Figure 5.2.6B**). 246D maximal inhibitory effect (~85-fold reduction) was reached 10 days post-infection with the vpu-defective virus. At the end of the experiment (day 11), 246D treatment induced on average a 41-fold decrease in PVLs in mice infected with the *vpu*-defective virus but no difference in hu-mice infected with the Vpu+ virus. These results highlight the role played by Vpu in promoting viral replication in presence of nnAbs.

Harnessing non-neutralizing antibody Fc-effector functions by improving epitope exposure and FcγRIIIa interaction.

Enhancing the affinity of the Fc fragment of antibodies for FcγRs was shown to increase Fc-effector functions of bNAbs in HIV-1-infected humanized mice (Bournazos et al., 2014; Wang

et al., 2020). To evaluate if this strategy could apply to nnAbs, we introduced well-characterized IgG1 Fc mutations in the 246D heavy chain to modulate its interaction with FcγRs. The GRLR mutations (G236R/L328R) and the GASDALIE mutations (G236A/S239D/A330L/I332E) are respectively known to decrease and increase the affinity for activating FcγRs (Bournazos et al., 2014; Horton et al., 2010; Smith et al., 2012). To characterize these Fc variants, primary $CD4^+$ T cells were infected with the HIV-$1_{NL4/3}$YU2 constructs expressing Vpu or not. As expected, Fc modifications did not alter the ability of 246D to recognize infected cells, but it modulated the interaction with the soluble dimeric FcγR probe, with the GRLR mutations abrogating FcγRIIIa binding and the GASDALIE mutations improving it (**Figure 5.2.7A-B**). Introduction of the GASDALIE mutations enhanced ADCC against cells infected with the *vpu*-defective virus. Interestingly, it also allowed 246D to mediate ADCC against cells infected with the Vpu+ IMC, while the unaltered native 246D failed to do so (**Figure 5.2.7C**). To evaluate if the 246D GASDALIE was able to mediate ADCC against cells infected with a primary isolate, we infected primary $CD4^+$ T cells with the transmitted/founder virus CH058, a strain shown to be resistant to 246D-mediated ADCC responses (**Figure 5.2.5B**). CH058-infected cells were poorly recognized by 246D and resistant to ADCC mediated by all 246D Fc variants tested, including 246D GASDALIE (**Figure 5.2.S4**). Consistent with the role of Nef and Vpu in preventing the exposure of epitopes recognized by nnAbs, disruption of the expression of both accessory proteins enhanced recognition and ADCC susceptibility of infected cells by 246D (**Figure 5.2.S4**). These results agree with the requirement of Env-CD4 interaction to expose the gp41 cluster I region. 246D recognizes with picomolar affinity a highly conserved linear peptide (^{596}WGCSGKLICTT^{606}) which corresponds to the gp41 C-C loop, located between HR1 and HR2 helices (**Figure 5.2.S3A-C**). This epitope is occluded in the "closed" Env trimer structure but can be exposed upon CD4-triggered conformational changes (**Figure 5.2.S3D-E**).

While it is becoming increasingly clear that HIV-1 successfully evades nnAbs responses by keeping its Env in a "closed" conformation (Bruel et al., 2017; Dufloo et al., 2020; Veillette et al., 2015; Veillette et al., 2014; von Bredow et al., 2016), new strategies are currently being tested to harness their potential antiviral activity. Small CD4 mimetic compounds have been optimized to "open up" Env trimers, therefore exposing otherwise occluded epitopes recognized by nnAbs (Ding et al., 2019b; Fritschi et al., 2021; Jette et al., 2021; Laumaea et al., 2020; Melillo et al.,

2016). Using this strategy, CD4mc were shown to synergize with monoclonal CD4i Abs or nnAbs found in plasma from infected individuals to eliminate HIV-1-infected cells *in vitro*, *ex vivo* and *in vivo* in humanized mice (Alsahafi et al., 2019; Anand et al., 2019; Ding et al., 2016b; Lee et al., 2015; Madani et al., 2018; Prevost et al., 2020b; Rajashekar et al., 2021; Richard et al., 2016; Richard et al., 2017; Richard et al., 2015). Since 246D was unable to efficiently recognize cells infected with a Vpu+ virus, we combined it with the CD4mc BNM-III-170, which greatly improved its capacity to bind to cells infected with HIV-$1_{NL4/3}$YU2 Vpu+ or the primary isolate CH058 (**Figure 5.2.7A and 5.2.S4A**). Accordingly, FcγRIIIa engagement and ADCC responses against WT-infected cells were significantly enhanced upon CD4mc addition (**Figure 5.2.7B-C and 5.2.S4B-C**). Given these observations, we investigated whether CD4mc and Fc modifications could improve the ability of 246D to alter HIV-1 WT replication *in vivo*. To do so, NSG-15 humanized mice engrafted with hu-PBL were infected with HIV-$1_{NL4/3}$YU2 Vpu+ and were administered with 246D nnAb alongside or without CD4mc BNM-III-170 at day 3, 5 and 7 post-infection (**Figure 5.2.7D**). In line with the data obtained *in vitro* (**Figure 5.2.7A-C**), we observed that co-administration of BNM-III-170 with 246D WT or GASDALIE considerably reduced PVLs at day 7 (18-fold and 219-fold, respectively), as compared to the antibody alone (**Figure 5.2.7E-F**). In both cases, treatment interruption led to a significant increase of PVLs in the following days. To evaluate the contribution of Fc-effector functions to this phenotype, infected humanized mice were co-administered with BNM-III-170 and 246D Fc variants (WT, GRLR or GASDALIE). At day 7 post-infection, PVLs were 15-fold higher in presence of 246D GRLR and 6-fold lower in presence of 246D GASDALIE, as compared to 246D WT, confirming the primordial role of Fc-effector functions in limiting HIV-1 replication in presence of nnAbs and CD4mc (**Figure 5.2.7G**). Altogether, our results indicate that Fc-effector functions mediated by nnAbs *in vivo* are limited by the occluded nature of their epitopes.

5.3.5 DISCUSSION

The HIV-1 accessory protein Vpu is a multi-functional protein that promotes viral replication by interfering with the intracellular trafficking of various host proteins (Dube et al., 2010). CD4 and BST-2 downregulation by Vpu was shown to increase viral release in cell culture systems (Bour et al., 1999; Neil et al., 2008; Van Damme et al., 2008). Humanized mouse models of acute HIV-1 infection using HIV-1-infected humanized mice confirmed the role of Vpu in

promoting viral replication in the initial phase of infection (Dave et al., 2013; Sato et al., 2012; Yamada et al., 2018). Similarly, chronic infection of NHPs with SHIV constructs encoding a defective or mutated vpu gene were found to be less pathogenic and exhibit lower viral loads (Hout et al., 2005; Shingai et al., 2011). In these in vivo studies, elevated viral loads were linked to Vpu-mediated CD4 and BST-2 downregulation, but the potential contribution of nnAbs to PVLs were not addressed. Beyond its effect on viral release, Vpu protects HIV-1-infected cells from nnAbs-mediated ADCC responses by limiting the presence of Env-CD4 complexes at the plasma membrane (Prevost et al., 2022; Veillette et al., 2015; Veillette et al., 2014). Here, we show that Vpu expression enhances HIV-1 viral replication *in vivo* by limiting nnAbs recognition of infected cells and therefore their capacity to mediate Fc-effector functions. Beyond infected cell elimination, the absence of Vpu could also affect the level of circulating infectious viral particles. While we did not observe any changes in the neutralization by anti-gp41 nnAbs against virions produced in 293T cells in vitro (**Figure 5.2.S1B-C**), one could speculate that the capacity of nnAbs to neutralize viral particles originating from primary cells could also be altered in the absence of Vpu. Indeed, CD4 incorporation into virions has been shown to sensitize them to neutralization by various CD4i mAbs and HIV-IG (Ding et al., 2019a). While this was observed with nef-defective viruses, CD4 incorporation is also modulated by Vpu expression and this could apply to vpu-defective viruses (Levesque et al., 2003). Our results highlight the importance of carefully selecting viruses for *in vitro* and *in vivo* studies, since several widely used HIV-1 strains are defective for Vpu expression (e.g. HXB2, YU2, ADA) (Li et al., 1991; Shaw et al., 1984; Theodore et al., 1996).

Different approaches aimed at generating bNAbs by vaccination are being investigated using germline-targeting Env immunogens (Dosenovic et al., 2015; Jardine et al., 2016; Steichen et al., 2016) followed by sequential Env trimer immunization (Escolano et al., 2016; Haynes et al., 2012b; Saunders et al., 2019; Williams et al., 2017) to guide antibody maturation. However, none of these vaccine studies have yet resulted in the consistent elicitation of bNAbs. Facing the difficulty in eliciting bNAbs by vaccination, nnAbs have been studied as an alternative for vaccine development. If ADCC activity contributes to vaccine protection, as suggested in the RV144 trial (Haynes et al., 2012a), our results suggest that elicitation of nnAbs are unlikely to confer protection in vaccine settings unless strategies to "open" the Env trimer are in place. Supporting this, NHP

immunized with monomeric gp120 were completely protected from a heterologous SHIV infection if a CD4mc was combined with the challenge viral stock (Madani et al., 2018). This study showed that nnAbs elicited by the gp120 immunogen did not protect in the absence of CD4mc. In addition, it was suggested that the modest protection observed in the RV144 trial could be linked to the circulating strains in Thailand (clade CRF01_AE) which harbors Env in a more "open" conformation, while a similar vaccine trial (HVTN 702) was unsuccessful when performed in South Africa, where Env from the circulating strains (clade C) samples a more "closed" conformation (Gray et al., 2021; Prevost et al., 2017).

In this study, we selected the SRG-15 and NSG-15 humanized mouse models over other humanized mouse models because of their endogenous expression of human IL-15, which allows the development of a functional NK cell compartment (Brehm et al., 2018; Herndler-Brandstetter et al., 2017). NK cells play a central role in the ADCC responses in vitro and *in vivo*¸ and their specific depletion has been shown to abrogate the elimination of HIV-1 reservoirs by a combination of CD4mc and nnAbs in SRG-15 humanized mice (Rajashekar et al., 2021). Human IL-15 expression likely also increases HIV-1 replication by regulating the susceptibility of $CD4^+$ T cells to infection (Manganaro et al., 2018). This could explain the higher viral load peak (~10^7 copies/mL) (**Figure 5.2.6B**) compared to those achieved in the NRG humanized mice using the same HIV-$1_{NL4/3}$YU2 IMC (~10^5 copies/mL) in previous studies (Halper-Stromberg et al., 2014; Horwitz et al., 2017). We also used humanized mice as a model of HIV-1 infection since it allows the use of clinically-relevant HIV-1 isolates and does not require Env adaptation to replicate.

In addition to accessory proteins, Env conformation is a critical factor when studying nnAbs Fc-effector functions (Alsahafi et al., 2016; Ding et al., 2016a; Dufloo et al., 2020; Prevost et al., 2021; Prevost et al., 2018a; Prevost et al., 2018b; Prevost et al., 2017; Richard et al., 2015; Veillette et al., 2015; Veillette et al., 2014). Multiple studies reported significant effects of nnAbs in limiting HIV-1/SHIV replication *in vivo* using viruses coding for easy-to-neutralize tier 1 Env from lab-adapted strains, which are readily recognized by nnAbs (Burton et al., 2011; Eda et al., 2006; Hessell et al., 2018; Hioe et al., 2022; Moog et al., 2014; Santra et al., 2015). A recent study showed that tier 2 primary virus can be impacted *in vivo* by nnAbs but only when combined with CD4mc (Rajashekar et al., 2021). The combination of nnAbs or HIV+ plasma with CD4mc

significantly reduced plasma viral loads and the size of the viral reservoir in an Fc-effector functions and NK cells dependent manner (Rajashekar et al., 2021). These results emphasize the need to utilize fully functional viruses in ADCC assays to preclude Vpu-related artifacts. However, one could speculate that the development of broad-spectrum Vpu inhibitors may enhance the efficacy of nnAbs to eliminate HIV-1-infected cells (Robinson et al., 2022). Overall, our study indicates that it is unlikely for nnAbs-based immunotherapies to alter HIV-1 viral replication *in vivo* in the absence of strategies aimed at exposing the vulnerable epitopes they recognize.

5.3.6 LIMITATIONS OF THE STUDY

The humanized mice experiments were performed with only one nnAb (246D) and using a chimeric virus (HIV-$1_{NL4/3}$YU2). Further *in vivo* experiments with additional nnAbs of different epitope specificities and using clinically relevant HIV-1 primary isolates are needed to confirm our observations. Moreover, our study mainly focuses on the role of the accessory protein Vpu to evade humoral responses *in vivo* but Nef is also known to affect Env conformation at the surface of HIV-1-infected cells. Nef plays a major role in CD4 downregulation form the cell surface and we cannot rule out the possibility that Nef could also contribute to HIV-1 evasion of nnAbs responses *in vivo*, especially when using primary viruses.

5.3.7 ACKNOWLEDGMENTS

The authors thank the CRCHUM BSL3 and Flow Cytometry Platforms for technical assistance, and Mario Legault from the FRQS AIDS and Infectious Diseases network for cohort coordination and clinical samples. We thank the following collaborators for kindly providing antibodies: Julie Overbaugh (Fred Hutchinson Cancer Research Center) for QA255-006, QA255-067 and QA255-072, James Robinson (Tulane University) for 7B2, 2.2B, 12.3D, 12.4H, A32, C11 and 17b, George Lewis (University of Maryland) for M785U1, M785U2, M785U3, M785U4, N5U1, N5U2, N5U3, N10U1 and N10U2, Gunilla Karlsson Hedestam (Karolinska Institutet) for GE2-JG8, John Mascola (Vaccine Research Center, NIAID) for VRC01, VRC03, VRC07-523, VRC13, VRC16 and VRC34, Mark Connors (NIAID) for 10E8, N6 and 35O22, Florian Klein (University of Cologne) for 1-18, and the International AIDS Vaccine Initiative (IAVI) for PG9, PG16, PGT121, PGT122, PGT123, PGT125, PGT126, PGT128, PGT130, PGT135, PGT136, PGT145 and PGT151. We thank P. Mark Hogarth (Burnet Institute) for kindly providing

recombinant dimeric FcγRIIIa. The graphical abstract, Figure 5.2.6 and Figure 5.2.7 were prepared using illustrations from BioRender.com.

This study was supported by a Canadian Institutes of Health Research (CIHR) foundation grant #352417 to A.F. Funds were also provided by a CIHR Team grant #422148 to P.K. and A.F., a Canada Foundation for Innovation (CFI) grant #41027 to A.F and by the National Institutes of Health to A.F. (R01 AI148379 and R01 AI150322), to M.P. and A.F. (R01 AI129769), M.P. (AI116274) and to P.K. (R01 AI145164, R33 AI122384 and P50 AI150464 [CHEETAH]). Support for this work was also provided by P01 GM56550/AI150471 to A.B.S. and A.F. This work was partially supported by 1UM1AI164562-01, co-funded by National Heart, Lung and Blood Institute, National Institute of Diabetes and Digestive and Kidney Diseases, National Institute of Neurological Disorders and Stroke, National Institute on Drug Abuse and the National Institute of Allergy and Infectious Diseases to A.F. A.F. is the recipient of a Canada Research Chair on Retroviral Entry #RCHS0235 950-232424. F.K. is supported by the German Research Foundation (DFG CRC 1279 and SPP 1923) and the Baden-Württemberg Foundation (BWST-ISF2018-032). J.P. and S.P.A. are recipients of CIHR doctoral fellowships. M.W.G. is a recipient of the Gruber Science Fellowship. The funders had no role in study design, data collection and analysis, decision to publish, or preparation of the manuscript.

5.3.8 STAR METHODS

Table 5.2.1 - Key resources table

REAGENT or RESOURCE	SOURCE	IDENTIFIER
Antibodies		
Monoclonal anti-Env gp41 246D	NIH AIDS Reagent Program (Xu et al., 1991)	Cat# 1245
Monoclonal anti-Env gp41 246D GRLR	This paper	N/A
Monoclonal anti-Env gp41 246D GASDALIE	This paper	N/A
Monoclonal anti-Env gp41 F240	NIH AIDS Reagent Program (Cavacini et al., 1998)	Cat# 7623
Anti-Env gp41 F240 Fab fragment	(Gohain et al.,2016)	N/A
Monoclonal anti-Env gp41 240D	NIH AIDS Reagent Program (Xu et al., 1991)	Cat# 1242
Monoclonal anti-Env gp41 167D	NIH AIDS Reagent Program (Xu et al., 1991)	Cat# 11681
Monoclonal anti-Env gp41 50-69	NIH AIDS Reagent Program (Gorny et al., 1989)	Cat# 531
Monoclonal anti-Env gp41 QA255-006, QA255-067 and QA255-072	Dr Julie Overbaugh (Williams et al., 2019)	N/A
Monoclonal anti-Env gp41 7B2	NIH AIDS Reagent Program	Cat# 12556
Monoclonal anti-Env gp41 2.2B, 12.3D and 12.4H	Dr James E. Robinson	N/A
Monoclonal anti-Env gp41 M785U1, M785U2, M785U3, M785U4, N10U1, N10U2, N5U1, N5U2 and N5U3	Dr George Lewis (Ding et al., 2016a)	N/A
Monoclonal anti-Env cluster A A32	NIH AIDS Reagent Program	Cat# 11438
Monoclonal anti-Env cluster A N5i5	(Guan et al., 2013)	N/A
Monoclonal anti-Env cluster A C11	Dr James E. Robinson (Robinson JE,1992)	N/A
Monoclonal anti-Env co-receptor binding site 17b	NIH AIDS Reagent Program	Cat# 4091
Monoclonal anti-Env co-receptor binding site X5	(Huang et al., 2004)	N/A
Monoclonal anti-Env V3 loop GE2-JG8	Dr Gunilla Karlsson Hedestam (Phad et al., 2015)	N/A
Monoclonal anti-Env CD4 binding site 3BNC117	(Scheid et al.,2011)	RRID:AB_2491033
Monoclonal anti-Env CD4 binding site N49-P7	(Sajadi et al., 2018)	N/A
Monoclonal anti-Env CD4 binding site VRC01	NIH AIDS Reagent Program (Wu et al., 2010b)	Cat# 12033; RRID:AB_2491019

Monoclonal anti-Env CD4 binding site VRC03	NIH AIDS Reagent Program (Wu et al., 2010b)	Cat# 12032; RRID:AB_2491021
Monoclonal anti-Env CD4 binding site VRC07-523	Dr John Mascola (Rudicell et al., 2014)	N/A
Monoclonal anti-Env CD4 binding site VRC13 and VRC16	Dr John Mascola (Zhou et al., 2015)	N/A
Monoclonal anti-Env CD4 binding site N6	NIH AIDS Reagent Program (Huang et al., 2016)	Cat# 12968
Monoclonal anti-Env CD4 binding site NC-Cow1	(Sok et al., 2017)	RRID:AB_2687423
Monoclonal anti-Env CD4 binding site b12	NIH AIDS Reagent Program (Burton et al., 1994)	Cat# 2640; RRID:AB_2491069
Monoclonal anti-Env CD4 binding site 1-18	Dr Florian Klein (Schommers et al., 2020)	N/A
Monoclonal anti-Env CD4 binding site HJ16	NIH AIDS Reagent Program (Corti et al., 2010)	Cat# 12138; RRID:AB_2491032
Monoclonal anti-Env CD4 binding site CH106	NIH AIDS Reagent Program (Liao et al., 2013)	Cat# 12566
Monoclonal anti-Env V3 glycan PGT121, PGT122, PGT123, PGT125, PGT126, PGT128, PGT130, PGT135 and PGT136	International AIDS Vaccine Initiative (Walker et al.,2011)	RRID:AB_2491041 RRID:AB_2491042 RRID:AB_2491043 RRID:AB_2491044 RRID:AB_2491045 RRID:AB_2491047 RRID:AB_2491048 RRID:AB_2491050 RRID:AB_2491060
Monoclonal anti-Env V3 glycan BG18	(Freund et al.,2017)	N/A
Monoclonal anti-Env V3 glycan 10-1074	(Mouquet et al., 2012)	RRID:AB_2491062
Anti-Env V2 apex PGT145 monoclonal Ab	International AIDS Vaccine Initiative (Walker et al.,2011)	RRID:AB_2491054
Anti-Env V2 apex PG9 and PG16 monoclonal Ab	International AIDS Vaccine Initiative (Walker et al.,2009)	RRID:AB_2491030 RRID:AB_2491031
Anti-Env silent face SF12 monoclonal Ab	(Schoofs et al., 2019)	N/A
Monoclonal anti-Env gp120-gp41 interface PGT151	International AIDS Vaccine Initiative (Falkowska et al., 2014)	N/A
Monoclonal anti-Env gp120-gp41 interface 8ANC195	(Scheid et al.,2011)	RRID:AB_2491037
Monoclonal anti-Env gp120-gp41 interface 35O22	Dr Mark Connors (Huang et al., 2014)	N/A
Monoclonal anti-Env gp120-gp41 interface VRC34	Dr John Mascola (Kong et al., 2016)	RRID:AB_2819225

Monoclonal anti-Env gp41 MPER 10E8	NIH AIDS Reagent Program (Huang et al., 2012)	Cat# 12294; RRID:AB_2491067
Monoclonal anti-Env gp41 MPER 4E10	NIH AIDS Reagent Program(Stiegler et al., 2001)	Cat# 10091; RRID:AB_2491029
Monoclonal anti-Env gp41 MPER 2F5	NIH AIDS Reagent Program (Buchacher et al., 1994)	Cat# 1475; RRID:AB_2491015
Polyclonal Anti-HIV Immune Globulin, Pooled Inactivated Human Sera (HIV-IG)	NIH AIDS Reagent Program	Cat# 3957; RRID:AB_2890264
Mouse anti-Human CD4 clone OKT4	Thermo Fisher Scientific	Cat# 14-0048-82; RRID:AB_467075
PE-Cy7 Mouse anti-Human CD317 (BST-2) clone RS38E	Biolegend	Cat# 348416; RRID:AB_2716221
Mouse anti-human CD155 (PVR) clone SKII.4	Biolegend	Cat# 337602; RRID:AB_2300508
Mouse anti-human CD352 (NTB-A) clone NT-7	Biolegend	Cat# 317202; RRID:AB_571931
Rabbit Anti-HIV-1 Nef Polyclonal Antibody	NIH AIDS Reagent Program	Cat# 2949
Rabbit Anti-HIV-1 Vpu Polyclonal Antibody	(Prevost et al., 2020a)	N/A
Goat anti-Human IgG (H+L) Cross-Adsorbed Secondary Antibody, Alexa Fluor 647	Thermo Fisher Scientific	Cat# A21445; RRID:AB_2535862
Goat anti-Mouse IgG (H+L) Cross-Adsorbed Secondary Antibody, Alexa Fluor 647	Thermo Fisher Scientific	Cat# A21235; RRID:AB_2535804
Alexa Fluor 647 anti-Human IgG Fc Antibody	Biolegend	Cat# 409319; RRID:AB_2563329
Brilliant Violet 421 Donkey anti-Rabbit IgG (minimal x-reactivity) Antibody	Biolegend	Cat# Poly4064; RRID:AB_10643424
Goat anti-Human IgG Fc Cross-Adsorbed Secondary Antibody, HRP	Thermo Fisher Scientific	Cat# A18823; RRID:AB_2535600
Streptavidin, Alexa Fluor 647 conjugate	Thermo Fisher Scientific	Cat# S32357; RRID:AB_2336066
PE Mouse anti-HIV-1 p24 clone KC57	Beckman Coulter	Cat# 6604667; RRID:AB_1575989
APC Mouse Anti-Human CD45 Clone HI30	BD Biosciences	Cat# 561864; RRID:AB_11153499
FITC Mouse Anti-Human CD3 Clone HIT3a	BD Biosciences	Cat# 555339; RRID:AB_395745
PE Mouse Anti-Human CD8 Clone RPA-T8	Biolegend	Cat# 555367; RRID:AB_395770
PerCP Mouse Anti-human CD4 Clone RPA-T4	Biolegend	Cat# 300527; RRID:AB_893327
Biological samples		
Human PBMCs from HIV-1-infected and uninfected individuals	FRQS AIDS network and New York Blood Bank	N/A
Plasma form HIV-1-infected individuals	FRQS AIDS network	N/A
Chemicals, peptides, and recombinant proteins		
Dulbecco's modified Eagle's medium (DMEM)	Wisent	Cat# 319-005-CL

Gibco™ Roswell Park Memorial Institute 1640 medium (RPMI)	Thermo Fisher Scientific	Cat# 11875-093
Fetal bovine serum (FBS)	VWR	Cat# 97068-085
Penicillin/streptomycin	Wisent	Cat# 450-200-EL
Tris-buffered saline (TBS)	Thermo Fisher Scientific	Cat# BP24711
Bovine Serum Albumin (BSA)	BioShop	Cat# ALB001.100
Tween20	Thermo Fisher Scientific	Cat# BP337-500
Western Lightning Plus-ECL, Enhanced Chemiluminescence Substrate	Perkin Elmer Life Sciences	Cat# NEL105001EA
Phosphate buffered saline (PBS)	Wisent	Cat# 311-010-CL
Lymphocyte separation medium	Wisent	Cat# 305-010-CL
FreeStyle 293F expression medium	ThermoFisher Scientific	Cat# 12338002
ExpiFectamine 293 transfection reagent	ThermoFisher Scientific	Cat# A14525
Passive lysis buffer	Promega	Cat# E1941
Firefly D-Luciferin Free Acid	Prolume	Cat# 306
eBioscience™ Cell proliferation dye eFluor670	Thermo Fisher Scientific	Cat# 65-0840-90
eBioscience™ Cell proliferation dye eFluor450	Thermo Fisher Scientific	Cat# 65-0842-85
LIVE/DEAD Fixable Aqua Dead Cell Stain	Thermo Fisher Scientific	Cat# L34966
Formaldehyde 37%	Thermo Fisher Scientific	Cat# F79-500
Biotininylated recombinant soluble dimeric FcγRIIIa (V^{158}) protein	(Wines et al., 2016)	N/A
CD4 mimetic BNM-III-170	Dr Amos B. Smith III (Chen et al., 2019)	N/A
Dimethyl sulfoxide (DMSO)	Thermo Fisher Scientific	Cat# D1391
Phytohemagglutinin-L (PHA-L)	Sigma	Cat# L2769
Recombinant IL-2 (rIL-2)	NIH AIDS Reagent Program	Cat# 136
Protein A Sepharose CL-4B	Cytiva	Cat # 17096303
Papain-agarose resin	Thermo Fisher Scientific	Cat # 20341
β-mercaptoethanol	Bio-Rad	Cat# #1610710
Acrylamide/Bis-Acrylamide	Thermo Fisher Scientific	Cat# BP1410-1
Sodium dodecyl sulfate (SDS)	Thermo Fisher Scientific	Cat # BP166-500
Ammonium Persulfate	Bio-Rad	Cat# 1610700
TEMED	Bio-Rad	Cat# 1610801
Coomassie Brilliant Blue R-250	Thermo Fisher Scientific	Cat# BP101-50
Magnesium phosphate ($MgSO_4$)	Bioshop	Cat# MAG511.500
Potassium phosphate monobasic (KH_2PO_4)	Thermo Fisher Scientific	Cat# P285-500

Adenosine 5-triphosphate disodium salt hydrate (ATP)	Sigma	Cat# A3377-10G
Dithiothreitol (DTT)	Thermo Fisher Scientific	Cat# BP172-5
HIV-1 Env gp41 peptide (583-618)	(Gohain et al.,2016)	N/A
HIV-1 Env gp41 peptide (587-597)	Genscript	N/A
HIV-1 Env gp41 peptide (596-606)	Genscript	N/A
SARS-CoV-2 Spike S2 peptide (1153-1163)	(Li et al., 2021)	N/A
Critical commercial assays		
QuikChange II XL Site-Directed Mutagenesis Kit	Agilent Technologies	Cat # #200522
Alexa Fluor 647 Protein Labeling Kit	Thermo Fisher Scientific	Cat# A20173
EasySep human CD4+ T cell enrichment kit	StemCell Technologies	Cat# 19052
Cytofix/Cytoperm Fixation/ Permeabilization Kit	BD Biosciences	Cat# 554714
QIAamp viral RNA mini kit	QIAGEN	Cat# 52906
Quantitect SYBR green RT-PCR Master Mix	QIAGEN	Cat# 204245
Experimental models: Cell lines		
293T human embryonic kidney cells	ATCC	Cat# CRL-3216; RRID: CVCL_0063
TZM-bl cells	NIH AIDS Reagent Program	Cat# 8129; RRID:CVCL_B478
FreeStyle 293F cells	Thermo Fisher Scientific	Cat# R79007; RRID: CVCL_D603
Experimental models: Organisms/strains		
SIRPA $^{h/m}$ Rag2$^{-/-}$ Il2rg$^{-/-}$ IL15 $^{h/m}$ (SRG-15) mice	(Herndler-Brandstetter et al., 2017)	N/A
NOD.Cg-*Prkdc*^{scid} IL2rg$^{-/-}$ Tg(Hu-IL15) (NSG-15) mice	Jackson Laboratory	Cat# 030890; RRID:IMSR_JAX:030890
Oligonucleotides		
246D heavy chain G236R FWD: 5'-CCTGAACTCCTGCGGGGACCGTCAGTC-3' REV: 5'-GACTGACGGTCCCCGCAGGAGTTCAGG-3'	Integrated DNA Technologies	N/A
246D heavy chain L328R FWD: 5'-CCAACAAAGCCCGCCCAGCCCCCATC-3' REV: 5'-GATGGGGGCTGGGCGGGCTTTGTTGG-3'	Integrated DNA Technologies	N/A
246D heavy chain G236A/S239D FWD: 5'-CTCCTGGCGGGACCGGATGTCTTCCTCTTC-3' REV: 5'-GAAGAGGAAGACATCCGGTCCCGCCAGGAG-3'	Integrated DNA Technologies	N/A
246D heavy chain A330L/I332E FWD: 5'-GCCCTCCCACTCCCCGAAGAGAAAACCATC-3' REV: 5'-GATGGTTTTCTCTTCGGGGAGTGGGAGGGC-3'	Integrated DNA Technologies	N/A
HIV-1 IMC JR-CSF Vpu- primers FWD:5'-GTGCATGTAATGTAACCTTTACAAATATTAGC-3' REV: 5'-GCTAATATTTGTAAAGGTTACATTACATGCAC-3'	Integrated DNA Technologies	N/A
HIV-1$_{NL4/3}$YU2 Vpu+ primers FWD: 5'-GTAAGTAGTACATGTAATGCAACCTATACC-3' REV: 5'-GGTATAGGTTGCATTACATGTACTACTTAC-3'	Integrated DNA Technologies	N/A

HIV-1 *gag* primers FWD: 5'-TGCTATGTCAGTTCCCCTTGGTTCTCT-3' REV: 5'-AGTTGGAGGACATCAAGCAGCCATGCAAAT-3'	(Rajashekar et al., 2021)	N/A
Recombinant DNA		
246D mAb Light Chain Expression Vector	NIH AIDS Reagent Program	Cat# 13742
246D mAb Heavy Chain Expression Vector	NIH AIDS Reagent Program	Cat# 13741
246D GRLR mAb Heavy Chain Expression Vector	This paper	N/A
246D GASDALIE mAb Heavy Chain Expression Vector	This paper	N/A
HIV-$1_{NL4/3}$YU2	(Horwitz et al., 2017)	N/A
HIV-$1_{NL4/3}$YU2 Vpu+	This paper	N/A
HIV-1 IMC JR-CSF	NIH AIDS Reagent Program (Koyanagi et al., 1987)	Cat# 2708
HIV-1 IMC JR-CSF Vpu-	This paper	N/A
HIV-1 IMC NL4/3	NIH AIDS Reagent Program (Adachi et al., 1986)	Cat# 114
HIV-1 IMC NL4/3 Vpu-	(Neil et al., 2006)	N/A
HIV-1 IMC YU2	(Li et al., 1991)	N/A
HIV-1 IMC YU2 Vpu+	(Krapp et al., 2016)	N/A
HIV-1 IMC AD8	(Theodore et al., 1996)	N/A
HIV-1 IMC AD8 Vpu+	(Krapp et al., 2016)	N/A
HIV-1 IMC CH058	(Ochsenbauer et al., 2012)	N/A
HIV-1 IMC CH058 Vpu-	(Kmiec et al., 2016)	N/A
HIV-1 IMC CH058 Nef-	(Heigele et al., 2016)	N/A
HIV-1 IMC CH058 Nef- Vpu-	(Heigele et al., 2016)	N/A
HIV-1 IMC CH077	(Ochsenbauer et al., 2012)	N/A
HIV-1 IMC CH077 Vpu-	(Kmiec et al., 2016)	N/A
HIV-1 IMC REJO	(Ochsenbauer et al., 2012)	N/A
HIV-1 IMC REJO Vpu-	(Yamada et al., 2018)	N/A
HIV-1 IMC STCO	(Parrish et al.,2013)	N/A
HIV-1 IMC STCO Vpu-	(Kmiec et al., 2016)	N/A
HIV-1 IMC CH198	(Parrish et al.,2013)	N/A
HIV-1 IMC CH198 Vpu-	(Sauter et al., 2015)	N/A
HIV-1 IMC ZM246F	(Parrish et al.,2012)	N/A
HIV-1 IMC ZM246F Vpu-	(Langer et al.,2015)	N/A
HIV-1 IMC CH167	(Parrish et al.,2013)	N/A
HIV-1 IMC CH167 Vpu-	(Kmiec et al., 2016)	N/A
HIV-1 IMC CH293	(Parrish et al.,2013)	N/A
HIV-1 IMC CH293 Vpu-	(Sauter et al., 2015)	N/A
VSV G glycoprotein expression vector	(Emi et al., 1991)	N/A

Software and algorithms		
BD FACSDiva v9.0	BD Biosciences	RRID: SCR_001456
FlowJo v10.5.3	Tree Star	https://www.flowjo.com/; RRID:SCR_008520
GraphPad Prism v9.1.0	GraphPad	https://www.graphpad.com/; RRID:SCR_002798
Other		
BD LSR II Flow Cytometer	BD Biosciences	N/A
TriStar LB 942 Microplate Reader	Berthold Technologies	N/A
Applied Biosystems 7500 real-time PCR system	Thermo Fisher Scientific	N/A
Biacore 3000	Cytiva	RRID: SCR_019954
Protein A sensor chip	Cytiva	Cat # 29127558
Superdex 200 16/60 column	Cytiva	Cat# 17-1069-01
Superdex 200 10/300 GL column	Cytiva	Cat# 17-5175-01
Clear V-bottom 96-well plates (cell culture-treated)	Corning	Cat# 0720096
White flat-bottom 96-well plates (cell culture-treated)	Corning	Cat# 0877126
White Maxisorp™ Nunc™ 96-well plates	Thermo Fisher Scientific	Cat# 437796

EXPERIMENTAL MODELS AND SUBJECT DETAILS

Ethics Statement

Written informed consent was obtained from all study participants and research adhered to the ethical guidelines of CRCHUM and was reviewed and approved by the CRCHUM institutional review board (ethics committee, approval number CE 16.164 - CA). Research adhered to the standards indicated by the Declaration of Helsinki. All participants were adult and provided informed written consent prior to enrolment in accordance with Institutional Review Board approval.

Cell lines and primary cells

293T human embryonic kidney cells (obtained from ATCC) and TZM-bl cells (NIH AIDS Reagent Program) were maintained at 37°C under 5% CO_2 in Dulbecco's Modified Eagle Medium (DMEM) (Wisent, St. Bruno, QC, Canada), supplemented with 5 % fetal bovine serum (FBS) (VWR, Radnor, PA, USA) and 100 U/mL penicillin/streptomycin (Wisent). 293T cells were derived from 293 cells, into which the simian virus 40 T-antigen was inserted. TZM-bl cells were

derived from HeLa cells and were engineered to stably express high levels of human CD4 and CCR5 and to contain the firefly luciferase reporter gene under the control of the HIV-1 promoter (Platt et al., 1998). Human peripheral blood mononuclear cells (PBMCs) from ten HIV-negative individuals (8 males and 2 females) and five antiretroviral therapy (ART)-treated HIV-positive individuals (all males) obtained by leukapheresis and Ficoll-Paque density gradient isolation were cryopreserved in liquid nitrogen until further use. $CD4^+$ T lymphocytes were purified from resting PBMCs by negative selection using immunomagnetic beads per the manufacturer's instructions (StemCell Technologies, Vancouver, BC) and were activated with phytohemagglutinin-L (10 µg/mL) for 48 h and then maintained in RPMI 1640 (Thermo Fisher Scientific, Waltham, MA, USA) complete medium supplemented with rIL-2 (100 U/mL).

Human plasma samples

The FRQS-AIDS and Infectious Diseases Network supports a representative cohort of newly-HIV-infected subjects with clinical indication of primary infection [the Montreal Primary HIV Infection Cohort (Fontaine et al., 2011; Fontaine et al., 2009)]. Cross-sectional plasma samples from 50 HIV-1-infected individuals were segregated in five groups based on infection duration and treatment with antiretroviral therapy (ART). Plasma samples were obtained from treatment-naive subjects during the acute phase of infection (first 3 months after HIV acquisition), the early phase of infection (3–6 and 6-12 months after acquisition) and during the chronic phase of infection (>2 years after acquisition). Another group of chronically-infected individuals (>2 years after acquisition) received ART treatment. Plasma samples were also obtained from ten age- and sex-matched HIV-negative healthy volunteers.

Experimental animal models

SRG-15 mice encoding human SIRPA and IL-15 in a 129xBALB/c (N3) genetic background were originally generated in the laboratory of Dr Richard Flavell (Yale University) (Herndler-Brandstetter et al., 2017). NSG-15 mice with expression of the human IL15 gene in the NOD/ShiLtJ background were purchased from the Jackson Laboratory (Bar Harbor, ME, USA) (Brehm et al., 2018). The mice were bred and maintained under specific pathogen-free conditions. All animal studies were performed with authorization from Institutional Animal Care and Use Committees (IACUC) of Yale University. The mice were a mix of male and female randomly

distributed between groups. SRG-15-Hu-PBL and NSG-15-Hu-PBL mice were engrafted as described (Rajashekar et al., 2021). Briefly, 1×10^7 PBMCs, purified by Ficoll density gradient centrifugation of healthy donor blood buffy coats (two anonymous donors, obtained from the New York Blood Bank) were injected IP in a 200-µL volume into 6- to 8-week-old SRG-15 or NSG-15 mice, using a 1-cm^3 syringe and 25-gauge needle. Cell engraftment was tested 15 days post-transplant. 100 µL of blood was collected by retroorbital bleeding. PBMCs were isolated by Ficoll density gradient centrifugation; stained with fluorescently-labelled anti-human CD45, CD3, CD4, CD8 and CD56 antibodies and analyzed by flow cytometry to confirm engraftment. Humanized mice were intraperitoneally challenged with 30,000 PFU of HIV-$1_{NL4/3}$YU2 Vpu- or Vpu+. Infection profile was analyzed for plasma viral load (PVL) analysis of serially collected plasma samples.

METHOD DETAILS

Plasmids and proviral constructs

The HIV-$1_{NL4/3}$YU2 proviral construct has been previously reported (Horwitz et al., 2017). A mutation was introduced in the putative vpu start codon (ACG → ATG) to restore the vpu open reading frame (ORF) in the HIV-$1_{NL4/3}$YU2 IMC using the QuikChange II XL site-directed mutagenesis protocol (Agilent Technologies, Santa Clara, CA). Transmitted/Founder (T/F) and chronic infectious molecular clones (IMCs) of patients CH058, CH077, CH198, ZM246F, CH167, CH293, REJO, STCO were inferred and constructed as previously described (Ochsenbauer et al., 2012; Parrish et al., 2013; Parrish et al., 2012; Salazar-Gonzalez et al., 2009). The generation of vpu-defective IMCs was previously described (Kmiec et al., 2016; Langer et al., 2015; Sauter et al., 2015; Yamada et al., 2018) and consists in the introduction of premature stop codons in the vpu reading frame using the QuikChange II XL site-directed mutagenesis protocol. CH058 IMCs defective for Vpu and/or Nef expression were previously described (Heigele et al., 2016; Kmiec et al., 2016). The IMCs encoding for HIV-1 reference strains NL4/3, AD8, YU2 and JR-CSF were described elsewhere (Adachi et al., 1986; Koyanagi et al., 1987; Krapp et al., 2016; Li et al., 1991; Theodore et al., 1996). To generate *vpu*-defective JR-CSF IMC, a stop-codon was introduced directly after the start-codon of *vpu* using the QuikChange II XL site-directed mutagenesis protocol. The plasmids encoding for the heavy and light chains of the 246D antibody are available

through the NIH AIDS Reagent Program. Site-directed mutagenesis was performed on the plasmid expressing 246D antibody heavy chain to introduce the GRLR mutations (G236R/L328R) or the GASDALIE mutations (G236A/S239D/A330L/I332E) using the QuikChange II XL site-directed mutagenesis protocol. The presence of the desired mutations was determined by automated DNA sequencing. The vesicular stomatitis virus G (VSV-G)-encoding plasmid was previously described (Emi et al., 1991).

Viral production, infections and ex vivo amplification.

For *in vitro* infection, vesicular stomatitis virus G (VSV-G)-pseudotyped HIV-1 viruses were produced by co-transfection of 293T cells with an HIV-1 proviral construct and a VSV-G-encoding vector using the calcium phosphate method. Two days post-transfection, cell supernatants were harvested, clarified by low-speed centrifugation (300 × g for 5 min), and concentrated by ultracentrifugation at 4°C (100,605 × g for 1 h) over a 20% sucrose cushion. Pellets were resuspended in fresh RPMI, and aliquots were stored at −80°C until use. Viruses were then used to infect activated primary CD4+ T cells from healthy HIV-1 negative donors by spin infection at 800 × g for 1 h in 96-well plates at 25 °C. Viral preparations were titrated directly on primary CD4+ T cells to achieve similar levels of infection among the different IMCs tested (around 10% of $p24^+$ cells). To expand endogenously infected $CD4^+$ T cells, primary $CD4^+$ T cells obtained from ART-treated HIV-1-infected individuals were isolated from PBMCs by negative selection. Purified $CD4^+$ T cells were activated with PHA-L at 10 µg/mL for 48 h and then cultured for at least 6 days in RPMI 1640 complete medium supplemented with rIL-2 (100 U/ml) to reach greater than 10% infection for the ADCC assay.

Antibodies

The following Abs were used to assess cell-surface Env staining: anti-gp41 nnAbs QA255-006, QA255-067, QA255-072 (kindly provided by Julie Overbaugh), 7B2, 2.2B, 12.3D, 12.4H (kindly provided by James Robinson), F240 (NIH AIDS Reagent Program), M785U1, M785U2, M785U3, M785U4, N10U1, N10U2, N5U1, N5U2, N5U3 (kindly provided by George Lewis), 246D, 240D, 167D, and 50-69; anti-cluster A A32 (NIH AIDS Reagent Program), C11 (kindly provided by James Robinson) and N5i5; anti-co-receptor binding site 17b (NIH AIDS Reagent Program) and X5; anti-V3 loop GE2-JG8 (kindly provided by Gunilla Karlsson Hedestam); anti-

CD4 binding site VRC01, VRC03, VRC07-523, VRC13, VRC16 (kindly provided by John Mascola), N6 (kindly provided by Mark Connors), 1-18 (kindly provided by Florian Klein), HJ16, CH106 (NIH AIDS Reagent Program), NC-Cow1, b12, 3BNC117 and N49-P7; anti-V3 glycan PGT121, PGT122, PGT123, PGT125, PGT126, PGT128, PGT130, PGT135, PGT136 (IAVI), BG18 and 10-1074; anti-V2 apex PGT145, PG9 and PG16 (IAVI); anti-gp120-gp41 interface PGT151 (IAVI), 35O22 (kindly provided by Mark Connors), VRC34 (kindly provided by John Mascola) and 8ANC195; anti-silent face SF12; anti-MPER 10E8 (kindly provided by Mark Connors), 4E10 and 2F5 (NIH AIDS Reagent Program). The HIV-IG polyclonal antibody consists of anti-HIV immunoglobulins purified from a pool of plasma from HIV^+ asymptomatic donors (NIH AIDS Reagent Program). Mouse anti-human CD4 (clone OKT4; Thermo Fisher Scientific), mouse anti-human BST-2 (clone RS38E, PE-Cy7-conjugated; Biolegend, San Diego, CA, USA), mouse anti-human NTB-A (clone NT-7, Biolegend) and mouse anti-PVR (clone SKII.4, Biolegend) were also used as primary antibodies for cell-surface staining. Goat anti-mouse IgG (H+L), goat anti-human IgG (H+L) (Thermo Fisher Scientific) and mouse anti-human IgG Fc (Biolegend) antibodies pre-coupled to Alexa Fluor 647 were used as secondary antibodies in flow cytometry experiments. Rabbit antisera raised against Nef (NIH AIDS Reagent Program) or Vpu (Prevost et al., 2020a) were used as primary antibodies in intracellular staining. BrillantViolet 421 (BV421)-conjugated donkey anti-rabbit antibodies (Biolegend) were used as secondary antibodies to detect Nef and Vpu antisera binding by flow cytometry. Goat anti-human IgG Fc antibodies conjugated to horseradish peroxidase (HRP; Thermo Fisher Scientific) were used as secondary antibodies in ELISA experiments.

Small CD4-mimetics

The small-molecule CD4-mimetic compound (CD4mc) BNM-III-170 was synthesized as described previously (Chen et al., 2019). The compounds were dissolved in dimethyl sulfoxide (DMSO) at a stock concentration of 10 mM and diluted to 50 µM in phosphate-buffered saline (PBS) for cell-surface staining or in RPMI-1640 complete medium for ADCC assays.

Protein production of recombinant proteins

FreeStyle 293F cells (Thermo Fisher Scientific) were grown in FreeStyle 293F medium (Thermo Fisher Scientific) to a density of 1×10^6 cells/ml at 37 °C with 8 % CO_2 with regular

agitation (150 rpm). Cells were transfected with plasmids expressing the light and heavy chains of a given antibody using ExpiFectamine 293 transfection reagent, as directed by the manufacturer (Thermo Fisher Scientific). One week later, the cells were pelleted and discarded. The supernatants were filtered (0.22-µm-pore-size filter), and antibodies were purified by protein A affinity columns, as directed by the manufacturer (Cytiva, Marlborough, MA, USA). The recombinant protein preparations were dialyzed against phosphate-buffered saline (PBS) and stored in aliquots at −80°C. To assess purity, recombinant proteins were loaded on SDS-PAGE polyacrylamide gels in the presence or absence of β-mercaptoethanol and stained with Coomassie blue. Purified F240 and 2.2B IgG were conjugated with Alexa Fluor 647 dye according to the manufacturer's protocol (Thermo Fisher Scientific). The F240 Fab fragments were prepared from purified IgG (10 mg/mL) by proteolytic digestion with immobilized papain (Pierce, Rockford, IL) and purified using protein A, followed by gel filtration chromatography on a Superdex 200 16/60 column (Cytiva). The biotin-tagged dimeric recombinant soluble FcγRIIIa (V158) protein was produced and characterized as described (Wines et al., 2016) with additional purification step using a Superdex 200 10/300 GL column (Cytiva).

Flow cytometry analysis of cell-surface staining

Cell surface staining was performed at 48h post-infection. Mock-infected or HIV-1-infected primary $CD4^+$ T cells were incubated for 30 min at 37°C with anti-CD4 (0.5 µg/mL), anti-BST-2 (2 µg/mL), anti-NTB-A (5 µg/mL), anti-PVR (10 µg/mL), anti-Env mAbs (5 µg/mL), HIV-IG (50 µg/mL) or plasma (1:1000 dilution). Cells were then washed once with PBS and stained with the appropriate Alexa Fluor 647-conjugated secondary antibody (2 µg/mL), when needed, for 20 min at room temperature. After one more PBS wash, cells were fixed in a 2% PBS-formaldehyde solution. Alternatively, the binding of anti-Env Abs was detected using a biotin-tagged dimeric recombinant soluble FcγRIIIa (0.2 µg/mL) followed by the addition of Alexa Fluor 647-conjugated streptavidin (Thermo Fisher Scientific; 2 µg/mL). Anti-human IgG Fc secondary antibodies (3 µg/mL) were used when cell surface binding was performed in presence of F240 Fab blockade. Infected cells were then permeabilized using the Cytofix/Cytoperm Fixation/ Permeabilization Kit (BD Biosciences, Mississauga, ON, Canada) and stained intracellularly using PE-conjugated mouse anti-p24 mAb (clone KC57; Beckman Coulter, Brea, CA, USA; 1:100 dilution) in combination with Nef or Vpu rabbit antisera (1:1000 dilution). The percentage of

infected cells ($p24^+$) was determined by gating on the living cell population according to a viability dye staining (Aqua Vivid; Thermo Fisher Scientific). Alternatively, cells were stained intracellularly with rabbit antisera raised against Nef or Vpu (1:1000) followed by BV421-conjugated anti-rabbit secondary antibody. Samples were acquired on an LSR II cytometer (BD Biosciences), and data analysis was performed using FlowJo v10.5.3 (Tree Star, Ashland, OR, USA).

Antibody-dependant cellular cytotoxicity (ADCC) assay

Measurement of ADCC using a fluorescence-activated cell sorting (FACS)-based infected cell elimination (ICE) assay was performed at 48 h post-infection. Briefly, HIV-1-infected primary $CD4^+$ T cells were stained with AquaVivid viability dye and cell proliferation dye eFluor670 (Thermo Fisher Scientific) and used as target cells. Cryopreserved autologous PBMC effectors cells, stained with cell proliferation dye eFluor450 (Thermo Fisher Scientific), were added at an effector: target ratio of 10:1 in 96-well V-bottom plates (Corning, Corning, NY). A 1:1000 final dilution of plasma or 5 µg/mL of anti-Env mAbs was added to appropriate wells and cells were incubated for 5 min at room temperature. The plates were subsequently centrifuged for 1 min at 300 × g, and incubated at 37 °C, 5 % CO_2 for 5 h before being fixed in a 2 % PBS-formaldehyde solution. Infected cells were identified by intracellular p24 staining as described above. Samples were acquired on an LSR II cytometer (BD Biosciences) and data analysis was performed using FlowJo v10.5.3 (Tree Star). The percentage of ADCC was calculated with the following formula: [(% of $p24^+$ cells in Targets plus Effectors) − (% of $p24^+$ cells in Targets plus Effectors plus plasma) / (% of $p24^+$ cells in Targets) × 100] by gating on infected lived target cells.

Virus neutralization assay

TZM-bl target cells were seeded at a density of 2×10^4 cells/well in 96-well luminometer-compatible tissue culture plates (PerkinElmer, Waltham, MA, USA) 24 h before infection. HIV-$1_{NL4/3}$YU2 Vpu- or Vpu+ (in a final volume of 50 µl) was pre-incubated with the indicated amounts of mAbs for 1 h at 37 °C before adding to the target cells. Following an incubation of 24 h at 37 °C, 100 µl of media was added to each well. Two days later, the medium was removed from each well, and the cells were lysed by the addition of 30 µl of passive lysis buffer (Promega, Madison, WI, USA) followed by one freeze-thaw cycle. An LB 942 TriStar luminometer (Berthold

Technologies, Bad Wildbad, Germany) was used to measure the luciferase activity in each well after the addition of 100 µL of Luciferin buffer (15 mM $MgSO_4$, 15 mM KH_2PO_4 [pH 7.8], 1 mM ATP, and 1 mM dithiothreitol) and 50 µL of 1 mM Firefly D-luciferin (Prolume, Pinetop, AZ, USA).

Plasma viral load measurements

Quantification of PVLs was done using the method described previously (Gibellini et al., 2004). Briefly, 100 µL of blood was collected from mice at each time point by retroorbital bleed. Plasma viral RNA was extracted using the QIAamp viral RNA mini kit (QIAGEN, Hilden Germany) following the manufacturer's protocol. SYBR green real-time PCR assay was carried out in a 20-µL PCR mixture volume consisting of 10 µL of 2× Quantitect SYBR green RT-PCR Master Mix (QIAGEN) containing HotStarTaq DNA polymerase, 0.5 µL of 500 nM each oligonucleotide primer, 0.2 µL of 100× QuantiTect RT Mix (containing Omniscript and Sensiscript RTs), and 8 µL of RNA extracted from plasma samples or standard HIV-1 RNA (from 5×10^5 to 5 copies per 1 mL). Highly conserved sequences on the *gag* region of HIV-1 were chosen, and specific HIV-1 *gag* primers were selected. The sequences of HIV-1 *gag* primers are 5' TGCTATGTCAGTTCCCCTTGGTTCTCT 3' and 5'AGTTGGAGGACATCAAGCAGCCATGCAAAT 3'. Amplification was done in an Applied Biosystems 7500 real-time PCR system, and it involved activation at 45 °C for 15 min and 95 °C for 15 min followed by 40 amplification cycles of 95 °C for 15s, 60 °C for 15s, and 72 °C for 30s. For the detection and quantification of viral RNA, the real-time PCR of each sample was compared with threshold cycle value of a standard curve.

Sequence analysis

The LOGO plot (Crooks et al., 2004) was created using the Analyze Align tool at the Los Alamos National Laboratory - HIV database which is based on the WebLogo program (https://www.hiv.lanl.gov/content/sequence/ANALYZEALIGN/analyze_align.html) and the HIV-1 database global curated and filtered 2019 alignment, including 6,223 individual Env protein sequences. The relative height of each letter within individual stack represents the frequency of the indicated amino acid at that position. The numbering of Env amino acid sequences is based on the HXB2 reference strain of HIV-1, where 1 is the initial methionine.

gp41 peptide ELISA

Peptides corresponding to the gp41 C-C loop region (residues 583-618) were either previously described (Gohain et al., 2016) or purchased from Genscript (Piscataway, NJ, USA). A peptide corresponding to the SARS-CoV-2 Spike S2 stem helix (residues 1153-1163) was used as a negative control and was previously reported (Li et al., 2021). Peptides were prepared in PBS at a concentration of 1 µg/mL and were adsorbed to white 96-well plates (MaxiSorp Nunc) overnight at 4 °C. Coated wells were subsequently blocked with blocking buffer (Tris buffered saline [TBS] containing 0.1% Tween20 and 2% BSA) for 1 hour at room temperature. Wells were then washed four times with washing buffer (TBS containing 0.1% Tween20). Anti-gp41 246D and F240 or anti-gp120 A32 (50 ng/mL) were prepared in a diluted solution of blocking buffer (0.1 % BSA) and incubated with the peptide-coated wells for 90 minutes at room temperature. Plates were washed four times with washing buffer followed by incubation with horseradish peroxidase (HRP)-conjugated anti-human IgG secondary Ab (0.3 µg/mL in a diluted solution of blocking buffer [0.4% BSA]) for 1 h at room temperature, followed by four washes. HRP enzyme activity was determined after the addition of a 1:1 mix of Western Lightning Plus-ECL oxidizing and luminol reagents (Perkin Elmer Life Sciences). Light emission was measured with a LB942 TriStar luminometer (Berthold Technologies).

Surface plasmon resonance (SPR)

Surface plasmon resonance assays were performed on a Biacore 3000 (Cytiva) with a running buffer of 10 mM HEPES pH 7.5 and 150 mM NaCl, supplemented with 0.05% Tween20 at 25 °C. The binding kinetics between the gp41 C-C loop and the 246D antibody were obtained in a format where 246D IgG was immobilized onto a Protein A sensor chip (Cytiva) with ~300 response units (RU) and serial dilutions of gp41 (583-618) synthetic peptide were injected with concentrations ranging from 0.488 to 31.25 nM. The protein A chip was regenerated with a wash step of 0.1 M glycine pH 2.0 and reloaded with IgG after each cycle. Kinetic constants were determined using a 1:1 Langmuir model in bimolecular interaction analysis (BIA) evaluation software.

QUANTIFICATION AND STATISTICAL ANALYSIS

Statistics were analyzed using GraphPad Prism version 9.3.1 (GraphPad, San Diego, CA, USA). Every data set was tested for statistical normality and this information was used to apply the appropriate (parametric or nonparametric) statistical test. Statistical details of experiments are indicated in the figure legends. P values < 0.05 were considered significant; significance values are indicated as * $P < 0.05$, ** $P < 0.01$, *** $P < 0.001$, **** $P < 0.0001$.

5.3.9 REFERENCES

Acharya, P., Tolbert, W.D., Gohain, N., Wu, X., Yu, L., Liu, T., Huang, W., Huang, C.C., Kwon, Y.D., Louder, R.K.*, et al.* (2014). Structural Definition of an Antibody-Dependent Cellular Cytotoxicity Response Implicated in Reduced Risk for HIV-1 Infection. J Virol *88*, 12895-12906.

Adachi, A., Gendelman, H.E., Koenig, S., Folks, T., Willey, R., Rabson, A., and Martin, M.A. (1986). Production of acquired immunodeficiency syndrome-associated retrovirus in human and nonhuman cells transfected with an infectious molecular clone. J Virol *59*, 284-291.

Alsahafi, N., Bakouche, N., Kazemi, M., Richard, J., Ding, S., Bhattacharyya, S., Das, D., Anand, S.P., Prevost, J., Tolbert, W.D.*, et al.* (2019). An Asymmetric Opening of HIV-1 Envelope Mediates Antibody-Dependent Cellular Cytotoxicity. Cell Host Microbe *25*, 578-587 e575.

Alsahafi, N., Ding, S., Richard, J., Markle, T., Brassard, N., Walker, B., Lewis, G.K., Kaufmann, D.E., Brockman, M.A., and Finzi, A. (2016). Nef Proteins from HIV-1 Elite Controllers Are Inefficient at Preventing Antibody-Dependent Cellular Cytotoxicity. J Virol *90*, 2993-3002.

Alvarez, R.A., Hamlin, R.E., Monroe, A., Moldt, B., Hotta, M.T., Rodriguez Caprio, G., Fierer, D.S., Simon, V., and Chen, B.K. (2014). HIV-1 Vpu antagonism of tetherin inhibits antibody-dependent cellular cytotoxic responses by natural killer cells. J Virol *88*, 6031-6046.

Anand, S.P., Prevost, J., Baril, S., Richard, J., Medjahed, H., Chapleau, J.P., Tolbert, W.D., Kirk, S., Smith, A.B., III, Wines, B.D.*, et al.* (2019). Two Families of Env Antibodies Efficiently Engage Fc-Gamma Receptors and Eliminate HIV-1-Infected Cells. J Virol *93*.

Arias, J.F., Heyer, L.N., von Bredow, B., Weisgrau, K.L., Moldt, B., Burton, D.R., Rakasz, E.G., and Evans, D.T. (2014). Tetherin antagonism by Vpu protects HIV-infected cells from antibody-dependent cell-mediated cytotoxicity. Proc Natl Acad Sci U S A *111*, 6425-6430.

Asokan, M., Dias, J., Liu, C., Maximova, A., Ernste, K., Pegu, A., McKee, K., Shi, W., Chen, X., Almasri, C.*, et al.* (2020). Fc-mediated effector function contributes to the in vivo antiviral effect of an HIV neutralizing antibody. Proc Natl Acad Sci U S A *117*, 18754-18763.

Bar, K.J., Sneller, M.C., Harrison, L.J., Justement, J.S., Overton, E.T., Petrone, M.E., Salantes, D.B., Seamon, C.A., Scheinfeld, B., Kwan, R.W.*, et al.* (2016). Effect of HIV Antibody VRC01 on Viral Rebound after Treatment Interruption. N Engl J Med *375*, 2037-2050.

Barouch, D.H., Whitney, J.B., Moldt, B., Klein, F., Oliveira, T.Y., Liu, J., Stephenson, K.E., Chang, H.W., Shekhar, K., Gupta, S.*, et al.* (2013). Therapeutic efficacy of potent neutralizing HIV-1-specific monoclonal antibodies in SHIV-infected rhesus monkeys. Nature *503*, 224-228.

Beaudoin-Bussieres, G., Prevost, J., Gendron-Lepage, G., Melillo, B., Chen, J., Smith Iii, A.B., Pazgier, M., and Finzi, A. (2020). Elicitation of Cluster A and Co-Receptor Binding Site Antibodies are Required to Eliminate HIV-1 Infected Cells. Microorganisms *8*.

Bolton, D.L., Pegu, A., Wang, K., McGinnis, K., Nason, M., Foulds, K., Letukas, V., Schmidt, S.D., Chen, X., Todd, J.P.*, et al.* (2016). Human Immunodeficiency Virus Type 1 Monoclonal Antibodies Suppress Acute Simian-Human Immunodeficiency Virus Viremia and Limit Seeding of Cell-Associated Viral Reservoirs. J Virol *90*, 1321-1332.

Bour, S., Perrin, C., and Strebel, K. (1999). Cell surface CD4 inhibits HIV-1 particle release by interfering with Vpu activity. J Biol Chem *274*, 33800-33806.

Bournazos, S., Gazumyan, A., Seaman, M.S., Nussenzweig, M.C., and Ravetch, J.V. (2016). Bispecific Anti-HIV-1 Antibodies with Enhanced Breadth and Potency. Cell *165*, 1609-1620.

Bournazos, S., Klein, F., Pietzsch, J., Seaman, M.S., Nussenzweig, M.C., and Ravetch, J.V. (2014). Broadly neutralizing anti-HIV-1 antibodies require Fc effector functions for in vivo activity. Cell *158*, 1243-1253.

Brehm, M.A., Aryee, K.-E., Bruzenksi, L., Greiner, D.L., Shultz, L.D., and Keck, J. (2018). Transgenic expression of human IL15 in NOD-*scid* IL2rg^{null} (NSG) mice enhances the development and survival of functional human NK cells. The Journal of Immunology 200, 103.120-103.120.

Bruel, T., Guivel-Benhassine, F., Lorin, V., Lortat-Jacob, H., Baleux, F., Bourdic, K., Noel, N., Lambotte, O., Mouquet, H., and Schwartz, O. (2017). Lack of ADCC breadth of human non-neutralizing anti-HIV-1 antibodies. J Virol.

Buchacher, A., Predl, R., Strutzenberger, K., Steinfellner, W., Trkola, A., Purtscher, M., Gruber, G., Tauer, C., Steindl, F., Jungbauer, A., and et al. (1994). Generation of human

monoclonal antibodies against HIV-1 proteins; electrofusion and Epstein-Barr virus transformation for peripheral blood lymphocyte immortalization. AIDS Res Hum Retroviruses *10*, 359-369.

Burton, D.R., Hessell, A.J., Keele, B.F., Klasse, P.J., Ketas, T.A., Moldt, B., Dunlop, D.C., Poignard, P., Doyle, L.A., Cavacini, L.*, et al.* (2011). Limited or no protection by weakly or nonneutralizing antibodies against vaginal SHIV challenge of macaques compared with a strongly neutralizing antibody. Proc Natl Acad Sci U S A *108*, 11181-11186.

Burton, D.R., Pyati, J., Koduri, R., Sharp, S.J., Thornton, G.B., Parren, P.W., Sawyer, L.S., Hendry, R.M., Dunlop, N., Nara, P.L., and et al. (1994). Efficient neutralization of primary isolates of HIV-1 by a recombinant human monoclonal antibody. Science *266*, 1024-1027.

Caskey, M., Klein, F., Lorenzi, J.C., Seaman, M.S., West, A.P., Jr., Buckley, N., Kremer, G., Nogueira, L., Braunschweig, M., Scheid, J.F.*, et al.* (2015). Viraemia suppressed in HIV-1-infected humans by broadly neutralizing antibody 3BNC117. Nature *522*, 487-491.

Caskey, M., Schoofs, T., Gruell, H., Settler, A., Karagounis, T., Kreider, E.F., Murrell, B., Pfeifer, N., Nogueira, L., Oliveira, T.Y.*, et al.* (2017). Antibody 10-1074 suppresses viremia in HIV-1-infected individuals. Nat Med *23*, 185-191.

Cavacini, L.A., Emes, C.L., Wisnewski, A.V., Power, J., Lewis, G., Montefiori, D., and Posner, M.R. (1998). Functional and molecular characterization of human monoclonal antibody reactive with the immunodominant region of HIV type 1 glycoprotein 41. AIDS Res Hum Retroviruses *14*, 1271-1280.

Chan, D.C., Fass, D., Berger, J.M., and Kim, P.S. (1997). Core structure of gp41 from the HIV envelope glycoprotein. Cell *89*, 263-273.

Chen, J., Park, J., Kirk, S.M., Chen, H.C., Li, X., Lippincott, D.J., Melillo, B., and Smith, A.B., III (2019). Development of an Effective Scalable Enantioselective Synthesis of the HIV-1 Entry Inhibitor BNM-III-170 as the Bis-Trifluoroacetate Salt. Org Process Res Dev *23*, 2464-2469.

Corti, D., Langedijk, J.P., Hinz, A., Seaman, M.S., Vanzetta, F., Fernandez-Rodriguez, B.M., Silacci, C., Pinna, D., Jarrossay, D., Balla-Jhagjhoorsingh, S.*, et al.* (2010). Analysis of memory B cell responses and isolation of novel monoclonal antibodies with neutralizing breadth from HIV-1-infected individuals. PLoS One *5*, e8805.

Crooks, G.E., Hon, G., Chandonia, J.M., and Brenner, S.E. (2004). WebLogo: a sequence logo generator. Genome Res *14*, 1188-1190.

Dave, V.P., Hajjar, F., Dieng, M.M., Haddad, E., and Cohen, E.A. (2013). Efficient BST2 antagonism by Vpu is critical for early HIV-1 dissemination in humanized mice. Retrovirology *10*, 128.

Davis, K.L., Gray, E.S., Moore, P.L., Decker, J.M., Salomon, A., Montefiori, D.C., Graham, B.S., Keefer, M.C., Pinter, A., Morris, L.*, et al.* (2009). High titer HIV-1 V3-specific antibodies with broad reactivity but low neutralizing potency in acute infection and following vaccination. Virology *387*, 414-426.

Decker, J.M., Bibollet-Ruche, F., Wei, X., Wang, S., Levy, D.N., Wang, W., Delaporte, E., Peeters, M., Derdeyn, C.A., Allen, S.*, et al.* (2005). Antigenic conservation and immunogenicity of the HIV coreceptor binding site. J Exp Med *201*, 1407-1419.

Ding, S., Gasser, R., Gendron-Lepage, G., Medjahed, H., Tolbert, W.D., Sodroski, J., Pazgier, M., and Finzi, A. (2019a). CD4 Incorporation into HIV-1 Viral Particles Exposes Envelope Epitopes Recognized by CD4-Induced Antibodies. J Virol *93*.

Ding, S., Grenier, M.C., Tolbert, W.D., Vezina, D., Sherburn, R., Richard, J., Prevost, J., Chapleau, J.P., Gendron-Lepage, G., Medjahed, H.*, et al.* (2019b). A New Family of Small-Molecule CD4-Mimetic Compounds Contacts Highly Conserved Aspartic Acid 368 of HIV-1 gp120 and Mediates Antibody-Dependent Cellular Cytotoxicity. J Virol *93*.

Ding, S., Veillette, M., Coutu, M., Prevost, J., Scharf, L., Bjorkman, P.J., Ferrari, G., Robinson, J.E., Sturzel, C., Hahn, B.H.*, et al.* (2016a). A Highly Conserved Residue of the HIV-1 gp120 Inner Domain Is Important for Antibody-Dependent Cellular Cytotoxicity Responses Mediated by Anti-cluster A Antibodies. J Virol *90*, 2127-2134.

Ding, S., Verly, M.M., Princiotto, A., Melillo, B., Moody, T., Bradley, T., Easterhoff, D., Roger, M., Hahn, B.H., Madani, N.*, et al.* (2016b). Small Molecule CD4-Mimetics Sensitize HIV-1-infected Cells to ADCC by Antibodies Elicited by Multiple Envelope Glycoprotein Immunogens in Non-Human Primates. AIDS Res Hum Retroviruses.

Diskin, R., Klein, F., Horwitz, J.A., Halper-Stromberg, A., Sather, D.N., Marcovecchio, P.M., Lee, T., West, A.P., Jr., Gao, H., Seaman, M.S.*, et al.* (2013). Restricting HIV-1 pathways for escape using rationally designed anti-HIV-1 antibodies. J Exp Med *210*, 1235-1249.

Doores, K.J. (2015). The HIV glycan shield as a target for broadly neutralizing antibodies. FEBS J *282*, 4679-4691.

Dosenovic, P., von Boehmer, L., Escolano, A., Jardine, J., Freund, N.T., Gitlin, A.D., McGuire, A.T., Kulp, D.W., Oliveira, T., Scharf, L.*, et al.* (2015). Immunization for HIV-1 Broadly Neutralizing Antibodies in Human Ig Knockin Mice. Cell *161*, 1505-1515.

Dube, M., Bego, M.G., Paquay, C., and Cohen, E.A. (2010). Modulation of HIV-1-host interaction: role of the Vpu accessory protein. Retrovirology *7*, 114.

Dufloo, J., Guivel-Benhassine, F., Buchrieser, J., Lorin, V., Grzelak, L., Dupouy, E., Mestrallet, G., Bourdic, K., Lambotte, O., Mouquet, H.*, et al.* (2020). Anti-HIV-1 antibodies trigger non-lytic complement deposition on infected cells. EMBO Rep *21*, e49351.

Earl, P.L., Doms, R.W., and Moss, B. (1990). Oligomeric structure of the human immunodeficiency virus type 1 envelope glycoprotein. Proc Natl Acad Sci U S A *87*, 648-652.

Eda, Y., Murakami, T., Ami, Y., Nakasone, T., Takizawa, M., Someya, K., Kaizu, M., Izumi, Y., Yoshino, N., Matsushita, S.*, et al.* (2006). Anti-V3 humanized antibody KD-247 effectively suppresses ex vivo generation of human immunodeficiency virus type 1 and affords sterile protection of monkeys against a heterologous simian/human immunodeficiency virus infection. J Virol *80*, 5563-5570.

Emi, N., Friedmann, T., and Yee, J.K. (1991). Pseudotype formation of murine leukemia virus with the G protein of vesicular stomatitis virus. J Virol *65*, 1202-1207.

Escolano, A., Steichen, J.M., Dosenovic, P., Kulp, D.W., Golijanin, J., Sok, D., Freund, N.T., Gitlin, A.D., Oliveira, T., Araki, T.*, et al.* (2016). Sequential Immunization Elicits Broadly Neutralizing Anti-HIV-1 Antibodies in Ig Knockin Mice. Cell *166*, 1445-1458 e1412.

Falkowska, E., Le, K.M., Ramos, A., Doores, K.J., Lee, J.H., Blattner, C., Ramirez, A., Derking, R., van Gils, M.J., Liang, C.H.*, et al.* (2014). Broadly neutralizing HIV antibodies define a glycan-dependent epitope on the prefusion conformation of gp41 on cleaved envelope trimers. Immunity *40*, 657-668.

Fontaine, J., Chagnon-Choquet, J., Valcke, H.S., Poudrier, J., and Roger, M. (2011). High expression levels of B lymphocyte stimulator (BLyS) by dendritic cells correlate with HIV-related B-cell disease progression in humans. Blood *117*, 145-155.

Fontaine, J., Coutlee, F., Tremblay, C., Routy, J.P., Poudrier, J., and Roger, M. (2009). HIV infection affects blood myeloid dendritic cells after successful therapy and despite nonprogressing clinical disease. J Infect Dis *199*, 1007-1018.

Freed, E.O., Myers, D.J., and Risser, R. (1989). Mutational analysis of the cleavage sequence of the human immunodeficiency virus type 1 envelope glycoprotein precursor gp160. J Virol *63*, 4670-4675.

Freund, N.T., Horwitz, J.A., Nogueira, L., Sievers, S.A., Scharf, L., Scheid, J.F., Gazumyan, A., Liu, C., Velinzon, K., Goldenthal, A.*, et al.* (2015). A New Glycan-Dependent CD4-Binding Site Neutralizing Antibody Exerts Pressure on HIV-1 In Vivo. PLoS Pathog *11*, e1005238.

Freund, N.T., Wang, H., Scharf, L., Nogueira, L., Horwitz, J.A., Bar-On, Y., Golijanin, J., Sievers, S.A., Sok, D., Cai, H.*, et al.* (2017). Coexistence of potent HIV-1 broadly neutralizing antibodies and antibody-sensitive viruses in a viremic controller. Sci Transl Med *9*.

Frey, G., Chen, J., Rits-Volloch, S., Freeman, M.M., Zolla-Pazner, S., and Chen, B. (2010). Distinct conformational states of HIV-1 gp41 are recognized by neutralizing and non-neutralizing antibodies. Nat Struct Mol Biol *17*, 1486-1491.

Fritschi, C.J., Liang, S., Mohammadi, M., Anang, S., Moraca, F., Chen, J., Madani, N., Sodroski, J.G., Abrams, C.F., Hendrickson, W.A., and Smith, A.B., 3rd (2021). Identification of gp120 Residue His105 as a Novel Target for HIV-1 Neutralization by Small-Molecule CD4-Mimics. ACS Med Chem Lett *12*, 1824-1831.

Gibellini, D., Vitone, F., Gori, E., La Placa, M., and Re, M.C. (2004). Quantitative detection of human immunodeficiency virus type 1 (HIV-1) viral load by SYBR green real-time RT-PCR technique in HIV-1 seropositive patients. J Virol Methods *115*, 183-189.

Gohain, N., Tolbert, W.D., Orlandi, C., Richard, J., Ding, S., Chen, X., Bonsor, D.A., Sundberg, E.J., Lu, W., Ray, K.*, et al.* (2016). Molecular basis for epitope recognition by non-neutralizing anti-gp41 antibody F240. Sci Rep *6*, 36685.

Gorny, M.K., Gianakakos, V., Sharpe, S., and Zolla-Pazner, S. (1989). Generation of human monoclonal antibodies to human immunodeficiency virus. Proc Natl Acad Sci U S A *86*, 1624-1628.

Gray, G.E., Bekker, L.G., Laher, F., Malahleha, M., Allen, M., Moodie, Z., Grunenberg, N., Huang, Y., Grove, D., Prigmore, B., et al. (2021). Vaccine Efficacy of ALVAC-HIV and Bivalent Subtype C gp120-MF59 in Adults. N Engl J Med 384, 1089-1100.

Guan, Y., Pazgier, M., Sajadi, M.M., Kamin-Lewis, R., Al-Darmarki, S., Flinko, R., Lovo, E., Wu, X., Robinson, J.E., Seaman, M.S., *et al.* (2013). Diverse specificity and effector function among human antibodies to HIV-1 envelope glycoprotein epitopes exposed by CD4 binding. Proc Natl Acad Sci U S A *110*, E69-78.

Halper-Stromberg, A., Lu, C.L., Klein, F., Horwitz, J.A., Bournazos, S., Nogueira, L., Eisenreich, T.R., Liu, C., Gazumyan, A., Schaefer, U., *et al.* (2014). Broadly neutralizing antibodies and viral inducers decrease rebound from HIV-1 latent reservoirs in humanized mice. Cell *158*, 989-999.

Haynes, B.F., Gilbert, P.B., McElrath, M.J., Zolla-Pazner, S., Tomaras, G.D., Alam, S.M., Evans, D.T., Montefiori, D.C., Karnasuta, C., Sutthent, R., *et al.* (2012a). Immune-correlates analysis of an HIV-1 vaccine efficacy trial. N Engl J Med *366*, 1275-1286.

Haynes, B.F., Kelsoe, G., Harrison, S.C., and Kepler, T.B. (2012b). B-cell-lineage immunogen design in vaccine development with HIV-1 as a case study. Nat Biotechnol *30*, 423-433.

Heigele, A., Kmiec, D., Regensburger, K., Langer, S., Peiffer, L., Sturzel, C.M., Sauter, D., Peeters, M., Pizzato, M., Learn, G.H., *et al.* (2016). The Potency of Nef-Mediated SERINC5 Antagonism Correlates with the Prevalence of Primate Lentiviruses in the Wild. Cell Host Microbe *20*, 381-391.

Herndler-Brandstetter, D., Shan, L., Yao, Y., Stecher, C., Plajer, V., Lietzenmayer, M., Strowig, T., de Zoete, M.R., Palm, N.W., Chen, J., *et al.* (2017). Humanized mouse model supports development, function, and tissue residency of human natural killer cells. Proc Natl Acad Sci U S A *114*, E9626-E9634.

Hessell, A.J., Jaworski, J.P., Epson, E., Matsuda, K., Pandey, S., Kahl, C., Reed, J., Sutton, W.F., Hammond, K.B., Cheever, T.A., *et al.* (2016). Early short-term treatment with neutralizing human monoclonal antibodies halts SHIV infection in infant macaques. Nat Med *22*, 362-368.

Hessell, A.J., Shapiro, M.B., Powell, R., Malherbe, D.C., McBurney, S.P., Pandey, S., Cheever, T., Sutton, W.F., Kahl, C., Park, B., *et al.* (2018). Reduced Cell-Associated DNA and Improved Viral Control in Macaques following Passive Transfer of a Single Anti-V2

Monoclonal Antibody and Repeated Simian/Human Immunodeficiency Virus Challenges. J Virol *92*.

Hioe, C.E., Li, G., Liu, X., Tsahouridis, O., He, X., Funaki, M., Klingler, J., Tang, A.F., Feyznezhad, R., Heindel, D.W.*, et al.* (2022). Non-neutralizing antibodies targeting the immunogenic regions of HIV-1 envelope reduce mucosal infection and virus burden in humanized mice. PLoS Pathog *18*, e1010183.

Horton, H.M., Bernett, M.J., Peipp, M., Pong, E., Karki, S., Chu, S.Y., Richards, J.O., Chen, H., Repp, R., Desjarlais, J.R., and Zhukovsky, E.A. (2010). Fc-engineered anti-CD40 antibody enhances multiple effector functions and exhibits potent in vitro and in vivo antitumor activity against hematologic malignancies. Blood *116*, 3004-3012.

Horwitz, J.A., Bar-On, Y., Lu, C.L., Fera, D., Lockhart, A.A.K., Lorenzi, J.C.C., Nogueira, L., Golijanin, J., Scheid, J.F., Seaman, M.S.*, et al.* (2017). Non-neutralizing Antibodies Alter the Course of HIV-1 Infection In Vivo. Cell *170*, 637-648 e610.

Horwitz, J.A., Halper-Stromberg, A., Mouquet, H., Gitlin, A.D., Tretiakova, A., Eisenreich, T.R., Malbec, M., Gravemann, S., Billerbeck, E., Dorner, M.*, et al.* (2013). HIV-1 suppression and durable control by combining single broadly neutralizing antibodies and antiretroviral drugs in humanized mice. Proc Natl Acad Sci U S A *110*, 16538-16543.

Hout, D.R., Gomez, M.L., Pacyniak, E., Gomez, L.M., Inbody, S.H., Mulcahy, E.R., Culley, N., Pinson, D.M., Powers, M.F., Wong, S.W., and Stephens, E.B. (2005). Scrambling of the amino acids within the transmembrane domain of Vpu results in a simian-human immunodeficiency virus (SHIVTM) that is less pathogenic for pig-tailed macaques. Virology *339*, 56-69.

Huang, C.C., Venturi, M., Majeed, S., Moore, M.J., Phogat, S., Zhang, M.Y., Dimitrov, D.S., Hendrickson, W.A., Robinson, J., Sodroski, J.*, et al.* (2004). Structural basis of tyrosine sulfation and VH-gene usage in antibodies that recognize the HIV type 1 coreceptor-binding site on gp120. Proc Natl Acad Sci U S A *101*, 2706-2711.

Huang, J., Kang, B.H., Ishida, E., Zhou, T., Griesman, T., Sheng, Z., Wu, F., Doria-Rose, N.A., Zhang, B., McKee, K.*, et al.* (2016). Identification of a CD4-Binding-Site Antibody to HIV that Evolved Near-Pan Neutralization Breadth. Immunity *45*, 1108-1121.

Huang, J., Kang, B.H., Pancera, M., Lee, J.H., Tong, T., Feng, Y., Imamichi, H., Georgiev, I.S., Chuang, G.Y., Druz, A.*, et al.* (2014). Broad and potent HIV-1 neutralization by a human antibody that binds the gp41-gp120 interface. Nature *515*, 138-142.

Huang, J., Ofek, G., Laub, L., Louder, M.K., Doria-Rose, N.A., Longo, N.S., Imamichi, H., Bailer, R.T., Chakrabarti, B., Sharma, S.K.*, et al.* (2012). Broad and potent neutralization of HIV-1 by a gp41-specific human antibody. Nature *491*, 406-412.

Jardine, J.G., Kulp, D.W., Havenar-Daughton, C., Sarkar, A., Briney, B., Sok, D., Sesterhenn, F., Ereno-Orbea, J., Kalyuzhniy, O., Deresa, I.*, et al.* (2016). HIV-1 broadly neutralizing antibody precursor B cells revealed by germline-targeting immunogen. Science *351*, 1458-1463.

Jette, C.A., Barnes, C.O., Kirk, S.M., Melillo, B., Smith, A.B., 3rd, and Bjorkman, P.J. (2021). Cryo-EM structures of HIV-1 trimer bound to CD4-mimetics BNM-III-170 and M48U1 adopt a CD4-bound open conformation. Nat Commun *12*, 1950.

Klein, F., Halper-Stromberg, A., Horwitz, J.A., Gruell, H., Scheid, J.F., Bournazos, S., Mouquet, H., Spatz, L.A., Diskin, R., Abadir, A.*, et al.* (2012). HIV therapy by a combination of broadly neutralizing antibodies in humanized mice. Nature *492*, 118-122.

Klein, F., Nogueira, L., Nishimura, Y., Phad, G., West, A.P., Jr., Halper-Stromberg, A., Horwitz, J.A., Gazumyan, A., Liu, C., Eisenreich, T.R.*, et al.* (2014). Enhanced HIV-1 immunotherapy by commonly arising antibodies that target virus escape variants. J Exp Med *211*, 2361-2372.

Kmiec, D., Iyer, S.S., Sturzel, C.M., Sauter, D., Hahn, B.H., and Kirchhoff, F. (2016). Vpu-Mediated Counteraction of Tetherin Is a Major Determinant of HIV-1 Interferon Resistance. MBio *7*.

Kong, R., Xu, K., Zhou, T., Acharya, P., Lemmin, T., Liu, K., Ozorowski, G., Soto, C., Taft, J.D., Bailer, R.T.*, et al.* (2016). Fusion peptide of HIV-1 as a site of vulnerability to neutralizing antibody. Science *352*, 828-833.

Koyanagi, Y., Miles, S., Mitsuyasu, R.T., Merrill, J.E., Vinters, H.V., and Chen, I.S. (1987). Dual infection of the central nervous system by AIDS viruses with distinct cellular tropisms. Science *236*, 819-822.

Krapp, C., Hotter, D., Gawanbacht, A., McLaren, P.J., Kluge, S.F., Sturzel, C.M., Mack, K., Reith, E., Engelhart, S., Ciuffi, A.*, et al.* (2016). Guanylate Binding Protein (GBP) 5 Is an Interferon-Inducible Inhibitor of HIV-1 Infectivity. Cell Host Microbe *19*, 504-514.

Kwong, P.D., Wyatt, R., Robinson, J., Sweet, R.W., Sodroski, J., and Hendrickson, W.A. (1998). Structure of an HIV gp120 envelope glycoprotein in complex with the CD4 receptor and a neutralizing human antibody. Nature *393*, 648-659.

Landais, E., and Moore, P.L. (2018). Development of broadly neutralizing antibodies in HIV-1 infected elite neutralizers. Retrovirology *15*, 61.

Langer, S.M., Hopfensperger, K., Iyer, S.S., Kreider, E.F., Learn, G.H., Lee, L.H., Hahn, B.H., and Sauter, D. (2015). A Naturally Occurring rev1-vpu Fusion Gene Does Not Confer a Fitness Advantage to HIV-1. PLoS One *10*, e0142118.

Laumaea, A., Smith, A.B., III, Sodroski, J., and Finzi, A. (2020). Opening the HIV envelope: potential of CD4 mimics as multifunctional HIV entry inhibitors. Curr Opin HIV AIDS *15*, 300-308.

Lee, J.H., Ozorowski, G., and Ward, A.B. (2016). Cryo-EM structure of a native, fully glycosylated, cleaved HIV-1 envelope trimer. Science *351*, 1043-1048.

Lee, W.S., Richard, J., Lichtfuss, M., Smith, A.B., III, Park, J., Courter, J.R., Melillo, B.N., Sodroski, J.G., Kaufmann, D.E., Finzi, A.*, et al.* (2015). Antibody-Dependent Cellular Cytotoxicity against Reactivated HIV-1-Infected Cells. J Virol *90*, 2021-2030.

Levesque, K., Zhao, Y.S., and Cohen, E.A. (2003). Vpu exerts a positive effect on HIV-1 infectivity by down-modulating CD4 receptor molecules at the surface of HIV-1-producing cells. J Biol Chem *278*, 28346-28353.

Li, W., Chen, Y., Prevost, J., Ullah, I., Lu, M., Gong, S.Y., Tauzin, A., Gasser, R., Vezina, D., Anand, S.P.*, et al.* (2021). Structural basis and mode of action for two broadly neutralizing antibodies against SARS-CoV-2 emerging variants of concern. Cell Rep, 110210.

Li, Y., Kappes, J.C., Conway, J.A., Price, R.W., Shaw, G.M., and Hahn, B.H. (1991). Molecular characterization of human immunodeficiency virus type 1 cloned directly from uncultured human brain tissue: identification of replication-competent and -defective viral genomes. J Virol *65*, 3973-3985.

Li, Z., Li, W., Lu, M., Bess, J., Jr., Chao, C.W., Gorman, J., Terry, D.S., Zhang, B., Zhou, T., Blanchard, S.C., *et al.* (2020). Subnanometer structures of HIV-1 envelope trimers on aldrithiol-2-inactivated virus particles. Nat Struct Mol Biol *27*, 726-734.

Liao, H.X., Lynch, R., Zhou, T., Gao, F., Alam, S.M., Boyd, S.D., Fire, A.Z., Roskin, K.M., Schramm, C.A., Zhang, Z., *et al.* (2013). Co-evolution of a broadly neutralizing HIV-1 antibody and founder virus. Nature *496*, 469-476.

Lu, C.L., Murakowski, D.K., Bournazos, S., Schoofs, T., Sarkar, D., Halper-Stromberg, A., Horwitz, J.A., Nogueira, L., Golijanin, J., Gazumyan, A., *et al.* (2016). Enhanced clearance of HIV-1-infected cells by broadly neutralizing antibodies against HIV-1 in vivo. Science *352*, 1001-1004.

Lu, M., Ma, X., Castillo-Menendez, L.R., Gorman, J., Alsahafi, N., Ermel, U., Terry, D.S., Chambers, M., Peng, D., Zhang, B., *et al.* (2019). Associating HIV-1 envelope glycoprotein structures with states on the virus observed by smFRET. Nature.

Lynch, R.M., Boritz, E., Coates, E.E., DeZure, A., Madden, P., Costner, P., Enama, M.E., Plummer, S., Holman, L., Hendel, C.S., *et al.* (2015). Virologic effects of broadly neutralizing antibody VRC01 administration during chronic HIV-1 infection. Science translational medicine *7*, 319ra206.

Madani, N., Princiotto, A.M., Easterhoff, D., Bradley, T., Luo, K., Williams, W.B., Liao, H.X., Moody, M.A., Phad, G.E., Vazquez Bernat, N., *et al.* (2016). Antibodies Elicited by Multiple Envelope Glycoprotein Immunogens in Primates Neutralize Primary Human Immunodeficiency Viruses (HIV-1) Sensitized by CD4-Mimetic Compounds. J Virol *90*, 5031-5046.

Madani, N., Princiotto, A.M., Mach, L., Ding, S., Prevost, J., Richard, J., Hora, B., Sutherland, L., Zhao, C.A., Conn, B.P., *et al.* (2018). A CD4-mimetic compound enhances vaccine efficacy against stringent immunodeficiency virus challenge. Nat Commun *9*, 2363.

Manganaro, L., Hong, P., Hernandez, M.M., Argyle, D., Mulder, L.C.F., Potla, U., Diaz-Griffero, F., Lee, B., Fernandez-Sesma, A., and Simon, V. (2018). IL-15 regulates susceptibility of CD4(+) T cells to HIV infection. Proc Natl Acad Sci U S A *115*, E9659-E9667.

Matusali, G., Potesta, M., Santoni, A., Cerboni, C., and Doria, M. (2012). The human immunodeficiency virus type 1 Nef and Vpu proteins downregulate the natural killer cell-activating ligand PVR. J Virol *86*, 4496-4504.

McCune, J.M., Rabin, L.B., Feinberg, M.B., Lieberman, M., Kosek, J.C., Reyes, G.R., and Weissman, I.L. (1988). Endoproteolytic cleavage of gp160 is required for the activation of human immunodeficiency virus. Cell *53*, 55-67.

Melillo, B., Liang, S., Park, J., Schon, A., Courter, J.R., LaLonde, J.M., Wendler, D.J., Princiotto, A.M., Seaman, M.S., Freire, E.*, et al.* (2016). Small-Molecule CD4-Mimics: Structure-Based Optimization of HIV-1 Entry Inhibition. ACS Med Chem Lett *7*, 330-334.

Moog, C., Dereuddre-Bosquet, N., Teillaud, J.L., Biedma, M.E., Holl, V., Van Ham, G., Heyndrickx, L., Van Dorsselaer, A., Katinger, D., Vcelar, B.*, et al.* (2014). Protective effect of vaginal application of neutralizing and nonneutralizing inhibitory antibodies against vaginal SHIV challenge in macaques. Mucosal Immunol *7*, 46-56.

Mouquet, H., Scharf, L., Euler, Z., Liu, Y., Eden, C., Scheid, J.F., Halper-Stromberg, A., Gnanapragasam, P.N., Spencer, D.I., Seaman, M.S.*, et al.* (2012). Complex-type N-glycan recognition by potent broadly neutralizing HIV antibodies. Proc Natl Acad Sci U S A *109*, E3268-3277.

Munro, J.B., Gorman, J., Ma, X., Zhou, Z., Arthos, J., Burton, D.R., Koff, W.C., Courter, J.R., Smith, A.B., III, Kwong, P.D.*, et al.* (2014). Conformational dynamics of single HIV-1 envelope trimers on the surface of native virions. Science *346*, 759-763.

Neil, S.J., Eastman, S.W., Jouvenet, N., and Bieniasz, P.D. (2006). HIV-1 Vpu promotes release and prevents endocytosis of nascent retrovirus particles from the plasma membrane. PLoS Pathog *2*, e39.

Neil, S.J., Zang, T., and Bieniasz, P.D. (2008). Tetherin inhibits retrovirus release and is antagonized by HIV-1 Vpu. Nature *451*, 425-430.

Nishimura, Y., Gautam, R., Chun, T.W., Sadjadpour, R., Foulds, K.E., Shingai, M., Klein, F., Gazumyan, A., Golijanin, J., Donaldson, M.*, et al.* (2017). Early antibody therapy can induce long-lasting immunity to SHIV. Nature *543*, 559-563.

Ochsenbauer, C., Edmonds, T.G., Ding, H., Keele, B.F., Decker, J., Salazar, M.G., Salazar-Gonzalez, J.F., Shattock, R., Haynes, B.F., Shaw, G.M.*, et al.* (2012). Generation of Transmitted/Founder HIV-1 Infectious Molecular Clones and Characterization of Their Replication Capacity in CD4 T Lymphocytes and Monocyte-Derived Macrophages. J Virol *86*, 2715-2728.

Parrish, N.F., Gao, F., Li, H., Giorgi, E.E., Barbian, H.J., Parrish, E.H., Zajic, L., Iyer, S.S., Decker, J.M., Kumar, A.*, et al.* (2013). Phenotypic properties of transmitted founder HIV-1. Proc Natl Acad Sci U S A *110*, 6626-6633.

Parrish, N.F., Wilen, C.B., Banks, L.B., Iyer, S.S., Pfaff, J.M., Salazar-Gonzalez, J.F., Salazar, M.G., Decker, J.M., Parrish, E.H., Berg, A.*, et al.* (2012). Transmitted/founder and chronic subtype C HIV-1 use CD4 and CCR5 receptors with equal efficiency and are not inhibited by blocking the integrin alpha4beta7. PLoS Pathog *8*, e1002686.

Parsons, M.S., Lee, W.S., Kristensen, A.B., Amarasena, T., Khoury, G., Wheatley, A.K., Reynaldi, A., Wines, B.D., Hogarth, P.M., Davenport, M.P., and Kent, S.J. (2019). Fc-dependent functions are redundant to efficacy of anti-HIV antibody PGT121 in macaques. J Clin Invest *129*, 182-191.

Pauthner, M.G., Nkolola, J.P., Havenar-Daughton, C., Murrell, B., Reiss, S.M., Bastidas, R., Prevost, J., Nedellec, R., von Bredow, B., Abbink, P.*, et al.* (2019). Vaccine-Induced Protection from Homologous Tier 2 SHIV Challenge in Nonhuman Primates Depends on Serum-Neutralizing Antibody Titers. Immunity *50*, 241-252 e246.

Phad, G.E., Vazquez Bernat, N., Feng, Y., Ingale, J., Martinez Murillo, P.A., O'Dell, S., Li, Y., Mascola, J.R., Sundling, C., Wyatt, R.T., and Karlsson Hedestam, G.B. (2015). Diverse antibody genetic and recognition properties revealed following HIV-1 envelope glycoprotein immunization. J Immunol *194*, 5903-5914.

Pham, T.N., Lukhele, S., Dallaire, F., Perron, G., and Cohen, E.A. (2016). Enhancing Virion Tethering by BST2 Sensitizes Productively and Latently HIV-infected T cells to ADCC Mediated by Broadly Neutralizing Antibodies. Sci Rep *6*, 37225.

Platt, E.J., Wehrly, K., Kuhmann, S.E., Chesebro, B., and Kabat, D. (1998). Effects of CCR5 and CD4 cell surface concentrations on infections by macrophage-tropic isolates of human immunodeficiency virus type 1. J Virol *72*, 2855-2864.

Prevost, J., Edgar, C.R., Richard, J., Trothen, S.M., Jacob, R.A., Mumby, M.J., Pickering, S., Dube, M., Kaufmann, D.E., Kirchhoff, F.*, et al.* (2020a). HIV-1 Vpu Downregulates Tim-3 from the Surface of Infected CD4(+) T Cells. J Virol *94*.

Prevost, J., Medjahed, H., Vezina, D., Chen, H.C., Hahn, B.H., Smith, A.B., 3rd, and Finzi, A. (2021). HIV-1 Envelope Glycoproteins Proteolytic Cleavage Protects Infected Cells from ADCC Mediated by Plasma from Infected Individuals. Viruses *13*.

Prevost, J., Pickering, S., Mumby, M.J., Medjahed, H., Gendron-Lepage, G., Delgado, G.G., Dirk, B.S., Dikeakos, J.D., Sturzel, C.M., Sauter, D.*, et al.* (2019). Upregulation of BST-2 by Type I Interferons Reduces the Capacity of Vpu To Protect HIV-1-Infected Cells from NK Cell Responses. mBio *10*.

Prevost, J., Richard, J., Ding, S., Pacheco, B., Charlebois, R., Hahn, B.H., Kaufmann, D.E., and Finzi, A. (2018a). Envelope glycoproteins sampling states 2/3 are susceptible to ADCC by sera from HIV-1-infected individuals. Virology *515*, 38-45.

Prevost, J., Richard, J., Gasser, R., Medjahed, H., Kirchhoff, F., Hahn, B.H., Kappes, J.C., Ochsenbauer, C., Duerr, R., and Finzi, A. (2022). Detection of the HIV-1 accessory proteins Nef and Vpu by flow cytometry represents a new tool to study their functional interplay within a single infected CD4+ T cell. J Virol, jvi0192921.

Prevost, J., Richard, J., Medjahed, H., Alexander, A., Jones, J., Kappes, J.C., Ochsenbauer, C., and Finzi, A. (2018b). Incomplete Downregulation of CD4 Expression Affects HIV-1 Env Conformation and Antibody-Dependent Cellular Cytotoxicity Responses. J Virol *92*.

Prevost, J., Tolbert, W.D., Medjahed, H., Sherburn, R.T., Madani, N., Zoubchenok, D., Gendron-Lepage, G., Gaffney, A.E., Grenier, M.C., Kirk, S.*, et al.* (2020b). The HIV-1 Env gp120 Inner Domain Shapes the Phe43 Cavity and the CD4 Binding Site. mBio *11*.

Prevost, J., Zoubchenok, D., Richard, J., Veillette, M., Pacheco, B., Coutu, M., Brassard, N., Parsons, M.S., Ruxrungtham, K., Bunupuradah, T.*, et al.* (2017). Influence of the Envelope gp120 Phe 43 Cavity on HIV-1 Sensitivity to Antibody-Dependent Cell-Mediated Cytotoxicity Responses. J Virol *91*.

Rajashekar, J.K., Richard, J., Beloor, J., Prevost, J., Anand, S.P., Beaudoin-Bussieres, G., Shan, L., Herndler-Brandstetter, D., Gendron-Lepage, G., Medjahed, H.*, et al.* (2021). Modulating HIV-1 envelope glycoprotein conformation to decrease the HIV-1 reservoir. Cell Host Microbe *29*, 904-916 e906.

Rerks-Ngarm, S., Pitisuttithum, P., Nitayaphan, S., Kaewkungwal, J., Chiu, J., Paris, R., Premsri, N., Namwat, C., de Souza, M., Adams, E.*, et al.* (2009). Vaccination with ALVAC and AIDSVAX to prevent HIV-1 infection in Thailand. N Engl J Med *361*, 2209-2220.

Richard, J., Pacheco, B., Gohain, N., Veillette, M., Ding, S., Alsahafi, N., Tolbert, W.D., Prevost, J., Chapleau, J.P., Coutu, M.*, et al.* (2016). Co-receptor Binding Site Antibodies Enable

CD4-Mimetics to Expose Conserved Anti-cluster A ADCC Epitopes on HIV-1 Envelope Glycoproteins. EBioMedicine *12*, 208-218.

Richard, J., Prevost, J., von Bredow, B., Ding, S., Brassard, N., Medjahed, H., Coutu, M., Melillo, B., Bibollet-Ruche, F., Hahn, B.H.*, et al.* (2017). BST-2 Expression Modulates Small CD4-Mimetic Sensitization of HIV-1-Infected Cells to Antibody-Dependent Cellular Cytotoxicity. J Virol *91*.

Richard, J., Veillette, M., Brassard, N., Iyer, S.S., Roger, M., Martin, L., Pazgier, M., Schon, A., Freire, E., Routy, J.P.*, et al.* (2015). CD4 mimetics sensitize HIV-1-infected cells to ADCC. Proc Natl Acad Sci U S A *112*, E2687-2694.

Robinson, C.A., Lyddon, T.D., Gil, H.M., Evans, D.T., Kuzmichev, Y.V., Richard, J., Finzi, A., Welbourn, S., Rasmussen, L., Nebane, N.M., et al. (2022). Novel Compound Inhibitors of HIV-1NL4-3 Vpu. Viruses 14.

Robinson JE, Y.H., Holton D, Elliott S, Ho DD (1992). Distinct antigenic sites on HIV gp120 identified by a panel of human monoclonal antibodies. Journal of Cellular Biochemistry Supplement *16E*, Q449.

Rudicell, R.S., Kwon, Y.D., Ko, S.Y., Pegu, A., Louder, M.K., Georgiev, I.S., Wu, X., Zhu, J., Boyington, J.C., Chen, X.*, et al.* (2014). Enhanced Potency of a Broadly Neutralizing HIV-1 Antibody In Vitro Improves Protection against Lentiviral Infection In Vivo. J Virol *88*, 12669-12682.

Sajadi, M.M., Dashti, A., Rikhtegaran Tehrani, Z., Tolbert, W.D., Seaman, M.S., Ouyang, X., Gohain, N., Pazgier, M., Kim, D., Cavet, G.*, et al.* (2018). Identification of Near-Pan-neutralizing Antibodies against HIV-1 by Deconvolution of Plasma Humoral Responses. Cell *173*, 1783-1795 e1714.

Salazar-Gonzalez, J.F., Salazar, M.G., Keele, B.F., Learn, G.H., Giorgi, E.E., Li, H., Decker, J.M., Wang, S., Baalwa, J., Kraus, M.H.*, et al.* (2009). Genetic identity, biological phenotype, and evolutionary pathways of transmitted/founder viruses in acute and early HIV-1 infection. J Exp Med *206*, 1273-1289.

Santra, S., Tomaras, G.D., Warrier, R., Nicely, N.I., Liao, H.X., Pollara, J., Liu, P., Alam, S.M., Zhang, R., Cocklin, S.L.*, et al.* (2015). Human Non-neutralizing HIV-1 Envelope Monoclonal Antibodies Limit the Number of Founder Viruses during SHIV Mucosal Infection in Rhesus Macaques. PLoS Pathog *11*, e1005042.

Sato, K., Misawa, N., Fukuhara, M., Iwami, S., An, D.S., Ito, M., and Koyanagi, Y. (2012). Vpu augments the initial burst phase of HIV-1 propagation and downregulates BST2 and CD4 in humanized mice. J Virol *86*, 5000-5013.

Saunders, K.O., Wiehe, K., Tian, M., Acharya, P., Bradley, T., Alam, S.M., Go, E.P., Scearce, R., Sutherland, L., Henderson, R.*, et al.* (2019). Targeted selection of HIV-specific antibody mutations by engineering B cell maturation. Science *366*.

Sauter, D., Hotter, D., Van Driessche, B., Sturzel, C.M., Kluge, S.F., Wildum, S., Yu, H., Baumann, B., Wirth, T., Plantier, J.C.*, et al.* (2015). Differential regulation of NF-kappaB-mediated proviral and antiviral host gene expression by primate lentiviral Nef and Vpu proteins. Cell Rep *10*, 586-599.

Scheid, J.F., Horwitz, J.A., Bar-On, Y., Kreider, E.F., Lu, C.L., Lorenzi, J.C., Feldmann, A., Braunschweig, M., Nogueira, L., Oliveira, T.*, et al.* (2016). HIV-1 antibody 3BNC117 suppresses viral rebound in humans during treatment interruption. Nature *535*, 556-560.

Scheid, J.F., Mouquet, H., Ueberheide, B., Diskin, R., Klein, F., Oliveira, T.Y., Pietzsch, J., Fenyo, D., Abadir, A., Velinzon, K.*, et al.* (2011). Sequence and structural convergence of broad and potent HIV antibodies that mimic CD4 binding. Science *333*, 1633-1637.

Schommers, P., Gruell, H., Abernathy, M.E., Tran, M.K., Dingens, A.S., Gristick, H.B., Barnes, C.O., Schoofs, T., Schlotz, M., Vanshylla, K.*, et al.* (2020). Restriction of HIV-1 Escape by a Highly Broad and Potent Neutralizing Antibody. Cell *180*, 471-489 e422.

Schoofs, T., Barnes, C.O., Suh-Toma, N., Golijanin, J., Schommers, P., Gruell, H., West, A.P., Jr., Bach, F., Lee, Y.E., Nogueira, L.*, et al.* (2019). Broad and Potent Neutralizing Antibodies Recognize the Silent Face of the HIV Envelope. Immunity *50*, 1513-1529 e1519.

Shah, A.H., Sowrirajan, B., Davis, Z.B., Ward, J.P., Campbell, E.M., Planelles, V., and Barker, E. (2010). Degranulation of natural killer cells following interaction with HIV-1-infected cells is hindered by downmodulation of NTB-A by Vpu. Cell Host Microbe *8*, 397-409.

Shaik, M.M., Peng, H., Lu, J., Rits-Volloch, S., Xu, C., Liao, M., and Chen, B. (2019). Structural basis of coreceptor recognition by HIV-1 envelope spike. Nature *565*, 318-323.

Shaw, G.M., Hahn, B.H., Arya, S.K., Groopman, J.E., Gallo, R.C., and Wong-Staal, F. (1984). Molecular characterization of human T-cell leukemia (lymphotropic) virus type III in the acquired immune deficiency syndrome. Science *226*, 1165-1171.

Shingai, M., Nishimura, Y., Klein, F., Mouquet, H., Donau, O.K., Plishka, R., Buckler-White, A., Seaman, M., Piatak, M., Jr., Lifson, J.D.*, et al.* (2013). Antibody-mediated immunotherapy of macaques chronically infected with SHIV suppresses viraemia. Nature *503*, 277-280.

Shingai, M., Yoshida, T., Martin, M.A., and Strebel, K. (2011). Some human immunodeficiency virus type 1 Vpu proteins are able to antagonize macaque BST-2 in vitro and in vivo: Vpu-negative simian-human immunodeficiency viruses are attenuated in vivo. J Virol *85*, 9708-9715.

Smith, P., DiLillo, D.J., Bournazos, S., Li, F., and Ravetch, J.V. (2012). Mouse model recapitulating human Fcgamma receptor structural and functional diversity. Proc Natl Acad Sci U S A *109*, 6181-6186.

Sojar, H., Baron, S., Sullivan, J.T., Garrett, M., van Haaren, M.M., Hoffman, J., Overbaugh, J., Doranz, B.J., and Hicar, M.D. (2019). Monoclonal Antibody 2C6 Targets a Cross-Clade Conformational Epitope in gp41 with Highly Active Antibody-Dependent Cell Cytotoxicity. J Virol *93*.

Sok, D., Le, K.M., Vadnais, M., Saye-Francisco, K.L., Jardine, J.G., Torres, J.L., Berndsen, Z.T., Kong, L., Stanfield, R., Ruiz, J.*, et al.* (2017). Rapid elicitation of broadly neutralizing antibodies to HIV by immunization in cows. Nature *548*, 108-111.

Stadtmueller, B.M., Bridges, M.D., Dam, K.M., Lerch, M.T., Huey-Tubman, K.E., Hubbell, W.L., and Bjorkman, P.J. (2018). DEER Spectroscopy Measurements Reveal Multiple Conformations of HIV-1 SOSIP Envelopes that Show Similarities with Envelopes on Native Virions. Immunity *49*, 235-246 e234.

Steichen, J.M., Kulp, D.W., Tokatlian, T., Escolano, A., Dosenovic, P., Stanfield, R.L., McCoy, L.E., Ozorowski, G., Hu, X., Kalyuzhniy, O.*, et al.* (2016). HIV Vaccine Design to Target Germline Precursors of Glycan-Dependent Broadly Neutralizing Antibodies. Immunity *45*, 483-496.

Stiegler, G., Kunert, R., Purtscher, M., Wolbank, S., Voglauer, R., Steindl, F., and Katinger, H. (2001). A potent cross-clade neutralizing human monoclonal antibody against a novel epitope on gp41 of human immunodeficiency virus type 1. AIDS Res Hum Retroviruses *17*, 1757-1765.

Theodore, T.S., Englund, G., Buckler-White, A., Buckler, C.E., Martin, M.A., and Peden, K.W. (1996). Construction and characterization of a stable full-length macrophage-tropic HIV

type 1 molecular clone that directs the production of high titers of progeny virions. AIDS Res Hum Retroviruses *12*, 191-194.

Tolbert, W.D., Sherburn, R., Gohain, N., Ding, S., Flinko, R., Orlandi, C., Ray, K., Finzi, A., Lewis, G.K., and Pazgier, M. (2020). Defining rules governing recognition and Fc-mediated effector functions to the HIV-1 co-receptor binding site. BMC Biol *18*, 91.

Tomaras, G.D., and Haynes, B.F. (2009). HIV-1-specific antibody responses during acute and chronic HIV-1 infection. Curr Opin HIV AIDS *4*, 373-379.

Tomaras, G.D., Yates, N.L., Liu, P., Qin, L., Fouda, G.G., Chavez, L.L., Decamp, A.C., Parks, R.J., Ashley, V.C., Lucas, J.T.*, et al.* (2008). Initial B-cell responses to transmitted human immunodeficiency virus type 1: virion-binding immunoglobulin M (IgM) and IgG antibodies followed by plasma anti-gp41 antibodies with ineffective control of initial viremia. J Virol *82*, 12449-12463.

Van Damme, N., Goff, D., Katsura, C., Jorgenson, R.L., Mitchell, R., Johnson, M.C., Stephens, E.B., and Guatelli, J. (2008). The interferon-induced protein BST-2 restricts HIV-1 release and is downregulated from the cell surface by the viral Vpu protein. Cell Host Microbe *3*, 245-252.

Vanshylla, K., Held, K., Eser, T.M., Gruell, H., Kleipass, F., Stumpf, R., Jain, K., Weiland, D., Munch, J., Gruttner, B.*, et al.* (2021). CD34T+ Humanized Mouse Model to Study Mucosal HIV-1 Transmission and Prevention. Vaccines (Basel) *9*.

Veillette, M., Coutu, M., Richard, J., Batraville, L.A., Dagher, O., Bernard, N., Tremblay, C., Kaufmann, D.E., Roger, M., and Finzi, A. (2015). The HIV-1 gp120 CD4-Bound Conformation Is Preferentially Targeted by Antibody-Dependent Cellular Cytotoxicity-Mediating Antibodies in Sera from HIV-1-Infected Individuals. J Virol *89*, 545-551.

Veillette, M., Desormeaux, A., Medjahed, H., Gharsallah, N.E., Coutu, M., Baalwa, J., Guan, Y., Lewis, G., Ferrari, G., Hahn, B.H.*, et al.* (2014). Interaction with cellular CD4 exposes HIV-1 envelope epitopes targeted by antibody-dependent cell-mediated cytotoxicity. J Virol *88*, 2633-2644.

Visciano, M.L., Gohain, N., Sherburn, R., Orlandi, C., Flinko, R., Dashti, A., Lewis, G.K., Tolbert, W.D., and Pazgier, M. (2019). Induction of Fc-Mediated Effector Functions Against a Stabilized Inner Domain of HIV-1 gp120 Designed to Selectively Harbor the A32 Epitope Region. Front Immunol *10*, 677.

von Bredow, B., Arias, J.F., Heyer, L.N., Moldt, B., Le, K., Robinson, J.E., Zolla-Pazner, S., Burton, D.R., and Evans, D.T. (2016). Comparison of Antibody-Dependent Cell-Mediated Cytotoxicity and Virus Neutralization by HIV-1 Env-Specific Monoclonal Antibodies. J Virol *90*, 6127-6139.

Walker, L.M., Huber, M., Doores, K.J., Falkowska, E., Pejchal, R., Julien, J.P., Wang, S.K., Ramos, A., Chan-Hui, P.Y., Moyle, M.*, et al.* (2011). Broad neutralization coverage of HIV by multiple highly potent antibodies. Nature *477*, 466-470.

Walker, L.M., Phogat, S.K., Chan-Hui, P.Y., Wagner, D., Phung, P., Goss, J.L., Wrin, T., Simek, M.D., Fling, S., Mitcham, J.L.*, et al.* (2009). Broad and potent neutralizing antibodies from an African donor reveal a new HIV-1 vaccine target. Science *326*, 285-289.

Wang, P., Gajjar, M.R., Yu, J., Padte, N.N., Gettie, A., Blanchard, J.L., Russell-Lodrigue, K., Liao, L.E., Perelson, A.S., Huang, Y., and Ho, D.D. (2020). Quantifying the contribution of Fc-mediated effector functions to the antiviral activity of anti-HIV-1 IgG1 antibodies in vivo. Proc Natl Acad Sci U S A *117*, 18002-18009.

Weissenhorn, W., Dessen, A., Harrison, S.C., Skehel, J.J., and Wiley, D.C. (1997). Atomic structure of the ectodomain from HIV-1 gp41. Nature *387*, 426-430.

Williams, K.L., Stumpf, M., Naiman, N.E., Ding, S., Garrett, M., Gobillot, T., Vezina, D., Dusenbury, K., Ramadoss, N.S., Basom, R.*, et al.* (2019). Identification of HIV gp41-specific antibodies that mediate killing of infected cells. PLoS Pathog *15*, e1007572.

5.3.10 FIGURES

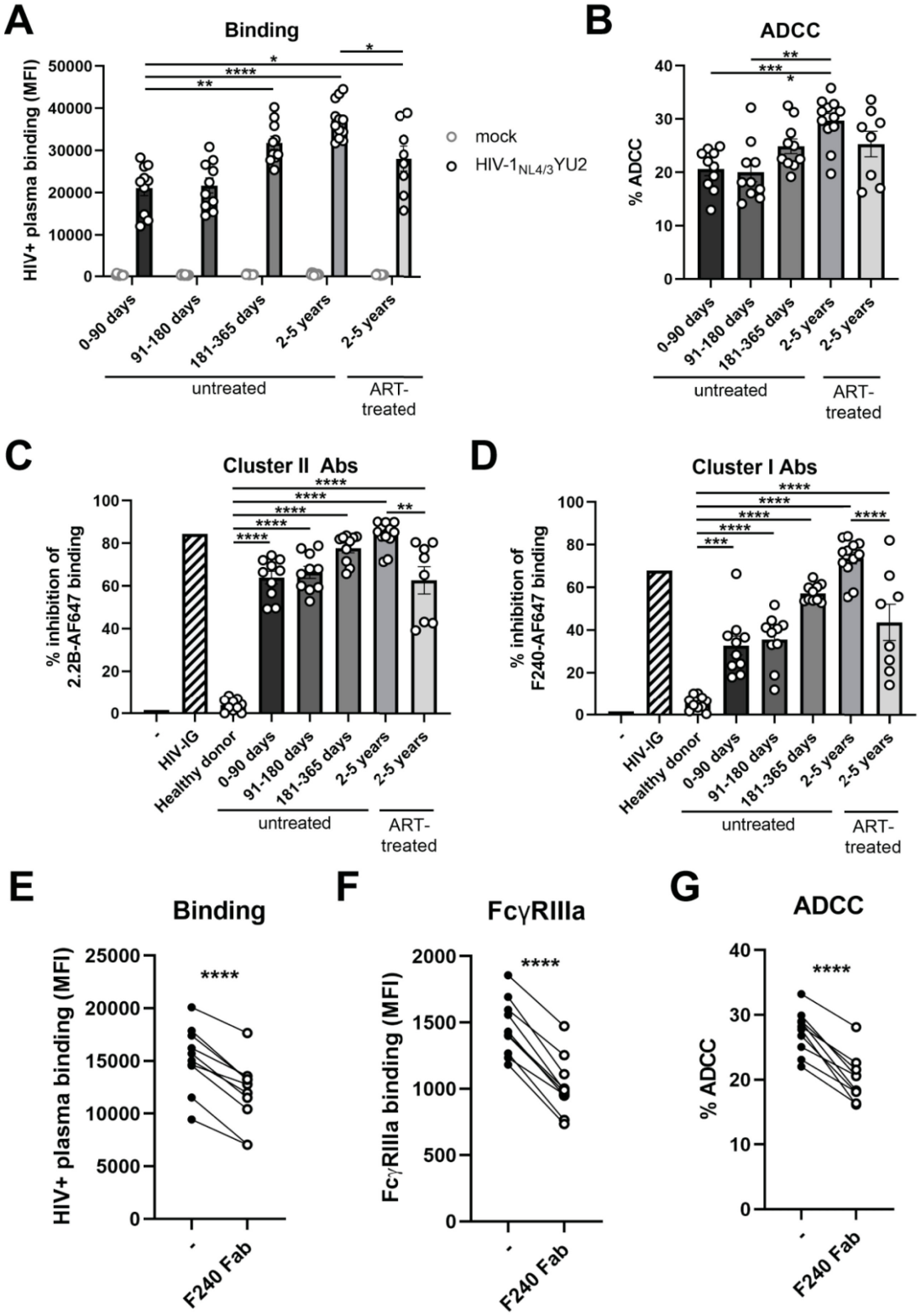

Figure 5.2.1 - Cells infected with HIV-$1_{NL4/3}$YU2 are susceptible to nnAb-mediated ADCC responses.

Primary $CD4^+$ T cells were either mock-infected (grey symbols) or infected with the HIV-$1_{NL4/3}$YU2 virus (black symbols). (**A**) Cell-surface staining and (**B**) ADCC responses mediated by plasma from 50 different HIV-1-infected individuals categorized by the time post-infection and the antiretroviral therapy (ART) treatment status. (**A**) The graph shows the mean fluorescence intensities (MFI) on the whole cell population (mock) or infected $p24^+$ cell population (HIV-$1_{NL4/3}$YU2). (**C-D**) The binding of Alexa Fluor 647 (AF647)-precoupled (**C**) anti-gp41 cluster II 2.2B mAb or (**D**) anti-gp41 cluster I F240 mAb was evaluated in presence of unlabeled human plasma from healthy controls or HIV-1-infected individuals. A pool of purified immunoglobulins from HIV-1-infected individuals (HIV-IG) was used as a positive control. (**E**) Plasma binding, (**F**) FcγRIIIa binding and (**G**) ADCC responses mediated by plasma from 10 untreated HIV-1-infected individuals (2-5 years) were evaluated in presence of competing anti-gp41 cluster I F240 Fab fragment. Error bars indicate means +/- standard errors of the means (SEM). Statistical significance was tested using (**A-D**) one-way ANOVA with a Holm-Sidak post-test or (**E-G**) a paired t test (*, $P < 0.05$; **, $P < 0.01$; ***, $P < 0.001$; ****, $P < 0.0001$; ns, nonsignificant).

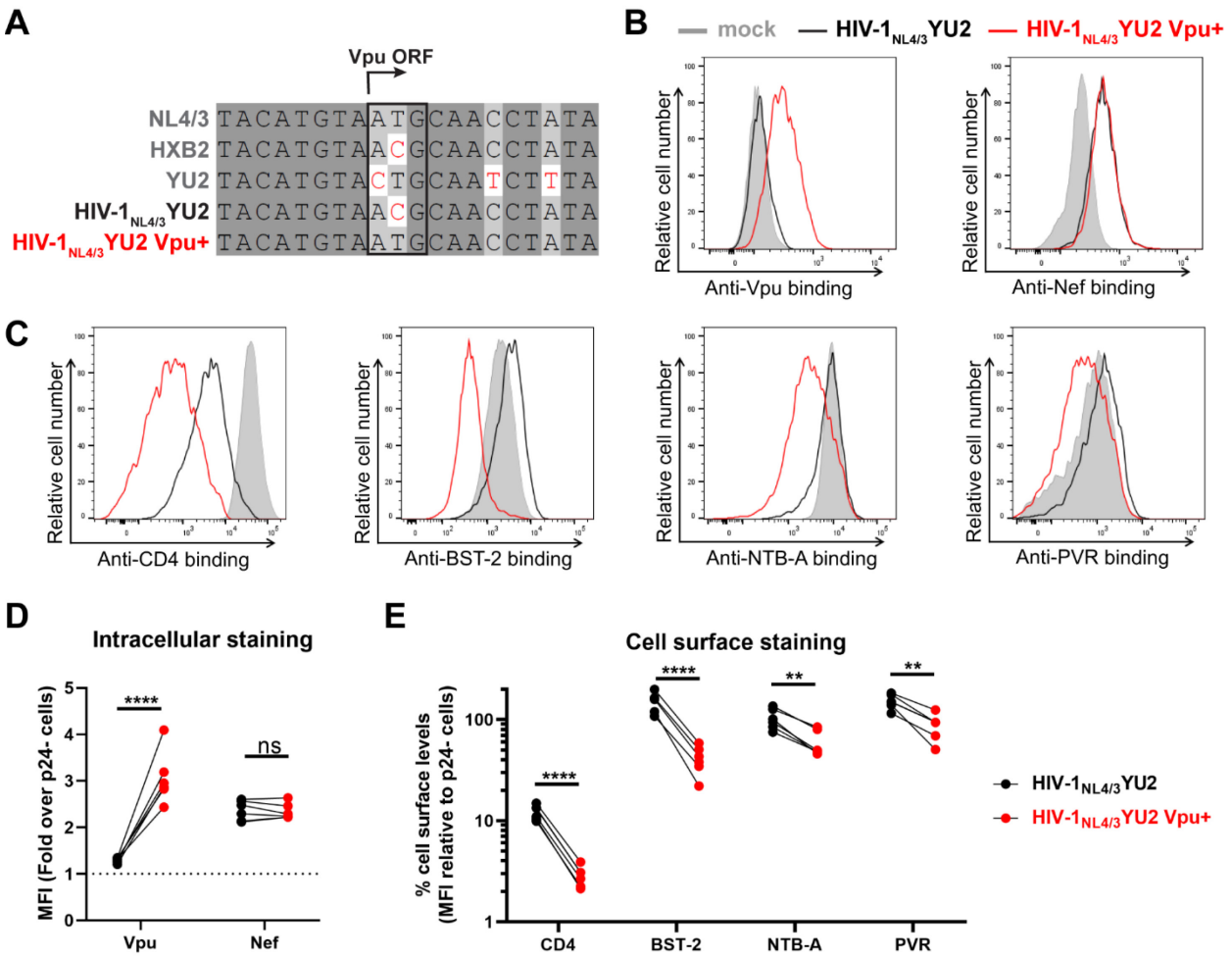

Figure 5.2.2 - Reversion of Vpu open reading frame in the HIV-1$_{NL4/3}$YU2 construct.
(**A**) Sequence alignment of the Vpu open reading frame (ORF) region of selected HIV-1 reference isolates (NL4/3, HXB2, YU2) with the HIV-1$_{NL4/3}$YU2 construct and its Vpu+ counterpart. Identical nucleotides are shaded in dark gray, conserved nucleotides in light gray and non-identical nucleotides are highlighted in red. The *vpu* start codon is highlighted by a black box. (**B-E**) Primary CD4$^+$ T cells either mock-infected or infected with the HIV-1$_{NL4/3}$YU2 virus or its Vpu+ counterpart were stained for intracellular detection of (**B**,**D**) viral proteins Vpu and Nef and cell-surface detection of (**C**,**E**) cellular proteins CD4, BST-2, NTB-A and PVR. (**B-C**) Histograms depicting representative stainings for (**B**) viral proteins and (**C**) their target substrates. (**D-E**) The graphs show the mean fluorescence intensities (MFI) obtained from five independent experiments using primary cells from five different healthy donors. (**D**) Viral protein levels were reported as a fold increase in the signal detected on infected p24$^+$ cells compared to uninfected p24$^-$ cells. (**E**) Cellular protein levels were reported as a percentage of detection at the surface of infected p24$^+$ cells compared to uninfected p24$^-$ cells. Error bars indicate means +/- standard errors of the means (SEM). Statistical significance was tested using an unpaired t test or a Mann-Whitney U test based on statistical normality (**, $P < 0.01$; ****, $P < 0.0001$; ns, nonsignificant).

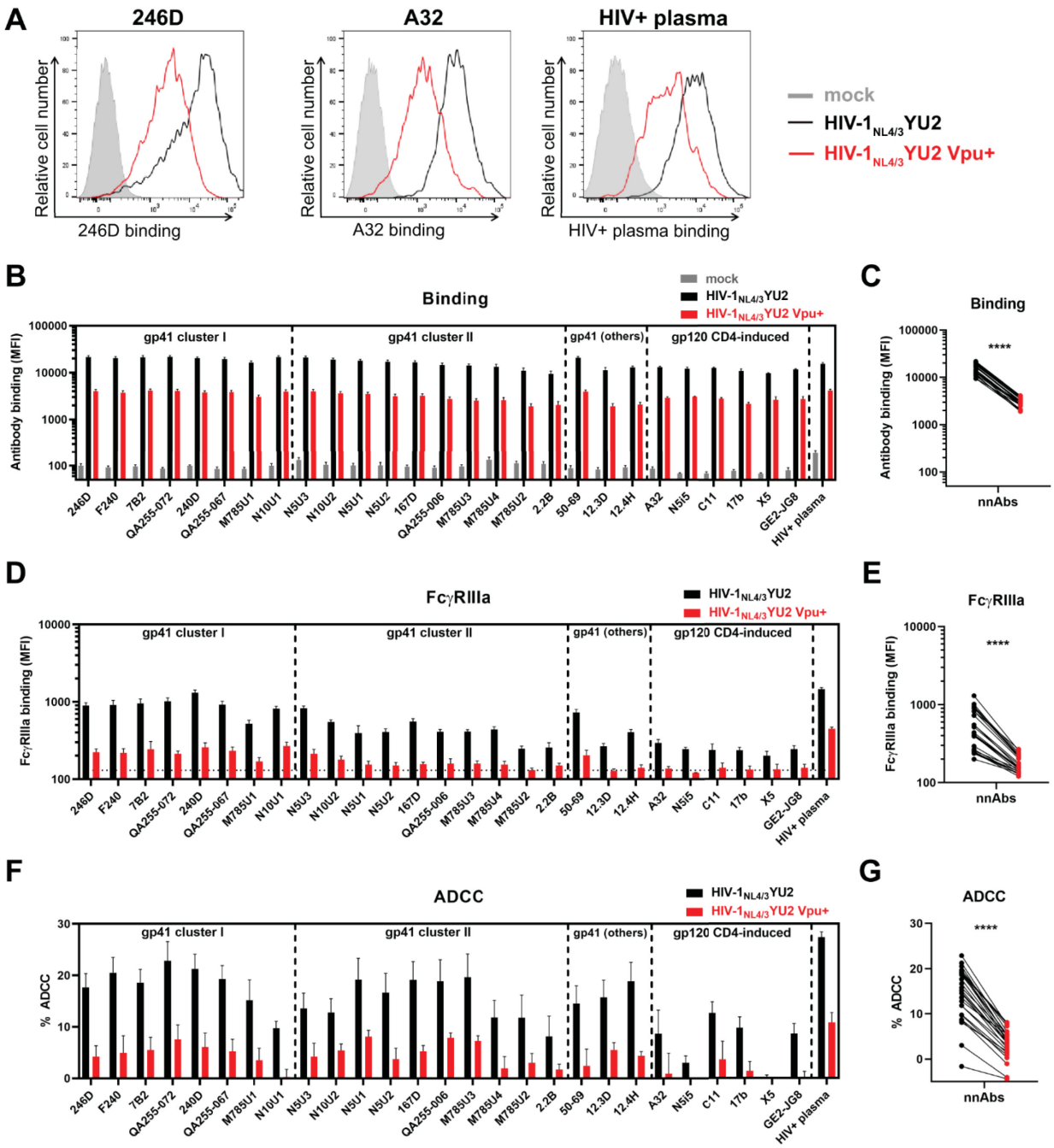
A
246D
A32
HIV+ plasma
Relative cell number
246D binding
A32 binding
HIV+ plasma binding
mock
HIV-1NL4/3YU2
HIV-1NL4/3YU2 Vpu+
B
Binding
Antibody binding (MFI)
gp41 cluster I
gp41 cluster II
gp41 (others)
gp120 CD4-induced
246D F240 7B2 QA255-072 240D QA255-067 M785U1 N10U1 N5U3 N10U2 N5U1 N5U2 167D QA255-006 M785U3 M785U4 M785U2 2.2B 50-69 12.3D 12.4H A32 N5i5 C11 17b X5 GE2-JG8 HIV+ plasma
C
Binding
****
nnAbs
D
FcγRIIIa
FcγRIIIa binding (MFI)
E
FcγRIIIa
****
nnAbs
F
ADCC
% ADCC
G
ADCC
****
nnAbs

Figure 5.2.3 - Vpu expression impairs Env recognition and Fc-effector functions mediated by anti-Env nnAbs.
Primary $CD4^+$ T cells were either mock-infected or infected with the HIV-$1_{NL4/3}$YU2 virus or its Vpu+ counterpart. (**A-E**) Cell surface staining performed using anti-gp41 non-neutralizing antibodies targeting the gp41 cluster I, cluster II or other gp41 regions as well as anti-gp120 CD4-induced antibodies and plasma from 10 HIV-1-infected individuals (HIV+ plasma). Antibody binding was detected either by using (**A**-**C**) Alexa Fluor 647-conjugated anti-human secondary Abs or (**D**-**E**) by using biotinylated recombinant soluble dimeric FcγRIIIa followed by the addition of Alexa Fluor 647-conjugated streptavidin. (**A**) Histograms depicting representative stainings using anti-gp41 cluster I 246D mAb, anti-gp120 cluster A A32 mAb and HIV+ plasma. (**B**,**D**) The graphs represent the mean fluorescence intensities (MFI) obtained from the infected $p24^+$ cell population using cells from five different healthy donors. (**D**) The horizontal dotted line represents the signal obtained in absence of mAb. (**F-G**) Primary $CD4^+$ T cells infected with HIV-$1_{NL4/3}$YU2 viruses were used as target cells. Autologous PBMCs were used as effector cells in a FACS-based ADCC assay. (**F**) The graph represents the percentages of ADCC obtained in the presence of the respective antibodies using cells from five different healthy donors. Error bars indicate means +/- standard errors of the means (SEM). (**C**,**E,G**) Statistical significance was tested using a paired t test (****, $P < 0.0001$).

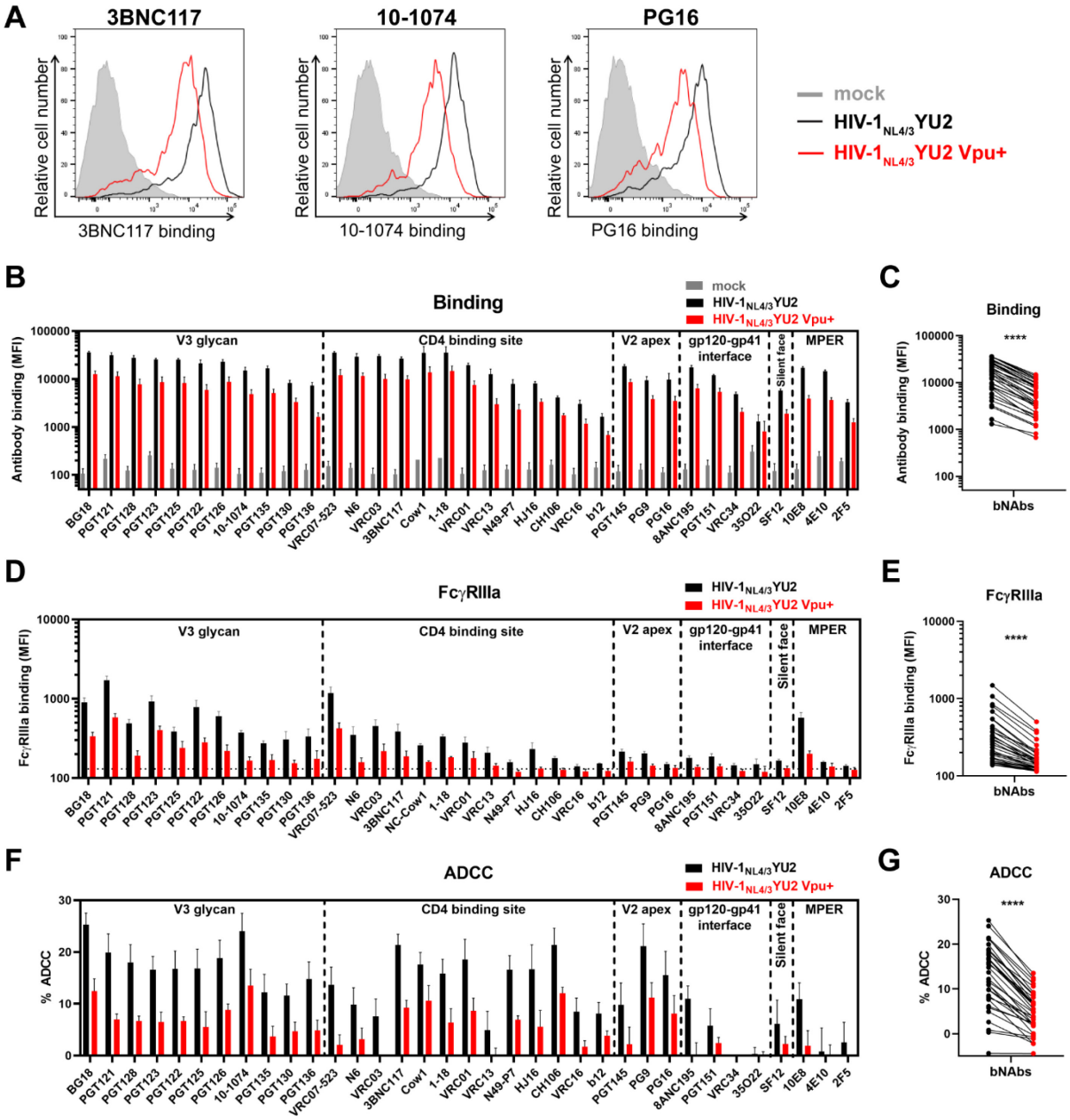
A
3BNC117
10-1074
PG16
Relative cell number
3BNC117 binding
10-1074 binding
PG16 binding
mock
HIV-1NL4/3YU2
HIV-1NL4/3YU2 Vpu+
B
Binding
Antibody binding (MFI)
V3 glycan
CD4 binding site
V2 apex
gp120-gp41 interface
Silent face
MPER
BG18 PGT121 PGT128 PGT123 PGT125 PGT122 PGT126 10-1074 PGT135 PGT130 PGT136 VRC07-523 N6 VRC03 3BNC117 Cow1 1-18 VRC01 VRC13 N49-P7 HJ16 CH106 VRC16 b12 PGT145 PG9 PG16 8ANC195 PGT151 VRC34 35O22 SF12 10E8 4E10 2F5
C
Binding
****
bNAbs
D
FcγRIIIa
FcγRIIIa binding (MFI)
NC-Cow1
E
FcγRIIIa
F
ADCC
% ADCC
G
ADCC

Figure 5.2.4 - Vpu expression decreases Env recognition and Fc-effector functions mediated by anti-Env bNAbs.
Primary $CD4^+$ T cells were either mock-infected or infected with the HIV-$1_{NL4/3}$YU2 virus or its Vpu+ counterpart. (**A-E**) Cell surface staining performed using broadly neutralizing antibodies targeting the gp120 V3 glycan supersite, CD4 binding site, V2 apex and silent face, the gp120-gp41 interface and the gp41 MPER. Antibody binding was detected either by using (**A**-**C**) Alexa Fluor 647-conjugated anti-human secondary Abs or (**D**-**E**) by using biotinylated recombinant soluble dimeric FcγRIIIa followed by the addition of Alexa Fluor 647-conjugated streptavidin. (**A**) Histograms depicting representative stainings using anti-CD4 binding site 3BNC117, anti-V3 glycan 10-1074 and anti-V2 apex PG16 mAbs. (**B**,**D**) The graphs represent the mean fluorescence intensities (MFI) obtained from the infected $p24^+$ cell population using cells from five different healthy donors. (**D**) The horizontal dotted line represents the signal obtained in absence of mAb. (**F-G**) Primary $CD4^+$ T cells infected with HIV-$1_{NL4/3}$YU2 viruses were used as target cells. Autologous PBMCs were used as effector cells in a FACS-based ADCC assay. (**F**) The graph represents the percentages of ADCC obtained in the presence of the respective antibodies using cells from five different healthy donors. Error bars indicate means +/- standard errors of the means (SEM). (**C**,**E,G**) Statistical significance was tested using a paired t test (****, $P < 0.0001$).

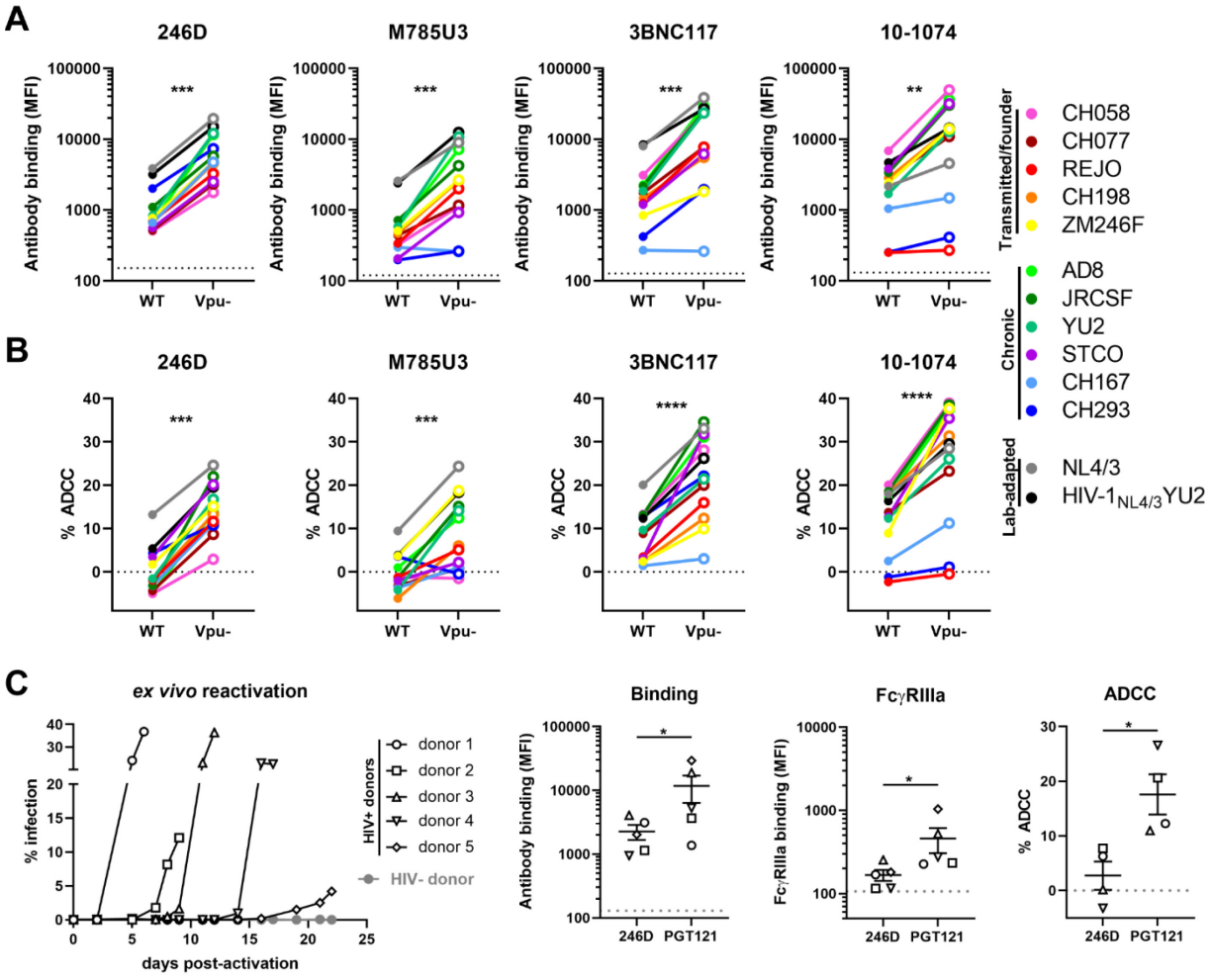
A
246D
M785U3
3BNC117
10-1074
Antibody binding (MFI)
WT
Vpu-
Transmitted/founder
CH058
CH077
REJO
CH198
ZM246F
Chronic
AD8
JRCSF
YU2
STCO
CH167
CH293
Lab-adapted
NL4/3
HIV-1NL4/3YU2
B
% ADCC
C
ex vivo reactivation
% infection
days post-activation
HIV+ donors
donor 1
donor 2
donor 3
donor 4
donor 5
HIV- donor
Binding
FcγRIIIa
ADCC
FcγRIIIa binding (MFI)
246D
PGT121

Figure 5.2.5 - The ability of Vpu to limit anti-Env ADCC responses is conserved among different HIV-1 strains.
(**A-B**) Primary $CD4^+$ T cells were infected with HIV-1 clade B and clade C transmitted/founder (CH058, CH077, REJO, CH198, ZM246F), chronic (AD8, JR-CSF, YU2, STCO, CH167, CH293) and lab-adapted (NL4/3, HIV-$1_{NL4/3}$YU2) wild-type (WT) strains or their Vpu- counterpart. (**A**) Cell surface staining performed using anti-gp41 nnAbs 246D and M785U3, as well as bNAbs 3BNC117 and 10-1074. Antibody binding was detected by using Alexa Fluor 647-conjugated anti-human secondary Abs. (**B**) Infected primary $CD4^+$ T cells were used as target cells and autologous PBMCs were used as effector cells in a FACS-based ADCC assay. (**C**) Primary $CD4^+$ T cells from five different ART-treated HIV-1-infected individuals were isolated and activated with PHA-L/IL-2 to expand the endogenous virus. Cell surface staining and ADCC experiments were performed upon reactivation. Antibody binding was detected using Alexa Fluor 647-conjugated anti-human secondary Abs or biotinylated recombinant soluble dimeric FcγRIIIa followed by the addition of Alexa Fluor 647-conjugated streptavidin. *Ex vivo*-expanded infected primary $CD4^+$ T cells from four HIV-1-infected individuals were used as target cells and autologous PBMCs were used as effector cells in a FACS-based ADCC assay. ADCC susceptibility was only measured when the percentage of infection ($p24^+$ cells) was higher than 10%. (**A,C**) The horizontal dotted lines represent the signal obtained in absence of mAb. (**A-C**) The antibody binding and FcγRIIIa graphs represent the mean fluorescence intensities (MFI) obtained from the infected $p24^+$ cell population. The ADCC graphs represent the percentages of ADCC obtained in the presence of the respective antibodies. Error bars indicate means +/- standard errors of the means (SEM). Statistical significance was tested using (**A-B**) a paired t test or Wilcoxon signed-rank test based on statistical normality or (**C**) a Mann-Whitney U test (*, $P < 0.05$; **, $P < 0.01$; ***, $P < 0.001$; ****, $P < 0.0001$; ns, nonsignificant).

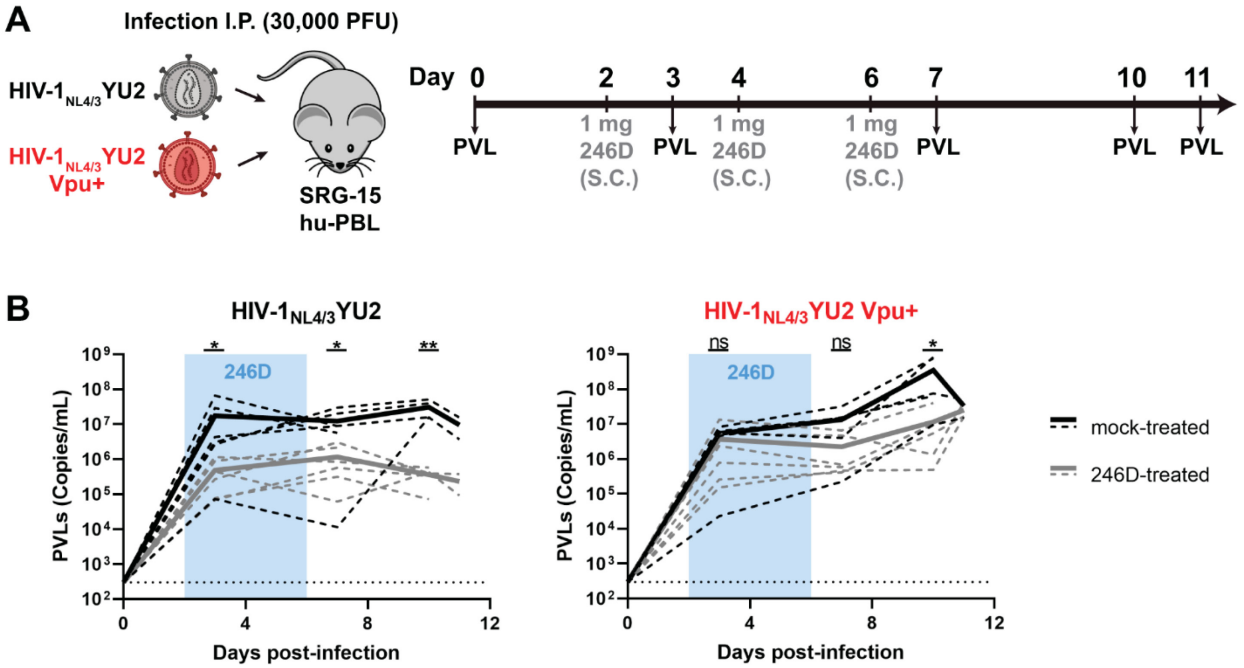

Figure 5.2.6 - Vpu promotes HIV-1 replication in humanized mice treated with non-neutralizing antibody 246D.

(**A**) Experimental outline. SRG-15-Hu-PBL mice were infected with HIV-$1_{NL4/3}$YU2 or its Vpu+ counterpart intraperitoneally. At day 2, 4 and 6 post-infection, mice were administered 1mg of 246D mAb subcutaneously (S.C.). Mice were bled routinely for plasma viral load (PVL) quantification. (**B**) PVL levels were measured by quantitative real-time PCR (limit of detection = 300 copies/mL, dotted line). Twelve mice were infected using each virus; six of them were mock-treated (black lines) and the other six were treated with 246D mAb (gray lines). PVL measurements for individual mice are shown as dashed lines and mean values for each regimen are shown as solid lines. Statistical significance was tested using an unpaired t test or a Mann-Whitney U test based on statistical normality (*, $P < 0.05$;**, $P < 0.01$; ns, nonsignificant).

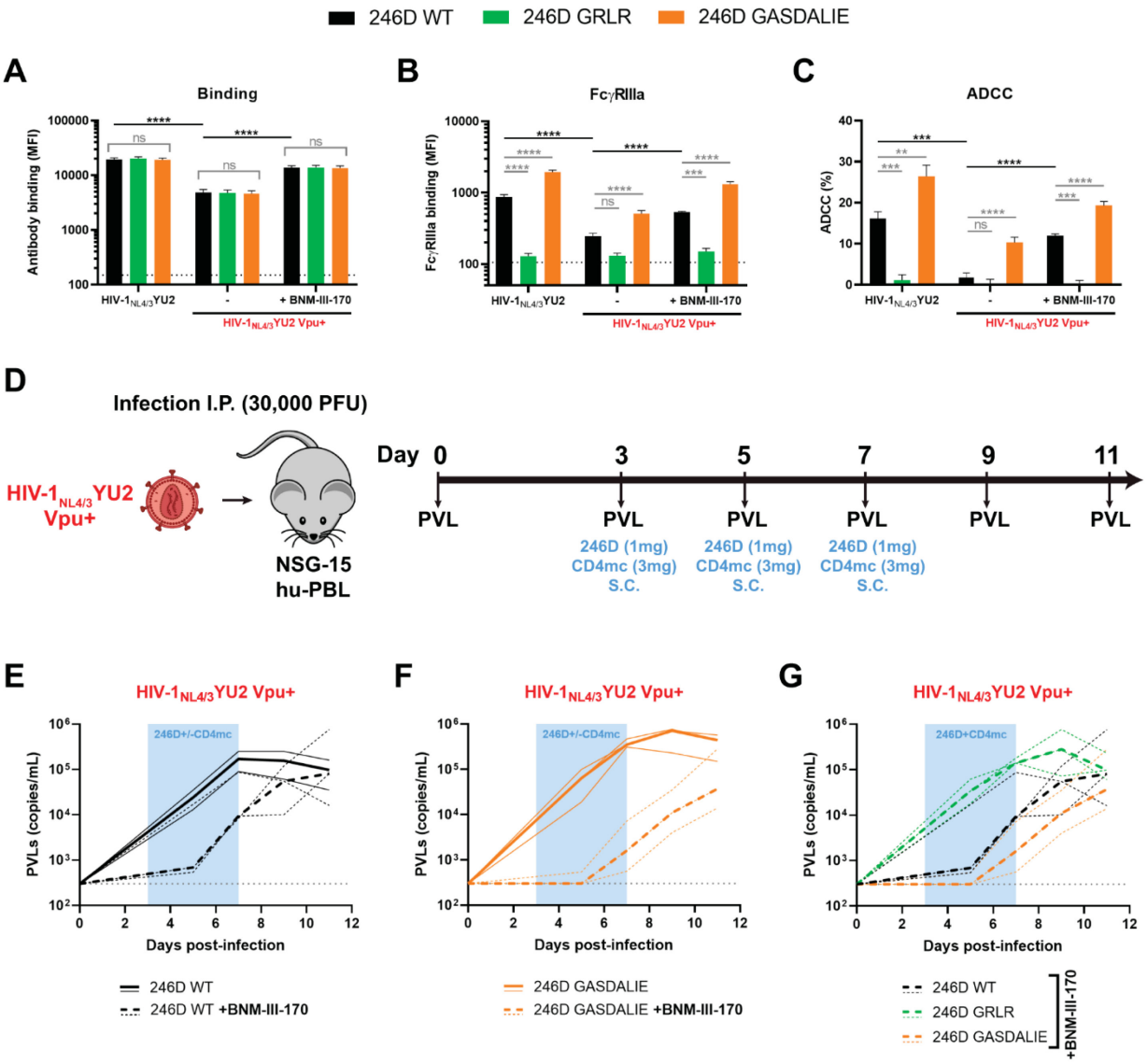
246D WT
246D GRLR
246D GASDALIE
A
Binding
Antibody binding (MFI)
HIV-1NL4/3YU2
HIV-1NL4/3YU2 Vpu+
+ BNM-III-170
B
FcγRIIIa
FcγRIIIa binding (MFI)
C
ADCC
ADCC (%)
D
Infection I.P. (30,000 PFU)
HIV-1NL4/3YU2 Vpu+
NSG-15 hu-PBL
Day 0 3 5 7 9 11
PVL
246D (1mg) CD4mc (3mg) S.C.
E
F
G
PVLs (copies/mL)
Days post-infection
246D+/-CD4mc
246D+CD4mc
246D WT
246D WT +BNM-III-170
246D GASDALIE
246D GASDALIE +BNM-III-170
246D GRLR
+BNM-III-170

Figure 5.2.7 - CD4 mimetics and Fc engineering enhance the antiviral activity of anti-gp41 nnAbs *in vivo*.

(**A-C**) Primary CD4+ T cells were either infected with HIV-$1_{NL4/3}$YU2 virus or its Vpu+ counterpart. Forty-eight hours post-infection, cell surface staining and ADCC responses were measured in presence of the anti-gp41 nnAb 246D WT or its Fc-mutated variants to impair (G236R/L328R; GRLR) or to enhance (G236A/S239D/A330L/I332E; GASDALIE) Fc-effector functions. Alternatively, cells infected with HIV-$1_{NL4/3}$YU2 Vpu+ were treated with CD4mc BNM-III-170 during staining and ADCC experiments. Antibody binding was detected using (**A**) Alexa Fluor 647-conjugated anti-human secondary Abs or (**B**) by using biotinylated recombinant soluble dimeric FcγRIIIa followed by the addition of Alexa Fluor 647-conjugated streptavidin. (**A-B**) The graphs represent the mean fluorescence intensities (MFI) obtained from the infected p24+ cell population using cells from five different healthy donors. The horizontal dotted lines represent the signal obtained in absence of mAb. (**C**) Infected primary CD4+ T cells were used as target cells and autologous PBMCs were used as effector cells in a FACS-based ADCC assay. The graph represents the percentages of ADCC obtained in the presence of the respective antibodies using cells from five different healthy donors. Error bars indicate means ± standard errors of the means (SEM). (**A-C**) Statistical significance was tested using a one-way ANOVA with a Holm-Sidak post-test or a Kruskal-Wallis test with a Dunn's post-test when comparing between the different 246D Fc variants and an unpaired t test or a Mann-Whitney U test when comparing between viruses or treatment. Appropriate statistical test (parametric or nonparametric) was applied based on dataset distribution normality (**, $P < 0.01$; ***, $P < 0.001$; ****, $P < 0.0001$; ns, nonsignificant). (**D**) Experimental outline. NSG-15-Hu-PBL mice were infected with HIV-$1_{NL4/3}$YU2 Vpu+ intraperitoneally. At day 3, 5 and 7 post-infection, mice were administered 1 mg of 246D mAb subcutaneously (S.C.) alongside or without of 3 mg of CD4mc BNM-III-170 (n=2-3 per cohort). (**E-G**) Plasma viral loads (PVL) were measured by quantitative real-time PCR (limit of detection = 300 copies/mL, dotted gray line) upon treatment with (**E**) 246D WT +/- CD4mc BNM-III-170, (**F**) 246D GASDALIE +/- CD4mc BNM-III-170 or (**G**) 246D WT, GRLR or GASDALIE in presence of CD4mc BNM-III-170. PVL measurements for individual mice are shown as thin lines and median values for each cohort as thick lines.

5.3.11 GRAPHICAL ABSTRACT

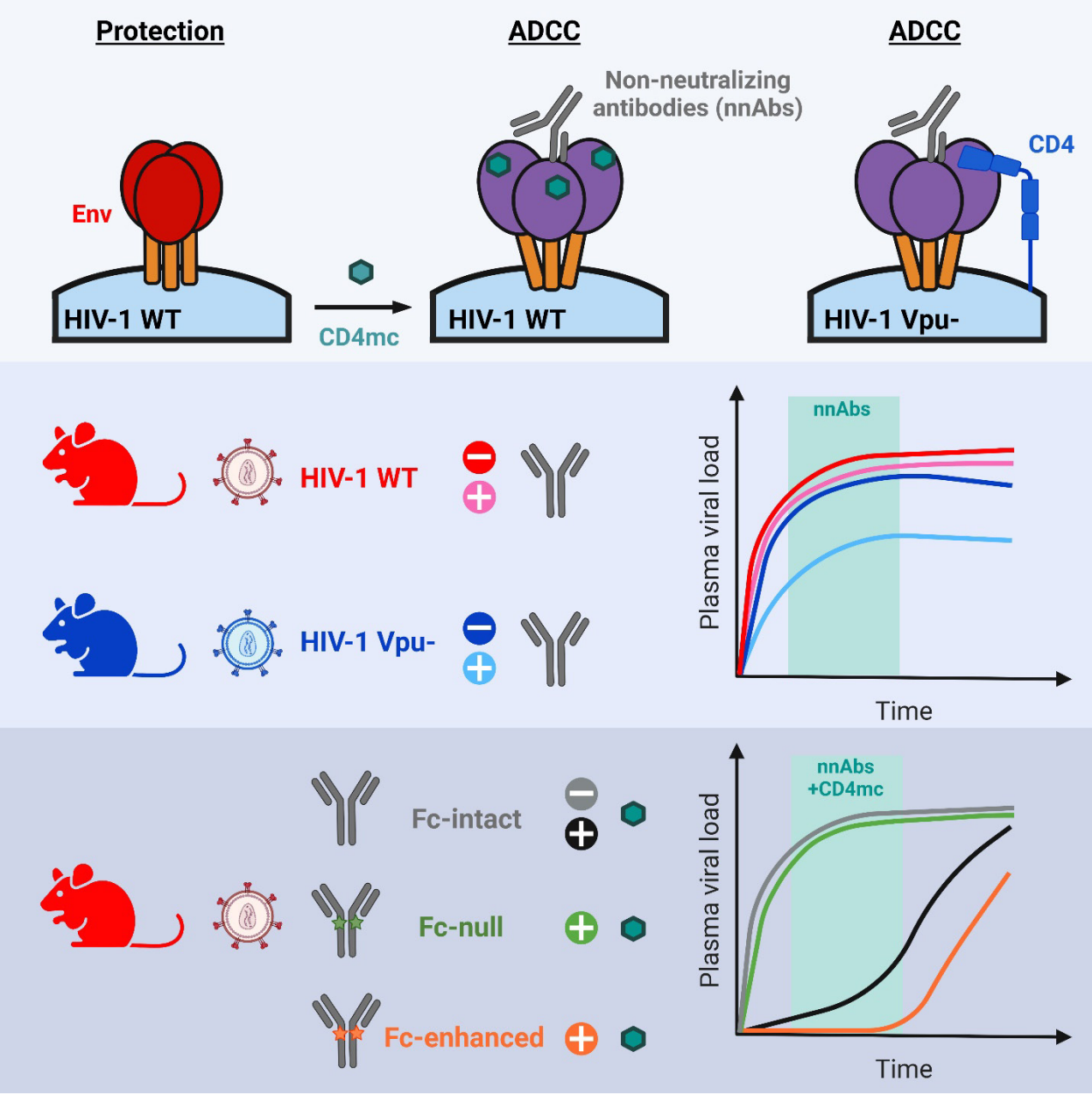

Figure 5.2.8 - Graphical abstract

HIV-1 Vpu restricts Fc-mediated effector functions mediated by anti-Env non-neutralizing antibodies *in vivo*

5.3.12 HIGHLIGHTS AND ETOC BLURB

Highlights

- Vpu limits HIV-1 Env recognition and ADCC responses mediated by nnAbs and bNAbs
- Vpu deletion impairs HIV-1 replication in humanized mice in presence of nnAbs
- CD4 mimetics and Fc engineering boost nnAbs antiviral activities *in vivo*

eTOC blurb

Prévost et al. demonstrate that the HIV-1 accessory protein Vpu protects infected cells from Fc-effector functions both *in vitro* and *in vivo*. Furthermore, it shows that non-neutralizing antibodies (nnAb) fail to alter HIV replication in humanized mice unless small CD4-mimetics are used to "open-up" Env and enable nnAb interaction.

5.3.13 SUPPLEMENTAL TABLE

Table 5.2.S1 - Cohort of HIV-1-infected individuals.

Group	Gender		Age (years)[a]	Days since infection[a]	Days since ART[a]	Days between infection and ART[a]	Viral load (copies/mL)[a]	CD4 count (cells/mm^3)[a]
	Male	Female						
Group 1 0-90 days untreated	10	0	40 [18-55]	68 [42-97]	N/A	N/A	60848 [132-391113]	470 [430-829]
Group 2 91-180 days untreated	10	0	38 [20-58]	135 [109-177]	N/A	N/A	21663 [6641-195302]	650 [420-1235]
Group 3 181-365 days untreated	10	0	31 [24-45]	240 [203-314]	N/A	N/A	27785 [1866-260852]	490 [230-770]
Group 4 2-5 years untreated	11	1	36 [23-54]	1158 [856-1810]	N/A	N/A	29234 [14255-809600]	421 [200-1311]
Group 5 2-5 years ART-treated	7	1	37 [23-60]	983 [794-1570]	690 [19-879]	428 [192-986]	50 [40-3337]	615 [170-1149]

[a]Values shown are group medians with ranges in bracket.

ART: antiretroviral therapy
N/A: not applicable

5.3.14 SUPPLEMENTAL FIGURES

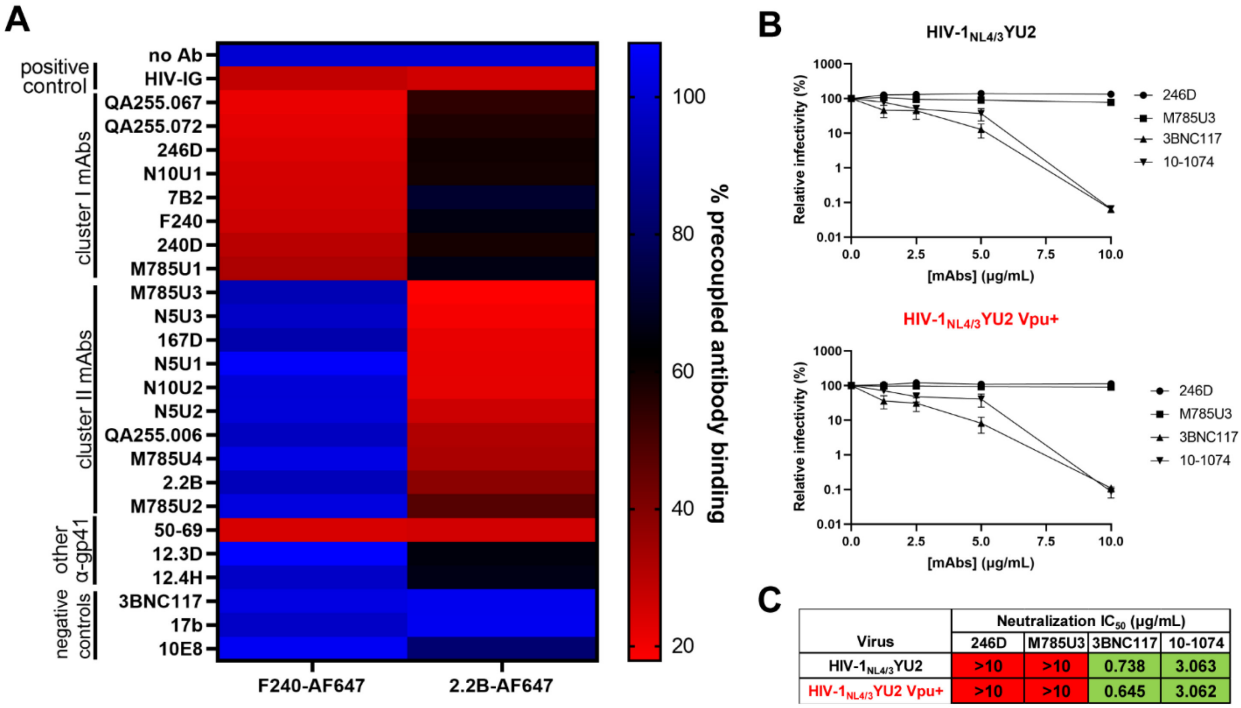

Figure 5.2.S1 - Classification of anti-gp41 non-neutralizing antibodies in two main clusters. (**A**) The binding of Alexa Fluor 647 (AF647)-precoupled anti-gp41 cluster I F240 mAb or anti-gp41 cluster II 2.2B mAb was evaluated on HIV-$1_{NL4/3}$YU2-infected cells in presence of a panel of unlabeled anti-gp41 nnAbs to determine epitope cross-competition. A pool of purified immunoglobulins from HIV-1-infected individuals (HIV-IG) was used as a positive control. Monoclonal antibodies with known non-competing epitopes (3BNC117, 17b, 10E8) were used as negative controls. (**B**) Lentiviral particles were produced from HIV-$1_{NL4/3}$YU2 IMC expressing Vpu or not. Viruses were incubated with serial dilutions of anti-Env mAbs (246D, M785U3, 3BNC117, 10-1074) at 37°C for 1 h prior to infection of TZM-bl target cells. The infectivity at each Ab concentration tested is shown as the percentage of infection without Ab for each virus. Quadruplicate samples were analyzed in each experiment. The data shown are the means of results obtained in three independent experiments. Error bars indicate means +/- the SEM. Neutralization half maximal inhibitory concentration (IC_{50}) values are summarized in (**C**).

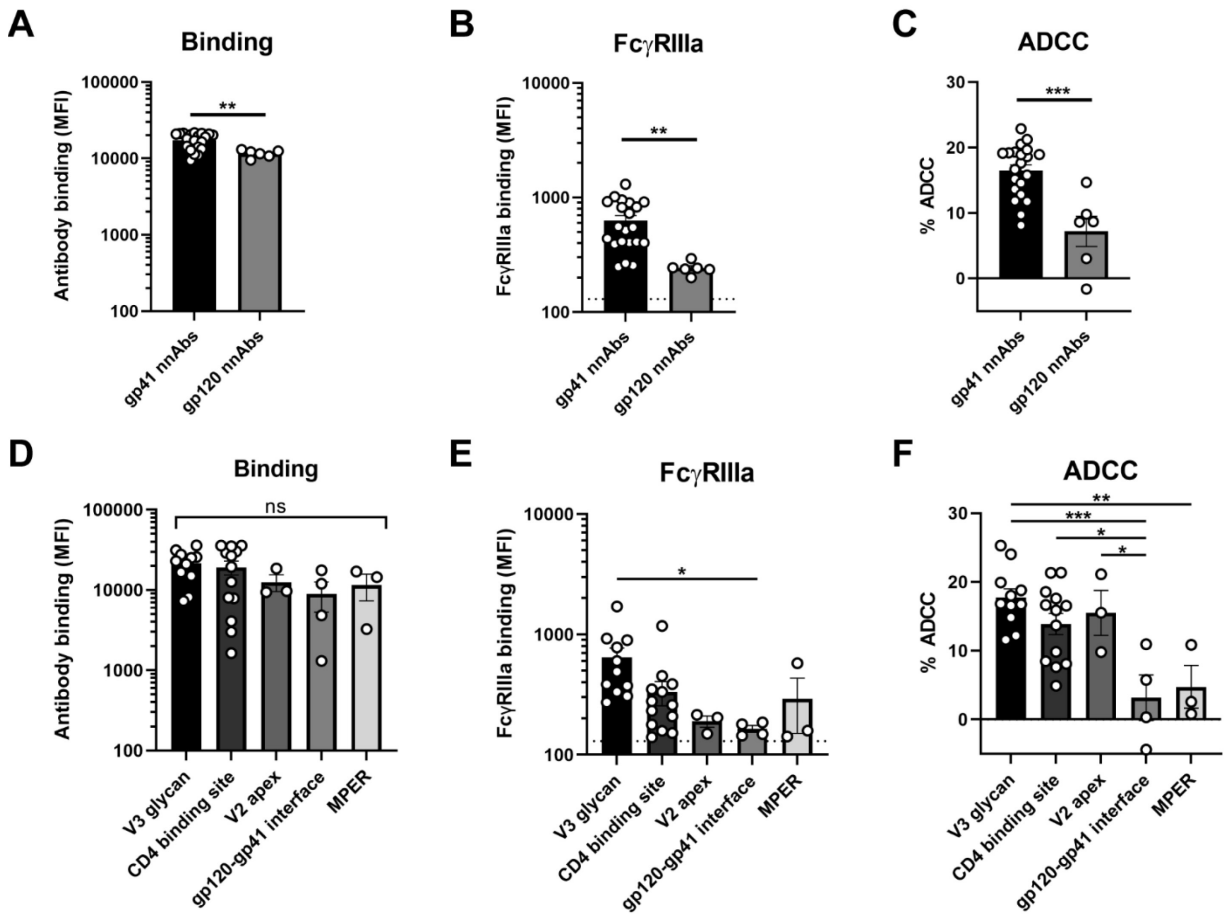

Figure 5.2.S2 - Epitope specificity dictates anti-Env ADCC responses mediated by nnAbs and bNAbs.

(**A-F**) Levels of antibody binding, FcγRIIIa binding and ADCC responses mediated by (**A-C**) nnAbs and (**D-F**) bNAbs as classified by epitope specificity (gp41 nnAbs, gp120 nnAbs; V3 glycan, CD4-binding site, V2 apex, gp120-gp41 interface, MPER) as performed on primary $CD4^+$ T cells infected with HIV-$1_{NL4/3}$YU2. Statistical significance was tested using (**A-C**) an unpaired t test or a Mann-Whitney U test and (**D-F**) a one-way ANOVA with a Holm-Sidak post-test or a Kruskal-Wallis test with a Dunn's post-test based on statistical normality (*, $P < 0.05$; **, $P < 0.01$; ***, $P < 0.001$; ****, $P < 0.0001$; ns, nonsignificant).

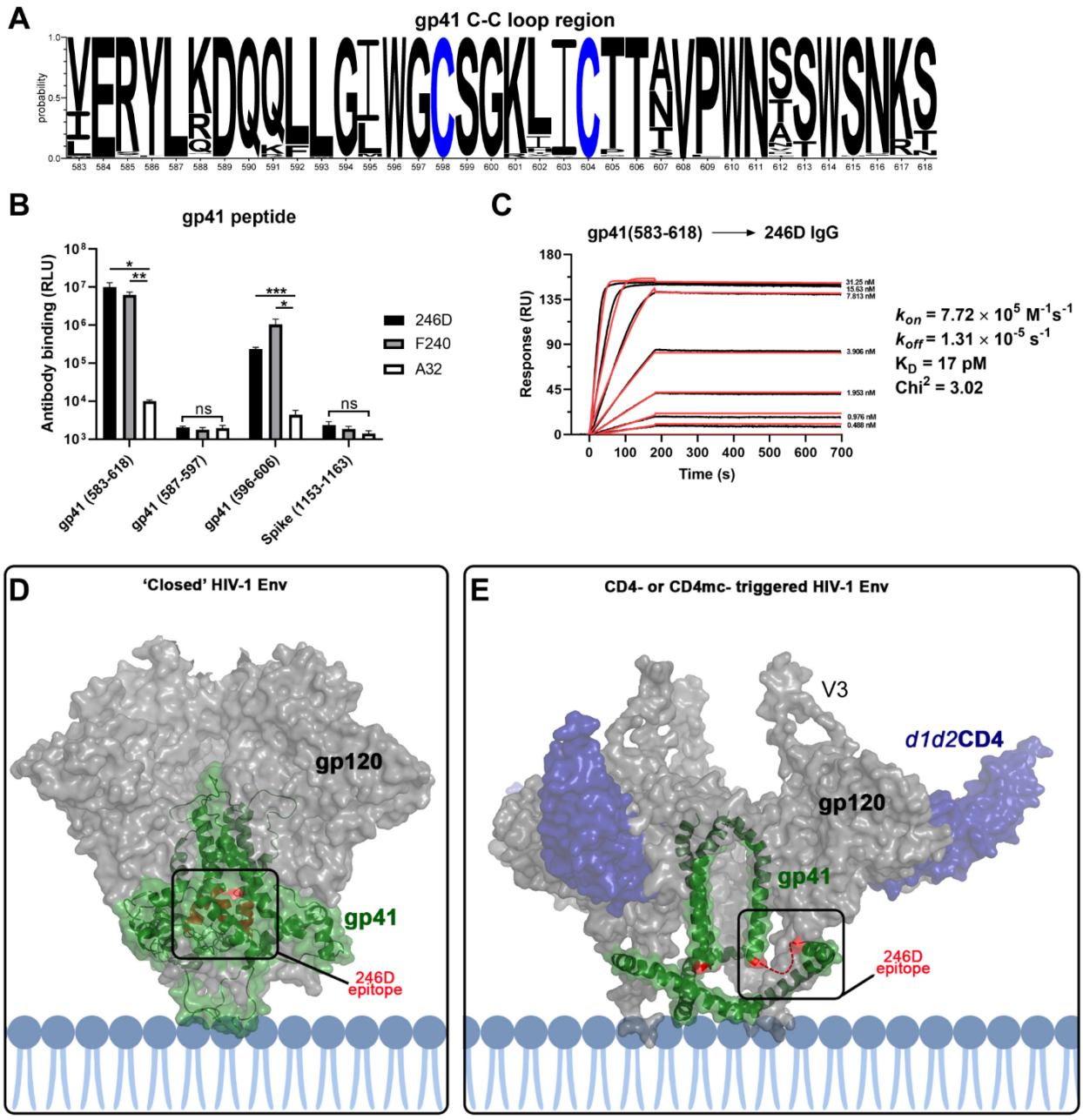
A
gp41 C-C loop region
probability
583 584 585 586 587 588 589 590 591 592 593 594 595 596 597 598 599 600 601 602 603 604 605 606 607 608 609 610 611 612 613 614 615 616 617 618
B
gp41 peptide
Antibody binding (RLU)
246D
F240
A32
ns
ns
gp41 (583-618)
gp41 (587-597)
gp41 (596-606)
Spike (1153-1163)
C
gp41(583-618) → 246D IgG
Response (RU)
Time (s)
31.25 nM
15.63 nM
7.813 nM
3.906 nM
1.953 nM
0.976 nM
0.488 nM
k_{on} = 7.72 × 10^5 M^{-1}s^{-1}
k_{off} = 1.31 × 10^{-5} s^{-1}
K_D = 17 pM
Chi^2 = 3.02
D
'Closed' HIV-1 Env
gp120
gp41
246D epitope
E
CD4- or CD4mc- triggered HIV-1 Env
V3
d1d2CD4
gp120
gp41
246D epitope

Figure 5.2.S3 - Monoclonal antibody 246D recognizes a gp41 linear peptide occluded in the closed Env trimer.
(**A**) Logo depiction of the frequency of each amino acid from the HIV-1 Env gp41 C-C loop region (residues 583-618) in all HIV-1 isolates. The height of the letter indicates its frequency among all strains. The 2019 Los Alamos database-curated filtered web Env alignment was used as the basis for this figure, which contains 6,223 individual Env amino acid sequences. Residue numbering is based on the HXB2 reference strain of HIV-1. (**B**) Indirect ELISA was performed using HIV-1 Env gp41 peptides corresponding to the C-C loop region, or a SARS-CoV-2 Spike S2 peptide as a negative control. Peptide-coated wells were incubated with anti-gp41 246D and F240 mAbs, as well as anti-gp120 cluster A A32 mAb as a negative control. Antibody binding was detected using HRP-conjugated anti-human IgG and was quantified by relative light units (RLU). The data shown are the means of results obtained in three independent experiments. Error bars indicate means ± the SEM. (**C**) 246D binding affinity and kinetics to gp41 C-C loop using surface plasmon resonance (SPR). The 246D IgG was immobilized as the ligand on a Protein A chip and HIV-1 gp41 (583-618) peptide used as analyte from 0.488 to 31.25 nM (2-fold serial dilution). Kinetic constants were determined using a 1:1 Langmuir model in bimolecular interaction analysis (BIA) evaluation software (experimental readings depicted in black and fitted curves in red). (**D-E**) Mapping of the ^{596}WGCSGKLICTT^{606} epitope within available structures of HIV-1 Env. (**D**) The closed conformation of HIV-1 Env (PDB: 6ULC) (PMID: 31931014) from a cryo-EM structure of full-length HIV-1 Env bound to the Fab of the antibody PG16 (not shown), with the 246D epitope highlighted in red. The 246D epitope is fully occluded in the closed the trimer and not accessible for antibody binding. (**E**) The CD4-triggered HIV-1 Env trimer (PDB: 3J70) (PMID: 26039348) from a computational model of full-length HIV-1 Env bound to the d1d2 domain of CD4 and the Fab of antibody 17b (not shown). In the CD4 triggered trimer the 246D epitope is largely disordered (highlighted with a broken red line for one of three gp41 protomers), but it is exposed at the surface of trimer and available for antibody recognition.

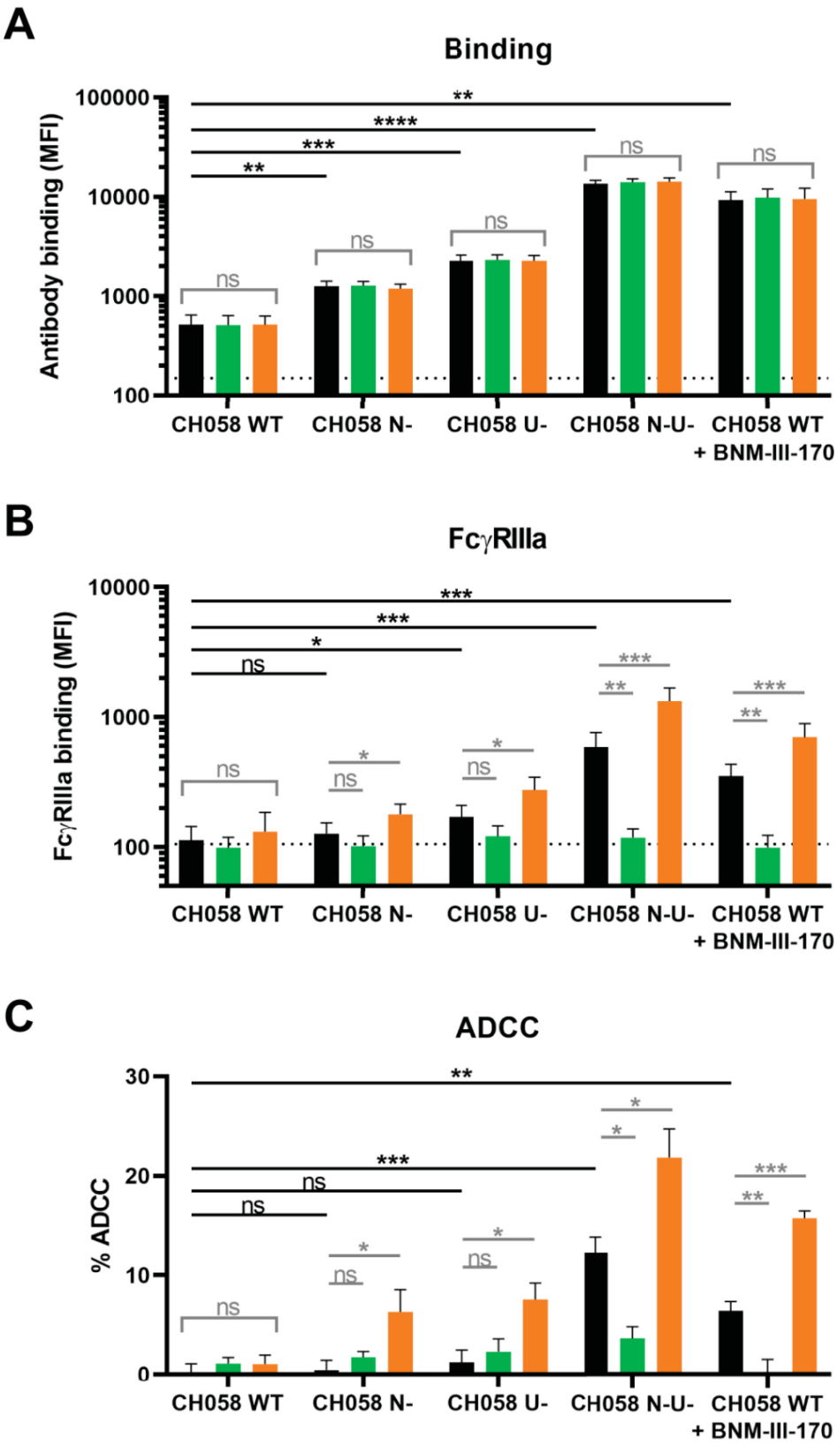
A
Binding
Antibody binding (MFI)
100000
10000
1000
100
**
****
***
**
ns
ns
ns
ns
ns
CH058 WT
CH058 N-
CH058 U-
CH058 N-U-
CH058 WT + BNM-III-170
B
FcγRIIIa
FcγRIIIa binding (MFI)
10000
1000
100
***
***
*
ns
***
**
***
**
*
*
ns
ns
ns
*
ns
CH058 WT
CH058 N-
CH058 U-
CH058 N-U-
CH058 WT + BNM-III-170
C
ADCC
% ADCC
30
20
10
0
**
*
*
***
ns
ns
*
ns
*
ns
***
**
ns
CH058 WT
CH058 N-
CH058 U-
CH058 N-U-
CH058 WT + BNM-III-170

Figure 5.2.S4 - CD4 mimetics and Fc modifications boost the capacity of anti-gp41 nnAbs to mediate ADCC responses.
(**A-C**) Primary CD4+ T cells were either infected with transmitted/founder virus CH058 wild-type (WT) or its Nef and/or Vpu-deleted counterparts (N-, U-, N-U-). Forty-eight hours post-infection, cell surface staining and ADCC responses were measured in presence of the anti-gp41 nnAb 246D WT or Fc-mutated to impair (G236R/L328R; GRLR) or enhance (G236A/S239D/A330L/I332E; GASDALIE) Fc-effector functions. Alternatively, cells infected with CH058 WT were treated with CD4mc BNM-III-170 during staining and ADCC experiments. Antibody binding was detected using (**A**) Alexa Fluor 647-conjugated anti-human secondary Abs or (**B**) by using biotinylated recombinant soluble dimeric FcγRIIIa followed by the addition of Alexa Fluor 647-conjugated streptavidin. (**A-B**) The graphs represent the mean fluorescence intensities (MFI) obtained from the infected p24+ cell population using cells from five different healthy donors. The horizontal dotted lines represent the signal obtained in absence of mAb. (**C**) Infected primary CD4+ T cells were used as target cells and autologous PBMCs were used as effector cells in a FACS-based ADCC assay. The graph represents the percentages of ADCC obtained in the presence of the respective antibodies using cells from five different healthy donors. Error bars indicate means ± standard errors of the means (SEM). (**A-C**) Statistical significance was tested using a one-way ANOVA with a Holm-Sidak post-test or a Kruskal-Wallis test with a Dunn's post-test when comparing between the different 246D Fc variants and an unpaired t test or a Mann-Whitney U test when comparing between viruses or treatment. Appropriate statistical test (parametric or nonparametric) was applied based on dataset distribution normality (*, $P < 0.05$; **, $P < 0.01$; ***, $P < 0.001$; ****, $P < 0.0001$; ns, nonsignificant).

CHAPITRE VI - UTILISATION DES MIMÉTIQUES MOLÉCULAIRES DE CD4 POUR OUVRIR ENV

6.1 Préambule

Dans ce chapitre, nous explorons de nouvelles stratégies afin de sensibiliser les cellules infectées à l'ADCC médiée par les nnAbs en modulant la conformation d'Env avec des mimétiques moléculaires de CD4 (CD4mc). Les CD4mc sont de petites molécules versatiles capables de neutraliser les particules virales en s'insérant dans la cavité Phe43 d'Env, ce qui leur permet de compétitionner directement avec la liaison de CD4 et également de libérer l'énergie nécessaire à la fusion en induisant des changements conformationnels menant à « l'ouverture » du trimère d'Env. Les CD4mc ont également été démontrés comme étant capable de sensibiliser spécifiquement les cellules infectées à la réponse ADCC médiées par le sérum HIV^+, tout en protégeant les cellules non-infectées avoisinantes de l'ADCC en empêchant la gp120 soluble d'interagir avec le CD4 présent à leur surface. Afin de continuer le développement de CD4mc plus puissants et à plus large spectre, nous avons identifié des mécanismes potentiels dictant la sensibilité et la résistance à ces molécules. Nous avons également développé des stratégies complémentaires pour promouvoir l'élimination des cellules infectées en présence de CD4mc et de nnAbs. Dans l'**article 10**, nous avons étudié certains résidus polymorphiques situés à l'intérieur et au pourtour de la cavité Phe43, présent naturellement dans une proportion non-négligeable des souches prédominantes en circulation. La présence d'une histidine en position 375, observée chez les souches CRF01_AE, confère une résistance complète au CD4mc en « remplissant » la cavité Phe43, tandis qu'une thréonine à cette position confère une sensibilité accrue au CD4mc en stabilisant l'insertion de la molécule dans cette cavité. La présence de polymorphismes dans les couches topologiques du domaine interne de la gp120 bordant la cavité Phe43 peut mener à une restructuration du site de liaison à CD4 et contribuer à la résistance de certaines souches au CD4mc. De nouveaux CD4mc pouvant accommoder ces variations sont présentement en développement. Dans l'**article 11**, nous avons identifié les niveaux d'Env présents à la surface des cellules infectées comme un autre facteur limitant dans l'induction de la réponse ADCC par les CD4mc. Afin de remédier à ce problème, nous proposons l'utilisation d'IFN-I ou d'IL-27, tous deux capables de stimuler l'expression du facteur de restriction BST-2. En dépit de l'activité de Vpu, l'augmentation de BST-2 par ces cytokines a pour effet d'augmenter l'accumulation d'antigènes viraux à la surface cellulaire, ce qui augmente significativement la capacité du CD4mc à sensibiliser les cellules infectées à la réponse ADCC médiée par les nnAbs.

ARTICLE 10

Le domaine interne de l'enveloppe du VIH-1 façonne la cavité Phe43 et le site de liaison à CD4

The HIV-1 Env gp120 Inner Domain Shapes the Phe43 Cavity and the CD4 Binding Site

Auteurs:

Jérémie Prévost[1,2], William D. Tolbert[3], Halima Medjahed[1], Rebekah T. Sherburn[3], Navid Madani[4,5], Daria Zoubchenok[1,2], Gabrielle Gendron-Lepage[1], Althea E. Gaffney[6], Melissa C. Grenier[6], Sharon Kirk[6], Natasha Vergara[9], Changze Han[12], Brendan T. Mann[7,8], Agnès L. Chénine[7,8], Adel Ahmed[9], Irwin Chaiken[9], Frank Kirchhoff[10], Beatrice H. Hahn[11], Hillel Haim[12], Cameron F. Abrams[9], Amos B. Smith III[6], Joseph Sodroski[4,5], Marzena Pazgier[3], Andrés Finzi[1,2,13]

Affiliations:

[1]Centre de Recherche du CHUM, Montreal, QC, Canada; [2]Département de Microbiologie, Infectiologie et Immunologie, Université de Montréal, Montreal, QC, Canada; [3]Infectious Diseases Division, Department of Medicine of Uniformed Services, University of the Health Sciences, Bethesda, MD, USA; [4]Department of Cancer Immunology and Virology, Dana-Farber Cancer Institute, Boston, MA, USA; [5]Department of Microbiology, Harvard Medical School, Boston, MA, USA; [6]Department of Chemistry, University of Pennsylvania, Philadelphia, PA, USA; [7]U.S. Military HIV Research Program, Walter Reed Army Institute of Research, Silver Spring, MD, USA; [8]Henry M. Jackson Foundation for the Advancement of the Military Medicine, Bethesda, MD, USA; [9]Department of Biochemistry and Molecular Biology, Drexel University College of Medicine, Philadelphia, PA, USA; [10]Institute of Molecular Virology, Ulm University Medical Center, Ulm, Germany; [11]Departments of Medicine and Microbiology, Perelman School of Medicine, University of Pennsylvania, Philadelphia, PA, USA; [12]Department of Microbiology, Carver College of Medicine, University of Iowa, Iowa City, IA, USA; [13]Department of Microbiology and Immunology, McGill University, Montreal, QC, Canada.

Contribution des auteurs:

Conceptualisation: **J.P.** et A.F.; Méthodologie: **J.P.**, M.P. et A.F.; Recherche: **J.P.**, W.D.T., H.M., R.T.S. N.M. et D.Z.; Ressources: **J.P.**, H.M., G.G.-L., A.E.G., M.C.G., S.K., B.T.M., A.L.C., A.A., I.C., F.K., B.H.H., A.B.S. et A.F.; Analyse formelle: **J.P.**, N.V. et C.H.; Visualisation: **J.P.**; Supervision: H.H., C.F.A., A.B.S., J.S., M.P. et A.F.; Obtention du financement: I.C., C.F.A.,

A.B.S., J.S., M.P. et A.F.; Rédaction - version originale: **J.P.**, J.S., M.P. et A.F.; Rédaction - révision et édition: **Tous les auteurs**.

Statut: Cet article a été publié dans *mBio*, le 26 mai 2020.
https://doi.org/10.1128/mBio.00280-20

6.2.1 RÉSUMÉ

Les glycoprotéines d'enveloppe du VIH-1 (Env) subissent des changements de conformation lors de l'interaction de la sous-unité gp120 avec le récepteur CD4. Les couches topologiques du domaine interne de la gp120 facilitent la transition d'Env vers la conformation liée à CD4. Le CD4 interagit avec la gp120 en introduisant sa phénylalanine 43 (Phe43) dans une cavité ("la cavité Phe43") située à l'interface entre les domaines interne et externe de la gp120. Les mimétiques moléculaires de CD4 (CD4mc) peuvent se lier dans la cavité Phe43 et déclencher des changements de conformation similaires à ceux induits par CD4. L'obtention de structures atomiques de CD4mc en complexe avec la gp120 CRF01_AE modifiée a révélé l'importance de ces couches du domaine interne de la gp120 dans la stabilisation de la cavité Phe43 et la formation du site de liaison à CD4. Notre étude révèle une interaction complexe entre le domaine interne de la gp120 et la cavité Phe43 et met en lumière des informations utiles pour le développement de CD4mc plus puissants.

6.2.2 ABSTRACT

The HIV-1 envelope glycoproteins (Env) undergo conformational changes upon interaction of the gp120 exterior glycoprotein with the CD4 receptor. The gp120 inner domain topological layers facilitate the transition of Env to the CD4-bound conformation. CD4 engages gp120 by introducing its phenylalanine 43 (Phe43) in a cavity ("the Phe43 cavity") located at the interface between the inner and outer gp120 domains. Small CD4-mimetic compounds (CD4mc) can bind within the Phe43 cavity and trigger conformational changes similar to those induced by CD4. Crystal structures of CD4mc in complex with a modified CRF01_AE gp120 core revealed the importance of these gp120 inner domain layers in stabilizing the Phe43 cavity and shaping the CD4 binding site. Our studies reveal a complex interplay between the gp120 inner domain and the Phe43 cavity and generate useful information for the development of more-potent CD4mc.

6.2.3 IMPORTANCE

The Phe43 cavity of HIV-1 envelope glycoproteins (Env) is an attractive druggable target. New promising compounds, including small CD4 mimetics (CD4mc), were shown to insert deeply into this cavity. Here, we identify a new network of residues that helps to shape this highly

conserved CD4 binding pocket and characterize the structural determinants responsible for Env sensitivity to small CD4 mimetics.

6.2.4 INTRODUCTION

The human immunodeficiency virus type 1 (HIV-1) envelope glycoproteins (Env) mediate virus entry into host cells to initiate the viral replication cycle. The gp120 exterior Env subunit mediates the initial interaction with the CD4 receptor. The gp120 phenylalanine 43 (Phe43) cavity is a conserved region of 150 $Å^3$ where Phe43 of CD4 makes numerous contacts with conserved gp120 residues and is connected with the gp120 inner domain and the coreceptor binding site via a water-filled solvent channel (1, 2). This interaction triggers major conformational changes allowing coreceptor (i.e., CCR5 and CXCR4) binding (3–10). Subsequent conformational changes in gp41 lead to the formation of the six-helix bundle, resulting in the fusion of the viral envelope and the target cell membrane (11, 12). CD4-induced (CD4i) conformational changes in the gp120 inner domain involve three flexible topological layers (layers 1, 2, and 3). Despite a lack of contact with CD4, the gp120 inner domain layers govern CD4 triggering by participating in conformational transitions within gp120 and regulating the interaction with gp41 (13, 14). Structural rearrangements between layer 1 and layer 2 were previously shown to facilitate the transition of the envelope glycoprotein trimer from the unliganded state to the CD4-bound state and to stabilize gp120-CD4 interactions (14–16). Layer 3 was previously shown to govern the efficiency of the initial gp120 interaction with CD4, a function that can also be fulfilled by filling the Phe43 cavity with a bulky residue at position 375 (13, 14, 17).

Env represents the only viral antigen exposed on the surface of virions and infected cells and thus is the primary target for antibodies (Abs). Despite targeting different epitopes, most broadly neutralizing antibodies (bNAbs) preferentially recognize the “closed” conformation of Env (18, 19). Conversely, CD4 binding forces Env to adopt “open” conformations (20, 21), allowing its recognition by non-neutralizing Abs (nnAbs) (22, 23). Env-CD4 complexes at the surface of HIV-1-infected cells were previously shown to be efficiently recognized by CD4-induced (CD4i) Abs, which are present in sera from HIV-1-infected individuals and can mediate potent antibody-dependent cellular cytotoxicity (ADCC) responses (24–28). HIV-1 evolved to minimize the exposure of these CD4i epitopes by limiting Env-CD4 interaction. HIV-1

accomplishes this through its Nef and Vpu accessory proteins, which decrease the overall amounts of Env (via Vpu-mediated BST-2 downregulation) and CD4 at the cell surface (23, 29, 30). In addition, efficient Env internalization also limits ADCC responses (31, 32). Motivated by the vulnerability of the CD4-bound conformation of Env to ADCC, new approaches to "force" Env to adopt this conformation using small CD4-mimetic compounds (CD4mc) have been developed (33). The antiviral activity of CD4mc is not limited to ADCC; these compounds can compete for Env-CD4 interaction, mediate viral particle inactivation by prematurely triggering Env, and sensitize infectious viral particles to neutralization by otherwise nnAbs (34–37). The potential clinical benefit of CD4mc was highlighted in two recent *in vivo* studies showing how CD4mc can act as prophylactic agents to decrease HIV-1 acquisition in humanized mice and simian-human immunodeficiency virus (SHIV)-challenged nonhuman primates (NHP) (38, 39).

Interestingly, Env transitions to the CD4-bound conformation can be modulated by single-residue substitutions. For example, the replacement of the well-conserved group M serine at position 375 by a large hydrophobic residue, such as tryptophan, fills the Phe43 cavity; this substitution alters Env conformation by predisposing gp120 to spontaneously assume a state closer to the CD4-bound conformation (13, 14, 40). While S375 is well conserved in the majority of group M HIV-1 isolates, CRF01_AE Env possesses a Phe43 cavity-filling residue at position 375 (H375) (41–43). The presence of H375 was linked to the natural exposure of CD4i epitopes in CRF01_AE strains, resulting in their enhanced susceptibility to ADCC responses (42). Besides modulating Env interaction with human CD4 (41), residue 375 was shown to modulate SHIV binding to rhesus monkey CD4 and replication in nonhuman primates (44), highlighting its critical role in viral pathogenesis. By performing structural, *in silico*, and functional analyses, using CD4mc as probes, we uncovered how the gp120 inner domain shapes the Phe43 cavity and the CD4 binding site.

6.2.5 RESULTS

Comparison of Phe43 cavity and coevolving inner domain layer residues among HIV-1 clades.

We previously reported that six residues within the gp120 inner domain layers coevolved with Phe43 cavity residue 375 to facilitate CD4 interaction (41). We analyzed all available HIV-1 sequences together or segregated by clades using the NIH Los Alamos HIV database to determine the degree of conservation of these residues located in layer 1 (residue 61), layer 2 (residues 105 and 108), and layer 3 (residues 474, 475, and 476) (collectively named LM, for layer mutants) and in the Phe43 cavity (residue 375). The consensus sequences of these residues from CRF01_AE strains diverge from those of all other major HIV-1 subtypes (clades A, B, C, D, F, G, and CRF02_AG) (**Fig. 6.1.1A**). Among the coevolving inner domain residues, most of the clades (except clade F [N474 and K476]) share the same consensus sequence (Y61, H105, I108, D474, M475, and R476), which differs from that seen with the residues found in CRF01_AE strains (H/Q61, Q105, V108, N474, I475, K476). Serine 375 is the predominant residue (75%) in all HIV-1 major subtypes, except for CRF01_AE (**Fig. 6.1.1A to C**). Other residues were found to occupy position 375 (T375, N375, I375, and M375), with T375 being present in more than 8% of all HIV-1 strains (**Fig. 6.1.1B**). T375 is present in clade B (16.9%), clade A1 (5%), and clade C (4.87%) but also in clade D (7.76%), CRF02_AG (5.26%), and clade F (2.27%). Interestingly, CRF01_AE strains have a highly conserved histidine at position 375 (H375; >99%) (41–43).

Phe43 cavity and gp120 inner domain layer changes render CRF01_AE strains susceptible to CD4mc antiviral activities.

To evaluate the potential impact of the LM residues on shaping the Phe43 cavity, we decided to use CD4mc as probes. Several cocrystals of different CD4 mimics and gp120 cores exist, providing detailed structural information regarding their mode of interaction within the cavity (1, 37, 45–51). Briefly, both CD4mc (molecular weight [MW], ~500 Da) and CD4 miniproteins (~3 kDa) were optimized to display a large hydrophobic group (phenyl or cyclohexyl ring) that projects deeply into the Phe43 cavity, allowing them to reach the cavity edge where residue 375 is located. These projections were found to go deeper into the Phe43 cavity than CD4 Phe43 residue itself, rendering these molecules more sensitive to changes occurring within the

cavity. It has been previously reported that the presence of bulky cavity-filling residues at this position (H375, W375, Y375, R375) confers resistance to CD4mc and CD4 miniproteins by abrogating their interaction deep within the Phe43 cavity (34, 36, 47, 48, 50, 52, 53). Replacement of the naturally occurring CRF01_AE H375 with a serine residue (H375S) has been shown to reduce CD4 binding. Introduction of the LM substitutions (H/Q61Y, Q105H, V108I, N474D, I475M, and K476R) restored this interaction (41). However, whether these Phe43 cavity and inner domain changes affect CD4mc sensitivity has not yet been determined. First, we evaluated the effect of the H375S change on the sensitivity of two CRF01_AE isolates (tier 1 92TH023 and tier 2 CM244) to neutralization by different CD4 mimics, including soluble CD4 (sCD4), CD4mc (BNM-III-170), and a CD4 miniprotein (M48U1) (33, 54). In agreement with previous results (41), replacement of histidine 375 by a serine residue (H375S) in both HIV-1_{CRF01_AE} Envs completely abolished the susceptibility of pseudotyped virions to sCD4 neutralization (**Fig. 6.1.2A and B to G**). Viral particles bearing both CRF01_AE Envs were resistant to neutralization by BNM-III-170 and M48U1; this was expected due to the presence of the cavity-filling histidine at position 375 (H375). Interestingly, replacement of the bulky histidine by a serine at this position (H375S) did not restore neutralization sensitivity to these CD4 mimics (**Fig. 6.1.2C to G**). However, the H375S change in combination with the LM mutations (LM plus HS [LM+HS]) dramatically enhanced the susceptibility of both CRF01_AE strains to neutralization by both CD4 mimics. Of note, the presence of different combinations of single-layer or multiple-layer changes together with the H375S change was not sufficient to restore sensitivity to neutralization by BNM-III-170 or M48U1 (see **Fig. 6.1.S1C to G** in the supplemental material). This was different from the results seen with respect to sCD4 neutralization, where viruses bearing LM changes without the Q61Y change were also sensitive to sCD4 neutralization (**Fig. 6.1.S1A and G**). These data highlight subtle differences in the mode of CD4mc and sCD4 recognition of Env. Altogether, these results indicate that all of the LM changes are required to restore CD4mc sensitivity to CRF01_AE strains presenting an "empty" (H375S) Phe43 cavity.

As a small residue at position 375 such as serine appears to be required for CD4mc sensitivity, we investigated the possibility that another naturally occurring small residue such as threonine (T), isoleucine (I), or asparagine (N) might affect HIV-1 sensitivity to CD4mc. We first introduced these changes into clade B HIV-1_{JRFL} Env and performed neutralization assays using

the CD4mc BNM-III-170. Among all the residue 375 substitutions tested, T375 was found to be more sensitive to BNM-III-170 inhibition than the wild type (WT) (S375) and all the other variants (**Fig. 6.1.3A**). We then introduced this change into a CRF01_AE Env alone (H375T) and in combination with the six layer mutations (LM+HT). Strikingly, the H375T change was sufficient to sensitize the CRF01_AE strain to BNM-III-170 neutralization in the absence of the LM mutations. Thus, despite having similar small side chains, T375 was found to be sufficient to sensitize the CRF01_AE virus to neutralization by BNM-III-170 whereas S375 required the LM mutations to do so. Addition of the LM changes together with H375T (LM+HT) further increased the sensitivity of the CRF01_AE virus to BNM-III-170 neutralization, resulting in levels comparable to those seen with the LM+HS mutant (**Fig. 6.1.3B and D**). We confirmed the enhanced susceptibility of T375-bearing viruses to BNM-III-170 with additional clade B (YU2) and clade A1 (BG505) strains. Increased neutralization by CD4mc was seen in the presence of T375 in these two strains (**Fig. 6.1.3C and D**). Strikingly, HIV-1_{BG505} has intrinsic resistance to CD4mc BNM-III-170 which can be overcome by the presence of T375.

Since CD4mc were also shown to sensitize HIV-1-infected cells to ADCC by CD4-induced (CD4i) Abs present in HIV-positive (HIV^+) sera (27, 33, 55–57), we evaluated the impact of the Phe43 and LM changes on the susceptibility of CRF01_AE-infected primary $CD4^+$ T cells to ADCC mediated by HIV^+ sera in the presence of the CD4mc BNM-III-170. Briefly, primary $CD4^+$ T cells cultured from uninfected individuals were infected with the wild-type (WT) CRF01_AE transmitted/founder (TF) 40061 strain or with an isogenic virus with the LM and 375 changes. This infectious molecular clone (IMC) was isolated from a participant in the acute HIV-1 infection RV217 cohort (58). In line with the results presented in **Fig. 6.1.2 and 6.1.3** (see also **Fig. 6.1.S1**), replacement of CRF01_AE H375 with a threonine, but not a serine, was sufficient to gain sensitivity to CD4mc, leading to an increase in binding and ADCC mediated by HIV^+ sera (**Fig. 6.1.4**). Addition of the LM changes to the resistant H375S variant conferred BNM-III-170 sensitivity but did not further enhance the susceptibility of the H375T variant.

To gain a better understanding of the impact that the LM and 375 changes have on Env conformation, we developed an assay to indirectly measure the capacity of BNM-III-170 to interact with Env. Briefly, CD4-negative cells were transfected with HIV-1_{CRF01_AE} 92TH023 or

CM244 Env variants. At 48 h post-transfection, Env-expressing cells were incubated with sCD4 in the presence of the CD4mc BNM-III-170 or an equivalent amount of the vehicle (dimethyl sulfoxide [DMSO]). Binding of sCD4 to cell surface Env was detected using an anti-CD4 mAb (OKT4), which recognizes the CD4 D3 domain and therefore does not compete for gp120 binding. The ability of BNM-III-170 to interact with Env was inferred by calculating the decrease in the level of sCD4 binding to Env in the absence of CD4mc (DMSO) or in its presence (**Fig. 6.1.3E to G**). In agreement with neutralization results, the occupancy of the Phe43 cavity of CRF01_AE strains by BNM-III-170 was increased as a consequence of a combination of Phe43 cavity and inner domain changes (LM+HS and LM+HT) or of the H375T mutation change alone. We observed a decrease of at least 50% in sCD4 binding for both CRF01_AE strains with these mutants (**Fig. 6.1.3E and F**). Similarly, CD4mc competed more efficiently for sCD4 binding in the presence of the S375T change for the three additional Envs tested (JRFL, YU2, BG505) (**Fig. 6.1.3G**). Using this assay, we also tested a panel of anti-Env antibodies, where bNAbs (3BNC117, NIH45-46 G54W, PG16, PGT151, and PGT128) preferentially recognize the "closed" trimer (18, 19, 59) and nnAbs (17b, 19b, F240, and A32) preferentially recognize the "open" trimer (18, 19, 27, 60). In agreement with the higher level of occupancy of the Phe43 cavity by BNM-III-170 in the presence of T375 or the LM+HS mutations, for these mutants, treatment of Env-expressing cells with the CD4mc BNM-III-170 more effectively decreased binding of bNAbs to the "closed" Env conformation (**Fig. 6.1.S2A and B and E to G**) and concomitantly enhanced binding of nnAbs to the "open" conformation (**Fig. 6.1.S2C and D and H to J**). Overall, the nature of the residue 375 and its coevolving inner domain residues regulate the susceptibility of the CRF01_AE strains to both neutralization and ADCC.

Phe43 cavity and layer residues modulate the sensitivity of HIV-1 of major clades to CD4mc antiviral activities.

In contrast with CRF01_AE strains, most strains from pandemic HIV-1 major clades (clades A, B, C, D, G, and CRF02_AG) harbor inner domain residues that coevolved with the presence of a small residue at position 375 (e.g., S375), making them potentially sensitive targets for CD4mc antagonist action. The presence of naturally occurring T375 in a significant fraction of these clades (up to 16.9% in clade B) might affect the susceptibility of these strains to CD4mc. Considering that T375 was found to be the residue that conferred the highest sensitivity to CD4mc

in the clade B JRFL strain (**Fig. 6.1.3**) and among all CRF01_AE strains tested (**Fig. 6.1.3 and 6.1.4**), we introduced the T375 change into the HIV-1_{JRFL} IMC and evaluated the capacity of BNM-III-170 to expose epitopes recognized by sera from 10 HIV-1-infected individuals at the surface of infected primary $CD4^+$ T cells. In line with the neutralization data (**Fig. 6.1.3**), replacement of S375 with a threonine residue (S375T) significantly enhanced the recognition of JRFL-infected cells by HIV^+ sera in the presence of BNM-III-170 (**Fig. 6.1.5A and B**). We also tested two additional primary clade B viruses (HIV-1_{CH58} and HIV-1_{CH77}) that naturally harbor T375 (**Fig. 6.1.6A**). Replacement of T375 in these two different TF viruses with a serine (T375S) strongly reduced the sensitivity of HIV-1_{CH77} to CD4mc but appeared to have no effect on HIV-1_{CH58} (**Fig. 6.1.5B**). However, the CH58 T375S mutant was less sensitive to CD4mc BNM-III-170 at concentrations lower than the concentration used in the staining and ADCC assays (50 μM) (**Fig. 6.1.6B**). A similar phenotype was also observed with another clade B strain (HIV-1_{YU2}), where the variant with T375 was more sensitive to BNM-III-170 at low concentrations (**Fig. 6.1.6C**). In all cases, a threonine residue at position 375 enhanced Env recognition by HIV^+ sera in the presence of BNM-III-170 (**Fig. 6.1.5A and B and 6.1.6B and C**). Importantly, enhanced recognition translated into enhanced susceptibility to ADCC responses (**Fig. 6.1.5C and D**).

Next, we evaluated a panel of 12 clade B and clade C primary viruses, including viruses from acute infections (transmitted/founder strains) (CH40, CH58, CH77, CH185, CH198, CH236, CH470, CH505, and CH850) and chronic infections (CH167, RHGA, STCO), for their susceptibility to BNM-III-170. We observed a significant increase in binding of HIV^+ sera by BNM-III-170 with all viruses tested but one (CH198) (**Fig. 6.1.5E**); the increase was greater for viruses harboring a naturally occurring T375 (**Fig. 6.1.5F**). The higher responsiveness of viruses harboring a T375 (CH58, RHGA, STCO, CH77, and CH236) to BNM-III-170 led to a significant increase in ADCC responses for all HIV^+ sera tested, whereas only a few (2/7) viruses harboring a S375 showed a significant increase in ADCC upon CD4mc addition (**Fig. 6.1.5G and H**). In brief, the presence of a naturally occurring T375 residue in clade B and clade C primary virus Envs increases susceptibility to CD4mc.

Since T375 was found to confer the highest sensitivity to BNM-III-170 in all strains tested, we sought to determine whether this was specific to this CD4mc or applicable to others as well.

Therefore, we selected different generations and families of CD4mc known to engage gp120 within the Phe43 cavity. The NBD-556 compound was originally identified through a screen for Env-CD4 interaction inhibitors (61) and consists of a halogenated phenyl ring linked with a tetramethyl-piperidine via an oxalamide linker (**Fig. 6.1.7A**). The DMJ-II-121 compound was derived from the NBD-556 analog JRC-II-191 through the substitution of the piperidine ring for an indane ring with a guanidinium group at position 2 (**Fig. 6.1.7B**) to improve its Env antagonism potency (46). Other DMJ-II-121 analogs were synthesized to harbor additional chemical groups on the indane ring at position 5 (BNM-III-170, BNM-IV-147, SMK-II-48, MCG-III-051), position 6 (BNM-IV-197, JP-III-48, AEG-I-249, AEG-I-259), or position 7 (MCG-III-051) (45). To this panel of small molecules, we added a new compound (MCG-IV-210) derived from a recent high-throughput screen aimed to identify small molecules able to stabilize the CD4-bound conformation (37). Its structure resembles that of the NBD-556 analogs, but it has a shorter amide linker and an N-substituted piperidine ring (**Fig. 6.1.7C**). The panel of CD4mc was tested for the ability to induce Env conformational changes at the surface of primary $CD4^+$ T cells infected with HIV-1_{CH58} WT or its T375S variant. Strikingly, all CD4mc tested were able to increase the exposure of the epitope recognized by the CD4i 17b mAb at the surface of WT-infected cells to similar extents (**Fig. 6.1.7D to F**). Introduction of the T375S change significantly diminished this ability for the less potent compounds, including MCG-IV-210, both NBD-556 analogs, and two DMJ-II-121 analogs (AEG-I-259 and MCG-III-051). The ability of these five CD4mc to enhance 17b binding to HIV-1_{JRFL}-infected cells was increased by the replacement of S375 with a threonine residue (**Fig. 6.1.7F**). Similar results were obtained in experiments evaluating the ability of these CD4mc to increase the binding of HIV^+ sera to CH58-infected and JRFL-infected cells (**Fig. 6.1.7G to I**). Altogether, our binding and functional analyses indicate that natural HIV-1 polymorphism in Ser/Thr 375 modulates Env interaction with CD4mc of different classes.

As shown in **Fig. 6.1.2 to 6.1.4** (see also **Fig. 6.1.S1**), specific inner domain layer residues (LM mutations) also modulate Env sensitivity to CD4mc in CRF01_AE strains. We investigated whether this could be extended to strains from other HIV-1 major clades. We replaced HIV-1 consensus inner domain residues in the clade B HIV-1_{YU2} Env with the residues that specifically coevolved with H375 in CRF01_AE strains (Y61H, H105Q, I108V, D474N, M475I, R476K). These changes (LM mutations) were introduced in combination with different residues at position

375 (S375, T375, or H375). Remarkably, using the sCD4 binding competition assay, the introduction of these LM changes totally abrogated the sensitivity of YU2 Env to CD4mc, but the presence of the S375T change (LM+ST) restored sensitivity to BNM-III-170 (**Fig. 6.1.6D**). The S375H change completely abrogated CD4mc interaction regardless of the LM mutations (**Fig. 6.1.6D**), as seen with CRF01_AE strains (**Fig. 6.1.2, 6.1.3, and 6.1.4**; see also **Fig. 6.1.S1**). Revisiting the data shown in **Fig. 6.1.5F**, the three strains that were the least sensitive to BNM-III-170 were found to have inner domain residues shared with the CRF01_AE consensus sequence (**Fig. 6.1.1C and 6.1.6A**): CH505 (V108, N474, and K476), CH470 (N474 and K476), and CH198 (N474 and K476). Some of the LM mutations were also naturally found in two clade B strains used in this study: JRFL (Q105) and CH77 (V108, N474, and K476) (**Fig. 6.1.6A**). Interestingly, replacement of these residues with residues that coevolved with S375 was found to increase CD4mc sensitivity for both strains, regardless of the nature of the residue at position 375 (**Fig. 6.1.6E and F**). Altogether, our data show that the nature of the residue at position 375 and the coevolving gp120 inner domain layers modulate the susceptibility of HIV-1 major clades to CD4mc.

Structural analysis of the interaction of CD4mc and HIV-1 gp120 with Phe43 cavity and inner domain layer changes.

Functional analysis clearly indicates that the LM+HT Env variant is the most effective at binding CD4mc. To better understand the structural basis for the role of the LM, HS, and HT mutations in reshaping the Phe43 cavity and in CD4mc binding, we solved the crystal structures of the CRF01_AE 93TH057 gp120 extended core ($gp120_{93TH057}$ $core_e$ [49]) containing the LM+HS changes in complex with two CD4mc compounds: MCG-IV-210 and BNM-III-170. The LM+HS $gp120_{93TH057}$ $core_e$–MCG-IV-210 complex was solved to 2.5-Å resolution (see **Table 6.1.S1** in the supplemental material; see also **Fig. 6.1.S3**), enabling an assessment of the impact of the HS mutation by comparison to the LM+HT $gp120_{93TH057}$ $core_e$–MCG-IV210 complex structure solved by us previously to 2.65-Å resolution (PDB identifier [ID] 6P9N) (37). We also solved the structure of the LM+HS $gp120_{93TH057}$ $core_e$–BNM-III-170 complex to 2.65-Å resolution (**Table 6.1.S1**), allowing a comparison with the structure of the HS $gp120_{93TH057}$ $core_e$ (the CRF01_AE 93TH057 gp120 $core_e$ with a single-point H375S mutation) in complex with DMJ-II-121, a compound closely related to BNM-III-170 (PDB ID 4I54). DMJ-II-121 lacks a (methylamino)-

methyl addition to position 5 of the indane ring but is identical to BNM-III-170 in all other respects. We first sought to understand the exclusive role of residue 375, in the context of the CRF01_AE LM gp120 variant, in influencing the interaction with CD4mc. We analyzed the complex structures of LM+HS and LM+HT $gp120_{93TH057}$ $core_e$s bound to the same MCG-IV-210 compound, which displayed the highest sensitivity to position 375 changes among all CD4mc tested (**Fig. 6.1.7**). As shown in **Fig. 6.1.8A**, MCG-IV-210 bound within the hydrophobic Phe43 cavity of both gp120 mutants, anchoring deeply into the cleft. The buried surface area (BSA) measurements of the complexes were 678 $Å^2$ (243 $Å^2$ from gp120 and 435 $Å^2$ from the compound) and 699 $Å^2$ (252 $Å^2$ from gp120 and 447 $Å^2$ from the compound) for the complexes of LM+HS $gp120_{93TH057}$ $core_e$–MCG-IV-210 and LM+HT $gp120_{93TH057}$ $core_e$–MCG-IV-210, respectively, indicating that more surface was buried by the LM+HT variant (**Fig. 6.1.8C**). In addition, while the orientations of MCG-IV-210 in the binding pocket of both complexes were identical, the shapes of the pockets differed. The H375T mutation added one methyl group compared with the H375S mutation, and this addition led to the closing of the Phe43 cavity from the top. The T375 γ-carbon methyl group made a number of additional contacts with the halogenated aromatic ring of the compound, but this did not lead to an increase in the BSA at position 375 due to rearrangement of the Phe43 cavity. In fact, the presence of Thr375 led to a notable decrease in the BSA within the cavity, where residues Thr257 on the left side, Phe382 and Asn425 on the right side, and Trp427 on the bottom made more contact with the compound in the LM+HS mutant. However, residues surrounding the cavity vestibule, including Asp368, Glu370, and Ile371 at the top of the Phe43 cavity, Asn424 on the right side, and Gly472, Gly473, and Met475 at the bottom (as orientated in **Fig. 6.1.8B**), made more contact with MCG-IV-210 and increased the BSA in the LM+HT mutant. The increases in BSA for residues lining the Phe43 cavity may further augment the LM mutant stabilization of layer 3, which may provide an explanation for the added potency for MCG-IV-210 in the LM+HT mutant.

Next, to better understand the exclusive role of the LM residues in reshaping the Phe43 cavity for effective interaction with CD4mc, we analyzed the complex structures of BNM-III-170 and DMJ-II-121 co-crystalized with $gp120_{93TH057}$ $core_e$s that differed only in the LM residues (**Fig. 6.1.8D**). Structural analyses indicated that the LM+HS gp120 $core_e$–BNM-III-170 complex buried more BSA and was stabilized by more contacts than the HS gp120 $core_e$–DMJ-II-121 complex

(**Fig. 6.1.8E and F**). Although some contacts observed in LM+HS gp120 $core_e$–BNM-III-170 complex were not present in HS gp120 $core_e$–DMJ-II-121 complex due to its smaller size [i.e., the hydrogen bond extending from the carbonyl of Gly472 to the (methylamino)methyl addition to BNM-III-170 and contacts extending from the (methylamino)methyl to Ala281, Thr283, and Thr455; **Fig. 6.1.8F**]**,** there was a significant increase in the BSA of the remaining contact residues; these contacted equivalent compound atoms in the BNM-III-170 LM+HS gp120 $core_e$ complex (313 $Å^2$ for BNM-III-170 [296 $Å^2$ when the methylamino-methyl contribution is subtracted] versus 271 $Å^2$ for DMJ-II-121). These included contacts mediated by the highly conserved Glu370 and Ile424 residues as well as Ser375 itself, all capping the CD4mc in the Phe43 cavity from the top. There were also increased contacts to the 470-to-475 loop region (e.g., residues Gly472, Asp474, and Met475). Interestingly, two of the LM residues, Asp474 and Met475, contributed directly to CD4mc binding and increased BSA. The LM Ile475-to-Met mutation decreased the size of the Phe43 cavity and increased the hydrophobic surface available for CD4mc binding. On the other hand, Asp474 stabilized the interlayer interactions by forming a hydrogen bond to Arg476. This tightening of one side of the Phe43 binding pocket likely also led to the increase in BSA for residues on the opposite side of the pocket, including Ser375 and Gly429 (**Fig. 6.1.8F**). Thus, although only two of the LM residues interacted directly with BNM-III-170, their combination had an additive effect on binding and resulted in an overall increase in the complex BSA and compound affinity.

Furthermore, we conducted *in silico* analysis to predict the interaction energies present upon docking of CD4mc BNM-III-170 with our different gp120 variants. All-atom, explicit-solvent molecular dynamics (MD) simulations of BNM-III-170-bound complexes were conducted for the WT, H375S, H375T, LM, LM+HS, and LM+HT versions of gp120 $core_e$. Average protein-ligand interaction energies were computed from these simulations under the generalized Born surface area (GBSA) implicit solvent model. The average relative interaction energies ranked from least to most favorable in the order WT < H375S < LM < H375T < LM+HS < LM+HT, as shown in **Fig. 6.1.8G**. This ordering is consistent with the ordering in half-maximal inhibitory concentration (IC_{50}) values indicated in **Fig. 6.1.3D**, suggesting that enthalpic interactions are of high importance in determining how these residues change and how they reshape the CD4-binding site (CD4BS) to affect the activity of CD4mc.

Phe43 cavity and inner domain substitutions shape the highly conserved CD4 binding site.

The CD4-binding site (CD4BS) region of Env represents a highly complex quaternary arrangement of five different loops that meet to form this highly conserved structure. The following three loops converge to form the Phe43 cavity: the CD4-binding loop (residues 365 to 371), which makes critical contacts with CD4 residues F43 and R59 (1); the β20-β21 loop (residues 424 to 432), which acts as a conformational regulatory switch between the inner domain and the outer domain of gp120 (62); and the outer domain exit loop (residues 470 to 475), linking the outer domain to inner domain layer 3. Two other loops in the periphery of the Phe43 cavity were shown to be implicated in CD4 binding: loop D (residues 275 to 283) and the V5 loop (residues 457 to 468) (1). On the basis of structural analysis presented in **Fig. 6.1.8**, the LM+HS/T changes appear to have increased the interaction of CD4mc with the Phe43 cavity by restructuring the CD4BS, most particularly the outer domain exit loop. To better understand the molecular basis of this phenomenon, we solved crystal structures of $gp120_{93TH057}$ $core_e$s containing the LM mutations in combination with H375S (LM+HS) or H375T (LM+HT) in their unliganded state (**Table 6.1.S1**). Unliganded structures of the LM+HS and LM+HT cores were solved at 2.2-Å and 2.5-Å resolution, respectively. The structures of LM+HS and LM+HT $gp120_{93TH057}$ $core_e$s compared to the wildtype $gp120_{93TH057}$ $core_e$ (PDB code 3TGT [49]), which carries a His at position 375, are shown in **Fig. 6.1.9**.

There is close similarity between the structures of the LM+HS and LM+HT $core_e$s. Indeed, alignments showed that they have a root mean square deviation (RMSD) of 0.43 Å for their main chain atoms. Alignments to the wild-type $gp120_{93TH057}$ $core_e$, resulted in RMSD values of 0.45 Å and 0.54 Å for the LM+HS and LM+HT mutants, respectively, indicating a larger dissimilarity between the LM+HT and wild-type $core_e$ structures. Interestingly, a closer look into interactions formed by mutated residues in the LM+HS and LM+HT $core_e$s (**Fig. 6.1.9A**, magnified view) reveals a new network of interactions mediated by Asp474 and Arg476 that stabilize the inner domain mobile layer 2 and 3 interface in the CD4-bound conformation (51, 63, 64). Asp474 in combination with Glu102 in layer 2 formed a network of hydrogen bonds with Arg476 in both LM mutants that bridged the two layers. This network of hydrogen bonds is absent from other clade gp120 $core_e$ structures, with the exception of the clade B YU2 gp120 (PDB ID 3TGQ). In wild-

type CRF01_AE gp120, Lys476 formed a hydrogen bond with Glu102, but without the added stability made possible by the Arg476 guanidinium group, leaving Asn474 out of the interface. Other LM mutant changes that potentially add to the interface stability are the Gln105-to-His mutation, which changes the character of the Trp479 amide hydrogen bond, and the Val108-to-Ile mutation, which increases the hydrophobic surface available for interaction with Pro253. CRF01_AE 93TH057 gp120 has a histidine at residue 375, in contrast to the more common Ser or Thr, which only partially fills the Phe43 cavity, leaving the space required for CD4mc compound binding. The H375S/T mutation most likely induces a loss in stability of the CD4 binding pocket in the absence of CD4 or CD4mc that in LM variants is partially compensated for by the Ile475-to-Met mutation. Both Ile475 in the wild-type gp120 and Met475 in the LM mutant pack against Trp479, which links the Phe43 pocket to the layer 3-layer 2 interface through the Trp479 amide bond to Gln105 (wild type) or His105 (LM). The bulkier side chain of Met475 provides more hydrophobic surface to the network, stabilizing and reshaping the Phe43 cavity.

The added stability of the LM mutations can be visualized by the crystallographic temperature or B-factors which describe the spread of electron density attributed to each atom (**Fig. 6.1.9B**). Outside the V1/V2 and V4 loop regions, which differ greatly between structures, one region formed by residues 470 to 475 stands out in the normalized B-factor plot (65). The levels of main chain atom B-factors corresponding to the residues in this region are much lower for the LM+HS and LM+HT mutants than for wild-type Env, implying that there is a greater degree of structural stability in this region in the LM mutants. It was shown previously that residues of the outer domain exit loop contribute to CD4mc binding, as also seen in the unliganded LM+HS and LM+HT $core_e$s (37, 45, 48). This raises the possibility that the observed rigidification constitutes an element that reshapes the Phe43 cavity, leading to preferential binding of CD4 or CD4mc; conversely, binding of CD4 or CD4mc might stabilize layer 3, which can lead to downstream conformational changes in the gp120 inner domain. Interestingly, another region of the CD4BS was found to be significantly rigidified in the presence of the LM+HS/T mutations: the V5 loop region (residues 457 to 468). This region has previously been described as being implicated in CD4 attachment but also as being recognized by most known broadly neutralizing Abs targeting the CD4BS (e.g., VRC01). Notably, alterations in the V5 region have been associated with resistance to members of the VRC01 class of Abs (66–71) and b12 (72), consistent

with a potential effect of V5 loop rigidification on gp120 recognition by CD4BS Abs. To validate our model, we evaluated the ability of a panel of CD4BS Abs to bind to CRF01_AE Envs harboring one of several different residues at position 375 (H375, S375, and T375) in combination with the LM mutations or not. Consistent with the CD4BS restructuring shown in **Fig. 6.1.9A**, the presence of the LM mutations was shown to increase the binding of all CD4BS Abs, except b12, regardless of the nature of the residue at position 375 in both CRF01_AE strains tested (**Fig. 6.1.9C**). CD4BS recognition of Env-expressing cells correlated with the neutralization profile of these mutants (**Fig. 6.1.9D**).

Finally, since changes in the gp120 inner domain layers in combination with changes at position 375 have a global effect on the CD4BS, we tested the sensitivity of our panel of CRF01_AE Env mutants to another class of Env antagonists targeting the CD4BS: cyclic peptide triazoles (cPTs) (73, 74). Again, the introduction of the LM mutations in combination with a small residue at position 375 (LM+HS and LM+HT) in a CRF01_AE Env was found to dramatically increase the sensitivity to neutralization by all cPTs tested (AAR029N2 and AAR029N3) (**Fig. 6.1.S4**). However, the presence of a bulky residue at position 375 (H375) was found to abrogate this effect and conferred total resistance to the members of this class of compound (**Fig. 6.1.S4B to D**). In summary, supported by structural data and functional assays using a wide variety of CD4BS probes, our data show that residue 375 and its inner domain coevolving residues act together to shape the highly conserved CD4BS.

6.2.6 DISCUSSION

Previous studies have indicated that the gp120 inner domain plays a role in modulating the transition of Env from its unbound to its CD4-bound conformation (13–15, 75, 76). Here, we add a detailed structural understanding of this mechanism by identifying six gp120 inner domain residues able to shape the Phe43 cavity and the CD4 binding site. Collectively named layer mutants (LM), these residues determine the efficiency with which HIV-1 Envs negotiate transitions from the pre-triggered state 1 conformation to CD4-bound conformations (states 2 and 3). Structures of trimeric Env stabilized in the native state 1 conformation might be required for observation of the conformational rearrangement of the gp120 inner domain layers upon CD4 or CD4mc binding. The efficiency with which a given HIV-1 variant undergoes these conformational changes influences virus susceptibility to a number of antiviral agents directed against the CD4-binding region of gp120, including CD4mc, CD4 miniproteins, cPTs, and different CD4BS antibodies. Our report documents the significant impact of the LM residues on the susceptibility of HIV-1 strain variants to this major class of virus entry inhibitors and opens the door to the rational design of agents with improved antiviral potency and breadth.

The LM residues also modulate the susceptibility of infected cells to ADCC mediated by HIV^+ sera. Small-molecule CD4mc have been shown to enhance dramatically the ADCC-mediating potency of the antibodies present at high titers in the sera of almost all HIV-1-infected individuals (33). CD4mc are under investigation as a means to use ADCC to effect a functional "cure" of HIV-1 infection, as an adjunct to highly active antiretroviral therapy. Knowledge of the identity of the LM residues in the HIV-1 strains present in infected individuals could assist in the identification of subjects most likely to benefit from available CD4mc. The structural information on LM residues provided by our study can assist the design of CD4mc tailored to be effective against particular HIV-1 strains.

Many epitopes of Env have changed at a population level during the AIDS pandemic (77). Notably, a significant decline in sensitivity of clade B circulating strains to CD4BS antibodies was observed. We examined the historical changes in residue occupancy at position 375 in diverse clades and distinct geographic regions. Among CRF01_AE strains, H375 remained highly conserved during the pandemic (**Fig. 6.1.10A**). In contrast, striking changes occurred in other

group M major clades, most importantly in clade B, where a gradual but constant loss of S375 occurred, with S375 progressively replaced by T375 (**Fig. 6.1.10A**). The different patterns observed in the HIV-1 major clades and CRF01_AE, which follow similar patterns in distinct geographic regions (**Fig. 6.1.10B**), likely reflect differences in the constraints applied to the Phe43 cavity in the unique context of their Envs. They suggest an ongoing evolution of theCD4BS, which might need to be taken into account in developing CD4mc or immunogens designed to elicit CD4BS Abs. With respect to the issue of why T375 seems especially able to induce susceptibility to CD4mc irrespective of the LM, one clue from the structures presented here offers a possible explanation: space in the Phe43 cavity near S375 is strongly occupied by a density that may represent water or a crystallization solute, and this density is largely lacking for T375; these observations suggest higher susceptibility for T375 because it has fewer solvent molecules to eject in permitting CD4mc binding.

Taking the data together, here we show that residue 375 and its inner domain coevolving residues act together to shape the highly conserved CD4BS. This new structural understanding will assist ongoing efforts to improve CD4mc and other agents directed against the CD4BS and to design immunogens aimed at eliciting CD4BS antibodies.

6.2.7 MATERIALS AND METHODS

Ethics statement

Written informed consent was obtained from all study participants (the Montreal Primary HIV Infection Cohort [78, 79] and the Canadian Cohort of HIV Infected Slow Progressors [80–82]), and research adhered to the ethical guidelines of CRCHUM and was reviewed and approved by the CRCHUM institutional review board (ethics committee, approval number CE 16.164 –CA). Research adhered to the standards indicated by the Declaration of Helsinki. All participants were adults and provided informed written consent prior to enrollment in accordance with Institutional Review Board approval.

Sequence analysis

The Logo plots (83) for HIV were made using the Analyze Align tool at the HIV database and are based on the WebLogo 3 program (https://www.hiv.lanl.gov/content/sequence/ANALYZEALIGN/analyze_align.html) and the HIV-1 database global curated and filtered 2017 alignment published circa June 2018, including 1 HIV-1 Env protein sequence per person from 5,471 individuals. The relative height of each letter within individual stack represents the frequency of the indicated amino acid at that position. The numbering of all the Env amino acid sequences is based on the prototypic HXBc2 strain of HIV-1, where 1 is the initial methionine (84).

Analysis of historical changes in amino acid sequence

HIV-1 Env sequences were obtained from the Los Alamos National Lab (LANL) database (https://www.hiv.lanl.gov). Non-functional Envs and sequences with nucleotide ambiguities were removed. Nucleotide sequences were aligned using a hidden Markov model with HMMER3 software (85), and phylogenetic relationships between sequences were inferred by the maximum-likelihood method using PhyML3 (86). A single env gene from each patient and a single sequence from known transmission pairs were used. In addition, a minimal distance of 0.03 nucleotide substitutions per site was applied as a cutoff for selection. Sequences were archived and residue frequencies at all Env positions in each population were determined using software developed in-house, as previously described (77).

Cell lines and isolation of primary cells

HEK293T human embryonic kidney cells and Cf2Th canine thymocytes (obtained from ATCC) were grown as previously described (14). Cf2Th cells stably expressing human CD4 and CCR5 (Cf2Th-CD4/CCR5) (87) were grown in medium supplemented with 0.4 mg/ml of G418 (Invitrogen) and 0.15 mg/ml of hygromycin B (Roche Diagnostics). Primary human peripheral blood mononuclear cells (PBMCs) and $CD4^+$ T cells were isolated, activated, and cultured as previously described (23, 33). Briefly, PBMCs were obtained by leukapheresis and $CD4^+$ T lymphocytes were purified from resting PBMCs by negative selection using immunomagnetic beads per the instructions of the manufacturer (StemCell Technologies, Vancouver, BC, Canada) and were activated with phytohemagglutinin-L (10 µg/ml) for 48 h and then maintained in RPMI 1640 complete medium supplemented with recombinant interleukin-2 (rIL-2) (100 U/ml).

Plasmids and proviral constructs

The plasmids expressing the CRF01_AE Envs HIV-$1_{92TH023}$ and HIV-1_{CM244} were previously reported (41, 88). Plasmid pSVIIIenv expressing the full-length HIV-1_{YU2} Env and Tat-expressing plasmid pLTR-Tat were previously described (14). The sequence of full-length clade B HIV-1_{JRFL} (21) and clade A HIV-1_{BG505} Envs (89) were codon optimized (GenScript) and cloned into expression plasmid pcDNA3.1(-) (Invitrogen). An asparagine residue was introduced at position 332 (N332) to allow recognition of 2G12 antibody. Vesicular stomatitis virus G (VSV-G)-encoding plasmid pSVCMV-IN-VSV-G was previously described (90). For crystallographic studies, the plasmid used to express gp120 extended core ($core_e$) from CRF01_AE strain 93TH057 (gp120 lacking the N and C termini and variable loops 1, 2, and 3) was previously described (49). The transmitted/founder (TF) CRF01_AE 40061 full viral genome was retrieved by single-genome amplification and cloned to generate full-length infectious molecular clone (IMC) as previously reported (91). TF and chronic IMCs of patients CH40, CH58, CH77, CH167, CH185, CH198, CH236, CH470, CH505, CH850, RHGA, and STCO were inferred, constructed, and biologically characterized as previously described (92–98). The JRFL IMC was also previously described (99). Mutations were introduced individually or in combination into the different Env expressors or IMCs using the QuikChange II XL site-directed mutagenesis protocol (Stratagene). The presence of the desired mutations was determined by automated DNA sequencing. The numbering of all the Env amino acid sequence is based on the prototypic HXBc2 strain of HIV-1, where 1 is the initial methionine (84).

Viral production and infections

To achieve similar levels of infection in primary $CD4^+$ T cells among the different IMCs tested, VSV-G-pseudotyped HIV-1 was produced and titrated as previously described (24). Viruses were then used to infect activated primary $CD4^+$ T cells from healthy HIV-1- negative donors by spin infection at 800 × *g* for 1 h in 96-well plates at 25°C. For the viral neutralization assay, Cf2Th-CD4/CCR5 cells were infected with single-round luciferase-expressing HIV-1 (14). Briefly, 293T cells were transfected by the calcium phosphate method with the proviral vector pNL4.3(Env-)Luc and a plasmid expressing wild-type or mutant HIV-1 Env at a ratio of 2:1. Two days after transfection, the cell supernatants were harvested. The reverse transcriptase activities of

all virus preparations were measured as described previously (100). Each virus preparation was frozen and stored in aliquots at -80°C until use.

Antibodies and sera

The following Abs were used to assess cell surface Env staining: A32, 17b, 19b, F240, PG16, N6, NIH45-46^{G54W}, VRC01, VRC03, HJ16, VRC-CH31, F105 (NIH AIDS Reagent Program), PGT151, PGT128 (IAVI), 3BNC117 (kindly provided by M. Nussenzweig, The Rockefeller University, New York, NY), b6, b12 (kindly provided by D. Burton, The Scripps Research Institute, La Jolla, CA), VRC07-523-LS, VRC13, VRC16 (kindly provided by J. Mascola, Vaccine Research Center, Bethesda, MD), GE2.JG8 (kindly provided by G. Karlsson Hedestam, Karolinska Institutet, Sweden), and N49P7 (kindly provided by M. Sajadi, University of Maryland, Baltimore, MD). The anti-CD4 OKT4 monoclonal antibody (recognizing the D3 domain of CD4) (eBioscience) was used to measure the binding of sCD4 to cell surface Env. Goat anti-mouse and anti-human antibodies pre-coupled to Alexa Fluor 647 (Invitrogen) were used as secondary antibodies in flow cytometry experiments. Sera from HIV-infected individuals were collected, heat inactivated, and conserved at -80°C until use. A random number generator (GraphPad; QuickCalcs, San Diego, CA, USA) was used to randomly select a number of sera for each experiment.

CD4 mimetics and other small molecules

Soluble CD4 (sCD4) and the miniprotein M48U1 were produced and purified as previously described (14, 101). The CD4 mimetic compounds (CD4mc) NBD-556, JRC-II-191, DMJ-II-121, JP-III-48, BNM-III-170, BNM-IV-147, BNM-IV-197, MCG-IV-210, SMK-II-48, AEG-I-249, AEG-I-259, and MCG-III-051 were developed and synthesized as described previously (37, 45–47, 52, 61, 102) or as described in the "Chemical synthesis" section below. The CD4mc were analyzed, dissolved in dimethyl sulfoxide (DMSO) at a stock concentration of 10 mM, aliquoted, and stored at -80°C. Cyclic peptide triazoles (cPTs) AAR029N2 and AAR029N3 were synthesized, purified (95% homogeneity by reverse-phase HPLC), and structurally validated as previously described (73, 74). The cPTs were analyzed, dissolved in DMSO at a stock concentration of 10 mM, aliquoted, and stored at -80°C. Each compound was then diluted to the

indicated concentrations in phosphate-buffered saline (PBS) for cell surface staining, in RPMI 1640 complete medium for ADCC assays, or in complete Dulbecco's modified Eagle's medium (DMEM) for viral neutralization assays.

Viral neutralization assay

Cf2Th-CD4/CCR5 target cells were seeded at a density of 5×10^3 cells/well in 96-well luminometer-compatible tissue culture plates (Perkin Elmer) 24 h before infection. Luciferase-expressing recombinant viruses (10,000 reverse transcriptase units) in a final volume of 100 l were incubated with the indicated amounts of different proteins, compounds, or antibodies for 1h at 37°C and were then added to the target cells followed by incubation for 48 h at 37°C; the medium was then removed from each well, and the cells were lysed by the addition of 30 µl of passive lysis buffer (Promega) followed by three freeze-thaw cycles. An LB 941 TriStar luminometer (Berthold Technologies) was used to measure the luciferase activity of each well after the addition of 100 µl of luciferin buffer (15 mM $MgSO_4$, 15 mM KPO_4 [pH 7.8], 1 mM ATP, and 1 mM dithiothreitol) and 50 µl of 1 mM D-luciferin potassium salt (Prolume). The neutralization half-maximal inhibitory concentration (IC_{50}) represents the amount of protein, compound, or antibody needed to inhibit 50% of the infection of Cf2Th-CD4/CCR5 cells by recombinant luciferase-expressing HIV-1 bearing the indicated Env.

Flow cytometry analysis of cell surface staining

Cell surface staining of infected cells was performed as previously described (24, 33). Binding of cell surface HIV-1 Env by sera (1:1,000 dilution) or anti-Env mAbs (5 µg/ml) was performed at 48 h post-infection in the presence of CD4mc or of an equal amount of the vehicle (DMSO). Infected cells were stained intracellularly for HIV-1 p24, using a Cytofix/ Cytoperm fixation/permeabilization kit (BD Biosciences, Mississauga, ON, Canada) and fluorescent antip24 mAb (phycoerythrin [PE]-conjugated anti-p24, clone KC57; Beckman Coulter/Immunotech). The percentage of infected cells ($p24^+$) was determined by gating the living cell population on the basis of viability dye staining (Aquavivid; Thermo Fisher Scientific). Samples were acquired on an LSR II cytometer (BD Biosciences), and data analysis was performed using FlowJo vX.0.7 (Tree Star, Ashland, OR, USA).

Cell surface staining of Env-expressing 293T cells was performed as previously described (103). Briefly, 2×10^6 cells were transfected with 7 µg of Env expressor and 1 µg of a green fluorescent protein (GFP) expressor (pIRES2-GFP) with the calcium-phosphate method. When the pSVIII Env expressor was used, it was co-transfected with 0.25 µg of a Tat-expressing plasmid. At 48 h post-transfection, 293T cells were stained with anti-Env antibodies (5 µg/ml). Alternatively, to evaluate sCD4 binding to the different cell surface Envs, transfected 293T cells were incubated with sCD4 (5 µg/ml), followed by staining performed with the monoclonal anti-CD4 OKT4 antibody (0.5 µg/ml). In experiments using transfected cells, all mean fluorescent intensities (MFI) were normalized to the MFI of 2G12 for each Env mutant.

FACS-based ADCC assay

Measurement of ADCC using the fluorescence-activated cell sorter (FACS)-based assay was performed at 48 h post-infection as previously described. Briefly, infected primary $CD4^+$ T cells were stained with Aquavivid viability dye and cell proliferation dye (eFluor670; eBioscience) and used as target cells. Autologous PBMC effector cells, stained with another cellular marker (cell proliferation dye eFluor450; eBioscience), were added at an effector/target ratio of 10:1 in 96-well V-bottom plates (Corning, Corning, NY). A 1:1,000 final dilution of sera was added to appropriate wells, and the cells were incubated for 15 min at room temperature. The plates were subsequently centrifuged for 1 min at 300 × *g* and incubated at 37°C and 5% CO_2 for 5 h before being fixed in a 2% PBS– formaldehyde solution. Samples were acquired on an LSR II cytometer (BD Biosciences), and data analysis was performed using FlowJo vX.0.7 (Tree Star). The percentage of ADCC resulting from gating performed on infected lived target cells was calculated with the following formula: (percentage of $p24^+$ cells in targets plus effectors) × (percentage of $p24^+$ cells in targets plus effectors plus sera) / (percentage of $p24^+$ cells in targets).

Protein expression and purification

Plasmids encoding the layer mutant gp120 extended core ($core_e$) proteins, HIV-$1_{93TH057}$ gp120 $core_e$ LM+HS and LM+HT, were transfected into $GnT1^-$ cells using Xtremegene transfection reagent (Sigma-Aldrich) per the manufacturer's instructions. Following 7 days of culture growth at 37°C and 8% CO_2, cells were pelleted by centrifugation and cell supernatant was filtered. Expressed gp120 was purified by passage over a 17b affinity column made by cross-

linking mAb 17b to protein A (Pierce protein A IgG plus orientation kit; Thermo Fisher). gp120 was eluted with 0.1 M glycine (pH 3.0) into tubes containing 1/10 the final volume of 1 M Tris-HCl (pH 8.5) to raise the pH. The protein was then deglycosylated with 10 units/µg of Endo H_f (New England Biolabs) overnight at 37°C in a mixture of deglycosylation buffer, 50 mM sodium acetate (pH 6.0), and 350 mM sodium chloride. Endo H_f was removed by passage over an amylose resin column, and the protein was further purified by gel filtration chromatography on a Superdex 200 16/60 column (GE Healthcare, Piscataway, NJ) equilibrated with 5 mM Tris-HCl (pH 7.2) and 150 mM sodium chloride. The protein was concentrated to approximately 5 mg/ml for use in crystallization trials.

X-ray crystallography

Deglycosylated HIV-$1_{93TH057}$ gp120 $core_e$ LM+HS or LM+HT (5 mg/ml) was crystalized by the hanging drop method in a mixture containing 5 to 10% polyethylene glycol (PEG) 1500, 6% PEG 400 (LM+HT), and 0.1 M HEPES (pH 7.5) or 5 to 10% PEG 3350, 6% PEG 400, and 0.1 M HEPES (pH 7.5) (LM+HS). CD4 mimetics were solubilized with DMSO at a concentration of 10 mM and diluted with crystallization buffer to 100 nM prior to use in crystal soaks. When CD4mc was added to the crystal, an equal volume of the 100 nM mimetic in crystallization buffer was added to the hanging drop and the crystals were allowed to soak for 4 h before being frozen. Crystals were flash frozen in liquid nitrogen after a brief soak in crystallization buffer containing 18% MPD (2-methyl-2,4-pentanediol) for cryoprotection and a 50 nM concentration of CD4mc when CD4mc was added.

Data collection, structure solution, and refinement

Data were collected on National Synchrotron Light Source II (NSLS II) highly automated macromolecular crystallography (AMX) beamline 17-ID-1 on an Eiger 9M detector system or on Stanford Synchrotron Radiation Light Source (SSRL) beamline 12-2 on a Dectris Pilatus 6M detector system. Data were integrated and processed with MOSFLM and SCALA from the CCP4 suite (104) or HKL2000 (105). Crystals were orthorhombic, belonging to space group $P2_12_12_1$, with cell dimensions of a = 64.0 to 66.8 Å, b = 65.6 to 67.5 Å, and c = 86.2 to 87.8 Å, with diffraction to 2.2 to 2.65 Å. Structures were solved by molecular replacement with the program PHASER from the CCP4 suite using PDB ID 3TGT as a starting model. Model building was done

using the program COOT (106). Refinement was done using the program REFMAC from the CCP4 suite or PHENIX (65).

Structure validation and analysis

The quality of the final refined models was monitored using the program MolProbity (107). Structural alignments were performed using the Dali server and the program LSQKAB from the CCP4 suite (104) The PISA webserver was used to determine contact surfaces and residues. All illustrations were prepared with the PyMol molecular graphic suite (DeLano Scientific, San Carlos, CA, USA). The Ramachandran plot was obtained by the use of the validation program "MolProbity" and shows that 92.8 to 97.0% of the total amino acids are in the most favored region, 3 to 6.6% in the generously allowed region, and 0 to 0.6% in the disallowed region, depending on the structure, with better values corresponding to the higher-resolution structures. Complete data collection and refinement statistics can be found in **Table S1**.

***In silico* analysis**

Starting with the H375S clade A/E HIV-1 core gp120 monomer in PDB entry 4H8W (108), we generated via residue mutation the WT, H375S, H375T, LM, LM+HS, and LM+HT variants and docked BNM-III-170 to each via alignment to the 5F4P PDB entry (45). For each variant, five independent fully TIP3P-solvated MD systems were generated and run for 500 ns each using NAMD 2.13 with the CHARM36 force field, with configurations saved every 0.1 ns. For each system, molecular mechanics-generalized Born surface area (MMGBSA) interaction energy data were computed by reprocessing trajectories through NAMD and computing protein-only, ligand-only, and protein-plus-ligand potential energies under the generalized Born implicit solvent (GBIS) model. The GBIS parameters included a solvent dielectric constant of 74.69, a total molar ion concentration of 0.3, a screening cutoff of 14 Å, and surface tension of 0.0072 kcal/mol/Å^2.

Statistical analysis

Statistics were analyzed using GraphPad Prism version 6.0.1 (GraphPad, San Diego, CA, USA). Every data set was tested for statistical normality, and this information was used to apply the appropriate (parametric or nonparametric) statistical test. P values of < 0.05 were considered

significant, and significance values are indicated as follows: *, $P < 0.05$; **, $P < 0.01$; ***, $P < 0.001$; ****, $P < 0.0001$.

Chemical synthesis

For details about chemical synthesis, see Text S1 in the supplemental material.

6.2.8 ACKNOWLEDGMENTS

We thank the staff members of the CRCHUM BSL3 and Flow Cytometry Platforms for technical assistance, Mario Legault from the FRQS AIDS and Infectious Diseases network for cohort coordination and clinical samples, Michel Nussenzweig for 3BNC117, and Dennis Burton for infectious molecular clone JRFL. This work was supported by CIHR foundation grant 352417 to A.F. Support for this work was also provided by NIH R01 to A.F. and M.P. (AI129769) and J.S. (AI124982 and AI145547) and by NIAID R01 to M.P. (AI116274). This study was also supported by NIH R01-GM56550 to A.B.S. and by grant P01-GM56550/AI150741 to A.F., A.B.S., I.C., J.S., and C.F.A. A.F. is the recipient of a Canada Research Chair on Retroviral Entry RCHS0235. J.P. is the recipient of a CIHR doctoral fellowship. C.H. was supported by a Development Grant from the University of Iowa (MI-2019). F.K. is supported by grants from the DFG (CRC 1279 and SPP 1923). The funders had no role in study design, data collection and analysis, decision to publish, or preparation of the manuscript. The views expressed in this presentation are those of the authors and do not reflect the official policy or position of the Uniformed Services University, U.S. Army, the Department of Defense, or the U.S. Government.

6.2.9 REFERENCES

1. Kwong PD, Wyatt R, Robinson J, Sweet RW, Sodroski J, Hendrickson WA. 1998. Structure of an HIV gp120 envelope glycoprotein in complex with the CD4 receptor and a neutralizing human antibody. Nature 393: 648 – 659.
2. Madani N, Perdigoto AL, Srinivasan K, Cox JM, Chruma JJ, LaLonde J, Head M, Smith AB, III, Sodroski JG. 2004. Localized changes in the gp120 envelope glycoprotein confer resistance to human immunodeficiency virus entry inhibitors BMS-806 and #155. J Virol 78:3742–3752.

3. Choe H, Farzan M, Sun Y, Sullivan N, Rollins B, Ponath PD, Wu L, Mackay CR, LaRosa G, Newman W, Gerard N, Gerard C, Sodroski J. 1996. The beta-chemokine receptors CCR3 and CCR5 facilitate infection by primary HIV-1 isolates. Cell 85:1135–1148.
4. Deng H, Liu R, Ellmeier W, Choe S, Unutmaz D, Burkhart M, Di Marzio P, Marmon S, Sutton RE, Hill CM, Davis CB, Peiper SC, Schall TJ, Littman DR, Landau NR. 1996. Identification of a major co-receptor for primary isolates of HIV-1. Nature 381:661–666.
5. Doranz BJ, Rucker J, Yi Y, Smyth RJ, Samson M, Peiper SC, Parmentier M, Collman RG, Doms RW. 1996. A dual-tropic primary HIV-1 isolate that uses fusin and the beta-chemokine receptors CKR-5, CKR-3, and CKR-2b as fusion cofactors. Cell 85:1149 – 1158.
6. Dragic T, Litwin V, Allaway GP, Martin SR, Huang Y, Nagashima KA, Cayanan C, Maddon PJ, Koup RA, Moore JP, Paxton WA. 1996. HIV-1 entry into CD4+ cells is mediated by the chemokine receptor CCCKR-5. Nature 381:667– 673.
7. Alkhatib G, Combadiere C, Broder CC, Feng Y, Kennedy PE, Murphy PM, Berger EA. 1996. CC CKR5: a RANTES, MIP-1alpha, MIP-1beta receptor as a fusion cofactor for macrophage-tropic HIV-1. Science 272:1955–1958.
8. Feng Y, Broder CC, Kennedy PE, Berger EA. 1996. HIV-1 entry cofactor: functional cDNA cloning of a seven-transmembrane, G protein-coupled receptor. Science 272:872–877.
9. Trkola A, Dragic T, Arthos J, Binley JM, Olson WC, Allaway GP, Cheng-Mayer C, Robinson J, Maddon PJ, Moore JP. 1996. CD4-dependent, antibody-sensitive interactions between HIV-1 and its co-receptor CCR-5. Nature 384:184 –187.
10. Wu L, Gerard NP, Wyatt R, Choe H, Parolin C, Ruffing N, Borsetti A, Cardoso AA, Desjardin E, Newman W, Gerard C, Sodroski J. 1996. CD4-induced interaction of primary HIV-1 gp120 glycoproteins with the chemokine receptor CCR-5. Nature 384:179 –183.
11. Lu M, Blacklow SC, Kim PS. 1995. A trimeric structural domain of the HIV-1 transmembrane glycoprotein. Nat Struct Biol 2:1075–1082.
12. Weissenhorn W, Dessen A, Harrison SC, Skehel JJ, Wiley DC. 1997. Atomic structure of the ectodomain from HIV-1 gp41. Nature 387: 426 – 430.
13. Desormeaux A, Coutu M, Medjahed H, Pacheco B, Herschhorn A, Gu C, Xiang SH, Mao Y, Sodroski J, Finzi A. 2013. The highly conserved layer-3 component of the HIV-1 gp120

inner domain is critical for CD4-required conformational transitions. J Virol 87:2549 – 2562.

14. Finzi A, Xiang SH, Pacheco B, Wang L, Haight J, Kassa A, Danek B, Pancera M, Kwong PD, Sodroski J. 2010. Topological layers in the HIV-1 gp120 inner domain regulate gp41 interaction and CD4-triggered conformational transitions. Mol Cell 37:656 – 667.
15. Ding S, Tolbert WD, Prevost J, Pacheco B, Coutu M, Debbeche O, Xiang SH, Pazgier M, Finzi A. 2016. A highly conserved gp120 inner domain residue modulates Env conformation and trimer stability. J Virol. 90:8395-409.
16. Finzi A, Pacheco B, Xiang SH, Pancera M, Herschhorn A, Wang L, Zeng X, Desormeaux A, Kwong PD, Sodroski J. 2012. Lineage-specific differences between human and simian immunodeficiency virus regulation of gp120 trimer association and CD4 binding. J Virol 86:8974 – 8986.
17. Ding S, Medjahed H, Prevost J, Coutu M, Xiang SH, Finzi A. 2016. Lineage-specific differences between the gp120 inner domain layer 3 of human immunodeficiency virus and that of simian immunodeficiency virus. J Virol 90:10065–10073.
18. Lu M, Ma X, Castillo-Menendez LR, Gorman J, Alsahafi N, Ermel U, Terry DS, Chambers M, Peng D, Zhang B, Zhou T, Reichard N, Wang K, Grover JR, Carman BP, Gardner MR, Nikic-Spiegel I, Sugawara A, Arthos J, Lemke EA, Smith AB, III, Farzan M, Abrams C, Munro JB, McDermott AB, Finzi A, Kwong PD, Blanchard SC, Sodroski JG, Mothes W. 2019. Associating HIV-1 envelope glycoprotein structures with states on the virus observed by smFRET. Nature 568:415– 419.
19. Munro JB, Gorman J, Ma X, Zhou Z, Arthos J, Burton DR, Koff WC, Courter JR, Smith AB, III, Kwong PD, Blanchard SC, Mothes W. 2014. Conformational dynamics of single HIV-1 envelope trimers on the surface of native virions. Science 346:759 –763.
20. Liu J, Bartesaghi A, Borgnia MJ, Sapiro G, Subramaniam S. 2008. Molecular architecture of native HIV-1 gp120 trimers. Nature 455:109 –113.
21. Mao Y, Wang L, Gu C, Herschhorn A, Xiang SH, Haim H, Yang X, Sodroski J. 2012. Subunit organization of the membrane-bound HIV-1 envelope glycoprotein trimer. Nat Struct Mol Biol 19:893– 899.

22. Veillette M, Coutu M, Richard J, Batraville LA, Desormeaux A, Roger M, Finzi A. 2014. Conformational evaluation of HIV-1 trimeric envelope glycoproteins using a cell-based ELISA assay. J Vis Exp 14:51995.
23. Veillette M, Desormeaux A, Medjahed H, Gharsallah NE, Coutu M, Baalwa J, Guan Y, Lewis G, Ferrari G, Hahn BH, Haynes BF, Robinson JE, Kaufmann DE, Bonsignori M, Sodroski J, Finzi A. 2014. Interaction with cellular CD4 exposes HIV-1 envelope epitopes targeted by antibody-dependent cell-mediated cytotoxicity. J Virol 88:2633–2644.
24. Veillette M, Coutu M, Richard J, Batraville LA, Dagher O, Bernard N, Tremblay C, Kaufmann DE, Roger M, Finzi A. 2015. The HIV-1 gp120 CD4-bound conformation is preferentially targeted by antibody-dependent cellular cytotoxicity-mediating antibodies in sera from HIV-1-infected individuals. J Virol 89:545–551.
25. Alsahafi N, Ding S, Richard J, Markle T, Brassard N, Walker B, Lewis GK, Kaufmann DE, Brockman MA, Finzi A. 2015. Nef proteins from HIV-1 elite controllers are inefficient at preventing antibody-dependent cellular cytotoxicity. J Virol 90:2993–3002.
26. Ding S, Veillette M, Coutu M, Prevost J, Scharf L, Bjorkman PJ, Ferrari G, Robinson JE, Sturzel C, Hahn BH, Sauter D, Kirchhoff F, Lewis GK, Pazgier M, Finzi A. 2016. A highly conserved residue of the HIV-1 gp120 inner domain is important for antibody-dependent cellular cytotoxicity responses mediated by anti-cluster A antibodies. J Virol 90:2127–2134.
27. Alsahafi N, Bakouche N, Kazemi M, Richard J, Ding S, Bhattacharyya S, Das D, Anand SP, Prevost J, Tolbert WD, Lu H, Medjahed H, Gendron-Lepage G, Ortega Delgado GG, Kirk S, Melillo B, Mothes W, Sodroski J, Smith AB, III, Kaufmann DE, Wu X, Pazgier M, Rouiller I, Finzi A, Munro JB. 2019. An asymmetric opening of HIV-1 envelope mediates antibody-dependent cellular cytotoxicity. Cell Host Microbe 25: 578 –587.e5.
28. Prevost J, Richard J, Medjahed H, Alexander A, Jones J, Kappes JC, Ochsenbauer C, Finzi A. 2018. Incomplete downregulation of CD4 expression affects HIV-1 Env conformation and antibody-dependent cellular cytotoxicity responses. J Virol 92:e00484-18.
29. Arias JF, Heyer LN, von Bredow B, Weisgrau KL, Moldt B, Burton DR, Rakasz EG, Evans DT. 2014. Tetherin antagonism by Vpu protects HIV-infected cells from antibody-dependent cell-mediated cytotoxicity. Proc Natl Acad Sci USA 111:6425– 6430.

30. Alvarez RA, Hamlin RE, Monroe A, Moldt B, Hotta MT, Rodriguez Caprio G, Fierer DS, Simon V, Chen BK. 2014. HIV-1 Vpu antagonism of tetherin inhibits antibody-dependent cellular cytotoxic responses by natural killer cells. J Virol 88:6031– 6046.
31. von Bredow B, Arias JF, Heyer LN, Gardner MR, Farzan M, Rakasz EG, Evans DT. 2015. Envelope glycoprotein internalization protects human and simian immunodeficiency virus-infected cells from antibody-dependent cell-mediated cytotoxicity. J Virol 89:10648 – 10655.
32. Anand SP, Grover JR, Tolbert WD, Prevost J, Richard J, Ding S, Baril S, Medjahed H, Evans DT, Pazgier M, Mothes W, Finzi A. 2019. Antibody-induced internalization of HIV-1 Env proteins limits surface expression of the closed conformation of Env. J Virol 93:e00293-19.
33. Richard J, Veillette M, Brassard N, Iyer SS, Roger M, Martin L, Pazgier M, Schon A, Freire E, Routy JP, Smith AB, III, Park J, Jones DM, Courter JR, Melillo BN, Kaufmann DE, Hahn BH, Permar SR, Haynes BF, Madani N, Sodroski JG, Finzi A. 2015. CD4 mimetics sensitize HIV-1-infected cells to ADCC. Proc Natl Acad Sci USA 112:E2687–E2694.
34. Madani N, Princiotto AM, Zhao C, Jahanbakhshsefidi F, Mertens M, Herschhorn A, Melillo B, Smith AB, III, Sodroski J. 2017. Activation and inactivation of primary human immunodeficiency virus envelope glycoprotein trimers by CD4-mimetic compounds. J Virol 91:e01880-16.
35. Madani N, Princiotto AM, Easterhoff D, Bradley T, Luo K, Williams WB, Liao HX, Moody MA, Phad GE, Vazquez Bernat N, Melillo B, Santra S, Smith AB, III, Karlsson Hedestam GB, Haynes B, Sodroski J. 2016. Antibodies elicited by multiple envelope glycoprotein immunogens in primates neutralize primary human immunodeficiency viruses (HIV-1) sensitized by CD4-mimetic compounds. J Virol 90:5031–5046.
36. Madani N, Princiotto AM, Schon A, LaLonde J, Feng Y, Freire E, Park J, Courter JR, Jones DM, Robinson J, Liao HX, Moody MA, Permar S, Haynes B, Smith AB, III, Wyatt R, Sodroski J. 2014. CD4-mimetic small molecules sensitize human immunodeficiency virus to vaccine-elicited antibodies. J Virol 88:6542– 6555.
37. Ding S, Grenier MC, Tolbert WD, Vezina D, Sherburn R, Richard J, Prevost J, Chapleau JP, Gendron-Lepage G, Medjahed H, Abrams C, Sodroski J, Pazgier M, Smith AB, III,

Finzi A. 2019. A new family of small-molecule CD4-mimetic compounds contacts highly conserved aspartic acid 368 of HIV-1 gp120 and mediates antibody-dependent cellular cytotoxicity. J Virol 93:e01325-19.

38. Madani N, Princiotto AM, Mach L, Ding S, Prevost J, Richard J, Hora B, Sutherland L, Zhao CA, Conn BP, Bradley T, Moody MA, Melillo B, Finzi A, Haynes BF, Smith AB, III, Santra S, Sodroski J. 2018. A CD4-mimetic compound enhances vaccine efficacy against stringent immunodeficiency virus challenge. Nat Commun 9:2363.
39. Princiotto AM, Vrbanac VD, Melillo B, Park J, Tager AM, Smith AB, III, Sodroski J, Madani N. 2018. A small-molecule CD4-mimetic compound protects bone marrow-liver-thymus humanized mice from HIV-1 infection. J Infect Dis 218:471– 475.
40. Xiang SH, Kwong PD, Gupta R, Rizzuto CD, Casper DJ, Wyatt R, Wang L, Hendrickson WA, Doyle ML, Sodroski J. 2002. Mutagenic stabilization and/or disruption of a CD4-bound state reveals distinct conformations of the human immunodeficiency virus type 1 gp120 envelope glycoprotein. J Virol 76:9888 –9899.
41. Zoubchenok D, Veillette M, Prevost J, Sanders-Buell E, Wagh K, Korber B, Chenine AL, Finzi A. 2017. Histidine 375 modulates CD4 binding in HIV-1 CRF01_AE envelope glycoproteins. J Virol 91:e02151-16.
42. Prevost J, Zoubchenok D, Richard J, Veillette M, Pacheco B, Coutu M, Brassard N, Parsons MS, Ruxrungtham K, Bunupuradah T, Tovanabutra S, Hwang KK, Moody MA, Haynes BF, Bonsignori M, Sodroski J, Kaufmann DE, Shaw GM, Chenine AL, Finzi A. 2017. Influence of the envelope gp120 Phe43 cavity on HIV-1 sensitivity to antibody-dependent cell-mediated cytotoxicity responses. J Virol 91:e02452-16.
43. Schader SM, Colby-Germinario SP, Quashie PK, Oliveira M, Ibanescu R-I, Moisi D, Mespléde T, Wainberg MA. 2012. HIV gp120 H375 is unique to HIV-1 subtype CRF01_AE and confers strong resistance to the entry inhibitor BMS-599793, a candidate microbicide drug. Antimicrob Agents Chemother 56:4257–4267.
44. Li H, Wang S, Kong R, Ding W, Lee FH, Parker Z, Kim E, Learn GH, Hahn P, Policicchio B, Brocca-Cofano E, Deleage C, Hao X, Chuang GY, Gorman J, Gardner M, Lewis MG, Hatziioannou T, Santra S, Apetrei C, Pandrea I, Alam SM, Liao HX, Shen X, Tomaras GD, Farzan M, Chertova E, Keele BF, Estes JD, Lifson JD, Doms RW, Montefiori DC, Haynes BF, Sodroski JG, Kwong PD, Hahn BH, Shaw GM. 2016. Envelope residue 375

substitutions in simian-human immunodeficiency viruses enhance CD4 binding and replication in rhesus macaques. Proc Natl Acad Sci USA 113:E3413–E3422.

45. Melillo B, Liang S, Park J, Schon A, Courter JR, LaLonde JM, Wendler DJ, Princiotto AM, Seaman MS, Freire E, Sodroski J, Madani N, Hendrickson WA, Smith AB, III. 2016. Small-molecule CD4-mimics: structure-based optimization of HIV-1 entry inhibition. ACS Med Chem Lett 7:330 –334.
46. Lalonde JM, Le-Khac M, Jones DM, Courter JR, Park J, Schon A, Princiotto AM, Wu X, Mascola JR, Freire E, Sodroski J, Madani N, Hendrickson WA, Smith AB, III. 2013. Structure-based design and synthesis of an HIV-1 Entry inhibitor exploiting X-ray and thermodynamic characterization. ACS Med Chem Lett 4:338 –343.
47. Lalonde JM, Kwon YD, Jones DM, Sun AW, Courter JR, Soeta T, Kobayashi T, Princiotto AM, Wu X, Schon A, Freire E, Kwong PD, Mascola JR, Sodroski J, Madani N, Smith AB, III. 2012. Structure-based design, synthesis, and characterization of dual hotspot small-molecule HIV-1 entry inhibitors. J Med Chem 55:4382– 4396.
48. Kwon YD, LaLonde JM, Yang Y, Elban MA, Sugawara A, Courter JR, Jones DM, Smith AB, III, Debnath AK, Kwong PD. 2014. Crystal structures of HIV-1 gp120 envelope glycoprotein in complex with NBD analogues that target the CD4-binding site. PLoS One 9:e85940.
49. Kwon YD, Finzi A, Wu X, Dogo-Isonagie C, Lee LK, Moore LR, Schmidt SD, Stuckey J, Yang Y, Zhou T, Zhu J, Vicic DA, Debnath AK, Shapiro L, Bewley CA, Mascola JR, Sodroski JG, Kwong PD. 2012. Unliganded HIV-1 gp120 core structures assume the CD4-bound conformation with regulation by quaternary interactions and variable loops. Proc Natl Acad Sci U S A 109:5663–5668.
50. Curreli F, Kwon YD, Zhang H, Yang Y, Scacalossi D, Kwong PD, Debnath AK. 2014. Binding mode characterization of NBD series CD4-mimetic HIV-1 entry inhibitors by X-ray structure and resistance study. Antimicrob Agents Chemother 58:5478 –5491.
51. Acharya P, Luongo TS, Louder MK, McKee K, Yang Y, Kwon YD, Mascola JR, Kessler P, Martin L, Kwong PD. 2013. Structural basis for highly effective HIV-1 neutralization by CD4-mimetic miniproteins revealed by 1.5 A cocrystal structure of gp120 and M48U1. Structure 21:1018 –1029.

52. Madani N, Schon A, Princiotto AM, Lalonde JM, Courter JR, Soeta T, Ng D, Wang L, Brower ET, Xiang SH, Do Kwon Y, Huang CC, Wyatt R, Kwong PD, Freire E, Smith AB, III, Sodroski J. 2008. Small-molecule CD4 mimics interact with a highly conserved pocket on HIV-1 gp120. Structure 16:1689 –1701.
53. Grupping K, Selhorst P, Michiels J, Vereecken K, Heyndrickx L, Kessler P, Vanham G, Martin L, Arien KK. 2012. MiniCD4 protein resistance mutations affect binding to the HIV-1 gp120 CD4 binding site and decrease entry efficiency. Retrovirology 9:36.
54. Richard J, Veillette M, Ding S, Zoubchenok D, Alsahafi N, Coutu M, Brassard N, Park J, Courter JR, Melillo B, Smith AB, III, Shaw GM, Hahn BH, Sodroski J, Kaufmann DE, Finzi A. 2016. Small CD4 mimetics prevent HIV-1 uninfected bystander CD4 T cell killing mediated by antibody-dependent cell-mediated cytotoxicity. EBioMedicine 3:122–134.
55. Anand SP, Prevost J, Baril S, Richard J, Medjahed H, Chapleau JP, Tolbert WD, Kirk S, Smith AB, III, Wines BD, Kent SJ, Hogarth PM, Parsons MS, Pazgier M, Finzi A. 2018. Two families of Env antibodies efficiently engage Fc-gamma receptors and eliminate HIV-1-infected cells. J Virol 93:e01823-18.
56. Richard J, Prevost J, von Bredow B, Ding S, Brassard N, Medjahed H, Coutu M, Melillo B, Bibollet-Ruche F, Hahn BH, Kaufmann DE, Smith AB, III, Sodroski J, Sauter D, Kirchhoff F, Gee K, Neil SJ, Evans DT, Finzi A. 2017. BST-2 expression modulates small CD4-mimetic sensitization of HIV-1-infected cells to antibody-dependent cellular cytotoxicity. J Virol 91:e00219-17.
57. Richard J, Pacheco B, Gohain N, Veillette M, Ding S, Alsahafi N, Tolbert WD, Prevost J, Chapleau JP, Coutu M, Jia M, Brassard N, Park J, Courter JR, Melillo B, Martin L, Tremblay C, Hahn BH, Kaufmann DE, Wu X, Smith AB, III, Sodroski J, Pazgier M, Finzi A. 2016. Co-receptor binding site antibodies enable CD4-mimetics to expose conserved anti-cluster A ADCC epitopes on HIV-1 envelope glycoproteins. EBioMedicine 12: 208 – 218.
58. Kijak GH, Sanders-Buell E, Chenine A-L, Eller MA, Goonetilleke N, Thomas R, Leviyang S, Harbolick EA, Bose M, Pham P, Oropeza C, Poltavee K, O'Sullivan AM, Billings E, Merbah M, Costanzo MC, Warren JA, Slike B, Li H, Peachman KK, Fischer W, Gao F, Cicala C, Arthos J, Eller LA, O'Connell RJ, Sinei S, Maganga L, Kibuuka H, Nitayaphan

S, Rao M, Marovich MA, Krebs SJ, Rolland M, Korber BT, Shaw GM, Michael NL, Robb ML, Tovanabutra S, Kim JH. 2017. Rare HIV-1 transmitted/founder lineages identified by deep viral sequencing contribute to rapid shifts in dominant quasispecies during acute and early infection. PLoS Pathog 13:e1006510.

59. Derking R, Ozorowski G, Sliepen K, Yasmeen A, Cupo A, Torres JL, Julien JP, Lee JH, van Montfort T, de Taeye SW, Connors M, Burton DR, Wilson IA, Klasse PJ, Ward AB, Moore JP, Sanders RW. 2015. Comprehensive antigenic map of a cleaved soluble HIV-1 envelope trimer. PLoS Pathog 11:e1004767.
60. Ma X, Lu M, Gorman J, Terry DS, Hong X, Zhou Z, Zhao H, Altman RB, Arthos J, Blanchard SC, Kwong PD, Munro JB, Mothes W. 2018. HIV-1 Env trimer opens through an asymmetric intermediate in which individual protomers adopt distinct conformations. eLife 7:e34271.
61. Zhao Q, Ma L, Jiang S, Lu H, Liu S, He Y, Strick N, Neamati N, Debnath AK. 2005. Identification of N-phenyl-N'-(2,2,6,6-tetramethyl-piperidin-4- yl)-oxalamides as a new class of HIV-1 entry inhibitors that prevent gp120 binding to CD4. Virology 339:213–225.
62. Herschhorn A, Gu C, Moraca F, Ma X, Farrell M, Smith AB, III, Pancera M, Kwong PD, Schon A, Freire E, Abrams C, Blanchard SC, Mothes W, Sodroski JG. 2017. The beta20-beta21 of gp120 is a regulatory switch for HIV-1 Env conformational transitions. Nat Commun 8:1049.
63. Shrivastava IH, Wendel K, LaLonde JM. 2012. Spontaneous rearrangement of the beta20/beta21 strands in simulations of unliganded HIV-1 glycoprotein, gp120. Biochemistry 51:7783–7793.
64. Tolbert WD, Sherburn RT, Van V, Pazgier M. 2019. Structural basis for epitopes in the gp120 cluster A region that invokes potent effector cell activity. Viruses 11:69.
65. Adams PD, Grosse-Kunstleve RW, Hung LW, Ioerger TR, McCoy AJ, Moriarty NW, Read RJ, Sacchettini JC, Sauter NK, Terwilliger TC. 2002. PHENIX: building new software for automated crystallographic structure determination. Acta Crystallogr D Biol Crystallogr 58:1948 –1954.
66. Guo D, Shi X, Arledge KC, Song D, Jiang L, Fu L, Gong X, Zhang S, Wang X, Zhang L. 2012. A single residue within the V5 region of HIV-1 envelope facilitates viral escape from the broadly neutralizing monoclonal antibody VRC01. J Biol Chem 287:43170 – 43179.

67. Zhou P, Wang H, Fang M, Li Y, Wang H, Shi S, Li Z, Wu J, Han X, Shi X, Shang H, Zhou T, Zhang L. 2019. Broadly resistant HIV-1 against CD4-binding site neutralizing antibodies. PLoS Pathog 15:e1007819.
68. Otsuka Y, Schmitt K, Quinlan BD, Gardner MR, Alfant B, Reich A, Farzan M, Choe H. 2018. Diverse pathways of escape from all well characterized VRC01-class broadly neutralizing HIV-1 antibodies. PLoS Pathog 14:e1007238.
69. Klein F, Nogueira L, Nishimura Y, Phad G, West AP, Jr, Halper-Stromberg A, Horwitz JA, Gazumyan A, Liu C, Eisenreich TR, Lehmann C, Fatkenheuer G, Williams C, Shingai M, Martin MA, Bjorkman PJ, Seaman MS, Zolla-Pazner S, Karlsson Hedestam GB, Nussenzweig MC. 2014. Enhanced HIV-1 immunotherapy by commonly arising antibodies that target virus escape variants. J Exp Med 211:2361–2372.
70. Klein F, Halper-Stromberg A, Horwitz JA, Gruell H, Scheid JF, Bournazos S, Mouquet H, Spatz LA, Diskin R, Abadir A, Zang T, Dorner M, Billerbeck E, Labitt RN, Gaebler C, Marcovecchio PM, Incesu RB, Eisenreich TR, Bieniasz PD, Seaman MS, Bjorkman PJ, Ravetch JV, Ploss A, Nussenzweig MC. 2012. HIV therapy by a combination of broadly neutralizing antibodies in humanized mice. Nature 492:118 –122.
71. Caskey M, Klein F, Lorenzi JCC, Seaman MS, West AP, Buckley N, Kremer G, Nogueira L, Braunschweig M, Scheid JF, Horwitz JA, Shimeliovich I, Ben-Avraham S, Witmer-Pack M, Platten M, Lehmann C, Burke LA, Hawthorne T, Gorelick RJ, Walker BD, Keler T, Gulick RM, Fätkenheuer G, Schlesinger SJ, Nussenzweig MC. 2015. Viraemia suppressed in HIV-1- infected humans by broadly neutralizing antibody 3BNC117. Nature 522:487– 491.
72. Yuan T, Li J, Zhang MY. 2013. HIV-1 envelope glycoprotein variable loops are indispensable for envelope structural integrity and virus entry. PLoS One 8:e69789.
73. Rashad AA, Acharya K, Haftl A, Aneja R, Dick A, Holmes AP, Chaiken I. 2017. Chemical optimization of macrocyclic HIV-1 inactivators for improving potency and increasing the structural diversity at the triazole ring. Org Biomol Chem 15:7770 –7782.
74. Rashad AA, Kalyana Sundaram RV, Aneja R, Duffy C, Chaiken I. 2015. Macrocyclic envelope glycoprotein antagonists that irreversibly inactivate HIV-1 before host cell encounter. J Med Chem 58:7603–7608.

75. Kassa A, Finzi A, Pancera M, Courter JR, Smith AB, III, Sodroski J. 2009. Identification of a human immunodeficiency virus (HIV-1) envelope glycoprotein variant resistant to cold inactivation. J Virol 83:4476-88.
76. Kassa A, Madani N, Schon A, Haim H, Finzi A, Xiang SH, Wang L, Princiotto A, Pancera M, Courter J, Smith AB, III, Freire E, Kwong PD, Sodroski J. 2009. Transitions to and from the CD4-bound conformation are modulated by a single-residue change in the human immunodeficiency virus type 1 gp120 inner domain. J Virol 83:8364 – 8378.
77. DeLeon O, Hodis H, O'Malley Y, Johnson J, Salimi H, Zhai Y, Winter E, Remec C, Eichelberger N, Van Cleave B, Puliadi R, Harrington RD, Stapleton JT, Haim H. 2017. Accurate predictions of population-level changes in sequence and structural properties of HIV-1 Env using a volatility-controlled diffusion model. PLoS Biol 15:e2001549.
78. Fontaine J, Chagnon-Choquet J, Valcke HS, Poudrier J, Roger M; Montreal Primary HIV Infection and Long-Term Non-Progressor Study Groups. 2011. High expression levels of B lymphocyte stimulator (BLyS) by dendritic cells correlate with HIV-related B-cell disease progression in humans. Blood 117:145–155.
79. Fontaine J, Coutlee F, Tremblay C, Routy JP, Poudrier J, Roger M; Montreal Primary HIV Infection and Long-Term Non-progressor Study Groups. 2009. HIV infection affects blood myeloid dendritic cells after successful therapy and despite non-progressing clinical disease. J Infect Dis 199:1007–1018.
80. Pereyra F, Jia X, McLaren PJ, Telenti A, de Bakker PIW, Walker BD, Ripke S, Brumme CJ, Pulit SL, Carrington M, Kadie CM, Carlson JM, Heckerman D, Graham RR, Plenge RM, Deeks SG, Gianniny L, Crawford G, Sullivan J, Gonzalez E, Davies L, Camargo A, Moore JM, Beattie N, Gupta S, Crenshaw A, Burtt NP, Guiducci C, Gupta N, Gao X, Qi Y, Yuki Y, Piechocka-Trocha A, Cutrell E, Rosenberg R, Moss KL, Lemay P, O'Leary J, Schaefer T, Verma P, Toth I, Block B, Baker B, Rothchild A, Lian J, Proudfoot J, Alvino DML, Vine S, Addo MM, Allen TM, et al. 2010. The major genetic determinants of HIV-1 control affect HLA class I peptide presentation. Science 330:1551–1557.
81. Kamya P, Boulet S, Tsoukas CM, Routy JP, Thomas R, Cote P, Boulassel MR, Baril JG, Kovacs C, Migueles SA, Connors M, Suscovich TJ, Brander C, Tremblay CL, Bernard N; Canadian Cohort of HIV Infected Slow Progressors. 2011. Receptor-ligand requirements

for increased NK cell polyfunctional potential in slow progressors infected with HIV-1 coexpressing KIR3DL1*h/*y and HLA-B*57. J Virol 85:5949 –5960.

82. Peretz Y, Ndongala ML, Boulet S, Boulassel MR, Rouleau D, Cote P, Longpre D, Routy JP, Falutz J, Tremblay C, Tsoukas CM, Sekaly RP, Bernard NF. 2007. Functional T cell subsets contribute differentially to HIV peptide-specific responses within infected individuals: correlation of these functional T cell subsets with markers of disease progression. Clin Immunol 124:57– 68.
83. Crooks GE, Hon G, Chandonia JM, Brenner SE. 2004. WebLogo: a sequence logo generator. Genome Res 14:1188 –1190.
84. Korber B, Foley BT, Kuiken C, Pillai SK, Sodroski JG. 1998. Numbering positions in HIV relative to HXB2CG, p 102–111. In Korber B, Kuiken CL, Foley B, Hahn B, McCutchan F, Mellors JW, Sodroski J (ed), Human Retroviruses and AIDS 1998. Theoretical Biology and Biophysics Group, Los Alamos National Laboratory, Los Alamos, NM.
85. Eddy SR. 2011. Accelerated profile HMM searches. PLoS Comput Biol 7:e1002195.
86. Guindon S, Dufayard JF, Lefort V, Anisimova M, Hordijk W, Gascuel O. 2010. New algorithms and methods to estimate maximum-likelihood phylogenies: assessing the performance of PhyML 3.0. Syst Biol 59: 307–321.
87. Farzan M, Mirzabekov T, Kolchinsky P, Wyatt R, Cayabyab M, Gerard NP, Gerard C, Sodroski J, Choe H. 1999. Tyrosine sulfation of the amino terminus of CCR5 facilitates HIV-1 entry. Cell 96:667– 676.
88. Montefiori DC, Karnasuta C, Huang Y, Ahmed H, Gilbert P, de Souza MS, McLinden R, Tovanabutra S, Laurence-Chenine A, Sanders-Buell E, Moody MA, Bonsignori M, Ochsenbauer C, Kappes J, Tang H, Greene K, Gao H, LaBranche CC, Andrews C, Polonis VR, Rerks-Ngarm S, Pitisuttithum P, Nitayaphan S, Kaewkungwal J, Self SG, Berman PW, Francis D, Sinangil F, Lee C, Tartaglia J, Robb ML, Haynes BF, Michael NL, Kim JH. 2012. Magnitude and breadth of the neutralizing antibody response in the RV144 and Vax003 HIV-1 vaccine efficacy trials. J Infect Dis 206: 431– 441.
89. Wu X, Parast AB, Richardson BA, Nduati R, John-Stewart G, MboriNgacha D, Rainwater SM, Overbaugh J. 2006. Neutralization escape variants of human immunodeficiency virus type 1 are transmitted from mother to infant. J Virol 80:835– 844.

90. Lodge R, Lalonde JP, Lemay G, Cohen EA. 1997. The membrane-proximal intracytoplasmic tyrosine residue of HIV-1 envelope glycoprotein is critical for basolateral targeting of viral budding in MDCK cells. EMBO J 16:695–705.
91. Chenine AL, Merbah M, Wieczorek L, Molnar S, Mann B, Lee J, O'Sullivan AM, Bose M, Sanders-Buell E, Kijak GH, Herrera C, McLinden R, O'Connell RJ, Michael NL, Robb ML, Kim JH, Polonis VR, Tovanabutra S. 2018. Neutralization sensitivity of a novel HIV-1 CRF01_AE panel of infectious molecular clones. J Acquir Immune Defic Syndr 78:348 –355.
92. Salazar-Gonzalez JF, Salazar MG, Keele BF, Learn GH, Giorgi EE, Li H, Decker JM, Wang S, Baalwa J, Kraus MH, Parrish NF, Shaw KS, Guffey MB, Bar KJ, Davis KL, Ochsenbauer-Jambor C, Kappes JC, Saag MS, Cohen MS, Mulenga J, Derdeyn CA, Allen S, Hunter E, Markowitz M, Hraber P, Perelson AS, Bhattacharya T, Haynes BF, Korber BT, Hahn BH, Shaw GM. 2009. Genetic identity, biological phenotype, and evolutionary pathways of transmitted/ founder viruses in acute and early HIV-1 infection. J Exp Med 206: 1273–1289.
93. Ochsenbauer C, Edmonds TG, Ding H, Keele BF, Decker J, Salazar MG, Salazar-Gonzalez JF, Shattock R, Haynes BF, Shaw GM, Hahn BH, Kappes JC. 2012. Generation of transmitted/founder HIV-1 infectious molecular clones and characterization of their replication capacity in CD4 T lymphocytes and monocyte-derived macrophages. J Virol 86: 2715–2728.
94. Liao HX, Lynch R, Zhou T, Gao F, Alam SM, Boyd SD, Fire AZ, Roskin KM, Schramm CA, Zhang Z, Zhu J, Shapiro L, Mullikin JC, Gnanakaran S, Hraber P, Wiehe K, Kelsoe G, Yang G, Xia SM, Montefiori DC, Parks R, Lloyd KE, Scearce RM, Soderberg KA, Cohen M, Kamanga G, Louder MK, Tran LM, Chen Y, Cai F, Chen S, Moquin S, Du X, Joyce MG, Srivatsan S, Zhang B, Zheng A, Shaw GM, Hahn BH, Kepler TB, Korber BT, Kwong PD, Mascola JR, Haynes BF; NISC Comparative Sequencing Program. 2013. Co-evolution of a broadly neutralizing HIV-1 antibody and founder virus. Nature 496:469 – 476.
95. Bar KJ, Tsao CY, Iyer SS, Decker JM, Yang Y, Bonsignori M, Chen X, Hwang KK, Montefiori DC, Liao HX, Hraber P, Fischer W, Li H, Wang S, Sterrett S, Keele BF, Ganusov VV, Perelson AS, Korber BT, Georgiev I, McLellan JS, Pavlicek JW, Gao F,

Haynes BF, Hahn BH, Kwong PD, Shaw GM. 2012. Early low-titer neutralizing antibodies impede HIV-1 replication and select for virus escape. PLoS Pathog 8:e1002721.

96. Fenton-May AE, Dibben O, Emmerich T, Ding H, Pfafferott K, Aasa-Chapman MM, Pellegrino P, Williams I, Cohen MS, Gao F, Shaw GM, Hahn BH, Ochsenbauer C, Kappes JC, Borrow P. 2013. Relative resistance of HIV-1 founder viruses to control by interferon-alpha. Retrovirology 10:146.
97. Parrish NF, Gao F, Li H, Giorgi EE, Barbian HJ, Parrish EH, Zajic L, Iyer SS, Decker JM, Kumar A, Hora B, Berg A, Cai F, Hopper J, Denny TN, Ding H, Ochsenbauer C, Kappes JC, Galimidi RP, West AP, Bjorkman PJ, Wilen CB, Doms RW, O'Brien M, Bhardwaj N, Borrow P, Haynes BF, Muldoon M, Theiler JP, Korber B, Shaw GM, Hahn BH. 2013. Phenotypic properties of transmitted founder HIV-1. Proc Natl Acad Sci USA 110:6626 – 6633.
98. Gao F, Bonsignori M, Liao HX, Kumar A, Xia SM, Lu X, Cai F, Hwang KK, Song H, Zhou T, Lynch RM, Alam SM, Moody MA, Ferrari G, Berrong M, Kelsoe G, Shaw GM, Hahn BH, Montefiori DC, Kamanga G, Cohen MS, Hraber P, Kwong PD, Korber BT, Mascola JR, Kepler TB, Haynes BF. 2014. Cooperation of B cell lineages in induction of HIV-1-broadly neutralizing antibodies. Cell 158:481– 491.
99. O'Brien WA, Koyanagi Y, Namazie A, Zhao JQ, Diagne A, Idler K, Zack JA, Chen IS. 1990. HIV-1 tropism for mononuclear phagocytes can be determined by regions of gp120 outside the CD4-binding domain. Nature 348:69 –73.
100. Rho HM, Poiesz B, Ruscetti FW, Gallo RC. 1981. Characterization of the reverse transcriptase from a new retrovirus (HTLV) produced by a human cutaneous T-cell lymphoma cell line. Virology 112:355–360.
101. Martin L, Stricher F, Misse D, Sironi F, Pugniere M, Barthe P, Prado-Gotor R, Freulon I, Magne X, Roumestand C, Menez A, Lusso P, Veas F, Vita C. 2003. Rational design of a CD4 mimic that inhibits HIV-1 entry and exposes cryptic neutralization epitopes. Nat Biotechnol 21:71–76.
102. Schon A, Madani N, Klein JC, Hubicki A, Ng D, Yang X, Smith AB, III, Sodroski J, Freire E. 2006. Thermodynamics of binding of a lowmolecular-weight CD4 mimetic to HIV-1 gp120. Biochemistry 45: 10973–10980.

103. Prevost J, Richard J, Ding S, Pacheco B, Charlebois R, Hahn BH, Kaufmann DE, Finzi A. 2018. Envelope glycoproteins sampling states 2/3 are susceptible to ADCC by sera from HIV-1-infected individuals. Virology 515:38 – 45.
104. Collaborative Computational Project, Number 4. 1994. The CCP4 suite: programs for protein crystallography. Acta Crystallogr D Biol Crystallogr 50:760 –763.
105. Otwinowski Z, Minor W. 1997. Processing of X-ray diffraction data collected in oscillation mode. Methods Enzymol 276:307–326.
106. Emsley P, Cowtan K. 2004. Coot: model-building tools for molecular graphics. Acta Crystallogr D Biol Crystallogr 60:2126 –2132.
107. Chen VB, Arendall WB, III, Headd JJ, Keedy DA, Immormino RM, Kapral GJ, Murray LW, Richardson JS, Richardson DC. 2010. MolProbity: all-atom structure validation for macromolecular crystallography. Acta Crystallogr D Biol Crystallogr 66:12–21.
108. Acharya P, Tolbert WD, Gohain N, Wu X, Yu L, Liu T, Huang W, Huang CC, Kwon YD, Louder RK, Luongo TS, McLellan JS, Pancera M, Yang Y, Zhang B, Flinko R, Foulke JS, Jr, Sajadi MM, Kamin-Lewis R, Robinson JE, Martin L, Kwong PD, Guan Y, DeVico AL, Lewis GK, Pazgier M. 2014. Structural definition of an antibody-dependent cellular cytotoxicity response implicated in reduced risk for HIV-1 infection. J Virol 88: 12895–12906.

6.2.10 FIGURES

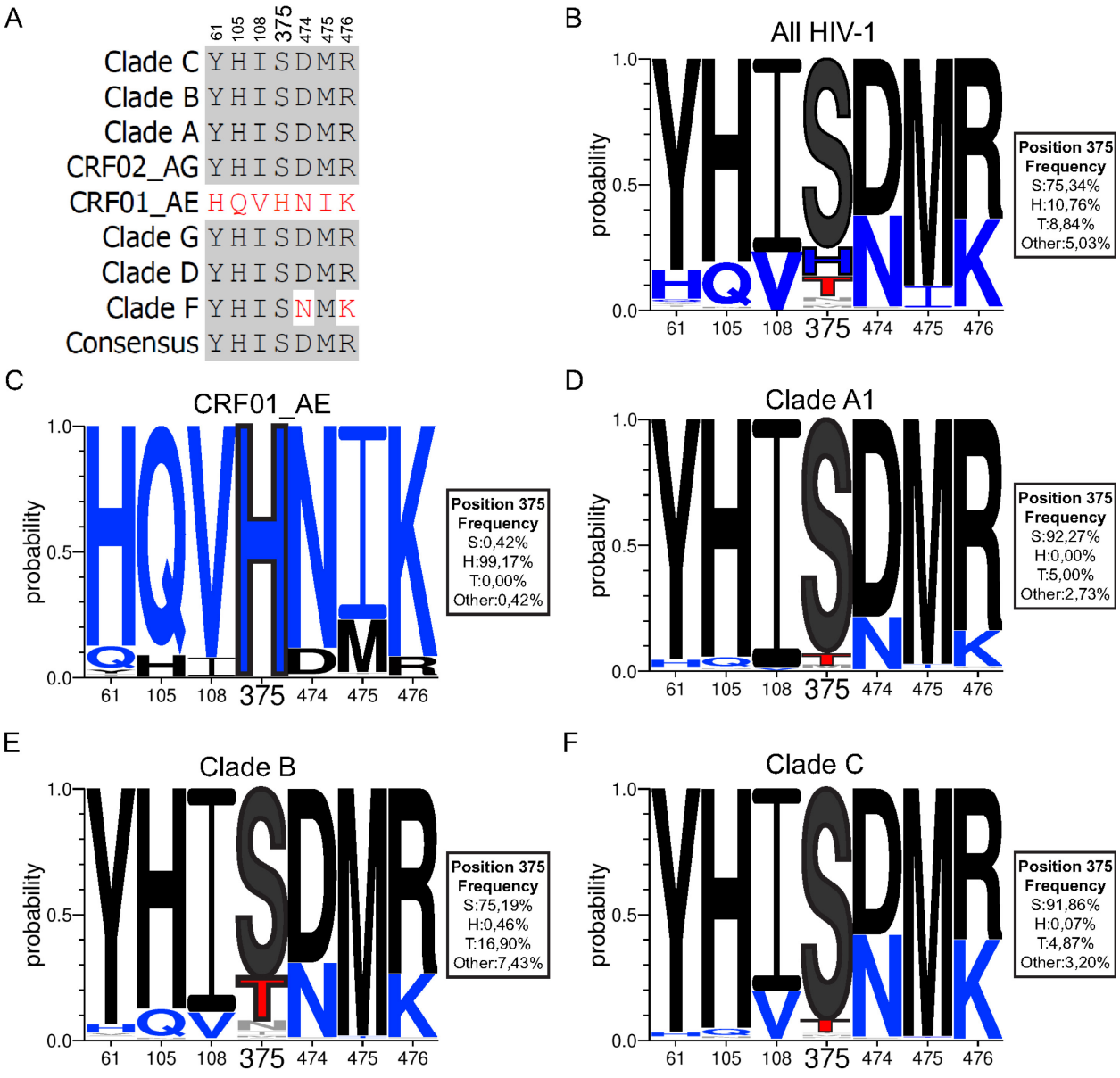

Figure 6.1.1 - Sequence alignment of gp120 Phe43 cavity and inner domain layer residues of different HIV-1 isolates.
(**A**) Sequence alignment of selected gp120 residues located in the Phe43 cavity (375) or the inner domain layers (61, 105, 108, 474, 475, and 476) based on the Env consensus sequence of each of the HIV-1 group M major subtypes (clades A, B, C, D, F, G, CRF01_AE, and CRF02_AG). The 2017 Los Alamos database-curated Env alignment was used as the basis for this figure, which contains 5,471 amino acid HIV-1 group M sequences (including 481 sequences of CRF01_AE, 220 of subtype A1, 1,937 of subtype B, and 1,377 of subtype C). Residue numbering is based on that of the HXBc2 strain of HIV-1. Identical residues are shaded in dark gray, and nonidentical residues are highlighted in red. (**B to F**) Logo depictions of the frequency of each amino acid from the Phe43 cavity at positions 61, 105, 108, 375, 474, 475, and 476 in all HIV-1 isolates (**B**) or in isolates from CRF01_AE (**C**), clade A1 (**D**), clade B (**E**), and clade C (**F**). The height of the letter indicates its frequency within the clade. S375 and its coevolving residues are shown in black, H375 and its coevolving residues are shown in blue, and T375 is shown in red. The box beside each logo indicates the frequency of all the amino acids at position 375.

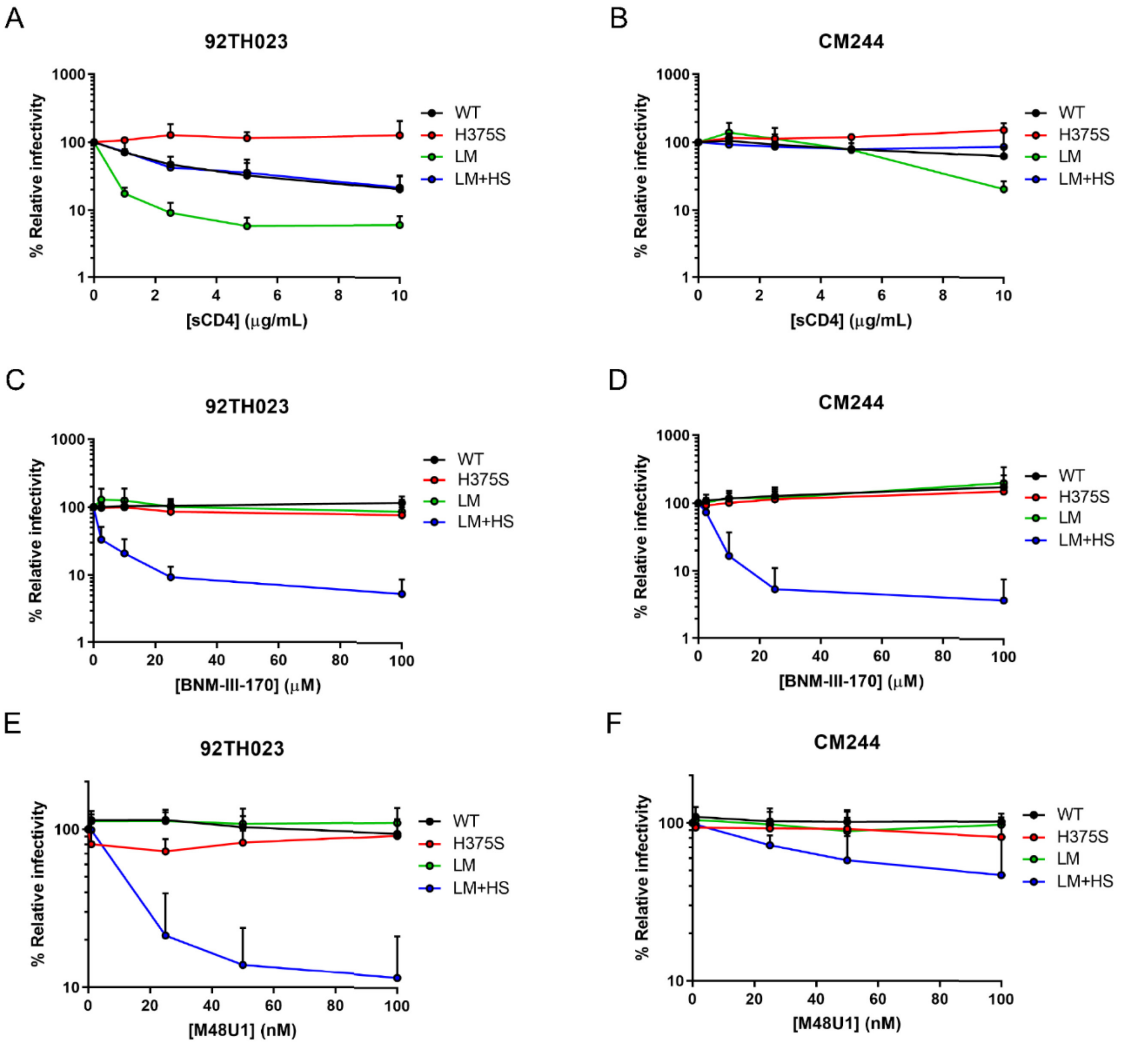

G

Neutralization IC_{50}			
92TH023	sCD4 µg/mL	BNM-III-170 µM	M48U1 nM
WT	2,32	>100	>100
H375S	>10	>100	>100
LM	0,61	>100	>100
LM+HS	2,12	1,88	16,11

Legend	
sCD4	CD4mc
IC_{50}<5	IC_{50}<50
5< IC_{50} <10	50< IC_{50} <100
IC_{50} >10	IC_{50} >100

Neutralization IC_{50}			
CM244	sCD4 µg/mL	BNM-III-170 µM	M48U1 nM
WT	>10	>100	>100
H375S	>10	>100	>100
LM	7,39	>100	>100
LM+HS	>10	1,88	86,21

Figure 6.1.2 - Effect of gp120 layer mutations on neutralization by CD4 and CD4mc.
Recombinant HIV-1 strains expressing luciferase and bearing wild-type or mutant CRF01_AE Envs (92TH023 and CM244 isolates) were normalized by reverse transcriptase activity. Normalized amounts of viruses were incubated with serial dilutions of sCD4 (**A and B**), BNM-III-170 (**C and D**), or M48U1 (**E and F**) at 37°C for 1 h prior to infection of Cf2Th-CD4/CCR5 cells. Infectivity at each dilution of sCD4 or CD4mc tested is shown as the percentage of infection without sCD4 or CD4mc for each particular mutant. Quadruplicate samples were analyzed in each experiment. Data shown are the means of results obtained in at least 3 independent experiments. The error bars represent the standard deviations. Neutralization half-maximal inhibitory concentration (IC_{50}) values are summarized in panel **G**.

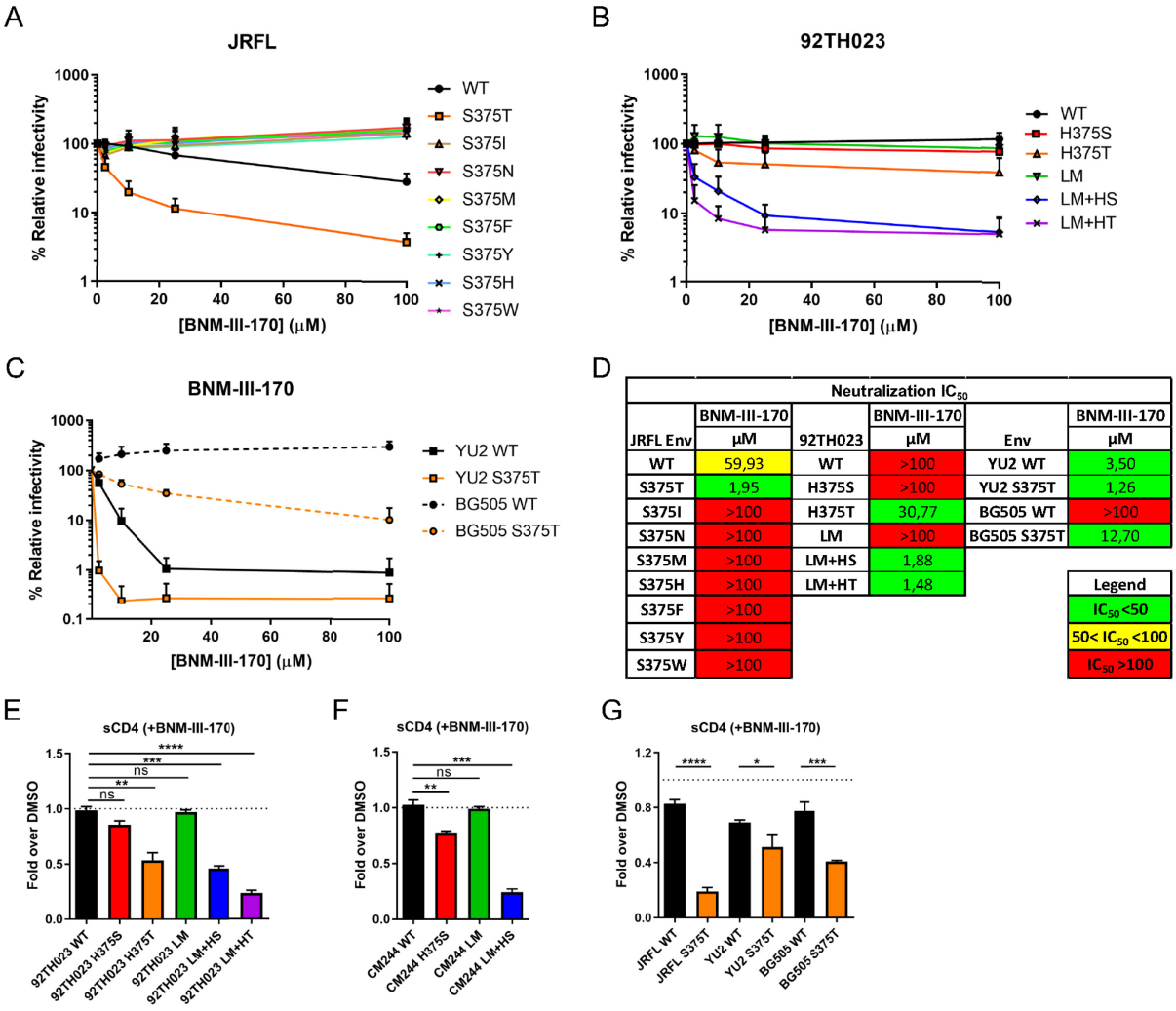

Figure 6.1.3 - Effect of Env residue 375 on CD4mc neutralization sensitivity.

(**A to D**) Recombinant HIV-1 strains expressing luciferase and bearing wild-type or mutant Envs (JRFL, 92TH023, YU2, and BG505 isolates) were normalized by reverse transcriptase activity. Normalized amounts of viruses were incubated with serial dilutions of BNM-III-170 (**A to C**) at 37°C for 1 h prior to infection of Cf2Th-CD4/CCR5 cells. Infectivity at each dilution of CD4mc tested is shown as the percentage of infection without CD4mc for each particular mutant. Quadruplicate samples were analyzed in each experiment. Data shown are the means of results obtained in at least 3 independent experiments. The error bars represent the standard deviations. Neutralization half-maximal inhibitory concentrations (IC_{50}) are summarized in panel **D**. (**E to G**) Cell surface staining of 293T cells transfected with different Env expressors (92TH023, CM244, JRFL, YU2, and BG505 isolates [WT or their mutated counterparts]). Binding of sCD4 in the presence of BNM-III-170 (50 µM) or in its absence (DMSO) was detected with the anti-CD4 OKT4 mAb. Shown are the mean fluorescence intensities (MFI) obtained in the presence of BNM-III-170 normalized to the MFI in the absence of BNM-III-170 (DMSO) from the transfected (GFP^+) population for staining obtained in at least 3 independent experiments. All MFI data were normalized to 2G12 MFI for each Env mutant. Error bars indicate means +/- standard errors of the means (SEM). Statistical significance was tested using an unpaired t test (*, $P < 0.05$; **, $P < 0.01$; ***, $P < 0.001$; ****, $P < 0.0001$; ns, nonsignificant).

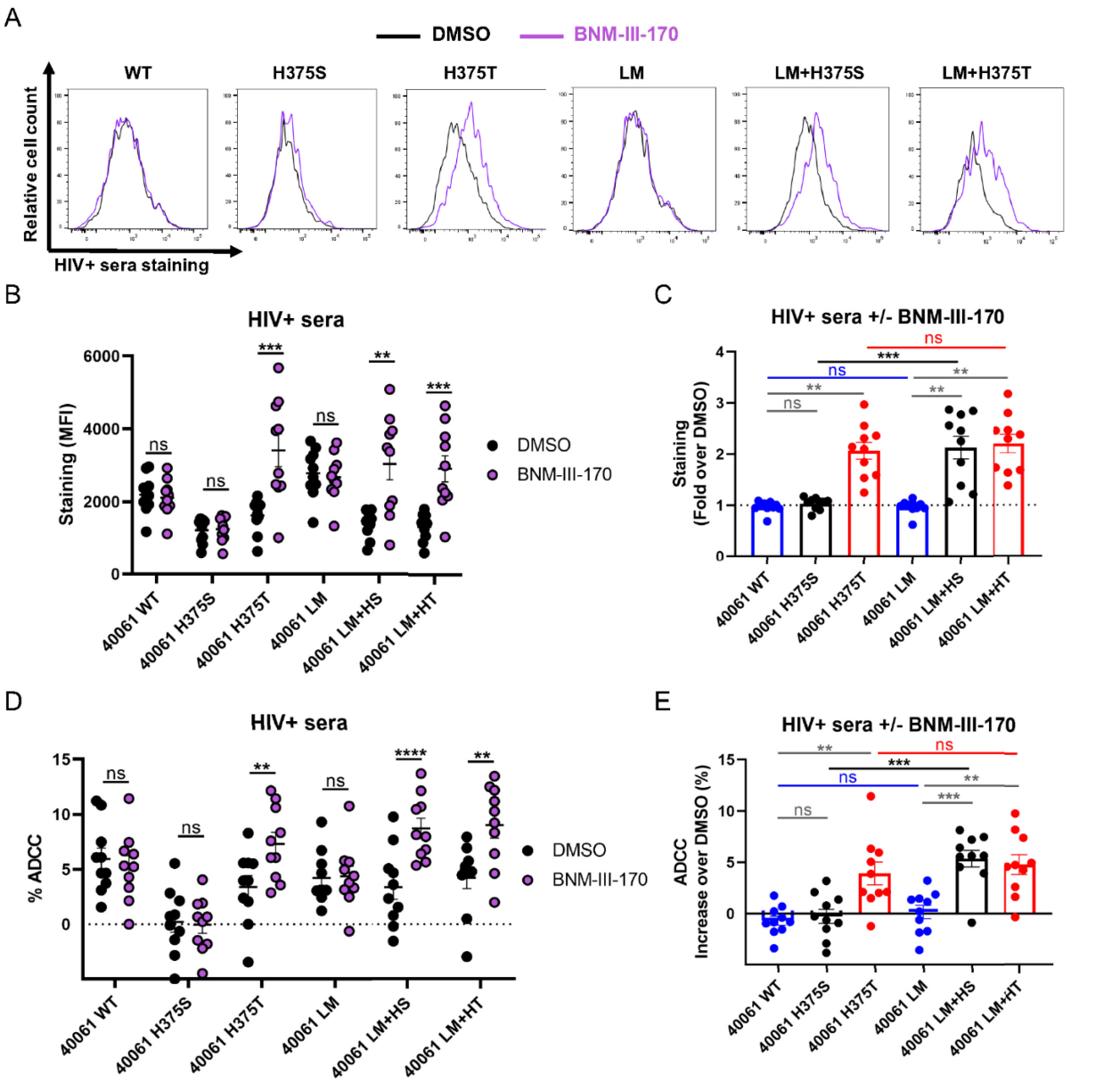

Figure 6.1.4 - Phe43 cavity and inner domain changes enhance susceptibility of the CRF01_AE HIV-1 strain to ADCC responses mediated by HIV$^+$ sera in the presence of CD4mc.

(**A to C**) Cell surface staining of primary CD4$^+$ T cells infected with a CRF01_AE transmitted-founder (TF) strain (40061) and variants with 10 different HIV$^+$ sera. (**A**) Histograms depicting representative HIV$^+$ serum staining. (**B and C**) The graphs shown represent the compiled mean fluorescence intensities (MFI) obtained with 10 HIV$^+$ sera (**B**) and the fold increase in MFI in the presence of CD4mc calculated for the infected (p24$^+$) population (**C**). (**D and E**) Infected primary CD4$^+$ T cells were also used as target cells, and autologous PBMCs were used as effector cells in a FACS-based ADCC assay. The graphs shown represent (**D**) the ADCC values and (**E**) the increase (in percentage points) of ADCC levels obtained in the presence of CD4mc with 10 HIV$^+$ sera. These results were obtained in at least 2 independent experiments. Error bars indicate means +/- SEM. Statistical significance was tested using a paired t test or a Wilcoxon rank test based on statistical normality (**, $P < 0.01$; ***, $P < 0.001$; ****, $P < 0.0001$; ns, nonsignificant).

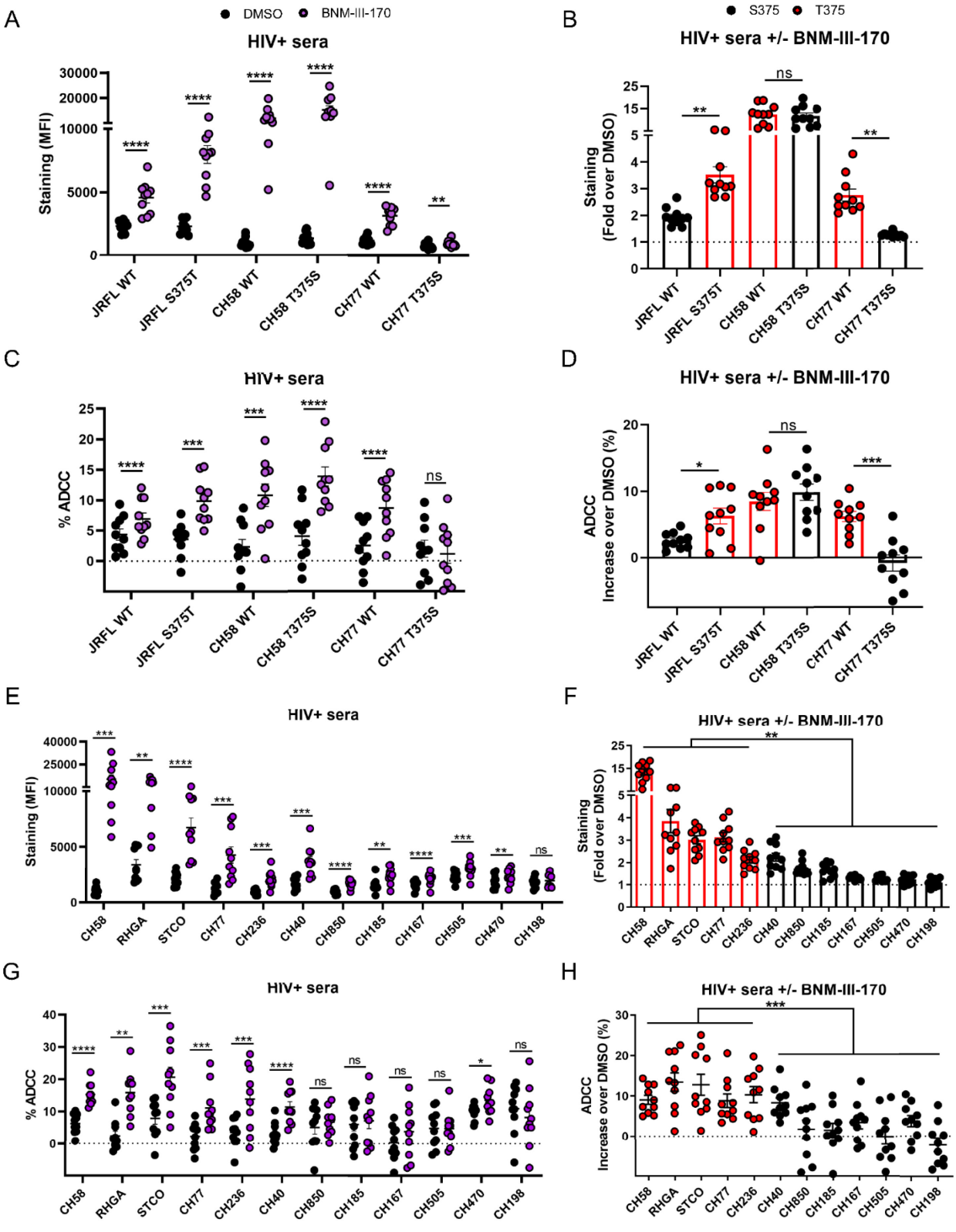
A
DMSO
BNM-III-170
HIV+ sera
Staining (MFI)
JRFL WT
JRFL S375T
CH58 WT
CH58 T375S
CH77 WT
CH77 T375S
B
S375
T375
HIV+ sera +/- BNM-III-170
Staining (Fold over DMSO)
C
HIV+ sera
% ADCC
D
HIV+ sera +/- BNM-III-170
ADCC Increase over DMSO (%)
E
HIV+ sera
Staining (MFI)
CH58
RHGA
STCO
CH77
CH236
CH40
CH850
CH185
CH167
CH505
CH470
CH198
F
HIV+ sera +/- BNM-III-170
Staining (Fold over DMSO)
G
HIV+ sera
% ADCC
H
HIV+ sera +/- BNM-III-170
ADCC Increase over DMSO (%)

Figure 6.1.5 - Primary viruses harboring a T375 residue are highly susceptible to ADCC responses mediated by HIV$^+$ sera in the presence of CD4mc.
Primary CD4$^+$ T cells were infected with clade B primary HIV-1 and their variants (**A to D**) or with a panel of TF and chronic viruses from clades B and C (**E to H**). At 48 h post-infection, cell surface staining was performed with 10 different HIV$^+$ sera. The graphs shown represent (**A and E**) the compiled mean fluorescence intensities (MFI) obtained with 10 HIV$^+$ sera and (**B and F**) the fold increase in MFI in the presence of CD4mc calculated on the infected (p24$^+$) population. Infected primary CD4$^+$ T cells were also used as target cells, and autologous PBMCs were used as effector cells in a FACS-based ADCC assay. The graphs shown represent (**C and G**) the ADCC values and (**D and H**) the increases (in percentage points) in the levels of ADCC obtained in the presence of CD4mc with 10 HIV$^+$ sera. These results were obtained in at least 2 independent experiments. Error bars indicate means +/- SEM. Statistical significance was tested using a paired t test or a Wilcoxon signed-rank test (**A to E and G**) or an unpaired t test or Mann-Whitney U test (**F and H**), based on statistical normality (*, $P < 0.05$; **, $P < 0.01$; ***, $P < 0.001$; ****, $P < 0.0001$; ns, nonsignificant).

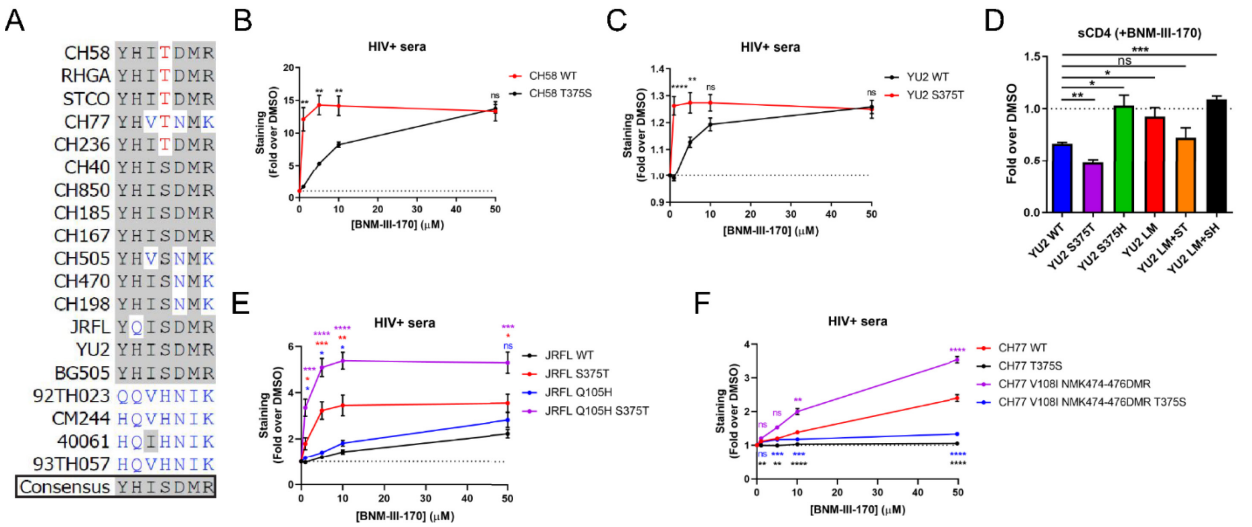

Figure 6.1.6 - Phe43 cavity and inner domain residues modulate the susceptibility of clade B strains to CD4mc.

(**A**) Sequence alignment of selected gp120 residues located in the Phe43 cavity (375) or the inner domain layers (61, 105, 108, 474, 475, and 476) for all HIV-1 strains used in this study. S375 and its coevolving residues are shown in black, H375 and its coevolving residues are shown in blue, and T375 is shown in red. Residues corresponding to the HIV-1 consensus sequence are shaded in gray. (**B, C, E, and F**) Cell surface staining with HIV$^+$ sera of primary CD4$^+$ T cells infected with clade B primary viruses (CH58, YU2, JRFL, and CH77) or their variants in the presence of increasing concentrations of BNM-III-170 (0, 1, 5, 10, and 50 μM). The graphs shown represent the compiled mean fluorescence intensities (MFI) obtained with 5 different HIV$^+$ sera in the presence of BNM-III-170 normalized to the MFI in the absence of BNM-III-170 (DMSO) from the infected (p24$^+$) population. These results were obtained in at least 2 independent experiments. (**D**) Cell surface staining of 293T cells transfected with an expressor of the HIV-1$_{YU2}$ Env WT or its mutated counterparts. Binding of sCD4 in the presence of BNM-III-170 (50 μM) or in its absence (DMSO) was detected with the anti-CD4 OKT4 mAb. Shown are the mean fluorescence intensities (MFI) obtained in the presence of BNM-III-170 normalized to the MFI in the absence of BNM-III-170 (DMSO) from the transfected (GFP$^+$) population for staining obtained in at least 3 independent experiments. All MFI data were normalized to 2G12 MFI for each Env mutant. Error bars indicate means +/- SEM. Statistical significance was tested using an unpaired t test or Mann-Whitney U test based on statistical normality (*, $P < 0.05$; **, $P < 0.01$; ***, $P < 0.001$; ****, $P < 0.0001$; ns, nonsignificant).

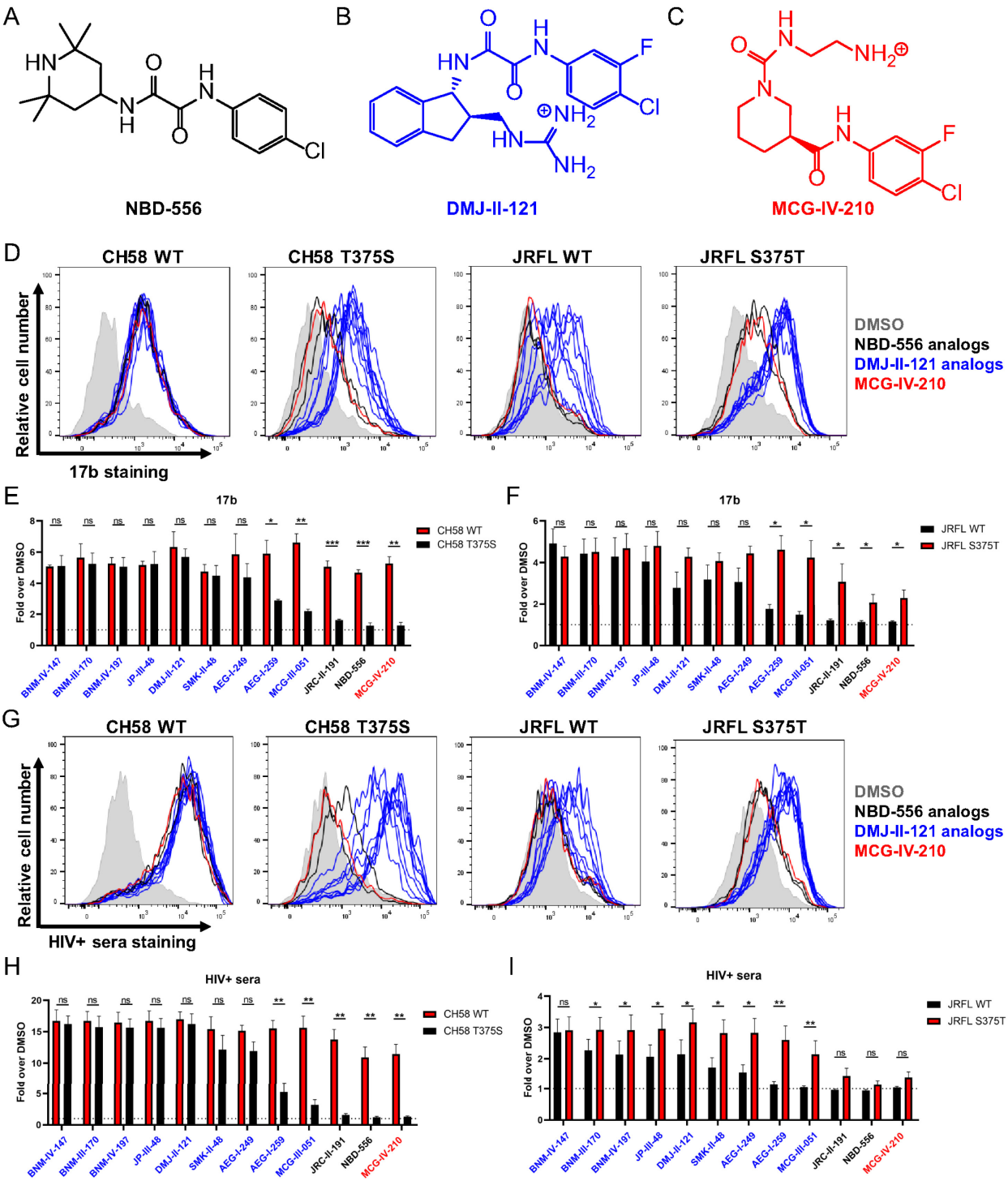
A
B
C
NBD-556
DMJ-II-121
MCG-IV-210
D
CH58 WT
CH58 T375S
JRFL WT
JRFL S375T
Relative cell number
17b staining
DMSO
NBD-556 analogs
DMJ-II-121 analogs
MCG-IV-210
E
17b
Fold over DMSO
CH58 WT
CH58 T375S
BNM-IV-147
BNM-III-170
BNM-IV-197
JP-III-48
DMJ-II-121
SMK-II-48
AEG-I-249
AEG-I-259
MCG-III-051
JRC-II-191
NBD-556
MCG-IV-210
F
17b
JRFL WT
JRFL S375T
G
HIV+ sera staining
H
HIV+ sera
I
HIV+ sera

Figure 6.1.7 - Residue 375 modulates Env sensitivity to different families of CD4mc.
(**A to C**) Chemical structures of representative members of the different families of CD4mc tested. (**D to I**) Cell surface staining of primary $CD4^+$ T cells infected with CH58 or JRFL viruses and their variants with anti-Env 17b mAb (**D to F**) or HIV^+ sera (**G to I**) was performed. Shown in panels D and G are histograms depicting representative 17b and HIV^+ serum staining results. The graphs shown represent the fold increase in mean fluorescence intensities (MFI) in the presence of CD4mc calculated on the infected ($p24^+$) population obtained with 17b (**E and F**) or with 5 different HIV^+ sera (**H and I**). These results were obtained in at least 3 independent experiments. Error bars indicate means +/- SEM. Statistical significance was tested using a paired t test or a Wilcoxon signed-rank test based on statistical normality (*, $P < 0.05$; **, $P < 0.01$; ***, $P < 0.001$; ns, nonsignificant).

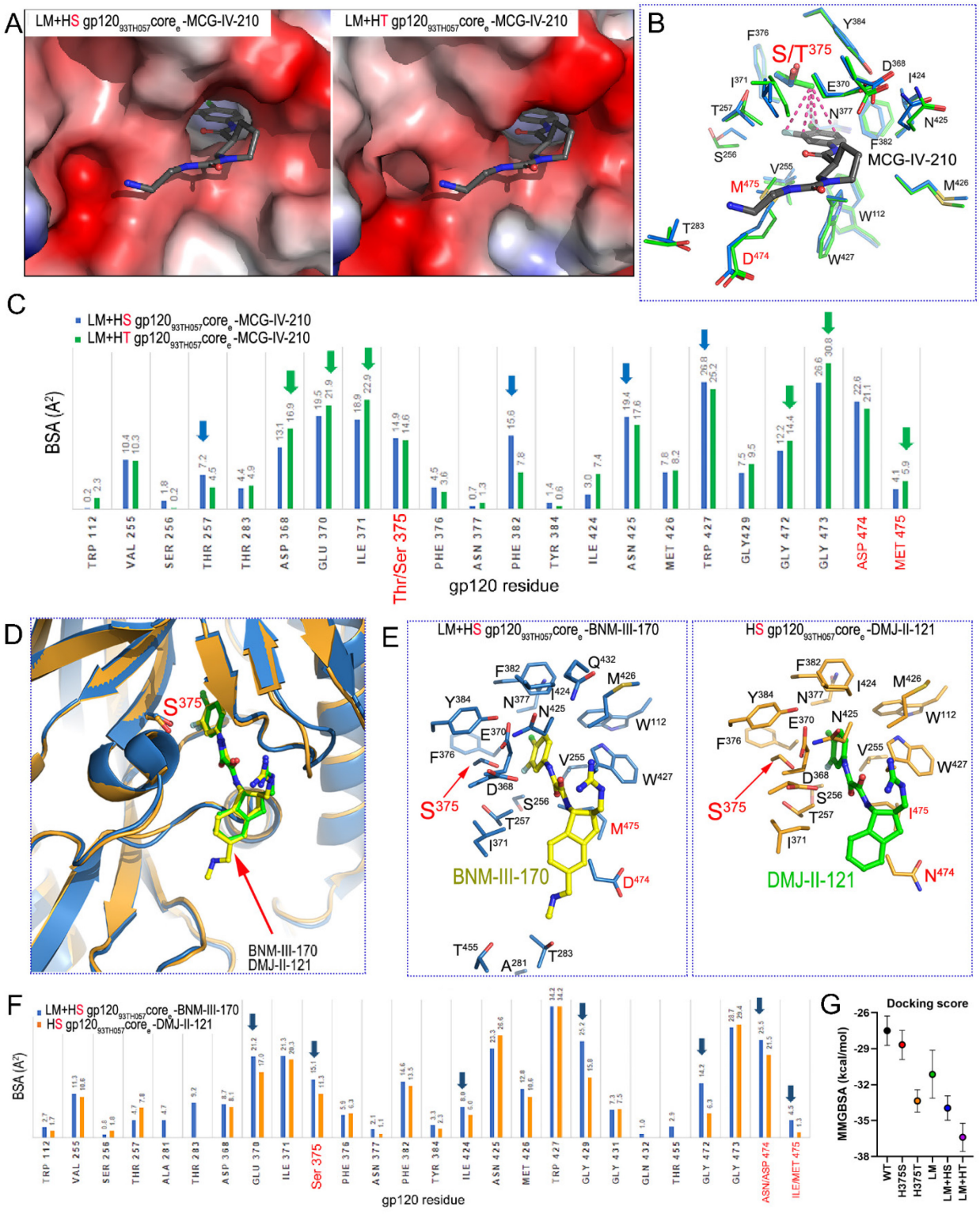
A
LM+HS gp120 93TH057 core e -MCG-IV-210
LM+HT gp120 93TH057 core e -MCG-IV-210
B
S/T375
MCG-IV-210
C
LM+HS gp120 93TH057 core e -MCG-IV-210
LM+HT gp120 93TH057 core e -MCG-IV-210
BSA (A2)
gp120 residue
Thr/Ser 375
D
S375
BNM-III-170
DMJ-II-121
E
LM+HS gp120 93TH057 core e -BNM-III-170
HS gp120 93TH057 core e -DMJ-II-121
BNM-III-170
DMJ-II-121
F
LM+HS gp120 93TH057 core e -BNM-III-170
HS gp120 93TH057 core e -DMJ-II-121
BSA (A2)
gp120 residue
Ser 375
G
Docking score
MMGBSA (kcal/mol)
WT
H375S
H375T
LM
LM+HS
LM+HT

Figure 6.1.8 - Structural effects of Phe43 cavity and inner domain changes on CD4mc docking into the Phe43 cavity.
(**A**) Magnified views of the CD4 binding pocket of LM+HS and LM+HT $gp120_{93TH057}$ core with MCG-IV-210 bound. Complexes are superimposed based on the gp120 core, and electrostatic surfaces are displayed over the gp120 molecule, with blue for electropositive and red for electronegative. The MGC-IV-210 compound is shown as balls and sticks. The LM+HT $gp120_{93TH057}$ core–MCG-IV-210 complex shown is from PDB ID 6P9N. (**B**) Details of MCG-IV-210 interactions within the binding pocket. The side chains of gp120 residues that interact with MCG-IV-210 are shown as sticks; LM+HS is depicted in green and LM+HT in blue. MCG-IV-210 is shown with balls and sticks. MCG-IV-210 atoms that interact with the T375 -carbon methyl group are shown with dashes connecting to the methyl group. (**C**) Analysis of the MCG-IV-210 interface for binding to LM+HS and LM+HT gp120. The relative contributions of gp120 residues to compound binding are shown as buried surface area (BSA) data as calculated by PISA. BSA data represent the solvent-accessible surface area of the corresponding residue that is buried upon interface formation. (**D**) Structural comparison of LM+HS $gp120_{93TH057}$ $core_e$–BNM-III-170 and HS $gp120_{93TH057}$ $core_e$–DMJ-II-121 (PDB ID 4I54) complex structures. Complexes are superimposed based on the gp120 core. CD4mc compounds and Ser375 are shown as sticks. (**E**) Details of binding of BNM-III-170 (left panel) and DMJ-II-121 (right panel) to LM+HS $gp120_{93TH057}$ $core_e$ and HS $gp120_{93TH057}$ $core_e$, respectively. Residues forming the binding site for the CD4mc compound are shown as sticks (with Gly residues omitted) with LM residues labeled in red. (**F**) Analysis of the gp120 $core_e$s-CD4mc binding interfaces. The relative contributions of gp120 residues to BNM-III-170 and DMJ-II-121 binding are shown by the buried surface area (BSA) as calculated by PISA. BSA represents the solvent-accessible surface area of the corresponding residue that is buried upon interface formation. (**G**) Docking score based on MMGBSA interaction energies, showing five replica simulations each along with averages, for six BNM-III-170-bound gp120 models.

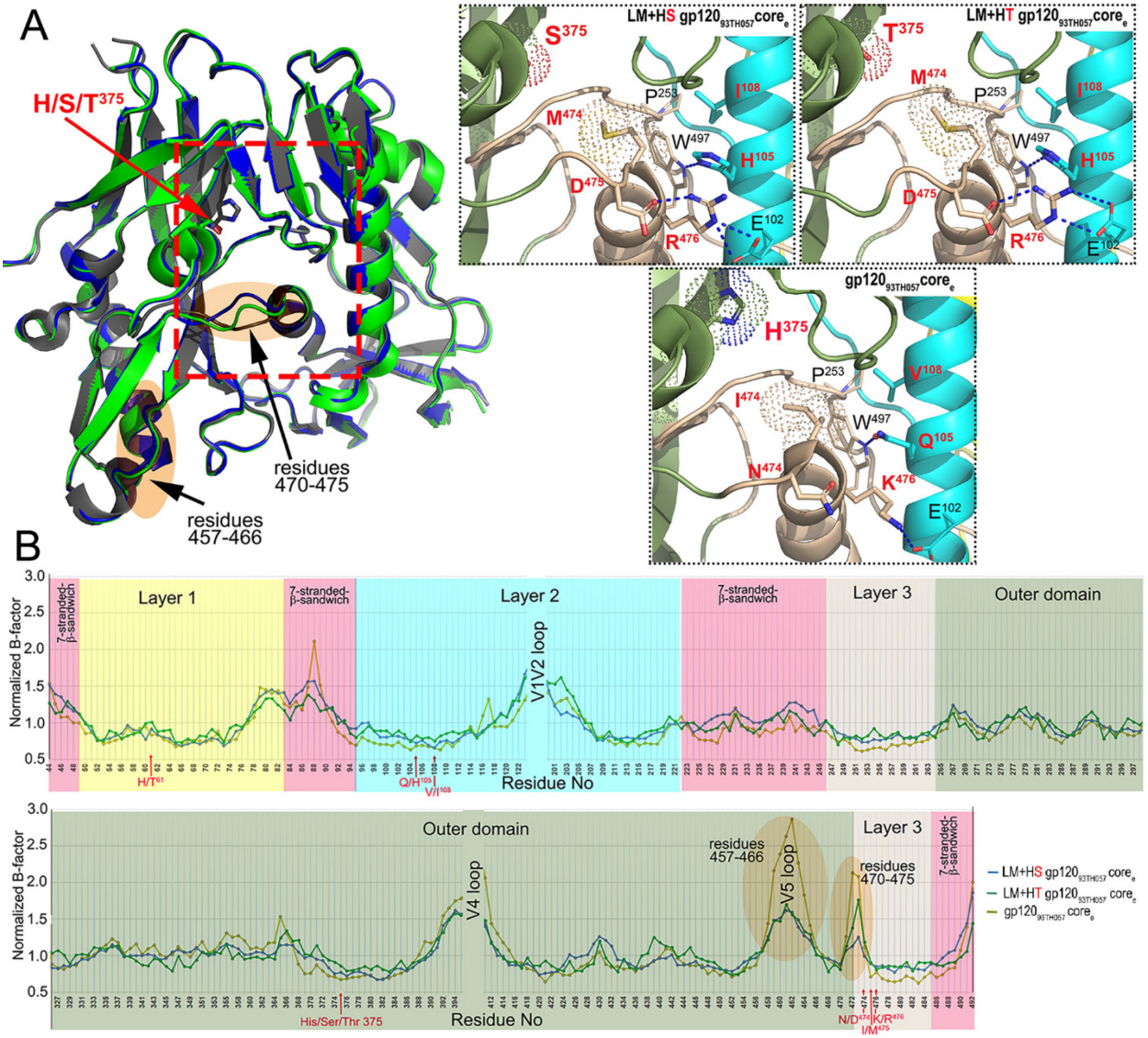

Neutralization IC_{50} (μg/mL)				
92TH023	VRC01	VRC13	VRC16	b12
WT	4,08	3,83	>10	>10
LM	2,10	3,60	3,44	>10
H375S	>10	3,59	>10	3,74
LM+HS	3,55	3,44	9,97	9,98

Legend	IC_{50} <5	5< IC_{50} <10	IC_{50} >10

Figure 6.1.9 - Effect of gp120 layer mutations on the highly conserved CD4 binding site.
(**A**) Structures of LM+HS and LM+HT $gp120_{93TH057}$ unliganded $core_e$s are superimposed onto wild-type $gp120_{93TH057}$ $core_e$ (PDB code: 3TGT). Residue 375 is shown as sticks, and the gp120 regions proximal to the CD4 binding site that shows the lowest B-factors in the LM core mutants compared to the unmutated core are highlighted in orange. The magnified views (right panel) show the network of interactions in each core mediated by LM+HS/T residues. The hydrogen bonds are shown as blue dashes. LM+HS/T residues are labeled in red. (**B**) Plot of the normalized B-factors for the main chain atoms of residues of $core_e$ structures. The rigidified region is highlighted in orange. (**C**) Cell surface staining of 293T cells transfected with CRF01_AE Env expressors (92TH023 and CM244 isolates [WT or their mutated counterparts]) using a panel of CD4-binding site antibodies (CD4BS Abs). Shown are the mean fluorescence intensities (MFI) normalized to 2G12 MFI obtained in the transfected (GFP^+) population for staining obtained in at least 3 independent experiments. All MFI data were normalized to 2G12 MFI for each Env mutant. Error bars indicate means +/- SEM. Statistical significance was tested using a paired t test or a Wilcoxon signed-rank test based on statistical normality (*, $P < 0.05$; **, $P < 0.01$; ***, $P < 0.001$). (**D**) Recombinant HIV-1 strains expressing luciferase and bearing wild-type or mutant CRF01_AE Envs (92TH023 and CM244 isolates) were normalized by reverse transcriptase activity. Normalized amounts of viruses were incubated with serial dilutions of VRC01, VRC16, VRC13, or b12 at 37°C for 1 h prior to infection of Cf2Th-CD4/CCR5 cells. Neutralization half-maximal inhibitory concentration (IC_{50}) data are summarized.

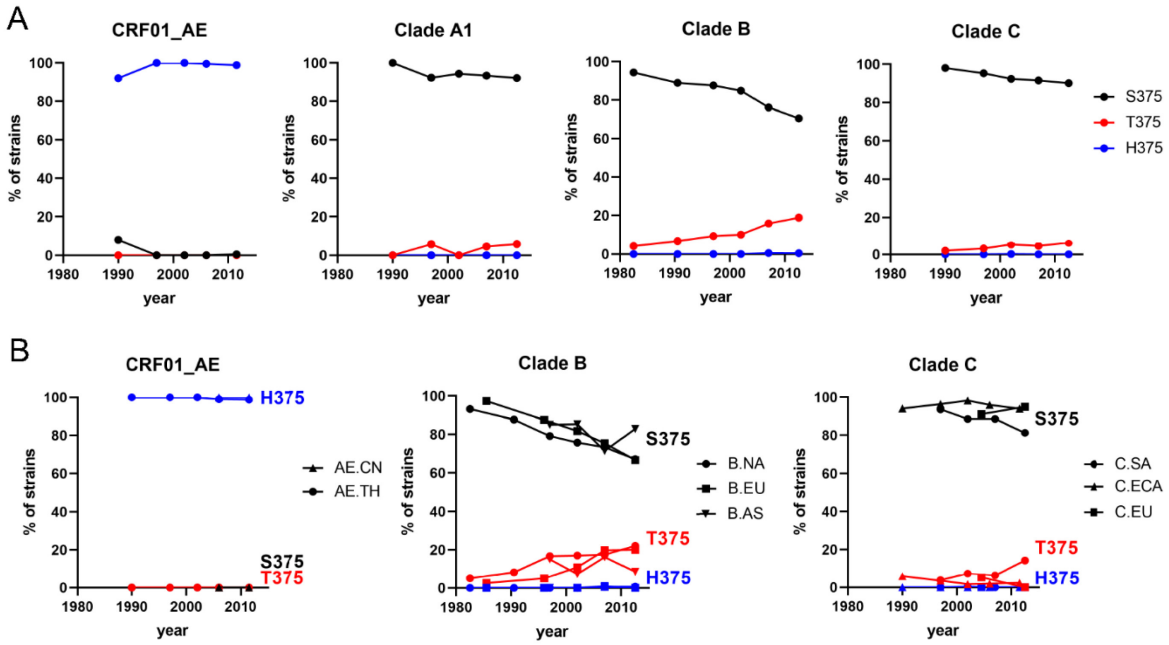

Figure 6.1.10 - Historical changes in amino acid sequence at position 375 in diverse clades and distinct geographic regions.

Env sequences from samples collected worldwide between 1979 and 2015 were examined. Totals of 335, 1,942, 1,248, and 543 Envs were used, from clades A1, B, C, and CRF01_AE, respectively. (**A**) Changes in frequencies of residues at position 375 in different clades. Values represent percentages of isolates from each 5-to-7-year period that contained the indicated residue. (**B**) Changes in frequencies of residues at position 375 in the indicated geographic regions. The residues shown in panels A and B account in most cases for more than 95% of all circulating strains. Sequences were analyzed phylogenetically to include a single Env from each patient (see Materials and Methods). For accuracy, only data from time periods with more than 25 patients are included for each clade and region. The following abbreviations are used: for clade B, NA, North America; EU, Europe; AS, Asia; for clade C, SA, Southern Africa (South Africa and Botswana); ECA, Eastern and Central Africa; IN/NP, India and Nepal; for CRF01_AE, CN, China; TH, Thailand.

6.2.11 SUPPLEMENTAL MATERIAL

Chemical synthesis

General Considerations

All reactions were conducted in oven-dried glassware under an inert atmosphere of nitrogen, unless otherwise stated. All solvents were reagent or high-performance liquid chromatography (HPLC) grade. Anhydrous CH_2Cl_2, toluene, ether and THF were obtained from the Pure SolveTM PS-400 system under an argon atmosphere. All reagents were purchased from commercially available sources and used as received. Reactions were magnetically stirred under a nitrogen atmosphere, unless otherwise noted and reactions were monitored by either thin layer chromatography (TLC) with 250 μm SiliaPlateTM pre-coated TLC plates or analytical ultraperformance liquid chromatography (UPLC). Yields refer to chromatographically or spectroscopically pure compounds. Optical rotations were measured on a JASCO P-2000 polarimeter. Proton (^{1}H) and carbon (^{13}C) NMR spectra were recorded on a Bruker Avance III 500-MHz spectrometer. Chemical shifts (δ) are reported in parts per million (ppm) relative to chloroform (δ 7.26), dimethyl sulfoxide (δ 2.50), acetone (δ 2.05) or methanol (δ 3.31) for ^{1}H-NMR, and chloroform (δ 77.0), dimethyl sulfoxide (δ 39.4), acetone (δ 29.8) or methanol (δ 49.0) for ^{13}C NMR. Infrared spectra were recorded using a JASCO 480-Plus FT-IR spectrometer, or a Perkin- Elmer Spectrum Two FT-IR spectrometer. Accurate mass measurements (AMM) were recorded at the University of Pennsylvania Mass Spectroscopy Service Center on either a Waters LCT Premier XE LC/MS or a Waters GC-TOF Premier system. Waters software calibrates and reports by use of neutral atomic masses. The mass of the electron is not included. Preparative scale HPLC was performed with a Gilson 333/334 preparative pump system equipped with a 5 mL injection loop, Sunfire C18 OBD column (10 μm packing material, 30 x 150 mm column dimensions) equipped with a UV-Vis dual wavelength (210 and 254 nm) detector and 215 liquid handling module. Solvent systems were comprised of H_2O and acetonitrile containing 0.1% trifluoroacetic acid. Lyophilization was performed in a Labconco FreeZone 12 Plus lyophilizer (0.035 mbar). The purity of new compounds was judged by NMR and LCMS (>95%).

Previously Reported Compounds

The synthesis and characterization of BNM-III-170, JP-III-048, BNM-IV-147, BNM-IV-197 (45), DMJ-II-121 (46), NBD-556 (101), JRC-II-191 (52) and MCG-IV-210 (37) have been previously reported.

Synthesis of SMK-II-048

Synthesis of aldehyde **1A** has been reported.[6]

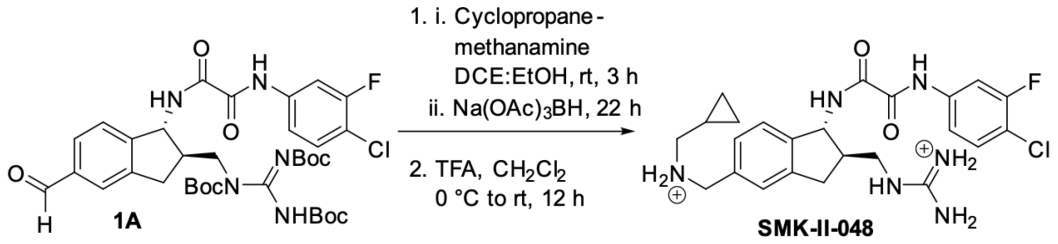

SMK-II-048. To a flask charged with aldehyde **1A** (30 mg, 0.041 mmol), cyclopropanemethylamine hydrochloride (44 mg, 0.41 mmol) at room temperature under nitrogen atmosphere was added dichloroethane (2 mL) and ethanol (2 mL). The reaction mixture was stirred at room temperature for 3 h before addition of sodium triacetoxyborohydride (6.0 mg, 0.103 mmol). The resulting reaction mixture was stirred at room temperature for 22 h, then cooled to 0 °C and quenched with aq. sat. $NaHCO_3$ and diluted with CH_2Cl_2. The biphasic solution was then adjusted to pH 10 with aq. 1M NaOH and stirred for 30 min. The layers were then separated and the resulting aqueous layer was extracted with CH_2Cl_2. The combined organic layers were washed with aq. sat. NaCl, dried over Na_2SO_4, and concentrated *in vacuo*. The reside was run through a plug of silica gel, eluting with 20:80 hexanes:EtOAc containing 1% triethylamine, then concentrated *in vacuo* and used in the next step without further purification. The residue was taken up in CH_2Cl_2 and cooled to 0 °C before addition of trifluoroacetic acid (0.075 mL, 1.0 mmol). The solution was stirred for 12 h at room temperature, then cooled to 0 °C before addition of trifluoroacetic acid (0.05 mL, 0.6 mmol). The solution was stirred at room temperature for 24 h, then concentrated *in vacuo* and taken up in H_2O/CH_3CN (80:20) and subjected to HPLC purification. Conditions: eluent H_2O/CH_3CN (90:10 to 20:80, linear gradient); flow rate: 15 mL/min; run time: 17 min. Product-containing fractions were combined and the resulting solution

was deep-frozen (-78 °C bath) and lyophilized to afford product as a white powder (3.7 mg, 12% yield from **1A**).

^{1}H NMR (500 MHz, Acetone-*d*6) δ 10.33 (s, 1H), 9.72 (s, 2H), 8.87 – 8.75 (m, 2H), 7.93 (s, 1H), 7.83 (s, 2H), 7.70 (d, J = 22.1 Hz, 2H), 7.51 (t, J = 8.5 Hz, 1H), 7.46 (s, 1H), 7.36 (d, J = 8.0 Hz, 1H), 7.23 (d, J = 7.7 Hz, 1H), 5.15 (d, J = 16.1 Hz, 1H), 4.26 (s, 2H), 3.57 (d, J = 29.7 Hz, 2H), 3.29 (dd, J = 15.9, 8.3 Hz, 1H), 2.82 – 2.74 (m, 2H), 0.62 (d, J = 8.4 Hz, 2H), 0.39 (s, 2H).

1) J. Chen, J. Park, S. M. Kirk, H. C. Chen, X. Li, D. Lippincott, B. Melillo and A.B. Smith, III. *Org. Process Res. Dev.* **2019**.(doi: 10.1021/acs.oprd.9b00353)

Synthesis of AEG-I-249 / AEG-I-259

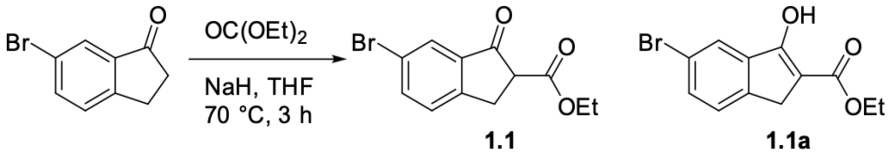

α-ketoester **1.1**. To a mixture of NaH (0.684 g, 17.1 mmol, 2.2 eq., 60% in mineral oil) in diethyl carbonate (5.65 mL, 46.6 mmol, 6 eq.) in a round bottom flask equipped with a reflux condenser under nitrogen gas at room temperature was added a solution of 6-bromoindanone (1.64 g, 7.77 mmol) in THF (13 mL). The reaction mixture was gradually warmed to 80 °C over 45 minutes. After another 2 hours the reaction was quenched with water. The reaction mixture was acidified to pH 2 with 1M aqueous HCl. This mixture was diluted with ethyl acetate and the layers were separated. The aqueous layer was washed with ethyl acetate (2 x 50 mL). The organic layers were combined, dried over sodium sulfate, decanted, and concentrated. Flash column chromatography (SiO_2, 100% hexanes to 25% ethyl acetate/hexanes) afforded a red solid (2.18 g, 99%).

^{1}H NMR (500 MHz, $CDCl_3$) 1:0.5 mixture of tautomers. δ 10.31 (br. s, 0.5 H), 7.89 (s, 1 H), 7.77 (s, 1 H), 7.72 (d, *J* = 8.1 Hz, 1 H), 7.52 (d, *J* = 8.1 Hz, 0.5 H), 7.39 (d, *J* = 8.1 Hz, 1 H), 7.32 (d, *J* = 8.1 Hz, 0.5 H), 4.33 (q, *J* = 7.1 Hz, 1 H), 4.25 (q, *J* = 7.1 Hz, 2 H), 3.74 (dd, *J* = 4.0, 8.2 Hz, 1 H), 3.50 (dd, *J* = 4.0, 17.4 Hz, 2 H), 3.32 (dd, *J* = 8.3, 17.4 Hz, 1 H), 1.38 (t, *J* = 7.1 Hz, 1.5 H), 1.31 (t, *J* = 7.1 Hz, 3 H).
^{13}C NMR (500 MHz, $CDCl_3$): δ 198.2, 168.8, 152.3, 141.8, 139.1, 138.3, 137.2, 132.2, 128.2, 127.6, 126.3, 123.9, 122.1, 120.9, 104.0, 62.1, 60.5, 53.7, 32.5, 30.1, 14.6, 14.3
IR ν_{max} 3379, 2922, 2845, 2300, 1564, 1399, 1108, 803
AMM (ESI) *m/z* 281.9892 [calcd for $C_{12}H_{11}BrO_3$ $(M+H)^+$ 281.98916]

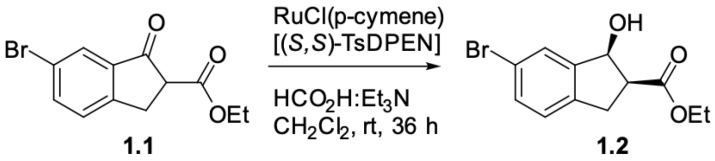

α-hydroxyester **1.2**. To a solution of **1.1** (1.19 g, 4.22 mol) and RuCl(*p*-cymene)[(*S,S*)-Ts-DPEN] (0.0537 g, 0.0843 mmol, 0.02 eq.) in dichloromethane (4.0 mL, 1.0 M) under nitrogen at room temperature was added 5:2 formic acid:triethylamine (1.2 mL). After three days, the reaction mixture was diluted with dichloromethane and water. The layers were separated and the aqueous layer was washed three times with dichloromethane. The organic layers were combined, dried with sodium sulfate, decanted and concentrated. The crude product mixture was purified using flash column chromatography (SiO_2, 100% hexanes to 20% ethyl acetate/hexanes) to afford a yellow solid (1.16 g, 97%).

^{1}H NMR (500 MHz, $CDCl_3$) δ 7.55 (s, 1 H), 7.40 (d, *J* = 8.0 Hz, 1 H), 7.13 (d, *J* = 7.7 Hz, 1 H), 5.29 (d, *J* = 5.8 Hz, 1 H), 4.22 (q, *J* = 7.1 Hz, 2 H), 3.35 (m, 2H), 3.04 (dd, *J* = 7.1, 14.9 Hz, 1 H), 1.31 (t, *J* = 7.0 Hz, 3 H).
^{13}C NMR (500 MHz, $CDCl_3$): δ 172.9, 145.1, 140.7, 132.1, 128.3, 126.5, 120.8, 75.6, 61.2, 49.6, 32.7, 14.4.
IR ν_{max} 3409, 2917, 2843, 2362, 2350, 2335, 1365
AMM (ESI) *m/z* 284.0048 [calcd for $C_{12}H_{13}BrO_3$ $(M+H)^+$ 284.00481]
[α]$_D^{23}$ = - 1 ° (*c*, 2.2 CH_2Cl_2)

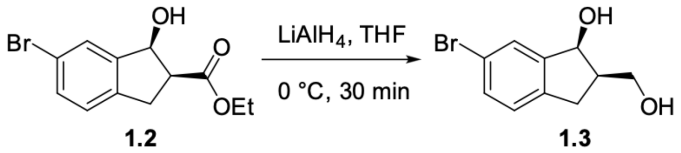

Diol **1.3**. To a solution of **1.2** (0.501 g, 1.76 mmol) in tetrahydrofuran (8.8 mL, 0.2 M) at 0 °C was added lithium aluminum hydride (0.100 g, 2.63 mmol, 1.5 eq.) in 5 equal aliquots in 5 minute intervals. After one hour the reaction was quenched at 0 °C with water, then saturated aqueous sodium potassium tartrate. The biphasic mixture was allowed to stir at room temperature for 30 minutes. The mixture was diluted with ethyl acetate and the layers were separated. The aqueous layer was washed three times with ethyl acetate. The organic layers were combined, dried over sodium sulfate, decanted, and concentrated. Flash column chromatography (SiO_2, 20% ethyl acetate / hexanes to 10% methanol / ethyl acetate) to afford the desired product (0.309 g, 72%).

^{1}H NMR (500 MHz, $CDCl_3$) δ 7.55 (s, 1 H), 7.40 (dd, *J* = 1.9, 8.0 Hz, 1 H), 7.13 (d, *J* = 8.0 Hz, 1 H), 5.31 (d, *J* = 5.9 Hz, 1 H), 3.93 (m, 2 H), 2.88 (m, 2 H), 2.75 (m, 1 H).
^{13}C NMR (500 MHz, $CDCl_3$): δ 146.4, 141.8, 131.9, 128.0, 126.7, 120.5, 77.2, 63.0, 45.4, 32.5
IR ν_{max} 3386, 2910, 2844, 2361, 2340, 1655, 1548
AMM (ESI) *m/z* 241.9640 [calcd for $C_{10}H_{11}BrO_2$ $(M+H)^+$ 241.99424]
[α]$_D^{23}$ = + 41 ° (*c* 0.2, CH_2Cl_2)

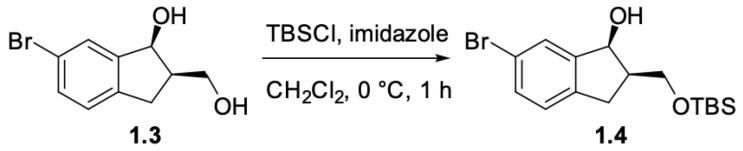

1.3 **1.4**

Alcohol **1.4**. To a solution of **1.3** (1.08 g, 4.44 mmol) in dichloromethane (44 mL, 0.1 M) under nitrogen at 0 °C was added imidazole (0.605 g, 8.88 mmol, 1.2 eq.) then TBSCl (0.803 g, 5.33 mmol, 1.2 eq.). After 1.5 hours, the reaction was quenched with water and diluted with dichloromethane. The layers were separated. The aqueous layer was washed three times with dichloromethane. The organic layers were combined, dried over sodium sulfate, decanted, and concentrated. Flash column chromatography (SiO_2, 100% hexanes to 10% ethyl acetate / hexanes) to afford the desired product as an oil (1.45 g, 91%).

^{1}H NMR (500 MHz, $CDCl_3$) δ 7.55 (s, 1 H), 7.35 (d, 1 H, *J* = 8.0 Hz), 7.08 (d, 1 H, *J* = 8.0 Hz), 5.25 (d, 1 H, *J* = 6.5 Hz), 3.96 (dd, 1 H, *J* = 7.0, 10.4 Hz), 3.37 (br s, 1 H), 2.88 (dd, 1 H, *J* = 8.1, 16.0 Hz), 2.77 (dd, 1 H, *J* = 6.1, 16.0 Hz), 2.70 (m, 1 H), 0.87 (s, 9 H), 0.10 (s, 3 H), 0.06 (s, 3 H).
^{13}C NMR (500 MHz, $CDCl_3$): δ 147.2, 141.3, 131.3, 128.1, 126.4, 120.4, 77.1, 63.7, 45.1, 33.0, 29.8, 25.9, 18.2, -5.4, -5.5
IR ν_{max} 3414.35, 2955.38, 2921.63, 2850.27, 2362.37, 2335.37, 1470.46, 1254.47, 1168.65, 1089.58
AMM (ESI) *m/z* 355.0758 obs. $C_{16}H_{23}BrO_2Si$ [356.0807 calcd for $C_{16}H_{25}BrO_2Si$ $(M+H)^+$]
[α]$_D^{23}$ = - 16 ° (*c* 0.07, CH_2Cl_2)

1.4 **1.5**

Azide **1.5**. To a solution of **1.4** (4.64 g, 13.0 mmol) in toluene under nitrogen at room temperature was added diphenylphosphoryl azide (5.6 mL, 26.0 mmol, 2 eq.). After ten minutes 1,8-diazabicyclo[5.4.0]undec-7-ene (5.4 mL, 36.4 mmol, 2.8 eq.) was added. The reaction mixture was then warmed to 85 °C and allowed to proceed overnight. The heating bath was removed and the reaction was quenched with water. The crude reaction mixture was diluted with water and ethyl

acetate. The layers were separated and the aqueous layer was washed four times with ethyl acetate. The organic layers were combined, dried over sodium sulfate, decanted, and concentrated. Flash column chromatography (SiO_2, 10% to 15 ethyl acetate / hexanes) to afford the desired product as an oil (4.69 g, 94%).

^{1}H NMR (500 MHz, $CDCl_3$) δ 7.51 (s, 1 H) 7.40 (d, 1 H, *J* = 8.1 Hz), 7.11 (d, 1 H, *J* = 8.4 Hz), 4.74 (d, 1 H, *J* = 6.0 Hz), 3.81 (dd, 1 H, *J* = 5.1, 10.3 Hz), 3.67 (dd, 1 H, *J* = 5.9, 10.3 Hz), 2.69 (dd, 1 H, *J* = 7.0, 15.8 Hz), 2.63 (m, 1 H), 0.91 (s, 9 H), 0.09 (overlapping s, 3 H), 0.08 (overlapping s, 3 H).
^{13}C NMR (500 MHz, $CDCl_3$): δ 143.0, 141.4, 131.8, 128.0, 126.7, 120.6, 61.7, 63.38, 49.7, 32.9, 26.0, -5.3
IR ν_{max} 2928, 2857, 2359, 2095, 1472, 1388, 1252, 1113, 984, 837, 777, 668
AMM(ESI)**:** sample did not ionize.
[α]$_D^{23}$ = - 40 ° (*c* 0.22, CH_2Cl_2)

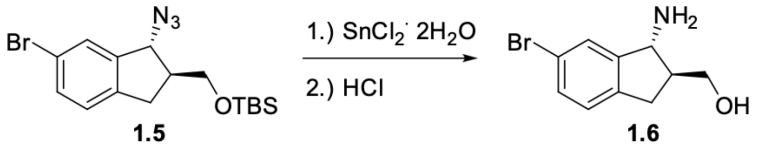

Aminol **1.6**. To a solution of **1.5** (3.32 g, 8.69 mmol) in methanol (29 mL, 0.3 M) under nitrogen at 0 °C was added tin chloride dihydrate (3.92 g, 17.4 mmol, 2 eq.). The reaction was allowed to proceed overnight. To the reaction mixture was then added 1 M aqueous HCl (15 mL). After five hours no starting material was observed. The pH of the reaction mixture was adjusted to 12 with 1 M aqueous NaOH. This solution was diluted with ethyl acetate and brine. The layers were separated. The aqueous layer was washed three times with ethyl acetate. The organic layers were combined, dried with magnesium sulfate, decanted and concentrated to afford the product (1.59 g, 75%).

^{1}H NMR (500 MHz, DMSO): δ 7.48 (s, 1 H), 7.30 (d, 1 H, *J* = 8.0 Hz), 7.12 (d, 1 H, *J* = 7.9 Hz), 3.93 (d, 1 H, *J* = 8.5 Hz), 3.66 (dd, 1 H, 5.1, 10.6 Hz), 3.58 (dd, 1 H, *J* = 6.2, 10.6 Hz), 2.84 (dd, 1 H, *J* = 8.1, 16.0 Hz), 2.54 (partially obscured dd, 1 H, *J* = 9.5, 16.0 Hz), 2.10 (m, 1 H).
^{13}C NMR (500 MHz, DMSO):δ 151.8, 141.5, 129.9, 127.3, 127.0, 119.7, 62.8, 59.3, 54.0.
IR ν_{max} 3393, 2945, 2843, 2369, 2329, 1659, 1420, 1375, 1247, 1127
AMM(ESI) *m/z* 242.0204 [calcd for $C_{10}H_{12}BrNO$ $(M+H)^+$ 242.0181]
[α]$_D^{23}$ = + 1 ° (*c* 0.18, CH_2Cl_2)

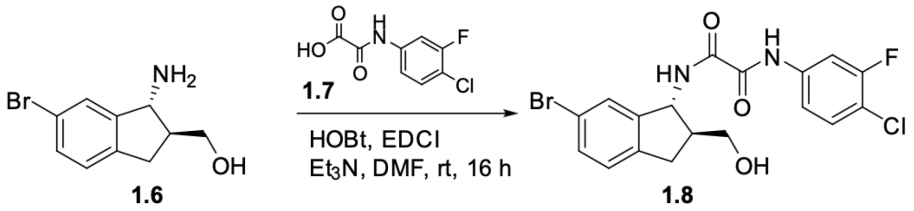

Alcohol **1.8**. To a solution of **1.6** (0.643 g, 2.65 mmol) and **1.7** (0.693 g, 3.18 mmol, 1.2 eq.) in dimethylformamide (6.6 mL, 0.5 M) at 0 °C under nitrogen was added EDCI hydrochloride (0.978 g, 6.36 mmol, 2.4 eq.) and hydroxybenzotriazole hydrate (1.22 g, 6.36 mmol, 2.4 eq.). After five minutes triethylamine was added (1.3 mL, 6.36 mmol, 2.4 eq.) and the reaction was allowed to proceed overnight. The reaction mixture was quenched with saturated aqueous sodium bicarbonate. The reaction mixture was diluted with water and ethyl acetate. The layers were separated and the aqueous layer was washed with ethyl acetate. The aqueous layer was adjusted to pH 9 with 1 M aqueous sodium hydroxide and washed twice with ethyl acetate. The organic layers were combined, dried with magnesium sulfate, and decanted. The organic layer was loaded onto celite and the product was purified with a silica gel plug (50% ethyl acetate / hexanes to 10% methanol / ethyl acetate) to afford the product as a white solid (0.763 g, 65%).

^{1}H NMR (500 MHz, DMSO): δ 11.06 (s, 1 H), 9.42 (d, 1 H, J = 8.7 Hz), 7.97 (dd, 1 H, J =2.3, 11.8 Hz), 7.75 (app. d, 1 H, J = 8.8 Hz), 7.60 (t, 1 H, J = 8.7 Hz), 7.39 (app. d, 1 H, J = 7.6 Hz), 7.32 (s, 1 H), 7.21 (d, 1 H, J = 8.0 Hz), 5.22 (t, 1 H, J = 8.4 Hz), 4.75 (t, 1 H, J = 5.0 Hz), 3.54 (m, 2 H), 3.00 (m, 1 H), 2.70 (m, 2 H).
^{13}C NMR (500 MHz, DMSO): δ 160.6, 159.5, 157.4 (d, J_{CF} = 244 Hz), 156.4, 146.5, 142.3, 139.0 (d, J_{CF} = 10 Hz), 131.2, 130.9, 127.4, 127.2, 119.7, 118.0 (d, J_{CF} = 3 Hz), 114.9 (d, J_{CF} = 17 Hz), 109.1 (d, J_{CF} = 26 Hz), 62.1, 56.5, 49.1, 33.5.
IR ν_{max} 3372, 3258, 2919, 2367, 1660, 1515, 1060, 956, 674, 441, 426
AMM(ESI) *m/z* 441.0021 [calcd for $C_{18}H_{15}BrClFN_2O_3$ $(M+H)^+$ 441.0017]
[α]$_D^{23}$ = + 16 ° (*c* 0.26, CH_2Cl_2)

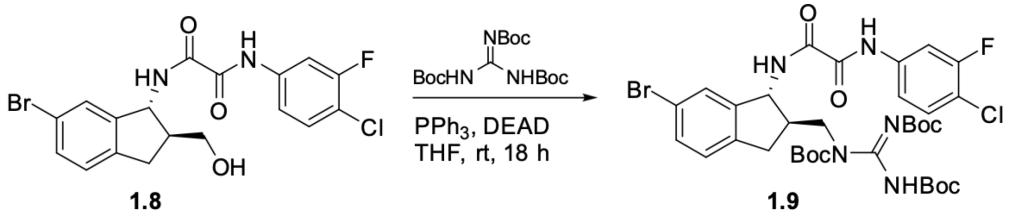

Bromide **1.9**. To a solution of alcohol **1.8** (0.180 g, 0.407 mmol) and triphenylphosphine (0.427 g, 1.63 mmol, 4 eq.) in tetrahydrofuran (15 mL, 0.02 M) under nitrogen at room temperature was added tribocguanidine (0.242 g, 0.403 mmol, 0.99 eq.). To this mixture was slowly added diethyl

azodicarboxylate (0.43 mL, 1.63 mmol, 4 eq.) and the reaction was allowed to proceed overnight. The reaction was quenched with aqueous sodium bicarbonate and diluted with ethyl acetate and water. The layers were separated and the aqueous layer was washed three times with ethyl acetate. The organic layers were combined, dried with sodium sulfate, decanted and concentrated. The crude reaction mixture was purified using flash column chromatography (SiO_2, dry loading on celite, 10% ethyl acetate / hexanes) to afford a white solid (0.108 g, 68%).

^{1}H NMR (500 MHz, $CDCl_3$): δ 10.61 (br s, 1 H), 9.38 (s, 1 H), 7.89 (d, 1 H, J = 9.0 Hz), 7.76 (dd, 1 H, J = 2.4, 10.6 Hz), 7.37 (m, 2 H), 7.33 (s, 1 H), 7.27 (m, 1 H), 7.11 (d, 1 H, J = 8.7 Hz), 5.24 (t, 1 H, J = 8.1 Hz), 4.13 (m, 2 H), 3.14 (dd, 1 H, J = 7.9, 15.8 Hz), 2.91 (m, 1 H), 2.74 (dd, 1 H, J = 9.0, 15.8 Hz), 1.51 (m, 27 H).
^{13}C NMR (500 MHz, $CDCl_3$): δ 159.74, 158.2 (d, J_{CF} = 248 Hz), 157.32, 153.39, 153.25, 143.64, 140.81, 136.5 (d, J_{CF} = 9.6 Hz), 131.52, 130.94, 127.20, 126.55, 120.70, 117.2 (d, J_{CF} = 18.1 Hz), 116.04 (d, J_{CF} = 3.5 Hz), 108.59 (d, J_{CF} = 26.1 Hz), 83.79, 58.44, 49.78, 48.12, 34.72, 29.84, 28.38, 28.19, 28.16, 28.13, 28.09, 27.96.
IR ν_{max} 3277, 2972, 2927, 2852, 2360, 1762, 1664, 1610, 1517, 1251, 1148, 664
AMM(ESI) *m/z* 782.1984 [calcd for $C_{34}H_{42}BrClFN_5O_8$ $(M+H)^+$ 782.1968]
[α]$_D^{23}$ = + 15 ° (*c* 0.4, CH_2Cl_2)

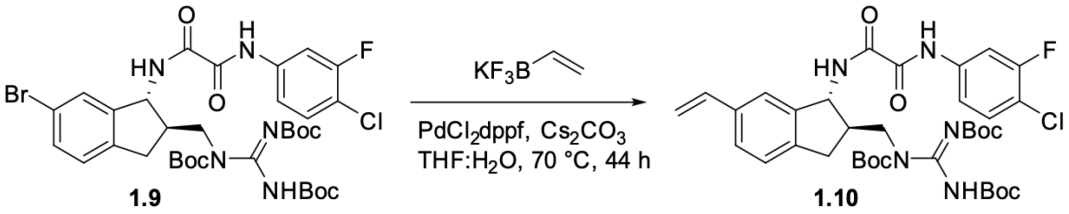

Alkene **1.10**. Bromide **1.9** (0.0987 g, 0.126 mmol), $Pd(dppf)Cl_2$ (0.0082 g, 0.0101 mmol, 0.08 eq.), vinyltrifluoroborate (0.0506 g, 0.378 mmol, 3 eq.) and cesium carbonate (0.164 g, 0.504 mmol, 4 eq.) under nitrogen at room temperature were dissolved in nitrogen-sparged THF/water (32 mL, 10:1, 0.004 M) in a round bottom flask equipped with a reflux condenser. The reaction mixture was heated to reflux overnight. After 21 h, the reaction mixture was cooled to room temperature and diluted with water. The reaction mixture was then filtered through celite with diethyl ether and diluted with water. The layers were separated and the aqueous layer was washed three times with diethyl ether. The organic layers were combined, dried over sodium sulfate, decanted and concentrated. The crude product mixture was purified using flash column chromatography (SiO_2, 20% hexanes / ethyl acetate) to afford product as a white solid (0.058 g, 63%).

^{1}H NMR (500 MHz, $CDCl_3$): δ10.55 (br s, 1 H), 9.38 (s, 1 H), 7.82 (d, 1 H, J = 9.1 Hz), 7.76 (dd, 1 H, J = 2.5 , 10.6 Hz), 7.38 (t, 1 H, J = 8.3 Hz), 7.30 (m, 1 H), 7.25 (m, 1 H), 7.23 (s, 1H), 7.19 (d, 1 H, J = 7.8 Hz), 6.67 (dd, 1 H, J = 10.9, 17.5 Hz), 5.69 (app. d, 1 H, J = 17.6 Hz), 5.25 (t, 1 H, J = 8.7 Hz), 5.20 (d, 1 H, J = 10.9 Hz), 4.14 (m, 1 H), 3.17 (dd, 1 H, J = 7.8, 15.8 Hz), 2.88 (m, 1 H), 2.79 (dd, 1 H, J = 8.8, 15.7 Hz), 1.56 - 1.44 (m, 27 H).
^{13}C NMR (500 MHz, $CDCl_3$):δ 159.7, 158.2 (d, J_{CF} = 248 Hz), 157.5, 153.3, 153.2, 141.7 (d, J_{CF} = 8 Hz), 137.0, 136.6, 136.5, 130.9, 126.8, 125.1, 121.5, 117.1 (d, J_{CF} = 18 Hz), 116.0 (d, J_{CF} = 3 Hz), 113.8, 108.4 (d, J_{CF} = 26 Hz), 83.7, 58.5, 50.0, 48.4, 35.0, 28.2, 28.2, 28.1
IR ν_{max} 3277, 2977. 2924, 2857, 2360, 2336, 1757, 1664, 1517, 1366, 1243, 1150 668
AMM(ESI) *m/z* 752.2864 [calcd for $C_{36}H_{45}ClFN_5O_8$ $(M+Na)^+$ 752.2838]
[α]$_D^{23}$ = + 19 ° (*c* 0.5, CH_2Cl_2)

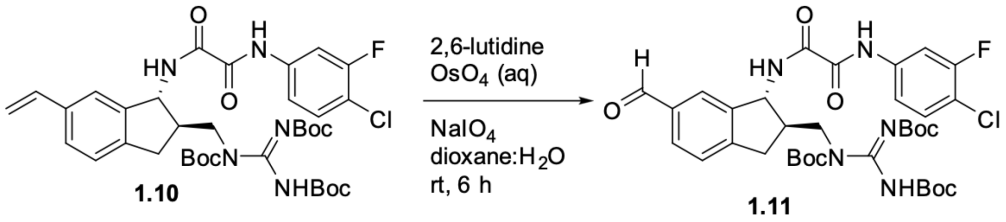

Aldehyde **1.11**. To a solution of alkene **1.10** (0.136 g, 0.186 mmol) in THF/water (3:1, 3 mL, 0.05 M) was added osmium tetroxide (2 mol% in water, 0.95 mL, 0.019 mmol, 0.1 eq.) then sodium periodate (0.120 g, 0.559 mmol, 3 eq). After three hours, the reaction was quenched with saturated aqueous sodium thiosulfate and allowed to stir overnight. The reaction mixture was diluted with ethyl acetate and the layers were separated. The aqueous layer was washed three times with ethyl acetate. The organic layers were combined, dried with magnesium sulfate, decanted and concentrated. The crude product mixture was purified using flash column chromatography (SiO_2, 100% hexanes to 30% ethyl acetate / hexanes, ethyl acetate flush) to afford the product as a solid (0.112 g, 82%).

^{1}H NMR (500 MHz, $CDCl_3$): δ 10.59 (br s, 1 H), 9.96 (s, 1 H), 9.31 (s, 1 H), 7.90 (d, 1 H, J = 8.7 Hz), 7.79 (d, 1 H, J = 7.7 Hz), 7.75 (m, 1 H), 7.72 (s, 1 H), 7.39 (t, 2 H, J = 8.3 Hz), 7.24 (d, 1 H, J = 8.6 Hz), 5.31 (t, 1 H, J = 8.7 Hz), 4.16 (m, 1 H), 3.27 (dd, 1 H, J = 7.5, 16.1 Hz), 2.92 (m, 2 H), 1.59 – 1.43 (m, 27 H).
^{13}C NMR (500 MHz, $CDCl_3$): δ 191.7, 159.8, 158.3 (d, J_{CF} = 248 Hz), 157.3, 153.6, 153.2, 149.2, 142.7, 136.4 (d, J_{CF} = 10 Hz), 136.1, 131.0, 130.7, 125.7, 125.1, 117.2 (d, J_{CF} = 18 Hz), 116.0 (d, J_{CF} = 4 Hz), 108.5 (d, J_{CF} = 26 Hz), 83.8, 58.3, 49.8, 48.0, 35.5, 28.2, 28.12, 28.08
IR ν_{max} 3393, 3284, 2979, 2932, 2852,1792, 1725, 1666, 1606, 1517, 1369, 1295, 1248, 1147, 775
AMM(ESI) *m/z* 732.2798 [calcd for $C_{35}H_{43}ClFN_5O_9$ $(M+H)^+$ 732.2812]
[α]$_D^{23}$ = + 31 ° (*c* 2.0, CH_2Cl_2)

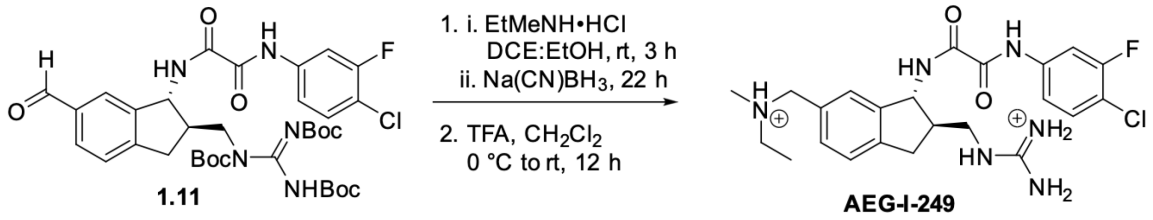

AEG-I-249. To a solution of **1.11** (0.030 g, 0.039 mmol) in dichloroethane (3 mL, 0.02 M) with 3 Å molecular sieves under nitrogen atmosphere at room temperature was added ethylmethylamine (0.08 mL, 0.948 mmol, 20 eq.). After stirring for one hour, sodium triacetoxyborohydride (0.016 g, 0.26 mmol, 5 eq.) was added. After 7 hours, no starting material was observed by TLC or LC/MS. The reaction was quenched with saturated aqueous sodium bicarbonate and diluted with ethyl acetate. The layers were separated, and the aqueous layer was washed three times with ethyl acetate. The organic layers were combined, dried over sodium sulfate, decanted, and concentrated. Flash column chromatography (SiO_2, 0% to 5% MeOH in dichloromethane) afforded a partially purified amine. This amine was dissolved in dichloromethane (3.9 mL, 0.01 M). To this solution was added trifluoroacetic acid (0.12 mL, 1.6 mmol, 40 eq.). After two days complete conversion was observed by LC/MS. The reaction mixture was concentrated, dissolved in 2.3 mL 1:1 acetonitrile/water and purified by reverse phase HPLC (15 mL/min, 15-70% H_2O/ACN + 0.1% TFA, 10 min gradient). The isolated fractions were frozen and concentrated by lyophilization to afford **AEG-I-249** as a white solid (10 mg, 37% over two steps).

^{1}H NMR (500 MHz, acetone-d6): δ 11.79 (s, 1 H), 10.30 (s, 1 H), 8.80 (m, 2 H), 7.99 (ddd, 1 H, J = 1.0, 2.4, 11.6 Hz), 7.90 – 7.65 (br s, 2 H), 7.72 (m, 1 H), 7.55 – 7.46 (m, 3 H), 7.33 (d, 1 H, J = 7.7 Hz), 5.34 (t, 1 H, J = 8.4 Hz), 4.55 – 4.23 (br d, J = 80.9 Hz), 3.68 – 3.55 (m, 2 H), 3.41 – 3.24 (br s, 1 H), 3.30 (dd, 1 H, J = 8.0, 15.9 Hz) 3.21 – 3.08 (br s, 1 H), 2.96 (m, 1 H), 2.84 (dd, 1 H, J = 9.0, 15.9 Hz), 2.78 (s, 3 H), 1.37 (t, 3 H, J = 7.2 Hz)
^{13}C NMR (500 MHz, acetone-d6, mixture of rotamers): δ 161.7 (q, J_{CF} = 34.0 Hz, TFA), 161.0609, 160.0 (d, J_{CF} = 249 Hz), 158.6 (d, J_{CF} = 245 Hz), 159.3, 159.2, 159.2, 159.1, 159.1, 144.5, 143.8, 139.2 (d, J_{CF} = 10.1 Hz), 139.1 (d, J_{CF} = 10.0 Hz), 132.0, 131.6, 129.8, 127.7, 126.3, 117.9 (q, J_{CF} = 294 Hz), 117.9 (d, J_{CF} = 3.5 Hz), 117.1 (d, J_{CF} = 3.5 Hz), 116.3 (d, J_{CF} = 18.0 Hz), 109.3 (d, J_{CF} = 26.2 Hz), 109.2 (d, J_{CF} = 26.1 Hz), 59.4, 58.8, 58.7, 51.2, 51.0, 48.0, 48.0, 44.6, 44.5, 38.7, 35.1, 35.1, 9.4.
IR ν_{max} 3355, 2359, 2341, 1682, 1517, 1428, 1203, 1135, 975, 837, 801, 722, 668
AMM(ESI) *m/z* 475.2011 [calcd for $C_{23}H_{29}ClFN_6O_2$ $(M+H)^+$ 475.2025]
[α]$_D^{23}$ = + 9 ° (*c* 0.09, MeOH)

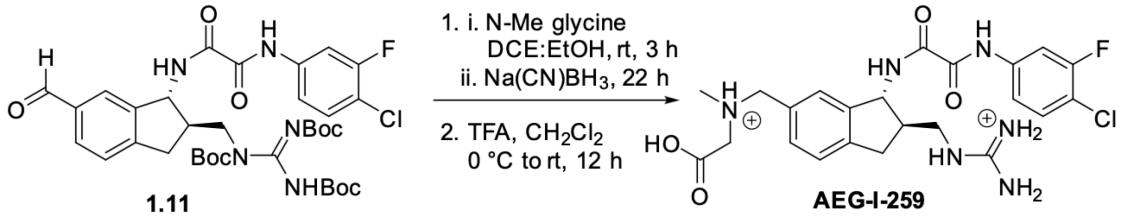

AEG-I-259. To a solution of **1.11** (0.060 g, 0.079 mmol) in dichloroethane (2 mL, 0.04 M) with 3 Å molecular sieves under nitrogen atmosphere at room temperature was added a solution of sarcosine (0.140 g, 1.57 mmol, 20 eq.) in methanol (2 mL). After stirring for 30 minutes, sodium triacetoxyborohydride (0.083 g, 0.39 mmol, 5 eq.) was added. After 24 hours, no conversion was observed by LC/MS. Sodium cyanoborohydride (0.030 g, 0.48 mmol, 6 eq.) was then added. After two hours, no starting material was observed by TLC or LC/MS. The reaction was quenched with saturated aqueous sodium bicarbonate and diluted with ethyl acetate. The layers were separated, and the aqueous layer was washed three times with ethyl acetate. The organic layers were combined, dried over sodium sulfate, decanted, and concentrated. Flash column chromatography (SiO_2, 0% to 10% MeOH in dichloromethane) afforded a partially purified amine. This amine was dissolved in dichloromethane (5.5 mL, 0.01 M). To this solution was added trifluoroacetic acid (0.16 mL, 2.2 mmol, 40 eq.). After two days complete conversion was observed by LC/MS. The reaction mixture was concentrated, dissolved in 2.3 mL 1:1 acetonitrile/water and purified by reverse phase HPLC (15 mL/min, 5-80% H_2O/ACN + 0.1% TFA, 20 min gradient). The isolated fractions were frozen and concentrated by lyophilization to afford **AEG-I-259** as a white solid (6.8 mg, 12% over two steps).

^{1}H NMR (500 MHz, acetone-d6): δ 11.10 (s, 1 H), 9.47 (d, 1 H, J = 9.1 Hz), 7.98 (dd, 1 H, J = 2.4, 11.8 Hz), 7.83 (m, 1 H), 7.77 (dd, 1 H, J = 2.3, 8.9 Hz), 7.60 (t, 1 H, J = 8.7 Hz), 7.31 (s, 1 H), 7.25 (s, 1 H), 5.20 (t, 1 H, J = 8.8 Hz), 4.09 (s, 2 H), 3.66 (s, 2 H), 3.39 (m, 1 H), 3.12 (dd, 1 H, J = 8.0, 15.8 Hz), 2.83 (m, 1 H), 2.68 (dd, 1 H, J = 9.3, 15.7 Hz), 2.58 (s, 3 H).
^{13}C NMR (500 MHz, acetone-d6): δ 168.5, 159.9, 158.8, 156.8 (q, J_{CF} = 34.0 Hz, TFA), 157.1, 156.8 (d, J_{CF} = 244 Hz),143.0, 142.9, 142.1,138.3 (d, J_{CF} = 10.0 Hz),130.7, 130.2, 125.6, 124.9, 117.3 (d, J_{CF} = 10.0 Hz), 117.2 (q, J_{CF} = 299.7 Hz, TFA), 114.4 (d, J_{CF} = 18.0 Hz), 108.5 (d, J_{CF} = 25.8 Hz), 59.1, 56.9, 55.2, 45.6, 42.9, 40.5, 33.7.
IR ν_{max} 3398, 2917, 2849 2359, 2342, 1683, 1672, 1645, 1635, 1626, 1203, 1138 cm^{-1}
AMM (ESI) *m/z* 505.1772 [calcd for $C_{23}H_{27}ClFN_6O_2$ $(M+H)^+$ 505.1766]
[α]$_D^{23}$ = + 9 ° (*c* 0.2, MeOH)

Synthesis of MCG-III-051

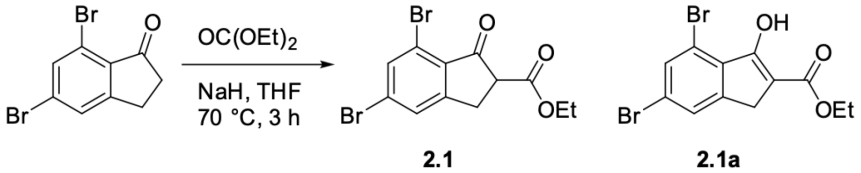

2.1 **2.1a**

Tautomers **2.1** and **2.1a.** To a stirred suspension of sodium hydride (60% dispersion in mineral oil, 82.8 mg, 2.07 mmol) and diethyl carbonate (1.3 mL, 10. mmol) in THF (3 mL) in a sealed microwave vial at room temperature under N_2 atmosphere was added dropwise a solution of 5,7-dibromo-1*H*-indanone (500. mg, 1.72 mmol) in THF (5.6 mL). The reaction mixture was heated to 70 °C for 3 h, then cooled and diluted with EtOAc and H_2O and neutralized with aq. 1N HCl. Layers were separated and the resulting aqueous layer was extracted with EtOAc. The combined organic layers were washed with sat. aq. NaCl and dried over anhydrous $MgSO_4$ then concentrated *in vacuo* to afford the desired product as an off-white solid (588 mg, 94% yield). The product was isolated as a mixture of keto and enol tautomers (ratio 2:1 by ^{1}H-NMR).

^{1}H NMR (500 MHz, Chloroform-*d*): keto tautomer δ 7.72 (s, 1H), 7.61 (s, 1H), 4.24 (q, *J* = 6.9 Hz, 2H), 3.74 (dd, *J* = 8.6, 4.2 Hz, 1H), 3.50 (dd, *J* = 17.7, 4.3 Hz, 1H), 3.28 (dd, *J* = 17.5, 8.4 Hz, 1H), 1.31 (t, *J* = 7.2 Hz, 3H); enol tautomer δ 10.76 (broad s, 1H), 7.68 (s, 1H), 7.53 (s, 1H), 4.32 (q, *J* = 7.2 Hz, 2H), 3.47 (s, 2H), 1.36 (t, *J* = 7.2 Hz, 3H);
^{13}C NMR (126 MHz, $CDCl_3$) δ 195.41, 169.05, 168.25, 157.17, 147.04, 135.58, 134.39, 134.26, 131.65, 130.30, 128.76, 127.02, 123.61, 120.98, 116.05, 103.77, 99.95, 61.99, 60.48, 53.92, 32.21, 29.01, 14.35, 14.14;
IR (ATR) ν_{max} 3300, 2983, 1653, 1418, 1243, 1018, 771 cm^{-1};
AMM (ESI) *m/z* 359.9018 [calcd for $C_{12}H_{10}Br_2O_3$ $(M+H)^+$ 359.8997].

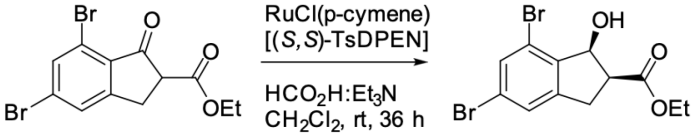

2.1/2.1a **2.2**

b-*Hydroxyester* **2.2.** To a stirred solution of tautomers **2.1** and **2.1a** (92.9 mg, 0.257 mmol) and RuCl(p-cymene)[(*S*,*S*)-TsDPEN] (3.3 mg, 0.005 mmol) in CH_2Cl_2 (2.5 mL) at room temperature under N_2 atmosphere was added formic acid:triethyl amine complex 5:2 (0.03 mL, 0.5 mmol). The reaction mixture was stirred at room temperature for 36 h, then diluted with sat. aq. $NaHCO_3$. Layers were separated and the resulting aqueous layer was extracted with CH_2Cl_2. The combined organic layers were washed with sat. aq. NaCl and dried over anhydrous $MgSO_4$ then concentrated

in vacuo. Flash column chromatography (SiO_2, 80:20 hexanes:EtOAc) afforded the product as a colorless oil (0.085 g, 91% yield).

[α]D^{23} +21.82 (c. 0.21, CH_2Cl_2);
^{1}H NMR (500 MHz, $CDCl_3$): ^{1}H NMR (500 MHz, Chloroform-*d*) δ 7.55 (s, 1H), 7.36 (s, 1H), 5.38 (dd, *J* = 5.8, 4.6 Hz, 1H), 4.26 (q, *J* = 7.1 Hz, 2H), 3.58 (dd, *J* = 16.3, 9.8 Hz, 1H), 3.35 (ddd, *J* = 9.9, 8.3, 5.9 Hz, 1H), 3.11 (dd, *J* = 16.4, 8.3 Hz, 1H), 2.77 (d, *J* = 4.6 Hz, 1H), 1.33 (t, *J* = 7.1 Hz, 3H);
^{13}C NMR (126 MHz, $CDCl_3$) δ 171.52, 146.13, 141.37, 132.92, 127.23, 123.54, 120.76, 75.35, 61.17, 48.92, 33.34, 14.24;
IR (thin film, KBr) ν_{max} 3460, 2929, 1730, 1216, 1038, 853 cm^{-1};
AMM (ESI) m/z 384.9057 [calcd for $C_{12}H_{12}Br_2O_3Na$ $(M+Na)^+$ 384.9051].

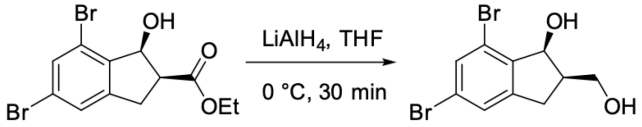

2.2 **2.3**

Diol **2.3**. To a precooled (0 °C) solution of **2.2** (373 mg, 1.02 mmol) in THF (5.1 mL) under N_2 atmosphere was added portion wise lithium aluminum hydride (31 mg, 0.82 mmol). The reaction mixture was stirred for 30 min at 0 °C then quenched with sat. aq. sodium potassium tartrate and stirred at room temperature for 10 min. The quenched solution was diluted with H_2O then EtOAc. The layers were separated, and the resulting aqueous layer was extracted with EtOAc. The combined organic layers were washed with sat. aq. NaCl dried over $MgSO_4$ and concentrated *in vacuo*. Flash column chromatography (SiO_2 20:80 hexanes:EtOAc) afforded the product as a white solid (285 mg, 86% yield).

[α]D^{23} +25.21 (c. 0.15, CH_2Cl_2);
^{1}H NMR (500 MHz, Chloroform-*d*) δ 7.53 (s, 1H), 7.36 (s, 1H), 5.34 (dd, *J* = 6.7, 2.9 Hz, 1H), 4.07 – 3.99 (m, 1H), 3.97 – 3.84 (m, 1H), 3.17 (dd, *J* = 16.4, 9.1 Hz, 1H), 2.94 (dd, *J* = 16.4, 8.3 Hz, 1H), 2.76 – 2.64 (m, 1H), 2.57 – 2.43 (m, 2H);
^{13}C NMR (126 MHz, $CDCl_3$) δ 147.61, 142.70, 132.45, 127.50, 123.28, 120.37, 77.09, 61.95, 44.40, 33.42.
IR (ATR) ν_{max} 3220, 1586, 1557, 1309, 1158, 849, 686, 561 cm^{-1};

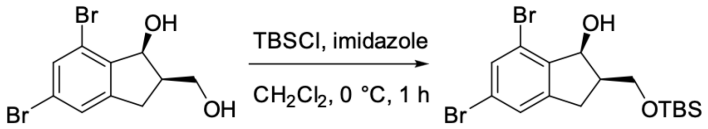

2.3 **2.4**

Silyl ether **2.4**. To a precooled solution (0 °C) of **2.3** (166 mg, 0.516 mmol) and 1H-imidazole (70.2 mg, 1.03 mmol) in CH_2Cl_2 (5 mL) under N_2 atmosphere was added *tert*-butylchlorodimethylsilane (78 mg, 0.52 mmol). The resulting mixture was stirred at 0 °C for 1 h, then diluted with CH_2Cl_2 and aq. sat. NH_4Cl. The layers were separated and the resulting aqueous layer was extracted with CH_2Cl_2. The combined organic layers were washed with sat. aq. NaCl, dried over $MgSO_4$, and concentrated *in vacuo*. Flash chromatography (SiO_2, 80:20 hexanes:EtOAc) afforded the product as a colorless oil (182 mg, 81% yield).

[α]D^{23} +24.15 (c. 0.094, CH_2Cl_2);
^{1}H NMR (500 MHz, Chloroform-*d*) δ 7.53 (s, 1H), 7.33 (s, 1H), 5.24 (t, *J* = 5.1 Hz, 1H), 4.09 – 3.91 (m, 2H), 3.12 (d, *J* = 4.2 Hz, 1H), 3.06 (dd, *J* = 16.2, 9.6 Hz, 1H), 2.90 (dd, *J* = 16.2, 8.0 Hz, 1H), 2.67 – 2.53 (m, 1H), 0.91 (s, 9H), 0.11 (d, *J* = 3.7 Hz, 6H);
^{13}C NMR (126 MHz, $CDCl_3$) δ 147.24, 143.43, 132.56, 127.17, 122.82, 120.85, 76.60, 62.45, 44.78, 33.79, 25.82, 18.17, -5.47, -5.54;
IR (ATR) ν_{max} 2952, 2927, 2855, 1590, 1252, 1079, 833, 774 cm^{-1};
AMM (ESI) *m/z* 456.9801 [calcd for $C_{16}H_{24}Br_2O_2NaSi$ $(M+Na)^+$ 456.9810].

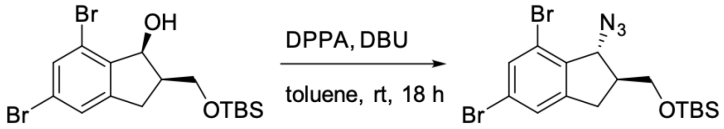

2.4 **2.5**

Azide **2.5**. To a solution of **2.4** (160. mg, 0.367 mmol) in toluene (1.8 mL) at room temperature under N_2 atmosphere was added diphenylphosphoryl azide (0.24 mL, 1.1 mmol) then 1,8-diazabicyclo[5.4.0]undec-7-ene (0.16 mL, 1.1 mmol). The resulting mixture was stirred at room temperature for 18 h, then diluted with EtOAc and aq. sat. NH_4Cl. The layers were separated and the resulting aqueous layer was extracted with EtOAc. The combined organic layers were washed with sat. aq. NaCl, dried over $MgSO_4$, and concentrated *in vacuo*. Flash chromatography (SiO_2, 95:5 hexanes:EtOAc) afforded the product as a colorless oil (124 mg, 78% yield).

[α]D^{23} +19.44 (c. 0.31, CH_2Cl_2);
^{1}H NMR (500 MHz, Chloroform-*d*) δ 7.57 (s, 1H), 7.32 (s, 1H), 4.78 (s, 1H), 3.68 (dd, *J* = 10.3, 5.6 Hz, 1H), 3.47 (t, *J* = 8.8 Hz, 1H), 3.25 (dd, *J* = 17.5, 8.7 Hz, 1H), 2.68 (d, *J* = 13.8 Hz, 2H), 0.86 (s, 10H), 0.04 (d, *J* = 3.7 Hz, 6H);
^{13}C NMR (126 MHz, $CDCl_3$) δ 147.11, 139.01, 133.04, 127.33, 123.37, 121.40, 68.76, 63.86, 48.04, 34.03, 25.75, 18.15, -5.44, -5.50;
IR (ATR) ν_{max} 2953, 2929, 2856, 2096, 1559, 1395, 1106, 814, 687 cm^{-1};

AMM (ESI) *m/z* 430.9930 [calcd for $C_{16}H_{23}Br_2ONSi$ (M-N_2) 430.9916].

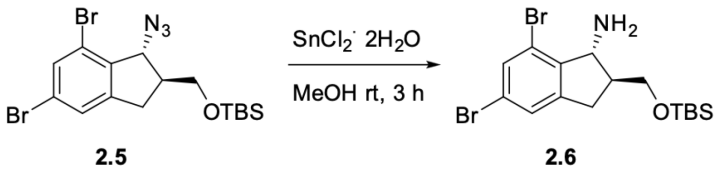

2.5 **2.6**

Amine **2.6**. To a precooled solution of **2.5** (500. mg, 1.08 mmol) in MeOH (2 mL) under N_2 atmosphere was added dropwise a solution of tin (II) chloride (366 mg, 1.63 mmol) in MeOH (3.5 mL). The resulting mixture was stirred at room temperature for 3 h, then concentrated *in vacuo*. The resulting solid was taken up in CH_2Cl_2 and H_2O, then treated with 1N aq. NaOH to remove emulsions. The layers were separated, and the resulting aqueous phase was extracted with CH_2Cl_2. The combined organic layers were washed with sat. aq. NaCl dried over $MgSO_4$ and concentrated *in vacuo* to afford the product as a white solid (433 mg, 92% yield).

[α]$_D^{24}$ +56.85 (c. 0.11, CH_3OH);
^{1}H NMR (500 MHz, Chloroform-*d*) δ 7.47 (s, 1H), 7.27 (s, 1H), 4.19 (d, *J* = 3.8 Hz, 1H), 3.61 (d, *J* = 6.5 Hz, 2H), 3.18 (dd, *J* = 16.8, 8.2 Hz, 1H), 2.70 (dd, *J* = 16.8, 4.8 Hz, 1H), 2.41 – 2.28 (m, 1H), 1.87 (s, 2H), 0.85 (s, 9H), 0.03 (s, 6H);
^{13}C NMR (126 MHz, $CDCl_3$) δ 146.52, 144.62, 132.51, 127.34, 121.64, 120.38, 64.56, 60.14, 50.15, 33.70, 25.81, 18.20, -5.41, -5.45;
IR (ATR) ν_{max} 2951, 2927, 2855, 1587, 1557, 1252, 1102, 834, 748 cm^{-1};
AMM (ESI) *m/z* 434.0139 [calcd for $C_{11}H_{26}N_3O_3Br_2Si$ $(M+H)^+$ 434.0110].

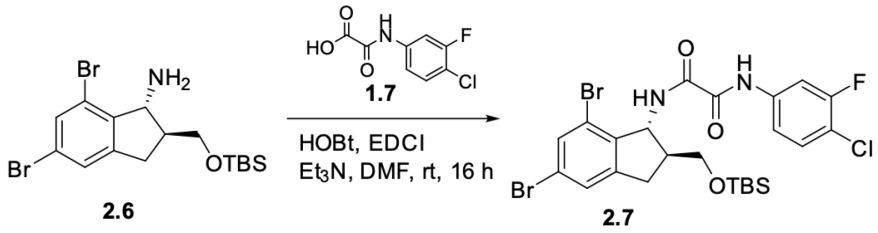

2.6 **2.7**

Oxalamide **2.7**. To a solution of **2.6** (693 mg, 1.50 mmol), **1.7** (339 mg, 1.50 mmol), 1-hydroxybenzotriazole hydrate (785 mg, 3.61 mmol), and N-(3-dimethylaminopropyl)-N'-ethylcarbodiimide hydrochloride (691 mg, 3.61 mmol) in DMF (7.5 mL) at room temperature under N_2 atmosphere was added triethylamine (0.96 mL, 6.9 mmol). The resulting mixture was stirred at room temperature for 16 h, then concentrated *in vacuo*. The crude resident was taken up in EtOAc and quenched with sat. aq. NH_4Cl. The layers were separated and the resulting aqueous phase was extracted with EtOAc. The combined organic layers were washed with H_2O then sat.

aq. NaCl, dried over Na_2SO_4, and concentrated *in vacuo*. Flash chromatography (SiO_2, 90:10 hexanes:EtOAc) afforded the product as a white solid (779 mg, 82% yield).

[α]$_D^{23}$ +3.04 (c. 0.10, CH_2Cl_2);
^{1}H NMR (500 MHz, Chloroform-*d*) δ 9.38 (s, 1H), 7.75 – 7.66 (m, 2H), 7.52 (s, 1H), 7.36 (t, *J* = 8.3 Hz, 1H), 7.34 (s, 1H), 7.26 – 7.22 (m, 1H), 5.23 (dd, *J* = 9.0, 4.0 Hz, 1H), 3.75 – 3.64 (m, 2H), 3.27 (dd, *J* = 16.9, 8.4 Hz, 1H), 2.85 (dd, *J* = 16.8, 4.8 Hz, 1H), 2.64 – 2.53 (m, 1H), 0.83 (s, 9H), 0.04 (d, *J* = 3.8 Hz, 6H);
^{13}C NMR (126 MHz, $CDCl_3$) δ 159.12, 158.75, 157.36, 157.14, 147.74, 138.88, 136.30, 136.22, 133.18, 130.82, 127.33, 123.32, 120.75, 117.24, 117.10, 115.95, 115.92, 108.53, 108.32, 64.13, 58.32, 48.74, 34.13, 25.73, 18.15, -5.49;
IR (ATR) ν_{max} 3279, 2928, 2855, 1667, 1593, 1517, 1154, 1110, 835, 665 cm^{-1};
AMM (ESI) *m/z* 630.9836 [calcd for $C_{24}H_{27}N_2O_3FClBr_2Si$ $(M-H)^-$ 630.9830].

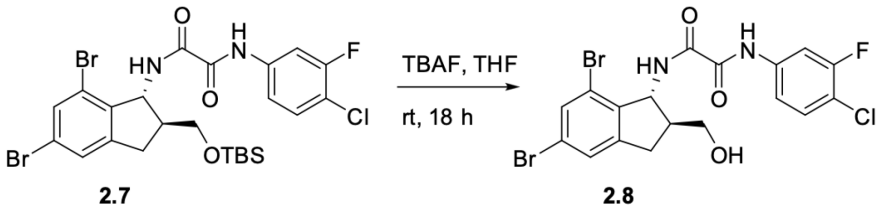

2.7 **2.8**

Alcohol **2.8**. To a solution of **2.7** (432 mg, 0.680 mmol) in THF (6.8 mL) at room temperature under N_2 atmosphere was added tetra-*n*-butylammonium fluoride (1 M solution in THF, 2.0 mL, 2.0 mmol). The resulting mixture was stirred at room temperature for 18 h, then diluted with EtOAc and quenched with H_2O. The layers were separated and the resulting aqueous phase was extracted with EtOAc. The combined organic layers were washed with sat. aq. NaCl, dried over Na_2SO_4, and concentrated *in vacuo*. Flash chromatography (SiO_2, 50:50 hexanes:EtOAc) afforded the product as a white solid (467 mg, 88% yield).

[α]$_D^{23}$ +95.19 (c. 0.059, DMSO);
^{1}H NMR (500 MHz, DMSO-*d*6) δ 11.06 (s, 1H), 9.45 (d, *J* = 9.0 Hz, 1H), 7.95 (d, *J* = 11.8 Hz, 1H), 7.74 (d, *J* = 8.9 Hz, 1H), 7.64 – 7.52 (m, 2H), 7.49 (s, 1H), 5.19 (dd, *J* = 9.2, 5.0 Hz, 1H), 4.80 (t, *J* = 5.2 Hz, 1H), 3.52 – 3.40 (m, 2H), 3.25 (dd, *J* = 16.8, 8.6 Hz, 1H), 2.76 (dd, *J* = 16.7, 6.0 Hz, 1H);
^{13}C NMR (126 MHz, DMSO) δ 158.75, 157.70, 155.75, 148.81, 140.19, 138.24, 138.16, 131.79, 130.50, 127.02, 121.50, 120.06, 117.21, 114.34, 114.19, 108.45, 108.25, 62.16, 56.95, 48.32, 33.91;
IR (ATR) ν_{max} 3259, 1662, 1591, 1512, 1426, 857, 800, 746 cm^{-1};
AMM (ESI) *m/z* 516.8973 [calcd for $C_{18}H_{13}N_2O_3FClBr_2$ $(M-H)^-$ 516.8965].

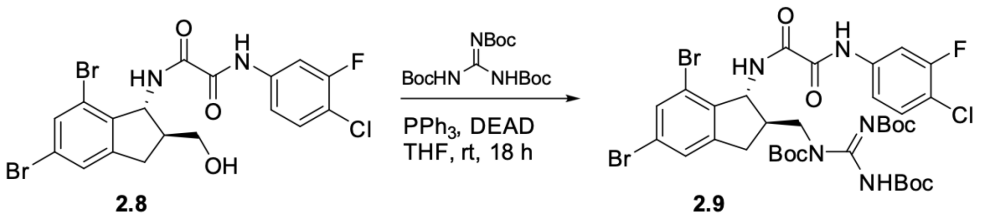

Common Intermediate **2.9**. To a precooled (0 °C) solution of **2.8** (287 mg, 0.551 mmol), N,N',N''-triBocguanidine (198 mg, 0.551 mmol), and triphenylphosphine (217 mg, 0.827 mmol) in THF (11 mL) under N_2 atmosphere was added dropwise a diethylazidocarboxylate (0.13 mL, 0.83 mmol). The resulting mixture was stirred at room temperature 18 h, then diluted with EtOAc and quenched with H_2O. The layers were separated and the aqueous phase was extracted with EtOAc. The combined organic layers were washed with sat. aq. NaCl, dried over Na_2SO_4, and concentrated *in vacuo*. Flash chromatography (SiO_2, 80:20 hexanes:EtOAc) afforded the product as a white solid (338 mg 71% yield).

[α]D23 +49.65 (c. 0.08, $CHCl_3$);
^{1}H NMR (500 MHz, DMSO-*d*6) δ 11.04 (s, 1H), 10.20 (s, 1H), 9.50 (d, *J* = 8.7 Hz, 1H), 7.94 (dd, *J* = 11.7, 2.4 Hz, 1H), 7.72 (dd, *J* = 8.9, 2.3 Hz, 1H), 7.61 (s, 1H), 7.58 (t, *J* = 8.7 Hz, 1H), 7.48 (s, 1H), 4.98 (dd, *J* = 8.7, 4.9 Hz, 1H), 3.77 – 3.58 (m, 2H), 2.74 – 2.63 (m, 1H), 1.49 – 1.32 (m, 9H);
^{13}C NMR (126 MHz, DMSO) δ 158.85, 158.62, 158.26, 157.75, 155.81, 152.52, 150.44, 148.23, 147.38, 146.37, 139.51, 138.30, 138.22, 131.99, 130.60, 127.03, 121.64, 120.12, 117.30, 117.27, 114.42, 114.28, 108.51, 108.30, 82.14, 81.05, 79.07, 58.01, 49.34, 45.77, 34.96, 27.86, 27.76, 27.67, 27.62;
IR (ATR) ν_{max} 3275, 2980, 1664, 1514, 1368, 1244, 1121, 762 cm^{-1};
AMM (ESI) *m/z* 860.1066 [calcd for $C_{34}H_{42}N_5O_8FClBr_2$ $(M+H)^+$ 860.1073].

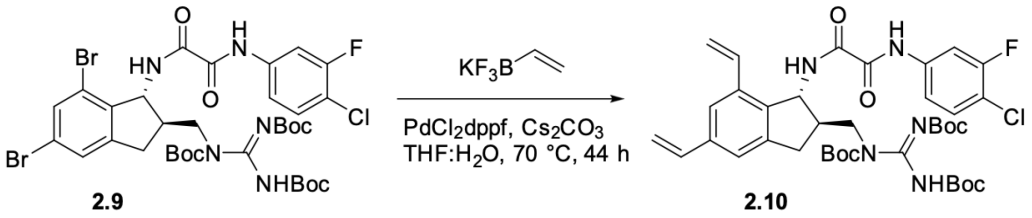

Divinyl **2.10**. To a flask charged with **2.9** (200. mg, 0.232 mmol), potassium vinyltrifluoroborate (93 mg, 0.70 mmol), [1,1'-bis(diphenylphosphino)ferrocene]dichloropalladium (II) (19 mg, 0.023 mmol) and cesium carbonate (454 mg, 1.39 mmol) at room temperature under N_2 atmosphere was added THF (10 mL) and H_2O (1.5 mL). The flask was affixed with a reflux condenser and backfilled and purged with N_2 (4x) then the reaction mixture was heated to 70 °C and stirred for

44 h. The reaction mixture was allowed to cool then quenched with H_2O and diluted with EtOAc. The layers were separated, and the resulting aqueous layer was extracted with EtOAc. The combined organic layers were washed with aq. sat. NaCl, dried over Na_2SO_4, and concentrated *in vacuo*. Flash chromatography (SiO_2, 90:10 hexanes:EtOAc) afforded the product as a white solid (82 mg, 47% yield).

[α]D^{23} +36.87 (c. 0.025, CH_2Cl_2);
^{1}H NMR (500 MHz, Chloroform-*d*) δ 10.41 (broad s, 1H), 9.35 (s, 2H), 7.67 (t, *J* = 8.8 Hz, 2H), 7.40 – 7.32 (m, 2H), 7.24 – 7.17 (m, 2H), 6.78 – 6.60 (m, 2H), 5.73 (dd, *J* = 31.0, 17.6 Hz, 2H), 5.40 (dd, *J* = 8.7, 3.6 Hz, 1H), 5.27 (dd, *J* = 11.0, 4.7 Hz, 2H), 4.00 – 3.85 (m, 2H), 3.26 (dd, *J* = 16.5, 8.0 Hz, 1H), 2.90 – 2.78 (m, 1H), 2.69 (dd, *J* = 16.5, 4.2 Hz, 1H), 1.52 – 1.43 (m, 27H);
^{13}C NMR (126 MHz, $CDCl_3$) δ 158.99, 158.49, 157.24, 157.02, 153.32, 152.00, 143.89, 138.76, 136.71, 136.44, 136.34, 136.26, 135.32, 133.12, 130.70, 122.30, 121.76, 116.96, 116.82, 116.41, 115.81, 114.34, 108.37, 108.17, 83.48, 56.89, 49.81, 46.61, 34.58, 29.65, 28.03, 27.96, 27.89;
IR (ATR) ν_{max} 3267, 1661, 1607, 1514, 1368, 1257, 1139, 763 cm^{-1};
AMM (ESI) *m/z* 754.3037 [calcd for $C_{38}H_{46}N_5O_8FCl$ $(M-H)^-$ 754.3019].

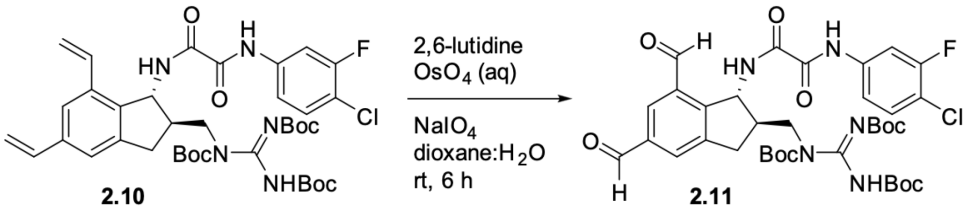

Dialdehyde **2.11**. To a precooled (0 °C) of **2.10** (81 mg, 0.11 mmol) in 1,4-dioxane (1.6 mL) and H_2O (0.5 mL) under N_2 atmosphere was added osmium tetroxide (0.5% in H_2O, 0.22 mL, 0.004 mmol) sodium periodate (182 mg, 0.861 mmol) and 2,6-lutidine (0.05 mL, 0.4 mmol). The resulting heterogeneous mixture was allowed to warm to room temperature and vigorously stirred for 6 h, then quenched with H_2O and diluted with CH_2Cl_2. The layers were separated and the resulting aqueous layer was extracted with CH_2Cl_2. The combined organic layers were washed with aq. sat. NaCl, dried over Na_2SO_4, and concentrated *in vacuo*. Flash chromatography (75:25 hexanes: EtOAc) afforded the desired product as a white solid (43 mg, 52% yield).

[α]D^{22} +70.68 (c. 0.074, CH_2Cl_2);
^{1}H NMR (500 MHz, Chloroform-*d*) δ 10.18 (s, 1H), 10.09 (s, 1H), 9.18 (s, 1H), 8.23 (s, 1H), 8.11 (d, *J* = 8.0 Hz, 1H), 8.03 (s, 1H), 7.65 (dd, *J* = 10.7, 2.5 Hz, 1H), 7.34 (t, *J* = 8.3 Hz, 2H), 7.14 (d, *J* = 8.7 Hz, 1H), 5.77 (dd, *J* = 8.1, 3.4 Hz, 1H), 4.01 (dd, *J* = 14.2, 6.6 Hz, 1H), 3.80 (dd, *J* = 14.1, 9.2 Hz, 1H), 3.50 (dd, *J* = 16.9, 8.2 Hz, 1H), 3.04 (s, 1H), 2.82 (dd, *J* = 17.2, 3.8 Hz, 2H), 1.48 (d, *J* = 19.8 Hz, 27H);
^{13}C NMR (126 MHz, $CDCl_3$) δ 190.81, 190.37, 159.12, 158.84, 157.20, 157.15, 153.54, 153.09,

147.15, 146.88, 137.64, 136.65, 136.38, 136.30, 133.56, 131.79, 130.87, 130.43, 120.26, 117.18, 117.04, 115.96, 108.50, 108.29, 83.86, 77.16, 57.48, 49.96, 46.04, 34.68, 28.28, 28.16, 28.07, 28.02, 24.51;
IR (ATR) ν_{max} 3460, 2921, 2850, 1730, 1591, 1558, 1450, 1397, 1061, 897, 850 cm^{-1};
AMM (ESI) *m/z* 760.2785 [calcd for $C_{36}H_{44}N_5O_{10}FCl$ $(M+H)^+$ 760.2761].

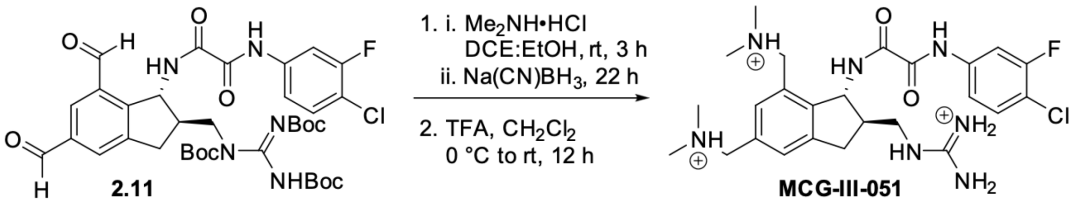

MCG-III-051. To a flask charged with **2.11** (42 mg, 0.056 mmol), dimethylamine hydrochloride (91 mg, 1.1 mmol) at room temperature under nitrogen atmosphere was added dichloroethane (2 mL) and ethanol (2 mL). The reaction mixture was stirred at room temperature for 3 h before addition of sodium cyanoborohydride (7.0 mg, 0.11 mmol). The resulting reaction mixture was stirred at room temperature for 22 h, then cooled to 0 °C and quenched with aq. sat. $NaHCO_3$ and diluted with CH_2Cl_2. The biphasic solution was then adjusted to pH 10 with aq. 1M NaOH and stirred for 30 min. The layers were then separated and the resulting aqueous layer was extracted with CH_2Cl_2. The combined organic layers were washed with aq. sat. NaCl, dried over Na_2SO_4, and concentrated *in vacuo*. The reside was run through a plug of silica gel, eluting with 20:80 hexanes:EtOAc containing 1% triethylamine, then concentrated *in vacuo* and used in the next step without further purification. The residue was taken up in CH_2Cl_2 and cooled to 0 °C before addition of trifluoroacetic acid (0.09 mL, 0.8 mmol). The solution was stirred for 12 h at room temperature, then cooled to 0 °C before addition of trifluoroacetic acid (0.05 mL, 0.6 mmol). The solution was stirred at room temperature for 24 h, then concentrated *in vacuo* and taken up in H_2O/CH_3CN (80:20) and subjected to HPLC purification. Conditions: eluent H_2O/CH_3CN (80:20 to 50:50, linear gradient); flow rate: 15 mL/min; run time: 15 min. Product-containing fractions were combined and the resulting solution was deep-frozen (-78 °C bath) and lyophilized to afford product as a white powder (6 mg, 12% yield from **1.23**).

^{1}H NMR (500 MHz, Acetone-*d*6) δ 10.29 (s, 1H), 9.19 – 9.05 (m, 1H), 7.97 (dd, *J* = 11.6, 2.4 Hz, 1H), 7.81 (s, 1H), 7.74 – 7.69 (m, 1H), 7.61 (s, 1H), 7.51 (t, *J* = 8.6 Hz, 1H), 5.73 (dd, *J* = 8.9, 3.3 Hz, 1H), 4.53 (dd, *J* = 27.9, 13.1 Hz, 2H), 4.40 (d, *J* = 13.2 Hz, 2H), 3.64 – 3.47 (m, 2H), 3.44 – 3.29 (m, 1H), 2.99 (s, 2H), 2.81 (dd, *J* = 16.9, 3.9 Hz, 1H).
AMM (ESI) *m/z* 518.2444 [calcd for $C_{25}H_{34}N_7O_2FCl$ $(M-2H)^-$ 518.2447]

6.2.12 SUPPLEMENTAL FIGURES

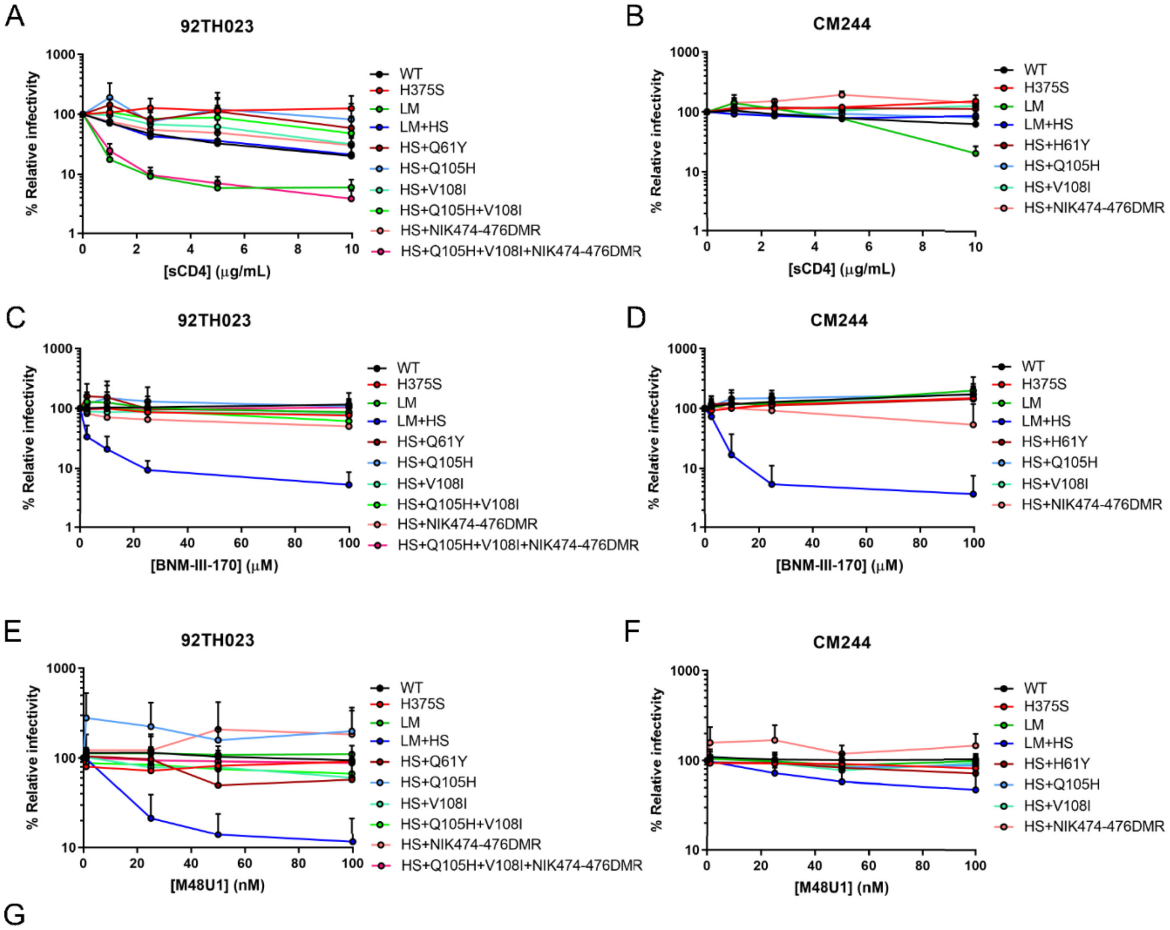

G

Neutralization IC_{50}			
92TH023	sCD4 µg/mL	BNM-III-170 µM	M48U1 nM
WT	2,32	>100	>100
H375S	>10	>100	>100
LM	0,61	>100	>100
LM+HS	2,12	1,88	16,11
H375S H61Y	>10	>100	>100
H375S Q105H	>10	>100	>100
H375S V108I	6,93	>100	>100
H375S Q105H-V108I	9,76	>100	>100
H375S NIK474-476DMR	4,49	96,97	>100
H375S Q105H-V108I-NIK474-476DMR	0,66	>100	>100

Legend	
sCD4	CD4mc
IC_{50} <5	IC_{50} <50
5< IC_{50} <10	50< IC_{50} <100
IC_{50} >10	IC_{50} >100

Neutralization IC_{50}			
CM244	sCD4 µg/mL	BNM-III-170 µM	M48U1 nM
WT	>10	>100	>100
H375S	>10	>100	>100
LM	7,39	>100	>100
LM+HS	>10	1,88	86,21
H375S H61Y	>10	>100	>100
H375S Q105H	>10	>100	>100
H375S V108I	>10	>100	>100
H375S NIK474-476DMR	>10	>100	>100

Figure 6.1.S1 - Effect of single gp120 layer mutations on neutralization by CD4 and CD4mc. Recombinant HIV-1 strains expressing luciferase and bearing wild-type or mutant CRF01_AE Envs (92TH023 and CM244 isolates) were normalized by reverse transcriptase activity. Normalized amounts of viruses were incubated with serial dilutions of sCD4 (**A, B**), BNM-III-170 (**C,D**), or M48U1 (**E,F**) at 37°C for 1 h prior to infection of Cf2Th-CD4/CCR5 cells. Infectivity at each dilution of sCD4 or CD4mc tested is shown as the percentage of infection without sCD4 or CD4mc for each particular mutant. Quadruplicate samples were analyzed in each experiment. Data shown are the means of results obtained in at least 3 independent experiments. The error bars represent the standard deviations. Neutralization half maximal inhibitory concentrations (IC_{50}) are summarized in (**G**).

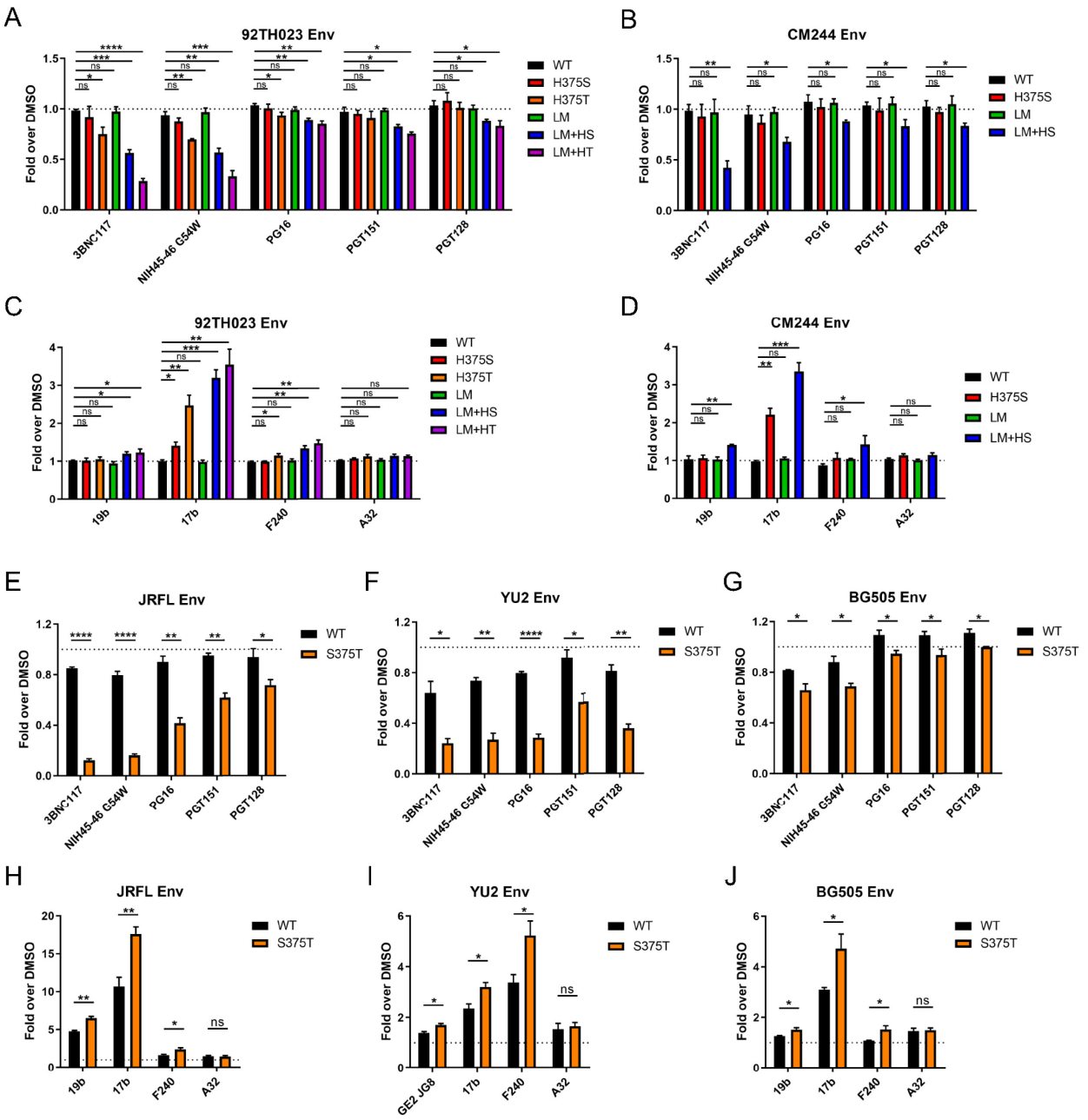

Figure 6.1.S2 - Phe43 cavity and inner domain changes render the CRF01_AE HIV-1 strain susceptible to CD4mc-induced Env conformational changes.

Cell-surface staining of 293T cells transfected with different Env expressors (92TH023, CM244, JRFL, YU2 and BG505 isolates) WT or their mutated counterparts using a panel of Env ligands. Binding of bNAbs (**A-B, E-G**) and nnAbs (**C-D, H-J**) was performed in presence of BNM-III-170 (50 µM) or not (DMSO). Shown are the mean fluorescence intensities (MFI) obtained in presence of BNM-III-170 normalized to the MFI in absence of BNM-III-170 (DMSO) from the transfected (GFP^+) population for staining obtained in at least 3 independent experiments. All MFI were normalized to 2G12 MFI for each Env mutants. Error bars indicate mean ± SEM. Statistical significance was tested using an unpaired t-test (*, $P < 0.05$, **, $P < 0.01$, ***, $P < 0.001$, ****, $P < 0.0001$, ns: non significant).

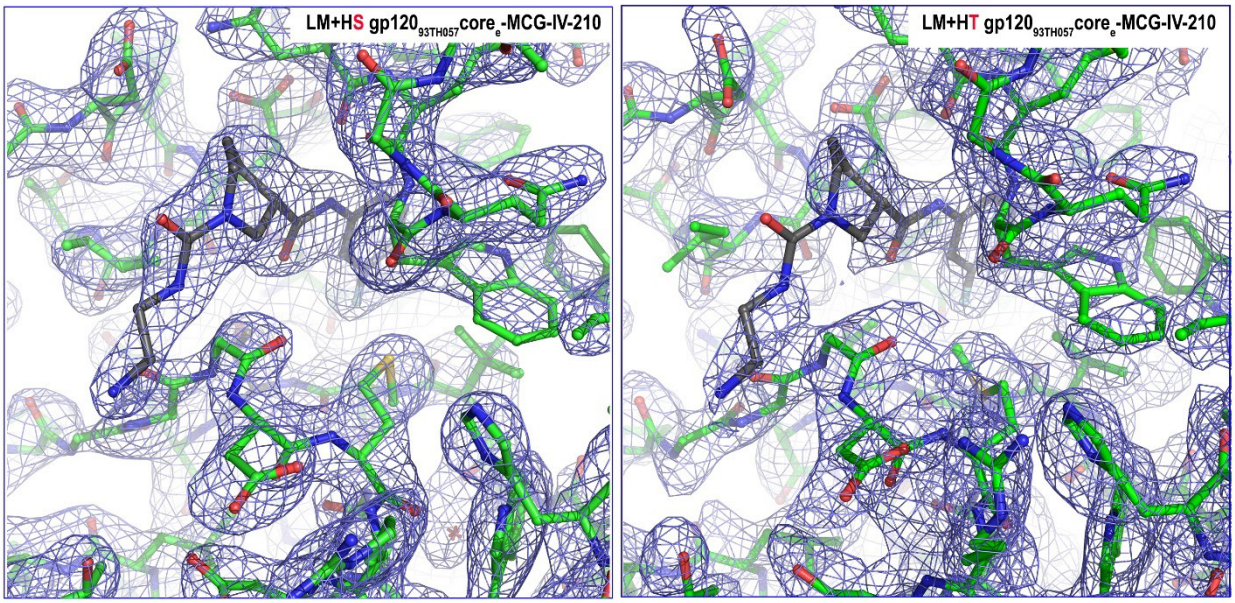

Figure 6.1.S3 - Electron density maps of CD4mc in complex with gp120.
A 2Fo-Fc electron density map contoured at 1s showing the density around MCG-IV-210 for the LM+HS gp120$_{93TH057}$ core$_e$ (left) and LM+HT gp120$_{93TH057}$ core$_e$ (right). MCG-IV-210 is colored grey and gp120 green. Nitrogens are colored blue and oxygens red.

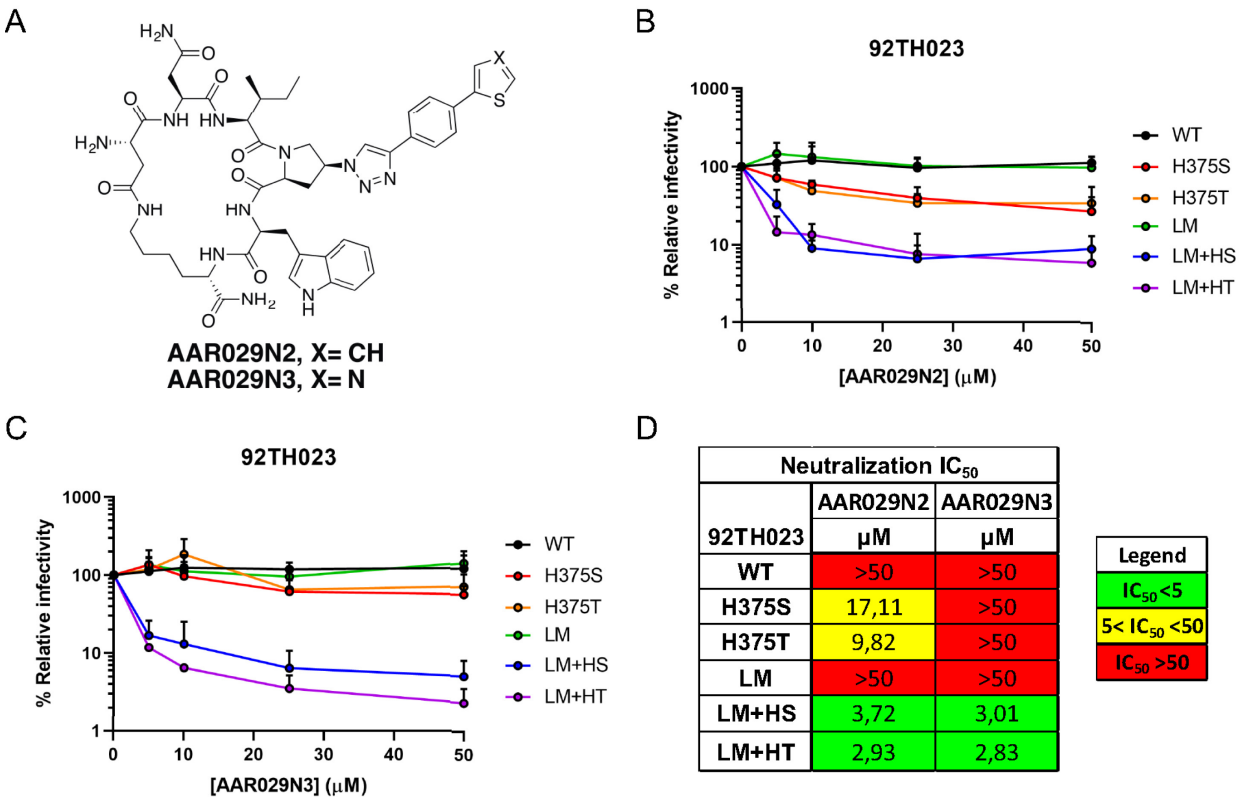

Figure 6.1.S4 - Phe43 cavity and inner domain changes enhance the sensitivity of CRF01_AE strains to neutralization by cPTs.

(**A**) Chemical structure of the different cPTs tested. (**B-D**) Recombinant HIV-1 strains expressing luciferase and bearing wild-type or mutant CRF01_AE Envs (92TH023 isolate) were normalized by reverse transcriptase activity. Normalized amounts of viruses were incubated with serial dilutions of the cyclic peptide triazoles (cPTs) AAR029N2 (**B**), or AAR029N3 (**C**) at 37°C for 1 h prior to infection of Cf2Th-CD4/CCR5 cells. Infectivity at each dilution of cPTs tested is shown as the percentage of infection without cPTs for each particular mutant. Quadruplicate samples were analyzed in each experiment. Data shown are the means of results obtained in at least 3 independent experiments. The error bars represent the standard deviations. Neutralization half maximal inhibitory concentration (IC_{50}) are summarized in (**D**).

Table 6.1.S1 - Data collection and refinement statistics

	LM+HT gp120$_{CRF01_AE}$ core$_e$	LM+HS gp120$_{CRF01_AE}$ core$_e$	LM+HS gp120$_{CRF01_AE}$ core$_e$ - BNM-III-170	LM+HS gp120$_{CRF01_AE}$ core$_e$ - (S)-MCG-IV-210
Data collection				
Wavelength, Å	0.920	1.033	0.979	0.979
Space group	$P2_12_12_1$	$P2_12_12_1$	$P2_12_12_1$	$P2_12_12_1$
Cell parameters				
a, b, c,	66.7, 67.5, 86.8	64.0, 65.6, 87.8	66.8, 66.5, 87.1	65.8, 66.6, 86.2
	90, 90, 90	90, 90, 90	90, 90, 90	90, 90, 90
α, β, γ, °	1	1	1	1
Complexes/a.u.	50-2.5 (2.56-2.5)	50-2.2 (2.24-2.2)	50-2.65 (2.79-2.65)	50-2.5 (2.54-2.5)
Resolution, (Å)				
	55,245	59,449	32,067	38,658
# of reflections	13,726	17,485	10,207	10,448
Total	16.5 (89.6)	11.3 (85.6)	13.3 (89.9)	11.8 (100)
Unique	— (—)	6.7 (59.8)	8.2 (57.1)	6.0 (60.0)
R_{merge}[a], %	0.98 (0.70)	0.99 (0.61)	0.99 (0.49)	0.97 (0.59)
R_{pim}[b], %	6.1 (1.0)	14.3 (0.8)	3.9 (0.8)	14.5 (0.8)
$CC_{1/2}$[c]				
I/σ	96.7 (62.3)	88.0 (66.6)	88.6 (90.0)	76.5 (81.2)
Completeness, %	4.0 (3.2)	3.4 (2.5)	3.1 (3.2)	3.7 (3.5)
Redundancy				
Refinement				
Statistics				
Resolution, Å	50.0 – 2.5	50.0 – 2.2	50.0 – 2.65	50.0 – 2.5
R[d] %	26.3	22.8	20.2	24.6
R_{free}[e], %	30.5	27.0	26.2	30.0
# of atoms				
Protein	2,674	2,668	2,651	2,673
Water	46	33	24	3
Ligand/Ion	155	155	186	178
Overall B value (Å)^2				
Protein	45	64	49	61
Water	40	54	46	58
Ligand/Ion	59	82	65	67
RMSD[f]				
Bond lengths, Å	0.006	0.006	0.006	0.007
Bond angles, °	1.0	0.9	0.83	0.95
Ramachandran[g]				
favored, %	92.8	97.0	94.9	94.9
allowed, %	6.6	3.0	4.8	5.1
outliers, %	0.6	0.0	0.3	0.0
PDB ID	**6UTB**	**6UTD**	**6UT1**	**6USW**

Values in parentheses are for highest-resolution shell

[a] $R_{merge} = \sum | I - \langle I \rangle | / \sum I$, where I is the observed intensity and $\langle I \rangle$ is the average intensity obtained from multiple observations of symmetry-related reflections after rejections

[b] R_{pim} = as defined in (Weiss. J Appl Cryst 2001)

[c] $CC_{1/2}$ = as defined by (Karplus and Diederichs. Science 2012)

[d] $R = \sum \| F_o | - | F_c \| / \sum | F_o |$, where F_o and F_c are the observed and calculated structure factors, respectively

[e] R_{free} = as defined by (Brünger. Methods in Enzymology 1997)

[f] RMSD = Root mean square deviation

[g] Calculated with MolProbity

ARTICLE 11

L'expression de BST-2 module la capacité des mimétiques moléculaires de CD4 à sensibiliser les cellules infectées par le VIH-1 à la réponse ADCC

BST-2 Expression Modulates Small CD4-Mimetic Sensitization of HIV-1-Infected Cells to Antibody-Dependent Cellular Cytotoxicity

Auteurs:

Jonathan Richard[1,2], Jérémie Prévost[1,2], Benjamin von Bredow[3], Shilei Ding[1,2], Nathalie Brassard[1], Halima Medjahed[1], Mathieu Coutu[1], Bruno Melillo[4], Frédéric Bibollet-Ruche[5], Beatrice H. Hahn[5], Daniel E. Kaufmann[1,6,7], Amos B. Smith III[4], Joseph Sodroski[8,9], Daniel Sauter[10], Frank Kirchhoff[10], Katrina Gee[11], Stuart J.D. Neil[12], David T. Evans[3,13], Andrés Finzi[1,2,,14]

Affiliation:

[1]Centre de Recherche du CHUM, Montreal, QC, Canada; [2]Department of Microbiology, Infectiology and Immunology, Université de Montréal, Montreal, QC, Canada; [3]Department of Pathology and Laboratory Medicine, University of Wisconsin—Madison, Madison, WI, USA; [4]Department of Chemistry, School of Arts and Sciences, University of Pennsylvania, Philadelphia, PA, USA; [5]Departments of Medicine and Microbiology, Perelman School of Medicine, University of Pennsylvania, Philadelphia, PA, USA; [6]Department of Medicine, Université de Montréal, Montreal, QC, Canada; [7]Center for HIV/AIDS Vaccine Immunology and Immunogen Discovery, The Scripps Research Institute, La Jolla, CA, USA; [8]Department of Cancer Immunology and Virology, Dana-Farber Cancer Institute, and Department of Microbiology and Immunobiology, Division of AIDS, Harvard Medical School, Boston, MA, USA; [9]Department of Immunology and Infectious Diseases, Harvard School of Public Health, Boston, MA, USA; [10]Institute of Molecular Virology, Ulm University Medical Center, Ulm, Germany; [11]Department of Biomedical and Molecular Sciences, Queen's University, Kingston, ON, Canada; [12]Department of Infectious Disease, King's College London School of Life Sciences and Medicine, Guy's Hospital, London, United Kingdom; [13]Wisconsin National Primate Research Center, University of Wisconsin—Madison, Madison, WI, USA; [14]Department of Microbiology and Immunology, McGill University, Montreal, QC, Canada.

Contribution des auteurs:

Conceptualisation: J.R. et A.F.; Méthodologie: J.R. et A.F.; Recherche: J.R., **J.P.**, B.V.B., et S.D.; Ressources: N.B., H.M., M.C., B.M., F.B.-R., B.H.H., D.E.K., A.B.S., D.S., F.K., K.G., S.J.D.N. et A.F.; Analyse formelle: J.R.; Visualisation: J.R.; Supervision: D.E.K., A.B.S., D.T.E. et A.F.; Obtention du financement: J.R., D.E.K., B.H.H., A.B.S., J.S., D.T.E. et A.F.; Rédaction - version originale: J.R. et A.F.; Rédaction - révision et édition: **Tous les auteurs**.

Statut: Cet article a été publié dans *Journal of Virology*, le 12 mai 2017.
https://doi.org/10.1128/JVI.00219-17

6.3.1 RÉSUMÉ

Il a été démontré que les anticorps reconnaissant les épitopes conservés induits par CD4 (CD4i) de l'Env du virus de l'immunodéficience humaine de type 1 (VIH-1) et capables de médier la réponse cytotoxique cellulaire dépendante des anticorps (ADCC) sont présents dans le sérum de la plupart des individus infectés par le VIH-1. Ces anticorps reconnaissent préférentiellement Env dans sa conformation liée à CD4. La régulation négative de CD4 par Nef et Vpu réduit considérablement l'exposition des épitopes CD4i de l'Env du VIH-1 et, par conséquent, réduit aussi la susceptibilité des cellules infectées par le VIH-1 à l'ADCC médiée par le sérum de personnes séropositives (sérum VIH^+). Il est important de noter que ce mécanisme d'évasion immunitaire peut être contourné à l'aide de mimétiques moléculaires de CD4 (CD4mc) qui sont capables de faire passer Env dans la conformation liée à CD4 et de sensibiliser les cellules infectées par le VIH-1 à l'ADCC médiée par les sérums VIH^+. Cependant, le VIH-1 a développé des mécanismes supplémentaires pour éviter l'ADCC, notamment l'antagonisme de BST-2 médié par Vpu, qui diminue la quantité globale d'Env présente à la surface des cellules. En conséquence, il a été démontré que la régulation à la hausse de la BST-2 en réponse à l'interféron alpha (IFN-α) augmente la susceptibilité des cellules infectées par le VIH-1 à l'ADCC malgré l'activité de Vpu. Nous montrons ici que la régulation à la hausse de BST-2 par l'IFN-β et l'interleukine-27 (IL-27) augmente également l'expression de surface d'Env et augmente ainsi la capacité des CD4mc à sensibiliser les cellules infectées par le VIH-1 à l'ADCC par des sérums provenant de personnes infectées par le VIH-1.

6.3.2 ABSTRACT

Antibodies recognizing conserved CD4-induced (CD4i) epitopes on human immunodeficiency virus type 1 (HIV-1) Env and able to mediate antibody-dependent cellular cytotoxicity (ADCC) have been shown to be present in sera from most HIV-1-infected individuals. These antibodies preferentially recognize Env in its CD4-bound conformation. CD4 downregulation by Nef and Vpu dramatically reduces exposure of CD4i HIV-1 Env epitopes and therefore reduce the susceptibility of HIV-1-infected cells to ADCC mediated by HIV-positive (HIV^+) sera. Importantly, this mechanism of immune evasion can be circumvented with small-molecule CD4 mimetics (CD4mc) that are able to transition Env into the CD4-bound conformation and sensitize HIV-1-infected cells to ADCC mediated by HIV^+ sera. However, HIV-1 developed

additional mechanisms to avoid ADCC, including Vpu-mediated BST-2 antagonism, which decreases the overall amount of Env present at the cell surface. Accordingly, BST-2 upregulation in response to alpha interferon (IFN-α) was shown to increase the susceptibility of HIV-1-infected cells to ADCC despite the activity of Vpu. Here we show that BST-2 upregulation by IFN-β and interleukin-27 (IL-27) also increases the surface expression of Env and thus boosts the ability of CD4mc to sensitize HIV-1-infected cells to ADCC by sera from HIV-1-infected individuals.

6.3.3 IMPORTANCE

HIV-1 evolved sophisticated strategies to conceal Env epitopes from ADCC-mediating antibodies present in HIV sera. Vpu-mediated BST-2 downregulation was shown to decrease ADCC responses by limiting the amount of Env present at the cell surface. This effect of Vpu was shown to be attenuated by IFN- treatment. Here we show that in addition to IFN-, IFN- and IL-27 also affect Vpu-mediated BST-2 downregulation and greatly enhance ADCC responses against HIV-1-infected cells in the presence of CD4mc. These findings may inform strategies aimed at HIV prevention and eradication.

6.3.4 INTRODUCTION

Antibodies that preferentially recognize the CD4-bound conformation of human immunodeficiency virus type 1 (HIV-1) envelope glycoproteins (Env) can eliminate HIV-1-infected cells through antibody-dependent cellular cytotoxicity (ADCC) responses (1–4). These antibodies are present in serum (1, 5), breast milk (5), and cervicovaginal lavage fluid (2, 5) samples from HIV-1-infected individuals and have been proposed to be part of the pressure exerted on HIV-1 to efficiently downregulate CD4 from the cell surface (6). Accordingly, Nef- and Vpu-mediated CD4 downregulation conceal the exposure of Env epitopes recognized by these antibodies (1, 3, 7). In addition, HIV-1 decreases ADCC responses by diminishing the overall amount of Env present at the cell surface. This is achieved through Vpu-mediated BST-2 (tetherin/CD317/HM1.24) downregulation (7–9), which allows for efficient release of viral particles (10, 11), and also through efficient Env internalization mediated by an endocytosis motif in the cytoplasmic tail of gp41 (12).

A better understanding of the importance that the CD4-bound conformation of HIV-1 envelope glycoproteins has on ADCC responses prompted us to "force" this Env conformation on the surface of infected cells using small-molecule CD4 mimetics (CD4mc). CD4mc induction of the CD4-bound conformation results in enhanced recognition of HIV-1-infected cells by serum, breast milk, and cervicovaginal fluid samples from HIV-1-infected subjects. Most importantly, CD4mc sensitizes HIV-1-infected cells to ADCC responses mediated by these biological fluids (4, 5, 13).

The effect of CD4mc on ADCC responses may be influenced by the amount of Env available at the cell surface. Only limited amounts of Env are presented at the cell surface due to efficient Env internalization (12) and Vpu-mediated BST-2 downregulation (7–9); this places an upper limit on the amount of Env that can be rendered susceptible to ADCC by CD4mc. Interestingly, two BST-2 isoforms possessing distinct biological properties have been described (14, 15). While the long isoform of BST-2 (L-BST-2) contains a cytoplasmic tyrosine motif mediating endocytic recycling, sensitivity to HIV-1 M Vpu and innate immune sensing, the short isoform of BST-2 (S-BST-2) lacks this motif due to the utilization of an alternative start codon (14, 15). How these two isoforms modulate Env recognition on the surface of HIV-1-infected cells by HIV-positive (HIV^+) sera and how this affects the activity of CD4mc remain unknown.

Type I interferons (IFNs) are an important part of the early host immune response observed during acute HIV-1 infection (16). The antiviral effect exerted by IFN is highlighted by the observation that transmitted/founder HIV-1 strains that initiate host infection have been shown to be more resistant to type I IFN responses than HIV-1 strains found during the chronic phase of infection (17–19). Furthermore, Vpu enhances viral replication particularly during early stages of infection, probably by counteracting the IFN-inducible restriction factor BST-2 (18, 20). The induction of BST-2 expression by type I IFN treatment was also shown to sensitize infected cells to ADCC (8). In addition, interleukin-27 (IL-27) also enhances BST-2 levels on the surface of human monocytes and $CD4^+$ T cells (21). IL-27 is a member of the IL-12 family of cytokines and drives the differentiation of Th1 $CD4^+$ T cells (22, 23). Interestingly, IL-27 induces an antiviral gene expression profile similar to that induced by alpha interferon (IFN-α), including the *apobec3g* gene (24). Furthermore, IL-27 inhibited the replication of HIV-1 in cultures of primary $CD4^+$ T

cells and monocytes/macrophages through the induction of APOBEC (apolipoprotein B mRNA-editing, enzyme-catalytic, polypeptide-like) proteins (24, 25). Notably, IL-27-mediated BST-2 upregulation was shown to be independent from type I IFN responses (21). However, the effect of IL-27 on ADCC responses during viral infection has not been determined.

Here we evaluated the role of BST-2 on Env accumulation on the surface of HIV-1-infected cells and tested whether type I IFNs or IL-27 could be exploited in conjunction with CD4mc to further enhance ADCC responses mediated by HIV-positive (HIV^+) sera.

6.3.5 RESULTS

BST-2 expression modulates Env accumulation on the surface of HIV-1-infected cells and its recognition by HIV^+ sera in the presence of CD4mc.

In the absence of Vpu, Env accumulates at the plasma membrane of HIV-1-infected cells (7–9) in large part due to the inhibitory effects of BST-2 on virus release (10, 11). This surface accumulation results in increased susceptibility of HIV-1-infected cells to ADCC (7–9). To further evaluate the role of BST-2 on Env surface expression, we infected Jurkat cell lines expressing no BST-2 (Jurkat Tag) or expressing the long isoform of BST-2 (Jurkat Tag L-BST-2) or the short isoform of BST-2 (Jurkat Tag S-BST-2) (15). Cells were infected with the transmitted/founder virus CH58 (CH58 TF) (5) expressing the Vpu accessory protein (wild-type [wt] CH58 TF) or containing a *vpu* deletion (Vpu-). Forty-eight hours postinfection, BST-2 and Env levels were evaluated by cell surface staining followed by intracellular p24 staining to identify infected (p24-positive [$p24^+$]) cells. As expected, while BST-2 was not detected on the surface of Jurkat Tag cells (**Fig. 6.2.1A and D**), it was equivalently detected on the surface of uninfected (mock) Jurkat Tag L-BST-2 and S-BST-2 cells, indicating that these two cell lines express similar levels of BST-2 (**Fig. 6.2.1B to D**). However, in agreement with previous reports, HIV-1 infection significantly decreased expression of L-BST-2 but not that of S-BST-2. The S-BST-2 isoform lacks 12 residues of the cytoplasmic tail required for Vpu group M-mediated BST-2 endosomal degradation (14, 15) (**Fig. 6.2.1C and D**). As expected, a virus lacking Vpu (Vpu-) was unable to decrease cell surface levels of BST-2 (**Fig. 6.2.1B to D**).

When we evaluated Env levels on the surface of infected cells with the conformation-independent 2G12 antibody (**Fig. 6.2.2A**), we observed a significant correlation with BST-2 levels (**Fig. 6.2.2B**). This supports previous observations indicating that BST-2 modulates the overall amount of Env on the surfaces of infected cells (7, 8). We then assessed whether enhanced accumulation of Env affected recognition of HIV-1-infected cells by HIV^+ sera. Despite different amounts of BST-2 and Env present on the surface of Jurkat cell lines expressing S-BST-2, L-BST-2, or no BST-2, cells infected with a wild-type virus were barely recognized by HIV^+ sera (**Fig. 6.2.2C**). This is believed to reflect the ability of HIV-1 to downregulate CD4 in infected cells such that only closed Env trimers remain (1, 3, 5, 7, 26). Antibodies present in HIV^+ sera preferentially recognize Env in its CD4-bound conformation (1, 27). Infection with a *vpu*- virus led to a small increase in recognition of HIV-1-infected cells by HIV^+ sera (**Fig. 6.2.2C**). In order to expose epitopes recognized by antibodies present in HIV^+ sera, infected cells were incubated in parallel with the potent CD4mc BNM-III-170 which forces Env to adopt a CD4-bound-like conformation (4, 28) and in conjunction with coreceptor binding site antibodies (CoRBS) efficiently expose anti-cluster A epitopes (4). CD4mc addition enhanced recognition of all three infected cell lines (**Fig. 6.2.2C**). In agreement with decreased sensitivity of S-BST-2 to Vpu-mediated downregulation, Jurkat Tag S-BST-2 cells infected with a wild-type virus responded significantly better to CD4mc than Jurkat Tag L-BST-2 cells infected with the same virus. This likely results from an enhanced Env accumulation on the surfaces of Jurkat Tag S-BST-2 cells due to the inability of Vpu to downregulate S-BST-2 (**Fig. 6.2.2A and C**). Likely due to the absence of BST-2 in the Jurkat Tag empty vector (EV) cell line, infection with a *vpu*- virus has a minor effect on Env levels (as evaluated by 2G12) and therefore recognition of infected cells by HIV^+ sera in the absence of CD4mc. Infection with a Vpu- virus of Jurkat Tag S-BST-2 and L cells led to a slightly better recognition of infected cells in the absence of CD4mc. Upon addition of CD4mc, however, all infected cells were significantly better recognized by HIV^+ sera. This finding confirms previous observations indicating that antibodies present in HIV^+ sera preferentially recognize Env in the CD4-bound conformation (1). Of note, the difference in HIV^+ serum recognition in the presence of CD4mc between wild-type and *vpu*- virus infected cells was higher in Jurkat L-BST-2 cells that express the BST-2 isoform susceptible to Vpu action (**Fig. 6.2.2C**). Accumulation of Env (as measured by 2G12) correlated significantly with recognition of infected cells by HIV^+ sera (**Fig.**

6.2.2D). Recognition of infected cells by HIV$^+$ sera also correlated with BST-2 expression (**Fig. 6.2.2E**).

BST-2 levels regulate Env accumulation and its recognition by HIV sera on the surface of HIV-1-infected primary CD4$^+$ T cells.

Figures 6.2.1 and 6.2.2 showed that BST-2 levels, and its sensitivity to Vpu downregulation, dictated Env accumulation on the surfaces of HIV-1-infected cell lines. Moreover, Env accumulation on the surfaces of infected cells increased the amount of Env available to engage CD4mc and henceforth sample the CD4-bound conformation, which is preferentially recognized by HIV$^+$ sera (1, 27). IFN-α treatment has been shown to enhance BST-2 levels, resulting in an accumulation of Env on the surfaces of HIV-1-infected cells and thus increasing the sensitivity of HIV-1-infected cells to ADCC (8). Similar observations were recently reported (29). Therefore, we decided to take advantage of the type 1 interferon responsiveness of BST-2 (10, 11). Primary CD4$^+$ T cells from healthy HIV-1 uninfected individuals were mock infected or infected with HIV-1 (CH58 TF), and BST-2 levels were modulated by stimulation with type 1 IFNs (IFN-α and IFN-β) or with IL-27 (21). As expected, BST-2 levels were significantly higher in uninfected than HIV-1-infected cells. Interestingly, IFN-α, IFN-β, and IL-27 treatment enhanced BST-2 detection in both uninfected and HIV-1-infected cells (**Fig. 6.2.3A**). BST-2 upregulation resulted in Env accumulation on the surfaces of infected cells, as measured with the 2G12 antibody (**Fig. 6.2.3B**).

We then evaluated whether IFN-α, IFN-β, and IL-27 treatment enhanced recognition of HIV-1-infected cells by HIV$^+$ sera. Despite a significant increase in Env accumulation on the surfaces of infected cells (**Fig. 6.2.3B**), treatment with IFN-β and IL-27 failed to enhance recognition of infected cells by HIV$^+$ sera, and the effect of IFN-α treatment was relatively minor (**Fig. 6.2.4**). However, addition of the CD4mc BNM-III-170 significantly increased recognition of HIV-1-infected cells by HIV$^+$ sera; these results are in agreement with previous reports demonstrating the ability of HIV$^+$ sera to recognize CD4i epitopes on primary HIV-1 Env that are not spontaneously exposed (1, 3) and the capacity of CD4mc to promote the CD4-bound conformation of Env on the surfaces of HIV-1-infected cells (4, 5, 13, 30). Remarkably, the

combination of IFN-α, IFN-β, or IL-27 with BNM-III-170 further increased recognition of HIV-1-infected cells by all sera tested compared to any one of these treatments (**Fig. 6.2.4**).

BST-2 upregulation boosts the capacity of CD4mc to sensitize HIV-1-infected cells to ADCC mediated by HIV$^+$ sera.

To evaluate whether the enhanced recognition of HIV-1-infected cells induced by the combination of IFN-α, IFN-β, and IL-27 treatments and BNM-III-170 would result in enhanced ADCC killing, we infected primary CD4$^+$ T cells with HIV-1 CH58 TF and evaluated their susceptibility to ADCC mediated by autologous peripheral blood mononuclear cells (PBMCs) using a previously described fluorescence-activated cell sorting (FACS)-based assay (5, 31). As reported (5, 13), CD4mc BNM-III-170 significantly increased ADCC mediated by all HIV$^+$ sera tested (**Fig. 6.2.5**). In agreement with the recognition of infected cells by HIV$^+$ sera (**Fig. 6.2.4**), IFN-α treatment alone had a minor but significant effect on ADCC responses (**Fig. 6.2.5**), but IFN-β and IL-27 treatment failed to do so (**Fig. 6.2.5**). Remarkably, addition of BNM-III-170 further enhanced the susceptibility of infected cells to ADCC for cells treated with IFN-α, IFN-β, or IL-27 (**Fig. 6.2.5**). As expected, enhanced recognition of HIV-1-infected cells by HIV$^+$ sera positively correlated with enhanced ADCC responses (**Fig. 6.2.6**). These results highlight the potential of combining type I IFNs and IL-27 with CD4mc to sensitize HIV-1-infected cells to ADCC.

6.3.6 DISCUSSION

Increasing evidence suggests that Fcγ receptor-dependent functions of antibodies play a role in controlling human immunodeficiency virus type 1 (HIV-1) infection and replication (32–40). Analysis of the correlates of protection in the RV144 vaccine trial suggested that decreased HIV-1 acquisition was linked to increased ADCC activity in protected vaccinees (41). ADCC-mediating antibodies (Abs) targeting anti-cluster A epitopes were isolated from some RV144 vaccinees (42) and were shown to preferentially recognize the HIV-1 envelope glycoproteins sampling the CD4-bound conformation (7). CD4i antibodies represent a significant portion of the anti-Env Abs elicited during natural HIV-1 infection (1, 27, 43). This elicitation of CD4i Abs could result from transitional exposure of CD4i Env epitope during viral entry (44) or, most likely, after binding of shed gp120 with CD4 on uninfected bystander cells (30). However, not all CD4i antibodies are able to mediate ADCC against HIV-1-infected cells. While anti-cluster A antibodies

have been shown to mediate potent ADCC responses against infected cells exposing Env in the CD4-bound conformation (3, 4, 7, 45), CD4i antibodies targeting the coreceptor binding site appear to be unable to do so (3, 4, 45, 46). While the reasons for these differences are not fully understood, the angle of approach of the antibody toward Env might differentially expose the Fc region which must be engaged by the Fcγ receptor in order to activate effector cells. Nevertheless, to limit the exposure of anti-cluster A epitopes that are exposed in the CD4-bound conformation of Env at the surface of infected cells, HIV-1 evolved sophisticated mechanisms to efficiently internalize Env (12) to counteract the host restriction factor BST-2 with the viral Vpu protein (7–9) and to downregulate CD4 by Nef and Vpu (1, 7). The requirement to evade ADCC provides one plausible explanation of why the vast majority of circulating HIV-1 strains worldwide express functional Nef and Vpu proteins, which limit the exposure of CD4i Env epitopes on the surfaces of infected cells.

In agreement with the necessity for HIV-1 to avoid exposing the CD4-bound conformation of Env, we recently showed that forcing Env to adopt this conformation with CD4mc sensitizes HIV-1-infected cells to ADCC by sera from HIV-1-infected subjects (5). Here we show that increasing the amounts on Env at the cell surface, once this Env is induced by CD4mc to adopt the CD4-bound conformation, results in increased recognition of HIV-1-infected cells by HIV^+ sera. We found that enhanced recognition of infected cells by HIV sera translates into enhanced susceptibility of infected cells to ADCC. This was achieved by exploiting the type 1 interferon responsiveness of the restriction factor BST-2, known to trap mature viral particles on the surfaces of infected cells. IFN-α and -β enhance BST-2 levels on the surfaces of infected cells, which translates into enhanced levels of Env potentially able to be targeted by ADCC after engaging the CD4mc. Interestingly, similar results were obtained using IL-27, a cytokine known to modulate BST-2 levels in an IFN-independent manner. Altogether, our results suggest a model (**Fig. 6.2.7**) where the conformation and availability of Env at the cell surface dictates the sensitivity of HIV-1-infected cells to ADCC. HIV-1 limits the amount of Env present at the cell surface and tightly controls its conformation. By preventing Env from assuming the CD4-bound conformation, HIV-1 avoids Env recognition by CD4i ADCC-mediating Abs present in the sera of the majority of HIV-1-infected individuals. Small CD4mc sensitize HIV-1-infected cells to ADCC by forcing Env to expose CD4i anti-cluster A-mediating epitopes. IFN-α, IFN-β, and IL-27 treatment, through

upregulation of BST-2, increases the total amounts of Env available for CD4mc to induce ADCC-susceptible Env conformations at the surface of infected cells. While HIV-1-infected cells are protected from ADCC responses, we recently demonstrated that uninfected bystander $CD4^+$ T cells bind gp120 shed from productively infected cells and are efficiently recognized by ADCC-mediating antibodies (30). Importantly, we also demonstrated that this phenomenon can be blocked by CD4mc that abrogates the binding of gp120 to uninfected cells and effectively redirects the immune system to infected cells. Therefore, the combination of CD4mc and type I IFN or IL-27 would represent an effective strategy to specifically target and eliminate HIV-1-infected cells by ADCC.

Robust type I interferon responses are among the earliest host immune defenses observed during acute HIV-1 infection (16). Accordingly, transmitted/founder viruses, including those used in the present study, were found to be more resistant to IFN treatment than viruses from chronic HIV-1 infection (17–19). In that context, Vpu counteraction of BST-2 was recently identified as a major determinant of this IFN resistance (18, 20) and was found to play a crucial role in enhancing virus replication and release in human $CD4^+$ T cells, particularly in the presence of IFN (18). Here we found that IFN-α, IFN-β, or IL-27 treatment enhanced BST-2 levels and, in combination with CD4mc, similarly sensitized HIV-1-infected cells to ADCC. However, there are many other IFN-α subtypes, and some of them inhibit HIV-1 replication more efficiently in vitro and in animal models than IFN-α2 (47, 48). Thus, it will be important to evaluate to what extent the different IFN-α subtypes sensitize HIV-1-infected cells to ADCC in the presence of CD4mc.

CD4mc were recently shown to enhance the viral neutralization and ADCC activities of antibodies elicited in nonhuman primates (NHP) by several different Env immunogens (49), suggesting that combining a vaccine with a small-molecule CD4mc, administered orally or in a microbicide formulation, might be useful as a prophylactic strategy against HIV-1 transmission. Interestingly, mucosal application of IFN-β protected macaques from intrarectal and intravaginal simian-human immunodeficiency virus (SHIV) challenges (50). Similarly, IFN-α2 treatment of rhesus macaques prevented systemic infection by simian immunodeficiency virus (SIV) (51). Whereas a combination of IFNs or IL-27 with CD4mc might further limit HIV-1 transmission or help decrease the size of the viral reservoir in HIV-1-infected individuals remains to be evaluated,

our results support performing future experiments aimed at evaluating whether sensitization of HIV-infected cells to ADCC could affect viral transmission and/or replication in animal models.

6.3.7 MATERIALS AND METHODS

Cell lines and isolation of primary cells

HEK293T human embryonic kidney (obtained from ATCC) and primary cells were grown as previously described (7, 52). Peripheral blood mononuclear cells (PBMCs) were obtained by leukapheresis. All participants provided informed written consent prior to enrollment in accordance with Institutional Review Board approval. CD4 T lymphocytes were purified from resting PBMCs by negative selection and activated as previously described (5). Jurkat Tag cells stably expressing the long isoform of BST-2 (L-BST-2) or the short isoform of BST-2 (S-BST-2) and the Jurkat Tag empty vector (EV) cell line expressing no BST-2 were previously described (15).

Viral production, infections, and detection of infected cells

In order to achieve the same level of infection between wild-type (wt) and Vpu viruses, vesicular stomatitis virus G (VSVG)-pseudotyped HIV-1 replicating competent viruses were produced. Briefly, proviral vectors and a VSVG-encoding plasmid were co-transfected in 293T cells by standard calcium phosphate transfection. Two days after transfection, cell supernatants were harvested, clarified by low-speed centrifugation (5 min at 1,500 rpm), and concentrated by ultracentrifugation for 1 h at 4°C at 100,605 × g over a 20% sucrose cushion. Pellets were resuspended in fresh RPMI 1640 medium, and aliquots were stored at -80°C until use (1). Viruses were then used to infect Jurkat Tag cell lines or primary $CD4^+$ T cells from healthy donors by spin infection at 800 × g for 1 h in 96-well plates at 25°C.

CD4 mimetic, type I IFN, or IL-27 treatments

The CD4mc BNM-III-170 was synthesized as described previously (28). BNM-III-170 was dissolved in dimethyl sulfoxide (DMSO) at a stock concentration of 10 mM, aliquoted, and stored at 20°C. BNM-III-170 was then diluted to 50 µM in phosphate-buffered saline (PBS) for cell surface staining or in complete RPMI 1640 medium for ADCC assays. IFN-α (PBL Assay Science) was reconstituted in complete RPMI 1640 medium at 1×10^7 U/ml, aliquoted, and stored at 80°C. IFN-α was then added to the cells at 1,000 U/ml. IFN-β (Rebif; EMD Serono Inc.) (19) was added to the cells at 1 ng/ml. IL-27 (R&D Systems) was reconstituted at 100 µg/ml in sterile

PBS containing 0.1% bovine serum albumin and stored at -80°C. IL-27 was then added to the cells at 100 ng/mL. Type I IFN or IL-27 was added to the cells 24 h post-infection, 24 h before cell surface staining or ADCC assays.

Antibodies and sera

The following antibodies (Abs) were used as the primary Abs for cell surface staining: 5 µg/ml of human anti-HIV-1 Env monoclonal antibody (mAb) 2G12 (National Institutes of Health [NIH] AIDS and Research and Reference Reagent Program), 2 µg/ml rabbit anti-BST-2 Ab (sc-99191; Santa Cruz), or sera from HIV-1-infected individuals (1:1,000 dilution), whereas 1 µg/ml of either Alexa Fluor 647-labeled goat anti-human mAbs (Invitrogen, San Diego, CA, USA) or Brilliant Violet 421-labeled donkey anti-rabbit mAbs (Biolegend, San Diego, CA, USA) were used as secondary Abs, and AquaVivid (Invitrogen, San Diego, CA, USA) was used as a viability dye. All sera were heat inactivated for 30 min at 56°C and stored at 4°C until ready to use in subsequent experiments. Written informed consent was obtained from all study participants (the Montreal Primary HIV Infection Cohort [53, 54] and the Canadian Cohort of HIV Infected Slow Progressors [55–57]), and research adhered to the ethical guidelines of Centre de Recherche du CHUM (CRCHUM) and was reviewed and approved by the CRCHUM institutional review board (ethics committee). A random-number generator (QuickCalcs; GraphPad) was used to randomly select a number of sera for experiments.

Plasmids

The plasmid encoding the HIV-1 transmitted founder (T/F) CH58 was previously described (5, 17, 58–60).

Flow cytometry analysis of cell surface staining and ADCC responses

Cell surface staining was performed as previously described (1, 5). Binding of HIV-1-infected cells by HIV^+ sera, anti-Env mAbs (2G12) or anti-BST-2 mAbs was performed 48 h after infection, 24 h after treatment with type I IFNs or IL-27, in the presence or absence of BNM-III-170 (50 µM) or an equivalent volume of vehicle (DMSO). Detection of p24 infected cells was performed as described previously (5). The percentage of infected cells ($p24^+$ cells) was determined by gating the living cell population based on the viability dye staining (Aqua Vivid;

Invitrogen). Samples were analyzed on a LSRII cytometer (BD Biosciences, Mississauga, ON, Canada), and data analysis was performed using FlowJo vX.0.7 (Tree Star, Ashland, OR, USA).

Measurement of ADCC-mediated killing was performed with a previously described assay (5). Briefly, primary CD4 T cells infected for 48 h and treated for 24 h with type I IFNs or IL-27 or not treated with type I IFNs or IL-27 were incubated with autologous PBMCs (effector/target cell ratio of 10:1) in the presence or absence of HIV^+ sera (1:1,000), in the presence of CD4mc BNM-III-170 (50 μM), or with an equivalent volume of vehicle (DMSO). The percentage of cytotoxicity was calculated as described previously (5).

Statistical analyses

Statistics were analyzed using GraphPad Prism version 6.0.1 (GraphPad, San Diego, CA, USA). Every data set was tested for statistical normality, and this information was used to apply the appropriate (parametric or nonparametric) statistical test. P values of < 0.05 were considered significant; significance values are indicated as follows: *, $P < 0.05$; **, $P < 0.01$, ***, $P < 0.001$; ****, $P < 0.0001$.

6.3.8 ACKNOWLEDGMENTS

We thank Elizabeth Carpelan for help with manuscript preparation. We thank Dominique Gauchat from the CRCHUM Flow Cytometry Platform for technical assistance and Mario Legault for cohort coordination and clinical samples. This work was supported by CIHR foundation grant 352417 and by amfAR Innovation Grant 109343-59-RGRL with support from FAIR to A.F. and by a FRQS AIDS and Infectious Diseases Network grant to J.R. and A.F. A.F. is the recipient of a Canada Research Chair on Retroviral Entry. J.R. is the recipient of a CIHR Fellowship Award 135349. D.E.K. is supported by a Research Scholar Career Award of the Quebec Health Research Fund (FRQS). This study was also supported by the National Institute of Allergy and Infectious Diseases of the National Institutes of Health and by the Center for HIV/AIDS Vaccine Immunology and Immunogen Discovery (CHAVI-ID), grants UM1- AI100645 and AI100663, by the National Institutes of Health grant GM56550, the late William F. McCarty-Cooper, NIH R01AI116274, HL-092565, R01 AI114266, and by NIH grants AI121135, AI098485, and AI095098 to D.T.E. F.K. is supported by the DFG and an ERC Advanced grant, and D.S. is

supported by the junior professorship program of the state Baden-Wuerttemberg, Germany. Our funding sources had no role in data collection, analysis or interpretation and were not involved in the writing of the manuscript. The content is solely the responsibility of the authors and does not necessarily represent the official views of the National Institutes of Health. We have no conflicts of interest to report.

6.3.9 REFERENCES

1. Veillette M, Coutu M, Richard J, Batraville LA, Dagher O, Bernard N, Tremblay C, Kaufmann DE, Roger M, Finzi A. 2015. The HIV-1 gp120 CD4-bound conformation is preferentially targeted by antibody-dependent cellular cytotoxicity-mediating antibodies in sera from HIV-1-infected individuals. J Virol 89:545–551.
2. Batraville LA, Richard J, Veillette M, Labbe AC, Alary M, Guedou F, Kaufmann DE, Poudrier J, Finzi A, Roger M. 2014. Anti-HIV-1 envelope immunoglobulin Gs in blood and cervicovaginal samples of Beninese commercial sex workers. AIDS Res Hum Retroviruses 30:1145–1149.
3. Ding S, Veillette M, Coutu M, Prevost J, Scharf L, Bjorkman PJ, Ferrari G, Robinson JE, Sturzel C, Hahn BH, Sauter D, Kirchhoff F, Lewis GK, Pazgier M, Finzi A. 2015. A highly conserved residue of the HIV-1 gp120 inner domain is important for antibody-dependent cellular cytotoxicity responses mediated by anti-cluster A antibodies. J Virol 90:2127–2134.
4. Richard J, Pacheco B, Gohain N, Veillette M, Ding S, Alsahafi N, Tolbert WD, Prevost J, Chapleau JP, Coutu M, Jia M, Brassard N, Park J, Courter JR, Melillo B, Martin L, Tremblay C, Hahn BH, Kaufmann DE, Wu X, Smith AB, III, Sodroski J, Pazgier M, Finzi A. 2016. Co-receptor binding site antibodies enable CD4-mimetics to expose conserved anti-cluster A ADCC epitopes on HIV-1 envelope glycoproteins. EBioMedicine 12: 208 – 218.
5. Richard J, Veillette M, Brassard N, Iyer SS, Roger M, Martin L, Pazgier M, Schon A, Freire E, Routy JP, Smith AB, III, Park J, Jones DM, Courter JR, Melillo BN, Kaufmann DE, Hahn BH, Permar SR, Haynes BF, Madani N, Sodroski JG, Finzi A. 2015. CD4 mimetics sensitize HIV-1-infected cells to ADCC. Proc Natl Acad Sci USA 112:E2687–E2694.

6. Veillette M, Richard J, Pazgier M, Lewis GK, Parsons MS, Finzi A. 2016. Role of HIV-1 envelope glycoproteins conformation and accessory proteins on ADCC responses. Curr HIV Res 14:9 –23.
7. Veillette M, Desormeaux A, Medjahed H, Gharsallah NE, Coutu M, Baalwa J, Guan Y, Lewis G, Ferrari G, Hahn BH, Haynes BF, Robinson JE, Kaufmann DE, Bonsignori M, Sodroski J, Finzi A. 2014. Interaction with cellular CD4 exposes HIV-1 envelope epitopes targeted by antibody-dependent cell-mediated cytotoxicity. J Virol 88:2633–2644.
8. Arias JF, Heyer LN, von Bredow B, Weisgrau KL, Moldt B, Burton DR, Rakasz EG, Evans DT. 2014. Tetherin antagonism by Vpu protects HIV-infected cells from antibody-dependent cell-mediated cytotoxicity. Proc Natl Acad Sci USA 111:6425– 6430.
9. Alvarez RA, Hamlin RE, Monroe A, Moldt B, Hotta MT, Rodriguez Caprio G, Fierer DS, Simon V, Chen BK. 2014. HIV-1 Vpu antagonism of tetherin inhibits antibody-dependent cellular cytotoxic responses by natural killer cells. J Virol 88:6031– 6046.
10. Neil SJ, Zang T, Bieniasz PD. 2008. Tetherin inhibits retrovirus release and is antagonized by HIV-1 Vpu. Nature 451:425– 430.
11. Van Damme N, Goff D, Katsura C, Jorgenson RL, Mitchell R, Johnson MC, Stephens EB, Guatelli J. 2008. The interferon-induced protein BST-2 restricts HIV-1 release and is downregulated from the cell surface by the viral Vpu protein. Cell Host Microbe 3:245–252.
12. von Bredow B, Arias JF, Heyer LN, Gardner MR, Farzan M, Rakasz EG, Evans DT. 2015. Envelope glycoprotein internalization protects human and simian immunodeficiency virus-infected cells from antibody-dependent cell-mediated cytotoxicity. J Virol 89:10648 –10655.
13. Lee WS, Richard J, Lichtfuss M, Smith AB, III, Park J, Courter JR, Melillo BN, Sodroski JG, Kaufmann DE, Finzi A, Parsons MS, Kent SJ. 2015. Antibody-dependent cellular cytotoxicity against reactivated HIV-1-infected cells. J Virol 90:2021–2030.
14. Cocka LJ, Bates P. 2012. Identification of alternatively translated Tetherin isoforms with differing antiviral and signaling activities. PLoS Pathog 8:e1002931.
15. Weinelt J, Neil SJ. 2014. Differential sensitivities of tetherin isoforms to counteraction by primate lentiviruses. J Virol 88:5845–5858.

16. Stacey AR, Norris PJ, Qin L, Haygreen EA, Taylor E, Heitman J, Lebedeva M, DeCamp A, Li D, Grove D, Self SG, Borrow P. 2009. Induction of a striking systemic cytokine cascade prior to peak viremia in acute human immunodeficiency virus type 1 infection, in contrast to more modest and delayed responses in acute hepatitis B and C virus infections. J Virol 83:3719 –3733.
17. Parrish NF, Gao F, Li H, Giorgi EE, Barbian HJ, Parrish EH, Zajic L, Iyer SS, Decker JM, Kumar A, Hora B, Berg A, Cai F, Hopper J, Denny TN, Ding H, Ochsenbauer C, Kappes JC, Galimidi RP, West AP, Jr, Bjorkman PJ, Wilen CB, Doms RW, O'Brien M, Bhardwaj N, Borrow P, Haynes BF, Muldoon M, Theiler JP, Korber B, Shaw GM, Hahn BH. 2013. Phenotypic properties of transmitted founder HIV-1. Proc Natl Acad Sci USA 110:6626 –6633.
18. Kmiec D, Iyer SS, Sturzel CM, Sauter D, Hahn BH, Kirchhoff F. 2016. Vpu-mediated counteraction of tetherin is a major determinant of HIV-1 interferon resistance. mBio 7:e00934 –16.
19. Iyer SS, Bibollet-Ruche F, Sherrill-Mix S, Learn GH, Plenderleith L, Smith AG, Barbian HJ, Russell RM, Gondim MV, Bahari CY, Shaw CM, Li Y, Decker T, Haynes BF, Shaw GM, Sharp PM, Borrow P, Hahn BH. 2017. Resistance to type 1 interferons is a major determinant of HIV-1 transmission fitness. Proc Natl Acad Sci USA 114:E590 –E599.
20. Sato K, Misawa N, Fukuhara M, Iwami S, An DS, Ito M, Koyanagi Y. 2012. Vpu augments the initial burst phase of HIV-1 propagation and downregulates BST2 and CD4 in humanized mice. J Virol 86:5000 –5013.
21. Guzzo C, Jung M, Graveline A, Banfield BW, Gee K. 2012. IL-27 increases BST-2 expression in human monocytes and T cells independently of type I IFN. Sci Rep 2:974.
22. Pflanz S, Hibbert L, Mattson J, Rosales R, Vaisberg E, Bazan JF, Phillips JH, McClanahan TK, de Waal Malefyt R, Kastelein RA. 2004. WSX-1 and glycoprotein 130 constitute a signal-transducing receptor for IL-27. J Immunol 172:2225–2231.
23. Owaki T, Asakawa M, Morishima N, Hata K, Fukai F, Matsui M, Mizuguchi J, Yoshimoto T. 2005. A role for IL-27 in early regulation of Th1 differentiation. J Immunol 175:2191–2200.

24. Imamichi T, Yang J, Huang DW, Brann TW, Fullmer BA, Adelsberger JW, Lempicki RA, Baseler MW, Lane HC. 2008. IL-27, a novel anti-HIV cytokine, activates multiple interferon-inducible genes in macrophages. AIDS 22: 39 – 45.
25. Greenwell-Wild T, Vazquez N, Jin W, Rangel Z, Munson PJ, Wahl SM. 2009. Interleukin-27 inhibition of HIV-1 involves an intermediate induction of type I interferon. Blood 114:1864 –1874.
26. Alsahafi N, Ding S, Richard J, Markle T, Brassard N, Walker B, Lewis GK, Kaufmann DE, Brockman MA, Finzi A. 2015. Nef proteins from HIV-1 elite controllers are inefficient at preventing antibody-dependent cellular cytotoxicity. J Virol 90:2993–3002.
27. Decker JM, Bibollet-Ruche F, Wei X, Wang S, Levy DN, Wang W, Delaporte E, Peeters M, Derdeyn CA, Allen S, Hunter E, Saag MS, Hoxie JA, Hahn BH, Kwong PD, Robinson JE, Shaw GM. 2005. Antigenic conservation and immunogenicity of the HIV coreceptor binding site. J Exp Med 201:1407–1419.
28. Melillo B, Liang S, Park J, Schon A, Courter JR, LaLonde JM, Wendler DJ, Princiotto AM, Seaman MS, Freire E, Sodroski J, Madani N, Hendrickson WA, Smith AB, III. 2016. Small-molecule CD4-mimics: structure-based optimization of HIV-1 entry inhibition. ACS Med Chem Lett 7:330 –334.
29. Pham TN, Lukhele S, Dallaire F, Perron G, Cohen EA. 2016. Enhancing virion tethering by BST2 sensitizes productively and latently HIV-infected T cells to ADCC mediated by broadly neutralizing antibodies. Sci Rep 6:37225.
30. Richard J, Veillette M, Ding S, Zoubchenok D, Alsahafi N, Coutu M, Brassard N, Park J, Courter JR, Melillo B, Smith AB, III, Shaw GM, Hahn BH, Sodroski J, Kaufmann DE, Finzi A. 2016. Small CD4 mimetics prevent HIV-1 uninfected bystander CD4 T cell killing mediated by antibody-dependent cell-mediated cytotoxicity. EBioMedicine 3:122–134.
31. Richard J, Veillette M, Batraville LA, Coutu M, Chapleau JP, Bonsignori M, Bernard N, Tremblay C, Roger M, Kaufmann DE, Finzi A. 2014. Flow cytometry-based assay to study HIV-1 gp120 specific antibody-dependent cellular cytotoxicity responses. J Virol Methods 208:107–114.
32. Alpert MD, Harvey JD, Lauer WA, Reeves RK, Piatak M, Jr, Carville A, Mansfield KG, Lifson JD, Li W, Desrosiers RC, Johnson RP, Evans DT. 2012. ADCC develops over time

during persistent infection with live-attenuated SIV and is associated with complete protection against SIV(mac)251 challenge. PLoS Pathog 8:e1002890.

33. Banks ND, Kinsey N, Clements J, Hildreth JE. 2002. Sustained antibodydependent cell-mediated cytotoxicity (ADCC) in SIV-infected macaques correlates with delayed progression to AIDS. AIDS Res Hum Retroviruses 18:1197–1205.
34. Baum LL, Cassutt KJ, Knigge K, Khattri R, Margolick J, Rinaldo C, Kleeberger CA, Nishanian P, Henrard DR, Phair J. 1996. HIV-1 gp120- specific antibody-dependent cell-mediated cytotoxicity correlates with rate of disease progression. J Immunol 157:2168 – 2173.
35. Chung AW, Isitman G, Navis M, Kramski M, Center RJ, Kent SJ, Stratov I. 2011. Immune escape from HIV-specific antibody-dependent cellular cytotoxicity (ADCC) pressure. Proc Natl Acad Sci USA 108:7505–7510.
36. Forthal DN, Landucci G, Haubrich R, Keenan B, Kuppermann BD, Tilles JG, Kaplan J. 1999. Antibody-dependent cellular cytotoxicity independently predicts survival in severely immunocompromised human immunodeficiency virus-infected patients. J Infect Dis 180:1338 –1341.
37. Mabuka J, Nduati R, Odem-Davis K, Peterson D, Overbaugh J. 2012. HIV-specific antibodies capable of ADCC are common in breastmilk and are associated with reduced risk of transmission in women with high viral loads. PLoS Pathog 8:e1002739.
38. Sun Y, Asmal M, Lane S, Permar SR, Schmidt SD, Mascola JR, Letvin NL. 2011. Antibody-dependent cell-mediated cytotoxicity in simian immunodeficiency virus-infected rhesus monkeys. J Virol 85:6906 – 6912.
39. Williams KL, Cortez V, Dingens AS, Gach JS, Rainwater S, Weis JF, Chen X, Spearman P, Forthal DN, Overbaugh J. 2015. HIV-specific CD4-induced antibodies mediate broad and potent antibody-dependent cellular cytotoxicity activity and are commonly detected in plasma from HIVinfected humans. EBioMedicine 2:1464 –1477.
40. Lewis GK, Pazgier M, Evans D, Ferrari G, Bournazos S, Parsons MS, Bernard NF, Finzi A. 2017. Beyond viral neutralization. AIDS Res Hum Retroviruses 33:760-764.
41. Haynes BF, Gilbert PB, McElrath MJ, Zolla-Pazner S, Tomaras GD, Alam SM, Evans DT, Montefiori DC, Karnasuta C, Sutthent R, Liao HX, DeVico AL, Lewis GK, Williams C, Pinter A, Fong Y, Janes H, DeCamp A, Huang Y, Rao M, Billings E, Karasavvas N, Robb

ML, Ngauy V, de Souza MS, Paris R, Ferrari G, Bailer RT, Soderberg KA, Andrews C, Berman PW, Frahm N, De Rosa SC, Alpert MD, Yates NL, Shen X, Koup RA, Pitisuttithum P, Kaewkungwal J, Nitayaphan S, Rerks-Ngarm S, Michael NL, Kim JH. 2012. Immune-correlates analysis of an HIV-1 vaccine efficacy trial. N Engl J Med 366:1275–1286.

42. Bonsignori M, Pollara J, Moody MA, Alpert MD, Chen X, Hwang KK, Gilbert PB, Huang Y, Gurley TC, Kozink DM, Marshall DJ, Whitesides JF, Tsao CY, Kaewkungwal J, Nitayaphan S, Pitisuttithum P, Rerks-Ngarm S, Kim JH, Michael NL, Tomaras GD, Montefiori DC, Lewis GK, Devico A, Evans DT, Ferrari G, Liao HX, Haynes BF. 2012. Antibody-dependent cellular cytotoxicity-mediating antibodies from an HIV-1 vaccine efficacy trial target multiple epitopes and preferentially use the VH1 gene family. J Virol 86:11521–11532.
43. Ferrari G, Pollara J, Kozink D, Harms T, Drinker M, Freel S, Moody MA, Alam SM, Tomaras GD, Ochsenbauer C, Kappes JC, Shaw GM, Hoxie JA, Robinson JE, Haynes BF. 2011. An HIV-1 gp120 envelope human monoclonal antibody that recognizes a C1 conformational epitope mediates potent antibody-dependent cellular cytotoxicity (ADCC) activity and defines a common ADCC epitope in human HIV-1 serum. J Virol 85: 7029 – 7036.
44. Mengistu M, Ray K, Lewis GK, DeVico AL. 2015. Antigenic properties of the human immunodeficiency virus envelope glycoprotein gp120 on virions bound to target cells. PLoS Pathog 11:e1004772.
45. Guan Y, Pazgier M, Sajadi MM, Kamin-Lewis R, Al-Darmarki S, Flinko R, Lovo E, Wu X, Robinson JE, Seaman MS, Fouts TR, Gallo RC, DeVico AL, Lewis GK. 2013. Diverse specificity and effector function among human antibodies to HIV-1 envelope glycoprotein epitopes exposed by CD4 binding. Proc Natl Acad Sci USA 110:E69 –E78.
46. Bruel T, Guivel-Benhassine F, Lorin V, Lortat-Jacob H, Baleux F, Bourdic K, Noel N, Lambotte O, Mouquet H, Schwartz O. 25 January 2017. Lack of ADCC breadth of human non-neutralizing anti-HIV-1 antibodies. J Virol 91:e02440-16.
47. Lavender KJ, Gibbert K, Peterson KE, Van Dis E, Francois S, Woods T, Messer RJ, Gawanbacht A, Muller JA, Munch J, Phillips K, Race B, Harper MS, Guo K, Lee EJ, Trilling M, Hengel H, Piehler J, Verheyen J, Wilson CC, Santiago ML, Hasenkrug KJ,

Dittmer U. 2016. Interferon alpha subtype-specific suppression of HIV-1 infection in vivo. J Virol 90:6001– 6013.

48. Harper MS, Guo K, Gibbert K, Lee EJ, Dillon SM, Barrett BS, McCarter MD, Hasenkrug KJ, Dittmer U, Wilson CC, Santiago ML. 2015. Interferon-alpha subtypes in an ex vivo model of acute HIV-1 infection: expression, potency and effector mechanisms. PLoS Pathog 11:e1005254.
49. Ding S, Verly MM, Princiotto A, Melillo B, Moody AM, Bradley T, Easterhoff D, Roger M, Hahn BH, Madani N, Smith AB, III, Haynes BF, Sodroski JMD, Finzi A. 19 December 2016. Small-molecule CD4 mimetics sensitize HIV-1-infected cells to antibody-dependent cellular cytotoxicity by antibodies elicited by multiple envelope glycoprotein immunogens in nonhuman primates. AIDS Res Hum Retroviruses 33:428-431
50. Veazey RS, Pilch-Cooper HA, Hope TJ, Alter G, Carias AM, Sips M, Wang X, Rodriguez B, Sieg SF, Reich A, Wilkinson P, Cameron MJ, Lederman MM. 2016. Prevention of SHIV transmission by topical IFN-beta treatment. Mucosal Immunol 9:1528 –1536.
51. Sandler NG, Bosinger SE, Estes JD, Zhu RT, Tharp GK, Boritz E, Levin D, Wijeyesinghe S, Makamdop KN, del Prete GQ, Hill BJ, Timmer JK, Reiss E, Yarden G, Darko S, Contijoch E, Todd JP, Silvestri G, Nason M, Norgren RB, Jr, Keele BF, Rao S, Langer JA, Lifson JD, Schreiber G, Douek DC. 2014. Type I interferon responses in rhesus macaques prevent SIV infection and slow disease progression. Nature 511:601– 605.
52. Richard J, Sindhu S, Pham TN, Belzile JP, Cohen EA. 2010. HIV-1 Vpr up-regulates expression of ligands for the activating NKG2D receptor and promotes NK cell-mediated killing. Blood 115:1354 –1363.
53. Fontaine J, Chagnon-Choquet J, Valcke HS, Poudrier J, Roger M, Montreal Primary HIV Infection and Long-Term Non-Progressor Study Groups. 2011. High expression levels of B lymphocyte stimulator (BLyS) by dendritic cells correlate with HIV-related B-cell disease progression in humans. Blood 117:145–155.
54. Fontaine J, Coutlee F, Tremblay C, Routy JP, Poudrier J, Roger M, Montreal Primary HIV Infection and Long-Term Non-progressor Study Groups. 2009. HIV infection affects blood myeloid dendritic cells after successful therapy and despite non-progressing clinical disease. J Infect Dis 199:1007–1018.

55. Peretz Y, Ndongala ML, Boulet S, Boulassel MR, Rouleau D, Cote P, Longpre D, Routy JP, Falutz J, Tremblay C, Tsoukas CM, Sekaly RP, Bernard NF. 2007. Functional T cell subsets contribute differentially to HIV peptide-specific responses within infected individuals: correlation of these functional T cell subsets with markers of disease progression. Clin Immunol 124:57– 68.
56. Kamya P, Boulet S, Tsoukas CM, Routy JP, Thomas R, Cote P, Boulassel MR, Baril JG, Kovacs C, Migueles SA, Connors M, Suscovich TJ, Brander C, Tremblay CL, Bernard N, Canadian Cohort of HIV Infected Slow Progressors. 2011. Receptor-ligand requirements for increased NK cell polyfunctional potential in slow progressors infected with HIV-1 coexpressing KIR3DL1*h/*y and HLA-B*57. J Virol 85:5949 –5960.
57. International HIV Controllers Study, Pereyra F, Jia X, McLaren PJ, Telenti A, de Bakker PI, Walker BD, Ripke S, Brumme CJ, Pulit SL, Carrington M, Kadie CM, Carlson JM, Heckerman D, Graham RR, Plenge RM, Deeks SG, Gianniny L, Crawford G, Sullivan J, Gonzalez E, Davies L, Camargo A, Moore JM, Beattie N, Gupta S, Crenshaw A, Burtt NP, Guiducci C, Gupta N, Gao X, Qi Y, Yuki Y, Piechocka-Trocha A, Cutrell E, Rosenberg R, Moss KL, Lemay P, O'Leary J, Schaefer T, Verma P, Toth I, Block B, Baker B, Rothchild A, Lian J, Proudfoot J, Alvino DM, Vine S, Addo MM, Allen TM, et al. 2010. The major genetic determinants of HIV-1 control affect HLA class I peptide presentation. Science 330:1551–1557.
58. Ochsenbauer C, Edmonds TG, Ding H, Keele BF, Decker J, Salazar MG, Salazar-Gonzalez JF, Shattock R, Haynes BF, Shaw GM, Hahn BH, Kappes JC. 2012. Generation of transmitted/founder HIV-1 infectious molecular clones and characterization of their replication capacity in CD4 T lymphocytes and monocyte-derived macrophages. J Virol 86:2715–2728.
59. Bar KJ, Tsao CY, Iyer SS, Decker JM, Yang Y, Bonsignori M, Chen X, Hwang KK, Montefiori DC, Liao HX, Hraber P, Fischer W, Li H, Wang S, Sterrett S, Keele BF, Ganusov VV, Perelson AS, Korber BT, Georgiev I, McLellan JS, Pavlicek JW, Gao F, Haynes BF, Hahn BH, Kwong PD, Shaw GM. 2012. Early low-titer neutralizing antibodies impede HIV-1 replication and select for virus escape. PLoS Pathog 8:e1002721.
60. Fenton-May AE, Dibben O, Emmerich T, Ding H, Pfafferott K, Aasa-Chapman MM, Pellegrino P, Williams I, Cohen MS, Gao F, Shaw GM, Hahn BH, Ochsenbauer C, Kappes JC, Borrow P. 2013. Relative resistance of HIV-1 founder viruses to control by interferon-alpha. Retrovirology 10: 146.

6.3.10 FIGURES

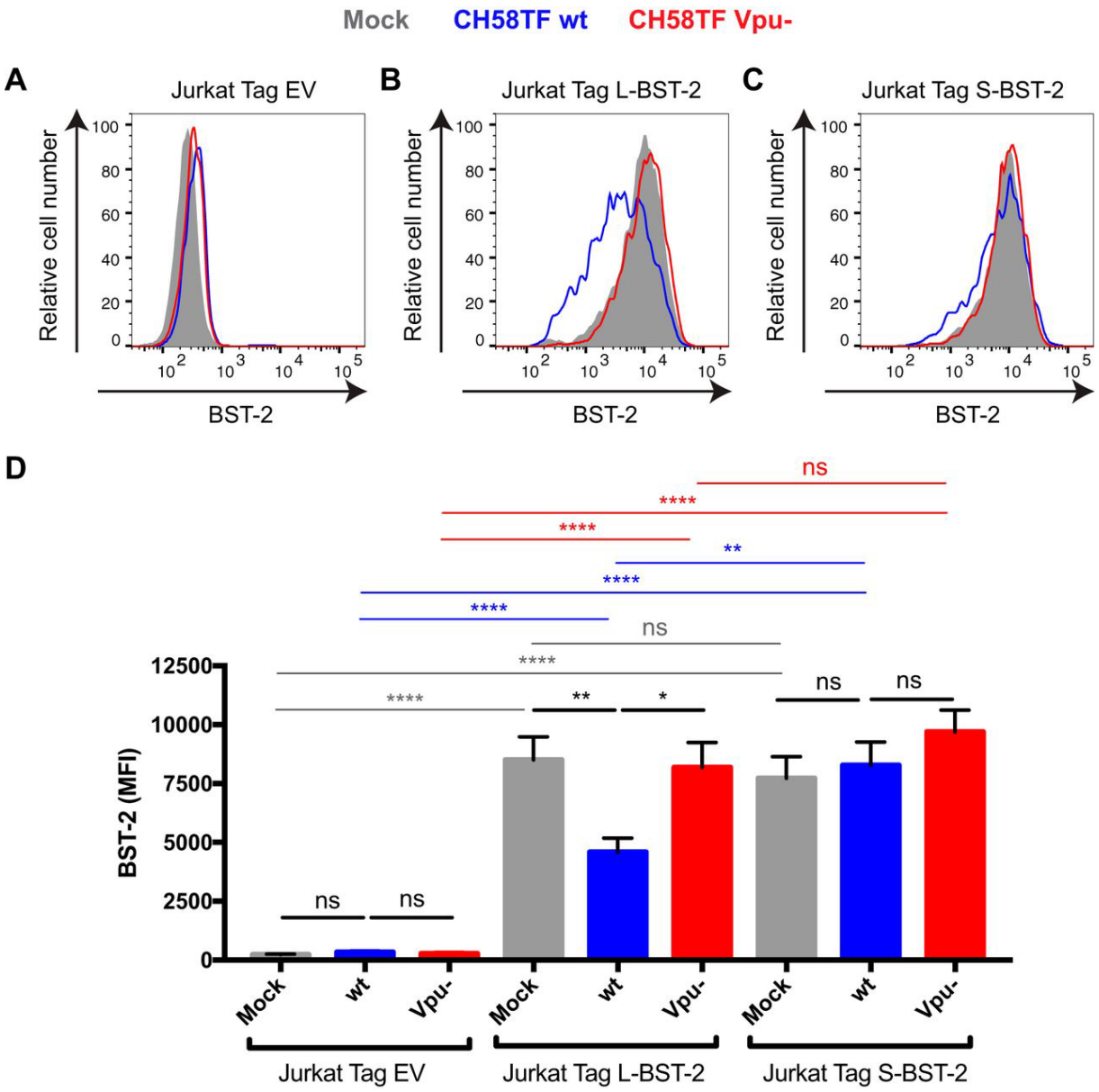

Figure 6.2.1 - Differential sensitivity of BST-2 isoforms to HIV-1 Vpu in Jurkat cell lines. Jurkat Tag cells (**A and D**) expressing no BST-2 (Jurkat Tag EV [empty vector]) or stably expressing the L-BST-2 (**B and D**) or S-BST-2 (**C and D**) were mock infected or infected with the transmitted/founder virus HIV-1 CH58 (CH58TF) expressing Vpu (wild-type CH58TF [CH58TF wt]) or not expressing Vpu (CH58TF Vpu^{-}). Forty-eight hours post-infection, cells were stained with anti-BST-2 Ab, followed with appropriate secondary Abs. (**A to C**) Histograms depicting representative staining; (**D**) mean fluorescence intensity (MFI) obtained in at least six independent experiments. Values are means +/- standard error of the means (SEM) (error bars). Statistical significance was tested using an unpaired t test (*, $P < 0.05$; **, $P < 0.01$, ****, $P < 0.0001$; ns, nonsignificant).

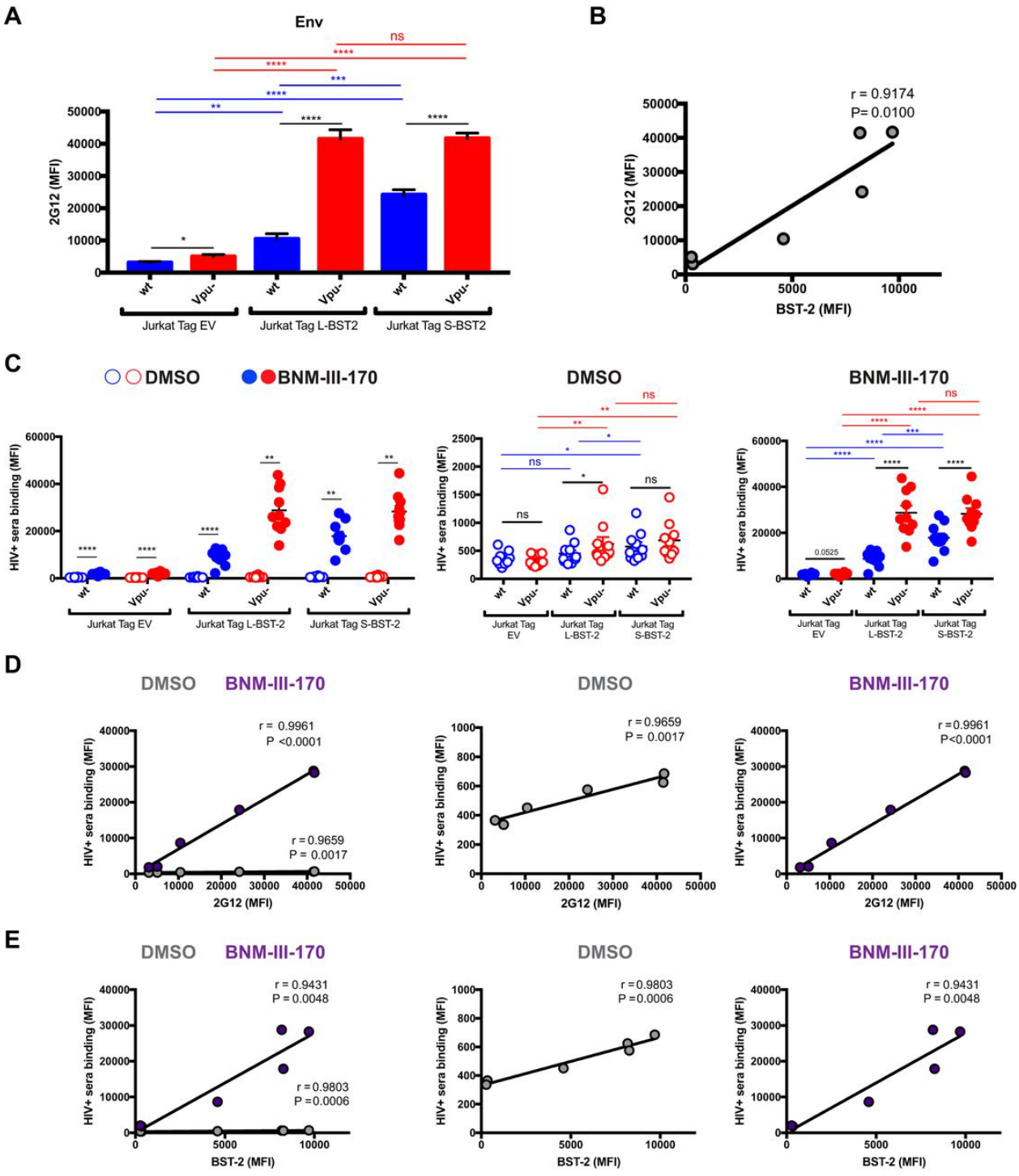
A
Env
2G12 (MFI)
wt
Vpu-
Jurkat Tag EV
Jurkat Tag L-BST2
Jurkat Tag S-BST2
B
r = 0.9174
P= 0.0100
2G12 (MFI)
BST-2 (MFI)
C
DMSO
BNM-III-170
HIV+ sera binding (MFI)
Jurkat Tag EV
Jurkat Tag L-BST-2
Jurkat Tag S-BST-2
0.0525
D
DMSO
BNM-III-170
r = 0.9961
P <0.0001
r = 0.9659
P = 0.0017
r = 0.9659
P = 0.0017
r = 0.9961
P<0.0001
2G12 (MFI)
E
DMSO
BNM-III-170
r = 0.9431
P = 0.0048
r = 0.9803
P =0.0006
r = 0.9803
P =0.0006
r = 0.9431
P = 0.0048
BST-2 (MFI)

Figure 6.2.2 - BST-2 expression correlates with cell surface Env level and recognition of HIV-1-infected cells by HIV$^+$ sera.
Jurkat Tag cells expressing no BST-2 (Jurkat Tag EV [empty vector]) or stably expressing L-BST-2 or S-BST-2 were mock infected or infected with the transmitted/founder virus HIV-1 CH58 (CH58 T/F) expressing Vpu (wild-type CH58 T/F [wt]) or not expressing Vpu (Vpu$^-$). Forty-eight hours post-infection, cells were stained with the anti-Env Ab 2G12 (**A and B**) or with sera from 10 HIV-1-infected individuals (**C**) in the presence of the CD4mc BNM-III-170 (50 μM) or equivalent volume of DMSO, followed with appropriate secondary Abs. (**A**) Mean fluorescence intensity (MFI) of 2G12 binding obtained in at least six independent experiments; (**B**) correlation between 2G12 binding and BST-2 level. (**C**) MFIs obtained with all the different sera in the presence of CD4mc BNM-III-170 or DMSO; (**D and E**) correlation between HIV$^+$ serum binding and 2G12 level or BST-2 level, respectively, in the presence of 50 μM CD4mc BNM-III-170 or DMSO. Values are means +/- standard error of the means (SEM) (error bars). Statistical significance was tested using an unpaired t test (**A**), a Pearson correlation test (**B, D, and E**), or a paired t test or Wilcoxon matched-pair signed-rank test based on statistical normality (**C**) (*, $P < 0.05$; **, $P < 0.01$, ***, $P < 0.001$; ****, $P < 0.0001$; ns, nonsignificant).

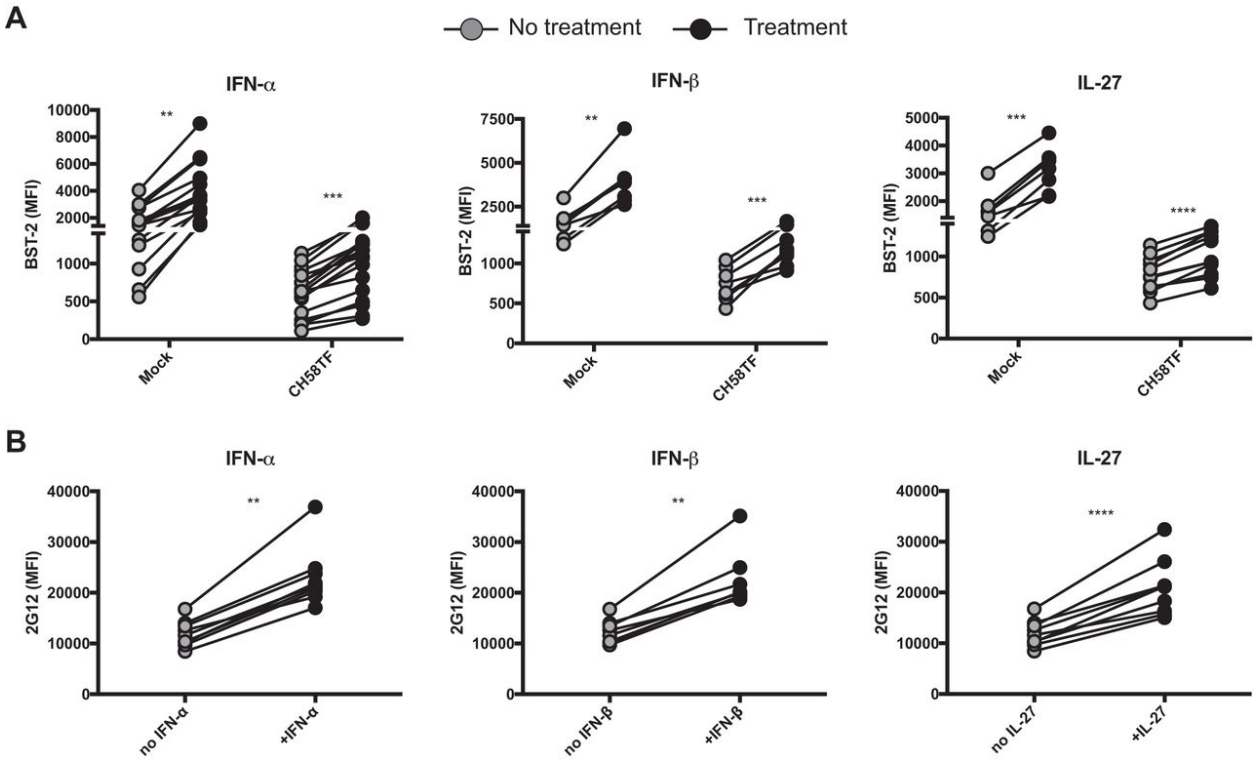

Figure 6.2.3 - Treatment with type I IFNs or IL-27 enhances Env levels on the surface of HIV-1-infected cells through BST-2 upregulation.

Primary $CD4^+$ T cells were mock infected or infected with the transmitted/founder virus CH58 (CH58TF) and either treated for 24 h with type I IFNs (IFN-α and IFN-β) or IL-27 or not treated. Forty-eight hours post-infection, cells were stained with anti-BST-2 Ab (**A**) or anti-Env Ab 2G12 (**B**), followed with appropriate secondary Abs. The graphs shown represent the mean fluorescence intensities obtained for at least eight independent experiments. Statistical significance was tested using a paired t test or Wilcoxon matched-pair signed-rank test based on statistical normality (**, $P < 0.01$; ***, $P < 0.001$; ****, $P < 0.0001$).

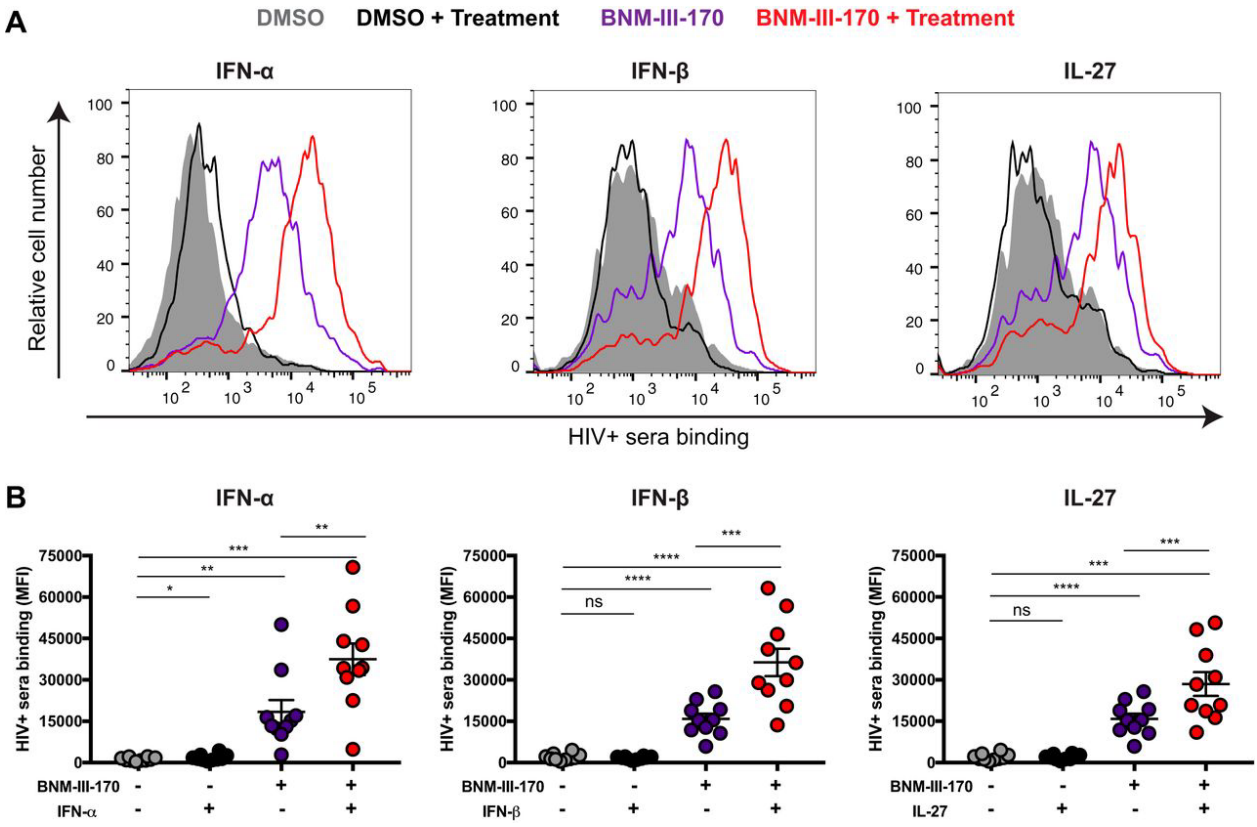

Figure 6.2.4 - Treatment with type I IFN or IL-27 enhances recognition of HIV-1-infected cells by sera from HIV-1-infected individuals in the presence of CD4mc.
Primary $CD4^+$ T cells were mock-infected or infected with the transmitted/founder virus HIV-1 CH58 (CH58 T/F) and either treated for 24 h with type I IFNs (IFN-α and IFN-β) or IL-27 or not treated. Forty-eight hours post-infection, cells were stained with sera from 10 HIV-1-infected individuals in the presence of the CD4mc BNM-III-170 (50 µM) or an equivalent volume of DMSO, followed with appropriate secondary Abs. (**A**) Histograms depicting representative staining; (**B**) mean fluorescence intensities (MFI) obtained with all the different sera. Values are means +/- standard error of the means (SEM) (error bars). Statistical significance was tested using a paired t test or Wilcoxon matched-pair signed-rank test based on statistical normality (*, $P < 0.05$; **, $P < 0.01$, ***, $P < 0.001$; ****, $P < 0.0001$; ns, nonsignificant).

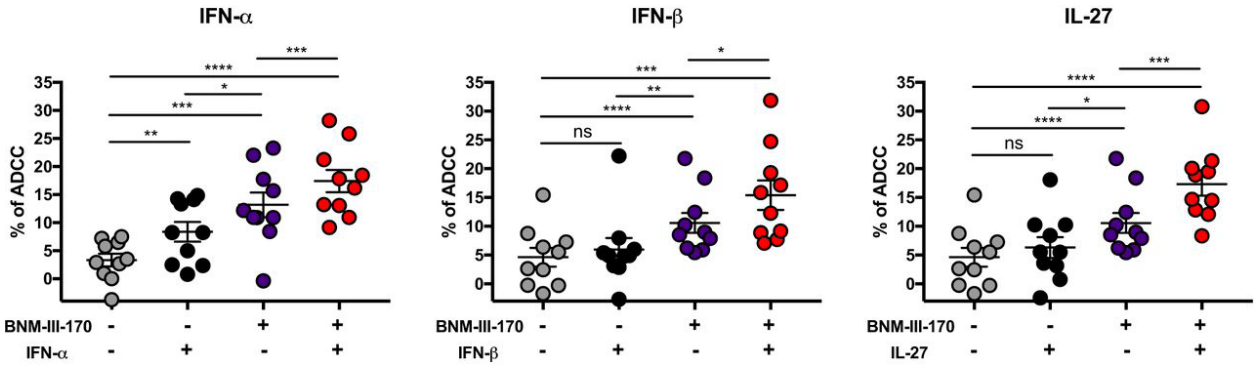

Figure 6.2.5 - Treatment with type I IFNs or IL-27 boosts CD4mc sensitization of HIV-1-infected cells to ADCC.

Primary $CD4^+$ T cells infected with the transmitted/founder virus CH58 (CH58 T/F), either treated for 24 h with type I IFNs (IFN-α and IFN-β) or IL-27 or not treated, were used as target cells, and autologous PBMCs were used as effector cells in our FACS-based ADCC assay. Shown are the percentages of ADCC-mediated killing obtained with sera from 10 HIV-1-infected individuals in the presence of the CD4mc BNM-III-170 (50 μM) or an equivalent volume of DMSO. Values are means +/- standard error of the means (SEM) (error bars). Statistical significance was tested using a paired t test or Wilcoxon matched-pair signed-rank test based on statistical normality (*, $P < 0.05$; **, $P < 0.01$, ***, $P < 0.001$; ****, $P < 0.0001$; ns, nonsignificant).

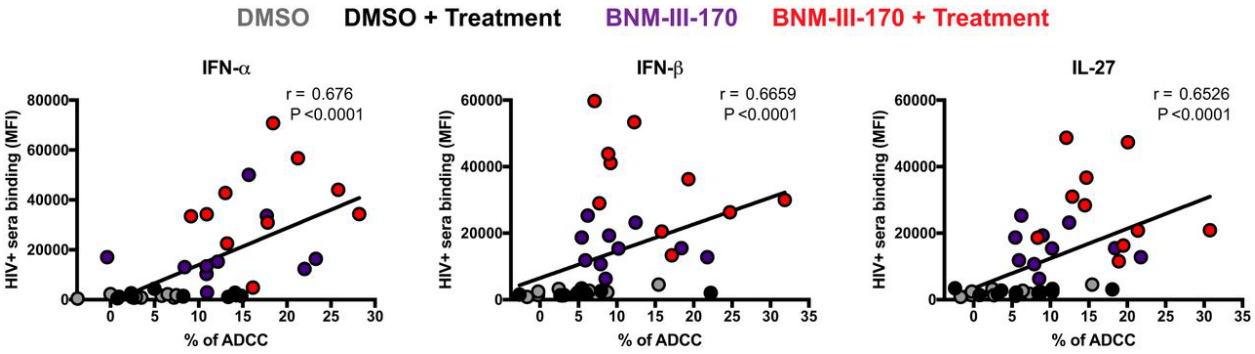

Figure 6.2.6 - Enhanced recognition of HIV-1-infected cells positively correlates with enhanced ADCC responses.

A positive correlation was observed between the recognition of primary $CD4^+$ T cells infected with the transmitted/founder virus CH58 (CH58 T/F) by HIV^+ sera and their ability to mediate an ADCC response. The correlations obtained for the different treatments (IFN-α, IFN-β, or IL-27) are shown. Statistical analysis was tested utilizing a Spearman rank correlation.

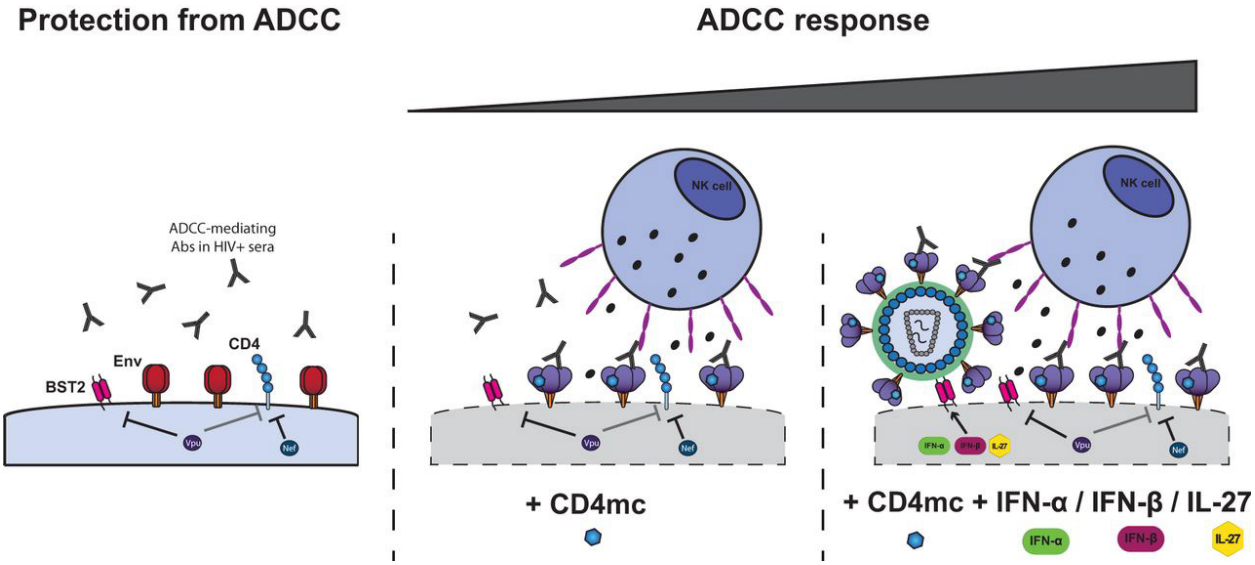

Figure 6.2.7 - Env conformation and its accumulation at the cell surface dictates sensitivity of HIV-1-infected cells to ADCC.

ADCC-mediating Abs present in sera from HIV-1-infected individuals preferentially recognize Env in its CD4-bound conformation (1). To limit the exposure of this conformation, HIV-1 has evolved sophisticated mechanisms to counteract the host restriction factor BST-2 with the viral Vpu protein (7–9) and to downregulate CD4 by Nef and Vpu (7). Nef and Vpu decrease the accumulation of Env and its interaction with CD4 at the cell surface, two factors that determine the susceptibility of HIV-1-infected cells to ADCC. Small CD4 mimetics sensitize HIV-1-infected cells to ADCC mediated by HIV^+ sera by forcing Env to sample its CD4-bound conformation (5). Type I IFNs or IL-27 treatment, through upregulation of BST-2 despite Vpu activity, boosts the ability of CD4mc by increasing the amounts of CD4mc-sensitized Env available on the cell surface.

CHAPITRE VII - DISCUSSION ET PERSPECTIVES

Malgré les nombreux mécanismes connus du VIH-1 pour évader la réponse humorale non-neutralisante, un pan de la littérature suggère que les nnAbs peuvent jouer un rôle important dans l'élimination des cellules infectées par le VIH-1, affectant ainsi l'efficacité de la transmission, la réplication virale et la progression de la maladie. Les travaux présentés dans cette thèse avaient pour objectif général de caractériser en détail les différents déterminants viraux et cellulaires agissants sur la conformation d'Env et sur la susceptibilité des cellules infectées à la réponse ADCC médiée par les nnAbs afin de déterminer leur utilité dans l'élaboration de vaccins pour limiter l'acquisition du virus ou d'immunothérapies à base d'anticorps dans le but d'une guérison fonctionnelle. Les résultats présentés dans le cadre des précédents chapitres nous ont permis de faire la lumière sur ces divergences théoriques par l'identification de biais expérimentaux et de particularités propres à certaines souches virales. Ces informations ont été utilisées afin d'optimiser des stratégies permettant d'augmenter l'activité antivirale des nnAbs dans le cadre d'approches thérapeutiques innovantes visant l'éradication des réservoirs viraux.

7.1 Contributions majeures de cette thèse

L'objectif du **chapitre III** était de déterminer les manières les plus adéquates de quantifier la réponse ADCC dirigée contre les cellules infectées. Pour ce faire, il semble plus qu'important de connaître la conformation d'Env exposée à la surface des cellules cibles, d'identifier clairement les populations cellulaires à cibler et de s'assurer que le virus utilisé soit pleinement infectieux puisque ces paramètres dicteront la reconnaissance antigénique. Nous avons identifié un nombre important de biais inhérents à certaines techniques d'ADCC pouvant altérer l'interprétation et la pertinence biologique des résultats obtenus. En effet, certaines méthodes quantifient principalement la réponse ADCC dirigée contre les cellules non-infectées recouvertes de gp120 monomérique soluble et potentiellement de particules virales (**article 2**). Ces systèmes ne sont pas représentatifs de la réponse anticorps dirigée contre les cellules productivement infectées puisqu'Env se lie au CD4 et adopte sa conformation « ouverte », ce qui amène à surestimer la réponse ADCC médiée par les nnAbs et sous-estimer celle médiée par les bNAbs. Les techniques spécifiques aux cellules infectées peuvent également surestimer la réponse ADCC médiée par les nnAbs lorsque la construction virale (IMC) utilisée est incapable d'induire une suppression complète des niveaux de surface de CD4 et de BST-2 (**article 3**). L'utilisation d'IMC du VIH-1 comportant un gène rapporteur comme celui de la luciférase est envisageable dans le contexte où

l'expression de Nef et Vpu demeure similaire aux niveaux d'expression des virus de type sauvage. À cet effet, le nouveau marquage intracellulaire développé dans l'**article 4** représente un outil pratique permettant de confirmer que ces deux protéines accessoires soient exprimées à des niveaux physiologiques.

Le **chapitre IV** avait pour but d'identifier les déterminants structuraux d'Env, qu'ils soient hautement conservés ou polymorphiques, affectant sa conformation et l'élimination des cellules infectées par les nnAbs présents chez les individus infectés ou vaccinés. En utilisant une technique d'ADCC spécifique aux cellules infectées, nous avons démontré qu'en plus de réguler négativement l'expression de CD4 à la surface des cellules infectées, le VIH-1 se doit de garder l'Env non-liée dans sa conformation « fermée » afin de protéger les cellules infectées de la réponse ADCC médiée par les nnAbs (**Figure 7.1 - panel du haut**). En effet, la substitution de résidus hautement conservés de la cavité Phe43 dans le site d'interaction à CD4 (S375), du domaine d'association du trimère (L193) ou du site de clivage de la furine (R508/R511) favorise les transitions vers la conformation « ouverte » et augmente la susceptibilité aux activités effectrices du sérum VIH^{+}. Parmi ceux-ci, le résidu 375 a la particularité d'être conservé à travers la majorité des clades prédominants du VIH-1 à l'exception des souches CRF01_AE. En effet, un polymorphisme naturel est présent chez le sous-type CRF01_AE (H375), ce qui accroît la reconnaissance et l'élimination des cellules infectées par les nnAbs par rapport aux autres sous-types. Ceci suggère que le clade CRF01_AE pourrait être plus sensible à des interventions vaccinales ou thérapeutiques dépendant des réponses non-neutralisantes.

Comme la conformation d'Env n'est pas le seul facteur impliqué dans la susceptibilité des cellules infectées à la réponse humorale, l'objectif du **chapitre V** était de déterminer les déterminants fonctionnels de Vpu jouant un rôle dans l'évasion de la réponse ADCC. Vpu est une petite protéine multifonctionnelle capable de cibler une grande variété de protéines cellulaires par leur séquestration dans des compartiments périnucléaires des voies de sécrétion et par la dégradation de certains de ses substrats. Nous montrons que la capacité de Vpu à cibler simultanément les protéines NTB-A et PVR, en plus de CD4 et BST-2, permet de protéger efficacement les cellules infectées de la réponse ADCC médiée par les nnAbs et de limiter l'activité effectrice Fc-dépendante des bNAbs (**Figure 7.1 - panel du milieu**). Leurs récepteurs

respectifs (NTB-A et DNAM-1) présents à la surface des cellules NK peuvent agir à titre de corécepteurs dans l'activation des fonctions effectrices par le récepteur Fc CD16. La présence d'IFN-I débalance la polyfonctionnalité de Vpu en augmentant BST-2, qui est préférentiellement ciblé par rapport à NTB-A et PVR, ce qui augmente l'élimination des cellules infectées par les anticorps dirigés contre Env. Nous démontrons également que l'importance de Vpu pour la réplication du VIH-1 *in vivo* va au-delà de sa capacité à augmenter la relâche et l'infectivité des particules virales. En effet, l'absence de Vpu rend la réplication du virus sous-optimale en présence de nnAbs, du moins pendant la phase aiguë de l'infection. L'utilisation de stratégies affectant ou contournant la polyfonctionnalité de Vpu semble être importante pour exploiter l'activité antivirale des nnAbs.

Comme Env, Nef et Vpu agissent de concert afin de garder Env dans sa conformation « fermée » et de limiter son expression de surface, le but du **chapitre VI** était d'optimiser de nouvelles approches expérimentales utilisant des CD4mc afin d'exploiter les activités antivirales des nnAbs. Pour ce faire, nous avons caractérisé la contribution de certains résidus polymorphiques d'Env, présents naturellement chez certaines souches, affectant sa sensibilité au CD4mc afin d'informer le développement de molécules plus puissantes et à plus large spectre (**Figure 7.1 - panel du bas**). Nous avons identifié des résidus polymorphiques à l'intérieur et au pourtour de la cavité Phe43, où le CD4mc s'insère. Entre autres, le clade CRF01_AE est complètement résistant au CD4mc grâce notamment au résidu H375, tandis qu'une certaine proportion des isolats des clades prédominants (A, B et C) possède un résidu T375 les rendant particulièrement sensibles au CD4mc et ainsi à l'élimination des cellules infectées par les nnAbs. Nous avons également montré qu'il est possible d'améliorer la capacité du cocktail combinant CD4mc et nnAbs à cibler les cellules infectées en augmentant les niveaux d'Env présents à leur surface à l'aide de cytokines comme les IFN-I ou l'IL-27. La combinaison de stratégies affectant la conformation d'Env, la polyfonctionnalité de Vpu et le recrutement des cellules effectrices pourrait s'avérer utile dans le cadre d'immunothérapies à base de nnAbs pour éliminer les réservoirs du VIH-1.

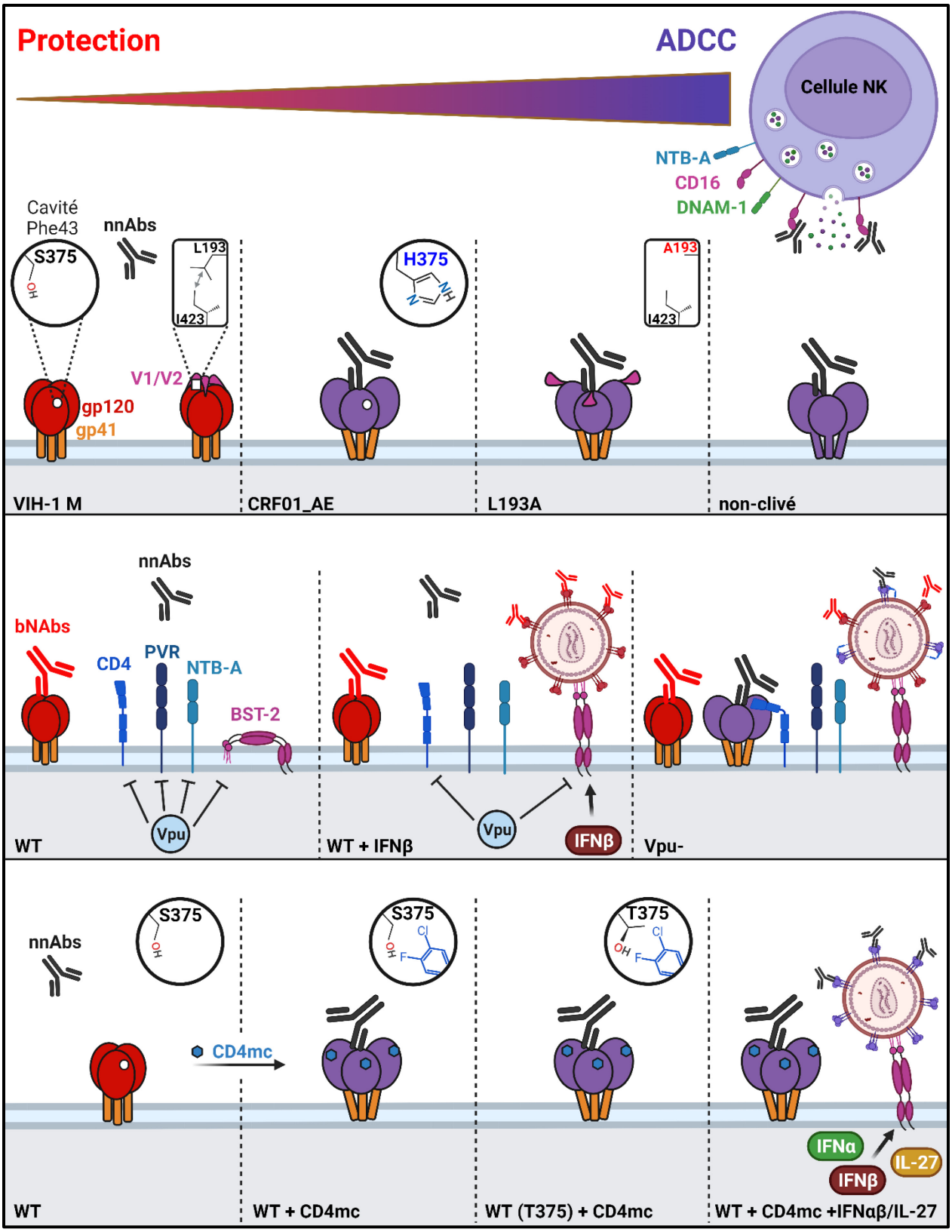
Protection
ADCC
Cellule NK
NTB-A
CD16
DNAM-1
Cavité
Phe43
nnAbs
S375
L193
I423
H375
A193
I423
V1/V2
gp120
gp41
VIH-1 M
CRF01_AE
L193A
non-clivé
nnAbs
bNAbs
CD4
PVR
NTB-A
BST-2
Vpu
WT
WT + IFNβ
Vpu
IFNβ
Vpu-
nnAbs
S375
S375
T375
CD4mc
WT
WT + CD4mc
WT (T375) + CD4mc
IFNα
IL-27
IFNβ
WT + CD4mc +IFNαβ/IL-27

Figure 7.1 - Contributions majeures de cette thèse.
Vue d'ensemble des principales contributions de cette thèse à la compréhension de la susceptibilité des cellules infectées à la réponse ADCC. (**Panel du haut**) Plusieurs éléments conservées de l'Env du VIH-1 contribuent à stabiliser sa conformation « fermée », notamment la cavité Phe43, le domaine d'association du trimère et le site de clivage de la furine. L'altération d'un de ces éléments permet d'exposer Env dans sa conformation « ouverte », ce qui rend les cellules infectées susceptibles à la réponse ADCC médiée par les nnAbs présents dans le sérum VIH^{+}. (**Panel du milieu**) La protéine accessoire Vpu cible CD4, PVR, NTB-A et BST-2 de manière simultanée, permettant d'évader l'ADCC médiée par les nnAbs et de diminuer l'ADCC médiée par les bNAbs. L'augmentation de BST-2 par les IFN-I diminue la polyfonctionnalité de Vpu en compétitionnant pour l'interaction avec son domaine transmembranaire, ce qui empêche la régulation négative de PVR et NTB-A. L'absence de Vpu rend les cellules infectées hypersensibles à l'ADCC médiée par les nnAbs et bNAbs. (**Panel du bas**) Les CD4mc peuvent être utilisés pour « ouvrir » Env et diriger la réponse ADCC médiée contre les cellules infectées. Des polymorphismes naturels à l'intérieur ou au pourtour de la cavité Phe43 modulent la sensibilité d'Env pour les CD4mc. La régulation positive de BST-2 par les IFN-I ou l'IL-27 permet d'augmenter la capacité des CD4mc à induire une réponse ADCC médiée par les nnAbs contre les cellules infectées. ADCC : Cytotoxicité cellulaire dépendante des anticorps; nnAbs : anticorps non-neutralisants; VIH-1 M : groupe M du VIH-1; bNAbs : anticorps neutralisants à large spectre; WT : virus de type sauvage; IFN :interféron; CD4mc: mimétique moléculaire de CD4. Diagramme créé avec BioRender.com.

7.2 Implications pour l'évasion des fonctions effectrices immunitaires

Le VIH-1 utilise une variété de stratégies pour protéger les cellules infectées des fonctions effectrices médiées par les anticorps ciblant Env, notamment en masquant des épitopes conformationnels hautement conservés et en réduisant la quantité d'Env accessible à la surface des cellules. Les présents travaux aident à mieux comprendre les résultats divergents dans la littérature et proposent un modèle unificateur postulant que la conformation d'Env est le principal facteur limitant la réponse humorale non-neutralisante, telle que dictée par ses propriétés intrinsèques (**articles 5, 6 et 7**) et son interaction avec CD4 (**articles 3, 4 et 9**). Ces résultats aident à comprendre pourquoi les isolats de laboratoire classifiés dans le tiers 1 (par exemple : HXB2, NL4-3, Ba-L, SF162, 89.6) sont particulièrement sensibles à la réponse ADCC médiée par les nnAbs comparativement aux isolats primaires de tiers 2 et 3 (1241, 1435, 1438). Il faut savoir que les virus adaptés en laboratoire sont généralement isolés à partir d'échantillons biologiques prélevés chez des patients dans la phase SIDA et sont subséquemment mis en culture *in vitro* pendant plusieurs semaines (37, 1439-1442), ce qui suggère qu'ils ont évolué en absence d'une pression immunitaire humorale adéquate autant *in vivo* qu'*in vitro*. Ainsi, il a été démontré que l'Env de

ces souches présente une propension plus grande à adopter la conformation « ouverte » par rapport à la majorité des souches en circulation (217, 218), qui s'accompagne occasionnellement de la délétion ou de l'atténuation des fonctions de certaines protéines accessoires comme Nef et Vpu (37, 1443-1446). La sensibilité accrue des souches de VIH-1 du tiers 1 à la réponse ADCC médiée par les nnAbs n'est donc pas représentative des quasi-espèces retrouvées chez les individus infectés, ce qui plaide en faveur de l'utilisation de souches de type sauvage de tiers 2 et 3 possédant une pertinence biologique comme les souches T/F ou les souches responsables du rebond viral à la suite de l'interruption du traitement ART (789, 1003). À cet effet, nous montrons qu'il est possible d'induire un phénotype semblable aux virus du tiers 1 chez des souches T/F du tiers 2 en mutant des résidus clés d'Env (**articles 5, 6 et 7**), en bloquant l'expression de Nef et/ou Vpu (**articles 2, 3, 4 et 9**) ou en utilisant des petites molécules mimant CD4 (**articles 10 et 11**).

La conformation « fermée » du trimère d'Env peut être déstabilisée aisément lorsqu'on introduit des substitutions dans ses domaines structuraux conservés. Entre autres, on y retrouve le domaine d'association du trimère qui est situé à l'apex des protomères de gp120 et qui joue un rôle prépondérant dans l'intégrité du trimère d'Env. Cette structure est composée des boucles V1/V2, V3 et β20-β21, qui forment des interactions intra- et inter-protomères stabilisées via d'imposants clusters de résidus hydrophobiques (1447) et des résidus modifiés de manière post-traductionnelles comme des tyrosines sulfatées (Y173, Y177) et des asparagines glycosylées (N156, N197) (1448-1451). Par exemple, le résidu L193 de la boucle V1/V2 (**article 5**) forme une interaction cruciale avec un autre résidu hydrophobe (I423) de la boucle β20-β21 afin de stabiliser l'apex du trimère d'Env (1452, 1453). À l'instar du résidu L193, la mutation du résidu I423 chez des souches T/F du tiers 2 induit « l'ouverture » prématurée d'Env, ce qui mène à une meilleure reconnaissance de celles-ci par les nnAbs (**annexe I**). Il existe également plusieurs autres éléments conservés d'Env que ceux étudiés dans le **chapitre IV**. L'une des caractéristiques remarquables d'Env est sa très longue queue cytoplasmique (CT) qui joue un rôle notamment dans son interaction avec la membrane lipidique, son endocytose par la voie de la clathrine et son incorporation efficace dans les particules virales (162, 195, 1454-1456). Plusieurs évidences suggèrent que la troncature de la CT peut également influencer la structure antigénique de l'ectodomaine d'Env (1457, 1458), ce qui pourrait avoir comme effet d'augmenter la capacité des nnAbs à reconnaître les cellules infectées. En écourtant séquentiellement la CT, nous avons observé que la troncature quasi-

complète de la CT (^{712}STOP) était nécessaire pour augmenter la liaison des nnAbs de manière significative, suggérant la présence d'une structure charnière à l'extrémité 5'de la CT d'Env (**annexe II - Figures 1 et 2**). Il a déjà été démontré que le motif d'endocytose de la CT (^{712}YXXΦ^{715}) est essentiel pour l'internalisation constitutive d'Env par la voie dépendante de la clathrine, ce qui permet de limiter les niveaux d'Env à la surface des cellules infectées (1101). Cette étude montre que la mutation du résidu Y712 de ce motif est suffisante pour sensibiliser les cellules infectées à la réponse ADCC médiée par les nnAbs présents chez les individus infectés par le VIH-1 (1101). Or, tel qu'observé dans les chapitres précédents, l'augmentation d'Env n'est pas suffisante pour induire une réponse ADCC médiée par les nnAbs, mais peut rehausser la susceptibilité des cellules infectées si Env adopte sa conformation « ouverte » (**articles 4, 9 et 11**). En suivant cette logique, nous montrons que le résidu Y712 affecte non seulement l'endocytose d'Env, mais également sa conformation, ce qui rend les cellules infectées hautement susceptibles à la réponse ADCC médiée par le sérum VIH+ (**annexe II - Figures 2 et 3**). Malgré tout, il existe très peu de données structurelles permettant de comprendre le rôle du résidu Y712 dans la conformation d'Env. Cela pourrait dépendre de sa localisation à l'interface du trimère de CT (195) ou encore de son interaction avec un partenaire cellulaire (AP-2) (414). Mis ensemble, ces exemples additionnels viennent renforcer le rôle central joué par la conformation d'Env dans la réponse ADCC médiée par les nnAbs tel que proposé dans le **chapitre IV**.

En plus de la réponse ADCC, il semble évident que la conformation d'Env puisse agir comme facteur limitant dans l'activation d'autres fonctions effectrices Fc-dépendantes comme celles impliquant la phagocytose (ADCP) ou la cascade du complément (ADCML). Tout comme c'est le cas pour la quantification de l'ADCC (**article 2**), la plupart des techniques mesurant la réponse ADCP ne prennent pas en compte la conformation d'Env et très peu d'études utilisent des cellules infectées avec des virus de type sauvage comme cellules cibles. Les méthodes d'ADCP les plus répandues utilisent plutôt des billes de latex recouvertes de protéines recombinantes biotinylées (1459), souvent sous forme de gp120 monomérique, d'ectodomaine de gp41, de gp140 non-clivée, ou même de peptides; tous ces antigènes sont connus pour exposer abondamment les épitopes CD4i comparativement au trimère d'Env natif (1460-1462). Dans cet ordre d'idées, il a été démontré que certains nnAbs sont capables d'induire la phagocytose de billes recouvertes de gp120 ou de gp41 recombinantes, mais pas celles recouvertes d'Env trimérique adoptant la

conformation « fermée » (1463). Néanmoins, l'utilisation de ces billes recouvertes d'antigènes d'Env peut devenir problématique du fait qu'elles sont peu représentatives des cellules infectées à cause de leur taille beaucoup plus petite, de l'immobilité de l'antigène et de l'absence de protéines cellulaires régulant l'activation de la réponse ADCP. Par exemple, la molécule CD47 agit à titre de marqueur du soi capable d'inhiber la phagocytose des cellules infectées lorsqu'elle interagit avec son récepteur SIRPα sur les cellules phagocytaires (1464-1466). Bien que Vpu soit connu pour diminuer légèrement les niveaux de surface de CD47, les cellules infectées conservent une certaine résistance à la phagocytose en absence d'anticorps (1467). Il a été démontré que les cellules non-infectées recouvertes de particules virales sont hautement susceptibles à l'ADCP médiée par les nnAbs présents dans le sérum VIH+ (1468), mais leur capacité à induire la phagocytose des cellules infectées par le VIH-1 n'est pas bien définie dans la littérature. On peut spéculer sur le fait que les cellules infectées de manière productive devraient être résistantes à la réponse ADCP par les nnAbs, à moins d'utiliser les CD4mc pour « ouvrir » Env (**articles 6, 9, 10 et 11**). Pour ce qui est de la réponse ADCML, à l'instar de la réponse ADCC, le recrutement du complément et la déposition de molécules C3b médiée par les nnAbs présents dans le sérum VIH+ sont largement dépendants de la reconnaissance d'Env et de l'action des protéines accessoires Nef et Vpu (1276). Or, il s'avère que la déposition du C3b n'est pas suffisante pour induire la lyse des cellules infectées et est souvent utilisée à tort pour mimer la réponse ADCML (1276). Même lorsque la liaison des anticorps et la déposition du C3b sont élevées, la présence de CD59 à la surface des cellules infectées est connue pour prévenir complètement leur élimination par le complément, que ce soit par les nnAbs (en absence de Nef et Vpu) ou par les bNAbs (1274-1276). Des études utilisant des modèles *in vivo* ont confirmé que la réponse ADCML avait très peu d'impact sur la transmission et la réplication du VIH-1, autant lors de l'administration passive de nnAbs que de bNAbs (1248, 1469, 1470). Dans l'ensemble, l'incapacité des nnAbs à reconnaître la conformation « fermée » d'Env semble prévenir l'activation des différentes fonctions effectrices Fc-dépendantes et ces mécanismes impliquent également des protéines cellulaires régulatrices dont la contribution devrait être non-négligeable.

Comme la réponse cytotoxique médiée par les lymphocytes T $CD8^+$ est particulièrement efficace pour éliminer les cellules infectées par le VIH-1 et pour contrôler la réplication du virus, certaines stratégies à base d'anticorps ont été mises à l'essai pour exploiter cette réponse CTL. On

peut penser aux DARTs (*dual-affinity re-targeting molecules*), qui sont des molécules bispécifiques comportant le fragment variable (Fv) d'un anticorps dirigé contre l'Env du VIH-1 et un autre Fv dirigé contre le TCR afin de favoriser le recrutement des CTL effectrices pour éliminer les cellules infectées (1471). Deux DARTs sont présentement en essai clinique de phase 1 (ClinicalTrials.gov : NCT03570918, NCT05261191) et ceux-ci reconnaissent des épitopes CD4i de la gp120 (A32xCD3) ou de la gp41 (7B2xCD3). Or, il s'avère que les études précliniques effectuées pour vérifier leur activité antivirale ont principalement été faites sans tenir compte de la conformation d'Env présente à la surface des cellules cibles. On note plusieurs biais favorisant la réponse nnAbs dans la sélection des souches virales et des méthodes de quantification de la cytotoxicité, souvent sans discrimination entre les cellules infectées et les cellules non-infectées (1472-1474). Parmi les virus utilisés, on peut remarquer l'utilisation de souches adaptées en laboratoire (HXB2, Ba-L), de souches mutées (S375H), de souches du clade CRF01_AE ou encore de souches n'exprimant pas Nef (IMC-LucR.T2A) (1472-1476), et toutes ces conditions favorisent la conformation « ouverte » d'Env, donc la liaison des nnAbs (**articles 3, 4, 7, 9 et 10**). Les souches déficientes pour Nef sont non seulement incapables de moduler CD4 à la baisse aux mêmes niveaux que les souches de type sauvage, mais également plusieurs récepteurs contribuant à l'activation de la réponse CTL. En effet, les constructions virales de type IMC-LucR.T2A ne peuvent cibler ni les molécules HLA-A et HLA-B dû à l'absence de Nef (1477) ni les molécules HLA-C puisqu'elles codent pour la protéine Vpu de la souche de laboratoire NL4-3 (711, 712, 1088). Nous avons généré des données préliminaires confirmant que les niveaux de surface des molécules classiques du CMH-I ne sont pas altérés lorsque les cellules sont infectées par les IMC-LucR.T2A (**annexe III**), ce qui pourrait augmenter fortement leur susceptibilité à la réponse CTL. L'augmentation des niveaux des ligands de NKG2D en absence de Nef (**article 3**) pourrait aussi contribuer à la sensibilité accrue des cellules infectées à la réponse CTL puisque les lymphocytes T $CD8^+$ expriment le récepteur activateur NKG2D, qui agit à titre de molécule costimulatrice du TCR (1478, 1479). En bref, ceci suggère que les DARTs à base de nnAbs devraient être inefficaces à purger les réservoirs du VIH-1 chez les individus infectés à moins de les combiner avec une stratégie pour « ouvrir » Env comme par l'utilisation des CD4mc.

7.3 Implications évolutives

Encore aujourd'hui, il n'est toujours pas clair pourquoi les souches du VIH-1 du groupe M (VIH-1 M) sont plus prévalentes et plus pathogéniques que les souches du VIH-1 des groupes N, O et P ainsi que les souches du VIH-2 (39, 89, 117, 1480-1482). Leurs capacités réplicatives supérieures pourraient être liées à leur habilité à évader certaines réponses immunitaires plus efficacement comme la réponse ADCC. Les fonctions effectrices Fc-dépendantes pourraient exercer une pression sélective sur la conformation d'Env et la régulation de plusieurs protéines cellulaires par Nef et Vpu, ce qui pourrait avoir façonné l'évolution du VIH-1 du groupe M à partir de son précurseur SIVcpzPtt et des ancêtres de celui-ci. En effet, la réplication du VIH-1 *in vivo* en présence de nnAbs à tendance à sélectionner pour des mutations échappatoires stabilisant la conformation « fermée » d'Env et réduisant sa réactivité au CD4 (1242, 1483). Également, l'intégrité du sillon hydrophobe du TMD de Vpu, nécessaire à l'antagonisme de BST-2, NTB-A et PVR, confère un avantage réplicatif au VIH-1 dans les modèles de souris humanisées (669). Une étude utilisant une souche du SIVcpzPtt pour infecter de manière expérimentale des souris humanisées a également mis en lumière l'importance des mutations adaptatives dans le site de liaison à CD4 d'Env et le TMD de Vpu (1484).

Plusieurs domaines structuraux d'Env étudiés dans cette thèse pourraient avoir été soumis à une pression évolutive pour échapper à la réponse ADCC autant chez l'humain que chez les singes. Parmi ceux-ci, le site de clivage polybasique de la furine (RXK/RR) (**article 6**) et le motif d'endocytose à base de tyrosine de la CT (YXXΦ) (**annexe II**) sont des caractéristiques hautement conservées à travers les différentes lignées de VIH et de SIV (**annexe IV – Tableau 1**), et sont également communes avec les glycoprotéines d'enveloppe provenant d'autres lentivirus et rétrovirus simples (1456, 1485-1488). Le point de contrôle conformationnel formé par les résidus L193 et I423 (**article 5 et annexe I**), situé dans les groupements hydrophobes de l'apex du trimère d'Env, est une structure partiellement conservée parmi les lentivirus de primates puisque l'identité de ces résidus varie à travers les espèces, mais leur caractère hydrophobe demeure. De son côté, la cavité Phe43 est soumise à une pression évolutive plus stricte puisqu'il existe d'importantes variations alléliques dans le domaine D1 du récepteur CD4 chez les chimpanzés, les gorilles et les guenons arboricoles (1489-1491). La présence de polymorphismes à la position 375 et dans les couches topologiques du domaine interne de la gp120 pourrait permettre une certaine flexibilité

nécessaire pour s'adapter au CD4 d'autres espèces de primates (**articles 7 et 10**). Le VIH-1 du groupe M diffère des autres lentivirus humains et simiens par la présence d'un petit résidu polaire (S) à la position 375 d'Env, comparativement aux larges résidus hydrophobes (W, H, Y, F, M) retrouvés chez ces derniers. Sur les bases de l'identité du résidu 375 d'Env, nos résultats suggèrent que le groupe M du VIH-1 devrait être capable d'évader la réponse ADCC médiée par les nnAbs plus efficacement que les autres lentivirus de primates, à l'exception du clade CRF01_AE (**articles 7 et 10**). Malgré sa susceptibilité plus élevée aux nnAbs, plusieurs raisons pourraient expliquer pourquoi les souches du clade CRF01_AE sont autant prévalentes, notamment par une transition vers le tropisme X4 et une déplétion des lymphocytes T $CD4^+$ plus rapides (1492-1495).

Parmi les fonctions de Nef et Vpu impliquées dans la réponse ADCC, plusieurs semblent avoir été héritées directement des précurseurs simiens du VIH-1 tandis que d'autres semblent avoir été acquises lors de la transmission inter-espèces (**annexe IV – Tableau 2**). Le VIH-1 M semble être le lentivirus humain ayant réussi à mieux s'adapter à son hôte pour prévenir la réponse ADCC par les nnAbs en ciblant simultanément CD4 et BST-2, pour garder Env dans sa conformation « fermée » et réduire son expression de surface, ainsi que NTB-A, PVR et les ligands NKG2D, pour limiter l'activation des cellules NK (**articles 3, 4, 8 et 9**). Puisque la queue cytoplasmique de CD4 est bien conservée parmi les différents primates, les protéines Nef et Vpu de la majorité des souches de VIH sont capables de cibler CD4, à l'exception du Vpu provenant du VIH-1 N et de l'absence de Vpu chez le VIH-2 (534, 537, 1496). De son côté, le facteur de restriction BST-2 est beaucoup plus variable, notamment au niveau de sa CT et de son TMD, et représente donc une barrière de transmission plus grande (537, 1497). Puisque les ancêtres proches du VIH (SIVcpzPtt, SIVgor et SIVsmm) utilisent Nef pour cibler le BST-2 de leur hôte respectif, mais sont incapables de cibler le BST-2 humain, le VIH-1 M a acquis la capacité d'antagoniser efficacement BST-2 par Vpu (536-538, 1498). Certaines souches du VIH ont également développé des antagonistes de BST-2, incluant Vpu (VIH-1 N), Nef (VIH-1 O) ou Env (VIH-2), mais ayant une activité sous-optimale (531, 534, 537, 1496, 1499-1501). De surcroît, le VIH-1 M est connu comme étant le seul lentivirus humain capable de cibler NTB-A et PVR (709, 710, 1500). En somme, il est possible que les fonctions effectrices Fc-dépendantes médiées par les nnAbs aient pu servir de barrière dans les transmissions intra- et inter-espèces, et que des adaptations dans les séquences d'Env, Nef et Vpu aient été nécessaires afin d'augmenter la réplication du virus en présence de nnAbs. Nos

résultats proposent que l'acquisition du résidu S375 d'Env et l'augmentation de la polyfonctionnalité de Nef et Vpu puissent avoir conféré un avantage évolutif au VIH-1 M contre la réponse humorale comparativement aux autres souches de lentivirus humains.

7.4 Implications pour les modèles animaux

L'évaluation de l'efficacité des différentes approches prophylactiques ou thérapeutiques à base d'anticorps ciblant Env nécessite la mise au point de modèles animaux capables de récapituler le plus fidèlement possible l'infection par le VIH-1 chez l'humain. Les infections lentivirales de souris humanisées ou de NHP (comme les macaques rhésus) sont les deux principaux modèles animaux utilisés pour mimer l'infection du VIH-1 *in vivo*, chacun possédant leurs propres avantages et limitations (1502-1505). Le modèle de souris humanisées semble un modèle plus adéquat pour tester des immunothérapies à base de nnAbs puisqu'il permet l'utilisation de souches du VIH-1 non-modifiés et cliniquement pertinentes, tandis que l'infection de NHP nécessite l'utilisation de virus chimériques (SHIV) dont le génome ne comporte que les protéines Env, Vpu, Tat et Rev du VIH-1 (669, 1323, 1506-1511). De plus, l'infection de souris humanisées par le VIH-1 ne nécessitent aucune d'adaptation d'Env pour se répliquer, contrairement aux modèles conventionnels d'infection de NHP par le SHIV. En fait, la plupart des Env du VIH-1 ne se lient pas efficacement au CD4 de macaque rhésus (rhCD4) à cause d'un résidu polymorphique distinctif (I39) présent dans le CD4 de macaque par rapport au CD4 humain (1512, 1513). Cette particularité semble causer une réorientation de la boucle Phe43 de CD4 dont l'accommodation pourrait nécessiter une inévitable restructuration du site de liaison à CD4 d'Env, favorisant une conformation plus « ouverte » (1512, 1514, 1515). Pour cette raison, les premières générations de SHIV ont été construites à partir d'Env ayant un tropisme pour les macrophages (SF162, Ba-L, 89.6, AD8), connues pour leur réactivité intrinsèque plus prononcée (1516-1520). Ces souches particulières ont évolué pour utiliser des faibles densités de CD4 à la surface des cellules myéloïdes, ce qui a tendance à sélectionner des variants d'Env dont la conformation est plus « ouverte » et donc plus sensibles aux nnAbs (1521-1524). On retrouve ce type de souches principalement dans les sanctuaires immunitaires comme le cerveau ou dans la circulation sanguine pendant la phase SIDA, faisant face à une pression humorale moins importante (1525-1529). Ces souches sont donc peu représentatives des isolats cliniques du VIH-1 tels que les virus T/F, dont l'Env adopte une conformation plus compacte et résistante aux nnAbs (787, 1241, 1530,

1531). Afin d'augmenter la pertinence biologique du modèle, les SHIV de nouvelle génération ont été élaborés avec des isolats de la phase aigüe de l'infection (1514, 1532-1537). Or, la vaste majorité de ces SHIV sont incapable de générer une infection productive et une réplication soutenue dans les modèles de NHP par manque d'affinité pour le rhCD4 (1514, 1532-1536). Afin de remédier à ce problème, ces SHIV ont été modifiés par l'introduction de résidus hydrophobes de grande taille à la position 375 de la cavité Phe43 (1514, 1535, 1536, 1538). Or, nos résultats montrent que ces modifications (S375H, S375W, S375Y) favorisent la conformation « ouverte » d'Env, rendant les cellules infectées hautement sensibles à la réponse ADCC par les nnAbs (**article 7 et annexe V**). De plus, des études récentes ont montré que des mutations dans le domaine d'association du trimère d'Env (e.g. L193A, I423A) (**article 5 et annexe I**) permettent également d'augmenter l'infection des lymphocytes T $CD4^+$ de macaque, confirmant que la conformation d'Env est un déterminant majeur dans l'utilisation du rhCD4 par les SHIV (1539-1541). La présence de mutations en position 375 chez cette nouvelle génération de SHIV empêche également l'utilisation de ce modèle animal dans la caractérisation de petites molécules comme les CD4mc en comblant la cavité Phe43 (**article 10**). En quête d'alternatives, certains ont suggéré l'utilisation de nouvelles espèces de NHP dont le récepteur CD4 est compatible à l'entrée virale par des isolats primaires du VIH-1 sans adaptation, comme les singes-chouettes (1542-1544).

L'utilisation de virus primaires non-modifiés dans les modèles de souris humanisées permet également de prendre en compte la contribution des protéines accessoires Nef et Vpu à l'évasion de la réponse humorale en présence de leurs substrats cellulaires correspondants, tandis que ce n'est pas le cas dans les modèles de NHP. En effet, la dynamique fonctionnelle entre le Vpu du VIH-1 et les protéines cellulaires de macaque reste largement inconnue. Même si certains SHIV codent pour Vpu, son rôle reste ambigu puisque la protéine BST-2 présente chez les macaques est résistante à son antagonisme (**article 8**) (536, 547, 1545). La capacité de Vpu à cibler d'autres substrats comme NTB-A et PVR chez le macaque pourrait également être mitigée à cause de variations au niveau du TMD de leurs orthologues simiens. Malgré une certaine redondance fonctionnelle entre les protéines Nef du VIH-1 et du SIVmac, celles-ci semblent posséder quelques fonctions divergentes, notamment par la régulation négative du TCR observée exclusivement chez le Nef du SIVmac (693, 1546-1548). En ce sens, nous avons généré des données préliminaires montrant que contrairement au VIH-1, les SHIV de nouvelle génération sont incapables de réguler

négativement le ligand activateur PVR (**annexe VI**). De plus, nous ne savons pas si la protéine Nef de SIVmac est capable de cibler les ligands de NKG2D chez le macaque. Des études plus approfondies évaluant la susceptibilité des cellules infectées par les SHIV à la cytotoxicité médiée par les cellules NK s'imposent afin de répondre à ces questionnements. Néanmoins, peu importe le modèle animal, il faut faire preuve de prudence lors de la sélection de virus, car même les souches de VIH-1 utilisées chez les souris humanisées peuvent s'avérer défectueuses pour l'expression de Vpu ou de Nef (1242, 1549-1551).

Une importante limitation des modèles de souris humanisées est la reconstitution du système immunitaire humain dans les souris immunodéficientes et plus particulièrement les cellules responsables des réponses effectrices dépendantes des anticorps. Les plus récents modèles de souris humanisées tendent à corriger ce problème par des modifications génétiques permettant aux souris d'exprimer des cytokines humaines importantes pour le développement de certains compartiments cellulaires fonctionnels comme les cellules NK (IL-15) ainsi que les macrophages et monocytes (IL-3, GM-CSF, M-CSF) (1552-1554). Ces modèles sont également conçus pour limiter la phagocytose des cellules humaines par les cellules phagocytaires murines par la délétion du CD47 murin ou en par l'introduction du SIRPα humain (1552, 1553, 1555, 1556). Cela limite les risques de réaction du greffon contre l'hôte (GvHD) et augmente ainsi la longévité du modèle, permettant l'évaluation de stratégies thérapeutiques de cure fonctionnelle. En utilisant un de ces modèles (SRG-15), il a été démontré que les nnAbs sont capables de réduire la taille des réservoirs du VIH-1, mais seulement en présence de CD4mc, requérant une contribution importante des fonctions effectrices dépendantes des cellules NK (1323). C'est également avec ce modèle que nous avons démontré le rôle de Vpu dans l'évasion de la réponse humorale non-neutralisante *in vivo* (**article 9**).

7.5 Implications pour les stratégies vaccinales

Parmi tous les essais vaccinaux de phases 2 et 3 ayant été testés au fil des années, seul l'essai vaccinal RV144 a démontré une efficacité modeste (31,2 %) à réduire le risque de transmission du VIH-1 (78). Des analyses ultérieures ont établi que les principaux corrélats immunitaires de la protection observée étaient les niveaux de nnAbs dirigés contre la boucle V1/V2 d'Env et une forte réponse ADCC chez les participants ayant une réponse IgA réduite

(1359, 1360). Or, nos résultats suggèrent que cette protection modeste pourrait être due au fait que les souches prédominantes circulant en Thaïlande appartiennent au clade CRF01_AE, dont la sensibilité à la réponse ADCC médiée par les nnAbs est plus élevée par rapport aux autres clades (**article 7 et annexe V**). À la suite du succès modeste de l'essai RV144, de nombreuses études ont examiné la possibilité d'utiliser les nnAbs comme traitement préventif contre l'infection par le VIH-1 par immunisation passive ou par vaccination. L'administration prophylactique de nnAbs, sous forme monoclonale ou polyclonale, n'a montré aucune capacité à prévenir l'acquisition du VIH-1 dans les modèles animaux exposés à des virus du clade B (1234, 1245-1248, 1437). Une étude préclinique utilisant le même protocole de vaccination que celui de l'essai RV144 dans un modèle de NHP exposés à un SHIV du clade C n'a démontré aucun effet protecteur malgré l'induction d'une forte réponse nnAbs (1433). De même, l'essai vaccinal HVTN 702, dont l'approche expérimentale était calquée sur celle du RV144, a été incapable de protéger contre l'infection par les souches du clade C prédominantes en Afrique du Sud et il a dû être arrêté pour cause de futilité (1363, 1364). Dans l'ensemble, si l'activité ADCC est nécessaire à la protection vaccinale, comme l'a suggéré l'essai vaccinal RV144, nos résultats suggèrent qu'il est peu probable que la génération de nnAbs confère une protection à moins que des stratégies visant à « ouvrir » le trimère d'Env soient en place (**articles 6, 9, 10 et 11**). À l'appui de cette hypothèse, des NHP immunisés avec de la gp120 monomérique ont été complètement protégés contre une infection hétérologue par un SHIV, codant pour l'Env d'une souche T/F de clade C, seulement en présence de CD4mc (1321). Cette étude a montré que les nnAbs induits par l'immunogène gp120 ne protégeaient pas en l'absence de CD4mc, mais qu'ils étaient capables de neutraliser et de médier des fonctions effectrices en présence de CD4mc (1321). Il est difficile de déterminer si une stratégie vaccinale combinant le CD4mc et des immunogènes capables d'induire des nnAbs est une approche vaccinale viable, mais cette étude confirme que la conformation adoptée par Env sur les particules virales représente un paramètre critique à prendre en compte dans la conception de vaccin anti-VIH-1. Comme l'Env des souches T/F adopte préférentiellement sa conformation « fermée », il est donc préférable de choisir des stratégies permettant l'induction de bNAbs. En effet, une étude dans un modèle de NHP à laquelle j'ai contribuée a permis d'identifier la neutralisation comme déterminant majeur de la protection vaccinale induite par l'immunogène d'Env trimérique SOSIP.664 (1369) et cette conclusion a été corroborée par une méta-analyse de treize études d'immunisation passive de bNAbs (1557). Or, seulement 2,5% des singes immunisés

avec le trimère SOSIP.664 ont réussi à générer une réponse neutralisante suffisante pour atteindre le seuil nécessaire à la protection contre une exposition répétée à un SHIV autologue (1369, 1375). Une étude plus récente a montré des progrès encourageants en utilisant un schéma de vaccination complexe combinant la technologie d'ARNm et une stratégie d'immunisation séquentielle dans un modèle simien, car la protection contre l'infection corrélait avec la génération de bNAbs ciblant le site de liaison à CD4 d'Env (1384).

Malgré que certaines études d'immunisation passive à l'aide de bNAbs aient montré que leur activité neutralisante peut être suffisante pour prévenir l'infection par le VIH-1 dans les modèles animaux (1201, 1558, 1559), les fonctions effectrices Fc-dépendantes peuvent contribuer à la protection par des bNAbs dont l'activité neutralisante est moins puissante (1469, 1560). Le développement d'une nouvelle plateforme de sérologie des systèmes permet de caractériser les réponses humorales effectrices induites par différents protocoles de vaccination (1149, 1561-1565). Celle-ci se concentre sur le profilage des anticorps induits par la vaccination via une variété de paramètres biophysiques (spécificité antigénique, isotype, glycosylation, affinité pour les FcγRs) et fonctionnels (cytotoxicité, phagocytose, déposition du complément). Cette plateforme a notamment été utilisée pour la sélection et la validation des approches expérimentales des essais vaccinaux HVTN 705 (interrompu pour cause de futilité) et HVTN 706 (1365-1367), en plus d'identifier les fonctions effectrices des anticorps comme corrélats de protection de ces vaccins dans les modèles animaux (1566, 1567). Malheureusement, les méthodes de quantification des réponses effectrices Fc-dépendantes inclues dans cette plateforme ne prennent pas en compte la conformation d'Env et utilisent typiquement des cellules cibles ou des billes d'agarose recouvertes d'antigènes recombinants (gp120, gp41, gp140, gp70) favorisant la détection de réponses non-neutralisantes (**article 2**). Il est donc peu probable que les données générées à l'aide de cette plateforme aient une pertinence biologique concernant l'immunité humorale nécessaire à prévenir l'acquisition des souches T/F du VIH-1. Afin d'augmenter son utilité dans l'évaluation de futures stratégies vaccinales, certains correctifs doivent être appliqués au niveau des analyses fonctionnelles, notamment par l'usage de techniques spécifiques aux cellules infectées et ciblant la conformation native « fermée » d'Env (**article 2**). Un autre outil intéressant dans la caractérisation des réponses effectrices vaccinales est l'établissement d'un panel standardisé de souches du VIH-1 de différents clades pour évaluer la réponse ADCC à large spectre (1568),

similairement au panel de neutralisation déjà existant (1161). Or, le premier panel développé en ce sens est composé exclusivement de constructions virales IMC-LucR.T2A défectives pour l'expression de Nef (1568), et il est donc peu probable que des données probantes et ayant une pertinence biologique quelconque soient générées à l'aide de ce panel. Nos résultats démontrent qu'il existe plusieurs alternatives afin de résoudre cette problématique, notamment via l'utilisation d'IMC possédant la cassette LucR.6ATRi ou d'IMC non-modifiés (**articles 3 et 4**). Quoi qu'il en soit, il semble logique que les panels de neutralisation et d'ADCC soient composés de souches T/F de type sauvage puisqu'elles sont responsables de l'infection initiale par le VIH-1.

7.6 Implications pour les stratégies thérapeutiques

La persistance des cellules réservoirs infectées de manière latente chez les PVVIH sous traitement ART est un obstacle à la guérison fonctionnelle de l'infection par le VIH-1. La stratégie du « shock and kill » vise à éradiquer ces réservoirs par l'activation transcriptionnelle et traductionnelle du provirus latent à l'aide de LRA et la destruction subséquente des cellules réactivées hébergeant le virus via le système immunitaire. Les travaux présentés dans les chapitres précédents se concentrent plus précisément sur l'optimisation de l'élimination des cellules infectées par le biais des fonctions effectrices Fc-dépendantes médiées par des anticorps dirigés contre l'Env du VIH-1. Plusieurs études réalisées dans des modèles animaux ont démontré la nécessité des fonctions effectrices pour une activité thérapeutique optimale des bNAbs *in vivo*, notamment par l'élimination des cellules infectées et le contrôle de la charge virale (1199, 1470, 1569-1572). Devant ces résultats encourageants, les bNAbs 3BNC117 et 10-1074 ont été testés dans des essais cliniques de phase 1b chez des individus infectés sous ART et ont montré une capacité à retarder le rebond viral jusqu'à 48 semaines après l'interruption du traitement ART chez certains patients, un phénomène possiblement attribuable à une modeste diminution des réservoirs viraux intacts (1212, 1214, 1573). Or, ces bénéfices thérapeutiques se limitent à une minorité d'individus puisque des souches résistantes à ces bNAbs sont déjà présentes chez certains individus ou se développent en cours de traitement chez d'autres (1212-1214, 1573). Comme ils sont facilement induits par l'infection ou la vaccination et que certains de leurs épitopes sont hautement conservés, les nnAbs sont présentement étudiés comme alternatives aux bNAbs dans des stratégies d'éradication des réservoirs du VIH-1 (1233, 1316, 1323, 1574, 1575). Or, nous avons démontré que les nnAbs utilisés seuls ne possèdent qu'une activité antivirale limitée *in vivo*

contre un virus de type sauvage (**article 9**), contrairement à ce qui avait été observé contre un virus défectif pour l'expression de Vpu (1242). En effet, une étude récente a permis de montrer que les fonctions effectrices des nnAbs peuvent avoir un impact sur l'élimination des réservoirs viraux, mais uniquement en présence de CD4mc (1323), rappelant encore une fois que la conformation d'Env est le principal facteur limitant pour les immunothérapies à base de nnAbs. En plus de la conformation d'Env, plusieurs paramètres additionnels sont à considérer dans l'optimisation d'une stratégie thérapeutique de « shock and kill » à base de nnAbs, concernant les propriétés intrinsèques des cellules réservoirs, la fonctionnalité des cellules effectrices et des anticorps, les niveaux d'antigènes et la contribution des protéines accessoires virales.

7.6.1 Propriétés intrinsèques des réservoirs

La nature du réservoir responsable de la persistance et du rebond viral suite à l'interruption du traitement ART est extrêmement complexe et les stratégies d'éradication se doivent de prendre en compte les capacités réplicatives, l'expression de marqueurs phénotypiques et la localisation anatomique de ces cellules. La population de provirus qui persiste dans le cadre du traitement ART est dominée par des provirus défectifs qui sont incapables de provoquer un rebond viral, contrairement aux provirus intacts compétents à la réplication qui forment le réservoir à cibler de manière thérapeutique (1576-1586). Une série d'études plutôt controversée rapporte des observations selon lesquelles les réservoirs viraux seraient enrichis dans les populations de lymphocytes T $CD4^+$ exprimant CD32a (FcγRIIa) (870, 1587-1591), ce qui pourrait les rendre plus résistantes à l'élimination par les fonctions effectrices humorales, probablement en compétitionnant avec les FcγR des cellules effectrices pour la liaison du fragment Fc des anticorps (1592). De manière intéressante, deux récentes études indépendantes ont montré à l'aide d'analyses transcriptomiques que les provirus intacts étaient enrichis dans des clones de lymphocytes T $CD4^+$ effecteurs mémoires cytotoxiques, possédant d'excellentes capacités de prolifération et comportant des granules lytiques composés de granzymes et de perforines (1593, 1594). Par leur nature cytotoxique, ces cellules expriment également de hauts niveaux du facteur anti-apoptotique BCL2 et de protéines inhibitrices de granzymes (SERPINB9) et de cathepsines (CST7), leur conférant une certaine résistance aux fonctions effectrices dépendant de l'apoptose comme les réponses ADCC et CTL (1593, 1594). L'utilisation d'inhibiteurs de BCL2 et de SERPINB9 pourrait faciliter l'élimination de ces cellules réservoirs par la réponse ADCC (1595-

1601). De manière encourageante, les stratégies de réactivation répandues combinant un agoniste de PKC et un inhibiteur de HDAC ont été montrées comme étant efficaces pour induire la traduction de protéines du VIH-1 chez les lymphocytes T_{EM} (869, 872, 1602), toutefois il reste à déterminer si les niveaux d'expression d'Env induits seraient suffisants pour sensibiliser ces cellules infectées à l'ADCC (1603). Puisque les cellules réservoirs sont connues pour exprimer des niveaux élevés de molécules de point de contrôle immunitaire (PD-1, LAG-3, TIGIT, TIM-3) (851, 858, 902, 904), l'utilisation d'anticorps bloquants dirigés contre ces molécules inhibitrices pourrait permettre d'améliorer significativement la capacité des LRA à réactiver l'expression provirale chez les cellules réservoirs latentes (1604, 1605).

7.6.2 Fonctionnalité des cellules effectrices

Les stratégies utilisées pour réactiver les réservoirs latents ainsi que pour augmenter la susceptibilité des cellules infectées à la réponse ADCC se doivent également d'être compatibles avec la fonctionnalité des cellules NK effectrices. Il faut d'abord être prudent dans la sélection des LRA puisque certains d'entre eux peuvent avoir un effet délétère sur les fonctions cytotoxiques des cellules NK (1606-1608). En effet, les agonistes de PKC ont tendance à induire une diminution des niveaux de CD16 et une augmentation des niveaux de NKG2D sur les cellules NK, ce qui pourrait globalement nuire à leur capacité à médier la réponse ADCC (1607, 1608). De plus, plusieurs inhibiteurs de HDAC ont des effets variables sur les niveaux de récepteurs activateurs des NK (1606, 1608). Par exemple, la romidepsine augmente l'expression de NKG2D, tandis que le panabinostat diminue l'expression de NKG2D et DNAM-1 (1608). Les LRA peuvent aussi avoir un effet sur l'expression des ligands de ces récepteurs activateurs puisqu'un agoniste de PKC (prostratine) et plusieurs inhibiteurs de HDAC peuvent augmenter de manière importante les niveaux des ligands de NKG2D sur les cellules infectées par le VIH-1 (1606-1608). Comme cette augmentation semble dépendante de l'activation de la voie des dommages à l'ADN via ATR, il serait intéressant de déterminer l'effet de ces LRA sur l'expression de PVR, aussi régulé par l'activation d'ATR (636, 1606). D'autre part, le blocage des points de contrôle immunitaires pour réactiver les cellules infectées latentes pourrait également être avantageux pour les cellules NK. Effectivement, le récepteur inhibiteur TIGIT est augmenté durant la phase chronique de l'infection sur les cellules NK cytotoxiques co-exprimant le récepteur activateur DNAM-1 (1609-1612). Comme ces deux récepteurs partagent un ligand commun (PVR), certaines études ont évalué les

bénéfices d'utiliser un anticorps bloquant ciblant TIGIT sur les cellules NK et ont observé un regain dans leur capacité à médier les réponses cytotoxiques directes et dépendantes des anticorps dirigées contre les cellules infectées (1609, 1611). Les fonctions effectrices des cellules NK peuvent également être revigorées par une panoplie de cytokines, notamment l'IL-15 et les IFN-I, connues pour stimuler l'activation des cellules NK et pour augmenter l'expression de récepteurs activateurs, de cytokines et de granules cytolytiques (1414-1416, 1613-1618). Plusieurs études ont permis de confirmer que le traitement des cellules NK avec ces cytokines renforce leur capacité à éliminer les cellules infectées par la réponse ADCC médiée par les bNAbs et nnAbs (1613-1617).

7.6.3 Optimisation du cocktail thérapeutique

L'utilisation d'un modèle de souris humanisées supportant la latence du VIH-1 et comportant un compartiment de cellules NK fonctionnelles a permis de démontrer l'efficacité d'une combinaison de nnAbs et de CD4mc pour éliminer les réservoirs viraux (1323). Comme l'activité thérapeutique de ce cocktail dépend grandement de la capacité du CD4mc à « ouvrir » Env, il est important de continuer le développement de CD4mc plus puissants et à plus large spectre. En effet, la présence de polymorphismes naturels ou l'émergence de mutations échappatoires dans la cavité Phe43 et le domaine interne de la gp120 peuvent conférer une résistance aux différents CD4mc, incluant les composés les plus prometteurs comme BNM-III-170 et M48U1 (**article 10**) (1330, 1619-1621). L'optimisation de nouveaux dérivés de BNM-III-170 est en cours et certains d'entre eux démontrent déjà un spectre d'activité augmenté grâce à l'ajout de groupements capables d'accommoder certains polymorphismes en bordure de la cavité Phe43 (1622). L'identification d'un nouveau CD4mc issu d'un criblage à haut débit offre des possibilités intéressantes dans le développement de molécules plus puissantes (1623, 1624). D'ailleurs, le développement de cette nouvelle famille de CD4mc a été rendu possible grâce à nos travaux sur l'identification de résidus polymorphiques à l'intérieur et au pourtour de la cavité Phe43 d'Env (**article 10**). Ces informations ont mené à la conception d'une gp120 recombinante du clade CRF01_AE modifiée (LM+HT), ayant une hypersensibilité au CD4mc et pouvant être utilisée aisément pour des analyses structurelles par cristallographie à rayons X (**article 10**). Les structures générées avec les premiers analogues de ce nouveau CD4mc ont permis le développement guidé de molécules de plus en plus puissantes et dont le mode de liaison permet d'entrer en contact avec les résidus D368 et E370 (1623, 1624). Comme ces deux résidus sont

hautement conservés dans les souches du VIH-1 en circulation, cela pourrait garantir à ces molécules un spectre d'activité plus large que les composés des générations précédentes. Mis à part leur activité antivirale, il faut également explorer les propriétés pharmacocinétiques des CD4mc plus en profondeur. Comme les réservoirs viraux sont disséminés dans une grande variété d'organes et de tissus (1625), il est important de surveiller la biodistribution, la demi-vie et la toxicité potentielle des CD4mc *in vivo*. Des données préliminaires dans les souris ont démontré une bonne pénétration de BNM-III-170 dans les différents tissus lymphoïdes, excepté la moelle osseuse, sans toxicité observable dans les conditions testées (1323). Pour ce qui est de sa durée de vie, des données non-publiées suggèrent une persistance de la molécule dans l'organisme pendant environ 48 heures après l'administration, ce qui est semblable à ce qui a été rapporté précédemment pour d'autres CD4mc (1324, 1325). Considérant ce déclin rapide, il serait logique d'envisager la conjugaison du CD4mc à une protéine de plus longue demi-vie comme un anticorps. Certains groupes ont déjà développé des protéines de fusion à partir de nnAbs comportant un CD4 soluble (sCD4) lié au fragment Fab de l'anticorps via un peptide flexible de longueur variable (1233, 1626-1628). Ces protéines hybrides multivalentes possèdent ainsi des capacités accrues à neutraliser les particules virales et à médier l'élimination des cellules infectées par la réponse ADCC (1233, 1626-1628). Par le fait même, il serait intéressant de générer des nnAbs conjugués au CD4mc afin de voir si ces molécules conservent leurs fonctions effectrices tout en prolongeant la demi-vie des CD4mc.

D'autre part, nous cherchons également à améliorer le volet anticorps du cocktail thérapeutique, présentement composé de nnAbs ciblant le CoRBS et le cluster A (1323, 1574, 1575, 1629, 1630). Nous avons évalué la possibilité d'utiliser des nnAbs de spécificités diverses, mais dont les épitopes ne se chevauchent pas, comme les anticorps dirigés contre la boucle V3 ou le cluster I de la gp41 (**Figure 1.1.10**). Nous avons observé que la combinaison de ces quatre classes de nnAbs avec le CD4mc permettait d'augmenter la reconnaissance et l'élimination des cellules infectées par la réponse ADCC par rapport au cocktail original contenant uniquement deux classes d'anticorps (**annexe VII**). Cette amélioration semble être dépendante d'une meilleure mobilisation du FcγRIIIa par ce nouveau cocktail. Plusieurs études utilisant des bNAbs ont démontré que l'interaction des anticorps avec le FcγRIIIa puisse être optimisée par l'altération de la glycosylation ou par la mutation de résidus du fragment Fc des anticorps (1253, 1255, 1256,

1569, 1571, 1631, 1632). Ici, nous montrons que les fonctions effectrices Fc-dépendantes du cocktail composé de quatre nnAbs peuvent être décuplées par l'introduction des mutations GASDALIE (G236A/S239D/A330L/I332E) dans leur portion Fc respective (**annexe VII**). Il pourrait être intéressant de tester l'effet de ce cocktail d'anticorps optimisé en combinaison avec les nouvelles générations de CD4mc sur la réduction des réservoirs du VIH-1 *in vivo*.

7.6.4 Augmentation des niveaux de surface d'Env

L'expression d'Env à la surface des cellules infectées est restreinte par l'antagonisme de BST-2 par Vpu et par l'endocytose constitutive d'Env grâce au motif YXXΦ de sa queue cytoplasmique, ce qui participe à l'évasion des réponses humorales effectrices (756, 757, 1099-1101, 1633, 1634). Nous montrons que ces niveaux réduits d'Env limitent également la capacité des CD4mc à stimuler la réponse ADCC médiée par les nnAbs (**article 11**). Étant donné que les niveaux d'Env exprimés lors de la réactivation des cellules réservoirs risquent également d'être limités, il faut élaborer des stratégies permettant d'augmenter significativement son exposition de surface afin de favoriser la reconnaissance des cellules infectées par les anticorps. Nos résultats démontrent qu'il est possible d'augmenter substantiellement les niveaux d'Env en stimulant l'expression de BST-2 à l'aide d'IFN-I ou d'IL-27 (**article 11**). De plus, de par leur effet délétère sur la polyfonctionnalité de Vpu, les IFN-I augmentent les niveaux de CD62L (**article 8**) et TIM-3 (593), tous deux ayant un rôle inhibiteur sur la relâche virale, ce qui pourrait également contribuer à l'augmentation d'Env (209, 705). Comme BST-2 peut être régulé à la hausse par d'autres molécules, comme l'IFNγ ou un antagoniste de PPARγ (1635-1637), il serait intéressant de déterminer s'il existe un effet additif entre celles-ci et les IFN-I ainsi que l'IL-27 dans l'augmentation des niveaux d'Env. De manière intéressante, le traitement avec ces différentes cytokines (IFNα, IL-27 et IFNγ) est connu pour induire l'expression des facteurs de résistance de la famille GBP (556, 1638). Les molécules GBP2 et GBP5 agissent en tant qu'inhibiteurs de la furine, la protéase cellulaire nécessaire au clivage protéolytique du précurseur d'Env (562, 563). Comme nous avons montré que l'Env non-clivée adopte une conformation plus « ouverte » et plus sensible aux CD4mc (**article 6**), ces cytokines pourraient favoriser l'exposition des épitopes CD4i, contribuant ainsi à sensibiliser les cellules infectées à la réponse ADCC médiée par les nnAbs. D'autre part, il pourrait être envisageable d'augmenter Env par d'autres moyens, comme par l'inhibition pharmacologique des voies d'endocytose ou du bourgeonnement viral. Par exemple,

l'utilisation de l'inhibiteur de dynamine prochlorpérazine pourrait ralentir l'endocytose d'Env, qu'elle soit constitutive ou induite par les anticorps (1101, 1102, 1639), et augmenter la densité des antigènes de surface, tel que démontré dans des modèles de cancer (1640). De même, l'utilisation de l'inhibiteur de Tsg101 ilaprazole pourrait bloquer le bourgeonnement des particules virales à la surface par la machinerie ESCRT (1641). Néanmoins, des études de toxicité seraient nécessaires pour confirmer leur potentiel thérapeutique. Dans l'ensemble, l'inhibition du bourgeonnement, de la relâche virale ou des voies d'endocytose a le potentiel d'augmenter l'élimination des cellules infectées en présence de CD4mc et de nnAbs.

7.6.5 Inhibiteurs de Nef et Vpu

En plus de cibler Env, il pourrait également être intéressant de cibler d'autres protéines virales impliquées dans l'évasion de la réponse ADCC comme Nef et Vpu. Il n'existe toujours pas d'inhibiteurs autorisés de Nef ou Vpu, tandis qu'une seule molécule ciblant l'activité viroporine de Vpu (BIT225) est actuellement testée en essai clinique de phase II en combinaison avec ART (1308, 1309). Or, les résultats de cette étude n'ont démontré aucun effet de BIT225 sur la diminution de la charge virale du VIH-1 (1308, 1309). Cela est probablement explicable par le fait que la fonction de viroporine de Vpu ne semble pas particulièrement importante pour la réplication dans les lymphocytes T $CD4^+$ ou pour l'évasion immunitaire (1305-1307). Dans le contexte d'une stratégie thérapeutique, les inhibiteurs de protéines accessoires devraient idéalement être capable d'altérer des fonctions de Nef et Vpu liées à l'activité ADCC des nnAbs, c'est-à-dire la régulation négative de CD4 et des ligands de NKG2D par Nef ainsi que l'antagonisme de CD4, BST-2, NTB-A et PVR par Vpu (**articles 2, 3, 4, 8, 9 et 11**). Entre autres, il pourrait être intéressant d'évaluer l'effet d'inhibiteurs d'endocytose sur la régulation de CD4 par Nef. Comme Nef diminue l'expression de surface de CD4 par la voie d'endocytose dépendante de la clathrine, l'utilisation de l'inhibiteur de dynamine prochlorpérazine pourrait atténuer l'internalisation de CD4 et ainsi augmenter son interaction avec Env pour exposer les épitopes CD4i (1640). Autrement, le mécanisme sous-jacent à la suppression des ligands de NKG2D par Nef est largement inconnu et une meilleure caractérisation des motifs de Nef impliqués pourrait faciliter le développement d'inhibiteur ciblant spécifiquement cette fonction (773, 1097). Pour ce qui est de Vpu, un récent criblage à haut débit basé sur la capacité de Vpu à recruter la E3 ubiquitine ligase $SCF^{\beta TrCP}$ a permis d'identifier deux inhibiteurs inhibant complètement l'activité anti-CD4 de Vpu et

partiellement son activité anti-BST-2 (1642). Par conséquent, ces nouvelles molécules sont capables d'augmenter significativement la susceptibilité des cellules infectées à la réponse ADCC médiée par les nnAbs (1642). Toutefois, étant donné la variabilité de Vpu (1445, 1643), le spectre d'activité de ces molécules se limite pour l'instant à la souche NL4-3 utilisée lors du criblage (1642). Afin d'outrepasser cette limitation, certains ont suggéré l'utilisation du pevonedistat (MLN4924), un inhibiteur de la E3 ubiquitine ligase $SCF^{\beta TrCP}$ utilisé en essai clinique pour le traitement de différentes leucémies (1644-1647), afin d'affecter les fonctions de Vpu (1633). Dans les faits, le pevonedistat affecte majoritairement l'antagonisme de CD4 par Vpu, augmentant ainsi l'élimination des cellules infectées par les nnAbs (1633). Malgré un effet minimal sur l'activité anti-BST-2 de Vpu, cette étude a également révélé qu'un traitement combinant le pevonedistat et l'IFNα avait un effet synergique sur l'augmentation de BST-2 et d'Env à la surface des cellules infectées (1633). En lien avec nos résultats (**articles 8 et 11**), l'association du pevonedistat avec les IFN-I ou l'IL-27 pourrait permettre de cibler les deux domaines fonctionnels principaux de Vpu (son motif phosphosérine et son TMD) et ainsi affecter la régulation négative de CD4, BST-2, NTB-A et PVR simultanément, ce qui aurait comme effet d'augmenter considérablement la reconnaissance et la susceptibilité des cellules infectées à la réponse ADCC médiée par les nnAbs.

7.7 Conclusions

Les travaux présentés dans cette thèse ont permis d'établir que la conformation de l'Env du VIH-1 est le déterminant majeur dictant la susceptibilité des cellules infectées à la réponse ADCC. L'adoption de la conformation « ouverte » d'Env permet l'exposition d'épitopes conservés reconnus par les nnAbs présents chez les individus infectées ou vaccinés. Toutefois, la majorité des souches du VIH-1 en circulation préviennent la reconnaissance des cellules infectées par les nnAbs en stabilisant la conformation « fermée » d'Env grâce à ses domaines structuraux hautement conservés et à la dégradation du récepteur CD4 par les protéines accessoires Nef et Vpu. Cependant, la présence de polymorphismes naturels chez certaines souches du virus peut altérer la conformation d'Env et ainsi augmenter leur susceptibilité à la réponse ADCC, ce qui apporte une explication plausible à la modeste protection observée dans le seul essai vaccinal efficace contre la transmission du VIH-1. L'évasion de la réponse humorale dépend également de la capacité de Vpu à limiter les niveaux d'Env présents à la surface des cellules infectées et à réguler l'expression de ligands activateurs des cellules effectrices. Au courant de ces études, nous

avons développé des stratégies efficaces afin de contourner ces mécanismes viraux d'évasion immunitaire, notamment via l'utilisation de CD4mc capable d'induire l'adoption de la conformation « ouverte » d'Env et de cytokines capables d'affecter la polyfonctionnalité de Vpu. Ces résultats représentent des avancées majeures pour le développement d'approches immunothérapeutiques afin d'éradiquer les réservoirs viraux et dans l'optique d'une guérison fonctionnelle de l'infection par le VIH-1.

CHAPITRE VIII - RÉFÉRENCES

RÉFÉRENCES

1. Taubenberger JK, Morens DM. 1918 Influenza: the mother of all pandemics. Emerg Infect Dis. 2006;12(1):15-22.
2. Global HIV & AIDS statistics — Fact sheet 2021. Geneva, Switzerland: Joint United Nations Programme on HIV/AIDS (UNAIDS); 2021 [Available from: https://www.unaids.org/sites/default/files/media_asset/JC3032_AIDS_Data_book_2021_En.pdf.
3. Coronavirus Resource Center Baltimore, MD, USA: Center for Systems Science and Engineering (CSSE) at Johns Hopkins University (JHU); 2022 [Available from: https://coronavirus.jhu.edu/.
4. 90–90–90 - An ambitious treatment target to help end the AIDS epidemic Geneva, Switzerland: Joint United Nations Programme on HIV/AIDS (UNAIDS); 2014 [Available from: https://www.unaids.org/sites/default/files/media_asset/90-90-90_en.pdf.
5. Levi J, Raymond A, Pozniak A, Vernazza P, Kohler P, Hill A. Can the UNAIDS 90-90-90 target be achieved? A systematic analysis of national HIV treatment cascades. BMJ Glob Health. 2016;1(2):e000010.
6. Marsh K, Eaton JW, Mahy M, Sabin K, Autenrieth CS, Wanyeki I, et al. Global, regional and country-level 90-90-90 estimates for 2018: assessing progress towards the 2020 target. AIDS. 2019;33 Suppl 3:S213-S26.
7. Understanding Fast-Track: accelerating action to end the AIDS epidemic by 2030 Geneva, Switzerland: Joint United Nations Programme on HIV/AIDS (UNAIDS); 2015 [Available from: https://www.unaids.org/sites/default/files/media_asset/201506_JC2743_Understanding_FastTrack_en.pdf.
8. Heath K, Levi J, Hill A. The Joint United Nations Programme on HIV/AIDS 95-95-95 targets: worldwide clinical and cost benefits of generic manufacture. AIDS. 2021;35(Suppl 2):S197-S203.
9. Lebelonyane R, Bachanas P, Block L, Ussery F, Alwano MG, Marukutira T, et al. To achieve 95-95-95 targets we must reach men and youth: High level of knowledge of HIV status, ART coverage, and viral suppression in the Botswana Combination Prevention Project through universal test and treat approach. PLoS One. 2021;16(8):e0255227.
10. Cohen MS, Shaw GM, McMichael AJ, Haynes BF. Acute HIV-1 Infection. N Engl J Med. 2011;364(20):1943-54.
11. Hladik F, McElrath MJ. Setting the stage: host invasion by HIV. Nat Rev Immunol. 2008;8(6):447-57.
12. Irungu EM, Mugwanya KK, Mugo NR, Bukusi EA, Donnell D, Odoyo J, et al. Integration of pre-exposure prophylaxis services into public HIV care clinics in Kenya: a pragmatic stepped-wedge randomised trial. Lancet Glob Health. 2021;9(12):e1730-e9.
13. Irungu EM, Baeten JM. PrEP rollout in Africa: status and opportunity. Nat Med. 2020;26(5):655-64.
14. Cork MA, Wilson KF, Perkins S, Collison ML, Deshpande A, Eaton JW, et al. Mapping male circumcision for HIV prevention efforts in sub-Saharan Africa. BMC Med. 2020;18(1):189.
15. Mashaphu S, Wyatt GE, Zhang M, Liu H. Condom use consistency among South African HIV serodiscordant couples following an HIV risk-reduction intervention. Int J STD AIDS. 2022:9564624221076617.

16. Johnson LF, Meyer-Rath G, Dorrington RE, Puren A, Seathlodi T, Zuma K, et al. The effect of HIV programmes in South Africa on national HIV incidence trends, 2000-2019. J Acquir Immune Defic Syndr. 2022.
17. Guaraldi G, Borghi V, Milic J, Carli F, Cuomo G, Menozzi M, et al. The Impact of COVID-19 on UNAIDS 90-90-90 Targets: Calls for New HIV Care Models. Open Forum Infect Dis. 2021;8(7):ofab283.
18. Moitra E, Tao J, Olsen J, Shearer RD, Wood BR, Busch AM, et al. Impact of the COVID-19 pandemic on HIV testing rates across four geographically diverse urban centres in the United States: An observational study. Lancet Reg Health Am. 2022;7:100159.
19. Simoes D, Stengaard AR, Combs L, Raben D, Euro TC-iacop. Impact of the COVID-19 pandemic on testing services for HIV, viral hepatitis and sexually transmitted infections in the WHO European Region, March to August 2020. Euro Surveill. 2020;25(47).
20. Wagner Z, Mukasa B, Nakakande J, Stecher C, Saya U, Linnemayr S. Impact of the COVID-19 Pandemic on Use of HIV Care, Antiretroviral Therapy Adherence, and Viral Suppression: An Observational Cohort Study From Uganda. J Acquir Immune Defic Syndr. 2021;88(5):448-56.
21. Shi L, Tang W, Hu H, Qiu T, Marley G, Liu X, et al. The impact of COVID-19 pandemic on HIV care continuum in Jiangsu, China. BMC Infect Dis. 2021;21(1):768.
22. Harris TG, Jaszi E, Lamb MR, Laudari CA, Furtado MLM, Nijirazana B, et al. Effects of the COVID-19 Pandemic on HIV Services: Findings from 11 Sub-Saharan African Countries. Clin Infect Dis. 2021.
23. Hajizadeh M, Sia D, Heymann SJ, Nandi A. Socioeconomic inequalities in HIV/AIDS prevalence in sub-Saharan African countries: evidence from the Demographic Health Surveys. Int J Equity Health. 2014;13:18.
24. Kavanagh MM, Agbla SC, Joy M, Aneja K, Pillinger M, Case A, et al. Law, criminalisation and HIV in the world: have countries that criminalise achieved more or less successful pandemic response? BMJ Glob Health. 2021;6(8).
25. Bernard EJ, Beyrer C, Cameron E, Clayton M, Volgina A. Ending unjust HIV criminalization: leave no-one behind. J Int AIDS Soc. 2021;24(2):e25681.
26. Mahajan AP, Sayles JN, Patel VA, Remien RH, Sawires SR, Ortiz DJ, et al. Stigma in the HIV/AIDS epidemic: a review of the literature and recommendations for the way forward. AIDS. 2008;22 Suppl 2:S67-79.
27. Bonnington O, Wamoyi J, Ddaaki W, Bukenya D, Ondenge K, Skovdal M, et al. Changing forms of HIV-related stigma along the HIV care and treatment continuum in sub-Saharan Africa: a temporal analysis. Sex Transm Infect. 2017;93(Suppl 3).
28. Centers for Disease C. Kaposi's sarcoma and Pneumocystis pneumonia among homosexual men--New York City and California. MMWR Morb Mortal Wkly Rep. 1981;30(25):305-8.
29. Gottlieb MS, Schroff R, Schanker HM, Weisman JD, Fan PT, Wolf RA, et al. Pneumocystis carinii pneumonia and mucosal candidiasis in previously healthy homosexual men: evidence of a new acquired cellular immunodeficiency. N Engl J Med. 1981;305(24):1425-31.
30. Siegal FP, Lopez C, Hammer GS, Brown AE, Kornfeld SJ, Gold J, et al. Severe acquired immunodeficiency in male homosexuals, manifested by chronic perianal ulcerative herpes simplex lesions. N Engl J Med. 1981;305(24):1439-44.
31. Centers for Disease C. Possible transfusion-associated acquired immune deficiency syndrome (AIDS) - California. MMWR Morb Mortal Wkly Rep. 1982;31(48):652-4.

32. Centers for Disease C. Update on acquired immune deficiency syndrome (AIDS) among patients with hemophilia A. MMWR Morb Mortal Wkly Rep. 1982;31(48):644-6, 52.
33. Hardy AM, Allen JR, Morgan WM, Curran JW. The incidence rate of acquired immunodeficiency syndrome in selected populations. JAMA. 1985;253(2):215-20.
34. Barre-Sinoussi F, Chermann JC, Rey F, Nugeyre MT, Chamaret S, Gruest J, et al. Isolation of a T-lymphotropic retrovirus from a patient at risk for acquired immune deficiency syndrome (AIDS). Science. 1983;220(4599):868-71.
35. Gallo RC, Salahuddin SZ, Popovic M, Shearer GM, Kaplan M, Haynes BF, et al. Frequent detection and isolation of cytopathic retroviruses (HTLV-III) from patients with AIDS and at risk for AIDS. Science. 1984;224(4648):500-3.
36. Popovic M, Sarngadharan MG, Read E, Gallo RC. Detection, isolation, and continuous production of cytopathic retroviruses (HTLV-III) from patients with AIDS and pre-AIDS. Science. 1984;224(4648):497-500.
37. Shaw GM, Hahn BH, Arya SK, Groopman JE, Gallo RC, Wong-Staal F. Molecular characterization of human T-cell leukemia (lymphotropic) virus type III in the acquired immune deficiency syndrome. Science. 1984;226(4679):1165-71.
38. Brown F, for the International Committee on Taxonomy of Viruses. AIDS virus nomenclature. Nature. 1986;321(6071):644.
39. Barin F, M'Boup S, Denis F, Kanki P, Allan JS, Lee TH, et al. Serological evidence for virus related to simian T-lymphotropic retrovirus III in residents of west Africa. Lancet. 1985;2(8469-70):1387-9.
40. Clavel F, Guetard D, Brun-Vezinet F, Chamaret S, Rey MA, Santos-Ferreira MO, et al. Isolation of a new human retrovirus from West African patients with AIDS. Science. 1986;233(4761):343-6.
41. Schupbach J, Popovic M, Gilden RV, Gonda MA, Sarngadharan MG, Gallo RC. Serological analysis of a subgroup of human T-lymphotropic retroviruses (HTLV-III) associated with AIDS. Science. 1984;224(4648):503-5.
42. Sarngadharan MG, Popovic M, Bruch L, Schupbach J, Gallo RC. Antibodies reactive with human T-lymphotropic retroviruses (HTLV-III) in the serum of patients with AIDS. Science. 1984;224(4648):506-8.
43. Brun-Vezinet F, Rouzioux C, Barre-Sinoussi F, Klatzmann D, Saimot AG, Rozenbaum W, et al. Detection of IgG antibodies to lymphadenopathy-associated virus in patients with AIDS or lymphadenopathy syndrome. Lancet. 1984;1(8389):1253-6.
44. Goedert JJ, Gallo RC. Epidemiological evidence that HTLV-III is the AIDS agent. Eur J Epidemiol. 1985;1(3):155-9.
45. Stankaitis JA, Bigos JP. HTLV III/LAV screening and blood banking. Am J Public Health. 1987;77(2):239.
46. Hahn BH, Shaw GM, Arya SK, Popovic M, Gallo RC, Wong-Staal F. Molecular cloning and characterization of the HTLV-III virus associated with AIDS. Nature. 1984;312(5990):166-9.
47. Luciw PA, Potter SJ, Steimer K, Dina D, Levy JA. Molecular cloning of AIDS-associated retrovirus. Nature. 1984;312(5996):760-3.
48. Alizon M, Sonigo P, Barre-Sinoussi F, Chermann JC, Tiollais P, Montagnier L, et al. Molecular cloning of lymphadenopathy-associated virus. Nature. 1984;312(5996):757-60.
49. Wain-Hobson S, Sonigo P, Danos O, Cole S, Alizon M. Nucleotide sequence of the AIDS virus, LAV. Cell. 1985;40(1):9-17.

50. Rabson AB, Martin MA. Molecular organization of the AIDS retrovirus. Cell. 1985;40(3):477-80.
51. Mitsuya H, Weinhold KJ, Furman PA, St Clair MH, Lehrman SN, Gallo RC, et al. 3'-Azido-3'-deoxythymidine (BW A509U): an antiviral agent that inhibits the infectivity and cytopathic effect of human T-lymphotropic virus type III/lymphadenopathy-associated virus in vitro. Proc Natl Acad Sci U S A. 1985;82(20):7096-100.
52. Yarchoan R, Klecker RW, Weinhold KJ, Markham PD, Lyerly HK, Durack DT, et al. Administration of 3'-azido-3'-deoxythymidine, an inhibitor of HTLV-III/LAV replication, to patients with AIDS or AIDS-related complex. Lancet. 1986;1(8481):575-80.
53. Yarchoan R, Mitsuya H, Thomas RV, Pluda JM, Hartman NR, Perno CF, et al. In vivo activity against HIV and favorable toxicity profile of 2',3'-dideoxyinosine. Science. 1989;245(4916):412-5.
54. van Leeuwen R, Lange JM, Hussey EK, Donn KH, Hall ST, Harker AJ, et al. The safety and pharmacokinetics of a reverse transcriptase inhibitor, 3TC, in patients with HIV infection: a phase I study. AIDS. 1992;6(12):1471-5.
55. Havlir D, Cheeseman SH, McLaughlin M, Murphy R, Erice A, Spector SA, et al. High-dose nevirapine: safety, pharmacokinetics, and antiviral effect in patients with human immunodeficiency virus infection. J Infect Dis. 1995;171(3):537-45.
56. Kitchen VS, Skinner C, Ariyoshi K, Lane EA, Duncan IB, Burckhardt J, et al. Safety and activity of saquinavir in HIV infection. Lancet. 1995;345(8955):952-5.
57. Markowitz M, Saag M, Powderly WG, Hurley AM, Hsu A, Valdes JM, et al. A preliminary study of ritonavir, an inhibitor of HIV-1 protease, to treat HIV-1 infection. N Engl J Med. 1995;333(23):1534-9.
58. Collier AC, Coombs RW, Fischl MA, Skolnik PR, Northfelt D, Boutin P, et al. Combination therapy with zidovudine and didanosine compared with zidovudine alone in HIV-1 infection. Ann Intern Med. 1993;119(8):786-93.
59. Yarchoan R, Lietzau JA, Nguyen BY, Brawley OW, Pluda JM, Saville MW, et al. A randomized pilot study of alternating or simultaneous zidovudine and didanosine therapy in patients with symptomatic human immunodeficiency virus infection. J Infect Dis. 1994;169(1):9-17.
60. Hammer SM, Katzenstein DA, Hughes MD, Gundacker H, Schooley RT, Haubrich RH, et al. A trial comparing nucleoside monotherapy with combination therapy in HIV-infected adults with CD4 cell counts from 200 to 500 per cubic millimeter. AIDS Clinical Trials Group Study 175 Study Team. N Engl J Med. 1996;335(15):1081-90.
61. Delta: a randomised double-blind controlled trial comparing combinations of zidovudine plus didanosine or zalcitabine with zidovudine alone in HIV-infected individuals. Delta Coordinating Committee. Lancet. 1996;348(9023):283-91.
62. D'Aquila RT, Hughes MD, Johnson VA, Fischl MA, Sommadossi JP, Liou SH, et al. Nevirapine, zidovudine, and didanosine compared with zidovudine and didanosine in patients with HIV-1 infection. A randomized, double-blind, placebo-controlled trial. National Institute of Allergy and Infectious Diseases AIDS Clinical Trials Group Protocol 241 Investigators. Ann Intern Med. 1996;124(12):1019-30.
63. Collier AC, Coombs RW, Schoenfeld DA, Bassett RL, Timpone J, Baruch A, et al. Treatment of human immunodeficiency virus infection with saquinavir, zidovudine, and zalcitabine. AIDS Clinical Trials Group. N Engl J Med. 1996;334(16):1011-7.

64. Gulick RM, Mellors JW, Havlir D, Eron JJ, Gonzalez C, McMahon D, et al. Treatment with indinavir, zidovudine, and lamivudine in adults with human immunodeficiency virus infection and prior antiretroviral therapy. N Engl J Med. 1997;337(11):734-9.
65. LeMessurier J, Traversy G, Varsaneux O, Weekes M, Avey MT, Niragira O, et al. Risk of sexual transmission of human immunodeficiency virus with antiretroviral therapy, suppressed viral load and condom use: a systematic review. CMAJ. 2018;190(46):E1350-E60.
66. Cohen MS, Chen YQ, McCauley M, Gamble T, Hosseinipour MC, Kumarasamy N, et al. Prevention of HIV-1 infection with early antiretroviral therapy. N Engl J Med. 2011;365(6):493-505.
67. Grant RM, Lama JR, Anderson PL, McMahan V, Liu AY, Vargas L, et al. Preexposure chemoprophylaxis for HIV prevention in men who have sex with men. N Engl J Med. 2010;363(27):2587-99.
68. Baeten JM, Donnell D, Ndase P, Mugo NR, Campbell JD, Wangisi J, et al. Antiretroviral prophylaxis for HIV prevention in heterosexual men and women. N Engl J Med. 2012;367(5):399-410.
69. Thigpen MC, Kebaabetswe PM, Paxton LA, Smith DK, Rose CE, Segolodi TM, et al. Antiretroviral preexposure prophylaxis for heterosexual HIV transmission in Botswana. N Engl J Med. 2012;367(5):423-34.
70. Molina JM, Charreau I, Spire B, Cotte L, Chas J, Capitant C, et al. Efficacy, safety, and effect on sexual behaviour of on-demand pre-exposure prophylaxis for HIV in men who have sex with men: an observational cohort study. Lancet HIV. 2017;4(9):e402-e10.
71. McCormack S, Dunn DT, Desai M, Dolling DI, Gafos M, Gilson R, et al. Pre-exposure prophylaxis to prevent the acquisition of HIV-1 infection (PROUD): effectiveness results from the pilot phase of a pragmatic open-label randomised trial. Lancet. 2016;387(10013):53-60.
72. Francis DP, Gregory T, McElrath MJ, Belshe RB, Gorse GJ, Migasena S, et al. Advancing AIDSVAX to phase 3. Safety, immunogenicity, and plans for phase 3. AIDS Res Hum Retroviruses. 1998;14 Suppl 3:S325-31.
73. Berman PW, Huang W, Riddle L, Gray AM, Wrin T, Vennari J, et al. Development of bivalent (B/E) vaccines able to neutralize CCR5-dependent viruses from the United States and Thailand. Virology. 1999;265(1):1-9.
74. Flynn NM, Forthal DN, Harro CD, Judson FN, Mayer KH, Para MF, et al. Placebo-controlled phase 3 trial of a recombinant glycoprotein 120 vaccine to prevent HIV-1 infection. J Infect Dis. 2005;191(5):654-65.
75. Pitisuttithum P, Gilbert P, Gurwith M, Heyward W, Martin M, van Griensven F, et al. Randomized, double-blind, placebo-controlled efficacy trial of a bivalent recombinant glycoprotein 120 HIV-1 vaccine among injection drug users in Bangkok, Thailand. J Infect Dis. 2006;194(12):1661-71.
76. Buchbinder SP, Mehrotra DV, Duerr A, Fitzgerald DW, Mogg R, Li D, et al. Efficacy assessment of a cell-mediated immunity HIV-1 vaccine (the Step Study): a double-blind, randomised, placebo-controlled, test-of-concept trial. Lancet. 2008;372(9653):1881-93.
77. Gray GE, Allen M, Moodie Z, Churchyard G, Bekker LG, Nchabeleng M, et al. Safety and efficacy of the HVTN 503/Phambili study of a clade-B-based HIV-1 vaccine in South Africa: a double-blind, randomised, placebo-controlled test-of-concept phase 2b study. Lancet Infect Dis. 2011;11(7):507-15.

78. Rerks-Ngarm S, Pitisuttithum P, Nitayaphan S, Kaewkungwal J, Chiu J, Paris R, et al. Vaccination with ALVAC and AIDSVAX to prevent HIV-1 infection in Thailand. N Engl J Med. 2009;361(23):2209-20.
79. Hutter G, Nowak D, Mossner M, Ganepola S, Mussig A, Allers K, et al. Long-term control of HIV by CCR5 Delta32/Delta32 stem-cell transplantation. N Engl J Med. 2009;360(7):692-8.
80. Allers K, Hutter G, Hofmann J, Loddenkemper C, Rieger K, Thiel E, et al. Evidence for the cure of HIV infection by CCR5Delta32/Delta32 stem cell transplantation. Blood. 2011;117(10):2791-9.
81. Gupta RK, Abdul-Jawad S, McCoy LE, Mok HP, Peppa D, Salgado M, et al. HIV-1 remission following CCR5Delta32/Delta32 haematopoietic stem-cell transplantation. Nature. 2019;568(7751):244-8.
82. Jensen BEO, Knops E, Lübke N, Wensing A, Martinez-Picado J, Kaiser R, et al. Analytic treatment interruption (ATI) after allogeneic CCR5-Δ32 HSCT for AML in 2013 [CROI Abstract 394]. In Special Issue: Abstracts From the 2019 Conference on Retroviruses and Opportunistic Infections, Top Antiv Med. 2019;27(1s):141.
83. Hsu JM, Van Besien K, Glesby MJ, Coletti A, Pahwa SG, Warshaw M, et al. HIV-1 Remission with CCR5Δ32Δ32 Haplo-Cord Transplant in a U.S. Woman: IMPAACT P1107 [CROI Abstract 65]. In Special Issue: Abstracts From the 2022 Conference on Retroviruses and Opportunistic Infections, Top Antiv Med. 2022;30(1s):11.
84. Baltimore D. RNA-dependent DNA polymerase in virions of RNA tumour viruses. Nature. 1970;226(5252):1209-11.
85. Mizutani S, Boettiger D, Temin HM. A DNA-depenent DNA polymerase and a DNA endonuclease in virions of Rous sarcoma virus. Nature. 1970;228(5270):424-7.
86. Panganiban AT, Temin HM. The retrovirus pol gene encodes a product required for DNA integration: identification of a retrovirus int locus. Proc Natl Acad Sci U S A. 1984;81(24):7885-9.
87. Schwartzberg P, Colicelli J, Goff SP. Construction and analysis of deletion mutations in the pol gene of Moloney murine leukemia virus: a new viral function required for productive infection. Cell. 1984;37(3):1043-52.
88. Elangovan R, Jenks M, Yun J, Dickson-Tetteh L, Kirtley S, Hemelaar J, et al. Global and Regional Estimates for Subtype-Specific Therapeutic and Prophylactic HIV-1 Vaccines: A Modeling Study. Front Microbiol. 2021;12:690647.
89. Visseaux B, Damond F, Matheron S, Descamps D, Charpentier C. Hiv-2 molecular epidemiology. Infect Genet Evol. 2016;46:233-40.
90. Kanki PJ, Travers KU, S MB, Hsieh CC, Marlink RG, Gueye NA, et al. Slower heterosexual spread of HIV-2 than HIV-1. Lancet. 1994;343(8903):943-6.
91. Popper SJ, Sarr AD, Travers KU, Gueye-Ndiaye A, Mboup S, Essex ME, et al. Lower human immunodeficiency virus (HIV) type 2 viral load reflects the difference in pathogenicity of HIV-1 and HIV-2. J Infect Dis. 1999;180(4):1116-21.
92. Gilbert PB, McKeague IW, Eisen G, Mullins C, Gueye NA, Mboup S, et al. Comparison of HIV-1 and HIV-2 infectivity from a prospective cohort study in Senegal. Stat Med. 2003;22(4):573-93.
93. van der Loeff MF, Larke N, Kaye S, Berry N, Ariyoshi K, Alabi A, et al. Undetectable plasma viral load predicts normal survival in HIV-2-infected people in a West African village. Retrovirology. 2010;7:46.

94. Esbjornsson J, Mansson F, Kvist A, da Silva ZJ, Andersson S, Fenyo EM, et al. Long-term follow-up of HIV-2-related AIDS and mortality in Guinea-Bissau: a prospective open cohort study. Lancet HIV. 2018.
95. Daniel MD, Letvin NL, King NW, Kannagi M, Sehgal PK, Hunt RD, et al. Isolation of T-cell tropic HTLV-III-like retrovirus from macaques. Science. 1985;228(4704):1201-4.
96. VandeWoude S, Apetrei C. Going wild: lessons from naturally occurring T-lymphotropic lentiviruses. Clin Microbiol Rev. 2006;19(4):728-62.
97. Sharp PM, Hahn BH. Origins of HIV and the AIDS pandemic. Cold Spring Harb Perspect Med. 2011;1(1):a006841.
98. Bell SM, Bedford T. Modern-day SIV viral diversity generated by extensive recombination and cross-species transmission. PLoS Pathog. 2017;13(7):e1006466.
99. Keele BF, Van Heuverswyn F, Li Y, Bailes E, Takehisa J, Santiago ML, et al. Chimpanzee reservoirs of pandemic and nonpandemic HIV-1. Science. 2006;313(5786):523-6.
100. Rey-Cuille MA, Berthier JL, Bomsel-Demontoy MC, Chaduc Y, Montagnier L, Hovanessian AG, et al. Simian immunodeficiency virus replicates to high levels in sooty mangabeys without inducing disease. J Virol. 1998;72(5):3872-86.
101. Silvestri G, Sodora DL, Koup RA, Paiardini M, O'Neil SP, McClure HM, et al. Nonpathogenic SIV infection of sooty mangabeys is characterized by limited bystander immunopathology despite chronic high-level viremia. Immunity. 2003;18(3):441-52.
102. Goldstein S, Brown CR, Ourmanov I, Pandrea I, Buckler-White A, Erb C, et al. Comparison of simian immunodeficiency virus SIVagmVer replication and CD4+ T-cell dynamics in vervet and sabaeus African green monkeys. J Virol. 2006;80(10):4868-77.
103. Pandrea I, Silvestri G, Onanga R, Veazey RS, Marx PA, Hirsch V, et al. Simian immunodeficiency viruses replication dynamics in African non-human primate hosts: common patterns and species-specific differences. J Med Primatol. 2006;35(4-5):194-201.
104. Apetrei C, Sumpter B, Souquiere S, Chahroudi A, Makuwa M, Reed P, et al. Immunovirological analyses of chronically simian immunodeficiency virus SIVmnd-1- and SIVmnd-2-infected mandrills (Mandrillus sphinx). J Virol. 2011;85(24):13077-87.
105. Gao F, Bailes E, Robertson DL, Chen Y, Rodenburg CM, Michael SF, et al. Origin of HIV-1 in the chimpanzee Pan troglodytes troglodytes. Nature. 1999;397(6718):436-41.
106. Worobey M, Gemmel M, Teuwen DE, Haselkorn T, Kunstman K, Bunce M, et al. Direct evidence of extensive diversity of HIV-1 in Kinshasa by 1960. Nature. 2008;455(7213):661-4.
107. Faria NR, Rambaut A, Suchard MA, Baele G, Bedford T, Ward MJ, et al. HIV epidemiology. The early spread and epidemic ignition of HIV-1 in human populations. Science. 2014;346(6205):56-61.
108. D'Arc M, Ayouba A, Esteban A, Learn GH, Boue V, Liegeois F, et al. Origin of the HIV-1 group O epidemic in western lowland gorillas. Proc Natl Acad Sci U S A. 2015;112(11):E1343-52.
109. Takehisa J, Kraus MH, Ayouba A, Bailes E, Van Heuverswyn F, Decker JM, et al. Origin and biology of simian immunodeficiency virus in wild-living western gorillas. J Virol. 2009;83(4):1635-48.
110. Van Heuverswyn F, Li Y, Neel C, Bailes E, Keele BF, Liu W, et al. Human immunodeficiency viruses: SIV infection in wild gorillas. Nature. 2006;444(7116):164.
111. Plantier JC, Leoz M, Dickerson JE, De Oliveira F, Cordonnier F, Lemee V, et al. A new human immunodeficiency virus derived from gorillas. Nat Med. 2009;15(8):871-2.

112. Bailes E, Gao F, Bibollet-Ruche F, Courgnaud V, Peeters M, Marx PA, et al. Hybrid origin of SIV in chimpanzees. Science. 2003;300(5626):1713.
113. Ayouba A, Akoua-Koffi C, Calvignac-Spencer S, Esteban A, Locatelli S, Li H, et al. Evidence for continuing cross-species transmission of SIVsmm to humans: characterization of a new HIV-2 lineage in rural Cote d'Ivoire. AIDS. 2013;27(15):2488-91.
114. Apetrei C, Kaur A, Lerche NW, Metzger M, Pandrea I, Hardcastle J, et al. Molecular epidemiology of simian immunodeficiency virus SIVsm in U.S. primate centers unravels the origin of SIVmac and SIVstm. J Virol. 2005;79(14):8991-9005.
115. Thippeshappa R, Kimata JT, Kaushal D. Toward a Macaque Model of HIV-1 Infection: Roadblocks, Progress, and Future Strategies. Front Microbiol. 2020;11:882.
116. Robertson DL, Anderson JP, Bradac JA, Carr JK, Foley B, Funkhouser RK, et al. HIV-1 nomenclature proposal. Science. 2000;288(5463):55-6.
117. Hemelaar J, Elangovan R, Yun J, Dickson-Tetteh L, Fleminger I, Kirtley S, et al. Global and regional molecular epidemiology of HIV-1, 1990-2015: a systematic review, global survey, and trend analysis. Lancet Infect Dis. 2019;19(2):143-55.
118. Gray RR, Tatem AJ, Lamers S, Hou W, Laeyendecker O, Serwadda D, et al. Spatial phylodynamics of HIV-1 epidemic emergence in east Africa. AIDS. 2009;23(14):F9-F17.
119. Wilkinson E, Engelbrecht S, de Oliveira T. History and origin of the HIV-1 subtype C epidemic in South Africa and the greater southern African region. Sci Rep. 2015;5:16897.
120. Shen C, Craigo J, Ding M, Chen Y, Gupta P. Origin and dynamics of HIV-1 subtype C infection in India. PLoS One. 2011;6(10):e25956.
121. Gilbert MT, Rambaut A, Wlasiuk G, Spira TJ, Pitchenik AE, Worobey M. The emergence of HIV/AIDS in the Americas and beyond. Proc Natl Acad Sci U S A. 2007;104(47):18566-70.
122. Delatorre E, Mir D, Bello G. Spatiotemporal dynamics of the HIV-1 subtype G epidemic in West and Central Africa. PLoS One. 2014;9(2):e98908.
123. Han C, Johnson J, Dong R, Kandula R, Kort A, Wong M, et al. Key Positions of HIV-1 Env and Signatures of Vaccine Efficacy Show Gradual Reduction of Population Founder Effects at the Clade and Regional Levels. mBio. 2020;11(3).
124. Li X, Liu H, Liu L, Feng Y, Kalish ML, Ho SYW, et al. Tracing the epidemic history of HIV-1 CRF01_AE clusters using near-complete genome sequences. Sci Rep. 2017;7(1):4024.
125. An M, Han X, Zhao B, English S, Frost SDW, Zhang H, et al. Cross-Continental Dispersal of Major HIV-1 CRF01_AE Clusters in China. Front Microbiol. 2020;11:61.
126. Mir D, Jung M, Delatorre E, Vidal N, Peeters M, Bello G. Phylodynamics of the major HIV-1 CRF02_AG African lineages and its global dissemination. Infect Genet Evol. 2016;46:190-9.
127. Ge Z, Feng Y, Zhang H, Rashid A, Zaongo SD, Li K, et al. HIV-1 CRF07_BC transmission dynamics in China: two decades of national molecular surveillance. Emerg Microbes Infect. 2021;10(1):1919-30.
128. Korber B, B. T. Foley, C. Kuiken, S. K. Pillai, J. G. Sodroski. Numbering Positions in HIV Relative to HXB2CG. Human Retroviruses and AIDS. 1998;pp. III:102-11.
129. Nikolaitchik OA, Dilley KA, Fu W, Gorelick RJ, Tai SH, Soheilian F, et al. Dimeric RNA recognition regulates HIV-1 genome packaging. PLoS Pathog. 2013;9(3):e1003249.
130. Mansky LM, Temin HM. Lower in vivo mutation rate of human immunodeficiency virus type 1 than that predicted from the fidelity of purified reverse transcriptase. J Virol. 1995;69(8):5087-94.

131. Kumar M, Keller B, Makalou N, Sutton RE. Systematic determination of the packaging limit of lentiviral vectors. Hum Gene Ther. 2001;12(15):1893-905.
132. Tripathi K, Balagam R, Vishnoi NK, Dixit NM. Stochastic simulations suggest that HIV-1 survives close to its error threshold. PLoS Comput Biol. 2012;8(9):e1002684.
133. Purcell DF, Martin MA. Alternative splicing of human immunodeficiency virus type 1 mRNA modulates viral protein expression, replication, and infectivity. J Virol. 1993;67(11):6365-78.
134. Fernandes JD, Faust TB, Strauli NB, Smith C, Crosby DC, Nakamura RL, et al. Functional Segregation of Overlapping Genes in HIV. Cell. 2016;167(7):1762-73 e12.
135. Ho JSY, Zhu Z, Marazzi I. Unconventional viral gene expression mechanisms as therapeutic targets. Nature. 2021;593(7859):362-71.
136. Chiu YL, Ho CK, Saha N, Schwer B, Shuman S, Rana TM. Tat stimulates cotranscriptional capping of HIV mRNA. Mol Cell. 2002;10(3):585-97.
137. Brown PH, Tiley LS, Cullen BR. Efficient polyadenylation within the human immunodeficiency virus type 1 long terminal repeat requires flanking U3-specific sequences. J Virol. 1991;65(6):3340-3.
138. Hu WS, Hughes SH. HIV-1 reverse transcription. Cold Spring Harb Perspect Med. 2012;2(10).
139. Erickson-Viitanen S, Manfredi J, Viitanen P, Tribe DE, Tritch R, Hutchison CA, 3rd, et al. Cleavage of HIV-1 gag polyprotein synthesized in vitro: sequential cleavage by the viral protease. AIDS Res Hum Retroviruses. 1989;5(6):577-91.
140. Louis JM, Wondrak EM, Kimmel AR, Wingfield PT, Nashed NT. Proteolytic processing of HIV-1 protease precursor, kinetics and mechanism. J Biol Chem. 1999;274(33):23437-42.
141. McCune JM, Rabin LB, Feinberg MB, Lieberman M, Kosek JC, Reyes GR, et al. Endoproteolytic cleavage of gp160 is required for the activation of human immunodeficiency virus. Cell. 1988;53(1):55-67.
142. Mattei S, Tan A, Glass B, Muller B, Krausslich HG, Briggs JAG. High-resolution structures of HIV-1 Gag cleavage mutants determine structural switch for virus maturation. Proc Natl Acad Sci U S A. 2018;115(40):E9401-E10.
143. Krausslich HG, Facke M, Heuser AM, Konvalinka J, Zentgraf H. The spacer peptide between human immunodeficiency virus capsid and nucleocapsid proteins is essential for ordered assembly and viral infectivity. J Virol. 1995;69(6):3407-19.
144. de Marco A, Heuser AM, Glass B, Krausslich HG, Muller B, Briggs JA. Role of the SP2 domain and its proteolytic cleavage in HIV-1 structural maturation and infectivity. J Virol. 2012;86(24):13708-16.
145. Jacks T, Power MD, Masiarz FR, Luciw PA, Barr PJ, Varmus HE. Characterization of ribosomal frameshifting in HIV-1 gag-pol expression. Nature. 1988;331(6153):280-3.
146. Park J, Morrow CD. The nonmyristylated Pr160gag-pol polyprotein of human immunodeficiency virus type 1 interacts with Pr55gag and is incorporated into viruslike particles. J Virol. 1992;66(11):6304-13.
147. Allan JS, Coligan JE, Barin F, McLane MF, Sodroski JG, Rosen CA, et al. Major glycoprotein antigens that induce antibodies in AIDS patients are encoded by HTLV-III. Science. 1985;228(4703):1091-4.
148. Sodroski J, Patarca R, Rosen C, Wong-Staal F, Haseltine W. Location of the trans-activating region on the genome of human T-cell lymphotropic virus type III. Science. 1985;229(4708):74-7.

149. Sodroski J, Goh WC, Rosen C, Dayton A, Terwilliger E, Haseltine W. A second post-transcriptional trans-activator gene required for HTLV-III replication. Nature. 1986;321(6068):412-7.
150. Cohen EA, Terwilliger EF, Jalinoos Y, Proulx J, Sodroski JG, Haseltine WA. Identification of HIV-1 vpr product and function. J Acquir Immune Defic Syndr. 1990;3(1):11-8.
151. Cohen EA, Terwilliger EF, Sodroski JG, Haseltine WA. Identification of a protein encoded by the vpu gene of HIV-1. Nature. 1988;334(6182):532-4.
152. Arya SK, Gallo RC. Three novel genes of human T-lymphotropic virus type III: immune reactivity of their products with sera from acquired immune deficiency syndrome patients. Proc Natl Acad Sci U S A. 1986;83(7):2209-13.
153. Strebel K, Klimkait T, Martin MA. A novel gene of HIV-1, vpu, and its 16-kilodalton product. Science. 1988;241(4870):1221-3.
154. Guyader M, Emerman M, Sonigo P, Clavel F, Montagnier L, Alizon M. Genome organization and transactivation of the human immunodeficiency virus type 2. Nature. 1987;326(6114):662-9.
155. Briggs JA, Wilk T, Welker R, Krausslich HG, Fuller SD. Structural organization of authentic, mature HIV-1 virions and cores. EMBO J. 2003;22(7):1707-15.
156. Zhu P, Liu J, Bess J, Jr., Chertova E, Lifson JD, Grise H, et al. Distribution and three-dimensional structure of AIDS virus envelope spikes. Nature. 2006;441(7095):847-52.
157. Carlson LA, Briggs JA, Glass B, Riches JD, Simon MN, Johnson MC, et al. Three-dimensional analysis of budding sites and released virus suggests a revised model for HIV-1 morphogenesis. Cell Host Microbe. 2008;4(6):592-9.
158. Jouvenet N, Neil SJ, Bess C, Johnson MC, Virgen CA, Simon SM, et al. Plasma membrane is the site of productive HIV-1 particle assembly. PLoS Biol. 2006;4(12):e435.
159. Finzi A, Orthwein A, Mercier J, Cohen EA. Productive human immunodeficiency virus type 1 assembly takes place at the plasma membrane. J Virol. 2007;81(14):7476-90.
160. Chojnacki J, Staudt T, Glass B, Bingen P, Engelhardt J, Anders M, et al. Maturation-dependent HIV-1 surface protein redistribution revealed by fluorescence nanoscopy. Science. 2012;338(6106):524-8.
161. Zhu P, Chertova E, Bess J, Jr., Lifson JD, Arthur LO, Liu J, et al. Electron tomography analysis of envelope glycoprotein trimers on HIV and simian immunodeficiency virus virions. Proc Natl Acad Sci U S A. 2003;100(26):15812-7.
162. Mangala Prasad V, Leaman DP, Lovendahl KN, Croft JT, Benhaim MA, Hodge EA, et al. Cryo-ET of Env on intact HIV virions reveals structural variation and positioning on the Gag lattice. Cell. 2022;185(4):641-53 e17.
163. Shehu-Xhilaga M, Crowe SM, Mak J. Maintenance of the Gag/Gag-Pol ratio is important for human immunodeficiency virus type 1 RNA dimerization and viral infectivity. J Virol. 2001;75(4):1834-41.
164. Pettit SC, Sheng N, Tritch R, Erickson-Viitanen S, Swanstrom R. The regulation of sequential processing of HIV-1 Gag by the viral protease. Adv Exp Med Biol. 1998;436:15-25.
165. Qu K, Ke Z, Zila V, Anders-Osswein M, Glass B, Mucksch F, et al. Maturation of the matrix and viral membrane of HIV-1. Science. 2021;373(6555):700-4.
166. Tedbury PR, Novikova M, Ablan SD, Freed EO. Biochemical evidence of a role for matrix trimerization in HIV-1 envelope glycoprotein incorporation. Proc Natl Acad Sci U S A. 2016;113(2):E182-90.

167. Ganser BK, Li S, Klishko VY, Finch JT, Sundquist WI. Assembly and analysis of conical models for the HIV-1 core. Science. 1999;283(5398):80-3.
168. Li S, Hill CP, Sundquist WI, Finch JT. Image reconstructions of helical assemblies of the HIV-1 CA protein. Nature. 2000;407(6802):409-13.
169. Briggs JA, Simon MN, Gross I, Krausslich HG, Fuller SD, Vogt VM, et al. The stoichiometry of Gag protein in HIV-1. Nat Struct Mol Biol. 2004;11(7):672-5.
170. Pornillos O, Ganser-Pornillos BK, Yeager M. Atomic-level modelling of the HIV capsid. Nature. 2011;469(7330):424-7.
171. Feng YX, Copeland TD, Henderson LE, Gorelick RJ, Bosche WJ, Levin JG, et al. HIV-1 nucleocapsid protein induces "maturation" of dimeric retroviral RNA in vitro. Proc Natl Acad Sci U S A. 1996;93(15):7577-81.
172. De Guzman RN, Wu ZR, Stalling CC, Pappalardo L, Borer PN, Summers MF. Structure of the HIV-1 nucleocapsid protein bound to the SL3 psi-RNA recognition element. Science. 1998;279(5349):384-8.
173. Blakemore RJ, Burnett C, Swanson C, Kharytonchyk S, Telesnitsky A, Munro JB. Stability and conformation of the dimeric HIV-1 genomic RNA 5'UTR. Biophys J. 2021;120(21):4874-90.
174. Kessl JJ, Kutluay SB, Townsend D, Rebensburg S, Slaughter A, Larue RC, et al. HIV-1 Integrase Binds the Viral RNA Genome and Is Essential during Virion Morphogenesis. Cell. 2016;166(5):1257-68 e12.
175. Das K, Martinez SE, DeStefano JJ, Arnold E. Structure of HIV-1 RT/dsRNA initiation complex prior to nucleotide incorporation. Proc Natl Acad Sci U S A. 2019;116(15):7308-13.
176. Khan MA, Aberham C, Kao S, Akari H, Gorelick R, Bour S, et al. Human immunodeficiency virus type 1 Vif protein is packaged into the nucleoprotein complex through an interaction with viral genomic RNA. J Virol. 2001;75(16):7252-65.
177. Paxton W, Connor RI, Landau NR. Incorporation of Vpr into human immunodeficiency virus type 1 virions: requirement for the p6 region of gag and mutational analysis. J Virol. 1993;67(12):7229-37.
178. Kondo E, Gottlinger HG. A conserved LXXLF sequence is the major determinant in p6gag required for the incorporation of human immunodeficiency virus type 1 Vpr. J Virol. 1996;70(1):159-64.
179. Welker R, Harris M, Cardel B, Krausslich HG. Virion incorporation of human immunodeficiency virus type 1 Nef is mediated by a bipartite membrane-targeting signal: analysis of its role in enhancement of viral infectivity. J Virol. 1998;72(11):8833-40.
180. Brandenberg OF, Magnus C, Rusert P, Regoes RR, Trkola A. Different infectivity of HIV-1 strains is linked to number of envelope trimers required for entry. PLoS Pathog. 2015;11(1):e1004595.
181. Magnus C, Rusert P, Bonhoeffer S, Trkola A, Regoes RR. Estimating the stoichiometry of human immunodeficiency virus entry. J Virol. 2009;83(3):1523-31.
182. Freed EO, Myers DJ, Risser R. Mutational analysis of the cleavage sequence of the human immunodeficiency virus type 1 envelope glycoprotein precursor gp160. J Virol. 1989;63(11):4670-5.
183. Bosch V, Pawlita M. Mutational analysis of the human immunodeficiency virus type 1 env gene product proteolytic cleavage site. J Virol. 1990;64(5):2337-44.
184. Earl PL, Doms RW, Moss B. Oligomeric structure of the human immunodeficiency virus type 1 envelope glycoprotein. Proc Natl Acad Sci U S A. 1990;87(2):648-52.

185. Lyumkis D, Julien JP, de Val N, Cupo A, Potter CS, Klasse PJ, et al. Cryo-EM Structure of a Fully Glycosylated Soluble Cleaved HIV-1 Envelope Trimer. Science. 2013.
186. Julien JP, Cupo A, Sok D, Stanfield RL, Lyumkis D, Deller MC, et al. Crystal structure of a soluble cleaved HIV-1 envelope trimer. Science. 2013;342(6165):1477-83.
187. Starcich BR, Hahn BH, Shaw GM, McNeely PD, Modrow S, Wolf H, et al. Identification and characterization of conserved and variable regions in the envelope gene of HTLV-III/LAV, the retrovirus of AIDS. Cell. 1986;45(5):637-48.
188. Willey RL, Rutledge RA, Dias S, Folks T, Theodore T, Buckler CE, et al. Identification of conserved and divergent domains within the envelope gene of the acquired immunodeficiency syndrome retrovirus. Proc Natl Acad Sci U S A. 1986;83(14):5038-42.
189. Pancera M, Majeed S, Ban YE, Chen L, Huang CC, Kong L, et al. Structure of HIV-1 gp120 with gp41-interactive region reveals layered envelope architecture and basis of conformational mobility. Proc Natl Acad Sci U S A. 2010;107(3):1166-71.
190. Lee JH, Ozorowski G, Ward AB. Cryo-EM structure of a native, fully glycosylated, cleaved HIV-1 envelope trimer. Science. 2016;351(6277):1043-8.
191. Pancera M, Zhou T, Druz A, Georgiev IS, Soto C, Gorman J, et al. Structure and immune recognition of trimeric pre-fusion HIV-1 Env. Nature. 2014;514(7523):455-61.
192. Piai A, Fu Q, Cai Y, Ghantous F, Xiao T, Shaik MM, et al. Structural basis of transmembrane coupling of the HIV-1 envelope glycoprotein. Nat Commun. 2020;11(1):2317.
193. Murphy RE, Samal AB, Vlach J, Saad JS. Solution Structure and Membrane Interaction of the Cytoplasmic Tail of HIV-1 gp41 Protein. Structure. 2017;25(11):1708-18 e5.
194. Weissenhorn W, Dessen A, Harrison SC, Skehel JJ, Wiley DC. Atomic structure of the ectodomain from HIV-1 gp41. Nature. 1997;387(6631):426-30.
195. Piai A, Fu Q, Sharp AK, Bighi B, Brown AM, Chou JJ. NMR Model of the Entire Membrane-Interacting Region of the HIV-1 Fusion Protein and Its Perturbation of Membrane Morphology. J Am Chem Soc. 2021;143(17):6609-15.
196. Buzon V, Natrajan G, Schibli D, Campelo F, Kozlov MM, Weissenhorn W. Crystal structure of HIV-1 gp41 including both fusion peptide and membrane proximal external regions. PLoS Pathog. 2010;6(5):e1000880.
197. Weissenhorn W, Hinz A, Gaudin Y. Virus membrane fusion. FEBS Lett. 2007;581(11):2150-5.
198. Harrison SC. Viral membrane fusion. Nat Struct Mol Biol. 2008;15(7):690-8.
199. Patel M, Yanagishita M, Roderiquez G, Bou-Habib DC, Oravecz T, Hascall VC, et al. Cell-surface heparan sulfate proteoglycan mediates HIV-1 infection of T-cell lines. AIDS Res Hum Retroviruses. 1993;9(2):167-74.
200. Ohshiro Y, Murakami T, Matsuda K, Nishioka K, Yoshida K, Yamamoto N. Role of cell surface glycosaminoglycans of human T cells in human immunodeficiency virus type-1 (HIV-1) infection. Microbiol Immunol. 1996;40(11):827-35.
201. Saphire AC, Bobardt MD, Zhang Z, David G, Gallay PA. Syndecans serve as attachment receptors for human immunodeficiency virus type 1 on macrophages. J Virol. 2001;75(19):9187-200.
202. Geijtenbeek TB, Kwon DS, Torensma R, van Vliet SJ, van Duijnhoven GC, Middel J, et al. DC-SIGN, a dendritic cell-specific HIV-1-binding protein that enhances trans-infection of T cells. Cell. 2000;100(5):587-97.

203. Pohlmann S, Baribaud F, Lee B, Leslie GJ, Sanchez MD, Hiebenthal-Millow K, et al. DC-SIGN interactions with human immunodeficiency virus type 1 and 2 and simian immunodeficiency virus. J Virol. 2001;75(10):4664-72.
204. Pohlmann S, Soilleux EJ, Baribaud F, Leslie GJ, Morris LS, Trowsdale J, et al. DC-SIGNR, a DC-SIGN homologue expressed in endothelial cells, binds to human and simian immunodeficiency viruses and activates infection in trans. Proc Natl Acad Sci U S A. 2001;98(5):2670-5.
205. Zou Z, Chastain A, Moir S, Ford J, Trandem K, Martinelli E, et al. Siglecs facilitate HIV-1 infection of macrophages through adhesion with viral sialic acids. PLoS One. 2011;6(9):e24559.
206. Guo MM, Hildreth JE. HIV acquires functional adhesion receptors from host cells. AIDS Res Hum Retroviruses. 1995;11(9):1007-13.
207. Kondo N, Melikyan GB. Intercellular adhesion molecule 1 promotes HIV-1 attachment but not fusion to target cells. PLoS One. 2012;7(9):e44827.
208. Thibault S, Tardif MR, Gilbert C, Tremblay MJ. Virus-associated host CD62L increases attachment of human immunodeficiency virus type 1 to endothelial cells and enhances trans infection of CD4+ T lymphocytes. J Gen Virol. 2007;88(Pt 9):2568-73.
209. Li M, Ablan SD, Miao C, Zheng YM, Fuller MS, Rennert PD, et al. TIM-family proteins inhibit HIV-1 release. Proc Natl Acad Sci U S A. 2014;111(35):E3699-707.
210. Hioe CE, Bastiani L, Hildreth JE, Zolla-Pazner S. Role of cellular adhesion molecules in HIV type 1 infection and their impact on virus neutralization. AIDS Res Hum Retroviruses. 1998;14 Suppl 3:S247-54.
211. Martin-Moreno A, Munoz-Fernandez MA. Dendritic Cells, the Double Agent in the War Against HIV-1. Front Immunol. 2019;10:2485.
212. Dalgleish AG, Beverley PC, Clapham PR, Crawford DH, Greaves MF, Weiss RA. The CD4 (T4) antigen is an essential component of the receptor for the AIDS retrovirus. Nature. 1984;312(5996):763-7.
213. Klatzmann D, Champagne E, Chamaret S, Gruest J, Guetard D, Hercend T, et al. T-lymphocyte T4 molecule behaves as the receptor for human retrovirus LAV. Nature. 1984;312(5996):767-8.
214. Wu H, Kwong PD, Hendrickson WA. Dimeric association and segmental variability in the structure of human CD4. Nature. 1997;387(6632):527-30.
215. Sattentau QJ, Moore JP. Conformational changes induced in the human immunodeficiency virus envelope glycoprotein by soluble CD4 binding. J Exp Med. 1991;174(2):407-15.
216. Liu J, Bartesaghi A, Borgnia MJ, Sapiro G, Subramaniam S. Molecular architecture of native HIV-1 gp120 trimers. Nature. 2008;455(7209):109-13.
217. Munro JB, Gorman J, Ma X, Zhou Z, Arthos J, Burton DR, et al. Conformational dynamics of single HIV-1 envelope trimers on the surface of native virions. Science. 2014;346(6210):759-63.
218. Ma X, Lu M, Gorman J, Terry DS, Hong X, Zhou Z, et al. HIV-1 Env trimer opens through an asymmetric intermediate in which individual protomers adopt distinct conformations. Elife. 2018;7.
219. Kwong PD, Wyatt R, Robinson J, Sweet RW, Sodroski J, Hendrickson WA. Structure of an HIV gp120 envelope glycoprotein in complex with the CD4 receptor and a neutralizing human antibody. Nature. 1998;393(6686):648-59.

220. Ozorowski G, Pallesen J, de Val N, Lyumkis D, Cottrell CA, Torres JL, et al. Open and closed structures reveal allostery and pliability in the HIV-1 envelope spike. Nature. 2017;547(7663):360-3.
221. Wang H, Cohen AA, Galimidi RP, Gristick HB, Jensen GJ, Bjorkman PJ. Cryo-EM structure of a CD4-bound open HIV-1 envelope trimer reveals structural rearrangements of the gp120 V1V2 loop. Proc Natl Acad Sci U S A. 2016.
222. Rizzuto CD, Wyatt R, Hernandez-Ramos N, Sun Y, Kwong PD, Hendrickson WA, et al. A conserved HIV gp120 glycoprotein structure involved in chemokine receptor binding. Science. 1998;280(5371):1949-53.
223. Huang CC, Lam SN, Acharya P, Tang M, Xiang SH, Hussan SS, et al. Structures of the CCR5 N terminus and of a tyrosine-sulfated antibody with HIV-1 gp120 and CD4. Science. 2007;317(5846):1930-4.
224. Shaik MM, Peng H, Lu J, Rits-Volloch S, Xu C, Liao M, et al. Structural basis of coreceptor recognition by HIV-1 envelope spike. Nature. 2019;565(7739):318-23.
225. Alkhatib G, Combadiere C, Broder CC, Feng Y, Kennedy PE, Murphy PM, et al. CC CKR5: a RANTES, MIP-1alpha, MIP-1beta receptor as a fusion cofactor for macrophage-tropic HIV-1. Science. 1996;272(5270):1955-8.
226. Choe H, Farzan M, Sun Y, Sullivan N, Rollins B, Ponath PD, et al. The beta-chemokine receptors CCR3 and CCR5 facilitate infection by primary HIV-1 isolates. Cell. 1996;85(7):1135-48.
227. Deng H, Liu R, Ellmeier W, Choe S, Unutmaz D, Burkhart M, et al. Identification of a major co-receptor for primary isolates of HIV-1. Nature. 1996;381(6584):661-6.
228. Doranz BJ, Rucker J, Yi Y, Smyth RJ, Samson M, Peiper SC, et al. A dual-tropic primary HIV-1 isolate that uses fusin and the beta-chemokine receptors CKR-5, CKR-3, and CKR-2b as fusion cofactors. Cell. 1996;85(7):1149-58.
229. Dragic T, Litwin V, Allaway GP, Martin SR, Huang Y, Nagashima KA, et al. HIV-1 entry into CD4+ cells is mediated by the chemokine receptor CC-CKR-5. Nature. 1996;381(6584):667-73.
230. Trkola A, Dragic T, Arthos J, Binley JM, Olson WC, Allaway GP, et al. CD4-dependent, antibody-sensitive interactions between HIV-1 and its co-receptor CCR-5. Nature. 1996;384(6605):184-7.
231. Wu L, Gerard NP, Wyatt R, Choe H, Parolin C, Ruffing N, et al. CD4-induced interaction of primary HIV-1 gp120 glycoproteins with the chemokine receptor CCR-5. Nature. 1996;384(6605):179-83.
232. Feng Y, Broder CC, Kennedy PE, Berger EA. HIV-1 entry cofactor: functional cDNA cloning of a seven-transmembrane, G protein-coupled receptor. Science. 1996;272(5263):872-7.
233. Berson JF, Long D, Doranz BJ, Rucker J, Jirik FR, Doms RW. A seven-transmembrane domain receptor involved in fusion and entry of T-cell-tropic human immunodeficiency virus type 1 strains. J Virol. 1996;70(9):6288-95.
234. Finzi A, Xiang SH, Pacheco B, Wang L, Haight J, Kassa A, et al. Topological layers in the HIV-1 gp120 inner domain regulate gp41 interaction and CD4-triggered conformational transitions. Mol Cell. 2010;37(5):656-67.
235. Finzi A, Pacheco B, Xiang SH, Pancera M, Herschhorn A, Wang L, et al. Lineage-specific differences between human and simian immunodeficiency virus regulation of gp120 trimer association and CD4 binding. J Virol. 2012;86(17):8974-86.

236. Desormeaux A, Coutu M, Medjahed H, Pacheco B, Herschhorn A, Gu C, et al. The highly conserved layer-3 component of the HIV-1 gp120 inner domain is critical for CD4-required conformational transitions. J Virol. 2013;87(5):2549-62.
237. Ding S, Tolbert WD, Prevost J, Pacheco B, Coutu M, Debbeche O, et al. A Highly Conserved gp120 Inner Domain Residue Modulates Env Conformation and Trimer Stability. J Virol. 2016.
238. Gallo SA, Puri A, Blumenthal R. HIV-1 gp41 six-helix bundle formation occurs rapidly after the engagement of gp120 by CXCR4 in the HIV-1 Env-mediated fusion process. Biochemistry. 2001;40(41):12231-6.
239. Ladinsky MS, Gnanapragasam PN, Yang Z, West AP, Kay MS, Bjorkman PJ. Electron tomography visualization of HIV-1 fusion with target cells using fusion inhibitors to trap the pre-hairpin intermediate. Elife. 2020;9.
240. Lu M, Blacklow SC, Kim PS. A trimeric structural domain of the HIV-1 transmembrane glycoprotein. Nat Struct Biol. 1995;2(12):1075-82.
241. Chan DC, Fass D, Berger JM, Kim PS. Core structure of gp41 from the HIV envelope glycoprotein. Cell. 1997;89(2):263-73.
242. Melikyan GB, Markosyan RM, Hemmati H, Delmedico MK, Lambert DM, Cohen FS. Evidence that the transition of HIV-1 gp41 into a six-helix bundle, not the bundle configuration, induces membrane fusion. J Cell Biol. 2000;151(2):413-23.
243. Markosyan RM, Cohen FS, Melikyan GB. HIV-1 envelope proteins complete their folding into six-helix bundles immediately after fusion pore formation. Mol Biol Cell. 2003;14(3):926-38.
244. Markosyan RM, Cohen FS, Melikyan GB. Time-resolved imaging of HIV-1 Env-mediated lipid and content mixing between a single virion and cell membrane. Mol Biol Cell. 2005;16(12):5502-13.
245. McClure MO, Marsh M, Weiss RA. Human immunodeficiency virus infection of CD4-bearing cells occurs by a pH-independent mechanism. EMBO J. 1988;7(2):513-8.
246. Stein BS, Gowda SD, Lifson JD, Penhallow RC, Bensch KG, Engleman EG. pH-independent HIV entry into CD4-positive T cells via virus envelope fusion to the plasma membrane. Cell. 1987;49(5):659-68.
247. Maddon PJ, McDougal JS, Clapham PR, Dalgleish AG, Jamal S, Weiss RA, et al. HIV infection does not require endocytosis of its receptor, CD4. Cell. 1988;54(6):865-74.
248. Daecke J, Fackler OT, Dittmar MT, Krausslich HG. Involvement of clathrin-mediated endocytosis in human immunodeficiency virus type 1 entry. J Virol. 2005;79(3):1581-94.
249. Marechal V, Prevost MC, Petit C, Perret E, Heard JM, Schwartz O. Human immunodeficiency virus type 1 entry into macrophages mediated by macropinocytosis. J Virol. 2001;75(22):11166-77.
250. Carter GC, Bernstone L, Baskaran D, James W. HIV-1 infects macrophages by exploiting an endocytic route dependent on dynamin, Rac1 and Pak1. Virology. 2011;409(2):234-50.
251. Gobeil LA, Lodge R, Tremblay MJ. Macropinocytosis-like HIV-1 internalization in macrophages is CCR5 dependent and leads to efficient but delayed degradation in endosomal compartments. J Virol. 2013;87(2):735-45.
252. Herold N, Anders-Osswein M, Glass B, Eckhardt M, Muller B, Krausslich HG. HIV-1 entry in SupT1-R5, CEM-ss, and primary CD4+ T cells occurs at the plasma membrane and does not require endocytosis. J Virol. 2014;88(24):13956-70.

253. Zaitseva E, Zaitsev E, Melikov K, Arakelyan A, Marin M, Villasmil R, et al. Fusion Stage of HIV-1 Entry Depends on Virus-Induced Cell Surface Exposure of Phosphatidylserine. Cell Host Microbe. 2017;22(1):99-110 e7.
254. Lee B, Sharron M, Montaner LJ, Weissman D, Doms RW. Quantification of CD4, CCR5, and CXCR4 levels on lymphocyte subsets, dendritic cells, and differentially conditioned monocyte-derived macrophages. Proc Natl Acad Sci U S A. 1999;96(9):5215-20.
255. Berger EA, Doms RW, Fenyo EM, Korber BT, Littman DR, Moore JP, et al. A new classification for HIV-1. Nature. 1998;391(6664):240.
256. Mariani SA, Vicenzi E, Poli G. Asymmetric HIV-1 co-receptor use and replication in CD4(+) T lymphocytes. J Transl Med. 2011;9 Suppl 1:S8.
257. Keele BF, Giorgi EE, Salazar-Gonzalez JF, Decker JM, Pham KT, Salazar MG, et al. Identification and characterization of transmitted and early founder virus envelopes in primary HIV-1 infection. Proc Natl Acad Sci U S A. 2008;105(21):7552-7.
258. Sun H, Kim D, Li X, Kiselinova M, Ouyang Z, Vandekerckhove L, et al. Th1/17 Polarization of CD4 T Cells Supports HIV-1 Persistence during Antiretroviral Therapy. J Virol. 2015;89(22):11284-93.
259. Gosselin A, Monteiro P, Chomont N, Diaz-Griffero F, Said EA, Fonseca S, et al. Peripheral blood CCR4+CCR6+ and CXCR3+CCR6+CD4+ T cells are highly permissive to HIV-1 infection. J Immunol. 2010;184(3):1604-16.
260. Sabo Y, Walsh D, Barry DS, Tinaztepe S, de Los Santos K, Goff SP, et al. HIV-1 induces the formation of stable microtubules to enhance early infection. Cell Host Microbe. 2013;14(5):535-46.
261. Fernandez J, Portilho DM, Danckaert A, Munier S, Becker A, Roux P, et al. Microtubule-associated proteins 1 (MAP1) promote human immunodeficiency virus type I (HIV-1) intracytoplasmic routing to the nucleus. J Biol Chem. 2015;290(8):4631-46.
262. Naghavi MH. HIV-1 capsid exploitation of the host microtubule cytoskeleton during early infection. Retrovirology. 2021;18(1):19.
263. Sweeney HL, Holzbaur ELF. Motor Proteins. Cold Spring Harb Perspect Biol. 2018;10(5).
264. Malikov V, da Silva ES, Jovasevic V, Bennett G, de Souza Aranha Vieira DA, Schulte B, et al. HIV-1 capsids bind and exploit the kinesin-1 adaptor FEZ1 for inward movement to the nucleus. Nat Commun. 2015;6:6660.
265. Huang PT, Summers BJ, Xu C, Perilla JR, Malikov V, Naghavi MH, et al. FEZ1 Is Recruited to a Conserved Cofactor Site on Capsid to Promote HIV-1 Trafficking. Cell Rep. 2019;28(9):2373-85 e7.
266. Dharan A, Opp S, Abdel-Rahim O, Keceli SK, Imam S, Diaz-Griffero F, et al. Bicaudal D2 facilitates the cytoplasmic trafficking and nuclear import of HIV-1 genomes during infection. Proc Natl Acad Sci U S A. 2017;114(50):E10707-E16.
267. Carnes SK, Zhou J, Aiken C. HIV-1 Engages a Dynein-Dynactin-BICD2 Complex for Infection and Transport to the Nucleus. J Virol. 2018;92(20).
268. Malikov V, Naghavi MH. Localized Phosphorylation of a Kinesin-1 Adaptor by a Capsid-Associated Kinase Regulates HIV-1 Motility and Uncoating. Cell Rep. 2017;20(12):2792-9.
269. Li Y, Kar AK, Sodroski J. Target cell type-dependent modulation of human immunodeficiency virus type 1 capsid disassembly by cyclophilin A. J Virol. 2009;83(21):10951-62.

270. Shah VB, Shi J, Hout DR, Oztop I, Krishnan L, Ahn J, et al. The host proteins transportin SR2/TNPO3 and cyclophilin A exert opposing effects on HIV-1 uncoating. J Virol. 2013;87(1):422-32.
271. Liu C, Perilla JR, Ning J, Lu M, Hou G, Ramalho R, et al. Cyclophilin A stabilizes the HIV-1 capsid through a novel non-canonical binding site. Nat Commun. 2016;7:10714.
272. Dick RA, Zadrozny KK, Xu C, Schur FKM, Lyddon TD, Ricana CL, et al. Inositol phosphates are assembly co-factors for HIV-1. Nature. 2018;560(7719):509-12.
273. Mallery DL, Marquez CL, McEwan WA, Dickson CF, Jacques DA, Anandapadamanaban M, et al. IP6 is an HIV pocket factor that prevents capsid collapse and promotes DNA synthesis. Elife. 2018;7.
274. Ni T, Zhu Y, Yang Z, Xu C, Chaban Y, Nesterova T, et al. Structure of native HIV-1 cores and their interactions with IP6 and CypA. Sci Adv. 2021;7(47):eabj5715.
275. Levin JG, Guo J, Rouzina I, Musier-Forsyth K. Nucleic acid chaperone activity of HIV-1 nucleocapsid protein: critical role in reverse transcription and molecular mechanism. Prog Nucleic Acid Res Mol Biol. 2005;80:217-86.
276. Gien H, Morse M, McCauley MJ, Kitzrow JP, Musier-Forsyth K, Gorelick RJ, et al. HIV-1 Nucleocapsid Protein Binds Double-Stranded DNA in Multiple Modes to Regulate Compaction and Capsid Uncoating. Viruses. 2022;14(2).
277. Isel C, Lanchy JM, Le Grice SF, Ehresmann C, Ehresmann B, Marquet R. Specific initiation and switch to elongation of human immunodeficiency virus type 1 reverse transcription require the post-transcriptional modifications of primer tRNA3Lys. EMBO J. 1996;15(4):917-24.
278. Jacques DA, McEwan WA, Hilditch L, Price AJ, Towers GJ, James LC. HIV-1 uses dynamic capsid pores to import nucleotides and fuel encapsidated DNA synthesis. Nature. 2016;536(7616):349-53.
279. Xu C, Fischer DK, Rankovic S, Li W, Dick RA, Runge B, et al. Permeability of the HIV-1 capsid to metabolites modulates viral DNA synthesis. PLoS Biol. 2020;18(12):e3001015.
280. Starnes MC, Cheng YC. Human immunodeficiency virus reverse transcriptase-associated RNase H activity. J Biol Chem. 1989;264(12):7073-7.
281. DeStefano JJ, Buiser RG, Mallaber LM, Bambara RA, Fay PJ. Human immunodeficiency virus reverse transcriptase displays a partially processive 3' to 5' endonuclease activity. J Biol Chem. 1991;266(36):24295-301.
282. Tian L, Kim MS, Li H, Wang J, Yang W. Structure of HIV-1 reverse transcriptase cleaving RNA in an RNA/DNA hybrid. Proc Natl Acad Sci U S A. 2018;115(3):507-12.
283. Peliska JA, Benkovic SJ. Mechanism of DNA strand transfer reactions catalyzed by HIV-1 reverse transcriptase. Science. 1992;258(5085):1112-8.
284. van Wamel JL, Berkhout B. The first strand transfer during HIV-1 reverse transcription can occur either intramolecularly or intermolecularly. Virology. 1998;244(2):245-51.
285. Panganiban AT, Fiore D. Ordered interstrand and intrastrand DNA transfer during reverse transcription. Science. 1988;241(4869):1064-9.
286. Huber HE, Richardson CC. Processing of the primer for plus strand DNA synthesis by human immunodeficiency virus 1 reverse transcriptase. J Biol Chem. 1990;265(18):10565-73.
287. Fuentes GM, Rodriguez-Rodriguez L, Fay PJ, Bambara RA. Use of an oligoribonucleotide containing the polypurine tract sequence as a primer by HIV reverse transcriptase. J Biol Chem. 1995;270(47):28169-76.
288. Charneau P, Alizon M, Clavel F. A second origin of DNA plus-strand synthesis is required for optimal human immunodeficiency virus replication. J Virol. 1992;66(5):2814-20.

289. Sarafianos SG, Das K, Tantillo C, Clark AD, Jr., Ding J, Whitcomb JM, et al. Crystal structure of HIV-1 reverse transcriptase in complex with a polypurine tract RNA:DNA. EMBO J. 2001;20(6):1449-61.
290. Furfine ES, Reardon JE. Human immunodeficiency virus reverse transcriptase ribonuclease H: specificity of tRNA(Lys3)-primer excision. Biochemistry. 1991;30(29):7041-6.
291. Smith JS, Roth MJ. Specificity of human immunodeficiency virus-1 reverse transcriptase-associated ribonuclease H in removal of the minus-strand primer, tRNA(Lys3). J Biol Chem. 1992;267(21):15071-9.
292. Onafuwa-Nuga A, Telesnitsky A. The remarkable frequency of human immunodeficiency virus type 1 genetic recombination. Microbiol Mol Biol Rev. 2009;73(3):451-80, Table of Contents.
293. Miller MD, Farnet CM, Bushman FD. Human immunodeficiency virus type 1 preintegration complexes: studies of organization and composition. J Virol. 1997;71(7):5382-90.
294. Popov S, Rexach M, Zybarth G, Reiling N, Lee MA, Ratner L, et al. Viral protein R regulates nuclear import of the HIV-1 pre-integration complex. EMBO J. 1998;17(4):909-17.
295. Haffar OK, Popov S, Dubrovsky L, Agostini I, Tang H, Pushkarsky T, et al. Two nuclear localization signals in the HIV-1 matrix protein regulate nuclear import of the HIV-1 pre-integration complex. J Mol Biol. 2000;299(2):359-68.
296. Selyutina A, Persaud M, Lee K, KewalRamani V, Diaz-Griffero F. Nuclear Import of the HIV-1 Core Precedes Reverse Transcription and Uncoating. Cell Rep. 2020;32(13):108201.
297. Francis AC, Marin M, Prellberg MJ, Palermino-Rowland K, Melikyan GB. HIV-1 Uncoating and Nuclear Import Precede the Completion of Reverse Transcription in Cell Lines and in Primary Macrophages. Viruses. 2020;12(11).
298. Dharan A, Bachmann N, Talley S, Zwikelmaier V, Campbell EM. Nuclear pore blockade reveals that HIV-1 completes reverse transcription and uncoating in the nucleus. Nat Microbiol. 2020;5(9):1088-95.
299. Francis AC, Melikyan GB. Single HIV-1 Imaging Reveals Progression of Infection through CA-Dependent Steps of Docking at the Nuclear Pore, Uncoating, and Nuclear Transport. Cell Host Microbe. 2018;23(4):536-48 e6.
300. Burdick RC, Li C, Munshi M, Rawson JMO, Nagashima K, Hu WS, et al. HIV-1 uncoats in the nucleus near sites of integration. Proc Natl Acad Sci U S A. 2020;117(10):5486-93.
301. Muller TG, Zila V, Peters K, Schifferdecker S, Stanic M, Lucic B, et al. HIV-1 uncoating by release of viral cDNA from capsid-like structures in the nucleus of infected cells. Elife. 2021;10.
302. Li C, Burdick RC, Nagashima K, Hu WS, Pathak VK. HIV-1 cores retain their integrity until minutes before uncoating in the nucleus. Proc Natl Acad Sci U S A. 2021;118(10).
303. Zila V, Margiotta E, Turonova B, Muller TG, Zimmerli CE, Mattei S, et al. Cone-shaped HIV-1 capsids are transported through intact nuclear pores. Cell. 2021;184(4):1032-46 e18.
304. Bichel K, Price AJ, Schaller T, Towers GJ, Freund SM, James LC. HIV-1 capsid undergoes coupled binding and isomerization by the nuclear pore protein NUP358. Retrovirology. 2013;10:81.
305. Meehan AM, Saenz DT, Guevera R, Morrison JH, Peretz M, Fadel HJ, et al. A cyclophilin homology domain-independent role for Nup358 in HIV-1 infection. PLoS Pathog. 2014;10(2):e1003969.
306. Matreyek KA, Engelman A. The requirement for nucleoporin NUP153 during human immunodeficiency virus type 1 infection is determined by the viral capsid. J Virol. 2011;85(15):7818-27.

307. Matreyek KA, Yucel SS, Li X, Engelman A. Nucleoporin NUP153 phenylalanine-glycine motifs engage a common binding pocket within the HIV-1 capsid protein to mediate lentiviral infectivity. PLoS Pathog. 2013;9(10):e1003693.
308. Di Nunzio F, Fricke T, Miccio A, Valle-Casuso JC, Perez P, Souque P, et al. Nup153 and Nup98 bind the HIV-1 core and contribute to the early steps of HIV-1 replication. Virology. 2013;440(1):8-18.
309. Buffone C, Martinez-Lopez A, Fricke T, Opp S, Severgnini M, Cifola I, et al. Nup153 Unlocks the Nuclear Pore Complex for HIV-1 Nuclear Translocation in Nondividing Cells. J Virol. 2018;92(19).
310. Price AJ, Fletcher AJ, Schaller T, Elliott T, Lee K, KewalRamani VN, et al. CPSF6 defines a conserved capsid interface that modulates HIV-1 replication. PLoS Pathog. 2012;8(8):e1002896.
311. De Iaco A, Santoni F, Vannier A, Guipponi M, Antonarakis S, Luban J. TNPO3 protects HIV-1 replication from CPSF6-mediated capsid stabilization in the host cell cytoplasm. Retrovirology. 2013;10:20.
312. Bhattacharya A, Alam SL, Fricke T, Zadrozny K, Sedzicki J, Taylor AB, et al. Structural basis of HIV-1 capsid recognition by PF74 and CPSF6. Proc Natl Acad Sci U S A. 2014;111(52):18625-30.
313. Chin CR, Perreira JM, Savidis G, Portmann JM, Aker AM, Feeley EM, et al. Direct Visualization of HIV-1 Replication Intermediates Shows that Capsid and CPSF6 Modulate HIV-1 Intra-nuclear Invasion and Integration. Cell Rep. 2015;13(8):1717-31.
314. Achuthan V, Perreira JM, Sowd GA, Puray-Chavez M, McDougall WM, Paulucci-Holthauzen A, et al. Capsid-CPSF6 Interaction Licenses Nuclear HIV-1 Trafficking to Sites of Viral DNA Integration. Cell Host Microbe. 2018;24(3):392-404 e8.
315. Jang S, Cook NJ, Pye VE, Bedwell GJ, Dudek AM, Singh PK, et al. Differential role for phosphorylation in alternative polyadenylation function versus nuclear import of SR-like protein CPSF6. Nucleic Acids Res. 2019;47(9):4663-83.
316. Bejarano DA, Peng K, Laketa V, Borner K, Jost KL, Lucic B, et al. HIV-1 nuclear import in macrophages is regulated by CPSF6-capsid interactions at the nuclear pore complex. Elife. 2019;8.
317. Zimmerli CE, Allegretti M, Rantos V, Goetz SK, Obarska-Kosinska A, Zagoriy I, et al. Nuclear pores dilate and constrict in cellulo. Science. 2021;374(6573):eabd9776.
318. von Appen A, Kosinski J, Sparks L, Ori A, DiGuilio AL, Vollmer B, et al. In situ structural analysis of the human nuclear pore complex. Nature. 2015;526(7571):140-3.
319. Blanco-Rodriguez G, Gazi A, Monel B, Frabetti S, Scoca V, Mueller F, et al. Remodeling of the Core Leads HIV-1 Preintegration Complex into the Nucleus of Human Lymphocytes. J Virol. 2020;94(11).
320. Guedan A, Donaldson CD, Caroe ER, Cosnefroy O, Taylor IA, Bishop KN. HIV-1 requires capsid remodelling at the nuclear pore for nuclear entry and integration. PLoS Pathog. 2021;17(9):e1009484.
321. Shen Q, Xu C, Jang S, Xiong Q, Devarkar SC, Tian T, et al. A DNA-origami nuclear pore mimic reveals nuclear entry mechanisms of HIV-1 capsid. bioRxiv. 2020.
322. Craigie R, Bushman FD. HIV DNA integration. Cold Spring Harb Perspect Med. 2012;2(7):a006890.
323. Bushman FD, Fujiwara T, Craigie R. Retroviral DNA integration directed by HIV integration protein in vitro. Science. 1990;249(4976):1555-8.

324. Bukrinsky MI, Sharova N, McDonald TL, Pushkarskaya T, Tarpley WG, Stevenson M. Association of integrase, matrix, and reverse transcriptase antigens of human immunodeficiency virus type 1 with viral nucleic acids following acute infection. Proc Natl Acad Sci U S A. 1993;90(13):6125-9.
325. Carteau S, Batson SC, Poljak L, Mouscadet JF, de Rocquigny H, Darlix JL, et al. Human immunodeficiency virus type 1 nucleocapsid protein specifically stimulates Mg2+-dependent DNA integration in vitro. J Virol. 1997;71(8):6225-9.
326. Llano M, Saenz DT, Meehan A, Wongthida P, Peretz M, Walker WH, et al. An essential role for LEDGF/p75 in HIV integration. Science. 2006;314(5798):461-4.
327. Lahouassa H, Blondot ML, Chauveau L, Chougui G, Morel M, Leduc M, et al. HIV-1 Vpr degrades the HLTF DNA translocase in T cells and macrophages. Proc Natl Acad Sci U S A. 2016;113(19):5311-6.
328. Richetta C, Thierry S, Thierry E, Lesbats P, Lapaillerie D, Munir S, et al. Two-long terminal repeat (LTR) DNA circles are a substrate for HIV-1 integrase. J Biol Chem. 2019;294(20):8286-95.
329. Pauza CD. Two bases are deleted from the termini of HIV-1 linear DNA during integrative recombination. Virology. 1990;179(2):886-9.
330. Hare S, Maertens GN, Cherepanov P. 3'-processing and strand transfer catalysed by retroviral integrase in crystallo. EMBO J. 2012;31(13):3020-8.
331. Passos DO, Li M, Yang R, Rebensburg SV, Ghirlando R, Jeon Y, et al. Cryo-EM structures and atomic model of the HIV-1 strand transfer complex intasome. Science. 2017;355(6320):89-92.
332. Yoder KE, Bushman FD. Repair of gaps in retroviral DNA integration intermediates. J Virol. 2000;74(23):11191-200.
333. Schroder AR, Shinn P, Chen H, Berry C, Ecker JR, Bushman F. HIV-1 integration in the human genome favors active genes and local hotspots. Cell. 2002;110(4):521-9.
334. Albanese A, Arosio D, Terreni M, Cereseto A. HIV-1 pre-integration complexes selectively target decondensed chromatin in the nuclear periphery. PLoS One. 2008;3(6):e2413.
335. Marini B, Kertesz-Farkas A, Ali H, Lucic B, Lisek K, Manganaro L, et al. Nuclear architecture dictates HIV-1 integration site selection. Nature. 2015;521(7551):227-31.
336. Pradeepa MM, Sutherland HG, Ule J, Grimes GR, Bickmore WA. Psip1/Ledgf p52 binds methylated histone H3K36 and splicing factors and contributes to the regulation of alternative splicing. PLoS Genet. 2012;8(5):e1002717.
337. van Nuland R, van Schaik FM, Simonis M, van Heesch S, Cuppen E, Boelens R, et al. Nucleosomal DNA binding drives the recognition of H3K36-methylated nucleosomes by the PSIP1-PWWP domain. Epigenetics Chromatin. 2013;6(1):12.
338. Eidahl JO, Crowe BL, North JA, McKee CJ, Shkriabai N, Feng L, et al. Structural basis for high-affinity binding of LEDGF PWWP to mononucleosomes. Nucleic Acids Res. 2013;41(6):3924-36.
339. Sapp N, Burge N, Cox K, Thapa S, Prakash P, Balasubramaniam M, et al. HIV-1 preintegration complex preferentially integrates the viral DNA into nucleosomes containing trimethylated histone 3-lysine 36 modification. bioRxiv. 2022.
340. Dutilleul A, Rodari A, Van Lint C. Depicting HIV-1 Transcriptional Mechanisms: A Summary of What We Know. Viruses. 2020;12(12).

341. Berkhout B, Jeang KT. Functional roles for the TATA promoter and enhancers in basal and Tat-induced expression of the human immunodeficiency virus type 1 long terminal repeat. J Virol. 1992;66(1):139-49.
342. van Opijnen T, Kamoschinski J, Jeeninga RE, Berkhout B. The human immunodeficiency virus type 1 promoter contains a CATA box instead of a TATA box for optimal transcription and replication. J Virol. 2004;78(13):6883-90.
343. Perkins ND, Edwards NL, Duckett CS, Agranoff AB, Schmid RM, Nabel GJ. A cooperative interaction between NF-kappa B and Sp1 is required for HIV-1 enhancer activation. EMBO J. 1993;12(9):3551-8.
344. Sune C, Garcia-Blanco MA. Sp1 transcription factor is required for in vitro basal and Tat-activated transcription from the human immunodeficiency virus type 1 long terminal repeat. J Virol. 1995;69(10):6572-6.
345. Van Lint C, Amella CA, Emiliani S, John M, Jie T, Verdin E. Transcription factor binding sites downstream of the human immunodeficiency virus type 1 transcription start site are important for virus infectivity. J Virol. 1997;71(8):6113-27.
346. Hidalgo-Estevez AM, Gonzalez E, Punzon C, Fresno M. Human immunodeficiency virus type 1 Tat increases cooperation between AP-1 and NFAT transcription factors in T cells. J Gen Virol. 2006;87(Pt 6):1603-12.
347. Ocwieja KE, Sherrill-Mix S, Mukherjee R, Custers-Allen R, David P, Brown M, et al. Dynamic regulation of HIV-1 mRNA populations analyzed by single-molecule enrichment and long-read sequencing. Nucleic Acids Res. 2012;40(20):10345-55.
348. Emery A, Zhou S, Pollom E, Swanstrom R. Characterizing HIV-1 Splicing by Using Next-Generation Sequencing. J Virol. 2017;91(6).
349. Efthymiadis A, Briggs LJ, Jans DA. The HIV-1 Tat nuclear localization sequence confers novel nuclear import properties. J Biol Chem. 1998;273(3):1623-8.
350. Smith KM, Himiari Z, Tsimbalyuk S, Forwood JK. Structural Basis for Importin-alpha Binding of the Human Immunodeficiency Virus Tat. Sci Rep. 2017;7(1):1650.
351. Henderson BR, Percipalle P. Interactions between HIV Rev and nuclear import and export factors: the Rev nuclear localisation signal mediates specific binding to human importin-beta. J Mol Biol. 1997;274(5):693-707.
352. Arizala JAC, Takahashi M, Burnett JC, Ouellet DL, Li H, Rossi JJ. Nucleolar Localization of HIV-1 Rev Is Required, Yet Insufficient for Production of Infectious Viral Particles. AIDS Res Hum Retroviruses. 2018;34(11):961-81.
353. Truant R, Cullen BR. The arginine-rich domains present in human immunodeficiency virus type 1 Tat and Rev function as direct importin beta-dependent nuclear localization signals. Mol Cell Biol. 1999;19(2):1210-7.
354. Sodroski J, Rosen C, Wong-Staal F, Salahuddin SZ, Popovic M, Arya S, et al. Trans-acting transcriptional regulation of human T-cell leukemia virus type III long terminal repeat. Science. 1985;227(4683):171-3.
355. Kuppuswamy M, Subramanian T, Srinivasan A, Chinnadurai G. Multiple functional domains of Tat, the trans-activator of HIV-1, defined by mutational analysis. Nucleic Acids Res. 1989;17(9):3551-61.
356. Ruben S, Perkins A, Purcell R, Joung K, Sia R, Burghoff R, et al. Structural and functional characterization of human immunodeficiency virus tat protein. J Virol. 1989;63(1):1-8.

357. Selby MJ, Bain ES, Luciw PA, Peterlin BM. Structure, sequence, and position of the stem-loop in tar determine transcriptional elongation by tat through the HIV-1 long terminal repeat. Genes Dev. 1989;3(4):547-58.
358. Schulze-Gahmen U, Hurley JH. Structural mechanism for HIV-1 TAR loop recognition by Tat and the super elongation complex. Proc Natl Acad Sci U S A. 2018;115(51):12973-8.
359. Ping YH, Rana TM. DSIF and NELF interact with RNA polymerase II elongation complex and HIV-1 Tat stimulates P-TEFb-mediated phosphorylation of RNA polymerase II and DSIF during transcription elongation. J Biol Chem. 2001;276(16):12951-8.
360. Parada CA, Roeder RG. Enhanced processivity of RNA polymerase II triggered by Tat-induced phosphorylation of its carboxy-terminal domain. Nature. 1996;384(6607):375-8.
361. Malim MH, Hauber J, Le SY, Maizel JV, Cullen BR. The HIV-1 rev trans-activator acts through a structured target sequence to activate nuclear export of unspliced viral mRNA. Nature. 1989;338(6212):254-7.
362. Dayton ET, Powell DM, Dayton AI. Functional analysis of CAR, the target sequence for the Rev protein of HIV-1. Science. 1989;246(4937):1625-9.
363. Neville M, Stutz F, Lee L, Davis LI, Rosbash M. The importin-beta family member Crm1p bridges the interaction between Rev and the nuclear pore complex during nuclear export. Curr Biol. 1997;7(10):767-75.
364. Askjaer P, Jensen TH, Nilsson J, Englmeier L, Kjems J. The specificity of the CRM1-Rev nuclear export signal interaction is mediated by RanGTP. J Biol Chem. 1998;273(50):33414-22.
365. Daugherty MD, Liu B, Frankel AD. Structural basis for cooperative RNA binding and export complex assembly by HIV Rev. Nat Struct Mol Biol. 2010;17(11):1337-42.
366. Guerrero S, Batisse J, Libre C, Bernacchi S, Marquet R, Paillart JC. HIV-1 replication and the cellular eukaryotic translation apparatus. Viruses. 2015;7(1):199-218.
367. Schwartz S, Felber BK, Fenyo EM, Pavlakis GN. Env and Vpu proteins of human immunodeficiency virus type 1 are produced from multiple bicistronic mRNAs. J Virol. 1990;64(11):5448-56.
368. Schwartz S, Felber BK, Pavlakis GN. Mechanism of translation of monocistronic and multicistronic human immunodeficiency virus type 1 mRNAs. Mol Cell Biol. 1992;12(1):207-19.
369. Krummheuer J, Johnson AT, Hauber I, Kammler S, Anderson JL, Hauber J, et al. A minimal uORF within the HIV-1 vpu leader allows efficient translation initiation at the downstream env AUG. Virology. 2007;363(2):261-71.
370. Anderson JL, Johnson AT, Howard JL, Purcell DF. Both linear and discontinuous ribosome scanning are used for translation initiation from bicistronic human immunodeficiency virus type 1 env mRNAs. J Virol. 2007;81(9):4664-76.
371. Reil H, Kollmus H, Weidle UH, Hauser H. A heptanucleotide sequence mediates ribosomal frameshifting in mammalian cells. J Virol. 1993;67(9):5579-84.
372. Wilson W, Braddock M, Adams SE, Rathjen PD, Kingsman SM, Kingsman AJ. HIV expression strategies: ribosomal frameshifting is directed by a short sequence in both mammalian and yeast systems. Cell. 1988;55(6):1159-69.
373. Gheysen D, Jacobs E, de Foresta F, Thiriart C, Francotte M, Thines D, et al. Assembly and release of HIV-1 precursor Pr55gag virus-like particles from recombinant baculovirus-infected insect cells. Cell. 1989;59(1):103-12.
374. Sundquist WI, Krausslich HG. HIV-1 assembly, budding, and maturation. Cold Spring Harb Perspect Med. 2012;2(7):a006924.

375. Ono A, Ablan SD, Lockett SJ, Nagashima K, Freed EO. Phosphatidylinositol (4,5) bisphosphate regulates HIV-1 Gag targeting to the plasma membrane. Proc Natl Acad Sci U S A. 2004;101(41):14889-94.
376. Saad JS, Miller J, Tai J, Kim A, Ghanam RH, Summers MF. Structural basis for targeting HIV-1 Gag proteins to the plasma membrane for virus assembly. Proc Natl Acad Sci U S A. 2006;103(30):11364-9.
377. Chan R, Uchil PD, Jin J, Shui G, Ott DE, Mothes W, et al. Retroviruses human immunodeficiency virus and murine leukemia virus are enriched in phosphoinositides. J Virol. 2008;82(22):11228-38.
378. Yandrapalli N, Lubart Q, Tanwar HS, Picart C, Mak J, Muriaux D, et al. Self assembly of HIV-1 Gag protein on lipid membranes generates PI(4,5)P2/Cholesterol nanoclusters. Sci Rep. 2016;6:39332.
379. Ono A, Freed EO. Plasma membrane rafts play a critical role in HIV-1 assembly and release. Proc Natl Acad Sci U S A. 2001;98(24):13925-30.
380. Nguyen DH, Hildreth JE. Evidence for budding of human immunodeficiency virus type 1 selectively from glycolipid-enriched membrane lipid rafts. J Virol. 2000;74(7):3264-72.
381. Lindwasser OW, Resh MD. Multimerization of human immunodeficiency virus type 1 Gag promotes its localization to barges, raft-like membrane microdomains. J Virol. 2001;75(17):7913-24.
382. Gamble TR, Yoo S, Vajdos FF, von Schwedler UK, Worthylake DK, Wang H, et al. Structure of the carboxyl-terminal dimerization domain of the HIV-1 capsid protein. Science. 1997;278(5339):849-53.
383. Huang M, Martin MA. Incorporation of Pr160(gag-pol) into virus particles requires the presence of both the major homology region and adjacent C-terminal capsid sequences within the Gag-Pol polyprotein. J Virol. 1997;71(6):4472-8.
384. Wright ER, Schooler JB, Ding HJ, Kieffer C, Fillmore C, Sundquist WI, et al. Electron cryotomography of immature HIV-1 virions reveals the structure of the CA and SP1 Gag shells. EMBO J. 2007;26(8):2218-26.
385. Pak AJ, Gupta M, Yeager M, Voth GA. Inositol hexakisphosphate (IP6) accelerates immature HIV-1 Gag protein assembly towards kinetically-trapped morphologies. bioRxiv. 2022.
386. Bachand F, Yao XJ, Hrimech M, Rougeau N, Cohen EA. Incorporation of Vpr into human immunodeficiency virus type 1 requires a direct interaction with the p6 domain of the p55 gag precursor. J Biol Chem. 1999;274(13):9083-91.
387. Lu YL, Bennett RP, Wills JW, Gorelick R, Ratner L. A leucine triplet repeat sequence (LXX)4 in p6gag is important for Vpr incorporation into human immunodeficiency virus type 1 particles. J Virol. 1995;69(11):6873-9.
388. Jenkins Y, Pornillos O, Rich RL, Myszka DG, Sundquist WI, Malim MH. Biochemical analyses of the interactions between human immunodeficiency virus type 1 Vpr and p6(Gag). J Virol. 2001;75(21):10537-42.
389. Salgado GF, Marquant R, Vogel A, Alves ID, Feller SE, Morellet N, et al. Structural studies of HIV-1 Gag p6ct and its interaction with Vpr determined by solution nuclear magnetic resonance. Biochemistry. 2009;48(11):2355-67.
390. Wanaguru M, Bishop KN. HIV-1 Gag Recruits Oligomeric Vpr via Two Binding Sites in p6, but Both Mature p6 and Vpr Are Rapidly Lost upon Target Cell Entry. J Virol. 2021;95(17):e0055421.

391. Berkowitz RD, Luban J, Goff SP. Specific binding of human immunodeficiency virus type 1 gag polyprotein and nucleocapsid protein to viral RNAs detected by RNA mobility shift assays. J Virol. 1993;67(12):7190-200.
392. Checkley MA, Luttge BG, Freed EO. HIV-1 envelope glycoprotein biosynthesis, trafficking, and incorporation. J Mol Biol. 2011;410(4):582-608.
393. Li Y, Bergeron JJ, Luo L, Ou WJ, Thomas DY, Kang CY. Effects of inefficient cleavage of the signal sequence of HIV-1 gp 120 on its association with calnexin, folding, and intracellular transport. Proc Natl Acad Sci U S A. 1996;93(18):9606-11.
394. Pfeiffer T, Pisch T, Devitt G, Holtkotte D, Bosch V. Effects of signal peptide exchange on HIV-1 glycoprotein expression and viral infectivity in mammalian cells. FEBS Lett. 2006;580(15):3775-8.
395. Snapp EL, McCaul N, Quandte M, Cabartova Z, Bontjer I, Kallgren C, et al. Structure and topology around the cleavage site regulate post-translational cleavage of the HIV-1 gp160 signal peptide. Elife. 2017;6.
396. McCaul N, Quandte M, Bontjer I, van Zadelhoff G, Land A, Crooks ET, et al. Intramolecular quality control: HIV-1 envelope gp160 signal-peptide cleavage as a functional folding checkpoint. Cell Rep. 2021;36(9):109646.
397. Leonard CK, Spellman MW, Riddle L, Harris RJ, Thomas JN, Gregory TJ. Assignment of intrachain disulfide bonds and characterization of potential glycosylation sites of the type 1 recombinant human immunodeficiency virus envelope glycoprotein (gp120) expressed in Chinese hamster ovary cells. J Biol Chem. 1990;265(18):10373-82.
398. Earl PL, Moss B, Doms RW. Folding, interaction with GRP78-BiP, assembly, and transport of the human immunodeficiency virus type 1 envelope protein. J Virol. 1991;65(4):2047-55.
399. Otteken A, Moss B. Calreticulin interacts with newly synthesized human immunodeficiency virus type 1 envelope glycoprotein, suggesting a chaperone function similar to that of calnexin. J Biol Chem. 1996;271(1):97-103.
400. Land A, Zonneveld D, Braakman I. Folding of HIV-1 envelope glycoprotein involves extensive isomerization of disulfide bonds and conformation-dependent leader peptide cleavage. FASEB J. 2003;17(9):1058-67.
401. Bernstein HB, Tucker SP, Hunter E, Schutzbach JS, Compans RW. Human immunodeficiency virus type 1 envelope glycoprotein is modified by O-linked oligosaccharides. J Virol. 1994;68(1):463-8.
402. Behrens AJ, Vasiljevic S, Pritchard LK, Harvey DJ, Andev RS, Krumm SA, et al. Composition and Antigenic Effects of Individual Glycan Sites of a Trimeric HIV-1 Envelope Glycoprotein. Cell Rep. 2016;14(11):2695-706.
403. Struwe WB, Chertova E, Allen JD, Seabright GE, Watanabe Y, Harvey DJ, et al. Site-Specific Glycosylation of Virion-Derived HIV-1 Env Is Mimicked by a Soluble Trimeric Immunogen. Cell Rep. 2018;24(8):1958-66 e5.
404. Zhang S, Nguyen HT, Ding H, Wang J, Zou S, Liu L, et al. Dual Pathways of Human Immunodeficiency Virus Type 1 Envelope Glycoprotein Trafficking Modulate the Selective Exclusion of Uncleaved Oligomers from Virions. J Virol. 2021;95(3).
405. Hallenberger S, Bosch V, Angliker H, Shaw E, Klenk HD, Garten W. Inhibition of furin-mediated cleavage activation of HIV-1 glycoprotein gp160. Nature. 1992;360(6402):358-61.
406. Decroly E, Vandenbranden M, Ruysschaert JM, Cogniaux J, Jacob GS, Howard SC, et al. The convertases furin and PC1 can both cleave the human immunodeficiency virus (HIV)-1

envelope glycoprotein gp160 into gp120 (HIV-1 SU) and gp41 (HIV-I TM). J Biol Chem. 1994;269(16):12240-7.
407. Decroly E, Wouters S, Di Bello C, Lazure C, Ruysschaert JM, Seidah NG. Identification of the paired basic convertases implicated in HIV gp160 processing based on in vitro assays and expression in CD4(+) cell lines. J Biol Chem. 1996;271(48):30442-50.
408. Decroly E, Benjannet S, Savaria D, Seidah NG. Comparative functional role of PC7 and furin in the processing of the HIV envelope glycoprotein gp160. FEBS Lett. 1997;405(1):68-72.
409. Helseth E, Olshevsky U, Furman C, Sodroski J. Human immunodeficiency virus type 1 gp120 envelope glycoprotein regions important for association with the gp41 transmembrane glycoprotein. J Virol. 1991;65(4):2119-23.
410. Yang X, Mahony E, Holm GH, Kassa A, Sodroski J. Role of the gp120 inner domain beta-sandwich in the interaction between the human immunodeficiency virus envelope glycoprotein subunits. Virology. 2003;313(1):117-25.
411. Dubay JW, Dubay SR, Shin HJ, Hunter E. Analysis of the cleavage site of the human immunodeficiency virus type 1 glycoprotein: requirement of precursor cleavage for glycoprotein incorporation. J Virol. 1995;69(8):4675-82.
412. Herrera C, Klasse PJ, Michael E, Kake S, Barnes K, Kibler CW, et al. The impact of envelope glycoprotein cleavage on the antigenicity, infectivity, and neutralization sensitivity of Env-pseudotyped human immunodeficiency virus type 1 particles. Virology. 2005;338(1):154-72.
413. Buttler CA, Pezeshkian N, Fernandez MV, Aaron J, Norman S, Freed EO, et al. Single molecule fate of HIV-1 envelope reveals late-stage viral lattice incorporation. Nat Commun. 2018;9(1):1861.
414. Boge M, Wyss S, Bonifacino JS, Thali M. A membrane-proximal tyrosine-based signal mediates internalization of the HIV-1 envelope glycoprotein via interaction with the AP-2 clathrin adaptor. J Biol Chem. 1998;273(25):15773-8.
415. Berlioz-Torrent C, Shacklett BL, Erdtmann L, Delamarre L, Bouchaert I, Sonigo P, et al. Interactions of the cytoplasmic domains of human and simian retroviral transmembrane proteins with components of the clathrin adaptor complexes modulate intracellular and cell surface expression of envelope glycoproteins. J Virol. 1999;73(2):1350-61.
416. Qi M, Williams JA, Chu H, Chen X, Wang JJ, Ding L, et al. Rab11-FIP1C and Rab14 direct plasma membrane sorting and particle incorporation of the HIV-1 envelope glycoprotein complex. PLoS Pathog. 2013;9(4):e1003278.
417. Qi M, Chu H, Chen X, Choi J, Wen X, Hammonds J, et al. A tyrosine-based motif in the HIV-1 envelope glycoprotein tail mediates cell-type- and Rab11-FIP1C-dependent incorporation into virions. Proc Natl Acad Sci U S A. 2015;112(24):7575-80.
418. Kirschman J, Qi M, Ding L, Hammonds J, Dienger-Stambaugh K, Wang JJ, et al. HIV-1 Envelope Glycoprotein Trafficking through the Endosomal Recycling Compartment Is Required for Particle Incorporation. J Virol. 2018;92(5).
419. Vishwanathan SA, Thomas A, Brasseur R, Epand RF, Hunter E, Epand RM. Large changes in the CRAC segment of gp41 of HIV do not destroy fusion activity if the segment interacts with cholesterol. Biochemistry. 2008;47(45):11869-76.
420. Vishwanathan SA, Hunter E. Importance of the membrane-perturbing properties of the membrane-proximal external region of human immunodeficiency virus type 1 gp41 to viral fusion. J Virol. 2008;82(11):5118-26.
421. Rousso I, Mixon MB, Chen BK, Kim PS. Palmitoylation of the HIV-1 envelope glycoprotein is critical for viral infectivity. Proc Natl Acad Sci U S A. 2000;97(25):13523-5.

422. Murakami T, Freed EO. Genetic evidence for an interaction between human immunodeficiency virus type 1 matrix and alpha-helix 2 of the gp41 cytoplasmic tail. J Virol. 2000;74(8):3548-54.
423. Pezeshkian N, Groves NS, van Engelenburg SB. Single-molecule imaging of HIV-1 envelope glycoprotein dynamics and Gag lattice association exposes determinants responsible for virus incorporation. Proc Natl Acad Sci U S A. 2019;116(50):25269-77.
424. Nieto-Garai JA, Arboleya A, Otaegi S, Chojnacki J, Casas J, Fabrias G, et al. Cholesterol in the Viral Membrane is a Molecular Switch Governing HIV-1 Env Clustering. Adv Sci (Weinh). 2021;8(3):2003468.
425. Gottlinger HG, Dorfman T, Sodroski JG, Haseltine WA. Effect of mutations affecting the p6 gag protein on human immunodeficiency virus particle release. Proc Natl Acad Sci U S A. 1991;88(8):3195-9.
426. Huang M, Orenstein JM, Martin MA, Freed EO. p6Gag is required for particle production from full-length human immunodeficiency virus type 1 molecular clones expressing protease. J Virol. 1995;69(11):6810-8.
427. Prescher J, Baumgartel V, Ivanchenko S, Torrano AA, Brauchle C, Muller B, et al. Super-resolution imaging of ESCRT-proteins at HIV-1 assembly sites. PLoS Pathog. 2015;11(2):e1004677.
428. Garrus JE, von Schwedler UK, Pornillos OW, Morham SG, Zavitz KH, Wang HE, et al. Tsg101 and the vacuolar protein sorting pathway are essential for HIV-1 budding. Cell. 2001;107(1):55-65.
429. Martin-Serrano J, Zang T, Bieniasz PD. HIV-1 and Ebola virus encode small peptide motifs that recruit Tsg101 to sites of particle assembly to facilitate egress. Nat Med. 2001;7(12):1313-9.
430. VerPlank L, Bouamr F, LaGrassa TJ, Agresta B, Kikonyogo A, Leis J, et al. Tsg101, a homologue of ubiquitin-conjugating (E2) enzymes, binds the L domain in HIV type 1 Pr55(Gag). Proc Natl Acad Sci U S A. 2001;98(14):7724-9.
431. von Schwedler UK, Stuchell M, Muller B, Ward DM, Chung HY, Morita E, et al. The protein network of HIV budding. Cell. 2003;114(6):701-13.
432. Strack B, Calistri A, Craig S, Popova E, Gottlinger HG. AIP1/ALIX is a binding partner for HIV-1 p6 and EIAV p9 functioning in virus budding. Cell. 2003;114(6):689-99.
433. Morita E, Sandrin V, McCullough J, Katsuyama A, Baci Hamilton I, Sundquist WI. ESCRT-III protein requirements for HIV-1 budding. Cell Host Microbe. 2011;9(3):235-42.
434. Debouck C, Gorniak JG, Strickler JE, Meek TD, Metcalf BW, Rosenberg M. Human immunodeficiency virus protease expressed in Escherichia coli exhibits autoprocessing and specific maturation of the gag precursor. Proc Natl Acad Sci U S A. 1987;84(24):8903-6.
435. Louis JM, Clore GM, Gronenborn AM. Autoprocessing of HIV-1 protease is tightly coupled to protein folding. Nat Struct Biol. 1999;6(9):868-75.
436. Pettit SC, Everitt LE, Choudhury S, Dunn BM, Kaplan AH. Initial cleavage of the human immunodeficiency virus type 1 GagPol precursor by its activated protease occurs by an intramolecular mechanism. J Virol. 2004;78(16):8477-85.
437. Wlodawer A, Miller M, Jaskolski M, Sathyanarayana BK, Baldwin E, Weber IT, et al. Conserved folding in retroviral proteases: crystal structure of a synthetic HIV-1 protease. Science. 1989;245(4918):616-21.

438. Babe LM, Rose J, Craik CS. Trans-dominant inhibitory human immunodeficiency virus type 1 protease monomers prevent protease activation and virion maturation. Proc Natl Acad Sci U S A. 1995;92(22):10069-73.
439. Strisovsky K, Tessmer U, Langner J, Konvalinka J, Krausslich HG. Systematic mutational analysis of the active-site threonine of HIV-1 proteinase: rethinking the "fireman's grip" hypothesis. Protein Sci. 2000;9(9):1631-41.
440. Pettit SC, Gulnik S, Everitt L, Kaplan AH. The dimer interfaces of protease and extra-protease domains influence the activation of protease and the specificity of GagPol cleavage. J Virol. 2003;77(1):366-74.
441. Pettit SC, Moody MD, Wehbie RS, Kaplan AH, Nantermet PV, Klein CA, et al. The p2 domain of human immunodeficiency virus type 1 Gag regulates sequential proteolytic processing and is required to produce fully infectious virions. J Virol. 1994;68(12):8017-27.
442. Wiegers K, Rutter G, Kottler H, Tessmer U, Hohenberg H, Krausslich HG. Sequential steps in human immunodeficiency virus particle maturation revealed by alterations of individual Gag polyprotein cleavage sites. J Virol. 1998;72(4):2846-54.
443. de Marco A, Muller B, Glass B, Riches JD, Krausslich HG, Briggs JA. Structural analysis of HIV-1 maturation using cryo-electron tomography. PLoS Pathog. 2010;6(11):e1001215.
444. Fontana J, Jurado KA, Cheng N, Ly NL, Fuchs JR, Gorelick RJ, et al. Distribution and Redistribution of HIV-1 Nucleocapsid Protein in Immature, Mature, and Integrase-Inhibited Virions: a Role for Integrase in Maturation. J Virol. 2015;89(19):9765-80.
445. Doyle T, Goujon C, Malim MH. HIV-1 and interferons: who's interfering with whom? Nat Rev Microbiol. 2015;13(7):403-13.
446. Sheehy AM, Gaddis NC, Choi JD, Malim MH. Isolation of a human gene that inhibits HIV-1 infection and is suppressed by the viral Vif protein. Nature. 2002;418(6898):646-50.
447. Stremlau M, Owens CM, Perron MJ, Kiessling M, Autissier P, Sodroski J. The cytoplasmic body component TRIM5alpha restricts HIV-1 infection in Old World monkeys. Nature. 2004;427(6977):848-53.
448. Laguette N, Sobhian B, Casartelli N, Ringeard M, Chable-Bessia C, Segeral E, et al. SAMHD1 is the dendritic- and myeloid-cell-specific HIV-1 restriction factor counteracted by Vpx. Nature. 2011;474(7353):654-7.
449. Hrecka K, Hao C, Gierszewska M, Swanson SK, Kesik-Brodacka M, Srivastava S, et al. Vpx relieves inhibition of HIV-1 infection of macrophages mediated by the SAMHD1 protein. Nature. 2011;474(7353):658-61.
450. Neil SJ, Zang T, Bieniasz PD. Tetherin inhibits retrovirus release and is antagonized by HIV-1 Vpu. Nature. 2008;451(7177):425-30.
451. Van Damme N, Goff D, Katsura C, Jorgenson RL, Mitchell R, Johnson MC, et al. The interferon-induced protein BST-2 restricts HIV-1 release and is downregulated from the cell surface by the viral Vpu protein. Cell Host Microbe. 2008;3(4):245-52.
452. Friew YN, Boyko V, Hu WS, Pathak VK. Intracellular interactions between APOBEC3G, RNA, and HIV-1 Gag: APOBEC3G multimerization is dependent on its association with RNA. Retrovirology. 2009;6:56.
453. Huthoff H, Autore F, Gallois-Montbrun S, Fraternali F, Malim MH. RNA-dependent oligomerization of APOBEC3G is required for restriction of HIV-1. PLoS Pathog. 2009;5(3):e1000330.

454. Zhang H, Yang B, Pomerantz RJ, Zhang C, Arunachalam SC, Gao L. The cytidine deaminase CEM15 induces hypermutation in newly synthesized HIV-1 DNA. Nature. 2003;424(6944):94-8.
455. Mangeat B, Turelli P, Caron G, Friedli M, Perrin L, Trono D. Broad antiretroviral defence by human APOBEC3G through lethal editing of nascent reverse transcripts. Nature. 2003;424(6944):99-103.
456. Yu Q, Konig R, Pillai S, Chiles K, Kearney M, Palmer S, et al. Single-strand specificity of APOBEC3G accounts for minus-strand deamination of the HIV genome. Nat Struct Mol Biol. 2004;11(5):435-42.
457. Harris RS, Bishop KN, Sheehy AM, Craig HM, Petersen-Mahrt SK, Watt IN, et al. DNA deamination mediates innate immunity to retroviral infection. Cell. 2003;113(6):803-9.
458. Lecossier D, Bouchonnet F, Clavel F, Hance AJ. Hypermutation of HIV-1 DNA in the absence of the Vif protein. Science. 2003;300(5622):1112.
459. Hultquist JF, Lengyel JA, Refsland EW, LaRue RS, Lackey L, Brown WL, et al. Human and rhesus APOBEC3D, APOBEC3F, APOBEC3G, and APOBEC3H demonstrate a conserved capacity to restrict Vif-deficient HIV-1. J Virol. 2011;85(21):11220-34.
460. Anderson BD, Ikeda T, Moghadasi SA, Martin AS, Brown WL, Harris RS. Natural APOBEC3C variants can elicit differential HIV-1 restriction activity. Retrovirology. 2018;15(1):78.
461. Koning FA, Newman EN, Kim EY, Kunstman KJ, Wolinsky SM, Malim MH. Defining APOBEC3 expression patterns in human tissues and hematopoietic cell subsets. J Virol. 2009;83(18):9474-85.
462. Oliva H, Pacheco R, Martinez-Navio JM, Rodriguez-Garcia M, Naranjo-Gomez M, Climent N, et al. Increased expression with differential subcellular location of cytidine deaminase APOBEC3G in human CD4(+) T-cell activation and dendritic cell maturation. Immunol Cell Biol. 2016;94(7):689-700.
463. Refsland EW, Stenglein MD, Shindo K, Albin JS, Brown WL, Harris RS. Quantitative profiling of the full APOBEC3 mRNA repertoire in lymphocytes and tissues: implications for HIV-1 restriction. Nucleic Acids Res. 2010;38(13):4274-84.
464. Marin M, Rose KM, Kozak SL, Kabat D. HIV-1 Vif protein binds the editing enzyme APOBEC3G and induces its degradation. Nat Med. 2003;9(11):1398-403.
465. Sheehy AM, Gaddis NC, Malim MH. The antiretroviral enzyme APOBEC3G is degraded by the proteasome in response to HIV-1 Vif. Nat Med. 2003;9(11):1404-7.
466. Stopak K, de Noronha C, Yonemoto W, Greene WC. HIV-1 Vif blocks the antiviral activity of APOBEC3G by impairing both its translation and intracellular stability. Mol Cell. 2003;12(3):591-601.
467. Yu X, Yu Y, Liu B, Luo K, Kong W, Mao P, et al. Induction of APOBEC3G ubiquitination and degradation by an HIV-1 Vif-Cul5-SCF complex. Science. 2003;302(5647):1056-60.
468. Mehle A, Strack B, Ancuta P, Zhang C, McPike M, Gabuzda D. Vif overcomes the innate antiviral activity of APOBEC3G by promoting its degradation in the ubiquitin-proteasome pathway. J Biol Chem. 2004;279(9):7792-8.
469. Stremlau M, Perron M, Lee M, Li Y, Song B, Javanbakht H, et al. Specific recognition and accelerated uncoating of retroviral capsids by the TRIM5alpha restriction factor. Proc Natl Acad Sci U S A. 2006;103(14):5514-9.

470. Goldstone DC, Walker PA, Calder LJ, Coombs PJ, Kirkpatrick J, Ball NJ, et al. Structural studies of postentry restriction factors reveal antiparallel dimers that enable avid binding to the HIV-1 capsid lattice. Proc Natl Acad Sci U S A. 2014;111(26):9609-14.
471. Sanchez JG, Okreglicka K, Chandrasekaran V, Welker JM, Sundquist WI, Pornillos O. The tripartite motif coiled-coil is an elongated antiparallel hairpin dimer. Proc Natl Acad Sci U S A. 2014;111(7):2494-9.
472. Wagner JM, Roganowicz MD, Skorupka K, Alam SL, Christensen D, Doss G, et al. Mechanism of B-box 2 domain-mediated higher-order assembly of the retroviral restriction factor TRIM5alpha. Elife. 2016;5.
473. Ganser-Pornillos BK, Chandrasekaran V, Pornillos O, Sodroski JG, Sundquist WI, Yeager M. Hexagonal assembly of a restricting TRIM5alpha protein. Proc Natl Acad Sci U S A. 2011;108(2):534-9.
474. Li YL, Chandrasekaran V, Carter SD, Woodward CL, Christensen DE, Dryden KA, et al. Primate TRIM5 proteins form hexagonal nets on HIV-1 capsids. Elife. 2016;5.
475. Skorupka KA, Roganowicz MD, Christensen DE, Wan Y, Pornillos O, Ganser-Pornillos BK. Hierarchical assembly governs TRIM5alpha recognition of HIV-1 and retroviral capsids. Sci Adv. 2019;5(11):eaaw3631.
476. Perez-Caballero D, Hatziioannou T, Zhang F, Cowan S, Bieniasz PD. Restriction of human immunodeficiency virus type 1 by TRIM-CypA occurs with rapid kinetics and independently of cytoplasmic bodies, ubiquitin, and proteasome activity. J Virol. 2005;79(24):15567-72.
477. Campbell EM, Weingart J, Sette P, Opp S, Sastri J, O'Connor SK, et al. TRIM5alpha-Mediated Ubiquitin Chain Conjugation Is Required for Inhibition of HIV-1 Reverse Transcription and Capsid Destabilization. J Virol. 2016;90(4):1849-57.
478. Jimenez-Guardeno JM, Apolonia L, Betancor G, Malim MH. Immunoproteasome activation enables human TRIM5alpha restriction of HIV-1. Nat Microbiol. 2019;4(6):933-40.
479. Li X, Gold B, O'HUigin C, Diaz-Griffero F, Song B, Si Z, et al. Unique features of TRIM5alpha among closely related human TRIM family members. Virology. 2007;360(2):419-33.
480. Yuan T, Yao W, Tokunaga K, Yang R, Sun B. An HIV-1 capsid binding protein TRIM11 accelerates viral uncoating. Retrovirology. 2016;13(1):72.
481. Ohainle M, Kim K, Komurlu Keceli S, Felton A, Campbell E, Luban J, et al. TRIM34 restricts HIV-1 and SIV capsids in a TRIM5alpha-dependent manner. PLoS Pathog. 2020;16(4):e1008507.
482. Kim K, Dauphin A, Komurlu S, McCauley SM, Yurkovetskiy L, Carbone C, et al. Cyclophilin A protects HIV-1 from restriction by human TRIM5alpha. Nat Microbiol. 2019;4(12):2044-51.
483. Selyutina A, Persaud M, Simons LM, Bulnes-Ramos A, Buffone C, Martinez-Lopez A, et al. Cyclophilin A Prevents HIV-1 Restriction in Lymphocytes by Blocking Human TRIM5alpha Binding to the Viral Core. Cell Rep. 2020;30(11):3766-77 e6.
484. Nisole S, Lynch C, Stoye JP, Yap MW. A Trim5-cyclophilin A fusion protein found in owl monkey kidney cells can restrict HIV-1. Proc Natl Acad Sci U S A. 2004;101(36):13324-8.
485. Sayah DM, Sokolskaja E, Berthoux L, Luban J. Cyclophilin A retrotransposition into TRIM5 explains owl monkey resistance to HIV-1. Nature. 2004;430(6999):569-73.
486. Liao CH, Kuang YQ, Liu HL, Zheng YT, Su B. A novel fusion gene, TRIM5-Cyclophilin A in the pig-tailed macaque determines its susceptibility to HIV-1 infection. AIDS. 2007;21 Suppl 8:S19-26.

487. Brennan G, Kozyrev Y, Hu SL. TRIMCyp expression in Old World primates Macaca nemestrina and Macaca fascicularis. Proc Natl Acad Sci U S A. 2008;105(9):3569-74.
488. Newman RM, Hall L, Kirmaier A, Pozzi LA, Pery E, Farzan M, et al. Evolution of a TRIM5-CypA splice isoform in old world monkeys. PLoS Pathog. 2008;4(2):e1000003.
489. Virgen CA, Kratovac Z, Bieniasz PD, Hatziioannou T. Independent genesis of chimeric TRIM5-cyclophilin proteins in two primate species. Proc Natl Acad Sci U S A. 2008;105(9):3563-8.
490. Wilson SJ, Webb BL, Ylinen LM, Verschoor E, Heeney JL, Towers GJ. Independent evolution of an antiviral TRIMCyp in rhesus macaques. Proc Natl Acad Sci U S A. 2008;105(9):3557-62.
491. Goldstone DC, Ennis-Adeniran V, Hedden JJ, Groom HC, Rice GI, Christodoulou E, et al. HIV-1 restriction factor SAMHD1 is a deoxynucleoside triphosphate triphosphohydrolase. Nature. 2011;480(7377):379-82.
492. Lahouassa H, Daddacha W, Hofmann H, Ayinde D, Logue EC, Dragin L, et al. SAMHD1 restricts the replication of human immunodeficiency virus type 1 by depleting the intracellular pool of deoxynucleoside triphosphates. Nat Immunol. 2012;13(3):223-8.
493. Cribier A, Descours B, Valadao AL, Laguette N, Benkirane M. Phosphorylation of SAMHD1 by cyclin A2/CDK1 regulates its restriction activity toward HIV-1. Cell Rep. 2013;3(4):1036-43.
494. Pauls E, Ruiz A, Badia R, Permanyer M, Gubern A, Riveira-Munoz E, et al. Cell cycle control and HIV-1 susceptibility are linked by CDK6-dependent CDK2 phosphorylation of SAMHD1 in myeloid and lymphoid cells. J Immunol. 2014;193(4):1988-97.
495. Schott K, Fuchs NV, Derua R, Mahboubi B, Schnellbacher E, Seifried J, et al. Dephosphorylation of the HIV-1 restriction factor SAMHD1 is mediated by PP2A-B55alpha holoenzymes during mitotic exit. Nat Commun. 2018;9(1):2227.
496. Coiras M, Bermejo M, Descours B, Mateos E, Garcia-Perez J, Lopez-Huertas MR, et al. IL-7 Induces SAMHD1 Phosphorylation in CD4+ T Lymphocytes, Improving Early Steps of HIV-1 Life Cycle. Cell Rep. 2016;14(9):2100-7.
497. Manganaro L, Hong P, Hernandez MM, Argyle D, Mulder LCF, Potla U, et al. IL-15 regulates susceptibility of CD4(+) T cells to HIV infection. Proc Natl Acad Sci U S A. 2018;115(41):E9659-E67.
498. Jowett JB, Planelles V, Poon B, Shah NP, Chen ML, Chen IS. The human immunodeficiency virus type 1 vpr gene arrests infected T cells in the G2 + M phase of the cell cycle. J Virol. 1995;69(10):6304-13.
499. He J, Choe S, Walker R, Di Marzio P, Morgan DO, Landau NR. Human immunodeficiency virus type 1 viral protein R (Vpr) arrests cells in the G2 phase of the cell cycle by inhibiting p34cdc2 activity. J Virol. 1995;69(11):6705-11.
500. Re F, Braaten D, Franke EK, Luban J. Human immunodeficiency virus type 1 Vpr arrests the cell cycle in G2 by inhibiting the activation of p34cdc2-cyclin B. J Virol. 1995;69(11):6859-64.
501. Greenwood EJ, Matheson NJ, Wals K, van den Boomen DJ, Antrobus R, Williamson JC, et al. Temporal proteomic analysis of HIV infection reveals remodelling of the host phosphoproteome by lentiviral Vif variants. Elife. 2016;5.
502. Salamango DJ, Ikeda T, Moghadasi SA, Wang J, McCann JL, Serebrenik AA, et al. HIV-1 Vif Triggers Cell Cycle Arrest by Degrading Cellular PPP2R5 Phospho-regulators. Cell Rep. 2019;29(5):1057-65 e4.

503. Nagata K, Shindo K, Matsui Y, Shirakawa K, Takaori-Kondo A. Critical role of PP2A-B56 family protein degradation in HIV-1 Vif mediated G2 cell cycle arrest. Biochem Biophys Res Commun. 2020;527(1):257-63.
504. Marelli S, Williamson JC, Protasio AV, Naamati A, Greenwood EJ, Deane JE, et al. Antagonism of PP2A is an independent and conserved function of HIV-1 Vif and causes cell cycle arrest. Elife. 2020;9.
505. Descours B, Cribier A, Chable-Bessia C, Ayinde D, Rice G, Crow Y, et al. SAMHD1 restricts HIV-1 reverse transcription in quiescent CD4(+) T-cells. Retrovirology. 2012;9:87.
506. Baldauf HM, Pan X, Erikson E, Schmidt S, Daddacha W, Burggraf M, et al. SAMHD1 restricts HIV-1 infection in resting CD4(+) T cells. Nat Med. 2012;18(11):1682-7.
507. Mlcochova P, Sutherland KA, Watters SA, Bertoli C, de Bruin RA, Rehwinkel J, et al. A G1-like state allows HIV-1 to bypass SAMHD1 restriction in macrophages. EMBO J. 2017;36(5):604-16.
508. Kupzig S, Korolchuk V, Rollason R, Sugden A, Wilde A, Banting G. Bst-2/HM1.24 is a raft-associated apical membrane protein with an unusual topology. Traffic. 2003;4(10):694-709.
509. Perez-Caballero D, Zang T, Ebrahimi A, McNatt MW, Gregory DA, Johnson MC, et al. Tetherin inhibits HIV-1 release by directly tethering virions to cells. Cell. 2009;139(3):499-511.
510. Sakuma T, Noda T, Urata S, Kawaoka Y, Yasuda J. Inhibition of Lassa and Marburg virus production by tetherin. J Virol. 2009;83(5):2382-5.
511. Jouvenet N, Neil SJ, Zhadina M, Zang T, Kratovac Z, Lee Y, et al. Broad-spectrum inhibition of retroviral and filoviral particle release by tetherin. J Virol. 2009;83(4):1837-44.
512. Mansouri M, Viswanathan K, Douglas JL, Hines J, Gustin J, Moses AV, et al. Molecular mechanism of BST2/tetherin downregulation by K5/MIR2 of Kaposi's sarcoma-associated herpesvirus. J Virol. 2009;83(19):9672-81.
513. Weidner JM, Jiang D, Pan XB, Chang J, Block TM, Guo JT. Interferon-induced cell membrane proteins, IFITM3 and tetherin, inhibit vesicular stomatitis virus infection via distinct mechanisms. J Virol. 2010;84(24):12646-57.
514. Radoshitzky SR, Dong L, Chi X, Clester JC, Retterer C, Spurgers K, et al. Infectious Lassa virus, but not filoviruses, is restricted by BST-2/tetherin. J Virol. 2010;84(20):10569-80.
515. Goffinet C, Schmidt S, Kern C, Oberbremer L, Keppler OT. Endogenous CD317/Tetherin limits replication of HIV-1 and murine leukemia virus in rodent cells and is resistant to antagonists from primate viruses. J Virol. 2010;84(21):11374-84.
516. Dafa-Berger A, Kuzmina A, Fassler M, Yitzhak-Asraf H, Shemer-Avni Y, Taube R. Modulation of hepatitis C virus release by the interferon-induced protein BST-2/tetherin. Virology. 2012;428(2):98-111.
517. Blondeau C, Pelchen-Matthews A, Mlcochova P, Marsh M, Milne RS, Towers GJ. Tetherin restricts herpes simplex virus 1 and is antagonized by glycoprotein M. J Virol. 2013;87(24):13124-33.
518. Zenner HL, Mauricio R, Banting G, Crump CM. Herpes simplex virus 1 counteracts tetherin restriction via its virion host shutoff activity. J Virol. 2013;87(24):13115-23.
519. Taylor JK, Coleman CM, Postel S, Sisk JM, Bernbaum JG, Venkataraman T, et al. Severe Acute Respiratory Syndrome Coronavirus ORF7a Inhibits Bone Marrow Stromal Antigen 2 Virion Tethering through a Novel Mechanism of Glycosylation Interference. J Virol. 2015;89(23):11820-33.
520. Hu S, Yin L, Mei S, Li J, Xu F, Sun H, et al. BST-2 restricts IAV release and is countered by the viral M2 protein. Biochem J. 2017;474(5):715-30.

521. Martin-Sancho L, Lewinski MK, Pache L, Stoneham CA, Yin X, Becker ME, et al. Functional landscape of SARS-CoV-2 cellular restriction. Mol Cell. 2021;81(12):2656-68 e8.
522. Dube M, Roy BB, Guiot-Guillain P, Mercier J, Binette J, Leung G, et al. Suppression of Tetherin-restricting activity upon human immunodeficiency virus type 1 particle release correlates with localization of Vpu in the trans-Golgi network. J Virol. 2009;83(9):4574-90.
523. Mitchell RS, Katsura C, Skasko MA, Fitzpatrick K, Lau D, Ruiz A, et al. Vpu antagonizes BST-2-mediated restriction of HIV-1 release via beta-TrCP and endo-lysosomal trafficking. PLoS Pathog. 2009;5(5):e1000450.
524. Mangeat B, Gers-Huber G, Lehmann M, Zufferey M, Luban J, Piguet V. HIV-1 Vpu neutralizes the antiviral factor Tetherin/BST-2 by binding it and directing its beta-TrCP2-dependent degradation. PLoS Pathog. 2009;5(9):e1000574.
525. Douglas JL, Viswanathan K, McCarroll MN, Gustin JK, Fruh K, Moses AV. Vpu directs the degradation of the human immunodeficiency virus restriction factor BST-2/Tetherin via a {beta}TrCP-dependent mechanism. J Virol. 2009;83(16):7931-47.
526. Goffinet C, Allespach I, Homann S, Tervo HM, Habermann A, Rupp D, et al. HIV-1 antagonism of CD317 is species specific and involves Vpu-mediated proteasomal degradation of the restriction factor. Cell Host Microbe. 2009;5(3):285-97.
527. Dube M, Roy BB, Guiot-Guillain P, Binette J, Mercier J, Chiasson A, et al. Antagonism of tetherin restriction of HIV-1 release by Vpu involves binding and sequestration of the restriction factor in a perinuclear compartment. PLoS Pathog. 2010;6(4):e1000856.
528. Hauser H, Lopez LA, Yang SJ, Oldenburg JE, Exline CM, Guatelli JC, et al. HIV-1 Vpu and HIV-2 Env counteract BST-2/tetherin by sequestration in a perinuclear compartment. Retrovirology. 2010;7:51.
529. Iwabu Y, Fujita H, Kinomoto M, Kaneko K, Ishizaka Y, Tanaka Y, et al. HIV-1 accessory protein Vpu internalizes cell-surface BST-2/tetherin through transmembrane interactions leading to lysosomes. J Biol Chem. 2009;284(50):35060-72.
530. Dube M, Paquay C, Roy BB, Bego MG, Mercier J, Cohen EA. HIV-1 Vpu antagonizes BST-2 by interfering mainly with the trafficking of newly synthesized BST-2 to the cell surface. Traffic. 2011;12(12):1714-29.
531. Le Tortorec A, Neil SJ. Antagonism to and intracellular sequestration of human tetherin by the human immunodeficiency virus type 2 envelope glycoprotein. J Virol. 2009;83(22):11966-78.
532. Gupta RK, Mlcochova P, Pelchen-Matthews A, Petit SJ, Mattiuzzo G, Pillay D, et al. Simian immunodeficiency virus envelope glycoprotein counteracts tetherin/BST-2/CD317 by intracellular sequestration. Proc Natl Acad Sci U S A. 2009;106(49):20889-94.
533. Exline CM, Yang SJ, Haworth KG, Rengarajan S, Lopez LA, Droniou ME, et al. Determinants in HIV-2 Env and tetherin required for functional interaction. Retrovirology. 2015;12:67.
534. Heusinger E, Deppe K, Sette P, Krapp C, Kmiec D, Kluge SF, et al. Preadaptation of Simian Immunodeficiency Virus SIVsmm Facilitated Env-Mediated Counteraction of Human Tetherin by Human Immunodeficiency Virus Type 2. J Virol. 2018;92(18).
535. Buffalo CZ, Sturzel CM, Heusinger E, Kmiec D, Kirchhoff F, Hurley JH, et al. Structural Basis for Tetherin Antagonism as a Barrier to Zoonotic Lentiviral Transmission. Cell Host Microbe. 2019;26(3):359-68 e8.

536. Jia B, Serra-Moreno R, Neidermyer W, Rahmberg A, Mackey J, Fofana IB, et al. Species-specific activity of SIV Nef and HIV-1 Vpu in overcoming restriction by tetherin/BST2. PLoS Pathog. 2009;5(5):e1000429.
537. Sauter D, Schindler M, Specht A, Landford WN, Munch J, Kim KA, et al. Tetherin-driven adaptation of Vpu and Nef function and the evolution of pandemic and nonpandemic HIV-1 strains. Cell Host Microbe. 2009;6(5):409-21.
538. Zhang F, Wilson SJ, Landford WC, Virgen B, Gregory D, Johnson MC, et al. Nef proteins from simian immunodeficiency viruses are tetherin antagonists. Cell Host Microbe. 2009;6(1):54-67.
539. Cocka LJ, Bates P. Identification of alternatively translated Tetherin isoforms with differing antiviral and signaling activities. PLoS Pathog. 2012;8(9):e1002931.
540. Weinelt J, Neil SJ. Differential sensitivities of tetherin isoforms to counteraction by primate lentiviruses. J Virol. 2014;88(10):5845-58.
541. Galao RP, Le Tortorec A, Pickering S, Kueck T, Neil SJ. Innate sensing of HIV-1 assembly by Tetherin induces NFkappaB-dependent proinflammatory responses. Cell Host Microbe. 2012;12(5):633-44.
542. Tokarev A, Suarez M, Kwan W, Fitzpatrick K, Singh R, Guatelli J. Stimulation of NF-kappaB activity by the HIV restriction factor BST2. J Virol. 2013;87(4):2046-57.
543. Sauter D, Hotter D, Van Driessche B, Sturzel CM, Kluge SF, Wildum S, et al. Differential regulation of NF-kappaB-mediated proviral and antiviral host gene expression by primate lentiviral Nef and Vpu proteins. Cell Rep. 2015;10(4):586-99.
544. Langer S, Hammer C, Hopfensperger K, Klein L, Hotter D, De Jesus PD, et al. HIV-1 Vpu is a potent transcriptional suppressor of NF-kappaB-elicited antiviral immune responses. Elife. 2019;8.
545. Guzzo C, Jung M, Graveline A, Banfield BW, Gee K. IL-27 increases BST-2 expression in human monocytes and T cells independently of type I IFN. Sci Rep. 2012;2:974.
546. Mariani R, Chen D, Schrofelbauer B, Navarro F, Konig R, Bollman B, et al. Species-specific exclusion of APOBEC3G from HIV-1 virions by Vif. Cell. 2003;114(1):21-31.
547. McNatt MW, Zang T, Hatziioannou T, Bartlett M, Fofana IB, Johnson WE, et al. Species-specific activity of HIV-1 Vpu and positive selection of tetherin transmembrane domain variants. PLoS Pathog. 2009;5(2):e1000300.
548. Westmoreland SV, Converse AP, Hrecka K, Hurley M, Knight H, Piatak M, et al. SIV vpx is essential for macrophage infection but not for development of AIDS. PLoS One. 2014;9(1):e84463.
549. Li J, Lord CI, Haseltine W, Letvin NL, Sodroski J. Infection of cynomolgus monkeys with a chimeric HIV-1/SIVmac virus that expresses the HIV-1 envelope glycoproteins. J Acquir Immune Defic Syndr. 1992;5(7):639-46.
550. Ho DD, Hartshorn KL, Rota TR, Andrews CA, Kaplan JC, Schooley RT, et al. Recombinant human interferon alfa-A suppresses HTLV-III replication in vitro. Lancet. 1985;1(8429):602-4.
551. Kornbluth RS, Oh PS, Munis JR, Cleveland PH, Richman DD. Interferons and bacterial lipopolysaccharide protect macrophages from productive infection by human immunodeficiency virus in vitro. J Exp Med. 1989;169(3):1137-51.
552. Shirazi Y, Pitha PM. Alpha interferon inhibits early stages of the human immunodeficiency virus type 1 replication cycle. J Virol. 1992;66(3):1321-8.

553. Meylan PR, Guatelli JC, Munis JR, Richman DD, Kornbluth RS. Mechanisms for the inhibition of HIV replication by interferons-alpha, -beta, and -gamma in primary human macrophages. Virology. 1993;193(1):138-48.
554. Goujon C, Malim MH. Characterization of the alpha interferon-induced postentry block to HIV-1 infection in primary human macrophages and T cells. J Virol. 2010;84(18):9254-66.
555. Cheney KM, McKnight A. Interferon-alpha mediates restriction of human immunodeficiency virus type-1 replication in primary human macrophages at an early stage of replication. PLoS One. 2010;5(10):e13521.
556. Krapp C, Hotter D, Gawanbacht A, McLaren PJ, Kluge SF, Sturzel CM, et al. Guanylate Binding Protein (GBP) 5 Is an Interferon-Inducible Inhibitor of HIV-1 Infectivity. Cell Host Microbe. 2016;19(4):504-14.
557. Lu J, Pan Q, Rong L, He W, Liu SL, Liang C. The IFITM proteins inhibit HIV-1 infection. J Virol. 2011;85(5):2126-37.
558. Tartour K, Appourchaux R, Gaillard J, Nguyen XN, Durand S, Turpin J, et al. IFITM proteins are incorporated onto HIV-1 virion particles and negatively imprint their infectivity. Retrovirology. 2014;11:103.
559. Compton AA, Bruel T, Porrot F, Mallet A, Sachse M, Euvrard M, et al. IFITM proteins incorporated into HIV-1 virions impair viral fusion and spread. Cell Host Microbe. 2014;16(6):736-47.
560. Yu J, Li M, Wilkins J, Ding S, Swartz TH, Esposito AM, et al. IFITM Proteins Restrict HIV-1 Infection by Antagonizing the Envelope Glycoprotein. Cell Rep. 2015;13(1):145-56.
561. Tartour K, Nguyen XN, Appourchaux R, Assil S, Barateau V, Bloyet LM, et al. Interference with the production of infectious viral particles and bimodal inhibition of replication are broadly conserved antiviral properties of IFITMs. PLoS Pathog. 2017;13(9):e1006610.
562. Braun E, Hotter D, Koepke L, Zech F, Gross R, Sparrer KMJ, et al. Guanylate-Binding Proteins 2 and 5 Exert Broad Antiviral Activity by Inhibiting Furin-Mediated Processing of Viral Envelope Proteins. Cell Rep. 2019;27(7):2092-104 e10.
563. Cui W, Braun E, Wang W, Tang J, Zheng Y, Slater B, et al. Structural basis for GTP-induced dimerization and antiviral function of guanylate-binding proteins. Proc Natl Acad Sci U S A. 2021;118(15).
564. Foster TL, Wilson H, Iyer SS, Coss K, Doores K, Smith S, et al. Resistance of Transmitted Founder HIV-1 to IFITM-Mediated Restriction. Cell Host Microbe. 2016;20(4):429-42.
565. Wang Y, Pan Q, Ding S, Wang Z, Yu J, Finzi A, et al. The V3 Loop of HIV-1 Env Determines Viral Susceptibility to IFITM3 Impairment of Viral Infectivity. J Virol. 2017;91(7).
566. Drouin A, Migraine J, Durand MA, Moreau A, Burlaud-Gaillard J, Beretta M, et al. Escape of HIV-1 envelope glycoprotein from the restriction of infection by IFITM3. J Virol. 2020.
567. Goujon C, Moncorge O, Bauby H, Doyle T, Ward CC, Schaller T, et al. Human MX2 is an interferon-induced post-entry inhibitor of HIV-1 infection. Nature. 2013;502(7472):559-62.
568. Kane M, Yadav SS, Bitzegeio J, Kutluay SB, Zang T, Wilson SJ, et al. MX2 is an interferon-induced inhibitor of HIV-1 infection. Nature. 2013;502(7472):563-6.
569. Liu Z, Pan Q, Ding S, Qian J, Xu F, Zhou J, et al. The interferon-inducible MxB protein inhibits HIV-1 infection. Cell Host Microbe. 2013;14(4):398-410.
570. Fricke T, White TE, Schulte B, de Souza Aranha Vieira DA, Dharan A, Campbell EM, et al. MxB binds to the HIV-1 core and prevents the uncoating process of HIV-1. Retrovirology. 2014;11:68.

571. Kane M, Rebensburg SV, Takata MA, Zang TM, Yamashita M, Kvaratskhelia M, et al. Nuclear pore heterogeneity influences HIV-1 infection and the antiviral activity of MX2. Elife. 2018;7.
572. Smaga SS, Xu C, Summers BJ, Digianantonio KM, Perilla JR, Xiong Y. MxB Restricts HIV-1 by Targeting the Tri-hexamer Interface of the Viral Capsid. Structure. 2019;27(8):1234-45 e5.
573. Li M, Kao E, Gao X, Sandig H, Limmer K, Pavon-Eternod M, et al. Codon-usage-based inhibition of HIV protein synthesis by human schlafen 11. Nature. 2012;491(7422):125-8.
574. Zhu Y, Chen G, Lv F, Wang X, Ji X, Xu Y, et al. Zinc-finger antiviral protein inhibits HIV-1 infection by selectively targeting multiply spliced viral mRNAs for degradation. Proc Natl Acad Sci U S A. 2011;108(38):15834-9.
575. Zhu Y, Wang X, Goff SP, Gao G. Translational repression precedes and is required for ZAP-mediated mRNA decay. EMBO J. 2012;31(21):4236-46.
576. Takata MA, Goncalves-Carneiro D, Zang TM, Soll SJ, York A, Blanco-Melo D, et al. CG dinucleotide suppression enables antiviral defence targeting non-self RNA. Nature. 2017;550(7674):124-7.
577. Ficarelli M, Wilson H, Pedro Galao R, Mazzon M, Antzin-Anduetza I, Marsh M, et al. KHNYN is essential for the zinc finger antiviral protein (ZAP) to restrict HIV-1 containing clustered CpG dinucleotides. Elife. 2019;8.
578. Ficarelli M, Antzin-Anduetza I, Hugh-White R, Firth AE, Sertkaya H, Wilson H, et al. CpG Dinucleotides Inhibit HIV-1 Replication through Zinc Finger Antiviral Protein (ZAP)-Dependent and -Independent Mechanisms. J Virol. 2020;94(6).
579. Kmiec D, Nchioua R, Sherrill-Mix S, Sturzel CM, Heusinger E, Braun E, et al. CpG Frequency in the 5' Third of the env Gene Determines Sensitivity of Primary HIV-1 Strains to the Zinc-Finger Antiviral Protein. mBio. 2020;11(1).
580. Xue G, Braczyk K, Goncalves-Carneiro D, Dawidziak DM, Sanchez K, Ong H, et al. Poly(ADP-ribose) potentiates ZAP antiviral activity. PLoS Pathog. 2022;18(2):e1009202.
581. Li M, Kao E, Malone D, Gao X, Wang JYJ, David M. DNA damage-induced cell death relies on SLFN11-dependent cleavage of distinct type II tRNAs. Nat Struct Mol Biol. 2018;25(11):1047-58.
582. Jordan-Paiz A, Franco S, Martinez MA. Synonymous Codon Pair Recoding of the HIV-1 env Gene Affects Virus Replication Capacity. Cells. 2021;10(7).
583. Jordan-Paiz A, Franco S, Martinez MA. Reducing HIV-1 env gene CpG frequency increases the replication capacity of the HXB2 virus strain. Virus Res. 2022;310:198685.
584. Rosa A, Chande A, Ziglio S, De Sanctis V, Bertorelli R, Goh SL, et al. HIV-1 Nef promotes infection by excluding SERINC5 from virion incorporation. Nature. 2015;526(7572):212-7.
585. Usami Y, Wu Y, Gottlinger HG. SERINC3 and SERINC5 restrict HIV-1 infectivity and are counteracted by Nef. Nature. 2015;526(7572):218-23.
586. Trautz B, Pierini V, Wombacher R, Stolp B, Chase AJ, Pizzato M, et al. Antagonism of the SERINC5 Particle Infectivity Restriction by HIV-1 Nef Involves Counteraction of Virion-associated Pools of the Restriction Factor. J Virol. 2016.
587. Ward AE, Kiessling V, Pornillos O, White JM, Ganser-Pornillos BK, Tamm LK. HIV-cell membrane fusion intermediates are restricted by Serincs as revealed by cryo-electron and TIRF microscopy. J Biol Chem. 2020;295(45):15183-95.
588. Leonhardt SA, Purdy MD, Grover JR, Yang Z, Poulos S, McIntire WE, et al. Cryo-EM structures of the human HIV-1 restriction factor SERINC3 and function as a lipid flippase Cold

Spring Harbor, NY: Cold Spring Harbor Laboratory - Retroviruses virtual meeting 2021; 2021 [Available from: https://meetings.cshl.edu/abstracts.aspx?meet=retro&year=21.
589. Pye VE, Rosa A, Bertelli C, Struwe WB, Maslen SL, Corey R, et al. A bipartite structural organization defines the SERINC family of HIV-1 restriction factors. Nat Struct Mol Biol. 2020;27(1):78-83.
590. Heigele A, Kmiec D, Regensburger K, Langer S, Peiffer L, Sturzel CM, et al. The Potency of Nef-Mediated SERINC5 Antagonism Correlates with the Prevalence of Primate Lentiviruses in the Wild. Cell Host Microbe. 2016;20(3):381-91.
591. Janaka SK, Palumbo AV, Tavakoli-Tameh A, Evans DT. Selective Disruption of SERINC5 Antagonism by Nef Impairs SIV Replication in Primary CD4(+) T Cells. J Virol. 2021.
592. Li M, Waheed AA, Yu J, Zeng C, Chen HY, Zheng YM, et al. TIM-mediated inhibition of HIV-1 release is antagonized by Nef but potentiated by SERINC proteins. Proc Natl Acad Sci U S A. 2019;116(12):5705-14.
593. Prevost J, Edgar CR, Richard J, Trothen SM, Jacob RA, Mumby MJ, et al. HIV-1 Vpu Downregulates Tim-3 from the Surface of Infected CD4(+) T Cells. J Virol. 2020;94(7).
594. Desrosiers RC, Lifson JD, Gibbs JS, Czajak SC, Howe AY, Arthur LO, et al. Identification of highly attenuated mutants of simian immunodeficiency virus. J Virol. 1998;72(2):1431-7.
595. Sato K, Izumi T, Misawa N, Kobayashi T, Yamashita Y, Ohmichi M, et al. Remarkable lethal G-to-A mutations in vif-proficient HIV-1 provirus by individual APOBEC3 proteins in humanized mice. J Virol. 2010;84(18):9546-56.
596. Krisko JF, Martinez-Torres F, Foster JL, Garcia JV. HIV restriction by APOBEC3 in humanized mice. PLoS Pathog. 2013;9(3):e1003242.
597. Krisko JF, Begum N, Baker CE, Foster JL, Garcia JV. APOBEC3G and APOBEC3F Act in Concert To Extinguish HIV-1 Replication. J Virol. 2016;90(9):4681-95.
598. Mehle A, Goncalves J, Santa-Marta M, McPike M, Gabuzda D. Phosphorylation of a novel SOCS-box regulates assembly of the HIV-1 Vif-Cul5 complex that promotes APOBEC3G degradation. Genes Dev. 2004;18(23):2861-6.
599. Yu Y, Xiao Z, Ehrlich ES, Yu X, Yu XF. Selective assembly of HIV-1 Vif-Cul5-ElonginB-ElonginC E3 ubiquitin ligase complex through a novel SOCS box and upstream cysteines. Genes Dev. 2004;18(23):2867-72.
600. Kobayashi M, Takaori-Kondo A, Miyauchi Y, Iwai K, Uchiyama T. Ubiquitination of APOBEC3G by an HIV-1 Vif-Cullin5-Elongin B-Elongin C complex is essential for Vif function. J Biol Chem. 2005;280(19):18573-8.
601. Shirakawa K, Takaori-Kondo A, Kobayashi M, Tomonaga M, Izumi T, Fukunaga K, et al. Ubiquitination of APOBEC3 proteins by the Vif-Cullin5-ElonginB-ElonginC complex. Virology. 2006;344(2):263-6.
602. Jager S, Kim DY, Hultquist JF, Shindo K, LaRue RS, Kwon E, et al. Vif hijacks CBF-beta to degrade APOBEC3G and promote HIV-1 infection. Nature. 2011;481(7381):371-5.
603. Zhang W, Du J, Evans SL, Yu Y, Yu XF. T-cell differentiation factor CBF-beta regulates HIV-1 Vif-mediated evasion of host restriction. Nature. 2011;481(7381):376-9.
604. Kim DY, Kwon E, Hartley PD, Crosby DC, Mann S, Krogan NJ, et al. CBFbeta stabilizes HIV Vif to counteract APOBEC3 at the expense of RUNX1 target gene expression. Mol Cell. 2013;49(4):632-44.
605. Guo Y, Dong L, Qiu X, Wang Y, Zhang B, Liu H, et al. Structural basis for hijacking CBF-beta and CUL5 E3 ligase complex by HIV-1 Vif. Nature. 2014;505(7482):229-33.

606. Fribourgh JL, Nguyen HC, Wolfe LS, Dewitt DC, Zhang W, Yu XF, et al. Core binding factor beta plays a critical role by facilitating the assembly of the Vif-cullin 5 E3 ubiquitin ligase. J Virol. 2014;88(6):3309-19.
607. Kaake RM, Echeverria I, Kim SJ, Von Dollen J, Chesarino NM, Feng Y, et al. Characterization of an A3G-VifHIV-1-CRL5-CBFbeta Structure Using a Cross-linking Mass Spectrometry Pipeline for Integrative Modeling of Host-Pathogen Complexes. Mol Cell Proteomics. 2021;20:100132.
608. Naamati A, Williamson JC, Greenwood EJ, Marelli S, Lehner PJ, Matheson NJ. Functional proteomic atlas of HIV infection in primary human CD4+ T cells. Elife. 2019;8.
609. Borel S, Robert-Hebmann V, Alfaisal J, Jain A, Faure M, Espert L, et al. HIV-1 viral infectivity factor interacts with microtubule-associated protein light chain 3 and inhibits autophagy. AIDS. 2015;29(3):275-86.
610. Okumura A, Alce T, Lubyova B, Ezelle H, Strebel K, Pitha PM. HIV-1 accessory proteins VPR and Vif modulate antiviral response by targeting IRF-3 for degradation. Virology. 2008;373(1):85-97.
611. Gargan S, Ahmed S, Mahony R, Bannan C, Napoletano S, O'Farrelly C, et al. HIV-1 Promotes the Degradation of Components of the Type 1 IFN JAK/STAT Pathway and Blocks Anti-viral ISG Induction. EBioMedicine. 2018;30:203-16.
612. Wang Y, Qian G, Zhu L, Zhao Z, Liu Y, Han W, et al. HIV-1 Vif suppresses antiviral immunity by targeting STING. Cell Mol Immunol. 2022;19(1):108-21.
613. Gibbs JS, Lackner AA, Lang SM, Simon MA, Sehgal PK, Daniel MD, et al. Progression to AIDS in the absence of a gene for vpr or vpx. J Virol. 1995;69(4):2378-83.
614. Hoch J, Lang SM, Weeger M, Stahl-Hennig C, Coulibaly C, Dittmer U, et al. vpr deletion mutant of simian immunodeficiency virus induces AIDS in rhesus monkeys. J Virol. 1995;69(8):4807-13.
615. Sato K, Misawa N, Iwami S, Satou Y, Matsuoka M, Ishizaka Y, et al. HIV-1 Vpr accelerates viral replication during acute infection by exploitation of proliferating CD4+ T cells in vivo. PLoS Pathog. 2013;9(12):e1003812.
616. Ali A, Ng HL, Blankson JN, Burton DR, Buckheit RW, 3rd, Moldt B, et al. Highly Attenuated Infection With a Vpr-Deleted Molecular Clone of Human Immunodeficiency Virus-1. J Infect Dis. 2018;218(9):1447-52.
617. Nodder SB, Gummuluru S. Illuminating the Role of Vpr in HIV Infection of Myeloid Cells. Front Immunol. 2019;10:1606.
618. Belzile JP, Duisit G, Rougeau N, Mercier J, Finzi A, Cohen EA. HIV-1 Vpr-mediated G2 arrest involves the DDB1-CUL4AVPRBP E3 ubiquitin ligase. PLoS Pathog. 2007;3(7):e85.
619. Le Rouzic E, Belaidouni N, Estrabaud E, Morel M, Rain JC, Transy C, et al. HIV1 Vpr arrests the cell cycle by recruiting DCAF1/VprBP, a receptor of the Cul4-DDB1 ubiquitin ligase. Cell Cycle. 2007;6(2):182-8.
620. Schrofelbauer B, Hakata Y, Landau NR. HIV-1 Vpr function is mediated by interaction with the damage-specific DNA-binding protein DDB1. Proc Natl Acad Sci U S A. 2007;104(10):4130-5.
621. DeHart JL, Zimmerman ES, Ardon O, Monteiro-Filho CM, Arganaraz ER, Planelles V. HIV-1 Vpr activates the G2 checkpoint through manipulation of the ubiquitin proteasome system. Virol J. 2007;4:57.

622. Hrecka K, Gierszewska M, Srivastava S, Kozaczkiewicz L, Swanson SK, Florens L, et al. Lentiviral Vpr usurps Cul4-DDB1[VprBP] E3 ubiquitin ligase to modulate cell cycle. Proc Natl Acad Sci U S A. 2007;104(28):11778-83.
623. Rogel ME, Wu LI, Emerman M. The human immunodeficiency virus type 1 vpr gene prevents cell proliferation during chronic infection. J Virol. 1995;69(2):882-8.
624. Roshal M, Kim B, Zhu Y, Nghiem P, Planelles V. Activation of the ATR-mediated DNA damage response by the HIV-1 viral protein R. J Biol Chem. 2003;278(28):25879-86.
625. Wang L, Mukherjee S, Jia F, Narayan O, Zhao LJ. Interaction of virion protein Vpr of human immunodeficiency virus type 1 with cellular transcription factor Sp1 and trans-activation of viral long terminal repeat. J Biol Chem. 1995;270(43):25564-9.
626. Vanitharani R, Mahalingam S, Rafaeli Y, Singh SP, Srinivasan A, Weiner DB, et al. HIV-1 Vpr transactivates LTR-directed expression through sequences present within -278 to -176 and increases virus replication in vitro. Virology. 2001;289(2):334-42.
627. Liu R, Tan J, Lin Y, Jia R, Yang W, Liang C, et al. HIV-1 Vpr activates both canonical and noncanonical NF-kappaB pathway by enhancing the phosphorylation of IKKalpha/beta. Virology. 2013;439(1):47-56.
628. Liu R, Lin Y, Jia R, Geng Y, Liang C, Tan J, et al. HIV-1 Vpr stimulates NF-kappaB and AP-1 signaling by activating TAK1. Retrovirology. 2014;11:45.
629. Bauby H, Ward CC, Hugh-White R, Swanson CM, Schulz R, Goujon C, et al. HIV-1 Vpr Induces Widespread Transcriptomic Changes in CD4(+) T Cells Early Postinfection. mBio. 2021;12(3):e0136921.
630. Conti L, Rainaldi G, Matarrese P, Varano B, Rivabene R, Columba S, et al. The HIV-1 vpr protein acts as a negative regulator of apoptosis in a human lymphoblastoid T cell line: possible implications for the pathogenesis of AIDS. J Exp Med. 1998;187(3):403-13.
631. Jacotot E, Ravagnan L, Loeffler M, Ferri KF, Vieira HL, Zamzami N, et al. The HIV-1 viral protein R induces apoptosis via a direct effect on the mitochondrial permeability transition pore. J Exp Med. 2000;191(1):33-46.
632. Muthumani K, Hwang DS, Desai BM, Zhang D, Dayes N, Green DR, et al. HIV-1 Vpr induces apoptosis through caspase 9 in T cells and peripheral blood mononuclear cells. J Biol Chem. 2002;277(40):37820-31.
633. Andersen JL, DeHart JL, Zimmerman ES, Ardon O, Kim B, Jacquot G, et al. HIV-1 Vpr-induced apoptosis is cell cycle dependent and requires Bax but not ANT. PLoS Pathog. 2006;2(12):e127.
634. Ward J, Davis Z, DeHart J, Zimmerman E, Bosque A, Brunetta E, et al. HIV-1 Vpr triggers natural killer cell-mediated lysis of infected cells through activation of the ATR-mediated DNA damage response. PLoS Pathog. 2009;5(10):e1000613.
635. Richard J, Sindhu S, Pham TN, Belzile JP, Cohen EA. HIV-1 Vpr up-regulates expression of ligands for the activating NKG2D receptor and promotes NK cell-mediated killing. Blood. 2010;115(7):1354-63.
636. Vassena L, Giuliani E, Matusali G, Cohen EA, Doria M. The human immunodeficiency virus type 1 Vpr protein upregulates PVR via activation of the ATR-mediated DNA damage response pathway. J Gen Virol. 2013;94(Pt 12):2664-9.
637. Schrofelbauer B, Yu Q, Zeitlin SG, Landau NR. Human immunodeficiency virus type 1 Vpr induces the degradation of the UNG and SMUG uracil-DNA glycosylases. J Virol. 2005;79(17):10978-87.

638. Wu Y, Zhou X, Barnes CO, DeLucia M, Cohen AE, Gronenborn AM, et al. The DDB1-DCAF1-Vpr-UNG2 crystal structure reveals how HIV-1 Vpr steers human UNG2 toward destruction. Nat Struct Mol Biol. 2016;23(10):933-40.
639. Laguette N, Bregnard C, Hue P, Basbous J, Yatim A, Larroque M, et al. Premature activation of the SLX4 complex by Vpr promotes G2/M arrest and escape from innate immune sensing. Cell. 2014;156(1-2):134-45.
640. Zhou X, DeLucia M, Ahn J. SLX4-SLX1 Protein-independent Down-regulation of MUS81-EME1 Protein by HIV-1 Viral Protein R (Vpr). J Biol Chem. 2016;291(33):16936-47.
641. Zhou X, DeLucia M, Hao C, Hrecka K, Monnie C, Skowronski J, et al. HIV-1 Vpr protein directly loads helicase-like transcription factor (HLTF) onto the CRL4-DCAF1 E3 ubiquitin ligase. J Biol Chem. 2017;292(51):21117-27.
642. Yan J, Shun MC, Zhang Y, Hao C, Skowronski J. HIV-1 Vpr counteracts HLTF-mediated restriction of HIV-1 infection in T cells. Proc Natl Acad Sci U S A. 2019;116(19):9568-77.
643. Yan J, Shun MC, Hao C, Zhang Y, Qian J, Hrecka K, et al. HIV-1 Vpr Reprograms CLR4(DCAF1) E3 Ubiquitin Ligase to Antagonize Exonuclease 1-Mediated Restriction of HIV-1 Infection. mBio. 2018;9(5).
644. Greenwood EJD, Williamson JC, Sienkiewicz A, Naamati A, Matheson NJ, Lehner PJ. Promiscuous Targeting of Cellular Proteins by Vpr Drives Systems-Level Proteomic Remodeling in HIV-1 Infection. Cell Rep. 2019;27(5):1579-96 e7.
645. Barbosa JAF, Sparapani S, Boulais J, Lodge R, Cohen EA. Human Immunodeficiency Virus Type 1 Vpr Mediates Degradation of APC1, a Scaffolding Component of the Anaphase-Promoting Complex/Cyclosome. J Virol. 2021;95(15):e0097120.
646. Zhang F, Bieniasz PD. HIV-1 Vpr induces cell cycle arrest and enhances viral gene expression by depleting CCDC137. Elife. 2020;9.
647. Huet T, Cheynier R, Meyerhans A, Roelants G, Wain-Hobson S. Genetic organization of a chimpanzee lentivirus related to HIV-1. Nature. 1990;345(6273):356-9.
648. Courgnaud V, Salemi M, Pourrut X, Mpoudi-Ngole E, Abela B, Auzel P, et al. Characterization of a novel simian immunodeficiency virus with a vpu gene from greater spot-nosed monkeys (Cercopithecus nictitans) provides new insights into simian/human immunodeficiency virus phylogeny. J Virol. 2002;76(16):8298-309.
649. Courgnaud V, Abela B, Pourrut X, Mpoudi-Ngole E, Loul S, Delaporte E, et al. Identification of a new simian immunodeficiency virus lineage with a vpu gene present among different cercopithecus monkeys (C. mona, C. cephus, and C. nictitans) from Cameroon. J Virol. 2003;77(23):12523-34.
650. Barlow KL, Ajao AO, Clewley JP. Characterization of a novel simian immunodeficiency virus (SIVmonNG1) genome sequence from a mona monkey (Cercopithecus mona). J Virol. 2003;77(12):6879-88.
651. Dazza MC, Ekwalanga M, Nende M, Shamamba KB, Bitshi P, Paraskevis D, et al. Characterization of a novel vpu-harboring simian immunodeficiency virus from a Dent's Mona monkey (Cercopithecus mona denti). J Virol. 2005;79(13):8560-71.
652. Zhang H, Lin EC, Das BB, Tian Y, Opella SJ. Structural determination of virus protein U from HIV-1 by NMR in membrane environments. Biochim Biophys Acta. 2015;1848(11 Pt A):3007-18.
653. Schubert U, Schneider T, Henklein P, Hoffmann K, Berthold E, Hauser H, et al. Human-immunodeficiency-virus-type-1-encoded Vpu protein is phosphorylated by casein kinase II. Eur J Biochem. 1992;204(2):875-83.

654. Schubert U, Strebel K. Differential activities of the human immunodeficiency virus type 1-encoded Vpu protein are regulated by phosphorylation and occur in different cellular compartments. J Virol. 1994;68(4):2260-71.
655. Schubert U, Henklein P, Boldyreff B, Wingender E, Strebel K, Porstmann T. The human immunodeficiency virus type 1 encoded Vpu protein is phosphorylated by casein kinase-2 (CK-2) at positions Ser52 and Ser56 within a predicted alpha-helix-turn-alpha-helix-motif. J Mol Biol. 1994;236(1):16-25.
656. Friborg J, Ladha A, Gottlinger H, Haseltine WA, Cohen EA. Functional analysis of the phosphorylation sites on the human immunodeficiency virus type 1 Vpu protein. J Acquir Immune Defic Syndr Hum Retrovirol. 1995;8(1):10-22.
657. Margottin F, Bour SP, Durand H, Selig L, Benichou S, Richard V, et al. A novel human WD protein, h-beta TrCp, that interacts with HIV-1 Vpu connects CD4 to the ER degradation pathway through an F-box motif. Mol Cell. 1998;1(4):565-74.
658. Butticaz C, Michielin O, Wyniger J, Telenti A, Rothenberger S. Silencing of both beta-TrCP1 and HOS (beta-TrCP2) is required to suppress human immunodeficiency virus type 1 Vpu-mediated CD4 down-modulation. J Virol. 2007;81(3):1502-5.
659. Kueck T, Neil SJ. A cytoplasmic tail determinant in HIV-1 Vpu mediates targeting of tetherin for endosomal degradation and counteracts interferon-induced restriction. PLoS Pathog. 2012;8(3):e1002609.
660. Jia X, Weber E, Tokarev A, Lewinski M, Rizk M, Suarez M, et al. Structural basis of HIV-1 Vpu-mediated BST2 antagonism via hijacking of the clathrin adaptor protein complex 1. Elife. 2014;3:e02362.
661. Kueck T, Foster TL, Weinelt J, Sumner JC, Pickering S, Neil SJ. Serine Phosphorylation of HIV-1 Vpu and Its Binding to Tetherin Regulates Interaction with Clathrin Adaptors. PLoS Pathog. 2015;11(8):e1005141.
662. Klimkait T, Strebel K, Hoggan MD, Martin MA, Orenstein JM. The human immunodeficiency virus type 1-specific protein vpu is required for efficient virus maturation and release. J Virol. 1990;64(2):621-9.
663. Varthakavi V, Smith RM, Martin KL, Derdowski A, Lapierre LA, Goldenring JR, et al. The pericentriolar recycling endosome plays a key role in Vpu-mediated enhancement of HIV-1 particle release. Traffic. 2006;7(3):298-307.
664. Willey RL, Maldarelli F, Martin MA, Strebel K. Human immunodeficiency virus type 1 Vpu protein induces rapid degradation of CD4. J Virol. 1992;66(12):7193-200.
665. Hout DR, Gomez ML, Pacyniak E, Gomez LM, Inbody SH, Mulcahy ER, et al. Scrambling of the amino acids within the transmembrane domain of Vpu results in a simian-human immunodeficiency virus (SHIVTM) that is less pathogenic for pig-tailed macaques. Virology. 2005;339(1):56-69.
666. Shingai M, Yoshida T, Martin MA, Strebel K. Some human immunodeficiency virus type 1 Vpu proteins are able to antagonize macaque BST-2 in vitro and in vivo: Vpu-negative simian-human immunodeficiency viruses are attenuated in vivo. J Virol. 2011;85(19):9708-15.
667. Sato K, Misawa N, Fukuhara M, Iwami S, An DS, Ito M, et al. Vpu augments the initial burst phase of HIV-1 propagation and downregulates BST2 and CD4 in humanized mice. J Virol. 2012;86(9):5000-13.
668. Dave VP, Hajjar F, Dieng MM, Haddad E, Cohen EA. Efficient BST2 antagonism by Vpu is critical for early HIV-1 dissemination in humanized mice. Retrovirology. 2013;10:128.

669. Yamada E, Nakaoka S, Klein L, Reith E, Langer S, Hopfensperger K, et al. Human-Specific Adaptations in Vpu Conferring Anti-tetherin Activity Are Critical for Efficient Early HIV-1 Replication In Vivo. Cell Host Microbe. 2018;23(1):110-20 e7.
670. Willey RL, Maldarelli F, Martin MA, Strebel K. Human immunodeficiency virus type 1 Vpu protein regulates the formation of intracellular gp160-CD4 complexes. J Virol. 1992;66(1):226-34.
671. Lenburg ME, Landau NR. Vpu-induced degradation of CD4: requirement for specific amino acid residues in the cytoplasmic domain of CD4. J Virol. 1993;67(12):7238-45.
672. Vincent MJ, Raja NU, Jabbar MA. Human immunodeficiency virus type 1 Vpu protein induces degradation of chimeric envelope glycoproteins bearing the cytoplasmic and anchor domains of CD4: role of the cytoplasmic domain in Vpu-induced degradation in the endoplasmic reticulum. J Virol. 1993;67(9):5538-49.
673. Willey RL, Buckler-White A, Strebel K. Sequences present in the cytoplasmic domain of CD4 are necessary and sufficient to confer sensitivity to the human immunodeficiency virus type 1 Vpu protein. J Virol. 1994;68(2):1207-12.
674. Yao XJ, Friborg J, Checroune F, Gratton S, Boisvert F, Sekaly RP, et al. Degradation of CD4 induced by human immunodeficiency virus type 1 Vpu protein: a predicted alpha-helix structure in the proximal cytoplasmic region of CD4 contributes to Vpu sensitivity. Virology. 1995;209(2):615-23.
675. Bour S, Schubert U, Strebel K. The human immunodeficiency virus type 1 Vpu protein specifically binds to the cytoplasmic domain of CD4: implications for the mechanism of degradation. J Virol. 1995;69(3):1510-20.
676. Margottin F, Benichou S, Durand H, Richard V, Liu LX, Gomas E, et al. Interaction between the cytoplasmic domains of HIV-1 Vpu and CD4: role of Vpu residues involved in CD4 interaction and in vitro CD4 degradation. Virology. 1996;223(2):381-6.
677. Tiganos E, Yao XJ, Friborg J, Daniel N, Cohen EA. Putative alpha-helical structures in the human immunodeficiency virus type 1 Vpu protein and CD4 are involved in binding and degradation of the CD4 molecule. J Virol. 1997;71(6):4452-60.
678. Hill MS, Ruiz A, Schmitt K, Stephens EB. Identification of amino acids within the second alpha helical domain of the human immunodeficiency virus type 1 Vpu that are critical for preventing CD4 cell surface expression. Virology. 2010;397(1):104-12.
679. Binette J, Dube M, Mercier J, Halawani D, Latterich M, Cohen EA. Requirements for the selective degradation of CD4 receptor molecules by the human immunodeficiency virus type 1 Vpu protein in the endoplasmic reticulum. Retrovirology. 2007;4:75.
680. Schubert U, Anton LC, Bacik I, Cox JH, Bour S, Bennink JR, et al. CD4 glycoprotein degradation induced by human immunodeficiency virus type 1 Vpu protein requires the function of proteasomes and the ubiquitin-conjugating pathway. J Virol. 1998;72(3):2280-8.
681. Meusser B, Sommer T. Vpu-mediated degradation of CD4 reconstituted in yeast reveals mechanistic differences to cellular ER-associated protein degradation. Mol Cell. 2004;14(2):247-58.
682. Magadan JG, Perez-Victoria FJ, Sougrat R, Ye Y, Strebel K, Bonifacino JS. Multilayered mechanism of CD4 downregulation by HIV-1 Vpu involving distinct ER retention and ERAD targeting steps. PLoS Pathog. 2010;6(4):e1000869.
683. Schmidt S, Fritz JV, Bitzegeio J, Fackler OT, Keppler OT. HIV-1 Vpu blocks recycling and biosynthetic transport of the intrinsic immunity factor CD317/tetherin to overcome the virion release restriction. mBio. 2011;2(3):e00036-11.

684. Vigan R, Neil SJ. Determinants of tetherin antagonism in the transmembrane domain of the human immunodeficiency virus type 1 Vpu protein. J Virol. 2010;84(24):12958-70.
685. Skasko M, Wang Y, Tian Y, Tokarev A, Munguia J, Ruiz A, et al. HIV-1 Vpu protein antagonizes innate restriction factor BST-2 via lipid-embedded helix-helix interactions. J Biol Chem. 2012;287(1):58-67.
686. Tokarev AA, Munguia J, Guatelli JC. Serine-threonine ubiquitination mediates downregulation of BST-2/tetherin and relief of restricted virion release by HIV-1 Vpu. J Virol. 2011;85(1):51-63.
687. Janvier K, Pelchen-Matthews A, Renaud JB, Caillet M, Marsh M, Berlioz-Torrent C. The ESCRT-0 component HRS is required for HIV-1 Vpu-mediated BST-2/tetherin down-regulation. PLoS Pathog. 2011;7(2):e1001265.
688. Gustin JK, Douglas JL, Bai Y, Moses AV. Ubiquitination of BST-2 protein by HIV-1 Vpu protein does not require lysine, serine, or threonine residues within the BST-2 cytoplasmic domain. J Biol Chem. 2012;287(18):14837-50.
689. Liu Y, Fu Y, Wang Q, Li M, Zhou Z, Dabbagh D, et al. Proteomic profiling of HIV-1 infection of human CD4(+) T cells identifies PSGL-1 as an HIV restriction factor. Nat Microbiol. 2019;4(5):813-25.
690. Fu Y, He S, Waheed AA, Dabbagh D, Zhou Z, Trinite B, et al. PSGL-1 restricts HIV-1 infectivity by blocking virus particle attachment to target cells. Proc Natl Acad Sci U S A. 2020;117(17):9537-45.
691. Murakami T, Carmona N, Ono A. Virion-incorporated PSGL-1 and CD43 inhibit both cell-free infection and transinfection of HIV-1 by preventing virus-cell binding. Proc Natl Acad Sci U S A. 2020;117(14):8055-63.
692. Krementsov DN, Weng J, Lambele M, Roy NH, Thali M. Tetraspanins regulate cell-to-cell transmission of HIV-1. Retrovirology. 2009;6:64.
693. Haller C, Muller B, Fritz JV, Lamas-Murua M, Stolp B, Pujol FM, et al. HIV-1 Nef and Vpu are functionally redundant broad-spectrum modulators of cell surface receptors, including tetraspanins. J Virol. 2014;88(24):14241-57.
694. Lambele M, Koppensteiner H, Symeonides M, Roy NH, Chan J, Schindler M, et al. Vpu is the main determinant for tetraspanin downregulation in HIV-1-infected cells. J Virol. 2015;89(6):3247-55.
695. Sato K, Aoki J, Misawa N, Daikoku E, Sano K, Tanaka Y, et al. Modulation of human immunodeficiency virus type 1 infectivity through incorporation of tetraspanin proteins. J Virol. 2008;82(2):1021-33.
696. Pawlak EN, Dirk BS, Jacob RA, Johnson AL, Dikeakos JD. The HIV-1 accessory proteins Nef and Vpu downregulate total and cell surface CD28 in CD4(+) T cells. Retrovirology. 2018;15(1):6.
697. Thoulouze MI, Sol-Foulon N, Blanchet F, Dautry-Varsat A, Schwartz O, Alcover A. Human immunodeficiency virus type-1 infection impairs the formation of the immunological synapse. Immunity. 2006;24(5):547-61.
698. Len ACL, Starling S, Shivkumar M, Jolly C. HIV-1 Activates T Cell Signaling Independently of Antigen to Drive Viral Spread. Cell Rep. 2017;18(4):1062-74.
699. Matheson NJ, Sumner J, Wals K, Rapiteanu R, Weekes MP, Vigan R, et al. Cell Surface Proteomic Map of HIV Infection Reveals Antagonism of Amino Acid Metabolism by Vpu and Nef. Cell Host Microbe. 2015;18(4):409-23.

700. Bour S, Perrin C, Akari H, Strebel K. The human immunodeficiency virus type 1 Vpu protein inhibits NF-kappa B activation by interfering with beta TrCP-mediated degradation of Ikappa B. J Biol Chem. 2001;276(19):15920-8.
701. Manganaro L, de Castro E, Maestre AM, Olivieri K, Garcia-Sastre A, Fernandez-Sesma A, et al. HIV Vpu Interferes with NF-kappaB Activity but Not with Interferon Regulatory Factor 3. J Virol. 2015;89(19):9781-90.
702. Ramirez PW, Famiglietti M, Sowrirajan B, DePaula-Silva AB, Rodesch C, Barker E, et al. Downmodulation of CCR7 by HIV-1 Vpu results in impaired migration and chemotactic signaling within CD4(+) T cells. Cell Rep. 2014;7(6):2019-30.
703. Tanabe R, Morikawa Y. Efficient Transendothelial Migration of Latently HIV-1-Infected Cells. Viruses. 2021;13(8).
704. Vassena L, Giuliani E, Koppensteiner H, Bolduan S, Schindler M, Doria M. HIV-1 Nef and Vpu Interfere with L-Selectin (CD62L) Cell Surface Expression To Inhibit Adhesion and Signaling in Infected CD4+ T Lymphocytes. J Virol. 2015;89(10):5687-700.
705. Kononchik J, Ireland J, Zou Z, Segura J, Holzapfel G, Chastain A, et al. HIV-1 targets L-selectin for adhesion and induces its shedding for viral release. Nat Commun. 2018;9(1):2825.
706. Zaongo SD, Liu Y, Harypursat V, Song F, Xia H, Ma P, et al. P-Selectin Glycoprotein Ligand 1: A Potential HIV-1 Therapeutic Target. Front Immunol. 2021;12:710121.
707. Shah AH, Sowrirajan B, Davis ZB, Ward JP, Campbell EM, Planelles V, et al. Degranulation of natural killer cells following interaction with HIV-1-infected cells is hindered by downmodulation of NTB-A by Vpu. Cell Host Microbe. 2010;8(5):397-409.
708. Matusali G, Potesta M, Santoni A, Cerboni C, Doria M. The human immunodeficiency virus type 1 Nef and Vpu proteins downregulate the natural killer cell-activating ligand PVR. J Virol. 2012;86(8):4496-504.
709. Bolduan S, Hubel P, Reif T, Lodermeyer V, Hohne K, Fritz JV, et al. HIV-1 Vpu affects the anterograde transport and the glycosylation pattern of NTB-A. Virology. 2013;440(2):190-203.
710. Bolduan S, Reif T, Schindler M, Schubert U. HIV-1 Vpu mediated downregulation of CD155 requires alanine residues 10, 14 and 18 of the transmembrane domain. Virology. 2014;464-465:375-84.
711. Apps R, Del Prete GQ, Chatterjee P, Lara A, Brumme ZL, Brockman MA, et al. HIV-1 Vpu Mediates HLA-C Downregulation. Cell Host Microbe. 2016;19(5):686-95.
712. Bachtel ND, Umviligihozo G, Pickering S, Mota TM, Liang H, Del Prete GQ, et al. HLA-C downregulation by HIV-1 adapts to host HLA genotype. PLoS Pathog. 2018;14(9):e1007257.
713. Moll M, Andersson SK, Smed-Sorensen A, Sandberg JK. Inhibition of lipid antigen presentation in dendritic cells by HIV-1 Vpu interference with CD1d recycling from endosomal compartments. Blood. 2010;116(11):1876-84.
714. Allan JS, Coligan JE, Lee TH, McLane MF, Kanki PJ, Groopman JE, et al. A new HTLV-III/LAV encoded antigen detected by antibodies from AIDS patients. Science. 1985;230(4727):810-3.
715. Deacon NJ, Tsykin A, Solomon A, Smith K, Ludford-Menting M, Hooker DJ, et al. Genomic structure of an attenuated quasi species of HIV-1 from a blood transfusion donor and recipients. Science. 1995;270(5238):988-91.
716. Kirchhoff F, Greenough TC, Brettler DB, Sullivan JL, Desrosiers RC. Brief report: absence of intact nef sequences in a long-term survivor with nonprogressive HIV-1 infection. N Engl J Med. 1995;332(4):228-32.

717. Salvi R, Garbuglia AR, Di Caro A, Pulciani S, Montella F, Benedetto A. Grossly defective nef gene sequences in a human immunodeficiency virus type 1-seropositive long-term nonprogressor. J Virol. 1998;72(5):3646-57.
718. Geffin R, Wolf D, Muller R, Hill MD, Stellwag E, Freitag M, et al. Functional and structural defects in HIV type 1 nef genes derived from pediatric long-term survivors. AIDS Res Hum Retroviruses. 2000;16(17):1855-68.
719. Casartelli N, Di Matteo G, Argentini C, Cancrini C, Bernardi S, Castelli G, et al. Structural defects and variations in the HIV-1 nef gene from rapid, slow and non-progressor children. AIDS. 2003;17(9):1291-301.
720. Crotti A, Neri F, Corti D, Ghezzi S, Heltai S, Baur A, et al. Nef alleles from human immunodeficiency virus type 1-infected long-term-nonprogressor hemophiliacs with or without late disease progression are defective in enhancing virus replication and CD4 down-regulation. J Virol. 2006;80(21):10663-74.
721. Mwimanzi P, Markle TJ, Martin E, Ogata Y, Kuang XT, Tokunaga M, et al. Attenuation of multiple Nef functions in HIV-1 elite controllers. Retrovirology. 2013;10:1.
722. Kestler HW, 3rd, Ringler DJ, Mori K, Panicali DL, Sehgal PK, Daniel MD, et al. Importance of the nef gene for maintenance of high virus loads and for development of AIDS. Cell. 1991;65(4):651-62.
723. Zou W, Denton PW, Watkins RL, Krisko JF, Nochi T, Foster JL, et al. Nef functions in BLT mice to enhance HIV-1 replication and deplete CD4+CD8+ thymocytes. Retrovirology. 2012;9:44.
724. Watkins RL, Zou W, Denton PW, Krisko JF, Foster JL, Garcia JV. In vivo analysis of highly conserved Nef activities in HIV-1 replication and pathogenesis. Retrovirology. 2013;10:125.
725. Watkins RL, Foster JL, Garcia JV. In vivo analysis of Nef's role in HIV-1 replication, systemic T cell activation and CD4(+) T cell loss. Retrovirology. 2015;12:61.
726. Lindemann D, Wilhelm R, Renard P, Althage A, Zinkernagel R, Mous J. Severe immunodeficiency associated with a human immunodeficiency virus 1 NEF/3'-long terminal repeat transgene. J Exp Med. 1994;179(3):797-807.
727. Hanna Z, Kay DG, Rebai N, Guimond A, Jothy S, Jolicoeur P. Nef harbors a major determinant of pathogenicity for an AIDS-like disease induced by HIV-1 in transgenic mice. Cell. 1998;95(2):163-75.
728. Hanna Z, Kay DG, Cool M, Jothy S, Rebai N, Jolicoeur P. Transgenic mice expressing human immunodeficiency virus type 1 in immune cells develop a severe AIDS-like disease. J Virol. 1998;72(1):121-32.
729. Simard MC, Chrobak P, Kay DG, Hanna Z, Jothy S, Jolicoeur P. Expression of simian immunodeficiency virus nef in immune cells of transgenic mice leads to a severe AIDS-like disease. J Virol. 2002;76(8):3981-95.
730. Yu G, Felsted RL. Effect of myristoylation on p27 nef subcellular distribution and suppression of HIV-LTR transcription. Virology. 1992;187(1):46-55.
731. Kaminchik J, Margalit R, Yaish S, Drummer H, Amit B, Sarver N, et al. Cellular distribution of HIV type 1 Nef protein: identification of domains in Nef required for association with membrane and detergent-insoluble cellular matrix. AIDS Res Hum Retroviruses. 1994;10(8):1003-10.

732. Bentham M, Mazaleyrat S, Harris M. Role of myristoylation and N-terminal basic residues in membrane association of the human immunodeficiency virus type 1 Nef protein. J Gen Virol. 2006;87(Pt 3):563-71.
733. Geyer M, Munte CE, Schorr J, Kellner R, Kalbitzer HR. Structure of the anchor-domain of myristoylated and non-myristoylated HIV-1 Nef protein. J Mol Biol. 1999;289(1):123-38.
734. Kent MS, Murton JK, Sasaki DY, Satija S, Akgun B, Nanda H, et al. Neutron reflectometry study of the conformation of HIV Nef bound to lipid membranes. Biophys J. 2010;99(6):1940-8.
735. Ren X, Park SY, Bonifacino JS, Hurley JH. How HIV-1 Nef hijacks the AP-2 clathrin adaptor to downregulate CD4. Elife. 2014;3:e01754.
736. Kwon Y, Kaake RM, Echeverria I, Suarez M, Karimian Shamsabadi M, Stoneham C, et al. Structural basis of CD4 downregulation by HIV-1 Nef. Nat Struct Mol Biol. 2020;27(9):822-8.
737. Garcia JV, Miller AD. Serine phosphorylation-independent downregulation of cell-surface CD4 by nef. Nature. 1991;350(6318):508-11.
738. Schwartz O, Marechal V, Le Gall S, Lemonnier F, Heard JM. Endocytosis of major histocompatibility complex class I molecules is induced by the HIV-1 Nef protein. Nat Med. 1996;2(3):338-42.
739. Aiken C, Konner J, Landau NR, Lenburg ME, Trono D. Nef induces CD4 endocytosis: requirement for a critical dileucine motif in the membrane-proximal CD4 cytoplasmic domain. Cell. 1994;76(5):853-64.
740. Rhee SS, Marsh JW. Human immunodeficiency virus type 1 Nef-induced down-modulation of CD4 is due to rapid internalization and degradation of surface CD4. J Virol. 1994;68(8):5156-63.
741. Greenberg ME, Bronson S, Lock M, Neumann M, Pavlakis GN, Skowronski J. Co-localization of HIV-1 Nef with the AP-2 adaptor protein complex correlates with Nef-induced CD4 down-regulation. EMBO J. 1997;16(23):6964-76.
742. Preusser A, Briese L, Baur AS, Willbold D. Direct in vitro binding of full-length human immunodeficiency virus type 1 Nef protein to CD4 cytoplasmic domain. J Virol. 2001;75(8):3960-4.
743. Burtey A, Rappoport JZ, Bouchet J, Basmaciogullari S, Guatelli J, Simon SM, et al. Dynamic interaction of HIV-1 Nef with the clathrin-mediated endocytic pathway at the plasma membrane. Traffic. 2007;8(1):61-76.
744. Chaudhuri R, Lindwasser OW, Smith WJ, Hurley JH, Bonifacino JS. Downregulation of CD4 by human immunodeficiency virus type 1 Nef is dependent on clathrin and involves direct interaction of Nef with the AP2 clathrin adaptor. J Virol. 2007;81(8):3877-90.
745. Gondim MV, Wiltzer-Bach L, Maurer B, Banning C, Arganaraz E, Schindler M. AP-2 Is the Crucial Clathrin Adaptor Protein for CD4 Downmodulation by HIV-1 Nef in Infected Primary CD4+ T Cells. J Virol. 2015;89(24):12518-24.
746. Piguet V, Gu F, Foti M, Demaurex N, Gruenberg J, Carpentier JL, et al. Nef-induced CD4 degradation: a diacidic-based motif in Nef functions as a lysosomal targeting signal through the binding of beta-COP in endosomes. Cell. 1999;97(1):63-73.
747. Schaefer MR, Wonderlich ER, Roeth JF, Leonard JA, Collins KL. HIV-1 Nef targets MHC-I and CD4 for degradation via a final common beta-COP-dependent pathway in T cells. PLoS Pathog. 2008;4(8):e1000131.
748. Benson RE, Sanfridson A, Ottinger JS, Doyle C, Cullen BR. Downregulation of cell-surface CD4 expression by simian immunodeficiency virus Nef prevents viral super infection. J Exp Med. 1993;177(6):1561-6.

749. Lama J, Mangasarian A, Trono D. Cell-surface expression of CD4 reduces HIV-1 infectivity by blocking Env incorporation in a Nef- and Vpu-inhibitable manner. Curr Biol. 1999;9(12):622-31.
750. Ross TM, Oran AE, Cullen BR. Inhibition of HIV-1 progeny virion release by cell-surface CD4 is relieved by expression of the viral Nef protein. Curr Biol. 1999;9(12):613-21.
751. Glushakova S, Munch J, Carl S, Greenough TC, Sullivan JL, Margolis L, et al. CD4 down-modulation by human immunodeficiency virus type 1 Nef correlates with the efficiency of viral replication and with CD4(+) T-cell depletion in human lymphoid tissue ex vivo. J Virol. 2001;75(21):10113-7.
752. Tanaka M, Ueno T, Nakahara T, Sasaki K, Ishimoto A, Sakai H. Downregulation of CD4 is required for maintenance of viral infectivity of HIV-1. Virology. 2003;311(2):316-25.
753. Arganaraz ER, Schindler M, Kirchhoff F, Cortes MJ, Lama J. Enhanced CD4 down-modulation by late stage HIV-1 nef alleles is associated with increased Env incorporation and viral replication. J Biol Chem. 2003;278(36):33912-9.
754. Wildum S, Schindler M, Munch J, Kirchhoff F. Contribution of Vpu, Env, and Nef to CD4 down-modulation and resistance of human immunodeficiency virus type 1-infected T cells to superinfection. J Virol. 2006;80(16):8047-59.
755. Cortes MJ, Wong-Staal F, Lama J. Cell surface CD4 interferes with the infectivity of HIV-1 particles released from T cells. J Biol Chem. 2002;277(3):1770-9.
756. Veillette M, Desormeaux A, Medjahed H, Gharsallah NE, Coutu M, Baalwa J, et al. Interaction with cellular CD4 exposes HIV-1 envelope epitopes targeted by antibody-dependent cell-mediated cytotoxicity. J Virol. 2014;88(5):2633-44.
757. Veillette M, Coutu M, Richard J, Batraville LA, Dagher O, Bernard N, et al. The HIV-1 gp120 CD4-Bound Conformation Is Preferentially Targeted by Antibody-Dependent Cellular Cytotoxicity-Mediating Antibodies in Sera from HIV-1-Infected Individuals. J Virol. 2015;89(1):545-51.
758. Alsahafi N, Ding S, Richard J, Markle T, Brassard N, Walker B, et al. Nef Proteins from HIV-1 Elite Controllers Are Inefficient at Preventing Antibody-Dependent Cellular Cytotoxicity. J Virol. 2016;90(6):2993-3002.
759. Ding S, Gasser R, Gendron-Lepage G, Medjahed H, Tolbert WD, Sodroski J, et al. CD4 Incorporation into HIV-1 Viral Particles Exposes Envelope Epitopes Recognized by CD4-Induced Antibodies. J Virol. 2019;93(22).
760. Shi J, Xiong R, Zhou T, Su P, Zhang X, Qiu X, et al. HIV-1 Nef Antagonizes SERINC5 Restriction by Downregulation of SERINC5 via the Endosome/Lysosome System. J Virol. 2018;92(11).
761. Staudt RP, Smithgall TE. Nef homodimers down-regulate SERINC5 by AP-2-mediated endocytosis to promote HIV-1 infectivity. J Biol Chem. 2020;295(46):15540-52.
762. Collins KL, Chen BK, Kalams SA, Walker BD, Baltimore D. HIV-1 Nef protein protects infected primary cells against killing by cytotoxic T lymphocytes. Nature. 1998;391(6665):397-401.
763. Cohen GB, Gandhi RT, Davis DM, Mandelboim O, Chen BK, Strominger JL, et al. The selective downregulation of class I major histocompatibility complex proteins by HIV-1 protects HIV-infected cells from NK cells. Immunity. 1999;10(6):661-71.
764. Cho S, Knox KS, Kohli LM, He JJ, Exley MA, Wilson SB, et al. Impaired cell surface expression of human CD1d by the formation of an HIV-1 Nef/CD1d complex. Virology. 2005;337(2):242-52.

765. Chen N, McCarthy C, Drakesmith H, Li D, Cerundolo V, McMichael AJ, et al. HIV-1 down-regulates the expression of CD1d via Nef. Eur J Immunol. 2006;36(2):278-86.
766. Wonderlich ER, Williams M, Collins KL. The tyrosine binding pocket in the adaptor protein 1 (AP-1) mu1 subunit is necessary for Nef to recruit AP-1 to the major histocompatibility complex class I cytoplasmic tail. J Biol Chem. 2008;283(6):3011-22.
767. van Stigt Thans T, Akko JI, Niehrs A, Garcia-Beltran WF, Richert L, Sturzel CM, et al. Primary HIV-1 Strains Use Nef To Downmodulate HLA-E Surface Expression. J Virol. 2019;93(20).
768. Le Gall S, Erdtmann L, Benichou S, Berlioz-Torrent C, Liu L, Benarous R, et al. Nef interacts with the mu subunit of clathrin adaptor complexes and reveals a cryptic sorting signal in MHC I molecules. Immunity. 1998;8(4):483-95.
769. Williams M, Roeth JF, Kasper MR, Fleis RI, Przybycin CG, Collins KL. Direct binding of human immunodeficiency virus type 1 Nef to the major histocompatibility complex class I (MHC-I) cytoplasmic tail disrupts MHC-I trafficking. J Virol. 2002;76(23):12173-84.
770. Roeth JF, Williams M, Kasper MR, Filzen TM, Collins KL. HIV-1 Nef disrupts MHC-I trafficking by recruiting AP-1 to the MHC-I cytoplasmic tail. J Cell Biol. 2004;167(5):903-13.
771. Jia X, Singh R, Homann S, Yang H, Guatelli J, Xiong Y. Structural basis of evasion of cellular adaptive immunity by HIV-1 Nef. Nat Struct Mol Biol. 2012;19(7):701-6.
772. Noviello CM, Benichou S, Guatelli JC. Cooperative binding of the class I major histocompatibility complex cytoplasmic domain and human immunodeficiency virus type 1 Nef to the endosomal AP-1 complex via its mu subunit. J Virol. 2008;82(3):1249-58.
773. Cerboni C, Neri F, Casartelli N, Zingoni A, Cosman D, Rossi P, et al. Human immunodeficiency virus 1 Nef protein downmodulates the ligands of the activating receptor NKG2D and inhibits natural killer cell-mediated cytotoxicity. J Gen Virol. 2007;88(Pt 1):242-50.
774. Alsahafi N, Richard J, Prevost J, Coutu M, Brassard N, Parsons MS, et al. Impaired downregulation of NKG2D ligands by Nef protein from elite controllers sensitizes HIV-1-infected cells to ADCC. J Virol. 2017.
775. Schrager JA, Marsh JW. HIV-1 Nef increases T cell activation in a stimulus-dependent manner. Proc Natl Acad Sci U S A. 1999;96(14):8167-72.
776. Fortin JF, Barat C, Beausejour Y, Barbeau B, Tremblay MJ. Hyper-responsiveness to stimulation of human immunodeficiency virus-infected CD4+ T cells requires Nef and Tat virus gene products and results from higher NFAT, NF-kappaB, and AP-1 induction. J Biol Chem. 2004;279(38):39520-31.
777. Fenard D, Yonemoto W, de Noronha C, Cavrois M, Williams SA, Greene WC. Nef is physically recruited into the immunological synapse and potentiates T cell activation early after TCR engagement. J Immunol. 2005;175(9):6050-7.
778. Olivieri KC, Mukerji J, Gabuzda D. Nef-mediated enhancement of cellular activation and human immunodeficiency virus type 1 replication in primary T cells is dependent on association with p21-activated kinase 2. Retrovirology. 2011;8:64.
779. Campbell GR, Rawat P, Bruckman RS, Spector SA. Human Immunodeficiency Virus Type 1 Nef Inhibits Autophagy through Transcription Factor EB Sequestration. PLoS Pathog. 2015;11(6):e1005018.
780. Castro-Gonzalez S, Shi Y, Colomer-Lluch M, Song Y, Mowery K, Almodovar S, et al. HIV-1 Nef counteracts autophagy restriction by enhancing the association between BECN1 and its inhibitor BCL2 in a PRKN-dependent manner. Autophagy. 2021;17(2):553-77.

781. Muratori C, Cavallin LE, Kratzel K, Tinari A, De Milito A, Fais S, et al. Massive secretion by T cells is caused by HIV Nef in infected cells and by Nef transfer to bystander cells. Cell Host Microbe. 2009;6(3):218-30.
782. Lee JH, Wittki S, Brau T, Dreyer FS, Kratzel K, Dindorf J, et al. HIV Nef, paxillin, and Pak1/2 regulate activation and secretion of TACE/ADAM10 proteases. Mol Cell. 2013;49(4):668-79.
783. Shaw GM, Hunter E. HIV transmission. Cold Spring Harb Perspect Med. 2012;2(11).
784. Derdeyn CA, Decker JM, Bibollet-Ruche F, Mokili JL, Muldoon M, Denham SA, et al. Envelope-constrained neutralization-sensitive HIV-1 after heterosexual transmission. Science. 2004;303(5666):2019-22.
785. Chohan B, Lang D, Sagar M, Korber B, Lavreys L, Richardson B, et al. Selection for human immunodeficiency virus type 1 envelope glycosylation variants with shorter V1-V2 loop sequences occurs during transmission of certain genetic subtypes and may impact viral RNA levels. J Virol. 2005;79(10):6528-31.
786. Liu Y, Curlin ME, Diem K, Zhao H, Ghosh AK, Zhu H, et al. Env length and N-linked glycosylation following transmission of human immunodeficiency virus Type 1 subtype B viruses. Virology. 2008;374(2):229-33.
787. Ochsenbauer C, Edmonds TG, Ding H, Keele BF, Decker J, Salazar MG, et al. Generation of Transmitted/Founder HIV-1 Infectious Molecular Clones and Characterization of Their Replication Capacity in CD4 T Lymphocytes and Monocyte-Derived Macrophages. J Virol. 2012;86(5):2715-28.
788. Parrish NF, Wilen CB, Banks LB, Iyer SS, Pfaff JM, Salazar-Gonzalez JF, et al. Transmitted/founder and chronic subtype C HIV-1 use CD4 and CCR5 receptors with equal efficiency and are not inhibited by blocking the integrin alpha4beta7. PLoS Pathog. 2012;8(5):e1002686.
789. Parrish NF, Gao F, Li H, Giorgi EE, Barbian HJ, Parrish EH, et al. Phenotypic properties of transmitted founder HIV-1. Proc Natl Acad Sci U S A. 2013;110(17):6626-33.
790. Fenton-May AE, Dibben O, Emmerich T, Ding H, Pfafferott K, Aasa-Chapman MM, et al. Relative resistance of HIV-1 founder viruses to control by interferon-alpha. Retrovirology. 2013;10:146.
791. Ping LH, Joseph SB, Anderson JA, Abrahams MR, Salazar-Gonzalez JF, Kincer LP, et al. Comparison of viral Env proteins from acute and chronic infections with subtype C human immunodeficiency virus type 1 identifies differences in glycosylation and CCR5 utilization and suggests a new strategy for immunogen design. J Virol. 2013;87(13):7218-33.
792. Iyer SS, Bibollet-Ruche F, Sherrill-Mix S, Learn GH, Plenderleith L, Smith AG, et al. Resistance to type 1 interferons is a major determinant of HIV-1 transmission fitness. Proc Natl Acad Sci U S A. 2017.
793. Wagh K, Kreider EF, Li Y, Barbian HJ, Learn GH, Giorgi E, et al. Completeness of HIV-1 Envelope Glycan Shield at Transmission Determines Neutralization Breadth. Cell Rep. 2018;25(4):893-908 e7.
794. Asmal M, Hellmann I, Liu W, Keele BF, Perelson AS, Bhattacharya T, et al. A signature in HIV-1 envelope leader peptide associated with transition from acute to chronic infection impacts envelope processing and infectivity. PLoS One. 2011;6(8):e23673.
795. Gaines H, von Sydow M, Pehrson PO, Lundbegh P. Clinical picture of primary HIV infection presenting as a glandular-fever-like illness. BMJ. 1988;297(6660):1363-8.

796. Clark SJ, Saag MS, Decker WD, Campbell-Hill S, Roberson JL, Veldkamp PJ, et al. High titers of cytopathic virus in plasma of patients with symptomatic primary HIV-1 infection. N Engl J Med. 1991;324(14):954-60.
797. Schacker T, Collier AC, Hughes J, Shea T, Corey L. Clinical and epidemiologic features of primary HIV infection. Ann Intern Med. 1996;125(4):257-64.
798. Little SJ, McLean AR, Spina CA, Richman DD, Havlir DV. Viral dynamics of acute HIV-1 infection. J Exp Med. 1999;190(6):841-50.
799. Lindback S, Thorstensson R, Karlsson AC, von Sydow M, Flamholc L, Blaxhult A, et al. Diagnosis of primary HIV-1 infection and duration of follow-up after HIV exposure. Karolinska Institute Primary HIV Infection Study Group. AIDS. 2000;14(15):2333-9.
800. Lindback S, Karlsson AC, Mittler J, Blaxhult A, Carlsson M, Briheim G, et al. Viral dynamics in primary HIV-1 infection. Karolinska Institutet Primary HIV Infection Study Group. AIDS. 2000;14(15):2283-91.
801. Haase AT. Targeting early infection to prevent HIV-1 mucosal transmission. Nature. 2010;464(7286):217-23.
802. Veazey RS, DeMaria M, Chalifoux LV, Shvetz DE, Pauley DR, Knight HL, et al. Gastrointestinal tract as a major site of CD4+ T cell depletion and viral replication in SIV infection. Science. 1998;280(5362):427-31.
803. Guadalupe M, Reay E, Sankaran S, Prindiville T, Flamm J, McNeil A, et al. Severe CD4+ T-cell depletion in gut lymphoid tissue during primary human immunodeficiency virus type 1 infection and substantial delay in restoration following highly active antiretroviral therapy. J Virol. 2003;77(21):11708-17.
804. Mehandru S, Poles MA, Tenner-Racz K, Horowitz A, Hurley A, Hogan C, et al. Primary HIV-1 infection is associated with preferential depletion of CD4+ T lymphocytes from effector sites in the gastrointestinal tract. J Exp Med. 2004;200(6):761-70.
805. Brenchley JM, Schacker TW, Ruff LE, Price DA, Taylor JH, Beilman GJ, et al. CD4+ T cell depletion during all stages of HIV disease occurs predominantly in the gastrointestinal tract. J Exp Med. 2004;200(6):749-59.
806. Mattapallil JJ, Douek DC, Hill B, Nishimura Y, Martin M, Roederer M. Massive infection and loss of memory CD4+ T cells in multiple tissues during acute SIV infection. Nature. 2005;434(7037):1093-7.
807. Li Q, Duan L, Estes JD, Ma ZM, Rourke T, Wang Y, et al. Peak SIV replication in resting memory CD4+ T cells depletes gut lamina propria CD4+ T cells. Nature. 2005;434(7037):1148-52.
808. Mehandru S, Poles MA, Tenner-Racz K, Manuelli V, Jean-Pierre P, Lopez P, et al. Mechanisms of gastrointestinal CD4+ T-cell depletion during acute and early human immunodeficiency virus type 1 infection. J Virol. 2007;81(2):599-612.
809. Ribeiro RM, Qin L, Chavez LL, Li D, Self SG, Perelson AS. Estimation of the initial viral growth rate and basic reproductive number during acute HIV-1 infection. J Virol. 2010;84(12):6096-102.
810. Kaur A, Hale CL, Ramanujan S, Jain RK, Johnson RP. Differential dynamics of CD4(+) and CD8(+) T-lymphocyte proliferation and activation in acute simian immunodeficiency virus infection. J Virol. 2000;74(18):8413-24.
811. Veazey RS, Lifson JD, Schmitz JE, Kuroda MJ, Piatak M, Jr., Pandrea I, et al. Dynamics of Simian immunodeficiency virus-specific cytotoxic T-cell responses in tissues. J Med Primatol. 2003;32(4-5):194-200.

812. Reynolds MR, Rakasz E, Skinner PJ, White C, Abel K, Ma ZM, et al. CD8+ T-lymphocyte response to major immunodominant epitopes after vaginal exposure to simian immunodeficiency virus: too late and too little. J Virol. 2005;79(14):9228-35.
813. Fiebig EW, Wright DJ, Rawal BD, Garrett PE, Schumacher RT, Peddada L, et al. Dynamics of HIV viremia and antibody seroconversion in plasma donors: implications for diagnosis and staging of primary HIV infection. AIDS. 2003;17(13):1871-9.
814. Chun TW, Engel D, Berrey MM, Shea T, Corey L, Fauci AS. Early establishment of a pool of latently infected, resting CD4(+) T cells during primary HIV-1 infection. Proc Natl Acad Sci U S A. 1998;95(15):8869-73.
815. Whitney JB, Hill AL, Sanisetty S, Penaloza-MacMaster P, Liu J, Shetty M, et al. Rapid seeding of the viral reservoir prior to SIV viraemia in rhesus monkeys. Nature. 2014;512(7512):74-7.
816. Ananworanich J, Sacdalan CP, Pinyakorn S, Chomont N, de Souza M, Luekasemsuk T, et al. Virological and immunological characteristics of HIV-infected individuals at the earliest stage of infection. J Virus Erad. 2016;2:43-8.
817. Shriner D, Liu Y, Nickle DC, Mullins JI. Evolution of intrahost HIV-1 genetic diversity during chronic infection. Evolution. 2006;60(6):1165-76.
818. Eller MA, Opollo MS, Liu M, Redd AD, Eller LA, Kityo C, et al. HIV Type 1 Disease Progression to AIDS and Death in a Rural Ugandan Cohort Is Primarily Dependent on Viral Load Despite Variable Subtype and T-Cell Immune Activation Levels. J Infect Dis. 2015;211(10):1574-84.
819. Brenchley JM, Price DA, Schacker TW, Asher TE, Silvestri G, Rao S, et al. Microbial translocation is a cause of systemic immune activation in chronic HIV infection. Nat Med. 2006;12(12):1365-71.
820. Brenchley JM, Paiardini M, Knox KS, Asher AI, Cervasi B, Asher TE, et al. Differential Th17 CD4 T-cell depletion in pathogenic and nonpathogenic lentiviral infections. Blood. 2008;112(7):2826-35.
821. Estes JD, Harris LD, Klatt NR, Tabb B, Pittaluga S, Paiardini M, et al. Damaged intestinal epithelial integrity linked to microbial translocation in pathogenic simian immunodeficiency virus infections. PLoS Pathog. 2010;6(8):e1001052.
822. Funderburg N, Luciano AA, Jiang W, Rodriguez B, Sieg SF, Lederman MM. Toll-like receptor ligands induce human T cell activation and death, a model for HIV pathogenesis. PLoS One. 2008;3(4):e1915.
823. Nettles RE, Kieffer TL, Kwon P, Monie D, Han Y, Parsons T, et al. Intermittent HIV-1 viremia (Blips) and drug resistance in patients receiving HAART. JAMA. 2005;293(7):817-29.
824. Munier ML, Kelleher AD. Acutely dysregulated, chronically disabled by the enemy within: T-cell responses to HIV-1 infection. Immunol Cell Biol. 2007;85(1):6-15.
825. Koup RA, Safrit JT, Cao Y, Andrews CA, McLeod G, Borkowsky W, et al. Temporal association of cellular immune responses with the initial control of viremia in primary human immunodeficiency virus type 1 syndrome. J Virol. 1994;68(7):4650-5.
826. Cummins NW, Badley AD. Mechanisms of HIV-associated lymphocyte apoptosis: 2010. Cell Death Dis. 2010;1:e99.
827. Doitsh G, Greene WC. Dissecting How CD4 T Cells Are Lost During HIV Infection. Cell Host Microbe. 2016;19(3):280-91.

828. Matrajt L, Younan PM, Kiem HP, Schiffer JT. The majority of CD4+ T-cell depletion during acute simian-human immunodeficiency virus SHIV89.6P infection occurs in uninfected cells. J Virol. 2014;88(6):3202-12.
829. Westendorp MO, Frank R, Ochsenbauer C, Stricker K, Dhein J, Walczak H, et al. Sensitization of T cells to CD95-mediated apoptosis by HIV-1 Tat and gp120. Nature. 1995;375(6531):497-500.
830. Li CJ, Friedman DJ, Wang C, Metelev V, Pardee AB. Induction of apoptosis in uninfected lymphocytes by HIV-1 Tat protein. Science. 1995;268(5209):429-31.
831. Varbanov M, Espert L, Biard-Piechaczyk M. Mechanisms of CD4 T-cell depletion triggered by HIV-1 viral proteins. AIDS Rev. 2006;8(4):221-36.
832. Doitsh G, Galloway NL, Geng X, Yang Z, Monroe KM, Zepeda O, et al. Cell death by pyroptosis drives CD4 T-cell depletion in HIV-1 infection. Nature. 2014;505(7484):509-14.
833. He X, Yang W, Zeng Z, Wei Y, Gao J, Zhang B, et al. NLRP3-dependent pyroptosis is required for HIV-1 gp120-induced neuropathology. Cell Mol Immunol. 2020;17(3):283-99.
834. Richard J, Veillette M, Ding S, Zoubchenok D, Alsahafi N, Coutu M, et al. Small CD4 Mimetics Prevent HIV-1 Uninfected Bystander CD4 + T Cell Killing Mediated by Antibody-dependent Cell-mediated Cytotoxicity. EBioMedicine. 2016;3:122-34.
835. 1993 revised classification system for HIV infection and expanded surveillance case definition for AIDS among adolescents and adults. MMWR Recomm Rep. 1992;41(RR-17):1-19.
836. Schuitemaker H, Koot M, Kootstra NA, Dercksen MW, de Goede RE, van Steenwijk RP, et al. Biological phenotype of human immunodeficiency virus type 1 clones at different stages of infection: progression of disease is associated with a shift from monocytotropic to T-cell-tropic virus population. J Virol. 1992;66(3):1354-60.
837. Daar ES, Kesler KL, Petropoulos CJ, Huang W, Bates M, Lail AE, et al. Baseline HIV type 1 coreceptor tropism predicts disease progression. Clin Infect Dis. 2007;45(5):643-9.
838. Wong KH, Chan KC, Lee SS. Delayed progression to death and to AIDS in a Hong Kong cohort of patients with advanced HIV type 1 disease during the era of highly active antiretroviral therapy. Clin Infect Dis. 2004;39(6):853-60.
839. Palella FJ, Jr., Delaney KM, Moorman AC, Loveless MO, Fuhrer J, Satten GA, et al. Declining morbidity and mortality among patients with advanced human immunodeficiency virus infection. HIV Outpatient Study Investigators. N Engl J Med. 1998;338(13):853-60.
840. Pantaleo G, Fauci AS. Immunopathogenesis of HIV infection. Annu Rev Microbiol. 1996;50:825-54.
841. Okulicz JF, Marconi VC, Landrum ML, Wegner S, Weintrob A, Ganesan A, et al. Clinical outcomes of elite controllers, viremic controllers, and long-term nonprogressors in the US Department of Defense HIV natural history study. J Infect Dis. 2009;200(11):1714-23.
842. Mendoza D, Johnson SA, Peterson BA, Natarajan V, Salgado M, Dewar RL, et al. Comprehensive analysis of unique cases with extraordinary control over HIV replication. Blood. 2012;119(20):4645-55.
843. Zaunders J, Dyer WB, Churchill M, Munier CML, Cunningham PH, Suzuki K, et al. Possible clearance of transfusion-acquired nef/LTR-deleted attenuated HIV-1 infection by an elite controller with CCR5 Delta32 heterozygous and HLA-B57 genotype. J Virus Erad. 2019;5(2):73-83.
844. Casado C, Galvez C, Pernas M, Tarancon-Diez L, Rodriguez C, Sanchez-Merino V, et al. Permanent control of HIV-1 pathogenesis in exceptional elite controllers: a model of spontaneous cure. Sci Rep. 2020;10(1):1902.

845. Kwaa AK, Garliss CC, Ritter KD, Laird GM, Blankson JN. Elite suppressors have low frequencies of intact HIV-1 proviral DNA. AIDS. 2020;34(4):641-3.
846. Jiang C, Lian X, Gao C, Sun X, Einkauf KB, Chevalier JM, et al. Distinct viral reservoirs in individuals with spontaneous control of HIV-1. Nature. 2020;585(7824):261-7.
847. Turk G, Seiger K, Lian X, Sun W, Parsons EM, Gao C, et al. A Possible Sterilizing Cure of HIV-1 Infection Without Stem Cell Transplantation. Ann Intern Med. 2022;175(1):95-100.
848. Finzi D, Hermankova M, Pierson T, Carruth LM, Buck C, Chaisson RE, et al. Identification of a reservoir for HIV-1 in patients on highly active antiretroviral therapy. Science. 1997;278(5341):1295-300.
849. Chun TW, Nickle DC, Justement JS, Meyers JH, Roby G, Hallahan CW, et al. Persistence of HIV in gut-associated lymphoid tissue despite long-term antiretroviral therapy. J Infect Dis. 2008;197(5):714-20.
850. Yukl SA, Gianella S, Sinclair E, Epling L, Li Q, Duan L, et al. Differences in HIV burden and immune activation within the gut of HIV-positive patients receiving suppressive antiretroviral therapy. J Infect Dis. 2010;202(10):1553-61.
851. Banga R, Procopio FA, Noto A, Pollakis G, Cavassini M, Ohmiti K, et al. PD-1(+) and follicular helper T cells are responsible for persistent HIV-1 transcription in treated aviremic individuals. Nat Med. 2016;22(7):754-61.
852. McManus WR, Bale MJ, Spindler J, Wiegand A, Musick A, Patro SC, et al. HIV-1 in lymph nodes is maintained by cellular proliferation during antiretroviral therapy. J Clin Invest. 2019;129(11):4629-42.
853. Estes JD, Kityo C, Ssali F, Swainson L, Makamdop KN, Del Prete GQ, et al. Defining total-body AIDS-virus burden with implications for curative strategies. Nat Med. 2017;23(11):1271-6.
854. Chaillon A, Gianella S, Dellicour S, Rawlings SA, Schlub TE, De Oliveira MF, et al. HIV persists throughout deep tissues with repopulation from multiple anatomical sources. J Clin Invest. 2020;130(4):1699-712.
855. Ruffin N, Thang PH, Rethi B, Nilsson A, Chiodi F. The impact of inflammation and immune activation on B cell differentiation during HIV-1 infection. Front Immunol. 2011;2:90.
856. Connick E, Mattila T, Folkvord JM, Schlichtemeier R, Meditz AL, Ray MG, et al. CTL fail to accumulate at sites of HIV-1 replication in lymphoid tissue. J Immunol. 2007;178(11):6975-83.
857. Luteijn R, Sciaranghella G, van Lunzen J, Nolting A, Dugast AS, Ghebremichael MS, et al. Early viral replication in lymph nodes provides HIV with a means by which to escape NK-cell-mediated control. Eur J Immunol. 2011;41(9):2729-40.
858. Perreau M, Savoye AL, De Crignis E, Corpataux JM, Cubas R, Haddad EK, et al. Follicular helper T cells serve as the major CD4 T cell compartment for HIV-1 infection, replication, and production. J Exp Med. 2013;210(1):143-56.
859. Fukazawa Y, Lum R, Okoye AA, Park H, Matsuda K, Bae JY, et al. B cell follicle sanctuary permits persistent productive simian immunodeficiency virus infection in elite controllers. Nat Med. 2015;21(2):132-9.
860. Kohler SL, Pham MN, Folkvord JM, Arends T, Miller SM, Miles B, et al. Germinal Center T Follicular Helper Cells Are Highly Permissive to HIV-1 and Alter Their Phenotype during Virus Replication. J Immunol. 2016;196(6):2711-22.

861. Schnell G, Price RW, Swanstrom R, Spudich S. Compartmentalization and clonal amplification of HIV-1 variants in the cerebrospinal fluid during primary infection. J Virol. 2010;84(5):2395-407.
862. Jenabian MA, Costiniuk CT, Mehraj V, Ghazawi FM, Fromentin R, Brousseau J, et al. Immune tolerance properties of the testicular tissue as a viral sanctuary site in ART-treated HIV-infected adults. AIDS. 2016;30(18):2777-86.
863. Ene L, Duiculescu D, Ruta SM. How much do antiretroviral drugs penetrate into the central nervous system? J Med Life. 2011;4(4):432-9.
864. Robillard KR, Chan GN, Zhang G, la Porte C, Cameron W, Bendayan R. Role of P-glycoprotein in the distribution of the HIV protease inhibitor atazanavir in the brain and male genital tract. Antimicrob Agents Chemother. 2014;58(3):1713-22.
865. Fletcher CV, Staskus K, Wietgrefe SW, Rothenberger M, Reilly C, Chipman JG, et al. Persistent HIV-1 replication is associated with lower antiretroviral drug concentrations in lymphatic tissues. Proc Natl Acad Sci U S A. 2014;111(6):2307-12.
866. Chomont N, El-Far M, Ancuta P, Trautmann L, Procopio FA, Yassine-Diab B, et al. HIV reservoir size and persistence are driven by T cell survival and homeostatic proliferation. Nat Med. 2009;15(8):893-900.
867. Buzon MJ, Sun H, Li C, Shaw A, Seiss K, Ouyang Z, et al. HIV-1 persistence in CD4+ T cells with stem cell-like properties. Nat Med. 2014;20(2):139-42.
868. Jaafoura S, de Goer de Herve MG, Hernandez-Vargas EA, Hendel-Chavez H, Abdoh M, Mateo MC, et al. Progressive contraction of the latent HIV reservoir around a core of less-differentiated CD4(+) memory T Cells. Nat Commun. 2014;5:5407.
869. Kulpa DA, Talla A, Brehm JH, Ribeiro SP, Yuan S, Bebin-Blackwell AG, et al. Differentiation into an Effector Memory Phenotype Potentiates HIV-1 Latency Reversal in CD4(+) T Cells. J Virol. 2019;93(24).
870. Cantero-Perez J, Grau-Exposito J, Serra-Peinado C, Rosero DA, Luque-Ballesteros L, Astorga-Gamaza A, et al. Resident memory T cells are a cellular reservoir for HIV in the cervical mucosa. Nat Commun. 2019;10(1):4739.
871. Hsiao F, Frouard J, Gramatica A, Xie G, Telwatte S, Lee GQ, et al. Tissue memory CD4+ T cells expressing IL-7 receptor-alpha (CD127) preferentially support latent HIV-1 infection. PLoS Pathog. 2020;16(4):e1008450.
872. Sannier G, Dube M, Dufour C, Richard C, Brassard N, Delgado GG, et al. Combined single-cell transcriptional, translational, and genomic profiling reveals HIV-1 reservoir diversity. Cell Rep. 2021;36(9):109643.
873. Rabezanahary H, Moukambi F, Palesch D, Clain J, Racine G, Andreani G, et al. Despite early antiretroviral therapy effector memory and follicular helper CD4 T cells are major reservoirs in visceral lymphoid tissues of SIV-infected macaques. Mucosal Immunol. 2020;13(1):149-60.
874. Amezcua Vesely MC, Pallis P, Bielecki P, Low JS, Zhao J, Harman CCD, et al. Effector TH17 Cells Give Rise to Long-Lived TRM Cells that Are Essential for an Immediate Response against Bacterial Infection. Cell. 2019;178(5):1176-88 e15.
875. Omenetti S, Bussi C, Metidji A, Iseppon A, Lee S, Tolaini M, et al. The Intestine Harbors Functionally Distinct Homeostatic Tissue-Resident and Inflammatory Th17 Cells. Immunity. 2019;51(1):77-89 e6.
876. El Hed A, Khaitan A, Kozhaya L, Manel N, Daskalakis D, Borkowsky W, et al. Susceptibility of human Th17 cells to human immunodeficiency virus and their perturbation during infection. J Infect Dis. 2010;201(6):843-54.

877. Monteiro P, Gosselin A, Wacleche VS, El-Far M, Said EA, Kared H, et al. Memory CCR6+CD4+ T cells are preferential targets for productive HIV type 1 infection regardless of their expression of integrin beta7. J Immunol. 2011;186(8):4618-30.
878. Alvarez Y, Tuen M, Shen G, Nawaz F, Arthos J, Wolff MJ, et al. Preferential HIV infection of CCR6+ Th17 cells is associated with higher levels of virus receptor expression and lack of CCR5 ligands. J Virol. 2013;87(19):10843-54.
879. Wacleche VS, Goulet JP, Gosselin A, Monteiro P, Soudeyns H, Fromentin R, et al. New insights into the heterogeneity of Th17 subsets contributing to HIV-1 persistence during antiretroviral therapy. Retrovirology. 2016;13(1):59.
880. Khoury G, Anderson JL, Fromentin R, Hartogenesis W, Smith MZ, Bacchetti P, et al. Persistence of integrated HIV DNA in CXCR3 + CCR6 + memory CD4+ T cells in HIV-infected individuals on antiretroviral therapy. AIDS. 2016;30(10):1511-20.
881. Gosselin A, Wiche Salinas TR, Planas D, Wacleche VS, Zhang Y, Fromentin R, et al. HIV persists in CCR6+CD4+ T cells from colon and blood during antiretroviral therapy. AIDS. 2017;31(1):35-48.
882. Planas D, Zhang Y, Monteiro P, Goulet JP, Gosselin A, Grandvaux N, et al. HIV-1 selectively targets gut-homing CCR6+CD4+ T cells via mTOR-dependent mechanisms. JCI Insight. 2017;2(15).
883. Anderson JL, Khoury G, Fromentin R, Solomon A, Chomont N, Sinclair E, et al. Human Immunodeficiency Virus (HIV)-Infected CCR6+ Rectal CD4+ T Cells and HIV Persistence On Antiretroviral Therapy. J Infect Dis. 2020;221(5):744-55.
884. Maric D, Grimm WA, Greco N, McRaven MD, Fought AJ, Veazey RS, et al. Th17 T Cells and Immature Dendritic Cells Are the Preferential Initial Targets after Rectal Challenge with a Simian Immunodeficiency Virus-Based Replication-Defective Dual-Reporter Vector. J Virol. 2021;95(19):e0070721.
885. Tokarev A, McKinnon LR, Pagliuzza A, Sivro A, Omole TE, Kroon E, et al. Preferential Infection of alpha4beta7+ Memory CD4+ T Cells During Early Acute Human Immunodeficiency Virus Type 1 Infection. Clin Infect Dis. 2020;71(11):e735-e43.
886. Stieh DJ, Matias E, Xu H, Fought AJ, Blanchard JL, Marx PA, et al. Th17 Cells Are Preferentially Infected Very Early after Vaginal Transmission of SIV in Macaques. Cell Host Microbe. 2016;19(4):529-40.
887. Vandergeeten C, Fromentin R, DaFonseca S, Lawani MB, Sereti I, Lederman MM, et al. Interleukin-7 promotes HIV persistence during antiretroviral therapy. Blood. 2013;121(21):4321-9.
888. Maldarelli F, Wu X, Su L, Simonetti FR, Shao W, Hill S, et al. HIV latency. Specific HIV integration sites are linked to clonal expansion and persistence of infected cells. Science. 2014;345(6193):179-83.
889. Wagner TA, McLaughlin S, Garg K, Cheung CY, Larsen BB, Styrchak S, et al. HIV latency. Proliferation of cells with HIV integrated into cancer genes contributes to persistent infection. Science. 2014;345(6196):570-3.
890. Henrich TJ, Hobbs KS, Hanhauser E, Scully E, Hogan LE, Robles YP, et al. Human Immunodeficiency Virus Type 1 Persistence Following Systemic Chemotherapy for Malignancy. J Infect Dis. 2017;216(2):254-62.
891. Wang Z, Gurule EE, Brennan TP, Gerold JM, Kwon KJ, Hosmane NN, et al. Expanded cellular clones carrying replication-competent HIV-1 persist, wax, and wane. Proc Natl Acad Sci U S A. 2018;115(11):E2575-E84.

892. Gantner P, Pagliuzza A, Pardons M, Ramgopal M, Routy JP, Fromentin R, et al. Single-cell TCR sequencing reveals phenotypically diverse clonally expanded cells harboring inducible HIV proviruses during ART. Nat Commun. 2020;11(1):4089.
893. Bosque A, Famiglietti M, Weyrich AS, Goulston C, Planelles V. Homeostatic proliferation fails to efficiently reactivate HIV-1 latently infected central memory CD4+ T cells. PLoS Pathog. 2011;7(10):e1002288.
894. Douek DC, Betts MR, Brenchley JM, Hill BJ, Ambrozak DR, Ngai KL, et al. A novel approach to the analysis of specificity, clonality, and frequency of HIV-specific T cell responses reveals a potential mechanism for control of viral escape. J Immunol. 2002;168(6):3099-104.
895. Hey-Nguyen WJ, Bailey M, Xu Y, Suzuki K, Van Bockel D, Finlayson R, et al. HIV-1 DNA Is Maintained in Antigen-Specific CD4+ T Cell Subsets in Patients on Long-Term Antiretroviral Therapy Regardless of Recurrent Antigen Exposure. AIDS Res Hum Retroviruses. 2019;35(1):112-20.
896. Chun TW, Finzi D, Margolick J, Chadwick K, Schwartz D, Siliciano RF. In vivo fate of HIV-1-infected T cells: quantitative analysis of the transition to stable latency. Nat Med. 1995;1(12):1284-90.
897. Chun TW, Stuyver L, Mizell SB, Ehler LA, Mican JA, Baseler M, et al. Presence of an inducible HIV-1 latent reservoir during highly active antiretroviral therapy. Proc Natl Acad Sci U S A. 1997;94(24):13193-7.
898. Chun TW, Carruth L, Finzi D, Shen X, DiGiuseppe JA, Taylor H, et al. Quantification of latent tissue reservoirs and total body viral load in HIV-1 infection. Nature. 1997;387(6629):183-8.
899. Siliciano JD, Kajdas J, Finzi D, Quinn TC, Chadwick K, Margolick JB, et al. Long-term follow-up studies confirm the stability of the latent reservoir for HIV-1 in resting CD4+ T cells. Nat Med. 2003;9(6):727-8.
900. Wong JK, Hezareh M, Gunthard HF, Havlir DV, Ignacio CC, Spina CA, et al. Recovery of replication-competent HIV despite prolonged suppression of plasma viremia. Science. 1997;278(5341):1291-5.
901. Finzi D, Blankson J, Siliciano JD, Margolick JB, Chadwick K, Pierson T, et al. Latent infection of CD4+ T cells provides a mechanism for lifelong persistence of HIV-1, even in patients on effective combination therapy. Nat Med. 1999;5(5):512-7.
902. Fromentin R, Bakeman W, Lawani MB, Khoury G, Hartogensis W, DaFonseca S, et al. CD4+ T Cells Expressing PD-1, TIGIT and LAG-3 Contribute to HIV Persistence during ART. PLoS Pathog. 2016;12(7):e1005761.
903. McGary CS, Deleage C, Harper J, Micci L, Ribeiro SP, Paganini S, et al. CTLA-4(+)PD-1(-) Memory CD4(+) T Cells Critically Contribute to Viral Persistence in Antiretroviral Therapy-Suppressed, SIV-Infected Rhesus Macaques. Immunity. 2017;47(4):776-88 e5.
904. Pardons M, Baxter AE, Massanella M, Pagliuzza A, Fromentin R, Dufour C, et al. Single-cell characterization and quantification of translation-competent viral reservoirs in treated and untreated HIV infection. PLoS Pathog. 2019;15(2):e1007619.
905. Chew GM, Fujita T, Webb GM, Burwitz BJ, Wu HL, Reed JS, et al. TIGIT Marks Exhausted T Cells, Correlates with Disease Progression, and Serves as a Target for Immune Restoration in HIV and SIV Infection. PLoS Pathog. 2016;12(1):e1005349.
906. Marban C, Suzanne S, Dequiedt F, de Walque S, Redel L, Van Lint C, et al. Recruitment of chromatin-modifying enzymes by CTIP2 promotes HIV-1 transcriptional silencing. EMBO J. 2007;26(2):412-23.

907. du Chene I, Basyuk E, Lin YL, Triboulet R, Knezevich A, Chable-Bessia C, et al. Suv39H1 and HP1gamma are responsible for chromatin-mediated HIV-1 transcriptional silencing and post-integration latency. EMBO J. 2007;26(2):424-35.
908. Tyagi M, Karn J. CBF-1 promotes transcriptional silencing during the establishment of HIV-1 latency. EMBO J. 2007;26(24):4985-95.
909. Kauder SE, Bosque A, Lindqvist A, Planelles V, Verdin E. Epigenetic regulation of HIV-1 latency by cytosine methylation. PLoS Pathog. 2009;5(6):e1000495.
910. Blazkova J, Trejbalova K, Gondois-Rey F, Halfon P, Philibert P, Guiguen A, et al. CpG methylation controls reactivation of HIV from latency. PLoS Pathog. 2009;5(8):e1000554.
911. Tyagi M, Pearson RJ, Karn J. Establishment of HIV latency in primary CD4+ cells is due to epigenetic transcriptional silencing and P-TEFb restriction. J Virol. 2010;84(13):6425-37.
912. Ylisastigui L, Archin NM, Lehrman G, Bosch RJ, Margolis DM. Coaxing HIV-1 from resting CD4 T cells: histone deacetylase inhibition allows latent viral expression. AIDS. 2004;18(8):1101-8.
913. Zhou M, Deng L, Lacoste V, Park HU, Pumfery A, Kashanchi F, et al. Coordination of transcription factor phosphorylation and histone methylation by the P-TEFb kinase during human immunodeficiency virus type 1 transcription. J Virol. 2004;78(24):13522-33.
914. Williams SA, Chen LF, Kwon H, Ruiz-Jarabo CM, Verdin E, Greene WC. NF-kappaB p50 promotes HIV latency through HDAC recruitment and repression of transcriptional initiation. EMBO J. 2006;25(1):139-49.
915. Pearson R, Kim YK, Hokello J, Lassen K, Friedman J, Tyagi M, et al. Epigenetic silencing of human immunodeficiency virus (HIV) transcription by formation of restrictive chromatin structures at the viral long terminal repeat drives the progressive entry of HIV into latency. J Virol. 2008;82(24):12291-303.
916. Honeycutt JB, Thayer WO, Baker CE, Ribeiro RM, Lada SM, Cao Y, et al. HIV persistence in tissue macrophages of humanized myeloid-only mice during antiretroviral therapy. Nat Med. 2017;23(5):638-43.
917. Cattin A, Wiche Salinas TR, Gosselin A, Planas D, Shacklett B, Cohen EA, et al. HIV-1 is rarely detected in blood and colon myeloid cells during viral-suppressive antiretroviral therapy. AIDS. 2019;33(8):1293-306.
918. Andrade VM, Mavian C, Babic D, Cordeiro T, Sharkey M, Barrios L, et al. A minor population of macrophage-tropic HIV-1 variants is identified in recrudescing viremia following analytic treatment interruption. Proc Natl Acad Sci U S A. 2020;117(18):9981-90.
919. Yin X, Langer S, Zhang Z, Herbert KM, Yoh S, Konig R, et al. Sensor Sensibility-HIV-1 and the Innate Immune Response. Cells. 2020;9(1).
920. Rustagi A, Gale M, Jr. Innate antiviral immune signaling, viral evasion and modulation by HIV-1. J Mol Biol. 2014;426(6):1161-77.
921. Li Q, Estes JD, Schlievert PM, Duan L, Brosnahan AJ, Southern PJ, et al. Glycerol monolaurate prevents mucosal SIV transmission. Nature. 2009;458(7241):1034-8.
922. Li G, Cheng M, Nunoya J, Cheng L, Guo H, Yu H, et al. Plasmacytoid dendritic cells suppress HIV-1 replication but contribute to HIV-1 induced immunopathogenesis in humanized mice. PLoS Pathog. 2014;10(7):e1004291.
923. Izaguirre A, Barnes BJ, Amrute S, Yeow WS, Megjugorac N, Dai J, et al. Comparative analysis of IRF and IFN-alpha expression in human plasmacytoid and monocyte-derived dendritic cells. J Leukoc Biol. 2003;74(6):1125-38.

924. Cella M, Jarrossay D, Facchetti F, Alebardi O, Nakajima H, Lanzavecchia A, et al. Plasmacytoid monocytes migrate to inflamed lymph nodes and produce large amounts of type I interferon. Nat Med. 1999;5(8):919-23.
925. Siegal FP, Kadowaki N, Shodell M, Fitzgerald-Bocarsly PA, Shah K, Ho S, et al. The nature of the principal type 1 interferon-producing cells in human blood. Science. 1999;284(5421):1835-7.
926. Hornung V, Rothenfusser S, Britsch S, Krug A, Jahrsdorfer B, Giese T, et al. Quantitative expression of toll-like receptor 1-10 mRNA in cellular subsets of human peripheral blood mononuclear cells and sensitivity to CpG oligodeoxynucleotides. J Immunol. 2002;168(9):4531-7.
927. Mitchell JL, Takata H, Muir R, Colby DJ, Kroon E, Crowell TA, et al. Plasmacytoid dendritic cells sense HIV replication before detectable viremia following treatment interruption. J Clin Invest. 2020;130(6):2845-58.
928. Pham TNQ, Meziane O, Miah MA, Volodina O, Colas C, Beland K, et al. Flt3L-Mediated Expansion of Plasmacytoid Dendritic Cells Suppresses HIV Infection in Humanized Mice. Cell Rep. 2019;29(9):2770-82 e5.
929. Beignon AS, McKenna K, Skoberne M, Manches O, DaSilva I, Kavanagh DG, et al. Endocytosis of HIV-1 activates plasmacytoid dendritic cells via Toll-like receptor-viral RNA interactions. J Clin Invest. 2005;115(11):3265-75.
930. Meier A, Alter G, Frahm N, Sidhu H, Li B, Bagchi A, et al. MyD88-dependent immune activation mediated by human immunodeficiency virus type 1-encoded Toll-like receptor ligands. J Virol. 2007;81(15):8180-91.
931. O'Brien M, Manches O, Sabado RL, Baranda SJ, Wang Y, Marie I, et al. Spatiotemporal trafficking of HIV in human plasmacytoid dendritic cells defines a persistently IFN-alpha-producing and partially matured phenotype. J Clin Invest. 2011;121(3):1088-101.
932. Guo H, Gao J, Taxman DJ, Ting JP, Su L. HIV-1 infection induces interleukin-1beta production via TLR8 protein-dependent and NLRP3 inflammasome mechanisms in human monocytes. J Biol Chem. 2014;289(31):21716-26.
933. Kawasaki T, Kawai T. Toll-like receptor signaling pathways. Front Immunol. 2014;5:461.
934. O'Brien M, Manches O, Wilen C, Gopal R, Huq R, Wu V, et al. CD4 Receptor is a Key Determinant of Divergent HIV-1 Sensing by Plasmacytoid Dendritic Cells. PLoS Pathog. 2016;12(4):e1005553.
935. Meas HZ, Haug M, Beckwith MS, Louet C, Ryan L, Hu Z, et al. Sensing of HIV-1 by TLR8 activates human T cells and reverses latency. Nat Commun. 2020;11(1):147.
936. Lepelley A, Louis S, Sourisseau M, Law HK, Pothlichet J, Schilte C, et al. Innate sensing of HIV-infected cells. PLoS Pathog. 2011;7(2):e1001284.
937. Kane M, Case LK, Wang C, Yurkovetskiy L, Dikiy S, Golovkina TV. Innate immune sensing of retroviral infection via Toll-like receptor 7 occurs upon viral entry. Immunity. 2011;35(1):135-45.
938. Sandler NG, Douek DC. Microbial translocation in HIV infection: causes, consequences and treatment opportunities. Nat Rev Microbiol. 2012;10(9):655-66.
939. Jakobsen MR, Bak RO, Andersen A, Berg RK, Jensen SB, Tengchuan J, et al. IFI16 senses DNA forms of the lentiviral replication cycle and controls HIV-1 replication. Proc Natl Acad Sci U S A. 2013;110(48):E4571-80.
940. Gao D, Wu J, Wu YT, Du F, Aroh C, Yan N, et al. Cyclic GMP-AMP synthase is an innate immune sensor of HIV and other retroviruses. Science. 2013;341(6148):903-6.

941. Wang MQ, Huang YL, Huang J, Zheng JL, Qian GX. RIG-I detects HIV-1 infection and mediates type I interferon response in human macrophages from patients with HIV-1-associated neurocognitive disorders. Genet Mol Res. 2015;14(4):13799-811.
942. Li P, Kaiser P, Lampiris HW, Kim P, Yukl SA, Havlir DV, et al. Stimulating the RIG-I pathway to kill cells in the latent HIV reservoir following viral reactivation. Nat Med. 2016;22(7):807-11.
943. Vermeire J, Roesch F, Sauter D, Rua R, Hotter D, Van Nuffel A, et al. HIV Triggers a cGAS-Dependent, Vpu- and Vpr-Regulated Type I Interferon Response in CD4(+) T Cells. Cell Rep. 2016;17(2):413-24.
944. Berg RK, Melchjorsen J, Rintahaka J, Diget E, Soby S, Horan KA, et al. Genomic HIV RNA induces innate immune responses through RIG-I-dependent sensing of secondary-structured RNA. PLoS One. 2012;7(1):e29291.
945. Rehwinkel J, Gack MU. RIG-I-like receptors: their regulation and roles in RNA sensing. Nat Rev Immunol. 2020;20(9):537-51.
946. Zahid A, Ismail H, Li B, Jin T. Molecular and Structural Basis of DNA Sensors in Antiviral Innate Immunity. Front Immunol. 2020;11:613039.
947. Cingoz O, Goff SP. HIV-1 Is a Poor Inducer of Innate Immune Responses. mBio. 2019;10(1).
948. Solis M, Nakhaei P, Jalalirad M, Lacoste J, Douville R, Arguello M, et al. RIG-I-mediated antiviral signaling is inhibited in HIV-1 infection by a protease-mediated sequestration of RIG-I. J Virol. 2011;85(3):1224-36.
949. Ringeard M, Marchand V, Decroly E, Motorin Y, Bennasser Y. FTSJ3 is an RNA 2'-O-methyltransferase recruited by HIV to avoid innate immune sensing. Nature. 2019;565(7740):500-4.
950. Chen S, Kumar S, Espada CE, Tirumuru N, Cahill MP, Hu L, et al. N6-methyladenosine modification of HIV-1 RNA suppresses type-I interferon induction in differentiated monocytic cells and primary macrophages. PLoS Pathog. 2021;17(3):e1009421.
951. Rasaiyaah J, Tan CP, Fletcher AJ, Price AJ, Blondeau C, Hilditch L, et al. HIV-1 evades innate immune recognition through specific cofactor recruitment. Nature. 2013;503(7476):402-5.
952. Lahaye X, Satoh T, Gentili M, Cerboni S, Conrad C, Hurbain I, et al. The capsids of HIV-1 and HIV-2 determine immune detection of the viral cDNA by the innate sensor cGAS in dendritic cells. Immunity. 2013;39(6):1132-42.
953. Lahaye X, Gentili M, Silvin A, Conrad C, Picard L, Jouve M, et al. NONO Detects the Nuclear HIV Capsid to Promote cGAS-Mediated Innate Immune Activation. Cell. 2018;175(2):488-501 e22.
954. Sumner RP, Harrison L, Touizer E, Peacock TP, Spencer M, Zuliani-Alvarez L, et al. Disrupting HIV-1 capsid formation causes cGAS sensing of viral DNA. EMBO J. 2020;39(20):e103958.
955. Doehle BP, Hladik F, McNevin JP, McElrath MJ, Gale M, Jr. Human immunodeficiency virus type 1 mediates global disruption of innate antiviral signaling and immune defenses within infected cells. J Virol. 2009;83(20):10395-405.
956. Park SY, Waheed AA, Zhang ZR, Freed EO, Bonifacino JS. HIV-1 Vpu accessory protein induces caspase-mediated cleavage of IRF3 transcription factor. J Biol Chem. 2014;289(51):35102-10.

957. Harman AN, Nasr N, Feetham A, Galoyan A, Alshehri AA, Rambukwelle D, et al. HIV Blocks Interferon Induction in Human Dendritic Cells and Macrophages by Dysregulation of TBK1. J Virol. 2015;89(13):6575-84.
958. Dhamanage AS, Thakar MR, Paranjape RS. HIV-1-Mediated Suppression of IFN-alpha Production Is Associated with Inhibition of IRF-7 Translocation and PI3K/akt Pathway in Plasmacytoid Dendritic Cells. AIDS Res Hum Retroviruses. 2019;35(1):40-8.
959. Martinelli E, Cicala C, Van Ryk D, Goode DJ, Macleod K, Arthos J, et al. HIV-1 gp120 inhibits TLR9-mediated activation and IFN-{alpha} secretion in plasmacytoid dendritic cells. Proc Natl Acad Sci U S A. 2007;104(9):3396-401.
960. Jin C, Li J, Cheng L, Liu F, Wu N. Gp120 binding with DC-SIGN induces reactivation of HIV-1 provirus via the NF-kappaB signaling pathway. Acta Biochim Biophys Sin (Shanghai). 2016;48(3):275-81.
961. Chung NP, Matthews K, Klasse PJ, Sanders RW, Moore JP. HIV-1 gp120 impairs the induction of B cell responses by TLR9-activated plasmacytoid dendritic cells. J Immunol. 2012;189(11):5257-65.
962. Lo CC, Schwartz JA, Johnson DJ, Yu M, Aidarus N, Mujib S, et al. HIV delays IFN-alpha production from human plasmacytoid dendritic cells and is associated with SYK phosphorylation. PLoS One. 2012;7(5):e37052.
963. Dhamanage A, Thakar M, Paranjape R. Human Immunodeficiency Virus-1 Impairs IFN-Alpha Production Induced by TLR-7 Agonist in Plasmacytoid Dendritic Cells. Viral Immunol. 2017;30(1):28-34.
964. Wang Q, Gao H, Clark KM, Mugisha CS, Davis K, Tang JP, et al. CARD8 is an inflammasome sensor for HIV-1 protease activity. Science. 2021;371(6535).
965. Doitsh G, Cavrois M, Lassen KG, Zepeda O, Yang Z, Santiago ML, et al. Abortive HIV infection mediates CD4 T cell depletion and inflammation in human lymphoid tissue. Cell. 2010;143(5):789-801.
966. Monroe KM, Yang Z, Johnson JR, Geng X, Doitsh G, Krogan NJ, et al. IFI16 DNA sensor is required for death of lymphoid CD4 T cells abortively infected with HIV. Science. 2014;343(6169):428-32.
967. Stunnenberg M, Sprokholt JK, van Hamme JL, Kaptein TM, Zijlstra-Willems EM, Gringhuis SI, et al. Synthetic Abortive HIV-1 RNAs Induce Potent Antiviral Immunity. Front Immunol. 2020;11:8.
968. Capobianchi MR, Uleri E, Caglioti C, Dolei A. Type I IFN family members: similarity, differences and interaction. Cytokine Growth Factor Rev. 2015;26(2):103-11.
969. Hardy MP, Owczarek CM, Jermiin LS, Ejdeback M, Hertzog PJ. Characterization of the type I interferon locus and identification of novel genes. Genomics. 2004;84(2):331-45.
970. de Weerd NA, Nguyen T. The interferons and their receptors--distribution and regulation. Immunol Cell Biol. 2012;90(5):483-91.
971. Majoros A, Platanitis E, Kernbauer-Holzl E, Rosebrock F, Muller M, Decker T. Canonical and Non-Canonical Aspects of JAK-STAT Signaling: Lessons from Interferons for Cytokine Responses. Front Immunol. 2017;8:29.
972. Mesev EV, LeDesma RA, Ploss A. Decoding type I and III interferon signalling during viral infection. Nat Microbiol. 2019;4(6):914-24.
973. Schoggins JW, Wilson SJ, Panis M, Murphy MY, Jones CT, Bieniasz P, et al. A diverse range of gene products are effectors of the type I interferon antiviral response. Nature. 2011;472(7344):481-5.

974. Nguyen NV, Tran JT, Sanchez DJ. HIV blocks Type I IFN signaling through disruption of STAT1 phosphorylation. Innate Immun. 2018;24(8):490-500.
975. Szubin R, Chang WL, Greasby T, Beckett L, Baumgarth N. Rigid interferon-alpha subtype responses of human plasmacytoid dendritic cells. J Interferon Cytokine Res. 2008;28(12):749-63.
976. Lavoie TB, Kalie E, Crisafulli-Cabatu S, Abramovich R, DiGioia G, Moolchan K, et al. Binding and activity of all human alpha interferon subtypes. Cytokine. 2011;56(2):282-9.
977. Moll HP, Maier T, Zommer A, Lavoie T, Brostjan C. The differential activity of interferon-alpha subtypes is consistent among distinct target genes and cell types. Cytokine. 2011;53(1):52-9.
978. Berry CM. Understanding Interferon Subtype Therapy for Viral Infections: Harnessing the Power of the Innate Immune System. Cytokine Growth Factor Rev. 2016;31:83-90.
979. Lavender KJ, Gibbert K, Peterson KE, Van Dis E, Francois S, Woods T, et al. Interferon Alpha Subtype-Specific Suppression of HIV-1 Infection In Vivo. J Virol. 2016;90(13):6001-13.
980. Abraham S, Choi JG, Ortega NM, Zhang J, Shankar P, Swamy NM. Gene therapy with plasmids encoding IFN-beta or IFN-alpha14 confers long-term resistance to HIV-1 in humanized mice. Oncotarget. 2016;7(48):78412-20.
981. Sutter K, Lavender KJ, Messer RJ, Widera M, Williams K, Race B, et al. Concurrent administration of IFNalpha14 and cART in TKO-BLT mice enhances suppression of HIV-1 viremia but does not eliminate the latent reservoir. Sci Rep. 2019;9(1):18089.
982. Tauzin A, Espinosa Ortiz A, Blake O, Soundaramourty C, Joly-Beauparlant C, Nicolas A, et al. Differential Inhibition of HIV Replication by the 12 Interferon Alpha Subtypes. J Virol. 2021;95(15):e0231120.
983. Rout SS, Di Y, Dittmer U, Sutter K, Lavender KJ. Distinct effects of treatment with two different interferon-alpha subtypes on HIV-1-associated T-cell activation and dysfunction in humanized mice. AIDS. 2022;36(3):325-36.
984. Harper MS, Guo K, Gibbert K, Lee EJ, Dillon SM, Barrett BS, et al. Interferon-alpha Subtypes in an Ex Vivo Model of Acute HIV-1 Infection: Expression, Potency and Effector Mechanisms. PLoS Pathog. 2015;11(11):e1005254.
985. von Sydow M, Sonnerborg A, Gaines H, Strannegard O. Interferon-alpha and tumor necrosis factor-alpha in serum of patients in various stages of HIV-1 infection. AIDS Res Hum Retroviruses. 1991;7(4):375-80.
986. Stacey AR, Norris PJ, Qin L, Haygreen EA, Taylor E, Heitman J, et al. Induction of a striking systemic cytokine cascade prior to peak viremia in acute human immunodeficiency virus type 1 infection, in contrast to more modest and delayed responses in acute hepatitis B and C virus infections. J Virol. 2009;83(8):3719-33.
987. Hardy GA, Sieg S, Rodriguez B, Anthony D, Asaad R, Jiang W, et al. Interferon-alpha is the primary plasma type-I IFN in HIV-1 infection and correlates with immune activation and disease markers. PLoS One. 2013;8(2):e56527.
988. Sandler NG, Bosinger SE, Estes JD, Zhu RT, Tharp GK, Boritz E, et al. Type I interferon responses in rhesus macaques prevent SIV infection and slow disease progression. Nature. 2014;511(7511):601-5.
989. Veazey RS, Pilch-Cooper HA, Hope TJ, Alter G, Carias AM, Sips M, et al. Prevention of SHIV transmission by topical IFN-beta treatment. Mucosal Immunol. 2016;9(6):1528-36.
990. Carnathan D, Lawson B, Yu J, Patel K, Billingsley JM, Tharp GK, et al. Reduced Chronic Lymphocyte Activation following Interferon Alpha Blockade during the Acute Phase of Simian Immunodeficiency Virus Infection in Rhesus Macaques. J Virol. 2018;92(9).

991. Sedaghat AR, German J, Teslovich TM, Cofrancesco J, Jr., Jie CC, Talbot CC, Jr., et al. Chronic CD4+ T-cell activation and depletion in human immunodeficiency virus type 1 infection: type I interferon-mediated disruption of T-cell dynamics. J Virol. 2008;82(4):1870-83.
992. Guo K, Shen G, Kibbie J, Gonzalez T, Dillon SM, Smith HA, et al. Qualitative Differences Between the IFNalpha subtypes and IFNbeta Influence Chronic Mucosal HIV-1 Pathogenesis. PLoS Pathog. 2020;16(10):e1008986.
993. Donaghy H, Pozniak A, Gazzard B, Qazi N, Gilmour J, Gotch F, et al. Loss of blood CD11c(+) myeloid and CD11c(-) plasmacytoid dendritic cells in patients with HIV-1 infection correlates with HIV-1 RNA virus load. Blood. 2001;98(8):2574-6.
994. Barron MA, Blyveis N, Palmer BE, MaWhinney S, Wilson CC. Influence of plasma viremia on defects in number and immunophenotype of blood dendritic cell subsets in human immunodeficiency virus 1-infected individuals. J Infect Dis. 2003;187(1):26-37.
995. Machmach K, Leal M, Gras C, Viciana P, Genebat M, Franco E, et al. Plasmacytoid dendritic cells reduce HIV production in elite controllers. J Virol. 2012;86(8):4245-52.
996. Asmuth DM, Murphy RL, Rosenkranz SL, Lertora JJ, Kottilil S, Cramer Y, et al. Safety, tolerability, and mechanisms of antiretroviral activity of pegylated interferon Alfa-2a in HIV-1-monoinfected participants: a phase II clinical trial. J Infect Dis. 2010;201(11):1686-96.
997. Boue F, Reynes J, Rouzioux C, Emilie D, Souala F, Tubiana R, et al. Alpha interferon administration during structured interruptions of combination antiretroviral therapy in patients with chronic HIV-1 infection: INTERVAC ANRS 105 trial. AIDS. 2011;25(1):115-8.
998. Goujard C, Emilie D, Roussillon C, Godot V, Rouzioux C, Venet A, et al. Continuous versus intermittent treatment strategies during primary HIV-1 infection: the randomized ANRS INTERPRIM Trial. AIDS. 2012;26(15):1895-905.
999. Azzoni L, Foulkes AS, Papasavvas E, Mexas AM, Lynn KM, Mounzer K, et al. Pegylated Interferon alfa-2a monotherapy results in suppression of HIV type 1 replication and decreased cell-associated HIV DNA integration. J Infect Dis. 2013;207(2):213-22.
1000. Papasavvas E, Azzoni L, Pagliuzza A, Abdel-Mohsen M, Ross BN, Fair M, et al. Safety, Immune, and Antiviral Effects of Pegylated Interferon Alpha 2b Administration in Antiretroviral Therapy-Suppressed Individuals: Results of Pilot Clinical Trial. AIDS Res Hum Retroviruses. 2021;37(6):433-43.
1001. Hua S, Vigano S, Tse S, Zhengyu O, Harrington S, Negron J, et al. Pegylated Interferon-alpha-Induced Natural Killer Cell Activation Is Associated With Human Immunodeficiency Virus-1 DNA Decline in Antiretroviral Therapy-Treated HIV-1/Hepatitis C Virus-Coinfected Patients. Clin Infect Dis. 2018;66(12):1910-7.
1002. Kmiec D, Iyer SS, Sturzel CM, Sauter D, Hahn BH, Kirchhoff F. Vpu-Mediated Counteraction of Tetherin Is a Major Determinant of HIV-1 Interferon Resistance. MBio. 2016;7(4).
1003. Gondim MVP, Sherrill-Mix S, Bibollet-Ruche F, Russell RM, Trimboli S, Smith AG, et al. Heightened resistance to host type 1 interferons characterizes HIV-1 at transmission and after antiretroviral therapy interruption. Sci Transl Med. 2021;13(576).
1004. Edlin BR, St Clair MH, Pitha PM, Whaling SM, King DM, Bitran JD, et al. In-vitro resistance to zidovudine and alpha-interferon in HIV-1 isolates from patients: correlations with treatment duration and response. Ann Intern Med. 1992;117(6):457-60.
1005. Kunzi MS, Farzadegan H, Margolick JB, Vlahov D, Pitha PM. Identification of human immunodeficiency virus primary isolates resistant to interferon-alpha and correlation of prevalence to disease progression. J Infect Dis. 1995;171(4):822-8.

1006. Borrow P, Lewicki H, Hahn BH, Shaw GM, Oldstone MB. Virus-specific CD8+ cytotoxic T-lymphocyte activity associated with control of viremia in primary human immunodeficiency virus type 1 infection. J Virol. 1994;68(9):6103-10.
1007. Matano T, Shibata R, Siemon C, Connors M, Lane HC, Martin MA. Administration of an anti-CD8 monoclonal antibody interferes with the clearance of chimeric simian/human immunodeficiency virus during primary infections of rhesus macaques. J Virol. 1998;72(1):164-9.
1008. Schmitz JE, Kuroda MJ, Santra S, Sasseville VG, Simon MA, Lifton MA, et al. Control of viremia in simian immunodeficiency virus infection by CD8+ lymphocytes. Science. 1999;283(5403):857-60.
1009. Goonetilleke N, Liu MK, Salazar-Gonzalez JF, Ferrari G, Giorgi E, Ganusov VV, et al. The first T cell response to transmitted/founder virus contributes to the control of acute viremia in HIV-1 infection. J Exp Med. 2009;206(6):1253-72.
1010. Lichterfeld M, Yu XG, Cohen D, Addo MM, Malenfant J, Perkins B, et al. HIV-1 Nef is preferentially recognized by CD8 T cells in primary HIV-1 infection despite a relatively high degree of genetic diversity. AIDS. 2004;18(10):1383-92.
1011. Turnbull EL, Wong M, Wang S, Wei X, Jones NA, Conrod KE, et al. Kinetics of expansion of epitope-specific T cell responses during primary HIV-1 infection. J Immunol. 2009;182(11):7131-45.
1012. Jones NA, Wei X, Flower DR, Wong M, Michor F, Saag MS, et al. Determinants of human immunodeficiency virus type 1 escape from the primary CD8+ cytotoxic T lymphocyte response. J Exp Med. 2004;200(10):1243-56.
1013. Bernardin F, Kong D, Peddada L, Baxter-Lowe LA, Delwart E. Human immunodeficiency virus mutations during the first month of infection are preferentially found in known cytotoxic T-lymphocyte epitopes. J Virol. 2005;79(17):11523-8.
1014. Streeck H, Jolin JS, Qi Y, Yassine-Diab B, Johnson RC, Kwon DS, et al. Human immunodeficiency virus type 1-specific CD8+ T-cell responses during primary infection are major determinants of the viral set point and loss of CD4+ T cells. J Virol. 2009;83(15):7641-8.
1015. Ndhlovu ZM, Kamya P, Mewalal N, Kloverpris HN, Nkosi T, Pretorius K, et al. Magnitude and Kinetics of CD8+ T Cell Activation during Hyperacute HIV Infection Impact Viral Set Point. Immunity. 2015;43(3):591-604.
1016. Tsomides TJ, Aldovini A, Johnson RP, Walker BD, Young RA, Eisen HN. Naturally processed viral peptides recognized by cytotoxic T lymphocytes on cells chronically infected by human immunodeficiency virus type 1. J Exp Med. 1994;180(4):1283-93.
1017. Honeyborne I, Codoner FM, Leslie A, Tudor-Williams G, Luzzi G, Ndung'u T, et al. HLA-Cw*03-restricted CD8+ T-cell responses targeting the HIV-1 gag major homology region drive virus immune escape and fitness constraints compensated for by intracodon variation. J Virol. 2010;84(21):11279-88.
1018. Berger CT, Carlson JM, Brumme CJ, Hartman KL, Brumme ZL, Henry LM, et al. Viral adaptation to immune selection pressure by HLA class I-restricted CTL responses targeting epitopes in HIV frameshift sequences. J Exp Med. 2010;207(1):61-75.
1019. Riou C, Ganusov VV, Campion S, Mlotshwa M, Liu MK, Whale VE, et al. Distinct kinetics of Gag-specific CD4+ and CD8+ T cell responses during acute HIV-1 infection. J Immunol. 2012;188(5):2198-206.

1020. Goulder PJ, Altfeld MA, Rosenberg ES, Nguyen T, Tang Y, Eldridge RL, et al. Substantial differences in specificity of HIV-specific cytotoxic T cells in acute and chronic HIV infection. J Exp Med. 2001;193(2):181-94.
1021. Kaslow RA, Carrington M, Apple R, Park L, Munoz A, Saah AJ, et al. Influence of combinations of human major histocompatibility complex genes on the course of HIV-1 infection. Nat Med. 1996;2(4):405-11.
1022. Migueles SA, Sabbaghian MS, Shupert WL, Bettinotti MP, Marincola FM, Martino L, et al. HLA B*5701 is highly associated with restriction of virus replication in a subgroup of HIV-infected long term nonprogressors. Proc Natl Acad Sci U S A. 2000;97(6):2709-14.
1023. Fellay J, Shianna KV, Ge D, Colombo S, Ledergerber B, Weale M, et al. A whole-genome association study of major determinants for host control of HIV-1. Science. 2007;317(5840):944-7.
1024. Pereyra F, Jia X, McLaren PJ, Telenti A, de Bakker PI, Walker BD, et al. The major genetic determinants of HIV-1 control affect HLA class I peptide presentation. Science. 2010;330(6010):1551-7.
1025. Saez-Cirion A, Bacchus C, Hocqueloux L, Avettand-Fenoel V, Girault I, Lecuroux C, et al. Post-treatment HIV-1 controllers with a long-term virological remission after the interruption of early initiated antiretroviral therapy ANRS VISCONTI Study. PLoS Pathog. 2013;9(3):e1003211.
1026. Brockman MA, Schneidewind A, Lahaie M, Schmidt A, Miura T, Desouza I, et al. Escape and compensation from early HLA-B57-mediated cytotoxic T-lymphocyte pressure on human immunodeficiency virus type 1 Gag alter capsid interactions with cyclophilin A. J Virol. 2007;81(22):12608-18.
1027. Schneidewind A, Brockman MA, Sidney J, Wang YE, Chen H, Suscovich TJ, et al. Structural and functional constraints limit options for cytotoxic T-lymphocyte escape in the immunodominant HLA-B27-restricted epitope in human immunodeficiency virus type 1 capsid. J Virol. 2008;82(11):5594-605.
1028. Battivelli E, Migraine J, Lecossier D, Yeni P, Clavel F, Hance AJ. Gag cytotoxic T lymphocyte escape mutations can increase sensitivity of HIV-1 to human TRIM5alpha, linking intrinsic and acquired immunity. J Virol. 2011;85(22):11846-54.
1029. Granier C, Battivelli E, Lecuroux C, Venet A, Lambotte O, Schmitt-Boulanger M, et al. Pressure from TRIM5alpha contributes to control of HIV-1 replication by individuals expressing protective HLA-B alleles. J Virol. 2013;87(18):10368-80.
1030. Merindol N, El-Far M, Sylla M, Masroori N, Dufour C, Li JX, et al. HIV-1 capsids from B27/B57+ elite controllers escape Mx2 but are targeted by TRIM5alpha, leading to the induction of an antiviral state. PLoS Pathog. 2018;14(11):e1007398.
1031. Schommers P, Martrus G, Matschl U, Sirignano M, Lutgehetmann M, Richert L, et al. Changes in HIV-1 Capsid Stability Induced by Common Cytotoxic-T-Lymphocyte-Driven Viral Sequence Mutations. J Virol. 2016;90(16):7579-86.
1032. Jin X, Bauer DE, Tuttleton SE, Lewin S, Gettie A, Blanchard J, et al. Dramatic rise in plasma viremia after CD8(+) T cell depletion in simian immunodeficiency virus-infected macaques. J Exp Med. 1999;189(6):991-8.
1033. Appay V, Dunbar PR, Callan M, Klenerman P, Gillespie GM, Papagno L, et al. Memory CD8+ T cells vary in differentiation phenotype in different persistent virus infections. Nat Med. 2002;8(4):379-85.

1034. Betts MR, Nason MC, West SM, De Rosa SC, Migueles SA, Abraham J, et al. HIV nonprogressors preferentially maintain highly functional HIV-specific CD8+ T cells. Blood. 2006;107(12):4781-9.
1035. Chowdhury A, Hayes TL, Bosinger SE, Lawson BO, Vanderford T, Schmitz JE, et al. Differential Impact of In Vivo CD8+ T Lymphocyte Depletion in Controller versus Progressor Simian Immunodeficiency Virus-Infected Macaques. J Virol. 2015;89(17):8677-86.
1036. Cartwright EK, Spicer L, Smith SA, Lee D, Fast R, Paganini S, et al. CD8(+) Lymphocytes Are Required for Maintaining Viral Suppression in SIV-Infected Macaques Treated with Short-Term Antiretroviral Therapy. Immunity. 2016;45(3):656-68.
1037. Cao Y, Cartwright EK, Silvestri G, Perelson AS. CD8+ lymphocyte control of SIV infection during antiretroviral therapy. PLoS Pathog. 2018;14(10):e1007350.
1038. Warren JA, Zhou S, Xu Y, Moeser MJ, MacMillan DR, Council O, et al. The HIV-1 latent reservoir is largely sensitive to circulating T cells. Elife. 2020;9.
1039. Deng K, Pertea M, Rongvaux A, Wang L, Durand CM, Ghiaur G, et al. Broad CTL response is required to clear latent HIV-1 due to dominance of escape mutations. Nature. 2015;517(7534):381-5.
1040. Lima NS, Takata H, Huang SH, Haregot A, Mitchell J, Blackmore S, et al. CTL Clonotypes with Higher TCR Affinity Have Better Ability to Reduce the HIV Latent Reservoir. J Immunol. 2020;205(3):699-707.
1041. Cocchi F, DeVico AL, Garzino-Demo A, Arya SK, Gallo RC, Lusso P. Identification of RANTES, MIP-1 alpha, and MIP-1 beta as the major HIV-suppressive factors produced by CD8+ T cells. Science. 1995;270(5243):1811-5.
1042. Paxton WA, Martin SR, Tse D, O'Brien TR, Skurnick J, VanDevanter NL, et al. Relative resistance to HIV-1 infection of CD4 lymphocytes from persons who remain uninfected despite multiple high-risk sexual exposure. Nat Med. 1996;2(4):412-7.
1043. Folkvord JM, Anderson DM, Arya J, MaWhinney S, Connick E. Microanatomic relationships between CD8+ cells and HIV-1-producing cells in human lymphoid tissue in vivo. J Acquir Immune Defic Syndr. 2003;32(5):469-76.
1044. Reuter MA, Del Rio Estrada PM, Buggert M, Petrovas C, Ferrando-Martinez S, Nguyen S, et al. HIV-Specific CD8(+) T Cells Exhibit Reduced and Differentially Regulated Cytolytic Activity in Lymphoid Tissue. Cell Rep. 2017;21(12):3458-70.
1045. Li S, Folkvord JM, Kovacs KJ, Wagstaff RK, Mwakalundwa G, Rendahl AK, et al. Low levels of SIV-specific CD8+ T cells in germinal centers characterizes acute SIV infection. PLoS Pathog. 2019;15(3):e1007311.
1046. Day CL, Kaufmann DE, Kiepiela P, Brown JA, Moodley ES, Reddy S, et al. PD-1 expression on HIV-specific T cells is associated with T-cell exhaustion and disease progression. Nature. 2006;443(7109):350-4.
1047. Trautmann L, Janbazian L, Chomont N, Said EA, Gimmig S, Bessette B, et al. Upregulation of PD-1 expression on HIV-specific CD8+ T cells leads to reversible immune dysfunction. Nat Med. 2006;12(10):1198-202.
1048. Petrovas C, Casazza JP, Brenchley JM, Price DA, Gostick E, Adams WC, et al. PD-1 is a regulator of virus-specific CD8+ T cell survival in HIV infection. J Exp Med. 2006;203(10):2281-92.
1049. Blackburn SD, Shin H, Haining WN, Zou T, Workman CJ, Polley A, et al. Coregulation of CD8+ T cell exhaustion by multiple inhibitory receptors during chronic viral infection. Nat Immunol. 2009;10(1):29-37.

1050. Sun JC, Lanier LL. NK cell development, homeostasis and function: parallels with CD8(+) T cells. Nat Rev Immunol. 2011;11(10):645-57.
1051. Poli A, Michel T, Theresine M, Andres E, Hentges F, Zimmer J. CD56bright natural killer (NK) cells: an important NK cell subset. Immunology. 2009;126(4):458-65.
1052. Michel T, Poli A, Cuapio A, Briquemont B, Iserentant G, Ollert M, et al. Human CD56bright NK Cells: An Update. J Immunol. 2016;196(7):2923-31.
1053. Jacobs R, Hintzen G, Kemper A, Beul K, Kempf S, Behrens G, et al. CD56bright cells differ in their KIR repertoire and cytotoxic features from CD56dim NK cells. Eur J Immunol. 2001;31(10):3121-7.
1054. Moretta L. Dissecting CD56dim human NK cells. Blood. 2010;116(19):3689-91.
1055. Lanier LL, Le AM, Civin CI, Loken MR, Phillips JH. The relationship of CD16 (Leu-11) and Leu-19 (NKH-1) antigen expression on human peripheral blood NK cells and cytotoxic T lymphocytes. J Immunol. 1986;136(12):4480-6.
1056. Krzewski K, Coligan JE. Human NK cell lytic granules and regulation of their exocytosis. Front Immunol. 2012;3:335.
1057. Cullen SP, Martin SJ. Mechanisms of granule-dependent killing. Cell Death Differ. 2008;15(2):251-62.
1058. Zwirner NW, Domaica CI. Cytokine regulation of natural killer cell effector functions. Biofactors. 2010;36(4):274-88.
1059. Hansen ML, Woetmann A, Krejsgaard T, Kopp KL, Sokilde R, Litman T, et al. IFN-alpha primes T- and NK-cells for IL-15-mediated signaling and cytotoxicity. Mol Immunol. 2011;48(15-16):2087-93.
1060. Kwaa AKR, Talana CAG, Blankson JN. Interferon Alpha Enhances NK Cell Function and the Suppressive Capacity of HIV-Specific CD8(+) T Cells. J Virol. 2019;93(3).
1061. Gosselin J, TomoIu A, Gallo RC, Flamand L. Interleukin-15 as an activator of natural killer cell-mediated antiviral response. Blood. 1999;94(12):4210-9.
1062. Ranson T, Vosshenrich CA, Corcuff E, Richard O, Muller W, Di Santo JP. IL-15 is an essential mediator of peripheral NK-cell homeostasis. Blood. 2003;101(12):4887-93.
1063. Zhang M, Wen B, Anton OM, Yao Z, Dubois S, Ju W, et al. IL-15 enhanced antibody-dependent cellular cytotoxicity mediated by NK cells and macrophages. Proc Natl Acad Sci U S A. 2018;115(46):E10915-E24.
1064. Wang X, Zhao XY. Transcription Factors Associated With IL-15 Cytokine Signaling During NK Cell Development. Front Immunol. 2021;12:610789.
1065. Anderson P, Caligiuri M, Ritz J, Schlossman SF. CD3-negative natural killer cells express zeta TCR as part of a novel molecular complex. Nature. 1989;341(6238):159-62.
1066. Hibbs ML, Selvaraj P, Carpen O, Springer TA, Kuster H, Jouvin MH, et al. Mechanisms for regulating expression of membrane isoforms of Fc gamma RIII (CD16). Science. 1989;246(4937):1608-11.
1067. Lanier LL, Corliss BC, Wu J, Leong C, Phillips JH. Immunoreceptor DAP12 bearing a tyrosine-based activation motif is involved in activating NK cells. Nature. 1998;391(6668):703-7.
1068. Long EO. Negative signaling by inhibitory receptors: the NK cell paradigm. Immunol Rev. 2008;224:70-84.
1069. Brumbaugh KM, Binstadt BA, Billadeau DD, Schoon RA, Dick CJ, Ten RM, et al. Functional role for Syk tyrosine kinase in natural killer cell-mediated natural cytotoxicity. J Exp Med. 1997;186(12):1965-74.

1070. Burshtyn DN, Yang W, Yi T, Long EO. A novel phosphotyrosine motif with a critical amino acid at position -2 for the SH2 domain-mediated activation of the tyrosine phosphatase SHP-1. J Biol Chem. 1997;272(20):13066-72.
1071. Dohring C, Colonna M. Human natural killer cell inhibitory receptors bind to HLA class I molecules. Eur J Immunol. 1996;26(2):365-9.
1072. Braud VM, Allan DS, O'Callaghan CA, Soderstrom K, D'Andrea A, Ogg GS, et al. HLA-E binds to natural killer cell receptors CD94/NKG2A, B and C. Nature. 1998;391(6669):795-9.
1073. Biassoni R, Pessino A, Malaspina A, Cantoni C, Bottino C, Sivori S, et al. Role of amino acid position 70 in the binding affinity of p50.1 and p58.1 receptors for HLA-Cw4 molecules. Eur J Immunol. 1997;27(12):3095-9.
1074. Vales-Gomez M, Reyburn HT, Erskine RA, Lopez-Botet M, Strominger JL. Kinetics and peptide dependency of the binding of the inhibitory NK receptor CD94/NKG2-A and the activating receptor CD94/NKG2-C to HLA-E. EMBO J. 1999;18(15):4250-60.
1075. Bottino C, Castriconi R, Pende D, Rivera P, Nanni M, Carnemolla B, et al. Identification of PVR (CD155) and Nectin-2 (CD112) as cell surface ligands for the human DNAM-1 (CD226) activating molecule. J Exp Med. 2003;198(4):557-67.
1076. Stanietsky N, Simic H, Arapovic J, Toporik A, Levy O, Novik A, et al. The interaction of TIGIT with PVR and PVRL2 inhibits human NK cell cytotoxicity. Proc Natl Acad Sci U S A. 2009;106(42):17858-63.
1077. Shibuya A, Shibuya K. DNAM-1 versus TIGIT: competitive roles in tumor immunity and inflammatory responses. Int Immunol. 2021;33(12):687-92.
1078. Cosman D, Mullberg J, Sutherland CL, Chin W, Armitage R, Fanslow W, et al. ULBPs, novel MHC class I-related molecules, bind to CMV glycoprotein UL16 and stimulate NK cytotoxicity through the NKG2D receptor. Immunity. 2001;14(2):123-33.
1079. Barrow AD, Martin CJ, Colonna M. The Natural Cytotoxicity Receptors in Health and Disease. Front Immunol. 2019;10:909.
1080. Brandt CS, Baratin M, Yi EC, Kennedy J, Gao Z, Fox B, et al. The B7 family member B7-H6 is a tumor cell ligand for the activating natural killer cell receptor NKp30 in humans. J Exp Med. 2009;206(7):1495-503.
1081. Yamashita Y, Anczurowski M, Nakatsugawa M, Tanaka M, Kagoya Y, Sinha A, et al. HLA-DP(84Gly) constitutively presents endogenous peptides generated by the class I antigen processing pathway. Nat Commun. 2017;8:15244.
1082. Niehrs A, Garcia-Beltran WF, Norman PJ, Watson GM, Holzemer A, Chapel A, et al. A subset of HLA-DP molecules serve as ligands for the natural cytotoxicity receptor NKp44. Nat Immunol. 2019;20(9):1129-37.
1083. Narni-Mancinelli E, Gauthier L, Baratin M, Guia S, Fenis A, Deghmane AE, et al. Complement factor P is a ligand for the natural killer cell-activating receptor NKp46. Sci Immunol. 2017;2(10).
1084. Kemper C, Atkinson JP, Hourcade DE. Properdin: emerging roles of a pattern-recognition molecule. Annu Rev Immunol. 2010;28:131-55.
1085. Brown MH, Boles K, van der Merwe PA, Kumar V, Mathew PA, Barclay AN. 2B4, the natural killer and T cell immunoglobulin superfamily surface protein, is a ligand for CD48. J Exp Med. 1998;188(11):2083-90.
1086. Flaig RM, Stark S, Watzl C. Cutting edge: NTB-A activates NK cells via homophilic interaction. J Immunol. 2004;172(11):6524-7.

1087. Bryceson YT, March ME, Ljunggren HG, Long EO. Synergy among receptors on resting NK cells for the activation of natural cytotoxicity and cytokine secretion. Blood. 2006;107(1):159-66.
1088. Hopfensperger K, Richard J, Sturzel CM, Bibollet-Ruche F, Apps R, Leoz M, et al. Convergent Evolution of HLA-C Downmodulation in HIV-1 and HIV-2. mBio. 2020;11(4).
1089. Xie G, Dong H, Liang Y, Ham JD, Rizwan R, Chen J. CAR-NK cells: A promising cellular immunotherapy for cancer. EBioMedicine. 2020;59:102975.
1090. Vieillard V, Strominger JL, Debre P. NK cytotoxicity against CD4+ T cells during HIV-1 infection: a gp41 peptide induces the expression of an NKp44 ligand. Proc Natl Acad Sci U S A. 2005;102(31):10981-6.
1091. Tremblay-McLean A, Bruneau J, Lebouche B, Lisovsky I, Song R, Bernard NF. Expression Profiles of Ligands for Activating Natural Killer Cell Receptors on HIV Infected and Uninfected CD4(+) T Cells. Viruses. 2017;9(10).
1092. Obiedat A, Charpak-Amikam Y, Tai-Schmiedel J, Seidel E, Mahameed M, Avril T, et al. The integrated stress response promotes B7H6 expression. J Mol Med (Berl). 2020;98(1):135-48.
1093. Borsa M, Ferreira PL, Petry A, Ferreira LG, Camargo MM, Bou-Habib DC, et al. HIV infection and antiretroviral therapy lead to unfolded protein response activation. Virol J. 2015;12:77.
1094. Stumptner-Cuvelette P, Morchoisne S, Dugast M, Le Gall S, Raposo G, Schwartz O, et al. HIV-1 Nef impairs MHC class II antigen presentation and surface expression. Proc Natl Acad Sci U S A. 2001;98(21):12144-9.
1095. Hussain A, Wesley C, Khalid M, Chaudhry A, Jameel S. Human immunodeficiency virus type 1 Vpu protein interacts with CD74 and modulates major histocompatibility complex class II presentation. J Virol. 2008;82(2):893-902.
1096. Fausther-Bovendo H, Sol-Foulon N, Candotti D, Agut H, Schwartz O, Debre P, et al. HIV escape from natural killer cytotoxicity: nef inhibits NKp44L expression on CD4+ T cells. AIDS. 2009;23(9):1077-87.
1097. Galaski J, Ahmad F, Tibroni N, Pujol FM, Muller B, Schmidt RE, et al. Cell Surface Downregulation of NK Cell Ligands by Patient-Derived HIV-1 Vpu and Nef Alleles. J Acquir Immune Defic Syndr. 2016;72(1):1-10.
1098. Ward J, Bonaparte M, Sacks J, Guterman J, Fogli M, Mavilio D, et al. HIV modulates the expression of ligands important in triggering natural killer cell cytotoxic responses on infected primary T-cell blasts. Blood. 2007;110(4):1207-14.
1099. Arias JF, Heyer LN, von Bredow B, Weisgrau KL, Moldt B, Burton DR, et al. Tetherin antagonism by Vpu protects HIV-infected cells from antibody-dependent cell-mediated cytotoxicity. Proc Natl Acad Sci U S A. 2014;111(17):6425-30.
1100. Alvarez RA, Hamlin RE, Monroe A, Moldt B, Hotta MT, Rodriguez Caprio G, et al. HIV-1 Vpu antagonism of tetherin inhibits antibody-dependent cellular cytotoxic responses by natural killer cells. J Virol. 2014;88(11):6031-46.
1101. von Bredow B, Arias JF, Heyer LN, Gardner MR, Farzan M, Rakasz EG, et al. Envelope Glycoprotein Internalization Protects Human and Simian Immunodeficiency Virus Infected Cells from Antibody-Dependent Cell-Mediated Cytotoxicity. J Virol. 2015.
1102. Anand SP, Grover JR, Tolbert WD, Prevost J, Richard J, Ding S, et al. Antibody-induced internalization of HIV-1 Env proteins limits the surface expression of the closed conformation of Env. J Virol. 2019.

1103. Sugden SM, Pham TNQ, Cohen EA. HIV-1 Vpu Downmodulates ICAM-1 Expression, Resulting in Decreased Killing of Infected CD4(+) T Cells by NK Cells. J Virol. 2017;91(8).
1104. Bryceson YT, March ME, Barber DF, Ljunggren HG, Long EO. Cytolytic granule polarization and degranulation controlled by different receptors in resting NK cells. J Exp Med. 2005;202(7):1001-12.
1105. Alter G, Teigen N, Ahern R, Streeck H, Meier A, Rosenberg ES, et al. Evolution of innate and adaptive effector cell functions during acute HIV-1 infection. J Infect Dis. 2007;195(10):1452-60.
1106. Alter G, Altfeld M. NK cells in HIV-1 infection: evidence for their role in the control of HIV-1 infection. J Intern Med. 2009;265(1):29-42.
1107. Oliva A, Kinter AL, Vaccarezza M, Rubbert A, Catanzaro A, Moir S, et al. Natural killer cells from human immunodeficiency virus (HIV)-infected individuals are an important source of CC-chemokines and suppress HIV-1 entry and replication in vitro. J Clin Invest. 1998;102(1):223-31.
1108. Quillay H, El Costa H, Duriez M, Marlin R, Cannou C, Madec Y, et al. NK cells control HIV-1 infection of macrophages through soluble factors and cellular contacts in the human decidua. Retrovirology. 2016;13(1):39.
1109. Huot N, Jacquelin B, Garcia-Tellez T, Rascle P, Ploquin MJ, Madec Y, et al. Natural killer cells migrate into and control simian immunodeficiency virus replication in lymph node follicles in African green monkeys. Nat Med. 2017;23(11):1277-86.
1110. Guo AL, Jiao YM, Zhao QW, Huang HH, Deng JN, Zhang C, et al. Implications of the accumulation of CXCR5(+) NK cells in lymph nodes of HIV-1 infected patients. EBioMedicine. 2022;75:103794.
1111. Rahman SA, Billinglsley J, Sharma AA, Styles TM, Govindaraj S, Shanmugasundaram U, et al. Lymph node CXCR5+ NK cells associate with control of chronic SHIV infection. JCI Insight. 2022.
1112. Martin MP, Gao X, Lee JH, Nelson GW, Detels R, Goedert JJ, et al. Epistatic interaction between KIR3DS1 and HLA-B delays the progression to AIDS. Nat Genet. 2002;31(4):429-34.
1113. Alter G, Martin MP, Teigen N, Carr WH, Suscovich TJ, Schneidewind A, et al. Differential natural killer cell-mediated inhibition of HIV-1 replication based on distinct KIR/HLA subtypes. J Exp Med. 2007;204(12):3027-36.
1114. Ravet S, Scott-Algara D, Bonnet E, Tran HK, Tran T, Nguyen N, et al. Distinctive NK-cell receptor repertoires sustain high-level constitutive NK-cell activation in HIV-exposed uninfected individuals. Blood. 2007;109(10):4296-305.
1115. Boulet S, Sharafi S, Simic N, Bruneau J, Routy JP, Tsoukas CM, et al. Increased proportion of KIR3DS1 homozygotes in HIV-exposed uninfected individuals. AIDS. 2008;22(5):595-9.
1116. Hu PF, Hultin LE, Hultin P, Hausner MA, Hirji K, Jewett A, et al. Natural killer cell immunodeficiency in HIV disease is manifest by profoundly decreased numbers of CD16+CD56+ cells and expansion of a population of CD16dimCD56- cells with low lytic activity. J Acquir Immune Defic Syndr Hum Retrovirol. 1995;10(3):331-40.
1117. Alter G, Teigen N, Davis BT, Addo MM, Suscovich TJ, Waring MT, et al. Sequential deregulation of NK cell subset distribution and function starting in acute HIV-1 infection. Blood. 2005;106(10):3366-9.
1118. Brunetta E, Fogli M, Varchetta S, Bozzo L, Hudspeth KL, Marcenaro E, et al. The decreased expression of Siglec-7 represents an early marker of dysfunctional natural killer-cell subsets associated with high levels of HIV-1 viremia. Blood. 2009;114(18):3822-30.

1119. De Maria A, Fogli M, Costa P, Murdaca G, Puppo F, Mavilio D, et al. The impaired NK cell cytolytic function in viremic HIV-1 infection is associated with a reduced surface expression of natural cytotoxicity receptors (NKp46, NKp30 and NKp44). Eur J Immunol. 2003;33(9):2410-8.
1120. Mavilio D, Benjamin J, Daucher M, Lombardo G, Kottilil S, Planta MA, et al. Natural killer cells in HIV-1 infection: dichotomous effects of viremia on inhibitory and activating receptors and their functional correlates. Proc Natl Acad Sci U S A. 2003;100(25):15011-6.
1121. Mavilio D, Lombardo G, Benjamin J, Kim D, Follman D, Marcenaro E, et al. Characterization of CD56-/CD16+ natural killer (NK) cells: a highly dysfunctional NK subset expanded in HIV-infected viremic individuals. Proc Natl Acad Sci U S A. 2005;102(8):2886-91.
1122. Fogli M, Mavilio D, Brunetta E, Varchetta S, Ata K, Roby G, et al. Lysis of endogenously infected CD4+ T cell blasts by rIL-2 activated autologous natural killer cells from HIV-infected viremic individuals. PLoS Pathog. 2008;4(7):e1000101.
1123. Nolting A, Dugast AS, Rihn S, Luteijn R, Carrington MF, Kane K, et al. MHC class I chain-related protein A shedding in chronic HIV-1 infection is associated with profound NK cell dysfunction. Virology. 2010;406(1):12-20.
1124. Matusali G, Tchidjou HK, Pontrelli G, Bernardi S, D'Ettorre G, Vullo V, et al. Soluble ligands for the NKG2D receptor are released during HIV-1 infection and impair NKG2D expression and cytotoxicity of NK cells. FASEB J. 2013;27(6):2440-50.
1125. Tomaras GD, Yates NL, Liu P, Qin L, Fouda GG, Chavez LL, et al. Initial B-cell responses to transmitted human immunodeficiency virus type 1: virion-binding immunoglobulin M (IgM) and IgG antibodies followed by plasma anti-gp41 antibodies with ineffective control of initial viremia. J Virol. 2008;82(24):12449-63.
1126. Decker JM, Bibollet-Ruche F, Wei X, Wang S, Levy DN, Wang W, et al. Antigenic conservation and immunogenicity of the HIV coreceptor binding site. J Exp Med. 2005;201(9):1407-19.
1127. Robinson JE, Elliott DH, Martin EA, Micken K, Rosenberg ES. High frequencies of antibody responses to CD4 induced epitopes in HIV infected patients started on HAART during acute infection. Hum Antibodies. 2005;14(3-4):115-21.
1128. Davis KL, Gray ES, Moore PL, Decker JM, Salomon A, Montefiori DC, et al. High titer HIV-1 V3-specific antibodies with broad reactivity but low neutralizing potency in acute infection and following vaccination. Virology. 2009;387(2):414-26.
1129. Moore JP, Cao Y, Ho DD, Koup RA. Development of the anti-gp120 antibody response during seroconversion to human immunodeficiency virus type 1. J Virol. 1994;68(8):5142-55.
1130. Wei X, Decker JM, Wang S, Hui H, Kappes JC, Wu X, et al. Antibody neutralization and escape by HIV-1. Nature. 2003;422(6929):307-12.
1131. Richman DD, Wrin T, Little SJ, Petropoulos CJ. Rapid evolution of the neutralizing antibody response to HIV type 1 infection. Proc Natl Acad Sci U S A. 2003;100(7):4144-9.
1132. Frost SD, Wrin T, Smith DM, Kosakovsky Pond SL, Liu Y, Paxinos E, et al. Neutralizing antibody responses drive the evolution of human immunodeficiency virus type 1 envelope during recent HIV infection. Proc Natl Acad Sci U S A. 2005;102(51):18514-9.
1133. Gray ES, Moore PL, Choge IA, Decker JM, Bibollet-Ruche F, Li H, et al. Neutralizing antibody responses in acute human immunodeficiency virus type 1 subtype C infection. J Virol. 2007;81(12):6187-96.

1134. Rong R, Li B, Lynch RM, Haaland RE, Murphy MK, Mulenga J, et al. Escape from autologous neutralizing antibodies in acute/early subtype C HIV-1 infection requires multiple pathways. PLoS Pathog. 2009;5(9):e1000594.
1135. Moore PL, Ranchobe N, Lambson BE, Gray ES, Cave E, Abrahams MR, et al. Limited neutralizing antibody specificities drive neutralization escape in early HIV-1 subtype C infection. PLoS Pathog. 2009;5(9):e1000598.
1136. Gray ES, Moody MA, Wibmer CK, Chen X, Marshall D, Amos J, et al. Isolation of a monoclonal antibody that targets the alpha-2 helix of gp120 and represents the initial autologous neutralizing-antibody response in an HIV-1 subtype C-infected individual. J Virol. 2011;85(15):7719-29.
1137. Bar KJ, Tsao CY, Iyer SS, Decker JM, Yang Y, Bonsignori M, et al. Early low-titer neutralizing antibodies impede HIV-1 replication and select for virus escape. PLoS Pathog. 2012;8(5):e1002721.
1138. Moody MA, Gao F, Gurley TC, Amos JD, Kumar A, Hora B, et al. Strain-Specific V3 and CD4 Binding Site Autologous HIV-1 Neutralizing Antibodies Select Neutralization-Resistant Viruses. Cell Host Microbe. 2015;18(3):354-62.
1139. Ringe RP, Pugach P, Cottrell CA, LaBranche CC, Seabright GE, Ketas TJ, et al. Closing and Opening Holes in the Glycan Shield of HIV-1 Envelope Glycoprotein SOSIP Trimers Can Redirect the Neutralizing Antibody Response to the Newly Unmasked Epitopes. J Virol. 2019;93(4).
1140. Schorcht A, Cottrell CA, Pugach P, Ringe RP, Han AX, Allen JD, et al. The Glycan Hole Area of HIV-1 Envelope Trimers Contributes Prominently to the Induction of Autologous Neutralization. J Virol. 2022;96(1):e0155221.
1141. Moore PL, Gray ES, Wibmer CK, Bhiman JN, Nonyane M, Sheward DJ, et al. Evolution of an HIV glycan-dependent broadly neutralizing antibody epitope through immune escape. Nat Med. 2012;18(11):1688-92.
1142. Liao HX, Lynch R, Zhou T, Gao F, Alam SM, Boyd SD, et al. Co-evolution of a broadly neutralizing HIV-1 antibody and founder virus. Nature. 2013;496(7446):469-76.
1143. Doria-Rose NA, Schramm CA, Gorman J, Moore PL, Bhiman JN, DeKosky BJ, et al. Developmental pathway for potent V1V2-directed HIV-neutralizing antibodies. Nature. 2014;509(7498):55-62.
1144. Bhiman JN, Anthony C, Doria-Rose NA, Karimanzira O, Schramm CA, Khoza T, et al. Viral variants that initiate and drive maturation of V1V2-directed HIV-1 broadly neutralizing antibodies. Nat Med. 2015;21(11):1332-6.
1145. Bonsignori M, Zhou T, Sheng Z, Chen L, Gao F, Joyce MG, et al. Maturation Pathway from Germline to Broad HIV-1 Neutralizer of a CD4-Mimic Antibody. Cell. 2016;165(2):449-63.
1146. MacLeod DT, Choi NM, Briney B, Garces F, Ver LS, Landais E, et al. Early Antibody Lineage Diversification and Independent Limb Maturation Lead to Broad HIV-1 Neutralization Targeting the Env High-Mannose Patch. Immunity. 2016;44(5):1215-26.
1147. Hraber P, Seaman MS, Bailer RT, Mascola JR, Montefiori DC, Korber BT. Prevalence of broadly neutralizing antibody responses during chronic HIV-1 infection. AIDS. 2014;28(2):163-9.
1148. Landais E, Moore PL. Development of broadly neutralizing antibodies in HIV-1 infected elite neutralizers. Retrovirology. 2018;15(1):61.

1149. Alter G, Dowell KG, Brown EP, Suscovich TJ, Mikhailova A, Mahan AE, et al. High-resolution definition of humoral immune response correlates of effective immunity against HIV. Mol Syst Biol. 2018;14(3):e7881.
1150. Methot SP, Di Noia JM. Molecular Mechanisms of Somatic Hypermutation and Class Switch Recombination. Adv Immunol. 2017;133:37-87.
1151. Saphire EO, Parren PW, Pantophlet R, Zwick MB, Morris GM, Rudd PM, et al. Crystal structure of a neutralizing human IGG against HIV-1: a template for vaccine design. Science. 2001;293(5532):1155-9.
1152. Vidarsson G, Dekkers G, Rispens T. IgG subclasses and allotypes: from structure to effector functions. Front Immunol. 2014;5:520.
1153. Ugurlar D, Howes SC, de Kreuk BJ, Koning RI, de Jong RN, Beurskens FJ, et al. Structures of C1-IgG1 provide insights into how danger pattern recognition activates complement. Science. 2018;359(6377):794-7.
1154. Sondermann P, Huber R, Oosthuizen V, Jacob U. The 3.2-A crystal structure of the human IgG1 Fc fragment-Fc gammaRIII complex. Nature. 2000;406(6793):267-73.
1155. Subedi GP, Barb AW. The Structural Role of Antibody N-Glycosylation in Receptor Interactions. Structure. 2015;23(9):1573-83.
1156. Martin WL, West AP, Jr., Gan L, Bjorkman PJ. Crystal structure at 2.8 A of an FcRn/heterodimeric Fc complex: mechanism of pH-dependent binding. Mol Cell. 2001;7(4):867-77.
1157. Oganesyan V, Damschroder MM, Cook KE, Li Q, Gao C, Wu H, et al. Structural insights into neonatal Fc receptor-based recycling mechanisms. J Biol Chem. 2014;289(11):7812-24.
1158. Roux KH, Strelets L, Michaelsen TE. Flexibility of human IgG subclasses. J Immunol. 1997;159(7):3372-82.
1159. Chu TH, Crowley AR, Backes I, Chang C, Tay M, Broge T, et al. Hinge length contributes to the phagocytic activity of HIV-specific IgG1 and IgG3 antibodies. PLoS Pathog. 2020;16(2):e1008083.
1160. Seaman MS, Janes H, Hawkins N, Grandpre LE, Devoy C, Giri A, et al. Tiered categorization of a diverse panel of HIV-1 Env pseudoviruses for assessment of neutralizing antibodies. J Virol. 2010;84(3):1439-52.
1161. deCamp A, Hraber P, Bailer RT, Seaman MS, Ochsenbauer C, Kappes J, et al. Global panel of HIV-1 Env reference strains for standardized assessments of vaccine-elicited neutralizing antibodies. J Virol. 2014;88(5):2489-507.
1162. Cai Y, Karaca-Griffin S, Chen J, Tian S, Fredette N, Linton CE, et al. Antigenicity-defined conformations of an extremely neutralization-resistant HIV-1 envelope spike. Proc Natl Acad Sci U S A. 2017;114(17):4477-82.
1163. Frey G, Peng H, Rits-Volloch S, Morelli M, Cheng Y, Chen B. A fusion-intermediate state of HIV-1 gp41 targeted by broadly neutralizing antibodies. Proc Natl Acad Sci U S A. 2008;105(10):3739-44.
1164. Julien JP, Sok D, Khayat R, Lee JH, Doores KJ, Walker LM, et al. Broadly neutralizing antibody PGT121 allosterically modulates CD4 binding via recognition of the HIV-1 gp120 V3 base and multiple surrounding glycans. PLoS Pathog. 2013;9(5):e1003342.
1165. Derking R, Ozorowski G, Sliepen K, Yasmeen A, Cupo A, Torres JL, et al. Comprehensive antigenic map of a cleaved soluble HIV-1 envelope trimer. PLoS Pathog. 2015;11(3):e1004767.

1166. Burton DR, Pyati J, Koduri R, Sharp SJ, Thornton GB, Parren PW, et al. Efficient neutralization of primary isolates of HIV-1 by a recombinant human monoclonal antibody. Science. 1994;266(5187):1024-7.
1167. Wu X, Yang ZY, Li Y, Hogerkorp CM, Schief WR, Seaman MS, et al. Rational design of envelope identifies broadly neutralizing human monoclonal antibodies to HIV-1. Science. 2010;329(5993):856-61.
1168. Scheid JF, Mouquet H, Ueberheide B, Diskin R, Klein F, Oliveira TY, et al. Sequence and structural convergence of broad and potent HIV antibodies that mimic CD4 binding. Science. 2011;333(6049):1633-7.
1169. Huang J, Kang BH, Ishida E, Zhou T, Griesman T, Sheng Z, et al. Identification of a CD4-Binding-Site Antibody to HIV that Evolved Near-Pan Neutralization Breadth. Immunity. 2016;45(5):1108-21.
1170. Sajadi MM, Dashti A, Rikhtegaran Tehrani Z, Tolbert WD, Seaman MS, Ouyang X, et al. Identification of Near-Pan-neutralizing Antibodies against HIV-1 by Deconvolution of Plasma Humoral Responses. Cell. 2018;173(7):1783-95 e14.
1171. Schommers P, Gruell H, Abernathy ME, Tran MK, Dingens AS, Gristick HB, et al. Restriction of HIV-1 Escape by a Highly Broad and Potent Neutralizing Antibody. Cell. 2020;180(3):471-89 e22.
1172. Walker LM, Phogat SK, Chan-Hui PY, Wagner D, Phung P, Goss JL, et al. Broad and potent neutralizing antibodies from an African donor reveal a new HIV-1 vaccine target. Science. 2009;326(5950):285-9.
1173. Walker LM, Huber M, Doores KJ, Falkowska E, Pejchal R, Julien JP, et al. Broad neutralization coverage of HIV by multiple highly potent antibodies. Nature. 2011;477(7365):466-70.
1174. Sok D, van Gils MJ, Pauthner M, Julien JP, Saye-Francisco KL, Hsueh J, et al. Recombinant HIV envelope trimer selects for quaternary-dependent antibodies targeting the trimer apex. Proc Natl Acad Sci U S A. 2014;111(49):17624-9.
1175. Mouquet H, Scharf L, Euler Z, Liu Y, Eden C, Scheid JF, et al. Complex-type N-glycan recognition by potent broadly neutralizing HIV antibodies. Proc Natl Acad Sci U S A. 2012;109(47):E3268-77.
1176. Freund NT, Wang H, Scharf L, Nogueira L, Horwitz JA, Bar-On Y, et al. Coexistence of potent HIV-1 broadly neutralizing antibodies and antibody-sensitive viruses in a viremic controller. Sci Transl Med. 2017;9(373).
1177. Zhou T, Zheng A, Baxa U, Chuang GY, Georgiev IS, Kong R, et al. A Neutralizing Antibody Recognizing Primarily N-Linked Glycan Targets the Silent Face of the HIV Envelope. Immunity. 2018;48(3):500-13 e6.
1178. Schoofs T, Barnes CO, Suh-Toma N, Golijanin J, Schommers P, Gruell H, et al. Broad and Potent Neutralizing Antibodies Recognize the Silent Face of the HIV Envelope. Immunity. 2019;50(6):1513-29 e9.
1179. Huang J, Kang BH, Pancera M, Lee JH, Tong T, Feng Y, et al. Broad and potent HIV-1 neutralization by a human antibody that binds the gp41-gp120 interface. Nature. 2014.
1180. Falkowska E, Le KM, Ramos A, Doores KJ, Lee JH, Blattner C, et al. Broadly neutralizing HIV antibodies define a glycan-dependent epitope on the prefusion conformation of gp41 on cleaved envelope trimers. Immunity. 2014;40(5):657-68.
1181. Scharf L, Scheid JF, Lee JH, West AP, Jr., Chen C, Gao H, et al. Antibody 8ANC195 reveals a site of broad vulnerability on the HIV-1 envelope spike. Cell Rep. 2014;7(3):785-95.

1182. Kong R, Xu K, Zhou T, Acharya P, Lemmin T, Liu K, et al. Fusion peptide of HIV-1 as a site of vulnerability to neutralizing antibody. Science. 2016;352(6287):828-33.
1183. Chen YH, Susanna A, Steindl F, Katinger H, Dierich MP. HIV-1 gp41 shares a common immunologic determinant with normal human blood lymphocytes and monocytes. AIDS. 1994;8(1):130-1.
1184. Zwick MB, Labrijn AF, Wang M, Spenlehauer C, Saphire EO, Binley JM, et al. Broadly neutralizing antibodies targeted to the membrane-proximal external region of human immunodeficiency virus type 1 glycoprotein gp41. J Virol. 2001;75(22):10892-905.
1185. Huang J, Ofek G, Laub L, Louder MK, Doria-Rose NA, Longo NS, et al. Broad and potent neutralization of HIV-1 by a gp41-specific human antibody. Nature. 2012;491(7424):406-12.
1186. Pinto D, Fenwick C, Caillat C, Silacci C, Guseva S, Dehez F, et al. Structural Basis for Broad HIV-1 Neutralization by the MPER-Specific Human Broadly Neutralizing Antibody LN01. Cell Host Microbe. 2019;26(5):623-37 e8.
1187. Chan KW, Luo CC, Lu H, Wu X, Kong XP. A site of vulnerability at V3 crown defined by HIV-1 bNAb M4008_N1. Nat Commun. 2021;12(1):6464.
1188. Jia M, Liberatore RA, Guo Y, Chan KW, Pan R, Lu H, et al. VSV-Displayed HIV-1 Envelope Identifies Broadly Neutralizing Antibodies Class-Switched to IgG and IgA. Cell Host Microbe. 2020;27(6):963-75 e5.
1189. Deimel LP, Xue X, Sattentau QJ. Glycans in HIV-1 vaccine design - engaging the shield. Trends Microbiol. 2022.
1190. Chuang GY, Zhou J, Acharya P, Rawi R, Shen CH, Sheng Z, et al. Structural Survey of Broadly Neutralizing Antibodies Targeting the HIV-1 Env Trimer Delineates Epitope Categories and Characteristics of Recognition. Structure. 2019;27(1):196-206 e6.
1191. Haynes BF, Kelsoe G, Harrison SC, Kepler TB. B-cell-lineage immunogen design in vaccine development with HIV-1 as a case study. Nat Biotechnol. 2012;30(5):423-33.
1192. Lorin V, Fernandez I, Masse-Ranson G, Bouvin-Pley M, Molinos-Albert LM, Planchais C, et al. Epitope convergence of broadly HIV-1 neutralizing IgA and IgG antibody lineages in a viremic controller. J Exp Med. 2022;219(3).
1193. Rossignol ED, Dugast AS, Compere H, Cottrell CA, Copps J, Lin S, et al. Mining HIV controllers for broad and functional antibodies to recognize and eliminate HIV-infected cells. Cell Rep. 2021;35(8):109167.
1194. Medina-Ramirez M, Sanchez-Merino V, Sanchez-Palomino S, Merino-Mansilla A, Ferreira CB, Perez I, et al. Broadly cross-neutralizing antibodies in HIV-1 patients with undetectable viremia. J Virol. 2011;85(12):5804-13.
1195. Trkola A, Purtscher M, Muster T, Ballaun C, Buchacher A, Sullivan N, et al. Human monoclonal antibody 2G12 defines a distinctive neutralization epitope on the gp120 glycoprotein of human immunodeficiency virus type 1. J Virol. 1996;70(2):1100-8.
1196. Murin CD, Julien JP, Sok D, Stanfield RL, Khayat R, Cupo A, et al. Structure of 2G12 Fab2 in complex with soluble and fully glycosylated HIV-1 Env by negative-stain single-particle electron microscopy. J Virol. 2014;88(17):10177-88.
1197. Williams WB, Meyerhoff RR, Edwards RJ, Li H, Manne K, Nicely NI, et al. Fab-dimerized glycan-reactive antibodies are a structural category of natural antibodies. Cell. 2021;184(11):2955-72 e25.
1198. Horwitz JA, Halper-Stromberg A, Mouquet H, Gitlin AD, Tretiakova A, Eisenreich TR, et al. HIV-1 suppression and durable control by combining single broadly neutralizing antibodies and antiretroviral drugs in humanized mice. Proc Natl Acad Sci U S A. 2013;110(41):16538-43.

1199. Halper-Stromberg A, Lu CL, Klein F, Horwitz JA, Bournazos S, Nogueira L, et al. Broadly neutralizing antibodies and viral inducers decrease rebound from HIV-1 latent reservoirs in humanized mice. Cell. 2014;158(5):989-99.
1200. Nishimura Y, Gautam R, Chun TW, Sadjadpour R, Foulds KE, Shingai M, et al. Early antibody therapy can induce long-lasting immunity to SHIV. Nature. 2017;543(7646):559-63.
1201. Parsons MS, Lee WS, Kristensen AB, Amarasena T, Khoury G, Wheatley AK, et al. Fc-dependent functions are redundant to efficacy of anti-HIV antibody PGT121 in macaques. J Clin Invest. 2019;129(1):182-91.
1202. Klein F, Halper-Stromberg A, Horwitz JA, Gruell H, Scheid JF, Bournazos S, et al. HIV therapy by a combination of broadly neutralizing antibodies in humanized mice. Nature. 2012;492(7427):118-22.
1203. Barouch DH, Whitney JB, Moldt B, Klein F, Oliveira TY, Liu J, et al. Therapeutic efficacy of potent neutralizing HIV-1-specific monoclonal antibodies in SHIV-infected rhesus monkeys. Nature. 2013;503(7475):224-8.
1204. Shingai M, Nishimura Y, Klein F, Mouquet H, Donau OK, Plishka R, et al. Antibody-mediated immunotherapy of macaques chronically infected with SHIV suppresses viraemia. Nature. 2013;503(7475):277-80.
1205. Hessell AJ, Jaworski JP, Epson E, Matsuda K, Pandey S, Kahl C, et al. Early short-term treatment with neutralizing human monoclonal antibodies halts SHIV infection in infant macaques. Nat Med. 2016;22(4):362-8.
1206. Bolton DL, Pegu A, Wang K, McGinnis K, Nason M, Foulds K, et al. Human Immunodeficiency Virus Type 1 Monoclonal Antibodies Suppress Acute Simian-Human Immunodeficiency Virus Viremia and Limit Seeding of Cell-Associated Viral Reservoirs. J Virol. 2016;90(3):1321-32.
1207. Lynch RM, Boritz E, Coates EE, DeZure A, Madden P, Costner P, et al. Virologic effects of broadly neutralizing antibody VRC01 administration during chronic HIV-1 infection. Sci Transl Med. 2015;7(319):319ra206.
1208. Bar KJ, Sneller MC, Harrison LJ, Justement JS, Overton ET, Petrone ME, et al. Effect of HIV Antibody VRC01 on Viral Rebound after Treatment Interruption. N Engl J Med. 2016;375(21):2037-50.
1209. Caskey M, Klein F, Lorenzi JC, Seaman MS, West AP, Jr., Buckley N, et al. Viraemia suppressed in HIV-1-infected humans by broadly neutralizing antibody 3BNC117. Nature. 2015;522(7557):487-91.
1210. Scheid JF, Horwitz JA, Bar-On Y, Kreider EF, Lu CL, Lorenzi JC, et al. HIV-1 antibody 3BNC117 suppresses viral rebound in humans during treatment interruption. Nature. 2016;535(7613):556-60.
1211. Caskey M, Schoofs T, Gruell H, Settler A, Karagounis T, Kreider EF, et al. Antibody 10-1074 suppresses viremia in HIV-1-infected individuals. Nat Med. 2017;23(2):185-91.
1212. Mendoza P, Gruell H, Nogueira L, Pai JA, Butler AL, Millard K, et al. Combination therapy with anti-HIV-1 antibodies maintains viral suppression. Nature. 2018;561(7724):479-84.
1213. Bar-On Y, Gruell H, Schoofs T, Pai JA, Nogueira L, Butler AL, et al. Safety and antiviral activity of combination HIV-1 broadly neutralizing antibodies in viremic individuals. Nat Med. 2018;24(11):1701-7.
1214. Gaebler C, Nogueira L, Stoffel E, Oliveira TY, Breton G, Millard KG, et al. Prolonged viral suppression with anti-HIV-1 antibody therapy. Nature. 2022.

1215. Li M, Gao F, Mascola JR, Stamatatos L, Polonis VR, Koutsoukos M, et al. Human immunodeficiency virus type 1 env clones from acute and early subtype B infections for standardized assessments of vaccine-elicited neutralizing antibodies. J Virol. 2005;79(16):10108-25.
1216. Li M, Salazar-Gonzalez JF, Derdeyn CA, Morris L, Williamson C, Robinson JE, et al. Genetic and neutralization properties of subtype C human immunodeficiency virus type 1 molecular env clones from acute and early heterosexually acquired infections in Southern Africa. J Virol. 2006;80(23):11776-90.
1217. Wang H, Barnes CO, Yang Z, Nussenzweig MC, Bjorkman PJ. Partially Open HIV-1 Envelope Structures Exhibit Conformational Changes Relevant for Coreceptor Binding and Fusion. Cell Host Microbe. 2018;24(4):579-92 e4.
1218. Yang Z, Wang H, Liu AZ, Gristick HB, Bjorkman PJ. Asymmetric opening of HIV-1 Env bound to CD4 and a coreceptor-mimicking antibody. Nat Struct Mol Biol. 2019;26(12):1167-75.
1219. Stanfield RL, Gorny MK, Williams C, Zolla-Pazner S, Wilson IA. Structural rationale for the broad neutralization of HIV-1 by human monoclonal antibody 447-52D. Structure. 2004;12(2):193-204.
1220. Stanfield RL, Gorny MK, Zolla-Pazner S, Wilson IA. Crystal structures of human immunodeficiency virus type 1 (HIV-1) neutralizing antibody 2219 in complex with three different V3 peptides reveal a new binding mode for HIV-1 cross-reactivity. J Virol. 2006;80(12):6093-105.
1221. Jiang X, Burke V, Totrov M, Williams C, Cardozo T, Gorny MK, et al. Conserved structural elements in the V3 crown of HIV-1 gp120. Nat Struct Mol Biol. 2010;17(8):955-61.
1222. Liao HX, Bonsignori M, Alam SM, McLellan JS, Tomaras GD, Moody MA, et al. Vaccine Induction of Antibodies against a Structurally Heterogeneous Site of Immune Pressure within HIV-1 Envelope Protein Variable Regions 1 and 2. Immunity. 2013;38(1):176-86.
1223. Pan R, Gorny MK, Zolla-Pazner S, Kong XP. The V1V2 Region of HIV-1 gp120 Forms a Five-Stranded Beta Barrel. J Virol. 2015;89(15):8003-10.
1224. Wibmer CK, Richardson SI, Yolitz J, Cicala C, Arthos J, Moore PL, et al. Common helical V1V2 conformations of HIV-1 Envelope expose the alpha4beta7 binding site on intact virions. Nat Commun. 2018;9(1):4489.
1225. Huang CC, Tang M, Zhang MY, Majeed S, Montabana E, Stanfield RL, et al. Structure of a V3-containing HIV-1 gp120 core. Science. 2005;310(5750):1025-8.
1226. Kwon YD, LaLonde JM, Yang Y, Elban MA, Sugawara A, Courter JR, et al. Crystal structures of HIV-1 gp120 envelope glycoprotein in complex with NBD analogues that target the CD4-binding site. PLoS One. 2014;9(1):e85940.
1227. Tolbert WD, Sherburn R, Gohain N, Ding S, Flinko R, Orlandi C, et al. Defining rules governing recognition and Fc-mediated effector functions to the HIV-1 co-receptor binding site. BMC Biol. 2020;18(1):91.
1228. Acharya P, Tolbert WD, Gohain N, Wu X, Yu L, Liu T, et al. Structural Definition of an Antibody-Dependent Cellular Cytotoxicity Response Implicated in Reduced Risk for HIV-1 Infection. J Virol. 2014;88(21):12895-906.
1229. Gohain N, Tolbert WD, Acharya P, Yu L, Liu T, Zhao P, et al. Cocrystal Structures of Antibody N60-i3 and Antibody JR4 in Complex with gp120 Define More Cluster A Epitopes Involved in Effective Antibody-Dependent Effector Function against HIV-1. J Virol. 2015;89(17):8840-54.

1230. Tolbert WD, Gohain N, Veillette M, Chapleau JP, Orlandi C, Visciano ML, et al. Paring Down HIV Env: Design and Crystal Structure of a Stabilized Inner Domain of HIV-1 gp120 Displaying a Major ADCC Target of the A32 Region. Structure. 2016;24(5):697-709.
1231. Tolbert WD, Gohain N, Alsahafi N, Van V, Orlandi C, Ding S, et al. Targeting the Late Stage of HIV-1 Entry for Antibody-Dependent Cellular Cytotoxicity: Structural Basis for Env Epitopes in the C11 Region. Structure. 2017;25(11):1719-31 e4.
1232. Tolbert WD, Van V, Sherburn R, Tuyishime M, Yan F, Nguyen DN, et al. Recognition Patterns of the C1/C2 Epitopes Involved in Fc-Mediated Response in HIV-1 Natural Infection and the RV114 Vaccine Trial. mBio. 2020;11(3).
1233. Richard J, Nguyen DN, Tolbert WD, Gasser R, Ding S, Vezina D, et al. Across Functional Boundaries: Making Nonneutralizing Antibodies To Neutralize HIV-1 and Mediate Fc-Mediated Effector Killing of Infected Cells. mBio. 2021;12(5):e0140521.
1234. Santra S, Tomaras GD, Warrier R, Nicely NI, Liao HX, Pollara J, et al. Human Non-neutralizing HIV-1 Envelope Monoclonal Antibodies Limit the Number of Founder Viruses during SHIV Mucosal Infection in Rhesus Macaques. PLoS Pathog. 2015;11(8):e1005042.
1235. Gohain N, Tolbert WD, Orlandi C, Richard J, Ding S, Chen X, et al. Molecular basis for epitope recognition by non-neutralizing anti-gp41 antibody F240. Sci Rep. 2016;6:36685.
1236. Cook JD, Khondker A, Lee JE. Conformational plasticity of the HIV-1 gp41 immunodominant region is recognized by multiple non-neutralizing antibodies. Commun Biol. 2022;5(1):291.
1237. Frey G, Chen J, Rits-Volloch S, Freeman MM, Zolla-Pazner S, Chen B. Distinct conformational states of HIV-1 gp41 are recognized by neutralizing and non-neutralizing antibodies. Nat Struct Mol Biol. 2010;17(12):1486-91.
1238. Oh SK, Cruikshank WW, Raina J, Blanchard GC, Adler WH, Walker J, et al. Identification of HIV-1 envelope glycoprotein in the serum of AIDS and ARC patients. J Acquir Immune Defic Syndr. 1992;5(3):251-6.
1239. Santosuosso M, Righi E, Lindstrom V, Leblanc PR, Poznansky MC. HIV-1 envelope protein gp120 is present at high concentrations in secondary lymphoid organs of individuals with chronic HIV-1 infection. J Infect Dis. 2009;200(7):1050-3.
1240. Rychert J, Strick D, Bazner S, Robinson J, Rosenberg E. Detection of HIV gp120 in plasma during early HIV infection is associated with increased proinflammatory and immunoregulatory cytokines. AIDS Res Hum Retroviruses. 2010;26(10):1139-45.
1241. Bruel T, Guivel-Benhassine F, Lorin V, Lortat-Jacob H, Baleux F, Bourdic K, et al. Lack of ADCC breadth of human non-neutralizing anti-HIV-1 antibodies. J Virol. 2017.
1242. Horwitz JA, Bar-On Y, Lu CL, Fera D, Lockhart AAK, Lorenzi JCC, et al. Non-neutralizing Antibodies Alter the Course of HIV-1 Infection In Vivo. Cell. 2017;170(4):637-48 e10.
1243. Moore PL, Crooks ET, Porter L, Zhu P, Cayanan CS, Grise H, et al. Nature of nonfunctional envelope proteins on the surface of human immunodeficiency virus type 1. J Virol. 2006;80(5):2515-28.
1244. Eda Y, Murakami T, Ami Y, Nakasone T, Takizawa M, Someya K, et al. Anti-V3 humanized antibody KD-247 effectively suppresses ex vivo generation of human immunodeficiency virus type 1 and affords sterile protection of monkeys against a heterologous simian/human immunodeficiency virus infection. J Virol. 2006;80(11):5563-70.
1245. Burton DR, Hessell AJ, Keele BF, Klasse PJ, Ketas TA, Moldt B, et al. Limited or no protection by weakly or nonneutralizing antibodies against vaginal SHIV challenge of macaques

compared with a strongly neutralizing antibody. Proc Natl Acad Sci U S A. 2011;108(27):11181-6.
1246. Moog C, Dereuddre-Bosquet N, Teillaud JL, Biedma ME, Holl V, Van Ham G, et al. Protective effect of vaginal application of neutralizing and nonneutralizing inhibitory antibodies against vaginal SHIV challenge in macaques. Mucosal Immunol. 2014;7(1):46-56.
1247. Hessell AJ, Shapiro MB, Powell R, Malherbe DC, McBurney SP, Pandey S, et al. Reduced Cell-Associated DNA and Improved Viral Control in Macaques following Passive Transfer of a Single Anti-V2 Monoclonal Antibody and Repeated Simian/Human Immunodeficiency Virus Challenges. J Virol. 2018;92(11).
1248. Hioe CE, Li G, Liu X, Tsahouridis O, He X, Funaki M, et al. Non-neutralizing antibodies targeting the immunogenic regions of HIV-1 envelope reduce mucosal infection and virus burden in humanized mice. PLoS Pathog. 2022;18(1):e1010183.
1249. Gillis C, Gouel-Cheron A, Jonsson F, Bruhns P. Contribution of Human FcgammaRs to Disease with Evidence from Human Polymorphisms and Transgenic Animal Studies. Front Immunol. 2014;5:254.
1250. Duchemin AM, Ernst LK, Anderson CL. Clustering of the high affinity Fc receptor for immunoglobulin G (Fc gamma RI) results in phosphorylation of its associated gamma-chain. J Biol Chem. 1994;269(16):12111-7.
1251. Kern N, Dong R, Douglas SM, Vale RD, Morrissey MA. Tight nanoscale clustering of Fcgamma receptors using DNA origami promotes phagocytosis. Elife. 2021;10.
1252. Bruhns P, Iannascoli B, England P, Mancardi DA, Fernandez N, Jorieux S, et al. Specificity and affinity of human Fcgamma receptors and their polymorphic variants for human IgG subclasses. Blood. 2009;113(16):3716-25.
1253. Forthal DN, Gach JS, Landucci G, Jez J, Strasser R, Kunert R, et al. Fc-glycosylation influences Fcgamma receptor binding and cell-mediated anti-HIV activity of monoclonal antibody 2G12. J Immunol. 2010;185(11):6876-82.
1254. Moldt B, Shibata-Koyama M, Rakasz EG, Schultz N, Kanda Y, Dunlop DC, et al. A nonfucosylated variant of the anti-HIV-1 monoclonal antibody b12 has enhanced FcgammaRIIIa-mediated antiviral activity in vitro but does not improve protection against mucosal SHIV challenge in macaques. J Virol. 2012;86(11):6189-96.
1255. Loos A, Gach JS, Hackl T, Maresch D, Henkel T, Porodko A, et al. Glycan modulation and sulfoengineering of anti-HIV-1 monoclonal antibody PG9 in plants. Proc Natl Acad Sci U S A. 2015;112(41):12675-80.
1256. Anand SP, Ding S, Tolbert WD, Prevost J, Richard J, Gil HM, et al. Enhanced Ability of Plant-Derived PGT121 Glycovariants To Eliminate HIV-1-Infected Cells. J Virol. 2021;95(18):e0079621.
1257. Forthal DN, Landucci G, Bream J, Jacobson LP, Phan TB, Montoya B. FcgammaRIIa genotype predicts progression of HIV infection. J Immunol. 2007;179(11):7916-23.
1258. French MA, Tanaskovic S, Law MG, Lim A, Fernandez S, Ward LD, et al. Vaccine-induced IgG2 anti-HIV p24 is associated with control of HIV in patients with a 'high-affinity' FcgammaRIIa genotype. AIDS. 2010;24(13):1983-90.
1259. Li SS, Gilbert PB, Carpp LN, Pyo CW, Janes H, Fong Y, et al. Fc Gamma Receptor Polymorphisms Modulated the Vaccine Effect on HIV-1 Risk in the HVTN 505 HIV Vaccine Trial. J Virol. 2019;93(21).
1260. Forthal DN, Finzi A. Antibody-Dependent Cellular Cytotoxicity (ADCC) in HIV Infection. AIDS. 2018.

1261. Parsons MS, Richard J, Lee WS, Vanderven H, Grant MD, Finzi A, et al. NKG2D acts as a co-receptor for natural killer cell-mediated anti-HIV-1 antibody-dependent cellular cytotoxicity. AIDS Res Hum Retroviruses. 2016.
1262. Tay MZ, Wiehe K, Pollara J. Antibody-Dependent Cellular Phagocytosis in Antiviral Immune Responses. Front Immunol. 2019;10:332.
1263. Niessl J, Baxter AE, Mendoza P, Jankovic M, Cohen YZ, Butler AL, et al. Combination anti-HIV-1 antibody therapy is associated with increased virus-specific T cell immunity. Nat Med. 2020;26(2):222-7.
1264. Tay MZ, Liu P, Williams LD, McRaven MD, Sawant S, Gurley TC, et al. Antibody-Mediated Internalization of Infectious HIV-1 Virions Differs among Antibody Isotypes and Subclasses. PLoS Pathog. 2016;12(8):e1005817.
1265. Duchemin M, Khamassi M, Xu L, Tudor D, Bomsel M. IgA Targeting Human Immunodeficiency Virus-1 Envelope gp41 Triggers Antibody-Dependent Cellular Cytotoxicity Cross-Clade and Cooperates with gp41-Specific IgG to Increase Cell Lysis. Front Immunol. 2018;9:244.
1266. Lohse S, Loew S, Kretschmer A, Jansen JHM, Meyer S, Ten Broeke T, et al. Effector mechanisms of IgA antibodies against CD20 include recruitment of myeloid cells for antibody-dependent cell-mediated cytotoxicity and complement-dependent cytotoxicity. Br J Haematol. 2018;181(3):413-7.
1267. Duchemin M, Tudor D, Cottignies-Calamarte A, Bomsel M. Antibody-Dependent Cellular Phagocytosis of HIV-1-Infected Cells Is Efficiently Triggered by IgA Targeting HIV-1 Envelope Subunit gp41. Front Immunol. 2020;11:1141.
1268. Mellors J, Tipton T, Longet S, Carroll M. Viral Evasion of the Complement System and Its Importance for Vaccines and Therapeutics. Front Immunol. 2020;11:1450.
1269. Krishnan V, Xu Y, Macon K, Volanakis JE, Narayana SV. The crystal structure of C2a, the catalytic fragment of classical pathway C3 and C5 convertase of human complement. J Mol Biol. 2007;367(1):224-33.
1270. Janssen BJ, Christodoulidou A, McCarthy A, Lambris JD, Gros P. Structure of C3b reveals conformational changes that underlie complement activity. Nature. 2006;444(7116):213-6.
1271. Menny A, Serna M, Boyd CM, Gardner S, Joseph AP, Morgan BP, et al. CryoEM reveals how the complement membrane attack complex ruptures lipid bilayers. Nat Commun. 2018;9(1):5316.
1272. Harada R, Okada N, Fujita T, Okada H. Purification of 1F5 antigen that prevents complement attack on homologous cell membranes. J Immunol. 1990;144(5):1823-8.
1273. Schmitz J, Zimmer JP, Kluxen B, Aries S, Bogel M, Gigli I, et al. Antibody-dependent complement-mediated cytotoxicity in sera from patients with HIV-1 infection is controlled by CD55 and CD59. J Clin Invest. 1995;96(3):1520-6.
1274. Lan J, Yang K, Byrd D, Hu N, Amet T, Shepherd N, et al. Provirus activation plus CD59 blockage triggers antibody-dependent complement-mediated lysis of latently HIV-1-infected cells. J Immunol. 2014;193(7):3577-89.
1275. Yang K, Lan J, Shepherd N, Hu N, Xing Y, Byrd D, et al. Blockage of CD59 Function Restores Activities of Neutralizing and Nonneutralizing Antibodies in Triggering Antibody-Dependent Complement-Mediated Lysis of HIV-1 Virions and Provirus-Activated Latently Infected Cells. J Virol. 2015;89(18):9393-406.

1276. Dufloo J, Guivel-Benhassine F, Buchrieser J, Lorin V, Grzelak L, Dupouy E, et al. Anti-HIV-1 antibodies trigger non-lytic complement deposition on infected cells. EMBO Rep. 2020;21(2):e49351.
1277. Deeks SG, Archin N, Cannon P, Collins S, Jones RB, de Jong M, et al. Research priorities for an HIV cure: International AIDS Society Global Scientific Strategy 2021. Nat Med. 2021;27(12):2085-98.
1278. Eggers C, Arendt G, Hahn K, Husstedt IW, Maschke M, Neuen-Jacob E, et al. HIV-1-associated neurocognitive disorder: epidemiology, pathogenesis, diagnosis, and treatment. J Neurol. 2017;264(8):1715-27.
1279. Wensing AM, Calvez V, Ceccherini-Silberstein F, Charpentier C, Gunthard HF, Paredes R, et al. 2019 update of the drug resistance mutations in HIV-1. Top Antivir Med. 2019;27(3):111-21.
1280. Lederman MM, Funderburg NT, Sekaly RP, Klatt NR, Hunt PW. Residual immune dysregulation syndrome in treated HIV infection. Adv Immunol. 2013;119:51-83.
1281. FDA-Approved HIV Medicines Rockville, Maryland: National Institutes of Health; 2022 [Available from: https://hivinfo.nih.gov/understanding-hiv/fact-sheets/fda-approved-hiv-medicines.
1282. Arts EJ, Hazuda DJ. HIV-1 antiretroviral drug therapy. Cold Spring Harb Perspect Med. 2012;2(4):a007161.
1283. Bertoletti N, Chan AH, Schinazi RF, Yin YW, Anderson KS. Structural insights into the recognition of nucleoside reverse transcriptase inhibitors by HIV-1 reverse transcriptase: First crystal structures with reverse transcriptase and the active triphosphate forms of lamivudine and emtricitabine. Protein Sci. 2019;28(9):1664-75.
1284. Bertoletti N, Chan AH, Schinazi RF, Anderson KS. Post-Catalytic Complexes with Emtricitabine or Stavudine and HIV-1 Reverse Transcriptase Reveal New Mechanistic Insights for Nucleotide Incorporation and Drug Resistance. Molecules. 2020;25(20).
1285. Kohlstaedt LA, Wang J, Friedman JM, Rice PA, Steitz TA. Crystal structure at 3.5 A resolution of HIV-1 reverse transcriptase complexed with an inhibitor. Science. 1992;256(5065):1783-90.
1286. Ren J, Milton J, Weaver KL, Short SA, Stuart DI, Stammers DK. Structural basis for the resilience of efavirenz (DMP-266) to drug resistance mutations in HIV-1 reverse transcriptase. Structure. 2000;8(10):1089-94.
1287. Passos DO, Li M, Jozwik IK, Zhao XZ, Santos-Martins D, Yang R, et al. Structural basis for strand-transfer inhibitor binding to HIV intasomes. Science. 2020;367(6479):810-4.
1288. Cook NJ, Li W, Berta D, Badaoui M, Ballandras-Colas A, Nans A, et al. Structural basis of second-generation HIV integrase inhibitor action and viral resistance. Science. 2020;367(6479):806-10.
1289. Sharma A, Slaughter A, Jena N, Feng L, Kessl JJ, Fadel HJ, et al. A new class of multimerization selective inhibitors of HIV-1 integrase. PLoS Pathog. 2014;10(5):e1004171.
1290. Gupta K, Turkki V, Sherrill-Mix S, Hwang Y, Eilers G, Taylor L, et al. Structural Basis for Inhibitor-Induced Aggregation of HIV Integrase. PLoS Biol. 2016;14(12):e1002584.
1291. Koneru PC, Francis AC, Deng N, Rebensburg SV, Hoyte AC, Lindenberger J, et al. HIV-1 integrase tetramers are the antiviral target of pyridine-based allosteric integrase inhibitors. Elife. 2019;8.

1292. Maehigashi T, Ahn S, Kim UI, Lindenberger J, Oo A, Koneru PC, et al. A highly potent and safe pyrrolopyridine-based allosteric HIV-1 integrase inhibitor targeting host LEDGF/p75-integrase interaction site. PLoS Pathog. 2021;17(7):e1009671.
1293. Miller M, Schneider J, Sathyanarayana BK, Toth MV, Marshall GR, Clawson L, et al. Structure of complex of synthetic HIV-1 protease with a substrate-based inhibitor at 2.3 A resolution. Science. 1989;246(4934):1149-52.
1294. Tie Y, Boross PI, Wang YF, Gaddis L, Hussain AK, Leshchenko S, et al. High resolution crystal structures of HIV-1 protease with a potent non-peptide inhibitor (UIC-94017) active against multi-drug-resistant clinical strains. J Mol Biol. 2004;338(2):341-52.
1295. Blair WS, Cao J, Fok-Seang J, Griffin P, Isaacson J, Jackson RL, et al. New small-molecule inhibitor class targeting human immunodeficiency virus type 1 virion maturation. Antimicrob Agents Chemother. 2009;53(12):5080-7.
1296. Keller PW, Adamson CS, Heymann JB, Freed EO, Steven AC. HIV-1 maturation inhibitor bevirimat stabilizes the immature Gag lattice. J Virol. 2011;85(4):1420-8.
1297. Purdy MD, Shi D, Chrustowicz J, Hattne J, Gonen T, Yeager M. MicroED structures of HIV-1 Gag CTD-SP1 reveal binding interactions with the maturation inhibitor bevirimat. Proc Natl Acad Sci U S A. 2018;115(52):13258-63.
1298. Guidelines for the Use of Antiretroviral Agents in Adults and Adolescents Living with HIV Rockville, Maryland: National Institutes of Health; 2021 [Available from: https://clinicalinfo.hiv.gov/en/guidelines/adult-and-adolescent-arv/what-start-initial-combination-regimens-antiretroviral-naive?view=full.
1299. Xiao T, Cai Y, Chen B. HIV-1 Entry and Membrane Fusion Inhibitors. Viruses. 2021;13(5).
1300. Yant SR, Mulato A, Hansen D, Tse WC, Niedziela-Majka A, Zhang JR, et al. A highly potent long-acting small-molecule HIV-1 capsid inhibitor with efficacy in a humanized mouse model. Nat Med. 2019;25(9):1377-84.
1301. Bester SM, Wei G, Zhao H, Adu-Ampratwum D, Iqbal N, Courouble VV, et al. Structural and mechanistic bases for a potent HIV-1 capsid inhibitor. Science. 2020;370(6514):360-4.
1302. Vidal SJ, Bekerman E, Hansen D, Lu B, Wang K, Mwangi J, et al. Long-acting capsid inhibitor protects macaques from repeat SHIV challenges. Nature. 2022;601(7894):612-6.
1303. Selyutina A, Hu P, Miller S, Simons LM, Yu HJ, Hultquist JF, et al. GS-CA1 and lenacapavir stabilize the HIV-1 core and modulate the core interaction with cellular factors. iScience. 2022;25(1):103593.
1304. Link JO, Rhee MS, Tse WC, Zheng J, Somoza JR, Rowe W, et al. Clinical targeting of HIV capsid protein with a long-acting small molecule. Nature. 2020;584(7822):614-8.
1305. Khoury G, Ewart G, Luscombe C, Miller M, Wilkinson J. Antiviral efficacy of the novel compound BIT225 against HIV-1 release from human macrophages. Antimicrob Agents Chemother. 2010;54(2):835-45.
1306. Kuhl BD, Cheng V, Donahue DA, Sloan RD, Liang C, Wilkinson J, et al. The HIV-1 Vpu viroporin inhibitor BIT225 does not affect Vpu-mediated tetherin antagonism. PLoS One. 2011;6(11):e27660.
1307. Khoury G, Ewart G, Luscombe C, Miller M, Wilkinson J. The antiviral compound BIT225 inhibits HIV-1 replication in myeloid dendritic cells. AIDS Res Ther. 2016;13:7.
1308. Wilkinson J, Ewart G, Luscombe C, McBride K, Ratanasuwan W, Miller M, et al. A Phase 1b/2a study of the safety, pharmacokinetics and antiviral activity of BIT225 in patients with HIV-1 infection. J Antimicrob Chemother. 2016;71(3):731-8.

1309. Luscombe CA, Avihingsanon A, Supparatpinyo K, Gatechompol S, Han WM, Ewart GD, et al. Human Immunodeficiency Virus Type 1 Vpu Inhibitor, BIT225, in Combination with 3-Drug Antiretroviral Therapy: Inflammation and Immune Cell Modulation. J Infect Dis. 2021;223(11):1914-22.
1310. Kozal M, Aberg J, Pialoux G, Cahn P, Thompson M, Molina JM, et al. Fostemsavir in Adults with Multidrug-Resistant HIV-1 Infection. N Engl J Med. 2020;382(13):1232-43.
1311. Pancera M, Lai YT, Bylund T, Druz A, Narpala S, O'Dell S, et al. Crystal structures of trimeric HIV envelope with entry inhibitors BMS-378806 and BMS-626529. Nat Chem Biol. 2017;13(10):1115-22.
1312. Lin PF, Blair W, Wang T, Spicer T, Guo Q, Zhou N, et al. A small molecule HIV-1 inhibitor that targets the HIV-1 envelope and inhibits CD4 receptor binding. Proc Natl Acad Sci U S A. 2003;100(19):11013-8.
1313. Si Z, Madani N, Cox JM, Chruma JJ, Klein JC, Schon A, et al. Small-molecule inhibitors of HIV-1 entry block receptor-induced conformational changes in the viral envelope glycoproteins. Proc Natl Acad Sci U S A. 2004;101(14):5036-41.
1314. Ho HT, Fan L, Nowicka-Sans B, McAuliffe B, Li CB, Yamanaka G, et al. Envelope conformational changes induced by human immunodeficiency virus type 1 attachment inhibitors prevent CD4 binding and downstream entry events. J Virol. 2006;80(8):4017-25.
1315. Madani N, Princiotto AM, Schon A, LaLonde J, Feng Y, Freire E, et al. CD4-mimetic small molecules sensitize human immunodeficiency virus to vaccine-elicited antibodies. J Virol. 2014;88(12):6542-55.
1316. Richard J, Veillette M, Brassard N, Iyer SS, Roger M, Martin L, et al. CD4 mimetics sensitize HIV-1-infected cells to ADCC. Proc Natl Acad Sci U S A. 2015;112(20):E2687-94.
1317. Jette CA, Barnes CO, Kirk SM, Melillo B, Smith AB, 3rd, Bjorkman PJ. Cryo-EM structures of HIV-1 trimer bound to CD4-mimetics BNM-III-170 and M48U1 adopt a CD4-bound open conformation. Nat Commun. 2021;12(1):1950.
1318. Haim H, Si Z, Madani N, Wang L, Courter JR, Princiotto A, et al. Soluble CD4 and CD4-mimetic compounds inhibit HIV-1 infection by induction of a short-lived activated state. PLoS Pathog. 2009;5(4):e1000360.
1319. Selhorst P, Grupping K, Tong T, Crooks ET, Martin L, Vanham G, et al. M48U1 CD4 mimetic has a sustained inhibitory effect on cell-associated HIV-1 by attenuating virion infectivity through gp120 shedding. Retrovirology. 2013;10:12.
1320. Madani N, Princiotto AM, Zhao C, Jahanbakhshsefidi F, Mertens M, Herschhorn A, et al. Activation and Inactivation of Primary Human Immunodeficiency Virus Envelope Glycoprotein Trimers by CD4-Mimetic Compounds. J Virol. 2017;91(3).
1321. Madani N, Princiotto AM, Mach L, Ding S, Prevost J, Richard J, et al. A CD4-mimetic compound enhances vaccine efficacy against stringent immunodeficiency virus challenge. Nat Commun. 2018;9(1):2363.
1322. Princiotto AM, Vrbanac VD, Melillo B, Park J, Tager AM, Smith AB, III, et al. A Small-Molecule CD4-Mimetic Compound Protects Bone Marrow-Liver-Thymus Humanized Mice From HIV-1 Infection. J Infect Dis. 2018;218(3):471-5.
1323. Rajashekar JK, Richard J, Beloor J, Prevost J, Anand SP, Beaudoin-Bussieres G, et al. Modulating HIV-1 envelope glycoprotein conformation to decrease the HIV-1 reservoir. Cell Host Microbe. 2021;29(6):904-16 e6.
1324. Dereuddre-Bosquet N, Morellato-Castillo L, Brouwers J, Augustijns P, Bouchemal K, Ponchel G, et al. MiniCD4 microbicide prevents HIV infection of human mucosal explants and

vaginal transmission of SHIV(162P3) in cynomolgus macaques. PLoS Pathog. 2012;8(12):e1003071.
1325. Arien KK, Baleux F, Desjardins D, Porrot F, Coic YM, Michiels J, et al. CD4-mimetic sulfopeptide conjugates display sub-nanomolar anti-HIV-1 activity and protect macaques against a SHIV162P3 vaginal challenge. Sci Rep. 2016;6:34829.
1326. Acharya P, Luongo TS, Louder MK, McKee K, Yang Y, Kwon YD, et al. Structural basis for highly effective HIV-1 neutralization by CD4-mimetic miniproteins revealed by 1.5 A cocrystal structure of gp120 and M48U1. Structure. 2013;21(6):1018-29.
1327. Courter JR, Madani N, Sodroski J, Schon A, Freire E, Kwong PD, et al. Structure-based design, synthesis and validation of CD4-mimetic small molecule inhibitors of HIV-1 entry: conversion of a viral entry agonist to an antagonist. Acc Chem Res. 2014;47(4):1228-37.
1328. Melillo B, Liang S, Park J, Schon A, Courter JR, LaLonde JM, et al. Small-Molecule CD4-Mimics: Structure-Based Optimization of HIV-1 Entry Inhibition. ACS Med Chem Lett. 2016;7(3):330-4.
1329. Madani N, Schon A, Princiotto AM, Lalonde JM, Courter JR, Soeta T, et al. Small-molecule CD4 mimics interact with a highly conserved pocket on HIV-1 gp120. Structure. 2008;16(11):1689-701.
1330. Grupping K, Selhorst P, Michiels J, Vereecken K, Heyndrickx L, Kessler P, et al. MiniCD4 protein resistance mutations affect binding to the HIV-1 gp120 CD4 binding site and decrease entry efficiency. Retrovirology. 2012;9:36.
1331. Curreli F, Kwon YD, Zhang H, Yang Y, Scacalossi D, Kwong PD, et al. Binding mode characterization of NBD series CD4-mimetic HIV-1 entry inhibitors by X-ray structure and resistance study. Antimicrob Agents Chemother. 2014;58(9):5478-91.
1332. Madani N, Princiotto AM, Easterhoff D, Bradley T, Luo K, Williams WB, et al. Antibodies Elicited by Multiple Envelope Glycoprotein Immunogens in Primates Neutralize Primary Human Immunodeficiency Viruses (HIV-1) Sensitized by CD4-Mimetic Compounds. J Virol. 2016;90(10):5031-46.
1333. Schader SM, Colby-Germinario SP, Quashie PK, Oliveira M, Ibanescu RI, Moisi D, et al. HIV gp120 H375 is unique to HIV-1 subtype CRF01_AE and confers strong resistance to the entry inhibitor BMS-599793, a candidate microbicide drug. Antimicrob Agents Chemother. 2012;56(8):4257-67.
1334. Zoubchenok D, Veillette M, Prevost J, Sanders-Buell E, Wagh K, Korber B, et al. Histidine 375 Modulates CD4 Binding in HIV-1 CRF01_AE Envelope Glycoproteins. J Virol. 2017;91(4).
1335. Reimann KA, Lin W, Bixler S, Browning B, Ehrenfels BN, Lucci J, et al. A humanized form of a CD4-specific monoclonal antibody exhibits decreased antigenicity and prolonged plasma half-life in rhesus monkeys while retaining its unique biological and antiviral properties. AIDS Res Hum Retroviruses. 1997;13(11):933-43.
1336. Freeman MM, Seaman MS, Rits-Volloch S, Hong X, Kao CY, Ho DD, et al. Crystal structure of HIV-1 primary receptor CD4 in complex with a potent antiviral antibody. Structure. 2010;18(12):1632-41.
1337. Emu B, Fessel J, Schrader S, Kumar P, Richmond G, Win S, et al. Phase 3 Study of Ibalizumab for Multidrug-Resistant HIV-1. N Engl J Med. 2018;379(7):645-54.
1338. Gathe JC, Hardwicke RL, Garcia F, Weinheimer S, Lewis ST, Cash RB. Efficacy, Pharmacokinetics, and Safety Over 48 Weeks With Ibalizumab-Based Therapy in Treatment-Experienced Adults Infected With HIV-1: A Phase 2a Study. J Acquir Immune Defic Syndr. 2021;86(4):482-9.

1339. Dorr P, Westby M, Dobbs S, Griffin P, Irvine B, Macartney M, et al. Maraviroc (UK-427,857), a potent, orally bioavailable, and selective small-molecule inhibitor of chemokine receptor CCR5 with broad-spectrum anti-human immunodeficiency virus type 1 activity. Antimicrob Agents Chemother. 2005;49(11):4721-32.
1340. Westby M, Lewis M, Whitcomb J, Youle M, Pozniak AL, James IT, et al. Emergence of CXCR4-using human immunodeficiency virus type 1 (HIV-1) variants in a minority of HIV-1-infected patients following treatment with the CCR5 antagonist maraviroc is from a pretreatment CXCR4-using virus reservoir. J Virol. 2006;80(10):4909-20.
1341. Tan Q, Zhu Y, Li J, Chen Z, Han GW, Kufareva I, et al. Structure of the CCR5 chemokine receptor-HIV entry inhibitor maraviroc complex. Science. 2013;341(6152):1387-90.
1342. Donzella GA, Schols D, Lin SW, Este JA, Nagashima KA, Maddon PJ, et al. AMD3100, a small molecule inhibitor of HIV-1 entry via the CXCR4 co-receptor. Nat Med. 1998;4(1):72-7.
1343. Hendrix CW, Collier AC, Lederman MM, Schols D, Pollard RB, Brown S, et al. Safety, pharmacokinetics, and antiviral activity of AMD3100, a selective CXCR4 receptor inhibitor, in HIV-1 infection. J Acquir Immune Defic Syndr. 2004;37(2):1253-62.
1344. Dhody K, Pourhassan N, Kazempour K, Green D, Badri S, Mekonnen H, et al. PRO 140, a monoclonal antibody targeting CCR5, as a long-acting, single-agent maintenance therapy for HIV-1 infection. HIV Clin Trials. 2018;19(3):85-93.
1345. Chang XL, Reed JS, Webb GM, Wu HL, Le J, Bateman KB, et al. Suppression of human and simian immunodeficiency virus replication with the CCR5-specific antibody Leronlimab in two species. PLoS Pathog. 2022;18(3):e1010396.
1346. Jiang S, Lin K, Strick N, Neurath AR. HIV-1 inhibition by a peptide. Nature. 1993;365(6442):113.
1347. Kilby JM, Hopkins S, Venetta TM, DiMassimo B, Cloud GA, Lee JY, et al. Potent suppression of HIV-1 replication in humans by T-20, a peptide inhibitor of gp41-mediated virus entry. Nat Med. 1998;4(11):1302-7.
1348. Sista PR, Melby T, Davison D, Jin L, Mosier S, Mink M, et al. Characterization of determinants of genotypic and phenotypic resistance to enfuvirtide in baseline and on-treatment HIV-1 isolates. AIDS. 2004;18(13):1787-94.
1349. Poveda E, Rodes B, Labernardiere JL, Benito JM, Toro C, Gonzalez-Lahoz J, et al. Evolution of genotypic and phenotypic resistance to Enfuvirtide in HIV-infected patients experiencing prolonged virologic failure. J Med Virol. 2004;74(1):21-8.
1350. Poveda E, Rodes B, Lebel-Binay S, Faudon JL, Jimenez V, Soriano V. Dynamics of enfuvirtide resistance in HIV-infected patients during and after long-term enfuvirtide salvage therapy. J Clin Virol. 2005;34(4):295-301.
1351. Xie D, Yao C, Wang L, Min W, Xu J, Xiao J, et al. An albumin-conjugated peptide exhibits potent anti-HIV activity and long in vivo half-life. Antimicrob Agents Chemother. 2010;54(1):191-6.
1352. Su B, Yao C, Zhao QX, Cai WP, Wang M, Lu HZ, et al. Efficacy and safety of the long-acting fusion inhibitor albuvirtide in antiretroviral-experienced adults with human immunodeficiency virus-1: interim analysis of the randomized, controlled, phase 3, non-inferiority TALENT study. Chin Med J (Engl). 2020;133(24):2919-27.
1353. Xue J, Chong H, Zhu Y, Zhang J, Tong L, Lu J, et al. Efficient treatment and pre-exposure prophylaxis in rhesus macaques by an HIV fusion-inhibitory lipopeptide. Cell. 2022;185(1):131-44 e18.

1354. Catanzaro AT, Koup RA, Roederer M, Bailer RT, Enama ME, Moodie Z, et al. Phase 1 safety and immunogenicity evaluation of a multiclade HIV-1 candidate vaccine delivered by a replication-defective recombinant adenovirus vector. J Infect Dis. 2006;194(12):1638-49.
1355. Priddy FH, Brown D, Kublin J, Monahan K, Wright DP, Lalezari J, et al. Safety and immunogenicity of a replication-incompetent adenovirus type 5 HIV-1 clade B gag/pol/nef vaccine in healthy adults. Clin Infect Dis. 2008;46(11):1769-81.
1356. Duerr A, Huang Y, Buchbinder S, Coombs RW, Sanchez J, del Rio C, et al. Extended follow-up confirms early vaccine-enhanced risk of HIV acquisition and demonstrates waning effect over time among participants in a randomized trial of recombinant adenovirus HIV vaccine (Step Study). J Infect Dis. 2012;206(2):258-66.
1357. Hammer SM, Sobieszczyk ME, Janes H, Karuna ST, Mulligan MJ, Grove D, et al. Efficacy trial of a DNA/rAd5 HIV-1 preventive vaccine. N Engl J Med. 2013;369(22):2083-92.
1358. Robb ML, Rerks-Ngarm S, Nitayaphan S, Pitisuttithum P, Kaewkungwal J, Kunasol P, et al. Risk behaviour and time as covariates for efficacy of the HIV vaccine regimen ALVAC-HIV (vCP1521) and AIDSVAX B/E: a post-hoc analysis of the Thai phase 3 efficacy trial RV 144. Lancet Infect Dis. 2012;12(7):531-7.
1359. Haynes BF, Gilbert PB, McElrath MJ, Zolla-Pazner S, Tomaras GD, Alam SM, et al. Immune-correlates analysis of an HIV-1 vaccine efficacy trial. N Engl J Med. 2012;366(14):1275-86.
1360. Tomaras GD, Ferrari G, Shen X, Alam SM, Liao HX, Pollara J, et al. Vaccine-induced plasma IgA specific for the C1 region of the HIV-1 envelope blocks binding and effector function of IgG. Proc Natl Acad Sci U S A. 2013.
1361. Rerks-Ngarm S, Pitisuttithum P, Excler JL, Nitayaphan S, Kaewkungwal J, Premsri N, et al. Randomized, Double-Blind Evaluation of Late Boost Strategies for HIV-Uninfected Vaccine Recipients in the RV144 HIV Vaccine Efficacy Trial. J Infect Dis. 2017;215(8):1255-63.
1362. Pitisuttithum P, Nitayaphan S, Chariyalertsak S, Kaewkungwal J, Dawson P, Dhitavat J, et al. Late boosting of the RV144 regimen with AIDSVAX B/E and ALVAC-HIV in HIV-uninfected Thai volunteers: a double-blind, randomised controlled trial. Lancet HIV. 2020;7(4):e238-e48.
1363. Bekker LG, Moodie Z, Grunenberg N, Laher F, Tomaras GD, Cohen KW, et al. Subtype C ALVAC-HIV and bivalent subtype C gp120/MF59 HIV-1 vaccine in low-risk, HIV-uninfected, South African adults: a phase 1/2 trial. Lancet HIV. 2018;5(7):e366-e78.
1364. Gray GE, Bekker LG, Laher F, Malahleha M, Allen M, Moodie Z, et al. Vaccine Efficacy of ALVAC-HIV and Bivalent Subtype C gp120-MF59 in Adults. N Engl J Med. 2021;384(12):1089-100.
1365. Barouch DH, Tomaka FL, Wegmann F, Stieh DJ, Alter G, Robb ML, et al. Evaluation of a mosaic HIV-1 vaccine in a multicentre, randomised, double-blind, placebo-controlled, phase 1/2a clinical trial (APPROACH) and in rhesus monkeys (NHP 13-19). Lancet. 2018;392(10143):232-43.
1366. Stephenson KE, Wegmann F, Tomaka F, Walsh SR, Tan CS, Lavreys L, et al. Comparison of shortened mosaic HIV-1 vaccine schedules: a randomised, double-blind, placebo-controlled phase 1 trial (IPCAVD010/HPX1002) and a preclinical study in rhesus monkeys (NHP 17-22). Lancet HIV. 2020;7(6):e410-e21.
1367. Baden LR, Stieh DJ, Sarnecki M, Walsh SR, Tomaras GD, Kublin JG, et al. Safety and immunogenicity of two heterologous HIV vaccine regimens in healthy, HIV-uninfected adults (TRAVERSE): a randomised, parallel-group, placebo-controlled, double-blind, phase 1/2a study. Lancet HIV. 2020;7(10):e688-e98.

1368. HIV Vaccine Candidate Does Not Sufficiently Protect Women Against HIV Infection Rockville, Maryland: National Institutes of Health; 2021 [Available from: https://www.nih.gov/news-events/news-releases/hiv-vaccine-candidate-does-not-sufficiently-protect-women-against-hiv-infection.
1369. Pauthner MG, Nkolola JP, Havenar-Daughton C, Murrell B, Reiss SM, Bastidas R, et al. Vaccine-Induced Protection from Homologous Tier 2 SHIV Challenge in Nonhuman Primates Depends on Serum-Neutralizing Antibody Titers. Immunity. 2019;50(1):241-52 e6.
1370. Behrens AJ, Harvey DJ, Milne E, Cupo A, Kumar A, Zitzmann N, et al. Molecular Architecture of the Cleavage-Dependent Mannose Patch on a Soluble HIV-1 Envelope Glycoprotein Trimer. J Virol. 2017;91(2).
1371. Alsahafi N, Anand SP, Castillo-Menendez L, Verly MM, Medjahed H, Prevost J, et al. SOSIP Changes Affect Human Immunodeficiency Virus Type 1 Envelope Glycoprotein Conformation and CD4 Engagement. J Virol. 2018;92(19).
1372. Lu M, Ma X, Castillo-Menendez LR, Gorman J, Alsahafi N, Ermel U, et al. Associating HIV-1 envelope glycoprotein structures with states on the virus observed by smFRET. Nature. 2019.
1373. Alsahafi N, Debbeche O, Sodroski J, Finzi A. Effects of the I559P gp41 change on the conformation and function of the human immunodeficiency virus (HIV-1) membrane envelope glycoprotein trimer. PLoS One. 2015;10(4):e0122111.
1374. Sanders RW, Derking R, Cupo A, Julien JP, Yasmeen A, de Val N, et al. A next-generation cleaved, soluble HIV-1 Env Trimer, BG505 SOSIP.664 gp140, expresses multiple epitopes for broadly neutralizing but not non-neutralizing antibodies. PLoS Pathog. 2013;9(9):e1003618.
1375. Pauthner M, Havenar-Daughton C, Sok D, Nkolola JP, Bastidas R, Boopathy AV, et al. Elicitation of Robust Tier 2 Neutralizing Antibody Responses in Nonhuman Primates by HIV Envelope Trimer Immunization Using Optimized Approaches. Immunity. 2017;46(6):1073-88 e6.
1376. Corrigan AR, Duan H, Cheng C, Gonelli CA, Ou L, Xu K, et al. Fusion peptide priming reduces immune responses to HIV-1 envelope trimer base. Cell Rep. 2021;35(1):108937.
1377. Dosenovic P, von Boehmer L, Escolano A, Jardine J, Freund NT, Gitlin AD, et al. Immunization for HIV-1 Broadly Neutralizing Antibodies in Human Ig Knockin Mice. Cell. 2015;161(7):1505-15.
1378. Steichen JM, Kulp DW, Tokatlian T, Escolano A, Dosenovic P, Stanfield RL, et al. HIV Vaccine Design to Target Germline Precursors of Glycan-Dependent Broadly Neutralizing Antibodies. Immunity. 2016;45(3):483-96.
1379. Escolano A, Steichen JM, Dosenovic P, Kulp DW, Golijanin J, Sok D, et al. Sequential Immunization Elicits Broadly Neutralizing Anti-HIV-1 Antibodies in Ig Knockin Mice. Cell. 2016;166(6):1445-58 e12.
1380. Jardine JG, Kulp DW, Havenar-Daughton C, Sarkar A, Briney B, Sok D, et al. HIV-1 broadly neutralizing antibody precursor B cells revealed by germline-targeting immunogen. Science. 2016;351(6280):1458-63.
1381. Williams WB, Zhang J, Jiang C, Nicely NI, Fera D, Luo K, et al. Initiation of HIV neutralizing B cell lineages with sequential envelope immunizations. Nat Commun. 2017;8(1):1732.
1382. Bonsignori M, Liao HX, Gao F, Williams WB, Alam SM, Montefiori DC, et al. Antibody-virus co-evolution in HIV infection: paths for HIV vaccine development. Immunol Rev. 2017;275(1):145-60.

1383. Saunders KO, Wiehe K, Tian M, Acharya P, Bradley T, Alam SM, et al. Targeted selection of HIV-specific antibody mutations by engineering B cell maturation. Science. 2019;366(6470).
1384. Zhang P, Narayanan E, Liu Q, Tsybovsky Y, Boswell K, Ding S, et al. A multiclade env-gag VLP mRNA vaccine elicits tier-2 HIV-1-neutralizing antibodies and reduces the risk of heterologous SHIV infection in macaques. Nat Med. 2021;27(12):2234-45.
1385. Saunders KO, Pardi N, Parks R, Santra S, Mu Z, Sutherland L, et al. Lipid nanoparticle encapsulated nucleoside-modified mRNA vaccines elicit polyfunctional HIV-1 antibodies comparable to proteins in nonhuman primates. NPJ Vaccines. 2021;6(1):50.
1386. Mu Z, Wiehe K, Saunders KO, Henderson R, Cain DW, Parks R, et al. mRNA-encoded HIV-1 Env trimer ferritin nanoparticles induce monoclonal antibodies that neutralize heterologous HIV-1 isolates in mice. Cell Rep. 2022;38(11):110514.
1387. Dean M, Carrington M, Winkler C, Huttley GA, Smith MW, Allikmets R, et al. Genetic restriction of HIV-1 infection and progression to AIDS by a deletion allele of the CKR5 structural gene. Hemophilia Growth and Development Study, Multicenter AIDS Cohort Study, Multicenter Hemophilia Cohort Study, San Francisco City Cohort, ALIVE Study. Science. 1996;273(5283):1856-62.
1388. Samson M, Libert F, Doranz BJ, Rucker J, Liesnard C, Farber CM, et al. Resistance to HIV-1 infection in caucasian individuals bearing mutant alleles of the CCR-5 chemokine receptor gene. Nature. 1996;382(6593):722-5.
1389. Liu R, Paxton WA, Choe S, Ceradini D, Martin SR, Horuk R, et al. Homozygous defect in HIV-1 coreceptor accounts for resistance of some multiply-exposed individuals to HIV-1 infection. Cell. 1996;86(3):367-77.
1390. Huang Y, Paxton WA, Wolinsky SM, Neumann AU, Zhang L, He T, et al. The role of a mutant CCR5 allele in HIV-1 transmission and disease progression. Nat Med. 1996;2(11):1240-3.
1391. Kordelas L, Verheyen J, Beelen DW, Horn PA, Heinold A, Kaiser R, et al. Shift of HIV tropism in stem-cell transplantation with CCR5 Delta32 mutation. N Engl J Med. 2014;371(9):880-2.
1392. Tebas P, Stein D, Tang WW, Frank I, Wang SQ, Lee G, et al. Gene editing of CCR5 in autologous CD4 T cells of persons infected with HIV. N Engl J Med. 2014;370(10):901-10.
1393. Xu L, Wang J, Liu Y, Xie L, Su B, Mou D, et al. CRISPR-Edited Stem Cells in a Patient with HIV and Acute Lymphocytic Leukemia. N Engl J Med. 2019;381(13):1240-7.
1394. Bitnun A, Samson L, Chun TW, Kakkar F, Brophy J, Murray D, et al. Early initiation of combination antiretroviral therapy in HIV-1-infected newborns can achieve sustained virologic suppression with low frequency of CD4+ T cells carrying HIV in peripheral blood. Clin Infect Dis. 2014;59(7):1012-9.
1395. Buzon MJ, Martin-Gayo E, Pereyra F, Ouyang Z, Sun H, Li JZ, et al. Long-term antiretroviral treatment initiated at primary HIV-1 infection affects the size, composition, and decay kinetics of the reservoir of HIV-1-infected CD4 T cells. J Virol. 2014;88(17):10056-65.
1396. Massanella M, Puthanakit T, Leyre L, Jupimai T, Sawangsinth P, de Souza M, et al. Continuous Prophylactic Antiretrovirals/Antiretroviral Therapy Since Birth Reduces Seeding and Persistence of the Viral Reservoir in Children Vertically Infected With Human Immunodeficiency Virus. Clin Infect Dis. 2021;73(3):427-38.
1397. Persaud D, Gay H, Ziemniak C, Chen YH, Piatak M, Jr., Chun TW, et al. Absence of detectable HIV-1 viremia after treatment cessation in an infant. N Engl J Med. 2013;369(19):1828-35.

1398. Frange P, Faye A, Avettand-Fenoel V, Bellaton E, Descamps D, Angin M, et al. HIV-1 virological remission lasting more than 12 years after interruption of early antiretroviral therapy in a perinatally infected teenager enrolled in the French ANRS EPF-CO10 paediatric cohort: a case report. Lancet HIV. 2016;3(1):e49-54.
1399. Violari A, Cotton MF, Kuhn L, Schramm DB, Paximadis M, Loubser S, et al. A child with perinatal HIV infection and long-term sustained virological control following antiretroviral treatment cessation. Nat Commun. 2019;10(1):412.
1400. Namazi G, Fajnzylber JM, Aga E, Bosch RJ, Acosta EP, Sharaf R, et al. The Control of HIV After Antiretroviral Medication Pause (CHAMP) Study: Posttreatment Controllers Identified From 14 Clinical Studies. J Infect Dis. 2018;218(12):1954-63.
1401. Luzuriaga K, Gay H, Ziemniak C, Sanborn KB, Somasundaran M, Rainwater-Lovett K, et al. Viremic relapse after HIV-1 remission in a perinatally infected child. N Engl J Med. 2015;372(8):786-8.
1402. Khoury G, Kulpa DA, Parsons MS. Potential Utility of Natural Killer Cells for Eliminating Cells Harboring Reactivated Latent HIV-1 Following the Removal of CD8(+) T Cell-Mediated Pro-Latency Effect(s). Viruses. 2021;13(8).
1403. Archin NM, Espeseth A, Parker D, Cheema M, Hazuda D, Margolis DM. Expression of latent HIV induced by the potent HDAC inhibitor suberoylanilide hydroxamic acid. AIDS Res Hum Retroviruses. 2009;25(2):207-12.
1404. Rasmussen TA, Schmeltz Sogaard O, Brinkmann C, Wightman F, Lewin SR, Melchjorsen J, et al. Comparison of HDAC inhibitors in clinical development: effect on HIV production in latently infected cells and T-cell activation. Hum Vaccin Immunother. 2013;9(5):993-1001.
1405. Wei DG, Chiang V, Fyne E, Balakrishnan M, Barnes T, Graupe M, et al. Histone deacetylase inhibitor romidepsin induces HIV expression in CD4 T cells from patients on suppressive antiretroviral therapy at concentrations achieved by clinical dosing. PLoS Pathog. 2014;10(4):e1004071.
1406. Banerjee C, Archin N, Michaels D, Belkina AC, Denis GV, Bradner J, et al. BET bromodomain inhibition as a novel strategy for reactivation of HIV-1. J Leukoc Biol. 2012;92(6):1147-54.
1407. Warrilow D, Gardner J, Darnell GA, Suhrbier A, Harrich D. HIV type 1 inhibition by protein kinase C modulatory compounds. AIDS Res Hum Retroviruses. 2006;22(9):854-64.
1408. Mehla R, Bivalkar-Mehla S, Zhang R, Handy I, Albrecht H, Giri S, et al. Bryostatin modulates latent HIV-1 infection via PKC and AMPK signaling but inhibits acute infection in a receptor independent manner. PLoS One. 2010;5(6):e11160.
1409. Pache L, Dutra MS, Spivak AM, Marlett JM, Murry JP, Hwang Y, et al. BIRC2/cIAP1 Is a Negative Regulator of HIV-1 Transcription and Can Be Targeted by Smac Mimetics to Promote Reversal of Viral Latency. Cell Host Microbe. 2015;18(3):345-53.
1410. Offersen R, Nissen SK, Rasmussen TA, Ostergaard L, Denton PW, Sogaard OS, et al. A Novel Toll-Like Receptor 9 Agonist, MGN1703, Enhances HIV-1 Transcription and NK Cell-Mediated Inhibition of HIV-1-Infected Autologous CD4+ T Cells. J Virol. 2016;90(9):4441-53.
1411. Tsai A, Irrinki A, Kaur J, Cihlar T, Kukolj G, Sloan DD, et al. Toll-Like Receptor 7 Agonist GS-9620 Induces HIV Expression and HIV-Specific Immunity in Cells from HIV-Infected Individuals on Suppressive Antiretroviral Therapy. J Virol. 2017;91(8).
1412. Rochat MA, Schlaepfer E, Speck RF. Promising Role of Toll-Like Receptor 8 Agonist in Concert with Prostratin for Activation of Silent HIV. J Virol. 2017;91(4).

1413. Macedo AB, Novis CL, De Assis CM, Sorensen ES, Moszczynski P, Huang SH, et al. Dual TLR2 and TLR7 agonists as HIV latency-reversing agents. JCI Insight. 2018;3(19).
1414. Tomescu C, Chehimi J, Maino VC, Montaner LJ. NK cell lysis of HIV-1-infected autologous CD4 primary T cells: requirement for IFN-mediated NK activation by plasmacytoid dendritic cells. J Immunol. 2007;179(4):2097-104.
1415. Tomescu C, Mavilio D, Montaner LJ. Lysis of HIV-1-infected autologous CD4+ primary T cells by interferon-alpha-activated NK cells requires NKp46 and NKG2D. AIDS. 2015;29(14):1767-73.
1416. Seay K, Church C, Zheng JH, Deneroff K, Ochsenbauer C, Kappes JC, et al. In Vivo Activation of Human NK Cells by Treatment with an Interleukin-15 Superagonist Potently Inhibits Acute In Vivo HIV-1 Infection in Humanized Mice. J Virol. 2015;89(12):6264-74.
1417. Jones RB, Mueller S, O'Connor R, Rimpel K, Sloan DD, Karel D, et al. A Subset of Latency-Reversing Agents Expose HIV-Infected Resting CD4+ T-Cells to Recognition by Cytotoxic T-Lymphocytes. PLoS Pathog. 2016;12(4):e1005545.
1418. Liu B, Zhang W, Xia B, Jing S, Du Y, Zou F, et al. Broadly neutralizing antibody-derived CAR T cells reduce viral reservoir in individuals infected with HIV-1. J Clin Invest. 2021;131(19).
1419. Vansant G, Bruggemans A, Janssens J, Debyser Z. Block-And-Lock Strategies to Cure HIV Infection. Viruses. 2020;12(1).
1420. Suzuki K, Juelich T, Lim H, Ishida T, Watanebe T, Cooper DA, et al. Closed chromatin architecture is induced by an RNA duplex targeting the HIV-1 promoter region. J Biol Chem. 2008;283(34):23353-63.
1421. Mousseau G, Clementz MA, Bakeman WN, Nagarsheth N, Cameron M, Shi J, et al. An analog of the natural steroidal alkaloid cortistatin A potently suppresses Tat-dependent HIV transcription. Cell Host Microbe. 2012;12(1):97-108.
1422. Ahlenstiel C, Mendez C, Lim ST, Marks K, Turville S, Cooper DA, et al. Novel RNA Duplex Locks HIV-1 in a Latent State via Chromatin-mediated Transcriptional Silencing. Mol Ther Nucleic Acids. 2015;4:e261.
1423. Mousseau G, Kessing CF, Fromentin R, Trautmann L, Chomont N, Valente ST. The Tat Inhibitor Didehydro-Cortistatin A Prevents HIV-1 Reactivation from Latency. mBio. 2015;6(4):e00465.
1424. Vargas B, Giacobbi NS, Sanyal A, Venkatachari NJ, Han F, Gupta P, et al. Inhibitors of Signaling Pathways That Block Reversal of HIV-1 Latency. Antimicrob Agents Chemother. 2019;63(2).
1425. Li Z, Li W, Lu M, Bess J, Jr., Chao CW, Gorman J, et al. Subnanometer structures of HIV-1 envelope trimers on aldrithiol-2-inactivated virus particles. Nat Struct Mol Biol. 2020;27(8):726-34.
1426. Ferrari G, Pollara J, Kozink D, Harms T, Drinker M, Freel S, et al. An HIV-1 gp120 envelope human monoclonal antibody that recognizes a C1 conformational epitope mediates potent antibody-dependent cellular cytotoxicity (ADCC) activity and defines a common ADCC epitope in human HIV-1 serum. J Virol. 2011;85(14):7029-36.
1427. Bonsignori M, Pollara J, Moody MA, Alpert MD, Chen X, Hwang KK, et al. Antibody-Dependent Cellular Cytotoxicity-Mediating Antibodies from an HIV-1 Vaccine Efficacy Trial Target Multiple Epitopes and Preferentially Use the VH1 Gene Family. J Virol. 2012;86(21):11521-32.

1428. Guan Y, Pazgier M, Sajadi MM, Kamin-Lewis R, Al-Darmarki S, Flinko R, et al. Diverse specificity and effector function among human antibodies to HIV-1 envelope glycoprotein epitopes exposed by CD4 binding. Proc Natl Acad Sci U S A. 2013;110(1):E69-78.
1429. Pollara J, Bonsignori M, Moody MA, Liu P, Alam SM, Hwang KK, et al. HIV-1 vaccine-induced C1 and V2 Env-specific antibodies synergize for increased antiviral activities. J Virol. 2014;88(14):7715-26.
1430. Williams KL, Cortez V, Dingens AS, Gach JS, Rainwater S, Weis JF, et al. HIV-specific CD4-induced Antibodies Mediate Broad and Potent Antibody-dependent Cellular Cytotoxicity Activity and are Commonly Detected in Plasma from HIV-infected Humans. EBioMedicine. 2015;2(10):1464-77.
1431. Huang Y, Ferrari G, Alter G, Forthal DN, Kappes JC, Lewis GK, et al. Diversity of Antiviral IgG Effector Activities Observed in HIV-Infected and Vaccinated Subjects. J Immunol. 2016;197(12):4603-12.
1432. Orlandi C, Flinko R, Lewis GK. A new cell line for high throughput HIV-specific antibody-dependent cellular cytotoxicity (ADCC) and cell-to-cell virus transmission studies. J Immunol Methods. 2016;433:51-8.
1433. Bradley T, Pollara J, Santra S, Vandergrift N, Pittala S, Bailey-Kellogg C, et al. Pentavalent HIV-1 vaccine protects against simian-human immunodeficiency virus challenge. Nat Commun. 2017;8:15711.
1434. Ding S, Veillette M, Coutu M, Prevost J, Scharf L, Bjorkman PJ, et al. A Highly Conserved Residue of the HIV-1 gp120 Inner Domain Is Important for Antibody-Dependent Cellular Cytotoxicity Responses Mediated by Anti-cluster A Antibodies. J Virol. 2016;90(4):2127-34.
1435. von Bredow B, Arias JF, Heyer LN, Moldt B, Le K, Robinson JE, et al. Comparison of Antibody-Dependent Cell-Mediated Cytotoxicity and Virus Neutralization by HIV-1 Env-Specific Monoclonal Antibodies. J Virol. 2016;90(13):6127-39.
1436. Williams KL, Stumpf M, Naiman NE, Ding S, Garrett M, Gobillot T, et al. Identification of HIV gp41-specific antibodies that mediate killing of infected cells. PLoS Pathog. 2019;15(2):e1007572.
1437. Dugast AS, Chan Y, Hoffner M, Licht A, Nkolola J, Li H, et al. Lack of protection following passive transfer of polyclonal highly functional low-dose non-neutralizing antibodies. PLoS One. 2014;9(5):e97229.
1438. Mayr LM, Decoville T, Schmidt S, Laumond G, Klingler J, Ducloy C, et al. Non-neutralizing Antibodies Targeting the V1V2 Domain of HIV Exhibit Strong Antibody-Dependent Cell-mediated Cytotoxic Activity. Sci Rep. 2017;7(1):12655.
1439. Gartner S, Markovits P, Markovitz DM, Kaplan MH, Gallo RC, Popovic M. The role of mononuclear phagocytes in HTLV-III/LAV infection. Science. 1986;233(4760):215-9.
1440. Adachi A, Gendelman HE, Koenig S, Folks T, Willey R, Rabson A, et al. Production of acquired immunodeficiency syndrome-associated retrovirus in human and nonhuman cells transfected with an infectious molecular clone. J Virol. 1986;59(2):284-91.
1441. Cheng-Mayer C, Weiss C, Seto D, Levy JA. Isolates of human immunodeficiency virus type 1 from the brain may constitute a special group of the AIDS virus. Proc Natl Acad Sci U S A. 1989;86(21):8575-9.
1442. Collman R, Balliet JW, Gregory SA, Friedman H, Kolson DL, Nathanson N, et al. An infectious molecular clone of an unusual macrophage-tropic and highly cytopathic strain of human immunodeficiency virus type 1. J Virol. 1992;66(12):7517-21.

1443. Li Y, Kappes JC, Conway JA, Price RW, Shaw GM, Hahn BH. Molecular characterization of human immunodeficiency virus type 1 cloned directly from uncultured human brain tissue: identification of replication-competent and -defective viral genomes. J Virol. 1991;65(8):3973-85.
1444. Theodore TS, Englund G, Buckler-White A, Buckler CE, Martin MA, Peden KW. Construction and characterization of a stable full-length macrophage-tropic HIV type 1 molecular clone that directs the production of high titers of progeny virions. AIDS Res Hum Retroviruses. 1996;12(3):191-4.
1445. Pickering S, Hue S, Kim EY, Reddy S, Wolinsky SM, Neil SJ. Preservation of Tetherin and CD4 Counter-Activities in Circulating Vpu Alleles despite Extensive Sequence Variation within HIV-1 Infected Individuals. PLoS Pathog. 2014;10(1):e1003895.
1446. Chen J, Tibroni N, Sauter D, Galaski J, Miura T, Alter G, et al. Modest attenuation of HIV-1 Vpu alleles derived from elite controller plasma. PLoS One. 2015;10(3):e0120434.
1447. Zhang P, Kwon AL, Guzzo C, Liu Q, Schmeisser H, Miao H, et al. Functional Anatomy of the Trimer Apex Reveals Key Hydrophobic Constraints That Maintain the HIV-1 Envelope Spike in a Closed State. mBio. 2021;12(2).
1448. Kolchinsky P, Kiprilov E, Bartley P, Rubinstein R, Sodroski J. Loss of a single N-linked glycan allows CD4-independent human immunodeficiency virus type 1 infection by altering the position of the gp120 V1/V2 variable loops. J Virol. 2001;75(7):3435-43.
1449. Li Y, Cleveland B, Klots I, Travis B, Richardson BA, Anderson D, et al. Removal of a single N-linked glycan in human immunodeficiency virus type 1 gp120 results in an enhanced ability to induce neutralizing antibody responses. J Virol. 2008;82(2):638-51.
1450. Huang X, Jin W, Hu K, Luo S, Du T, Griffin GE, et al. Highly conserved HIV-1 gp120 glycans proximal to CD4-binding region affect viral infectivity and neutralizing antibody induction. Virology. 2012;423(1):97-106.
1451. Liang Y, Guttman M, Williams JA, Verkerke H, Alvarado D, Hu SL, et al. Changes in Structure and Antigenicity of HIV-1 Env Trimers Resulting from Removal of a Conserved CD4 Binding Site-Proximal Glycan. J Virol. 2016;90(20):9224-36.
1452. Herschhorn A, Ma X, Gu C, Ventura JD, Castillo-Menendez L, Melillo B, et al. Release of gp120 Restraints Leads to an Entry-Competent Intermediate State of the HIV-1 Envelope Glycoproteins. MBio. 2016;7(5).
1453. Herschhorn A, Gu C, Moraca F, Ma X, Farrell M, Smith AB, 3rd, et al. The beta20-beta21 of gp120 is a regulatory switch for HIV-1 Env conformational transitions. Nat Commun. 2017;8(1):1049.
1454. Yu X, Yuan X, McLane MF, Lee TH, Essex M. Mutations in the cytoplasmic domain of human immunodeficiency virus type 1 transmembrane protein impair the incorporation of Env proteins into mature virions. J Virol. 1993;67(1):213-21.
1455. Rowell JF, Stanhope PE, Siliciano RF. Endocytosis of endogenously synthesized HIV-1 envelope protein. Mechanism and role in processing for association with class II MHC. J Immunol. 1995;155(1):473-88.
1456. Postler TS, Desrosiers RC. The tale of the long tail: the cytoplasmic domain of HIV-1 gp41. J Virol. 2013;87(1):2-15.
1457. Chen J, Kovacs JM, Peng H, Rits-Volloch S, Lu J, Park D, et al. HIV-1 ENVELOPE. Effect of the cytoplasmic domain on antigenic characteristics of HIV-1 envelope glycoprotein. Science. 2015;349(6244):191-5.

1458. Samal S, Das S, Boliar S, Qureshi H, Shrivastava T, Kumar N, et al. Cell surface ectodomain integrity of a subset of functional HIV-1 envelopes is dependent on a conserved hydrophilic domain containing region in their C-terminal tail. Retrovirology. 2018;15(1):50.
1459. McAndrew EG, Dugast AS, Licht AF, Eusebio JR, Alter G, Ackerman ME. Determining the phagocytic activity of clinical antibody samples. J Vis Exp. 2011(57):e3588.
1460. Sattentau QJ. Envelope Glycoprotein Trimers as HIV-1 Vaccine Immunogens. Vaccines (Basel). 2013;1(4):497-512.
1461. Crooks ET, Tong T, Osawa K, Binley JM. Enzyme digests eliminate nonfunctional Env from HIV-1 particle surfaces, leaving native Env trimers intact and viral infectivity unaffected. J Virol. 2011;85(12):5825-39.
1462. Ringe RP, Sanders RW, Yasmeen A, Kim HJ, Lee JH, Cupo A, et al. Cleavage strongly influences whether soluble HIV-1 envelope glycoprotein trimers adopt a native-like conformation. Proc Natl Acad Sci U S A. 2013;110(45):18256-61.
1463. Musich T, Li L, Liu L, Zolla-Pazner S, Robert-Guroff M, Gorny MK. Monoclonal Antibodies Specific for the V2, V3, CD4-Binding Site, and gp41 of HIV-1 Mediate Phagocytosis in a Dose-Dependent Manner. J Virol. 2017;91(8).
1464. Oldenborg PA, Zheleznyak A, Fang YF, Lagenaur CF, Gresham HD, Lindberg FP. Role of CD47 as a marker of self on red blood cells. Science. 2000;288(5473):2051-4.
1465. Tsao LC, Crosby EJ, Trotter TN, Agarwal P, Hwang BJ, Acharya C, et al. CD47 blockade augmentation of trastuzumab antitumor efficacy dependent on antibody-dependent cellular phagocytosis. JCI Insight. 2019;4(24).
1466. Cham LB, Torrez Dulgeroff LB, Tal MC, Adomati T, Li F, Bhat H, et al. Immunotherapeutic Blockade of CD47 Inhibitory Signaling Enhances Innate and Adaptive Immune Responses to Viral Infection. Cell Rep. 2020;31(2):107494.
1467. Cong L, Sugden SM, Leclair P, Lim CJ, Pham TNQ, Cohen EA. HIV-1 Vpu Promotes Phagocytosis of Infected CD4(+) T Cells by Macrophages through Downregulation of CD47. mBio. 2021;12(4):e0192021.
1468. Gach JS, Bouzin M, Wong MP, Chromikova V, Gorlani A, Yu KT, et al. Human immunodeficiency virus type-1 (HIV-1) evades antibody-dependent phagocytosis. PLoS Pathog. 2017;13(12):e1006793.
1469. Hessell AJ, Hangartner L, Hunter M, Havenith CE, Beurskens FJ, Bakker JM, et al. Fc receptor but not complement binding is important in antibody protection against HIV. Nature. 2007;449(7158):101-4.
1470. Spencer DA, Goldberg BS, Pandey S, Ordonez T, Dufloo J, Barnette P, et al. Phagocytosis by an HIV antibody is associated with reduced viremia irrespective of enhanced complement lysis. Nat Commun. 2022;13(1):662.
1471. Ferrari G, Haynes BF, Koenig S, Nordstrom JL, Margolis DM, Tomaras GD. Envelope-specific antibodies and antibody-derived molecules for treating and curing HIV infection. Nat Rev Drug Discov. 2016;15(12):823-34.
1472. Dashti A, Waller C, Mavigner M, Schoof N, Bar KJ, Shaw GM, et al. SMAC Mimetic Plus Triple-Combination Bispecific HIVxCD3 Retargeting Molecules in SHIV.C.CH505-Infected, Antiretroviral Therapy-Suppressed Rhesus Macaques. J Virol. 2020;94(21).
1473. Pollara J, Edwards RW, Jha S, Lam CK, Liu L, Diedrich G, et al. Redirection of Cord Blood T Cells and Natural Killer Cells for Elimination of Autologous HIV-1-Infected Target Cells Using Bispecific DART(R) Molecules. Front Immunol. 2020;11:713.

1474. Tuyishime M, Dashti A, Faircloth K, Jha S, Nordstrom JL, Haynes BF, et al. Elimination of SHIV Infected Cells by Combinations of Bispecific HIVxCD3 DART((R)) Molecules. Front Immunol. 2021;12:710273.
1475. Sung JA, Pickeral J, Liu L, Stanfield-Oakley SA, Lam CK, Garrido C, et al. Dual-Affinity Re-Targeting proteins direct T cell-mediated cytolysis of latently HIV-infected cells. J Clin Invest. 2015.
1476. Sloan DD, Lam CY, Irrinki A, Liu L, Tsai A, Pace CS, et al. Targeting HIV Reservoir in Infected CD4 T Cells by Dual-Affinity Re-targeting Molecules (DARTs) that Bind HIV Envelope and Recruit Cytotoxic T Cells. PLoS Pathog. 2015;11(11):e1005233.
1477. Alberti MO, Jones JJ, Miglietta R, Ding H, Bakshi RK, Edmonds TG, et al. Optimized Replicating Renilla Luciferase Reporter HIV-1 Utilizing Novel Internal Ribosome Entry Site Elements for Native Nef Expression and Function. AIDS Res Hum Retroviruses. 2015;31(12):1278-96.
1478. Bauer S, Groh V, Wu J, Steinle A, Phillips JH, Lanier LL, et al. Activation of NK cells and T cells by NKG2D, a receptor for stress-inducible MICA. Science. 1999;285(5428):727-9.
1479. Prajapati K, Perez C, Rojas LBP, Burke B, Guevara-Patino JA. Functions of NKG2D in CD8(+) T cells: an opportunity for immunotherapy. Cell Mol Immunol. 2018;15(5):470-9.
1480. Delaugerre C, De Oliveira F, Lascoux-Combe C, Plantier JC, Simon F. HIV-1 group N: travelling beyond Cameroon. Lancet. 2011;378(9806):1894.
1481. Bush S, Tebit DM. HIV-1 Group O Origin, Evolution, Pathogenesis, and Treatment: Unraveling the Complexity of an Outlier 25 Years Later. AIDS Rev. 2015;17(3):147-58.
1482. Alessandri-Gradt E, De Oliveira F, Leoz M, Lemee V, Robertson DL, Feyertag F, et al. HIV-1 group P infection: towards a dead-end infection? AIDS. 2018;32(10):1317-22.
1483. Mielke D, Bandawe G, Zheng J, Jones J, Abrahams MR, Bekker V, et al. ADCC-mediating non-neutralizing antibodies can exert immune pressure in early HIV-1 infection. PLoS Pathog. 2021;17(11):e1010046.
1484. Sato K, Misawa N, Takeuchi JS, Kobayashi T, Izumi T, Aso H, et al. Experimental Adaptive Evolution of Simian Immunodeficiency Virus SIVcpz to Pandemic Human Immunodeficiency Virus Type 1 by Using a Humanized Mouse Model. J Virol. 2018;92(4).
1485. Peng X, Pan J, Gong R, Liu Y, Kang S, Feng H, et al. Functional characterization of syncytin-A, a newly murine endogenous virus envelope protein. Implication for its fusion mechanism. J Biol Chem. 2007;282(1):381-9.
1486. Albritton LM. Chapter 1 - Retrovirus Receptor Interactions and Entry. 2018:1-49.
1487. Evans DT, Tillman KC, Desrosiers RC. Envelope glycoprotein cytoplasmic domains from diverse lentiviruses interact with the prenylated Rab acceptor. J Virol. 2002;76(1):327-37.
1488. Santos da Silva E, Mulinge M, Perez Bercoff D. The frantic play of the concealed HIV envelope cytoplasmic tail. Retrovirology. 2013;10:54.
1489. Bibollet-Ruche F, Russell RM, Liu W, Stewart-Jones GBE, Sherrill-Mix S, Li Y, et al. CD4 receptor diversity in chimpanzees protects against SIV infection. Proc Natl Acad Sci U S A. 2019;116(8):3229-38.
1490. Warren CJ, Meyerson NR, Stabell AC, Fattor WT, Wilkerson GK, Sawyer SL. A glycan shield on chimpanzee CD4 protects against infection by primate lentiviruses (HIV/SIV). Proc Natl Acad Sci U S A. 2019;116(23):11460-9.
1491. Russell RM, Bibollet-Ruche F, Liu W, Sherrill-Mix S, Li Y, Connell J, et al. CD4 receptor diversity represents an ancient protection mechanism against primate lentiviruses. Proc Natl Acad Sci U S A. 2021;118(13).

1492. Ng OT, Lin L, Laeyendecker O, Quinn TC, Sun YJ, Lee CC, et al. Increased rate of CD4+ T-cell decline and faster time to antiretroviral therapy in HIV-1 subtype CRF01_AE infected seroconverters in Singapore. PLoS One. 2011;6(1):e15738.
1493. Li X, Xue Y, Zhou L, Lin Y, Yu X, Wang X, et al. Evidence that HIV-1 CRF01_AE is associated with low CD4+T cell count and CXCR4 co-receptor usage in recently infected young men who have sex with men (MSM) in Shanghai, China. PLoS One. 2014;9(2):e89462.
1494. Joshi A, Cox EK, Sedano MJ, Punke EB, Lee RT, Maurer-Stroh S, et al. HIV-1 subtype CRF01_AE and B differ in utilization of low levels of CCR5, Maraviroc susceptibility and potential N-glycosylation sites. Virology. 2017;512:222-33.
1495. Song H, Ou W, Feng Y, Zhang J, Li F, Hu J, et al. Rapid CD4 cell loss is caused by specific CRF01_AE cluster with V3 signatures favoring CXCR4 usage. bioRxiv. 2018.
1496. Sauter D, Hue S, Petit SJ, Plantier JC, Towers GJ, Kirchhoff F, et al. HIV-1 Group P is unable to antagonize human tetherin by Vpu, Env or Nef. Retrovirology. 2011;8:103.
1497. Lim ES, Malik HS, Emerman M. Ancient adaptive evolution of tetherin shaped the functions of Vpu and Nef in human immunodeficiency virus and primate lentiviruses. J Virol. 2010;84(14):7124-34.
1498. Yang SJ, Lopez LA, Hauser H, Exline CM, Haworth KG, Cannon PM. Anti-tetherin activities in Vpu-expressing primate lentiviruses. Retrovirology. 2010;7:13.
1499. Yang SJ, Lopez LA, Exline CM, Haworth KG, Cannon PM. Lack of adaptation to human tetherin in HIV-1 group O and P. Retrovirology. 2011;8:78.
1500. Sauter D, Unterweger D, Vogl M, Usmani SM, Heigele A, Kluge SF, et al. Human tetherin exerts strong selection pressure on the HIV-1 group N Vpu protein. PLoS Pathog. 2012;8(12):e1003093.
1501. Kluge SF, Mack K, Iyer SS, Pujol FM, Heigele A, Learn GH, et al. Nef proteins of epidemic HIV-1 group O strains antagonize human tetherin. Cell Host Microbe. 2014;16(5):639-50.
1502. Hatziioannou T, Evans DT. Animal models for HIV/AIDS research. Nat Rev Microbiol. 2012;10(12):852-67.
1503. Kumar N, Chahroudi A, Silvestri G. Animal models to achieve an HIV cure. Curr Opin HIV AIDS. 2016;11(4):432-41.
1504. Policicchio BB, Pandrea I, Apetrei C. Animal Models for HIV Cure Research. Front Immunol. 2016;7:12.
1505. Marsden MD. Benefits and limitations of humanized mice in HIV persistence studies. Retrovirology. 2020;17(1):7.
1506. Bauer AM, Bar KJ. Advances in simian--human immunodeficiency viruses for nonhuman primate studies of HIV prevention and cure. Curr Opin HIV AIDS. 2020;15(5):275-81.
1507. Wu X, Liu L, Cheung KW, Wang H, Lu X, Cheung AK, et al. Brain Invasion by CD4(+) T Cells Infected with a Transmitted/Founder HIV-1BJZS7 During Acute Stage in Humanized Mice. J Neuroimmune Pharmacol. 2016;11(3):572-83.
1508. Honeycutt JB, Wahl A, Baker C, Spagnuolo RA, Foster J, Zakharova O, et al. Macrophages sustain HIV replication in vivo independently of T cells. J Clin Invest. 2016;126(4):1353-66.
1509. Honeycutt JB, Liao B, Nixon CC, Cleary RA, Thayer WO, Birath SL, et al. T cells establish and maintain CNS viral infection in HIV-infected humanized mice. J Clin Invest. 2018;128(7):2862-76.

1510. Ventura JD, Beloor J, Allen E, Zhang T, Haugh KA, Uchil PD, et al. Longitudinal bioluminescent imaging of HIV-1 infection during antiretroviral therapy and treatment interruption in humanized mice. PLoS Pathog. 2019;15(12):e1008161.
1511. Flerin NC, Bardhi A, Zheng JH, Korom M, Folkvord J, Kovacs C, et al. Establishment of a Novel Humanized Mouse Model To Investigate In Vivo Activation and Depletion of Patient-Derived HIV Latent Reservoirs. J Virol. 2019;93(6).
1512. Humes D, Emery S, Laws E, Overbaugh J. A species-specific amino acid difference in the macaque CD4 receptor restricts replication by global circulating HIV-1 variants representing viruses from recent infection. J Virol. 2012;86(23):12472-83.
1513. Fellinger CH, Gardner MR, Bailey CC, Farzan M. Simian Immunodeficiency Virus SIVmac239, but Not SIVmac316, Binds and Utilizes Human CD4 More Efficiently than Rhesus CD4. J Virol. 2017;91(18).
1514. Li H, Wang S, Kong R, Ding W, Lee FH, Parker Z, et al. Envelope residue 375 substitutions in simian-human immunodeficiency viruses enhance CD4 binding and replication in rhesus macaques. Proc Natl Acad Sci U S A. 2016;113(24):E3413-22.
1515. Gorman J, Mason RD, Nettey L, Cavett N, Chuang GY, Peng D, et al. Isolation and Structure of an Antibody that Fully Neutralizes Isolate SIVmac239 Reveals Functional Similarity of SIV and HIV Glycan Shields. Immunity. 2019;51(4):724-34 e4.
1516. Reimann KA, Li JT, Voss G, Lekutis C, Tenner-Racz K, Racz P, et al. An env gene derived from a primary human immunodeficiency virus type 1 isolate confers high in vivo replicative capacity to a chimeric simian/human immunodeficiency virus in rhesus monkeys. J Virol. 1996;70(5):3198-206.
1517. Harouse JM, Gettie A, Eshetu T, Tan RC, Bohm R, Blanchard J, et al. Mucosal transmission and induction of simian AIDS by CCR5-specific simian/human immunodeficiency virus SHIV(SF162P3). J Virol. 2001;75(4):1990-5.
1518. Pal R, Taylor B, Foulke JS, Woodward R, Merges M, Praschunus R, et al. Characterization of a simian human immunodeficiency virus encoding the envelope gene from the CCR5-tropic HIV-1 Ba-L. J Acquir Immune Defic Syndr. 2003;33(3):300-7.
1519. Song RJ, Chenine AL, Rasmussen RA, Ruprecht CR, Mirshahidi S, Grisson RD, et al. Molecularly cloned SHIV-1157ipd3N4: a highly replication- competent, mucosally transmissible R5 simian-human immunodeficiency virus encoding HIV clade C Env. J Virol. 2006;80(17):8729-38.
1520. Shingai M, Donau OK, Schmidt SD, Gautam R, Plishka RJ, Buckler-White A, et al. Most rhesus macaques infected with the CCR5-tropic SHIV(AD8) generate cross-reactive antibodies that neutralize multiple HIV-1 strains. Proc Natl Acad Sci U S A. 2012;109(48):19769-74.
1521. Beauparlant D, Rusert P, Magnus C, Kadelka C, Weber J, Uhr T, et al. Delineating CD4 dependency of HIV-1: Adaptation to infect low level CD4 expressing target cells widens cellular tropism but severely impacts on envelope functionality. PLoS Pathog. 2017;13(3):e1006255.
1522. O'Connell O, Repik A, Reeves JD, Gonzalez-Perez MP, Quitadamo B, Anton ED, et al. Efficiency of bridging-sheet recruitment explains HIV-1 R5 envelope glycoprotein sensitivity to soluble CD4 and macrophage tropism. J Virol. 2013;87(1):187-98.
1523. Quitadamo B, Peters PJ, Repik A, O'Connell O, Mou Z, Koch M, et al. HIV-1 R5 Macrophage-Tropic Envelope Glycoprotein Trimers Bind CD4 with High Affinity, while the CD4 Binding Site on Non-macrophage-tropic, T-Tropic R5 Envelopes Is Occluded. J Virol. 2018;92(2).

1524. Joseph SB, Arrildt KT, Swanstrom AE, Schnell G, Lee B, Hoxie JA, et al. Quantification of entry phenotypes of macrophage-tropic HIV-1 across a wide range of CD4 densities. J Virol. 2014;88(4):1858-69.
1525. Li S, Juarez J, Alali M, Dwyer D, Collman R, Cunningham A, et al. Persistent CCR5 utilization and enhanced macrophage tropism by primary blood human immunodeficiency virus type 1 isolates from advanced stages of disease and comparison to tissue-derived isolates. J Virol. 1999;73(12):9741-55.
1526. Peters PJ, Sullivan WM, Duenas-Decamp MJ, Bhattacharya J, Ankghuambom C, Brown R, et al. Non-macrophage-tropic human immunodeficiency virus type 1 R5 envelopes predominate in blood, lymph nodes, and semen: implications for transmission and pathogenesis. J Virol. 2006;80(13):6324-32.
1527. Gonzalez-Perez MP, O'Connell O, Lin R, Sullivan WM, Bell J, Simmonds P, et al. Independent evolution of macrophage-tropism and increased charge between HIV-1 R5 envelopes present in brain and immune tissue. Retrovirology. 2012;9:20.
1528. Gonzalez-Perez MP, Peters PJ, O'Connell O, Silva N, Harbison C, Cummings Macri S, et al. Identification of Emerging Macrophage-Tropic HIV-1 R5 Variants in Brain Tissue of AIDS Patients without Severe Neurological Complications. J Virol. 2017;91(20).
1529. Brese RL, Gonzalez-Perez MP, Koch M, O'Connell O, Luzuriaga K, Somasundaran M, et al. Ultradeep single-molecule real-time sequencing of HIV envelope reveals complete compartmentalization of highly macrophage-tropic R5 proviral variants in brain and CXCR4-using variants in immune and peripheral tissues. J Neurovirol. 2018;24(4):439-53.
1530. Musich T, O'Connell O, Gonzalez-Perez MP, Derdeyn CA, Peters PJ, Clapham PR. HIV-1 non-macrophage-tropic R5 envelope glycoproteins are not more tropic for entry into primary CD4+ T-cells than envelopes highly adapted for macrophages. Retrovirology. 2015;12:25.
1531. Peters PJ, Gonzalez-Perez MP, Musich T, Moore Simas TA, Lin R, Morse AN, et al. Infection of ectocervical tissue and universal targeting of T-cells mediated by primary non-macrophage-tropic and highly macrophage-tropic HIV-1 R5 envelopes. Retrovirology. 2015;12:48.
1532. Del Prete GQ, Ailers B, Moldt B, Keele BF, Estes JD, Rodriguez A, et al. Selection of unadapted, pathogenic SHIVs encoding newly transmitted HIV-1 envelope proteins. Cell Host Microbe. 2014;16(3):412-8.
1533. Chang HW, Tartaglia LJ, Whitney JB, Lim SY, Sanisetty S, Lavine CL, et al. Generation and evaluation of clade C simian-human immunodeficiency virus challenge stocks. J Virol. 2015;89(4):1965-74.
1534. Tartaglia LJ, Chang HW, Lee BC, Abbink P, Ng'ang'a D, Boyd M, et al. Production of Mucosally Transmissible SHIV Challenge Stocks from HIV-1 Circulating Recombinant Form 01_AE env Sequences. PLoS Pathog. 2016;12(2):e1005431.
1535. O'Brien SP, Swanstrom AE, Pegu A, Ko SY, Immonen TT, Del Prete GQ, et al. Rational design and in vivo selection of SHIVs encoding transmitted/founder subtype C HIV-1 envelopes. PLoS Pathog. 2019;15(4):e1007632.
1536. Li H, Wang S, Lee FH, Roark RS, Murphy AI, Smith J, et al. New SHIVs and Improved Design Strategy for Modeling HIV-1 Transmission, Immunopathogenesis, Prevention and Cure. J Virol. 2021.
1537. Asmal M, Luedemann C, Lavine CL, Mach LV, Balachandran H, Brinkley C, et al. Infection of monkeys by simian-human immunodeficiency viruses with transmitted/founder clade C HIV-1 envelopes. Virology. 2015;475:37-45.

1538. Tartaglia LJ, Gupte S, Pastores KC, Trott S, Abbink P, Mercado NB, et al. Differential Outcomes following Optimization of Simian-Human Immunodeficiency Viruses from Clades AE, B, and C. J Virol. 2020;94(10).
1539. Vilmen G, Smith AC, Benet HC, Shukla RK, Larue RC, Herschhorn A, et al. Conformation of HIV-1 Envelope Governs Rhesus CD4 Usage and Simian-Human Immunodeficiency Virus Replication. mBio. 2022:e0275221.
1540. Humes D, Overbaugh J. Adaptation of subtype a human immunodeficiency virus type 1 envelope to pig-tailed macaque cells. J Virol. 2011;85(9):4409-20.
1541. Boyd DF, Peterson D, Haggarty BS, Jordan AP, Hogan MJ, Goo L, et al. Mutations in HIV-1 envelope that enhance entry with the macaque CD4 receptor alter antibody recognition by disrupting quaternary interactions within the trimer. J Virol. 2015;89(2):894-907.
1542. Meyerson NR, Sharma A, Wilkerson GK, Overbaugh J, Sawyer SL. Identification of Owl Monkey CD4 Receptors Broadly Compatible with Early-Stage HIV-1 Isolates. J Virol. 2015;89(16):8611-22.
1543. Nahabedian J, Sharma A, Kaczmarek ME, Wilkerson GK, Sawyer SL, Overbaugh J. Owl monkey CCR5 reveals synergism between CD4 and CCR5 in HIV-1 entry. Virology. 2017;512:180-6.
1544. Warren CJ, Meyerson NR, Dirasantha O, Feldman ER, Wilkerson GK, Sawyer SL. Selective use of primate CD4 receptors by HIV-1. PLoS Biol. 2019;17(6):e3000304.
1545. Yoshida T, Kao S, Strebel K. Identification of Residues in the BST-2 TM Domain Important for Antagonism by HIV-1 Vpu Using a Gain-of-Function Approach. Front Microbiol. 2011;2:35.
1546. Bell I, Ashman C, Maughan J, Hooker E, Cook F, Reinhart TA. Association of simian immunodeficiency virus Nef with the T-cell receptor (TCR) zeta chain leads to TCR down-modulation. J Gen Virol. 1998;79 (Pt 11):2717-27.
1547. Schindler M, Munch J, Kutsch O, Li H, Santiago ML, Bibollet-Ruche F, et al. Nef-mediated suppression of T cell activation was lost in a lentiviral lineage that gave rise to HIV-1. Cell. 2006;125(6):1055-67.
1548. Laguette N, Bregnard C, Benichou S, Basmaciogullari S. Human immunodeficiency virus (HIV) type-1, HIV-2 and simian immunodeficiency virus Nef proteins. Mol Aspects Med. 2010;31(5):418-33.
1549. Sun Z, Denton PW, Estes JD, Othieno FA, Wei BL, Wege AK, et al. Intrarectal transmission, systemic infection, and CD4+ T cell depletion in humanized mice infected with HIV-1. J Exp Med. 2007;204(4):705-14.
1550. Thomas T, Seay K, Zheng JH, Zhang C, Ochsenbauer C, Kappes JC, et al. High-Throughput Humanized Mouse Models for Evaluation of HIV-1 Therapeutics and Pathogenesis. Methods Mol Biol. 2016;1354:221-35.
1551. Bardhi A, Wu Y, Chen W, Li W, Zhu Z, Zheng JH, et al. Potent In Vivo NK Cell-Mediated Elimination of HIV-1-Infected Cells Mobilized by a gp120-Bispecific and Hexavalent Broadly Neutralizing Fusion Protein. J Virol. 2017;91(20).
1552. Rongvaux A, Willinger T, Martinek J, Strowig T, Gearty SV, Teichmann LL, et al. Development and function of human innate immune cells in a humanized mouse model. Nat Biotechnol. 2014;32(4):364-72.
1553. Herndler-Brandstetter D, Shan L, Yao Y, Stecher C, Plajer V, Lietzenmayer M, et al. Humanized mouse model supports development, function, and tissue residency of human natural killer cells. Proc Natl Acad Sci U S A. 2017;114(45):E9626-E34.

1554. Matsuda M, Ono R, Iyoda T, Endo T, Iwasaki M, Tomizawa-Murasawa M, et al. Human NK cell development in hIL-7 and hIL-15 knockin NOD/SCID/IL2rgKO mice. Life Sci Alliance. 2019;2(2).
1555. Lavender KJ, Pang WW, Messer RJ, Duley AK, Race B, Phillips K, et al. BLT-humanized C57BL/6 Rag2-/-gammac-/-CD47-/- mice are resistant to GVHD and develop B- and T-cell immunity to HIV infection. Blood. 2013;122(25):4013-20.
1556. Lavender KJ, Pace C, Sutter K, Messer RJ, Pouncey DL, Cummins NW, et al. An advanced BLT-humanized mouse model for extended HIV-1 cure studies. AIDS. 2018;32(1):1-10.
1557. Pegu A, Borate B, Huang Y, Pauthner MG, Hessell AJ, Julg B, et al. A Meta-analysis of Passive Immunization Studies Shows that Serum-Neutralizing Antibody Titer Associates with Protection against SHIV Challenge. Cell Host Microbe. 2019;26(3):336-46 e3.
1558. Parsons MS, Kristensen AB, Selva KJ, Lee WS, Amarasena T, Esterbauer R, et al. Protective efficacy of the anti-HIV broadly neutralizing antibody PGT121 in the context of semen exposure. EBioMedicine. 2021;70:103518.
1559. Hangartner L, Beauparlant D, Rakasz E, Nedellec R, Hoze N, McKenney K, et al. Effector function does not contribute to protection from virus challenge by a highly potent HIV broadly neutralizing antibody in nonhuman primates. Sci Transl Med. 2021;13(585).
1560. Hessell AJ, Poignard P, Hunter M, Hangartner L, Tehrani DM, Bleeker WK, et al. Effective, low-titer antibody protection against low-dose repeated mucosal SHIV challenge in macaques. Nat Med. 2009;15(8):951-4.
1561. Chung AW, Kumar MP, Arnold KB, Yu WH, Schoen MK, Dunphy LJ, et al. Dissecting Polyclonal Vaccine-Induced Humoral Immunity against HIV Using Systems Serology. Cell. 2015;163(4):988-98.
1562. Ackerman ME, Barouch DH, Alter G. Systems serology for evaluation of HIV vaccine trials. Immunol Rev. 2017;275(1):262-70.
1563. Pittala S, Morrison KS, Ackerman ME. Systems serology for decoding infection and vaccine-induced antibody responses to HIV-1. Curr Opin HIV AIDS. 2019;14(4):253-64.
1564. Fischinger S, Dolatshahi S, Jennewein MF, Rerks-Ngarm S, Pitisuttithum P, Nitayaphan S, et al. IgG3 collaborates with IgG1 and IgA to recruit effector function in RV144 vaccinees. JCI Insight. 2020;5(21).
1565. Chung AW, Alter G. Systems serology: profiling vaccine induced humoral immunity against HIV. Retrovirology. 2017;14(1):57.
1566. Barouch DH, Alter G, Broge T, Linde C, Ackerman ME, Brown EP, et al. Protective efficacy of adenovirus/protein vaccines against SIV challenges in rhesus monkeys. Science. 2015;349(6245):320-4.
1567. Alter G, Yu WH, Chandrashekar A, Borducchi EN, Ghneim K, Sharma A, et al. Passive Transfer of Vaccine-Elicited Antibodies Protects against SIV in Rhesus Macaques. Cell. 2020;183(1):185-96 e14.
1568. Mielke D, Stanfield-Oakley S, Borate B, Fisher LH, Faircloth K, Tuyishime M, et al. Selection of HIV Envelope strains for standardized assessments of vaccine-elicited antibody-dependent cellular cytotoxicity (ADCC)-mediating antibodies. J Virol. 2021:JVI0164321.
1569. Bournazos S, Klein F, Pietzsch J, Seaman MS, Nussenzweig MC, Ravetch JV. Broadly neutralizing anti-HIV-1 antibodies require Fc effector functions for in vivo activity. Cell. 2014;158(6):1243-53.

1570. Lu CL, Murakowski DK, Bournazos S, Schoofs T, Sarkar D, Halper-Stromberg A, et al. Enhanced clearance of HIV-1-infected cells by broadly neutralizing antibodies against HIV-1 in vivo. Science. 2016;352(6288):1001-4.
1571. Wang P, Gajjar MR, Yu J, Padte NN, Gettie A, Blanchard JL, et al. Quantifying the contribution of Fc-mediated effector functions to the antiviral activity of anti-HIV-1 IgG1 antibodies in vivo. Proc Natl Acad Sci U S A. 2020;117(30):18002-9.
1572. Asokan M, Dias J, Liu C, Maximova A, Ernste K, Pegu A, et al. Fc-mediated effector function contributes to the in vivo antiviral effect of an HIV neutralizing antibody. Proc Natl Acad Sci U S A. 2020;117(31):18754-63.
1573. Sneller MC, Blazkova J, Justement JS, Shi V, Kennedy BD, Gittens K, et al. Combination anti-HIV antibodies provide sustained virological suppression. Nature. 2022;606(7913):375-81.
1574. Richard J, Pacheco B, Gohain N, Veillette M, Ding S, Alsahafi N, et al. Co-receptor Binding Site Antibodies Enable CD4-Mimetics to Expose Conserved Anti-cluster A ADCC Epitopes on HIV-1 Envelope Glycoproteins. EBioMedicine. 2016;12:208-18.
1575. Anand SP, Prevost J, Baril S, Richard J, Medjahed H, Chapleau JP, et al. Two Families of Env Antibodies Efficiently Engage Fc-Gamma Receptors and Eliminate HIV-1-Infected Cells. J Virol. 2019;93(3).
1576. Lorenzi JC, Cohen YZ, Cohn LB, Kreider EF, Barton JP, Learn GH, et al. Paired quantitative and qualitative assessment of the replication-competent HIV-1 reservoir and comparison with integrated proviral DNA. Proc Natl Acad Sci U S A. 2016;113(49):E7908-E16.
1577. Bruner KM, Murray AJ, Pollack RA, Soliman MG, Laskey SB, Capoferri AA, et al. Defective proviruses rapidly accumulate during acute HIV-1 infection. Nat Med. 2016;22(9):1043-9.
1578. Cohn LB, da Silva IT, Valieris R, Huang AS, Lorenzi JCC, Cohen YZ, et al. Clonal CD4(+) T cells in the HIV-1 latent reservoir display a distinct gene profile upon reactivation. Nat Med. 2018;24(5):604-9.
1579. Vibholm LK, Lorenzi JCC, Pai JA, Cohen YZ, Oliveira TY, Barton JP, et al. Characterization of Intact Proviruses in Blood and Lymph Node from HIV-Infected Individuals Undergoing Analytical Treatment Interruption. J Virol. 2019;93(8).
1580. Gaebler C, Lorenzi JCC, Oliveira TY, Nogueira L, Ramos V, Lu CL, et al. Combination of quadruplex qPCR and next-generation sequencing for qualitative and quantitative analysis of the HIV-1 latent reservoir. J Exp Med. 2019;216(10):2253-64.
1581. Simonetti FR, White JA, Tumiotto C, Ritter KD, Cai M, Gandhi RT, et al. Intact proviral DNA assay analysis of large cohorts of people with HIV provides a benchmark for the frequency and composition of persistent proviral DNA. Proc Natl Acad Sci U S A. 2020;117(31):18692-700.
1582. Gaebler C, Falcinelli SD, Stoffel E, Read J, Murtagh R, Oliveira TY, et al. Sequence Evaluation and Comparative Analysis of Novel Assays for Intact Proviral HIV-1 DNA. J Virol. 2021;95(6).
1583. Martin AR, Bender AM, Hackman J, Kwon KJ, Lynch BA, Bruno D, et al. Similar Frequency and Inducibility of Intact Human Immunodeficiency Virus-1 Proviruses in Blood and Lymph Nodes. J Infect Dis. 2021;224(2):258-68.
1584. Morcilla V, Bacchus-Souffan C, Fisher K, Horsburgh BA, Hiener B, Wang XQ, et al. HIV-1 Genomes Are Enriched in Memory CD4(+) T-Cells with Short Half-Lives. mBio. 2021;12(5):e0244721.

1585. Cho A, Gaebler C, Olveira T, Ramos V, Saad M, Lorenzi JCC, et al. Longitudinal clonal dynamics of HIV-1 latent reservoirs measured by combination quadruplex polymerase chain reaction and sequencing. Proc Natl Acad Sci U S A. 2022;119(4).
1586. Bruner KM, Wang Z, Simonetti FR, Bender AM, Kwon KJ, Sengupta S, et al. A quantitative approach for measuring the reservoir of latent HIV-1 proviruses. Nature. 2019;566(7742):120-5.
1587. Descours B, Petitjean G, Lopez-Zaragoza JL, Bruel T, Raffel R, Psomas C, et al. CD32a is a marker of a CD4 T-cell HIV reservoir harbouring replication-competent proviruses. Nature. 2017;543(7646):564-7.
1588. Noto A, Procopio FA, Banga R, Suffiotti M, Corpataux JM, Cavassini M, et al. CD32(+) and PD-1(+) Lymph Node CD4 T Cells Support Persistent HIV-1 Transcription in Treated Aviremic Individuals. J Virol. 2018;92(20).
1589. Darcis G, Kootstra NA, Hooibrink B, van Montfort T, Maurer I, Groen K, et al. CD32(+)CD4(+) T Cells Are Highly Enriched for HIV DNA and Can Support Transcriptional Latency. Cell Rep. 2020;30(7):2284-96 e3.
1590. Galvez C, Grau-Exposito J, Urrea V, Clotet B, Falco V, Buzon MJ, et al. Atlas of the HIV-1 Reservoir in Peripheral CD4 T Cells of Individuals on Successful Antiretroviral Therapy. mBio. 2021;12(6):e0307821.
1591. Adams P, Fievez V, Schober R, Amand M, Iserentant G, Rutsaert S, et al. CD32(+)CD4(+) memory T cells are enriched for total HIV-1 DNA in tissues from humanized mice. iScience. 2021;24(1):101881.
1592. Astorga-Gamaza A, Grau-Exposito J, Burgos J, Navarro J, Curran A, Planas B, et al. Identification of HIV-reservoir cells with reduced susceptibility to antibody-dependent immune response. Elife. 2022;11.
1593. Weymar GHJ, Bar-On Y, Oliveira TY, Gaebler C, Ramos V, Hartweger H, et al. Distinct gene expression by expanded clones of quiescent memory CD4⁺ T cells harboring intact latent HIV-1 proviruses. bioRxiv. 2022.
1594. Collora JA, Liu R, Pinto-Santini D, Ravindra N, Ganoza C, Lama JR, et al. Single-cell multiomics reveals persistence of HIV-1 in expanded cytotoxic T cell clones. Immunity. 2022;55(6):1013-31 e7.
1595. Cummins NW, Sainski AM, Dai H, Natesampillai S, Pang YP, Bren GD, et al. Prime, Shock, and Kill: Priming CD4 T Cells from HIV Patients with a BCL-2 Antagonist before HIV Reactivation Reduces HIV Reservoir Size. J Virol. 2016;90(8):4032-48.
1596. Ren Y, Huang SH, Patel S, Alberto WDC, Magat D, Ahimovic D, et al. BCL-2 antagonism sensitizes cytotoxic T cell-resistant HIV reservoirs to elimination ex vivo. J Clin Invest. 2020;130(5):2542-59.
1597. Ren Y, Huang SH, Macedo AB, Ward AR, Alberto WDC, Klevorn T, et al. Selective BCL-XL Antagonists Eliminate Infected Cells from a Primary-Cell Model of HIV Latency but Not from Ex Vivo Reservoirs. J Virol. 2021;95(15):e0242520.
1598. Nakamura A, Suzuki S, Kanasugi J, Ejiri M, Hanamura I, Ueda R, et al. Synergistic Effects of Venetoclax and Daratumumab on Antibody-Dependent Cell-Mediated Natural Killer Cytotoxicity in Multiple Myeloma. Int J Mol Sci. 2021;22(19).
1599. Jiang L, Wang YJ, Zhao J, Uehara M, Hou Q, Kasinath V, et al. Direct Tumor Killing and Immunotherapy through Anti-SerpinB9 Therapy. Cell. 2020;183(5):1219-33 e18.

1600. Masood A, Chitta K, Paulus A, Khan AN, Sher T, Ersing N, et al. Downregulation of BCL2 by AT-101 enhances the antileukaemic effect of lenalidomide both by an immune dependant and independent manner. Br J Haematol. 2012;157(1):59-66.
1601. Gomes SE, Simoes AE, Pereira DM, Castro RE, Rodrigues CM, Borralho PM. miR-143 or miR-145 overexpression increases cetuximab-mediated antibody-dependent cellular cytotoxicity in human colon cancer cells. Oncotarget. 2016;7(8):9368-87.
1602. Pardons M, Fromentin R, Pagliuzza A, Routy JP, Chomont N. Latency-Reversing Agents Induce Differential Responses in Distinct Memory CD4 T Cell Subsets in Individuals on Antiretroviral Therapy. Cell Rep. 2019;29(9):2783-95 e5.
1603. Gao H, Ozanturk AN, Wang Q, Harlan GH, Schmitz AJ, Presti RM, et al. Evaluation of HIV-1 latency reversal and antibody-dependent viral clearance by quantification of singly spliced HIV-1 vpu/env mRNA. J Virol. 2021.
1604. Fromentin R, DaFonseca S, Costiniuk CT, El-Far M, Procopio FA, Hecht FM, et al. PD-1 blockade potentiates HIV latency reversal ex vivo in CD4(+) T cells from ART-suppressed individuals. Nat Commun. 2019;10(1):814.
1605. Van der Sluis RM, Kumar NA, Pascoe RD, Zerbato JM, Evans VA, Dantanarayana AI, et al. Combination Immune Checkpoint Blockade to Reverse HIV Latency. J Immunol. 2020;204(5):1242-54.
1606. Desimio MG, Giuliani E, Doria M. The histone deacetylase inhibitor SAHA simultaneously reactivates HIV-1 from latency and up-regulates NKG2D ligands sensitizing for natural killer cell cytotoxicity. Virology. 2017;510:9-21.
1607. Desimio MG, Giuliani E, Ferraro AS, Adorno G, Doria M. In Vitro Exposure to Prostratin but Not Bryostatin-1 Improves Natural Killer Cell Functions Including Killing of CD4(+) T Cells Harboring Reactivated Human Immunodeficiency Virus. Front Immunol. 2018;9:1514.
1608. Covino DA, Desimio MG, Doria M. Combinations of Histone Deacetylase Inhibitors with Distinct Latency Reversing Agents Variably Affect HIV Reactivation and Susceptibility to NK Cell-Mediated Killing of T Cells That Exit Viral Latency. Int J Mol Sci. 2021;22(13).
1609. Yin X, Liu T, Wang Z, Ma M, Lei J, Zhang Z, et al. Expression of the Inhibitory Receptor TIGIT Is Up-Regulated Specifically on NK Cells With CD226 Activating Receptor From HIV-Infected Individuals. Front Immunol. 2018;9:2341.
1610. Vendrame E, Seiler C, Ranganath T, Zhao NQ, Vergara R, Alary M, et al. TIGIT is upregulated by HIV-1 infection and marks a highly functional adaptive and mature subset of natural killer cells. AIDS. 2020;34(6):801-13.
1611. Holder KA, Burt K, Grant MD. TIGIT blockade enhances NK cell activity against autologous HIV-1-infected CD4(+) T cells. Clin Transl Immunology. 2021;10(10):e1348.
1612. Zhang X, Lu X, Cheung AKL, Zhang Q, Liu Z, Li Z, et al. Analysis of the Characteristics of TIGIT-Expressing CD3(-)CD56(+)NK Cells in Controlling Different Stages of HIV-1 Infection. Front Immunol. 2021;12:602492.
1613. Wren L, Parsons MS, Isitman G, Center RJ, Kelleher AD, Stratov I, et al. Influence of cytokines on HIV-specific antibody-dependent cellular cytotoxicity activation profile of natural killer cells. PLoS One. 2012;7(6):e38580.
1614. Tomescu C, Tebas P, Montaner LJ. IFN-alpha augments natural killer-mediated antibody-dependent cellular cytotoxicity of HIV-1-infected autologous CD4+ T cells regardless of major histocompatibility complex class 1 downregulation. AIDS. 2017;31(5):613-22.

1615. Garrido C, Abad-Fernandez M, Tuyishime M, Pollara JJ, Ferrari G, Soriano-Sarabia N, et al. Interleukin-15-Stimulated Natural Killer Cells Clear HIV-1-Infected Cells following Latency Reversal Ex Vivo. J Virol. 2018;92(12).
1616. Fisher L, Zinter M, Stanfield-Oakley S, Carpp LN, Edwards RW, Denny T, et al. Vaccine-Induced Antibodies Mediate Higher Antibody-Dependent Cellular Cytotoxicity After Interleukin-15 Pretreatment of Natural Killer Effector Cells. Front Immunol. 2019;10:2741.
1617. Xie Z, Zheng J, Wang Y, Li D, Maermaer T, Li Y, et al. Deficient IL-2 Produced by Activated CD56(+) T Cells Contributes to Impaired NK Cell-Mediated ADCC Function in Chronic HIV-1 Infection. Front Immunol. 2019;10:1647.
1618. Harper J, Huot N, Micci L, Tharp G, King C, Rascle P, et al. IL-21 and IFNalpha therapy rescues terminally differentiated NK cells and limits SIV reservoir in ART-treated macaques. Nat Commun. 2021;12(1):2866.
1619. Yoshimura K, Harada S, Shibata J, Hatada M, Yamada Y, Ochiai C, et al. Enhanced exposure of human immunodeficiency virus type 1 primary isolate neutralization epitopes through binding of CD4 mimetic compounds. J Virol. 2010;84(15):7558-68.
1620. Harada S, Irahara Y, Boonchawalit S, Goryo M, Tamamura H, Matano T, et al. Mutations at the Bottom of the Phe43 Cavity Are Responsible for Cross-Resistance to NBD Analogues. In Special Issue: Abstracts From the 2015 Conference on Retroviruses and Opportunistic Infections, Top Antiv Med. 2015;24(1s):253.
1621. Anang S, Richard J, Bourassa C, Goyette G, Chiu T-J, Chen H-C, et al. Characterization of human immunodeficiency virus (HIV-1) envelope glycoprotein variants selected for resistance to a CD4-mimetic compound. bioRxiv. 2022.
1622. Fritschi CJ, Liang S, Mohammadi M, Anang S, Moraca F, Chen J, et al. Identification of gp120 Residue His105 as a Novel Target for HIV-1 Neutralization by Small-Molecule CD4-Mimics. ACS Med Chem Lett. 2021;12(11):1824-31.
1623. Ding S, Grenier MC, Tolbert WD, Vezina D, Sherburn R, Richard J, et al. A New Family of Small-Molecule CD4-Mimetic Compounds Contacts Highly Conserved Aspartic Acid 368 of HIV-1 gp120 and Mediates Antibody-Dependent Cellular Cytotoxicity. J Virol. 2019;93(24).
1624. Grenier MC, Ding S, Vezina D, Chapleau JP, Tolbert WD, Sherburn R, et al. Optimization of Small Molecules That Sensitize HIV-1 Infected Cells to Antibody-Dependent Cellular Cytotoxicity. ACS Med Chem Lett. 2020;11(3):371-8.
1625. Cohn LB, Chomont N, Deeks SG. The Biology of the HIV-1 Latent Reservoir and Implications for Cure Strategies. Cell Host Microbe. 2020;27(4):519-30.
1626. Dey B, Del Castillo CS, Berger EA. Neutralization of human immunodeficiency virus type 1 by sCD4-17b, a single-chain chimeric protein, based on sequential interaction of gp120 with CD4 and coreceptor. J Virol. 2003;77(5):2859-65.
1627. Lagenaur LA, Villarroel VA, Bundoc V, Dey B, Berger EA. sCD4-17b bifunctional protein: extremely broad and potent neutralization of HIV-1 Env pseudotyped viruses from genetically diverse primary isolates. Retrovirology. 2010;7:11.
1628. West AP, Jr., Galimidi RP, Foglesong CP, Gnanapragasam PN, Klein JS, Bjorkman PJ. Evaluation of CD4-CD4i antibody architectures yields potent, broadly cross-reactive anti-human immunodeficiency virus reagents. J Virol. 2010;84(1):261-9.
1629. Alsahafi N, Bakouche N, Kazemi M, Richard J, Ding S, Bhattacharyya S, et al. An Asymmetric Opening of HIV-1 Envelope Mediates Antibody-Dependent Cellular Cytotoxicity. Cell Host Microbe. 2019;25(4):578-87 e5.

1630. Vezina D, Gong SY, Tolbert WD, Ding S, Nguyen D, Richard J, et al. Stabilizing the HIV-1 envelope glycoprotein State 2A conformation. J Virol. 2020.
1631. Edwards JM, Heydarchi B, Khoury G, Salazar-Quiroz NA, Gonelli CA, Wines B, et al. Enhancement of Antibody-Dependent Cellular Cytotoxicity and Phagocytosis in Anti-HIV-1 Human-Bovine Chimeric Broadly Neutralizing Antibodies. J Virol. 2021;95(13):e0021921.
1632. Moldt B, Schultz N, Dunlop DC, Alpert MD, Harvey JD, Evans DT, et al. A panel of IgG1 b12 variants with selectively diminished or enhanced affinity for Fcgamma receptors to define the role of effector functions in protection against HIV. J Virol. 2011;85(20):10572-81.
1633. Tokarev A, Stoneham C, Lewinski MK, Mukim A, Deshmukh S, Vollbrecht T, et al. Pharmacologic Inhibition of Nedd8 Activation Enzyme Exposes CD4-Induced Epitopes within Env on Cells Expressing HIV-1. J Virol. 2015;90(5):2486-502.
1634. Pham TN, Lukhele S, Dallaire F, Perron G, Cohen EA. Enhancing Virion Tethering by BST2 Sensitizes Productively and Latently HIV-infected T cells to ADCC Mediated by Broadly Neutralizing Antibodies. Sci Rep. 2016;6:37225.
1635. Blasius AL, Giurisato E, Cella M, Schreiber RD, Shaw AS, Colonna M. Bone marrow stromal cell antigen 2 is a specific marker of type I IFN-producing cells in the naive mouse, but a promiscuous cell surface antigen following IFN stimulation. J Immunol. 2006;177(5):3260-5.
1636. Yoo H, Park SH, Ye SK, Kim M. IFN-gamma-induced BST2 mediates monocyte adhesion to human endothelial cells. Cell Immunol. 2011;267(1):23-9.
1637. Planas D, Fert A, Zhang Y, Goulet JP, Richard J, Finzi A, et al. Pharmacological Inhibition of PPARγ Boosts HIV Reactivation and Th17 Effector Functions, While Preventing Progeny Virion Release and de novo Infection. Pathog Immun. 2020;5(1):177-239.
1638. Cheng J, Myers TG, Levinger C, Kumar P, Kumar J, Goshu BA, et al. IL-27 induces IFN/STAT1-dependent genes and enhances function of TIGIT(+) HIVGag-specific T cells. iScience. 2022;25(1):103588.
1639. Anand SP, Prévost J, Descôteaux-Dinelle J, Richard J, Nguyen DN, Medjahed H, et al. HIV-1 Envelope Glycoprotein Cell Surface Localization Is Associated with Antibody-Induced Internalization. Viruses. 2021;13(10):1953.
1640. Chew HY, De Lima PO, Gonzalez Cruz JL, Banushi B, Echejoh G, Hu L, et al. Endocytosis Inhibition in Humans to Improve Responses to ADCC-Mediating Antibodies. Cell. 2020;180(5):895-914 e27.
1641. Leis J, Luan CH, Audia JE, Dunne SF, Heath CM. Ilaprazole and other novel prazole-based compounds that bind Tsg101 inhibit viral budding of HSV-1/2 and HIV from cells. J Virol. 2021.
1642. Robinson CA, Lyddon TD, Gil HM, Evans DT, Kuzmichev YV, Richard J, et al. Novel Compound Inhibitors of HIV-1NL4-3 Vpu. Viruses. 2022;14(4).
1643. Umviligihozo G, Cobarrubias KD, Chandrarathna S, Jin SW, Reddy N, Byakwaga H, et al. Differential Vpu-Mediated CD4 and Tetherin Downregulation Functions among Major HIV-1 Group M Subtypes. J Virol. 2020;94(14).
1644. Swords RT, Coutre S, Maris MB, Zeidner JF, Foran JM, Cruz J, et al. Pevonedistat, a first-in-class NEDD8-activating enzyme inhibitor, combined with azacitidine in patients with AML. Blood. 2018;131(13):1415-24.
1645. Sekeres MA, Watts J, Radinoff A, Sangerman MA, Cerrano M, Lopez PF, et al. Randomized phase 2 trial of pevonedistat plus azacitidine versus azacitidine for higher-risk MDS/CMML or low-blast AML. Leukemia. 2021;35(7):2119-24.

1646. Ades L, Girshova L, Doronin VA, Diez-Campelo M, Valcarcel D, Kambhampati S, et al. Pevonedistat plus azacitidine vs azacitidine alone in higher-risk MDS/chronic myelomonocytic leukemia or low-blast percentage AML. Blood Adv. 2022.
1647. Handa H, Cheong JW, Onishi Y, Iida H, Kobayashi Y, Kim HJ, et al. Pevonedistat in East Asian patients with acute myeloid leukemia or myelodysplastic syndromes: a phase 1/1b study to evaluate safety, pharmacokinetics and activity as a single agent and in combination with azacitidine. J Hematol Oncol. 2022;15(1):56.

CHAPITRE IX - ANNEXES

ANNEXE I

Effet de la mutation I423A sur la conformation d'Env et la reconnaissance par les anticorps

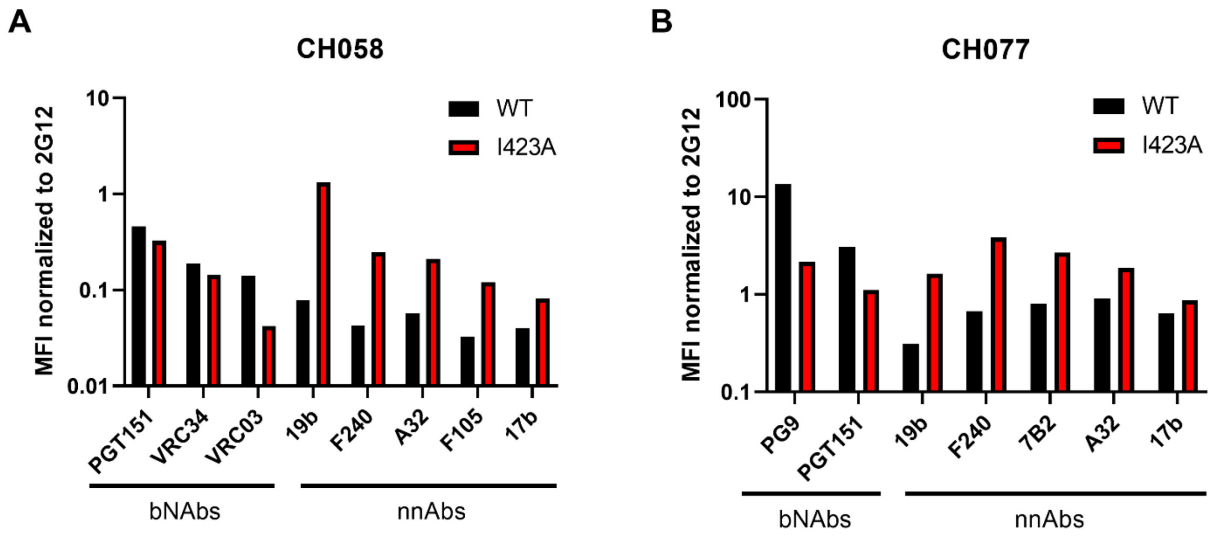

Figure 9.1.1 - La mutation I423A dans l'enveloppe du VIH-1 expose les épitopes reconnus par les anticorps non-neutralisants.
Des lymphocytes T $CD4^+$ primaires ont été infectés avec les souches du VIH-1 (**A**) CH058 ou (**B**) CH077 de type sauvage (WT) ou ayant la mutation I423A dans la séquence d'Env. (**A-B**) Quarante-huit heures après l'infection, un marquage de surface a été fait en utilisant des anticorps neutralisants (2G12, PGT151, VRC34, VRC03, PG9) ou des anticorps non-neutralisants (19b, F240, 7B2, 17b, A32, F105). Les graphiques montrent les moyennes d'intensité de la fluorescence (MFI) obtenues pour une seule expérience.

ANNEXE II

Rôle de la queue cytoplasmique d'Env dans la réponse ADCC contre les cellules infectées par le VIH-1

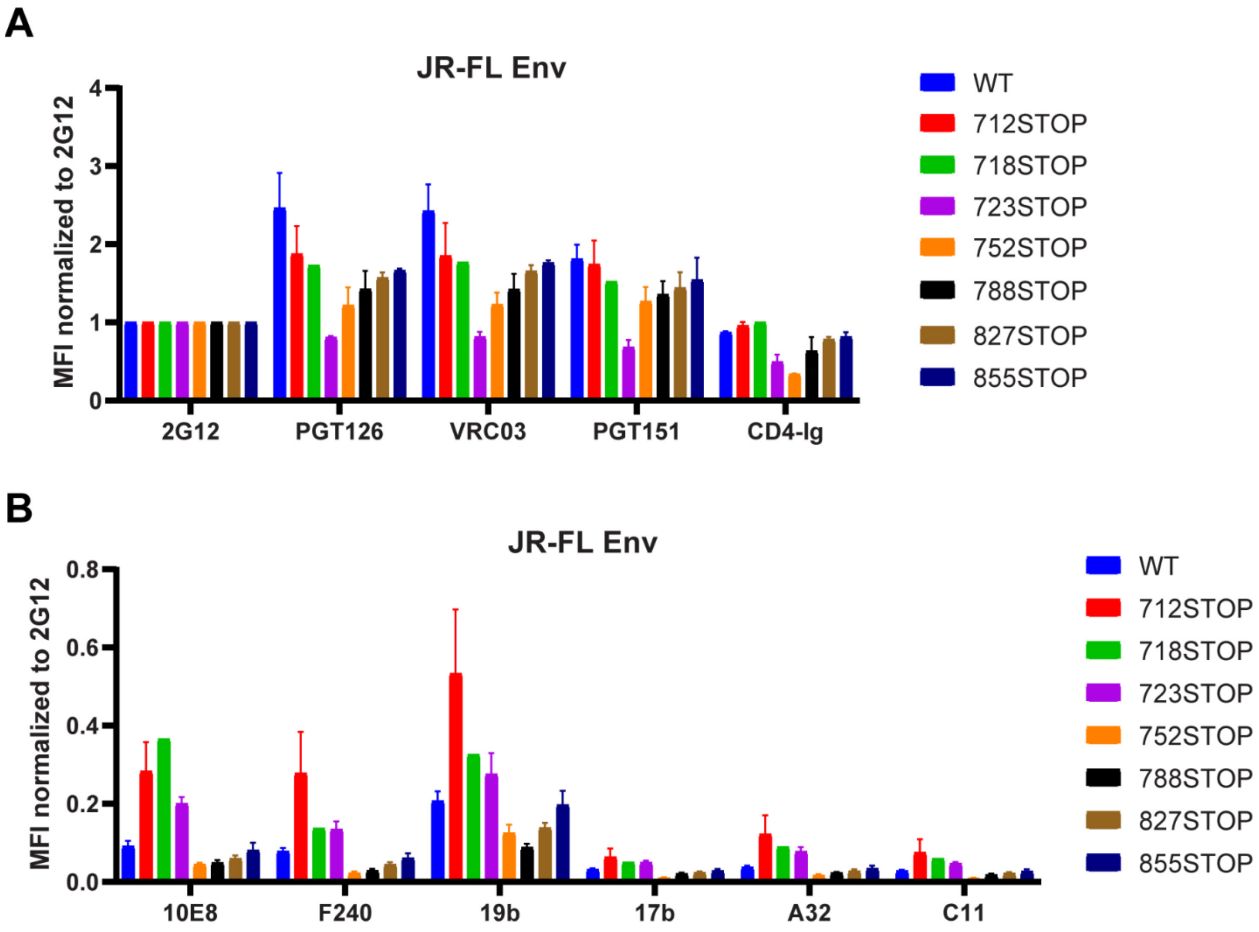

Figure 9.2.1 - La queue cytoplasmique de l'enveloppe du VIH-1 module sa reconnaissance par des bNAbs et nnAbs.

Des cellules HEK293T ont été co-transfectées avec un plasmide exprimant Env_{JR-FL} ayant une troncation graduelle de la queue cytoplasmique et un plasmide exprimant la protéine GFP. Quarante-huit heures après la transfection, un marquage de surface a été fait en utilisant (**A**) des anticorps neutralisants (2G12, PGT126, VRC03, PGT151) ou la protéine de fusion CD4-Ig et (**B**) des anticorps préférant la conformation ouverte d'Env (10E8, F240, 19b, 17b, A32, C11). (**A-B**) Les graphiques montrent les moyennes d'intensité de la fluorescence (MFI) obtenues d'au moins 2 expériences indépendantes. Les barres d'erreur représentent la moyenne des données +/- l'écart-type de la moyenne.

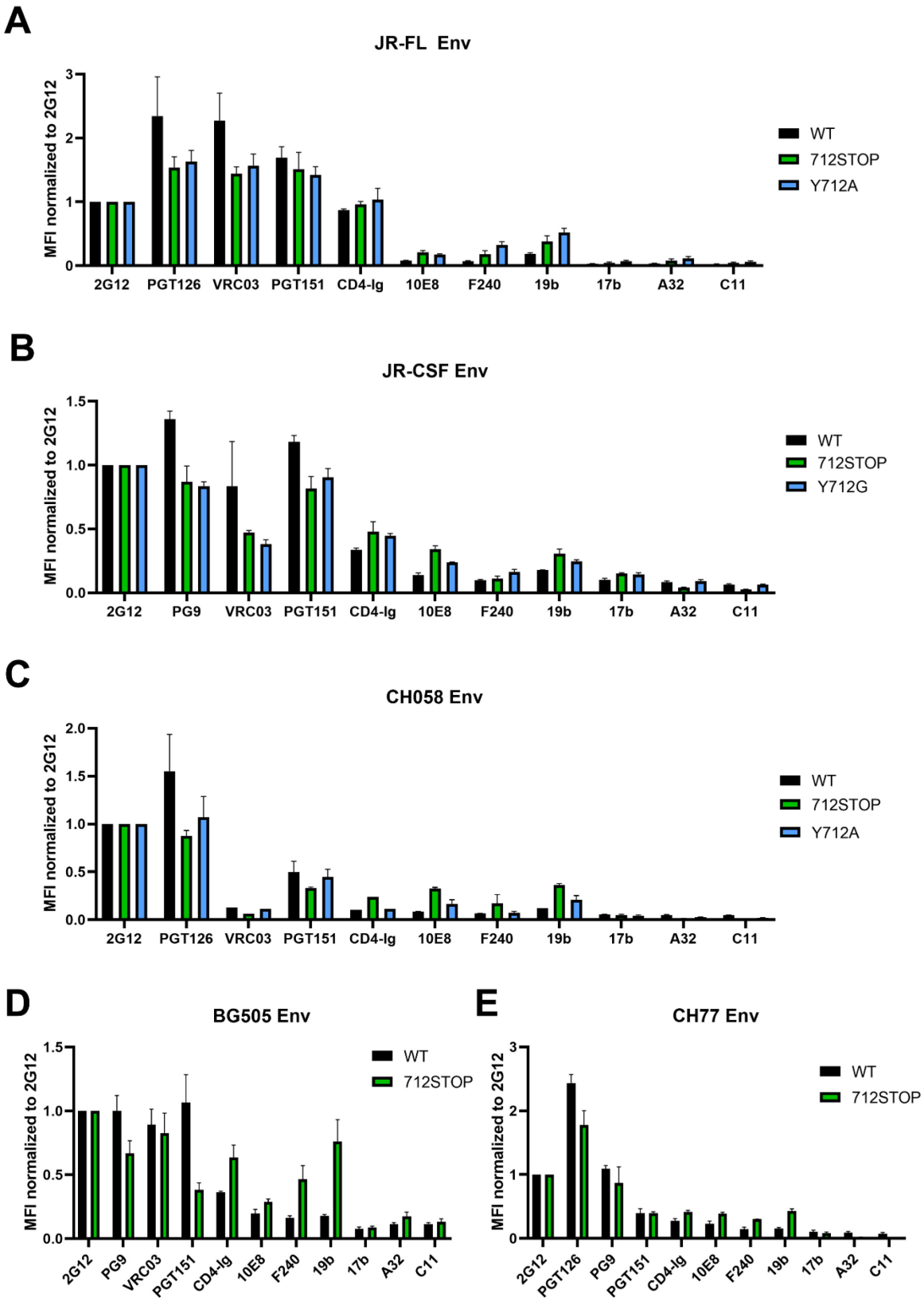
A
JR-FL Env
MFI normalized to 2G12
WT
712STOP
Y712A
2G12
PGT126
VRC03
PGT151
CD4-Ig
10E8
F240
19b
17b
A32
C11
B
JR-CSF Env
MFI normalized to 2G12
WT
712STOP
Y712G
2G12
PG9
VRC03
PGT151
CD4-Ig
10E8
F240
19b
17b
A32
C11
C
CH058 Env
MFI normalized to 2G12
WT
712STOP
Y712A
2G12
PGT126
VRC03
PGT151
CD4-Ig
10E8
F240
19b
17b
A32
C11
D
BG505 Env
MFI normalized to 2G12
WT
712STOP
2G12
PG9
VRC03
PGT151
CD4-Ig
10E8
F240
19b
17b
A32
C11
E
CH77 Env
MFI normalized to 2G12
WT
712STOP
2G12
PGT126
PG9
PGT151
CD4-Ig
10E8
F240
19b
17b
A32
C11

Figure 9.2.2 - Le motif d'endocytose de l'enveloppe du VIH-1 module son antigénicité.
Des cellules HEK293T ont été co-transfectées avec un plasmide exprimant l'Env des souches du VIH-1 (**A**) JR-FL, (**B**) JR-CSF, (**C**) CH058, (**D**) BG505 ou (**E**) CH077 ayant une troncation de la queue cytoplasmique (712STOP) ou une mutation dans le motif d'endocytose (Y712A/G) ainsi qu'un plasmide exprimant la protéine GFP. Quarante-huit heures après la transfection, un marquage de surface a été fait en utilisant des anticorps neutralisants (2G12, PGT126, VRC03, PGT151), la protéine de fusion CD4-Ig et des anticorps préférant la conformation ouverte d'Env (10E8, F240, 19b, 17b, A32, C11). Les graphiques montrent les moyennes d'intensité de la fluorescence (MFI) obtenues d'au moins 2 expériences indépendantes. Les barres d'erreur représentent la moyenne des données +/- l'écart-type de la moyenne.

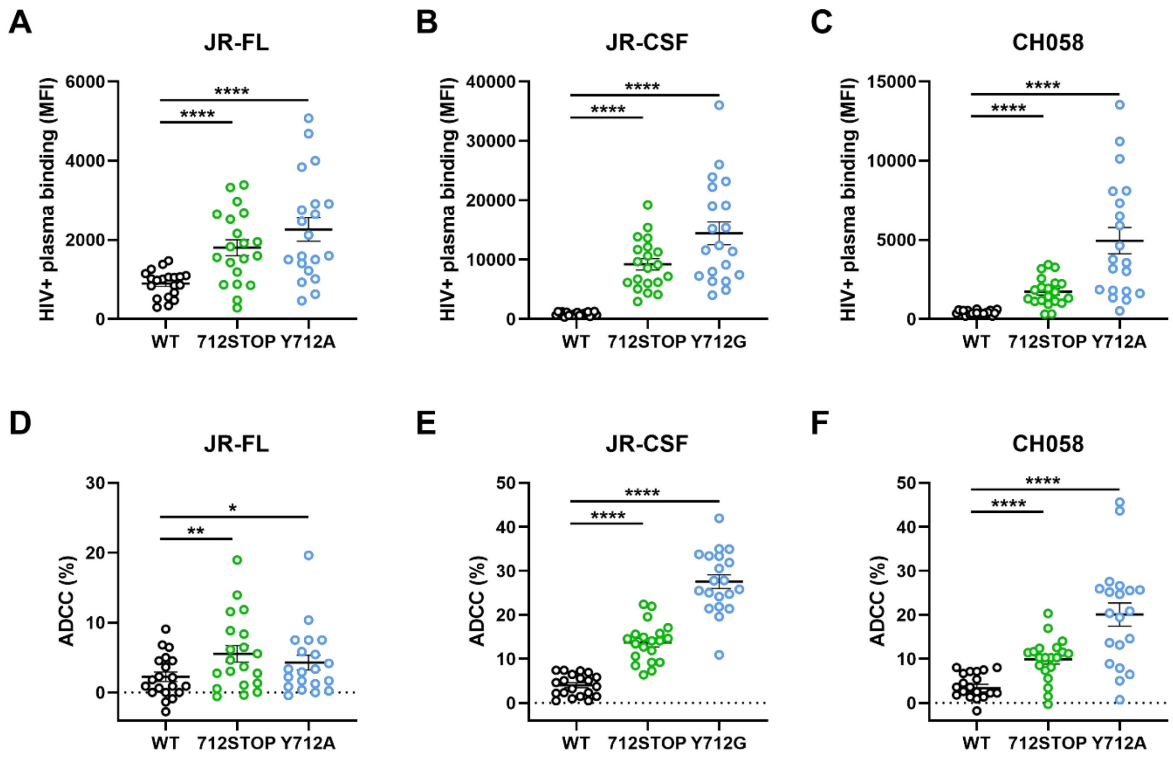

Figure 9.2.3 - La queue cytoplasmique d'Env prévient la reconnaissance et l'élimination des cellules infectées par le plasma d'individus infectés.

Des lymphocytes T $CD4^+$ primaires ont été infectés avec les souches du VIH-1 (**A,D**) JR-FL, (**B, E**) JR-CSF ou (**C,F**) CH058 ayant une troncation de la queue cytoplasmique d'Env (ΔCT) ou une mutation dans le motif d'endocytose (Y712A/G). (**A-C**) Quarante-huit heures après l'infection, un marquage de surface a été fait en utilisant 20 plasmas d'individus infectés par le VIH-1. Les graphiques montrent les moyennes d'intensité de la fluorescence (MFI). (**D-F**) La capacité de ces plasmas à induire l'élimination des cellules infectées par la réponse ADCC a également été mesurée en présence de cellules effectrices autologues. Ces résultats ont été obtenus à partir d'au moins trois expériences indépendantes. Les barres d'erreur représentent la moyenne des données +/- l'écart-type de la moyenne. L'analyse statistique a été faite en utilisant le test t de Student apparié (*, $p < 0.05$; **, $p < 0.01$; ****, $p < 0.0001$).

ANNEXE III

Absence de suppression des niveaux de surface du complexe d'histocompatibilité de classe I en utilisant des souches du VIH-1 comportant la cassette LucR.T2A

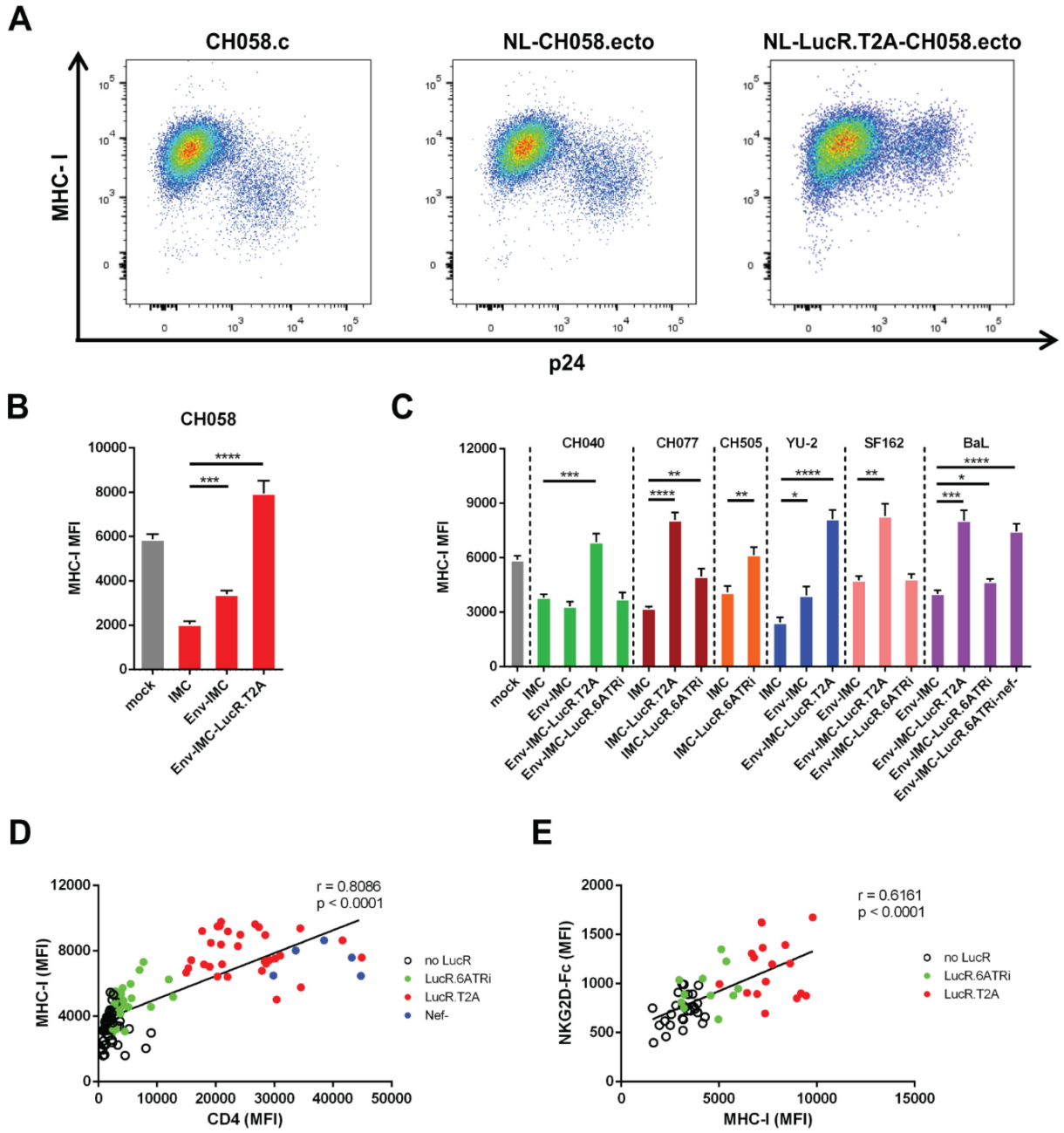

Figure 9.3.1 – Impact de la stratégie d'insertion de l'élément LucR sur la régulation du CMH-I.

Marquage de surface avec un anticorps contre HLA-A/B/C sur des lymphocytes T $CD4^+$ primaires infectés avec des clones moléculaires du VIH-1 (IMC) exprimant différents souches d'Env (CH058, CH040, CH077, CH0505, YU2, SF162 et BaL) et exprimant ou non le rapporteur LucR. (**A**) Données brutes de cytométrie en flux montrant l'expression du CMH-I sur les cellules infectées (p24+) par les IMC de CH058. (**B-C**) Les graphiques montre les moyennes d'intensité de la fluorescence (MFI) obtenues avec des cellules d'au moins 5 donneurs sains différents. (**D-E**) Les niveaux d'expression du CMH-I sont corrélés avec la détection de (**D**) CD4 ou (**E**) de NKG2D-Fc à la surface des cellules infectées (p24+) à l'aide d'un test de corrélation de Pearson. Les barres d'erreur représentent la moyenne des données +/- l'écart-type de la moyenne. L'analyse statistique a été faite en utilisant le test t de Student (*, $p < 0.05$; **, $p < 0.01$; ***, $p < 0.001$; ****, $p < 0.0001$).

ANNEXE IV

Évolution d'une sélection de résidus d'Env et de fonctions de Nef et Vpu chez les différentes souches de VIH et de SIV

Tableau 9.4.1 - Conservation de résidus d'Env pouvant affecter sa conformation et présence de la protéine accessoire Vpu chez les lentivirus infectant les primates.

Virus	Env 375	Env 193	Env 423	Site de clivage polybasique (RXK/RR)	Motif d'endocytose YXXΦ	Vpu ou Vpx
VIH-1 M	**S**	**L**	**I**	**R**E**KR**	**Y**S**PL**	**Vpu**
SIVcpzPtt	H	**L**	**I**	**R**E**KR**	**Y**S**PL**	**Vpu**
VIH-1 N	M	**L**	**I**	**R**E**KR**	**Y**S**PL**	**Vpu**
SIVcpzPtt	M	**L**	**I**	**R**E**KR**	**Y**S**PL**	**Vpu**
VIH-1 O	H	**L**	V	**R**E**KR**	**Y**Q**PL**	**Vpu**
VIH-1 P	H	**L**	V	**RKKR**	**Y**S**PV**	**Vpu**
SIVgor	H	**L**	V	**R**E**KR**	**Y**S**PL**	**Vpu**
SIVcpzPts	W	**L**	**I**	**RSKR**	**Y**M**PL**	**Vpu**
SIVmus2	W	I	F	V**KAR**	**Y**S**PL**	**Vpu**
SIVmus1	W	I	F	V**KAR**	**Y**S**PL**	**Vpu**
SIVgsn	W	I	F	V**KKR**	**Y**S**PL**	**Vpu**
SIVmon	W	**L**/I	L/M	**R**E**KR**	**Y**S**LL**	**Vpu**
SIVden	R	M	L	**RRRR**	**Y**S**PL**	**Vpu**
SIVdeb	W	M	L	**RQKR**	**Y**S**PL**	aucun
SIVtal	W	A	M	**K**E**KR**	**Y**L**PL**	aucun
SIVsyk	W	**L**	**I**	**KQKR**	**Y**S**PL**	aucun
SIVagmSab	F	M	V	**RQKR**	**Y**A**PL**	aucun
SIVagmTan	W	M	**I**	**R**E**KR**	**Y**F**PL**	aucun
SIVagmGri	W	M	V	**R**E**KR**	**Y**N**PL**	aucun
SIVagmVer	W	M	V	**RQKR**	**Y**T**PL**	aucun
SIVrcm	W	M	**I**/V	**KQKR**	**Y**T**PL**	Vpx
SIVmac	W	M	**I**	**RNKR**	**Y**R**PV**	Vpx
SIVsmm	W	M	**I**	**RNKR**	**Y**R**PV**	Vpx
VIH-2	W	M	**I**	**RNKR**	**Y**R**PV**	Vpx
SIVdrl	M	V	**I**	**RQKR**	**Y**R**PL**	Vpx
SIVmnd2	M	M	**I**	**RQKR**	**Y**R**PL**	Vpx
SIVmnd1	M	M	**I**	**K**E**KR**	**Y**R**PV**	aucun
SIVlho	M	M	**I**/V	**RQKR**	**Y**R**VL**	aucun
SIVsun	M	M	V	**K**E**KR**	**Y**R**VL**	aucun
SIVwrc	M	V/I	**I**	**R**E**KR**	**Y**S**KL**	aucun
SIVolc	M	M	N	**RNKR**	**Y**V**SL**	aucun
SIVcol	F	M	L	**RQKR**	**Y**L**LV**	aucun

Tableau 9.4.2 - Régulation négative de protéines de l'hôte par les protéines accessoires Nef et Vpu encodées par le VIH-1, VIH-2 et les SIV étroitement liés.

Virus	Vpu ⟶ CD4	Vpu ⟶ BST-2	Vpu ⟶ NTB-A	Vpu ⟶ PVR	Nef ⟶ CD4	Nef ⟶ BST-2	Nef ⟶ PVR
VIH-1 M	**oui**	**oui**	**oui**	**oui**	**oui**	**non**	**oui**
VIH-1 N	non	**oui**	non	non	**oui**	**non**	non
SIVcpzPtt	**oui**	non	**oui**	non	**oui**	oui	**oui**
VIH-1 O	**oui**	non	n.d.	n.d.	**oui**	oui	n.d.
VIH-1 P	**oui**	non	n.d.	non	**oui**	**non**	non
SIVgor	**oui**	non	**oui**	non	**oui**	oui	**oui**
SIVcpzPts	**oui**	non	**oui**	n.d.	**oui**	oui	n.d.
SIVgsn	**oui**	**oui**	**oui**	non	**oui**	**non**	non
VIH-2	N/A	N/A	N/A	N/A	**oui**	**non***	non
SIVmac	N/A	N/A	N/A	N/A	**oui**	oui	non
SIVsmm	N/A	N/A	N/A	N/A	**oui**	oui	n.d.

*La régulation négative de BST-2 par le VIH-2 est médiée par Env

N/A : non applicable (absence de Vpu)

n.d. : donnée non disponible

ANNEXE V

Influence de la cavité Phe43 de l'enveloppe du VIH-1 sur la susceptibilité des cellules infectées à la réponse ADCC

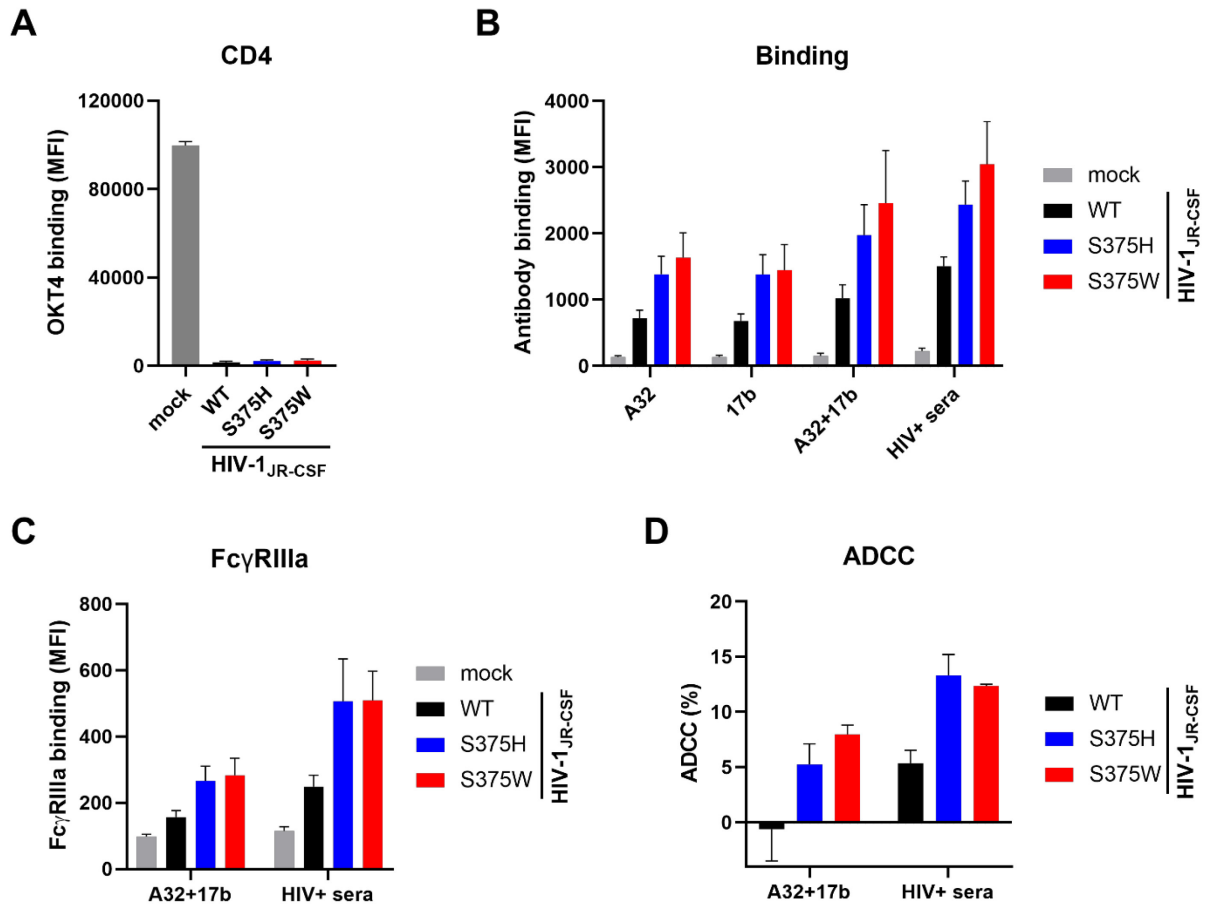

Figure 9.5.1 – La cavité Phe43 module la reconnaissance et l'élimination par ADCC des cellules infectées par un isolat du VIH-1 fréquemment utilisé dans les modèles de souris humanisées.

Des lymphocytes T CD4$^+$ primaires (mock) ont été infectés avec la souche du VIH-1 JR-CSF de type sauvage (WT) ou ayant une mutation du résidu 375 dans la séquence d'Env (S375H, S375W). 48h après l'infection, les cellules ont subi un marquage de surface total avec (**A**) un anticorps contre CD4 (OKT4) ainsi que (**B**) des anticorps monoclonaux (A32, 17b) ou du sérum de patients infectés par le VIH-1 (HIV$^+$ sera) reconnaissant l'enveloppe du VIH-1. (**C**) Alternativement, les cellules marquées avec les anticorps contre Env ont été détectées à l'aide d'une protéine de FcγRIIIa dimérique soluble. (**D**) La susceptibilité des cellules infectées à la réponse ADCC en présence de cellules effectrices autologues a été évaluée par cytométrie en flux. (**A-D**) Les graphiques montrent les moyennes d'intensité de la fluorescence (MFI) et les pourcentages (%) d'ADCC obtenus dans trois expériences indépendantes. Les barres d'erreur représentent la moyenne des données +/- l'écart-type de la moyenne.

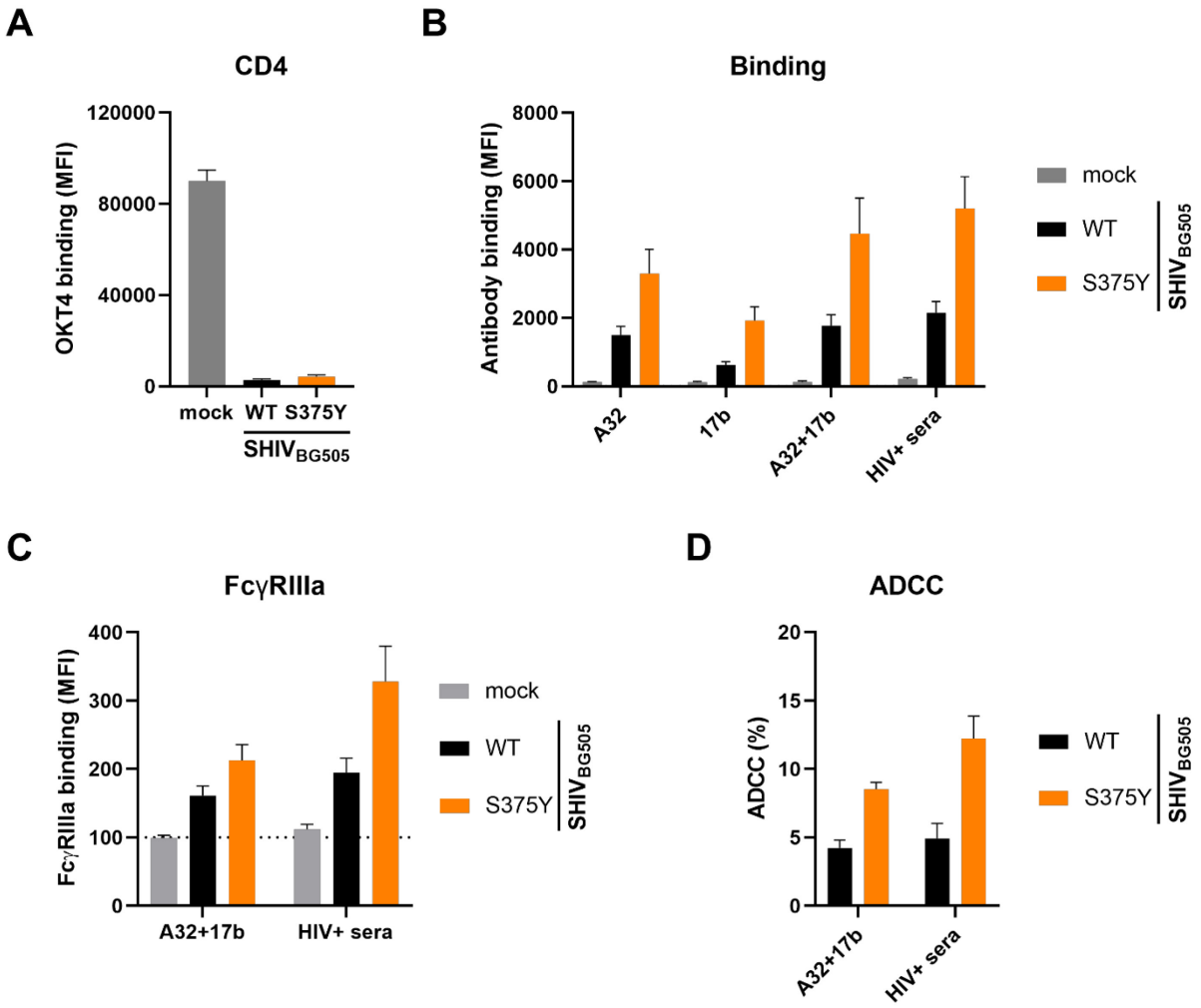

Figure 9.5.2 – La cavité Phe43 module la reconnaissance et l'élimination par ADCC des cellules infectées par un SHIV fréquemment utilisé dans les modèles de primates non-humains.

Des lymphocytes T CD4$^+$ primaires (mock) ont été infectés avec la souche du SHIV BG505 de type sauvage (WT) ou ayant une mutation du résidu 375 dans la séquence d'Env (S375Y). 48h après l'infection, les cellules ont subi un marquage de surface total avec (**A**) un anticorps contre CD4 (OKT4) ainsi que (**B**) des anticorps monoclonaux (A32, 17b) ou du sérum de patients infectés par le VIH-1 (HIV$^+$ sera) reconnaissant l'enveloppe du VIH-1. (**C**) Alternativement, les cellules marquées avec les anticorps contre Env ont été détectées à l'aide d'une protéine de FcγRIIIa dimérique soluble. (**D**) La susceptibilité des cellules infectées à la réponse ADCC en présence de cellules effectrices autologues a été évaluée par cytométrie en flux. (**A-D**) Les graphiques montrent les moyennes d'intensité de la fluorescence (MFI) et les pourcentages (%) d'ADCC obtenus dans cinq expériences indépendantes. Les barres d'erreur représentent la moyenne des données +/- l'écart-type de la moyenne.

ANNEXE VI

Régulation d'un ligand activateur des cellules NK par les SHIV de nouvelle génération

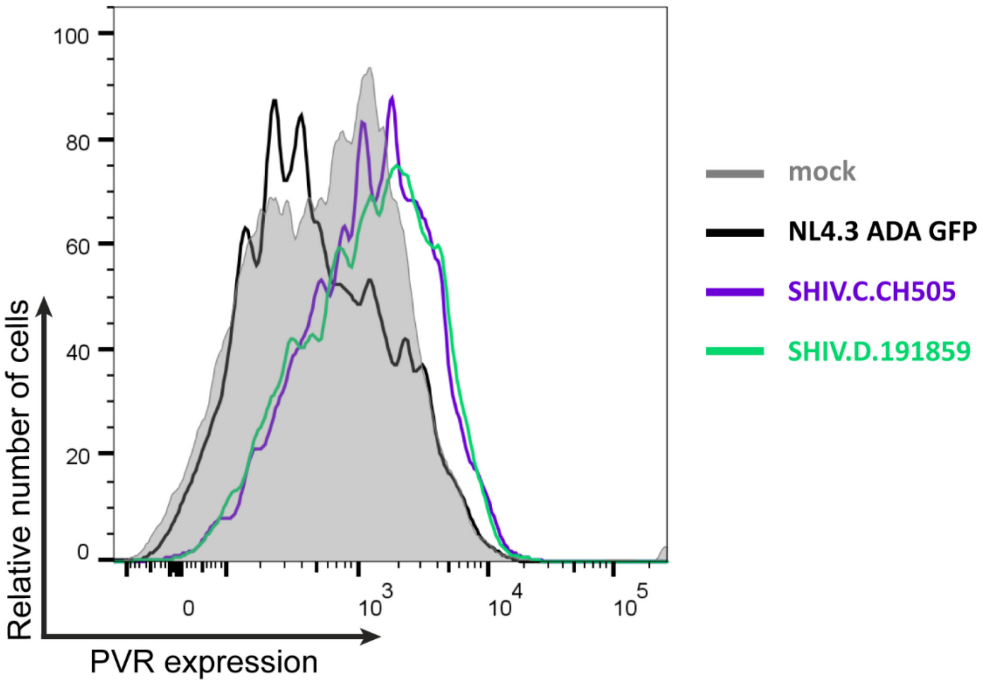

Figure 9.6.1 – Absence de régulation négative du ligand activateur PVR par les SHIV. Marquage de surface avec un anticorps contre PVR sur des lymphocytes T $CD4^+$ primaires infectés avec des clones moléculaires du VIH-1 (NL4.3 ADA GFP) ou de SHIV (SHIV.C.CH505 et SHIV.D.191859). Histogramme de cytométrie en flux montrant l'expression de PVR sur des cellules non-infectées (mock) ou infectées par le VIH-1 ou un SHIV (Gag+). Ce graphique montre des données provenant d'une seule expérience**.**

ANNEXE VII

Développement de nouvelles combinaisons d'anticorps non-neutralisants pour éliminer les cellules infectées par le VIH-1 via la réponse ADCC

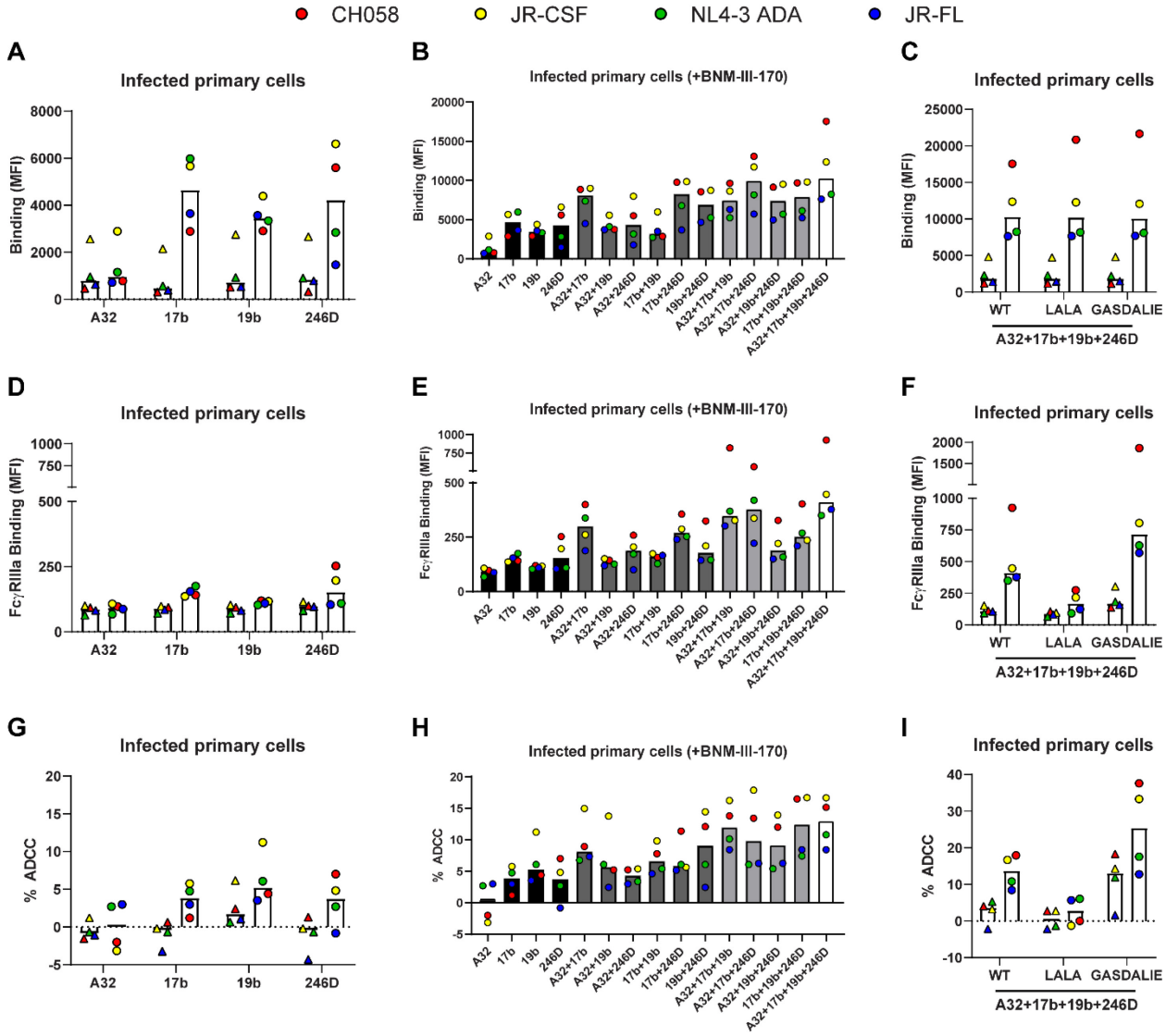

Figure 9.7.1 - La combinaison d'anticorps non-neutralisants de différentes spécificités augmente la réponse anticorps en présence de CD4mc.

Des lymphocytes T CD4$^+$ primaires ont été infectés avec différents isolats du VIH-1 de clade B (CH058, JR-CSF, NL4.3 ADA, JR-FL). 48h après l'infection, nous avons fait un marquage de surface total (**A-C**), un marquage FcγRIIIa (**D-F**) ou nous avons quantifié la susceptibilité des cellules infectées à la réponse ADCC en présence de cellules effectrices (**G-I**) par cytométrie en flux. Pour ce faire, nous avons utilisé (**A,D,G**) des anticorps non-neutralisants (A32, 17b, 19b, 246D) en présence du CD4mc BNM-III-170 (cercle) ou du solvant (DMSO; triangle), des combinaisons de plusieurs anticorps non-neutralisants en présence de CD4mc (**B,E,H**) ou encore des combinaisons d'anticorps non-neutralisants ayant des mutations dans la partie Fc (LALA ou GASDALIE) en présence de CD4mc (**C,F,I**).

ANNEXE VIII

Liste des articles additionnels auxquels le candidat a contribué

1. Ding S, Veillette M, Coutu M, **Prévost J**, Scharf L, Bjorkman PJ, Ferrari G, Robinson JE, Stürzel C, Hahn BH, Sauter D, Kirchhoff F, Lewis GK, Pazgier M, Finzi A. *A Highly Conserved Residue of the HIV-1 gp120 Inner Domain Is Important for Antibody-Dependent Cellular Cytotoxicity Responses Mediated by Anti-cluster A Antibodies*. **J Virol**. 2015 Dec 4;90(4):2127-34.

2. Ding S, Tolbert WD, **Prévost J**, Pacheco B, Coutu M, Debbeche O, Xiang SH, Pazgier M, Finzi A. *A Highly Conserved gp120 Inner Domain Residue Modulates Env Conformation and Trimer Stability*. **J Virol.** 2016 Sep 12;90(19):8395-409.

3. Richard J, Pacheco B, Gohain N, Veillette M, Ding S, Alsahafi N, Tolbert WD, **Prévost J**, Chapleau JP, Coutu M, Jia M, Brassard N, Park J, Courter JR, Melillo B, Martin L, Tremblay C, Hahn BH, Kaufmann DE, Wu X, Smith AB, III, Sodroski J, Pazgier M, Finzi A. *Co-receptor Binding Site Antibodies Enable CD4-Mimetics to Expose Conserved Anti-Cluster A ADCC Epitopes on HIV-1 Envelope Glycoproteins*. **EBioMedicine.** 2016 Oct;12:208-218.

4. Ding S, Medjahed H, **Prévost J**, Coutu M, Xiang SH, Finzi A. *Lineage-Specific Differences between the gp120 Inner Domain Layer 3 of Human Immunodeficiency Virus and That of Simian Immunodeficiency Virus*. **J Virol.** 2016 Oct 28;90(22):10065-10073.

5. Zoubchenok D*, Veillette M*, **Prévost J**, Sanders-Buell E, Wagh K, Korber B, Chenine AL, Finzi A. *Histidine 375 Modulates CD4 Binding in HIV-1 CRF01_AE Envelope Glycoproteins*. **J Virol**. 2017 Jan 31;91(4). *contribution égale

6. Pacheco B, Alsahafi N, Debbeche O, **Prévost J**, Ding S, Chapleau JP, Herschhorn A, Madani N, Princiotto A, Melillo B, Gu C, Zeng X, Mao Y, Smith AB, III, Sodroski J, Finzi A. *Residues in the gp41 Ectodomain Regulate HIV-1 Envelope Glycoprotein Conformational Transitions Induced by gp120-Directed Inhibitors*. **J Virol**. 2017 Feb 14;91(5).

7. Levast B*, Barblu L*, Coutu M, **Prévost J**, Brassard N, Peres A, Stegen C, Madrenas J, Kaufmann DE, Finzi A. *HIV-1 gp120 envelope glycoprotein determinants for cytokine burst in human monocytes*. **PLoS One**. 2017 Mar 27;12(3):e0174550. *contribution égale

8. Alsahafi N, Richard J, **Prévost J,** Coutu M, Brassard N, Parsons MS, Kaufmann DE, Brockman M, Finzi A. *Impaired Downregulation of NKG2D Ligands by Nef Proteins from Elite Controllers Sensitizes HIV-1-Infected Cells to Antibody-Dependent Cellular Cytotoxicity*. **J Virol**. 2017 Jul 27;91(16).

9. Madani N, Princiotto AM, Mach L, Ding S, **Prévost J**, Richard J, Hora B, Sutherland L, Zhao CA, Conn BP, Bradley T, Moody MA, Melillo B, Finzi A, Haynes BF, Smith AB, III, Santra S, Sodroski J. *A CD4-mimetic compound enhances vaccine efficacy against stringent immunodeficiency virus challenge*. **Nat Commun**. 2018 Jun 18;9(1):2363.

10. Alsahafi N, Anand SP, Castillo-Menendez L, Verly MM, Medjahed H, **Prévost J**, Herschhorn A, Richard J, Schön A, Melillo B, Freire E, Smith AB, III, Sodroski J, Finzi A. *SOSIP Changes Affect Human Immunodeficiency Virus Type 1 Envelope Glycoprotein Conformation and CD4 Engagement*. **J Virol.** 2018 Sep 12;92(19).

11. Anand SP, **Prévost J**, Baril S, Richard J, Medjahed H, Chapleau JP, Tolbert WD, Kirk S, Smith AB, III, Wines BD, Kent SJ, Hogarth PM, Parsons MS, Pazgier M, Finzi A. *Two Families of Env Antibodies Efficiently Engage Fc-Gamma Receptors and Eliminate HIV-1-Infected Cells*. **J Virol**. 2019 Jan 17;93(3).

12. Pauthner MG, Nkolola JP, Havenar-Daughton C, Murrell B, Reiss SM, Bastidas R, **Prévost J**, Nedellec R, von Bredow B, Abbink P, Cottrell CA, Kulp DW, Tokatlian T, Nogal B, Bianchi M, Li H, Lee JH, Butera ST, Evans DT, Hangartner L, Finzi A, Wilson IA, Wyatt RT, Irvine DJ, Schief WR, Ward AB, Sanders RW, Crotty S, Shaw GM, Barouch DH, Burton DR. *Vaccine-Induced Protection from Homologous Tier 2 SHIV Challenge in Nonhuman Primates Depends on Serum-Neutralizing Antibody Titers*. **Immunity**. 2019 Jan 15;50(1):241-252.e6.

13. Lee WS, **Prévost J**, Richard J, van der Sluis RM, Lewin SR, Pazgier M, Finzi A, Parsons MS, Kent SJ. *CD4- and Time-Dependent Susceptibility of HIV-1-Infected Cells to Antibody-Dependent Cellular Cytotoxicity*. **J Virol**. 2019 May 1;93(10).

14. Anand SP, Grover JR, Tolbert WD, **Prévost J**, Richard J, Ding S, Baril S, Medjahed H, Evans DT, Pazgier M, Mothes W, Finzi A. *Antibody-Induced Internalization of HIV-1 Env Proteins Limits Surface Expression of the Closed Conformation of Env*. **J Virol**. 2019 May 15;93(11).

15. Alsahafi N*, Bakouche N*, Kazemi M*, Richard J, Ding S, Bhattacharyya S, Das D, Anand SP, **Prévost J**, Tolbert WD, Lu H, Medjahed H, Gendron-Lepage G, Ortega Delgado GG, Kirk S, Melillo B, Mothes W, Sodroski J, Smith AB, III, Kaufmann DE, Wu X, Pazgier M, Rouiller I, Finzi A, Munro JB. *An Asymmetric Opening of HIV-1 Envelope Mediates Antibody-Dependent Cellular Cytotoxicity*. **Cell Host Microbe.** 2019 Apr 10;25(4):578-587.e5.

16. Ding S*, Grenier MC*, Tolbert WD, Vézina D, Sherburn R, Richard J, **Prévost J**, Chapleau JP, Gendron-Lepage G, Medjahed H, Abrams C, Sodroski J, Pazgier M, Smith AB, III, Finzi A. *A New Family of Small-Molecule CD4-Mimetic Compounds Contacts Highly Conserved Aspartic Acid 368 of HIV-1 gp120 and Mediates Antibody-Dependent Cellular Cytotoxicity*. **J Virol**. 2019 Nov 26;93(24).

17. **Prévost J*,** Edgar CR*, Richard J, Trothen SM, Jacob RA, Mumby MJ, Pickering S, Dubé M, Kaufmann DE, Kirchhoff F, Neil SJD, Finzi A, Dikeakos JD. *HIV-1 Vpu Downregulates Tim-3 from the Surface of Infected CD4+ T Cells*. **J Virol**. 2020 Mar 17;94(7):e01999-19. *contribution égale

18. Beaudoin-Bussières G*, **Prévost J*,** Gendron-Lepage G, Melillo B, Chen J, Smith AB, III, Pazgier M, Finzi A. *Elicitation of Cluster A and Co-Receptor Binding Site Antibodies are Required to Eliminate HIV-1 Infected Cells*. **Microorganisms**. 2020 May 11;8(5):710. *contribution égale

19. Perreault J, Tremblay T, Fournier MJ, Drouin M, Beaudoin-Bussières G, **Prévost J**, Lewin A, Bégin P, Finzi A, Bazin R. *Waning of SARS-CoV-2 RBD antibodies in longitudinal convalescent plasma samples within 4 months after symptom onset*. **Blood.** 2020 Nov 26;136(22):2588-2591.

20. Anand SP, Chen Y, **Prévost J,** Gasser R, Beaudoin-Bussières G, Abrams CF, Pazgier M, Finzi A. *Interaction of Human ACE2 to Membrane-Bound SARS-CoV-1 and SARS-CoV-2 S Glycoproteins*. **Viruses.** 2020 Sep 29;12(10):1104.

21. **Prévost J*,** Gasser R*, Beaudoin-Bussières G*, Richard J*, Duerr R*, Laumaea A*, Anand SP, Goyette G, Benlarbi M, Ding S, Medjahed H, Lewin A, Perreault J, Tremblay T, Gendron-Lepage G, Gauthier N, Carrier M, Marcoux D, Piché A, Lavoie M, Benoit A, Loungnarath V, Brochu G, Haddad E, Stacey HD, Miller MS, Desforges M, Talbot PJ, Maule GTG, Côté M, Therrien C, Serhir B, Bazin R, Roger M, Finzi A. *Cross-Sectional Evaluation of Humoral Responses against SARS-CoV-2 Spike*. **Cell Rep Med.** 2020 Oct 20;1(7):100126. *contribution égale

22. Beaudoin-Bussières G*, Laumaea A*, Anand SP*, **Prévost J*,** Gasser R*, Goyette G, Medjahed H, Perreault J, Tremblay T, Lewin A, Gokool L, Morrisseau C, Bégin P, Tremblay C, Martel-Laferrière V, Kaufmann DE, Richard J, Bazin R, Finzi A. *Decline of Humoral Responses against SARS-CoV-2 Spike in Convalescent Individuals*. **mBio.** 2020 Oct 16;11(5):e02590-20. *contribution égale

23. Lu M, Uchil PD, Li W, Zheng D, Terry DS, Gorman J, Shi W, Zhang B, Zhou T, Ding S, Gasser R, **Prévost J,** Beaudoin-Bussières G, Anand SP, Laumaea A, Grover JR, Liu L, Ho DD, Mascola JR, Finzi A, Kwong PD, Blanchard SC, Mothes W. *Real-Time Conformational Dynamics of SARS-CoV-2 Spikes on Virus Particles*. **Cell Host Microbe**. 2020 Dec 9;28(6):880-891.e8.

24. Anand SP*, **Prévost J*,** Richard J*, Perreault J, Tremblay T, Drouin M, Fournier MJ, Lewin A, Bazin R, Finzi A. *High-throughput detection of antibodies targeting the SARS-CoV-2 Spike in longitudinal convalescent plasma samples*. **Transfusion.** 2021 May;61(5):1377-1382. *contribution égale

25. Rébillard RM*, Charabati M*, Grasmuck C*, Filali-Mouhim A, Tastet O, Brassard N, Daigneault A, Bourbonnière L, Anand SP, Balthazard R, Beaudoin-Bussières G, Gasser R, Benlarbi M, Moratalla AC, Solorio YC, Boutin M, Farzam-Kia N, Descôteaux-Dinelle J, Fournier AP, Gowing E, Laumaea A, Jamann H, Lahav B, Goyette G, Lemaître F, Mamane VH, **Prévost J**, Richard J, Thai K, Cailhier JF, Chomont N, Finzi A, Chassé M, Durand M, Arbour N, Kaufmann DE, Prat A, Larochelle C. *Identification of SARS-CoV-2-specific immune alterations in acutely ill patients*. **J Clin Invest**. 2021 Apr 15;131(8):145853. *contribution égale

26. Gasser R*, Cloutier M*, **Prévost J,** Fink C, Ducas É, Ding S, Dussault N, Landry P, Tremblay T, Laforce-Lavoie A, Lewin A, Beaudoin-Bussières G, Laumaea A, Medjahed H, Larochelle C, Richard J, Dekaban GA, Dikeakos JD, Bazin R, Finzi A. *Major role of IgM in the neutralizing activity of convalescent plasma against SARS-CoV-2*. **Cell Rep.** 2021 Mar 2;34(9):108790. *contribution égale

27. **Prévost J,** Finzi A. *The great escape? SARS-CoV-2 variants evading neutralizing responses*. **Cell Host Microbe.** 2021 Mar 10;29(3):322-324.

28. Anand SP*, **Prévost J*,** Nayrac M*, Beaudoin-Bussières G*, Benlarbi M, Gasser R, Brassard N, Laumaea A, Gong SY, Bourassa C, Brunet-Ratnasingham E, Medjahed H, Gendron-Lepage G, Goyette G, Gokool L, Morrisseau C, Bégin P, Martel-Laferrière V, Tremblay C, Richard J, Bazin R, Duerr R, Kaufmann DE, Finzi A. *Longitudinal analysis of humoral immunity against SARS-CoV-2 Spike in convalescent individuals up to 8 months post-symptom onset*. **Cell Rep Med.** 2021 Jun 15;2(6):100290. *contribution égale

29. Lewin A, Therrien R, De Serres G, Grégoire Y, Perreault J, Drouin M, Fournier MJ, Tremblay T, Beaudoin J, Beaudoin-Bussières G, **Prévost J,** Gendron-Lepage G, Finzi A, Bernier F, Bazin R, Germain M, Delage G. *SARS-CoV-2 seroprevalence among blood donors in Québec, and analysis of symptoms associated with seropositivity: a nested case-control study*. **Can J Public Health.** 2021 Aug;112(4):576-586.

30. Rajashekar JK*, Richard J*, Beloor J, **Prévost J**, Anand SP, Beaudoin-Bussières G, Shan L, Herndler-Brandstetter D, Gendron-Lepage G, Medjahed H, Bourassa C, Gaudette F, Ullah I, Symmes K, Peric A, Lindemuth E, Bibollet-Ruche F, Park J, Chen HC, Kaufmann DE, Hahn BH, Sodroski J, Pazgier M, Flavell RA, Smith AB, III, Finzi A, Kumar P. *Modulating HIV-1 envelope glycoprotein conformation to decrease the HIV-1 reservoir*. **Cell Host Microbe.** 2021 Jun 9;29(6):904-916.e6. *contribution égale

31. Tauzin A*, Nayrac M*, Benlarbi M, Gong SY, Gasser R, Beaudoin-Bussières G, Brassard N, Laumaea A, Vézina D, **Prévost J**, Anand SP, Bourassa C, Gendron-Lepage G, Medjahed H, Goyette G, Niessl J, Tastet O, Gokool L, Morrisseau C, Arlotto P, Stamatatos L, McGuire AT, Larochelle C, Uchil P, Lu M, Mothes W, De Serres G, Moreira S, Roger M, Richard J, Martel-

Laferrière V, Duerr R, Tremblay C, Kaufmann DE, Finzi A. *A single dose of the SARS-CoV-2 vaccine BNT162b2 elicits Fc-mediated antibody effector functions and T cell responses*. **Cell Host Microbe**. 2021 Jun 4:S1931-3128(21)00279-1. *contribution égale

32. Papenburg J, Cheng MP, Corsini R, Caya C, Mendoza E, Manguiat K, Lindsay LR, Wood H, Drebot MA, Dibernardo A, Zaharatos G, Bazin R, Gasser R, Benlarbi M, Gendron-Lepage G, Beaudoin-Bussières G, **Prévost J,** Finzi A, Ndao M, Yansouni CP. *Evaluation of a Commercial Culture-Free Neutralization Antibody Detection Kit for Severe Acute Respiratory Syndrome-Related Coronavirus-2 and Comparison With an Antireceptor-Binding Domain Enzyme-Linked Immunosorbent Assay*. **Open Forum Infect Dis.** 2021 Apr 30;8(6):ofab220.

33. Anand SP*, Ding S*, Tolbert WD, **Prévost J**, Richard J, Gil HM, Gendron-Lepage G, Cheung WF, Wang H, Pastora R, Saxena H, Wakarchuk W, Medjahed H, Wines BD, Hogarth PM, Shaw GM, Martin MA, Burton DR, Hangartner L, Evans DT, Pazgier M, Cossar D, McLean MD, Finzi A. *Enhanced ability of plant-derived PGT121 glycovariants to eliminate HIV-1-infected cells*. **J Virol**. 2021 Jul 7:JVI0079621. *contribution égale

34. Jacob RA, Edgar CR, **Prévost J,** Trothen SM, Lurie A, Mumby MJ, Galbraith A, Kirchhoff F, Haeryfar SMM, Finzi A, Dikeakos JD. *The HIV-1 accessory protein Nef upregulates Tim-3 in infected CD4+ T cells*. **J Biol Chem**. 2021 Aug 3:101042.

35. Ullah I*, **Prévost J***, Ladinsky MS, Stone H, Lu M, Anand SP, Beaudoin-Bussières G, Benlarbi M, Ding S, Gasser R, Fink C, Chen Y, Tauzin A, Goyette G, Bourassa C, Medjahed H, Mack M, Chung K, Wilen CB, Dekaban GA, Dikeakos JD, Bruce EA, Kaufmann DE, Stamatatos L, McGuire AT, Richard J, Pazgier M, Bjorkman PJ, Mothes W, Finzi A, Kumar P, Uchil PD. *Live imaging of SARS-CoV-2 infection in mice reveals neutralizing antibodies require Fc function for optimal efficacy*. **Immunity**. 2021 Aug 18:S1074-7613(21)00347-2. *contribution égale

36. **Prévost J,** Richard J, Gasser R, Ding S, Fage C, Anand SP, Adam D, Gupta Vergara N, Tauzin A, Benlarbi M, Gong SY, Goyette G, Privé A, Moreira S, Charest H, Roger M, Mothes W, Pazgier M, Brochiero E, Boivin G, Abrams CF, Schön A, Finzi A. *Impact of temperature on the affinity of SARS-CoV-2 Spike for ACE2*. **J Biol Chem.** 2021 Aug 31:101151.

37. Gong SY*, Chatterjee D*, Richard J, **Prévost J**, Tauzin A, Gasser R, Bo Y, Vézina D, Goyette G, Gendron-Lepage G, Medjahed H, Roger M, Côté M, Finzi A. *Contribution of single mutations to selected SARS-CoV-2 emerging variants Spike antigenicity*. **Virology.** 2021 Sep 11;563:134-145. *contribution égale

38. Beaudoin-Bussières G, Richard J, **Prévost J**, Goyette G, Finzi A. *A new flow cytometry assay to measure antibody dependent cell-mediated cytotoxicity against SARS-CoV-2 Spike expressing cells*. **STAR Protoc.** 2021 Sep 13:100851.

39. Richard J*, Nguyen DN*, Tolbert WD, Gasser R, Ding S, Vézina D, Gong SY, **Prévost J**, Gendron-Lepage G, Medjahed H, Gottumukkala S, Finzi A, Pazgier M. *Across functional boundaries: making non-neutralizing antibodies to neutralize HIV-1 and mediate Fc mediated effector killing of infected cells*. **mBio.** 2021 Sep 28:e0140521. *contribution égale

40. Anand SP, **Prévost J**, Descôteaux-Dinelle J, Richard J, Nguyen DN, Medjahed H, Chen HC, Smith AB, III, Pazgier M, Finzi A. *HIV-1 Envelope Glycoprotein cell surface localization dictates its susceptibility to antibody-induced internalization*. **Viruses**. 2021 Sep 29, 13(10):1953.

41. **The CONCOR-1 Study Group.** CONCOR-1 writing committee : Bégin P, Callum J, Jamula E, Cook R, Heddle NM, Tinmouth A, Zeller MP, Beaudoin-Bussières G, Amorim L, Bazin R, Cadogan Loftsgard K, Carl R, Chassé M, Cushing MM, Daneman N, Devine DV, Dumaresq J, Fergusson DA, Gabe C, Glesby MJ, Li N, Liu Y, McGeer A, Robitaille N, Sachais BS, Scales DC, Schwartz L, Shehata N, Turgeon AF, Wood H, Zarychanski R, Finzi A, Arnold DM, for The CONCOR-1 Study Group. *Convalescent plasma for hospitalized patients with COVID-19 and the effect of plasma antibodies: a randomized controlled, open-label trial*. **Nat Med.** 2021 Nov;27(11):2012-2024.

42. **The REMAP-CAP Study Group.** REMAP-CAP writing committee: Estcourt LJ, Turgeon AF, McQuilten ZK, McVerry BJ, Al-Beidh F, Annane D, Arabi YM, Arnold DM, Beane A, Bégin P, van Bentum-Puijk W, Berry LR, Bhimani Z, Birchall JE, Bonten MJM, Bradbury CA, Brunkhorst FM, Buxton M, Callum JL, Chassé M, Cheng AC, Cove ME, Daly J, Derde L, Detry MA, De Jong M, Evans A, Fergusson DA, Fish M, Fitzgerald M, Foley C, Goossens H, Gordon AC, Gosbell IB, Green C, Haniffa R, Harvala H, Higgins AM, Hills TE, Hoad VC, Horvat C, Huang DT, Hudson CL, Ichihara N, Laing E, Lamikanra AA, Lamontagne F, Lawler PR, Linstrum K, Litton E, Lorenzi E, MacLennan S, Marshall J, McAuley DF, McDyer JF, McGlothlin A, McGuinness S, Miflin G, Montgomery S, Mouncey PR, Murthy S, Nichol A, Parke R, Parker JC, Priddee N, Purcell DFJ, Reyes LF, Richardson P, Robitaille N, Rowan KM, Rynne J, Saito H, Santos M, Saunders CT, Serpa Neto A, Seymour CW, Silversides JA, Tinmouth AA, Triulzi DJ, Turner AM, van de Veerdonk F, Walsh TS, Wood EM, Berry S, Lewis RJ, Menon DK, McArthur C, Zarychanski R, Angus DC, Webb SA, Roberts DJ, Shankar-Hari M. *Effect of Convalescent Plasma on Organ Support-Free Days in Critically Ill Patients With COVID-19: A Randomized Clinical Trial***. JAMA**. 2021 Nov 2;326(17):1690-1702

43. Valcourt EJ, Manguiat K, Robinson A, Lin YC, Abe KT, Mubareka S, Shigayeva A, Zhong Z, Girardin RC, DuPuis A, Payne A, McDonough K, Wang Z, Gasser R, Laumaea A, Benlarbi M, Richard J, **Prévost J**, Anand SP, Dimitrova K, Phillipson C, McGeer A, Gingras AC, Liang C, Petric M, Sekirov I, Morshed M, Finzi A, Drebot M, Wood H. *Evaluating humoral immunity against SARS-CoV-2: Validation of a plaque-reduction neutralization test and a multi-laboratory comparison of conventional and surrogate neutralization assays*. **Microbiol Spectr.** 2021 Nov 17;9(3):e0088621.

44. Brunet-Ratnasingham E*, Anand SP*, Gantner P*, Dyachenko A*, Moquin-Beaudry G, Brassard N, Beaudoin-Bussières G, Pagliuzza A, Gasser R, Benlarbi M, Point F, **Prévost J**, Laumaea A, Niessl J, Nayrac M, Sannier G, Orban C, Messier-Peet M, Butler-Laporte G, Morrison DR, Zhou S, Nakanishi T, Boutin M, Descôteaux-Dinelle J, Gendron-Lepage G, Goyette G, Bourassa C, Medjahed H, Laurent L, Rébillard RM, Richard J, Dubé M, Fromentin R, Arbour N, Prat A, Larochelle C, Durand M, Richards JB, Chassé M, Tétreault M, Chomont N, Finzi A, Kaufmann DE. *Integrated immunovirological profiling validates plasma SARS-CoV-2 RNA as an early predictor of COVID-19 mortality*. **Sci Adv.** 2021 Nov 26;7(48):eabj5629. *contribution égale

45. Tauzin A, Gong SY, Beaudoin-Bussières G, Vézina D, Gasser R, Nault L, Marchitto L, Benlarbi M, Chatterjee D, Nayrac M, Laumaea A, **Prévost J**, Boutin M, Sannier G, Nicolas A, Bourassa C, Gendron-Lepage G, Medjahed H, Goyette G, Bo Y, Perreault J, Gokool L, Morrisseau C, Arlotto P, Bazin R, Dubé M, De Serres G, Brousseau N, Richard J, Rovito R, Côté M, Tremblay C, Marchetti GC, Duerr R, Martel-Laferrière V, Kaufmann DE, Finzi A. *Strong humoral immune responses against SARS-CoV-2 Spike after BNT162b2 mRNA vaccination with a sixteen-week interval between doses*. **Cell Host Microbe**. 2021 Dec 3:S1931-3128(21)00569-2.

46. Li W*, Chen Y*, **Prévost J***, Ullah I, Lu M, Gong SY, Tauzin A, Gasser R, Vézina D, Anand SP, Goyette G, Chatterjee D, Ding S, Tolbert WD, Grunst MW, Bo Y, Zhang S, Richard J, Zhou F, Huang RK, Esser L, Zeher A, Côté M, Kumar P, Sodroski J, Xia D, Uchil PD, Pazgier M, Finzi A, Mothes W. *Structural Basis and Mode of Action for Two Broadly Neutralizing Antibodies Against SARS-CoV-2 Emerging Variants of Concern*. **Cell Rep**. 2021 Dec 15;110210. *contribution égale

47. Ding S, Adam D, Beaudoin-Bussières G, Tauzin A, Gong SY, Gasser R, Laumaea A, Anand SP, Privé A, Bourassa C, Medjahed H, **Prévost J**, Charest H, Richard J, Brochiero E, Finzi A. *SARS-CoV-2 Spike Expression at the Surface of Infected Primary Human Airway Epithelial Cells*. **Viruses** 2022, 14(1): 5.

48. Hioe CE, Li G, Liu X, Tsahouridis O, He X, Funaki M, Klingler J, Tang AF, Feyznezhad R, Heindel DW, Wang XH, Spencer DA, Hu G, Satija N, **Prévost J**, Finzi A, Hessell A, Wang S, Lu S, Chen BK, Zolla-Pazner S, Upadhyay C, Alvarez R, Su L. *Non-neutralizing antibodies targeting the immunogenic regions of HIV-1 envelope reduce mucosal infection and virus burden in humanized mice*. **PLoS Pathog**. 2022 Jan 5;18(1):e1010183.

49. Bégin P, Callum J, Cook R, Jamula E, Liu Y, Finzi A; **CONCOR-1 Study Group**, Arnold DM. *Reply to: Concerns about estimating relative risk of death associated with convalescent plasma for COVID-19*. **Nat Med**. 2022 Jan;28(1):53-58.

50. Beaudoin-Bussières G*, Chen Y*, Ullah I*, **Prévost J**, Tolbert WD, Symmes K, Ding S, Benlarbi M, Gong SY, Tauzin A, Gasser R, Chatterjee D, Vézina D, Goyette G, Richard J,

Zhou F, Stamatatos L, McGuire AT, Charest H, Roger M, Pazharski E, Kumar P, Mothes W, Uchil PD, Pazgier M, Finzi A. *A Fc-enhanced NTD-binding non-neutralizing antibody delays virus spread and synergizes with a nAb to protect mice from lethal SARS-CoV-2 infection*. **Cell Rep.** 2022 Feb 15;38(7):110368. *contribution égale

51. Chatterjee D, Tauzin A, Marchitto L, Gong SY, Boutin M, Bourassa C, Beaudoin-Bussières G, Bo Y, Ding S, Laumaea A, Vézina D, Perreault J, Gokool L, Morrisseau C, Arlotto P, Fournier É, Guilbault A, Delisle B, Levade I, Goyette G, Gendron-Lepage G, Medjahed H, De Serres G, Tremblay C, Martel-Laferrière V, Kaufmann DE, Bazin R, **Prévost J**, Moreira S, Richard J, Côté M, Finzi A. *SARS-CoV-2 Omicron Spike recognition by plasma from individuals receiving BNT162b2 mRNA vaccination with a 16-weeks interval between doses*. **Cell Rep**. 2022 Feb 8;38(9):110429

52. Boutin M, Vézina D, Ding S, **Prévost J**, Laumaea A, Marchitto L, Anand SP, Medjahed H, Gendron-Lepage G, Bourassa C, Goyette G, Clark A, Richard J, Finzi A. *Temsavir treatment of HIV-1-infected cells decreases envelope glycoproteins recognition by broadly neutralizing antibodies*. **mBio**. 2022 Jun 28;13(3):e0057722.

53. Nayrac M*, Dubé M*, Sannier G, Nicolas A, Marchitto L, Tastet O, Tauzin A, Brassard N, Lima-Barbosa R, Beaudoin-Bussières G, Vézina D, Gong SY, Benlarbi M, Gasser R, Laumaea A, **Prévost J**, Bourassa C, Gendron-Lepage G, Medjahed H, Goyette G, Ortega-Delgado GG, Laporte M, Niessl J, Gokool L, Morrisseau C, Arlotto P, Richard J, Bélair J, Tremblay C, Martel-Laferrière V, Finzi A, Kaufmann DE. *Temporal associations of B and T cell immunity with robust vaccine responsiveness in a 16-week interval BNT162b2 regimen*. **Cell Rep**. 2022 Jun 13;39(13):111013. *contribution égale

54. Benlarbi M*, Laroche G*, Fink C, Fu K, Mulloy RP, Phan A, Ariana A, Stewart CM, **Prévost J**, Beaudoin-Bussières G, Daniel R, Bo Y, El Ferri O, Yockell-Lelièvre J, Stanford WL, Giguère PM, Mubareka S, Finzi A, Dekaban GA, Dikeakos JD, Côté M. *Identification and differential usage of a host metalloproteinase entry pathway by SARS-CoV-2 Delta and Omicron*. **iScience**. 2022 Nov 18;25(11):105316. *contribution égale

55. Gong SY, Ding S, Benlarbi M, Chen Y, Vézina D, Marchitto L, Beaudoin-Bussières G, Goyette G, Bourassa C, Bo Y, Medjahed H, Levade I, Pazgier M, Côté M, Richard J, **Prévost J**, Finzi A. *Temperature influences the interaction between SARS-CoV-2 Spike from Omicron subvariants and human ACE2*. **Viruses**. 2022 Sep 30;14(10):2178.

56. Laumaea A, Marchitto L, Ding S, Beaudoin-Bussières G, **Prévost J**, Gasser R, Chatterjee D, Gendron-Lepage G, Medjahed H, Chen HC, Smith III AB, Ding H, Kappes JC, Hahn BH, Kirchhoff F, Richard J, Duerr R, Finzi A. *Small CD4 mimetics sensitize HIV-1-infected macrophages to antibody-dependent cellular cytotoxicity*. **Cell Rep.** *En révision*.

57. Chen Y*, **Prévost J***, Ullah I, Romero H, Lisi V, Tolbert WD, Grover JR, Ding S, Gong SY, Beaudoin-Bussières G, Gasser R, Benlarbi M, Vézina D, Anand SP, Chatterjee D, Goyette G, Grunst MW, Yang Z, Bo Y, Zhou F, Béland K, Bai X, Zeher AR, Huang RK, Nguyen DN, Sherburn R, Wu D, Piszczek G, Paré B, Matthies D, Xia D, Richard J, Kumar P, Mothes W, Côté M, Uchil PD, Lavallée VP, Smith MA, Pazgier M, Haddad E, Finzi A. *Molecular basis for antiviral activity of pediatric neutralizing antibodies targeting SARS-CoV-2 Spike receptor binding domain*. **iScience**. *En révision.* *contribution égale

58. Matsumoto K, Kuwata T, Tolbert WD, Richard J, Ding S, **Prévost J**, Takahama S, Judicate GP, Ueno T, Nakata H, Kobayakawa T, Tsuji K, Tamamura H, Smith III AB, Pazgier M, Finzi A, Matsushita S. *Characterization of a novel CD4 mimetic compound YIR-821 against HIV-1 clinical isolates*. **J Virol**. *En révision.*

59. Richard J*, **Prévost J***, Bourassa C, Brassard N, Goyette G, Medjahed H, Gendron-Lepage G, Gaudette F, Chen HC; Tolbert WD; Smith III AB; Pazgier M, Dubé M, Clark A, Mothes W, Kaufmann DE, Finzi A. *Temsavir blocks HIV-1 soluble gp120-induced immunomodulatory activities*. **Cell Chem Biol**. *En révision.* *contribution égale

ANNEXE IX

Liste des présentations orales et par affiche

1. **Prévost J**, Debbeche O, Coutu M, Finzi A. *A Highly Conserved gp120 Inner Domain Residue Modulates Interaction with CD4 and Conformation Changes.* Journée des étudiants du réseau SIDA/MI du FRSQ, Montréal, Québec, Canada (30 octobre 2015).

2. **Prévost J**, Debbeche O, Coutu M, Finzi A. *A Highly Conserved gp120 Inner Domain Residue Modulates Interaction with CD4 and Conformation Changes*. 4e journée de la recherche du département de Microbiologie, Infectiologie et Immunologie de l'Université de Montréal, Montréal, Québec, Canada (16 mars 2016).

3. **Prévost J**, Ding S, Tolbert WD, Coutu M, Debbeche O, Xiang SH, Pazgier M, Finzi A. *A Highly Conserved gp120 Inner Domain Residue Modulates Env Conformation and Trimer Stability*. Cold Spring Harbor meeting on Retroviruses, New York, NY, USA (23-28 mai 2016).

4. Ding S, Tolbert WD, **Prévost J**, Pacheco B, Coutu M, Debbeche O, Xiang SH, Pazgier M, Finzi A. *A Highly Conserved gp120 Inner Domain Residue Modulates Env Conformation and Trimer Stability.* 7e journée scientifique annuelle du CRCHUM, Vaccinologie et immunothérapie : de la recherche fondamentale à la médecine personnalisée, Montréal, Québec, Canada (20 octobre 2016).

5. **Prévost J**, Ding S, Tolbert WD, Pacheco B, Coutu M, Debbeche O, Xiang SH, Pazgier M, Finzi A. *A Highly Conserved gp120 Inner Domain Residue Modulates Env Conformation and Trimer Stability*. Journée des étudiants, stagiaires et résidents du réseau SIDA/MI du FRSQ, Montréal, Québec, Canada (4 novembre 2016).
   ***Présentation orale**

6. **Prévost J**, Ding S, Tolbert WD, Pacheco B, Coutu M, Debbeche O, Xiang SH, Pazgier M, Finzi A. *A Highly Conserved gp120 Inner Domain Residue Modulates Env Conformation and Trimer Stability*. 50e congrès COPSE des stagiaires de recherche du 1er cycle à la Faculté de Médecine, Montréal, Québec, Canada (27 janvier 2016).
   ***Présentation orale**

7. **Prévost J**, Zoubchenok D, Richard J, Veillette M, Pacheco B, Coutu M, Brassard N, Parsons MS, Ruxrungtham K, Bunupuradah T, Tovanabutra S, Hwang KK, Moody MA, Haynes BF, Bonsignori M, Sodroski J, Kaufmann DE, Shaw GM, Chenine AL, Finzi A. *Influence of the Envelope gp120 Phe 43 Cavity on HIV-1 Sensitivity to Antibody-Dependent Cell-Mediated Cytotoxicity Responses.* The 26th Annual Canadian Conference on HIV/AIDS Research, Montréal, Québec, Canada (6-9 avril 2017).
   ***Présentation orale**
   ****Bourse de voyage**

8. **Prévost J**, Zoubchenok D, Richard J, Veillette M, Pacheco B, Coutu M, Brassard N, Parsons MS, Ruxrungtham K, Bunupuradah T, Tovanabutra S, Hwang KK, Moody MA, Haynes BF, Bonsignori M, Sodroski J, Kaufmann DE, Shaw GM, Chenine AL, Finzi A. *Influence of the Envelope gp120 Phe 43 Cavity on HIV-1 Sensitivity to Antibody-Dependent Cell-Mediated Cytotoxicity Responses.* 19e congrès des étudiants, stagiaires et résidents du CRCHUM, Montréal, Québec, Canada (4 mai 2017).
***Prix d'excellence**

9. **Prévost J**, Zoubchenok D, Richard J, Veillette M, Pacheco B, Coutu M, Brassard N, Parsons MS, Ruxrungtham K, Bunupuradah T, Tovanabutra S, Hwang KK, Moody MA, Haynes BF, Bonsignori M, Sodroski J, Kaufmann DE, Shaw GM, Chenine AL, Finzi A. *Influence of the Envelope gp120 Phe 43 Cavity on HIV-1 Sensitivity to Antibody-Dependent Cell-Mediated Cytotoxicity Responses*. Cold Spring Harbor meeting on Retroviruses, New York, NY, USA (22-27 mai 2017).

10. **Prévost J**, Zoubchenok D, Richard J, Veillette M, Pacheco B, Coutu M, Brassard N, Parsons MS, Ruxrungtham K, Bunupuradah T, Tovanabutra S, Hwang KK, Moody MA, Haynes BF, Bonsignori M, Sodroski J, Kaufmann DE, Shaw GM, Chenine AL, Finzi A. *Influence of the Envelope gp120 Phe 43 Cavity on HIV-1 Sensitivity to Antibody-Dependent Cell-Mediated Cytotoxicity Responses*. Duke Center for HIV/AIDS Vaccine Immunology and Immunogen Design (CHAVI-ID) annual meeting, Durham, NC, USA (1-4 octobre 2017).
***Présentation orale**
****Prix d'excellence**

11. **Prévost J**, Zoubchenok D, Richard J, Veillette M, Pacheco B, Coutu M, Brassard N, Parsons MS, Ruxrungtham K, Bunupuradah T, Tovanabutra S, Hwang KK, Moody MA, Haynes BF, Bonsignori M, Sodroski J, Kaufmann DE, Shaw GM, Chenine AL, Finzi A. *Influence of the Envelope gp120 Phe 43 Cavity on HIV-1 Sensitivity to Antibody-Dependent Cell-Mediated Cytotoxicity Responses.* 5e journée de la recherche du département de Microbiologie, Infectiologie et Immunologie de l'Université de Montréal, Montréal, Québec, Canada (13 octobre 2017).
***Présentation orale**
****Prix d'excellence**

12. **Prévost J**, Richard J, Ding S, Pacheco B, Medjahed H, Brassard N, Hahn BH, Kaufmann DE, Finzi A. *Envelope Glycoproteins Sampling States 2/3 are Susceptible to ADCC mediated by sera from HIV-1- infected Individuals.* 8e journée scientifique annuelle du CRCHUM, Montréal, Québec, Canada (26 octobre 2017).

13. **Prévost J**, Zoubchenok D, Richard J, Veillette M, Pacheco B, Coutu M, Brassard N, Parsons MS, Ruxrungtham K, Bunupuradah T, Tovanabutra S, Hwang KK, Moody MA, Haynes BF, Bonsignori M, Sodroski J, Kaufmann DE, Shaw GM, Chenine AL, Finzi A. *Influence of the Envelope gp120 Phe 43 Cavity on HIV-1 Sensitivity to Antibody-Dependent Cell-Mediated*

Cytotoxicity Responses. Journée des étudiants, stagiaires et résidents du réseau SIDA/MI du FRSQ, Montréal, Québec, Canada (10 novembre 2017).
*** Présentation orale**
****Prix d'excellence**

14. **Prévost J**, Richard J, Ding S, Pacheco B, Medjahed H, Brassard N, Hahn BH, Kaufmann DE, Finzi A. *Envelope Glycoproteins Sampling States 2/3 are Susceptible to ADCC mediated by sera from HIV-1- infected Individuals*. Keystone Symposia: Progress and Pathways Toward an Effective HIV Vaccine, Banff, Alberta, Canada (28 janvier – 2 février 2018).

15. **Prévost J**, Richard J, Medjahed H, Jones J, Kappes JC, Ochsenbauer C, Finzi A. *Importance of CD4 downregulation for in vitro ADCC measurements.* Keystone Symposia: Emerging Technologies in Vaccine Discovery and Development, Banff, Alberta, Canada (28 janvier – 2 février 2018).

16. **Prévost J**, Richard J, Medjahed H, Jones J, Kappes JC, Ochsenbauer C, Finzi A. *Impact of CD4 downregulation on HIV-1 Env conformation and ADCC responses.* 20^{e} congrès des étudiants, stagiaires et résidents du CRCHUM, Montréal, Québec, Canada (3 mai 2018)

17. **Prévost J**, Richard J, Ding S, Pacheco B, Medjahed H, Brassard N, Hahn BH, Kaufmann DE, Finzi A. *Envelope Glycoproteins Sampling States 2/3 are Susceptible to ADCC mediated by sera from HIV-1- infected Individuals.* Cold Spring Harbor meeting on Retroviruses, New York, NY, USA (21-26 mai 2018).

18. **Prévost J**, Richard J, Medjahed H, Jones J, Kappes JC, Ochsenbauer C, Finzi A. *Impact of CD4 downregulation on HIV-1 Env conformation and ADCC responses.* Cold Spring Harbor meeting on Retroviruses, New York, NY, USA (21-26 mai 2018).

19. **Prévost J**, Richard J, Medjahed H, Jones J, Kappes JC, Ochsenbauer C, Finzi A. *Impact of CD4 downregulation on HIV-1 Env conformation and ADCC responses.* 1ère édition de la semaine Innove-action du CHUM, Montréal, Québec, Canada (30 novembre 2018).

20. **Prévost J**, Tolbert WD, Sherburn R, Madani N, Medjahed H, Zoubchenok D, Gendron-Lepage G, Kirk S, Mann BT, Chénine AG, Kirchhoff F, Hahn BH, Abrams CF, Smith III AB, Sodroski J, Pazgier M, Finzi A. *A Complex Interplay Between the HIV-1 Env gp120 Inner Domain and the Phe43 Cavity Modulates Its Sensitivity to Small CD4-Mimetic Compounds.* Keystone Symposia: Functional Cures and the Eradication of HIV, Whistler, BC, Canada (24-28 mars 2019).
***Bourse de voyage**

21. **Prévost J**, Tolbert WD, Sherburn R, Madani N, Medjahed H, Zoubchenok D, Gendron-Lepage G, Kirk S, Mann BT, Chénine AG, Kirchhoff F, Hahn BH, Abrams CF, Smith III AB, Sodroski

J, Pazgier M, Finzi A. *A Complex Interplay Between the HIV-1 Env gp120 Inner Domain and the Phe43 Cavity Modulates Its Sensitivity to Small CD4-Mimetic Compounds.* Les Journées Québécoises du VIH du réseau SIDA/MI du FRQS, Montréal, Québec, Canada (11-12 avril 2019).
***Présentation orale**
****Prix d'excellence**

22. **Prévost J**, Pickering S, Medjahed H, Gendron-Lepage G, Delgado GG, Dirk BS, Dikeakos JD, Stürzel CM, Sauter D, Kirchhoff F, Bibollet-Ruche F, Hahn BH, Dubé M, Kaufmann DE, Neil SD, Finzi A, Richard J. *Upregulation of BST-2 by type I IFNs reduce the capacity of Vpu to protect HIV-1-infected cells from NK cell responses.* 21e congrès des étudiants, stagiaires et résidents du CRCHUM, Montréal, Québec, Canada (9 mai 2019).

23. **Prévost J,** Tolbert WD, Sherburn R, Madani N, Medjahed H, Zoubchenok D, Gendron-Lepage G, Kirk S, Kirchhoff F, Hahn BH, Abrams CF, Smith III AB, Sodroski J, Pazgier M, Finzi A. *A complex interplay between the HIV-1 Env gp120 inner domain and the Phe43 cavity shapes the highly conserved CD4 binding site.* Cold Spring Harbor meeting on Retroviruses, New York, NY, USA (20-25 mai 2019).

24. **Prévost J**, Tolbert WD, Sherburn R, Madani N, Medjahed H, Zoubchenok D, Gendron-Lepage G, Kirk S, Mann BT, Chénine AG, Kirchhoff F, Hahn BH, Abrams CF, Smith III AB, Sodroski J, Pazgier M, Finzi A. *A Complex Interplay Between the HIV-1 Env gp120 Inner Domain and the Phe43 Cavity Modulates Its Sensitivity to Small CD4-Mimetic Compounds.* National Institute of General Medical Sciences Structural Biology Related to HIV/AIDS meeting, Bethesda, MD, USA (27-28 juin 2019).

25. Anand SP, Grover JR, Tolbert WD, **Prévost J**, Richard J, Ding S, Baril S, Medjahed H, Evans DT, Pazgier M, Mothes W, Finzi A. *Antibody-Induced Internalization of HIV-1 Env Proteins Limits Surface Expression of the Closed Conformation of Env.* 10e journée scientifique annuelle du CRCHUM, Montréal, Québec, Canada (17 octobre 2019).

26. **Prévost J**, Pickering S, Medjahed H, Gendron-Lepage G, Delgado GG, Dirk BS, Dikeakos JD, Stürzel CM, Sauter D, Kirchhoff F, Bibollet-Ruche F, Hahn BH, Dubé M, Kaufmann DE, Neil SD, Finzi A, Richard J. *Upregulation of BST-2 by type I IFNs reduce the capacity of Vpu to protect HIV-1-infected cells from NK cell responses.* 6e journée de la recherche du département de Microbiologie, Infectiologie et Immunologie de l'Université de Montréal, Montréal, Québec, Canada (27 novembre 2019).
***Présentation orale**

27. **Prévost J,** Tolbert WD, Medjahed H, Sherburn R, Madani N, Zoubchenok D, Gendron-Lepage G, Gaffney AE, Grenier MC, Kirk S, Vergara N, Han C, Mann BT, Chénine AL, Ahmed A, Chaiken I, Kirchhoff F, Hahn BH, Haim H, Abrams CF, Smith 3rd AB, Sodroski JG, Pazgier M, Finzi A. *A Complex Interplay Between the HIV-1 Env gp120 Inner Domain and the Phe43*

Cavity Modulates Its Sensitivity to Small CD4-Mimetic Compounds. The 29th Annual Canadian Conference on HIV/AIDS Research, conférence virtuelle (30 avril – 3 mai 2020).

28. **Prévost J,** Medjahed H, Smith, III AB, Finzi A. *Env Proteolytic Cleavage Protects HIV-1-Infected Cells from ADCC Mediated by Non-neutralizing Antibodies.* The 29th Annual Canadian Conference on HIV/AIDS Research, conférence virtuelle (30 avril – 3 mai 2020).

29. **Prévost J**, Tolbert WD, Medjahed H, Sherburn RT, Madani N, Zoubchenok D, Gendron-Lepage G, Vergara N, Han C, Chénine AL, Kirchhoff F, Hahn BH, Haim H, Abrams CF, Smith III AB, Sodroski J, Pazgier M, Finzi A. *The HIV-1 Env gp120 inner domain shapes the Phe43 cavity and the CD4-binding site.* Cold Spring Harbor meeting on Retroviruses, conférence virtuelle (18-21 mai 2020).

30. **Prévost J**, Medjahed H, Hahn BH, Smith III AB, Finzi A. *Env proteolytic cleavage protects HIV-1-infected cells from ADCC mediated by non-neutralizing antibodies.* Cold Spring Harbor meeting on Retroviruses, conférence virtuelle (18-21 mai 2020).

31. **Prévost J**, Edgar CR, Richard J, Trothen SM, Jacob RA, Mumby MJ, Pickering S, Dubé M, Kaufmann DE, Kirchhoff F, Neil SJD, Finzi A, Dikeakos JD. *HIV-1 Vpu downregulates Tim-3 from the surface of infected CD4+ T cells*. Cold Spring Harbor meeting on Retroviruses, conférence virtuelle (18-21 mai 2020).
***Présentation orale**
****Prix d'excellence**

32. **Prévost J**, Gasser R, Beaudoin-Bussières G, Richard J, Duerr R, Laumaea A, Anand SP, Goyette G, Benlarbi M, Ding S, Medjahed H, Lewin A, Perreault J, Tremblay T, Gendron-Lepage G, Gauthier N, Carrier M, Marcoux D, Piché A, Lavoie M, Benoit A, Loungnarath V, Brochu G, Haddad E, Stacey HD, Miller MS, Desforges M, Talbot PJ, Gould Maule GT, Côté M, Therrien C, Serhir B, Bazin R, Roger M, Finzi A. *Cross-sectional evaluation of humoral responses against SARS-CoV-2 Spike.* CITAC-CSCI Annual General Meeting: Young Investigators forum, conference virtuelle (12-13 novembre 2020).

33. **Prévost J**, Gasser R, Beaudoin-Bussières G, Richard J, Duerr R, Laumaea A, Anand SP, Goyette G, Benlarbi M, Ding S, Medjahed H, Lewin A, Perreault J, Tremblay T, Gendron-Lepage G, Gauthier N, Carrier M, Marcoux D, Piché A, Lavoie M, Benoit A, Loungnarath V, Brochu G, Haddad E, Stacey HD, Miller MS, Desforges M, Talbot PJ, Gould Maule GT, Côté M, Therrien C, Serhir B, Bazin R, Roger M, Finzi A. *Cross-sectional evaluation of humoral responses against SARS-CoV-2 Spike.* The 36th International Congress of the International Society of Blood Transfusion, conférence virtuelle (12-16 décembre 2020).

34. Ullah I**, Prévost J**, Ladinsky MS, Stone H, Lu M, Anand SP, Beaudoin-Bussières G, Benlarbi M, Ding S, Gasser R, Fink C, Chen Y, Tauzin A, Goyette G, Bourassa C, Medjahed H, Mack M, Chung K, Wilen CB, Dekaban GA, Dikeakos JD, Bruce EA, Kaufmann DE, Stamatatos L,

McGuire AT, Richard J, Pazgier M, Bjorkman PJ, Mothes W, Finzi A, Kumar P, Uchil PD. *Live imaging of SARS-CoV-2 infection in mice reveals neutralizing antibodies require Fc function for optimal efficacy*. 22e congrès des étudiants, stagiaires et résidents du CRCHUM, conference virtuelle (6 mai 2021)

35. **Prévost J**, Rajashekar JK, Anand SP, Richard J, Goyette G, Medjahed H, Gendron-Lepage G, Zolla-Pazner S, Smith III AB, Pazgier M, Nussenzweig MC, Kumar P, Finzi A. *HIV-1 Vpu limits Fc-mediated effector functions in vivo.* Cold Spring Harbor meeting on Retroviruses, conférence virtuelle (25-28 mai 2021).
***Présentation orale**

36. **Prévost J**, Rajashekar JK, Anand SP, Richard J, Goyette G, Medjahed H, Gendron-Lepage G, Zolla-Pazner S, Smith III AB, Pazgier M, Nussenzweig MC, Kumar P, Finzi A. *HIV-1 Vpu limits Fc-mediated effector functions in vivo.* Keystone eSymposia: HIV Vaccines, conférence virtuelle (1-4 juin 2021).
***Bourse d'inscription**

37. **Prévost J**, Richard J, Medjahed H, Gasser R, Gendron-Lepage G, Hahn BH, Shaw GM, Herschhorn A, Sodroski J, Smith III AB, Pazgier M, Mothes W, Finzi A. *Temsavir protects uninfected bystander cells from ADCC responses.* Keystone eSymposia: HIV Pathogenesis and Cure, conférence virtuelle (1-4 juin 2021).

38. **Prévost J**. *Réponses humorales et cellulaires contre la glycoprotéine S du SARS-CoV-2.* 4e édition de la semaine Innove-action du CHUM, conférence virtuelle, Montréal, QC, Canada (15-17 juin 2021).
***Conférencier invité**

39. **Prévost J**, Anand SP, Rajashekar JK, Richard J, Goyette G, Medjahed H, Gendron-Lepage G, Chen HC, Horwitz JA, Zolla-Pazner S, Burton DR, Kirchhoff F, Hahn BH, Smith III AB, Pazgier M, Nussenzweig MC, Kumar P, Finzi A. *HIV-1 Vpu limits Fc-mediated effector functions in vivo.* AIDS 2022, the 24th International AIDS Conference, Montréal, QC, Canada (29 juillet au 2 août 2022).

ANNEXE X

Autorisations d'utiliser des documents protégés par le droit d'auteur

CHAPITRE I

1. Richard J*, **Prévost J***, Alsahafi N, Ding S, Finzi A. *Impact of HIV-1 Envelope Conformation on ADCC Responses.* Trends Microbiol. 2018 Apr;26(4):253-265. *contribution égale

Les maisons d'édition Cell Press et Elsevier (qui publient *Trends in Microbiology*) accorde à l'auteur la permission de réutiliser leur propre matériel dans de nouvelles œuvres sans autorisation ni paiement (avec mention complète de l'article original). Ceci inclut l'utilisation ou le partage de leurs travaux à des fins académiques, comme par exemple, le droit de réutiliser l'article complet dans sa thèse ou dissertation.

CHAPITRE II

2. Richard J, **Prévost J**, Baxter AE, von Bredow B, Ding S, Medjahed H, Delgado GG, Brassard N, Stürzel CM, Kirchhoff F, Hahn BH, Parsons MS, Kaufmann DE, Evans DT, Finzi A. *Uninfected Bystander Cells Impact the Measurement of HIV-Specific Antibody-Dependent Cellular Cytotoxicity Responses*. mBio. 2018 Mar 20;9(2).

Depuis 2016, les articles publiés dans *mBio* sont couverts par une licence Creative Commons Attribution 4.0 International (CC BY 4.0). Les auteurs conservent les droits d'auteur sous cette licence. D'autres personnes peuvent lire, télécharger, copier, distribuer, imprimer, rechercher, adapter, créer des liens vers, réorganiser et s'appuyer sur l'œuvre publiée à toutes fins, même commerciales, tant que l'auteur et l'article original sont mentionnés.

3. **Prévost J**, Richard J, Medjahed H, Alexander A, Jones J, Kappes JC, Ochsenbauer C, Finzi A. *Incomplete Downregulation of CD4 Expression Affects HIV-1 Env Conformation and Antibody-Dependent Cellular Cytotoxicity Responses*. J Virol. 2018 Jun 13;92(13).

La maison d'édition ASM (qui détient *Journal of Virology*) accorde à l'auteur le droit de republier des portions de son article dans toute autre publication dont il est l'auteur, à condition que la publication originale publiée par ASM soit dûment citée. L'auteur conserve également le droit de réutiliser l'article complet dans sa dissertation ou sa thèse.

4. **Prévost J***, Richard J*, Gasser R, Medjahed H, Kirchhoff F, Hahn BH, Kappes JC, Ochsenbauer C, Duerr R, Finzi A. *Detection of the HIV-1 accessory proteins Nef and Vpu*

by flow cytometry represents a new tool to study their functional interplay within a single infected CD4$^+$ T cell. J Virol. 2022 Jan 26:jvi0192921. *contribution égale

La maison d'édition ASM (qui détient *Journal of Virology*) accorde à l'auteur le droit de republier des portions de son article dans toute autre publication dont il est l'auteur, à condition que la publication originale publiée par ASM soit dûment citée. L'auteur conserve également le droit de réutiliser l'article complet dans sa dissertation ou sa thèse.

CHAPITRE III

5. **Prévost J**, Richard J, Ding S, Pacheco B, Charlebois R, Hahn BH, Kaufmann DE, Finzi A. *Envelope glycoproteins sampling states 2/3 are susceptible to ADCC by sera from HIV-1-infected individuals*. Virology. 2018 Feb;515:38-45.

La maison d'édition Elsevier (qui publie *Virology*) accorde à l'auteur la permission de réutiliser leur propre matériel dans de nouvelles œuvres sans autorisation ni paiement (avec mention complète de l'article original). Ceci inclut l'utilisation ou le partage de leurs travaux à des fins académiques, comme par exemple, le droit de réutiliser l'article complet dans sa thèse ou dissertation.

6. **Prévost J**, Medjahed H, Vézina D, Chen HC, Hahn BH, Smith AB, III, Finzi A. *HIV-1 envelope glycoproteins proteolytic cleavage protects infected cells from ADCC mediated by plasma from infected individuals*. Viruses. 2021 Nov 6;13(11):2236.

Pour tous les articles publiés dans les revues de la maison d'édition MDPI (dont *Viruses*), les droits d'auteur sont conservés par les auteurs. Les articles sont soumis à une licence d'accès libre Creative Commons Attribution 4.0 International (CC BY 4.0), ce qui signifie que tout le monde peut télécharger et lire l'article gratuitement. En outre, l'article peut être réutilisé et cité à condition que la version originale publiée soit citée.

7. **Prévost J**, Zoubchenok D, Richard J, Veillette M, Pacheco B, Coutu M, Brassard N, Parsons MS, Ruxrungtham K, Bunupuradah T, Tovanabutra S, Hwang KK, Moody MA, Haynes BF, Bonsignori M, Sodroski J, Kaufmann DE, Shaw GM, Chenine AL, Finzi A. *Influence of the Envelope gp120 Phe43 Cavity on HIV-1 Sensitivity to Antibody-Dependent Cell-Mediated Cytotoxicity Responses*. J Virol. 2017 Mar 13;91(7).

La maison d'édition ASM (qui détient *Journal of Virology*) accorde à l'auteur le droit de republier des portions de son article dans toute autre publication dont il est l'auteur, à condition que la

publication originale publiée par ASM soit dûment citée. L'auteur conserve également le droit de réutiliser l'article complet dans sa dissertation ou sa thèse.

CHAPITRE IV

8. **Prévost J**, Pickering S, Mumby MJ, Medjahed H, Gendron-Lepage G, Delgado GG, Dirk BS, Dikeakos JD, Stürzel CM, Sauter D, Kirchhoff F, Bibollet-Ruche F, Hahn BH, Dubé M, Kaufmann DE, Neil SJD, Finzi A, Richard J. *Upregulation of BST-2 by Type I Interferons Reduces the Capacity of Vpu to Protect HIV-1-Infected Cells from NK Cell Responses*. mBio. 2019 Jun 18;10(3).

Depuis 2016, les articles publiés dans *mBio* sont couverts par une licence Creative Commons Attribution 4.0 International. Les auteurs conservent les droits d'auteur sous cette licence. D'autres personnes peuvent lire, télécharger, copier, distribuer, imprimer, rechercher, adapter, créer des liens vers, réorganiser et s'appuyer sur l'œuvre publiée à toutes fins, même commerciales, tant que l'auteur et l'article original sont mentionnés.

9. **Prévost J**, Anand SP, Rajashekar JK, Richard J, Goyette G, Medjahed H, Gendron-Lepage G, Chen HC, Chen Y, Horwitz JA, Grunst MW, Zolla-Pazner S, Haynes BF, Burton DR, Flavell RA, Kirchhoff F, Hahn BH, Smith AB, III, Pazgier M, Nussenzweig MC, Kumar P, Finzi A. *HIV-1 Vpu restricts Fc-mediated effector functions in vivo*. Cell Rep. 2022 Nov 8;41(6):111624.

Les maisons d'édition Cell Press et Elsevier (qui publient *Cell Reports*) accorde à l'auteur la permission de réutiliser leur propre matériel dans de nouvelles œuvres sans autorisation ni paiement (avec mention complète de l'article original). Ceci inclut l'utilisation ou le partage de leurs travaux à des fins académiques, comme par exemple, le droit de réutiliser l'article complet dans sa thèse ou dissertation.

CHAPITRE V

10. **Prévost J**, Tolbert WD, Medjahed H, Sherburn RT, Madani N, Zoubchenok D, Gendron-Lepage G, Gaffney AE, Grenier MC, Kirk S, Vergara N, Han C, Mann BT, Chénine AL, Ahmed A, Chaiken I, Kirchhoff F, Hahn BH, Haim H, Abrams CF, Smith AB, III, Sodroski J, Pazgier M, Finzi A. *The HIV-1 Env gp120 Inner Domain Shapes the Phe43 Cavity and the CD4 Binding Site*. mBio. 2020 May 26;11(3):e00280-20.

11. Richard J, **Prévost J**, von Bredow B, Ding S, Brassard N, Medjahed H, Coutu M, Melillo B, Bibollet-Ruche F, Hahn BH, Kaufmann DE, Smith AB, III, Sodroski J, Sauter D, Kirchhoff F, Gee K, Neil SJ, Evans DT, Finzi A. *BST-2 Expression Modulates Small CD4-Mimetic Sensitization of HIV-1-Infected Cells to Antibody-Dependent Cellular Cytotoxicity*. J Virol. 2017 May 12;91(11).